Handbook of Induction Heating

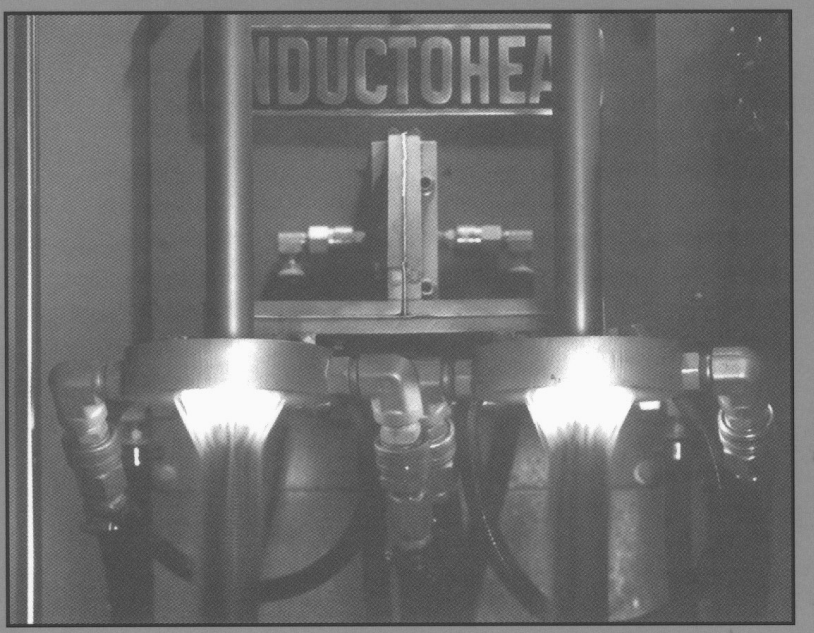

Valery Rudnev
Don Loveless
Raymond Cook

Handbook of Induction Heating

MANUFACTURING ENGINEERING AND MATERIALS PROCESSING

A Series of Reference Books and Textbooks

1. Computers in Manufacturing, *U. Rembold, M. Seth, and J. S. Weinstein*
2. Cold Rolling of Steel, *William L. Roberts*
3. Strengthening of Ceramics: Treatments, Tests, and Design Applications, *Harry P. Kirchner*
4. Metal Forming: The Application of Limit Analysis, *Betzalel Avitzur*
5. Improving Productivity by Classification, Coding, and Data Base Standardization: The Key to Maximizing CAD/CAM and Group Technology, *William F. Hyde*
6. Automatic Assembly, *Geoffrey Boothroyd, Corrado Poli, and Laurence E. Murch*
7. Manufacturing Engineering Processes, *Leo Alting*
8. Modern Ceramic Engineering: Properties, Processing, and Use in Design, *David W. Richerson*
9. Interface Technology for Computer-Controlled Manufacturing Processes, *Ulrich Rembold, Karl Armbruster, and Wolfgang Ülzmann*
10. Hot Rolling of Steel, *William L. Roberts*
11. Adhesives in Manufacturing, *edited by Gerald L. Schneberger*
12. Understanding the Manufacturing Process: Key to Successful CAD/CAM Implementation, *Joseph Harrington, Jr.*
13. Industrial Materials Science and Engineering, *edited by Lawrence E. Murr*
14. Lubricants and Lubrication in Metalworking Operations, *Elliot S. Nachtman and Serope Kalpakjian*
15. Manufacturing Engineering: An Introduction to the Basic Functions, *John P. Tanner*
16. Computer-Integrated Manufacturing Technology and Systems, *Ulrich Rembold, Christian Blume, and Ruediger Dillman*
17. Connections in Electronic Assemblies, *Anthony J. Bilotta*
18. Automation for Press Feed Operations: Applications and Economics, *Edward Walker*
19. Nontraditional Manufacturing Processes, *Gary F. Benedict*
20. Programmable Controllers for Factory Automation, *David G. Johnson*
21. Printed Circuit Assembly Manufacturing, *Fred W. Kear*
22. Manufacturing High Technology Handbook, *edited by Donatas Tijunelis and Keith E. McKee*
23. Factory Information Systems: Design and Implementation for CIM Management and Control, *John Gaylord*
24. Flat Processing of Steel, *William L. Roberts*
25. Soldering for Electronic Assemblies, *Leo P. Lambert*
26. Flexible Manufacturing Systems in Practice: Applications, Design, and Simulation, *Joseph Talavage and Roger G. Hannam*
27. Flexible Manufacturing Systems: Benefits for the Low Inventory Factory, *John E. Lenz*
28. Fundamentals of Machining and Machine Tools: Second Edition, *Geoffrey Boothroyd and Winston A. Knight*
29. Computer-Automated Process Planning for World-Class Manufacturing, *James Nolen*
30. Steel-Rolling Technology: Theory and Practice, *Vladimir B. Ginzburg*
31. Computer Integrated Electronics Manufacturing and Testing, *Jack Arabian*

32. In-Process Measurement and Control, *Stephan D. Murphy*
33. Assembly Line Design: Methodology and Applications, *We-Min Chow*
34. Robot Technology and Applications, *edited by Ulrich Rembold*
35. Mechanical Deburring and Surface Finishing Technology, *Alfred F. Scheider*
36. Manufacturing Engineering: An Introduction to the Basic Functions, Second Edition, Revised and Expanded, *John P. Tanner*
37. Assembly Automation and Product Design, *Geoffrey Boothroyd*
38. Hybrid Assemblies and Multichip Modules, *Fred W. Kear*
39. High-Quality Steel Rolling: Theory and Practice, *Vladimir B. Ginzburg*
40. Manufacturing Engineering Processes: Second Edition, Revised and Expanded, *Leo Alting*
41. Metalworking Fluids, *edited by Jerry P. Byers*
42. Coordinate Measuring Machines and Systems, *edited by John A. Bosch*
43. Arc Welding Automation, *Howard B. Cary*
44. Facilities Planning and Materials Handling: Methods and Requirements, *Vijay S. Sheth*
45. Continuous Flow Manufacturing: Quality in Design and Processes, *Pierre C. Guerindon*
46. Laser Materials Processing, *edited by Leonard Migliore*
47. Re-Engineering the Manufacturing System: Applying the Theory of Constraints, *Robert E. Stein*
48. Handbook of Manufacturing Engineering, *edited by Jack M. Walker*
49. Metal Cutting Theory and Practice, *David A. Stephenson and John S. Agapiou*
50. Manufacturing Process Design and Optimization, *Robert F. Rhyder*
51. Statistical Process Control in Manufacturing Practice, *Fred W. Kear*
52. Measurement of Geometric Tolerances in Manufacturing, *James D. Meadows*
53. Machining of Ceramics and Composites, *edited by Said Jahanmir, M. Ramulu, and Philip Koshy*
54. Introduction to Manufacturing Processes and Materials, *Robert C. Creese*
55. Computer-Aided Fixture Design, *Yiming (Kevin) Rong and Yaoxiang (Stephens) Zhu*
56. Understanding and Applying Machine Vision: Second Edition, Revised and Expanded, *Nello Zuech*
57. Flat Rolling Fundamentals, *Vladimir B. Ginzburg and Robert Ballas*
58. Product Design for Manufacture and Assembly: Second Edition, Revised and Expanded, *Geoffrey Boothroyd, Peter Dewhurst, and Winston Knight*
59. Process Modeling in Composites Manufacturing, *Suresh G. Advani and E. Murat Sozer*
60. Integrated Product Design and Manufacturing Using Geometric Dimensioning and Tolerancing, *Robert G. Campbell and Edward S. Roth*
61. Handbook of Induction Heating, *Valery Rudnev, Don Loveless, Raymond Cook, and Micah Black*

Additional Volumes in Preparation

Reengineering the Manufacturing System: Applying the Theory of Constraints, Second Edition, Revised and Expanded, *Robert E. Stein*

Handbook of Induction Heating

Valery Rudnev
Don Loveless
Raymond Cook
Micah Black

INDUCTOHEAT, Inc.
Madison Heights, Michigan, U.S.A.

MARCEL DEKKER, INC. NEW YORK • BASEL

Library of Congress Cataloging-in-Publication Data
A catalog record for this book is available from the Library of Congress.

ISBN: 0-8247-0848-2

This book is printed on acid-free paper.

Headquarters
Marcel Dekker, Inc.
270 Madison Avenue, New York, NY 10016
tel: 212-696-9000; fax: 212-685-4540

Eastern Hemisphere Distribution
Marcel Dekker AG
Hutgasse 4, Postfach 812, CH-4001 Basel, Switzerland
tel: 41-61-260-6300; fax: 41-61-260-6333

World Wide Web
http://www.dekker.com

The publisher offers discounts on this book when ordered in bulk quantities. For more information, write to Special Sales/Professional Marketing at the headquarters address above.

Current printed (last digit):
10 9 8 7 6 5 4 3 2 1

PRINTED IN THE UNITED STATES OF AMERICA

This book is dedicated to the customers of Inductoheat Group who through the years have provided the opportunity to study, learn, and develop the themes presented in this text. This includes customers of the past and present who have had the courage to venture into sometimes uncharted waters in the area of induction heating design and development in order to reap the projected gains provided by this technology.

Preface

In the beginning there is PRICE,
at the end there is COST.
The difference is QUALITY.
This quality insured the ability to
avoid unpleasant surprises by utilizing
the experience of previous jobs,
engineering expertise and awareness of
the latest advances in theoretical knowledge.

This handbook is a synthesis of information, discoveries, and technical insights that we have accumulated during the course of our tenure in industry and academia. Often technical books on induction heating deal with separate islands of information that must be further researched by the reader to discover the relationship and interaction of the different threads in order to tie them together into one design. This book is different.

Beginning with a brief introduction to the history of induction heating, it proceeds to connect related subjects such as metallurgy and principles of heat threatment, beginning with the basics and proceeding to the nonequilibrium nature of phase transformation processes incurred during induction heating.

Special attention has been paid to presenting a detailed description of important electromagnetic and heat transfer phenomena that take place during induction heating including the skin effect, electromagnetic "ring" and "slot" effects, proximity effects, electromagnetic end and edge effects, and many other phenomena that are imperative for a practitioner of induction heating to know. An attempt has been made to discuss complex interrelated effects in simple terms.

Other subjects of interest include surface and through hardening, tempering, stress relieving, annealing, shrink fitting, brazing, bonding, soldering, induction heating prior to bending, coating, forging, rolling, upsetting, and extrusion of ferrous and nonferrous metals. Emphasis is placed on the intricacies of irregularly shaped heating products such as crank shafts, cam shafts, gears, and other critical components, as well as billets, bars, slabs, blooms, strips, tubes, pipes, wires, and cables.

This handbook also embarks on the next step, the design of practical, cost-effective modern induction heating processes and equipment, providing many case

studies, ready-to-use tables, diagrams, simplified formulas, and graphs. Plots of electromagnetic fields, temperature profiles, and photographs of a variety of production installations are provided to show not only that the task has been previously accomplished but also why and how it has been done. Some materials presented here have never before been published.

It is recommended that the reader follow the order of the material presented in the text, which will allow completion of a thorough study of the material. At the same time, readers with a limited amount of available time can skip certain sections and turn to the subject of interest. Because this text is written as a handbook, each section has cross-references to other sections in which a particular phenomenon may be explained in more detail.

We present this work in the hope that it will be an aid to practitioners, students, engineers, and scientists of the art of induction heating to further the development of this technology in the next millennium. It is the most complete modern source of information on all the important aspects of the design process for induction heating systems.

Valery Rudnev
Don Loveless
Raymond Cook
Micah Black

Acknowledgment

We would like to give special thanks to those who have made this effort possible.

We first acknowledge the contribution of the employees of the INDUCTOHEAT organization. Their professional attitude and commitment to quality have made them the benchmark in the induction heating industry and have made this work possible.

Next we thank Byron Taylor, the CEO of the INDUCTOHEAT Group, who has taken the company from obscurity to the largest and most respected company in the industry. During this time he has provided us with many opportunities to stretch our thinking on new concepts, solve difficult technical problems, and, most of all, do the things that others are sure cannot be done.

Special thanks are also due to Henry (Hank) M. Rowan, the founder of Inductotherm Corporation and owner of Inductotherm Industries and all its related companies. His vision, drive, and demand for the best performance have propelled this group of companies to world dominance in the induction melting and heating arena. Hank has said, "This country doesn't just need more engineers, we need more great engineers."

May thanks must go to our families. It goes without saying that a technical book of this magnitude requires many hours of meticulous work, hours that often have infringed upon or restricted planned family activities.

We gratefully acknowledge the contribution of the Mikron Instrument Company Inc. of Oakland, New Jersey, for providing the sections on infrared thermometry and noncontact temperature measurement, authored on their behalf by John Merchant of Word Works. Thanks are also due to Scott Nagle, Mikron's Domestic Sales Director, for the providing tables, graphs, and photographs, and for editing the text.

We also acknowledge the contribution of the Leco Corporation of St. Joseph, Michigan, for providing the sections on metallographic sample preparation, hardness testing and microscopic analysis. Our special thanks go to Patrick Foster of

Leco's Metallographic Applications Lab management for facilitating the preparation of this material.

Finally we acknowledge and greatly appreciate the contribution and assistance of the following companies in the INDUCTOHEAT Group:

Inductoheat, Inc., USA
Radyne Corp., USA
Inductoheat Mass Heat Div., USA
Inductoheat–Brazil
Inductoheat–I.H.S., USA
HWG–Inductoheat, Germany
Radyne Ltd., UK
Welduction Corp, USA
Alpha-1, USA
Lepel Corp, USA
Inductoheat–India
Inductoheat–Taiwan
Inductoheat–Australia
Newelco, UK
Inductoheat–Japan
IRK Korea
Inductoheat Banyard, UK
Inductoheat–China

Contents

1

Introduction

This introduction provides a general background of the contents of the book and allows easy identification of the section or chapter that may be most appropriate for the question or problem at hand.

The basis for heating metal by induction was discovered in 1831 by the English physicist Michael Faraday. While experimenting in his laboratory with two coils of wire wrapped around a common iron core, he discovered that if the switch connecting a battery to the first coil was closed, a momentary current could be measured in one direction on a galvanometer placed in series with the second coil. If the switch remained closed, no current was detected in the second coil. When the switch was opened, a current was again detected in the second coil, but in the opposite direction to that measured when the switch was closed.

Faraday concluded from this that an electric current can be produced by a changing magnetic field. Since there was no physical connection between the two coils, the current in the second coil was said to be produced by a voltage that was "induced" from the first coil to the second coil. Faraday's law of induction states that "The electro-motive force (emf) induced in a circuit is directly proportional to the time rate of change of magnetic flux through the circuit."

The German physicist Heinrich Lenz later formulated Lenz's law, which states that "The polarity of the induced emf is such that it tends to produce a current that will create a magnetic flux to oppose the change in magnetic flux through the loop" [3, 6, 40].

Over the next several decades these effects were used to develop the design of transformers for the purpose of changing the level of voltage from one circuit to another for efficient transmission of electricity and operation of electrical machinery. A byproduct of this transformation process was the heat generated in the magnetic core of the transformer. These cores were made of laminated stacks of steel in an attempt to reduce heating from occurring in the core. In the latter part of the ninteenth century the exact opposite was attempted in order to utilize this heating effect for the purpose of melting metal.

Northrup, in the early 1900s, developed equipment to heat metal using a cylindrical crucible and a spark gap power supply. The development of these types of heating and melting systems was limited due to the low power attainable from the spark gap power supply. In 1922 the development of motor generators provided an ideal power source for these "coreless" induction furnaces.

After general acceptance of induction for the melting of metal, the attention of scientists and engineers was turned in another direction. Since the depth of current penetration in a given metal varies with the material electrical resistivity, magnetic permeability, and frequency, it is possible to heat specific areas of a piece of metal without heating others. This knowledge was used as successful attempts were made at Midvale Steel (1927) and the Ohio Crankshaft Company (mid-1930s) to use this technology to surface harden steel. Much of the early work was done in the hardening of crankshafts with frequencies of 1920 and 3000 Hz. In the late 1960s the development of high current, high voltage semiconductors led to the replacement of the motor generator by solid-state power supplies. The major factors promoting this change have been improved process efficiency and lower cost.

As illustrated above, the technology-involved induction heating phenomenon has changed through the years. In modern industry the requirements for the induction heating process have become quite stringent. Some of these requirements could not possibly have been satisfied 15 or even 10 years ago.

Many years ago a basic knowledge of electromagnetic fields, a calculator, and engineering intuition were all that were available to design an induction heating system. Now these alone are not enough. In order to provide a successful design for modern induction heating it is now necessary to take into account more details of the process. The designers of induction heating systems in this next millennium must have advanced software that allows the effective simulation of the heating and cooling processes, and they must be aware of the intricacies of the interrelated features of the induction heating process and new achievements in theory and practice in this area.

Several useful books have been published in the past on the basic principles of induction heating design [1–12]. Some of the most popular induction heating texts have been written by Chester Tudbury [1, 260] and Alexander Slukhotskii [4,5,449]. The first editions of these books were published at practically the same time (1960 and 1954, respectively) in countries that are situated thousands of miles apart: the USA and Russia. Both books have been reprinted numerous times. The tremendous success of these books deals with the unique ability of both authors to discuss the very complex phenomena existing in induction heating in simple terms.

In this present handbook, an attempt has been made to continue the tradition of those classical texts to educate specialists involved in induction heating technologies. Therefore, the major goal of this handbook is to embark upon the next step in the study and design of modern induction heating processes and equipment. Thus, there is a hope that this handbook will serve the industry as a complete contemporary guide to induction heating.

The study of basic principles, modern design concepts, and an introduction to advanced methods used in modeling and evaluation of different types of processes that utilize heating by induction are provided in this text. The study also includes the systematization of existing and new information, as well as a description of new knowledge that has been accumulated in recent years at the world's largest

manufacturer of induction heating equipment—INDUCTOHEAT, Inc. and by our colleagues around the world. Some materials presented here are new and have never been published before. Others have existed only in articles or internal reports of the INDUCTOHEAT Group (Figure 1.1) or published in engineering and scientific journals, as well as conference proceedings.

There has been an attempt to make this the most complete source book on heating and heat treating by induction. It is intended to reach a wide variety of readers including practitioners, designers, students, managers, and scientists.

Practitioners and first-time designers can find in this text a detailed "nuts-and-bolts" description of the basic phenomena involved in induction heating. Common sense and a basic knowledge of physics should be enough to understand the material presented in the sections that describe the basic phenomena (i.e., Secs. 3.1 through 3.3). Readers with a limited knowledge in advanced mathematics, including numerical modeling and partial differential equations, can skip Section 3.4, "Advanced Induction Principles and Mathematical Modeling," that is primarily oriented toward students, engineers, and scientists.

A reader with great experience in the field will also find this book useful because he or she will discover the reasons for intuitive engineering decisions made in the past. College students preparing for a career involving induction heating or metal heat treating will see how the theory and mathematical methods they are studying are used to solve problems encountered in everyday practice. This book consists of information that will be useful to a manager as well, because he or she will better understand the complexity of the process and the attention to detail required to obtain cost-effective, high-quality induction heating results.

It is recommended that the reader follow the order of the material presented in the text which will allow the completion of a thorough study of the material presented. At the same time, readers having a limited amount of time available can skip certain sections and turn to the desired subject (e.g., bar end heating, induction tempering, or wire/cable heating). Since this text is written as a handbook each section has cross-references to previous sections referring to related topics where a particular phenomenon may be explained in more detail.

At the same time, during the writing of this text the authors put the chapters and sections in a certain order from a logical and methodological perspective for presenting the material. Following the sequence would allow one to accumulate knowledge in a progressive manner. This approach is highly recommended.

This book is not intended to describe exhaustively the specific mathematical methods or in-depth theoretical aspects of electrodynamics, thermodynamics, metallurgy, or principles of optimal control involved in the process of designing modern induction heating equipment. For that the reader would need to be well versed in many advanced theoretical subjects. The authors would encourage any interested readers who would like to conduct an in-depth study of a certain theoretical aspect to the extensive reference list provided at the end of the handbook and indicated in the text by brackets []. Readers are also welcome to contact the authors of this book directly at INDUCTOHEAT, Inc. in Madison Heights, Michigan, USA, www.inductoheat.com.

As we mentioned above, a basic knowledge of physics and common sense is all that is required to grasp the great majority of material presented here.

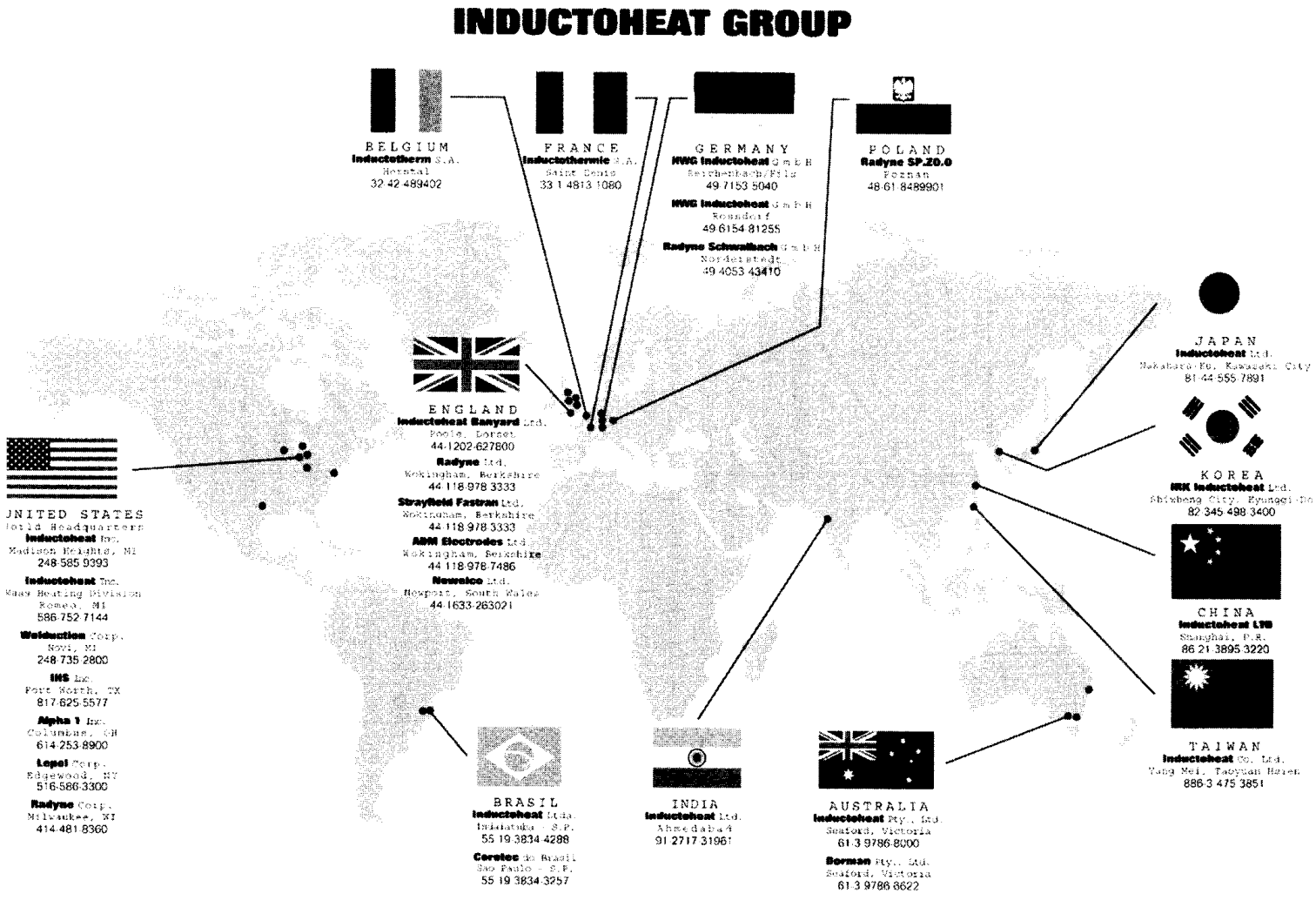

Figure 1.1 INDUCTOHEAT Group is the world's largest manufacturer of induction heating and heat treating equipment.

There is a hope that upon completion of this book, readers will have a solid knowledge of the most important electromagnetic and heat transfer principles, metallurgical aspects of induction heating and heat treating, an orientation to modern induction heating power supplies, load matching, process control, quality assurance, monitoring, and modern computational methods for electroheat problems encountered in induction heating. They will be able to evaluate the important features of the dynamics of the induction heating process and procure knowledge that will be helpful in avoiding many of the unpleasant surprises one might encounter in the design and operation of induction heating systems.

Probably the most comforting discovery for most engineers, designers, and practitioners is that someone has actually built a production system to accomplish the same task they are trying to perform.

Current information is presented on the use of magnetic field plots and temperature profiles with sketches, drawings, and numerous photographs of practical applications. The authors strongly believe that the information provided by one picture can be worth a thousand words. Plots of electromagnetic fields, temperature profiles and photographs of a variety of production installations are provided to show not only that the task has been previously accomplished but also why and how it has been done.

The book is divided into eight chapters. A brief description of the material contained in each chapter is presented below with some suggestions for the best approach for practitioners, students, engineers, and scientists.

Chapter 2. Industrial Applications of Induction Heating

This chapter provides a brief description of the specifics of induction heating and a variety of applications that utilize heating by induction. A brief description and classification of different induction heating applications divided into five large groups: induction heat treating, induction mass heating, special applications of induction heating, as well as induction melting and induction welding are also given in this chapter.

The heat treating section begins with a brief introduction to the basics of metallurgy and the principles of heat treatment. Special attention is paid to the limitations of commonly used guidelines, diagrams, charts, and graphs (e.g., the iron–iron carbide equilibrium diagram, TTT diagrams, CCT diagrams, etc.) when trying to use them for prediction of the required process parameters of heat treating by induction.

An overview of the most common heat treating applications is also provided in this section. This includes surface hardening, through hardening, tempering, stress relieving, normalizing, annealing, spherodizing, sintering, and so on.

Such applications as bar and billet heating, reheating of strip, slab, bloom, and plate, preheating and postheating for coating and curing applications, heating of wires, cables, and rods, as well as some other applications all belong to the group of induction mass heating. An overview of these applications is provided here.

Finally, descriptions are given in the section on special applications to facilitate understanding such terms as joining, shrink fitting, motor rotor heating, cap sealing, and a wide variety of others. Induction melting and welding are also briefly discussed in this chapter.

Chapter 3. Theoretical Background

Chapter 3 delves into the theoretical background and specific electromagnetic phenomena utilized to design the optimum induction system. Basic thermal phenomena and the three common modes of heat transfer are discussed here as well as changes of the material properties with a rise in temperature.

Many useful and practical recommendations are presented in Chapter 3 in regard to some subtle aspects of electromagnetic and heat transfer including the "skin" effect, proximity effect, electromagnetic "ring" effect, end and edge effects, and other phenomena that are imperative for modern induction heating practitioners and engineers to know.

An exceptionally useful part of this chapter is the section on mathematical modeling for the induction heating process. The majority of traditional methods for calculation of the induction heating process used in the past (e.g., the Baker and Williamson methods) were based on equations for an infinitely long coil and workpiece. Unfortunately, this assumption is rarely valid in induction hardening where inductors typically have no more than a few turns and cannot be considered infinitely long.

During the last decade a considerable amount of experience has been accumulated on the computation of induction heating and heat treatment problems using numerical techniques. Unfortunately descriptions of particular numerical methods and certain aspects of the different computation approaches are contained in a variety of internal reports, scientific journals, or literature specializing in a particular (typically quite narrow) area of computational work. These materials are often presented in a form that is nearly inaccessible to engineers with limited experience in numerical analysis. Also, the textbooks on numerical analysis usually emphasize the mathematical methods. They do not get into detail on the physical aspects of the problem that are often crucial to the success of the simulation.

It is not our aim to describe all of the available numerical methods. However, in order to make the right choice, one should have some orientation regarding the advantages and limitations of the methods that are most often used for modeling induction heating processes. An attempt has been made to bridge the gap between advanced theoretical information and information which is of practical use to the induction heating specialist conducting a mathematical modeling study.

A description and comparison of the different available numerical techniques including the finite element method (FEM), boundary element method (BEM), finite difference method (FDM) and mutual inductance method (MIM), is presented to allow the user to make an educated decision with respect to which computational technique is the best to use in a certain application.

In most previous publications, induction heating was introduced as an uncoupled process without emphasis on the interrelated features of the electromagnetic and heat transfer phenomena. Most studies consider the two phenomena separately. Such an approach could lead to substantial errors in predicting the variation of the principal process parameters, including the temperature profile, required power, optimal frequency, electrical current, and coil voltage because they fail to take into consideration the change in material properties during the heating cycle.

By nature, the induction heating process is characterized by a tight interrelation of the physical properties of the heated material. These properties are strongly

dependent upon magnetic field intensity, the temperature of the workpiece, and its microstructure. During the heating cycle significant changes occur in the specific heat, thermal conductivity, magnetic permeability, electrical resistivity, and other properties of the heated material. These changes are critical for the heating process and must be properly taken into consideration in the contemporary design of any induction system.

A discussion of different coupling techniques for the electromagnetic—thermal problem (i.e., two-step approach, indirect and direct coupling) is presented in this section as well. This will be helpful in making the reader aware of the dangerous pitfalls in using some of the commercially available software for computation of the induction heating problem.

Chapter 4. Temperature Measurement

One crucial requirement in the verification of theoretical calculations is the ability to accurately measure the temperature and rate of temperature change in the workpiece as it is being heated. Chapter 4 gives a basic description of the different methods of temperature measurement available ranging from temperature-sensitive paints to advanced multicolor infrared optical systems. A discussion of blackbody and graybody radiation is presented along with a description of the theory behind thermocouples and different types of pyrometers.

From a practical standpoint the care and maintenance of standard temperature measuring systems and fiber optic systems is discussed with special emphasis on induction heat treating and mass heating applications. Practical limits for the use of thermocouples and infrared systems are discussed here as well as typical measurement errors and methods to prevent them.

Chapter 5. Heat Treatment by Induction

This chapter describes a wide range of methods of heating metals with induction for the purpose of heat treatment, with emphasis on surface hardening, through hardening, tempering, stress relieving, and annealing of a variety of parts. This includes but is not limited to camshafts, crankshafts, axle shafts, gears, and other critical components made from steels and cast irons, as well as parts made from powder metals.

Induction heat treatment has many features that make it a unique process from the standpoint of coil design as well as computational methods, process operation, and equipment maintenance. Detailed information is presented in the areas of inductor design and coil fabrication, specifics of spray quenching, formation of residual stresses, induction tempering, coil maintenance, contradictions and intricacies of using magnetic flux concentrators, as well as different aspects of metallographic sample preparation and principles of microscopic analysis. Concrete engineering recommendations and guidelines to choose optimal process parameters, design criteria, and machine concepts are presented in this chapter as well.

Chapter 6. Special Applications of Induction Heating

Chapter 6 gives an overview of special applications such as brazing, soldering, bonding, shrink fitting, cap sealing, induction lost core melt out, and a wide variety of others. This gives a sufficient background to determine the effectiveness of using induction for applications of these kinds.

Chapter 7. Induction Mass Heating

This chapter provides detailed descriptions of applications that belong to the group of induction mass heating. Mass heating involves heating of bars, billets, rods, blooms, slabs, plates, and sheets prior to rolling, forging, extrusion, up-setting, and so on. A number of important electromagnetic effects are described since a knowledge of these is essential for a successful design of mass heating equipment. Special consideration is devoted to induction heating of tubes, wires, cables, ropes, and strips for a variety of applications including galvanizing, galvannealing, galvaluming, drying, and so on. In some cases, heating may vary from the necessity to heat the entire workpiece to a certain portion of the workpiece being required to be heated, for example, bar end heating or slab end or edge reheating.

A description of some of the unique applications of induction heating such as aluminum slug heating for semisolid forming and induction reheating for the world's largest carbon steel slabs is given here as well.

Chapter 8. Power Supplies for Modern Induction Heating

One of the most critical parts of any induction heating machine is the power supply. The old saying, *"It only takes a mouse in the elephant show to ruin the whole circus,"* can be rephrased as, "It only takes a bad power supply to totally ruin the most sophisticated induction heating machine." The power supply affects practically all critical parameters of the induction heating system, including reliability, maintainability, compactness, system flexibility, energy efficiency, and cost. Many different power supply types and models are available to meet the heating requirements of a nearly endless variety of induction heating and heat treating applications.

Chapter 8 rounds out the materials discussed in this handbook by providing a comparison of the different types of power supplies used for induction heating. Charts showing the "frequency–power" relationship for common induction mass heating and heat treating applications are provided in this chapter.

The discussion includes a description beginning with the basic elements such as inductors, capacitors, and resistors and proceeds to outline the various power semiconductors. A comparison is given between thyristorize-type (SCR) inverters, transistorized (IGBT and MOSFET) inverters, and vacuum tube oscillators to allow the user to quickly choose the best type of power supply for a given heat treat or mass heating application.

Most conventional types of inverters used in induction heating are discussed with coverage of circuit topology, operating characteristics, and load matching. Load matching is a particularly important subject, since some induction heating coils work well with certain types of power supplies and are ineffective with others. Therefore, the optimal design of an induction heating system should take into

consideration the features of induction heating not as a standalone process but as a combination of the inductor, load-matching station, and power supply. These components must then be integrated into the larger production process to provide one integrated package to the customer.

The characteristics of medium- and high-frequency transformers, their selection, and working conditions, and special considerations are discussed here as well.

Special attention has been paid to quality assurance, process control, and monitoring. This includes but is not limited to a discussion on the basic principles of "close-loop" and "open-loop" control approaches, various control modes such as proportional (P), integral (I), derivative (D), proportional-integral (PI), and proportional-integral-derivative (PID), as well as PLC controllers, energy monitoring, and "signature" monitoring.

Subsequent sections of Chapter 8 enter into a discussion of power supply maintenance, protective devices, specifics of cooling, power/energy quality, harmonics, and safety principles.

2

Industrial Applications of Induction Heating

There are many ways to heat metal parts including the use of induction heaters, gas-fired furnaces, fluidized bed furnaces, salt baths, infrared heaters, electric and fuel-fired furnaces, and so on. Each method has its own advantages. There is obviously no universal method that is best in all cases of metal heating and heat treating.

In the past three decades heating by induction has become more popular. A major reason is the ability to create high heat intensity very quickly at well-defined locations on the part. This leads to low process cycle time (high productivity) with repeatable quality. Induction heating is also more energy efficient and inherently more environmentally friendly than most other heat sources including gas-fired furnaces, salt and lead baths, carburizing, or nitriding systems. Any smoke and fumes that may occur due to residual lubricants or other surface contaminants can be easily removed. A considerable reduction of heat exposure is another factor that contributes to the environmental friendliness of induction heaters.

Gas-fired furnaces can result in poor surface quality due to scale formation, grain coarsening, oxidation, and decarburization. Induction heating provides much better surface quality of heated metal with a significant reduction of scale and decarburization, which in turn eliminates the need for recarburization. The reduction of scale results in substantial metal savings.

Induction systems usually require far less startup and shutdown time and lower labor cost for machine operators. Other important factors of induction heating machinery include quality assurance, automation capability, high reliability, and easy maintainability of the equipment. In many cases induction heating will require minimum shop floor space and produce less distortion in the workpiece.

Induction heat treatment is a complex combination of electromagnetic, heat transfer, and metallurgical phenomena involving many factors. The main components of an induction heating system are an induction coil, power supply, load-matching station, quenching system (for heat treating applications), and the workpiece itself. Induction coils or inductors are usually designed for specific applications and are, therefore, found in a wide variety of shapes and sizes.

The features involved in the design and operation of modern induction heating processes greatly depend upon the application specifics of the particular process. Industrial applications of induction heating can be divided into five groups: heat treating, mass heating, special heating applications, induction melting, and induction welding (Figure 2.1). A short description of each group is provided below.

2.1 HEAT TREATMENT BY INDUCTION

Prior to the discussion of the features of heat treatment by induction it is imperative for readers to refresh their knowledge of the basic metallurgical principles that play an important role in heat treatment. Due to space limitation only a brief introduction to the principles of metallurgy and certain aspects of heat treatment and material science are provided here. More detailed information can be found in classical books written by C. Brooks [20, 179, 180], G. Krauss [21], K. Thelming [23], G. Golovin [12], M. Grossman and E. Bain [186], G. Kurdyumov [103], R. Honeycombe and H. Bhadeshia [176], L. Samuels [181], A. Gulyaev [228], and W. Smith [215], as well as others [2, 6, 7, 11, 14, 19, 172–185, 215–220], where certain features of metal heat treatment have been thoroughly described.

2.1.1 The Basics of Metallurgy and Principles of Heat Treatment

Metallurgy as an art has been practiced since the beginning of the history of man but as a science it is relatively new, tracing its origin to the early 1860s when the microscope began to be used to inspect the structure of metals. The field of metallurgy today can be divided into two broad categories: the first deals with the process of extracting metals from the ores in which they are found, and the second, physical metallurgy, which deals with the physical and mechanical characteristics of metals and of various metallic mixtures referred to as alloys.

In physical metallurgy the three main variables that are considered are the chemical composition of the metal, any mechanical prior treatment, and prior thermal treatment (heat treatment). Any of these variables can be changed in order to produce a metal with certain desired properties such as hardness, strength, ductility,

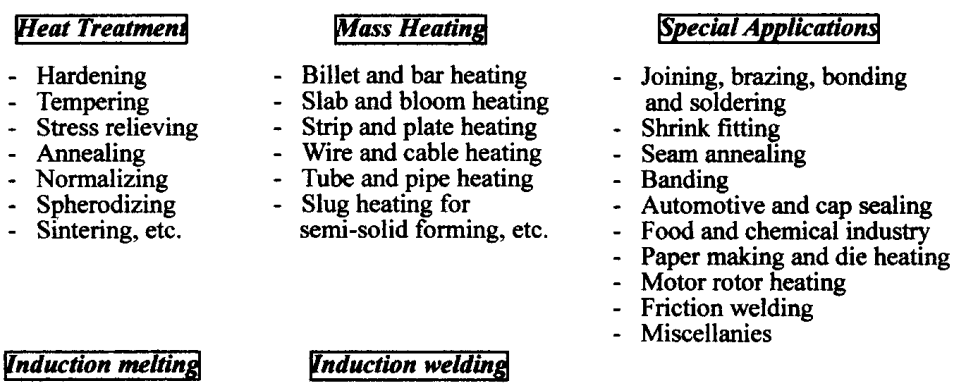

Figure 2.1 Industrial applications of induction heating.

toughness, corrosion and wear resistance. Prior thermal treatment, deals with the effect of temperature and the rate of heating and cooling of the metal in order to arrive at a specific microstructure and properties [22].

2.1.1.1 Crystalline Structure of Elements and Critical Temperatures

An element is a pure substance or material that cannot be separated chemically or by any other means to provide any other type of material. There are 103 elements recognized on the Periodic Table of the Elements (see Appendix A). These elements are composed of atoms that are arranged in a specific combination to produce the element. If the atoms are separated, they no longer maintain the characteristic properties of the element and may be very different in nature. The elements are arranged in the table by increasing atomic weight and tend to be grouped according to physical and chemical properties.

Atoms are composed of a solid nucleus containing neutrons and protons. Around this nucleus are various numbers of electrons circulating in specific orbits determined by their energy level. An example would be a helium atom, which has two orbiting electrons about its nucleus. The electrons carry a negative electrical charge that is balanced by the proton in the nucleus that carries a positive electrical charge. A neutral atom would contain an equal number of electrons and protons.

Two or more elements can combine to form a molecule. For example, in water (chemical formula H_2O) two hydrogen atoms combine with a single oxygen atom to form a molecule of water. A molecule is the smallest building block from which a compound is produced. Two or more elements are required to produce different compounds. A compound often has totally different properties than the elements of which it is constituted. In our example of water, which is composed of two gases, hydrogen and oxygen form the liquid phase of water.

Combining or mixing two or more elements or compounds that are not chemically joined together forms a mixture. A solution is a special kind of mixture in which one substance is totally dissolved in another. In a solution, the material that is dissolved is referred to as the solute. The material in which another material is dissolved is referred to as the solvent.

It is possible to have a mixture of two materials that are solid. The mixing of the two materials takes place at a high temperature when both materials are in a liquid phase. When the mixture is cooled and becomes a solid, the mixture is referred to as a solid solution. This is the case with materials commonly referred to as alloys that may involve the mixing of elements such as copper and tin to form the alloy called bronze.

Although the basic principles of heat treatment may be applicable to many different types of metals, the primary focus in our discussion is with respect to steels and cast irons since these are, by far, the area of greatest interest in the field of induction heating and heat treating.

When large groups of atoms cluster together they form a family. This family is then known as a crystal. In a crystal, the atoms are all oriented in a prescribed three-dimensional orderly fashion (Figure 2.2). For example, with metals such as iron and steel, there is a specific crystalline structure that is found in the material. At lower temperatures (below 912°C/1674°F) the crystalline structure of iron is described as body centered cubic, BCC (called α-iron or ferrite). The atoms are arranged in the form of a cube with an atom at each corner and one at the center of the cube. Besides

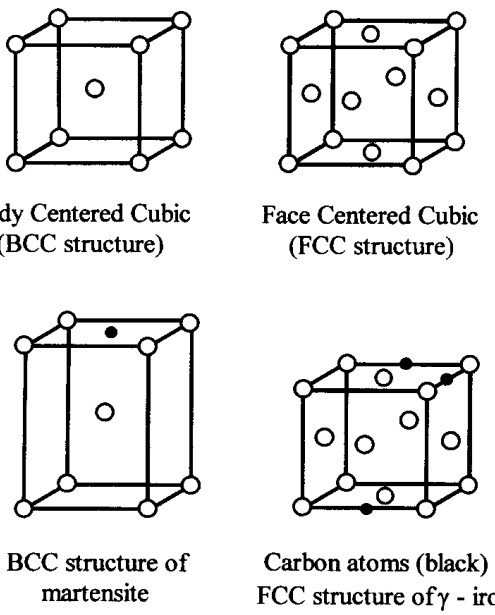

Figure 2.2 BBC and FCC structures: ○ = γ-Fe, • = C.

iron, some other metals including tungsten, molybdenum and chromium have BCC structure at room temperature. BCC structure is inherently brittle.

At higher temperatures (below 1392°C/2538°F) the atoms are still arranged in the shape of a cube with an atom at each corner and six additional atoms located at the center of each face of the cube and no atom at the center of the cube. This structure is referred to as a face centered cubic (FCC) structure which is called γ-iron or austenite (Figure 2.2). FCC structure is much more ductile than BCC structure. Upon further heating and after exceeding the temperature of about 1392°C (2538°F), the FCC structure of iron will transform back to the BCC structure known as δ-iron.

Changes occurring in the crystal structure are called allotropic transformation. It should be mentioned that it is not always necessary to heat metals in order to obtain a FCC crystalline structure. Such metals as copper, aluminum, gold, and nickel have FCC structure at room temperature.

When the iron structure changes from one type to another type there is a thermal effect called the latent heat of transformation. The appearance of the latent heat is different depending upon whether the iron is heated or cooled down. On steady heating with sufficiently low heat intensity, the temperature rise will be slowed down or even stopped when iron experiences a structural change. The first interruption in the temperature rise during heating of iron takes place when the iron loses its magnetic properties, becoming paramagnetic (Figure 2.3). This critical temperature is known as the A_2 temperature or the Curie point. A more detailed discussion regarding Curie temperatures of different metals is provided in Section 3.1.1.

In some publications, the paramagnetic form of α-iron is referred as β-iron. It is broadly agreed to avoid using the term β-iron by modern metallurgists. Since the paramagnetic state of α-iron still has a BCC structure it is probably proper to characterize the state of iron within the temperature range of 768°C (1414°F) to 912°C (1674°F) as a nonmagnetic form of α-iron.

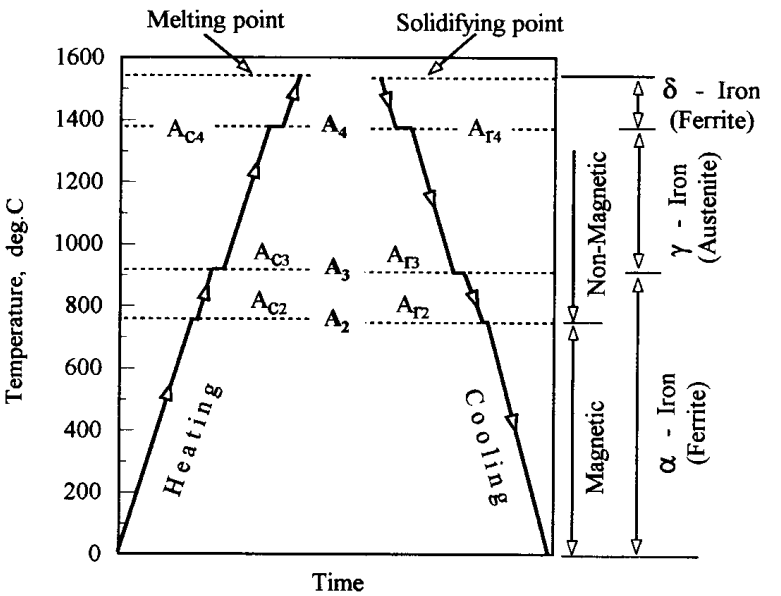

Figure 2.3 Heating and cooling curves for pure iron.

As can be seen from Figure 2.3, the second interruption in the temperature rise takes place after reaching a temperature of approximately 912°C (1674°F), when the iron structure undergoes a change from α-iron (ferrite) to γ-iron (austenite). The third and fourth interruptions occur during the transition of the iron structure from γ-iron to δ-iron (1392°C/2538°F) and at the melting point (1528°C/2782°F), correspondingly. Table 2.1 shows the states of the pure iron as a function of temperature.

The α-iron and γ-iron are two of the most important forms of iron that are presented in the majority of induction heating and heat treating applications. Since δ-iron exists only at temperatures above 1392°C (2538°F), induction heating practitioners seldom come across this structure unless melting or welding.

Interruptions observed in the temperature rise on slow heating using low heat intensities deal with the necessity of absorbing the additional energy required to support the processes taking place during crystalline transformation.

As one can see from Figure 2.3, cooling curves are almost identical to heating curves. At the same time, there are two principal differences:

- all critical temperatures on cooling are lower than critical temperatures on heating; and
- contrary to heating, during cooling when the iron undergoes a crystalline transformation, additional energy is freed and heat is generated. This additional energy accounts for the interruptions seen on the cooling curves.

Table 2.1 States of Pure Iron as Function of Temperature

Solid	α-Iron	BCC	Ferrite	Up to 912°C (1674°F)
Solid	γ-Iron	FCC	Austenite	912°C (1674°F) to 1392°C (2538°F)
Solid	δ-Iron	BCC		1392°C (2538°F) to 1528°C (2782°F)
Liquid				1528°C (2782°F) to 2880°C (5216°F)
Gas				Above 2880°C (5216°F)

As one can conclude from Figure 2.3 and the discussion above, critical (transformation) temperatures represent critical points, which are sometimes called delay or arrest points. At these points additional absorption of heat energy takes place when a specimen is heating and heat is generated when a specimen is cooling. Therefore, the existence of critical (transformation) points represents an inherent resistance of metal to any structural transformation or modification.

The symbol A representing critical temperatures (i.e., A_1, A_2, A_3, A_{cm}) originates from the French word *arret* (meaning arrest). In order to distinguish critical temperatures that appear during the heating cycle from similar temperatures in the cooling cycle, the symbol "c" (standing for French *chauffage*, heating) is used as a subscript of symbol A to designate the heating cycle. The symbol "r" (standing for French *refroidissement*, cooling) is used to represent a cooling cycle [20, 23, 181].

In addition to the phenomenon of interruption or delaying of heating/cooling curves, several other phenomena also occur at the critical temperatures. Marked changes in the behavior of several physical properties of metals including thermal conductivity, specific heat, electrical resistivity, magnetic permeability, volumetric changes, variation of density, and elongation might be observed at certain critical temperatures. Variations of thermal and electromagnetic properties with temperature are discussed in Sections 3.1.1 and 3.2.

Figure 2.4 shows an example of how the existence of the critical points affects the thermal expansion and density of steel during the heating/cooling cycle. At the beginning of the heating cycle (Figure 2.4, top) steel expands proportionally to the temperature rise. Upon reaching the A_{c1} critical point, the expansion of steel stops and the steel begins to experience a contraction of its volume until, reaching a critical temperature of A_{c3}, the steel then starts to expand again. When the steel undergoes a cooling cycle, the reverse changes occur (Figure 2.4, top).

Density and volumetric changes of metals taking place during the heating/cooling cycle result in contraction and expansion of different areas of the heated body. These changes play an important role in the appearance of transitional and residual stresses that might result in noticeable warping and shape distortion of the heated workpiece and even crack development. The nature of the transitional and residual stresses is discussed in Sections 5.3 through 5.5 and [18,369,470].

Idealistically speaking, in the case of a sufficiently slow heating/cooling that represents the equilibrium condition, transformation temperatures should be the same on heating as well as on cooling resulting in no real difference between A_c and A_r critical temperatures. Practically speaking, the equilibrium condition simply does not exist in the "real world", particularly when induction heating is used. During nonequilibrium conditions the phenomenon of thermal hysteresis takes place.

As mentioned earlier, A_c temperatures are always higher than A_r temperatures. The difference between A_c and A_r temperatures represents thermal hysteresis that is a function of several factors including the metal chemical composition, microstructure, and the heating/cooling rate. The greater the rate of heating/cooling the greater the difference between the A_c and A_r temperatures. It is especially important to take the phenomenon of thermal hysteresis into consideration for induction hardening applications utilizing intensive heating (heating rate frequently exceeds 150°C/sec) and severe cooling (200°C/sec and higher) when the hot metal is spray quenched in water that is near the ambient temperature.

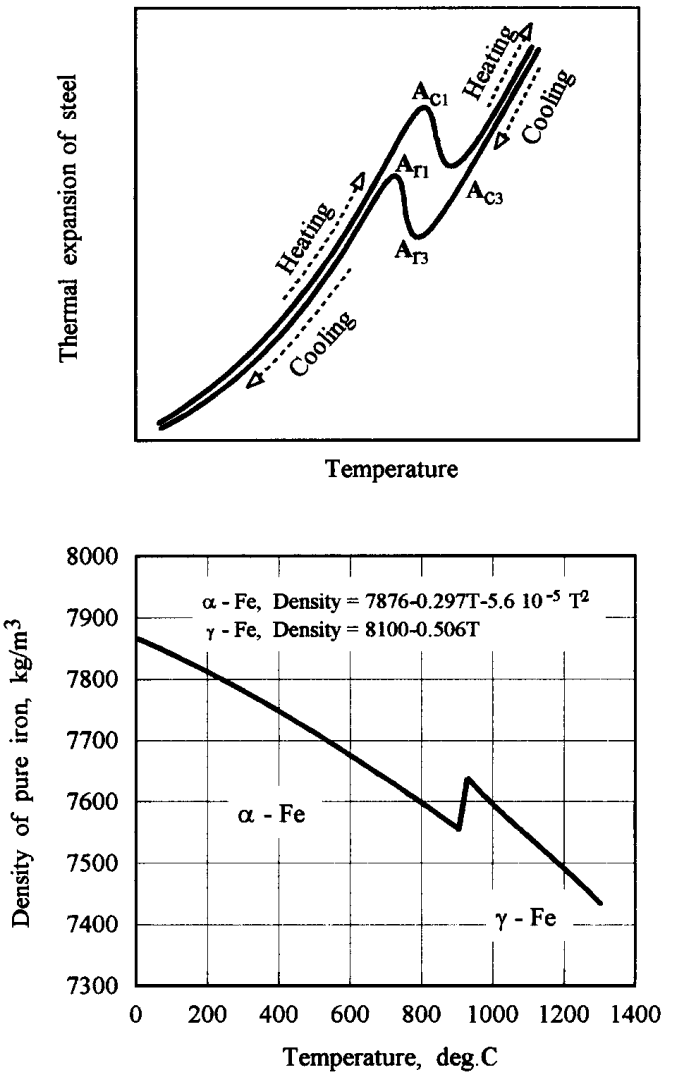

Figure 2.4 Thermal expansion of steel (top) and iron density (bottom) versus temperature. (From Ref. 444.)

Among all alloys, steel is the most commonly used in industry. Plain carbon steel is a binary alloy of iron and carbon. It is a solid solution that contains more than 90% iron and often more than 99%. The amount of carbon in steels varies from slightly above 0 to 2%. Most steel ranges from 0.08 to 1% carbon. Above 2% carbon, the mixture is referred to as cast iron. Above 6% carbon the mixture becomes so brittle that it has no real practical use [14, 17, 22].

It should be stated at this point that although carbon is the major alloying element in steel, depending upon the features of the steel manufacturing and rough materials, so-called plain carbon steel may consist of a limited amount of other chemical elements, including manganese (< 1%), silicon (< 0.3%), phosphorus (< 0.04%), sulfur (< 0.05%), and some other elements.

It is important to keep the amount of sulfur and phosphorus in plain carbon steel at a minimum since they introduce brittleness and crack sensitivity. A limited

amount of manganese plays an important role in plain carbon steels, since it prevents or minimizes the formation of iron sulfides (FeS) that appears at the grain boundaries. In addition, being very hard and brittle, FeS also has a relatively low melting temperature. A combination of these features can result in undesirable properties of steel such as brittleness and sensitivity to development of intergranule cracks and grain boundary liquation during intensive heat treating. When an adequate amount of manganese is present in the steel, sulfur combines with the manganese to form manganese sulfide (MnS) which is distributed within the grains creating a more desirable structure. A manganese to sulfur ratio of 4:1 to 5:1 is quite typical for carbon steels.

The effect of the most commonly used chemical elements in steel is discussed in Section 2.1.1.4.

2.1.1.2 Equilibrium Phase Transformation Diagram

When iron is alloyed with a different percentage of carbon the critical temperatures can be determined based on the iron–iron carbide phase transformation diagram (Figure 2.5). This diagram is valid only for the equilibrium condition of plain carbon steel at a pressure of one atmosphere. The existence of nonequilibrium conditions, appreciable amount of alloying elements, pressure, and certain prior treatment can noticeably shift the critical temperatures.

An iron–iron carbide equilibrium diagram, shown in Figures 2.5 and 2.6, may be used to predict the characteristics of plain carbon steel, but only under conditions mentioned above. The diagram presents a graph of temperature versus carbon content of the steel and shows the effect of heating the steel to elevated temperatures or

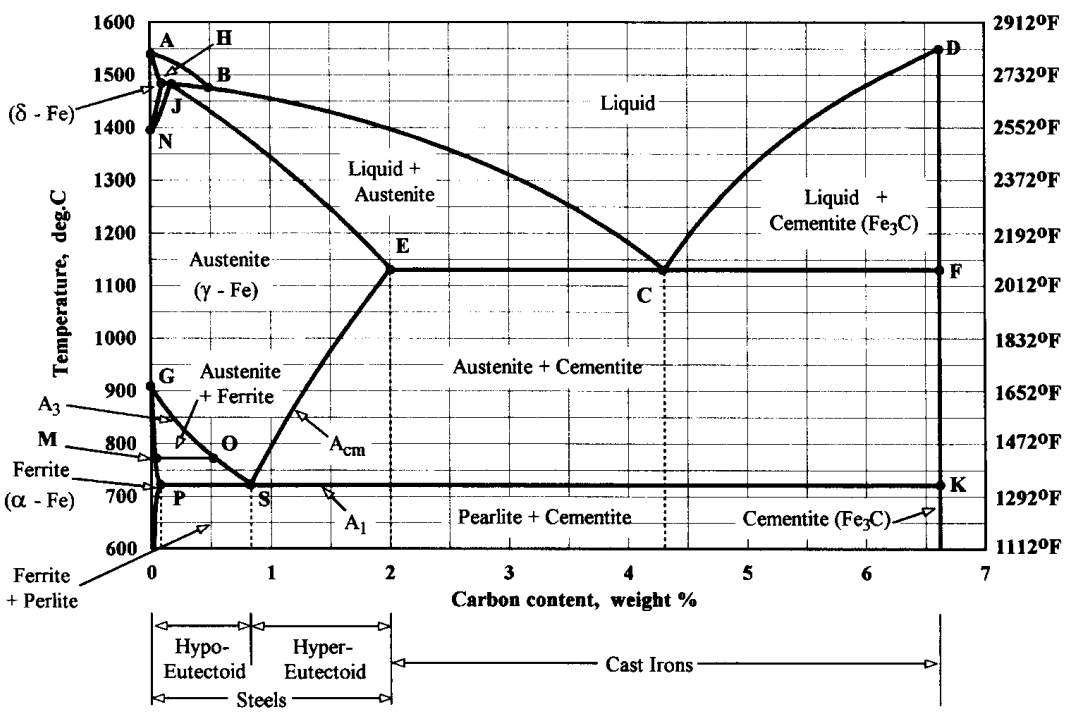

Figure 2.5 The iron–iron carbide equilibrium diagram (sufficiently slow heating/cooling).

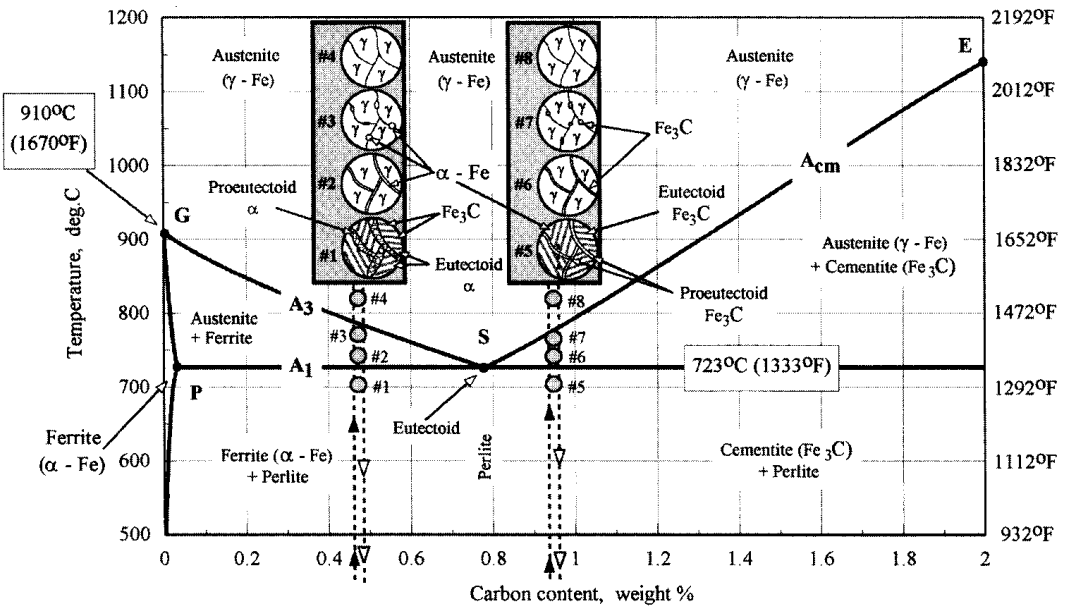

Figure 2.6 The lower left-hand part of the iron–iron carbide equilibrium diagram (compare with Figure 2.5).

steel cooling that may cause a transformation in its crystalline structure [14, 17]. It also can be used to determine the range of temperatures in which certain types of heat treatment of the steel may be carried out.

Steels with a carbon content below about 0.78% belong to the group of hypoeutectoid steels. If the steels contain more than 0.8% carbon they are called hypereutectoid steels and those with carbon content of about 0.78 to 0.8% are called eutectoid steels.

The number that is given to the carbon steel makes it easy to identify whether it is a plain carbon or alloy steel. The identification number of plain carbon and low-alloy steels starts with a number 10xx or 11xx. The last two or three numbers represent the percentage of carbon in the steel. For example, 1045 steel would be a plain carbon steel with about 0.45% carbon; 1080 steel would be a plain carbon steel with approximately 0.8% carbon.

Depending upon carbon content, plain carbon steels can be classified not only as hypoeutectoid, eutectoid, and hypereutectoid steels, but also as mild ($<0.2\%$C), low-carbon ($<0.35\%$C), medium-carbon (from 0.35 to 0.55%C), and high-carbon steels ($>0.55\%$C). This classification is not widely accepted and is used by heat treat practitioners only to indicate certain features of plain carbon steels, including the ability of a steel to be hardened to a certain hardness, how easily the steel responds to induction hardening, whether the steel may exhibit a pronounced tendency toward cracking during heating and quenching, and others.

The equilibrium phase transformation diagram is often called simply an iron–iron carbide diagram because it consists of several areas representing a range of carbon content, temperatures, and phases formed by iron and iron carbide (Fe_3C). As can be seen from Figure 2.6, the maximum amount of carbon that can be dissolved in α-iron (ferrite) is approximately 0.022% taking place at a temperature of about 727°C (1341°F) (at point P, Figure 2.6). Relative softness and good ductility

are two marked mechanical qualities of the ferrite. Ferrite is magnetic and exists at relatively low temperatures.

In contrast to α-iron (ferrite), γ-iron (austenite) being the solid solution of carbon in γ-iron, can dissolve a much greater amount of carbon with the maximum of carbon solubility slightly exceeding 2% at a temperature of 1147°C (2097°F) (point E). Austenite occupies the area of GSEJNG, as seen in Figure 2.5. Under equilibrium conditions, austenite does not exist in plain carbon steels at a temperature below the A_1 critical temperature.

The point S (Figure 2.6) of the intersection of lines representing the critical temperatures of A_1, A_2, A_3, and A_{cm} is called the eutectoid point (about 0.78% of carbon content on the equilibrium phase transformation diagram).

Figure 2.6 shows a simplified kinetics of the formation of austenite. In reality, when steel is heated to the temperatures of the austenitic range, the process of grain refinement and growth takes place. It is a diffusion-type process and is a function of temperature and time. Below the A_{c1} critical temperature grain growth is negligible. Even though ferritic grains can grow to some extent below a low critical temperature, during an austenitic formation those grains will be refined. Above the A_{c3} critical temperature a noticeable grain growth can be observed. ASTM E112 standard provides guidelines and procedures for determining an average grain size.

When heating eutectoid steel, a formation of austenite is completed at temperatures slightly above the A_{c1} critical point (due to the intersection of A_1, A_3, and A_{cm} lines at point *S*). When heating hypoeutectoid or hypereutectoid steels, austenitic grains could noticeably grow due to the necessity of heating a specimen to higher temperatures in order to complete a formation of austenite.

Upon cooling, the eutectoid point a eutectoid transformation of austenite takes place resulting in replacement of one solid phase by two different solid phases. According to the transformation diagram, upon slow cooling at the eutectoid point a homogeneous austenite transforms into perlite which is a lamellar mixture of α-iron (ferrite) and iron carbide (Fe_3C) often called cementite. Since cementite contains much more carbon than ferrite it is significantly harder but much more brittle than ferrite. This eutectoid transformation can be illustrated by the formula [175]

$$\gamma\ (0.78\ \text{wt\%\ C}) \underset{\text{cooling}}{\overset{\text{heating}}{\rightleftarrows}} \alpha\text{-iron}\ (0.022\ \text{wt.\%\ C}) + \text{Fe}_3\text{C}\ (6.7\ \text{wt.\%\ C}).$$

As can be seen from Figure 2.6, upon cooling the perlitic transformation starts at the grain boundaries of γ-iron (austenite). Being a mixture of α-iron and Fe_3C, the mechanical properties of the perlite are intermediate between the soft ductile ferrite and the hard brittle cementite.

The uniqueness of the area GSPG deals with the fact that having various carbon contents, both α-iron (ferrite) and γ-iron (austenite) can exist simultaneously there. Both α-iron and γ-iron are formed on sufficiently slow cooling of homogeneous austenite.

On the high-temperature side, a critical line A_3 limits the GSPG area. On the low-temperature side, critical line A_1, which is called the low transformation temperature line, limits this area. The existence of the GSPG area plays a very important

role in choosing the proper process parameters in a variety of steel heat treating applications, including annealing, normalizing, and hardening.

A similar phenomenon exists in the area of SEFKS (Figure 2.5), where γ-iron and iron carbide also exist simultaneously. The critical line A_{cm} (called the upper transformation temperature) limits this area on the high-temperature side determining the limit of solid solubility of carbon in γ-iron.

It is imperative to emphasize at this point that all three of the microstructures discussed above (ferrite–perlite, perlite, and perlite–cementite) obtained upon equilibrium cooling conditions, meaning a sufficiently slow cooling of homogeneous austenite, are produced by a diffusion-dependent transformation process [21].

From the standpoint of actually trying to predict the results of heat treatment upon the metal there is at least one crucial factor that is missing on the iron–iron carbide equilibrium diagram and that is the factor of time. In order to predict the effect of a certain heat treatment it is necessary to know something about the effect of different rates of heating and cooling of the metal.

2.1.1.3 Time-Temperature Transformation Diagram (TTT Diagram) and Continuous Cooling Transformation Diagram (CCT Diagram)

The isothermal transformation (IT) diagram shown in Figure 2.7, also called the time–temperature transformation diagram (TTT diagram), helps to predict the postheat treating microstructure based on the cooling rate (quench severity). The isothermal transformation diagram plots time on the X-axis (a logarithmic scale) versus temperature on the Y-axis. The characteristic S-shaped curve shows the effect of different cooling scenarios on the composition of the mixture of material in the steel. As there is no representation of carbon content for the steel under consideration, a different chart is required for each chemical composition and grain size to be analyzed.

TTT diagrams allow one to determine the end products of homogeneous austenitic transformation upon its cooling by holding the steel at a fixed temperature below the A_1 critical temperature.

It is imperative to remember that samples with small cross-sections were used to obtain these diagrams. Therefore, there will be some inherent errors in trying to apply those curves to moderate or large-sized parts.

In addition to TTT diagrams, the continuous-cooling transformation diagrams (CCT diagrams, Figure 2.8) were developed. CCT diagrams are more helpful for heat treating practitioners because they allow prediction of the final microstructure of the steel taking into account the continuous nature of the process during cooling of austenite [13, 14, 17, 19, 24].

As has been shown by several authors [181, 184, 186, 215], CCT diagrams can be slightly shifted to lower temperatures and longer times compared to TTT diagrams.

Although TTT (IT) and CCT diagrams are helpful, there are a few drawbacks when trying to apply those diagrams for the induction heat treating process.

- In addition to the assumptions discussed above, an assumption of a homogeneous austenite has been made in developing both the TTT and the CCT diagrams.
- TTT diagrams are of limited use for heat treatment by induction since induction is a nonisothermal process.

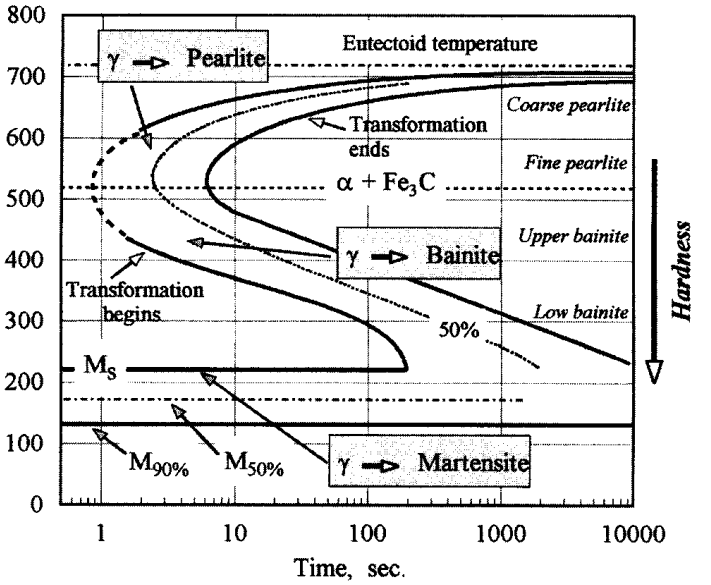

(A). Time-temperaure isothermal transformation diagram for plain carbon steel 1080, austenized at 900deg.C, grain size: 6 [6, 24]

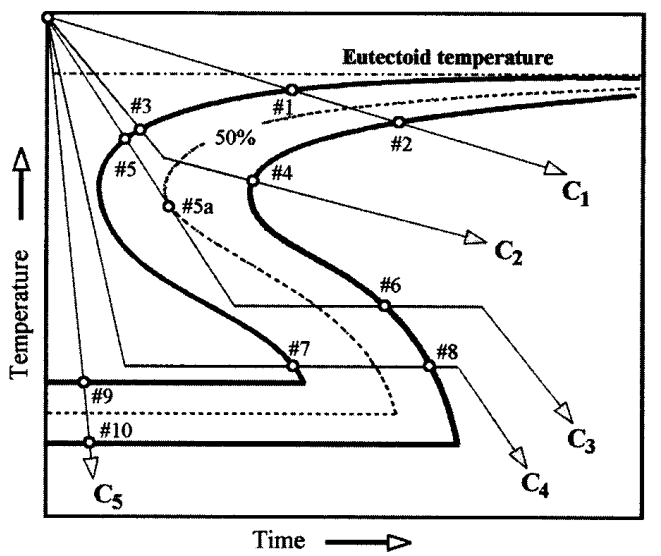

(B). Examples of cooling scenarii for isothermal transformations

Figure 2.7 Time–temperature isothermal transformation curves.

- Although CCT diagrams take into consideration continuous cooling during quenching, they presume that the cooling curve has a constant cooling rate, which in most cases of induction heat treating is not a correct assumption.
- In induction heat treating, the thermal heat exchange process between the surface of the heated workpiece and the quenchant, among other factors (e.g., type of quenchant, quenching temperature, pressure and flow rate of quenchant, size and density of quench holes, spray quench impingement,

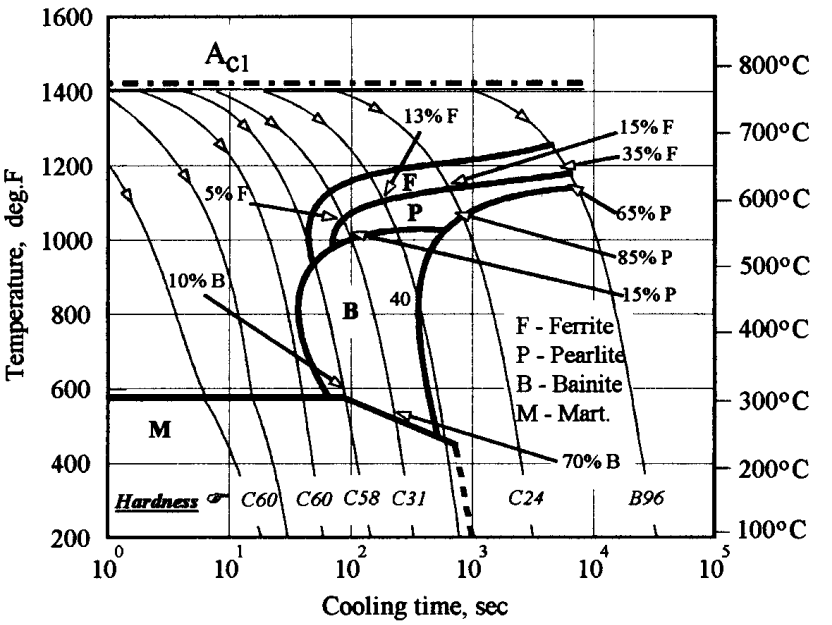

Figure 2.8 Continuous cooling transformation (CCT) diagram: AISI 15B41 steel, Grain size #7-8 (0.42% C, 1.61% Mn, 0.29% Si, 0.006% P, 0.019% S, 0.004% B). (From Ref. 13.)

etc.), is a function of the surface temperature, which obviously is not constant. In addition, the workpiece temperature (austenizing temperature) prior to applying the quenchant is not always the same as assumed in the CCT diagrams.

- Finally, in induction surface hardening the temperature distribution prior to quenching is nonuniform. The existence of a cold core that acts as a heat sink has a marked effect on the cooling rate during quenching, greatly affecting the hardened depth and pattern.

As mentioned above, regardless of the obvious limitations of TTT (IT) diagrams and CCT diagrams, they are useful in helping the heat treater to understand the basic phenomena and principles of heat treatment of steels and cast irons.

As an example, Figure 2.7A shows an IT diagram (or TTT diagram) for 1080 carbon steel (eutectoid steel) which was austenized at a temperature of 900°C (1652°F) [6, 24]. As one can see from Figure 2.7A, depending upon cooling conditions, a time–temperature transformation diagram (IT diagram) consists of several well-defined regions representing three important reactions:

- γ-iron into perlite (upper region),
- γ-iron into bainite (middle region), and
- γ-iron into martensite (low region).

Capital letters are used on TTT diagrams to represent a particular structure. For example, A stands for austenite, F for ferrite, P for perlite, B for bainite, and M for martensite. In order to emphasize a certain feature of a particular structure, double capital letters are sometimes utilized. For example, CP and FP stand for

coarse and fine perlite, respectively, and UB and LB stand for upper and low bainite, correspondingly.

Another distinguishing feature of the TTT diagrams deals with the fact that these diagrams consist of two S-shaped curves (sometimes also referred to as C-shaped curves). The left solid curve (Figure 2.7B) represents the beginning (the start) of the transformation process. The right solid curve designates the end of the isothermal transformation.

Often TTT diagrams show a curve that represents the completion of 50% of the transformation of the austenite. This curve is usually shown as a dotted curve located between the transformation beginning curve and the curve representing the end of the isothermal transformation.

A typical heat treatment procedure for hardening of steel involves heating the alloy up to an austenizing temperature (i.e., above the A_3 critical temperature) and then holding it at that temperature for a period of time long enough for completion of the transformation to austenite. Next the steel is rapidly cooled until it is near ambient temperature. This rapid cooling allows replacing the diffusion-dependent transformation process by a shear-type (diffusionless) transformation creating a hard constituent called martensite.

In the case of using a moderate (mild quenching) or interrupted quenching, a final microstructure of steels or cast irons can be represented as a complex combination of several different structures.

Figure 2.7B shows several examples of different cooling scenarios based on severity of quenching. The time-cooling line C_1 represents a slow cooling. This line crosses a left S-shaped (C-shaped) transformation curve in the upper region of the isothermal transformation diagram. At point 1, austenite starts its isothermal transformation. The phase transformation process continues until the time-cooling line C_1 crosses the right solid curve that represents the end of the transformation process. At point 2 all of the austenite transforms into coarse perlite.

Time-cooling curve C_2 represents a faster cooling condition compared to line C_1. It enters an isothermal transformation region at point 3, meaning that austenite will start to transform into fine perlite. After crossing a curve representing the end of isothermal transformation (point 4), all austenite will complete its transformation process transforming into fine perlite, which has closely spaced alternating lamellaes of ferrite and cementite.

The isothermal transformation "austenite-to-perlite" is a diffusion-controlled process for plain carbon steels that occurs within the temperature range of about 720°C (1328°F) to 550°C (1022°F). A temperature range of about 720°C (1328°F) to 620°C (1148°F) corresponds to coarse perlite transformation temperatures and a temperature range of about 620°C (1148°F) to 550°C (1022°F) corresponds to a fine perlite transformation range (formerly known as troostite). Perlite is a mechanical mixture of two phases: ferrite and cementite arranged in a lamellar matrix. Figure 2.9 shows a metallographic appearance of perlite in AISI 1050 steel.

Upon cooling of austenite below the A_1 critical temperature, colonies of perlite occur initially at the austenite grain boundaries. Thanks to the diffusion-controlled nature of perlitic transformation, initially developed colonies of perlite continue to grow, enlarging in size. At the same time, newly developed perlitic colonies continue to occur during transformation.

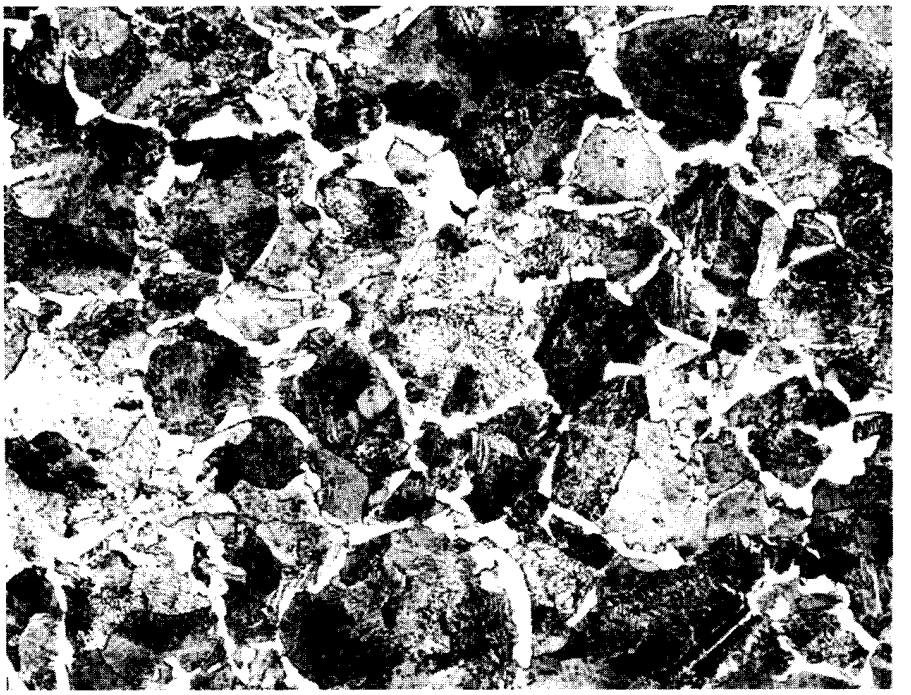

Figure 2.9 Metallographic appearance of perlite in AISI 1050 steel structure consists of perlite (dark gray) and ferrite (light). (Courtesy of LECO Corp.)

Fine perlite created upon more rapid cooling has superior properties over coarse perlite. This includes slightly higher hardness, better wear resistance, and impact strength.

It should be understood that depending upon a steel's carbon content, the perlitic region of the transformation diagram represents perlite–ferrite, perlite–cementite, and perlite microstructures.

Time-cooling curve C_3 crosses a left isothermal transformation curve in the area of fine perlite transformation (point 5). At point 5a, about of 50% of the austenite will transform into fine perlite. Then curve C_3 moves back from a dotted curve representing an isothermal transformation of 50% of austenite. When curve C_3 moves back from the dotted curve the transformation process will practically stop. The remaining 50% of the austenite will continue its transformation after crossing the 50% dotted curve. At point 6, the rest of the 50% of the austenite will complete its transformation into upper bainite.

In plain carbon and low-alloy steels the upper bainitic isothermal transformation occurs within the temperature range of about 550°C (1022°F) to 380°C (716°F). Upper bainite has a distinguishing feathery appearance.

Time-cooling curve C_4 represents even faster cooling conditions than the previous three scenarios. An important feature of curve C_4 deals with the fact that it "misses" the "nose" of the left isothermal transformation curve.

This means that austenite will not transform into any soft structures such as perlite or upper bainite. As shown in Figure 2.7B, just before reaching a region of martensitic transformation the cooling process has been interrupted or its severity has been drastically reduced resulting in entering and exiting an isothermal trans-

formation region in the lower bainitic area. At point 7 the steel still consists of 100% austenite. At point 8, all austenite will transform into lower bainite. An isothermal reaction "austenite-to-lower bainite" occupies the temperature range of about 380°C (716°F) to 220°C (428°F). Lower bainite has an acicular morphology and appears as a combination of plate-shaped entities looking somewhat similar to martensite [21]. An electron microscope is better suited to reveal a morphology of upper and, particularly, lower bainite.

Bainitic microstructures are tough and relatively hard (lower bainite being harder than upper bainite). The formation of bainite is governed by a complex combination of a diffusion-controlled and a diffusionless (shear-type) process. The bainitic transformation is probably the least explored reaction. A detailed discussion on the features of bainitic reactions, varieties of its morphologies, microstructures, and properties can be found in [14, 17, 19–21, 23, 103, 176, 181, 215, 228].

Time-cooling line C_5 represents a severe quenching condition that is typical for obtaining a fully martensitic structure. Line C_5 crosses the isothermal transformation curves in a martensitic region only. It enters and exits the TTT region at points 9 and 10, correspondingly. It is imperative to stress one more time the importance of "missing" the nose of the TTT curves in order to avoid soft upper transformation products such as perlite or upper bainite in an as-quenched structure.

Unfortunately, the isothermal time–temperature transformation diagrams of noneutectoid plain carbon steels (i.e., hypoeutectoid and hypereutectoid steels) are shifted so far to the left, that practically regardless of quench severity, the cooling curve will enter the region of the beginning of the transformation in the upper transformation area. This leads to an inability to obtain an entirely martensitic microstructure while isothermally transforming plain carbon steel (Figure 2.10). Therefore, in cases such as this, even upon severe quenching from austenitic tem-

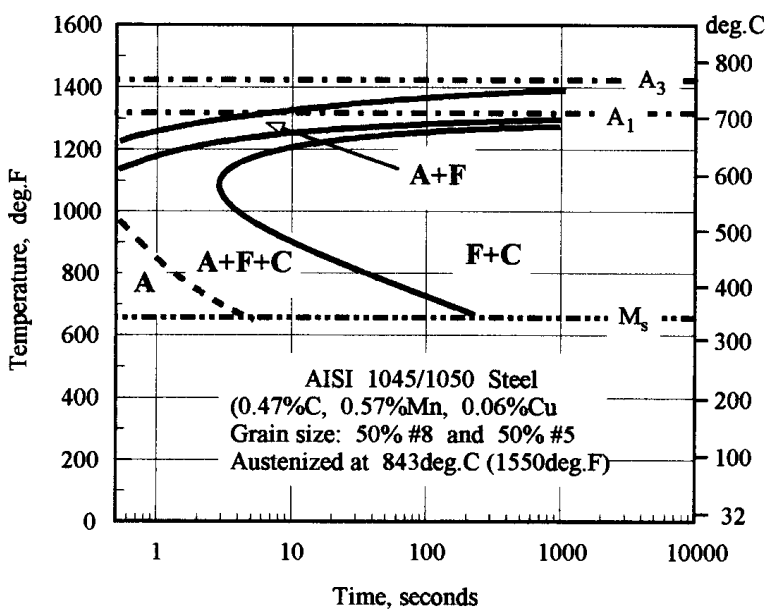

Figure 2.10 Isothermal time–temperature transformation diagram of AISI 1045/1050 steel. (From Ref. 24.)

perature down to ambient temperature, the final microstructure will consist of a combination of martensite and upper transformation products.

In hardening applications an ability to obtain a certain degree of martensitic structure is often the measure of how successful the heat treating process was. Martensite is a supersaturated solid solution of carbon in ferrite. The crystalline structure of martensite is referred to as a body-centered tetragonal structure. When the metal is rapidly cooled, the carbon is trapped in the crystal structure [19–21]. As shown in Figure 2.2, two dimensions of the unit cell are equal, but the third, because of the trapped carbon, is slightly expanded. This distortion of the martensitic crystalline structure is the reason for the high hardness that is developed when steel is transformed to martensite [174].

In an optical microscope, martensite appears as an acicular or needlelike structure. As mentioned above, the formation of martensite is governed by a shear-type (diffusionless) transformation of austenite, meaning that the transformation takes place almost instantaneously upon reaching a certain temperature.

Martensitic transformation takes place over a temperature range M_s (standing for "start") to M_f (standing for "finish") that depends upon the chemical composition of a given steel and cannot be changed by a variation of the quenching severity. If cooling upon quenching is interrupted at a certain temperature within the temperature range of a martensitic transformation, no further transformation to martensite will take place. Only upon cooling to a lower temperature will it be possible to initiate a martensitic transformation again. Being a diffusionless process, martensitic transformation is independent of time.

Figure 2.11 shows that the M_s–M_f temperature range is directly related to the steel's carbon content. The carbon content (Figure 2.12, top), actual amount of martensite formed, and grain size exclusively determine the maximum hardness of a given steel. In the range of 0.2 to 0.65% carbon, the hardness of the steel is proportional to the amount of carbon contained.

The M_s, M_{50}, and M_{90} lines on the time–temperature transformation diagram (Figure 2.7A) represent the temperatures at the start of transformation to martensite and the temperature at which 50 and 90% of the material has been transformed to martensite, respectively.

For plain carbon steels with a high carbon content, cast irons, and some alloy steels, the M_f temperatures are below room temperature (Figure 2.11). This means that under conventional heat treating conditions the existence of a noticeable amount of untransformed or retained austenite is unavoidable (Figure 2.13). In cases like these, the use of cryogenic treatment can transform the retained austenite into martensite providing a fully martensitic microstructure. This usually results in an additional increase in hardness (shaded area shown on Figure 2.12, bottom).

The M_s temperature of industrial plain carbon steels can be calculated using the following formula [20, 175, 181],

$$M_s(^\circ\mathrm{C}) = 512 - 453\mathrm{C} + 217(\mathrm{C})^2 - 71.5\,(\mathrm{C})(\mathrm{Mn}).$$

Identification of the stage of completion of the martensitic transformation is a more difficult task compared to determining M_s temperatures. Some investigators suggested the following correlation between the stage of martensitic transformation and M_s temperatures for hypoeutectoid steels.

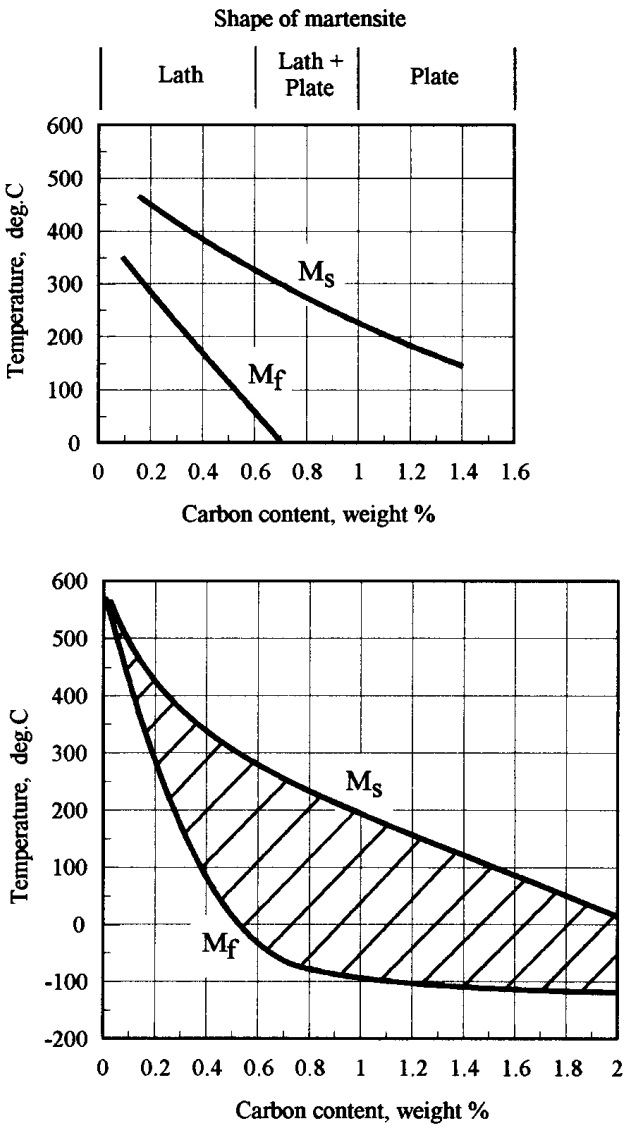

Figure 2.11 M_s and M_f temperature as a function of carbon content. (Top figure from Refs. 6 and 229; bottom figure from Ref. 228.)

$$M_{10\%}(^\circ\mathrm{C}) = M_s(^\circ\mathrm{C}) - 10 \quad (\text{error} \pm 3^\circ\mathrm{C})$$

$$M_{50\%}(^\circ\mathrm{C}) = M_s(^\circ\mathrm{C}) - 47 \quad (\text{error} \pm 6^\circ\mathrm{C})$$

$$M_{90\%}(^\circ\mathrm{C}) = M_s(^\circ\mathrm{C}) - 103 \quad (\text{error} \pm 12^\circ\mathrm{C})$$

$$M_f(^\circ\mathrm{C}) = M_s(^\circ\mathrm{C}) - 215 \quad (\text{error} \pm 15^\circ\mathrm{C}).$$

However, other researchers [175] found that, in reality, M_f temperatures are significantly lower than the values suggested in the above-mentioned formulas.

Martensitic transformation is accompanied by a volume increase. Table 2.2 shows a change in volume and length of a 1% plain carbon steel specimen [23].

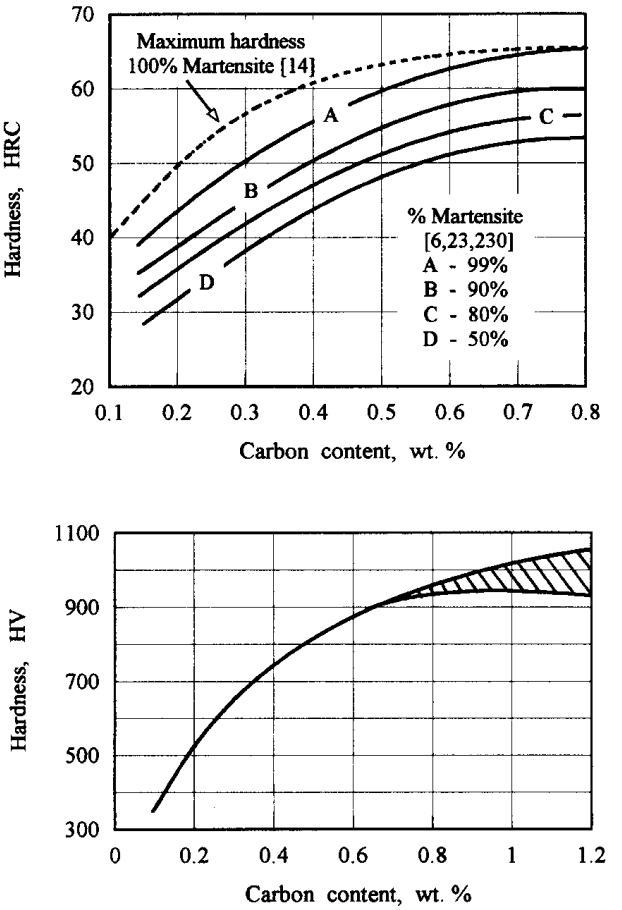

Figure 2.12 Relationship among hardness, carbon content, and amount of martensite. (Top figure: solid lines from Refs. 6, 23, and 230, dotted line from Ref. 14; bottom figure from Refs. 181 and 215.)

The phenomenon of volume change is responsible for the existence of residual stresses (e.g., for the presence of compressive residual stresses at the surface of case hardened parts) and shape/size distortion during and after heat treatment.

Depending upon the carbon content (Figure 2.11, top), there might be several different forms of martensite: lath martensite (in carbon steels with a carbon content up to 0.6%), plate martensite (when carbon content exceeds 1%), or a combination of both morphologies [21]. Both forms of martensite consist of numerous plates. Martensitic plates do not propagate beyond the austenitic grain boundaries. In the case of lath martensite, the martensitic plates are smaller in size and grouped together in martensitic units having approximately the same orientation within the unit. Conversely, the martensitic plates of plate martensite are much larger in size than the plates of lath martensite. Neighboring plates are randomly oriented.

Since the martensitic transformation is a diffusionless process, the initially created martensitic plates do not grow in size with time. Instead, upon further cooling new formations of plates continue to appear.

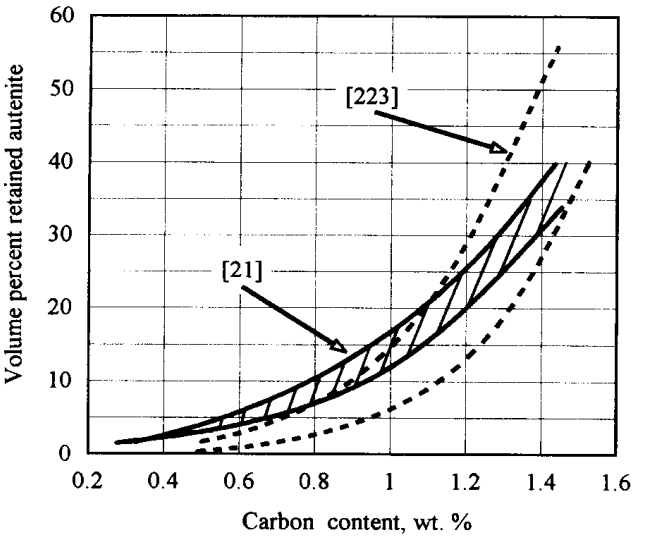

Figure 2.13 Retained austenite as a function of carbon content. (Solid curves from Ref. 21; dotted curves from Ref. 228.)

Although martensite is very hard, it is also quite brittle (particularly the plate martensite since numerous microcracks typically develop in the plate martensite of high carbon steels). This necessitates a subsequent heating and cooling operation referred to as tempering. Tempering relieves internal stresses caused by the hardening process, slightly reduces the hardness of the finished material, and provides the required balance of hardness, strength, ductility, and toughness. The real return in the tempering process is that instead of "as-hardened" martensite (also called "as-quenched" martensite) the finished structure consists of tempered martensite which is still quite hard and, in addition, is tough, durable, and much less brittle than "as-quenched" martensite. A higher tempering temperature leads to a greater hardness reduction and, at the same time, an increase in ductility.

Figure 2.14 shows the hardness variation of plain carbon steels as a function of the carbon content of the various phase transformation products [181].

2.1.1.4 Steel's Trace Elements and Alloying Elements

Although the percentage of carbon by far provides the most important influence on the properties of the steel, there are a number of other chemical elements that

Table 2.2 Incremental Changes in Volume and Length as a Result of Austenitic Transformation

Transformation	Change in Volume (%)	Change in Length (%)
γ-Iron into perlite	+2.4	+0.8
γ-Iron into lower bainite	+3.2	+1.07
γ-Iron into martensite	+4.2	+1.4

Source: Ref. 23.

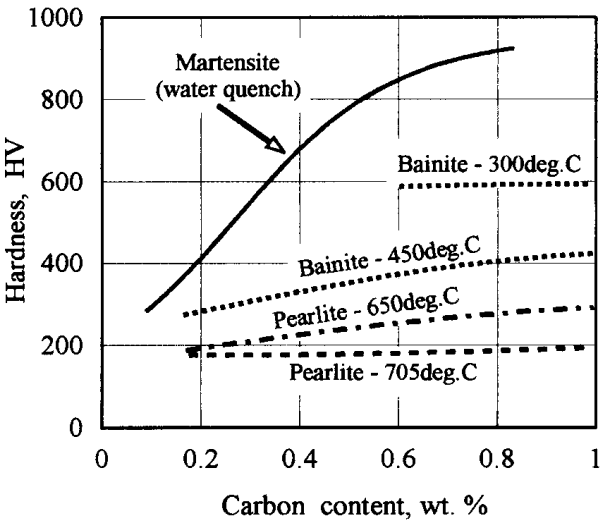

Figure 2.14 Hardness variation of plain carbon steel as a function of carbon content of the various phase transformation products. (From Ref. 181.)

depending upon their amount and combination can also notably affect the steel properties. All commercial grades of plain carbon steel, in addition to iron and carbon, may contain limited amounts of other chemical elements. Some of these additional chemical elements "happened to be" in the plain carbon steel as traces or residual impurities in the raw materials or were added to the melting pot for the creation of certain conditions during the steelmaking process. Inasmuch as the amount of these elements is normally limited and closely controlled, they normally do not greatly affect the process of heat treating or the basic microstructure of the steel and its properties. This allows us to consider plain carbon steel as a binary Fe–C alloy.

Another source of the presence of additional elements in plain carbon steel deals with the fact that although carbon steels, being the least expensive steels, are widely used in industry, there are many engineering applications where the properties of plain carbon steels are not suitable for meeting certain engineering requirements. Such requirements may include the necessity to increase the depth of hardness (hardenability); to reduce the tendency for grain growth; to improve corrosion resistance, abrasion resistance, or resistance to chemical attack; to increase impact strength; and to reduce oxidation and the susceptibility of heat treated parts to cracking and shape distortion. Often, it is required to achieve not just a certain property of the steel part but a combination of properties that are often contradictory, for example, obtaining a combination of strength, toughness, and ductility, as well as improving mechanical properties of the steel at elevated or low temperatures.

In order to provide steel with specific properties, an appreciable amount of certain chemical elements is purposely added to the steel. Chemical elements that typically serve as alloying elements include manganese, silicon, nickel, chromium, boron, molybdenum, and others. Alloy steels are more expensive to produce but are often worth the cost in applications requiring their use. Some examples of steels

consisting of a substantial amount of alloying elements are stainless steels, tool steels, maraging steels, bearing steels, and spring steels.

Due to the presence of a noticeably large amount of alloying elements, most alloy steel cannot be considered as a binary alloy, but more often as a ternary or quaternary alloy. Examples of ternary alloy steels are Fe–Co–Mn, Fe–Cr–Mo, and Fe–Cr–Ni steels.

An increased amount of alloying elements leads to a complex interaction among the different elements, which, in turn, provides a variety of microstructures and mechanical, chemical, thermal, and electromagnetic properties of steel.

Maraging steels can serve as an example of a steel that provides a unique combination of properties such as high strength, good ductility, and toughness thanks to substantial amounts of such alloying elements as nickel (8%), molybdenum (5%), and titanium (0.4%).

A detailed description of alloy steels and the effect of alloying elements on microstructure and the properties of the heat treated parts are discussed in [14, 17, 36, 96, 175–177, 183–186, 215–217, 228, 230].

The identification number of steel makes it easy to recognize not only the carbon content in a given steel but also the main alloying element as well (see Table 2.3).

When alloying elements are added to the mixture they often change the position of critical points of the phase transformation diagram with respect to temperature, carbon content, and the critical cooling rate that determines the hardened depth. The ability of some alloying elements to shift the nose of the C-shaped (S-shaped) curves to the right on the TTT diagram provides a significant practical benefit, as it makes it possible to harden the steel using less severe quenching techniques. Moderate quenching reduces the possibility of cracking and size/shape dis-

Table 2.3 General Classification of Steel Grades Based on Identification Number

Identification number	Type of Steel Grades Based on Principle Alloy Element
10xx	Plain carbon (nonresulfurized)
11xx	Plain carbon (resulfurized)
12xx	Resulphurized and rephosphorized
13xx	Manganese alloy
2xxx	Nickel alloy
3xxx	Nickel-chromium alloy
4xxx	Molybdenum alloy (may contain some nickel, chromium, or both)
5xxx	Chromium alloy
6xxx	Chromium–vanadium alloy
7xxx	Tungsten alloy
8xxx	Nickel–chromium–molybdenum alloy
92xx	Silicon–manganese alloy
94xxx/98xx	Nickel–chromium–molybdenum alloy (may contain some manganese)
14Bxx	Boron alloy
50Bxx/51Bxx	Chromium–boron alloy
8xBxx	Nickel–chromium–molybdenum–boron alloy

tortion on the heat treated part without sacrificing the ability to obtain the required martensitic structure. It should be mentioned here that some researchers (i.e. Dr. N. Kobasko [473], Dr. K. Shepelyakovskii [376]) believe that an effect of the cooling rate within the martensitic range on crack initiation appears as a bell-shape curve.

Depending upon the effect made by the alloying elements on the heat treatment process, microstructure, and properties of the steel, these elements can be divided into several groups based on their interaction with iron, carbon, and other alloying elements and their ability to promote or stabilize a certain phase (i.e., austenite formers, ferrite formers, carbide formers, etc.).

Such elements as manganese, nickel, copper, and cobalt belong to a group of austenite stabilizers. For example, due to an appreciable amount of nickel (from 7 to 20%), austenitic stainless steels (i.e., AISI 301, 302, 304, 310) retain an austenitic structure even at room temperature.

Other elements including silicon, chromium, tungsten, molybdenum, and aluminum act as ferrite formers. For example, silicon, being a strong ferrite former, serves as the principal alloying element (3 to 7% Si) and is used for manufacturing ferritic steel sheets used as laminations for magnetic flux concentrators, transformers, shunts, and flux diverters.

Some ferrite forming elements can at the same time promote the formation of carbides. Generally speaking, metals that stand to the left of iron in the Periodic Table of the Elements (Appendix A) are capable of forming carbides. Such elements as niobium, titanium, vanadium, molybdenum, tungsten, and chromium are called carbide formers. Under certain conditions complex carbides can be formed in steel.

The majority of elements that do not form chemical compounds with carbon and iron are presented in solid solution with iron [228].

In addition to the above-mentioned groups, alloying elements can also be subdivided into subgroups, based on their effect on the position of critical temperatures (i.e., A_1, A_3, A_{cm}), solubility in iron, the influence on the kinetics of austenitic transformation upon cooling, and susceptibility for grain growth.

Alloying elements affect the heat treatment process in many different ways. Some of these are described in [96, 181, 183–186, 215, 217, 228, 230]. Table 2.4 provides a brief summary of the effect of commonly used steel alloying elements.

Figures 2.15 and 2.16 show a graphical representation of the effect of alloying elements on eutectoid carbon content and eutectoid transformation temperature, respectively. A summary of observations is given below.

Analysis of Figure 2.15 leads to the important conclusion that the majority of alloying elements reduces eutectoid carbon content. This means that a perlitic structure may be developed with a relatively low carbon content providing more ductility for steel.

Such elements as nickel, which lowers the A_1 and A_3 critical temperatures, affect the process of austenization in a favorable way by lowering the austenizing temperature.

Similar to nickel, silicon does not form carbides, but it does noticeably slow the diffusion of carbon into the iron. This requires an increased austenizing temperature for a steel alloyed with silicon and/or a longer time at austenizing temperature compared to a plain carbon steel.

Carbide forming elements that develop stable carbides (i.e., vanadium and chromium) also require longer austenization time and/or higher temperatures for

Table 2.4 The Effect of Commonly Used Steel Alloying Elements

Element	Effect
Manganese (Mn)	Moderate carbide former. Deoxidizer in steel making. Lowers A_{c1}, A_{c3}, A_{r1}, and A_{r3} critical temperatures. Increases strength and decreases critical cooling rate. Improves hardenability and response to heat treatment. Lowers M_s temperature. Strongly increases amount of retained austenite. Reduces plasticity.
Nickel (Ni)	Does not form carbides. Austenite stabilizer. Lowers A_{c1}, A_{c3}, A_{r1}, and A_{r3} critical temperatures. Improves hardenability and corrosion resistance. Increases strength and toughness. Reduces eutectoid carbon content. Decreases critical cooling rate. Reduces amount of retained austenite and improves mechanical properties at low temperatures.
Silicon (Si)	Deoxidizer in steel making. Strong ferrite stabilizer. Does not form carbides. Reduces eutectoid carbon content. Slows the diffusion of carbon into ferrite, requiring longer time or higher temperatures for austenization (raises A_{c1}, A_{c3} critical temperatures). Improves hardenability. Promotes graphitization. Increases strength of ferrite and low-alloy steels but increases the steel's susceptibility to decarburization, and may lead to adverse effect on machinability. Provides some special electrical and magnetic properties.
Chromium (Cr)	Carbide former and strong carbide stabilizer. Raises A_{c1}, A_{c3} and lowers A_{r1}, A_{r3} critical temperatures. Requires longer time and/or higher temperatures for austenization since the chromium–iron carbides go more slowly into solution in austenite. Improves hardenability. Resists softening on tempering but may lead to secondary hardening. Slightly decreases M_s temperature. Increases wear resistance, corrosion resistance, cutting ability, and abrasion resistance. Decreases oxidation and increases high temperature strength.
Molybdenum (Mo)	Strong carbide former (forms stable carbides in steel). Nonoxidizing element. Raises A_{c1}, A_{c3} and lowers A_{r1}, A_{r3} critical temperatures. Decreases M_s temperature. Improves hardenability particularly in high-carbon steels. Has a pronounced effect on secondary hardening during tempering. Resists grain growth, temper brittleness, and undesirable tempering back. Increases the strength of steel at elevated temperatures.
Copper (Cu)	Increases atmospheric corrosion resistance and yield strength.
Aluminum (Al)	Strong deoxidizer in steel making. Improves hardenability. Decreases the critical cooling rate. Resists grain growth.
Boron (B)	Appreciably improves hardenability and machinability.

Table 2.4 Continued

Element	Effect
Vanadium (V)	Strong carbide former (forms stable carbides in steel). Raises A_{c1}, A_{c3} critical temperatures. Improves hardenability but to lesser extent than some other elements. has a pronounced effect on secondary hardening during tempering. Resists grain growth. Increases strength and toughness. Decreases eutectoid carbon content and increases hardenss at elevated temperatures.
Titanium (Ti)	Deoxidizer in steel making. Strong carbide former and carbide stabilizer (eliminates carbide percipitation). Nitride former. Drastically raises A_{c1} and A_{c3} critical temperatures. Improves hardenability. Promotes fine grains.
Niobium (Nb) (Columbium)	Raises A_{c3} and A_{r3} critical temperatures. Strong carbide stabilizer (eliminates carbide precipitation). Resists undesirable tempering back and grain growth. Increases impact strength and ductility.
Tungsten (Wolfram) (W)	Carbide former. Raises A_{c1}, A_{c3} and lowers A_{r1}, A_{r3} critical temperatures. Increases hardness, wear resistance, and strength at high temperatures. Resists grain growth. Primarily affects high-carbon steels.
Zirconium (Zr)	Deoxidizer. Strong carbide former. Nitride former. Improves hardenability. Resists grain growth. Improves mechanical properties at elevated temperatures.
Cobalt (Co)	Austenite former. Increases strength of ferrite. Increases wear resistance of steel. Resists softening at elevated temperatures. Increases the austenite precipitation rate. Reduces hardenability.
Lead (Pb)	Does not alloy with steel. Improves machinability.
Sulfur (S)	Improves machinability. Decreases ductility and impact strength. May lead to structural segregation. Its presence is often considered to be undesirable.
Phosphorus (P)	Increases strength and hardness but decreases toughness and ductility. Introduces noticeable brittleness. Promotes structural segregation. Its presence is often considered to be undesirable.

completion of the diffusion processes necessary for carbides to go into solution and for forming a structure of homogeneous austenite.

It is particularly important when choosing the appropriate process parameters for induction heat treating to take into account the existence of large carbides in the steels because of the short heat time of the induction process.

The effects of alloying elements shown in Table 2.4 and Figures 2.15 and 2.16 illustrate an independent action of each alloying element without taking into con-

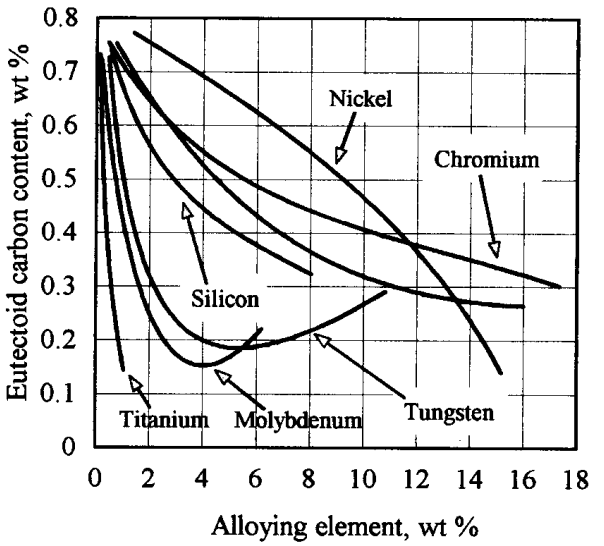

Figure 2.15 Effects of alloying elements on the eutectoid carbon content in steel. (From Refs. 21 and 184.)

sideration the potential interaction among elements. It is important to recognize the alloy interaction phenomenon when estimating the effect of a particular alloying element. The interaction between such elements as nickel–manganese, nickel–copper, boron–titanium, and tungsten–molybdenum–chromium can serve as a good example of strong alloy interaction.

The majority of alloying elements have a pronounced effect on the transformation of austenite during its cooling that includes the following transformations: γ-iron into perlite, γ-iron into bainite, and γ-iron into martensite.

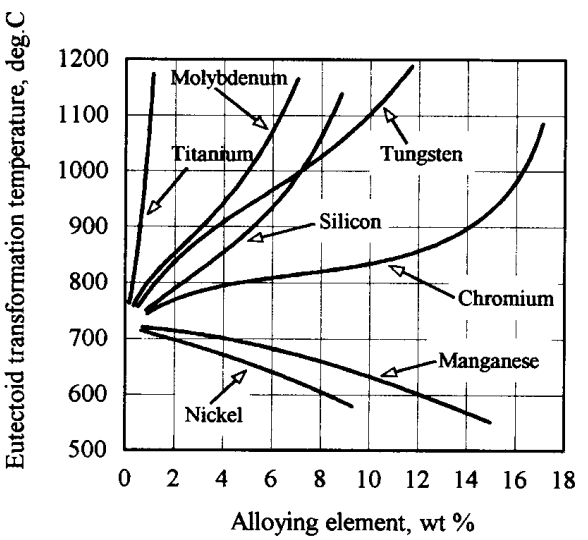

Figure 2.16 Effects of alloying elements on the eutectoid transformation temperature of steel. (From Refs. 21 and 184.)

As stated earlier, one of the most significant practical benefits of using alloying elements is the ability to shift the nose of the S-curve (C-curve) to the right. Some of the alloying elements increase the austenite precipitation rate (i.e., cobalt); however, the majority of the commonly used alloying elements slow the austenitic transformation. Figure 2.17 shows two scenarios of shifting the isothermal time–temperature transformation curves based on whether the alloying element belongs to the group of carbide formers.

Figure 2.18 shows the effect of alloying elements on the M_s temperature [96] and on the amount of the retained austenite in the as-quenched steel with 1% C [96].

Some carbide forming elements form stable carbides; others form relatively unstable carbides. Experimental data show [228] that the elements located further to the left of the row (see the Periodic Table of the Elements, Appendix A) form more stable carbides. Therefore, carbides formed by titanium and vanadium are more stable than carbides formed by chromium and manganese.

There have been several attempts to develop convenient mathematical expressions that would allow the heat treater to calculate the critical temperatures of transformation for different phases. Some of the formulas that can be used for a rough estimation of A_{c1}, A_{c3}, B_s, and M_s temperatures of industrial carbon steels are shown below.

Austenitic critical temperatures:

(from [232])
$$A_{c3}(^\circ\text{C}) = 910 - 203\sqrt{C} - 15.2\text{Ni} + 44.7\text{Si} + 104\text{V} + 31.5\text{Mo} + 13.1\text{W}$$
$$A_{c1}(^\circ\text{C}) = 723 - 10.7\text{Mn} - 16.9\text{Ni} + 29.1\text{Si} + 16.9\text{Cr} + 290\text{As} + 6.38\text{W}.$$

Critical temperatures for beginning bainitic transformation:

(from [176])
$$B_s(^\circ\text{C}) = 830 - 270C - 90\text{Mn} - 37\text{Ni} - 70\text{Cr} - 83\text{Mo}.$$

M_s transformation temperature:

$$M_s(^\circ\text{C}) = 539 - 423C - 30.4\text{Mn} - 12.1\text{Cr} - 17.7\text{Ni} - 7.5\text{Mo}$$

(from [232])
$$M_s(^\circ\text{C}) = 512 - 453C - 16.9\text{Ni} + 15\text{Cr} - 9.5\text{Mo} + 217(C)^2 - 71.5(C)(\text{Mn}) - 67.6(C)(\text{Cr})$$

(from [233])
$$M_s(^\circ\text{C}) = 561 - 474C - 33\text{Mn} - 17\text{Ni} - 17\text{Cr} - 21\text{Mo}$$

(from [234])
$$M_s(^\circ\text{C}) = 550 - 350C - 40\text{Mn} - 20\text{Cr} - 17\text{Ni} - 10\text{Mo} - 8\text{W} - 35\text{V} - 10\text{Cu} + 15\text{Co} + 30\text{Al}.$$

As opposed to other heat treating techniques, heat treatment by induction is appreciably affected by variations of metal chemical composition. Since the chemical composition of steel may vary to some extent, the heat treater should have a great deal of knowledge regarding this variation and its possible effect on the results of the heat treatment as well as on the performance of the part. Wide compositional limits cause surface hardness and case depth variation. Conversely, tight control of the composition eliminates possible variation of the heat treat pattern resulting from multiple steel/iron sources. If steel does not respond to heat treatment in an expected way, then the first step in finding the reason is to conduct a chemical analysis to ensure that the steel has the specified chemical composition.

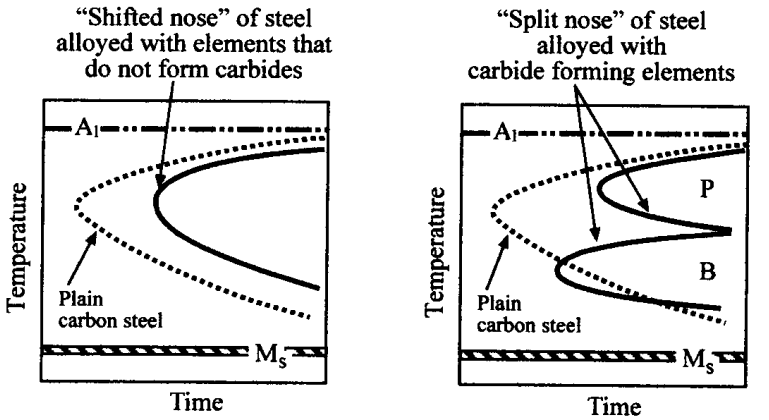

Figure 2.17 Isothermal ITT diagrams of alloyed steels compared to the ITT diagram of plain carbon steel. (From Ref. 228.)

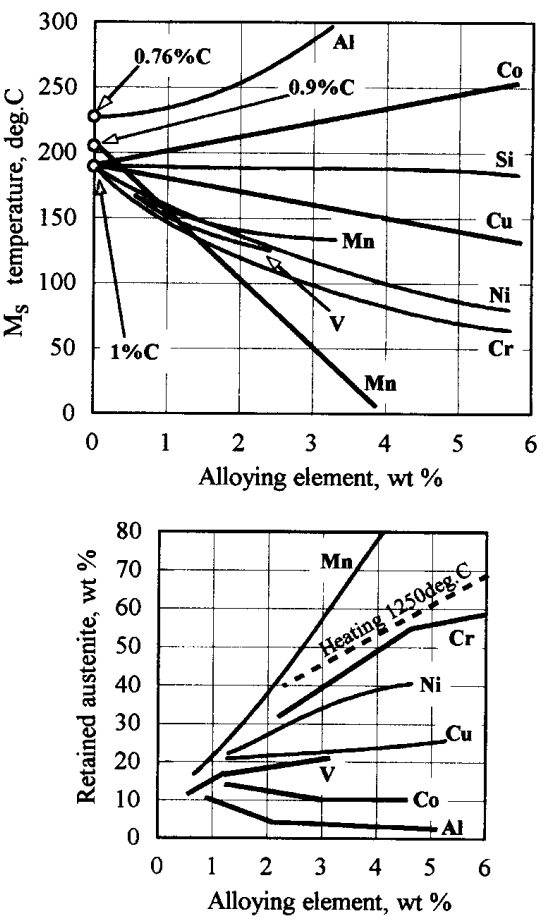

Figure 2.18 Effect of alloying elements on the M_s temperature (top and the amount of retained austenite in quenched steel (1% C) (bottom). (From Ref. 96.)

2.1.1.5 Hardenability

Hardenability is an important property of steel and cast iron defining the ability of the material to be hardened to a certain depth. It is measured as the distance from the surface where a certain hardness can be obtained or a specific percentage of martensite can be formed (e.g., the hardness of 50 HRC or 50% martensitic structure are often used to define the hardenability of steel). Hardenability is a function of chemical composition, grain size, the degree of the homogenization of the austenite, and the intensity of cooling during quenching.

When discussing the subject of hardenability, it is important to recognize certain differences that influence hardenability in the case of through hardening compared to induction surface hardening.

a. Through Hardening. In order to harden the workpiece throughout its entire cross-section, it is typically required to heat the workpiece as uniformly as possible to the austenizing temperature range and then to quench it to the ambient temperature.

During quenching, the cooling rate at the surface of the through heated workpiece is always more intense compared to the cooling rate of internal areas of the workpiece and, particularly, compared to the cooling rate at its core. If the workpiece is thin enough, then the intensity of cooling at the core might still be severe enough to "miss" the upper transformation region of the continuous cooling diagram and to form a sufficient amount of martensite within the workpiece core (Figure 2.19, left). As a result, a relatively uniform through harden pattern would take place. At the same time, since the cooling rate at the workpiece surface is always more intense compared to the cooling rate in its core, the amount of martensite formed in the surface and subsurface areas will be greater compared to the amount of martensite formed in the core. Therefore, the surface hardness is to some extent higher compared to the core hardness (assuming that the surface has not been overheated and oxidation or decarburization do not occur).

When the diameter or thickness of the workpiece increases then the thickness of the hardened layer (hardened depth) will also increase. At the same time, with increased workpiece diameter/thickness the hot core is situated farther from the quenched surface and, therefore, the thermal conductivity provides less intensive cooling of the core during surface quenching. As a result, at a certain point, the CCT curve that represents the core cooling conditions during surface quenching will be extended farther to the right and finally will enter a curve that indicates the beginning of transformation at temperatures that exceed the M_s temperature (Figure 2.19, right). As a result, depending upon the cooling rate, a certain amount of upper transformation products (i.e., bainite, perlite, ferrite) would be formed within the core leading to a softer core compared to the surface.

For a given steel, grain size, and quench intensity, and assuming that upon austenization a homogeneous austenite has been formed, there would be a cylinder of a particular diameter that would have 50% martensite at its core upon quenching. This "particular diameter" is commonly called the critical diameter D_{cr}. If the workpiece diameter exceeds the critical diameter, then the amount of martensite that would be formed in the core of the cylinder would be less than 50% resulting in an essentially "soft" core. Therefore, the value of D_{cr} represents the maximum diameter of a cylinder that can be through hardened.

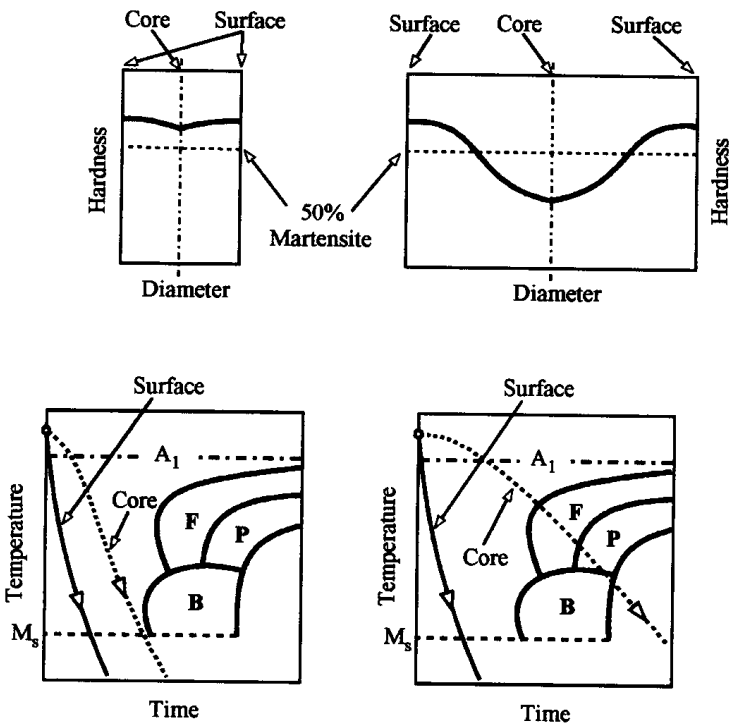

Figure 2.19 Effect of diameter on hardness profile and core cooling rate.

More intense quenching provides the ability to through harden cylinders of bigger diameters. Figure 2.20 shows the effect of different quenchants on the ability to through harden solid cylinders with different diameters made from the same steel.

Three parameters influencing the value of the critical diameter (chemical composition, grain size, and homogenization of austenite) can be relatively easily defined. The fourth factor (the quenching condition) is often the least-defined factor. This is particularly true in the case of induction hardening.

As discussed in Section 5, spray quenching is one of the most popular quenching modes used in the majority of induction hardening applications. The severity of cooling during spray quenching depends upon a combination of several factors including the surface temperature of the workpiece, quench pressure, flow rate, specifics of the quenching block design, number and distribution of quench holes, size of orifices and angle of drilled quench holes, type and purity of quenchant, quenchant temperature, and so on. The complexity of determining the particular quenching condition makes it difficult to use a value for the critical diameter for a description of the hardenability.

In order to eliminate the uncertainty of quenching conditions and provide a more practical and universal quantitative measure of hardenability of steels and cast irons, the term ideal critical diameter D_i has been commonly accepted in industry. A value of D_i represents the ideal quenching that would take place if upon quenching the surface of the workpiece it would be cooled instantly down to the temperature of the quenchant.

There are several experimental techniques that exist for the determination of the hardenability of steel and cast iron. Among these techniques the Grossmann's

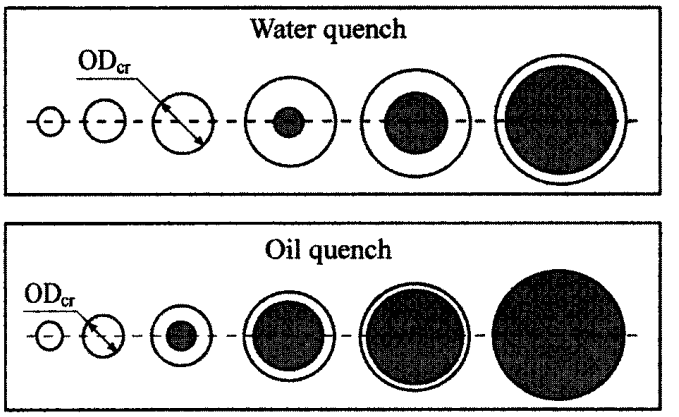

Figure 2.20 Effect of specimen diameter and quench media on hardenability (unhardened areas shaded in gray).

hardenability test and the Jominy end-quench test are two of the most well known.

The Grossmann's hardenability test implies the concept of the critical diameter. A variety of specified cylinders having different diameters are cooled from a certain austenitic temperature down to ambient temperature using a given quench medium (Figure 2.20). As mentioned above, for a specimen cooled with a particular quenchant, a cylinder with 50% martensite at its core would correspond to the critical diameter D_{cr}. A correlation between critical diameter and ideal critical diameter has been established.

Figure 2.21 shows the values of the ideal critical diameter as a function of carbon content and grain size for plain carbon steel. For example, the ideal diameter that corresponds to a maximum through harden diameter of plain carbon steel

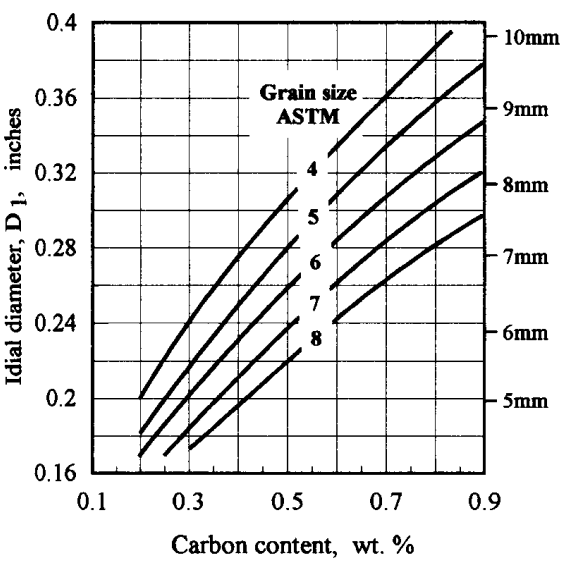

Figure 2.21 The dial critical diameter as a function of the carbon content and austenitic grain size. (From Refs. 23 and 186.)

consisting of 0.5% C with grain size of 6 would be equal to 0.26 in. (6.6 mm). Coarse grain steels exhibit superior hardenability than fine grain steels.

Alloying elements have a marked effect on hardenability. The effect of commonly used alloying elements on steel hardenability and the value of the ideal diameter can be calculated by using multiplying factors (Figure 2.22). For example, according to the charts shown in Figures 2.21 and 2.22, nickel–chromium–molybdenum alloy steel AISI 8645 (0.43–0.48% C, 0.75–1.0% Mn, 0.15–0.35% Si, 0.4–0.7% Ni, 0.4–0.6% Cr, 0.15–0.2% Mo) of grain size 6 would have the following range of ideal critical diameters D_i^{min} and D_i^{max} based on the extreme variation of the amounts of alloying elements.

Element	Mn	Ni	Cr	Si	Mo
Percentage	0.75	0.4	0.4	0.15	0.15
Multiplying factor	3.55	1.16	1.86	1.1	1.43

$D_1^{min} = 0.24*3.55*1.16*1.86*1.1*1.43 = 2.89$ in. (73 mm).

Element	Mn	Ni	Cr	Si	Mo
Percentage	1	0.7	0.6	0.35	0.2
Multiplying factor	4.4	1.28	2.3	1.25	1.6

$D_1^{max} = 0.257 \times 4.4 \times 1.28 \times 2.3 \times 1.25 \times 1.6 = 6.66$ in. (169 mm).

As one can see, the ideal critical diameter can vary drastically. Obviously the worst combinations of the amounts of alloying elements have been used in these examples. The probability of having such combinations is very low. At the same time, it is important to recognize that depending upon different steel manufacturers or even different batches of steel produced by the same manufacturer, having the same identification number, and satisfying the chemical composition requirements (ranges and limits of principal alloying elements) it is still possible to have a noticeably different hardenability. This means that the hardened case depth as well as the hardness pattern could be different. This variation depends on the steel manufacturing practice, the raw materials, and a number of other factors.

There are cases when certain applications could require having tight control of not only the chemical composition but hardenability as well. Steels that satisfy such requirements are called H-steels. H-steels have basically the same identification number as regular steels, however, the suffix "H" is added at the end of the H-steels' identification numbers.

Since the process of induction hardening is more sensitive to a steel's chemical composition and the ability of the steel to be hardened to a certain depth than other heat treat processes (carburizing, nitriding, etc.), H-steels are the preferable choice for induction hardening.

As one can imagine, in order to conduct a Grossmann's hardenability test, it is necessary to have a variety of cylindrical specimens with different diameters that are equally and uniformly heated and placed under identical quenching conditions. In

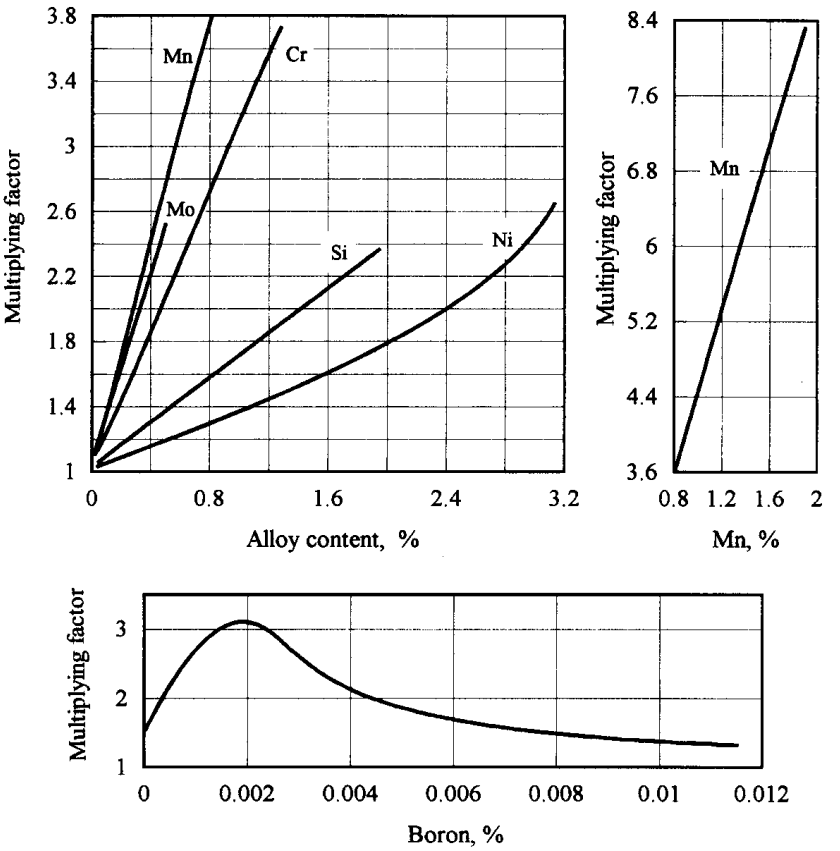

Figure 2.22 Multiplying factors for different alloying elements for hardenability calculations. (From Refs. 20, 23, 97 and 237.)

order to overcome the complexity of the Grossmann's hardenability test, the Jominy end-quench test was developed. Being one of the simplest and the least expensive, a Jominy end-quench test became one of the most popular techniques used for the determination of steel hardenability.

According to the Jominy end-quench test a cylindrical specimen (25 mm OD and 100 mm long) is uniformly heated to reach the condition of homogeneous austenite and then spray quenched from one end (Figure 2.23). As a result, a longitudinal hardness distribution as a function of the distance from the quenched end is obtained. Obviously, the Jominy end-quench test is much simpler compared to the more complicated Grossmann's hardenability test.

b. Induction Surface Hardening. Some applications require the formation of martensitic layers at specific areas of the workpiece (e.g., at its surface) while allowing the microstructure of the remainder of the part (i.e., core) to be unaffected. As shown in Sections 2.1.2.1, 3.1.2, and 5.1.2, thanks to the skin effect and some other electromagnetic phenomena, it is possible with induction heating to induce power in selected areas of the workpiece where the metallurgical changes are required.

Surface hardening is accomplished by raising the required depth of the material above the A_3 critical temperature to the point where it is transformed to austenite

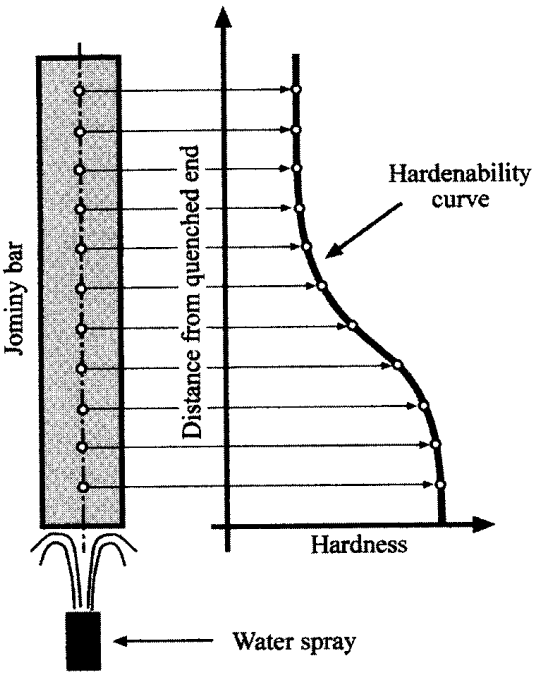

Figure 2.23 Sketch of Jominy end-quench test and an example of hardenability curve.

and then cooling the workpiece rapidly to produce martensite. The dynamics of the induction surface hardening process are shown in Figures 2.24 and 2.25.

Temperature profiles at different heating and quenching stages as well as hardness distribution at the end of quenching have been calculated using ADVANCE-H software, developed by the scientific group of Drs. S. Gurevich and N. Zimin. This software takes into consideration the shift of critical temperatures of the phase transformation diagram due to intensive heating, as well as the specifics of induction hardening, including spray quenching. The required electrical process parameters as well as the grain size growth and distribution of the structural phases (i.e., martensite, bainite, perlite, etc.) are among the parameters that can be predicted by using ADVANCE-H.

As has been discussed above, the main reason for a heat deficit in the core of a cylindrical part is the skin effect. This effect depends upon the metal properties and the frequency of the induction heating power. Due to the skin effect, about 86% of the power is induced within the surface layer that is referred to as the current penetration depth. The induced electrical current decreases from the surface toward the core.

At different stages of heating the value of the current penetration depth varies. Table 2.5 shows the current penetration depth versus frequency and heating stage for typical conditions of induction hardening of medium carbon steel.

The core of the solid cylinder is always heated due to thermal conduction. Since the heating time in induction surface hardening applications is often very short, the penetration depth of electrical currents induced within the heated workpiece by the induction coil is the major factor in obtaining a certain hardness depth. It is particularly true when the time of heating is less than 4 sec.

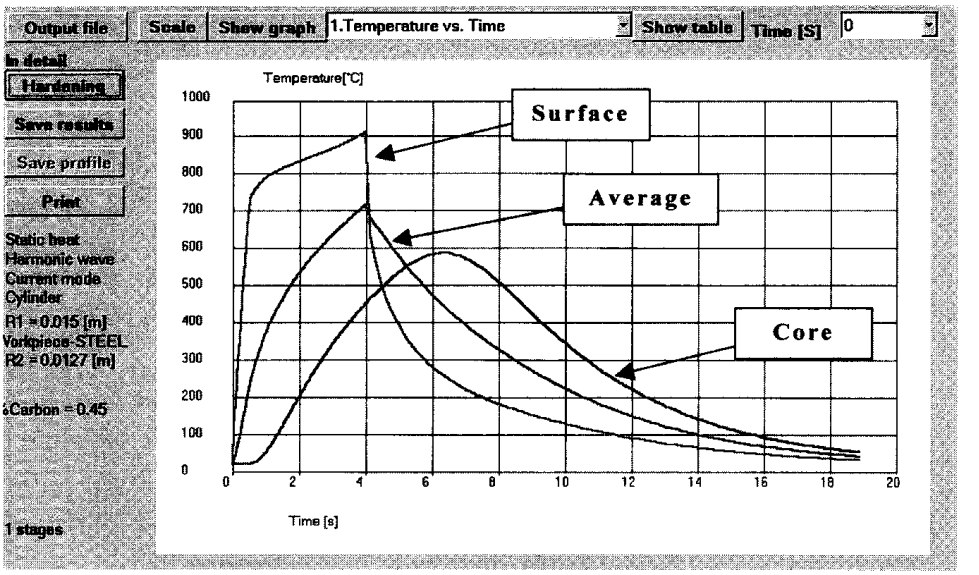

A) Temperature vs. time during induction hardening

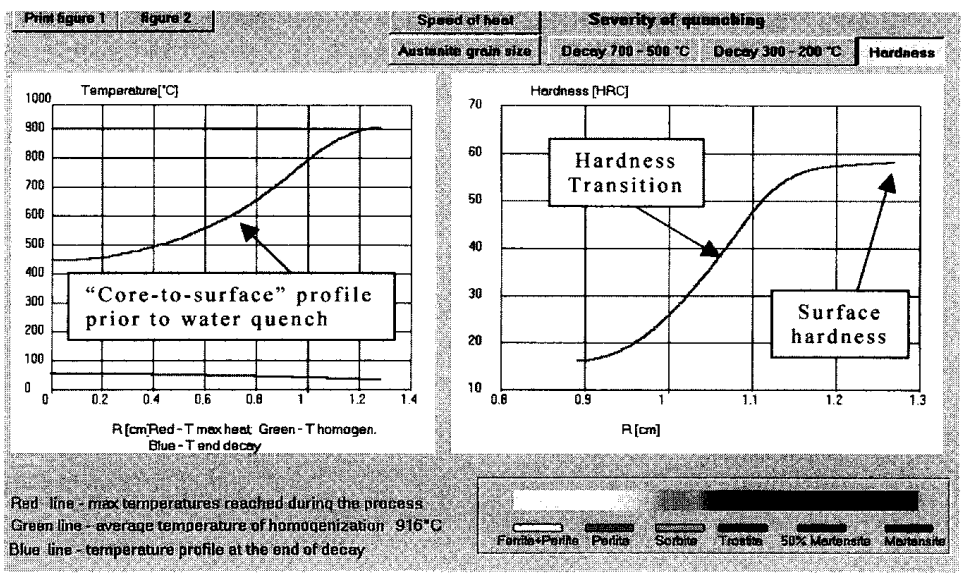

B) "Surface-to-core" temperature profiles and hardness distribution

Figure 2.24 Dynamics of induction hardening of the carbon steel shaft of OD = 25.4 mm (1 in.) using a frequency of 30 kHz (output files of the software ADVANCE-H).

A detailed analysis of the skin effect in induction surface hardening is provided in Sections 3.1.2 and 5.1.2.

The existence of the cold core has an important impact on the cooling conditions during quenching. In some surface hardening applications when the heat time is short and the skin effect is pronounced, the temperature of the core does not rise significantly during the heating stage. Therefore, upon quenching the cold core provides an additional cooling effect resulting in more severe quenching conditions

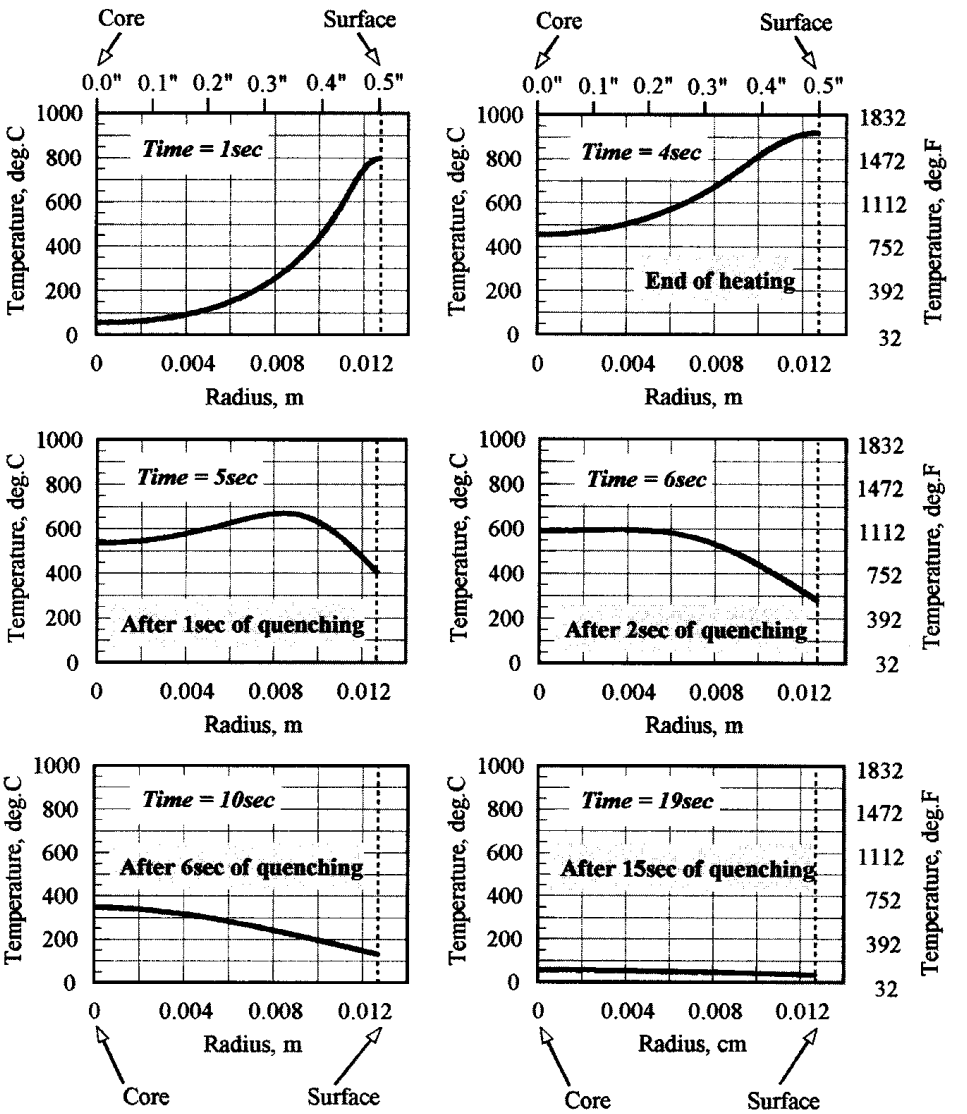

Figure 2.25 Temperature profiles at different stages of induction heating and quenching of steel shaft (1040) of 25.4 mm OD using a frequency of 30 kHz.

overall compared to the cooling intensity of the through heated parts. A more intensive quench increases the steel hardenability as well as other important parameters of the heat treatment process including the formation and distribution of residual stresses, specifics of austenite transformation, and so on.

c. Limitations of Standard Forms of Hardenability Tests. Unfortunately, the majority of techniques for measurement of hardenability should be applied for induction hardening (particularly induction surface hardening) with a great deal of caution due to the assumptions and features taking place when experiments have been conducted. Some of these features are discussed below.

- In its standard form, the Jominy end-quench test is only suitable for moderate cooling rates and can provide particularly misleading results when

Table 2.5 Current Penetration Depth (in mm) versus Frequency and Heating Stage for Typical Conditions of Induction Hardening of Medium Carbon Steel

	Frequency (kHz)					
Heating Stage	0.5	3	10	30	70	200
Initial heating stage (ambient temperature)	3.6–3.9	1.4–1.6	0.7–0.85	0.42–0.5	0.3–0.38	0.15–0.22
Final heating stage (surface above A_{c3})	17.5	10	5.6	3.2	2.1	1.2

cooling rates are about 100°C/sec or higher (which is the case of the majority of induction hardening applications).

- According to standard hardenability tests, a specimen is heated to austenitic temperature and held at that temperature for a sufficiently long time assuring that a homogeneous austenite has been formed. However, in the case of induction surface hardening when intense heating has been applied without any holding time, the structure of the austenite and its homogenization differ to some extent compared to austenite formed on slow heating with a sufficiently long holding time at austenitic temperature. This variation can cause some differences in the hardenability curves.
- The fact that heating during induction hardening is very intensive shifts the A_3 critical curve toward higher temperatures (this phenomenon is discussed in more detail in Section 2.1.1.6). Quenching of specimens from temperatures that are often 100 to 180°C higher than the temperature used during hardenability tests can also lead to certain errors in the prediction of the hardness pattern.
- The ability of the cold core to increase the severity of the cooling during quenching in surface hardening applications is another factor that results in modification of conventional hardenability curves. The effect of the cold core that often can have a detrimental effect on the intensity of cooling does make it possible to have "self-quenching" (also known as a "mass quenching") which allows elimination of spray quenching with liquid quenchants.
- Hardenability tests are primarily oriented toward specimens of cylindrical shape with limited ability to extend them to the square cross-sections. Unfortunately, these results cannot be easily transferred to such geometry as rectangular, conical, and, complex geometry such as gears and the like.

Taking into consideration the above-mentioned features and, in order to increase the accuracy of predicting a material's hardenability after induction surface hardening, nonstandard forms of the Grossmann's hardenability or Jominy end-quench tests can be conducted. These tests require the creation of certain temperature gradients before quenching, and are better suited to induction surface hardening needs, but they are cumbersome, complex, more expensive, time consuming, and still cannot provide universal recommendations. Due to these restrictions these types of

hardenability measurements are not widely conducted and therefore, their results are not readily available in the literature.

As a short summary on hardenability it should be mentioned that data obtained from a standard Jominy or Grossmann tests should primarily be used for reference purposes. Nevertheless, the hardenability curves are still quite useful as they provide orientation regarding an ability to estimate such important parameters as surface hardness, hardened pattern, and case depth (Figures 2.23 and 2.24).

2.1.1.6 Effect of Heat Intensity (Heating Rate) on Steel Induction Heat Treatment Results

As mentioned in Section 2.1.1.2, an equilibrium phase transformation diagram is only valid for equilibrium conditions. One of the major requirements of an equilibrium condition is sufficiently slow heating. However, induction heating is a very fast process. The intensity of induction hardening often exceeds 200°C/sec. A heat intensity of this magnitude by any means cannot be considered an equilibrium condition.

A high heating rate affects the kinetics of the austenite formation process requiring higher austenizing temperatures in order to create favorable conditions for the required diffusion processes. Figure 2.26 shows the effect of the heating rate on the A_{c3} critical temperature of steels having different structures [6, 186].

Figure 2.27 shows the influence of the heating rate on grain size growth of medium carbon steel (AISI 1040). A detailed discussion regarding the kinetics of the phase transformation processes during intensive heating can be found in [6,12,103,186,235,236].

2.1.1.7 Effect of Prior Microstructure of Steel

The microstructure of steel prior to heat treatment (sometimes also referred to as the initial structures or structure of the "green" part) has a pronounced effect on the results of the heat treatment and process parameters. This includes the austenizing

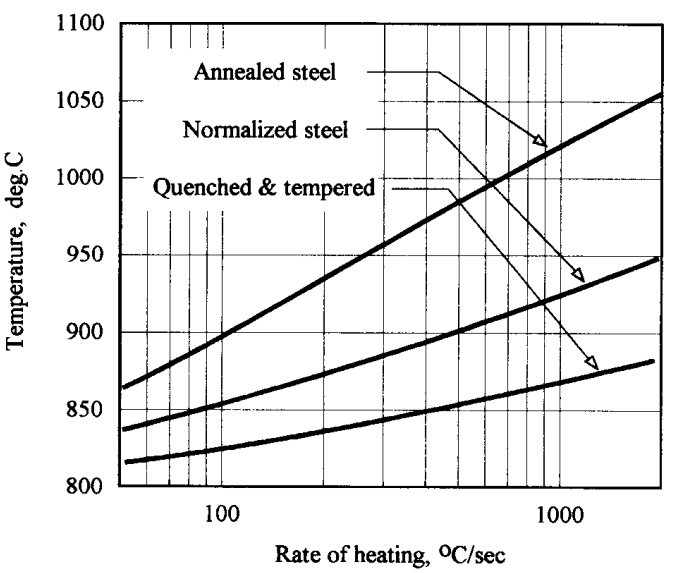

Figure 2.26 Effect of initial microstructure and heating rate on A_3 critical temperature for 1042 steel. (From Refs. 6 and 188.)

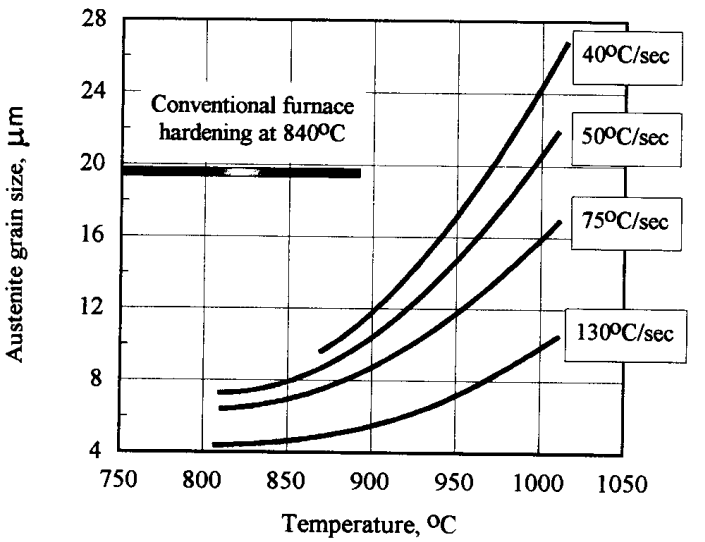

Figure 2.27 Influence of the heating rate on austenitic grain size of steel 1040. (From Ref. 12.)

temperature, the amount of time required at that temperature, hardness profile, length of the transition zone, and so on.

A "favorable" initial microstructure that includes homogeneous fine-grain quenched and tempered martensitic structure with a hardness of about 30 to 34 HRC allows one to reduce the austenizing temperature and leads to fast and consistent metal response to induction heat treatment with the smallest shape/size distortion, minimum amount of grain growth, and a well-defined (crisp) pattern with a short transition zone. This type of initial microstructure also results in higher hardness and deeper hardened case depth compared to a ferritic/perlitic initial microstructure. Figure 2.28 shows the effect of initial microstructure on an AISI 1070 carbon steel bar in response to surface hardening [6, 185].

H-steels having tight control of not only the chemical composition but on hardenability as well are preferable steels due to their tendency to provide more repeatable heat treat results.

If the initial microstructure of a part that is supposed to be induction heat treated has a significant amount of coarse perlite and, most important, coarse ferrites or clusters or bands of ferrites, then these microstructures cannot be considered "favorable" structures.

Ferrite is practically a pure iron and does not contain the carbon required for martensitic transformation. Pure ferrite consists of less than 0.025% carbon. Large areas (clusters or bands) of ferrite require a long time for carbon to be able to diffuse into the poor carbon area of the ferrite. Otherwise, clusters or bands of ferrites would act as one huge grain of ferrite and would be retained in the austenite. Upon quenching, a complex ferritic–martensitic microstructure would be formed. This structure is characterized by scattered soft and hard spots and poor mechanical properties. Therefore, segregated and banded initial microstructures of "green" parts should be avoided.

Steels with large stable carbides (i.e., spherodized microstructures) have poor response to induction hardening as well and also result in the necessity of having prolonged heating and higher temperatures for austenization. Longer heat time leads

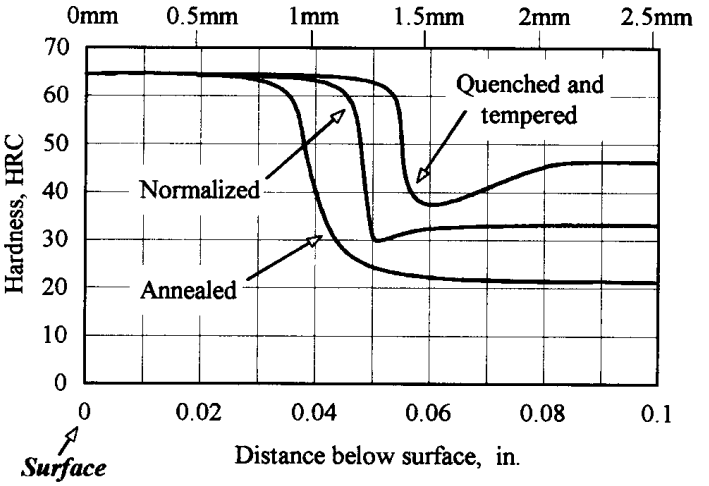

Figure 2.28 Effect of initial microstructure in 1070 steel bars in response to surface hardening using a 450 kHz induction generator operated at a power density of 2.5 kW/cm^2 (16 kW/in.^{2}). (From Refs. 6 and 187.)

to grain growth, the appearance of coarse martensite, data scatter, extended transition zone, surface oxidation/decarburization, and increased shape distortion of the heat treated part. Coarse martensite has a negative effect on such important properties as toughness, impact strength, and bending fatigue strength and is susceptible to crack development.

Figure 2.26 shows the effect of initial microstructure and heating rate on A_3 critical temperature for 1042 steel [6, 186]. It is obvious that heating should be conducted at a higher temperature for an annealed coarse microstructure as compared to a quenched and tempered fine grain microstructure.

2.1.1.8 Induction Heat Treatment of Cast Irons

Up to this point we have focused on some aspects of heat treating concentrating on the principles of steel hardening. The induction method may also be successfully used for hardening of cast irons. There are a number of induction surface hardening application heating parts manufactured from different types of cast irons [14, 17, 19–23, 98–106, 175, 176, 186, 215–220, 224–226].

It should be clarified at this point that the term "cast iron" does not represent one particular material but a large family of alloys that occupy the right side of the iron–iron carbide transformation diagram (Figure 2.5) featuring a high carbon content region (2% and higher) and a wide variety of properties.

Generally speaking, within the family of commercial cast irons it is possible to recognize six groups: white, gray, malleable, ductile (nodular), compacted graphite, and special alloy cast irons. It is important to remember, that the first five groups of cast irons have a moderate amount of alloying elements, whereas the amount of alloying elements represented in special alloy cast irons is significant and usually exceeds 3%.

Gray, ductile (nodular), and, to a lesser extent, the malleable and compacted graphite irons are four groups of cast irons that more frequently utilize heat treatment by induction.

The majority of commercial cast irons consist of a significant amount of silicon (typically from 0.6 to 3% Si) together with carbon as the two principal alloying elements. Moreover, in order to provide particular properties for a certain type of cast iron, some other alloying elements including manganese, phosphorus, copper, sulfur, nickel, and so on are added [14, 17, 19, 21, 98–106, 175, 215–220, 225]. For comparison purposes, Table 2.6 shows the typical chemical composition of the three most common unalloyed cast irons: gray, malleable, and ductile irons [17]. As one can see, unlike steels, different types of cast iron have very similar chemical composition. Specifics of cast iron microstructure and the appearance of a graphite and matrix distinguish one type of cast iron from another.

While discussing the main features of heat treatment of cast irons it is important to introduce the concept of carbon equivalence (CE). There are several mathematical expressions that have been developed to allow calculation of the carbon equivalent [14, 17, 19, 21, 103, 104, 218, 219]. The expression recommended in [17] is often used at INDUCTOHEAT, Inc. to calculate the value of CE:

$$CE = \%\,C + 0.3(\%\,Si) + 0.33(\%\,P) - 0.027(\%\,Mn) + 0.4(\%\,S),$$

where % C is the value of the total carbon content (TC).

CE establishes the relationship between the effect of alloying elements in cast iron and the amount of carbon that would provide a similar heat treatment effect. As follows from the equilibrium iron–iron carbide transformation diagram (Figure 2.5), the eutectic composition of unalloyed cast iron is approximately 4.3% C. Therefore, if a calculated carbon equivalent is about 4.3% C, then the composition of that cast iron can be roughly considered as eutectic. Somewhat similar to the classification of plain carbon steels, cast irons with CE $<$ 4.3% would be classified as hypoeutectic. If CE $>$ 4.3%, those cast irons would be considered as hypereutectic.

Many properties of cast irons can be related to CE. Table 2.7 shows the effect of a carbon equivalent on surface hardness of induction hardened gray irons [14, 19].

Generally speaking, there are seven basic forms of the appearance of graphite in cast irons. A description of these forms can be found in [17, 19, 219].

It is quite easy to distinguish gray iron from ductile iron. Gray iron is named after the appearance of the fracture surface of its broken piece, and it consists of carbon as graphite particles in flake form (Figure 2.29). Since graphite flakes serve as stress risers, most fractures occur along these flakes, which appear to be gray in color. Tensile strength is often used in order to classify gray irons.

The properties of gray iron greatly depend upon the type of matrix (ferritic, ferritic–perlitic, or perlitic), as well as on the amount, size, shape, and distribution of the graphite flakes. A perlitic matrix provides better response to heat treating by induction. A ferritic matrix is considered unsuitable for induction hardening. The shape, size, and distribution of the graphite flakes depend upon the specifics of the manufacturing practice (primarily alloy composition and the cooling rate during the casting operation) of the gray iron castings. The length of the graphite flakes is typically within the range of 0.06 to 1 mm.

ASTM specification (A247) establishes several types of graphite flakes designated by capital letters "A" through "E." Table 2.8 consists of a short description of the different types of graphite flakes. Fine graphite flakes uniformly distributed and randomly oriented (type "A") are the most preferable type of flakes for the majority of induction gray iron hardening applications.

Table 2.6 Typical Chemical Composition of Unalloyed Cast Irons

Cast Iron Type	Chemical Composition (%)										
	TC[a]	Mn	Si	Cr	Ni	Mo	Cu	P	S	Ce	Mg
Gray	3.25–3.50	0.50–0.90	1.80–2.30	0.05–0.45	0.05–0.20	0.05–0.10	0.15–0.40	≤ 0.12	≤ 0.15	—	—
Malleable	2.4–2.55	0.35–0.55	1.40–1.50	0.04–0.07	0.05–0.30	0.03–0.10	0.03–0.40	≤ 0.03	0.05–0.07	—	—
Ductile	3.60–3.80	0.15–1.00	1.80–2.80	0.03–0.07	0.05–0.20	0.01–0.10	0.15–1.00	≤ 0.03	≤ 0.002	0.0–0.20	0.03–0.06

[a]TC is a total carbon representing a sum of combined carbon (including carbon in solution and the free carbon [17].)
Source: Ref. 17.

Table 2.7 Effect of Carbon Equivalent on Surface Hardness of Induction Hardened Gray Irons

Composition (%)[a]			Hardness HRC, Converted from Rockwell		
C	Si	Carbon Equivalent[b]	As read	30 N	Microhardness
3.13	1.50	3.63	50	50	61
3.14	1.68	3.70	49	50	57
3.19	1.64	3.74	48	50	61
3.34	1.59	3.87	47	49	58
3.42	1.80	4.02	46	47	61
3.46	2.00	4.13	43	45	59
3.52	2.14	4.23	36	38	61

[a]Each iron also contained 0.5 to 0.9 Mn, 0.35 to 0.55 Ni, 0.08 to 0.15 Cr, and 0.15n to 0.30 Mo.
[b]Carbon equivalent has been calculated using expression CE = % C + 1.3% Si.
Source: Ref. 19.

In order to illustrate the effect of those flakes on some of the properties of gray iron castings, one may imagine that instead of being manufactured from solid metal, a workpiece were made from porous material with a disrupted matrix consisting of numerous sharp-cornered internal microcracks or notches. The larger the size of those microcracks and the bigger the ratio of the volume of microcracks to the volume of their solid matrix, the less the tensile strength of the workpiece will be. Using this analogy, it is possible to make an obvious conclusion that brittle graphite flakes weaken the matrix. The existence of those flakes with a combination of high carbon content makes the gray iron castings brittle and hard, with poor tensile strength and poor ability to withstand noticeable shock or impact loads. Gray irons have practically no ability to elongate resulting in poor ductility.

As indicated in [14, 17, 19, 224–226], cast irons with a low value of CE have better response to induction hardening. The achievable surface hardness after induction hardening of gray irons, as well as any other cast irons, is reduced with the increasing amount of graphite.

Being brittle, gray iron may introduce certain challenges to induction heat treat practitioners, due to the tendency toward cracking upon fast heating as well as during intense cooling. Preheating and soft quenching are often used for reduction of the thermal stresses and thermal shocks. At the same time, there are cases when gray irons have been successfully hardened using short heat time (less than 3 sec) and water quenched.

The size, shape, dispersion, and amount of the graphite flakes affect not only the mechanical properties, but electromagnetic and thermal properties of the gray iron castings as well. For example, gray iron with large graphite flakes is known for having higher thermal conductivity, lower electrical resistivity, and better damping capacity. It has been reported in [17] that a combination of high carbon content, excessive amount of silicon, high CE values, and slow cooling during manufacturing of iron castings tends to produce larger graphite flakes in larger quantities.

Regardless of the above-mentioned shortcomings, gray irons being relatively inexpensive ferrous materials with a remarkable machinability at the hardness levels

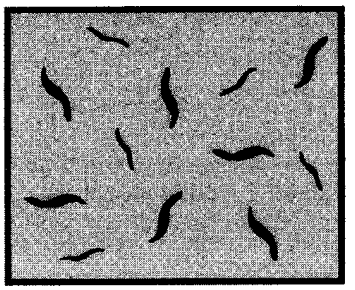

Gray iron
Un-etched appearance of the graphite flakes in pearlite matrix

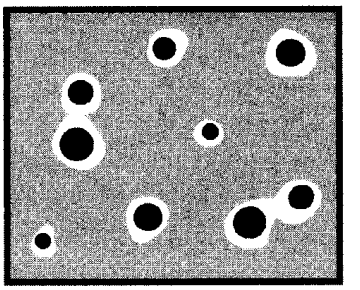

Ductile (nodule) iron
Etched appearance of the graphite nodules surrounded by ferrites in pearlite matrix

Metallographical appearence of gray iron

Figure 2.29 Appearance of gray iron and ductile iron.

that produce excellent wear resistance and resistance to galling and seizing are an attractive choice for a variety of applications. Their remarkable fluidity allows one to produce complex geometry including thin sections. The ability of gray irons to absorb energy caused by vibration (damping capacity) and outstanding compressive stresses are additional features that encourage the use of gray irons. An existence of graphite flakes helps prevent galling problems.

In contrast to gray irons, ductile (nodular) irons have carbon particles in the form of graphite nodules (Figures 2.29 and 2.37) instead of graphite flakes. Those nodules serve as "crack-arresters" providing ductile irons with important advantages over cast irons. Some of the advantages include but are not limited to ductility, relatively high tensile and bending strength, and moderate elongation.

As mentioned earlier, ductile (nodular) iron itself represents a large group of materials offering a wide variety of properties. The group of ductile irons can be

Table 2.8 Types of Graphite Flakes in Gray Iron

Type "A"	Type "B"	Type "C"	Type "D"	Type "E"
Flakes are uniformly distributed and randomly oriented	Flakes are randomly grouped into rosettes	Randomly oriented coarse and moderate flakes (kish graphite)	Interdentritic segregation of randomly oriented graphite flakes	Interdendritic segregation, preferred orientation

Source: Refs. 17, 218, and 223.

divided into five subgroups: ferritic, perlitic–ferritic, perlitic, martensitic, and austempered ductile irons. A detailed discussion regarding the properties of different types of ductile irons can be found in [14, 17, 19, 21, 98–105, 215–220, 224–226]. Induction hardening is usually applied to martensitic, perlitic, or to lesser extent, perlitic–ferritic ductile irons. It is possible to change one form of ductile iron to another by utilizing an appropriate heat treating procedure. At the same time, the shape of the graphite cannot be changed once it has been formed.

Being inherently strong, ductile iron can handle much greater stresses upon heating and quenching without cracking than gray iron. However, it is important to remember that although graphite nodules serve as "crack-arresters" their existence does not guarantee that ductile iron castings will not crack during intensive heating and/or severe quenching. Caution and common sense should be applied when choosing process parameters for induction surface hardening of ductile irons, particularly if cast irons consist of high phosphorous content.

Under normal circumstances, due to the appreciable amount of silicon, commercial cast irons cannot be considered to be binary alloys but at least as ternary Fe–C–Si alloys. The fact that cast irons typically consist of 0.6 to 3% silicon (Si) results in a shift of phase transformation curves compared to the ones shown in Figure 2.5. Figure 2.30 illustrates this phenomenon [17]. There is a noticeable difference between the two diagrams particularly with respect to the maximum solubility of carbon in austenite, as well as the occurrence of eutectic and eutectoid reactions.

In contrast to the iron–iron carbide diagram, both the eutectoid and eutectic reactions on the Fe–C–Si diagram occur at higher temperatures and over a range of temperatures that increases with an increase of both the carbon and silicon content. All of these features should be taken into consideration when choosing the proper parameters for heat treatment.

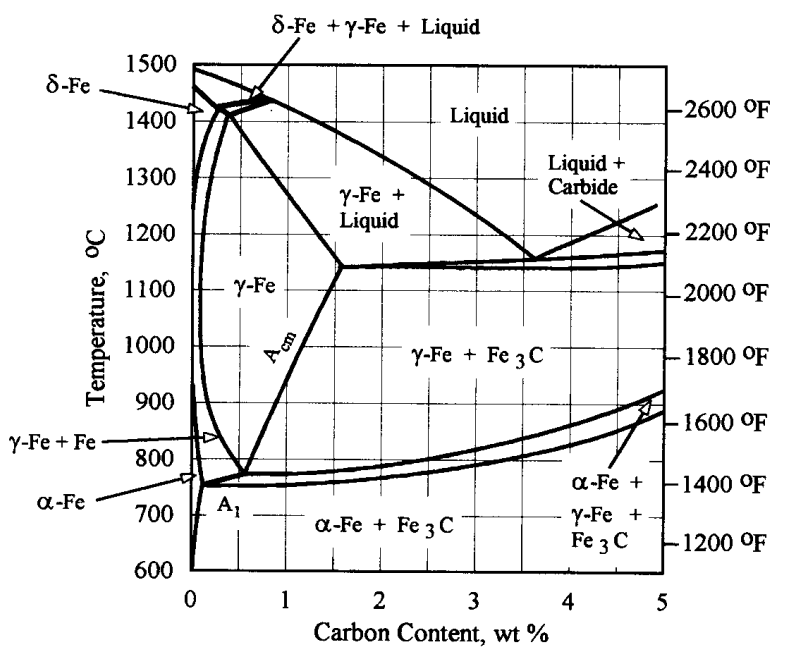

Figure 2.30 Fe–C–Si equilibrium phase transformation diagram at 2% silicon. (From Ref. 17.)

As mentioned above, besides carbon and silicon all commercial cast irons have to some extent an appreciable amount of other alloying elements that provide cast iron with specific properties. In addition to a limited amount of purposely added alloying elements, commercial cast irons may consist of an insignificant amount of residual impurities occurring from the raw materials and specifics of the casting operation. Table 2.9 lists information regarding the structural effects of the alloying elements in cast irons [219]. A thorough description of the effects of different alloying elements on the heat treating of cast irons can be found in [14, 17, 19, 21, 99–105, 175, 215–220].

Some heat treaters with extensive experience in induction hardening of cast irons might notice a phenomenon when seemingly identical cast iron parts having the same chemical composition, geometry, grain size, and microstructure, produced at the same foundry (even from the same lot or batch) respond differently to surface hardening. Some of them may be processed very easily whereas others may have a substantial amount of cracks with the same heating and quenching conditions. One of the reasons for such a "strange" response of cast irons deals with a phenomenon called age strengthening. W. Nicola and V. Rachards [224] have conducted a first systematic experimental study of this phenomenon.

It has been statistically shown that aging at room temperature for about 60 days can strengthen gray cast irons up to 12%. Approximately 87% of the cast irons evaluated have revealed the effect of age strengthening. The Brinell hardness did not change with aging time, resulting in an increased ratio of tensile strength to hardness.

Table 2.9 Structural Effects of Some Alloying Elements in Industrial Cast Irons

Element	Effect During Solidification	Effect During Eutectoid Reaction
Aluminum	Strong graphitizer	Promote ferrite and graphite formation
Antimony	Little effect in amounts used	Strong perlite stabilizer
Bismuth	Carbide promoter, but not carbide former	Very mild perlite stabilizer
Boron $<0.15\%$	Strong graphitizer	Promotes graphite formation
$>0.15\%$	Carbide stabilizer	Strong perlite retainer
Chromium	Strong carbide former. Forms very stable complex carbides	Strong perlite former
Copper	Mild graphitizer	Promotes perlite formation
Manganese	Mild carbide former	Strong perlite former
Nickel	Graphitizer	Mild perlite promoter
Silicon	Strong graphitizer	Promotes ferrite and graphite formation
Tellurium	Very strong carbide promoter, but not stabilizer	Very mild perlite stabilizer
Tin	Little effect with amount normally used	Strong perlite retainer
Titanium ($< 0.25\%$)	Graphitizer	Promotes graphite formation
Vanadium	Strong carbide former	Strong perlite former

Source: Ref. 219.

The age strengthening phenomenon occurs in both cupola and induction furnace melted irons. Interstitial (free) nitrogen appears to be a controlling factor in determining whether aging will take place [224]. Therefore, age strengthened castings would more easily withstand thermal gradients occurring during heating and quenching without cracking. The age strengthening phenomenon may explain the known practice in the past when heat treaters would store some cast irons and in particular gray iron parts for several months and then heat treat them.

2.1.2 Hardening

One of the most common applications of induction heat treatment is the hardening of steels and cast irons. Figure 2.31 shows a variety of parts that can undergo hardening and tempering by induction.

As mentioned above, a typical heat treatment procedure for hardening of steels and cast irons involves heating the alloy up to the austenizing temperature, holding it at a temperature for a period long enough for completion of the formation of austenite, then rapidly cooling the metal until it is below the M_s temperature. Rapid cooling allows replacement of the diffusion-dependent transformation process by a shear-type transformation of steel or cast iron into the much harder constituent called martensite.

Hardening of steel or cast iron parts may be done for purposes of obtaining certain properties such as strength, wear resistance, and so on, and may be done either on the surface of the workpiece or throughout the entire cross-section. Each of these techniques has been briefly discussed earlier and will be discussed further under Surface Hardening (Section 2.1.2.1) and Through Hardening (Section 2.1.2.2) as well as in Chapter 5.

Depending upon the heat treat requirements and part geometry, induction hardening equipment can be designed as a relatively simple apparatus or can involve sophisticated machinery. As an example, Figure 2.32 shows a typical unitized induction machine for hardening and tempering shafts. The system consists of a single shot hardening and tempering inductor, part shuttle mechanism, part unload device, electrical controls, quality monitoring, water recirculation system, and a 300 kW/10 kHz power supply.

2.1.2.1 Surface Hardening

The goal in surface hardening is to provide a martensitic layer on specific areas of the workpiece to increase the hardness and wear resistance while allowing the remainder of the part to be unaffected by the process [17–21]. Because of the physics of the induction phenomena the heating can be localized to areas where the metallurgical changes are desired. Surface hardening is a complex combination of electromagnetic, heat transfer, and metallurgical phenomena that occur when a workpiece surface is heated to a temperature above that which is required for a phase transformation to austenite and then rapidly quenched. For example, Figure 2.33 shows heating and quenching stages during induction hardening of shafts using a vertical scanning mode.

The first step in designing an induction surface hardening machine is to specify the required surface hardness and hardness profile including the case depth and transition zone. The hardness distribution along the workpiece radius or thickness depends upon the following factors: the temperature distribution, the microstructure

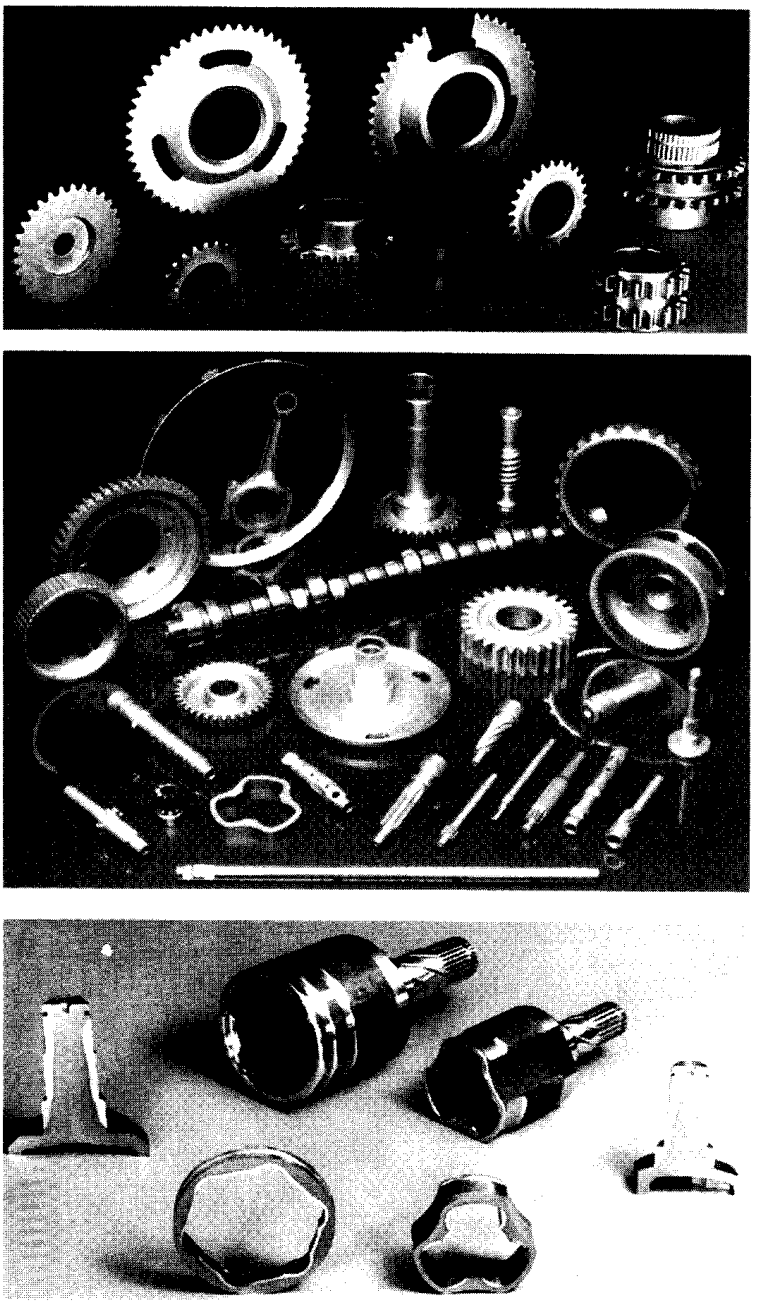

Figure 2.31 Variety of parts that can be induction hardened. (Courtesy of INDUCTOHEAT, Inc., Madison Heights, MI.)

of the metal, its chemical composition, quenching conditions, grain size, and the hardenability of the steel. Temperature distribution in induction surface hardening is controlled by selection of frequency, power density, and workpiece/coil geometry and is discussed in Section 5.

In induction surface hardening applications, the value of case depth (hardness depth) is typically defined as the surface area where the microstructure is at least

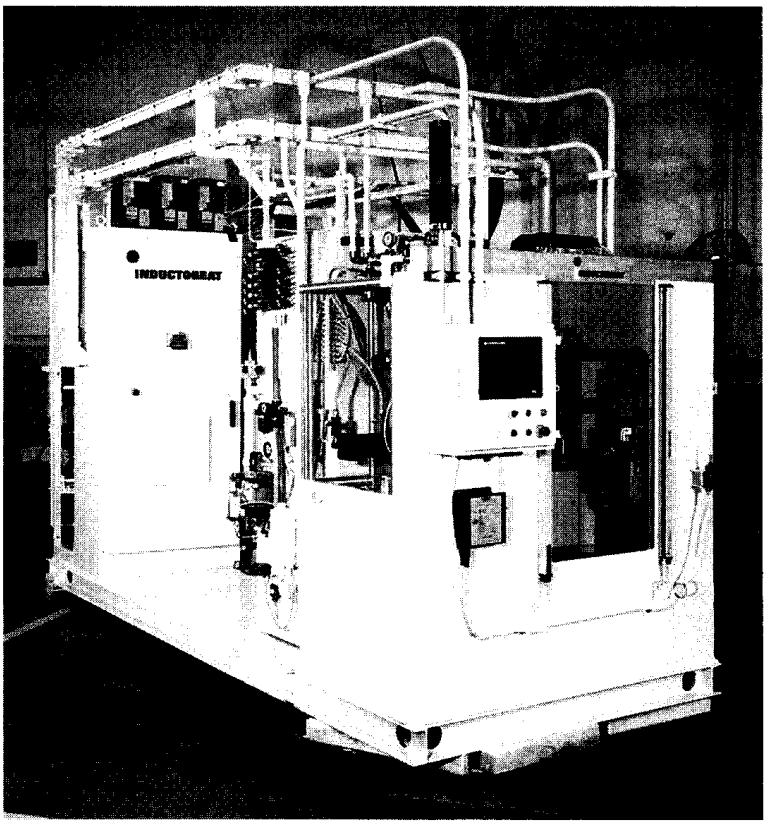

Figure 2.32 Modern unitized induction machine for hardening and tempering shafts. The system consists of a single shot hardening and tempering inductor, part shuttle mechanisms, part unload device, electrical controls, quality monitoring, water recirculating system, and a 300 kW, 10 kHz power supply.

50% martensite. Below the case depth the hardness begins to decrease drastically. This depth is measured in a cut section of the hardened workpiece using a hardness tester to determine the hardness at various distances from the surface. The distance below the part surface where the hardness drops to 10 HRC lower than the surface hardness is often called the effective case depth.

Different applications and part geometry require certain surface hardness and hardness profiles on the workpiece. As an example, Figure 2.34 shows a constant-velocity automotive front wheel drive component that has been cut and etched to show the pattern obtained by induction heat treating [93]. This component requires two areas of hardness with different strength, load, and wear requirements. The "stem" needs torsion strength as well as a hard outer surface, whereas the soft core must be ductile and therefore able to handle the mechanical shock from frequent pulsing. The inner surface of the "bell" needs hardness for wear purposes, as ball bearings ride in the track or raceways. The threads of this component hold the wheel on. For heavy-duty applications the thread is also hardened and then tempered back to produce a very tough thread. The tempering of these parts is nearly always done with induction, using a separate inductor.

Bearings, rocker arms, pump shafts, and skid plates are examples of parts that require a shallow-hardened case primarily for the purpose of wear resistance. Case

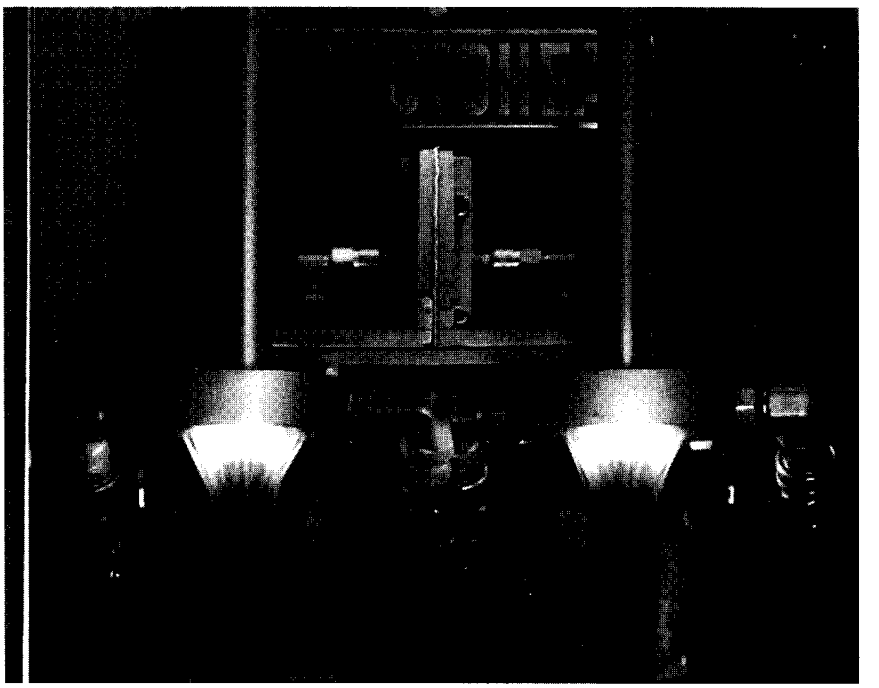

Figure 2.33 Dual shaft induction scanner.

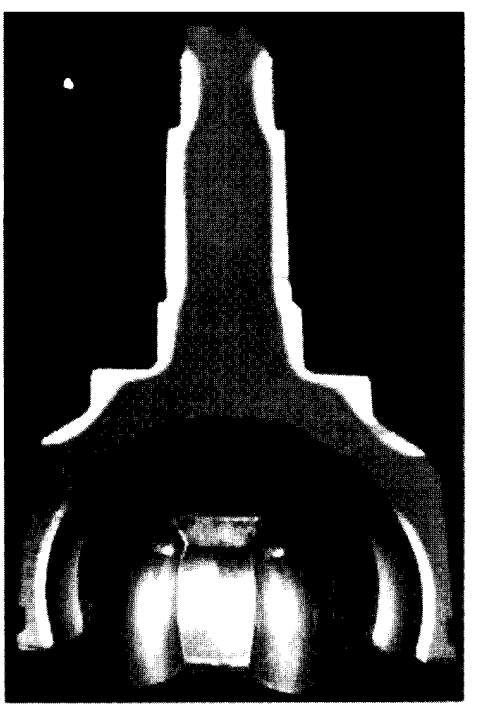

Figure 2.34 Induction hardened constant-velocity front wheel drive component (Courtesy of INDUCTOHEAT, Inc., Madison Heights, MI.)

depths of these parts that will enable them to handle light loads are usually in the range of 0.25 to 1 mm (0.010–0.040 in.).

Generally speaking, heating for shallow case depths requires high frequency, low energy, and high power density. In some cases of surface hardening of massive parts with a shallow case depth (typically less than 1.5 mm) it is possible to use self-quenching techniques (also called mass quenching). In cases like this, because the heated surface layer is very fine and its mass is negligibly small compared to the mass of the cold core, it is possible to have rapid surface cooling due to heat being conducted toward the cold core. The rate of cooling might be severe enough to form a martensitic structure. The mass of the cold core acts as a large heat sink. Therefore, self-quenching can make the use of fluid quenchants unnecessary except as a cool down to allow handling of parts.

Parts that require both wear resistance and moderate loading such as gears, camshafts, and crankshafts are usually induction hardened to case depths of 1.5 to 2.5 mm (0.060–0.1 in.). Because the load stresses drop exponentially from the surface, these deeper case depths strengthen the part dramatically compared to shallow-hardened cases. The induction heating frequency that is required to obtain case depths of 1.5 to 2.5 mm (0.06–0.1 in.) is usually in the range of 100 to 10 kHz, respectively.

Parts that must withstand a heavy load require greater case depths; these include axle shafts, wheel spindles, and large heavy-duty gears. The cross-sectional areas of the part and the magnitude of the load they must handle determine the appropriate case depth. These heavy workpiece applications usually require a depth in the range from 3.5 mm to as much as 12 mm (0.125–0.47 in.). Here a higher energy at frequencies of 10 to 500 Hz and in some cases even the line frequency is necessary.

In many of these applications the induction heating pattern can encompass a significant part of the cross-sectional area. As a result, an appreciable distortion may appear. Where noticeable distortion is present, it may be necessary to provide additional stock and case depth to allow for final grinding after hardening.

Induction surface hardening is typically characterized by high-dimensional accuracy of the heat treated parts. The ability to keep part distortion as low as possible after the heat treatment process is due to the fact that induction heating is a very fast process and concentrates the heat sources in a surface layer called the current penetration depth that greatly affects a hardened case depth. An analysis of this feature is provided in Sections 3.1.2 and 5.1.2.

As mentioned earlier, steel surface hardening is accomplished by raising the required depth of material above the transformation temperature (A_3 or A_{cm} critical temperatures of iron–iron carbide phase transformation diagram shown in Figure 2.6) to the point where it is transformed to austenite and then cooling the workpiece rapidly to produce martensite. This rapid quenching that appears in induction hardening is covered in detail in Chapter 5.

The heating time to complete a surface hardening process often ranges from 1 to 10 sec per component.

Steel selection depends upon specifics of the working conditions, required surface hardness, hardness profile, and cost. Plain carbon steels and low-alloy steels are the least expensive steels being successfully used for a variety of surface hardening applications. The general classification of plain carbon steels is discussed in Section 2.1.1. It is important to remember that the carbon content of steel plays an extremely

important role in the determination of the maximum achievable surface hardness (Figures 2.12 and 2.14), as well as affecting the amount of retained austenite (Figure 2.13), steel hardenability (Figure 2.21), hardness case depth, and transition zone. Figure 2.35 shows the effect of the carbon content of steel on hardness and the length of the transition zone when surface hardening eutectoid steel (solid line) and hypoeutectoid steel (dotted line). The temperature distribution and quenching conditions are the same in both cases.

A wide application range of high carbon steels in industry is limited by their extremely low ductility, poor machinability, and higher cost compared to medium carbon steels. In addition, there is a variety of applications including valve-spring wire, drill bits, and other cutting tools, where high-carbon steels (such as AISI 1060 to 1080) provide a noticeable advantage over medium- and low-carbon steels. It is wise to remember that high-carbon steels have a tendency toward cracking during heating as well as quenching. Therefore, care should be taken to avoid crack development when heat treating these steels.

Medium-carbon steels are the most common steels used in industry, including the automotive industry. These steels are applied, for example, to a variety of transmission components (e.g., input shafts, output shafts, gears, clutches), suspension, and steering (e.g., front wheel drive components-CV joints, steering racks, ball studs, and sockets), engine components (e.g., crankshaft, camshafts, connecting rods, rocker arms, etc.) as well as for fasteners (bolts, screws, and studs).

Low-carbon steels are used where toughness rather than high hardness is required such as in clutch plates or pins for farm equipment. These steels may be AISI 1020-1035.

When discussing induction hardening it is imperative to mention the importance of having "favorable" metal conditions prior to induction hardening. As

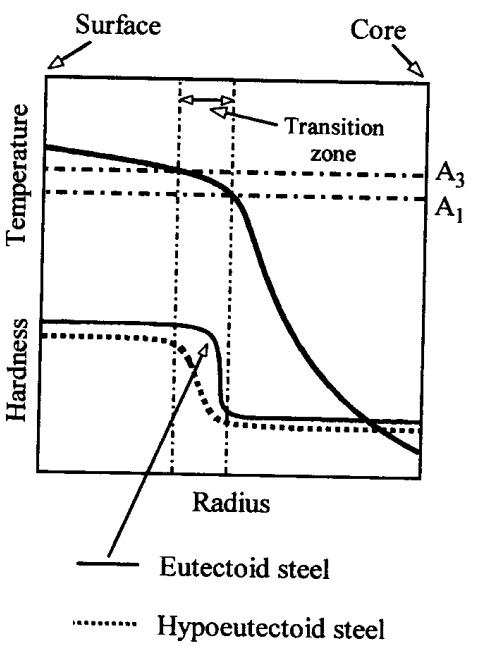

Figure 2.35 Temperature distribution and hardness profile along the radius. (From Ref. 217.)

shown in Section 2.1.1, "favorable" initial microstructure, including a homogeneous fine-grain quenched and tempered martensitic structure with hardness of 30 to 34 HRC, leads to fast and consistent metal response to heat treating with the smallest shape/size distortion and a minimum amount of grain growth. This type of initial microstructure results in higher hardness and deeper hardened case depth compared to the perlitic and, particularly, ferritic initial microstructure (see Figure 2.28).

In contrast to quenched and tempered prior microstructure, steels with large carbides (i.e., spherodized microstructures) have poor response to induction hardening and result in the necessity of having prolonged heating and require higher temperatures for austenization. The existence of large carbides may also lead to hardness data scatter.

Longer heat time results in grain growth, the appearance of coarse martensite, an extended transition zone, and shape distortion. Coarse martensite has a negative effect on toughness and creates favorable conditions for intergranule crack development during service.

As opposed to other heat treating techniques, heat treatment by induction is appreciably affected by variations in metal chemical composition. Therefore, "favorable" initial metal condition also includes tight control of the specified chemical composition of steels and irons. As in Section 2.1.1.4, wide compositional limits cause surface hardness and harden pattern variation. Conversely, tight control of the composition eliminates possible variation of the heat treat pattern resulting from multiple steel/iron sources. Therefore, H-steels are preferable steels due to their tendency to have more repeatable patterns and case depths.

Alloy steels are often induction hardened. As mentioned in Section 2.1.1.4, although plain carbon steels, being the least expensive steels, are widely used in industry, there are many engineering applications where the properties of plain carbon steels and low-alloy steels are not adequately suitable for meeting a particular engineering requirement or combination of requirements. Such requirements may include the necessity to increase the depth of hardness (hardenability), to reduce the tendency of the steel toward the grain growth, to improve its corrosion resistance, abrasion resistance, or resistance to chemical attack, increase impact strength, reduce oxidation and susceptibility of heat treated parts to cracking, and shape distortion. Often it is required to achieve not just a certain property of the steel part but a combination of properties that are often contradictory, for example, obtaining a combination of strength, toughness, and ductility, as well as improving mechanical properties of the steel at elevated or low temperatures.

The specifics of alloying elements on process parameters are discussed in Section 2.1.1.4.

Design factors that include complexity of the part's geometry, existence of holes, sharp corners, and so on noticeably affect the success of an induction surface hardening operation. The surface condition of the workpiece is another factor that can have a pronounced effect on heat treating practice and workpiece life during service. Voids, microcracks, notches, and other surface and subsurface discontinuities as well as other stress concentrators (including sharp corners, grooves, etc.) can initiate crack development during induction hardening when the metal goes through the "expansion–contraction" cycle; thermal gradients and stresses can reach critical values and "open" notches and microcracks. Conversely, a homogeneous metal structure with a smooth surface free of voids, microcracks, and notches improves

the heat treating conditions, and positively affects important part characteristics such as bending fatigue strength, endurance limit, and durability.

Alternating electrical currents of medium and particularly high frequency have a tendency to overheat sharp corners. Therefore, if possible, sharp corners should be generously rounded and chamfered for optimum results in the heating process as well as during quenching because the corners also have a tendency to have more severe cooling compared to the rest of the workpiece.

Complex-shaped parts can present some challenges in obtaining the required hardness pattern, because during heating the "thick" sections of the part may not come up to the required temperature as quickly as "thin" sections. Thus coil profiling and the use of special process settings can help to overcome this problem. Thickness variations of complex geometry workpieces may create some difficulties during quenching as well, since the thinner sections may cool down noticeably differently compared to massive areas and special adjustments in inductor design and quench blocks should be made. Figure 2.36 shows an induction machine for hardening the working surface of wrench jaws as well as etched surfaces that reveal

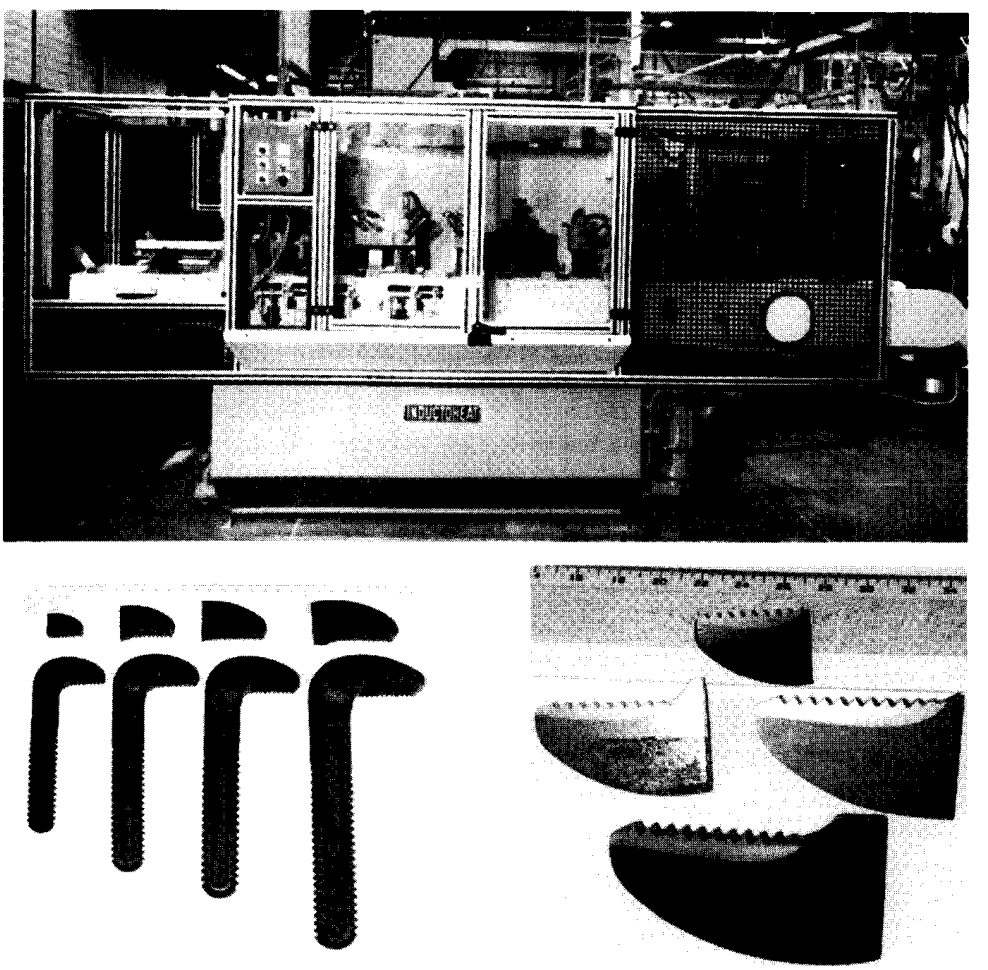

Figure 2.36 Induction machine for hardening and tempering the working surface of wrench jaws. (Courtesy of INDUCTOHEAT, Inc.)

hardness patterns of parts having appreciable differences in masses of metal near the hardened surface area.

Proper process parameters are obviously very important in order to ensure the required case hardening conditions and hardness pattern. Such important subjects as frequency selection, a choice of power density, heat time, specifics of spray quenching, particularities of the inductor design, and the optimal choice of the time settings and other process parameters is discussed in Chapter 5.

When discussing induction surface hardening of steel, it is necessary to mention the phenomenon that is usually called superhardening, which is not clearly understood. Due to this phenomenon, for a given carbon steel the surface hardness of the part that has been case hardened by induction is typically 3 to 4 HRC and in some cases even higher than for a through heated furnace hardened steels. Superhardening can be attributed to the fast heating cycle and severe quenching resulting in the ability to obtain steels with finer grain size. This occurs because in induction hardening the steel is at the austenizing temperature for a short time, which results in finer grain sizes [6, 12]. Another factor that might contribute to superhardening is the higher lattice strain from residual compressive stresses at the surface of the part when its internal regions and the core remain underheated or cold [12]. This phenomenon is particularly noticeable in steels with a carbon content of 0.35 to 0.6%. Formation of residual stresses during surface hardening is discussed in Section 5.3.

Up to this point we primarily discussed the subject of surface hardening based on the features of the surface hardening of steels. At the same time, a noticeable number of surface hardening applications (e.g., camshafts, cranckshafts, gears, sprockets, rollers, rocker arms, crane wheels, pinions, etc.) utilize different types of cast irons, including gray irons, ductile (nodular) irons, and (less frequently) malleable irons. Figure 2.37 shows an induction surface hardened crankshaft made from ductile (nodular) cast iron, its hardness pattern and microstructure of the hardened case, transition zone, and "green" core.

Induction surface hardening of cast iron has many similarities with induction hardening of steel; at the same time there are some specific features that should be taken into consideration. As discussed in Section 2.1.1, due to the fact that most commercial cast irons are ternary (Fe–C–Si) alloys compared to plain carbon steels or low-alloy steels, being binary alloys (Fe–C), the critical temperatures of cast irons differ from those of carbon steels.

The existence of 0.6 to 3% silicon in commercial cast iron deforms the equilibrium phase transformation diagram (Figure 2.30) to higher temperatures than those shown in Figure 2.5.

Table 2.10 shows the influence of silicon and three other elements commonly present in cast irons on the critical temperatures [219] upon slow heating.

The temperature range of 860°C (1580°F) to 960°C (1760°F) is typical for induction surface hardening of gray and ductile iron castings. Although the required case depth of inductively hardened iron castings does not normally exceed 4 mm (1/6 in.), the "mass quenching" is not typically used for induction surface hardening of the cast irons. Induction hardened cast irons have a well-defined case depth with a relatively short transition zone.

Similar to surface hardening of steels, the task of providing a successful surface hardening of cast irons will be simplified, if the following conditions are satisfied.

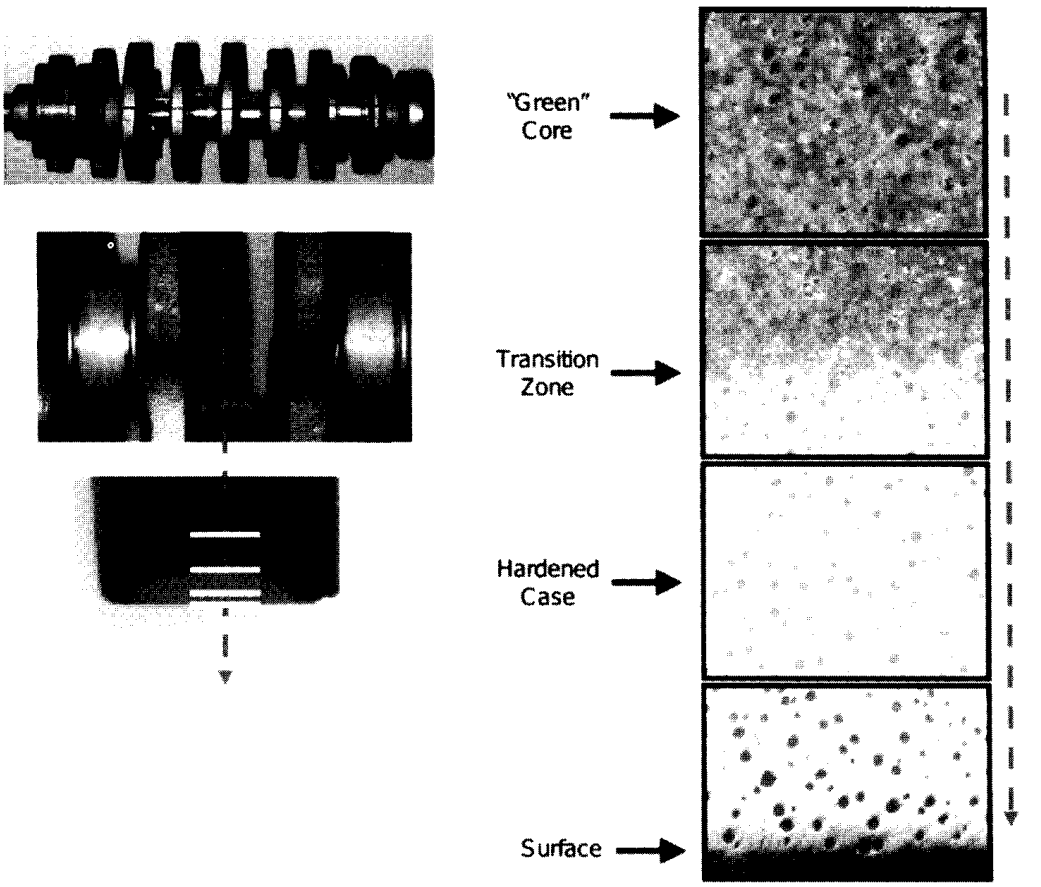

Figure 2.37 An induction surface hardened crankshaft made from ductile (nodular) cast iron, its hardened pattern, and the obtained microstructures of hardened case, transition zone, and "green" core.

a. Proper Chemical Composition. If, for some reason, cast iron does not respond to heat treatment in an expected way, the first step in determining the reason is to make sure that the cast iron has the proper chemical composition. Although carbon and silicon are two of the principal alloying elements of gray, malleable, and ductile irons and have the most significant influence on the hardened microstructure, the heat treater should not limit his or her examination to evaluating the chemical composition of these two elements. All commercial cast irons have, to some extent, an appreciable amount of alloying elements including manganese, chromium, nickel, copper, molybdenum, phosphorous, sulfur, and so on. In addition, besides a limited amount of alloying elements, commercial cast irons may consist of traces of residual impurities occurring from the raw materials. These residual impurities under certain conditions may act as alloying elements and markedly affect the response of the cast iron to induction surface hardening resulting in a variation of the critical temperatures of the phase transformation diagram and shifting the continuous cooling curves. All these factors may lead to a noticeable variation in the microstructure of surface hardened castings. As shown in [227], even a very small amount of such elements as bismuth, lead,

Table 2.10 Influence of Silicon and Three Other Elements Commonly Presented in Cast Irons on the Critical Temperature upon Slow Heating

Element	Silicon	Phosphorus	Manganese	Nickel
Range (%)	0.3–3.5	0–0.2	0–1.0	0–1.0
Upper temp. effect per %	37°C (67°F)	220°C (400°F)	37°C (67°F)	17°C (31°F)
Direction	Increase	Increase	Decrease	Decrease
Lower temp. effect per %	29°C (52°F)	220°C (400°F)	130°C (235°F)	24°C (43°F)
Direction	Increase	Increase	Decrease	Decrease

Source: Ref. 219.

titanium, tin, or nitrogen may have a marked effect on the microstructure of the hardened part. It has been reported that an excessive amount of phosphorous (the normally specified amount is less than 0.12% for gray and 0.04% for ductile irons) can result in increased brittleness of iron castings. In some cases, the same type of the cast iron purchased from two different suppliers can have appreciably different properties. The features of the casting process, including the rate of solidification and amount of residual elements may cause these differences. Therefore it is important that the heat treater have a clear picture regarding the chemical composition of the particular cast iron with which he or she working. Special attention should be paid to elements, which promote graphitization. It is also imperative to remember that some elements have a combined effect (i.e., carbon and silicon, sulfur and manganese, etc.), therefore it is important to control their combined effect. Close control must also be maintained over such properties as CE-value (carbon equivalent) and TC-value (total carbon).

b. Friendly Prior-Microstructure. In order to create a required amount of martensite upon quenching, austenite must contain enough carbon. This is why it is preferable that cast irons have a homogeneous quenched and tempered or fully perlitic microstructure (preferably a structure that consists of fine perlites) prior to induction surface hardening. Ferritic cast irons are not well suited for surface hardening by induction, because, as discussed in Sections 2.1.1 and 2.1.2.1, carbon has a poor solubility in ferrite. Therefore the only way for carbon to enter the austenite is to diffuse from eutectic graphite flakes or nodules. This reaction of carbon diffusion from eutectic graphite into the matrix requires a long time, which eliminates one of the main advantages of induction, the short heat time. Figure 2.38 illustrates this phenomenon [98, 221] showing the achievable hardness of ductile iron with a ferritic matrix as a function of the holding time at a temperature of 871°C (1600°F).

It should be mentioned at this point that a small amount of ferrite adjacent to the graphite nodules will not prevent reaching the required hardness, as the carbon will be able to quickly diffuse into the matrix from carbide flakes or nodules (assuming that the time at the austenizing temperature has been properly chosen).

Inevitably, a certain amount of ferrites will exist within some structure of cast iron. These ferrites should not exceed a maximum amount of about 8 to 9%, otherwise a lower hardness reading and hardness scatter can take place.

Alloy segregation and a microstructure consisting of large clusters cannot be considered a preferable prior-microstructure and should be avoided. Large graphite

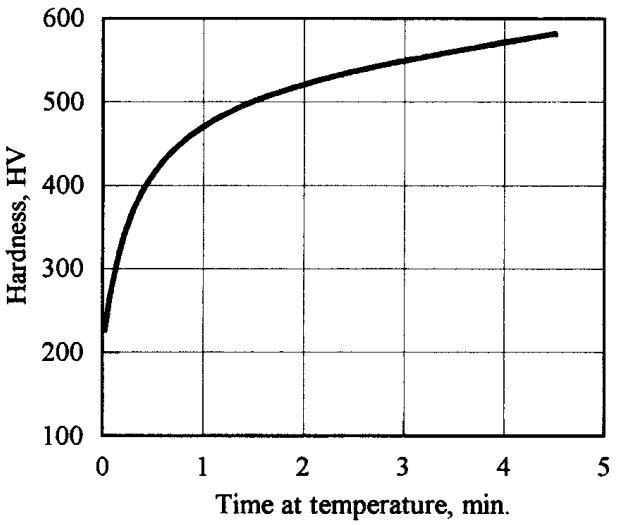

Figure 2.38 Hardness response of ferritic ductile iron held at the austenizing temperature of 871°C (1600°F). (From Refs. 98 and 221.)

flakes or clusters having a preferred orientation of flakes and located near the castings surface serve as stress raisers (Figure 2.39) and make gray iron castings more sensitive to crack development during rapid heating (particularly when frequencies of 30 kHz and higher are used) and during fast cooling (especially water quenching). Upon hardening of gray irons, soft spots may occur in areas in the location of large clusters.

It has been reported that eutectic carbides can encourage cracking in all types of cast irons suitable for surface hardening [102], due to insufficient holding time at the austenizing temperature. This phenomenon leads to the appearance of a complex stress distribution during quenching, due to the fact that the carbides' physical properties (i.e., thermal expansion, density, etc.) are quite different compared to martensite.

Dendritic structures as well as an undercooled graphite structure, which appears as the result of rapid solidification and insufficient inoculation, should

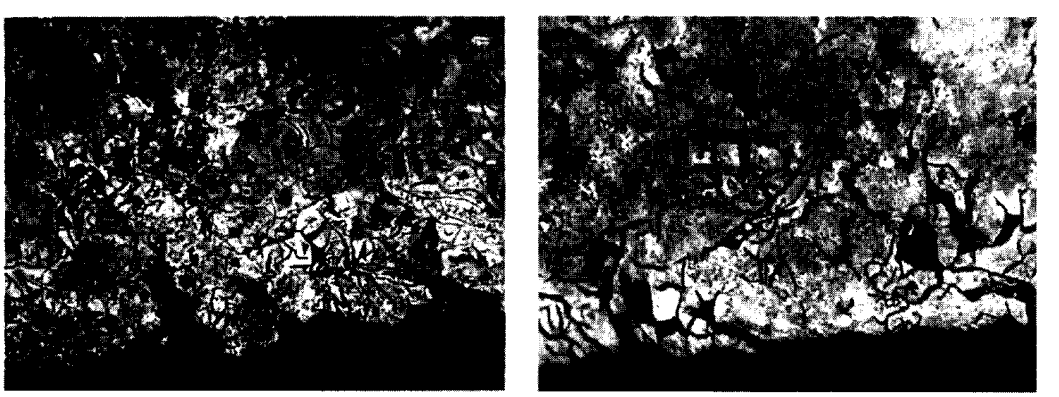

Figure 2.39 Undesirable subsurface microstructure of the gray iron part having stress raiser.

also be avoided since historically they have been a source for crack development and undesirable microstructure of induction hardened areas.

c. Proper Process Parameters. The proper parameters of the heat treating process include an appropriate austenizing temperature and time at this temperature, which are functions of the cast iron grade and particularities of the heating and quenching. The austenizing temperature should be sufficiently high and austenizing time should be sufficiently long to make sure that all diffusion-type processes required for the formation of homogeneous austenite will take place and upon quenching a martensitic structure will be free of the "ghost" perlite as well as free ferrites. Otherwise, an austenization process will not be completed and instead of a martensitic structure there will be a complex "martensitic–perlitic" structure consisting of islands of free ferrites. That structure features low hardness, scattered hardness readings, and a pronounced tendency toward crack development. There are several recommendations to estimate the required austenizing temperature when induction hardening cast irons [14, 17, 100, 101–104, 127, 219]. For a rough estimation of the minimum required austenizing temperature of unalloyed cast irons heated at a moderate heat intensity the following expressions are used at INDUCTOHEAT:

$$\text{Austenizing temperature, } °C = 800 + 28\,(\%\,\text{Si}) - 25\,(\%\,\text{Mn})$$

$$\text{Austenizing temperature, } °F = 1472 + 50\,(\%\,\text{Si}) - 45\,(\%\,\text{Mn}).$$

Similar to hardening of steels, there is a certain range of recommended austenitic temperatures for surface hardening of cast irons. This means that besides a minimum austenitic temperature, there is a maximum recommended temperature that should not be exceeded under any circumstances. Overheating of cast irons above that maximum temperature results in decarburization of the surface and the appearance of an excessive amount of retained austenite within the as-quenched structure resulting in a hardness reduction. As an example, Figure 2.40 shows the

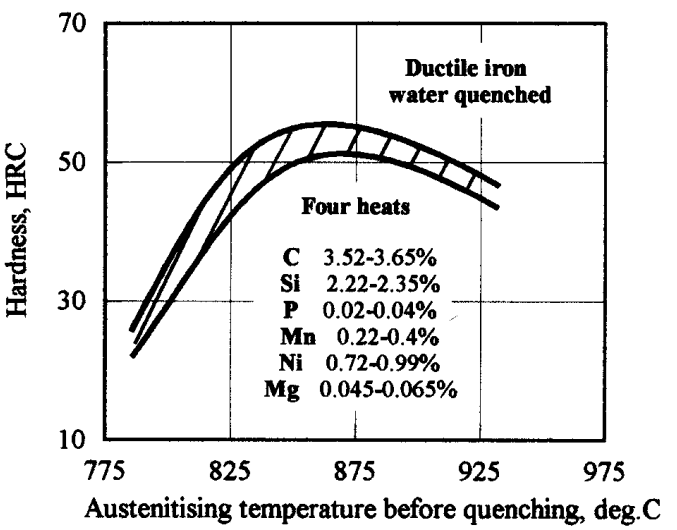

Figure 2.40 Influence of austenizing temperature on hardness of ductile iron. Specimens were slow heated, held in air for 1 hour, and water quenched. (From Ref. 19.)

influence of austenizing temperature on the hardness of water quenched ductile iron [19]. An overheating also leads to grain growth resulting in coarse martensite and in the formation of undesirable structures called white iron. The existences of high surface temperatures causes a large thermal gradient during the heating cycle and, especially, during the quenching cycle, which may initiate crack development.

As can be seen from the equilibrium phase transformation diagrams shown in Figures 2.5 and 2.30, the cast iron eutectic starts to melt at temperatures of about 150 to 250°C lower than the majority of carbon steels used for surface hardening. For example, in the case of moderate heat intensity the cast iron eutectic starts to melt at temperatures of approximately 1130°C (2066°F). Therefore if something goes wrong there is a distinct possibility of surface melting, incipient melting, or grain boundary liquation due to the low melting temperatures. The situation becomes more complicated, as some alloying elements (such as copper or tin, which are often added to gray and ductile irons as perlitic promoters) have low melting temperatures in the first place. As a result of the nonequilibrium nature of induction heating, all critical temperatures of the equilibrium phase transformation diagrams (i.e., diagrams shown in Figures 2.5 and 2.30) are shifted toward the higher temperatures. Therefore, when hardening cast irons at sufficiently high heating rates, in order to ensure the completion of the austenizing transformation, austenizing temperatures may approach a dangerously high level.

All these factors make it necessary to provide precise monitoring and reliable control systems when hardening cast irons. The importance of having a sufficiently reliable temperature control system for hardening of iron castings is even more pronounced than for surface hardening of steels. Moreover, the necessity of having precise monitoring becomes even more critical when surface hardening cast irons with a high silicon content and excessive amount of certain alloying elements, particularly when a scanning mode is used. Section 8.14 provides a detailed discussion on the monitoring principles and control systems used in modern induction surface hardening.

When heating cast irons susceptible to cracking (e.g., gray irons with large graphite flakes) it is sometimes useful to preheat the castings or to conduct a slow heating during the initial stage (from ambient to a temperature of about 600°C/1112°F).

Since cast irons and, in particular, gray irons are by far more susceptible to cracking upon quenching, preheating and "mild" quenching are often used. This allows the reduction of thermal stresses and thermal shocks. Oil at a temperature of 80°C (176°F) to 100°C (212°F) and concentrated polymer quenchants are often used for surface hardening of gray iron castings allowing minimization of the possibility of crack development and distortion. At the same time, there are numerous cases when gray iron castings have been successfully hardened using short heat time (less than 3 sec) and water as a quenchant. The appropriate prior-microstructure and the correct combination of process parameters (including scanning rate, pressure, flow rate, temperature of water, quenching block design, etc.) are required in order to eliminate the occurrence of cracking using water quench.

d. Design Factors and Quality of Castings. All design factors discussed above that influence the success of the surface hardening of steels are applied to induction hardening of cast irons. In addition, certain factors have specific fea-

tures that have an effect on the results of heat treatment. Because of space limitation, only some of these factors are discussed here. Poor quality of castings and defects occurring as a result might lead to inappropriate hardening results. Casting defects can cause problems by themselves or can contribute to an abnormal combination of factors that can cause the problem. For example, the presence of such casting defects as porosity, inclusions, sand and gas defects, blowholes, and dimensional errors within the case hardened area may cause local overheating, stress concentration, cracking, hardness scatter data, burns, and so on.

When iron castings have a complex shape featuring a combination of "thick" and "thin" areas, the regions with different masses have a tendency to heat differently. This promotes the appearance of the thermal gradients and thermal stresses, which in turn create favorable conditions for distortion and crack development, particularly in the areas where there is a change of mass. The situation can be complicated when transitional thermal stresses combine with residual stresses from previous operations (i.e., casting, machining, honing, surface peening, etc.). Long castings with thin complex cross-sections are more likely to have residual stresses compared to massive areas of iron castings. In order to reduce the probability of cracking during the induction hardening operation, stress relieving prior to induction hardening is highly recommended. Since stress relieving is a diffusion-type process, a certain time–temperature correlation is required. Stress relieving sufficiently relieves stresses prior to induction hardening without a significant reduction of the strength of the cast iron. In contrast to steels and some other metals, an induction heating is not always the best choice for stress relieving of cast irons prior to induction hardening; instead, ovens are often more suitable for this operation. The typical practice for stress relieving of iron castings includes heating the part and holding it at temperatures about 550°C (1022°F) for two hours and then slowly cooling down to ambient temperature.

2.1.2.2 Through Hardening

Through hardening may be needed for parts requiring high strength such as snowplow blades, springs, chain links, truck bed frames, certain fasteners (including nails and screws), and the like. In these cases the entire workpiece is raised above the transformation temperature and then quenched. Selection of the correct induction heating frequency is very important to achieve uniform "surface-to-core" temperature in the shortest time with the highest heating efficiency.

Guidelines for frequency selection for induction through hardening are quite different compared to frequency selection for surface hardening. When induction through hardening parts, care must be taken to avoid cancellation of eddy currents induced by the induction coil within the part. A frequency lower than the optimal results in increased current penetration depth and current cancellation may occur resulting in a significant decrease in coil electrical efficiency. The geometry of the workpiece plays a major role in choosing the frequency for through hardening. The factors related to frequency choice and selection of other process parameters are discussed in detail in Chapter 5.

The ability of the part to be through hardened depends upon the hardenability of material, quenching conditions, grain size, and geometry.

It is necessary to mention that during quenching the cooling intensity of the surface hardened workpiece is greater than the intensity of cooling of a through

hardened workpiece. This is because in surface hardening, additional cooling of the surface layers takes place due to the cold core, which plays the role of a heat sink.

In contrast to surface hardening, which typically displays compressive stresses at the workpiece surface, in the majority of through hardening applications the workpiece surface usually experiences tensile stresses after hardening.

2.1.3 Tempering and Stress Relieving

The tempering process takes place after steel is hardened, but is no less important in the metal heat treatment. The transformation to martensite through quenching creates a very hard and brittle structure. Untempered martensite is typically too brittle for commercial use and retains a high level of stress.

A variety of microstructures and mechanical properties of steels and cast irons can be produced by tempering. The main purposes of tempering are to increase the steel's toughness, yield strength, and ductility, to relieve internal stresses, and to eliminate brittleness.

As discussed above, in surface hardening only a thin surface layer of the workpiece is heated. The surface is raised to a relatively high temperature in a short period of time. A significant surface-to-core temperature difference and the steels' transformation phenomena upon quenching result in the buildup of internal residual stresses. Reheating the steel for tempering after hardening and quenching leads to a decrease or relaxation of these internal stresses. In other words, because of tempering it is possible to improve the mechanical properties of the workpiece and to reduce the stresses caused by the previous heat treatment stage without losing too much of the hardness. For a particular application, tempering can provide the optimal combination of hardness, strength, and toughness [6, 11, 18, 19, 21, 149–151].

Tempering temperatures are below the lower transformation temperature (A_1) and usually in the range of 120°C (248°F) to 600°C (1112°F). There are different stages of tempering [21, 181]. Depending upon the tempering stage, different amounts of iron carbides (Fe_3C) are formed affecting the properties of "as-hardened and tempered" structure. Low-temperature tempering of carbon steels occurs typically at 120°C (248°F) to 300°C (572°F). The main purposes of low-temperature tempering are stress relieving and generation of tempered martensite. The hardness reduction in this case typically does not exceed 1 to 3 points HRC.

If the carbon steel or cast iron is heated to less than 100°C (212°F), there is no change in microstructure, and no induction tempering will occur.

If carbon steel is tempered at above 600°C (1112°F), practically all of the residual stresses existing in the part will be removed and changes in microstructure may lead to a significant loss in hardness. The hardness reduction may exceed 15 points HRC. Note that tempering an alloyed steel above 600°C (1112°F) may not result in a significant hardness loss. Properties of tempered steels are greatly affected by not only temperature and time at tempering temperature but by the part's as-quenched microstructure as well (for example, by the amount of retained austenite).

During tempering of some alloy steels (i.e., tool steels) an effect known as secondary hardening may occur. According to this phenomenon, the hardness of a quenched part initially decreases with a rise of temperature. However, at a certain point the hardness starts to increase. After reaching its maximum value, the hardness will start to decrease again with a temperature increase.

Basically there are two ways to temper parts after induction hardening: self-tempering (also called slack quenching), where residual heat in the part is exploited, and induction tempering, where the hardened part is reheated. Section 5.5 discusses both techniques in detail as well as the time–temperature correlation of induction tempering compared to furnace tempering.

2.1.4 Normalizing

Normalizing can be done by heating the steel to a temperature of about 100°C above the upper transformation temperature and then allowing it to air cool to room temperature. Normalizing usually takes a very long time (much longer than tempering), and can take as long as several hours. Normalizing is done to refine the ferritic and austenitic grain sizes obtaining the relatively fine ferritic–perlitic metal structure to a state in which the next operation can take place. Parts are often normalized before hardening. Some parts are spheroidized to make them easier to form.

2.1.5 Annealing

Annealing is a broad term that is used by heat treat practitioners to describe a variety of processes and properties related to microstructure, machinability, formability, internal stresses, and the like. In some cases, heat treaters have misused the term "annealing" by using it in applications where the more proper terms (i.e., tempering or stress relieving) should be applied. There are two basic types of annealing:

- full annealing
- process annealing

The purpose of full annealing is much like that of normalizing in that the hardness is decreased, the ductility is increased, and the material's homogenization and machinability are improved [12, 19, 21].

Being cooled very slowly, a fully annealed workpiece is essentially free of stresses. In addition, the soak time during cooling is longer and the cooling rate is slower than in normalizing. Typically, full annealing is done in a gas-fired or electric furnace. Very seldom is induction used for full annealing.

As has been shown in [21] full annealing temperatures depend upon the carbon content of the steel. Full annealing temperatures of hypoeutectoid steels are just above the A_3 critical temperature. Fully annealing temperatures of hypereutectoid steels are just above the A_1 critical line.

A process often associated with a full annealing is homogenization, the major purpose of which is obtaining a homogeneous structure by eliminating alloy segregation. It is usually performed at higher temperatures than full annealing to create favorable conditions for diffusion processes required for homogenization. Homogenization usually occupies the temperature range of 1000 to 1150°C.

In applications that do not require achieving fully annealed parts, process annealing might be the preferable choice compared to full annealing. Process annealing represents an intermittent stage between a fully annealed condition and a cold worked condition (i.e., rolled or drawn). The main purpose of process annealing is to improve ductility of such cold worked workpieces as strips, plates, wires, rods, tubes, and so on). According to process annealing a workpiece is typically heated to tem-

peratures of 20 to 120°C below the low critical temperature A_1, held for some time at temperature, and then air cooled.

It should be mentioned that such processes as full annealing and homogenization require long holding times (e.g., many hours). The cost effectiveness of heating using induction for full annealing and homogenization is drastically reduced. Other heat sources including gas furnaces and resistive furnaces would then be the better choice. However, induction heating is often preferable for process annealing.

2.1.6 Spheroidizing

When steel is heated to higher temperatures (in the range of the transformation temperatures) and then cooled, iron carbide particles can form in the mixture. These particles are very hard. Spheroidizing is a softening process for steel that involves heating the steel to a temperature just below the lower transformation temperature (in some cases slightly above it) and holding it for a sufficient time period for the iron carbide particles to assume the shape of a spheroid. This leaves the metal in the ductile and softest possible state for later forming processes. As in the case of full annealing and homogenization, heating by induction is typically not the most cost-effective process for spheroidizing.

When a spheroidal structure is heated by induction, the required heat time is typically longer than for other microstructures and the required temperature is higher. The longer time at higher temperature is required to austenize the carbides to obtain a uniform structure throughout the mixture. Therefore, spheroidized structures are not considered friendly structures for induction hardening applications.

2.1.7 Sintering

Sintering is the bonding of the molecular structure in powdered metal. This bonding is done by heating the metal to a high temperature, below its melting point, to produce recrystallization. High temperature sintering produces a more consistent structure than casting or forging and provides added hardenability with more consistent heat treatment results. Sintering powdered metal is like normalizing carbon steel and is recommended if a subsequent heat treatment is to be performed.

2.1.8 Heat Treating of Light Metals

Many nonferrous alloys, including nickel-based alloys, aluminum and copper alloys, and titanium and cobalt-based alloys, can be heat treated using similar principles as cast irons and steels by using a sequence of heating, quenching, and aging operations. Some of the most common heat treatment techniques for light metals include annealing and recrystallization after cold working and casting and precipitation hardening.

Since a heat treating portion of this textbook concentrates on heat treatment of steels and cast irons, the specifics of heat treatment of light metals is not discussed here. Instead a detailed description of the features of heat treating of nonferrous metals including light metals can be found in the classical text written by C. Brooks [179].

2.2 INDUCTION MASS HEATING

Induction mass heating is a process that is used to heat various metals to temperatures that will allow hot or warm forming (i.e., forging, upsetting, rolling, extrusion, etc.) or pre- or post-heat for coating operations. In many cases, the main goal is to raise the part to the specified temperature with required temperature uniformity. This temperature uniformity may include maximum tolerable temperature differentials "surface-to-core," "end-to-end," and "side-to-side" temperature variations. Often it is desired to have a uniform temperature distribution within the heated body. Besides the temperature uniformity, the other major goal of induction heating is to provide the maximum production rate at which the metal can be processed. High powers (i.e., from hundreds to thousands of kilowatts) and relatively low frequencies (typically in the range of 200 Hz to 30 kHz) are the most commonly used for induction mass heating.

When designing modern inline induction heating systems, the requirement for temperature uniformity of the reheated product is only one of the goals. Additional design criteria include maximum production rate, minimum metal losses (due to scale, oxidation, burns, decarburization, etc.), and providing compact *systems* that have high electrical efficiency. Other important factors include quality assurance, environmental friendliness, automation capability, reliability, maintainability, and availability of the equipment. The last criteria, but not the least, are the competitive cost of an induction heating system and predictable rate of energy resources (i.e., prices for gas or electricity) [268,270]. The ways to optimize some of the above-described criteria are discussed below.

Although it may seem like an easy task to simply heat a metal to a given temperature, there are many nuances of the heating process that require indepth theoretical knowledge, an extensive engineering background, and the experience of previous jobs in order to build the optimum system to satisfy often contradictory design requirements. Heating of the stock to a given temperature requires careful calculation of the required power and frequency to heat the material with the highest efficiency and flexibility, occupying minimum floor space. The factors related to frequency selection are discussed in detail in Section 7.

A major consideration is where the heat will be dissipated in the workpiece. Most often there is a need for temperature uniformity to be able to easily form the heated metal. A piece of stock that is nonuniformly heated can cause problems with premature wear on hammers and presses and may cause problems by requiring excessive force to form the metal. At the same time, there are cases when obtaining certain temperature gradients is required. For example, when heating aluminum or steel billets prior to direct or continuous extrusion, certain thermal gradients along the billet's length are often desired.

A very important consideration when designing and building an induction heating system is employee safety and the prevention of any type of machine malfunction that could occur while attempting to forge a piece of stock that has not been properly heated.

Since the part usually goes on to a press, roll former, or hammer, there is not much concern about cooling the part down for handling in subsequent processes as may be required for induction heat treating systems. A brief description is provided below for some mass heating applications.

2.2.1 Bar, Rod, and Billet Reheating

Modern techniques for producing long products such as cylindrical bars and rods integrate three stages of production: casting, reheating, and rolling into a continuous line. The goal of re-heating is to provide the bar at the rolling stage with the desired (typically uniform) temperature across its diameter as well as along its length. In some cases, the initial temperature of the product prior to reheating is the ambient temperature. In other cases, the initial temperature is nonuniform due to uneven cooling of the bar as it progresses from the caster. Surface layers of the bar become much cooler than its core.

In the past, gas-fired furnaces were typically used because of the low cost of gas. However in recent years, bar/rod producers are shifting their preference toward induction heating systems.

First, gas-fired furnaces require a very long heating tunnel to achieve the desired temperature uniformity. The length of long products presents a great problem in plants due to the limited space between the caster and rolling mill. Also, gas-firing can result in poor bar surface quality (due to scale, decarburization, oxidation, coarse grains, etc.). Finally, gas heating faces ergonomical and environmental restrictions.

These factors have resulted in heating by induction becoming the popular approach to reheating bars and rods of both ferrous and nonferrous metals (Figure 2.41). The INDUCTOHEAT Group has supplied several hundred induction bar heaters of various types to the metal forming industry worldwide. Power ratings of these machines vary from less than 100 kilowatts up to 33 megawatts.

Depending upon the specifics of the application, an induction bar heating system may consist of one or numerous inline induction coils powered by several

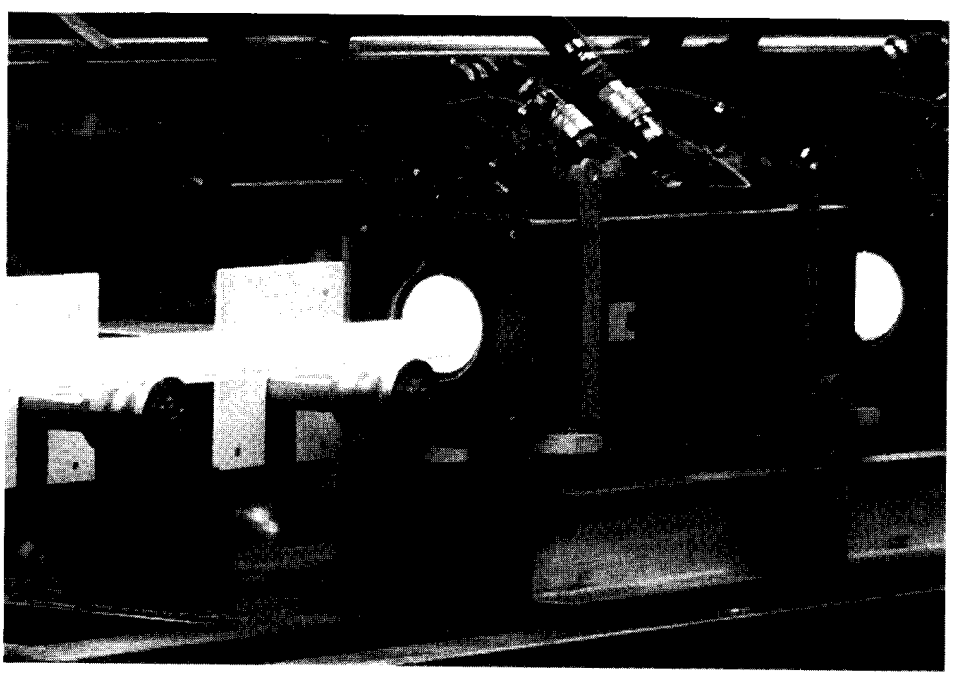

Figure 2.41 Inline induction bar heater.

inverters that have different frequencies. In some cases of high production of thick steel bars there can be more than 30 coils. The challenge in induction heating arises from the fact that the surface-to-core temperature profile continues to change as the bar passes through the line of induction coils. Due to the physics of the process, the bar core tends to be heated more slowly than its surface. At the same time, the leading and trailing ends have a tendency to heat faster than the body of the bar.

The process features, requirements, a variety of the design concepts, and an evaluation of different engineering decisions made when building induction bar heating machinery are discussed in Sections 7.1 and 7.2.

Billets are shorter pieces of bar stock that have been cut off for individual handling in the heating phase of the process. The billet may be heated to forging temperature and the entire billet fed into a forging press or hammer. The result at the end of the forming process is a part with a small amount of residual metal that must be trimmed away to yield the final forged part. As an example, Figure 2.42 shows a variety of final forged parts made from billets that have been induction heated prior to the forging operation.

Billets typically move through the induction heater using (depending upon application, heated metal, required temperature, etc.) continuous or incremental pushing systems, conveyors, belts, or walking beam systems, which carry billets through the induction coil (usually a solenoidal shaped inductor).

The diameters of the steel billets and bars usually vary from 12 mm (1/2 in.) to 150 mm (6 in.). However, the diameters of light metal billets can be much larger. For example, it is not unusual to induction heat aluminum and titanium billets of

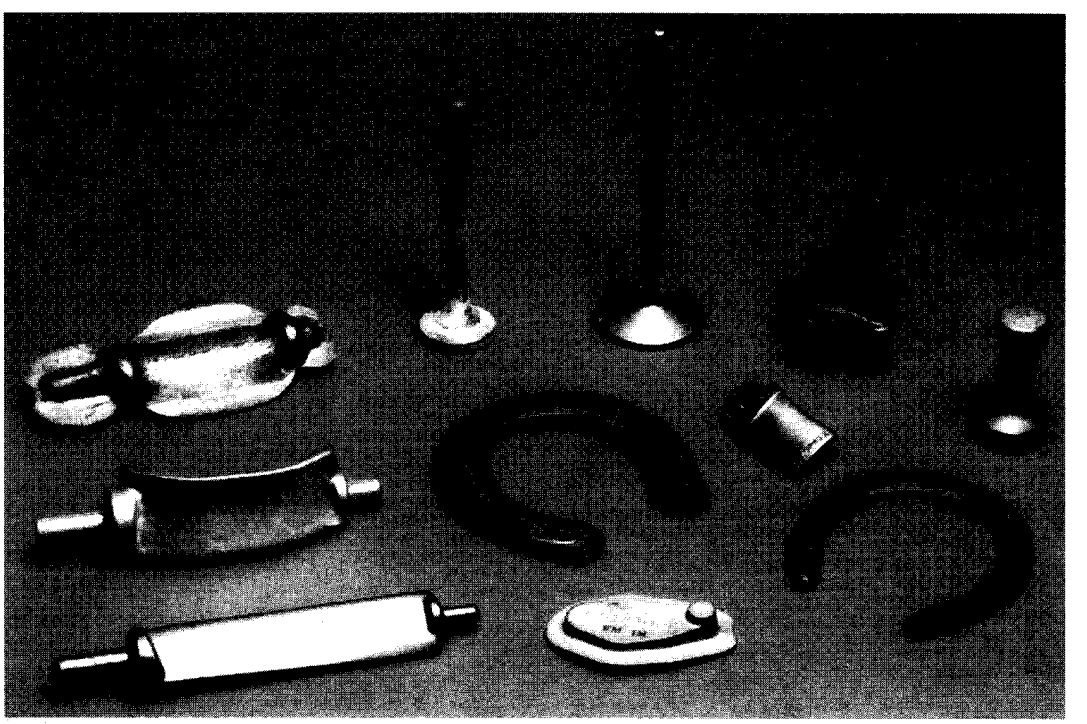

Figure 2.42 Variety of forged parts that have been heated by induction prior to forging.

diameters of 500 mm (19.5 in.) and larger. Figure 2.43 shows a multilayer inductor for preheating of aluminum billets prior to direct extrusion.

Final heated temperatures depend upon the kind of metal and application. For example, for steel bars and billets the final temperatures vary from 1050°C (1922°F) to 1260°C (2300°F). For aluminum billets final temperatures are usually in the range of 480°C (896°F) to 580°C (1076°F). Temperatures of 900°C (1652°F) to 1000°C (1832°F) and 950°C (1742°F) to 1050°C (1922°F) are typical temperatures for heating copper and titanium billets, respectively.

Instead of heating the whole billet or bar, another common approach is to heat the end of a bar to forging temperature and to insert it into a press or hammer to form the end of the bar into the desired shape. The excess metal is then removed from the part and the part is sheared off the end of the bar. The bar may then be heated again to forging temperature and the forming process repeated.

End heating of billets and bars share some similar features in the heating process. However, electromagnetic end and edge effects as well as thermal edge effect can result in a marked nonuniformity of the heating if care is not taken in the design process. The optimal choice of frequency, coil design, and power density can minimize these problems. These effects are discussed in detail in Chapters 3 and 7.

2.2.2 Slug Heating for Semisolid Forming

A relatively novel application of induction heating is the heating of various metal slugs (often aluminum or magnesium alloys) to a partially liquid state in order to easily form the slug into the desired final shape achieving a low level of product porosity without entrapment of gas and also providing high flow viscosity during casting. The semisolid metal casting process consists of preheating a metal slug up to a semisolid condition partially liquid and partially solid followed by the casting process.

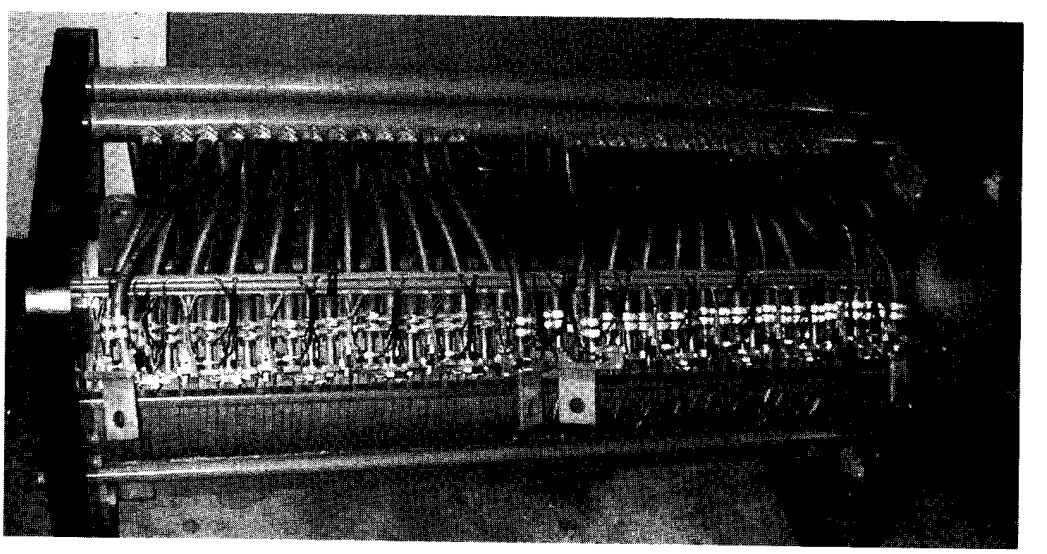

Figure 2.43 Multilayer inductor for heating aluminum billets prior to direct extrusion. (Courtesy of Inductoheat Banyard Ltd., UK.)

The heating is so close to the melting point that if the temperature is slightly higher than required, the slug can collapse to a puddle of liquid metal or sag into the inductor. The heating is continued until the slug is partially liquid inside the surface, but held together by the slightly cooler outer surface layer. The quality of semisolid casting is greatly affected by the ability to achieve temperature uniformity within the slug. Induction heating has been identified as the process that best meets the heating criteria for semisolid forming. There are two different types of induction coil arrangements: vertical and horizontal.

Automated systems control the temperature very closely (typically within 3°C) and usually involve multiple billets in process during the heating cycle (Figure 2.44).

2.2.3 Tube, Pipe, and Vessel Heating

There are many heating applications for tubular products that include annealing, normalizing, stress relieving, heating to prior sizing, piercing, parting, coating, bending, and so on. The heating of tubes, pipes, and vessels is somewhat different than the heating of solid bodies. With a solid object there is considerable conduction of heat toward the core or center of the object. With a hollow object, electromagnetic and thermal calculations must utilize different boundary conditions to properly describe the workpiece during the heat treating cycle. When the wall of the object being heated is relatively small compared to the eddy current penetration depth for

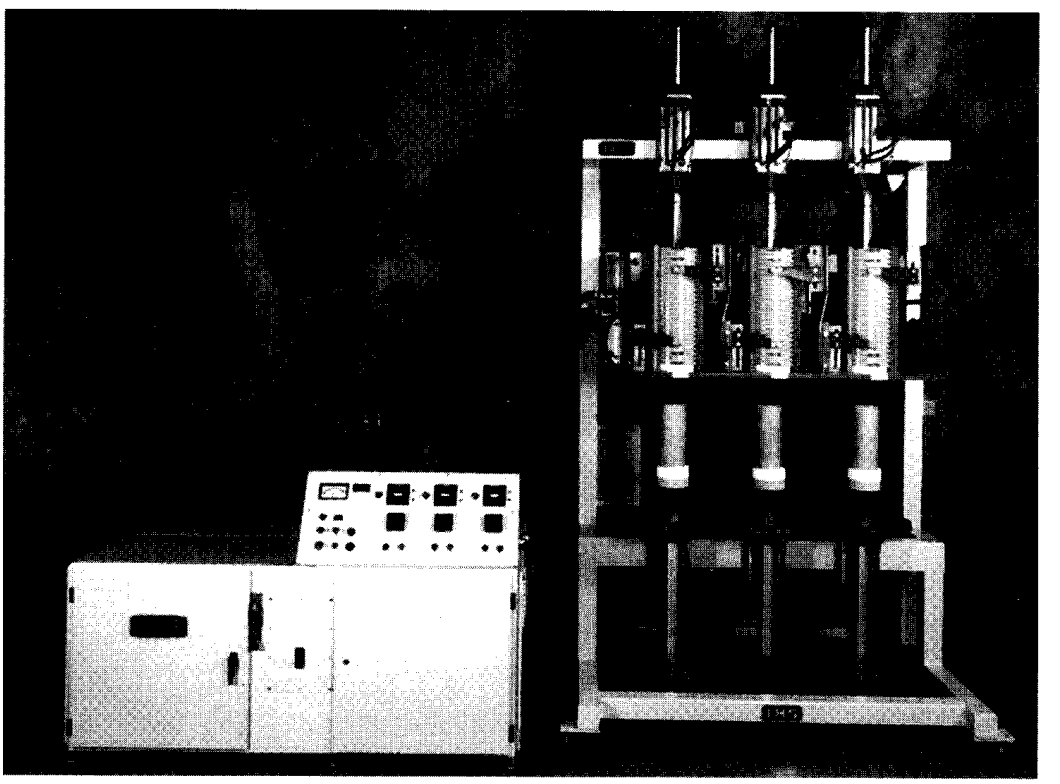

Figure 2.44 Vertical induction heating machine for semisolid forming of aluminum billets (Courtesy of INDUCTOHEAT–IHS Corp., Fort Worth, Texas.)

the chosen frequency, the reflected impedance of the load and electrical efficiency at a given frequency can be much different. These features make a marked difference on choosing the process parameters and designing the induction heating system for tubular products; these are discussed in Section 7.4.

2.2.4 Wire, Rod, and Cable Heating

The extensive use of induction for heating wire, rod, and cable products in such applications as heat treatment, coating, thermal diffusion, drying, plating, encapsulation, relaxation, and others demands a wide range of process concepts. The physical nature of wires, cables, and rods makes it reasonable to use a continuous-feed type system. In these cases, the induction heating often utilizes an oval bore coil with multiple openings for the wire to pass through. Typically, there are individual ceramic tubes (ceramic guides) for the wire to pass through. The ceramic tubes allow the heat loss to be minimized and assist somewhat with mechanically constraining the movement of the wire. Therefore, these tubes are advantageous both from a thermal and mechanical perspective.

The best electrical efficiency would result from a very tight inductor to wire coupling; often the mechanical requirements of a continuous process do not allow this without excessive wear on the inductor. Obviously a compromise is required.

Since the wire is usually small in diameter, it loses the induced heat relatively quickly. This dictates using frequencies in the range of 10 to 800 kHz with wires traveling through the inductor at speeds as high as 2 m per second and higher. As an example, Figure 2.45 shows an induction heat treatment line for the hardening and tempering of 1060 carbon steel spring wire in the diameter range of 4 mm (0.162 in.) to 8 mm (0.312 in.) at 1.39 to 2.6 tons per hour using a dual-frequency approach. Heating below Curie temperature is done using a 400 kW/10 kHz inverter. A 420 kW/200 kHz inverter is used for heating wires above the Curie temperature. Tempering is done using a 400 kW/10 kHz inverter.

Often the requirements of wire processing demand the use of a protective atmosphere that can be easily incorporated into the induction heating system.

A variety of process features and physical phenomena that distinguish induction heating of multiple wires and cables from conventional induction heating of solid cylinders, bars, and even single wire heating are discussed in Section 7.3.

2.2.5 Slab, Plate, Rectangular Bar, and Bloom Heating

Slabs, plates, and blooms of various shape and thickness may be heated and later rolled down to the final desired size. Some of these are cooled and later reheated for rolling or forming; others are reheated as a part of the continuous process to facilitate the subsequent rolling or forming operation. These types of systems utilize large low-frequency power supplies and often quite long coil lines. Figure 2.46 shows induction system for heating of the world's largest carbon steel slab.

When heating rectangular-shaped workpieces, the difficulty in obtaining heat uniformity is caused by a combination of "skin" effect, electromagnetic longitudinal end effects, transverse edge effects, and thermal edge effect. If the initial temperature of the slab or bloom is uniform, then in order to provide a uniform temperature distribution within the slab, it is necessary to ensure that each region within the

Figure 2.45 Radyne's induction heat treatment line for the hardening and tempering of AISI 1060 carbon steel spring wire in the diameter range 4 mm (0.6 in.) to 8 mm (0.31 in.) at 1.39 to 2.6 tons per hour. Pre-Curie inverter: 400 kW/10 kHz; post-Curie inverter: 420 kW/200 kHz; tempering stage: 400 kW/10 kHz.

workpiece absorbs the same energy during the heating cycle. Therefore, it is necessary to provide a balance of these effects.

There are several different coil arrangements available to heat slab by induction; however, the great majority of applications apply longitudinal flux inductors (rectangular solenoids). Depending upon the process requirements there are three major design concepts of the induction slab heating systems: static heating, inline progressive heating, and oscillating heating.

Frequently, the temperature distribution within the cast ingots, slabs, or blooms is nonuniform having a complex initial temperature profile depending upon the geometry and the specifics of cooling during the casting and production rate. Obviously it requires much less energy to reheat the slabs before they cool down to room temperature. However, in cases such as this the frequency should be selected based on the specifics of the initial temperature distribution. Slab edges tend to cool faster than the central areas and core. Therefore, it is often required during reheating to distribute energy induced in the slab in such a way as to compensate for its nonuniform initial temperature distribution.

Since workpieces that require reheating can come to the induction heater at different temperatures, special controls may be required to sense the incoming part temperature profile and to reset the power level of the heater to maintain a relatively constant output temperature.

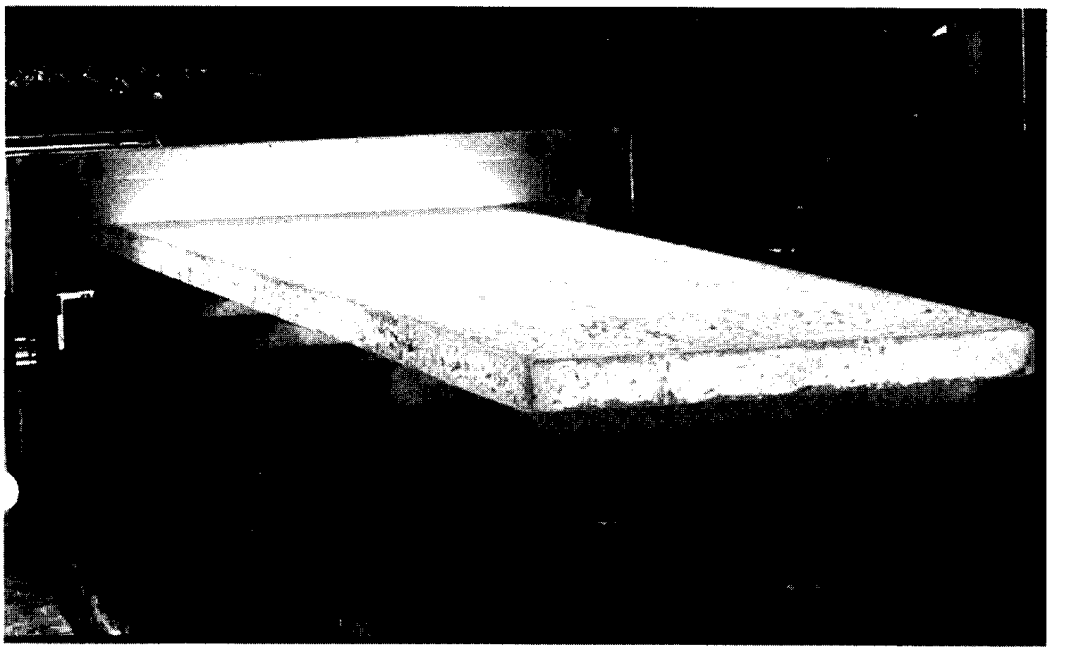

Figure 2.46 Induction re-heater of the world's largest carbon steel slab. Maximum slab width: 3.2 m (126″); thickness: 0.22 m (8.7″) @ 540 tons per hour; total power: 42,000 kW. Installed by Inductotherm Corp. in 1995 at Geneva Steel, Utah.

Section 7.5 is devoted to a discussion of the major features of induction heating of rectangular bodies.

2.2.6 Induction Heating of Strips, Thin Slabs, Plates, and Sheets

There is a variety of applications that require the heating of thin metal (e.g., copper, bronze, silver, carbon steel, aluminum, etc.) sheets and strips that are fed in a continuous process from large storage rolls. Since the heating process is continuous and may involve coating the sheet with a protective layer, curing of paints and varnishes, and annealing, pickling, or thermal spraying, it is necessary to tightly control the temperature across the width of the strip to ensure uniformity.

Induction heating of strips, plates, thin slabs, and sheets has many similarities compared to the heating of slabs and blooms. At the same time, there are some specific features.

A particular application calls for a specific coil design. Depending upon the orientation of the main magnetic flux with respect to the strip and the particularity of the coil design, there are five basic induction strip heating coil designs: longitudinal flux coils, transverse flux inductors, traveling wave coils, channel-type coils, and "C"-type inductors.

At lower temperatures relatively low frequencies can be used for thin carbon steel strips because the strips are in the magnetic stage and the efficiency is high. At higher temperatures (i.e., above Curie), in order to provide high efficiency, much higher frequencies are required to heat the strip or plate. In some cases it is necessary to change the direction of the magnetic flux in the workpiece to achieve better

efficiency at higher temperatures (i.e., transverse flux inductors or traveling wave inductors).

There are two major concerns faced by the designers of induction machinery for strip heating. One of them deals with the ability to provide temperature uniformity across the strip width. The ability to avoid eddy current cancellation and obtain high coil efficiency when heating nonmagnetic thin strips is another concern.

Because the strip is moving at a fast rate, large power supplies, often many on one line, are needed to provide the required energy input in order to guarantee the desired production rate. Section 7.6 discusses the intricacies of induction heating of strips, plates, sheets, and thin slabs.

2.2.7 Coating

Induction heating of strips, wires, and tubes has been used for a variety of systems involving the coating, spraying, and curing of various coatings such as paints, varnishes, and zinc alloys for galvanizing steel. Figure 2.47 shows an oil gas pipe field joint heat and coat head. This system has been designed to heat 610 mm (24 in.) diameter with 30 mm (1.2 in.) wall steel pipe and apply a coating of the powder in 90

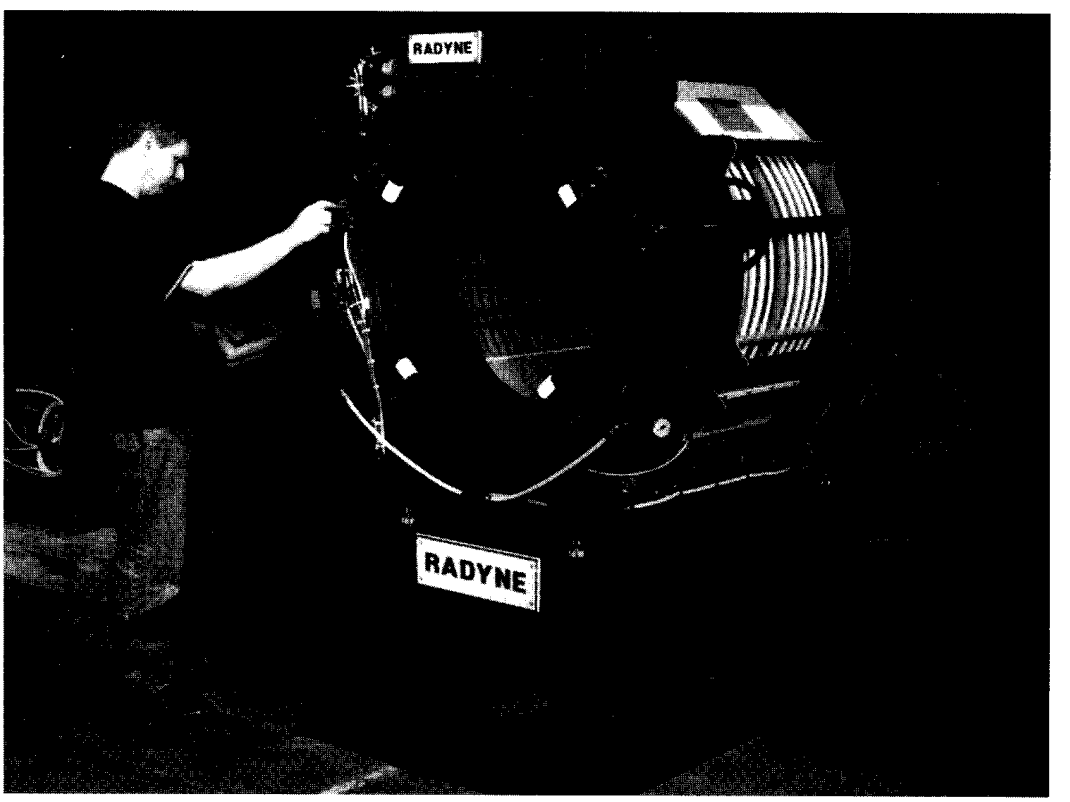

Figure 2.47 Oil gas pipe field joint heat and coat head. Designed to heat 610 mm (24 in.) diameter with 30 mm (1.2 in.) wall steel pipe and apply a coating of the powder in 90 seconds. Length of joint to be coated, 300 mm. Powered by Radyne standard 450 kW/3 kHz thyristor inverter.

seconds. The length of the joint to be coated is 300 mm. The system is powered by a Radyne standard 450 kW/3 kHz SCR-type inverter.

2.2.7.1 Curing of Paints and Varnishes

Curing of paints and varnishes requires special design considerations due to the potential for an explosion or fire if a spark or uncontrolled overheating of the metal occurs in the presence of paint or varnish fumes. The metal strip is painted on a continuous line, which later passes through the induction coil. The quality of the painted surface is very important and care must be taken to ensure that there are no surfaces above the painted surface that could allow water to condense and drop onto the painted surface. Because induction heats the substance, inside-out, there are no pin holes in the coating. The mechanical movement of the painted surface must be constrained and the heating coil opening must be sufficient to allow sample clearance for the painted strip to move within limits without touching the heating coil. Since the curing requires low temperatures the heating can be done with relatively low frequencies for the thin strip in the magnetic state. High power levels allow faster curing requiring in most cases only 1/3 the length of conventional ovens.

2.2.7.2 PreHeating Prior to Thermal Spraying

Thermal spraying involves the application of a coating material to the workpiece by spraying the coating material at an elevated temperature. The material adheres to the outer surface of the metal that it is sprayed on and provides a cost-effective way to increase resistance to wear, corrosion, and heat. These processes include electric arc combustion and plasma spray coating.

Preheating the surface prior to the application of the coating material can facilitate the application of spraycoating materials onto a moving part. This type of system often utilizes a stationary coil and spray system while the workpiece moves continuously through the coil. Systems for coating sections of pipe and tube have also been designed utilizing a moving inductor and high-frequency power supply along a stationary pipe or tube as the spray head, mounted very close to the moving inductor, applies the coating material.

2.2.7.3 Galvannealing, Galvanizing, and Galvaluming

The hot dip coating of steel with zinc and or aluminum involves the process of feeding a continuous steel strip through a variety of different stages to clean and prepare the material, anneal, coat, cool, anneal, inspect, and finally to apply a protective coating before storage.

Galvannealing is the continuous annealing of the steel strip after the dipping of the strip, wire, or tube into the molten zinc or zinc–aluminum bath. The strip temperature is raised to the point of remelting the zinc, which leads to the formation of different zinc–iron alloys. This coating facilitates uniform appearance and adhesion of paints as well as electrical welding of the strip when used in the automotive industry.

Galvanizing is the continuous process of coating the strip by transporting it through a molten zinc bath. As an example, Figure 2.48 shows a continuous galvanizing line of low carbon strips that includes solid-state power supplies, induction melting pot, and an induction strip heating system built by joint effort of INDUCTOHEAT, Inc. and Inductotherm Corp.

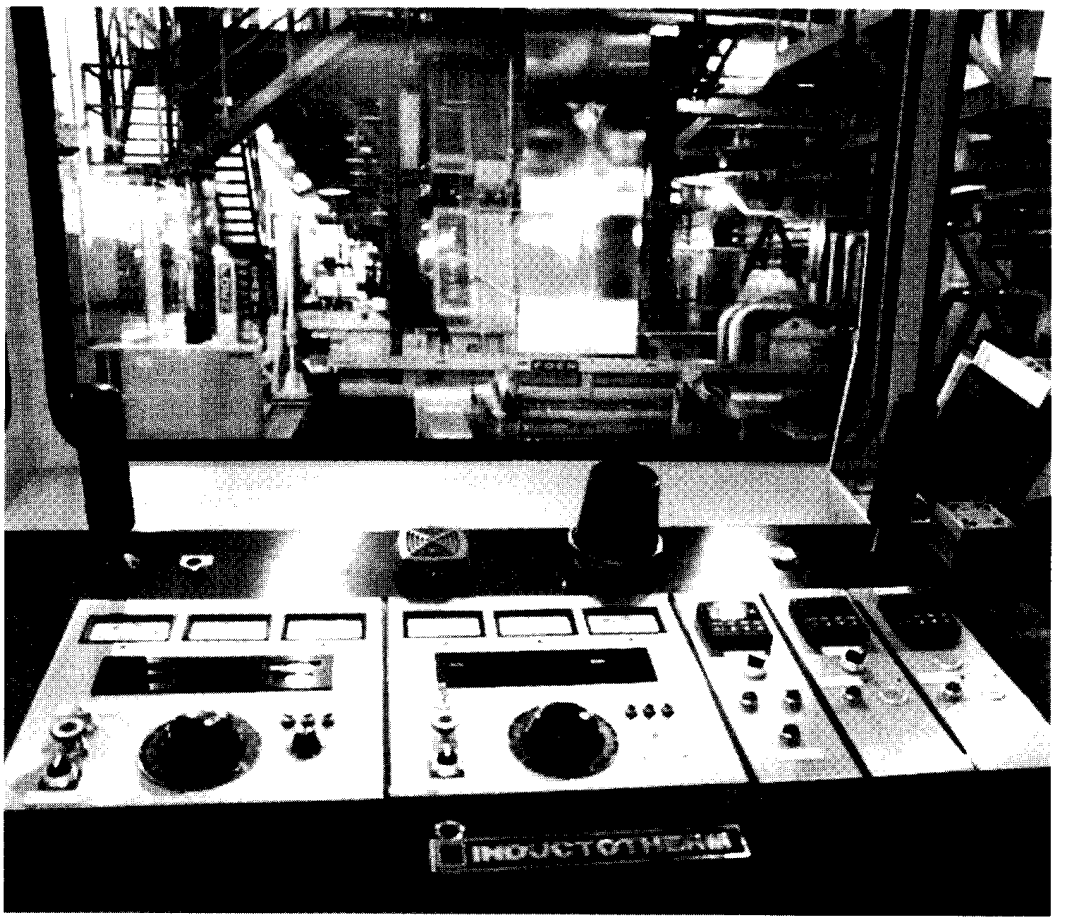

Figure 2.48 Induction strip galvanizing line. (Built in cooperation between INDUCTOHEAT, Inc. and Inductotherm Corp.)

Galvaluming is the same type of coating process but using coatings composed of zinc and various percentages of aluminum. The aluminum content helps to make the material more malleable during the continuous folding of the strip on the various rollers. Some coating jobs require a pure aluminum coating such as Alupur (171).

Virtually instantaneous changes in power allow changes in speed/temperature/materials with a minimum yield loss.

Due to the precarious location of heating and annealing coils in the vicinity of the hot zinc and/or aluminum bath, often high in the air, it is necessary to take safety precautions to prevent injury to maintenance workers. Also care must be taken to ensure that no water leakage from coil cooling lines occurs over the molten bath.

Since induction is a self-contained package requiring minimum space, it is often simple to add to an existing line.

2.3 SPECIAL APPLICATIONS OF INDUCTION HEATING

Induction heating lends itself well to many special applications that satisfy a variety of needs in a broad base of different industries. Some of these are described below.

2.3.1 Joining, Friction Welding, Brazing, Bonding, and Soldering

When joining and bonding different pieces of metal together, it is very common to apply induction as a heat source. Figure 2.49 shows a friction welded part preheated by induction. An example of induction joining would be the heating of the end of an axle hub before it is friction welded by spinning it at high speed and pressing it against the end of an axle housing.

Brazing and soldering are also typical joining applications of induction heating. In this process two pieces of metal are held very close together and heated to an appropriate temperature; a flux is applied to the joint to enhance the flow of the brazed material or solder into the joint. Very careful temperature control is necessary and placement of the two pieces to be joined is critical to achieving a successful joint. Figure 2.50 shows an induction machine for brazing the working tips of tool bits for the mining industry.

Bonding of two different sections of metal through the heat curing of an epoxy or adhesive has been done successfully for joining a variety of different surfaces and shapes. One typical example is the bonding of a rearview mirror in the automotive industry, which involves heating up a metal tab attached to the mirror support while it is held against the windshield. The metal tab is then bonded to the windshield glass to support the mirror. Figure 2.51 shows an example of using induction heating for brazing a brass cap to a steel body.

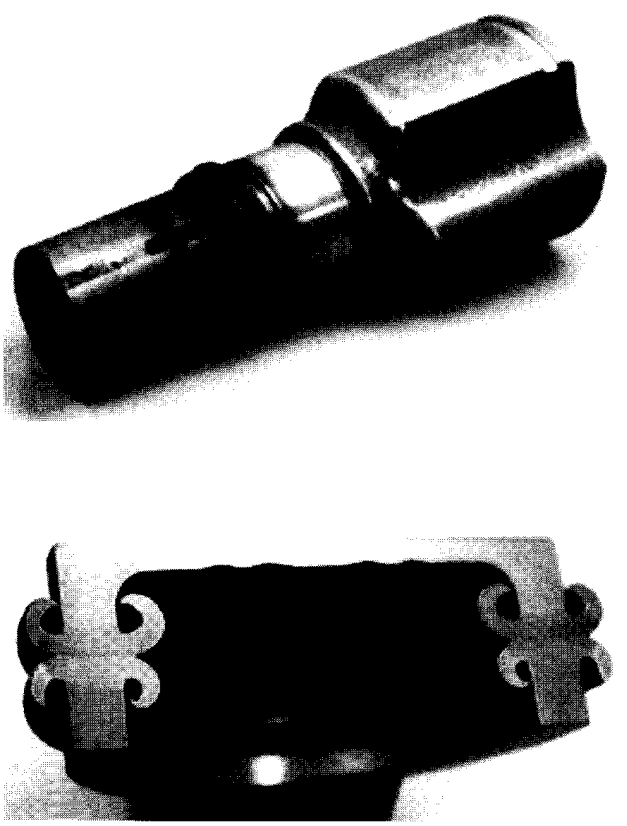

Figure 2.49 Friction welded parts preheated by induction.

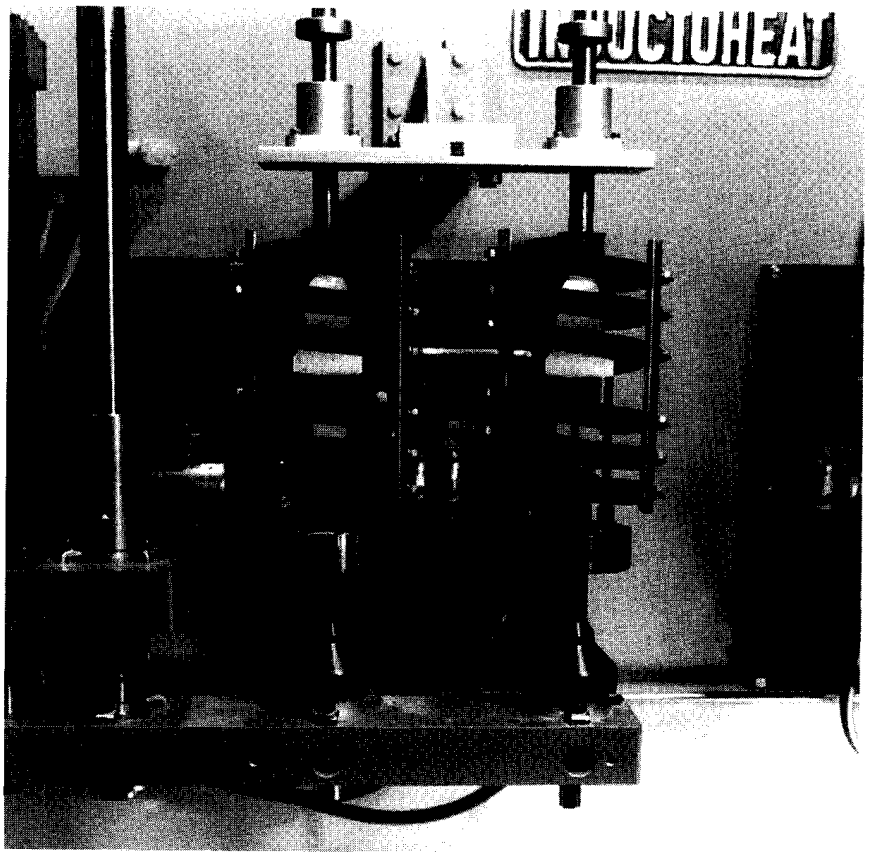

Figure 2.50 Induction machine for brazing the working tips of tool bits for the mining industry.

2.3.2 Shrink Fitting

A common application of induction heating is the heating of various types of housings and base assemblies for insertion of another component, such as a pin, into a properly sized hole. The part or base assembly with a mating hole is typically heated to about 200°C with low frequency to ensure uniformity of the heating in the desired area. When the area around the hole has been heated to allow the size of the hole to increase as the metal expands, a pin is inserted, usually with a small amount of pressure to press it into the hole to mate with the base assembly.

A typical assembly of this type would be an automotive steering knuckle which has a wheel spindle inserted into the hole in the knuckle. Another common use of shrink fitting is for the insertion of bearing assemblies into a parent housing.

In shrink fitting, sufficient mass around the hole must be heated for the size of the hole to increase. If local heating is done inside the hole for a short time, the reverse effect may be seen and the metal may expand in the direction of reducing the hole diameter and preventing the insertion of the pin or bearing assembly.

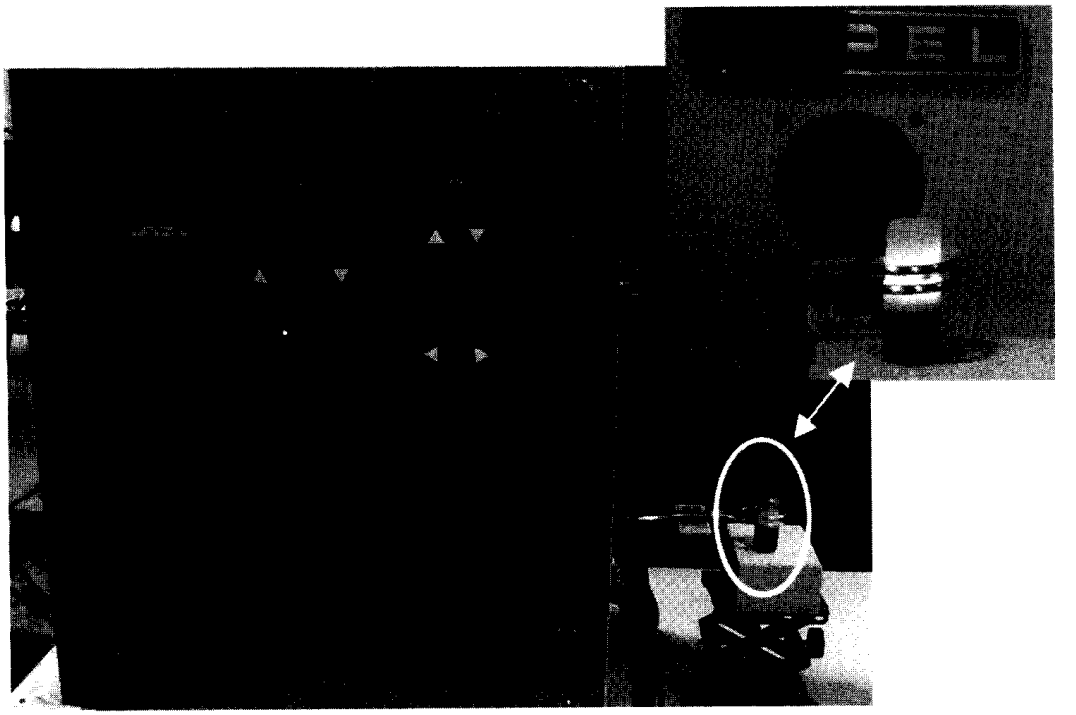

Figure 2.51 Induction brazing a brass cap to a steel body using the LSS 7.5 kW inverter.

2.3.3 Banding

In the manufacture of some types of cathode ray tubes (CRTs) the process requires the shrink fitting of a steel band around a joint in the neck of the tube in order to provide an air tight seal. The band is heated by induction to cause expansion of the band. When the band is fully expanded, it is placed around the end of the tube where the joint is required. As the band cools it compresses the pieces of glass and provides the desired sealing effect.

2.3.4 Motor Rotor Heating (Lamination Bluing and Bond Breaking)

In the production of small and moderate size motors, induction heating is used to heat the rotor of the motor for the purpose of die cast aluminum bond breaking and lamination bluing, as well as rotor shaft shrink fitting (Figure 2.52). Rotor heating systems are typically similar to forge billet heaters.

According to one approach of bond breaking (thermal shocking) and lamination bluing, motor rotors are placed end to end on a locating vee and indexed into the induction coil. Another approach utilizes coil design used for induction heating prior to semisolid forming. The parts are heated to the required temperature as they progress through the coil and are ready at the exit, after cooldown, to proceed to the next assembly operation.

Induction heating is often the preferable choice for curing of epoxy used in the assembly of the stator as well as for motor frame disassembly.

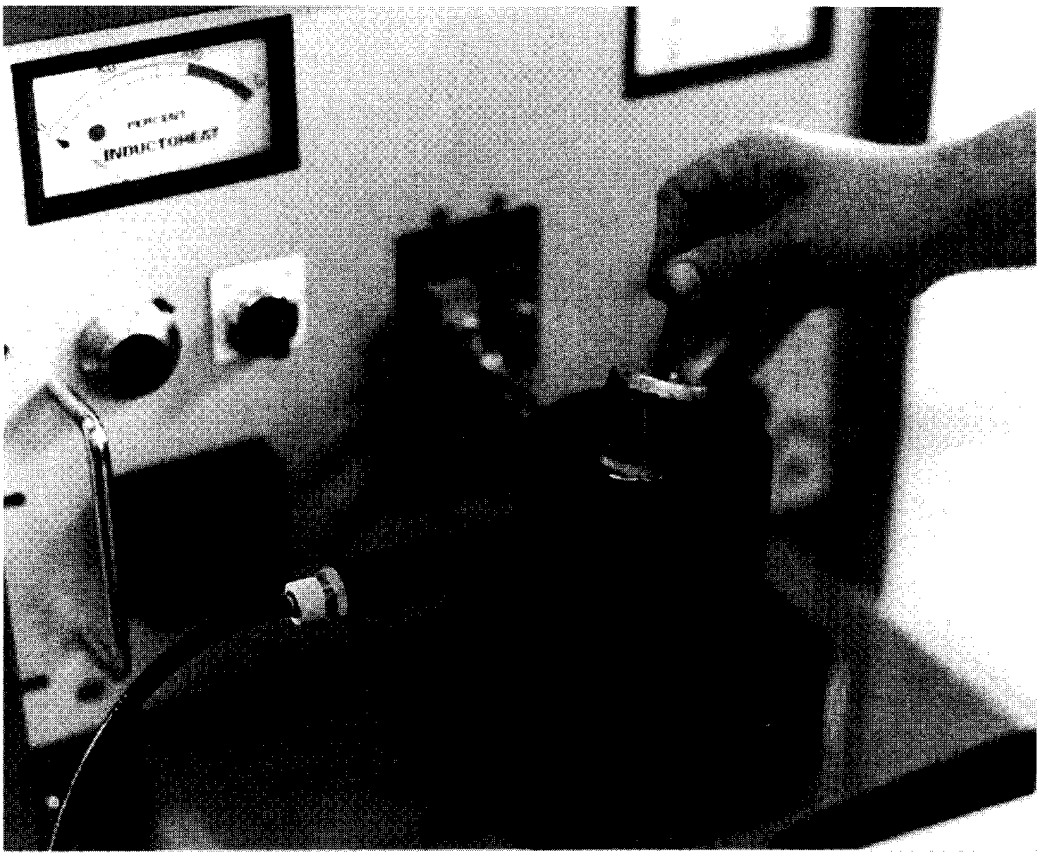

Figure 2.52 Portable induction rotor heater.

2.3.5 Seam Annealing

In the manufacture of pipe and tubular products it is often necessary to form the tube from a piece of flat metal strip or plate. A seam occurs at the point where the two ends of the strip meet to form the cylindrical shape of the tube forming a straight longitudinal or spiral seam. This seam is usually welded to form a closed tube or pipe.

After the welding process the welded area must be annealed in order to prevent brittleness at the welded joint.

A common type of inductor (or coil) used to anneal the longitudinal seam of pipes and tubes is a split return inductor (see Sec. 7.7.3). This type of coil arrangement provides high field strength under the single pass of the conductor, which is positioned over the welded joint. Flux concentrators are used to focus the heating in a narrow band along the welded seam. The current along the go and return path is half the magnitude of the current in the single pass section of the coil.

Since these coils are used in a continuous process it is essential that the reliability be very high and that there be some redundancy in the system in the event of a component failure in one of the power supply or coil assemblies.

2.3.6 Food Industry

A variety of applications of induction heating is found in the food industry. Many systems utilize susceptors that are heated by induction which in turn heat the food by conduction. Many induction food warmers and induction stoves work by this principle. Induction extruders are used to produce many types of grain-transformation and confectionery products. Large cauldrons are used for cooking caramel and other similar products and there are also fluid heating systems used in the production of milk. A final application in the food industry is the heating of rollers used to make thin products such as pizza dough and cookies.

2.3.7 Papermaking

In the papermaking industry the primary application is in the heating of calendar rolls to accurately control the thickness and quality of the paper produced. A variety of individual coils is spaced along the length of the calender roll. The roll temperature and paper quality are continually monitored and the power levels are adjusted accordingly to provide the desired temperature at each point along the length of the roll.

2.3.8 Wool and Wood Processing

It is possible to utilize induction heating in industries that require the drying of materials as they pass along a production line or in batches offline. The induction coil is used to heat a metal plate, which in turn may contact the material and heat it by conduction and/or convection.

2.3.9 Chemical Industry

In the chemical industry, induction heating is used to heat various types of reactors and distillation equipment, which is used in the production of pharmaceutical products. In most industrial systems, the heat that must be transferred to water in an induction system is an undesirable byproduct of the heating process. In the chemical and food industry it may itself be the desired end product. Some of the benefits of using induction as opposed to open flame heating are ease of control, safety and efficiency.

2.3.10 Automotive Sealing

In the automotive industry it is common to use induction heating to cure an epoxy or thermal setting glue that is used to bond different sections of sheet metal. The bond can be a complete seal around the entire panel or it can involve spot bonding, where the panel is fastened at a number of discrete locations around the periphery rather than a continuous loop around the entire panel. This process can be used to bond metal to metal or metal to another material.

A single power supply is used for continuous bonding whereas a number of small individual power supplies may be used for spot bonding. The advantage of individual power supplies is that they provide individual control of the temperature

at each bonding point rather than attempting to control the temperature at individual points by contouring the inductor or using flux concentrators.

2.3.11 Cap Sealing

Cap sealing is a very important application in the food and pharmaceutical industries. Fear in recent years, with respect to illegal tampering with food or drugs prior to consumer use, has led to the development of cap sealing.

This technology provides a way that consumers can be sure that the product they are using is coming to them in exactly the same form and purity in which it was packaged at the factory.

With this process, a small layer of aluminum foil is placed on the top of a container that has been filled and inspected (Figure 2.53). The container with the foil is passed under an induction coil, which heats the foil to a sufficient temperature to bond it to the top of the container. The contents are thus sealed and virtually guaranteed safe at the point of final use.

2.3.12 Die Heating

For consistent forging and hammering operations the die temperature must stabilize at a temperature suitable to produce a good forging. This can be done using flame,

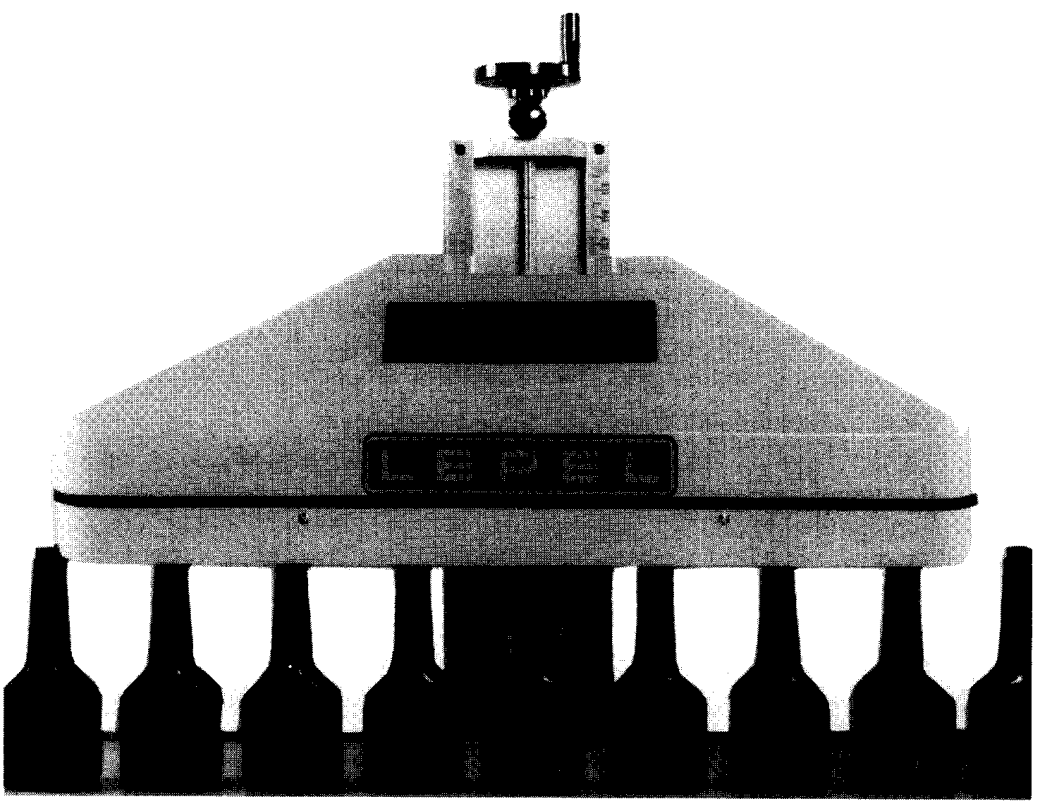

Figure 2.53 Lepel's induction cap sealing system.

gas firing or induction heating. Presses being very expensive machinery, their downtime is very costly. When flame or gas-fired furnaces are used, in order to minimize the downtime of presses, it is necessary to keep dies inside the heating furnace all the time. This negatively affects the die life, builds scale, and dicarburizes the die's surface. Induction is a faster and more economical approach to die heating when the geometry of the die will allow heating with reasonable uniformity. This can save considerable time at the start of each operation by bringing the dies quickly up to operating temperature (see Sec. 6.4).

2.3.13 Miscellaneous

Some other miscellaneous uses of induction would include lost core melt out systems, de-bonding paint from oil tanks and ship hulls, annealing of shell casings, crystal growing, induction pumping of liquid metal, levitation heating, induction plasma, and so on (Figure 2.54).

2.4 INDUCTION MELTING

In the production of metal it is necessary to raise the temperature of the metal or ore to the melting point and often to hold it at temperature to allow some type of metallurgical treatment. Electric furnaces used in the melting process are induction,

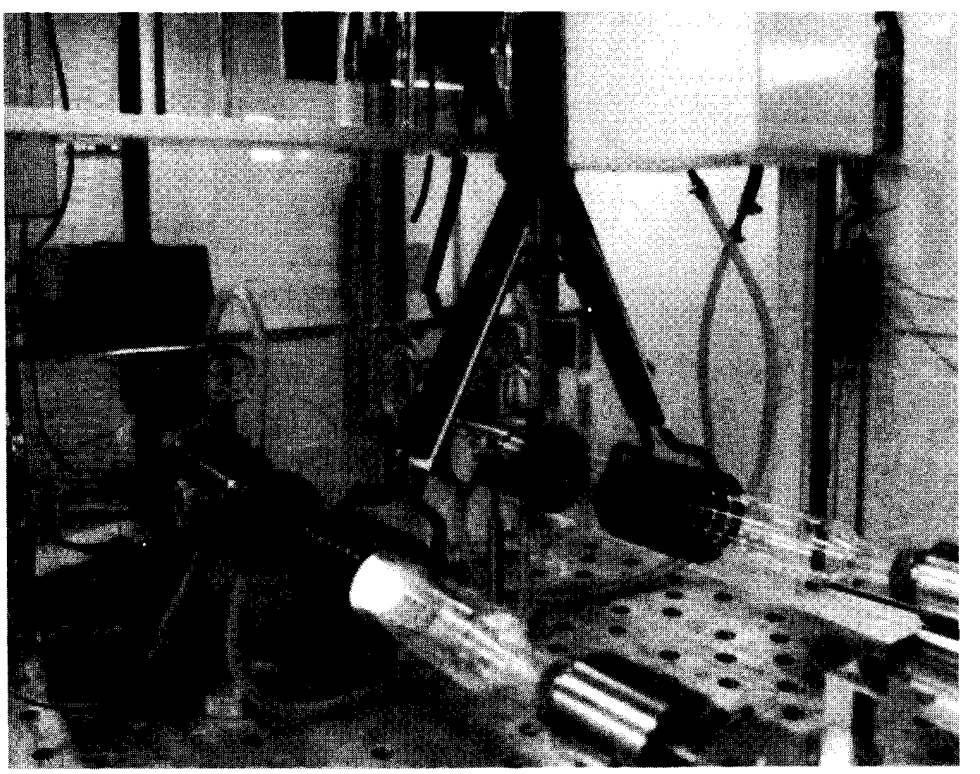

Figure 2.54 Induction plasma.

arc, or resistance furnaces. The typical induction melting furnaces in use are the channel type and the crucible type that allow one to melt irons, steels, aluminum, copper, zinc, nickel, and other metals and alloys.

2.4.1 Induction Channel-Type Furnace

The channel type induction furnace derives its name from the fact that it is constructed with a small channel of molten metal passing through the magnetic core, which has a primary winding (N_1) wound around it (Figure 2.55). This channel of molten metal acts like the secondary (N_2) of a short-circuited transformer causing current to flow through the metal in the channel and heat loss to occur by the Joule effect. The channel is usually located at the bottom of the molten metal bath to prevent known problems with the interruption of the current flow in the bath during heating.

Channel furnaces are primarily suitable for continuous use and may often be fed by other types of furnaces. Channel furnaces are a particularly good approach for melting metals in such cases when [21]

- high metal volumes are desired,
- only one product is produced,
- power outages are not expected, and
- temperature uniformity is not critical.

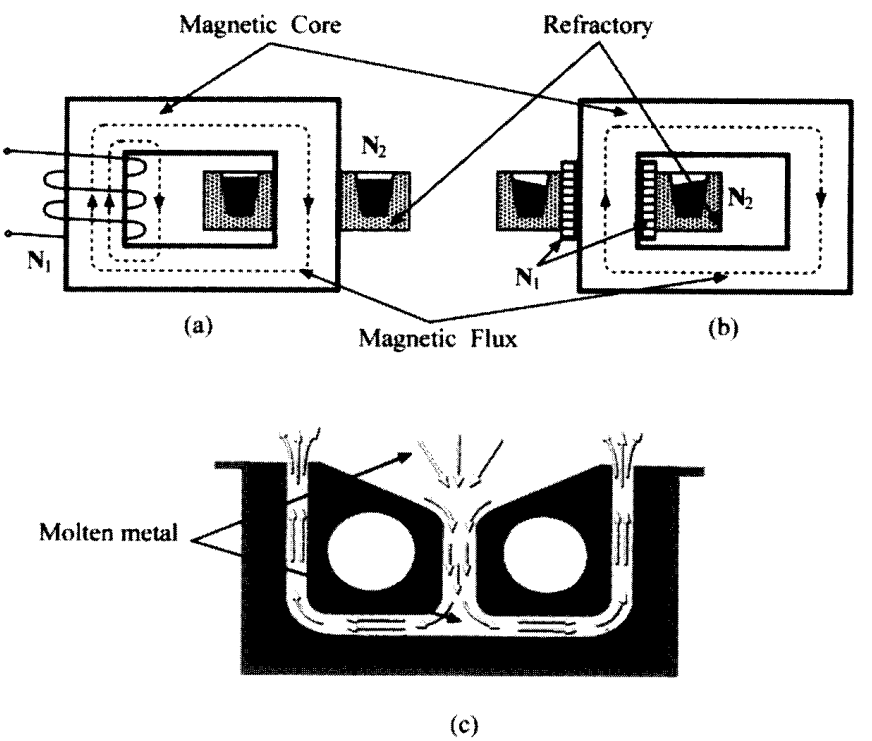

Figure 2.55 Simplified sketches of the channel-type induction melting furnaces.

2.4.2 Induction Crucible-Type (Coreless) Furnace

The crucible type, or coreless induction furnace, consists of a solenoidal induction heating coil surrounding a crucible (Figure 2.56). Depending upon the application, the crucible can be made from an electrically conductive material (for example, steel, graphite, etc.) or nonelectrically conductive material (for example, ceramics, etc.). Electrically conductive crucibles are heated due to eddy currents induced from the inductor and allow one to increase a coil electrical efficiency when melting low resistive materials (for example, aluminum, copper, bronze, magnesium, and some precious metals). The process of melting takes place thanks to thermal conduction from the heated crucible, to the metal required to melt. Refractory liners are used for coil protection from excessive heating by radiation and convection.

In the case of nonelectrically conductive crucibles, the metal mass to be melted is located inside the pot formed by the refractory material. The refractory material may differ depending on the type of material to be heated. This type of furnace requires no magnetic core like the channel-type furnace, although external magnetic shunts may be used to control the magnetic field exposure. The mixing or stirring action experienced in a coreless furnace is directly proportional to the power and inversely proportional to the square root of the applied frequency. A coreless furnace is a particularly good approach for melting metals in such cases when [15]

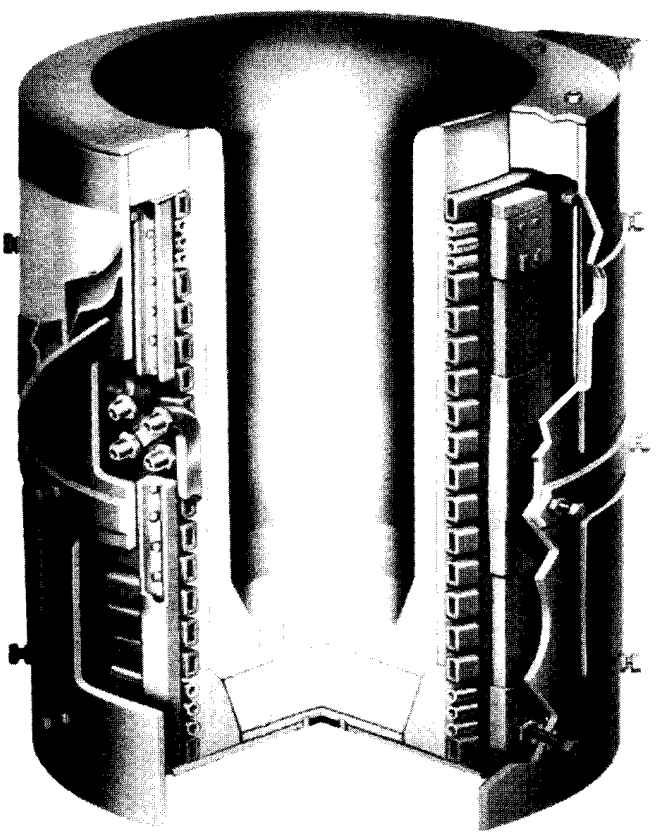

Figure 2.56 Sketch of Inductotherm's induction crucible-type (coreless) melting furnace.

- precise temperature control is required,
- dross generation is high,
- lower capital and installation costs are desired,
- pre-melt capability is needed, and
- power interruptions are expected.

Coreless furnaces can be emptied very quickly to handle alloy changes on short notice. This provides maximum alloy flexibility, reducing job turnaround time and decreasing nonproductive and off-shift holding time [15].

2.4.3 Induction Vacuum Furnace

The melting process can be carried out in a vacuum in order to eliminate concerns about oxidation and metal purity during the melting and casting processes. Due to the need to place the entire melting and casting system into one enclosure and to allow for any additions to the metal during the melt, this method can be quite costly and is reserved for use where the required purity of the product justifies the additional expense. Special methods of pouring the liquid metal are sometimes required when controlled amounts must be delivered to the mould at the time of casting.

2.5 INDUCTION WELDING

As mentioned earlier, one of the major uses of induction heating in the pipe and tube making industry involves the heating of a sheet of metal that has been formed into a tubular shape and constrained in such a way that eddy currents in the workpiece cause the two open ends of the sheet to be welded together producing the seam.

In order to do so, a cylindrical coil surrounds the tube's V-shaped open seam area. Squeeze rolls press the strip edges together in the area where there is a maximum density of the induced current providing a so-called "forge weld." Often a water-cooled magnetic flux concentrator (magnetic impedor) is placed inside the tube allowing it to increase the efficiency of the process.

Induction welding typically applies relatively high frequencies in the range of 200 to 600 kHz and power from 50 to 1500 kW. Figure 2.57 shows Thermatool's induction welder, bus work and induction coil.

Induction welding is usually a continuous operation. After welding, the seams are then subsequently annealed with a seam annealing system that follows the welding system in a continuous line.

2.6 CONCLUSION

As mentioned above, the industrial applications of induction heating can be divided into five groups: heat treating, mass heating, special heating applications, induction melting and induction welding. Because of space limitation, only the first three groups are discussed in this textbook in detail. A discussion of the features of induction melting and welding are outside the scope of this text. Although the basic thermal and electromagnetic phenomena (including the skin effect, proximity

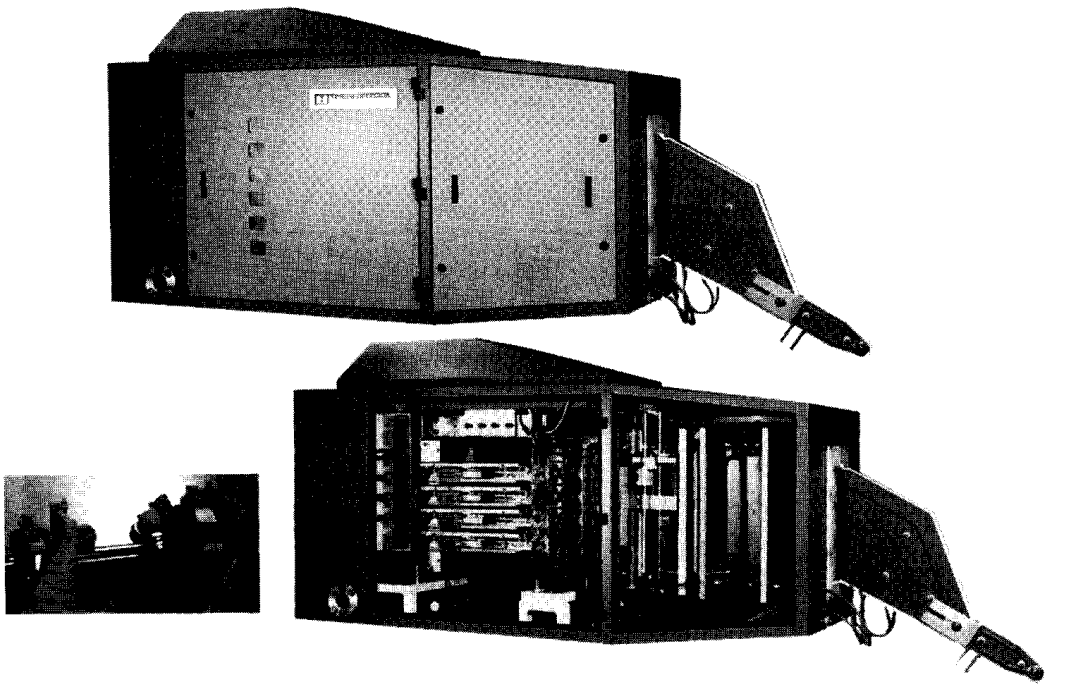

Figure 2.57 Thermatool's solid-state tube and pipe welder.

effect, electromagnetic slot and ring effects, as well as electromagnetic end and edge effects, etc.) are common for all induction applications, there are some distinguishing features in induction melting and welding that deal with technological uniqueness and process specifics.

If the reader has questions or is interested in certain aspects or features of the induction melting or induction welding processes the authors recommends the publications [4, 5, 7, 10, 15] or refers the reader to the leading manufacturers of this equipment such as Inductotherm Corp., Consarc Corp., Thermatool Corp., and others.

3

Theoretical Background

As mentioned above, induction heating is a complex combination of electromagnetic, heat transfer, and metallurgical phenomena. Heat transfer and electromagnetics are tightly interrelated because the physical properties of heat treated materials depend strongly on both magnetic field intensity and temperature. The metallurgical phenomenon is also a nonlinear function of temperature, heating intensity/cooling severity, chemical composition, and other factors. This chapter is devoted to a discussion of the electromagnetic and heat transfer phenomena and some other aspects relating to them.

3.1 BASIC ELECTROMAGNETIC PHENOMENA IN INDUCTION HEATING

The basic electromagnetic phenomena of induction heating are quite simple and discussed in several textbooks including college physics. An alternating voltage applied to an induction coil (e.g., solenoid coil) will result in an alternating current in the coil circuit. An alternating coil current will produce in its surroundings a time-variable magnetic field that has the same frequency as the coil current. This magnetic field induces eddy currents in the workpiece located inside the coil. Eddy currents will also be induced in other electrically conductive objects that are located near the coil. These induced currents have the same frequency as the coil current; however, their direction is opposite to the coil current. These currents produce heat by the Joule effect (I^2R). A conventional induction heating system that consists of a cylindrical load surrounded by a multiturn induction coil is shown in Figure 3.1.

Because of several electromagnetic phenomena, the current distribution within an inductor and workpiece is not uniform. This heat source nonuniformity causes a nonuniform temperature profile in the workpiece. A nonuniform current distribution can be caused by several electromagnetic phenomena, including (1) skin effect, (2) proximity effect, and (3) ring effect. These effects play an important role in

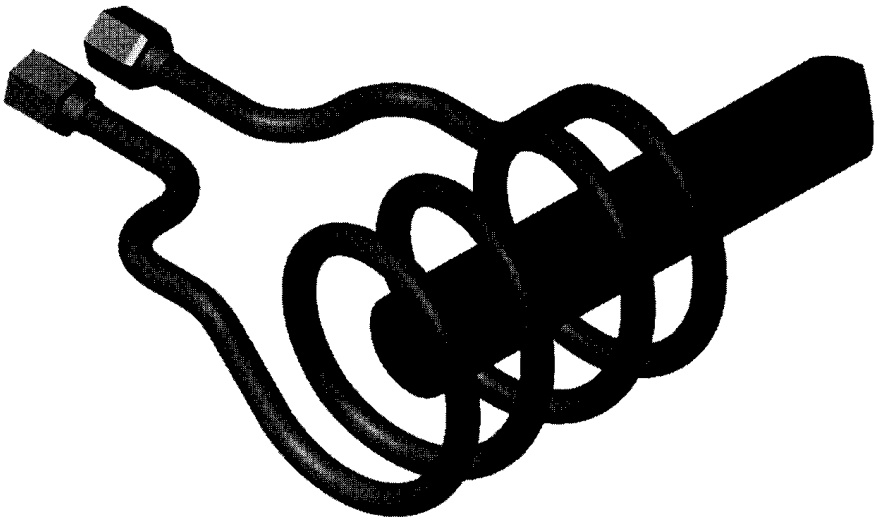

Figure 3.1 A conventional induction heating system consists of a cylindrical load surrounded by a multiturn induction coil.

understanding the induction heating phenomena [1–12, 40, 50–53, 92, 118–121]. Before exploring the distribution of the magnetic field and eddy current it is imperative to understand the nature of electromagnetic properties of heated metals.

3.1.1 Electromagnetic Properties of Metals

Electromagnetic properties of materials is quite a broad expression that refers to a number of electromagnetic characteristics including magnetic permeability, electrical resistivity (electrical conductivity), saturation flux density, coercive force, hysteresis loss, initial permeability, permittivity, magnetic susceptibility, magnetic dipole moment, and many others. Recognizing the importance of all electromagnetic properties, we concentrate in this text only on those properties that have the most pronounced effect on parameters of the induction heating systems.

3.1.1.1 Electrical Resistivity (Electrical Conductivity)

The ability of material to easily conduct electric current is specified by electrical conductivity σ [16,189,446]. The reciprocal of the conductivity σ is electrical resistivity ρ. The units for ρ and σ are Ω-meters and mho/m, respectively. Both characteristics can be used in engineering practice, however, the majority of data books consist of data for electrical resistivity. Therefore in this text the value of electrical resistivity is primarily used.

Metals and alloys are considered to be good conductors and have much less electrical resistance compared to other materials (e.g., ceramics, plastics, etc.). Table 3.1 shows values of electrical resistivities for common materials at ambient temperature. Although metals having low electrical resistivities are known to be good electrical conductors, they are, in turn, also divided based on their electrical resistivity. There are metals that we consider being low-resistive metals (e.g., silver, copper,

Table 3.1 Electrical Resistivites for Some Common Materials

Material (at Room Temperature)	Electrical Resistivity ($\mu\Omega * m$)	Material (at Room Temperature)	Electrical Resistivity ($\mu\Omega * m$)
Silver	0.015	Stainless steel	0.7
Copper	0.017	Lead	0.21
Gold	0.024	Titanium	0.42
Aluminum	0.027	Nichrome	1
Tungsten	0.054	Graphite	14,000
Zinc	0.059	Wood	10^{14}–10^{17}
Nickel	0.068	Glass	10^{16}–10^{20}
Cobalt	0.09	Mica	10^{17}–10^{21}
Mild carbon steel	0.16	Teflon	$> 10^{19}$

Source: Ref. 451.

gold, aluminum) and high-resistive metals (e.g., stainless steel, titanium, carbon steel).

Electrical resistivity of a particular metal varies with temperature, chemical composition, metal microstructure, and grain size. For most metals, ρ rises with temperature. Figure 3.2 shows electrical resistivities of some commonly used metals as a function of temperature.

The resistivity of the pure metals can often be represented as a linear function of the temperature (unless there is a change in a lattice of metal)

$$\rho(T) = \rho_0[1 + \alpha(T - T_0)], \tag{3.1}$$

where ρ_0 is the resistivity at ambient temperature T_0; $\rho(T)$ is the resistivity at temperature T; α is the temperature coefficient of the electrical resistivity. The unit for α is $1/^\circ C$. Table 3.2 consists of the values of α for some pure metals.

For some electrically conductive materials, an electrical resistivity decreases with temperature and, therefore, the value of α can be a negative. For other materials (including carbon steels, alloyed steels, graphite, etc.) α is a nonlinear function of temperature due to a nonlinear function of ρ versus temperature (Figure 3.3). At melting point the electrical resistivity of metals is sharply increased (Figure 3.4).

Impurities observed in metals distort the metal lattice and can affect the behavior of ρ to a considerable extent. This is particularly true for metal alloys [100]. For most binary alloys, the behavior of ρ versus the concentration of alloying elements is represented by a bell-shaped curve. This curve has maximum electrical resistivity at the concentration of alloying elements equal to 50% of the atomic weight [100]. Figures 3.5 and 3.6 illustrate this phenomenon.

In some cases, instead of the bell-shaped curve, electrical resistivity continuously decreases or increases with the concentration of alloys. For example, the electrical resistivity of plain carbon steels increases with an increase in the carbon content.

The value of electrical resistivity is also affected by the grain size (e.g., higher ρ corresponds to finer grains), plastic deformation, heat treatment, and some other factors, but to a smaller extent compared to the effect of temperature and chemical composition.

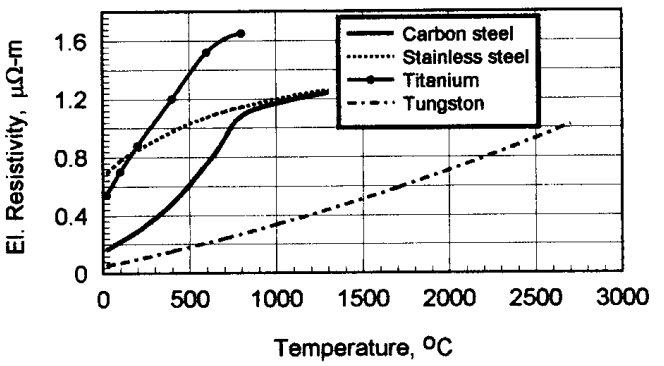

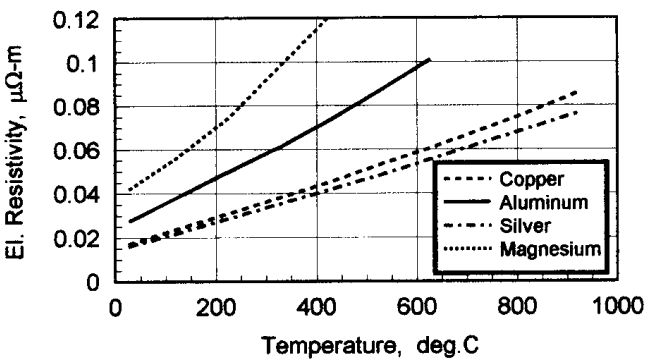

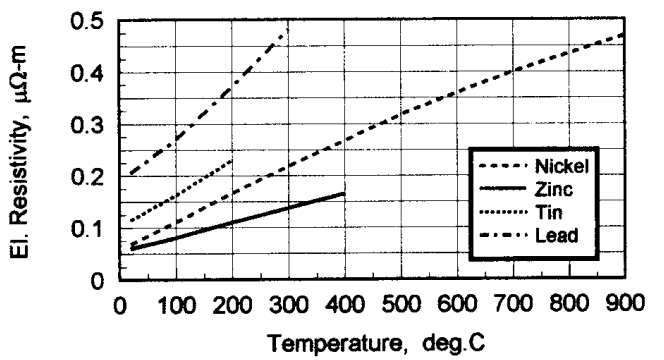

Figure 3.2 Electrical resistivities of some commercially used metals.

Table 3.2 Temperature Coefficient for Some Metals

Metals (at Room Temperature)	α (1/°C)	Metals (at Room Temperature)	α (1/°C)
Aluminum	0.0043	Nichrome	0.0004
Cobalt	0.0053	Nickel	0.0069
Copper	0.004	Silver	0.004
Gold	0.0035	Titanium	0.0035
Iron	0.005	Tungsten	0.0045
Lead	0.0037	Zinc	0.0042

Source: Ref. 450.

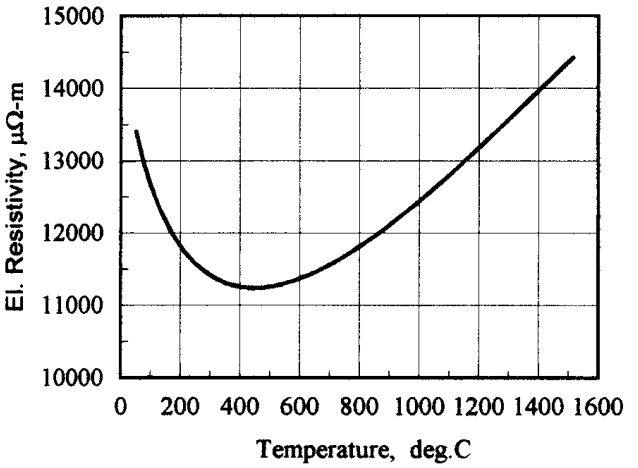

Figure 3.3 Electrical resistivity of graphite (ATL) versus temperature.

One should not confuse electrical resistivity $\rho(\Omega\text{-}m)$ with electrical resistance $R(\Omega)$. The relationship between these parameters can be expressed as

$$R = \frac{\rho l}{a}, \tag{3.2}$$

where l is the length of the current-carrying conductor and a is the area of the conductor's cross-section where the current is flowing through.

Electrical resistivity is an imperative physical property. It affects practically all important parameters of an induction heating system including depth of heating, heat uniformity, coil electrical efficiency, coil impedance, and others. An effect of ρ on a particular parameter of the induction system is discussed further in the text in the appropriate sections.

3.1.1.2 Magnetic Permeability and Relative Permittivity (Dielectric Constant)

Relative magnetic permeability μ_r indicates the ability of a material (e.g., metal) to conduct the magnetic flux better than a vacuum or air. Relative permittivity (or dielectric constant) ε indicates the ability of a material to conduct the electric field

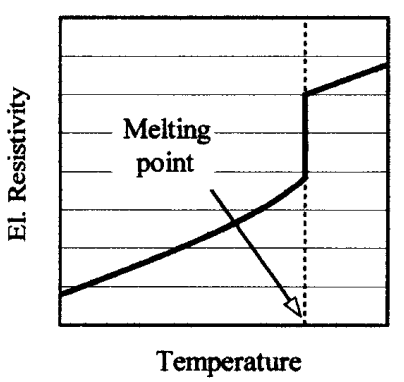

Figure 3.4 Electrical resistivity of metals versus temperature.

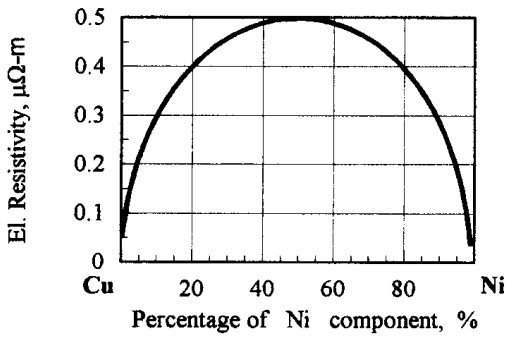

A). Electrical resistivity vs. percentage of nickel in a Cu-Ni binary alloy [16]

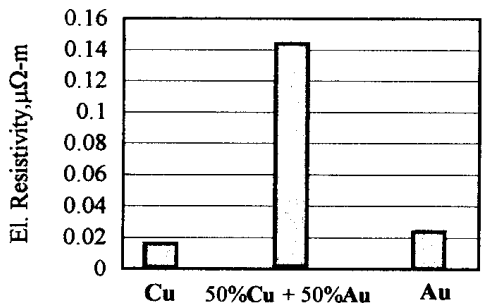

B). Electrical resistivity vs. percentage of alloying element in a Cu-Au binary alloy

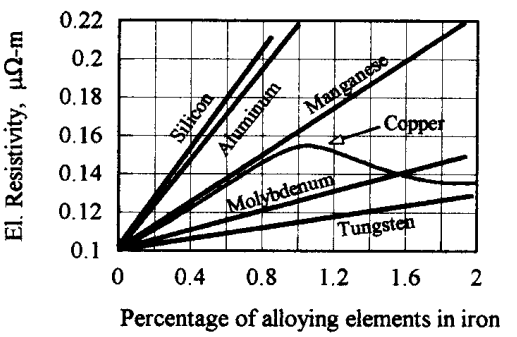

C). El. Resistivity vs. % of alloying element in iron [189]

Figure 3.5 Electrical resistivities of binary alloys.

better than a vacuum or air. Both relative magnetic permeability μ_r and relative permittivity ε are nondimensional parameters and have very similar meanings. Understanding the physics of these properties is important when designing heating systems.

Relative magnetic permeability has a marked effect on all basic induction phenomena, including the skin effect, electromagnetic edge, and end effect, as well as proximity and ring effects, and also has a marked effect on coil calculation and computation of electromagnetic field distribution. Relative permittivity is not as widely used in induction heating, but it plays a major role in dielectric heating applications.

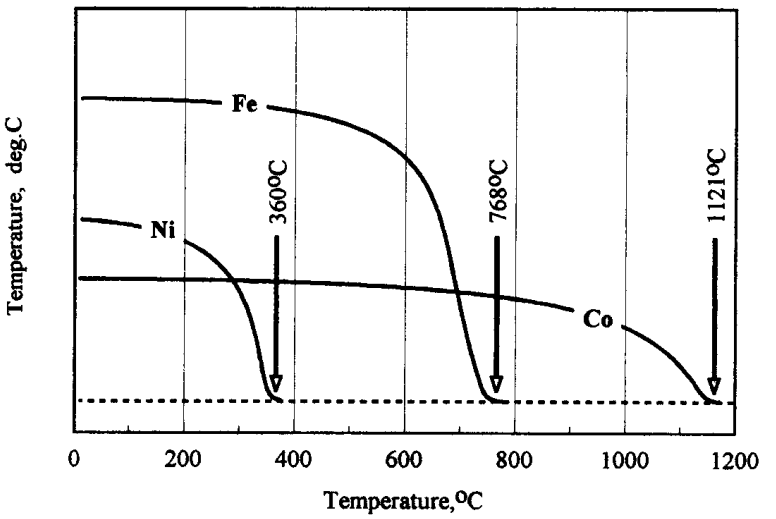

Figure 3.6 Relative magnetic permeability versus temperature of iron, nickel, and cobalt in moderate magnetic field.

The constant $\mu_0 = 4\pi \times 10^{-7}$ H/m [or Wb/(A.m)] is called the permeability of free space (the vacuum), and similarly the constant $\varepsilon_0 = 8.854 \times 10^{-12}$ F/m is called the permittivity of free space.

The product of relative magnetic permeability and permeability of the free space is called permeability μ and corresponds to the ratio of the magnetic flux density (B) to magnetic field intensity (H).

$$\frac{B}{H} = \mu_r \mu_0 \qquad \text{or} \qquad B = \mu_r \mu_0 H \tag{3.3}$$

Basic definitions, interrelations between these two properties of the magnetic field (B and H), as well as its designations are discussed in high school science textbooks and college physics textbooks and here we simply refer to those texts.

In everyday engineering language, the induction heating specialists often call the relative magnetic permeability simply magnetic permeability. The relative magnetic permeability is closely related to magnetic susceptibility by the expression:

$$\mu_r = \chi + 1 \quad \text{or} \quad \chi = \mu_r - 1. \tag{3.4}$$

In other words magnetic susceptibility shows the amount by which μ_r differs from unity.

All materials based on their magnetization ability can be divided into paramagnetic, diamagnetic, and ferromagnetic. Relative magnetic permeability of paramagnetic materials is slightly greater than 1($\mu_r > 1$). The value of μ_r for diamagnetic materials is slightly less than 1($\mu_r < 1$). Due to insignificant differences of μ_r for both paramagnetic and diamagnetic materials, in induction heating practice those materials are simply called nonmagnetic materials. Typical nonmagnetic metals are aluminum, copper, titanium, tungsten, and so on.

In contrast to paramagnetic and diamagnetic materials, ferromagnetic materials exhibit the high value of relative magnetic permeability ($\mu_r \gg 1$). There are only a few elements that reveal the ferromagnetic properties at room temperature. These

include iron, cobalt, and nickel. Some rare earth metals and gadolinium are ferromagnetic at temperatures much lower than room temperature.

The ferromagnetic property of the material is a complex function of structure, chemical composition, prior treatment, grain size, frequency, magnetic field intensity, and temperature. As one can see from Figure 3.7, the same kind of carbon steel at the same temperature and frequency can have a different value of relative magnetic permeability due to differences in the intensity of the magnetic field. For example, the magnetic permeability of magnetic steels commonly used in induction heating can vary from small values of μ_r (e.g., $\mu_r = 2$ or 3) to very high

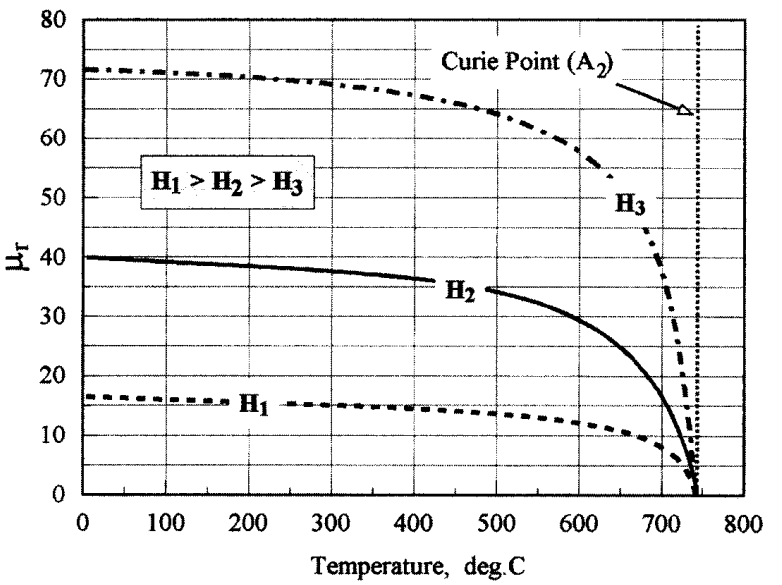

A). Effect of temperature and magnetic field intensity on relative magnetic permeability of medium carbon steel

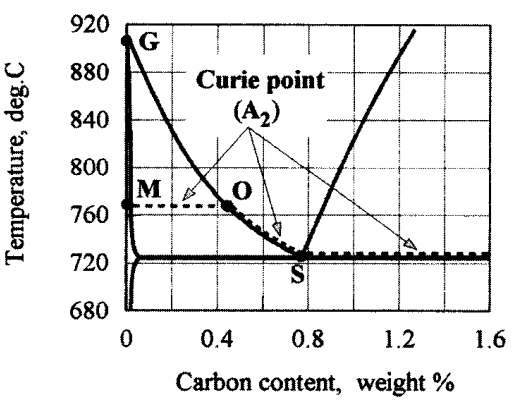

B). Curie temperature of plain carbon steel at heating rate less than 70deg.C per second

Figure 3.7 Effect of temperature, carbon content, and field intensity on relative magnetic permeability.

values of μ_r (e.g., more than 500), depending on the magnetic field intensity H and temperature.

The temperature at which a ferromagnetic body becomes nonmagnetic is called the Curie temperature (Curie point). Table 3.3 shows the Curie temperatures of some magnetic materials.

Depending upon the heat intensity (°C/sec) there can be some minor shifting of the Curie temperature. Chemical composition is another factor which has a marked effect on the Curie temperature. Even among the plain carbon steels the Curie temperature might be different due to the variation of carbon content. For example, as one can see from Table 3.3 the Curie temperature of plain carbon steel 1008 is noticeably different from steel 1060 (768°C/1414°F versus 732°C/1350°F). In the case of relatively slow heating (less then 70°C/sec) of plain carbon steels, irons, and alloyed steels, the Curie temperature can be determined based on A_{c2} and A_{r2} lines. In contrast to critical curves A_{c3} and A_{r3}, the critical curves A_{c2} and A_{r2} practically coincide with a majority of heat intensities (°C/sec) used in most induction heating and heat treating applications, thanks to a moderate thermal hysteresis.

The maximum value of relative magnetic permeability μ_r^{max} is affected by the chemical composition. For example, μ_r^{max} of high-carbon steel with 1.2% is more than three times lower compared to μ_r^{max} of low-carbon steel with 0.1% carbon content.

The magnetization curve describes the nonlinear relationship between magnetic flux density B and magnetic field intensity H. The nonlinear variation of $\mu_r = B/(H\mu_0)$ for a typical carbon steel is shown in Figure 3.8. The maximum of μ_r occurs at the "knee" of the curve. The magnetic field intensity H_{cr} that corresponds to the maximum permeability is called a critical value of H. When $H > H_{cr}$, the magnetic permeability will decrease with increasing H. If $H \to \infty$, then $\mu_r \to 1$. In conventional induction heat treating, the magnetic field intensity H_{surf} at the workpiece surface is much greater that H_{cr}. However, there are some induction heating applications where this is not true and this phenomenon will play an important role.

Similar to the current distribution, the magnetic field intensity is at its maximum value at the surface of the homogeneous workpiece and falls off exponentially toward the core (Figure 3.9). As a result, the magnetic permeability varies within the magnetic body. At the surface, μ_r^{surf} corresponds to the surface magnetic field intensity H_{surf}. In quick calculations H_{surf} can be considered as the field intensity in the air gap between the coil and the workpiece. With increasing distance from the surface, μ increases and after reaching its maximum value at $H = H_{cr}$ begins to fall off (Figure 3.9).

The complex nature of μ_r as a complex function of temperature and magnetic field intensity is shown in Figure 3.10.

Table 3.3 Curie Temperature of Some Magnetic Materials

Magnetic Material	1008	1060	Permalloy	Cobalt	Nickel
Temperature °C (°F)	768 (1414)	732 (1350)	440 (824)	1120 (2048)	358 (676)

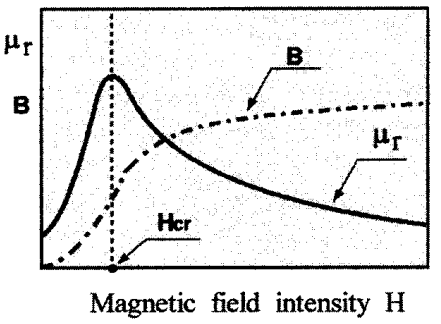

Figure 3.8 Magnetic field density (B) and relative magnetic permability (μ_r).

From Figures 3.7 and 3.10 one might think that magnetic permeability always decreases with temperature. In the majority of induction heating and heat treating applications it is the case. However, in a relatively "weak" magnetic field μ_r might first increase with temperature and only near the Curie point would magnetic permeability start to drastically decrease (Figure 3.11).

3.1.2 Skin Effect

As one may know from the basics of electricity, when a direct current flows through a conductor that stands alone (bus bar or cable), the current distribution within the conductor's cross-section is uniform. However, when an alternating current flows through the same conductor, the current distribution is not uniform. The maximum value of the current density will always be located on the surface of the conductor; the current density will decrease from the surface of the conductor toward its center. This phenomenon of nonuniform current distribution within the conductor cross-section is called the skin effect, which always occurs when there is an alternating current. Therefore, the skin effect will also be found in a workpiece located inside an induction coil (Figure 3.12). This is one of the major factors that causes the

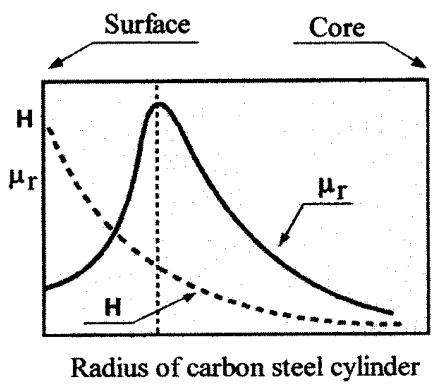

Figure 3.9 Distribution of magnetic field intensity (H) and relative magnetic permeability (μ_r) along the radius of a homogeneous carbon steel cylinder.

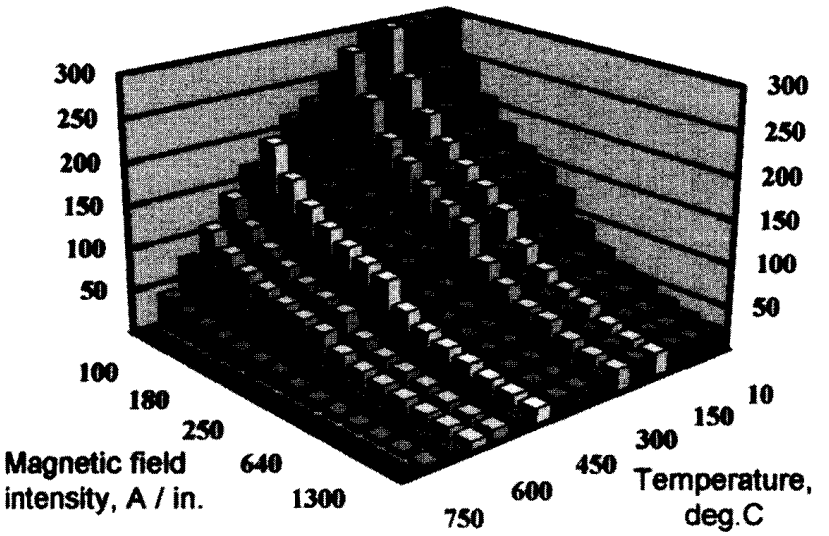

Figure 3.10 Relative magnetic permeability as a function of magnetic field intensity H = (100–1500) A/in. (39–590 A/cm) and temperature T = (10–750)°C (50–1382)°F.

concentration of eddy current in the surface layer ("skin") of the workpiece. Due to the circumferential nature of the eddy current induced in the workpiece, there is no current flow at the center of the workpiece.

The skin effect is of great practical importance in electrical applications using alternative current. Because of this effect, approximately 86% of the power will be concentrated in the surface layer of the conductor. This layer is called the reference (or penetration) depth δ. The degree of skin effect depends on the frequency and material properties (electrical resistivity ρ and relative magnetic permeability μ_r) of the conductor. There will be a pronounced skin effect when high frequency is applied or when the radius of the workpiece is relatively large (Figure 3.13). The distribution

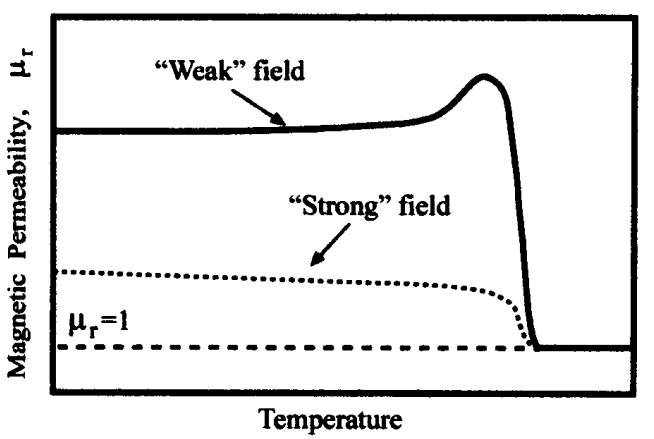

Figure 3.11 Comparison of magnetic permeabilities in relatively "weak" magnetic field and in "strong" field.

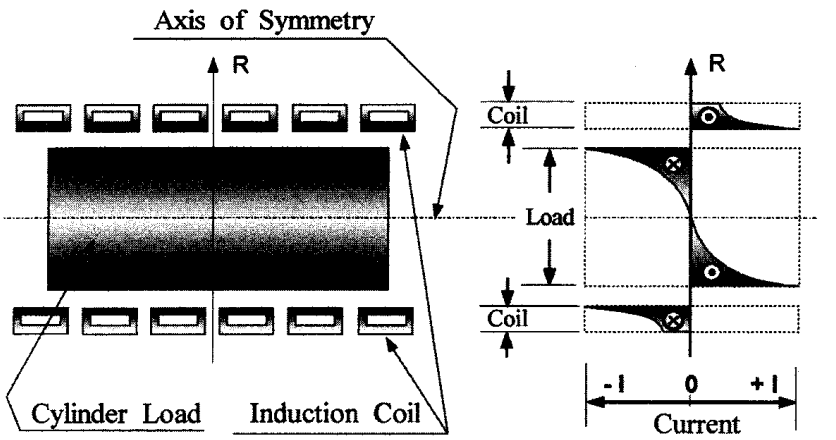

Figure 3.12 Current distribution in "coil–workpiece" induction system.

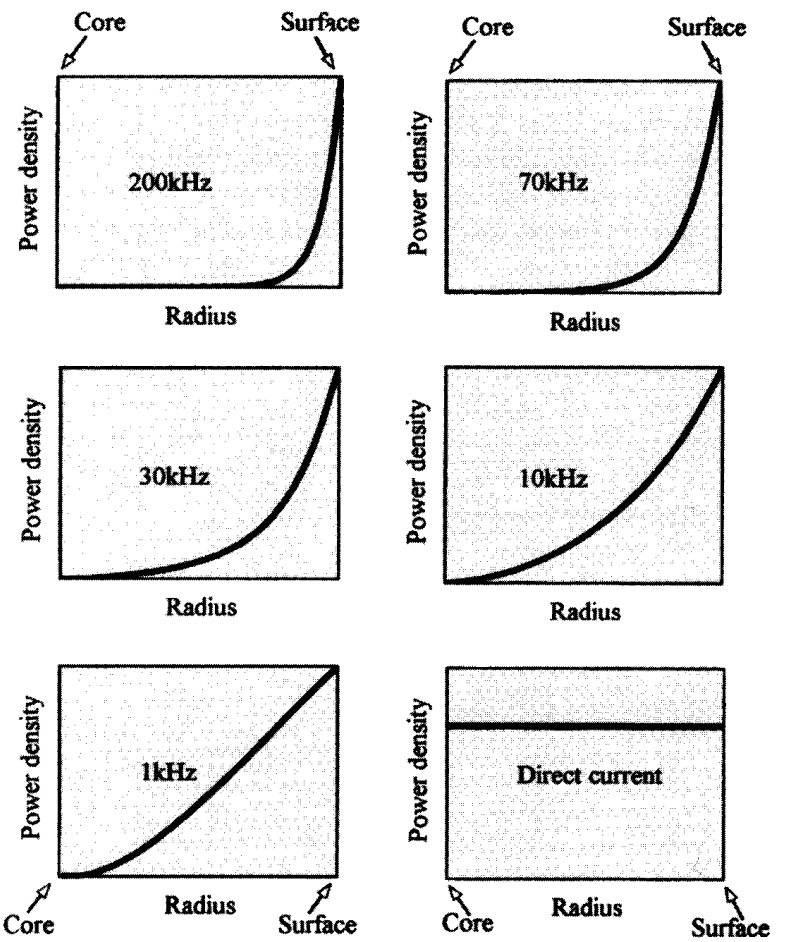

Figure 3.13 Power density (heat source) distribution along the radius of a stainless steel cylinder (OD = 20 mm).

of the current density along the workpiece thickness (radius) can be roughly calculated by the equation

$$\mathbf{I} = \mathbf{I}_0 \mathrm{e}^{-y/\delta}, \tag{3.5}$$

where $\mathbf{I}$ is current density at distance y from the surface A/m^2; $\mathbf{I}_0$ is current density at the workpiece surface A/m^2; y is the distance from the surface toward the core m, and δ is penetration depth m.

Penetration depth is described in meters as

$$\delta = 503\sqrt{\frac{\rho}{\mu_r F}}, \tag{3.6}$$

where

ρ = electrical resistivity of the metal Ω^*m,
μ_r = relative magnetic permeability, and
F = frequency, Hz (cycle/sec), or in inches

$$\delta = 3160\sqrt{\frac{\rho}{\mu_r F}}, \tag{3.7}$$

where electrical resistivity ρ is in Ω^*in.

As one can see, the value of penetration depth varies with the square root of electrical resistivity and inversely with the square root of frequency and relative magnetic permeability. Mathematically speaking, the penetration depth δ in Eq. (3.5) is the distance from the surface of the conductor toward its core at which the current decreases exponentially to "1/exp" its value at the surface. The power density at this distance will decrease to "$1/\exp^2$" its value at the surface. Figure 3.14 illustrates a skin effect appearance by showing distribution of current density and power density from the workpiece surface toward the core. As one can see from the figure, at one penetration depth from the surface ($y = \delta$) the current will equal 37% of its surface value. However, the power density will equal 14% of its surface value. From this we can conclude that 63% of the current and 86% of the power in the workpiece within a surface layer of thickness δ will be concentrated.

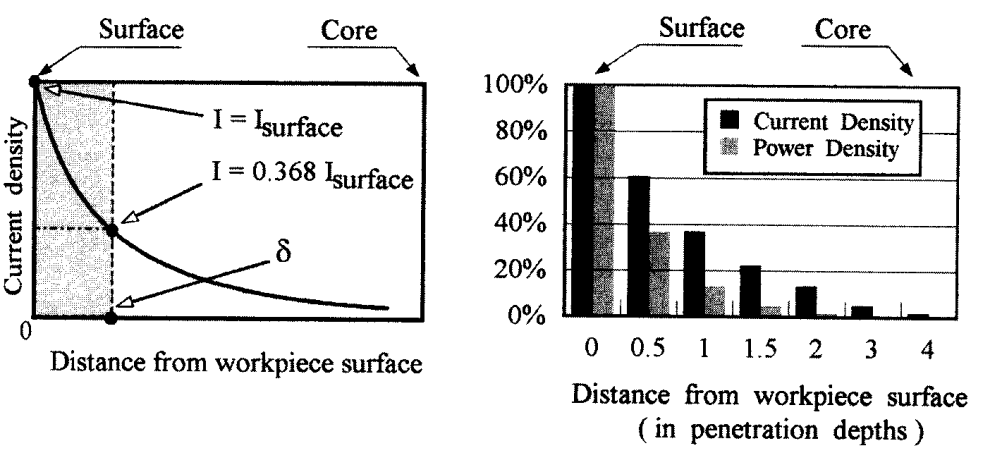

Figure 3.14 Current and power density distributions due to skin effect.

Analysis of Eqs. (3.6) and (3.7) shows that the penetration depth has different values for different materials and is a function of frequency. The magnetic permeability δ of nonmagnetic materials is equivalent to that of air and is assigned a value of 1. The electrical resistivity of metals ρ is a function of temperature (Figure 3.2). During the heating cycle ρ of most metals can increase to four to five times its initial value. Therefore, even for nonmagnetic metals, during the heating cycle the penetration depth can increase significantly. Table 3.4 shows some penetration depths of metals that are most commonly used with induction heating.

While discussing the behavior of μ_r within a ferromagnetic workpiece, it is necessary to mention that the definition of penetration depth of current in its classical form (Eqs. 3.6 and 3.7) does not have a fully determined meaning because of the nonconstant distribution of μ_r within the workpiece. In engineering practice, the value of relative magnetic permeability at the surface of the workpiece is typically used to give a determination of those equations in definite form. Here we also use the value of μ_r^{surf} to determine the penetration depth in the magnetic workpiece. Figure 3.15 and Table 3.5 show the value of the penetration depth in carbon steel (1045) at an ambient temperature (21°C or 70°F) as a function of frequency and magnetic field intensity H at the workpiece surface.

From another perspective, penetration depth is a function of temperature as well. At the beginning of the heating cycle, the current penetration into the carbon steel workpiece will increase slightly (Figure 3.16) because of the increase in electrical resistivity of the metal with temperature. With a further rise of temperature (at approximately 550°C or 1022°F), μ_r starts to decrease more and more. Near a critical temperature T_c, known as the Curie temperature or Curie point, permeability drastically drops to unity because the metal becomes nonmagnetic. As a result, the penetration depth will increase significantly. After heating above the Curie temperature, the penetration depth will continue to increase due to the increase in electrical resistivity of the metal (Figure 3.16). However, the rate of growth will not be as significant as it was during the transition through the Curie temperature.

The variation of δ during induction heating of a carbon steel workpiece drastically changes the degree of skin effect. Figure 3.17 shows how many times the current penetration depth of some metals can increase during heating. It is especially important to take this phenomenon into account when designing for induction through hardening of carbon steel where the core-to-surface temperature difference is primarily a result of skin effect.

In most publications devoted to induction heating and induction heat treating, distributions of current and power densities (heat source distribution) along the workpiece thickness/radius are simplified and introduced as being always exponentially decreasing from the surface into the workpiece. This assumption is correct only for a homogeneous nonmagnetic solid body with constant electrical resistivity within the workpiece.

However, realistically speaking this assumption can be made for only some unique cases because for the great majority of induction heating applications (thanks to the skin effect and some other electromagnetic phenomena which are discussed in the following chapters), the current density (heat source) distribution is not uniform and there are always thermal gradients within the heated workpiece. These thermal gradients result in nonuniform distribution of electrical resistivity and magnetic permeability within the workpiece.

Table 3.4 Penetration Depth of Nonmagnetic Metals (mm)

	T		ρ		Frequency (kHz)										
Metal	°C	°F	μΩ · m	μΩ · in.	0.06	0.50	1	2.5	4	8	10	30	70	200	500
Aluminum	20	68	0.027	1.06	10.7	3.70	2.61	1.65	1.30	0.92	0.83	0.48	0.31	0.18	0.12
	250	482	0.053	2.09	15.0	5.18	3.66	2.32	1.83	1.29	1.16	0.67	0.44	0.26	0.16
	500	932	0.087	3.43	19.2	6.64	4.69	2.97	2.35	1.66	1.48	0.86	0.56	0.33	0.21
Copper	20	68	0.018	0.71	8.81	3.05	2.16	1.36	1.08	0.76	0.68	0.39	0.26	0.15	0.10
	500	932	0.050	1.97	14.5	5.03	3.56	2.25	1.78	1.26	1.12	0.65	0.43	0.25	0.16
	900	1,652	0.085	3.35	19.3	6.67	4.72	2.98	2.36	1.67	1.49	0.86	0.56	0.33	0.21
Brass	20	68	0.065	2.56	16.6	5.74	4.06	2.56	2.03	1.43	1.28	0.74	0.48	0.29	0.18
	400	752	0.114	4.49	21.9	7.60	5.37	3.40	2.69	1.90	1.70	0.98	0.64	0.38	0.24
	900	1,632	0.203	7.99	29.3	10.1	7.17	4.53	3.58	2.53	2.27	1.31	0.86	0.51	0.32
Stainless steel	20	68	0.690	27.2	53.9	18.7	13.2	8.36	6.61	4.67	4.18	2.41	1.58	0.93	0.59
	800	1,472	1.150	45.3	69.6	24.1	17.1	10.8	8.53	6.03	5.39	3.11	2.04	1.21	0.76
	1,200	2,192	1.240	48.8	72.3	25.1	17.7	11.2	8.86	6.26	5.60	3.23	2.12	1.25	0.79
Silver	20	68	0.017	0.67	8.34	2.89	2.04	1.29	1.02	0.72	0.65	0.37	0.24	0.14	0.09
	300	572	0.038	1.50	12.7	4.39	3.10	1.96	1.55	1.10	0.98	0.57	0.37	0.22	0.14
	800	1,472	0.070	2.76	17.2	5.95	4.21	2.66	2.10	1.49	1.33	0.77	0.50	0.30	0.19
Tungsten	20	68	0.050	1.97	14.5	5.03	3.56	2.25	1.78	1.26	1.12	0.65	0.43	0.83	0.53
	1,500	5,072	1.550	21.7	48.2	16.7	11.8	7.46	5.90	4.17	3.73	2.15	1.41	0.83	0.53
	2,800	5,072	1.040	40.9	66.2	22.9	16.2	10.3	8.11	5.74	5.13	2.96	1.94	1.15	0.73
Titanium	20	68	0.500	19.7	45.9	15.9	11.3	7.11	5.62	3.98	3.56	2.05	1.34	0.80	0.50
	600	1,112	1.400	55.1	76.8	26.6	18.8	11.9	9.41	6.65	5.95	3.44	2.25	1.33	0.84
	1,200	2,192	1.800	70.9	87.1	30.2	21.3	13.5	10.7	7.54	6.75	3.90	2.55	1.51	0.95

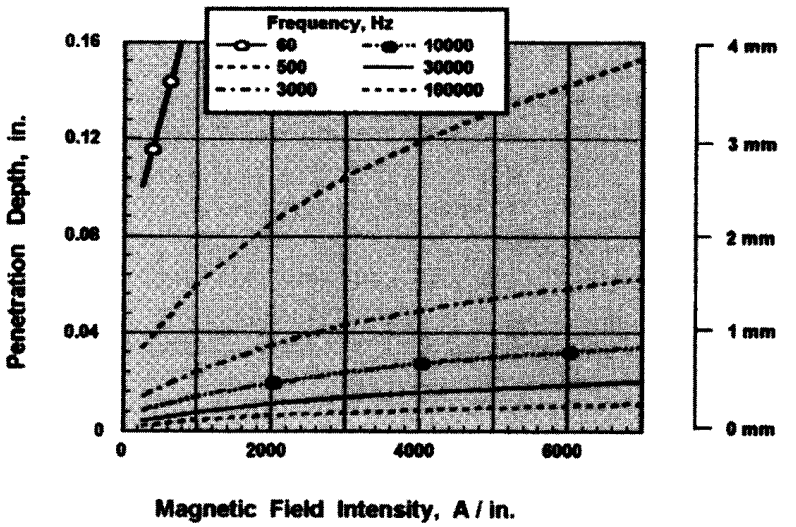

Figure 3.15 Current penetration in carbon steel (1045) at ambient temperature 21°C (70°F).

In addition, as shown in the previous section, relative magnetic permeability is nonuniform along the workpiece thickness due to a nonuniform distribution of the magnetic field intensity (Figure 3.9).

An assumption of exponential current density distribution (Eq. 3.5) can be used in induction heating calculations for the purpose of rough engineering estimations for heating of nonmagnetic materials and in through heating of carbon steels to forging temperatures.

However, in some applications, such as surface hardening, the power density distribution along the radius/thickness has a unique wave-shaped form, which is significantly different than the classical exponential distribution. The maximum power density is located at the surface. Then the power density decreases toward the core. However, once it reaches a certain distance from the surface, the power density starts to increase again and after reaching a maximum, it starts to decrease again.

This wave-shaped phenomenon was originally independently briefly discussed by M. Lozinskii and P. Simpson in their respective texts [2, 3]. Both authors intuitively felt that there should be situations when distribution of the power density (heat sources) would be different compared to traditionally accepted exponential form. Unfortunately, due to computer limitations at that time and the unavailability of sufficiently sophisticated software to model the induction heating processes, it was not possible to describe that phenomenon in more detail. Obviously, it was not possible to measure the power density distribution within the solid body as well.

The new generation of coupled software (e.g., ADVANCE software) allows one to make a quite accurate prediction regarding the physics of that power density wave-shaped phenomenon and quantify its appearance. An appearance of this phenomenon in different applications (surface hardening, bar heating, etc.) is discussed later in this text in corresponding sections. At this point, we mention only that this phenomenon is pronounced when the surface of the heated workpiece is heated above the Curie temperature; however, areas located just below the surface still retain their magnetic properties.

Table 3.5 Penetration Depth of Carbon Steel 1040 at Ambient Temperature of 21°C (70°F)

Magnetic Field Intensity		Frequency (Hz)											
		60		500		3,000		10,000		30,000		100,000	
		Penetration Depth											
A/mm	A/in.	mm	in.	mm	in.	mm	in.	mm	in.	mm	in.	mm	in.
10	250	2.50	0.100	0.88	0.034	0.36	0.014	0.2	0.008	0.11	0.004	0.06	0.002
40	1000	4.70	0.185	1.63	0.064	0.67	0.026	0.36	0.014	0.21	0.008	0.12	0.005
80	2000	6.30	0.249	2.20	0.086	0.9	0.035	0.49	0.019	0.28	0.011	0.16	0.006
160	4050	8.76	0.345	3.03	0.119	1.24	0.049	0.68	0.027	0.39	0.015	0.21	0.008
200	5100	9.63	0.379	3.33	0.131	1.36	0.054	0.75	0.029	0.43	0.017	0.24	0.009
280	7100	11.20	0.442	3.89	0.153	1.59	0.062	0.87	0.034	0.50	0.020	0.27	0.011

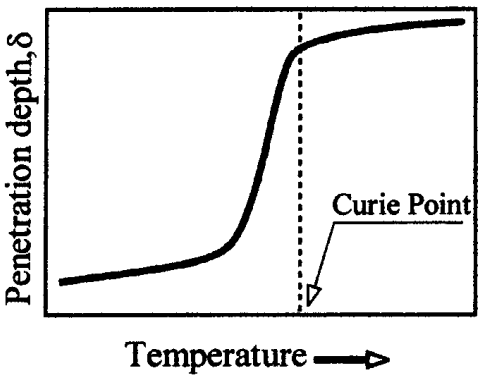

Figure 3.16 Typical variations of current penetration depth during induction heating of a carbon steel workpiece.

When discussing the skin effect it is proper to introduce the terms of electromagnetically *thick* and electromagnetically *thin* bodies [20]. Depending upon the chosen frequency and magnetic field orientation any body can be considered from the electromagnetic point of view as a *thick* body or *thin* body. If a current penetration depth is greater compared to the thickness or diameter of the solid body, then it is considered to be an electromagnetically *thin* body. There is a distinct current cancellation within the electromagnetically *thin* bodies and, therefore, only a negligible amount of energy will be absorbed by it. Being transparent to the external electromagnetic field, there will be only small amounts of the Joule effect appearing in electromagnetically *thin* bodies.

If the thickness or diameter of the solid electrically conductive body is six times the current penetration depth, then it can be considered as an electromagnetically *thick* body. Since current penetration depth can increase more than 15 times during the heating cycle, the workpiece that initially could be considered as an electromagnetically *thick* body can become at the end of the heating cycle an electromagnetically *thin* body.

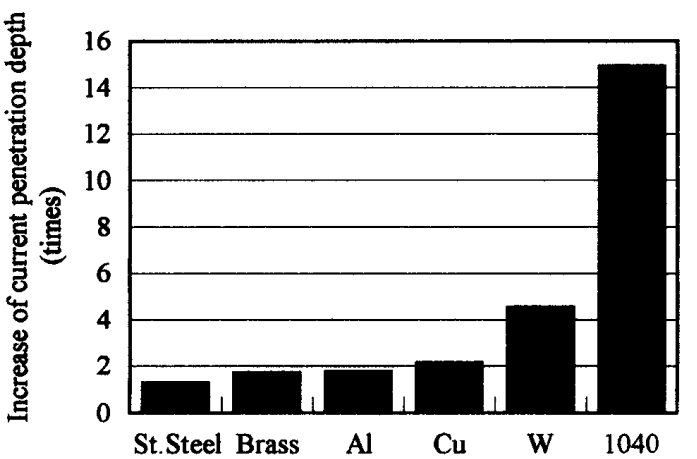

Figure 3.17 Variation of current penetration depths of different metals during induction heating.

Besides the frequency, the orientation of the body with respect to the electromagnetic field has a marked effect on considering the workpiece as a *thin* or *thick* body from an electromagnetic point of view. If orientation of the workpiece compared to the inductor results in a current cancellation, then the workpiece can be considered a *thin* body, otherwise it can be called a *thick* body. Figure 3.18 shows that depending upon plate or slab orientation compared to the inductor, it can be called a *thin* or *thick* body.

Geometry alone cannot determine whether a workpiece should be considered an electromagnetically *thin* or *thick* body. For example, when using a solenoidal coil, a stainless steel billet of 25mm (1 in.) diameter will act during induction heating as an electromagnetically *thin* body using line frequency. In contrast, a stainless steel billet of 12.7 mm (0.5 in.) diameter will be considered an electromagnetically *thick* body if a frequency of 70 kHz is applied.

3.1.3 Electromagnetic Proximity Effect

When we discussed the skin effect in conductors or cables, we assumed that a conductor stands alone and that there are no other current-carrying conductors in the

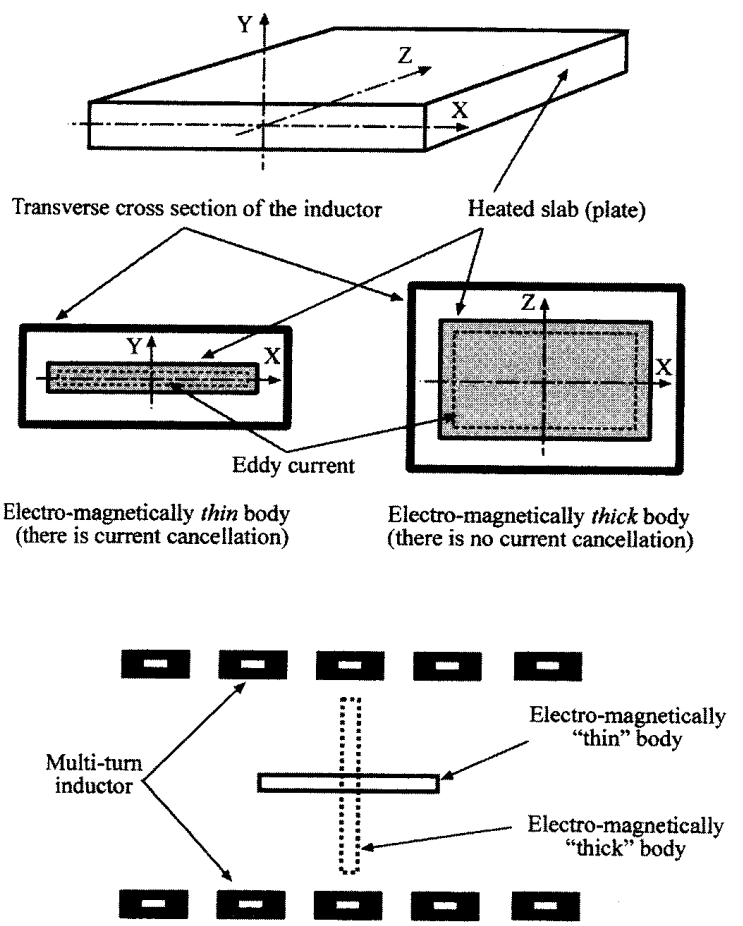

Figure 3.18 Electromagnetically *thin* and *thick* bodies.

surrounding area. In most practical applications this is not the case. Most often there are other conductors in close proximity. These conductors have their own magnetic fields, which interact with nearby fields, and as a result the current and power density distributions will be distorted.

An analysis of the effect on current distribution in a conductor when another conductor is placed nearby is given below. Figure 3.19a shows the skin effect and magnetic field distribution in a conductor (e.g., cylindrical bar) that stands alone. When another current carrying conductor is placed near the first one, the currents in both conductors will redistribute. If the currents flowing in the conductors have opposite directions, then both currents (Figure 3.19b) will be concentrated in the areas facing each other (internal areas). However, if the currents have the same direction, then these currents will be concentrated on opposite sides of the conductors (Figure 3.19c). The same will be true with bus bars (Figure 3.20).

When the currents flow in opposite directions, a strong magnetic field forms in the area between the bus bars (Figure 3.20). This occurs because in this area the magnetic field lines that are produced by each bus bar have the same direction. Therefore, the resulting magnetic field between the bus bars will be very strong. However, because the current is concentrated in the internal areas, the external magnetic field will be weak. The external magnetic fields will have opposite directions and will tend to cancel each other. The phenomena is used in coaxial cables. The

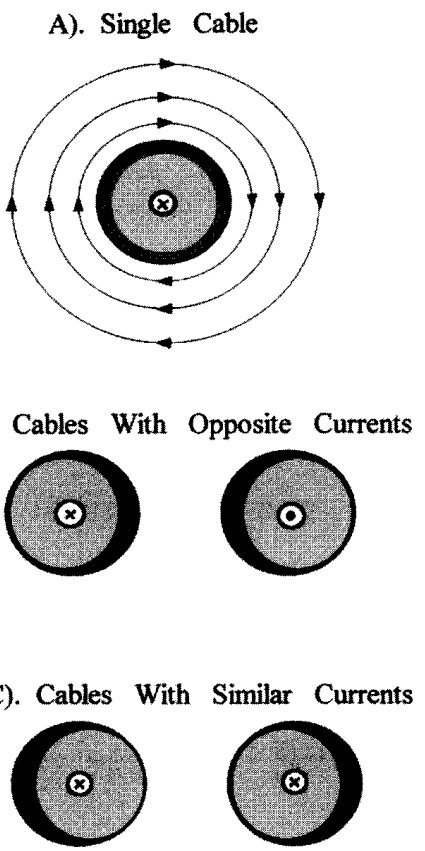

Figure 3.19 Proximity effects in cylindrical conductions.

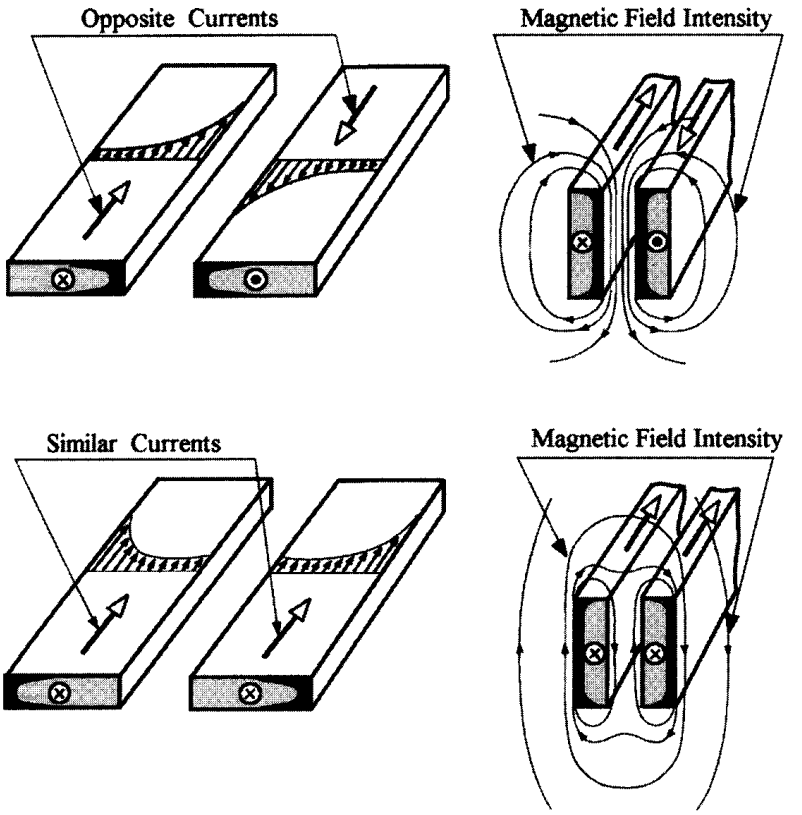

Figure 3.20 Current distribution in bus bars due to the proximity effect.

opposite is true if the currents have the same direction, for then the magnetic field lines will have opposite directions in the area between bus bars, and therefore they will cancel each other in that area. Because of this cancellation, a weak magnetic field will exist between the bus bars; however, the external magnetic field will be quite strong because the magnetic lines produced by the two conductors will have the same direction in the external area.

If the distance between bars increases, then the strength of the proximity effect will decrease. Proximity effect in the case of nonsymmetrical systems is shown in Figure 3.21.

The phenomenon of proximity effect can be directly applied in induction heating. Induction systems consist of two conductors [143]. One of these conductors is an inductor that carries the source current (Figure 3.22), and the other is the workpiece located near the inductor. Eddy currents are induced in the workpiece by an external alternating magnetic field of the source current (Figure 3.22b). As will be shown in Sec. 3.4.1, due to Faraday's law, eddy currents induced within the workpiece have an opposite direction to that of the source current of the inductor. Therefore, due to proximity effect, the coil current and workpiece eddy currents will concentrate in the areas facing each other (Figure 3.22a). This is the second factor that causes a current redistribution in an induction heating system as shown in Figure 3.12.

Figure 3.23 shows how the electromagnetic proximity effect produces different heating patterns. A carbon steel cylinder is located asymmetrically inside a single-

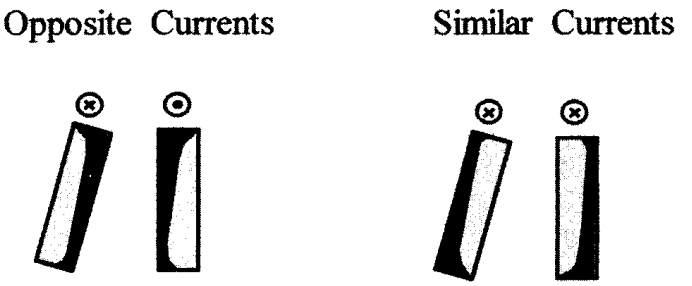

Figure 3.21 Proximity effect in nonsymmetrical systems.

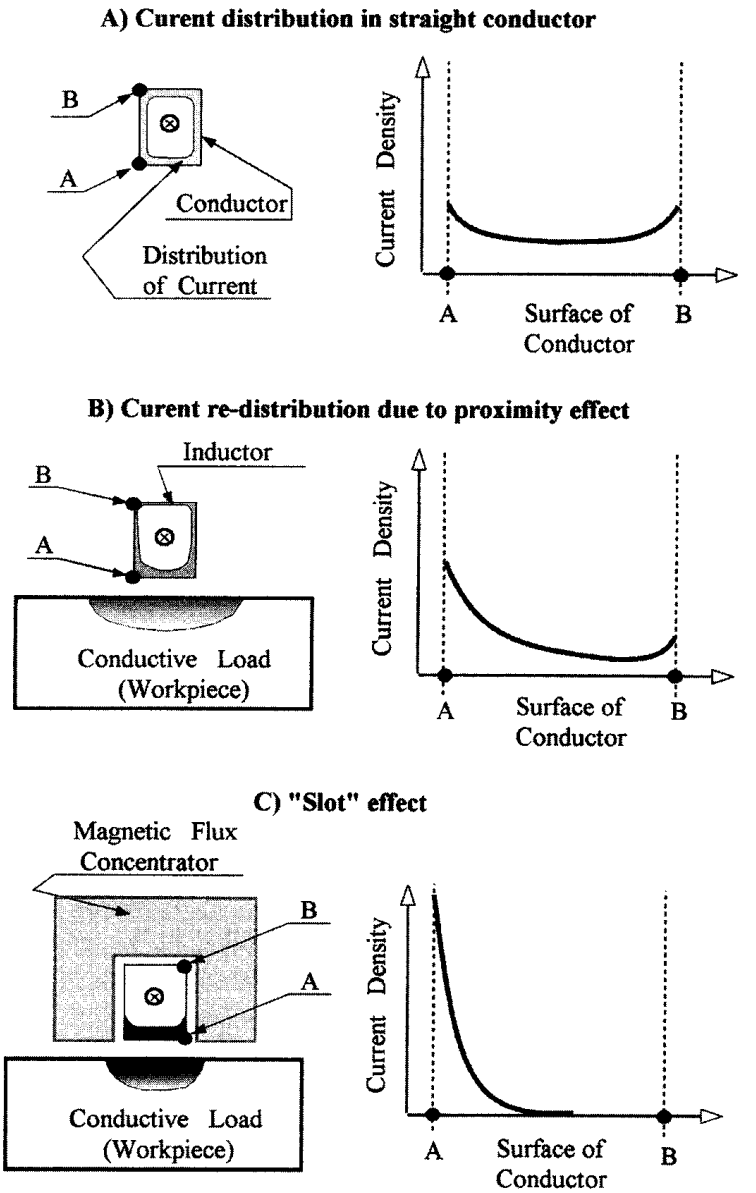

Figure 3.22 Current distribution due to proximity and slot effect.

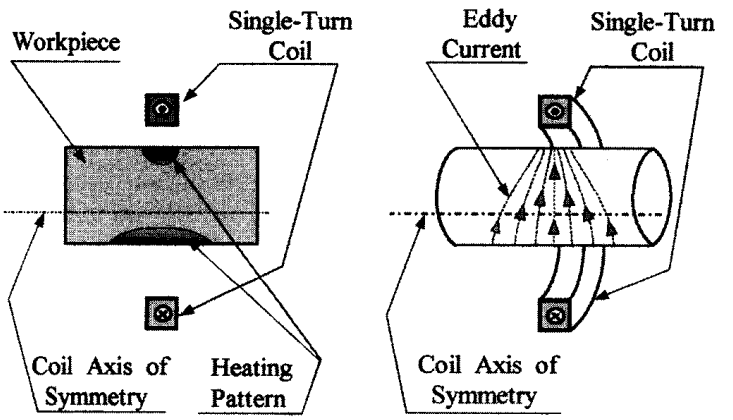

Figure 3.23 Proximity effect in nonsymmetrical single-turn inductor.

turn inductor. If the cylinder is statically heated (without rotation), then two different patterns will develop in its cross-section. The appearance of these patterns is caused by a difference in the eddy current distribution in the cylinder. As shown in Figure 3.23, the eddy currents have a higher density in the workpiece area where the coil-to-workpiece air gap is small (good coupling). Therefore, there will be intense heating due to the Joule effect. As a result, the heat pattern will be relatively narrow and deep.

In the area with the larger air gap (poor coupling) the temperature rise will not be as significant as in the case of good coupling. Also, the heat pattern will be much wider and more shallow.

In the case of an unequal coil–workpiece air gap, an almost identical heat pattern can be obtained by rotating the workpiece.

An understanding of the physics of the electromagnetic proximity and skin effects is important not only in induction heating but also in power supply and bus design. The proper design of a bus network will significantly decrease its impedance-minimizing voltage drop and power losses.

There is another electromagnetic effect that is related to the proximity effect. This is called the "slot" effect.

3.1.4 Electromagnetic Slot Effect

When we discussed the proximity effect, we first introduced the current distribution in a standalone conductor (Figure 3.22a) and then observed the current redistribution when an electrically conductive load (workpiece) was located near this conductor (Figure 3.22b). As shown in Figure 3.22b, a significant part of the conductor's current will flow near the surface of the conductor that faces the load. The remainder of the current will be concentrated in the sides of the conductor [143].

Continuing our study, let us locate an external magnetic flux concentrator (e.g., C-shaped laminations) around this conductor as shown in Figure 3.22c. As a result, practically all of the conductor's current will be concentrated on the surface facing the workpiece. The magnetic concentrator will squeeze the current to the "open surface" of the concentrator, in other words, to the open area of the slot. It is

necessary to mention here that the slot effect will also take place without the workpiece. In this case, the current will be slightly redistributed in the conductor, but most of it will still be concentrated in the "open surface" area. This effect always occurs when there is a conductor located within the magnetic slot. The actual current distribution in the conductor depends on the frequency, magnetic field intensity, geometry, and electromagnetic properties of the conductor and the concentrator.

Slot and proximity effects play a particularly important role in the proper design of coils for selective induction hardening including channel, hairpin, spiral–helical, and pancake types of inductors.

The slot effect is widely used not only in connection with induction heating but also in the design of other industrial machines such as motor generators and AC and DC machines.

3.1.5 Electromagnetic Ring Effect

Up to now we have discussed current density distribution in straight conductors. One such conductor, a rectangular bus bar, and its current distribution are shown in Figure 3.24. If that current-carrying bar is bent to shape it into a ring, then its current will be redistributed. Magnetic flux lines will be concentrated inside the ring, and therefore the density of the magnetic field will be higher inside the ring. Outside the ring, the magnetic flux lines will be disseminated. As a result, most of the current will flow within the thin inside surface layer of the ring [4]. As one can see, this ring effect is somewhat similar to the proximity effect. Figure 3.25 also shows the appearance of the electromagnetic ring effect in cylinders. As one can see, this effect leads to a concentration of current on the inside surface of the induction coil. The ring effect takes place not only in single-turn inductors but also in multiturn coils. Therefore, it is the third electromagnetic effect that is responsible for the current distribution in the induction system shown in Figure 3.12.

The appearance of the ring effect can have a positive or negative effect on the process. For example, in conventional induction heating of cylinders, when the

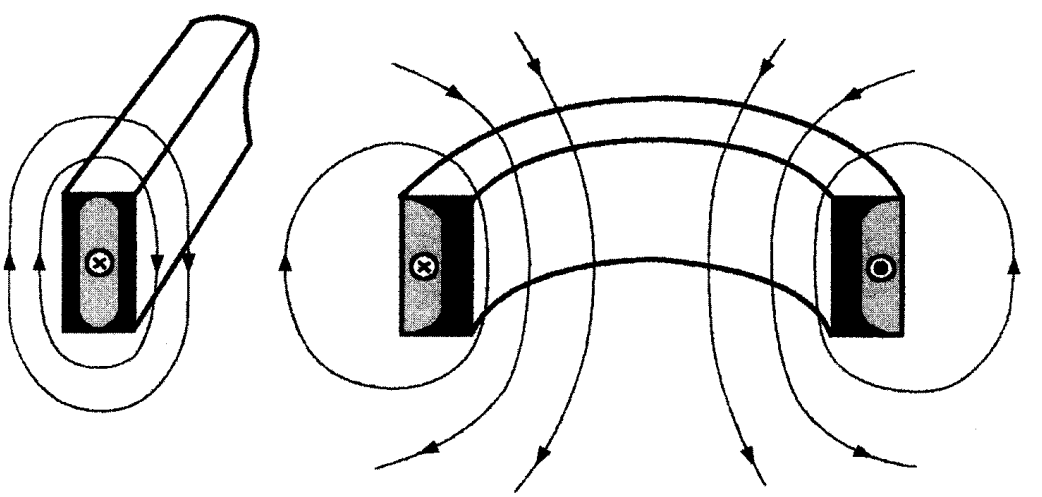

Figure 3.24 Ring effect in rectangular conductors.

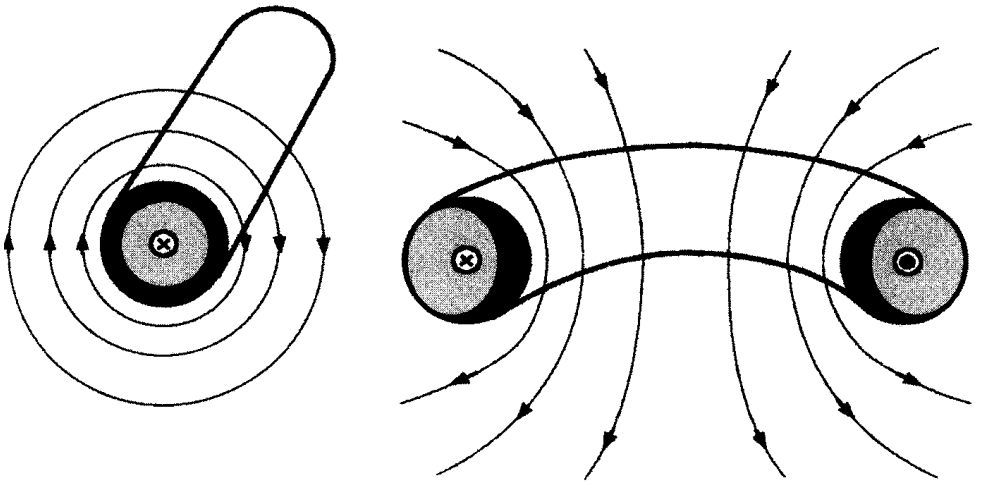

Figure 3.25 Ring effect in round conductors.

workpiece is located inside the induction coil this effect plays a positive role because in combination with the skin and proximity effects it will lead to a concentration of the coil current on the inside diameter of the coil. As a result, there will be close coil–workpiece coupling, which leads to good coil efficiency.

The ring effect plays a negative role in the induction heating of internal surfaces (so-called I.D. heating), where the induction coil is located inside the workpiece. In this case, this effect leads to a coil current concentration on the inside diameter of the coil. This makes the coil–workpiece coupling poor and, therefore, decreases coil efficiency. However, despite the ring effect, the proximity effect here tends to move the coil current to an outside surface of the coil. Therefore the coil current distribution in such applications is a result of two counteracting phenomena: the proximity and ring effects. It should be mentioned here that in order to "help" the proximity effect dominate the ring effect, in a great majority of I.D. heating applications a magnetic flux concentration is located inside the coil. This allows a slot effect to appear and "assist" the proximity effect to increase the coil efficiency and overcome the ring effect. The ring effect plays an important role in power supply design also. Because of this effect, the current is concentrated in areas where bus bars are bent, which leads to undesirable overheating of certain areas of the bus bar. To avoid local overheating it is necessary to take this effect into account when designing the cooling circuit for the bus bar.

3.1.6 Electromagnetic Force

A current-carrying conductor placed in a magnetic field experiences the force that is proportional to current and magnetic flux density. Thanks to an experimental study conducted by Ampère and Biot-Savart this force can be quantified. If current I carrying element dl is placed in the magnetic field B it will experience the force dF according to formula (3.8):

$$dF = I \times B\,dl = IB\,dl \sin\varphi, \tag{3.8}$$

where F, I, and B are vectors and φ is the angle between the direction of the current I and magnetic field B.

In SI units the force measures in newtons (N). Figure 3.26 shows that the direction of the force experienced by the element dl of the current-carrying conductor placed in an external magnetic field B can be determined based on the left-hand rule. According to the left-hand rule, if the middle finger follows the direction of the current flow and the pointer finger follows the direction of the magnetic flux of the external field (magnetic field lines head on into the palm) then the thumb will show the direction of the force.

As follows from formula (3.8), if the angle φ between the direction of the current I and magnetic field B is equal to zero, then $\sin\varphi = 0$ and therefore there will not be any force experience by the current-carrying conductor. In other words, if the current-carrying conductor is parallel to a magnetic field then conductor will not experience any forces from an external field.

Let's consider some of the most common cases of the appearance of magnetic forces in induction heating applications.

1. If two current-carrying conductors (e.g., bus bars or cables) with the currents oriented in opposite directions are located near each other then each conductor will experience forces oriented in the opposite direction (Figure 3.27, top) trying to separate both conductors $F_{12} = -F_{21}$.
2. In contrast, if two conductors carrying currents are oriented in the same direction, forces will be oriented in a way that tries to squeeze both conductors toward each other, experiencing an attractive (repulsive) force $F_{12} = F_{21}$ (Figure 3.27, bottom). The value of those forces in some cases might be so significant that they can result in shape distortion and even banding of bus bars. At this point, it will be imperative to conduct some simplified calculations of generated magnetic forces taking place between two thin wires carrying a current of 200 A each and separated by 20 mm. From the basics of the electromagnetics it is known [39–46] that each of the two parallel current-carrying wires produces a magnetic field according to Eq. (3.9),

$$B = \frac{\mu_0 I}{2\pi R}, \tag{3.9}$$

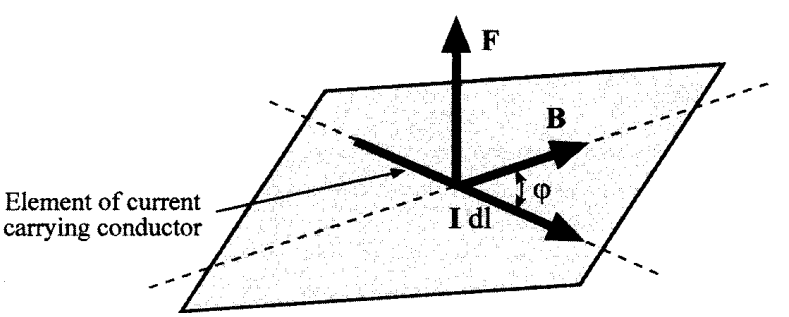

Figure 3.26 Left-hand (FBL) rule of magnetic force.

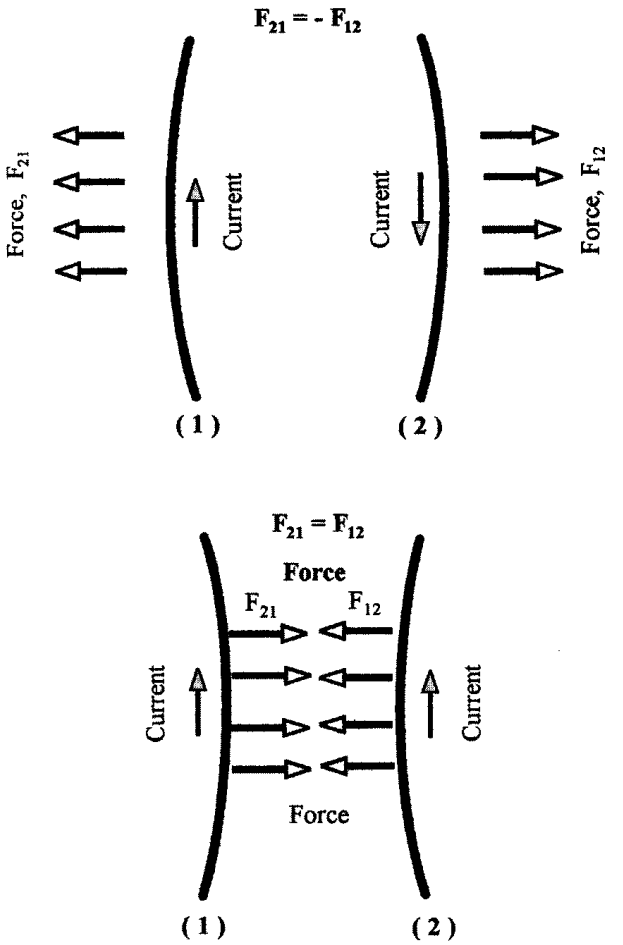

Figure 3.27 Magnetic force in current-carrying conductors.

where R is the radial distance between wires (Figure 3.28). Therefore the magnetic force experienced by the second wire will be according to formula (3.8) as

$$F = I_2 \frac{\mu_0 I_1}{2\pi R} l$$

or the force per unit length will be

$$\frac{F}{l} = I_2 \frac{\mu_0 I_1}{2\pi R}.$$

Therefore, in our case, the force per unit length will be

$$\frac{F}{l} = \frac{(4\pi \times 10^{-7}\ Wb/(\text{A} \times \text{m})(200\,\text{A})^2)}{2\pi(0.02\,\text{m})} = 0.4\,\text{N/m}.$$

3. Let's apply the above-discussed phenomena to a solenoid coil. When alternative voltage is applied to a multiturn solenoid resulting in a current flow within it, the distribution of forces will be as shown in Figure 3.29. Since current flowing in each turn of the multiturn solenoid is oriented in

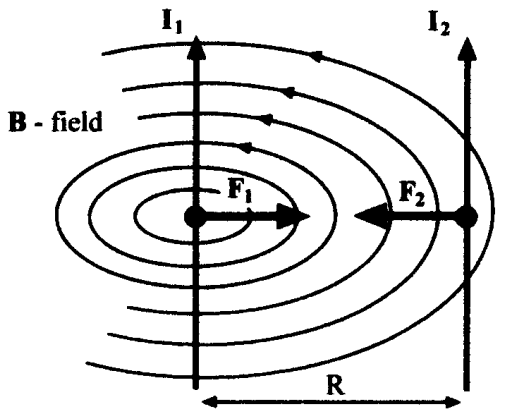

Figure 3.28 Magnetic interaction between two thin wires.

the same direction, turns will experience the longitudinal compressive stresses. It can be shown that assuming an infinitely long solenoid and a homogeneous magnetic field, the longitudinal magnetic pressure (density of the magnetic force measures in N/m^2) f_l inside the long solenoid can be determined as

$$f_l = F_l/\text{Area} = \mu_0 H_t^2/2 = B_t^2/(2\mu_0). \tag{3.10}$$

In the case of an infinitely long multiturn solenoid H_t is the r.m.s. tangential component of vector H,

$$H_t = NI/l. \tag{3.11}$$

At the same time, in the radial direction, turns of the solenoid experience tensile forces, because the current flowing on opposite side of each turn is oriented in the opposite direction. Interestingly enough, after some simple algebra, the radial tensile magnetic pressure f_R can be described as

$$f_R = \mu_0 H_t^2/2 = B_t^2/(2\mu_0). \tag{3.12}$$

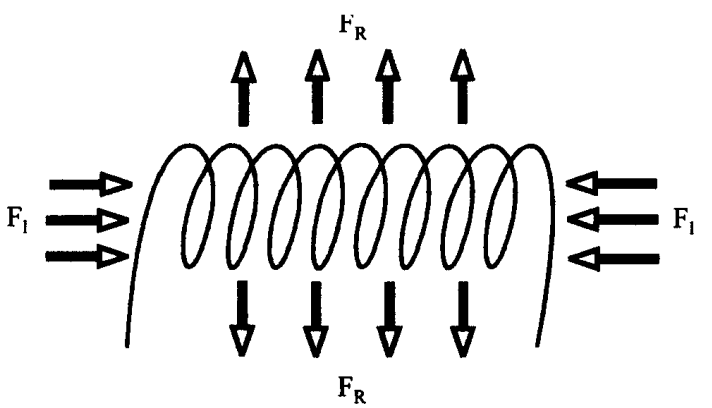

Figure 3.29 Magnetic forces in a solenidal coil.

Another assumption used while obtaining formulas (3.10) and (3.12) is that the solenoid is empty or consists of an infinitely long nonmagnetic load with a constant electrical resistivity. It is imperative to mention here that since eddy currents flowing within the heated workpiece are oriented in the opposite direction compared to the coil current, the coil turns experience tensile magnetic pressure but the workpiece is under compressive pressure. In order to provide a rigid and reliable coil design, this magnetic pressure should be taken into consideration particularly for inductors that apply proximity heating (e.g., pancake and butterfly coils) and when using low frequencies for heating low-resistive metals (e.g., induction billet heaters of copper, silver, and aluminum alloys).

4. So far we considered infinitely long solenoids and infinitely long nonmagnetic load. However, when the induction coil and workpiece are of finite length (which is the realistic case), the electromagnetic end and edge effects have a pronounced effect on the value and distribution of the magnetic forces. Since the electromagnetic end and edge effects are discussed in the next section, we limit our analysis here regarding magnetic forces in finite length induction systems to the following examples (Figure 3.30).
   4.1. If the nonmagnetic bar is partially placed inside a multiturn inductor (Figure 3.30, top) to provide the bar end heating, the magnetic force will act so as to eject the bar from the coil. The heating bars of low electrical resistive metals result in stronger forces.
   4.2. However, when a magnetic bar (e.g., carbon steel or iron) is partially placed inside a multiturn inductor (Figure 3.30, bottom) then the situation is quite different. The resulting force is a combination

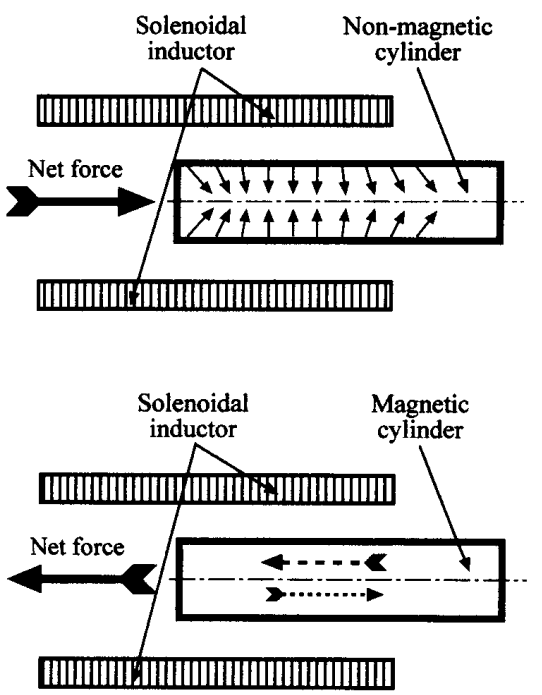

Figure 3.30 Magnetic forces in bar end heating of magnetic and nonmagnetic bars.

of forces: one resulting from the demagnetization effect and forcing the removal of the bar from the inductor, and another resulting from the magnetization effect. That force results in a sucking action towards the center of the induction core, forcing placement of a magnetic bar symmetrically inside the coil. An effect of the latter force is typically the stronger.

Depending upon the application, magnetic forces can have negative effects: being harmful to rigidity of the induction heating system, and causing intensive vibration and industrial noise. However, in other cases, those forces can be desirable and play an important technological part of the process (e.g., electromagnetic stirring effect in melting furnaces, applications using the principles of levitation, electromagnetic separation, induction plasma, etc.).

3.1.7 Introduction to Electromagnetic End and Edge Effects

In order to guarantee the required uniform induction heating of a workpiece (e.g., billet, bar, slab, etc.) it is necessary to accurately predict the electromagnetic field distribution produced by the induction coil under different operating conditions. As discussed in Section 3.1.2, the surface-to-core temperature difference is a result of the skin effect. The temperature profiles along the workpiece's length and width are affected by, among other factors, a distortion of the electromagnetic field (emf) in its end and edge areas. Those field distortions and corresponding distributions of induced currents and power are referred to as end and edge effects. These effects and the field distortion caused by them are primarily responsible for nonuniform temperature profiles in cylindrical, rectangular, and trapezoidal shaped workpieces. Due to the great importance of these effects in the induction heating applications, much effort has been devoted to their study. The first attempt to provide a systematic analysis of electromagnetic end effects was carried out by D. Lavers in the late 1960s and early 1970s [25]. Further analysis of electromagnetic end effects and edge effects has been reported [49–51, 53, 92, 117, 120–125, 169, 190–194]. It is convenient to introduce these effects studying induction heating of a slab.

Suppose a slab is placed in an initially uniform magnetic field (Figure 3.31). If the slab's length and width are much larger than its thickness, the emf in the slab can be viewed as an area consisting of three zones: central part, tranverse edge effect area, and longitudinal end effect area (Figure 3.31). In the central part, the emf distribution corresponds to the field in the infinite plate. Basically, end and edge effects have a two-dimensional space distribution excluding only the zone of three-edge corners where the field is three-dimensional and the corresponding field distribution is the result of a mixture of both the end and edge effects. For many practical applications the separate study of end and edge effects is of great engineering interest. Depending upon applications these effects can act differently.

The study of the electromagnetic end effect provided by estimating the power density distribution along the length of the cylindrical or rectangular workpiece (along the Z-axis in the Y–Z cross section, Figure 3.31). The analysis of the edge effect is provided by evaluation of the power density distribution along the slab width (along the X-axis in the Y–Z cross-section). The electromagnetic edge effect is typically negligible when heating cylindrical workpieces (e.g., billets or bars) in the

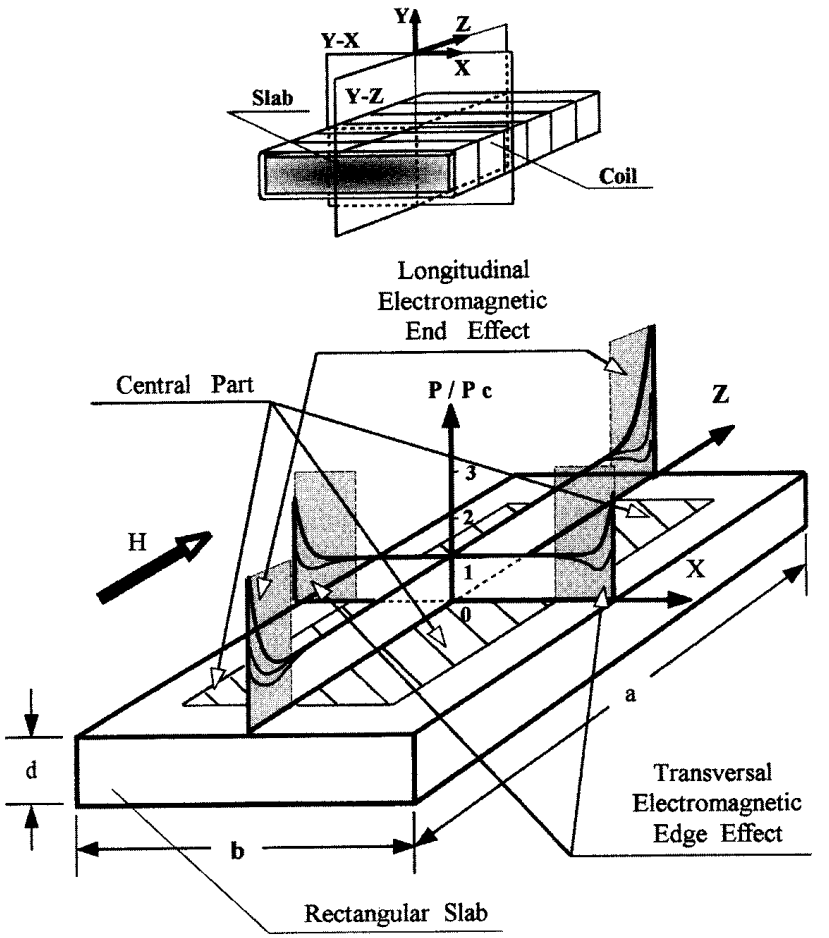

Figure 3.31 Electromagnetic end and edge effect of the slab [120].

longitudinal flux solenoidal inductors. However, this effect can play an essential role when heating billets in oval-type coils when billets are transferred transversally regarding the coil.

Sections 5.7, 7.2.4, 7.2.5, 7.2.8, 7.4.4, and 7.5 provide a detailed analysis of the main features of the electromagnetic end and edge effects in a particular application. In this section we provide a brief orientation regarding these effects.

3.1.7.1 Electromagnetic Longitudinal End Effect

Figure 3.32 shows an appearance of the electromagnetic end effect when heating cylinders. As mentioned above, an electromagnetic end effect represents distortion of the electromagnetic field in the extreme end of the cylinder. Basically, the end effect in the extreme end of the homogeneous electrically conductive cylinder is defined by four variables, the skin effect, the coil overhang, the ratio of coil inside the radius to the cylinder radius, and the coil turn space factor K_{space}. The coil turn space factor represents how tightly the coil turns are wound. For a single-turn coil, a space factor is equal to 1. The coil turn space factor for a multiturn coil can be determined according to Figure 3.33. An incorrect combination of these factors can lead to under heating or overheating the extreme end of the workpiece.

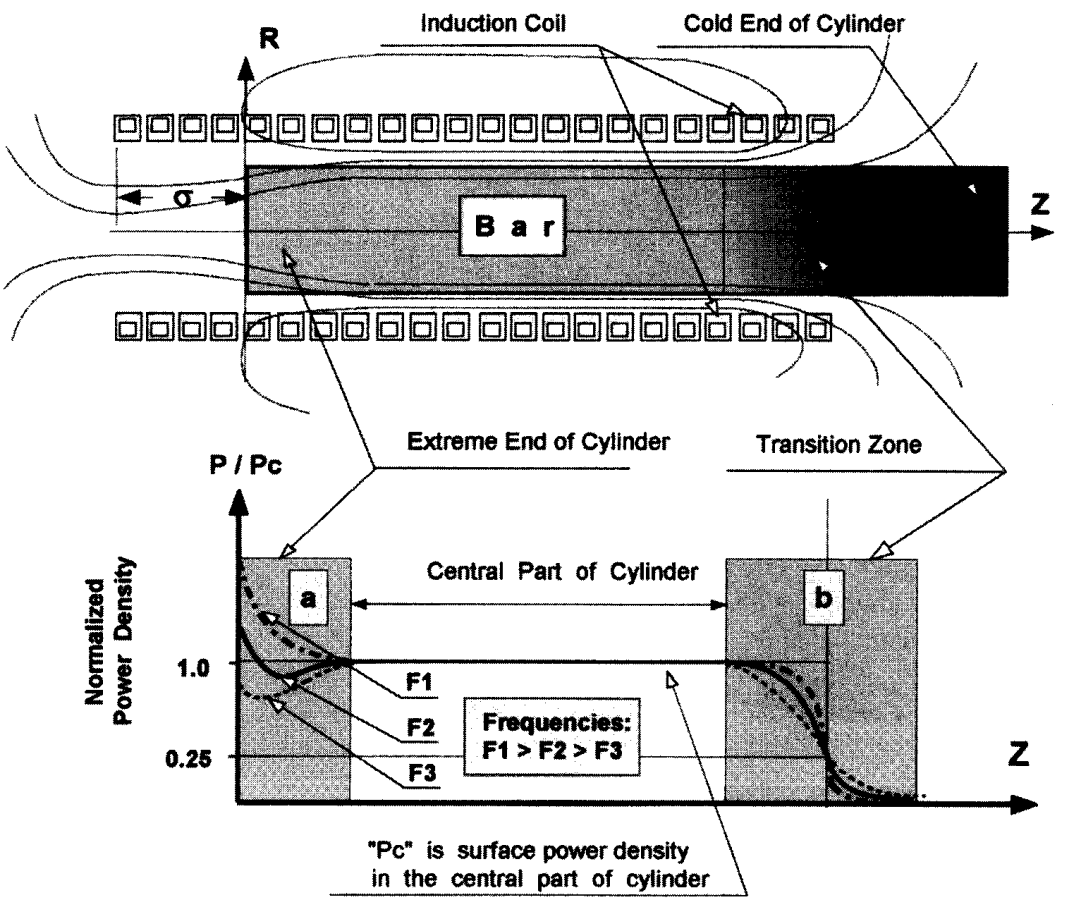

Figure 3.32 Sketch of induction heater and power distribution along the length of a cylinder.

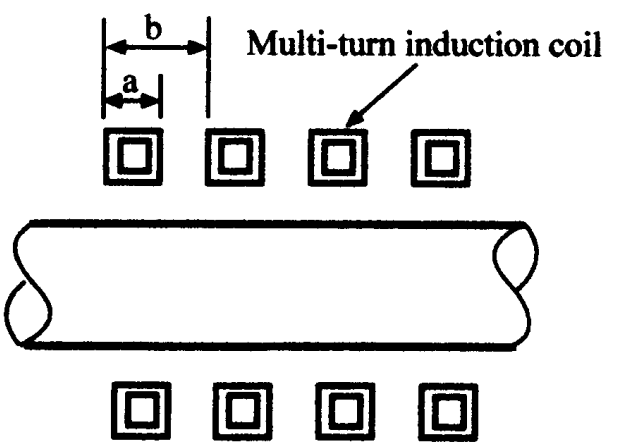

Figure 3.33 Coil turn space factor $\mathbf{K}_{\text{space}}$: $\mathbf{K}_{\text{space}} = a/b$.

As an example Figure 3.34 shows an effect of the coil overhang σ on the distribution of the surface power density along the length of the nonmagnetic cylinder using the line frequency (skin effect is pronounced). As one can see from Figure 3.34, the existence of the large coil overhang results in the overheating of the ends of the nonmagnetic cylinder. At the same time, there is a certain coil overhang (in the case shown in Figure 3.34 that overhang approximately corresponds to σ_4) that results in a reasonably uniform power density distribution. A low frequency in combination with small or negative coil overhangs results in a power density deficit at the extreme end of the cylinder. As one can see from this figure, that electromagnetic longitudinal end effect plays a major role in obtaining a required temperature profile in such applications as bar/billet end heater, as well as inline bar heating.

It is possible to show that in the case of a long multiturn inductor with a homogeneous nonmagnetic cylinder, the density of the induced eddy current in the workpiece area under the coil tail end near the cold end of the cylinder (Figure 3.32, zone **b**) is only half that in the central part. Therefore, the power density in that area is only one-fourth of the power in its central part (see Appendix B).

The electromagnetic end effect in a magnetic slab has several features compared to the nonmagnetic one. Magnetic materials have a tendency to gather the

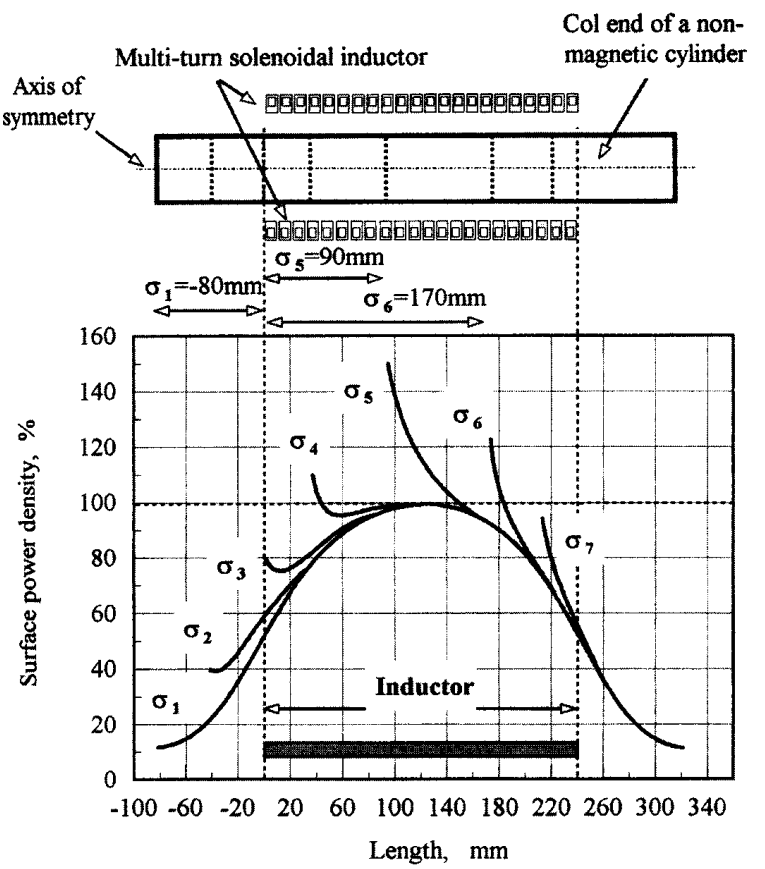

Figure 3.34 Longitudinal electromagnetic end effect at different coil overhangs of the nonmagnetic cylinder (in mm): $\sigma_1 = -80$, $\sigma_2 = -40$, $\sigma_3 = 0$, $\sigma_4 = 30$, $\sigma_3 = 90$, $\sigma_6 = 170$, $\sigma_7 = 210$.

magnetic flux lines thanks to magnetic permeability. Generally speaking, the electromagnetic end effect in a ferromagnetic workpiece is mainly affected by the factors:

1. The demagnetizing effect of eddy currents that tend to force the magnetic field out of the workpiece
2. The magnetizing effect of the surface and volumetric currents, which have a tendency to gather the magnetic field within the magnetic workpiece.

The first factor causes an increase in power at the workpiece's end (somewhat similar to the end effect of a nonmagnetic cylinder). The second factor causes a power reduction there. Therefore, unlike those of the nonmagnetic cylinder, the ends of the ferromagnetic cylinder, even in a uniform magnetic field having large coil overhangs, may be either overheated or underheated.

3.1.7.2 Electromagnetic Transverse Edge Effect

When heating a rectangular workpiece, besides the distortion of the magnetic field in the slab's end areas, similar distortion occurs at its edges (Figure 3.31). This phenomenon takes place due to the electromagnetic transverse edge effect that plays a major role in obtaining the required temperature profile across the slab or plate width.

The maximum value of the eddy current density is located on the surface of the slab's central part (it does not, however, mean that the maximum temperature is located there). The more pronounced the skin effect, the better induced currents match the contour of the slab. Figure 3.35 shows the distribution of the electric field intensity in the slab's cross-section with pronounced skin effect ($d/\delta = 10$, where the slab thickness d divided by penetration depth δ is equal to 10) and when the skin effect is not pronounced ($d/\delta = 3$).

If the skin effect is pronounced ($d/\delta > 5$), then the current and power density are approximately the same along the slab perimeter, except in the edge areas (two-dimensional corners, Figure 3.35), where the distortion of induced power takes place. The edge area is usually (1.5–4.0)* δ long.

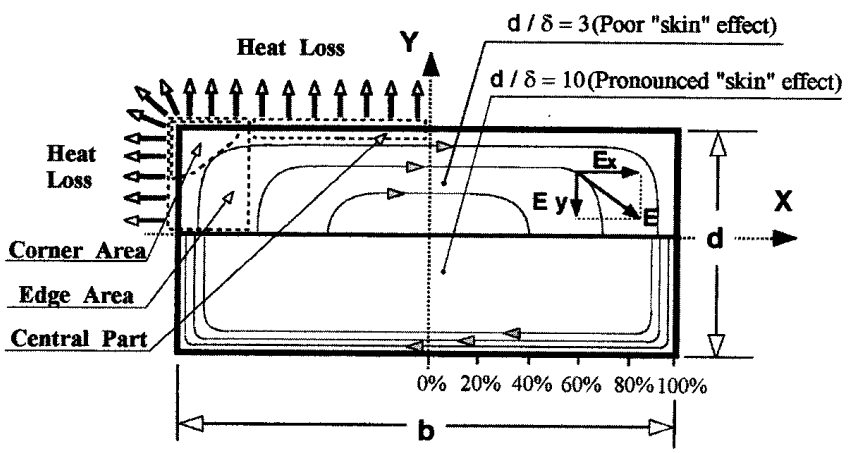

Figure 3.35 Distribution of the electric field intensity (E) in the transverse cross-section of the slab.

Even though heat losses at the edge area are higher than heat losses at the central part, the edge areas can be easily overheated compared to the central part. This occurs because in the central part the heat sources penetrate from two sides (from two surfaces) and at the edge areas the heat sources penetrate from three sides (two surfaces and butt edge). The phenomenon of edge overheating usually occurs in the induction heating of magnetic steel, aluminum, or copper slabs where the skin effect is typically marked.

If the skin effect is not distinct ($(d/\delta < 3)$, then underheating of the edge areas will occur. In this case, the current's path in the slab cross-section does not match the contour of the slab and most of the induced currents close their loops earlier, without reaching the corners and the edge areas (Figure 3.35). As a result, the power densities and heat sources in edge areas will be less than corresponding values in the central part of the slab. For example, in induction heating of thick titanium slabs (using the line frequency), in the final heating stage the temperature of the corners and edge areas could often be 20% lower compared to the temperature of the slab's central part.

3.1.7.3 The Electromagnetic Effect of Joined Materials with Different Electromagnetic Properties (EEJ Effect)

The electromagnetic effect of joined materials with different properties (EEJ effect) occurs when two different metals are located in a common magnetic field. To simplify the study of this effect, let us consider the electromagnetic process in a conventional solenoidal induction coil with two workpieces, for example, two cylindrical billets (Figure 3.36).

Assume that the billets have different material properties (e.g., different electrical resistivity ρ or magnetic permeability μ). When two billets with different material properties are joined or placed close to each other inside an induction coil, the electromagnetic field between the two billets becomes distorted [50, 51, 106].

For illustration purposes, let's have a look at what happens when two carbon steel billets (one billet, e.g., was heated above the Curie point and became nonmagnetic and the other billet still maintained its magnetic properties at ambient temperature) are placed in a multiturn solenoidal inductor. The distribution of the electromagnetic field in this case is shown in Figure 3.37. If the induction coil and both billets are long enough, then the magnetic field intensity at their central areas will be approximately the same and correspond to the coil current. At the same time,

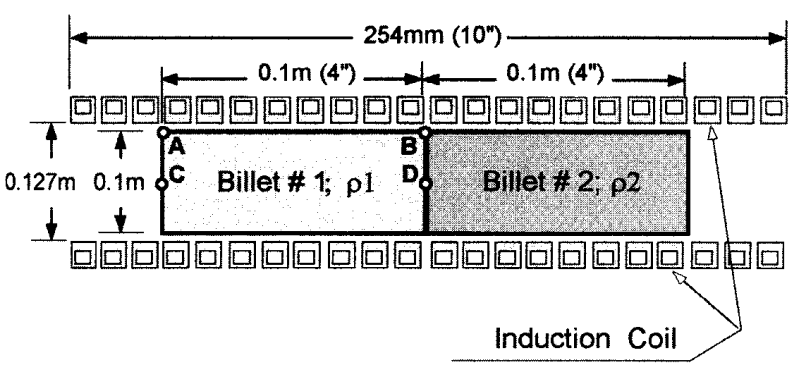

Figure 3.36 Sketch of an induction heating system.

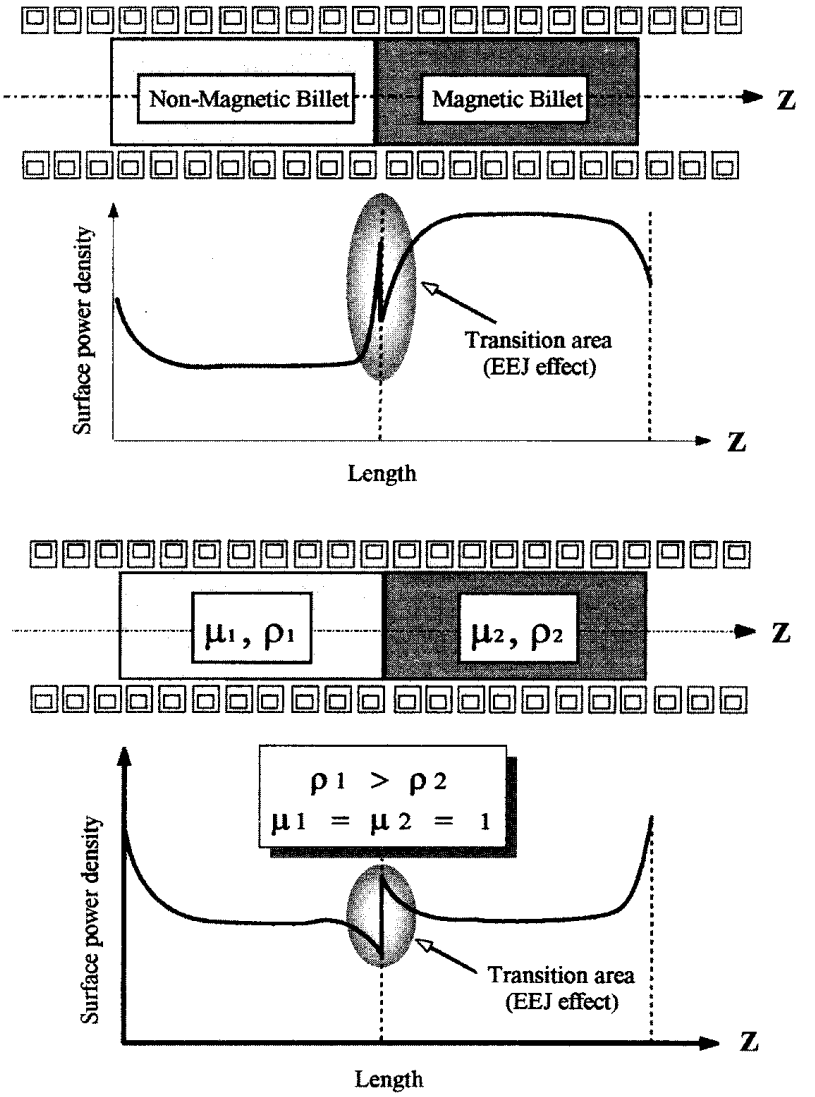

Figure 3.37 Electromagnetic effect of joined materials (EEJ).

the surface power densities of the magnetic and nonmagnetic billets will be rather different (Figure 3.37, top).

At the left end of the nonmagnetic billet (billet #1, Figure 3.36) and at the right end of the magnetic billet (billet #2), there will be a nonuniform power density distribution due to the end effects of the nonmagnetic and magnetic workpieces. Another area where the magnetic field is distorted and quite complicated is the transition area between the billets (the so-called billet's joint area). At the right end of the nonmagnetic cylinder (billet #1), the power density sharply increases. Simultaneously, in the left end of the magnetic cylinder (billet #2), surface power density sharply decreases. This phenomenon is called the electromagnetic effect of joined materials with different properties (EEJ effect).

Obviously, this effect plays an important role in the appearance of several phenomena including the striping phenomenon in induction hardening (Section

5.1.6) and temperature nonuniformities in inline induction billet heating systems. With the striping phenomenon, the workpiece area under the coil may unexpectedly start to heat nonuniformly. Shortly after the heating cycle begins, alternating "hot" bright areas (bright stripes) and "cold" areas (dark stripes) become visible. This combination of "hot" and "cold" stripes leads to a significant redistribution of the electromagnetic field in the area of the dark rings (which retain their magnetic properties) and in the bright high-temperature rings (which have become nonmagnetic) due to the EEJ effect.

When discussing the EEJ effect, it is necessary to mention that this effect also occurs when both workpieces are nonmagnetic but have noticeably different electrical resistivities (Figure 3.37, bottom). Figure 3.38 shows the power density distribution within billet #1 for the induction system shown in Figure 3.36. Both billets are nonmagnetic, but they have different electrical resistivities (ρ_1 and ρ_2). When the electrical resistivity of billet #1 (ρ_1) is three times that of billet #2, (Figure 3.38a), then the surface power density in the joint area of the billet with higher electrical resistivity (i.e., the right end of billet #1) is reduced (Figure 3.37, bottom). When $\rho_1 = 0.33 \times \rho_2$, there is an increase in surface power density there (Figure 3.38b).

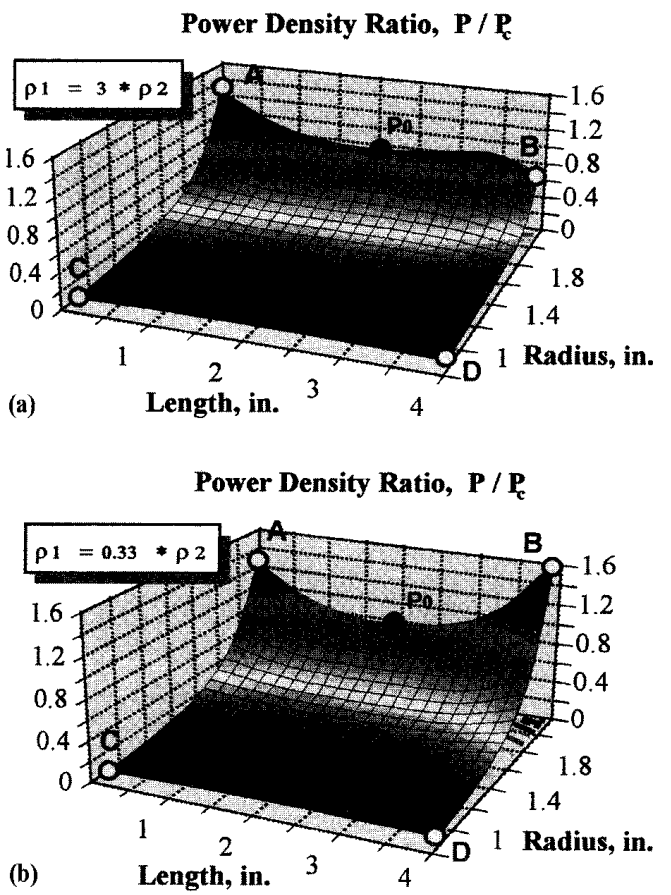

Figure 3.38 Power density distribution along the length of billet #1 (frequency = 60 Hz; $\rho = 1.1\ \mu\Omega$, compare to Figure 3.36).

The effect of joined materials with different electromagnetic properties does not play as important a role as electromagnetic end and edge effects; however, there are some applications where this phenomenon may have a marked influence on the transient and final temperature distribution within the workpiece. This is not only the striping phenomenon but also may affect the final temperature distribution of the billet heater, especially when it is required to heat relatively thin but long billets just above the Curie point [50, 51, 106].

3.2 BASIC THERMAL PHENOMENA IN INDUCTION HEATING

3.2.1 Thermal Properties of the Materials

3.2.1.1 Thermal Conductivity

Thermal conductivity k designates the rate at which heat travels across a thermally conductive workpiece. A material with a high k value will conduct heat faster than a material with a low k. In choosing a material for an inductor's refractory, a lower value of k is required and will correspond to high efficiency and lower heat loss. Conversely, when the thermal conductivity of the metal is high, it is easier to obtain a uniform temperature distribution along the workpiece thickness, which is important in through heating applications.

Therefore, from the point of view of obtaining temperature uniformity, a higher thermal conductivity of metal is preferable. However, in selective hardening applications, a high value of k is quite often a disadvantage because of its tendency to promote a soaking action and equalize the temperature distribution within the workpiece. As a result of heat soaking the temperature rise will take place not only in the required region of the workpiece, which is to be hardened, but in adjacent areas as well, which are not. The temperature increase in the adjacent areas of the workpiece results in the necessity of more power to heat the region to the desired final temperature. A large amount of heated mass in the workpiece can also cause a distortion of the workpiece geometry.

The values of the thermal conductivity of some commonly used metals are shown in Figure 3.39 [37, 38]. As one may note, the thermal conductivity is a nonlinear function of temperature.

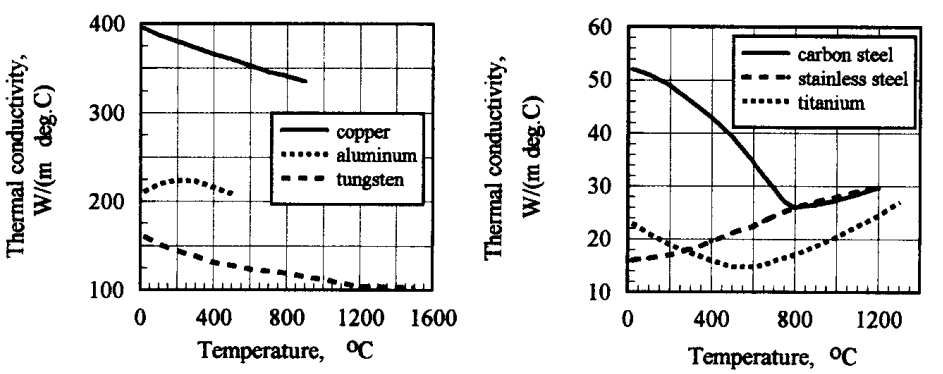

Figure 3.39 Thermal conductivities for some commonly used metals versus temperature.

3.2.1.2 Heat Capacity and Specific Heat

The value of heat capacity C indicates the amount of energy that would have to be absorbed by the workpiece to achieve a unit of required temperature change. Mathematically speaking,

$$C = \frac{dQ}{dT}, \tag{3.13}$$

where dQ is the required energy and dT is the required temperature change. Heat capacity is determined per mole of material. Therefore C is measured in J/(mol °C).

Heat capacity is closely related to a parameter called specific heat c which represents the heat capacity per unit mass meaning the amount of the required heat energy to be absorbed by a unit mass of the workpiece to achieve a unit temperature increase. The c is measured in J/(kg °C) or Btu/(lb °F).

A high value of specific heat corresponds to a high required power to heat a unit mass to a unit temperature. The values of the specific heat of some commonly used metals are shown in Figure 3.40 [37, 38].

3.2.2 Three Modes of Heat Transfer

In induction heating, all three modes of heat transfer—conduction, convection, and radiation—are present [26–35, 436].

3.2.2.1 Thermal Conduction

Heat is transferred by conduction from the high-temperature regions of the workpiece toward the low-temperature regions. The basic law that describes heat transfer by conduction is Fourier's law,

$$q_{\text{cond}} = -k \operatorname{grad}(T), \tag{3.14}$$

where q_{cond} is heat flux by conduction, k is thermal conductivity, and T is temperature.

As one can see from Eq. (3.14), according to Fourier's law the rate of heat transfer in a workpiece is proportional to the temperature gradient (temperature difference) and the thermal conductivity of the workpiece. In other words, a large

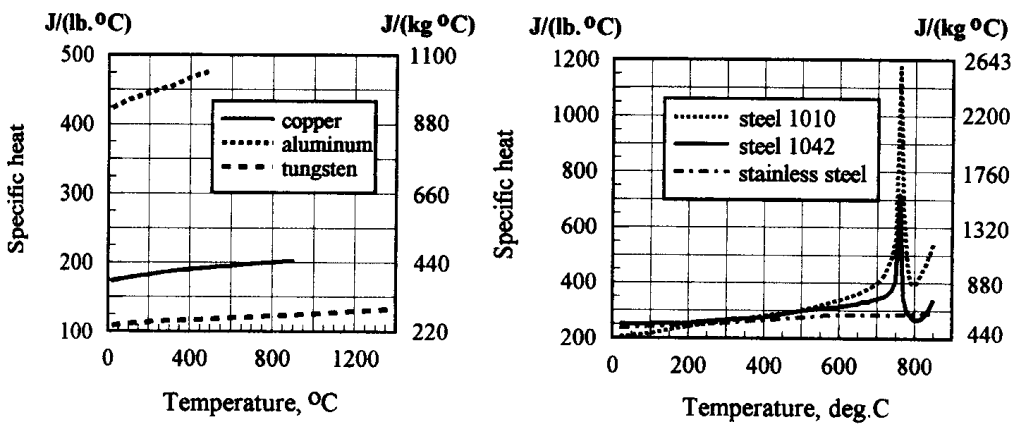

Figure 3.40 Specific heat for some commonly used metals versus temperature.

temperature difference between surface and core (which, e.g., typically takes place during surface hardening) and a high value of thermal conductivity of the metal result in intensive heat transfer from the hot surface of the workpiece toward the cold core. Conversely, the rate of heat transfer by conduction is inversely proportional to the distance between regions with different temperatures.

3.2.2.2 Convection Mode of the Heat Transfer

In contrast to conduction, heat transfer by convection is carried out by fluid, gas, or air (i.e., from the surface of the heated workpiece to the ambient area). The well-known Newton's law can describe convection heat transfer. This law states that the heat transfer rate is directly proportional to the temperature difference between the workpiece surface and the ambient area,

$$q_{\text{conv}} = \alpha(T_s - T_a), \tag{3.15}$$

where q_{conv} is heat flux density by convection, W/m^2 or W/in^2; α is the convection surface heat transfer coefficient, W/(m^2.°C) or W/(in^2.°F); T_s is surface temperature, °C or °F; and T_a is ambient temperature, °C or °F. The subscripts s and a denote surface and ambient, respectively.

The convection surface heat transfer coefficient is primarily a function of the thermal properties of the workpiece, the thermal properties of the surrounding fluids (i.e., quenchants), gas, or air, and their viscosity or the velocity of the heat-treated workpiece if the workpiece is moving at high speed (e.g., induction heat treating of a strip or spinning disk). It is particularly important to take this mode into account when designing low-temperature induction heating applications (e.g., tempering, stress relieving, paint curing, or other processes with a maximum temperature less than 500°C or 932°F). In these applications convection losses are equal to or exceed heat losses due to radiation.

With certain applications the value of convection losses can vary dramatically depending on the temperature of the workpiece and outside temperature, as well as workpiece geometry, surface conditions, and whether it is free or forced convection. Remember that in a number of induction heating applications (e.g., strip heating, wire heating, heating of the rotating disks, etc.) convection heat transfer cannot be considered as free convection. In some galvanizing, galvaluming, and galvannealing applications, the strip travels at a speed up to 5 m/sec (16 ft/sec). In cases like this, the heat losses due to forced convection are much higher (e.g., often 5–10 times higher) compared to free convection losses of the stationary heated workpiece.

There are several empirical formulas that provide a rough engineering estimate of the free convection losses q_{conv}, including formulas (3.16) [468] and (3.17) [8]

$$q_{\text{conv}} = 1.86(T_s - T_a)^{1.3} \quad [\text{W/m}^2] \tag{3.16}$$

$$q_{\text{conv}} = 1.54(T_s - T_a)^{1.33} \quad [\text{W/m}^2], \tag{3.17}$$

where T_s and T_a are surface temperature and ambient temperature, correspondingly, in °C. For example, free convection heat loss density from the workpiece surface heated to 600°C (1112°F) into the surrounding atmosphere ($T_a = 20$°C) is as shown in Table 3.6.

Table 3.6 Examples of Calculating Free Convection Loss Density

According to Formula (3.17)	According to Formula (3.18)
$q_{conv} = 1.86 \times 580^{1.3} = 7.3 \times 10^3$ W/m^2 or $q_{conv} = 7.3$ kW/m^2	$q_{conv} = 1.54 \times 580^{1.33} = 7.45 \times 10^3$ W/m^2 or $q_{conv} = 7.45$ kW/m^2

Convection heat transfer plays a particularly important role in the quenching process where the surface heat transfer coefficient describes the cooling process during quenching.

3.2.2.3 *Radiation Mode of the Heat Transfer*

In the third mode of heat transfer, which is heat radiation, the heat may be transferred from the hot workpiece into surrounding areas including a nonmaterial region (vacuum). The effect of heat transfer by radiation can be introduced as a phenomenon of electromagnetic energy propagation due to a temperature difference. This phenomenon is governed by the Stefan–Boltzmann law of thermal radiation, which states that the heat transfer rate by radiation is proportional to a radiation loss coefficient C_s and the value of $T_s^4 - T_a^4$.

Since radiation losses are proportional to the fourth power of temperature, these losses are a significant part of the total heat losses in high-temperature applications (e.g., surface hardening, through hardening, induction heating prior to forging upsetting, rolling, etc.). The radiation heat loss coefficient includes emissivity, radiation shape factor (the view factor), and surface conditions. For example, the value of emissivity increases with increase of surface oxidation. At the same time, polished metal will radiate less heat to the surroundings than will nonpolished metal. A comparison of emissivities of some commonly used polished metals versus nonpolished is shown in Table 3.7.

The radiation heat loss coefficient can be determined approximately as $C_s = \sigma_s \varepsilon$, where ε is the emissivity of the metal and σ_s is the Stefan–Boltzmann constant ($\sigma_s = 5.67 \times 10^{-8}$ W/(m^2 K^4)).

Radiation loss density as a function of temperature and ε is shown in Figure 3.41. Similar to convection losses, there is a formula that provides a rough engineering estimate of the free radiation losses q_{rad},

$$q_{rad} = 5.67 \times 10^{-8} \varepsilon [(T_s + 273)^4 - (T_a + 273)^4] \quad [\text{W/m}^2] \tag{3.18}$$

when T_S and T_a are measured in °C.

Table 3.7 Comparison of Emissivities ε of Some Commonly Used Polished Metals Versus Nonpolished Metals

Surface Condition	Aluminum	Carbon Steel	Copper	Brass and Zinc
Polished	0.042–0.053	0.062	0.026–0.042	0.03–0.039
Nonpolished, oxidized	0.082–0.40	0.71–0.8	0.24–0.65	0.21–0.50

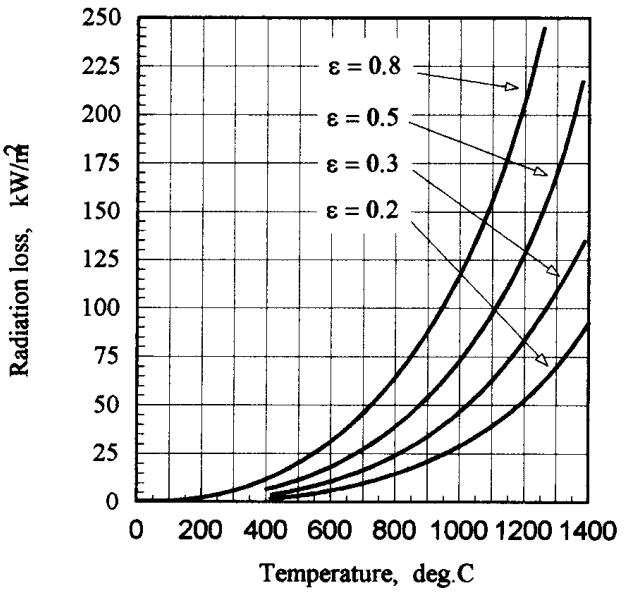

Figure 3.41 Variation of the radiation loss density versus temperature and emissivity.

For example, a free radiation carbon steel slab ($\varepsilon = 0.8$) heated to 1250°C (2282°F) into the surrounding atmosphere ($T_a = 20°C$) corresponds to a radiation loss density of

$$q_{\text{rad}} = 5.67 \times 10^{-8} \times 0.8 \times (1523^4 - 293^4) = 244 \times 10^3\ \text{W/m}^2 = 244\ \text{kW/m}^2.$$

The above-described determination of radiation heat loss is a valid assumption for classical workpiece geometry when there is free heat radiation from the heated body into the surroundings. However, there are some applications where the radiation heat transfer phenomenon can be complicated and such a simple approach would not be valid. Complete details of all three modes of heat transfer can be found in several references [26–35, 436]. The theory of thermal radiation is also discussed in detail in Section 4.1.3 while discussing the principles of infrared thermometry.

As discussed previously, in conventional induction heating and heat treatment, heat transfer by convection and radiation reflects the value of heat loss. A high value of heat loss reduces the total efficiency of the induction heater. These surface heat losses are highly variable because of the nonlinear behavior of convection and the radiation losses. The analysis shows that convection losses are the major part of the heat loss in low-temperature induction heating applications (i.e., aluminum, lead, zinc, tin, magnesium, and steel at a temperature lower than 350°C/662°F). In high-temperature applications (such as induction hardening and heating of steels, titanium, tungsten, nickel, and other metals) when it is required to heat the workpiece to the temperatures of hot forming or rolling, radiation losses are much more significant than convection losses (Figure 3.42).

In high-temperature applications, including induction bar/billet/slab heating prior to forging, rolling, and extrusion the use of thermal insulation (refractory) allows one to drastically reduce energy waste due to surface heat losses. The features of using thermal insulation are discussed in Section 7 of this handbook.

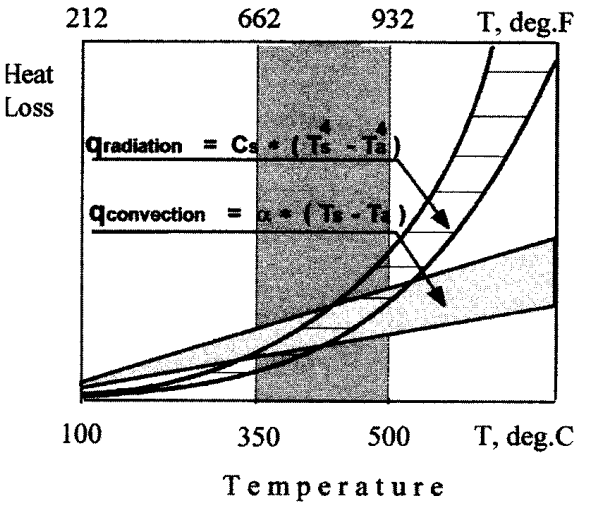

Figure 3.42 Convection and radiation heat losses in typical induction heating applications.

3.3 ESTIMATION OF THE REQUIRED POWER AND DYNAMICS OF INDUCTION HEATING

3.3.1 Estimation of the Required Power for Induction Heating

Since the value of specific heat c represents the amount of the required heat energy to be absorbed by a unit mass of the workpiece to achieve a unit temperature increase, an average value of specific heat c can be effectively used for a ballpark estimate of the required workpiece power (P_w) to heat a given shape workpiece to an average temperature rise at the required production rate. The formula (3.19) can be used for this purpose,

$$P_w = mc\,\frac{T_f - T_{\text{in}}}{t}, \tag{3.19}$$

where m is the mass of the heated body, kg; c is the average value of specific heat, J/(kg °C); T_{in} and T_f are average values of initial and final temperatures, °C; and t is the required heat time, seconds.

For example, in order to heat a solid copper cylinder (0.1 m diameter, 0.3 m long) from ambient temperature (20°C/68°F) to a temperature of 620°C/1148°F in 120 sec, the required power can be determined corresponding to formula (3.19).

In this case, the mass of the heated body can be calculated as

$$m = \frac{\pi D^2}{4}\,l\gamma = \frac{3.14 \times 0.1^2}{4} \times 0.3 \times 8.91 \times 10^3 = 21\ \text{kg},$$

where γ is the density in kg/m^3 (for copper $\gamma = 8.91 \times 10^3$ kg/m^3); D is the diameter in m; and l is the billet length in m.

$c = 420$ J/(kg °C) can be used as an average value of the specific heat of copper in the temperature range 20 to 620°C. Therefore, applying Eq. (3.19) the required power will be

$$P_w = mc\frac{T_f - T_{in}}{t} = 21 \times 420 \times \frac{620 - 20}{120} = 44100\,\text{W} = 44.1\,\text{kW}. \quad (3.20)$$

In engineering calculations, some practitioners prefer to use the value of the heat content of the material to determine the value of P_w. Heat content is measured in kW × hour/t. In this case, formula (3.19) can be rewritten as

$$P_w = HC \times \text{Production}. \quad (3.21)$$

Figure 3.43 shows the values of the heat content for commonly used metals used with Eq. 3.21 to determine the required power (P_w) to heat a copper billet (example above) based on the heat content value. From Figure 3.43 the required value of the heat content would be approximately equal to 70 kW × hour/t.

$$\text{Production} = \frac{21\,\text{kg}}{120\,\text{sec}} = \frac{0.021t}{0.033h} = 0.64t/h$$

$$P_w = HC \times \text{Production} = 70 \times 0.64 = 44.8\,\text{kW}.$$

Simplified formulas such as (3.19) and (3.21) are very convenient to use in applications such as induction heating of classically-shaped workpieces (e.g., billets, bars, slabs, blooms, etc.) where relatively uniform through heating is required. Such simplified formulas have the advantage of providing fast estimation of the required power (P_w). However, numerical computation can provide much more precise estimation particularly in cases such as surface hardening, selective hardening, induction reheating when initial temperature is not uniform (e.g., the case of induction slab/bar reheating after a continuous caster), and others.

It is important to remember that power P_w does not represent the power at coil terminals (so-called coil power). Formula (3.22) provides a correlation between the required coil power P_c and required workpiece power P_w:

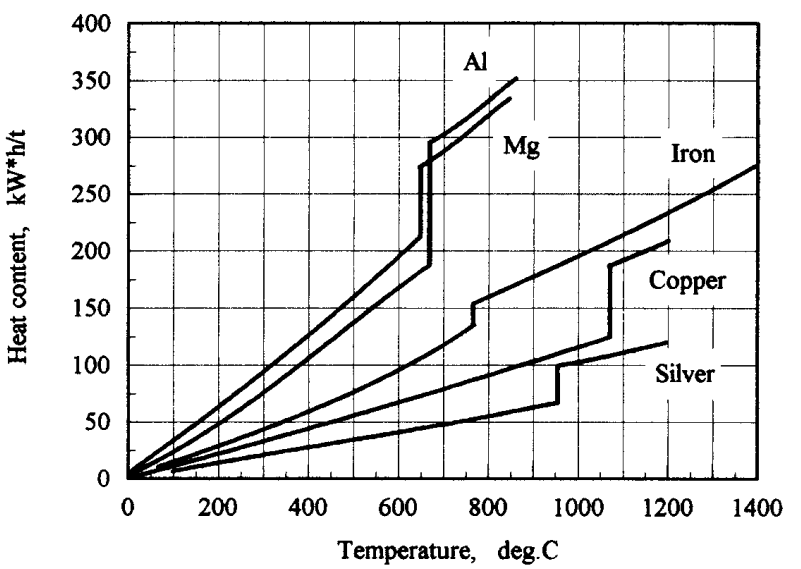

Figure 3.43 Heat content of metals at various temperatures.

$$P_c = \frac{P_w}{\eta_{el}\eta_{th}}, \tag{3.22}$$

where η_{el} is electrical efficiency and η_{th} is thermal efficiency. Both, η_{el} and η_{th} are in the range of 0 to 1.

The value of η_{el} represents the ratio of the power induced in the workpiece P_w, to the total of P_w and electrical losses (P_{loss}^{el}).

$$\eta_{el} = \frac{P_w}{P_w + P_{loss}^{el}}, \tag{3.23}$$

where P_{loss}^{el} includes power loss in the coil turns P_{loss}^{turns}, and power loss in conductive bodies located in the surrounding area P_{loss}^{sur} and can be determined as

$$P_{loss}^{el} = P_{loss}^{turns} + P_{loss}^{sur}. \tag{3.24}$$

The value of P_{loss}^{sur} represents undesirable heating of tools or other electrically conductive structures (i.e., shunts, flux concentrators, etc.).

As shown in [4], when heating a solid a cylinder in a long solenoidal coil the value of the η_{el} can be calculated according to the formula

$$\eta_{el} = \frac{1}{1 + \frac{D_1'}{D_2'}\frac{\rho_1}{\rho_2}\frac{\delta_1}{\delta_2}} = \frac{1}{1 + \frac{D_1'}{D_2'}\sqrt{\frac{\rho_1}{\mu_r\rho_2}}}, \tag{3.25}$$

where D_1' is an effective coil inside diameter, $D_1' = D_1 + \delta_1$; D_2' is an effective outside diameter of a cylinder, $D_2' = D_2 - \delta_2$; δ_1 and δ_2 are current penetration depths in the coil copper and cylinder (workpiece), respectively; ρ_1 and ρ_2 are the electrical resistivities of the coil and workpiece; and μ_r is the relative magnetic permeability of the heated cylinder.

Formula (3.25) has been obtained under the assumptions:

- a skin effect is pronounced;
- the coil is standing alone; there are no electrically conductive structures located in the coil proximity;
- inductor is a single-layer infinitely long solenoid producing a homogeneous magnetic field; and
- a thick wall copper tube is used for coil fabrication.

The ratio $(D_1'/D_2')(\sqrt{\rho_1/(\mu_r\rho_2)})$ is called the coil electrical efficiency factor. High coil electrical efficiency corresponds to a low value of the electrical efficiency factor. Therefore high coil electrical efficiency takes place when heating workpieces that are magnetic, have high electrical resistivity, and have the smallest possible gap between the coil and workpiece ($D_1/D_2 \to 1$). For example, the coil electrical efficiency η_{el} when heating carbon steel cylinders below the Curie temperature is usually in the range of 0.8 to 0.95. In contrast, when heating billets made from silver or copper, η_{el} is typically in the range of 0.35 to 0.45.

When heating rectangular bodies, including slabs and plates, instead of formula (3.25), formula (3.26) should be applied:

$$\eta_{el} = \frac{1}{1 + \frac{F_1}{F_2}\sqrt{\frac{\rho_1}{\mu_r \rho_2}}}, \tag{3.26}$$

where F_1 and F_2 are effective perimeters of the coil opening and the heated slab, respectively.

The value of η_{th} in (3.22) represents the amount of the heat losses (P_{loss}^{th}) compared to the heating power and can be determined as

$$\eta_{th} = \frac{P_w^{av}}{P_w^{av} + P_{loss}^{th}}. \tag{3.27}$$

P_{loss}^{th} includes heat losses from the workpiece surface due to radiation and convection as well as heat loss due to thermal conduction (e.g., the heat losses from the billet to a water-cooled liner). The next section shows that the power induced in the workpiece P_w is not a constant during the heating cycle and varies depending upon the change in electrical resistivity and relative magnetic permeability. This is why, instead of using P_w, the value of P_w^{av} (meaning the average power per heating cycle) is applied.

Thermal insulation or refractory materials can significantly decrease the heat losses. An accurate estimation of the value of the P_{loss}^{th} can be determined with numerical computation, at the same time, there are several empirical formulas that can allow one to obtain a rough value of those losses [192]. For cylindrical coils with concrete blocks as a refractory, the value of thermal losses can be determined as shown:

$$P_{loss}^{th} = 3.74 \times 10^{-2} \frac{l}{\log_{10}\left(\frac{D1}{D3}\right)}, \tag{3.28}$$

where P_{loss}^{th} is the heat loss from the workpiece surface in kW, l is the coil length in cm, $D1$ is the inside diameter of the induction coil in cm, and $D3$ is the inside diameter of the refractory in cm.

Total efficiency of the induction coil (η) is a combination of both coil thermal efficiency (η_{th}) and coil electrical efficiency (η_{el}),

$$\eta = \eta_{el}\, \eta_{th}. \tag{3.29}$$

As mentioned above, thermal insulation or refractory materials can significantly decrease heat losses. At the same time, the use of refractory results in a larger coil-to-workpiece air gap. This results in deterioration of electromagnetic coupling between the induction coil and heated workpiece, and as a result leads to a decrease in coil electrical efficiency (Figure 3.44).

Therefore refractory allows one to improve the coil thermal efficiency. On the other hand, it results in a reduction in coil electrical efficiency. A decision to use or not to use a refractory is always a reasonable compromise. In some cases, it is more energy and cost-efficient not to use a refractory at all and, therefore, have the smallest possible coil-to-workpiece air gap maximizing coil electrical efficiency (i.e., induction hardening and brazing applications). In other cases, it is wise to use a refractory to significantly decrease surface heat losses and more than compensate for the loss of energy due to a greater coil-to-workpiece air gap (i.e., induction

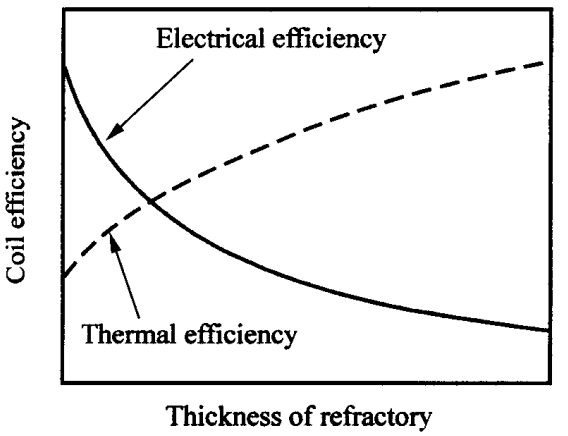

Figure 3.44 Coil electrical and thermal efficiencies versus thickness of refractory.

heating prior to forging, rolling, and extrusion). Numerical computation helps to make an intelligent decision as to whether to use a refractory.

3.3.2 Intricacies of the Dynamics of Induction Heating

Up to this point we have been discussing electromagnetic and thermal properties as well as describing the electromagnetic processes that take place in induction heating. These must now be combined with the generation of heat that is produced by the Joule effect in the workpiece (I^2R). To simplify this, let's discuss the features of induction heating of a carbon steel cylinder located inside a long multiturn solenoid coil. The process of induction heating a magnetic cylinder from a temperature below the Curie point (i.e., ambient temperature) to a temperature above it has several features that should be taken into account when designing an induction system.

The dynamics of the induction heating process are affected by several nonlinear factors, including but not limited to electromagnetic and thermal properties of the heated workpiece, power supply operational features and control mode. For educational purposes, at this point it is beneficial to evaluate the dynamics of induction heating considering simplified conditions. Having this in mind, it is possible to recognize three classical process modes: coil voltage is constant, coil current is constant, and coil power is constant. Figure 3.45 shows the variation of workpiece power versus time of heating for a carbon steel cylinder from ambient temperature to forging range temperatures (i.e., 1200°C/2190°F). A detailed study of these modes can be found in [4].

Figure 3.46 shows the change of surface and core temperatures with constant current applied to the coil. As shown above, if the temperature of carbon steel is changed, some of the properties that affect the electroheating process also change. The most significant of these are magnetic permeability, electrical resistivity, and specific heat (Figures 3.2 to 3.4, 3.7, 3.8, 3.10, 3.11, 3.39, and 3.40).

At the first stage of the heating cycle the entire workpiece is magnetic, magnetic permeability is quite large, current penetration depth is very small [according to Eqs. (3.6) and (3.7)], and therefore, the skin effect is pronounced. At the same

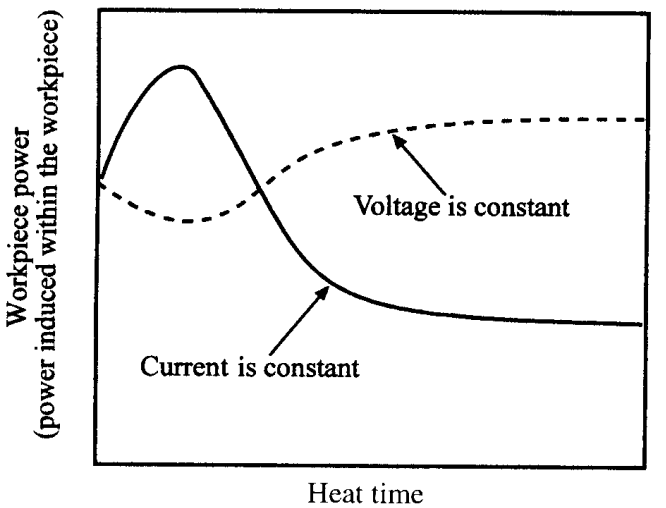

Figure 3.45 Power induced within the workpiece as a function of the heat time for two of the most common process modes: coil current is constant (solid line) and coil voltage is constant (dotted line).

time, because of the relatively low temperature, the heat losses from the cylinder surface at this stage are relatively low (Figure 3.42). Because of the pronounced skin effect, the induced power appears in the fine surface layer of the workpiece. This leads to a rapid increase in temperature at the surface with practically no change at the core. Figure 3.47a shows the temperature and power density (heat source) distribution along the radius of the workpiece at this stage. The maximum temperature is located at the surface. Intensive heating and the existence of a large temperature differential within the workpiece characterize this stage. As one can see from Figure 3.47a, the temperature profile does not match the heat source profile because of thermal conductivity k, which spreads the heat from the surface toward the core.

During this stage, the electrical efficiency (Figure 3.47b) increases due to an increase in electrical resistivity ρ of the metal with temperature (Figure 3.2). At the same time, the relative magnetic permeability μ_r remains high, and a slight reduction of μ_r does not affect the rise in electrical efficiency. After a short time, coil electrical efficiency reaches its maximum value and then starts to decrease (Figure 3.46). The surface reaches the Curie temperature first, and after that the heat intensity at the surface significantly decreases. This takes place primarily because

1. specific heat has its maximum value (a peak) near the Curie point (Figure 3.40). Since the value of the specific heat denotes the amount of energy that must be absorbed by the metal to achieve the required heat, the peak of the specific heat leads to a decrease in heat intensity in the surface; and
2. steel in the surface area loses its magnetic properties and μ_r drops to 1. As a result, the surface power density and heat sources will also be drastically reduced.

Figure 3.47b shows the temperature profile and heat source distribution along the radius of the cylinder after the surface temperature passes the Curie point

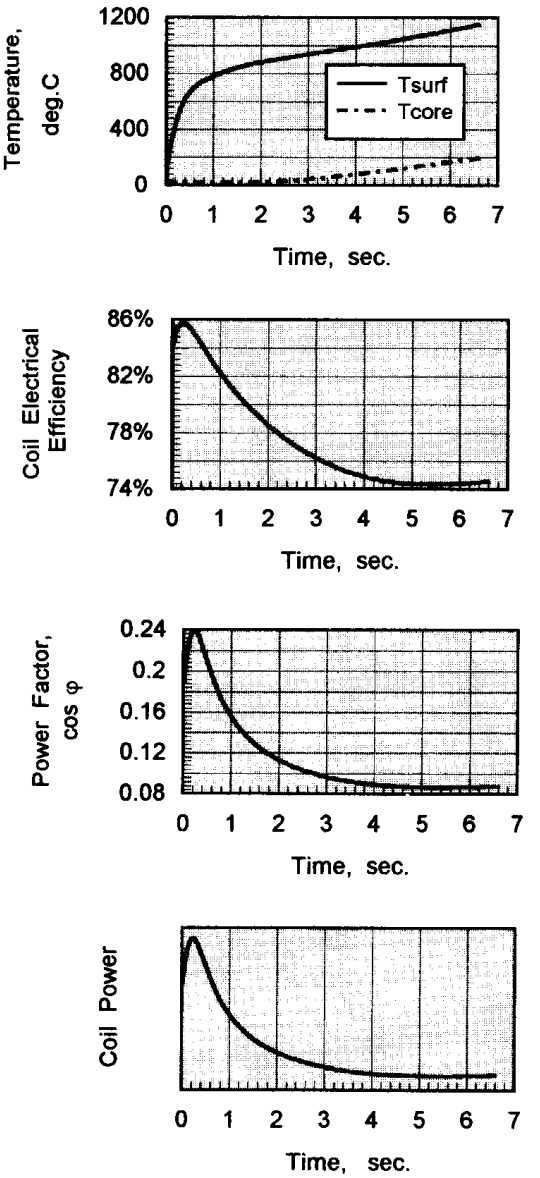

Figure 3.46 Change of coil parameters with time during surface hardening of a carbon steel cylinder (frequency is 25 kHz).

(second stage). At this stage, the electrical resistivity of the carbon steel increases approximately two- to threefold compared to its value in the initial stage. A decrease of μ_r and an increase of ρ cause a six- to tenfold increase in penetration depth from its value in the initial stage [93]. Most of the power is now induced in the surface and the internal layers of the workpiece. This stage can be characterized as the dual-properties (biproperties) stage of steel/iron heating.

The workpiece surface becomes nonmagnetic; however, its internal layers remain magnetic. This stage takes place until the thickness of the nonmagnetic layer is less than the penetration depth in hot steel. Heat sources have a unique wave shape (waveform) that is different from the classical exponential distribution.

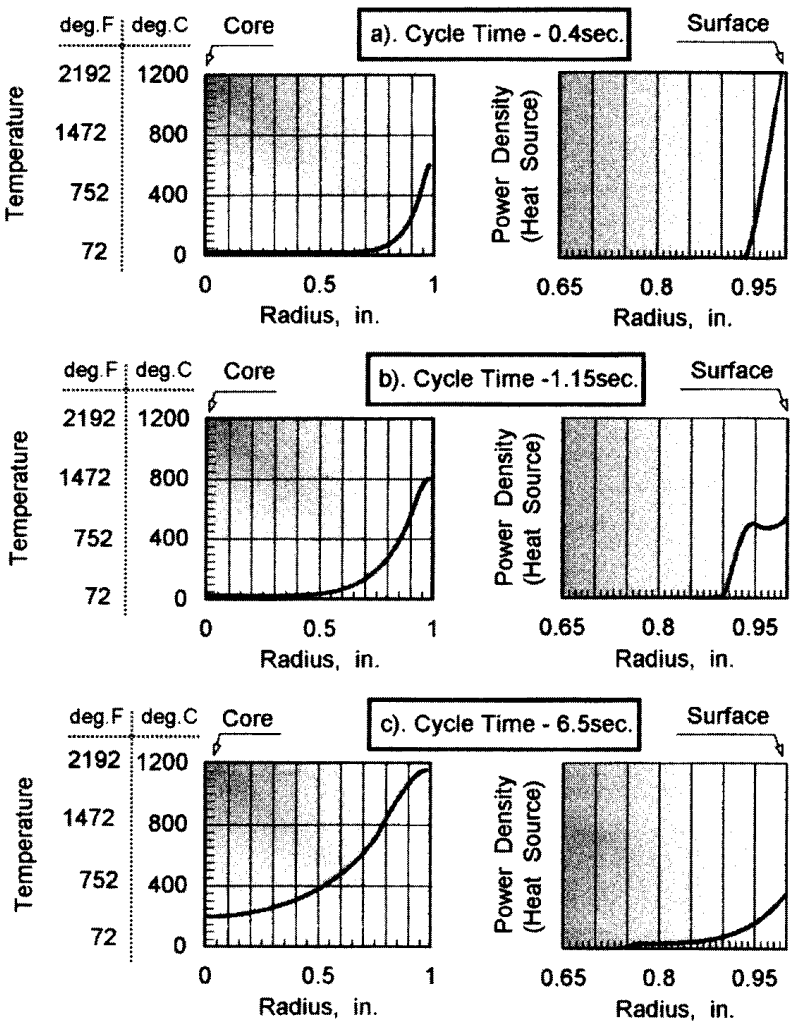

Figure 3.47 Temperature and power density profiles at different stages of induction heating of a 2-in. cylinder (frequency is 25 kHz).

Figure 3.47b shows that at the cylinder surface there is a maximum of the heat sources. Then the heat sources decrease toward the core. However, at a distance of 1.4 mm from the surface, the heat sources start to increase again. This takes place because of the remaining magnetic properties of the steel at this distance. It is necessary to mention here that in some applications, due to the dual-properties (biproperties) phenomenon, the maximum value of heat sources can be located in an internal layer of the workpiece and not on its surface.

It is particularly important to take into account the existence of the dual-properties structure in the heating of metal-plated parts as well as when designing the surface hardening processes.

Finally (the third stage), the thickness of the surface layer with nonmagnetic properties exceeds the penetration depth in hot steel and the dual-properties phenomenon becomes less pronounced and will finally disappear. The power density will then have its classical exponential distribution (Figure 3.47c).

The existence of the three stages of induction heating results in variation of both the workpiece power P_w and coil power P_c during the process of heating. All three stages should be taken into consideration when evaluating the process parameters. Workpiece power P_w can be obtained as a product of the surface power density and workpiece surface exposed to the magnetic field. Surface power density for ballpark estimation purposes can be found for a magnetic body heated inside the infinitely long solenoid inductor as a function of the magnetic field intensity, frequency, electrical resistivity, and relative magnetic permeability according to formula (3.30) [4],

$$p_0 = 2.72 \times 10^{-3} H_{\text{surf}}^2 \sqrt{\rho \mu_{\text{surf}} F}, \tag{3.30}$$

where p_0 is surface power density measured in W/m^2, H_{surf} is the magnetic field intensity at the surface of the workpiece, ρ is electrical resistivity, μ is relative magnetic permeability at the workpiece surface, and F is a frequency. All units are according to the SI system. Precise calculation of all the major process parameters including heating conditions can be conducted only by numerical computation.

To finalize the discussion on the dynamics of the induction heating process we should mention that a particular application often has specific features that affect the dynamics of the induction process and establish its uniqueness. Those features are discussed in detail later.

3.4 ADVANCED INDUCTION PRINCIPLES AND MATHEMATICAL MODELING

Mathematical modeling is one of the major factors in the successful design of induction heating systems. Theoretical models may vary from a simple hand-calculated formula to a very complicated numerical analysis which can require several hours of computational work using modern supercomputers. The choice of a particular theoretical model depends on several factors, including the complexity of the engineering problem, required accuracy, time limitations, and cost.

Before an engineer starts to provide a mathematical simulation of any process it is necessary to have a sound understanding of the nature and physics of that process. Engineers should also be aware of the limitations of applied mathematical models, assumptions, and possible errors and should consider correctness and sensitivity of the chosen model to poorly defined parameters such as boundary conditions, material properties, or initial temperature conditions. One model can work well in certain applications and give unrealistic results in another. Underestimation of features of the process or overly simple assumptions can lead to an incorrect mathematical model (including chosen governing equations) that will not provide the required accuracy.

It is important to remember that any computational analysis can at best produce only results that are derived from the governing equations. Therefore, the first and the most important step in any mathematical simulation is to choose an appropriate theoretical model that will correctly describe the technological process or phenomenon.

Computer modeling provides the ability to predict how different factors may influence the transitional and final heat treating conditions of the workpiece and what must be accomplished in the design of the induction heating system to improve the effectiveness of the process and guarantee the desired heating results.

As mentioned above, induction heating is a complex combination of electromagnetic, heat transfer, and metallurgical phenomena. These are tightly interrelated because the physical properties of heat-treated materials depend strongly on both magnetic field intensity and temperature as well as chemical composition. The metallurgical aspects have been discussed in Chapter 2. This chapter concentrates on mathematical modeling of the electromagnetic field and thermal processes that occur during induction heating.

Note. This section requires from the reader a knowledge of certain aspects of mathematics including differential calculus, integral calculus, and vector analysis, and can be skipped by the first-time reader or reader with limited knowledge of advanced mathematics and applied physics.

3.4.1 Mathematical Modeling of the Electromagnetic Field

The technique of calculating electromagnetic field depends on the ability to solve Maxwell's equations. For general time-varying electromagnetic fields, Maxwell's equations in differential form can be written as [39–52]

$$\nabla \times \mathbf{H} = \mathbf{J} + \frac{\partial \mathbf{D}}{\partial t} \qquad \text{(from Ampere's law)} \tag{3.31}$$

$$\nabla \times \mathbf{E} = -\frac{\partial B}{\partial t} \qquad \text{(from Faraday's law)} \tag{3.32}$$

$$\nabla \bullet \mathbf{B} = 0 \qquad \text{(from Gauss' law)} \tag{3.33}$$

$$\nabla \bullet \mathbf{D} = \rho^{\text{charge}} \qquad \text{(from Gauss' law),} \tag{3.34}$$

where **E** is electric field intensity, **D** is electric flux density, **H** is magnetic field intensity, **B** is magnetic flux density, **J** is conduction current density, and ρ^{charge} is electric charge density.

Equations (3.31) to (3.34) consist of special symbols: $\nabla\bullet$ and $\nabla\times$. These two useful symbols along with the third symbol of ∇ are popular in vector algebra and are used to shorten an expression of particular differential operation without having to carry out the details. For example, in the rectangular coordinate system these symbols represent the following operations.

$$\nabla U = \text{grad}\, U = i\frac{\partial U}{\partial X} + j\frac{\partial U}{\partial Y} + k\frac{\partial U}{\partial Z} \tag{3.35}$$

$$\nabla \bullet U = \text{div}\, U = \frac{\partial U_x}{\partial X} + \frac{\partial U_y}{\partial Y} + \frac{\partial U_z}{\partial Z} \tag{3.36}$$

$$\nabla \times U = \operatorname{curl} U = \begin{vmatrix} i & j & k \\ \dfrac{\partial}{\partial X} & \dfrac{\partial}{\partial Y} & \dfrac{\partial}{\partial Z} \\ U_X & U_Y & U_Z \end{vmatrix} =$$

$$= i\left(\frac{\partial U_Z}{\partial Y} - \frac{\partial U_Y}{\partial Z}\right) + j\left(\frac{\partial U_X}{\partial Z} - \frac{\partial U_Z}{\partial X}\right)$$

$$+ k\left(\frac{\partial U_Y}{\partial X} - \frac{\partial U_X}{\partial Y}\right). \tag{3.37}$$

The fundamental laws governing the general time-varying electromagnetic field (Eqs. 3.31 through 3.34) can be written not only in differential form but in integral form as well by applying Stokes' theorem [42–47].

Maxwell's equations not only have a purely mathematical meaning, they have a concrete physical interpretation as well. For example, Eq. (3.31) says that the curl of **H** always has two sources: conductive (**J**) and displacement ρ^{charge} currents. A magnetic field is produced whenever there are electric currents flowing in surrounding objects. From Eq. (3.32) one can conclude that a time rate of change in magnetic flux density **B** always produces the curling **E** field and induces currents in the surrounding area and, therefore, in other words it produces an electric field in the area where such changes take place. The minus sign in Eq. (3.32) determines the direction of that induced electric field. This fundamental result can be applied to any region in space.

Let us consider how Eqs. (3.31) and (3.32) can be used to support the basic explanation of some of the electromagnetic process in induction heating provided in Sec. 3.1. The application of alternating voltage to the induction coil will result in the appearance of an alternating current in the coil circuit. According to Eq. (3.31), an alternating coil current will produce in its surrounding area an alternating (changing) magnetic field that will have the same frequency as the source current (coil current). That magnetic field's strength depends on the current flowing in the induction coil, the coil geometry, and the distance from the coil. The changing magnetic field induces eddy currents in the workpiece and in other objects that are located near that coil. By Eq. (3.32), induced currents have the same frequency as the source coil current; however, their direction is opposite that of the coil current. This is determined by the minus sign in Eq. (3.32). According to Eq. (3.31), alternating eddy currents induced in the workpiece produce their own magnetic fields, which have opposite directions to the direction of the main magnetic field of the coil. The total magnetic field of the induction coil is a result of the source magnetic field and induced magnetic fields.

As one would expect from an analysis of Eq. (3.31), there can be an undesirable heating of tools, fasteners, or other electrically conductive structures located near the induction coil.

In induction heating and heat treatment applications, an engineer should pay particular attention to such simple relations as (3.33) or (3.34). The popular saying, "The best things come in small packages," is particularly true here. The short notation of Eq. (3.33) has real significance in induction heating and the heat treatment of electrically conductive body. To say that the divergence of magnetic flux density is zero is equivalent to saying that **B** lines have no source points at which they originate or end; in other words, **B** lines always form a continuous loop. A clear understanding of such a simple statement will allow one to explain and avoid many mistakes in

dealing with induction heat treatment and the induction heating of workpieces with irregular geometry as well as slabs, blooms, and strips.

The above-described Maxwell's equations are in indefinite form because the number of equations is less than the number of unknowns. These equations become definite when the relations between the field quantities are specified. The following constitutive relations are additional and hold true for a linear isotropic medium.

$$\mathbf{D} = \varepsilon\varepsilon_0\mathbf{E} \tag{3.38}$$

$$\mathbf{B} = \mu_r\mu_0\mathbf{H} \tag{3.39}$$

$$\mathbf{J} = \sigma\mathbf{E} \qquad \text{(Ohm's law)}, \tag{3.40}$$

where the parameters ε, μ_r, and σ denote, respectively, the relative permittivity, relative magnetic permeability, and electrical conductivity of the material; $\sigma = 1/\rho$, where ρ is electrical resistivity. The constant $\mu_0 = 4\pi \times 10^{-7}$ H/m [or Wb/(A × m)] is called the permeability of free space (the vacuum), and similarly the constant $\varepsilon_0 = 8.854 \times 10^{-12}$ F/m is called the permittivity of free space. Both relative magnetic permeability μ_r and relative permittivity ε are nondimensional parameters and have very similar meanings. Relative magnetic permeability indicates the ability of a material to conduct the magnetic flux better than a vacuum or air. This parameter is very important in choosing materials for magnetic flux concentrators. Relative permittivity (or dielectric constant) indicates the ability of a material to conduct the electric field better than a vacuum or air.

By taking Eqs. (3.38) and (3.40) into account, Eq. (3.31) can be rewritten as

$$\nabla \times \mathbf{H} = \sigma\mathbf{E} + \frac{\partial(\varepsilon_0\varepsilon\mathbf{E})}{\partial t}. \tag{3.41}$$

For most practical applications of the induction heating of metals, where the frequency of currents is less than 10 MHz, the induced conduction current density $\mathbf{J}$ is much greater than the displacement current density $\partial\mathrm{D}/\partial t$, so the last term on the right-hand side of Eq. (3.41) can be neglected. Therefore, Eq. (3.41) can be rewritten as

$$\nabla \times \mathbf{H} = \sigma\mathbf{E}, \tag{3.42}$$

After some vector algebra and using Eqs. (3.31), (3.32), and (3.39), it is possible to show that

$$\nabla \times \left(\frac{1}{\sigma}\nabla \times \mathbf{H}\right) = -\mu_r\mu_o\frac{\partial \mathbf{H}}{\partial t} \tag{3.43}$$

$$\nabla \times \left(\frac{1}{\mu_r}\nabla \times \mathbf{E}\right) = -\sigma\mu_o\frac{\partial \mathbf{E}}{\partial t}. \tag{3.44}$$

Since the magnetic flux density $\mathbf{B}$ satisfies a zero divergence condition [Eq. (3.33)], it can be expressed in terms of a magnetic vector potential $\mathbf{A}$ as

$$\mathbf{B} = \nabla \times \mathbf{A}. \tag{3.45}$$

And then, from (3.32) and (3.45), it follows that

$$\nabla \times \mathbf{E} = -\nabla \times \frac{\partial \mathbf{A}}{\partial \mathrm{t}}. \tag{3.46}$$

Therefore, after integration, one can obtain

$$\mathbf{E} = -\frac{\partial \mathbf{A}}{\partial t} - \nabla\varphi, \tag{3.47}$$

where φ is the electric scalar potential. Equation (3.40) can be written as

$$\mathbf{J} = -\sigma\frac{\partial \mathbf{A}}{\partial t} + \mathbf{J_s}, \tag{3.48}$$

where $\mathbf{J}_s = -\sigma\nabla\varphi$ is the source (excitation) current density in the induction coil.

Taking the material properties as being piecewise continuous and neglecting the hysteresis and magnetic saturation it can be shown that

$$\frac{1}{\mu_r\mu_0}(\nabla \times \nabla \times \mathbf{A}) = \mathbf{J}_s - \sigma\frac{\partial \mathbf{A}}{\partial t}. \tag{3.49}$$

It should be mentioned here that for the great majority of induction heating applications (such as through hardening and induction heating to prior to forging, rolling, and extrusion) a heat effect due to hysteresis losses does not typically exceed 7% compared to the heat effect due to eddy current losses. Therefore, an assumption of neglecting the hysteresis is valid.

However, in some cases, such as induction tempering, paint curing, stress relieving, heating prior to galvanizing, and lacquer coating, hysteresis losses can be quite significant compared to eddy current losses. In these cases, hysteresis losses should be taken into account since they can contain a significant portion of heat sources (in some cases contributing 40% or more of the total heat sources).

It can be shown that for the great majority of induction heating applications it is possible to further simplify the mathematical model by assuming that the currents have a steady-state quality. Therefore, with this assumption we can conclude that the electromagnetic field quantities in Maxwell's equations are harmonically oscillating functions with a single frequency. Thus a time-harmonic electromagnetic field can be introduced. This field can be described by the following equations, which are derived after some vector algebra from Eqs. (3.43), (3.44), and (3.49), respectively.

$$\frac{1}{\sigma}\nabla^2\mathbf{H} = \mathrm{j}\omega\mu_r\mu_o\mathbf{H} \tag{3.50}$$

$$\frac{1}{\mu_r}\nabla^2\mathbf{E} = \mathrm{j}\omega\mu_r\mu_o\mathbf{E} \tag{3.51}$$

$$\frac{1}{\mu_r\mu_0}\nabla^2\mathbf{A} = -\mathbf{J_s} + \mathrm{j}\omega\sigma\mathbf{A}, \tag{3.52}$$

where ∇^2 is the Laplacian, which has different forms in Cartesian and cylindrical coordinates. In Cartesian coordinates,

$$\nabla^2\mathbf{A} = \frac{\partial^2\mathbf{A}}{\partial X^2} + \frac{\partial^2\mathbf{A}}{\partial Y^2} + \frac{\partial^2\mathbf{A}}{\partial Z^2}. \tag{3.53}$$

In cylindrical coordinates (axisymmetric case),

$$\nabla^2 \mathbf{A} = \frac{1}{R}\frac{\partial}{\partial R}\left(R\frac{\partial \mathbf{A}}{\partial R}\right) + \frac{\partial^2 \mathbf{A}}{\partial Z^2}. \tag{3.54}$$

In other words, an assumption of harmonically oscillating currents with a single frequency means that harmonics are absent in both the impressed and induced currents and fields. The governing equations (3.50) to (3.52) for the time-harmonic field with the appropriate boundary condition can be solved with respect to **H**, **E**, or **A**.

Equations (3.50) to (3.52) are valid for general three-dimensional fields and allow one to find all of the required design parameters of the induction system such as current, power, coil impedance, and heat source density induced by eddy currents.

Although there is considerable practical interest in three-dimensional problems, a great majority of engineering problems in induction heating tend to be handled with a combination of two-dimensional assumptions. Several factors discourage three-dimensional field consideration.

1. Computing costs are much higher for three-dimensional cases (especially taking into account tightly interrelated features (including material properties) of electromagnetic and heat transfer phenomena in induction heating).
2. The user must have special knowledge in many theoretical subjects and should have specific experience working with three-dimensional software.
3. Representation of both results and geometric input data could create a well-known problem of working with three-dimensional images.

For many induction heating applications the quantities of the magnetic field (such as magnetic vector potential, electric field intensity, and magnetic field intensity) may be assumed to be entirely directed. For example, in the longitudinal cross-section of the solenoid coil, both **A** and **E** vectors have only one component, which is entirely **Z**-directed. In the case of a transverse section, **H** and **B** vectors have only one component (Figure 3.48). This allows one to reduce the three-dimensional field to a combination of two-dimensional forms. For example, in the case of magnetic vector potential, Eq. (3.52) can be expressed for a two-dimensional Cartesian system as

$$\frac{1}{\mu_r \mu_0}\left(\frac{\partial^2 \mathbf{A}}{\partial X^2} + \frac{\partial^2 \mathbf{A}}{\partial Y^2}\right) = -\mathbf{J}_s + j\omega\sigma\mathbf{A}, \tag{3.55}$$

and for an axisymmetric cylindrical system as

$$\frac{1}{\mu_r \mu_0}\left(\frac{\partial^2 \mathbf{A}}{\partial R^2} + \frac{1}{R}\frac{\partial \mathbf{A}}{\partial R} + \frac{\partial^2 \mathbf{A}}{\partial Z^2} - \frac{\mathbf{A}}{R^2}\right) = -\mathbf{J}_s + j\omega\sigma\mathbf{A}. \tag{3.56}$$

The boundary of the region is selected such that the magnetic vector potential **A** is zero along the boundary (Dirichlet condition) or its gradient is negligibly small along the boundary compared to its value elsewhere in the region (Neumann condition $\partial \mathbf{A}/\partial n = 0$). Therefore, the heat transfer equation which is discussed in Section

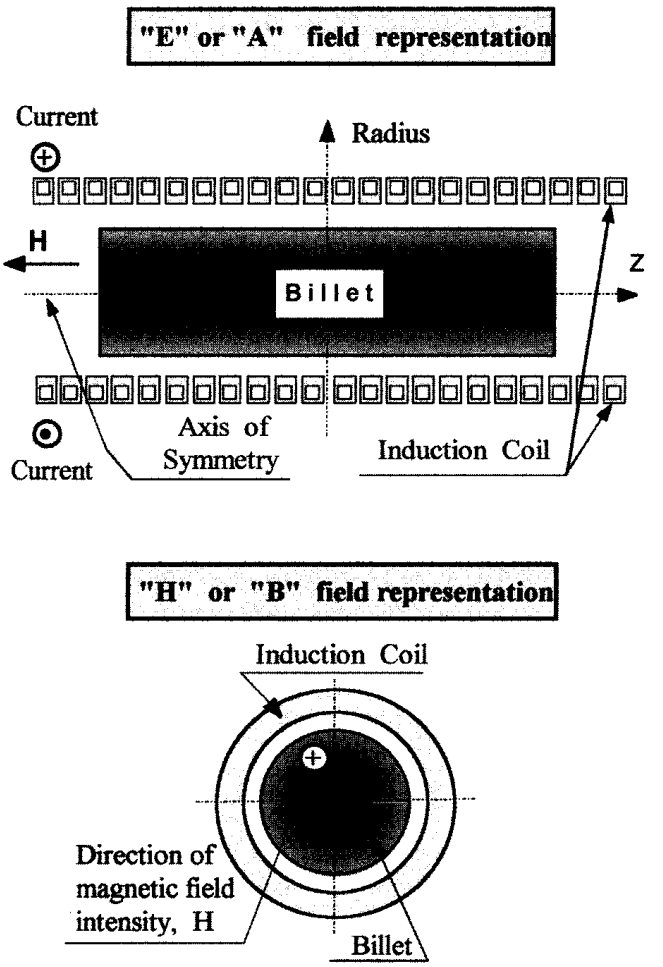

Figure 3.48 E, A and H, B field representations in a cylindrical system.

3.4.2 and Eq. (3.56) with their initial and boundary conditions fully describe the electrothermal processes in a great majority of conventional cylindrical induction heat treatment systems.

By using analogous vector algebra manipulations it is possible to obtain governing equations similar to (3.55) and (3.56) that can be formulated with respect to **E**, **B**, or **H**. Therefore, any given electromagnetic problem in induction heat treatment may be worked in terms of **A, E, B**, or **H**. Part of the art of mathematical modeling of electromagnetic fields derives from the right choice of field representation, which could be different for different applications.

Partial differential equations that are formulated with respect to **A** or **E** are very convenient for describing the electromagnetic field in a longitudinal cross-section of the induction heating system. However, the electromagnetic field distribution in a transverse cross-section of the workpiece can be more conveniently described by governing equations formulated with respect to **B** or **H** [49, 50] (Figure 3.48). Field representations that are typically used by induction heating designers for describing electromagnetic processes in a conventional induction surface or through hardening of cylindrical workpieces are shown in Figure 3.48.

3.4.2 Mathematical Modeling of the Thermal Processes

In general, the transient (time-dependent) heat transfer process in a metal workpiece can be described by the Fourier equation:

$$c\gamma\frac{\partial T}{\partial t} + \nabla \bullet (-k\nabla T) = Q, \tag{3.57}$$

where T is temperature, γ is the density of the metal, c is the specific heat, k is the thermal conductivity of the metal, and Q is the heat source density induced by eddy currents per unit time in a unit volume (so-called heat generation). This heat source density is obtained by solving the electromagnetic problem.

As one might conclude from Figures 3.39 and 3.40, both k and c are nonlinear functions of temperature. Our experience shows that in the great majority of tempering, stress relieving, annealing, and normalizing applications, as well as induction heating prior to metal hot forming, a rough approximation of thermal conductivity in simulations of the heating process will not lead to significant errors in temperature distributions. However, in surface hardening and through hardening a rough approximation of k (i.e., assumes $k = \text{const}$) can create unacceptable results.

At the same time, regardless of application, a rough approximation of specific heat (i.e., an assumption of $c = \text{const}$) could create significant errors in obtaining the required coil power and temperature profile within the workpiece.

Equation (3.57), with suitable boundary and initial conditions, represents the three-dimensional temperature distribution at any time and at any point in the workpiece. The initial temperature condition refers to the temperature profile within the workpiece at time t = 0; therefore that condition is required only when dealing with a transient heat transfer problem where the temperature is a function not only of the space coordinates but also of time. The initial temperature distribution is usually uniform and corresponds to the ambient temperature. In some cases, the initial temperature distribution is nonuniform due to the residual heat after the previous technological process (i.e., preheating, partial quenching, or continuous casting).

For most engineering induction heating problems, boundary conditions combine the heat losses due to convection and radiation (Figure 3.42). In this case the boundary condition can be expressed as

$$-k\frac{\partial T}{\partial n} = \alpha(T_s - T_a) + C_s\left(T_s^4 - T_a^4\right) + Q_s, \tag{3.58}$$

where $\partial T/\partial n$ is the temperature gradient in a direction normal to the surface at the point under consideration, α is the convection surface heat transfer coefficient, c_s is the radiation heat loss coefficient, Q_s is the surface loss (i.e., during quenching or as a result of workpiece contact with cold rolls or water-cooled guides, etc.), and n denotes the normal to the boundary surface.

As one may see from Eq. (3.58) and Figure 3.42, the heat losses at the workpiece surface are highly variable because of the nonlinear behavior of convection and the radiation losses.

If the heated body is geometrically symmetrical along the axis of symmetry, the Neumann boundary condition can be formulated as

$$\frac{\partial T}{\partial n} = 0. \tag{3.59}$$

The Neumann boundary condition implies that the temperature gradient in a direction normal to the axis of symmetry is zero. In other words, there is no heat exchange at the axis of symmetry. This boundary condition can also be applied in the case of a perfectly insulated workpiece.

In the case of heating a cylindrical workpiece, Eq. (3.57) can be rewritten as

$$c\gamma \frac{\partial T}{\partial t} = \frac{\partial T}{\partial Z}\left(k\frac{\partial T}{\partial Z}\right) + \frac{1}{R}\frac{\partial}{\partial R}\left(kR\frac{\partial T}{\partial R}\right) + Q. \tag{3.60}$$

The same Eq. (3.57) can be shown in Cartesian coordinates (i.e., heat transfer in slab, strip, or plate) as

$$c\gamma \frac{\partial T}{\partial t} = \frac{\partial T}{\partial X}\left(k\frac{\partial T}{\partial X}\right) + \frac{\partial}{\partial Y}\left(k\frac{\partial T}{\partial Y}\right) + \frac{\partial}{\partial Z}\left(k\frac{\partial T}{\partial Z}\right) + Q. \tag{3.61}$$

Equations (3.60) and (3.61) with boundary conditions (3.58) and (3.59) are the most popular equations for mathematical modeling of the heat transfer processes in induction heating and heat treatment applications.

3.4.3 Numerical Computation of the Process

3.4.3.1 Traditional Methods of Calculation

The analytical methods and equivalent circuit coil design methods popular in the 1960s and 1970s no longer satisfy the modern designer because of the inherent restrictions outlined above. The designer must be aware that in many applications, erroneous and inadequate results can be obtained when such methods are used. The development of modern computers and the increasing complexity in most modern induction heating applications have significantly restricted the solution to the application of simple formulas and analytical and seminumerical methods. These methods can be useful only in obtaining approximate results in simple cases.

Rather than use simple computational techniques with many restrictions and poor accuracy, modern induction heating specialists are currently turning to highly effective numerical methods such as finite difference, finite element, mutual impedance, and boundary element methods. These methods are widely and successfully used in the computation of electromagnetic and heat transfer problems. Each of these methods has certain advantages and has been used alone or in combination with others.

Because of the extraordinarily large amount of information that is available in the scientific literature, even an experienced engineer can be easily confused if too many of the nuances of computer modeling of induction heating problems are introduced. Therefore we briefly discuss the modern electroheat numerical computation techniques while simplifying the materials so they are understood by induction heating specialists who have limited experience in numerical modeling. Thus our goal is to provide the reader with a general orientation on advanced numerical simulation methods.

Before we discuss the features and applications of the most popular numerical methods it is necessary to point out one of their important qualities: all numerical methods give an approximate solution to the modeled problem (including heat transfer and electromagnetic problems). Therefore there is always the danger of

obtaining inappropriate results when those methods are used. The fact that the numerical solution is always approximate and not absolutely accurate should not discourage engineers from using numerical methods. On the contrary, it should stimulate them to carefully study the features of these methods and to transform them into a powerful computational tool that will allow analysts to control the accuracy of the simulation and to produce information that cannot be measured or obtained by using analytical, semianalytical, or other kinds of methods, including physical experiments. It is wise to remember that the correct use of numerical methods will provide approximate, but acceptable, engineering solutions that will satisfy the requirements of modern technology from a practical standpoint.

Many mathematical modeling methods and programs exist or are under development. Work in this field is done in universities, research institutes, inside large companies such as INDUCTOHEAT, Inc., and by specialized software companies such as Integrated Engineering Software Inc., Infolytica Inc., Magsoft Corp., Ansoft Corp., ANSYS Corp., SYSWELD, Cosmos Corp., Vector Fields Inc., and others.

For each problem or family of similar problems, certain numerical methods or software are preferred. It is obviously quite difficult if not impossible to find a single medicine that will be equally effective for both constipation and diarrhea. The medicine will most likely stop diarrhea or it will help constipation but not both. The same reasoning holds true in searching for an efficient and universal computational tool. There is not a single universal computational method that fits all cases and is optimum for solving all induction heating problems. Our experience in the use of different numerical methods has shown that it is preferable to have several methods and programs rather than searching for one universal program for solving a wide variety of tasks.

The right choice of computational method and software depends on the application and features of the specific problem or phenomenon. It is important for the designer of the induction heating equipment to know the advantages and limitations of a variety of computational techniques. This will allow the analyst to select an appropriate tool that will provide an accurate evaluation of the problem and allow the engineer to predetermine the temperature distribution within the workpiece at all stages of the process cycle, which includes heating, soaking, and quenching. This will also result in obtaining the required heating conditions and the desired metallurgical properties in the workpiece.

Because of space limitations, this chapter does not give an exhaustive list of the methods available for electromagnetic field and heat transfer calculations. There are many publications that describe the features and applications of mathematical modeling methods. An interested reader can study the description of the most popular computational techniques used for simulation of heat transfer and electromagnetic processes in References 5, 30, and 47–92. Here we briefly analyze and describe some of the methods that are successfully used at INDUCTOHEAT. We hope that the knowledge obtained will afford engineers and designers an understanding of how the numerical methods work and what kind of numerical methods can be the most suitable for a particular induction heating and heat treating application.

3.4.3.2 Finite Difference Method

The finite difference method (FDM) was the earliest numerical technique [27, 54–56] used for mathematical modeling of different processes. The finite difference method

has been used extensively for solving both heat transfer and electromagnetic problems [27, 49, 51–59]. It is particularly easy to apply when the modeling area has cylindrical or rectangular shapes.

The orthogonal mesh discretizes the area of modeling (i.e., induction coil, workpiece, flux concentrator, etc.) into a finite number of nodes (Figure 3.49). Because of the orthogonal mesh, the discretization algorithm is quite simple. An approximate solution of the governing equation is found at the mesh points defined by the intersections of the lines.

The computation procedure consists of replacing each partial derivative of the governing equations (3.55), (3.56), (3.60), or (3.61) by a finite difference "stencil" that couples the value of the unknown variable (i.e., temperature or magnetic vector potential) at an approximation node with its value in the surrounding area. This method provides a pointwise approximation of the partial differential equation and is quite universal because of its generality and its relative simplicity of application.

By Taylor's theorem for two variables, the value of a variable at a node on the mesh can be expressed in terms of its neighboring values and separation distance (called a space step) h as in the expressions (stencils):

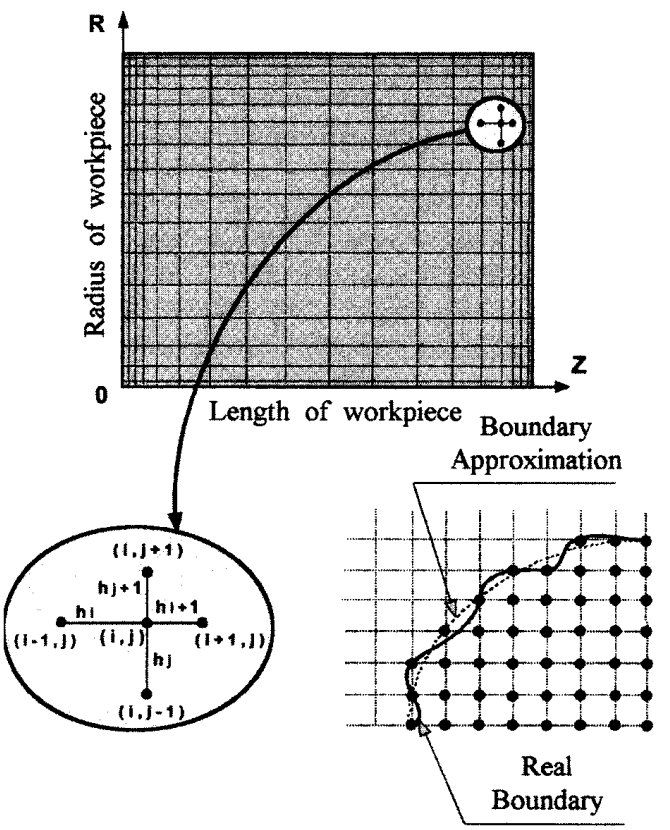

Figure 3.49 Finite difference approximation and rectangular mesh network.

$$\frac{\partial T}{\partial X} \Rightarrow \frac{T_{i+1} - T_i}{h} + O(h) \qquad \text{(Forward difference)} \tag{3.62}$$

$$\frac{\partial T}{\partial X} \Rightarrow \frac{T_i - T_{i-1}}{h} + O(h) \qquad \text{(Backward difference)} \tag{3.63}$$

$$\frac{\partial T}{\partial X} \Rightarrow \frac{T_{i+1} - T_{i-1}}{2h} + O(h) \qquad \text{(Central difference)} \tag{3.64}$$

$$\frac{\partial^2 T}{\partial X^2} \Rightarrow \frac{T_{i+1} - 2T_i + T_{i-1}}{h^2} + O(h^2). \tag{3.65}$$

Here the notation $O(h)$ is used to show that the error involved in the approximation is on the order of h. Similarly, $O(h^2)$ is for the approximation error on the order of h^2, which is more accurate than one on the order of h.

Substitution of the finite difference stencils into the electromagnetic and heat transfer partial differential equations gives the local approximation. By assembling all local approximations and taking into account the proper initial and boundary conditions, one can obtain a set of simultaneous algebraic equations that can be solved with respect to unknown variables (i.e., T, **A**, **E**, **H**, or **B**) at each node of the mesh. The solution can be obtained either by iterative techniques or by direct matrix inversion methods. Since the matrices are sparsely occupied (nonzeros only in the neighborhood of the diagonal), some simplification in the computational procedure can be used.

As an example, we illustrate using FDM for modeling heat transfer processes for cylindrical billet heating (Fourier equation). In order to mathematically describe a heat transfer process in a cylindrical billet, a governing equation (3.57) can be rewritten as

$$c\gamma \frac{\partial T}{\partial t} = \frac{\partial}{\partial Z}\left(k \frac{\partial T}{\partial Z}\right) + \frac{1}{R}\frac{\partial}{\partial R}\left(kR \frac{\partial T}{\partial R}\right) + Q(Z, R). \tag{3.66}$$

For describing a heat transfer process in rectangular bodies (i.e., slab, plate, and bloom), Eq. (3.57) can be rewritten as

$$c\gamma \frac{\partial T}{\partial t} = \frac{\partial}{\partial X}\left(k \frac{\partial T}{\partial X}\right) + \frac{\partial}{\partial Y}\left(k \frac{\partial T}{\partial Y}\right) + Q(X, Y). \tag{3.67}$$

As mentioned in Section 3.2.1, c and k are functions of the temperature. Partial differential equation (3.66) may be expressed in a more concise form by introducing the finite difference operators

$$\frac{1}{c\gamma}\frac{\partial}{\partial Z}\left(k \frac{\partial T}{\partial Z}\right) \Rightarrow \Lambda_Z T \tag{3.68}$$

$$\frac{1}{c\gamma}\frac{1}{R}\frac{\partial}{\partial R}\left(kR \frac{\partial T}{\partial R}\right) \Rightarrow \Lambda_R T. \tag{3.69}$$

Substitution of (3.68) and (3.69) into Eq. (3.66) results in the finite difference format:

$$\frac{\partial T}{\partial t} = \Lambda_Z T + \Lambda_R T + \frac{1}{c\gamma} Q(Z, R). \tag{3.70}$$

Figure 3.49 shows the rectangular mesh network. As mentioned above, the material properties are considered to be piecewise constants. Therefore the coefficients of Eqs. (3.66) and (3.67) vary at different mesh nodes. The finite difference stencil with respect to the Z-coordinate can be written as

$$\frac{1}{c\gamma}\frac{\partial}{\partial Z}\left(k\frac{\partial T}{\partial Z}\right) \Rightarrow \Lambda_Z T^{\tau}$$
$$= \frac{2}{c(T)\gamma(T)(h_i + h_{i+1})}\left(k_{i+1,j}\frac{T^{\tau}_{i+1,j} - T^{\tau}_{i,j}}{h_{i+1}} - k_{i,j}\frac{T^{\tau}_{i,j} - T^{\tau}_{i-1,j}}{h_i}\right). \tag{3.71}$$

In FDM, it is important that the boundaries of the mesh region coincide with the boundaries of the appropriate regions of the induction heating system. Experience in using FDM in induction heating computations has shown that noncoincidence of the boundaries has a strong negative effect on the accuracy of the calculation.

Approximations of the boundary conditions by Z = 0 and Z = ZZ are

$$\begin{aligned} Z = 0, \ &\Rightarrow \ k_{1,j}\frac{T^{\tau}_{1,j} - T^{\tau}_{0,j}}{h_{i+1}} = P_{z=0} \\ Z = ZZ, \ &\Rightarrow \ -k_{ZZ,j}\frac{T^{\tau}_{N,j} - T^{\tau}_{N-1,j}}{h_N} = P_{z=NN}, \end{aligned} \tag{3.72}$$

where i, j, τ are indexes corresponding to the Z-axis, the R-axis, and the time, respectively.

The finite difference expressions for differential operators with respect to the radius will be similar to (3.71) and (3.72) [56].

When mesh boundaries do not coincide with boundaries of the components of the induction heating system, then the values corresponding to the temperature at the boundary nodes are the values they have at the neighboring nodes of the real boundary (Figure 3.49, bottom right).

Since the accuracy of the numerical computation depends upon both the errors in the governing equation approximation and the error from approximating the boundary conditions, it is very important to treat boundary conditions at least as accurately as the governing equation.

Another factor that emphasizes the importance of a "good" approximation of the boundary condition and approximation of the subsurface area is the fact that according to the skin effect and some other phenomena discussed in Section 3.1, the heat sources penetrate from the workpiece surface toward the core. Therefore the most significant amount of heat sources are located at the surface and subsurface areas. So a rough approximation in these areas can have a detrimental effect on the overall accuracy of the calculations.

An important feature of heat transfer modeling deals with the fact that induction heating is a nonlinear time-dependent (transient) process. There are several formats available to address these features of nonlinearity and time-dependency. Each algorithm has its own advantages and disadvantages. The choice of a particular numerical procedure depends upon several factors, including the specifics of the application, computer capabilities, and individual experience using numerical methods.

Finite difference formats for the heat transfer transient problem range from explicit forms to the implicit forms [56]. Implicit forms require solving a set of algebraic equations at each time step.

The explicit approximation is the simplest technique. In explicit forms, the temperature distribution is obtained directly in a step-by-step manner. A forward difference approximation with respect to time leads to the explicit finite difference formulation

$$\frac{T_{i,j}^{\tau+1} - T_{i,j}^{\tau}}{h_\tau} = \Lambda_Z T_{i,j}^{\tau} + \Lambda_R T_{i,j}^{\tau} + \frac{1}{c\gamma} Q_{i,j}^{\tau}. \tag{3.73}$$

As one can see from Eq. (3.73), the unknown temperatures corresponding to the $(\tau + 1)$ time step are obtained as functions of the known material properties, heat sources, and temperatures at the time τ (Figure 3.50a). The temperatures are achieved by the workpiece after the first time step h_τ which is found by the given initial condition (initial temperature condition is often assumed to be ambient) and the appropriate boundary conditions. Therefore the unknown temperatures are obtained explicitly from their initially known or previously calculated values. No time-extensive procedures are required to execute a computer code.

The ability to provide a stable and accurate numerical solution is primarily a concern when using an explicit finite difference format. Accuracy is a measure of the closeness of the numerical approximation to the exact solution [56]. The finite difference format [i.e., finite difference formulation (3.73)] is said to be numerically stable if at sufficiently small time steps h_τ and space steps h that equation has a unique solution and that solution does not increase its magnitude with small variations of h_τ and/or h.

It should be pointed out here that the stability condition depends upon the properties of the finite difference format and is, in many cases, independent of the governing partial differential equation or physical phenomena. Unfortunately, explicit methods are accurate and stable only for certain relations between the time, space

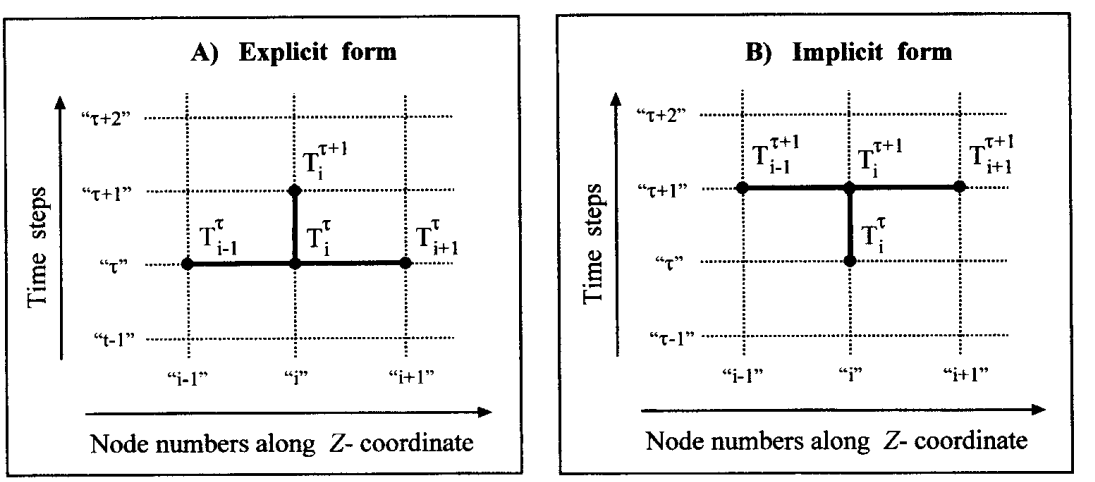

Figure 3.50 Examples of simplified explicit (A) and implicit (B) forms for one-dimensional approximation.

steps, and values of material properties. Sometimes those relations can contradict one another.

The stability condition usually leads to extremely small time steps. Otherwise a physically unrealistic oscillatory solution can occur. A fine mesh and small time step can require significant computational efforts.

With explicit formats it is not unusual to have a situation where the decreasing time steps and space steps will not improve the solution but rather worsen it. This is a typical case of unstable or ill-conditioned systems. In such cases, the use of different stencils may help. For example, instead of a central difference stencil a forward difference or backward difference approximation can be used and vice versa.

Thus, regardless of the simplicity and convenience of the explicit algorithms, a concern for obtaining an accurate and stable solution (particularly taking into consideration essentially nonlinear material properties) leads to a limited use of these algorithms as a computational tool for modeling induction heating processes.

Implicit methods are more popular due to their ability to provide more stable results compared to explicit algorithms and to have a relatively independent choice of mesh parameters (Figure 3.50b). Several implicit methods were developed to reduce computational efforts. The use of any implicit method requires the calculation of a system of algebraic equations.

When using implicit methods for modeling heat transfer problems, the finite difference format can be written as [56]

$$\frac{T_{i,j}^{\tau+1} - T_{i,j}^{\tau}}{h_\tau} = \xi(\Lambda_Z T_{i,j}^{\tau+1} + \Lambda_R T_{i,j}^{\tau+1}) + (1-\xi)(\Lambda_Z T_{i,j}^{\tau} + \Lambda_R T_{i,j}^{\tau}) + \frac{1}{c\gamma} Q_{i,j}^{\tau}. \tag{3.74}$$

The choice of the parameter ξ is a balance between accuracy and stability. The value of this parameter varies between 0 and 1. For $\xi = 0.5$, the well-known Crank–Nicolson format represents an intermediate approximation of the partial derivatives (halfway between two levels of time τ and $\tau + 1$). The complete implicit format is obtained when $\xi = 1$.

The implicit method is said to be unconditionally stable, however certain computational oscillations could appear when coarse mesh and large time steps are used. The time step is restricted by the desired accuracy. The following finite difference implicit formats are commonly used for solving the transient heat transfer problem.

a. A Locally One-Dimensional Format (Proposed by A. Samarskii [56]).

$$\frac{T_{i,j}^{\tau+0.5} - T_{i,j}^{\tau}}{h_\tau} = \Lambda_Z T_{i,j}^{\tau+0.5} + \frac{1}{2c\gamma} Q_{i,j}^{\tau} \tag{3.75}$$

$$\frac{T_{i,j}^{\tau+1} - T_{i,j}^{\tau+0.5}}{h_\tau} = \lambda_R T_{i,j}^{\tau+1} + \frac{1}{2c\gamma} Q_{i,j}^{\tau}. \tag{3.76}$$

The set of Eqs. (3.75) and (3.76) is said to be stable for all sizes of time step h_τ. The main restriction for choosing a large h_τ is avoiding significant truncation errors. Physically, Eqs. (3.75) and (3.76) can be interpreted as a complex combination of two heat transfer processes: along the Z-axis and along the R-axis [56]. The transition from time level τ to time level $\tau + 1$ is assumed to be made in two stages using

intermittent time step $0.5h_\tau$. This means that the transition from a known temperature field distribution of $T_{i,j}^{k}$ to an unknown temperature $T_{i,j}^{\tau+1}$, is made through the intermediate temperature distribution of $T_{i,j}^{\tau+0.5}$. In each direction, Fourier equation is approximated implicitly with the necessity of solving two sets of simultaneous algebraic equations.

After substituting the respective finite difference stencils into Eqs. (3.75) and (3.76) and after some simple algebraic operations, Eq. (3.75) can be rewritten as

$$\zeta_i T_{i-1,j}^{\tau+0.5} - \psi_i T_{i,j}^{\tau+0.5} + \upsilon_i T_{i+1,j}^{\tau+0.5} = -F_{i,j}^{\tau} \tag{3.77}$$

and, respectively, Eq. (3.76) will be

$$\zeta_i T_{i,j-1}^{\tau+1} - \psi_i T_{i,j}^{\tau+1} + \upsilon_i T_{i,j+1}^{\tau+1} = -F_{i,j}^{\tau}, \tag{3.78}$$

where ζ, ψ, and υ are coefficients

As one can see, the matrices of the algebraic equations (3.77) and (3.78) are sparsely occupied and have a tridiagonal matrix structure meaning that nonzeros occupy only the main diagonal and its neighborhood. Thanks to this feature, several simplified computational procedures can be effectively used [56] to solve Eqs. (3.77) and (3.78).

b. Peaceman–Rachford Format [56].

$$\frac{T_{i,j}^{\tau+0.5} - T_{i,j}^{\tau}}{0.5h_\tau} = \Lambda_Z T_{i,j}^{\tau+0.5} + \Lambda_R T_{i,j}^{\tau} + \frac{1}{c\gamma} Q_{i,k}^{\tau} \tag{3.79}$$

$$\frac{T_{i,j}^{\tau+1} - T_{i,j}^{\tau+0.5}}{0.5h_\tau} = \Lambda_Z T_{i,j}^{\tau+0.5} + \Lambda_R T_{i,j}^{\tau+1} + \frac{1}{c\gamma} Q_{i,k}^{\tau} \tag{3.80}$$

Equation (3.79) is implicit in direction Z and explicit in R. However, Eq. (3.80) is explicit in direction Z and implicit in R. A set of algebraic equations that corresponds to the Peaceman–Rachford format is similar to Eqs. (3.77) and (3.78).

As mentioned earlier, there have been two techniques used for solving algebraic equations obtained after substitution of the finite difference stencils into the partial differential equations: iterative algorithms (such as the Jacobi method, Gauss–Seidel method, over-relaxation techniques, etc.) and direct methods. One of the most widely used methods for solving a tridiagonal matrix is the Gaussian two-step elimination method. This algorithm is simple and effective. Its procedures take into account the features of the tridiagonal matrix and require a minimum computer memory and a short execution time.

The optimal choice of mesh generation and time steps has a pronounced effect on the accuracy and stability of the calculation using any of the numerical modeling techniques; however, these parameters become particularly critical when using FDM. Certainly, in FDM as in any of the numerical techniques, for greater accuracy the smaller space and time steps are recommended. In addition, it is quite clear that the large number of nodes results in a more complicated and time-consuming solution. Therefore there should be a reasonable compromise among mesh size, time steps, computation time, and accuracy of modeling. Naturally, it is recommended to select a smaller mesh size for regions with the greater gradients of variables (i.e., temperatures, magnetic vector potentials, or magnetic field intensities) and coarse mesh for areas where there is insignificant variation of variables.

The optimal combination of mesh parameters and time steps is usually determined by computational experiment. The calculations are provided for the different mesh sizes and time steps and the results are compared. If the comparison shows a large difference, then it is necessary to repeat the calculation for a finer mesh and/or smaller time steps until the difference between calculations is insignificant. The rule of thumb is: if the computation is done correctly, the values of the unknown variables (e.g., temperature) should converge as the space mesh becomes finer and time steps become smaller.

It is wise to remember that the reduction of the space steps leads to the reduction of truncation error. Furthermore, a finer mesh has a larger number of nodes and smaller space steps. The number of algebraic equations can grow tremendously; however, a computer deals with only a limited number of arithmetic units. All these can lead to a crucial level of round-off errors. Therefore the accuracy of the computations can be improved by refining the space mesh and reducing the time steps, unless the round-off errors become excessive (see Figure 3.51).

Often developers and users of numerical computation software have created certain "tricks" and know-how that allow them to overcome relatively quickly the problems resulting from computation failure due to round-off errors. For example, one can successfully rerun the program by only slightly changing some insignificant material properties or by a slight remeshing.

The other way to avoid computation failures cased by round-off error is using double precision arithmetic. Of course it will lead to an increase of software execution time.

The above-mentioned remarks regarding different aspects of mesh generation and computation errors are valid not only for FDM but for the majority of other numerical techniques as well (including finite element, boundary element, etc.).

When modeling problems that couple several different physical phenomena (e.g., electrothermal, heat transfer-phase transformation, electromechanical, etc.), it is very attractive to use a single universal mesh. This might seem like a time-saving approach and would allow one to save time on the mesh generation. However, from

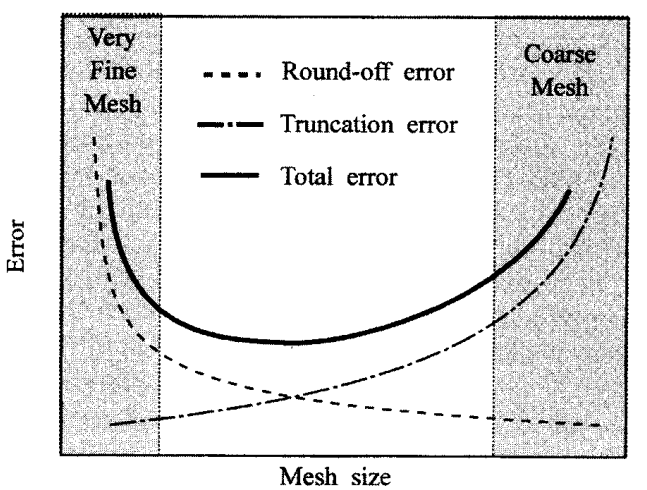

Figure 3.51 Correlation among the round-off error, truncation error, and mesh size.

a practical point of view, if the physical phenomena are inherently different (e.g., heat transfer phenomena and eddy current) it is often more efficient to use different, problem-optimized meshes.

The method of finite differences has been illustrated based on the most commonly used first- and second-order finite difference approximations (3.62) to (3.65). The accuracy of the numerical calculations may be improved by employing higher-order finite difference approximations. Such approximations will allow one to reduce truncation error, but at the same time, this approach results in an increase of the number of nodes involved in the local approximation. And therefore a matrix of algebraic equations will no longer be tridiagonal but five- or seven-diagonal. This makes the program code more complex with a noticeable increase in execution time and memory use. FDM is used for creating computational code; for modeling the induction heating process, first- and second-order finite difference approximations are typically used.

3.4.3.3 *Finite Element Method*

The finite element method (FEM) is another group of numerical techniques devoted to obtaining an approximate solution for different technical problems, including those encountered in induction heating. This numerical technique was originally applied in mechanical engineering. Later, applications of FEM have expanded to other areas of engineering. It has become one of the most popular numerical tools for a variety of scientific and engineering tasks. The tremendous improvement in computer capabilities (particularly within the last three decades) has boosted the development of several variations of the finite element method [55, 60–83].

Some of these are:

- Weighted residual method (weak form of the governing equations);
- Different kinds of the Ritz method;
- Different types of the Galerkin method;
- Pseudo-variational methods; and
- Methods based on minimization of the energy functional, and so on.

As described in Section 3.4.3.2, the finite difference method provides a point wise approximation; however, the FEM provides an elementwise approximation of the governing equations.

Different finite element approaches might be better suited for certain problems. For example, the weighted residuals formulation has been very effectively used for computation of heat transfer problems. An interested reader can find a description of different finite element techniques in [60–83]. Since induction heating is a complex combination of electromagnetic and heat transfer phenomena and taking into consideration that in the previous section, the use of FDM has been illustrated for modeling a heat transfer problem, in this chapter we discuss the use of FEM for solving electromagnetic problems.

Several different FEM codes have been developed for modeling electromagnetic processes taking place in electric machines, motors, circuit breakers, transformers, magnetic recording systems, test equipment, and electrical and induction heating machines.

Many worthwhile texts, conference proceedings, and articles have been written on the subject of finite element modeling [55, 60–83]. The large number of papers on

the subject of FEM applications for electromagnetic field computation makes it impossible to mention all of the contributions. However, some of the proposed finite element models are similar in form. It should be mentioned here that P. Silvester and M. Chari [60, 61] presented the first general nonlinear variational formulation of magnetic field analysis using FEM. Essential input into the development of FEM was provided by W. Lord, A. Konrad, S. Salon, S. Udpa, D. Lavers, J. Brauer, A. Bossavit, J. Sabonnadiere, and many others [63–66, 69, 70, 72, 73, 81, 83]. The following is short description of one form of FEM which has been successfully applied at INDUCTOHEAT, Inc. for computation of eddy current field problems for several years. This approach is based on a combination the finite-element concept proposed by W. Lord [63, 64], S. Udpa and coworkers [72, 73], and S. Gurevich and coworkers [467].

Due to the general postulate of the variational principle, the solution of electromagnetic field computation is typically obtained by minimizing the energy functional that corresponds to the governing equation [e.g., Eqs. (3.55) or (3.57)] instead of solving that equation directly. The energy functional is minimized for the integral over the total area of modeling, which includes the workpiece, coil, flux concentrators, cores, and surrounding area.

The well-known principle of minimum energy [55, 60–64, 66, 68, 71, 75, 80–82] requires that the vector potential distribution correspond to the minimum of the stored field energy per unit length. As a result of that assumption, it is necessary to solve the global set of simultaneous algebraic equations with respect to the unknown, for example, magnetic vector potential at each node. The formulation of the energy functional, its minimization to obtain a set of finite element equations, and the solution techniques (the solver) were created for both two-dimensional (Cartesian system) and axisymmetric (cylindrical system) induction heating problems.

Magnetic vector potential **A** in the two-dimensional case (longitudinal cross-section) acts in the direction of the current density **J** and is described by a two-dimensional partial differential equation (3.55). The boundary of the region can be selected so that the magnetic vector potential **A** is zero along the boundary (Dirichlet condition) or Neumann condition ($\partial A/\partial n = 0$), meaning that its gradient is negligibly small along the boundary compared to the value elsewhere in the region.

The energy functional corresponding to the two-dimensional governing equation (3.55) can be written in the form [60, 61]:

$$F = \int_V \left(\frac{1}{2\mu_r \mu_0} \left(\left| \frac{\partial A}{\partial X} \right|^2 + \left| \frac{\partial A}{\partial Y} \right|^2 \right) + j \frac{\omega \sigma}{2} |A|^2 - J_S A \right) dV, \tag{3.81}$$

where V is the total area of modeling and J_S is a source current density. The first, second, and third terms inside the integrand represent energy of the magnetic field, eddy currents, and the source current, respectively.

The minimization of the functional (3.81) corresponds to the solution of the two-dimensional eddy current field problem with respective boundary conditions.

According to FEM, the area of study is divided into nonoverlapping numerous finite elements (mesh), therefore the minimization of this functional provides minimization of energy at every node of each element.

Many geometric arrangements and shapes of finite elements are possible. Flexibility of their shapes allows them, in fact, to satisfy regions of practically any geometry, that is, any shape of induction heating system.

The most common two-dimensional finite element is the first-order triangle (Figure 3.52). In the axisymmetric cylindrical case, such a finite element mesh may be represented as a set of rings. Each ring revolves around the axis of symmetry and has a triangular cross-section (the so-called triangular torus element). The use of high-order isoparametric elements allows reduction of the required total number of elements at the expense of an increase in computation time and algorithm complexity.

Space discretization is a very important aspect of FEM analysis. The following are some general remarks concerning finite element discretization (mesh generation) that has some similarities with FDM.

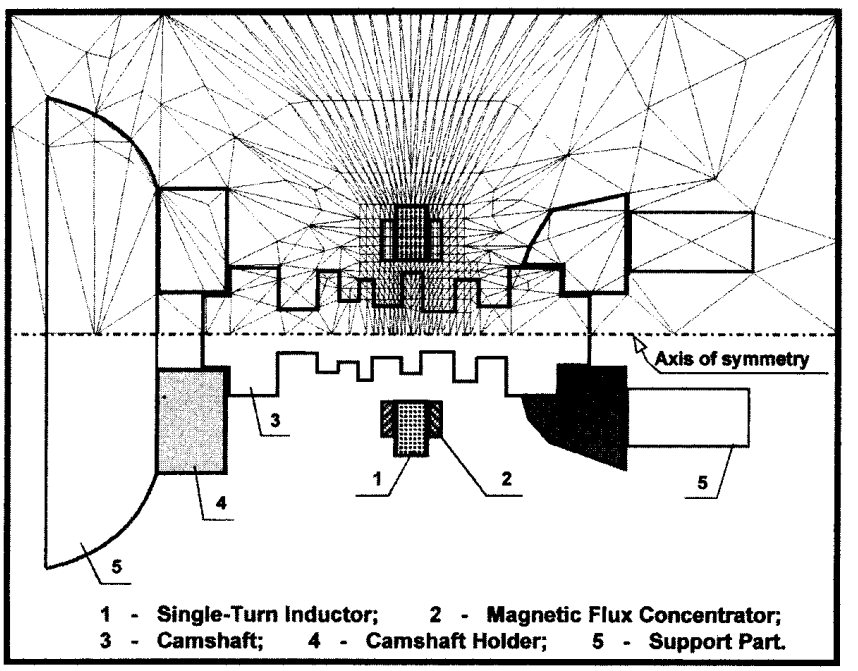

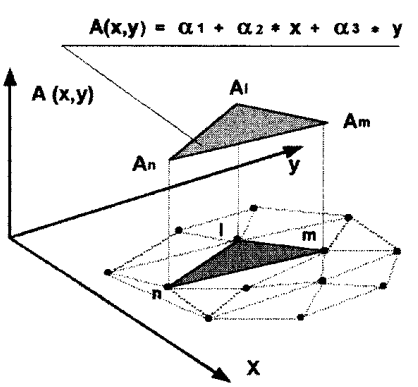

Figure 3.52 Finite element discretization.

The area of study is subdivided into nonoverlapping finite elements (finite element mesh, Figure 3.52). The sides of the finite elements intersect at nodes. The number and location of these elements depend upon personal judgment. However, in order to obtain reasonable accuracy of the numerical solution, the finite element mesh has to be relatively fine (sizes of finite elements must be smaller) in the regions where the rate of change of the unknown (i.e., the magnetic vector potential) is high. Experience using finite element software at INDUCTOHEAT, Inc. has shown that special effort should be made to obtain a fine mesh within three current penetration depths in the workpiece surface that faces the induction coil. A higher frequency requires a finer mesh.

- All the finite elements should have the same unit depth in the Z direction.
- The current density, flux density, electrical conductivity, magnetic permeability, and other material properties are postulated to be constant within each element. At the same time, they can be different from element to element.
- The designer should take advantage of the symmetry involved in the system geometry, for example, by making normal derivative values of **A** along the symmetry disappear.

In most typical cases, when it is necessary to obtain the electromagnetic field distribution and temperature profile along the length of a cylindrical workpiece (longitudinal cross-section), the finite element method has been used in solving the governing equation with respect to magnetic vector potential for the electromagnetic problem [Eqs. (3.55) and (3.56)].

Assuming that local behavior of the electromagnetic field is linear across each finite element and can be approximated by a linear law, and supposing that the chosen finite elements are first-order parametric triangulars, then the magnetic vector potential behavior within a triangular can be defined as

$$A(X, Y) = \alpha_1 + \alpha_2 X + \alpha_3 Y. \tag{3.82}$$

Based on two-dimensional linear approximation laws, the coefficients $\alpha_1, \alpha_2, \alpha_3$ are constant and can be calculated from the three independent simultaneous equations by assuming vertex values of $\mathbf{A}_l$, $\mathbf{A}_m$, $\mathbf{A}_n$ of a magnetic vector potential A at the three nodes of a triangular. Therefore the local set of equations can be rewritten as

$$\begin{aligned} A_l &= \alpha_1 + \alpha_2 X_l + \alpha_3 Y_l \\ A_m &= \alpha_1 + \alpha_2 X_m + \alpha_3 Y_m \\ A_n &= \alpha_1 + \alpha_2 X_n + \alpha_3 Y_n. \end{aligned} \tag{3.83}$$

The matrix notation of set (3.83) can be written as

$$\begin{bmatrix} A_l \\ A_m \\ A_n \end{bmatrix} = \begin{bmatrix} 1 & X_l & Y_l \\ 1 & X_m & Y_m \\ 1 & X_n & Y_n \end{bmatrix} \begin{bmatrix} \alpha_1 \\ \alpha_2 \\ \alpha_3 \end{bmatrix}. \tag{3.84}$$

The determinant of the square matrix in (3.84) can be introduced as a value of twice the triangular area. Knowing the geometry of elements and the magnetic vector potential at each node in every element, it is possible to obtain the value of A at any point inside the element. By extending a local approximation to all the elements that

represent the total area of interest, it is possible to obtain an approximation for the magnetic vector potential throughout the modeling area (Figure 3.52).

Energy balance within the modeling area is determined by minimizing the energy functional at every node. This can be arranged by setting the first partial derivative of the functional with respect to each node, equal to zero. Instead of performing the minimization of the functional node by node, it is reasonable to perform it element by element.

The total (global) energy associated with a whole area of modeling equals the sum of the energies of all elements. As a result, a set of the simultaneous algebraic equations with respect to the unknown values of magnetic vector potential at each node can be obtained.

After some algebraic operations, the local matrix equation, which represents the minimization of the energy functional within any triangular element, can be written as

$$[[V]_e + j[W]_e][A] = [Q]_e, \tag{3.85}$$

where

$$[V]_e = \frac{1}{4\mu_r\mu_0\Delta}\begin{bmatrix} (b_l b_l + c_l c_l) & (b_l b_m + c_l c_m) & (b_l b_n + c_l c_n) \\ (b_m b_l + c_m c_l) & (b_m b_m + c_m c_m) & (b_m b_n + c_m c_n) \\ (b_n b_l + c_n c_l) & (b_n b_m + c_n c_m) & (b_n b_n + c_n c_n) \end{bmatrix} \tag{3.86}$$

$$\begin{bmatrix} a_l & a_m & a_n \\ b_l & b_m & b_n \\ c_l & c_m & c_n \end{bmatrix} = \begin{bmatrix} (X_m Y_n - X_n Y_m) & (X_n Y_l - X_l Y_n) & (X_l Y_m - X_m Y_l) \\ (Y_m - Y_l) & (Y_n - Y_l) & (Y_l - Y_m) \\ (X_n - X_m) & (X_l - X_n) & (X_m - X_l) \end{bmatrix} \tag{3.87}$$

$$[W]_e = \frac{\omega\sigma\Delta}{12}\begin{bmatrix} 2 & 1 & 1 \\ 1 & 2 & 1 \\ 1 & 1 & 2 \end{bmatrix} \tag{3.88}$$

$$[Q]_e = \frac{J_S\Delta}{3}\begin{bmatrix} 1 \\ 1 \\ 1 \end{bmatrix} \tag{3.89}$$

$$[A]_e = \begin{bmatrix} A_l \\ A_m \\ A_n \end{bmatrix}. \tag{3.90}$$

Δ is a cross-sectional area of a particular triangular.

After assembling all local matrices of finite elements and specifying the corresponding boundary conditions, a global matrix equation can be obtained:

$$[G][A] = [Q]. \tag{3.91}$$

It is necessary to mention here that there are several commonly used ways to specify the boundary conditions in Eq. (3.91). One of the most popular techniques is called blasting the diagonal. This technique requires multiplying the diagonal terms of the equations representing the nodes where the value of the magnetic vector potential is known by a significantly large number (e.g., 10^{30}). At the same time,

the corresponding right-hand sides of those equations are replaced by known values of boundary conditions times the new diagonal. Such an artificial approach is very effective and easy to apply in computer code.

For the axisymmetric case the local and global matrices will be similar to Eqs. (3.85) through (3.91) [64]. Parameters of the local matrix of Eq. (3.85) for the axisymmetric problem (i.e., cylindrical system) are

$$[V]_e = \frac{R_c}{4\mu_r\mu_0\Delta}\begin{bmatrix} (\beta_l\beta_l + c_lc_l) & (\beta_l\beta_m + c_lc_m) & (\beta_l\beta_n + c_lc_n) \\ (\beta_m\beta_l + c_mc_l) & (\beta_m\beta_m + c_mc_m) & (\beta_m\beta_n + c_mc_n) \\ (\beta_n\beta_l + c_nc_l) & (\beta_n\beta_m + c_nc_m) & (\beta_n\beta_n + c_nc_n) \end{bmatrix}, \tag{3.92}$$

where R_c is the radius of the finite element centroid, and $\beta_i = b_i + 2\Delta/3R_c$, $i = l, m, n$.

$$\begin{bmatrix} a_l & a_m & a_n \\ b_l & b_m & b_n \\ c_l & c_m & c_n \end{bmatrix} = \begin{bmatrix} (R_mZ_n - R_nZ_m) & (R_nZ_l - R_lZ_n) & (R_lZ_m - R_mZ_l) \\ (Z_m - Z_n) & (Z_n - Z_l) & (Z_l - Z_m) \\ (R_n - R_m) & (R_l - R_n) & (R_m - R_l) \end{bmatrix} \tag{3.93}$$

$$[W]_e = \frac{\omega\sigma R_c\Delta}{12}\begin{bmatrix} 2 & 1 & 1 \\ 1 & 2 & 1 \\ 1 & 1 & 2 \end{bmatrix} \tag{3.94}$$

$$[Q]_e = \frac{J_S R_c\Delta}{3}\begin{bmatrix} 1 \\ 1 \\ 1 \end{bmatrix} \tag{3.95}$$

$$[A]_e = \begin{bmatrix} A_l \\ A_m \\ A_n \end{bmatrix}. \tag{3.96}$$

As with the FDM, the significant portion of the computation work for FEM consists of solving the large system of matrix equations. A global matrix in Eq. (3.85) can be solved using either iterative methods or direct matrix inversion techniques while taking into consideration the matrix's sparse nature and banded symmetry.

As mentioned above, the accuracy of the numerical approximation of the governing partial differential equations improves with a finer mesh. In other words, the more finite elements used in the simulation, the better the approximation will be and the closer a numerical solution gets to the exact solution of the governing equations. The optimum number of elements depends upon the problem of modeling. Our experience shows that a finite element mesh of 10,000 elements with about 5151 nodes is typically sufficient for the majority of induction heat treating problems. In the stage of developing and testing FE code, a developer can judge the obtained accuracy of the FE approximation based on its comparison with the available analytical solution.

After solving the system of algebraic equations and obtaining the distributions of the magnetic vector potential in the modeling region, it is possible to find all of the required output parameters of the electromagnetic field.

The induced current density in conductors,

$$J_e = -j\omega\sigma A. \tag{3.97}$$

The total current density in the conductor,

$$J = J_s - j\omega\sigma A. \tag{3.98}$$

The magnetic flux density components B_x and B_y can be calculated from relationship (3.45) as follows [63, 64],

$$\frac{\partial A}{\partial Y} = -B_x; \qquad \frac{\partial A}{\partial X} = B_y. \tag{3.99}$$

From (3.99) the flux density can be obtained as

$$B = \left[B_x^2 + B_y^2\right]^{1/2}. \tag{3.100}$$

For the axisymmetric case of a cylindrical workpiece, the magnetic flux density components B_R and B_Z can be calculated as

$$B_R = -\frac{\partial A}{\partial Z}; \qquad B_Z = \frac{\partial A}{\partial R} + \frac{A}{R}. \tag{3.101}$$

Magnetic field intensity,

$$H = \frac{B}{\mu_r \mu_0}. \tag{3.102}$$

Electric field intensity,

$$E = -j\omega A. \tag{3.103}$$

Electromagnetic force density in current-carrying conductors and the workpiece can be computed from the cross product of the vector of total current density and the vector of magnetic flux density:

$$F_x = J \times B_y; \qquad F_y = -J \times B_x. \tag{3.104}$$

From a vector potential solution it is possible to compute the other important quantities of the process such as stored energy, flux leakage, total power loss, and coil impedance.

As one can see, the above-described FEM requires using the current density of the source (induction coil) as the input parameter. This is often the case for induction hardening applications. At the same time, in the majority of induction heating applications prior to hot and warm forming when using multiturn coils it is necessary to have not a current density but the voltage of the coil as the input parameter. For cases such as these, special FEM procedures have been developed [73, 77, 78].

3.4.3.4 Mutual Impedance Method

The inductors involved in induction heating of billets, bars, slabs, and the like prior to the metal hot forming processes including forging, upsetting, rolling, and extrusion are quite different compared to inductors for heat treating (i.e., surface hardening). Induction billet/bar heaters are typically designed as multiturn solenoid coils

of cylindrical or rectangular shape. Such induction heaters can consist of one or several inline coils. The total length of a system sometimes exceeds 10 m. The inside diameter of some coils can be as large as 1 m. Depending upon the specifics of the application, coils can be fabricated as single or multilayer solenoids connected to a single and/or multiphase power source with normal and/or complex drive circuit connections (e.g., auto-transformer-type connections).

Two of the well-known disadvantages of both FDM and FEM are the problem of incorporating the circuit equations into general consideration and the difficulty of modeling long systems since an enormously large finite element or finite difference mesh is required.

For relatively short systems (e.g., 1–2 m) there have been some straightforward attempts to compute the induction system by combining circuit equations with finite difference or finite element equations. Such a large global matrix would consist of all the unknown parameters and can be solved all at once. Regardless of the seeming simplicity, such an approach results in an unrealistically large amount (from an engineering point of view) of computational work.

As an alternative to FDM and FEM, the mutual impedance method (MIM) can be used to solve a circuit analysis problem combined with an eddy current problem of induction heating for cylindrical-shaped systems (e.g., induction billet or bar heating). In some rare cases, MIM can be used for computer modeling of rectangular systems (heating of slabs and RCS bars).

As an alternative to FDM and FEM, the mutual impedance method applies an integral equation approach instead of using a differential formulation of the electromagnetic equations. The integral equation approach typically requires less computer memory and execution time. It is not required to make an artificial assumption for boundary conditions at infinitely propagating regions. The integral equation is complete as it is, thanks to the explicit appearance of the boundary values in the integrals.

Another advantage of using integral equations deals with the fact that the area of the integration (computation) is limited to surfaces of electrically conductive bodies. In other words, the electrically conductive bodies of the induction heating system limit the mesh of discretization. Therefore the areas requiring discretization include induction coils, workpieces, magnetic shunts, concentrators, fasteners, and so on. Unlike FEM and FDM, integral formulations do not generally have to consider free space areas (such as air).

As with FDM and FEM, there are several different formulations of MIM devoted to the simulation of the induction heating problem. One of the earliest texts describing this technique was by E. Kolbe and W. Reiss in 1962 [460]. Further development of this technique was done by O. Tozoni [462], R. Dudley [461], P. Burke [461], and several other researchers. A brief introduction to MIM is given here based on the concepts discussed in [165].

Let's first consider two axisymmetric multiturn coaxial coils (Figure 3.53) connected in series and driven by a sinusoidal voltage source. No harmonics are involved in the example. Both coils are placed around an axisymmetric nonmagnetic workpiece (i.e., copper, aluminum, or stainless steel billets). The electromagnetic field distribution in such a system can be described with respect to the current densities in the electrically conductive parts of the induction system by the Fredholm integral equation of the second kind:

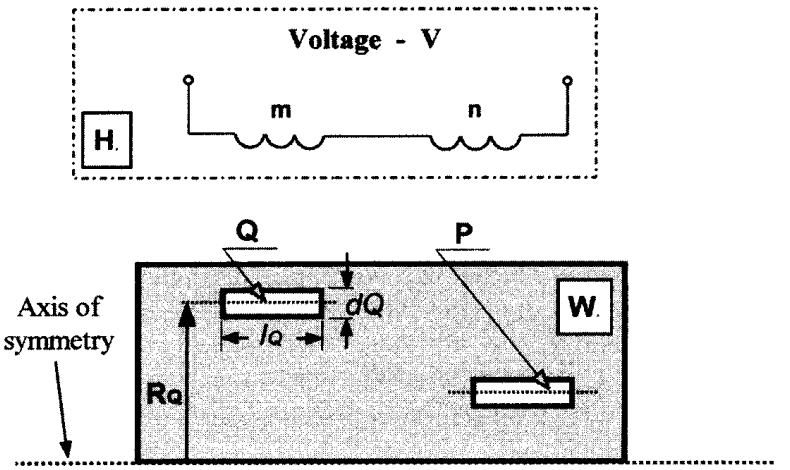

Figure 3.53 Representation of the induction system for mutual impedance method (MIM). **W** represents the cylinder workpiece. **H** represents the induction heater.

$$2\pi R_Q \rho_Q J + j\omega \int_{P \in H,W} M_{QP} J_P dS_P = V_Q, \tag{3.105}$$

where

$\rho_Q = 1/\sigma_Q$, resistivity of the element Q;
R_q = average radius of the element Q;
J_Q and J_P = current densities in the elements Q and P, respectively;
M_{QP} = mutual inductance between elements Q and P, respectively, representing a mutal interaction of the elements (current-carrying rings);
S_P = computation areas ($p \in H, W$, where H represents the induction heater and W represents the heated workpiece); and
V_Q = source voltage of the element. The value of V_Q is zero for all elements of the workpiece.

The method of solving the integral equation in the most complicated case has been described in [462]. The solution of Eq. (3.105) in its simplest form [165] is presented here.

The electrically conductive regions of the induction heating system, including the induction heater and workpiece (Figure 3.53, areas, $\boldsymbol{H}$ and $\boldsymbol{W}$, correspondingly) are subdivided into appropriate elements. As with FEM, eddy current densities and material properties are assumed to be constant within each element.

If the skin effect in the coil is pronounced then the multiturn induction coils can be considered to act as multiturn solenoids. The integral equation (3.105) can be rewritten as

$$r_Q I_Q + j\omega \sum_{P \in H,W} M_{QP} I_P = V_Q, \tag{3.106}$$

where r_Q = resistance of the element Q.

As seen from (3.105) and (3.106), the Fredholm integral equation of the second kind is converted into an impedance equation representing the well-known Kirchhoff's law. After assembling equations that correspond to all electrically

conductive elements of the induction system, the global set of impedance equations can be obtained.

In order to illustrate the procedure described above, a set of global equations representing the induction system in Figure 3.53 is obtained below. According to the sketch shown in Figure 3.53, the induction heating system consists of two elements of the workpiece (elements P and Q) and two induction coils m and n connected in series. The global set of the impedance equations for this case is

$$\begin{aligned}
(r_Q + j\omega M_{QQ})I_Q &+ j\omega M_{QP} I_P &+ j\omega(M_{Qn} + M_{Qm})I_{mn} &= 0 \\
j + \omega M_{PQ} I_Q &+ (r_P + j\omega M_{PP})I_P &+ j\omega(M_{Pn} + M_{Pm})I_{mn} &= 0 \\
j\omega(M_{nQ} + M_{mQ})I_Q &+ j\omega(M_{nP} + M_{mP})I_P &+ (r_n + r_m + j\omega(M_{mn} + M_{nm}))I_{mn} &= V,
\end{aligned} \tag{3.107}$$

where M_{QQ}, M_{PP}, M_{nn}, and M_{mm} are the self-inductances of the elements and coils, respectively; and M_{QP}, M_{Qn}, M_{Qm}, M_{PQ}, M_{Pn}, M_{Pm}, M_{nQ}, M_{nP}, M_{nm}, M_{mQ}, M_{mP}, and M_{mm} are the mutal inductances representing the interaction of all the current-carrying elements.

The formulas for calculation of the various self-inductances and mutual inductances with their range of applicability are given in [463–465]. The resistances of the rings (r_Q and r_P) and resistances of the coils (r_n and r_m) can be calculated as

$$r_Q = \frac{2\pi\rho_Q R_Q}{d_Q l_Q} \tag{3.108}$$

$$r_n = \frac{2\pi\rho_n R_n}{l_n \delta_n K_{\text{space}}} N, \tag{3.109}$$

where K_{space} is the space factor of the coil and N is the number of turns of the coil n.

After some simple algebraic operations, the resulting matrix equation can be rewritten as

$$\begin{bmatrix} \mathbf{a}_W & \mathbf{a}_{WH} \\ \mathbf{a}_{HW} & \mathbf{a}_H \end{bmatrix} \begin{bmatrix} I_W \\ I_H \end{bmatrix} = \begin{bmatrix} 0 \\ V_H \end{bmatrix}, \tag{3.110}$$

where $\mathbf{a}_W$, $\mathbf{a}_H$ are matrices of the self-impedances of the workpiece and induction coils and $\mathbf{a}_{WH}$, $\mathbf{a}_{HW}$ are matrices of the mutual inductances.

By evaluation of the equations for the mutual inductances between elements it is obvious that $M_{PQ} = M_{QP}$ and $\mathbf{a}_{WH} = \mathbf{a}_{HW}$. Therefore the matrix of

$$\begin{bmatrix} \mathbf{a}_W & \mathbf{a}_{WH} \\ \mathbf{a}_{HW} & \mathbf{a}_H \end{bmatrix}$$

is symmetric and the set of Eqs. (3.110) can be rewritten as

$$[\mathbf{S}_r + j\mathbf{S}_x][\mathbf{I}_r + j\mathbf{I}_x] = [\mathbf{V}_r + j\mathbf{V}_x], \tag{3.111}$$

where

$\mathbf{S}_r$ = diagonal matrix consisting of the resistivities of elements of coils and the workpiece

$\mathbf{S}_x$ = square matrix of the self-inductances and mutual inductances

$\mathbf{I}_r, \mathbf{I}_x$ = column matrices representing that the currents have both real and imaginary components ($\mathbf{I} = \mathbf{I}_r + j\mathbf{I}_x$)
$\mathbf{V}_r, \mathbf{V}_x$ = column matrices of the voltages ($\mathbf{V} = \mathbf{V}_r + j\mathbf{V}_x$) which are similar to the column matrices of the currents.

The set of Eqs. (3.111) can be rewritten as

$$\begin{bmatrix} \mathbf{S}_r & -\mathbf{S}_x \\ \mathbf{S}_x & \mathbf{S}_r \end{bmatrix} \begin{bmatrix} \mathbf{I}_r \\ \mathbf{I}_x \end{bmatrix} = \begin{bmatrix} \mathbf{V}_r \\ \mathbf{V}_x \end{bmatrix}. \tag{3.112}$$

Since the matrix $\mathbf{S}_r$ is a diagonal matrix and the matrix $\mathbf{S}_x$ is a symmetrical square matrix, in order to reduce the execution time and computer memory required for storage of all matrices a special computational procedure for solving the set of Equations (3.112) has been developed [165]:

$$[\mathbf{S}_r + \mathbf{S}_x\mathbf{S}_r^{-1}\mathbf{S}_x][\mathbf{I}_x] = [\mathbf{V}_r - \mathbf{S}_x\mathbf{S}_r^{-1}\mathbf{V}_r] \tag{3.113}$$

$$[\mathbf{I}_r] = [\mathbf{S}_r]^{-1}[\mathbf{V}_r + \mathbf{S}_x\mathbf{I}_x]. \tag{3.114}$$

After solving the set of Eqs. (3.113) and (3.114) one can obtain the coil currents and eddy currents as well as power densities, heat source distribution in the workpiece, and other important design parameters of the induction system including coil power, power induced within the workpiece, coil electrical efficiency, power factor, and so on.

As in any numerical technique, a proper space discretization is a very important aspect of the mutual impedance method. One of the obvious advantages of MIM is its ability to relatively easily incorporate circuit connection features into general consideration. Some of the typical circuits that have been studied using this technique are shown in Figure 3.54.

The MIM method was extended for the computation of induction heating of magnetic workpieces by combining the mutual inductance method with the boundary element method (BEM) [49, 51].

3.4.3.5 *Boundary Element Method*

The fourth family of numerical techniques devoted to induction heating computation is called the boundary element method (BEM). This method started to be widely used for modeling processes related to induction heating in the late 1980s to the early 1990s. The mathematics required to discuss the BEM are more advanced than those needed for FDM, FEM, or MIM. The interested reader will find several texts, conference proceedings, and journal articles [49, 51, 83–90] that describe various modifications of BEM.

Here we just mention that when applying BEM (in contrast to FDM or FEM), an integral form of Maxwell's equation is used as a governing equation for the electromagnetic problem. This allows one to take into consideration only conductive bodies in the computation. In this respect BEM has some similarity with MIM.

With the BEM unknown characteristics of the electromagnetic field (i.e., magnetic vector potential) are expressed in terms of an integral over the boundary of the area of interest. In this case, the problem of mathematical modeling of induction processes may be divided into two tasks: external and internal electromagnetic problems. Using an iterative procedure both tasks can be solved. The internal problem

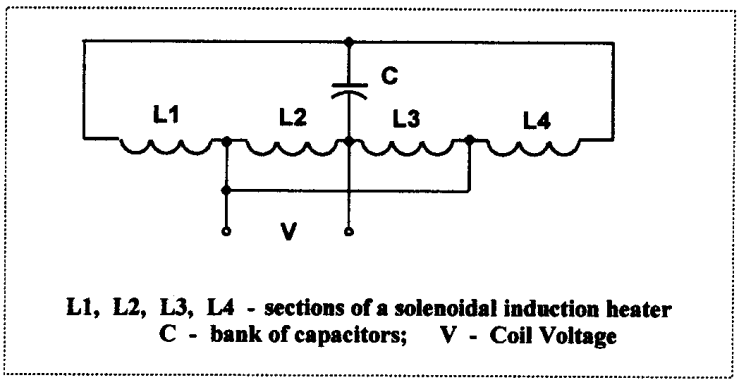

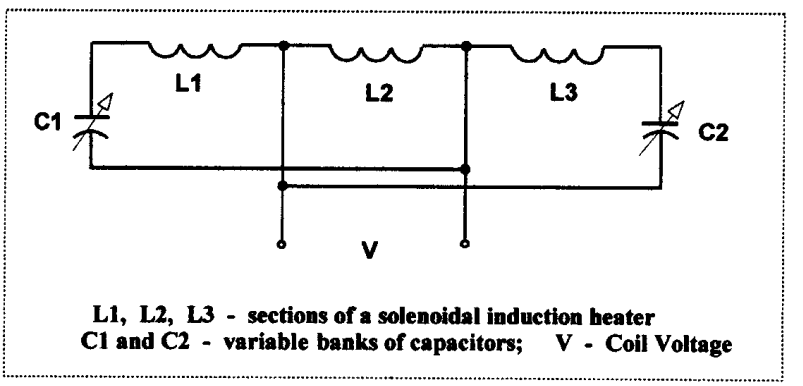

Figure 3.54 Examples of the circuit connections of induction heating coils.

describes the electromagnetic field distribution within the body of the workpiece. The external problem describes the field distribution in external regions.

Contrary to FEM, BEM only requires discretization of the boundaries of the components of the induction system. A computational procedure establishes the unknown surface qualities (i.e., equivalent current densities along surfaces) that would satisfy the global solution.

According to one of the many forms of the BEM [84–90], it is assumed that the surface impedance is initially known and could be determined as

$$Z_0 = \frac{E_t}{H_t}. \tag{3.115}$$

This assumption was proposed by Leontovich for problems exhibiting a pronounced skin effect. It is obvious that Z_0 is not constant along the workpiece surface and is a function of the electromagnetic field. For many induction heating applications, the surface impedance of the workpiece can be defined at a particular node ξ, similar to the surface impedance of an infinite conducting half plane as [466]

$$Z_0^{\xi} = \frac{\rho_{\xi}(U + jV)}{\delta_{\xi}}, \tag{3.116}$$

where U and V are coefficients, $U, V \leq 1$ depending upon the application, ρ_ξ is electrical resistivity, and δ_Q is current penetration depth at node Q.

As shown in [49, 51], if the skin effect in a nonmagnetic load is pronounced then $U = V = 1$ (Leontovich condition). In the case of a magnetic body placed in a relatively strong magnetic field those coefficients will be $U = 1.32 - 1.37$ and $V = 0.97$. In the edge and corner areas of the surface, the assumption (3.116) is not valid and different approaches should be used.

As mentioned above, a thorough discussion of the BEM is beyond the scope of this text. Details on the boundary element method can be found in [84–94]. Such advantages as the reduction of computation time, simplicity, and user-friendliness of mesh generation as well as good accuracy make this technique quite attractive in certain applications compared to other methods.

3.4.3.6 Coupling of the Electromagnetic and Thermal Problems

One of the major features of induction heating computation deals with the fact that both the electromagnetic and heat transfer phenomena are tightly coupled thanks to the interrelated nature of the material properties (see Secs. 3.1.1 and 3.2.1) such as

- Specific heat, thermal conductivity, and electric resistivity are functions of temperature.
- Magnetic permeability is a function of magnetic field intensity, temperature, and frequency

Obviously, these variations of physical properties make the induction heating problem nonlinear. This interrelated feature dictates the necessity of development of special computational algorithms that are able to deal with these coupled effects. An important observation that has a noticeable effect on consideration of the coupling phenomenon deals with the fact that the time scales (time constants) of the electromagnetic and heat transfer processes have different orders. Electromagnetic processes used in induction heating are very fast with time constants significantly less then 0.02 sec (depending upon the frequency). At the same time, the heat transfer processes are much longer. For example, time cycle for induction billet heaters can exceed 300 sec depending upon frequency, geometry, and material properties of the billet.

There are several ways to couple the electromagnetic and heat transfer problems. The simplest method is called a two-step approach (Figure 3.55). The first step is devoted to solving the electromagnetic problem. Then the obtained current densities and Joule loss distribution are used as heat sources for solving the thermal problem assuming that the electrical resistivity and magnetic permeability do not change during heating. The two-step approach is known for its short execution time and moderate computer memory requirements.

Even a cursory look at the behavior of the material properties in Figures 3.2 through 3.11, 3.39, and 3.40 reveals the danger in using a two-step approach. As shown in Sections 3.1.1 and 3.1.2, the electrical resistivity of some metals can vary during the process of heating more than 8 times. Furthermore, relative magnetic permeability can vary 60 times or more. Therefore an assumption that material properties are constant during the entire heating period is a very rough postulation and can result in significant calculation errors. Thus this approach can be used in a very limited number of induction heating applications. Low-temperature heating (i.e., heating from ambient temperature to about 200°C) of aluminum or copper

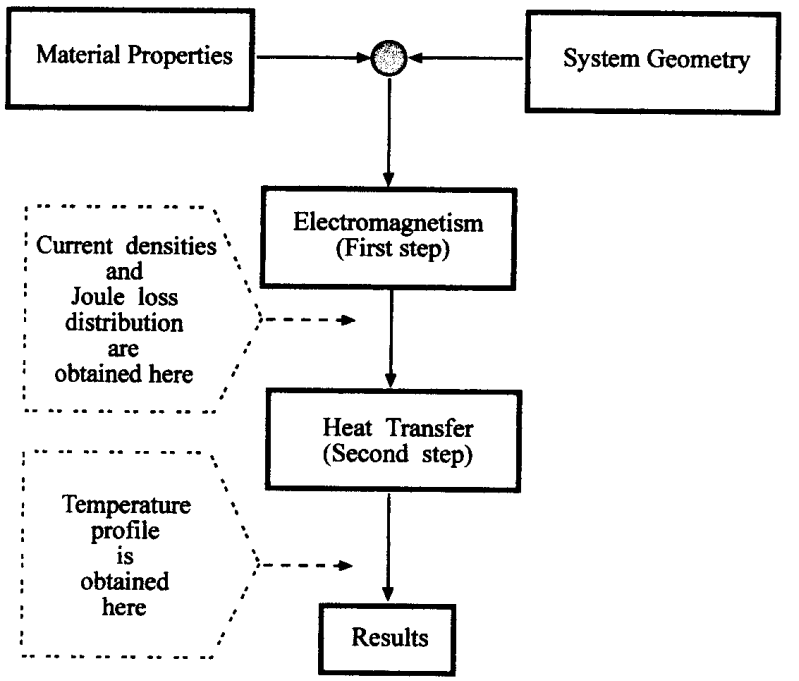

Figure 3.55 Two-step approach for coupling in induction heating.

strips or wires can serve as an example when a two-step coupling approach can be used quite effectively (the average values of the metal properties are used in the calculation in cases like this).

The most common approach to coupled electromagnetic and heat transfer problems is called the indirect coupling method. This method calls for an iteration process (Figure 3.56). An iteration process consists of an electromagnetic computation and then recalculation of heat sources in order to provide a heat transfer simulation. This approach assumes that temperature variations are not significant during certain stages of heat cycle, meaning that the electromagnetic properties remain approximately the same, and during certain times the heat transfer process continues to be solved without correcting the heat sources. The temperature distribution within the workpiece obtained from the time stepped heat transfer computation is used to update the values of specific heat and thermal conductivity at each time step. As soon as the heat source variations become significant (due to the variations of electrical conductivity and magnetic permeability), the convergence condition will no longer be satisfied, and recalculation of the electromagnetic field and heat sources will take place.

For most induction heating applications, an indirect coupling approach is valid and very effective. However, there are situations (e.g., intensive induction heating of carbon steel 1010 just above the Curie point, high-power density induction contour hardening, and pulse hardening as well as some low-power density strip annealing applications) where this approach could lead to noticeable errors. In these cases, the direct coupling method should be applied.

In order to provide direct coupling of the electromagnetic and heat transfer problems, it is necessary to formalize a set of governing equations in such a way that the unknown parameters of the electromagnetic field (e.g., a magnetic vector poten-

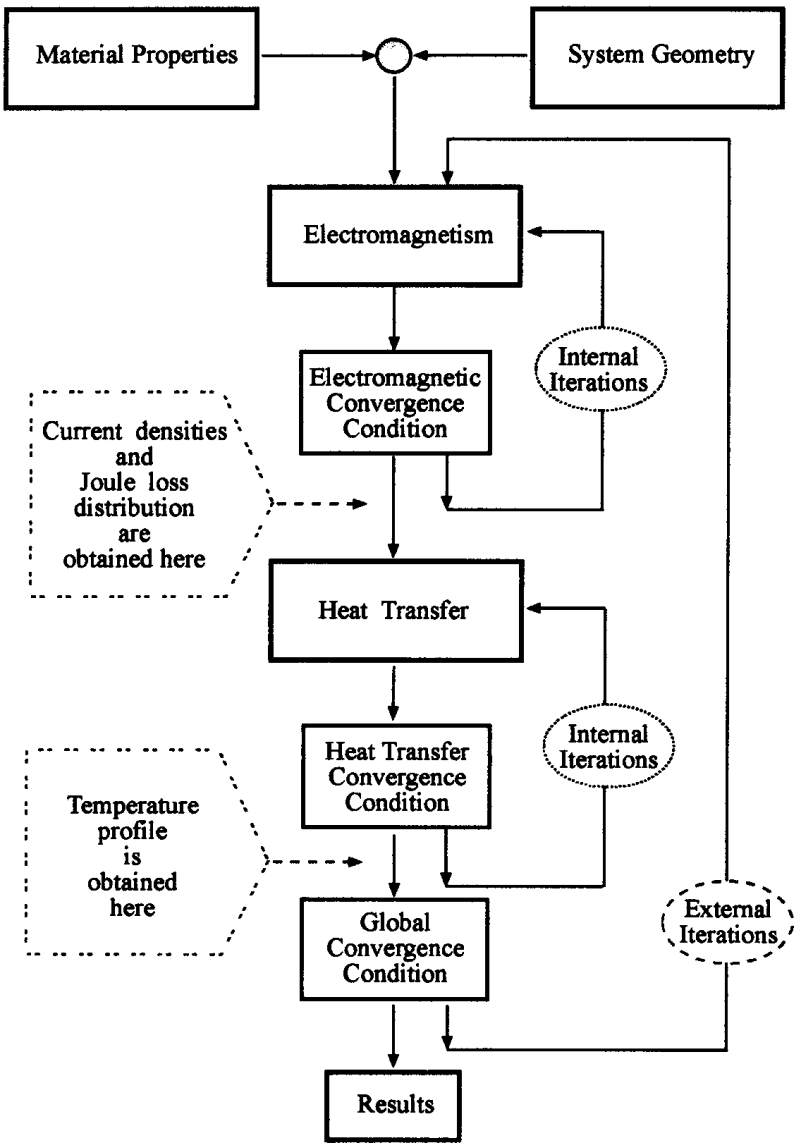

Figure 3.56 Indirect coupling process.

tial or magnetic field intensity) and unknown parameters of the thermal problem (i.e., temperature) will be part of one global matrix that will be solved simultaneously (Figure 3.57).

Direct coupling results in an extremely intensive computer execution time and is memory intensive. It should be used only in cases where it is needed.

3.4.3.7 Comparison of Differrent Numerical Techniques and Final Remarks Regarding Computer Modeling

Superficially, the FDM and FEM appear to be different; however, they are closely related. As outlined above, FDM starts with a differential statement of the problem of interest, and requires that the partial derivative of the governing equation be replaced by a finite difference stencil to provide a pointwise approximation. FEM

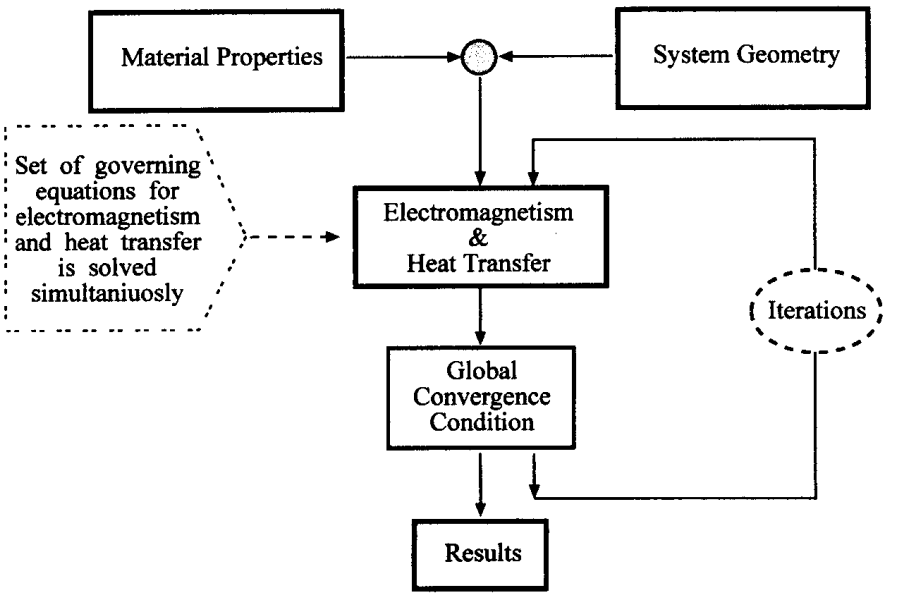

Figure 3.57 Direct coupling process.

starts with a variational statement and provides elementwise approximation. Both methods discretize a continuous function (e.g., magnetic vector potential or temperature) and result in a set of simultaneous algebraic equations to be solved with respect to its nodal values. Therefore the two methods are, in fact, quite similar.

Finite difference stencils overlap one another, and in the case of complicated workpiece geometry, they could have nodes outside the boundary of the workpiece, coil, or other components of the induction heating system. Finite elements do not overlap one another, do not have nodes outside the boundaries, and fit the complicated shape boundary perfectly. In electromagnetic field computation finite elements are usually introduced as a way to minimize a functional. In fact, FDM can also be described as a form of functional minimization (the so-called finite difference energy method).

Therefore FDM and FEM are different only in the choice of mesh generation and the way in which the global set of algebraic equations is obtained. They have approximately the same accuracy; however, the required computer time and memory are often less when FDM is used for modeling classical-shaped bodies. For example, the computer time needed to form global matrices is usually four to nine times greater with FEM than with FDM. As one would expect, a comparison of the efficiency of the two methods depends on the type of problem and program organization. Experience with both methods at INDUCTOHEAT shows that FDM is not well suited for an induction heat treatment system with complicated shaped boundaries or in the case of a mixture of materials and forms (e.g., heat treating of camshafts, crankshafts, gears, and other critical components). In this case, FEM has a distinct advantage over FDM.

As shown above, both finite difference and finite element methods require a network mesh of the modeling area. That network includes induction coils, the workpiece, flux concentrators, and so on. Unfortunately, to suit the conditions of smoothness criteria and continuity of the governing differential equation it is also

necessary to generate a mesh within electrically nonconductive areas, such as the airspace regions. Electromagnetic field distribution in the air, in most cases of coil design, can be considered useless information. Such information might be of interest only during the final design stage when evaluating electromagnetic field exposure from the induction heater. The need to always carry out computation of the electromagnetic field in the air can be considered a disadvantage of both the finite difference and finite element methods.

Another difficulty that appears when using FDM or FEM for electromagnetic field computation is how to treat an exterior region that extends to infinity. This deals with the infinite nature of electromagnetic wave propagation. Several methods have been used, taking into account the phenomena of an infinite exterior region. Some of those methods are the "ballooning" method, "mapping" technique, and combination of finite elements and infinite elements. However, each of the above-mentioned methods has certain shortcomings.

Both the mutual impedance and boundary element methods do not require taking the airspace into consideration. This can be taken as an advantage of these methods over FDM and FEM. Since MIM and BEM require discretization of only the boundaries of the components of the induction system, it makes the mesh generation procedure relatively fast and simple.

The mutual impedance method does not appear to be an effective computational technique for complex-shaped bodies due to the known limitations of calculating self-inductances and mutual inductances. However, it does allow one to easily incorporate circuit connection features into general consideration. This is an important feature for calculating systems such as line frequency induction heating of large aluminum billets using multiturn and multilayer coil arrangements (often four to six layers) connected to a multiphase power source.

We may summarize our introduction into numerical methods used for the simulation of induction heating problems very simply. Each of the above-described methods has certain advantages. In many applications it is effective to use a combination of methods. The right choice of method depends on the specific application and features of the induction heating process. Table 3.8 consists of recommendations on the suitability of numerical techniques based on experience using different mathematical methods at INDUCTOHEAT, Inc., Madison Heights, Michigan.

In induction heating simulation the thermal modeling is usually not as cumbersome as electromagnetics. Since the boundaries of the heated parts are always well defined, both FDM and FEM are well suited to compute the temperature profiles. Due to greater flexibility of the FEM to workpiece shape variation, this method is the most popular choice for mathematical modeling of heat transfer problems. Only in the case of classically shaped bodies does FDM have superior qualities over FEM.

It should be pointed out here that the use of modern software does not guarantee correct computational results. It must be used in conjunction with experience in numerical techniques and engineering knowledge to achieve the required accuracy of mathematical modeling. This is especially so because even in modern commercial software, regardless of the amount of testing and verification, a computation program may never have all its possible errors detected. The engineer must consequently be on guard against various kinds of errors: the more powerful the software, the

Table 3.8 Overview of Choices of Computer Modeling Techniques for Some Selective Induction Heating and Induction Heat Treating Applications

Application	Computation Method
Inline multicoil induction billet/bar heating prior to metal hot shearing or hot forming (i.e., forging)	FDM & MIM* or BEM
Induction bar and billet end heating prior to upsetting	FEM or BEM
Induction surface hardening of crankshafts and camshafts	FEM or BEM
Induction scan hardening of axle shafts	FEM or BEM or FDM
Induction hardening of gears and critical components	FEM or BEM
Induction tempering of complex-shaped parts	FEM or BEM
Induction slab, plate, and bloom heating prior to rolling	FEM or BEM
Induction pipe and tube heating	FDM & MIM or FEM or BEM
Induction strip heating for galvanizing, galvaluming, and galvannealing	FEM or BEM
Induction heating of large aluminum and copper billets prior to extrusion	FDM & MIM
Shrink fitting	FEM or BEM
Induction selective hardening	FEM or BEM
Induction wire/cable heating	FEM or BEM or FDM & MIM
Heating of inside surfaces	FEM or BEM
Induction heating for metallic or organic coating	FEM or BEM or FDM & MIM

*FDM & MIM stands for a combination of FDM and MIM methods.

greater the probability of errors. Common sense and engineering "gut feeling" are always the analyst's helpful assistants.

Computer modeling provides the ability to predict how different factors may affect the transient and final heat treating conditions of the workpiece and what must be accomplished in the design of the induction heating system to improve the effectiveness of the process and guarantee the desired heating results.

4

Temperature Measurement

One crucial requirement in the verification of theoretical calculations and ensuring the required metal heating conditions is the ability to accurately measure the temperature of the workpiece as it is being heated.

One of the simplest techniques for temperature measurement is based on the surface appearance of the heated metal. The color of surfaces of some metals (e.g., carbon steels) can be related to their temperature. At low-temperature applications the change of the surface color deals with its oxidation. At higher temperatures, the change of the color of the heated part deals with the radiation phenomena discussed later in this section. Table 4.1 illustrates the correlation between the surface colors of carbon steel and temperatures when heating to the levels typical for annealing, hardening, forging, and rolling. Table 4.2 shows the colors of carbon steel when heated to the range of the stress relieving, tempering and shrink fitting temperatures.

Obviously accuracy of visual temperature estimation based on color is very limited since it depends upon the workpiece surface condition and relies upon the human eye, providing a very subjective judgment. In addition, some metals (e.g., aluminum, titanium, etc.) do not have such a distinguishing correlation between the temperature and surface appearance. Therefore other means are used in practical applications for temperature measurement.

4.1 COLOR INDICATORS

Two of the most common noninstrument measurements involve the use of a temperature-sensitive paint applied to the metal surface to be heated and a temperature-sensitive pencil or stick that melts at a particular temperature. Either the paint or the stick appears to melt when the rated temperature is exceeded.

Parts are typically painted with several different colors that each melt at a specific temperature. For example, to measure a temperature of 400°C, the surface

Table 4.1 Correlation of Surface Colors and Temperatures

Temperature (°C)	Temperature (°F)	Color
560–680	1040–1256	Dark red
700–780	1292–1436	Cherry red
800–880	1472–1616	Bright cherry
900–980	1652–1796	Orange red
980–1100	1796–2012	Orange yellow
1100–1250	2012–2282	Bright yellow
1280	2336	White

may be coated with paint that melts at 375, 400, and 425°C. As the part is heated, the temperature is known to within 25°C if the 375 and 400°C paints melt and the 425°C paint remains unmelted.

The temperature-sensitive pencil or stick is touched to the hot metal surface during the heating process. The correct temperature is judged to be the rating of the pencil or stick when the stick begins to melt on contact with the hot metal. This technique is typically used during a development stage for providing a quick and inexpensive rough evaluation of the workpiece heating conditions. Care must be taken while using the temperature-sensitive pencils and sticks to prevent human contact with hot metal or radiant heat during the testing.

Other methods that do not require subjective operator evaluation of colors or melting point are described below.

4.2 CONTACT-TYPE SENSORS (THERMOCOUPLES)

4.2.1 Thermoelectric Principles and Seebeck Effect

The term "thermoelectric" refers to the fact that a thermocouple, by the Seebeck effect, can directly produce a voltage proportional to the temperature of the junction of two dissimilar metals "A" and "B" (Figure 4.1). This effect couples the thermal and electrical energies and allows temperature measurement with a simple analog or

Table 4.2 Carbon Steel Colors of Temperatures

Temperature (°C)	Temperature (°F)	Color
190–200	374–392	Faint straw
205–215	401–419	Straw
220–235	428–455	Dark straw
240–250	464–482	Bronze
255–275	491–527	Purple
280–295	536–563	Blue
300–330	572–626	Light blue

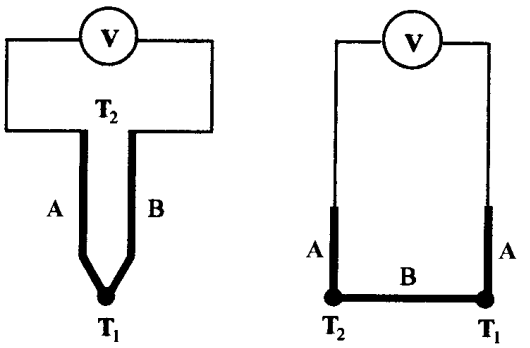

Figure 4.1 Simple thermocouple circuits.

digital meter in much the same way that the voltage in an electric circuit is measured. The Seebeck electromotive force (emf) is the electrical potential difference that is measured as a voltage (the so-called thermoelectric voltage) between the terminals of a thermocouple. This voltage depends upon the metal's properties and temperature differential at metal junctions (T_1–T_2). If the temperature of one junction stays constant, for example, $T_2 = 20°C/70°F$ (Figure 4.1), then the thermoelectric voltage will be a function of the temperature of the other junction (T_1).

The Seebeck, or thermoelectric, effect was discovered in 1821 by T. J. Seebeck. In experimenting with the effect of temperature on homogeneous wires of dissimilar metals he detected a current in a closed circuit by the effect of the magnetic field created by the current on a needle suspended on a wire external to the circuit but in proximity to it. Although this effect was originally related to and described by the current, it has subsequently been observed in open as well as closed circuits and is now related more as an emf phenomenon. It is important to distinguish between the relative Seebeck effect that is seen for dissimilar metals from the absolute Seebeck effect that is seen with nonhomogeneous sections of the same metal. In practice, the relative Seebeck effect is used in thermocouple arrangements for temperature measurement [155–161].

The three traditional laws of thermoelectric circuits as presented initially by Roesser and outlined in reference [155] are as follows.

The Law of Homogeneous Metals

A thermoelectric current cannot be sustained in a circuit of a single homogeneous material, however varying in cross-section, the application of heat alone.

The Law of Intermediate Metals

The algebraic sum of the thermoelectromotive forces in a circuit composed of any number of dissimilar materials is zero if all of the circuit is at a uniform temperature.

The Law of Successive or Intermediate Temperatures

If two dissimilar homogeneous metals produce a thermal emf of E1, when the junctions are at temperatures T1 and T2, and a thermal emf of E2, when the junctions are at T2 and T3, the emf generated when the junctions are at T1 and T3, will be E1 + E2 [157].

These laws provide a theoretical background of thermoelectricity and play a major role in helping to better appreciate many applications of thermoelectric thermometry including thermocouples.

4.2.2 Thermocouple Design, Alloys, and Element Groups

The most common types of alloys used for commercial thermocouples are Chrome–Constantan (E), Iron–Constantan (J), Copper–Constantan (T), Chromel–Alumel (K), Tungsten (5%) Rhenium–Tungsten (26%) Rhenium (C), Tungsten–Tungsten (26%) Rhenium (G), Platinum–Platinum (13%) Rhodium (R), Platinum–Platinum (10%) Rhodium (S), and so on. These combinations are listed in decreasing order of their emf output for a given temperature. Thermocouples are usually simply classified by a letter that identifies the alloys used in the construction. The thermocouple identifications such as T, J, E, K, S, R, B, G, D, and C are listed in order from the lowest to the highest temperature application.

There are three basic designs for round wire thremocouples: the exposed, grounded, and isolated junctions [155].

The *exposed junction* is the most commonly used design in induction heating. It consists of two round wires of dissimilar metals that are connected, usually by welding, at the sensing tip. The wires are electrically isolated at all other points except the sensing tip. The exposed junction thermocouple gives the quickest response but is quite fragile and sensitive to electromagnetic fields (particularly medium- and high-frequency fields), corrosive atmospheres, and mechanical fatigue and breakage.

The *grounded junction* is similar to the exposed unit except that the junction is enclosed in a protective metallic sheath. The thermocouple junction is electrically connected to the metal sheath. The metal sheath provides protection from mechanical abuse and corrosive atmospheres but due to the conduction required to heat the sheath and then the thermocouple junction, the response is typically much slower than exposed junction design. This type of unit can be sensitive to stray electromagnetic signals and larger conduction and radiation error.

The *ungrounded junction* is also enclosed in a protective metal sheath but is electrically insulated from the sheath. This arrangement provides significant electromagnetic shielding from signal interference. It also provides protection from mechanical abuse and corrosive atmospheres but is subject to large conduction and radiation errors and slow response time.

Since the thermoelectric effect is not isolated only to the tip of the thermocouple junction, care must be taken to avoid introducing errors by improper termination or extension of thermocouple leads before the measurement is made. Special polarized plugs are available for thermocouples to minimize the effect of terminations or joining of thermocouple wires since at each point a connection is made, another junction occurs [155].

Care must also be taken to avoid the introduction of errors in measurement by the insertion of large thermocouple assemblies through holes that may allow conduction of heat away from the point of interest and result in inaccuracies in the measurement.

4.2.3 Application Limits of Thermocouples and Review of Errors in Thermocouple Measurement (Including Transmission Errors, Noise, Response Time, etc.)

Thermocouples are designed to provide a temperature measurement in certain temperature intervals. The upper limitation is the proximity to the melting point of the specific alloy being used and can be found in the manufacturer's specifications [155].

There are several types of errors that can be of concern in the use of thermocouples, the most common of these being conduction, radiation, transmission, response time, and electrical noise errors.

Since induction heating is a relatively fast process, the time response is one of the major constraints when using thermocouples. The time constant of a sensor τ is defined as the time required for a sensor to respond to 63.2% of its total output signal when a step function is applied. In order to reach a level of 99% of the output five time constants are required (Figure 4.2). The larger the wire diameter results in the larger the time constant for a given thermocouple.

The required time constant for response to an input signal can limit the usefulness of thermocouples when attempting to measure high-speed, short-duration temperature changes. The response time for the thermocouple junction itself is dependent upon the thermal conductivity of the materials used in the junction and is typically in the range of 0.5 to 4 sec. Some small-sized specially designed thermocouples are capable of responding to a step change on the order of a fraction of a second.

Temperature measurements are often required in industrial applications that are very challenging from an environmental standpoint. Often there is moisture, high humidity, scale, electromagnetic interference, ground loops, high-temperature metal, and a host of other considerations. In the laboratory fragile instrumentation can survive through careful use. In industry a measurement system must be very robust and survive a variety of types of mechanical abuse as well as environmental concerns.

In order to measure elevated temperatures without damage to wiring and insulation it is necessary to use a variety of refractory materials in the construction of the thermocouple assemblies. These materials include Alumina, Beryllia, Zirconia, Silicon Carbide, Carbon Graphite, Titanium Carbide, Thoria, and several other materials. These materials are able to operate as high as 2700°C and even higher.

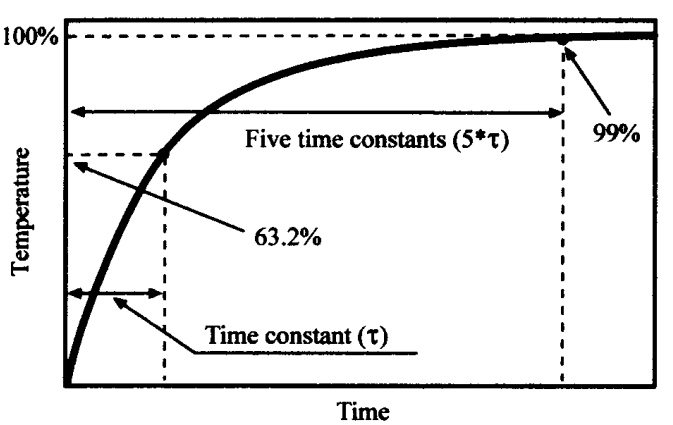

Figure 4.2 Time response of sensor.

Most ceramic and refractory types of material are relatively fragile in an industrial environment and care must be taken to avoid their breakage from mechanical shock, vibration, thermal shock, or handling.

Some of the industrial thermocouples utilize a fairly heavy outer metal sheath that protects the sensitive thermocouple junction and wiring from the environment. On higher temperature applications the typical insulation on lower temperature thermocouples is inadequate and ceramic beads are typically used to insulate the wires from each other to prevent physical contact.

Conduction errors have to do with the heat sinking effect of thermocouple leads, and the metal sheath surrounding the thermocouple. These can lead to a sinking of heat away from the object that is being measured and lead to erroneous readings of the actual temperature particularly when the object is small. Larger sizes of leads and sheath assemblies can lead to large conduction errors.

Radiation errors can occur when heat radiated from the object being measured causes a difference in temperature of lead wires or portions of the sheath assembly. Thermocouple measurements assume that the leads from the junction to the assembly remain at a controlled temperature during the measuring process.

Transmission errors can occur if the material in the thermocouple leads changes in composition, temperature, or size from the hot junction to the cold junction or reference.

Response time errors can occur when larger diameter leads are used or when a large diameter sheath is used with the thermocouple due to the thermal conduction time. They also can occur when a thin outside surface is measured in order to indicate the temperature on an inside surface. In any of these situations, if the reading is taken too early, an error will occur in the reading compared to the actual temperature.

Electrical noise errors can occur in the use of exposed junction and grounded thermocouples due to their susceptibility to induced currents and ground loop noise. This is particularly critical since an inductively heated workpiece is always placed in a relatively strong magnetic field. The ungrounded junction type offers electromagnetic shielding of the junction from the standpoint of electrical noise being induced in the loop between the lead wires and thermocouple junction.

In order to provide a reliable measurement the thermocouples typically require physical contact with the heated body and can be used in applications where the heated workpiece is static during heating. In cases where the heated body is moving during heating (e.g., inline heating of bars, slabs, ropes, wires, strips, etc.) or rotation of the workpiece is required during the heating cycle (e.g., surface hardening and through hardening) the noncontact temperature sensors (pyrometers) are more suitable for providing the temperature measurement.

4.3 INFRARED RADIATION THEORY AND NONCONTACT SENSORS (PYROMETERS)

4.3.1 Infrared Radiation Theory

The basics of thermal radiation have been discussed in Section 3.2. In order to describe the principles of the pyrometers it is necessary to have an in-depth under-

standing of the theory of infrared radiation such as can be found in [158–164]. Some elements of the theory of infrared radiation are provided below.

Infrared radiation (IR) is a component of the electromagnetic spectrum that falls between the frequencies of visible light radiation and radio waves. Electromagnetic radiation is sinusoidal in nature and the components of the total spectrum are differentiated by the frequency bands they occupy.

The relationship of wavelength to frequency is:

$$\lambda = \frac{c}{f},$$

where λ is the wavelength in micrometers (microns), c is the velocity of light $= 2.99793 \times 10^{14}$ μm/sec, and f is the frequency in Hz.

Figure 4.3 shows the electromagnetic spectrum. IR occupies the waveband between 0.7 and 1000 microns. Devices that respond to IR energy such as silicon photocells also react to visible light in the 0.6-micron region.

For practical temperature measurement purposes, only wavelengths between 0.6 and 20 microns are used. Radiation beyond 20 microns is too weak to be detected by conventional means at lower temperatures and is easily attenuated. Although IR energy is invisible to the human eye, it is helpful to think of it as visible light because it behaves in an identical manner. It can be reflected, absorbed, and attenuated by objects and conditions in its path.

4.3.1.1 Heat Tansfer by Radiation

When IR energy strikes an object or substance, a portion of the energy is reflected from the surface and a portion is absorbed. In the case of materials that are transparent to certain wavelengths of IR, some of the energy will be transmitted through the material. Of the energy that is absorbed, a portion is reradiated from the object's surface and a portion is reflected internally. This is true of visually opaque materials such as metals and refractories, and also of visually transparent materials such as

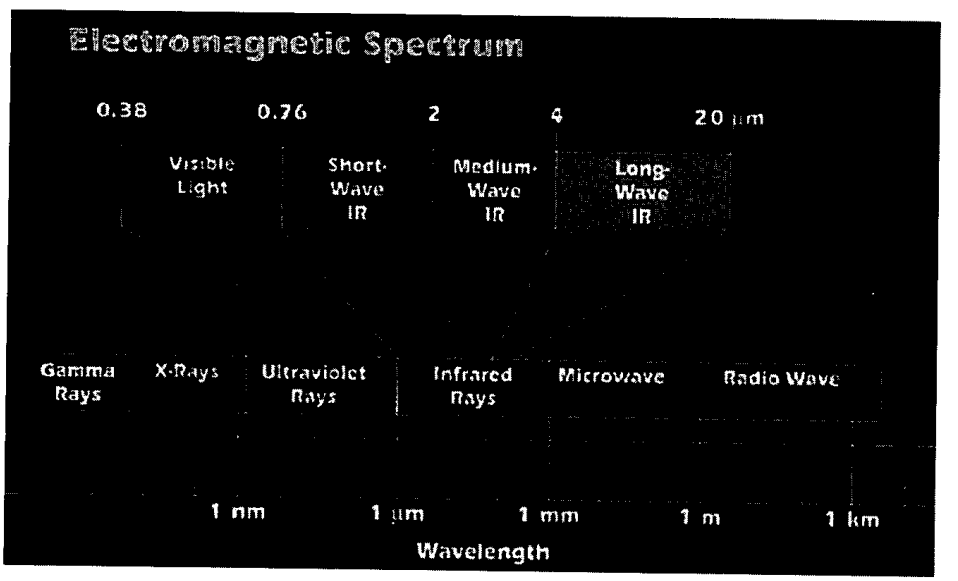

Figure 4.3 Electromagnetic spectrum.

glass and plastics. The absorption, reflection, and reradiation process continues until the object and its surroundings reach a state of temperature equilibrium. The laws governing this process are as follows:

Stefan–Boltzmann Law. The Stefan-Boltzmann law states that the hotter an object becomes, the more IR energy it emits, defined by the formula: $W = \varepsilon\sigma T^4$, where

W = radiant energy in watts/cm^2,
ε = emissivity factor,
σ = Stefan–Boltzmann constant (5.67×10^{-12} W/cm^{2}K^4), and
T = temperature in degrees Kelvin.

Wien's Displacement Law. Figure 4.4 shows a graph of IR energy radiated by a body at different temperatures. Wien's Displacement Law states that the wavelength at which the maximum amount of infrared energy is emitted becomes

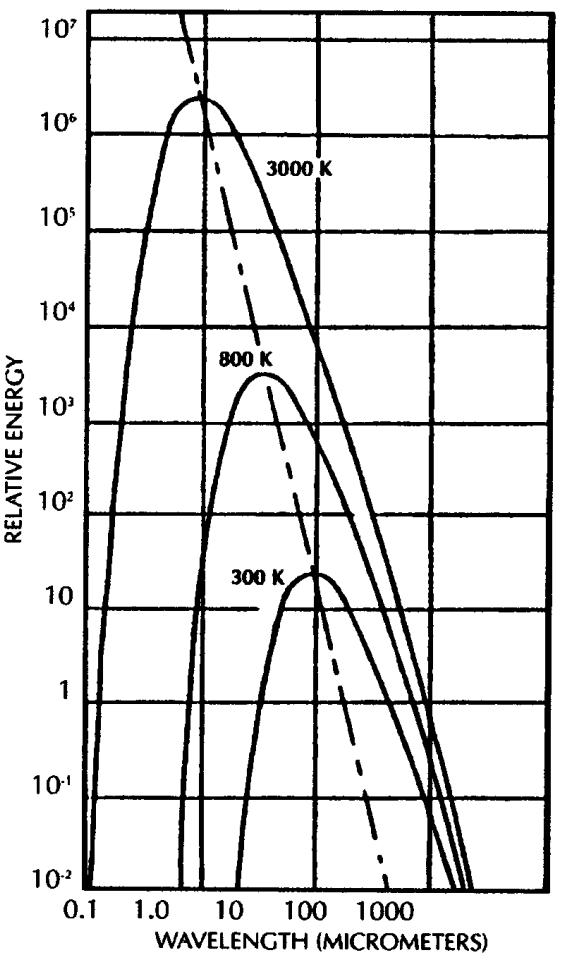

Figure 4.4 Infrared energy radiated by a body at different temperatures.

shorter as the temperature increases (Figure 4.4.). Mathematically, $\lambda_{max} = 2.89 \times 10^3\ \mu mK/T$, where

λ_{max} = maximum wavelength in micrometers,
T = temperature in degrees Kelvin.

Planck's Equation. Planck's equation describes the relationship between spectral emissivity, temperature, and radiant energy, expressing the radiant energy emitted per unit area of a blackbody as a function of wavelength and temperature.

$$W_\lambda = C_1 \varepsilon_\lambda [\lambda^5 (e^{C_2/\lambda T} - 1)]^{-1}, \tag{4.1}$$

where

W_λ = the radiation emitted by an object at a given wavelength (λ),
ε_λ = the emissivity of the object at the same wavelength (λ),
C_1 = Planck's first radiation constant ($3.75 \times 10^{-12}\ Wcm^2$),
C_2 = Planck's second radiation constant (1.438 cmK) equals wavelength in microns,
e = base of natural logarithms (2.718), and
T = temperature in degrees Kelvin.

Emissivity. A factor common to both the Stefan–Boltzmann law and Planck's equation is the term "emissivity." Emissivity is the propensity of an object or surface to absorb and emit infrared radiation. It can be expressed as the ratio of the radiant energy emitted by an object at a temperature T and the radiant energy emitted by a blackbody at the same temperature. This may be stated as $\varepsilon = W/W_{bb}$.

An object that absorbs all the IR energy that falls on it and reradiates all the IR energy it absorbs is termed a perfect blackbody, and is given an arbitrary emissivity value of $\varepsilon = 1.0$. Perfect blackbodies do not exist in nature. The degree to which materials approximate to an emissivity of 1.0 is a function of their molecular construction and their surface characteristics, that is, rough, pitted, or highly polished. Emissivity is also affected by the angle at which the IR energy strikes the surface, that is, the closer to perpendicular the higher the apparent emissivity. Some typical emissivity values for some metals are listed in Table 3.7.

A practical method for determining the emissivity of an object is to compare the temperature obtained from a carefully positioned thermocouple, attached to a sample, with data obtained from an IR thermometer from the same area. The thermometer emissivity setting can then be adjusted until both readings match. The thermocouple should be attached firmly (welded) to the piece, and should be of fine gauge wire so as not to conduct excessive heat away from the target area.

An alternative method is to coat part of a sample piece with a high emissivity coating and heat the piece to the desired temperature. Set the emissivity adjustment on the IR thermometer to the emissivity of the coating and document the temperature. Then view and measure the uncoated portion of the sample piece and readjust the emissivity on the IR thermometer to match the same temperature obtained from the coated portion.

4.3.1.2 Blackbody and Graybody Radiation

As noted above, the emissivity of an object depends on the molecular composition of the material, its surface characteristics (rough, smooth, shiny, etc.), and the amount of radiation, if any, that is transmitted through the object. A perfect blackbody radiator, if it existed, with an emissivity of $\varepsilon = 1$, would radiate energy with equal intensity at all wavelengths in the infrared spectrum. In practice, emissivity is always less than $\varepsilon = 1$, and is dependent on the wavelength, as stated in Planck's equation. Emissivity in this context is referred to as "spectral emissivity."

If the emissivity of an object remains constant, the radiated energy at a given wavelength will change proportionately with temperature and can therefore be detected and utilized for temperature measurement. Such objects are termed blackbody radiators. In the case of most metals, however, the emissivity changes with temperature as the surface oxidizes. This is because metal oxide has a different molecular composition than unoxidized metal. Not all metals have this characteristic, and these exceptions exhibit a constant emissivity less than $\varepsilon = 1$ at different wavelengths. Such rare materials are known as graybody radiators.

Many data are available on the spectral emissivity of blackbody radiators, but the same cannot be said for graybody radiators. The graybodyness of a material must generally be determined experimentally. The experiment consists of heating the material over the temperature range of interest, and comparing the temperature measured by a thermocouple embedded in the material with the temperature measured by an IR thermometer. If the two sets of readings correlate, the material is a graybody. IR thermometer manufacturers will generally provide spectral emissivity data and also will perform the graybodyness test on request.

4.3.1.3 Prelude to Discussion of Construction and Operation of Noncontact Infrared Thermometers

From the foregoing it can be seen that, providing the parameters of emissivity and wavelength are taken into account, a measurement of the IR energy radiated by an object can be used to determine the temperature. Simple thermocouples measure radiated as well as conducted energy, but have the disadvantage of needing to be in contact or at least in close proximity to the object being measured. This is impracticable if the object is moving or is at a considerable distance from the measurement instrument, or is located in an electromagnetic field as is the case in induction heating.

Since IR energy behaves like visible light, it can be focused by a lens. If the IR energy is focused by a lens onto an IR-sensitive detector capable of converting the energy to an electrical signal, then noncontact temperature measurement from a distance is feasible. The optical pyrometer is an early example of a noncontact temperature measurement instrument. At the time of its invention, devices to convert IR energy to an electrical signal did not exist, so a human operator performed the conversion. The optical pyrometer has a focusable lens and a filament in the field of view (FOV) that forms part of an electrical resistance bridge. Another arm of the bridge consists of a rheostat linked to a scale calibrated in temperature units, and that varies the flow of current from a battery through the filament.

The operator views the object to be measured through the lens and rotates the rheostat until the filament glows with the same intensity (color) as the object being measured. This action matches the object's "color" to that of the filament so that the

filament is indistinguishable to the operator, hence the alternative names for this device: "disappearing filament pyrometer" and "color pyrometer." Once the filament has been matched to the target, the temperature is read from the rheostat scale. Although still in fairly common use, the disadvantages of this device are obvious. Only objects hot enough to radiate energy in the visible light spectrum can be measured, and the measurement procedure is too slow to track rapidly changing temperatures typical for a majority of induction heating applications. Added to these shortcomings, the technique also requires the constant attendance of an operator, and its accuracy is dependent on the operator's visual acuity.

Modern IR thermometers avoid the shortcomings of optical pyrometers: they do not require human participation, they are able to track very rapid temperature variations in the microsecond domain, and they are capable of measuring temperatures even of materials that are below freezing. A theoretical IR thermometer would consist of a lens to focus energy emitted by the target onto a detector capable of converting the energy to an electrical signal. The detector output must also be compensated for changes in the ambient temperature of its location. A theoretical IR thermometer is illustrated in Figure 4.5. One of the earliest and still most commonly used detectors is the thermopile. Modern thermopiles consist of a series network of hairlike thermocouples deposited on a semiconductor substrate. Other commonly used detectors are silicon and germanium photo cells. The need to use a variety of detectors arises because no single type of detector meets all the necessary criteria; for example, silicon cells do not produce a usable electrical signal below about 300°C (572°F).

Practical IR thermometers are seldom as simple as the theoretical device described above. Many incorporate optical filters to restrict the bandwidth of IR reaching the detector. Most designs incorporate electronics to amplify and condition the detector signal, and some have complex optics and optical choppers. All but the most basic designs incorporate an emissivity gain adjustment to compensate the thermometer calibration for surfaces being measured that have an emissivity less than unity. Although basically rugged in construction, application extremes of ambient temperature, smoke, and fumes also dictate that the IR thermometer be cooled and its optics purged. Figure 4.6 illustrates a modern infrared thermometer design.

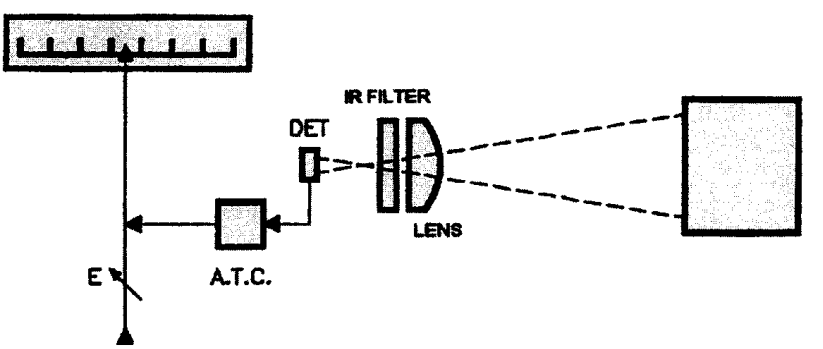

Figure 4.5 Theoretical IR thermometer.

Figure 4.6 Modern infrared thermometer design.

4.3.2 BandPass Single Detector IR Thermometers

As stated in the previous section, IR energy will be attenuated by objects, smoke, vapor, dust, and gases that intervene between the emitting source and the detecting device, or putting it another way, that obscure or impinge on the field of view. Target surface conditions such as scale, coatings, dirt, and oil will also change emittance. If accurate temperature measurements are to be obtained, these attenuating elements must be avoided or eliminated. Water vapor (not droplets) and gases commonly encountered in industrial heating processes, such as CO and CO_2, have predictable IR absorption bands. This also applies to glasses and plastics. Figure 4.7 shows the wavelengths of some common absorption bands.

If the amounts of vapor and/or gases in the FOV were constant, it would be possible to calibrate the sensor accordingly. However, since this is rarely true, the attenuation must be avoided. To circumvent the impact that the absorption bands can have on measurement accuracy, IR energy entering the thermometer is optically filtered so that only the unattenuated energy wavelengths reach the detector.

As stated in Section 4.3.1, out of the total IR spectrum of 0.7 to 1000 microns (μm), only the band between 0.7 and 20.0 is used for temperature measurement. Within this band, certain wavelengths and wavebands are selected because they avoid unwanted absorption bands. Conversely, if it is desired to measure the temperature of CO, CO_2, glass, or certain plastics, the wavelength sensitivity of the IR thermometer can be filtered to accept only the relevant absorption bands.

The band or wavelength of energy that the IR thermometer responds to is termed the "spectral response." Some typical wavelength spectral responses in com-

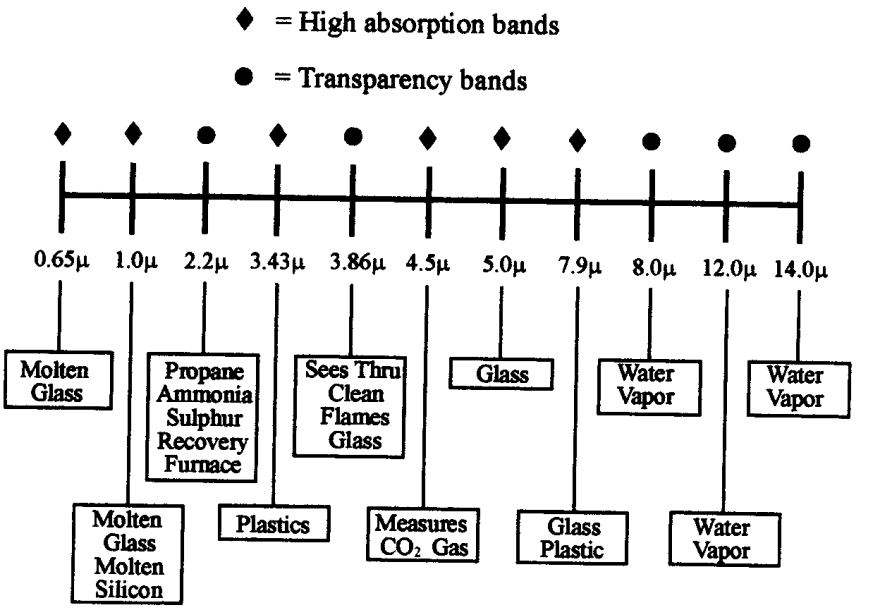

Figure 4.7 Infrared scale.

mon use are 0.65, 1.0, 4.5, 7.9, and 8–14 μm. 0.65 μm falls in the visible light part of the spectrum, but is useful for measuring very hot objects and avoids many of the atmospheric IR absorption bands. It also matches the spectral response of the old optical pyrometer, thus allowing direct comparison of data obtained by each technique.

Aside from the avoidance of signal attenuation, some infrared thermometers have an inherent spectral response dictated by the type of detector used. A good example is the silicon cell, which is only sensitive to very short wavelengths of IR, and is most responsive to visible light, thus acting as its own filter. It is therefore applied to narrowband, high-temperature applications.

Referring to Planck's equation, IR energy emission increases with temperature, and as the temperature increases, the emission peak shifts toward the short wavelength end of the spectrum. This is illustrated in Figure 4.4. Planck's equation also shows that apparent emissivity is highest at short wavelengths and that emissivity variations have less impact on narrowband than on broadband sensor accuracy. Table 4.3 shows the error attributable to a 1% change in surface emissivity for a range of spectral responses and temperatures.

In the best of all worlds then, if there could be an ideal infrared thermometer, it would seem that a narrowband, short-wavelength sensor would be preferred. In the real world, a variety of spectral responses are used: either to avoid attenuation problems or to take advantage of specific absorption bands for the measurement of gases, flames, glass, and plastics, or because a given type of detector predetermines the sensor spectral response by reason of its own, inherent spectral response. IR thermometer response speed also dictates certain detectors and therefore spectral responses; for example, thermopiles are broadband detectors and have relatively slow, millisecond-domain response speeds, whereas silicon and germanium detectors are capable of microsecond, or even nanosecond, responses.

Table 4.3 Temperature Errors Caused by 1% Emissivity Change[a]

	SPECTRAL RESPONSE CODE										
Mikron's Spectral Code	V	H	Q	P	M	D	L	E	F	B	R
Effective Wavelength	0.65 μm	0.9 μm	1.64 μm	2.3 μm	3.43 μm	3.86 μm	4.5 μm	5.0 μm	7.9 μm	10.6 μm	0.78–1.06
Target Temperature (°C)						Errors (°C)					
−50.0									1.8	1.3	
−40.0									1.3	1.0	
−30.0									1.0	0.8	
−20.0									0.7	0.6	
−10.0									0.5	0.4	
0.0									0.3	0.3	
10.0									0.2	0.2	
20.0									0.0	0.0	
30.0					0.0	0.0	0.0	0.0	0.0	0.0	
40.0					0.1	0.1	0.1	0.1	0.1	0.1	
50.0				0.1	0.2	0.2	0.2	0.2	0.2	0.2	
60.0				0.2	0.2	0.2	0.2	0.2	0.3	0.3	
70.0				0.2	0.2	0.3	0.3	0.3	0.4	0.4	
80.0				0.2	0.3	0.3	0.3	0.3	0.4	0.5	
90.0				0.2	0.3	0.3	0.3	0.4	0.5	0.5	
100.0			0.2	0.2	0.3	0.3	0.4	0.4	0.5	0.6	
120.0			0.2	0.3	0.4	0.4	0.4	0.5	0.6	0.7	
140.0			0.2	0.3	0.4	0.4	0.5	0.5	0.8	0.9	
160.0			0.2	0.3	0.4	0.5	0.6	0.6	0.9	1.0	
180.0			0.2	0.3	0.5	0.5	0.6	0.7	1.0	1.1	
200.0			0.3	0.4	0.5	0.6	0.7	0.8	1.1	1.2	

220.0			0.3	0.4	0.6	0.7	0.7	0.8	1.2	1.4	
240.0			0.3	0.4	0.6	0.7	0.8	0.9	1.3	1.5	
260.0			0.3	0.5	0.7	0.8	0.9	1.0	1.4	1.6	
280.0			0.4	0.5	0.7	0.8	0.9	1.0	1.5	1.8	
300.0			0.4	0.5	0.8	0.9	1.0	1.1	1.6	1.9	
320.0			0.4	0.6	0.8	0.9	1.1	1.2	1.8	2.0	
340.0			0.4	0.6	0.9	1.0	1.2	1.3	1.9	2.2	
360.0			0.5	0.7	1.0	1.1	1.2	1.4	2.0	2.3	
380.0			0.5	0.7	1.0	1.1	1.3	1.4	2.1	2.4	
400.0		0.3	0.5	0.7	1.1	1.2	1.4	1.5	2.2	2.6	
420.0		0.3	0.5	0.8	1.2	1.3	1.5	1.6	2.4	2.7	
440.0		0.4	0.6	0.8	1.2	1.4	1.6	1.7	2.5	2.9	
460.0		0.4	0.6	0.9	1.3	1.4	1.7	1.8	2.6	3.0	
480.0		0.4	0.6	0.9	1.4	1.5	1.7	1.9	2.8	3.2	
500.0		0.4	0.7	1.0	1.4	1.6	1.8	2.0	2.9	3.3	
550.0		0.5	0.7	1.1	1.6	1.8	2.1	2.3	3.2	3.7	
600.0		0.5	0.8	1.2	1.8	2.0	2.3	2.5	3.6	4.1	10.6
650.0		0.6	0.9	1.4	2.0	2.3	2.6	2.8	4.0	4.5	11.2
700.0		0.6	1.0	1.5	2.2	2.5	2.8	3.1	4.3	4.9	11.7
750.0		0.7	1.1	1.7	2.5	2.8	3.1	3.4	4.7	5.3	12.2
800.0	0.5	0.8	1.2	1.8	2.7	3.0	3.4	3.7	5.1	5.7	12.8
850.0	0.6	0.8	1.3	2.0	3.0	3.3	3.7	4.0	5.5	6.1	13.4
900.0	0.6	0.9	1.4	2.2	3.2	3.5	4.0	4.3	5.9	6.5	14.0
950.0	0.7	1.0	1.5	2.4	3.5	3.8	4.3	4.7	6.3	6.9	14.6
1000.0	0.7	1.1	1.7	2.5	3.7	4.1	4.6	5.0	6.7	7.4	15.3
1100.0	0.9	1.3	1.9	2.9	4.3	4.7	5.3	5.7	7.5	8.2	16.7
1200.0	1.0	1.4	2.2	3.4	4.9	5.4	6.0	6.4	8.4	9.1	18.1
1300.0	1.1	1.6	2.4	3.8	5.5	6.0	6.7	7.2	9.2	10.0	19.7
1400.0	1.3	1.8	2.7	4.3	6.2	6.7	7.4	7.9	10.1	10.9	21.3

Table 4.3 (Continued)

	SPECTRAL RESPONSE CODE										
Mikron's Spectral Code	V	H	Q	P	M	D	L	E	F	B	R
Effective Wavelength	0.65 μm	0.9 μm	1.64 μm	2.3 μm	3.43 μm	3.86 μm	4.5 μm	5.0 μm	7.9 μm	10.6 μm	0.78–1.06
Target Temperature (°C)	Errors (°C)										
1500.0	1.4	2.0	3.0	4.8	6.8	7.4	8.1	8.7	11.0	11.9	23.1
1600.0	1.6	2.3	3.4	5.3	7.5	8.1	8.9	9.5	11.9	12.7	24.9
1700.0	1.8	2.5	3.7	5.8	8.2	8.9	9.7	10.3	12.8	13.7	26.8
1800.0	1.9	2.8	4.0	6.4	8.9	9.6	10.5	11.1	13.7	14.6	28.8
1900.0	2.1	3.0	4.4	7.0	9.6	10.4	11.3	12.0	14.6	15.5	30.9
2000.0	2.3	3.3	4.8	7.6	10.4	11.2	12.1	12.8	15.5	16.5	33.1
2100.0	2.5	3.6	5.2	8.2	11.2	12.0	12.9	13.6	16.4	17.4	35.4
2200.0	2.8	3.9	5.6	8.8	12.0	12.7	13.8	14.5	17.3	18.3	37.8
2300.0	3.0	4.2	6.0	9.5	12.7	13.6	14.6	15.3	18.3	19.3	40.2
2400.0	3.2	4.5	6.4	10.1	13.5	14.4	15.5	16.2	19.2	20.3	42.7
2500.0	3.5	4.9	6.9	10.8	14.3	15.2	16.3	17.1	20.2	21.2	45.4
2600.0	3.7	5.2	7.3	11.5	15.1	16.1	17.2	18.0	21.1	22.2	48.1
2700.0	4.0	5.6	7.8	12.2	15.9	16.9	18.1	18.9	22.1	23.1	50.9
2800.0	4.2	5.9	8.3	12.8	16.8	17.8	19.0	19.8	23.0	24.1	53.8
2900.0	4.5	6.3	8.8	13.6	17.6	18.6	19.9	20.7	24.0	25.1	56.8
3000.0	4.8	6.7	9.3	14.3	18.4	19.5	20.7	21.6	24.9	26.0	59.9

[a]The magnitude of temperature error created by a given emissivity uncertainty depends on the spectral range of the infrared thermometer, and the temperature of the target. The error table shows temperature errors caused by a 1% emissivity error, for different spectral bands at different target temperatures. The error is given in degrees Celsius. For two-color instruments with spectral response Code R, 1% change represents change in the ratio of emissivities.

Source: Courtesy of Mikron Instrument Company, Inc.

4.3.3 Two-Color, Two-Detector Ratio Thermometers

The foregoing section dealt with bandpass, single-wavelength IR thermometers and how they are designed to avoid, or to measure, absorption by gases and vapors in the field of view. It has also been shown that careful selection of the spectral response can enhance the apparent emissivity of a target and minimize errors due to changing surface emissivity. However, this type of IR thermometer will not overcome errors due to dust, steam, water droplets, or solid objects in the field of view. Nor will it completely eliminate variable emissivity errors or function accurately if the FOV is not completely filled by the target.

At the present time, there is no good solution to the problem of water droplets and steam in the FOV, since the droplets constitute tiny blackbody cavities that absorb infrared energy and reflect most of it internally, allowing only a fraction of the energy to reach the detector. In dealing with the other sources of error, a two-color or ratio thermometer will be effective in many cases. The ratio thermometer differs from the single detector type in that its output signal is the ratio of energy from two detectors with close but different spectral responses. The name "two-color" is derived from the old, optical pyrometer technology when the temperature of metals and refractories was determined by their color, for example, cherry red, yellow, white hot and so on. Figure 4.8 illustrates a two-color ratio thermometer.

In operation, energy that enters the ratio thermometer from the target is directed by a beamsplitter to two short-wavelength detectors. One detector, D1, has a bandpass filter; the other, D2, does not, thus creating the difference in signals from a common energy source necessary for a ratio calculation. The two signals are then ratioed electronically and the product of that process becomes the thermometer

Figure 4.8 Two-color ratio thermometer. (Courtesy of Mikron Instrument Company, Inc.)

output. The close proximity of the two detectors' spectral responses is necessary to minimize errors attributable to differences in spectral emissivity, and the short-wavelength spectral response further reduces such errors.

If it can be said that the aberrant conditions in the thermometer's field of view will affect equally the energy striking each detector, then the ratio will be unchanged, the thermometer output will change only with temperature, and no errors will accrue. This is most effective in the case of errors due to a solid object in the FOV, or of a target that does not fill the FOV. In fact, ratio thermometers will continue to measure accurately when only a fraction of the target is visible, depending on the temperature range. Typically, only 50% of the FOV needs to be filled at the start of the thermometer's temperature range, and as little as 1% at the top of the range. The effectiveness of the technique in dealing with particulates, smoke, and steam in the FOV, and variable emissivity is more conditional.

Smoke and particulates tend to include particles that are the same size as the wavelength sensitivity of the detectors, for example, 1.0 μm. This results in unpredictable attenuation of the energy at specific wavelengths that can unbalance the ratio. Deposition on viewing ports and window seals constitutes a similar source of error. Steam contains water vapor and droplets that affect accuracy as has been previously stated. The ratio technique can be very effective in the case of variable emissivity, probably the most common phenomenon encountered in metallurgical processes. However, since the technique involves measurement at two wavelengths, and it has already been shown that emissivity is wavelength dependent, emissivity changes in blackbody radiators will unbalance the ratio. Graybody radiators, on the other hand, will not incur spectrally related errors because their emissivity values are identical at any two wavelengths.

Since the majority of metals are not graybodies, a means must be found to compensate the ratio for non-graybodyness if this technique is to be broadly useful. The compensation is achieved by biasing the ratio electronically via a user-accessible "slope" adjustment on the thermometer that replaces the emissivity setting. The term slope refers to the bias ratio gain relationship. The setting of this adjustment is arbitrary and must be arrived at experimentally as described in the section on graybodies.

In summary, it can be seen that the ratio technique has some clear benefits in dealing with variable emissivity targets, and in FOV and target size problems, but careful selection of a single detector sensor can sometimes produce comparable performance at less cost. It should be noted that because a ratio thermometer will measure accurately with only a partially filled FOV, it tends to measure the hottest area within the FOV, providing that the minimum target area requirements are fulfilled. This can be a critical factor in process measurements where the target is unevenly heated. In such applications a single-color thermometer is preferable because it will average the temperatures in the target area. However, despite the limitations of ratio thermometry, it is often the best solution for difficult application problems.

The most effective rule when selecting an IR thermometer for a given application is to choose the narrowest spectral band closest to the short-wavelength end of the spectrum, commensurate with the required temperature range and any atmospheric absorption considerations. Refer to Table 4.4 for guidance.

Table 4.4 Selection of the Shortest Wavelength

RULE OF THUMB:
(FOR METAL SURFACES)

SELECT THE SHORTEST WAVELENGTH TO RAISE APPARENT EMISSIVITY AND TO MINIMIZE TEMPERATURE ERRORS DUE TO CHANGES IN EMISSIVITY.

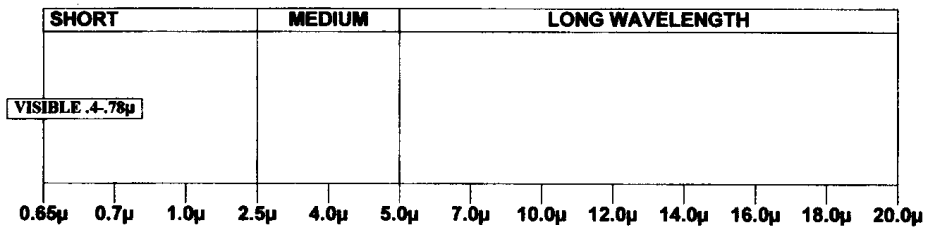

Source: Courtesy of Mikron Instrument Company, Inc.

4.3.4 Sources of Measurement Error in Noncontact Temperature Measurement and Some Solutions

4.3.4.1 Sight-Path Obscuration

The source of obscuration can be intermittent as in the case of smoke, fumes, and particulates; progressive as in the case of window or lens obscuration; or permanent as in the case of a collapsed refractory or an intervening object such as an induction coil. A fan sometimes can clear away smoke, fumes, and dust, but the thermometer purge, if supplied, should not be expected to do this. If a fan is not feasible or effective, consideration should be given to a peak picker. Peak pickers are electronic devices, either integral to the thermometer, or a separate add-on module, that respond in real-time to temperature signal increases and at a preset delayed rate to decreases. They effectively "smooth out" decreases in the thermometer output signal caused by intermittent obscuration.

Progressive obscuration of a view port or window seal is more difficult to handle. Purge systems will help to keep the window clean for longer periods and a ratio thermometer will be less affected by the obscuration than a single detector system. However, none of these methods is as reliable and effective as frequent inspection and manual cleaning of the window, although care must be taken not to scratch the window during cleaning.

Note. Some window materials such as pyrex act as filters to block certain wavelengths of IR used in the measurement and can cause errors. If in doubt, the window should be tested by the IR thermometer manufacturer. Alternatively, obtain an approved window from the thermometer vendor.

Partial blockage of the FOV can be solved by simply clearing the obstruction or resighting the thermometer. If neither of these solutions is possible, a ratio thermometer may be effective. The thermometer vendor will need to know the percentage of the FOV that is obscured and the temperature range of interest. A

thermometer with focusable optics and a through-the-lens sighting design will simplify sighting and the avoidance of objects in the FOV. Care in the selection of a FOV is also important and is discussed in the following section.

4.3.4.2 *Field of View Selection*

IR thermometers are designed with fixed, prefocused, or variable focus optics. In all cases, the minimum target diameter required to fill the FOV is determined by the combined factors of temperature range and spectral response. As a general rule, the higher the temperature range and the wider the spectral response, the smaller the minimum possible target diameter will be. Fixed focus instruments are either "close focused," in which case the FOV converges from the lens aperture to the target, or focused at infinity, in which case the FOV diverges from the lens.

Alternatives to lens optics are so-called "light pipes," which are rods of very pure quartz glass, sapphire, or germanium. Light pipes channel IR energy from the target to the detector by utilizing the internal reflection properties of the rods. Such devices have a FOV that is determined by the natural acceptance angle of the end of the rod, generally about 60°. The distance to target area ratio is typically 1:1; that is, at 100 mm distance between the tip of the rod and the target, the minimum target area necessary to fill the FOV is 100 mm diameter. Figure 4.9 illustrates the acceptance angle of a light pipe. For this reason, light pipes are generally installed with the tip in close proximity to the target, and are often inserted through small holes in the induction coils, so as to avoid attenuation of IR energy by smoke, fumes, or dust in the sight path. Light pipes are most often used with fiber optic cables as discussed later.

Unlike a camera, it is not necessary for the target to be in sharp visual focus to measure accurately. It is only necessary to ensure that the FOV is filled by the target at the sighting distance. The exception is the ratio thermometer, which need only have a prescribed fraction of the FOV filled by the target. If the minimum target size requirements are not met, temperature reading errors will result.

If the application in question is relatively permanent, and is not subject to unpredictable, job, or machine changes, a fixed-focus system is adequate and is usually lower in cost. A variable-focus system is more costly, but is also more adaptable to changes in application geometry. Care in selecting the FOV and focus of a fixed-focus thermometer is essential, but is also important when selecting variable-focus sensors. Vendor literature will usually define the lens aperture and

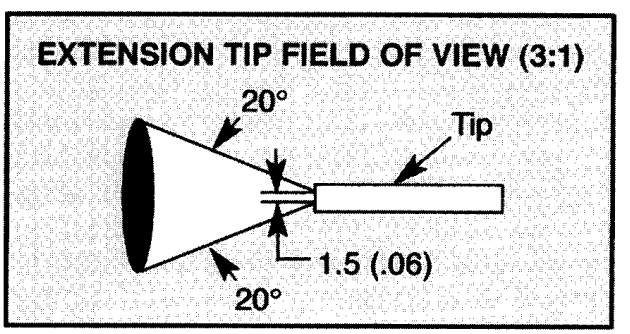

Figure 4.9 The acceptance angle of a light pipe.

field of view according to the selected temperature range and spectral response. This may be expressed diagrammatically or as a ratio of target diameter to distance from the lens. Figure 4.10 illustrates a typical thermometer FOV and shows how to calculate minimum target diameter for any given distance. Figure 4.11 shows correct and incorrect FOV selections.

Fields of view are most commonly circular in cross-section, but can be square or rectangular according to the special needs of the application. The sighting angle will influence the FOV shape as projected on the target; for example, the FOV will encompass a circular target if the line of sight is perpendicular to a flat target surface, and become progressively more oval as the angle of sighting is reduced. It is therefore important to take into account the increased target area at shallow angles in order to avoid hot or cold spots.

Very shallow angles of less than 45° are to be avoided due to the increased reflectivity of the target surface and therefore reduced emissivity. An analogous example is an asphalt road surface that may appear to be mirrorlike if viewed at a shallow angle, even though the surface is quite rough. The higher reflectivity can also produce errors attributable to background radiation emanating from hotter surfaces in the area of the measurement.

Square and rectangular FOVs are commonly applied to applications where the target is moving and cannot be constrained within the boundaries of a circular FOV, or is too small to fill the smallest possible FOV for a particular temperature range and spectral response. A typical example is wire drawing that often combines a small target with wire movement. In such applications the FOV is usually rectangular, with

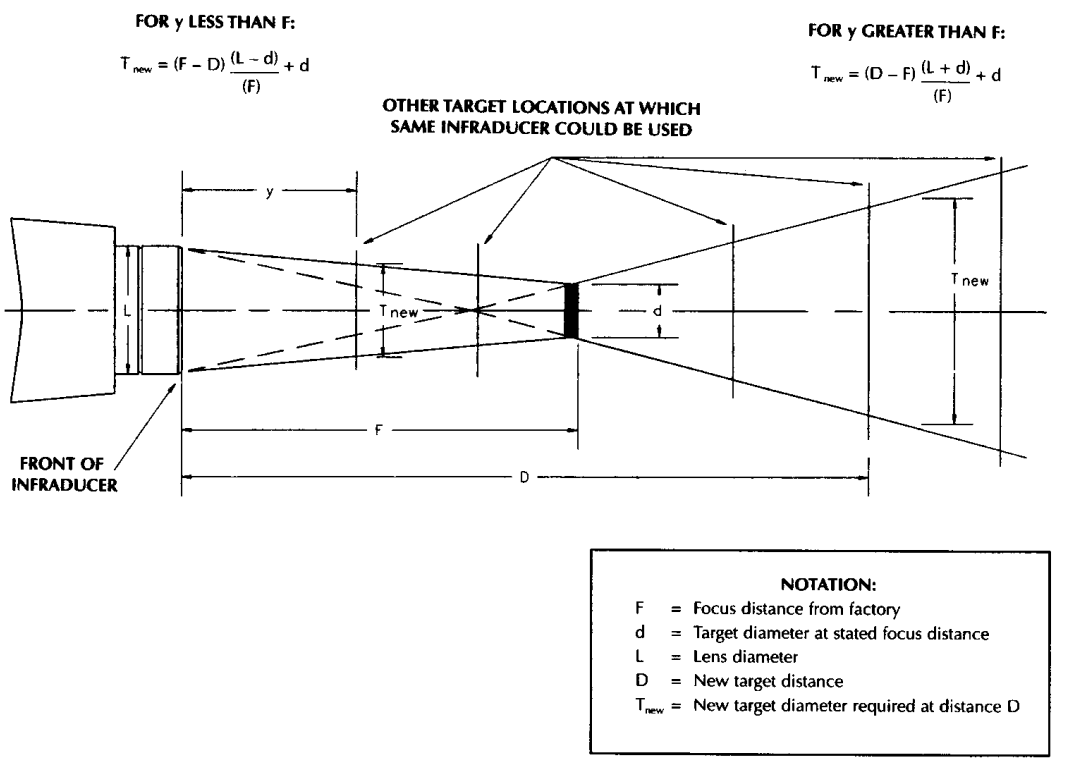

Figure 4.10 Typical thermometer FOV.

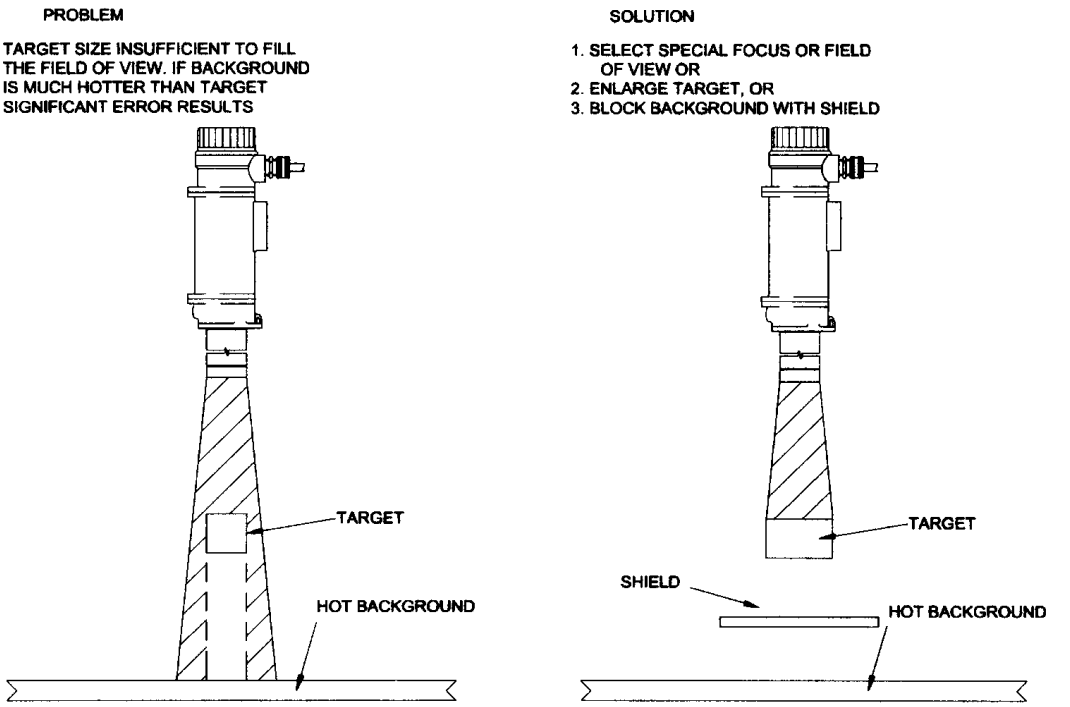

Figure 4.11 Examples of incorrect (left) and correct (right) FOV selections.

the long dimension in line with the direction in which the wire is being pulled. The shorter FOV dimension accommodates side to side "wandering" of the wire. In order to attain measurement accuracy with an incompletely filled FOV, a two-color IR thermometer must be used and the area behind the wire must be cooler than the wire.

4.3.4.3 Electromagnetic Interference

Despite their electronic content and low-level signals, well-designed IR thermometers are not especially prone to emf interference provided good wiring and grounding practices are followed. The vendor's manual will usually indicate how the system should be wired and grounded. In the event that emf interference persists, it may be necessary to relocate the sensor or to ensure that the lens, wiring, and sensor housing are adequately shielded. If relocation is not possible, the source of interference must be identified and either relocated or turned off when measurement is in progress. Another alternative is to resort to fiber optic IR thermometer systems, discussed later in this section.

4.3.4.4 Vibration

Properly designed IR thermometers are not especially sensitive to shock and vibration. They have been used for decades on rolling mills and forging presses without unacceptable failure rates. Specifications are typically 3 gs for any axis, continuous, for vibration, and 50 gs for shock, although it is naturally better to avoid such conditions if possible.

Shock and vibration are likely to have a more significant impact on the thermometer mountings, which can result in changes in the line of sight if mounting

jackets sag or rotate; for example, concentricity of the target alignment is lost. The best solution is to isolate the thermometer from the source of vibration. This is often impossible, and an alternative solution is the use of flexible fiber optics (see Sec. 4.3.5) that channel the radiated energy to the sensor which can be mounted several feet from the vibrating structures.

Shock-absorbing mountings can also be used, but care in selecting the characteristics of the mountings is important because a badly selected mounting can produce harmonics of the source vibration frequency that are potentially more damaging.

In the case of very small target applications where the target is vibrating in and out of the FOV, an electronic peak picker can be used to "capture" the highest target temperature during the brief period of the vibration cycle when the target passes into the FOV.

4.3.4.5 Background Radiation and Reflection

Probably the least understood source of error in any form of temperature measurement is the influence of background radiation. "Background" in this context applies to any surface that is in the line of sight of the object being measured. As has been shown earlier, object and material surfaces reflect a portion of the IR energy striking them. Therefore, if an area in the line of sight of the target is hotter than the target, the sensor will respond to energy emitted by that surface reflected by the target and will exhibit a high error. Plant lighting also can cause similar errors. Mercury vapor and fluorescent lights emit significant amounts of infrared energy at the short wavelengths typically used in induction heating temperature measurement applications.

Most often, the simplest solution to reflection error problems is to construct a shield, or simply to change the angle of the line of sight of the sensor. In the case of errors emanating from lights, changing the sensor's spectral response to the one that coincides with the absorption waveband of glass can be effective. Some sophisticated IR thermometer systems include a background compensation feature that electronically computes the background radiation factor and subtracts it from the final reading. Figure 4.12 shows an application where shielding is being used to eliminate reflection errors.

4.3.4.6 Low and Variable Emissivity

Unoxidized metal surfaces have emissivity values that can be as low as 0.2 (silver and gold). This results in relatively low emittance of infrared energy that is difficult or impossible for IR thermometers to detect and measure. When metals are heated, the metal surface will become oxidized, and the emissivity will increase accordingly as the oxide builds up, proportionately increasing the IR emittance. This phenomenon is most consequential when it is desired to track an object's temperature over a wide range, for example, from ambient to 1000°C (1832°F).

There are several approaches to solving this problem. Selecting a sensor with the shortest possible spectral response will increase the apparent emissivity and be less sensitive to emissivity change. This often involves a trade-off with temperature range; for example, a spectral response of 1.0 μm cannot be used for measurements below 300°C (572°F) because insufficient energy is available from such a narrow waveband at that temperature. Sighting on a part of the target that has a rough surface such as threading or knurling will also increase emissivity by reducing reflec-

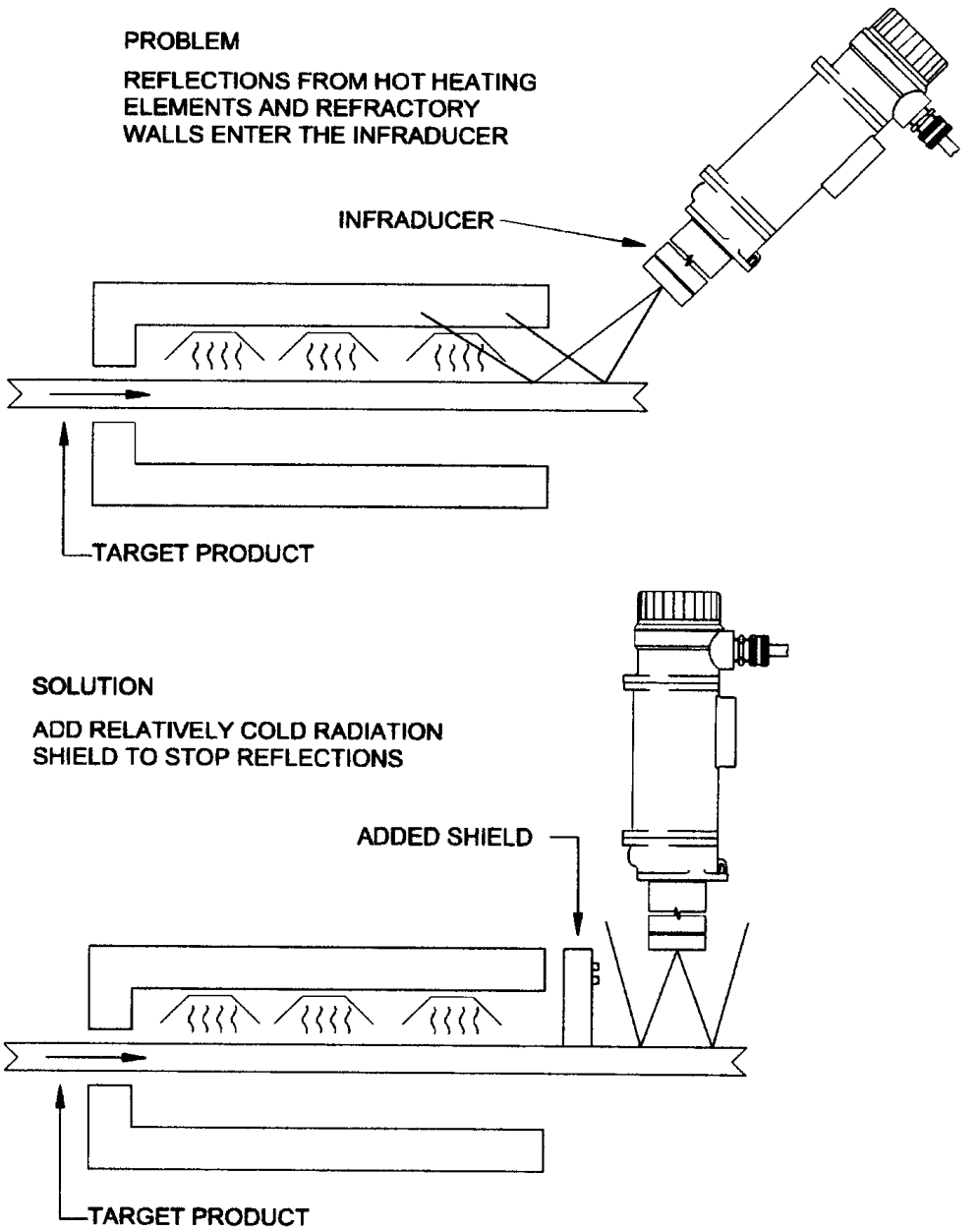

Figure 4.12 The use of shielding for reflection error elimination.

tion. Sighting into a hole will have the same effect. Sighting as nearly perpendicular to the surface as possible will also be helpful. If none of these solutions is applicable, it is sometimes acceptable to infer the true temperature by experimentally determining the IR thermometer reading that equates to the true temperature, in the knowledge that this will be repeatable for the same workpiece.

The error attributable to low emissivity can be determined by heating the piece to a preset temperature determined by an attached thermocouple, and noting the difference in temperature to that obtained by a simultaneous IR thermometer reading with the lowest emissivity setting. An alternative method for overcoming low

emissivity is to coat the workpiece target area with a high emissivity blackbody paint such as Infrablack. Table 4.5 shows two versions of Infrablack coating with temperature ratings and emissivity values.

The ratio thermometer offers an alternative approach, but it should be remembered that the graybodyness factor must be taken into account as stated in the earlier section on ratio thermometry.

4.3.4.7 Metallic Coatings

Galvanizing, galvannealing, and galvaluming are applications that are particularly problematic due to variable emissivity. These continuous processes typically involve the coating of a ferrous substrate such as steel strip, wire, or tubing with zinc or aluminum alloys as a rust preventative (see Section 7.9.1). Ferrous materials have emissivities of the order of 0.5 to 0.9 according to the degree of oxidation. The nonferrous coatings have emissivities that can be as low as 0.1 in this context. Emissivity of molten alloys is often unknown and is a complex function of alloy composition, rate of diffusion and temperature, resulting in potential wide emissivity disparity. A further complication is caused by the potential for the wavefront to change position relative to the target area being monitored, with the possibility for dramatic errors.

4.3.4.8 Infrared Thermometer Response Speed

IR thermometers are capable of extraordinary response speeds that are more than adequate for most industrial processes. However, it is important to bear in mind that the more sophisticated electronic versions that include signal amplification, ratioing, and signal conditioning will be slower in response than their basic counterparts. An IR thermometer that is too slow to capture the peak temperature of the workpiece, or has an incorrectly set peak picker, will produce low reading errors.

4.3.4.9 Ambient Temperature Compensation

As has been stated earlier, an IR thermometer's output signal, just like a thermocouple's, must be compensated for changes in the ambient temperature of its location in order to be accurate. The compensation circuit, although efficient, is encased within the IR thermometer housing, and is relatively slow acting compared with the thermometer response speed. Induction heating applications often subject the IR thermometer to intermittent and rapid high levels of radiant heating.

These variations in ambient temperature are usually out of phase with the changes being sensed by the ambient temperature compensation circuit, and this results in errors that are exhibited as thermometer instability. The solution to this problem lies in ensuring that an adequate mass insulates the thermometer from rapid ambient temperature changes. This can be achieved by locating the thermometer in a protective mounting enclosure or cooling jacket, even though the general ambient condition would not indicate the need for this.

Table 4.5 Infrablack Coatings

Description	Temperature Range (°C)	Emissivity Value
Infrablack I	Up to 300	0.95
Infrablack III	Up to 1700	0.93

4.3.4.10 Monitoring Irregularly Shaped Pieces

Irregularly shaped workpieces need particular consideration with regard to target area selection and the possibility of uneven temperature distribution and/or emissivity. A knurled or threaded target or one with holes and depressions will have a higher emissivity than a smooth-surfaced target. Protrusions from a surface or edges may reach a higher temperature in a given heating cycle than the greater mass of the whole workpiece. These factors are not often detrimental to the measurement as long as they are recognized and taken into account.

Target areas with higher than typical emissivity can be compensated by the emissivity adjustment or an offset in the heating cycle. Hot spot protrusions can be compensated for in a similar manner. If the piece is moving during the measurement period, a two-color ratio thermometer will ignore differences in emissivity, providing non-graybodyness is taken into account, but will measure the highest temperature in its FOV, if the "hot spot" fulfills the minimum target area requirements of the temperature range being used.

4.3.4.11 Application Questionnaire

Most IR thermometer manufacturers will provide an application questionnaire to assist the prospective user to supply all the salient information necessary to select the correct sensor and avoid any application problems. Although this may seem to be a tedious task, time spent in carefully completing the questionnaire will avoid subsequent problems and expense. The form opposite is an example of an application questionnaire.

4.3.4.12 Infrared Thermometer Calibration

It should be clear by now that emissivity is a significant variable in infrared measurement accuracy. In order to establish reliable IR calibration sources it is therefore desirable to have high and stable emissivity targets. A well-designed IR calibration standard is a best approximation to a perfect blackbody. An ideal blackbody calibration source would have an emissivity of $\varepsilon = 1.0$. In order to have practical use as a calibration tool, it is implicit that a part of the source must radiate to the device being calibrated, through an aperture of sufficient diameter to accommodate the thermometer FOV, thus incurring a loss of energy. This loss will result in an emissivity less than 1.0. However, with careful design and selection of materials, it is possible to achieve a source with an emissivity very close to 1.0.

In order to achieve this, it is necessary to construct the source from high emissivity materials and/or locate the source target inside a cavity such that incident energy will be reflected internally and therefore minimize reflection errors. Mathematically, $\varepsilon = 1 - R$, where R is the reflected component. Figure 4.13 shows this diagrammatically. The most efficient blackbody calibrator designs are based on spherical or semispherical cavities and can achieve an emissivity as high as $\varepsilon = 0.999$.

4.3.4.13 Transfer Standards and Traceability

High-temperature blackbody sources are not inexpensive, and the cost is not easy to justify for a user with only a small number of IR thermometers. A more affordable alternative is the transfer standard for use as a comparator to check process IR thermometers and, in fact, blackbody sources. Specially designed, very precise IR thermometers are used to transfer calibration from the primary calibration sources

APPLICATION ANALYSIS FORM

For Noncontact Temperature Measurement

Customer:_____ Date: _____

Name: _____ From: _____

Company: _____

Address: _____ **Analysis Completed by:**
□ Customer □ Rep

City: _____State: _____ Zip: _____

TYPE OF USE

□ Portable □ Process
□ Display: □ Analog □ Digital □ None
□ Output:_____mA_____mV_____Volts_____
T/C Specify Type_____
□ Control Capability: □ On/Off □ Ramp/ Soak
□ Proportional (PID) 4–20mA output
□ Recording Capability: □ Others _____

TARGET INFORMATION:

A. Process Description: (Reverse may be used to sketch your application setup configuration) _____
_____
_____

B. Nature of target surface: (Material name, size, shape, color, and surface condition) as seen by sensor _____
_____
_____

C. Sample enclosed: □ Sample sent under separate cover □ No Sample

D. Working temperature range from _____°___to_____°___; Critical temperature _____°___

E. Desired Target Size_____ at _____distance

F. Distance between sensor and target_____ min. _____ max.

G. Is target under direct infrared energy source: □ Yes □ No. If yes describe method of heating _____

H. Target is □ Stationary □ Moving at _____ per minute

I. Interference between sensor and target: _____

J. Target is □ in a vacuum □ behind a _____ window

ENVIRONMENTAL CONDITIONS:

A. Ambient temperature range at IR sensor location:_____°__ to _____°__

B. Atmospheric Contaminants: □ Dust □ Smoke □ Steam □ Other: _____
□ Periodic □ Continuous

C. Distance between sensor and electronics: min. _____ max. _____

D. Is Strong RFI, EMI radiant present □ Yes □ No

Courtesy of the Mikron Instrument Company, Inc.

located in accredited calibration laboratories, to field calibration devices and process instruments. Despite their inherent long-term stability and accuracy, transfer standards should not be treated like everyday process instruments and must be housed under controlled conditions and protected from abuse. Figure 4.14 shows the long-term stability of a Mikron M190-TS transfer standard checked at four metal freezing point temperatures over a period of several weeks.

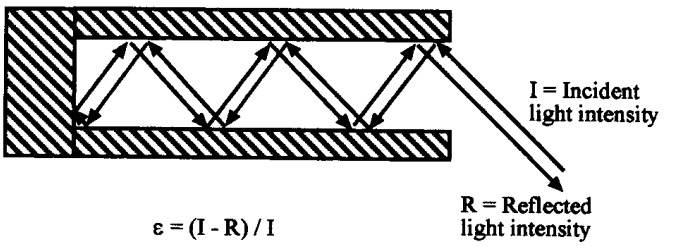

Figure 4.13 Graphical and mathematical representation of ε.

The transfer standard protocol will not provide reliable calibration assurance without the added discipline of calibration traceability. This is largely a matter of documentation and the establishment of a calibration hierarchy, with the appropriate national standards institute at the top of the tree. In practice, most national standards institutes are underfunded and overcommitted. It therefore falls to accredited calibration laboratories in the private sector to provide most of the routine calibration certification for primary references, albeit themselves traceable to national levels. A laboratory calibration traceability hierarchy is illustrated in Figure 4.15.

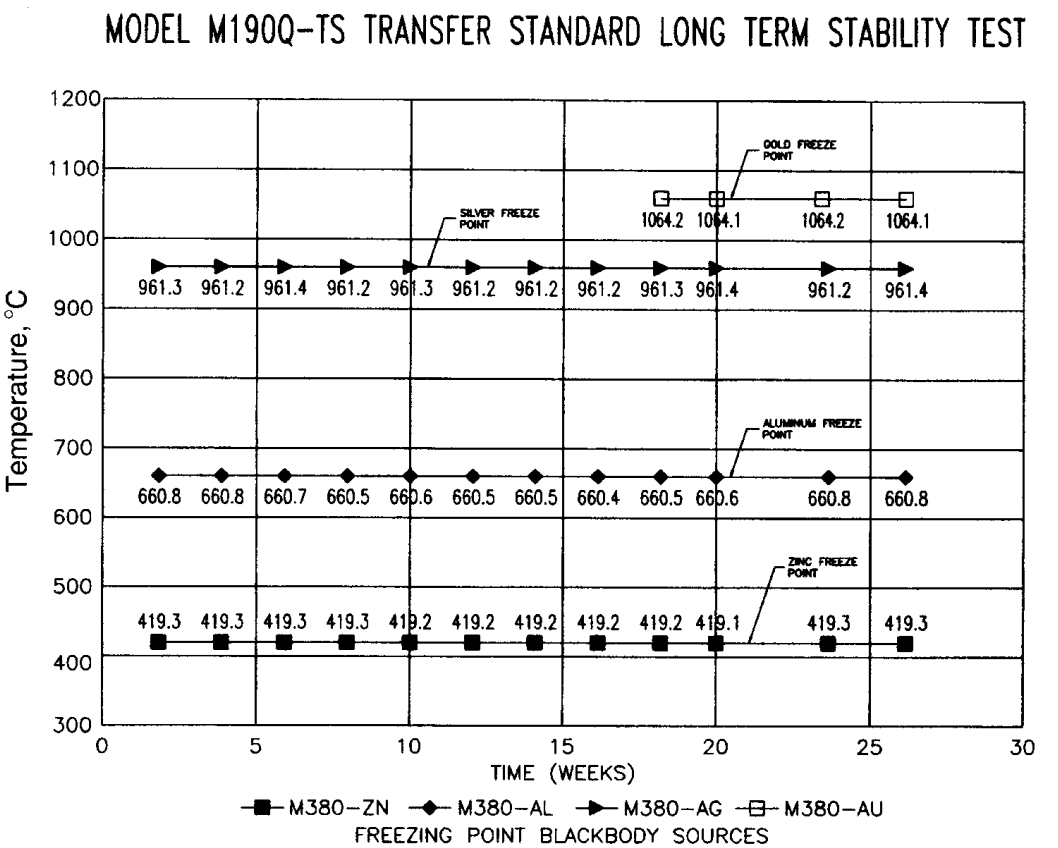

Figure 4.14 The long term stability of a Mikron M190-TS.

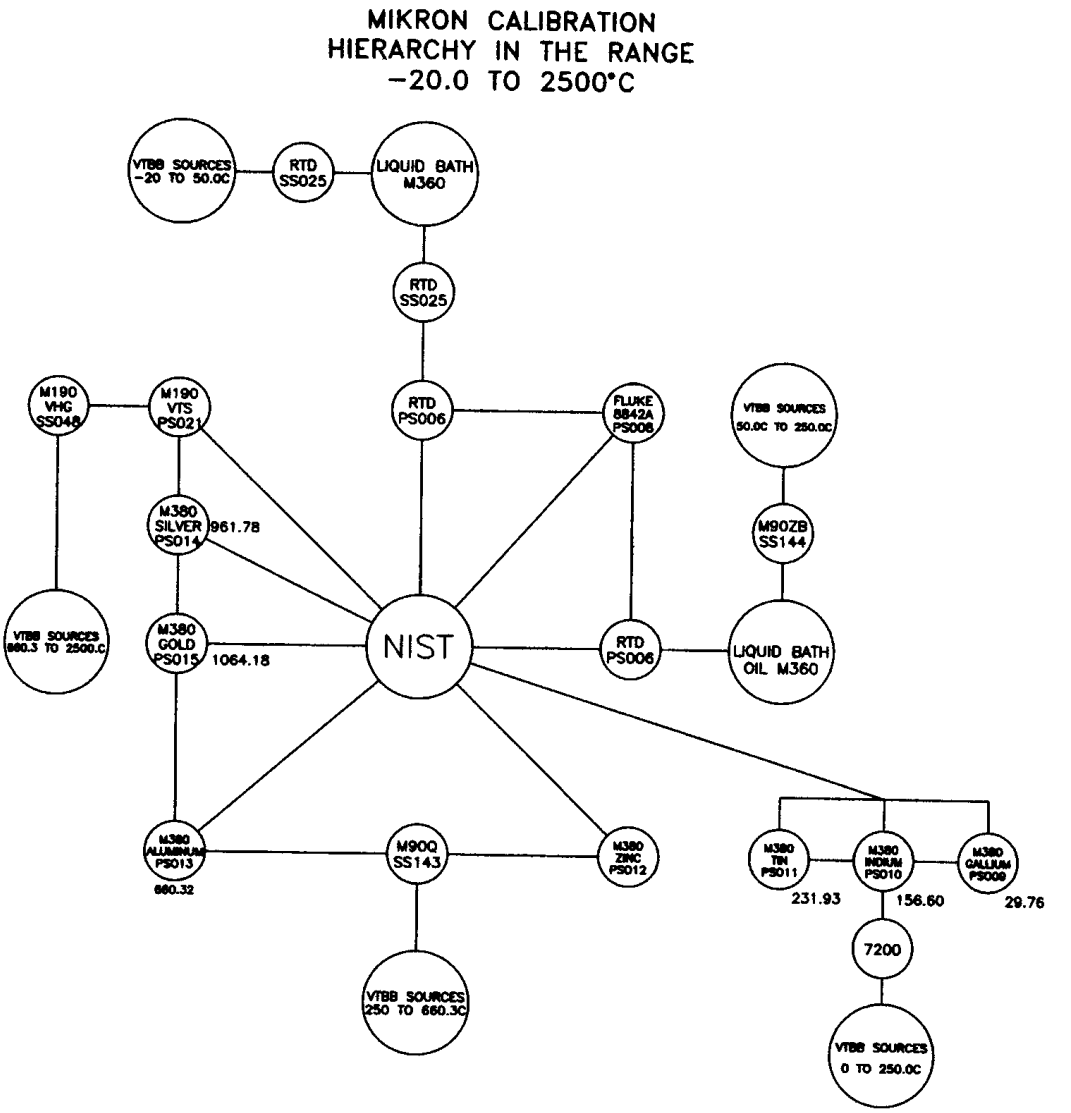

Figure 4.15 A laboratory calibration traceability hierarchy.

4.3.5 Fiber Optic IR Thermometer Systems

All the IR thermometer systems considered so far have been of the conventional lens type, where the lens is an integral part of the thermometer housing. This design dictates that the line of sight between the thermometer and the target be straight, or alternatively be reflected at an angle by a mirror. Induction heating applications in particular often preclude this arrangement due to intervening coils or machinery. In such cases the fiber optic approach can be advantageous.

In fiber optic systems, the lens is separated from the detector and electronics by a flexible, metal-sheathed bundle of glass fibers which can be several feet in length. Energy from the target is focused by the lens onto one end of the bundle and is carried by the glass fibers to the detector. Such an arrangement eliminates the need for a straight line of sight and allows the detector and electronics to be located away from severe environments of high temperature and/or emf interference. Fiber optic

systems can also incorporate the very useful feature of a light source that illuminates and defines the target area being measured.

Several fiber cables can be combined into a single electronics module. Figure 4.16 shows a Mikron Instrument Company, Inc. fiber optic system, and Figure 4.17 illustrates diagrammatically how a multicable unit can be deployed in a zoned heating application.

4.3.6 Thermography

Thermography, or thermal imaging, is a form of IR measurement that not only produces temperature data, but also is capable of producing a picture of the target in temperature-related contours, either in color or grayscale images. The technique has been used for many years for such tasks as power distribution equipment and building insulation surveys, but is now finding application in process measurements. In the case of induction heating, the thermal imager can be useful in job setup, as an aid in designing induction coils, or for monitoring heat distribution in zoned applications. Multiple images can be stored in either the thermal imager or a related computer for later study. Mikron's M9100 Pyrovision, illustrated in Figure 4.18, uniquely combines short wavelength, real-time IR imaging with a selectable visible light image. Figure 4.19 shows a thermal image of an induction heated aluminum billet.

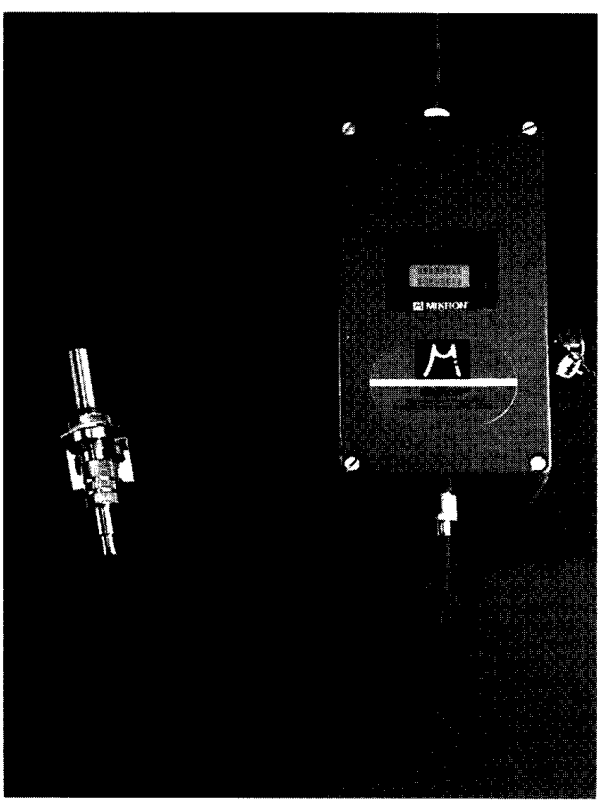

Figure 4.16 Mikron Instrument Company, Inc., fiber optic system.

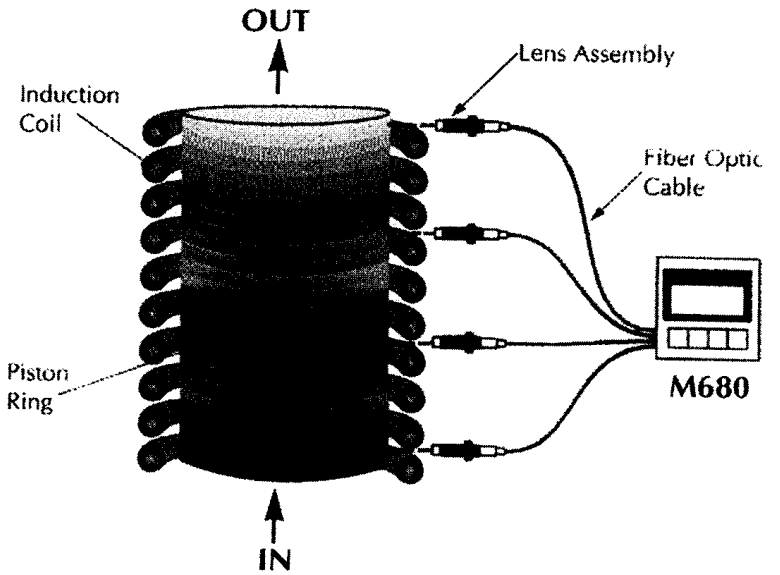

Figure 4.17 Deployment in a zoned heating application.

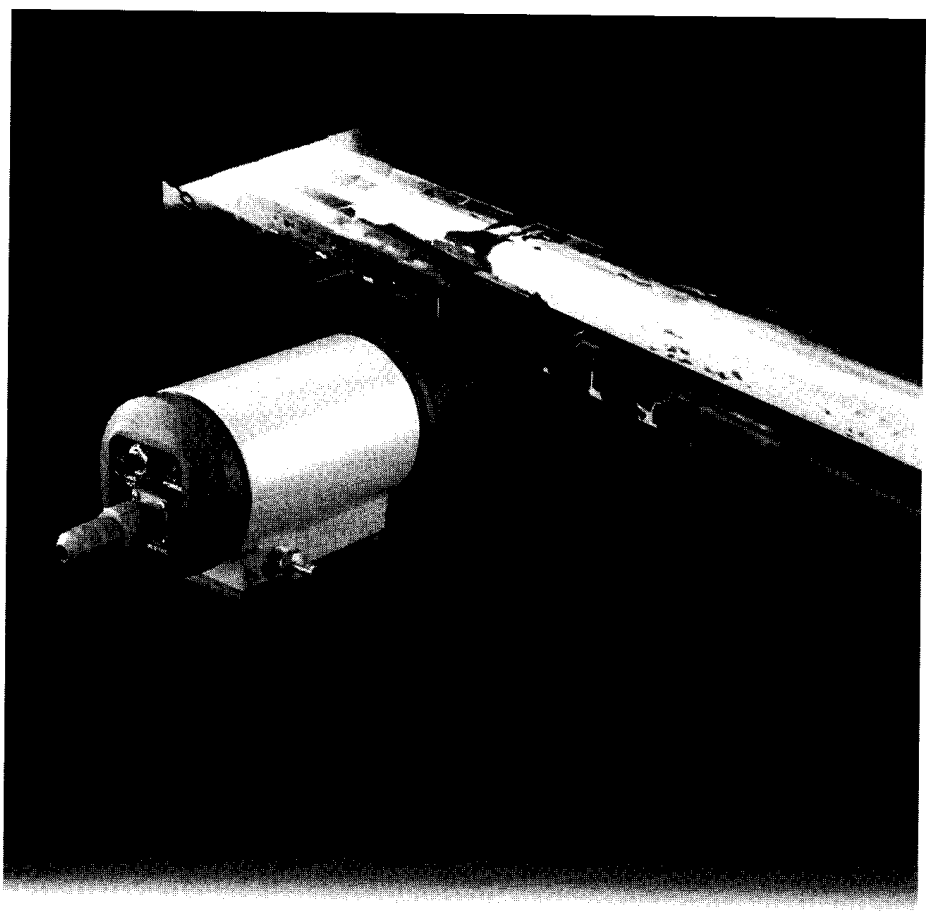

Figure 4.18 Mikron's M9100 Pyrovision.

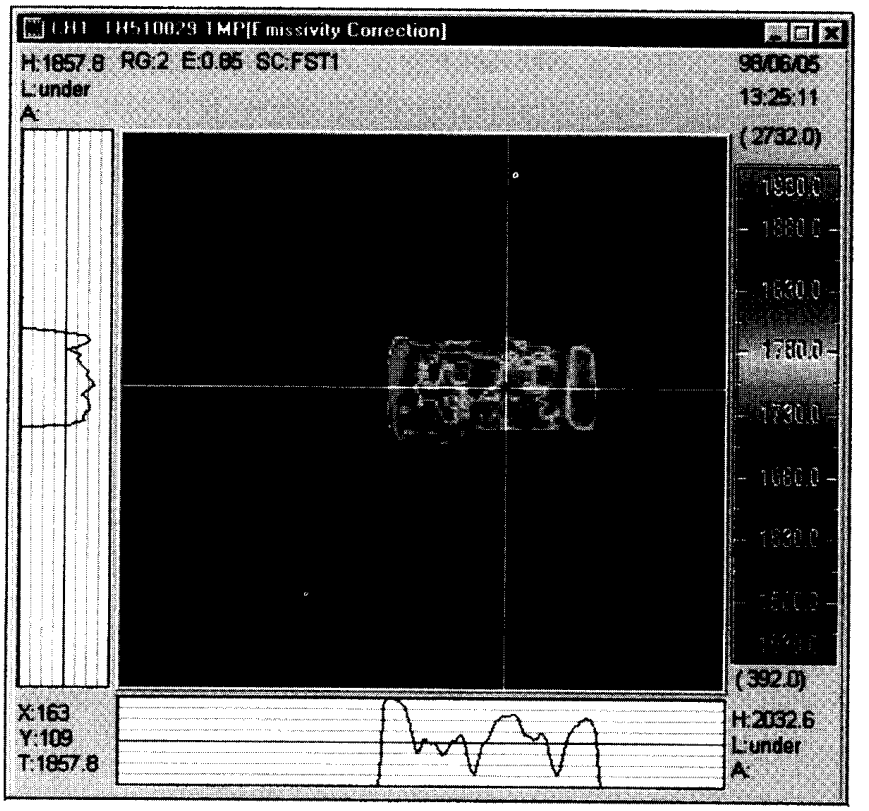

Figure 4.19 A thermal image of an induction heated aluminum billet (Courtesy of Mikron Instrument Company, Inc.).

4.3.7 IR Temperature Measurement in Induction Heat Treating and Mass Heating of Metals Prior to Forging, Rolling, and Extrusion

Although most of the foregoing sections apply to some or all IR thermometer applications, the information contained in them is very much directed toward induction heating. Induction heating, whether it is applied to the mass heating of billets, the melting of high duty alloys, or the heat treatment of parts, shares the basic fundamentals of the measurement technique. The aspects that separate say, mass heating from heat treatment, are application geometry, the amount of radiated heat in proximity to the measurement location, response speed, target shape and size, and the implications of quenching.

Rolling, forging, and extrusion, and heating of slabs, bars, and billets, for example, do not typically call for rapid response or small target measurement. Nor is it a problem to track temperature because the workpiece surface is heavily oxidized and has a relatively high and consistent emissivity. Mass heating often involves intense radiant heat in the measurement location requiring the thermometer to be protected by a reflective shield, or to be mounted at a distance from the target. When mounting a thermometer at a distance care must be taken to avoid interruption of the sight path by machinery or personnel.

Induction heating of small components in brazing, welding, soldering, and hardening applications, on the other hand, often calls for a very fast response system

combined with small target resolution. This usually goes hand in hand with needing to locate the sensor in close proximity to the target, with the associated problems of emf interference and the avoidance of splashes from quenching and cooling media.

Induction heat treating has some unique measurement requirements in that temperature distribution both laterally and in depth is often as important as the actual temperature reading. An example of the need to control heating depth is in case hardening of bearing shafts. Additionally, lateral heat distribution control is necessary in the manufacturing process of camshafts and saw blades. Such applications call for careful sighting of the system and sometimes the need for multiple systems or the use of a multichannel fiber optic IR thermometer. Quenching and water cooling of heated parts can add the complication of smoke or steam in the FOV and should be addressed by the methods indicated earlier.

When the bar and rod are passed through induction heating coils, the leading and trailing ends create disturbances in the magnetic field such that the ends are not heated uniformly (see Section 3.1.7) and will therefore have different heat content and metallurgical properties from the rest of the piece. IR thermometers can be applied to monitor the longitudinal temperature profile as the workpiece moves through the heating coil in order to determine the region of uneven heating and can allow one to quantify the amount of the end overheating or underheating. Coupling the IR thermometer signal to an automatic marking system will help to determine "GO" / "NO GO" status of the heated bar or rod and minimize metal waste when the ends are cut.

Data Acquisition and Storage

Most modern IR thermometer systems have industry standard output signals that are compatible with computers, data loggers, and other recording methods. Careful archiving of the data provides invaluable information for investigating quality problems, providing customer assurance, and assisting in repeat job setup.

4.3.8 Care and Maintenance of Infrared Thermometers

IR thermometers have been used in arduous conditions in industry for at least 70 years. Over that period, reliability and durability of IR devices have been constantly improved. Today's IR thermometer is rugged, and capable of giving extended service with little maintenance. However, the instrument is, after all, a precision electro-optic device that relies on clean optics and a controlled environment. IR thermometer suppliers provide an extensive range of accessories to protect the thermometer from environmental extremes and to keep the optics clean for acceptably long periods. It is false economy to ignore the need for the protection these accessories can provide.

Given that adequate protection has been provided, it is still good maintenance practice to routinely inspect the optics and the electrical connections. It is also important not to overcool systems. Overcooling can cause condensation to form on the optics and electronics with serious consequences. An easy basic check is to ensure that the cooling medium exiting the system is slightly warm to the touch. When manually cleaning optics, only optical tissues should be used and only ethyl alcohol used as a cleaning fluid. Other solvents can destroy the lens coating. If a system has an air purge to keep the lens clean, only oil-free, dry instrument air should be used. If this is not available, a fan or compressed nitrogen is a good alternative.

Well-designed IR thermometers usually have good, inherent long-term stability. Neglect, accidental damage, or abuse can have an impact on this performance, so it is recommended that systems be checked for calibration periodically. The interval between calibration checks will be dictated by the application conditions and the extent to which sensors have exhibited a calibration error for whatever reason. Calibration checks can be made either against a transfer standard as mentioned earlier, or against the user's or vendor's blackbody calibration source. It is prudent to have a standby thermometer if machine downtime is to be limited.

5

Heat Treatment by Induction

This chapter is devoted to the study of different design approaches, the selection of process parameters, equipment specifications, and phenomena that are imperative for building induction heat treat machinery that will provide heat treated parts conforming to the customer's specifications without incurring unpleasant surprises.

The study primarily focuses on the heat treating of steels and cast irons, since they represent, by far, the area of greatest interest in the field of induction heat treatment. The metallurgical aspects of induction heat treatment discussed in Section 2.1 are imperative for understanding why a certain design approach would be better suited to a particular application. Therefore, it is assumed that the readers have reviewed that material.

5.1 MACHINE DESIGN FOR INDUCTION SURFACE AND THROUGH HARDENING

Hardening of steels and cast irons represents the most popular application of induction heat treatment. Induction hardening is a complex combination of electromagnetic, heat transfer, and metallurgical phenomena. As mentioned in Section 2.1.2, a typical induction hardening procedure involves heating the entire component, or a part of the component that needs to be hardened, to the austenizing temperature, holding it for a period long enough for completion of the formation of austenite, and then rapidly cooling it below the temperature where martensitic transformation begins (M_s temperature).

Hardening of steels or cast iron parts may be done for the purpose of obtaining certain properties that include but are not limited to strength, fatigue, and wear resistance. Alternatives to the induction heating process such as gas furnaces or resistance heaters always require heating the entire part. After heating to the austenizing temperature the parts are batch quenched and then returned to a furnace for a stress relieving or tempering operation.

The necessity of heating the entire part does not always result in the optimal combination of mechanical properties that would correspond to long-lasting performance. Significant size and shape distortions are other disadvantages of furnace heat treatment discussed in Chapter 2.

In contrast, induction makes it is possible to create high heat intensity quickly at specific areas of the part, which in turn leads to high production rates with repeatable quality. Induction heat treating is often more energy efficient and environmentally friendly than other heat treat methods. In addition, induction equipment requires practically no startup and shutdown time; it uses minimum floor space and produces less distortion in the workpiece.

The three most common forms of induction hardening are: surface hardening, through hardening, and selective hardening [203]. Depending upon the specific application, selective hardening is sometimes considered a part of surface or through hardening.

The goal of induction surface hardening is to provide a martensitic layer on specific surface areas of the workpiece that allows one to improve mechanical properties without affecting the remainder of the part. This is accomplished by raising only the required depth of material above the transformation temperature to a point where it transforms to austenite and is then rapidly cooled.

Case depth (hardness depth) is typically defined as the surface area where the microstructure is at least 50% martensite. Below the case depth, the hardness begins to decrease drastically (see Figure 5.1). This depth is measured in a cut section of the hardened workpiece using a hardness tester to determine the hardness at various distances from the surface. The distance below the part surface where the hardness drops 10 HRC lower than the surface hardness is often called the effective case depth. The hardness distribution along the workpiece radius depends primarily on the temperature profile, the microstructure of the metal prior to heat treatment, its carbon content, the quenching conditions, and the hardenability.

High- to medium-carbon steel is typically used for induction surface hardening. Surface hardened parts, having a hard outer shell, are strong and typically have compressive stresses at the surface (see Figure 5.2). These stresses are important for improving the fatigue properties of the component, allowing the delay of crack initiation and the propagation of microcracks.

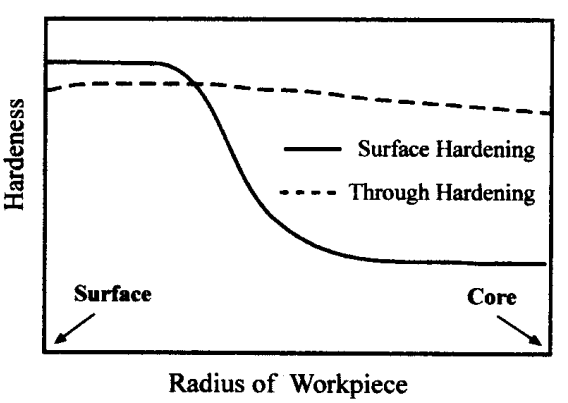

Figure 5.1 Comparison of hardness profiles after induction surface hardening and through hardening of a carbon steel cylinder.

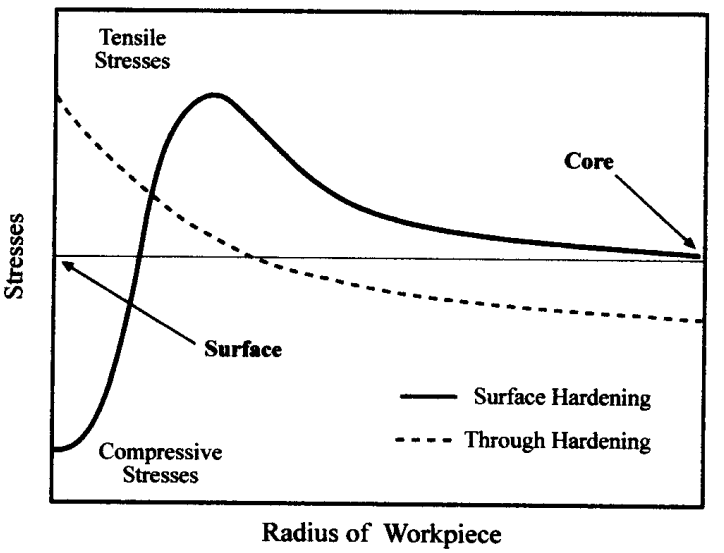

Figure 5.2 Typical distribution of residual stresses after induction surface hardening compared to through hardening of a carbon steel cylinder.

Whenever a metal is heated, some shape distortion occurs. At the same time, induction surface hardening offers high-dimensional stability, particularly on symmetrically shaped parts such as bar shafts, axle shafts, rods, pins, and the like. There are several factors that affect the distortion of the hardened component including geometry, metal properties, hardness profile, residual stresses prior to heat treatment, and so on. One of the most important factors having a pronounced effect on distortion is the amount of heat generated within a component: the greater the amount of heated metal, the greater the metal's expansion, which in turn causes the greater distortion. Some of the important advantages of induction surface hardening are the ability to generate heat in well-defined areas and have short heat times that usually range from 0.5 to 20 sec depending upon the application (heat time for hardening depends upon several factors including prior microstructure, component geometry, required hardness parameters, and the available power supply). Due to these features, distortion of the component is minimized because heating by induction occurs quickly with a minimum amount of metal being heated and the cold core acting as a shape stabilizer.

In contrast to surface hardening, the goal of through hardening is to provide a martensitic structure throughout the entire workpiece. For this to occur, the entire cross-section is raised above the transformation temperature and then rapidly cooled to produce a consistent martensitic structure through the entire cross-section. The ability of the component to be through hardened depends upon the hardenability of the material, the quenching conditions, grain size, and geometry. These features have been discussed in detail in Section 2.1.1.5.

Through hardening may be needed for parts that require high strength such as snowplow blades, springs, chain links, truckbed frames, fasteners, and the like.

Both induction through and surface hardening can be localized to selective areas that require hardening, a process often referred to as selective hardening.

Because induction has the ability to heat parts very quickly it lends itself readily to cellular workflow which is quite common in most manufacturing facilities. Most induction heating systems are capable of producing hundreds of parts per hour. The use of robots and conveyors can completely automate the induction heating operation. Induction equipment should follow standard machine tool design practices in that it should be robust and repeatable for continuous use.

5.1.1 Heating Modes

There are four basic heating modes for induction hardening: static (also called single-shot), scanning, progressive, and pulse heating.

When referring to static or "single-shot" heating, neither the workpiece nor the inductor moves linearly during heating; at the same time, however, the part can be rotated to provide the required heat uniformity. When a scanning mode is utilized, the workpiece or the inductor or both move linearly during the heating cycle. Progressive heating means that the heating is done in various stages and the workpiece is being progressively moved from one heating stage or heating station to another. In order to provide the required temperature distribution before quenching, the heat is sometimes applied in several short bursts with a timed delay between heats to allow the heat to conduct toward the areas that may act as a heat sink. This heat mode is called pulse heating.

In some cases the part to be heat treated is moved into an inductor, heated, and then moved into another position for the next operation, such as quenching. In other cases, the quench is integrated into the inductor and the process of quenching can be done in the same position or station without any movement of the part. In cases where delay time should be minimized and an instant quench is required a quench-integrated approach is the most beneficial.

Some of the main considerations in choosing the particular mode of heating are the shape and size of the part to be heated, the required hardness pattern, the production rate, the maximum allowable distortion, and any special customer considerations and preferences that might include the ability to handle irregularly shaped parts such as crank shafts or steering knuckles (see Figures 5.3 and 5.4). The shape of the components limits the number of ways they can be processed with induction heating. Components such as bar shafts have more options as to how to pass the part through a coil.

Whichever heating mode is used, it is imperative that the part-to-coil location be consistent because it drastically affects the heat treat pattern. All four heat modes are discussed in more detail in the following.

5.1.1.1 Static Heating Mode

The simplest way to heat a part is without any linear movement during heating. This is referred to as *static heating* or single-shot. This mode is efficiently used for selective hardening or localized heating when only a portion of the part is to be heated. Some components require hardness in certain areas of the part, such as the lobes of a cam shaft for wear or a fillet area of an axle shaft for added strength. Selective hardening of only the area that requires hardness rather than hardening the whole component drastically reduces distortion and saves time and energy.

Figure 5.3 Irregularly shaped parts to be selectively induction hardened.

This also allows the design of a part that has completely different mechanical properties within the same component.

Usually the part is moved into the coil, heated, quenched, and then moved out of the coil. Often rotation is added if the part to be heated is cylindrical or rotationally symmetric. The mechanism for moving the part in and out of the coil can be hydraulic, pneumatic, or electric. Figure 5.5 shows a simple lift rotate configuration. This system uses a cylinder to lift the part and an electric motor to rotate the part. An adjustable hard stop is used for part positioning. Figure 5.6 also has the lift rotate mechanics, however, a rotary turntable is used to increase the production rate. This

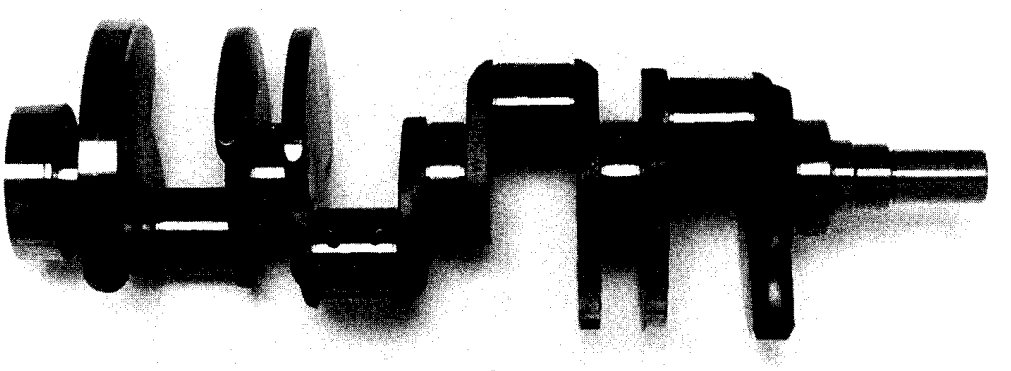

Figure 5.4 Irregularly shaped parts as shown require special consideration when designing material handling and inductors. The orientation of the components, once in the inductor, requires accuracy and repeatability.

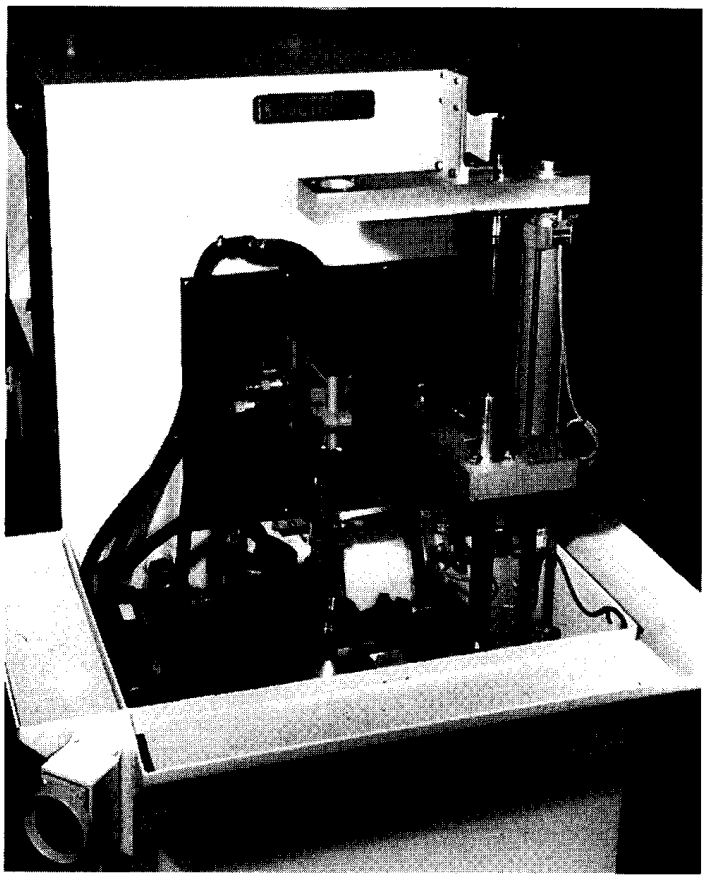

Figure 5.5 Simple lift rotate mechanism for hardening transmission components.

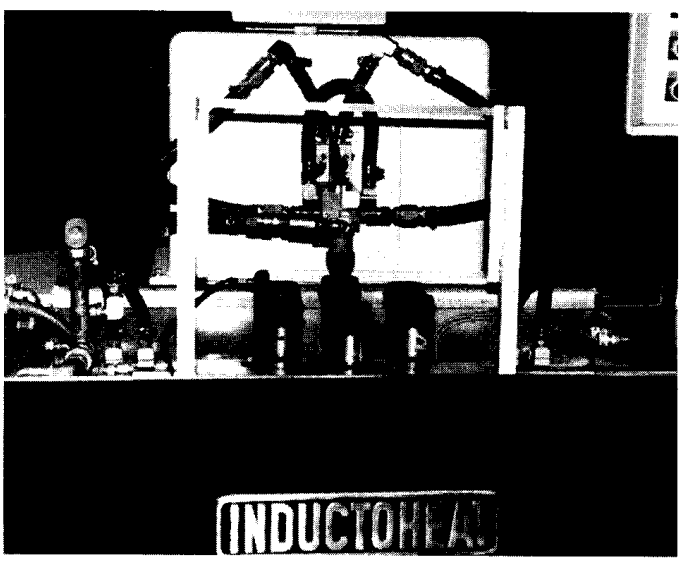

Figure 5.6 Six-position lift rotate mechanism with incorporated rotary table for hardening ball stud sockets used in steering assemblies.

type of system can also be used if there are different areas to be heated on the same part. Figure 5.7 shows a cross-sectional view of a simple single-turn inductor and the hardness pattern it would produce. The part being heated is rotated during the heating and quenching operations to ensure uniformity of heating and quenching.

5.1.1.2 Scan Heating Mode

The part to be heated is held between centers or some other locating feature and moved near the inductor, or the inductor is moved near the workpiece. The heat is applied while the part or inductor is moving; this is called *scan heating*. To keep the high-frequency electrical leads short it is usually preferred to move the part through the coil. This type of system is flexible with respect to part length and to some extent variations in the part outside diameter. In addition, the scanning mode provides the ability to vary speed and power, which controls the amount of heat applied to different areas of the part. Typically, systems have the ability to detect the end of the heat treated part. This feature allows one to process a wide variety of parts using a scanning mode without tooling changeover. The machine chooses the correct process recipe for whichever part is loaded. Depending on the workflow of parts the system can be built as vertical, horizontal, or even at an angle.

The use of servomotors is often required for increased speed and ease of control. High-speed movement is used for indexing IN and OUT of the coil to satisfy the required cycle time. Scanning is typically used for bar shafts, axle shafts, rails, bedways, or parts where the cross-section is somewhat consistent. Figure 5.8 shows a four-spindle scanning system for hardening axle shafts.

If the required hardness pattern lends itself to using the scanning mode of heating, there are a variety of ways to scan heat. This is discussed in Section 5.1.4.

5.1.1.3 Progressive Heating Mode

When induction surface hardening long bars with outside diameters varying from $\frac{1}{2}$ in. (25 mm) to 4 in. (100 mm) or more, the *progressive heating* mode is often selected. The progressive mode can be used for hardening and tempering such workpieces as

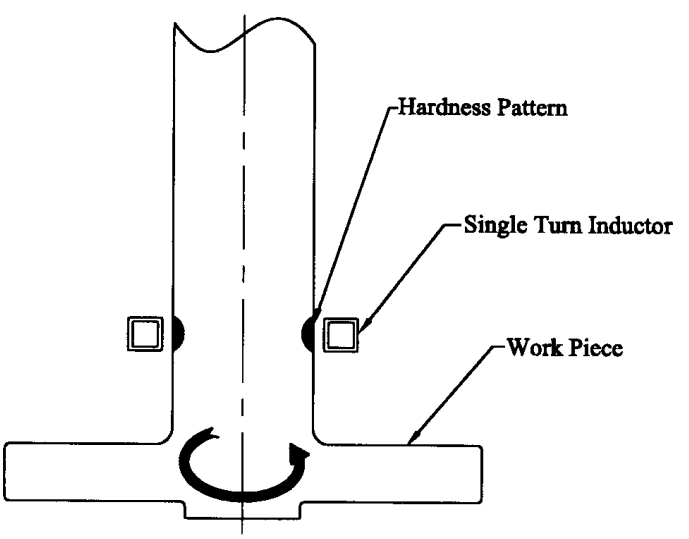

Figure 5.7 Cross-section of an inductor static heating bands of a workpiece.

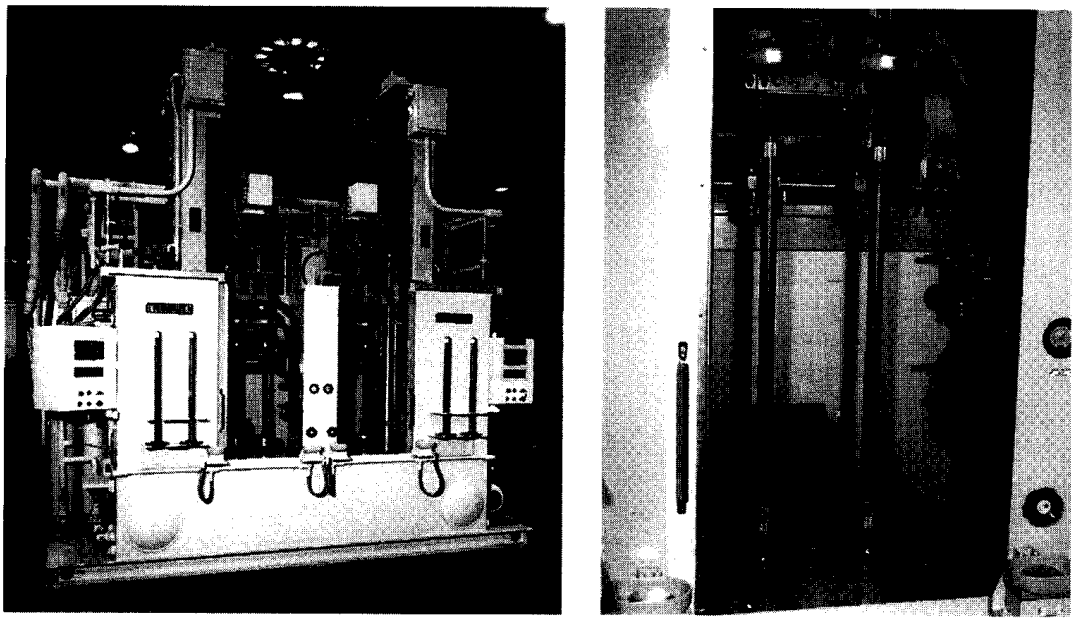

Figure 5.8 Four-spindle scanning system for hardening axle shafts (right); close-up view of coils and axle shafts (left).

tubes, pipes, rods, and bars with smaller outside diameters. Examples of long parts that require hardness include long tool holders used in deep oilwell drilling or in the mining industry.

With the progressive heating mode there are usually three stages corresponding to three categories: preheat, midheat, and final heat. Due to skin effect (discussed in chapter 3) most of the heat is induced in the surface layer of the workpiece. Therefore, the various stages are used with the progressive mode to allow the heat to soak toward the core of the workpiece (e.g., bar) being heated (see Figure 5.9).

Depending upon the application, the same power levels and frequency may be used for all three stages (preheat, midheat, and final heat) when the progressive mode is applied. In other cases, power levels, frequencies, and coil design are different at the different heating stages.

In surface hardening of irregularly shaped workpieces a preheat is used to let the heat conduct to areas of the part into which it is difficult to force eddy currents to flow. In this case conduction and dwell time are used for achieving the desired result. Some examples of this would be fillet hardening axle shafts or the root of gears. In this case the preheat may be done with a lower frequency than the final heat.

Preheating is also often a good choice when hardening cast irons and steels prone to cracking.

To protect the coils, when heating long parts in multiple inductors, guide rails can be added between each inductor. In order to keep them from heating due to the close proximity to the inductor these rails can be water-cooled and are made from nonmagnetic stainless steel. See Figure 5.9 for a simplistic inductor arrangement for progressive heating.

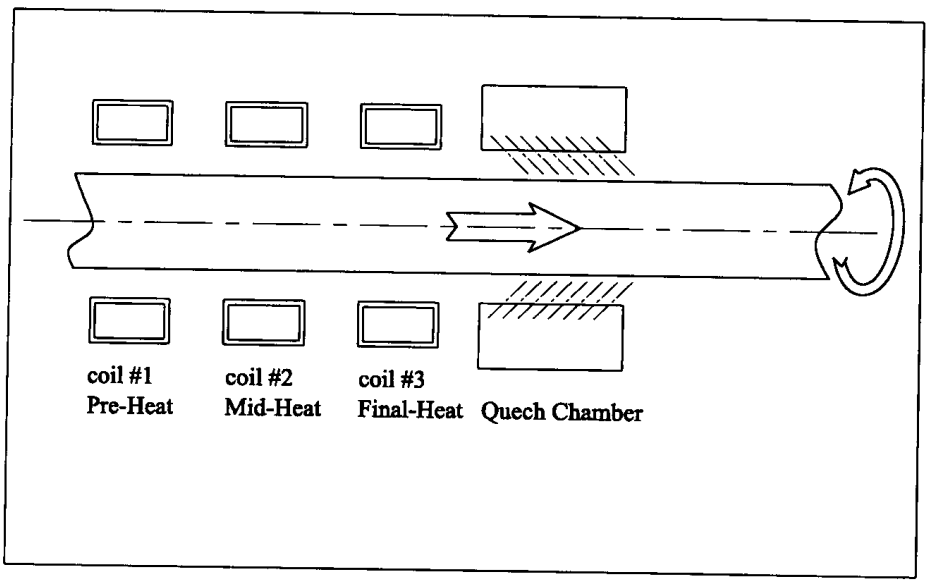

Figure 5.9 Horizontal progressive heating arrangement of coils: coil # 1 does the preheating, coil # 2 does the midheating, and coil # 3 completes the heating with the final heat followed by quenching.

5.1.1.4 Pulse Heating Mode

When the phrase *pulse heating* is used it is usually referring to the method of using short bursts of heat to control or maintain a desired surface temperature. It is often used in induction hardening of gears, critical components, and high-carbon steels and cast irons that have a pronounced tendency to crack. These bursts of heat allow the surface temperature to be maintained without overheating. The pulsing mode can be used in combination with dual-frequency heating. In some gear hardening applications preheating is done with a low frequency and then the heat is pulsed for the final heat at high frequency (see Section 5.4). The cycle time may be the same as a single heating time; however, the actual time the heat is on is very short. A typical pulse hardening cycle would include a series of heat on and heat off cycles until the desired metallurgy is obtained. The duration of each pulse for hardening typically ranges between 0.2 to 3 sec, depending on the size and geometrical complexity of the component.

For cast irons and steels that are prone to cracking, pulse heating can lead to the avoidance of critical thermal gradients by slowing the heat intensity and allowing the heat to conduct toward the core without overheating the surface of the workpiece.

Pulse heating is somewhat similar to progressive heating since the workpiece "sees" a pulsing of the applied power.

5.1.2 Frequency Choice and Power Density

For any induction heating application it is important to select the correct power required and the proper frequency. All induction heating equipment is rated in frequency and maximum power output. There is a variety of power supply designs available. These are described in detail in Chapter 8.

For a repetitive alternating voltage or current waveform the frequency is described as the number of cycles the waveform repeats per second. One cycle consists of the AC voltage or current going through a full 360 electrical degrees. A 10 kHz induction system operates at 10,000 cycles per second. The more cycles completed in one second the higher the frequency. Because frequency counts the number of cycles per second it was originally called cycles or cps (cycles per second) (see Figure 5.10). It was in the 1960s when the name Hertz (Hz) became widely accepted, to honor the great scientist, Heinrich Hertz.

The frequency, power density, and duration determine the actual depth of heating. The frequency is usually chosen first because, in induction surface hardening, the required frequency is primarily dictated by the hardened depth and is directly related to the current penetration depth (discussed in Section 3.1). The size and shape of the part being heated can also affect the choice of frequency. Larger parts can be heated with lower frequencies whereas it is typically more desirable to use higher frequencies on smaller parts and on hollow parts with thin walls.

When discussing the required depth of heating, power density is also a controlling factor. Power density is described as kilowatts per unit area (square meters or square inches) of the part being heated. The area can be calculated by multiplying the perimeter of the part or section of the part to be heated times the heated length. Since the heating condition of the part is a function not only of power density, but also of the duration of the applied power, the applied energy is often used to quantify the induction heating process. Applied energy is measured in kilowatt seconds (kWs). The actual kilowatt seconds may be calculated by multiplying the duration of heat (in seconds) by the power (kW). For example, if a part is heated for 2 sec with a power level of 150 kW, the applied energy would equal 300 kWs.

5.1.2.1 *Frequency Choice and Power Density Choice for Surface Hardening*

The effect of surface hardening (case hardening) using induction can be achieved because of the skin effect. As discussed in detail in Chapter 3, the skin effect is described as the tendency of current to flow near the outer surface of a conductor. The depth of the skin effect is related to the frequency and the material properties

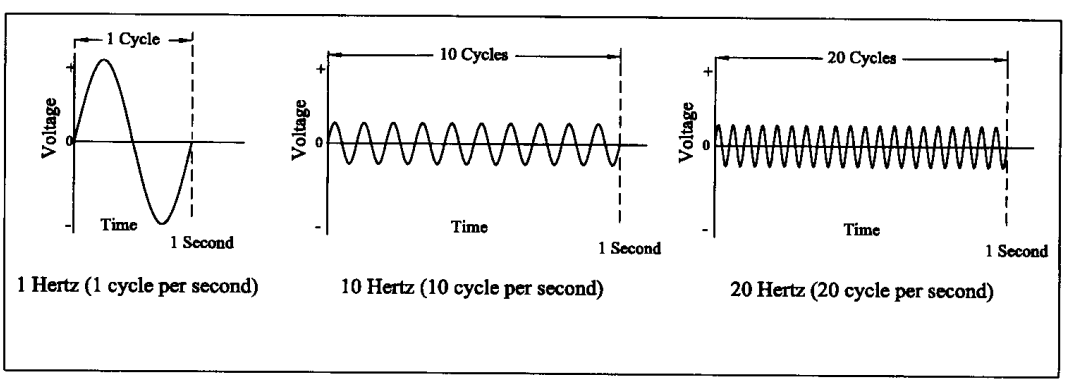

Figure 5.10 Frequency is the number of cycles per second (or Hertz). The more cycles per second the higher the frequency is said to be.

(electrical resistivity and relative magnetic permeability) and is measured in terms of reference depth. The skin effect is utilized for surface hardening because in most cases surface hardening requires a relatively shallow layer of the workpiece to be hardened. The maximum amount of the current induced into the workpiece is on the outer surface of the part being heated.

The frequency ranges for surface heat treatment are as high as 4000 kHz (hardening thin wires) to as low as 60 Hz (hardening large rolls). In the practice of induction heat treating, practitioners typically divide frequencies into three categories: low frequency to 10 kHz, medium frequency 10 to 70 kHz, and high frequency anything higher than 70 kHz. High frequency is also said to be the radio frequency (RF), because it is above the audible range for human hearing. As the frequency is increased the depth of heating is decreased. For example, a system designed to operate in the 600 kHz range would have a very shallow depth of heating whereas a 1 kHz system will produce relatively deep heating.

As mentioned earlier, when hardening small parts, care must be taken to avoid cancellation of current. It would not be practical to try to harden to a case depth of 0.06 in. (1.5 mm) on a $\frac{1}{4}$ in. (6.5 mm) diameter part or a thin wall part with a 1 kHz system. The current penetration depth in hot steel at 1 kHz is too great for this small diameter and current cancellation would occur. Care must be taken to avoid current paths that cancel each other (see Figure 5.11), because current cancellation can lead

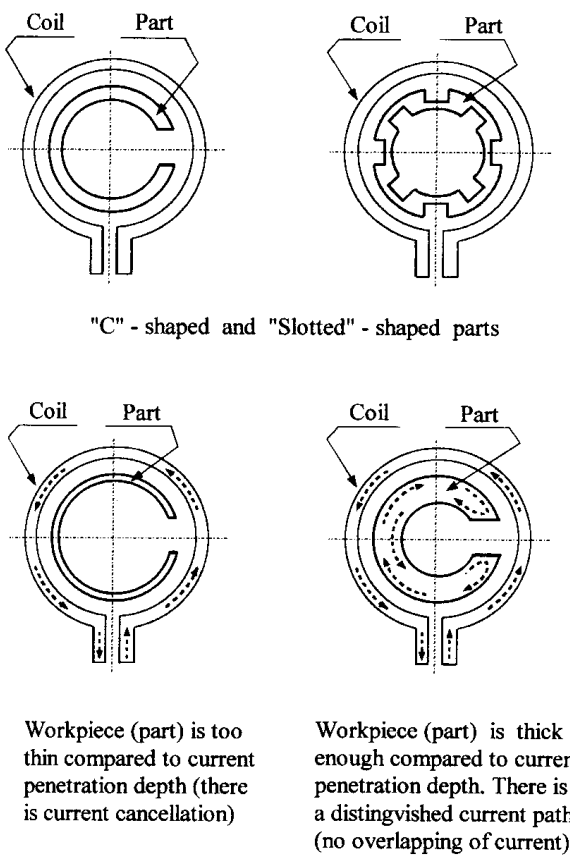

Figure 5.11 Current cancellation in induction heating of C-shaped parts.

to a significant decrease in electrical efficiency. Typically, the frequencies used in surface hardening applications result in a pronounced skin effect, which prevents eddy currents induced within the workpiece from canceling each other. Therefore, in surface hardening current cancellation does not typically occur.

If the workpiece has an irregular shape (e.g., C-shaped tubes, odd-shaped parts, or slotted cylinders; see Figure 5.11), the eddy current will flow on the inside area of the part in order to provide an uninterrupted current loop and current cancellation can take place. The basic rule of thumb that will allow one to avoid current cancellation is that the current penetration depth should be no more than one-fourth of the thickness of the current-conducting path.

In addition to current cancellation there are other dangers of using the wrong frequency. If the frequency is too high for the specified case depth, additional heating time is needed to allow the heat to conduct to the desired depth. Not only does this add unnecessary cycle time but there can also be significant overheating on the surface, which may lead to excessive grain growth. Overheating of the surface can also cause decarburization and excessive scale to be formed on the surface (see Figure 5.12, left).

Conversely, if the chosen frequency is too low the heating is deeper than necessary. The result is a large heat-affected zone, additional workpiece distortion, and unnecessary waste of energy (see Figure 5.12, middle).

In some cases, the penetration depth can be so large compared to the required hardened case depth that it will not be possible to meet the pattern specification. Generally speaking, the optimum frequency will result in a current penetration depth of 1.2 to 3 times the required case depth. This ratio is just enough to compensate for the cooling/soaking effect of the cold core. Figure 5.12 shows sketches of various hardness profiles as a function of applied frequencies.

In most publications devoted to the subject of induction heating, distribution of eddy current density and power density along the workpiece radius/thickness are simplified and introduced as being exponentially decreasing from the surface into the workpiece [according to formula (3.5)]. As mentioned in Section 3.1.2, this assumption is correct only for a nonmagnetic solid body with constant electrical resistivity and homogeneous external magnetic field. However, realistically speaking, this

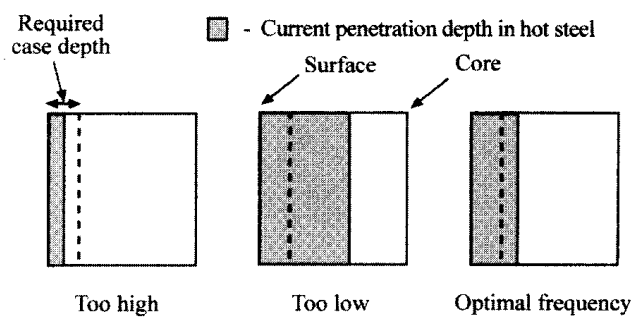

Figure 5.12 Current penetration depth compared to required case depth. If the frequency is too high it results in surface overheating (left); if frequency is too low it results in higher power density and a large heat-affected zone, and can cause excessive distortion and wasted energy (middle).

assumption of exponential current density distribution cannot be made for surface hardening applications. In these applications, during more than half of the heat time, the workpiece surface is nonmagnetic, being heated above the Curie temperature. At the same time, its internal layers remain magnetic.

If the frequency has been chosen correctly, the thickness of the nonmagnetic layer is less than the penetration depth in hot steel. In cases such as this, thanks to the dual-properties phenomenon, the power density has a unique waveshape (waveform) arrangement that is different from the classical exponential distribution. Figures 5.13 through 5.15 show the temperature profile and power density distribution along the radius of the 36 mm (1.42 in.) carbon steel shaft after 0.75 seconds and 1.75 seconds of heating using 10, 25 and 100 kHz. Required hardness depth and total heat time in all three cases were 2 mm and 1.75 sec, respectively. The dotted curves show the exponential distribution.

As one can see from Figures 5.13 through 5.15 the maximum power density is always located at the surface of the cylinder. In the subsurface area, the current density decreases toward the core. However, at a certain distance from the surface, the current density starts to increase again. This phenomenon takes place due to the

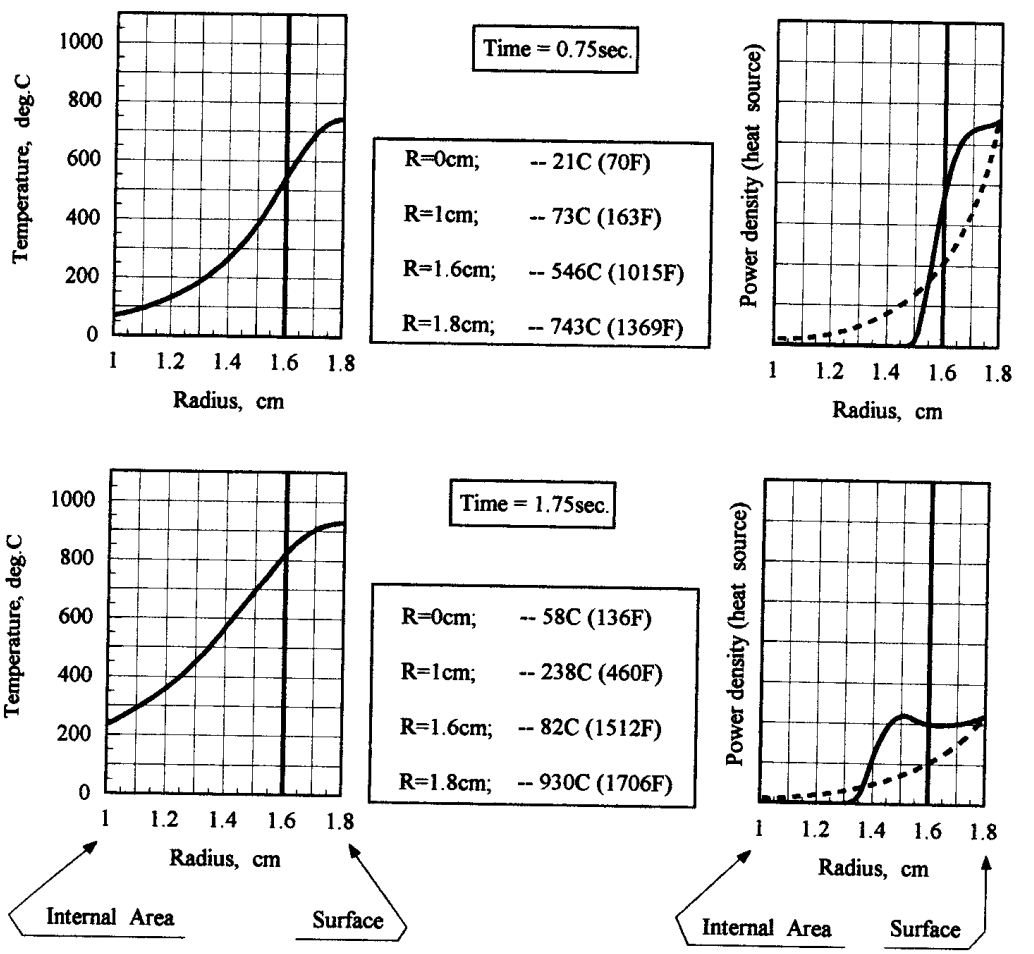

Figure 5.13 Temperature profiles and power density distribution of induction surface hardening using 10 kHz (case depth is 0.2 cm/2 mm).

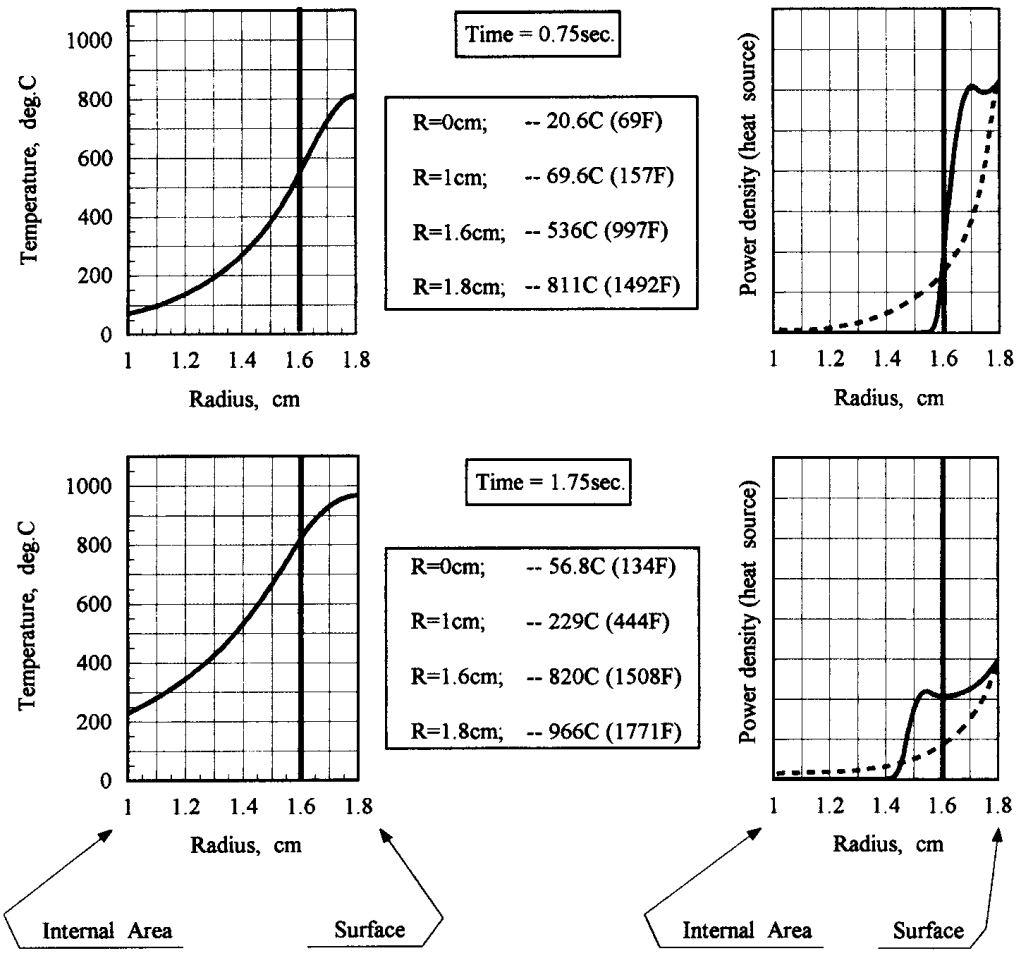

Figure 5.14 Temperature profiles and power density distribution of induction surface hardening using 25 kHz (case depth is 0.2 cm/2 mm).

remaining magnetic properties of the steel at this distance and is called the dual-properties (biproperties) phenomenon. It is necessary to mention here that in some applications, due to the dual-properties (biproperties) phenomenon, the maximum value of heat sources can be located in an internal layer of the workpiece and not on its surface.

The assumption of the existence of the "magnetic wave" phenomenon was announced by M. Losinskii [2] and J. Davies and P. Simpson [3]. The authors provided a qualitative description based on the authors' intuition and their understanding of the physics of the process. New software, such as ADVANCE allows one to provide a quantitative estimation of the magnetic wave phenomenon based on a coupled approach of solving electromagnetic and thermal problems as shown in Figures 5.13 through 5.15.

An ability to take into consideration a phenomenon of the waveshape distribution of power density has a marked affect on the choice of frequency in order to provide the required hardness depth. As one can see, the frequency choice is not as easy a task as it would seem to be at first glance and requires a detailed evaluation of the entire heating process.

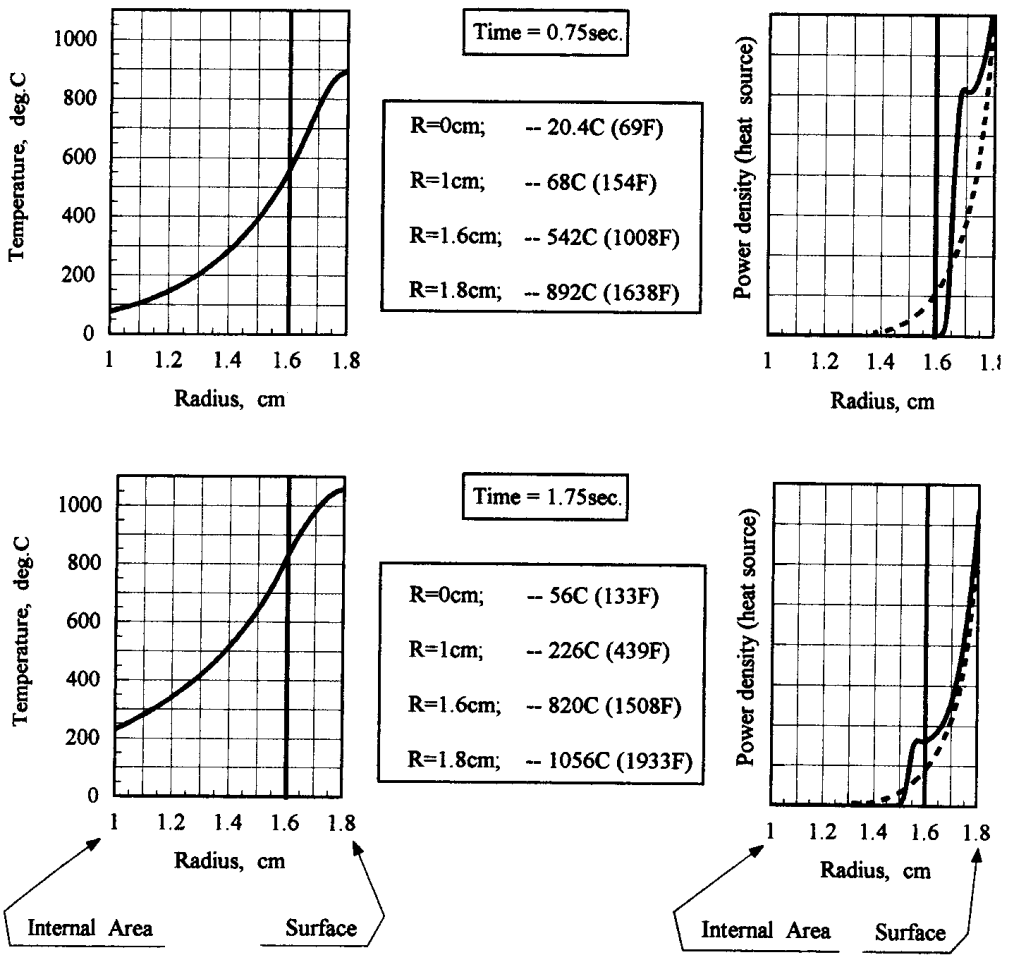

Figure 5.15 Temperature profiles and power density distribution of induction surface hardening using 100 kHz (case depth is 0.2 cm/2 mm).

The specifications for the hardened case depth are a function of the application and performance required by that part. Typically, very shallow case depths of 0.3 to 0.75 mm (0.01 to 0.03 in.) are for wear resistance. These case depths are obtained by using frequencies between 800 and 100 kHz.

Parts that require both wear resistance and moderate loading such as cam shafts and crank shafts are usually induction hardened to case depths of 1 to 3 mm (0.04 to 0.12 in.; See Figure 5.16).

Deeper case depths strengthen the part dramatically because load stresses drop exponentially from the surface. To obtain these case depths, the required frequency is usually between 8 and 50 kHz. Parts that withstand heavy loads such as axle shafts, wheel spindles, and large heavy-duty gears require even greater case depths. The cross-sectional areas of the parts and the magnitudes of the loads they must handle dictate the case depth. These heavy workpiece applications usually require a depth anywhere from 3.5 to 12 mm (0.12 to 0.47 in.), which requires a frequency between 500 Hz to 10 kHz.

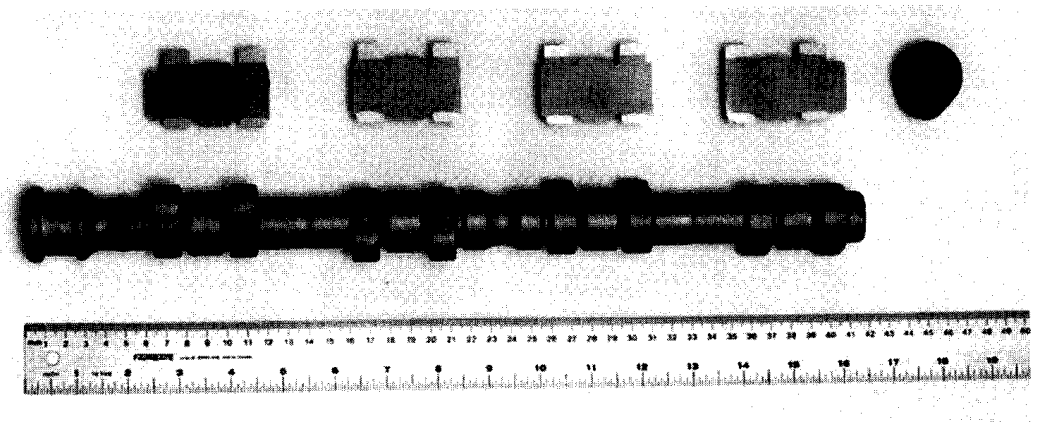

Figure 5.16 Automotive right and left-hand cam shafts that have been selectively induction surface hardened. The above-shown cam shaft was forged, heat treated, then final ground. No premachining was necessary. The equipment utilized a dual-spindle transfer mechanism; the coil was a four-turn coil heating four lobes per spindle at a time. Power was applied for each set of four lobes: 150 kW, 10 kHz. The result is a case depth in the base circle of the cam of 4.2 mm deep. (Courtesy of INDUCTOHEAT, Inc.)

As mentioned earlier case depth is a function of frequency, power density, and duration of heat. Table 5.1 can be used as ballpark data to approximately determine the required frequency and power density.

Higher power densities can result in coil life reduction. In cases like this, proper coil cooling becomes very critical. Specifics on coil cooling are discussed later in this text.

In many cases it is possible to achieve the desired results by a combination of power density and frequency. For instance, when a shallow case depth is required it may be possible to achieve the same results with a lower than recommended frequency by using a higher power density for a shorter time. Conversely, if a deeper

Table 5.1 Frequency and Power Density to Obtain Various Hardening Depths in Carbon Steel

Frequency (kHz)	Hardening Depth (in.)	Low Power Density	High Power Density
450	0.015–0.045	7	12
	0.045–0.090	3	8
10	0.060–0.090	8	15
	0.090–0.160	5	13
3	0.090–0.120	10	17
	0.160–0.200	5	14
1	0.200–0.280	5	12
	0.280–0.350	5	12
Contour Gear Hardening[a] 450–200	0.015–0.045	15	25

[a]A low power density preheat at 3 or 10 kHz is recommended for contour gear hardening.

pattern is required with a system that is designed for higher frequency, lower power density for a longer heat time may be used. As an example, Figure 5.17 shows various case depths achieved with the same inductor. The difference among them is accomplished by changing the frequency and power density.

When designing a new system the correct frequency choice is an economical one as well: a higher frequency rating usually reflects a higher cost for the equipment. As a rule of thumb, the required frequency for surface hardening applications can be found from the condition

$$\left(\frac{5}{X_{hd}}\right) < \text{Frequency (kHz)} < \left(\frac{16}{X_{hd}}\right), \text{ or Frequency (kHz)} = \left(\frac{8.5}{X_{hd}}\right)^2$$

where X_{hd} = required case depth [mm].

Example. If a 3 mm case depth is required the calculation for the frequency range is shown below:

$$\left(\frac{5}{3}\right)^2 < \text{Frequency (kHz)} < \left(\frac{16}{3}\right)^2$$

$$\left(\frac{5}{3}\right)^2 < \text{Frequency} < \left(\frac{16}{3}\right)^2,$$

where the frequency range = 2.78 kHz < Frequency < 28.44 kHz.

5.1.2.2 *Frequency and Power Density Choice for Through Hardening*

Through hardening is done when high strength is required in parts. Snowplow blades, springs, chain links, truckbed frames, and certain fasteners such as nails or screws are good examples of parts that require high strength. Tubes and pipes are also often through hardened. As mentioned earlier, when through hardening is required the entire cross-section of the workpiece is raised above the transformation temperature and then quenched. Because of this deep heating, selection of the correct induction heating frequency is important to achieve uniform surface-to-core temperature in the shortest process time while maintaining high electrical efficiency. Typically frequencies for through hardening are in the low to medium range from

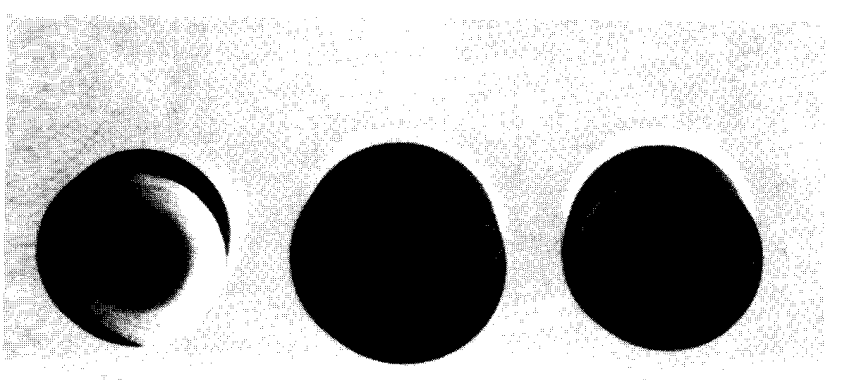

Figure 5.17 Various case depths achieved with the same inductor. The difference between them is accomplished by changing the frequency and power density.

500 Hz to 80 kHz. The size of the workpiece plays a major role in choosing the frequency for through hardening. With induction through hardening applications care must be taken when selecting the frequency to avoid current cancellation.

Figure 5.18 shows a small armature shaft, through hardened at the end. Since the end to be heated is only $\frac{1}{4}$ in. diameter (6.5 mm) a frequency of 150 to 200 kHz would be used in order to avoid current cancellation. In this example through hardening with a lower frequency (i.e., 10 kHz) would be extremely inefficient or even impossible. If using too high a frequency (i.e., 500 kHz) the duration of heat will be increased and overheating of the surface edges and corners might occur. Refer to Table 5.2 for recommended frequencies for through hardening of cylindrical workpieces.

The cooling rate of surface layers during quenching of a surface hardened workpiece is typically greater than the cooling rate of a through hardened workpiece because the cold core in surface hardening applications acts as a heat sink. Because of the greater cooling rate, a deeper martensitic structure occurs after induction surface hardening. Consequently, the surface hardness of through hardened parts is lower than surface hardened parts. This is not only due to more severe quenching but also due to compressive residual stresses at the surface with surface hardening compared to tensile residual stresses with through hardening.

In some through hardening applications, it is very effective to use a dual-frequency design concept. This requires the use of a low frequency during the stage when the workpiece surface layers retain their magnetic properties (below the Curie point). In the second stage, when the workpiece becomes nonmagnetic and penetration depth is increased up to 5 to 8 times, it is more efficient to use a higher frequency. It is at this stage when thermal conductivity has a major impact.

Typically, the power densities for through hardening applications are lower than surface hardening. As an example, Table 5.3 shows a range of typical power densities used for through hardening of medium-carbon steel bars with an outside diameter from $\frac{1}{2}$ to 2 in. (12 to 50 mm), assuming that the correct frequencies have been selected.

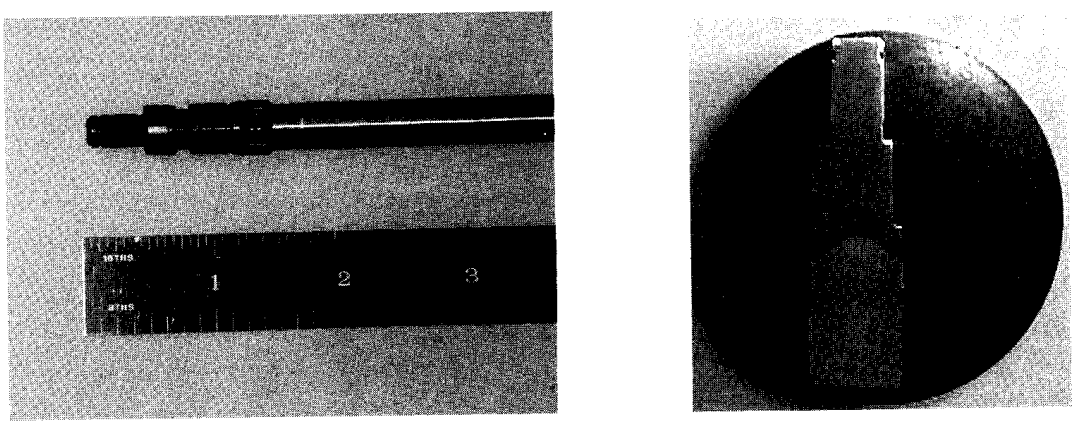

Figure 5.18 Small parts can be through hardened if the correct frequency is selected. Cut, mounted, and etched section of a through hardened small armature shaft. Hardness throughout the hardened zone ranges from 54 to 57 HRC. The material is medium carbon steel.

Table 5.2 Recommended Frequency for Through Hardening Steel Solid Cylinders

Part Diameter (in.)	Part Diameter (mm)	Recommended Frequency
3/32–1/4	2–6	400–200 kHz
1/4–1/2	6–12	200–30 kHz
1/2–1	12–25	30–8 kHz
1–2	25–50	8–3 kHz
2–3	50–75	3–1 kHz
3–6	75–150	1–0.18 kHz
Over 6	150+	0.18–0.06 kHz

5.1.3 Duration of Heat for Surface Hardening

After selecting the correct frequency and power density for the depth of heating that is required, based on the part case depth specification, the last parameter is the *duration of heat*. As previously stated, many induction heated components can be heated to hardening temperatures within several seconds. Thanks to thermal conductivity the longer heating time results in a deeper case depth. Time and temperature are the two major factors responsible for establishing the final metal structure and providing efficient control of process parameters such as distortion. Rapid heating tends to heat only the area where eddy currents have been induced (i.e., the outer surface layer). This results in a very small transition area of the hardened profile. With the increase of time, the thermal conductivity of metals starts to play a more dominant role allowing the heat to soak from higher-temperature areas toward lower-temperature regions. This leads to a fuzzy transition area of the hardened pattern.

As seen in Figure 5.19A, a heating time of 1.5 sec shows no rise in core temperature and a slight increase in temperature in the internal areas of the workpiece. A heating time of 3.0 sec (Figure 5.19B) leads to a small rise in core temperature, and a heating time of 10.0 sec (Figure 5.19C) leads to a significant rise in core temperature. In all three cases, the required temperature at the hardened depth (2 mm from the surface of the workpiece) is approximately the same. Below the hardened depth is where the difference is seen as the temperature of internal layers begins to increase. Physics indicates that the more heat induced in the workpiece,

Table 5.3 Power Densities for Through Harden Bars from $\frac{1}{2}$ to 2 in. Diameter, Assuming Correct Frequencies Were Selected

Frequency (kHz)	Power Density (kW/sq. in.)
1	1.2
3	0.6
10	0.5
30	0.4

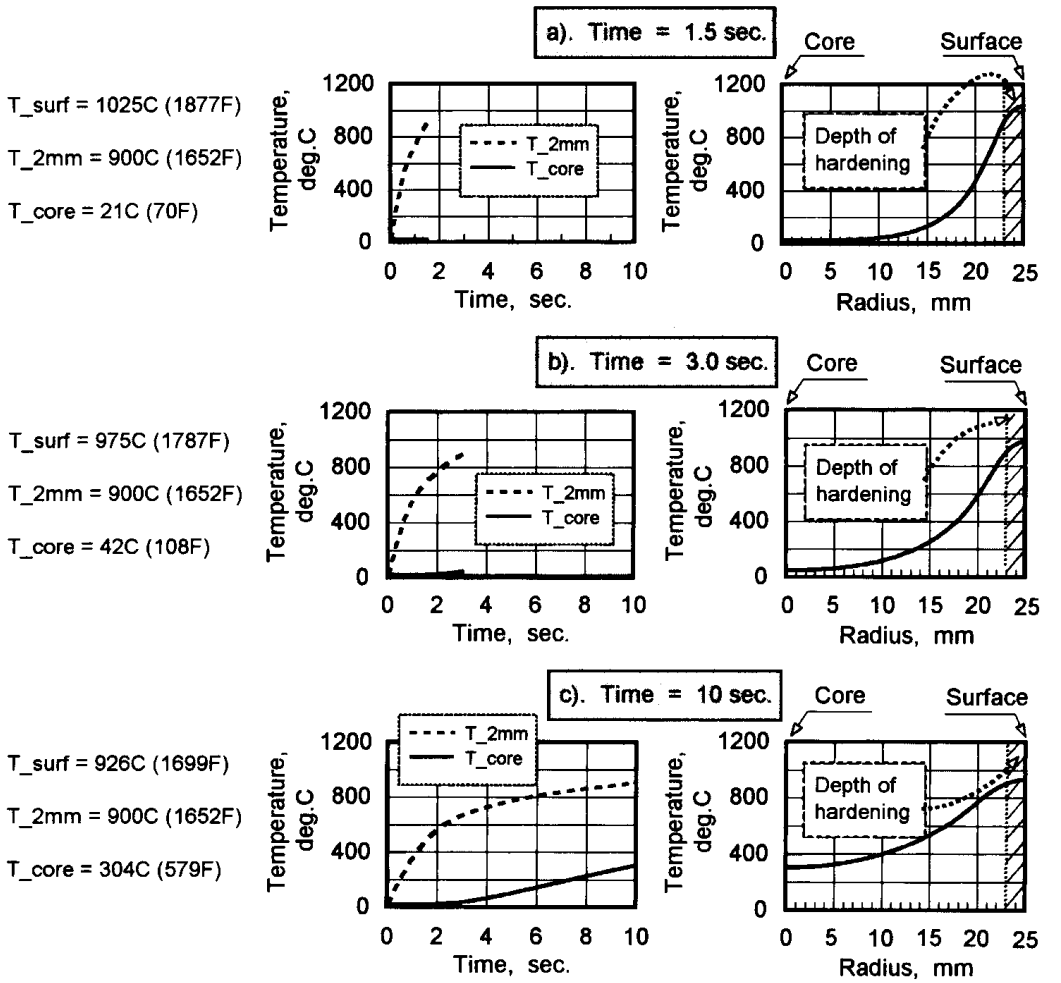

Figure 5.19 Temperature profiles during different stages of induction hardening (10 kHz) minimum required case depth of 2 mm will be achieved in all three cases.

the greater the mass heated and the greater the expansion, thus leading to more distortion.

In order to decrease the distortion of symmetrical parts, it is desirable to have the heating time as short as possible. However, there are some limitations. First, the material must reach the minimum required transformation temperature at the depth to be hardened. If the frequency or surface power density is unreasonably high the surface can be overheated even though the required temperature is held at the case depth. Also, as a result of the short cycle time, large temperature gradients can occur; thermal stresses can reach their critical value and cracking can develop.

When heating asymmetrical parts it may be desirable to use a longer heating time with lower power densities and frequencies. Irregularities such as sharp corners and edges will heat faster with an increase of frequency and power density due to local eddy current concentration in these areas. In these cases a slower heat is often desired, and possibly a dwell before quenching to allow the surface temperature to equalize any "hot" spots.

Every component that is induction heated has its own personality, with respect to material, shape, size, and thermal conductivity. To determine the best heating time for each component may require some experimentation with heating times as well as other process parameters. As long as the appropriate frequency and power size are selected, the duration of heat can usually be determined after several parts are sectioned and evaluated for case depth. Computer mathematical modeling can be very helpful in these cases.

5.1.4 Inductor Styles

An *inductor* or *induction coil* is described as an electrical current-carrying conductor located in close proximity to a part or workpiece to be heated. The alternating current flowing in the inductor creates a time-varying magnetic field that links the inductor and the workpiece. As shown earlier, by Faraday's law, this time-varying magnetic field causes a voltage to be induced into the workpiece or, in other words, to be magnetically coupled from the coil to the workpiece. The magnitude of this induced voltage is determined by the rate of change of the magnetic flux in the workpiece as well as the number of turns in the induction coil ($e = -N)\ d/dt$. The presence of a voltage or potential difference in the workpiece leads to the flow of current and subsequent I^2R loss or power dissipated in the workpiece. This power loss depends on the workpiece resistivity and manifests itself in the heating of the workpiece.

There are many types of inductors and each type is typically dependent upon the mode of induction heating, geometry of the heated part, required hardness pattern, or specifics of the application; these may include whether the part is heated throughout its entire length at one time or in a progressive manner, the number of parts to be heated in one cycle, and the power and frequency available. Inductor styles can be separated into the following categories: scanning, progressive, single-shot, and special inductors.

5.1.4.1 Scan Inductors

The main advantage of a scanning inductor is the ability to run various lengths of parts. This type of inductor provides a repeatable, easily automated process that can quickly adapt to new heat treatment tasks and be easily integrated into a work cell.

Scan inductors may be one (see Figure 5.20) or more turns. The required number of turns is determined by the ability to load match (load tune) the coils to the power supply or by other specific process requirements. This impedance matching process is important if maximum power is required from the power supply. There should be a balance in voltage, frequency, and current to achieve the desired power level. The term load matching or load tuning is used to describe this process. Load matching is discussed in detail in Section 8.4.

The longer (horizontal coil arrangement) or the higher (vertical coil arrangement) the scan coil is, the faster the scan rate is. This is due to the simple fact that the inductor is longer; the part will be in the inductor for a longer period of time; therefore, the scan rate can be higher.

Single-turn inductors are used where a sharp pattern runout is required. An example of this would be the case where a pattern must end near a snap ring groove. Single-turn inductors are typically machined from a solid copper bar, thus making

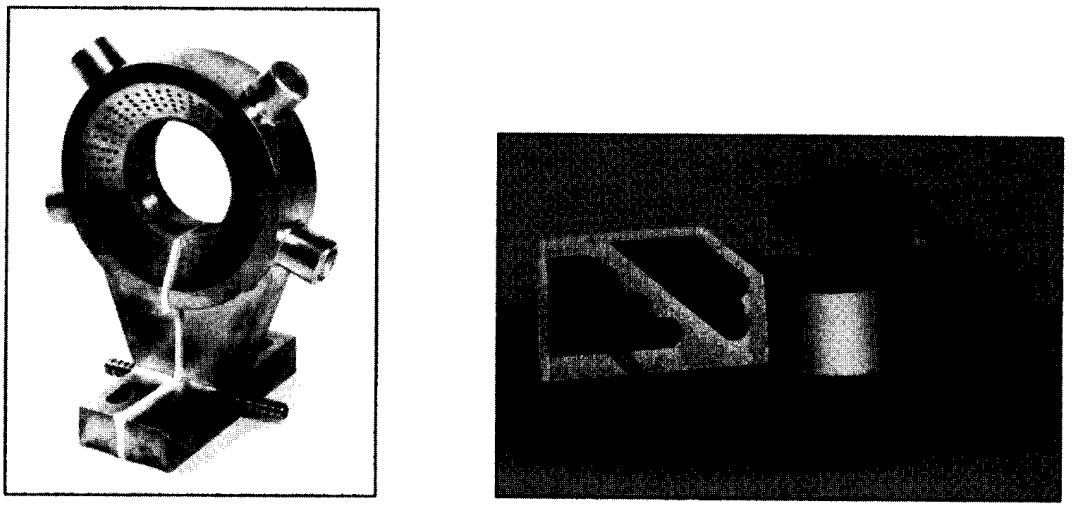

Figure 5.20 Typical machined scan inductor with integrated quench: cross-section (left) of a single-turn scan coil to show quench chamber and coil-cooling chamber (right).

them very rigid, durable, and repeatable. In other cases, a copper tube may be used in the coil fabrication.

The quench barrel and quench holes can be integrated into a single-turn scan inductor. This type of inductor is sometimes called an MIQ inductor (machined integral quench; see Figure 5.21, left). The quench spray should hit the part approximately $\frac{3}{4}$ in. from the heating face and be angled down to prevent the quench from splashing back into the inductor. This dimension can vary with different types of steel and with the scan rate. An additional quench follower may be added to inductors designed to run parts with varying diameters. The quench follower will ensure a proper quench for through hardened workpieces or parts with heavy case depth requirements (Figure 5.21, right). This will prevent problems with shallower parts too hot to be handled, or loss of hardness due to tempering back.

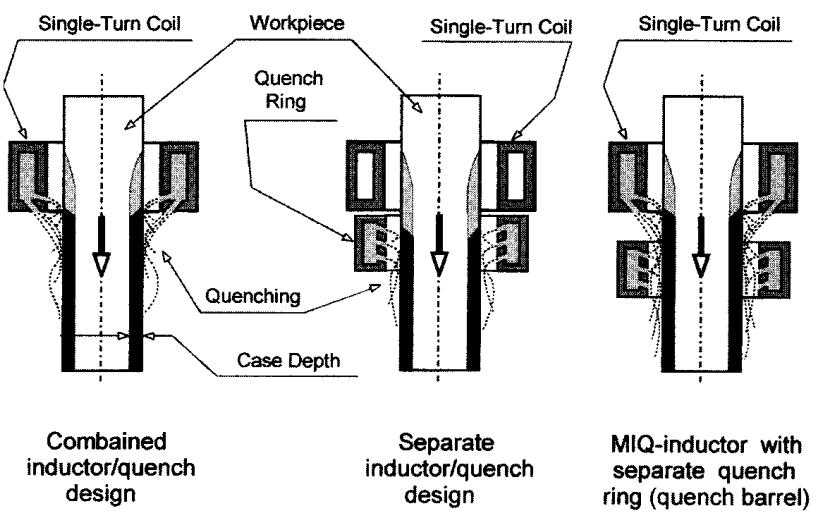

Figure 5.21 Combined and separate inductor/quench designs.

A narrow heating face is required for a sharp pattern cutoff or a short transition zone because of the small flux field and higher power density it provides. A wider heating face or more coil turns can be used when a faster scan rate is desired. The main disadvantage to the wide heating face is that it will produce a gradual pattern runout and may not meet pattern specifications.

For scan inductors that are intended to heat fillets, a radius or a flange must be focused into the fillet area. Flux intensifiers (flux concentrators) may be used to focus the magnetic field into the fillet. These are critical applications that require careful design because the current will try to take the shortest path and stay in the shaft area. Therefore, all efforts must be made to focus it into the fillet. Typically, lower frequencies work better in this application. Scan inductors have a good chance of working effectively to achieve the desired metallurgical results, without having to modify the coil. This is due to the flexibility that results from being able to vary power, scan rate, and quench delay in order to achieve the desired hardness pattern. One disadvantage of this inductor type is that it is generally limited to shafts or bars. Scanning is recommended for shafts where power is limited and/or shaft length is over 8 in. (200 mm).

When scan hardening parts that have a continuous pattern around the perimeter of the part, as in a bar shaft, the part is usually rotated. Rotating the part ensures consistent heating and quenching along the perimeter of the part. Rotation of the part is especially important if a single-turn inductor is used, due to the fact that the inductor has a gap separating the polarized power leads. If the part is not rotated there will be a tendency to develop a cold spot in the area of this split in the inductor. Induction practitioners sometimes refer to this phenomenon as the "fish-tail" effect.

In cases where rotating the part is not practical, concentric heat patterns can be achieved very effectively without rotation if the "split" of the coil is carefully designed. This also requires the workpiece to be oriented and accurately placed in the coil.

a. Vertical Scanning versus Horizontal Scanning. Scanners are typically either vertical or horizontal. The choice is usually decided based on the part shape and length, and the workflow throughout the plant or factory in which the equipment is being installed. Horizontal heating is often chosen when long workpieces are to be processed (6 ft or longer). In such cases, for a through hardening application, there can be several coils installed in line. Each solenoidal coil can have a multiturn or single-turn arrangement. With a horizontal arrangement, parts can be fed through the system with the parts being processed end to end. The loading system can push parts through the inductor by a pinch drive mechanism, conveyor, or mechanical pushers. In these systems the part to be heated is typically a consistent cross-section. Some examples would be bars, shafts, or pins. Parts can be fed by magazine, walking beam, or conveyor. Horizontal scanning can be easily incorporated into a walking beam system. When lifted off the beam it is indexed into the inductor and the heat can be applied to select areas of the workpiece or the entire length can be scanned. A walking beam system, as described above, can accommodate different sizes and irregularly shaped parts to be heated.

One of the main concerns with horizontal scanning is quenching. When scanning vertically the quenching is done below the inductor. This naturally allows

gravity to pull the quench fluid down. With vertical quenching the quench fluid continues to flow on the part long after it has passed the quench chamber (Figure 5.22, left). This can be a benefit if trying to reach ambient temperature before removal from the machine.

When quenching horizontally special care must be taken to provide uniform conditions and prevent quenchant from splashing back into the inductor while heating or onto the floor at the ends of the equipment (Figure 5.22, right).

Vertical scanners can process one to six parts at once. As an example, Figure 5.23 shows a Statiscan vertical scanner with dual spindles. This system has been used for hardening and tempering of a wide variety of parts such as shafts, rasp bars, axles, and hubs. Parts are located and held between centers while they are scanned during the cycle. The part is rotated during the cycle by using a variable-speed motor. This particular model is provided with several power ratings: from 50 kW to 250 kW at frequencies from 3 to 200 kHz. The Statiscan is equipped with a user-friendly onscreen program to provide quick setup, changeover, and diagnostic capability. To simplify setup, upper tooling centers can be adjusted without any extra tools. A selection of standard quick-change inductor mountings is also helpful in minimizing changeover time.

Whether vertical or horizontal, it does not affect the heating face: the heating face would be the same. The main difference in the process lies in the quenching and handling. With horizontal scanning, deflectors, shields, and drip trays may be needed to control quench fluids (see Figure 5.22, right).

b. Movable Inductor versus Movable Part. As previously stated, when a scan heating mode is chosen either the inductor or the part may be moved for the heating and quenching operations. When moving the inductor either flexible cables are used or the inductor is hard-bused to the transformer and it moves with the inductor. With the smaller transistorized power supplies the power supply itself may be moved to scan a stationary workpiece.

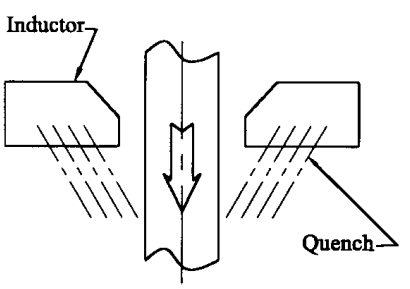

Vertical Scanning Inductor

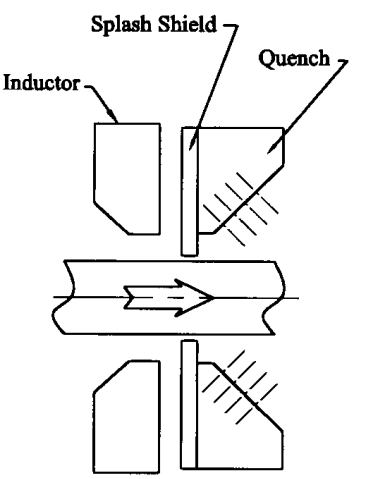

Horizontal Scanning Inductor

Figure 5.22 In both vertical and horizontal scanning, the heating portion of the coil is the same. The quenching is the main difference.

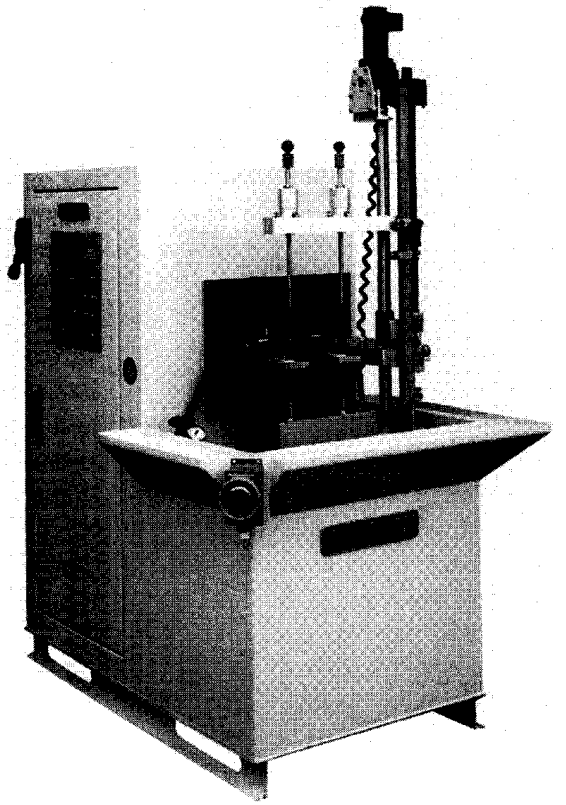

Figure 5.23 Statiscan unitized vertical scanner with dual spindles.

The choice to move the inductor or to move the part is primarily based on the size and geometry of the part compared to the size and shape of the inductor: in other words, which of the two is easier to move. The other consideration is the length of the leads or bus from the power source to the inductor. These should be as short as possible to conserve energy and to allow the power source to operate. If these leads are too long there may be more inductance in the leads themselves than in the inductor. This will net minimal power at the inductor, and thus no appreciable heat into the part.

In some cases it may not be practical to move very large components for heating such as scanning 20 ft (6 m) long bedways. The power leads for this would be too long and it would consume too much floor space to move the part through a stationary inductor. In this case the best choice is to move the inductor with the power supply attached. Another example of moving the inductor is when hardening trailer axles.

As an example, Figure 5.24 shows a system that hardens both ends of an axle. The machine has a walking beam mechanism for part transfer. At the heating station the axle is lifted off the beam and the power supply and inductor are indexed to position for scan heating and quenching. After one end is processed the axle is then lifted off the transfer mechanism and rotated 180 degrees to harden the other end. In such cases heavy-duty precision shafting and bearings are used for stability and

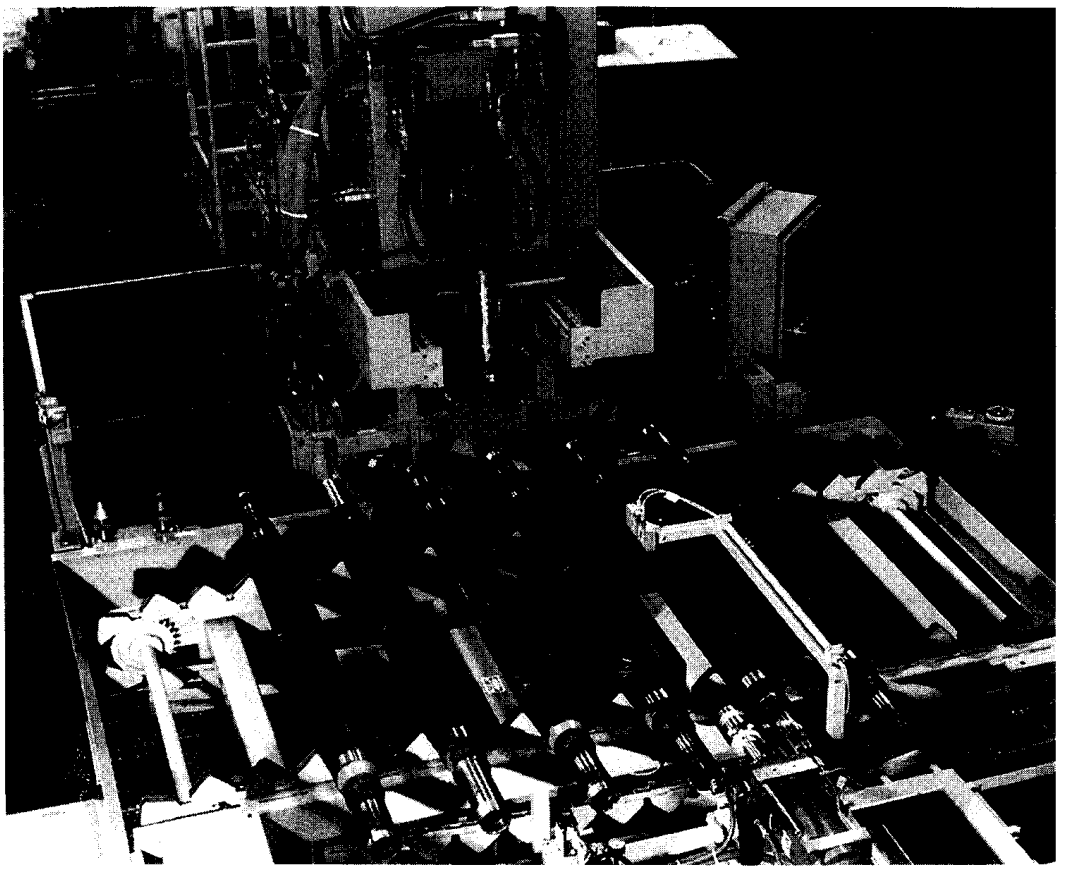

Figure 5.24 Walking beam equipment with movable inductor and power supply. This system uses a 200 kW/10 kHz power supply. A servomotor is used to move the power supply and coil assembly for scan hardening. (Courtesy of INDUCTOHEAT, Inc.)

consistency. Figures 5.25 and 5.26 show a typical movable inductor and pattern from such a system.

When scanning smaller components it is more practical and economical to move the part than the inductor and power supply. It is much easier to move a part that weighs 2 or 3 lbs (1 to 1.5 kg) rather than moving an entire power supply. The weight is an important issue because the movement can occur several hundred times each day.

The length of the part to be heated is also a consideration: when the component is 40 in. (1 m) or shorter it is usually desirable to move the part rather than the inductor. Whether moving the inductor or moving the part the system can be designed to be robust in order to ensure smooth and consistent movement.

c. Single-Frequency Scanners and Dual-Frequency Scanners. In many components case depths are specified to be a certain depth throughout the hardness pattern. Case depth is greatly affected by frequency. In order to have a low capital cost investment, scanning machines utilize a single frequency. Single-frequency scanners operate in a set frequency range. For example, a power supply that is said to be a 30 kHz unit may have a range from about 20 to 35 kHz. When scanning a part that has an irregular cross-section or large changes in diameter the

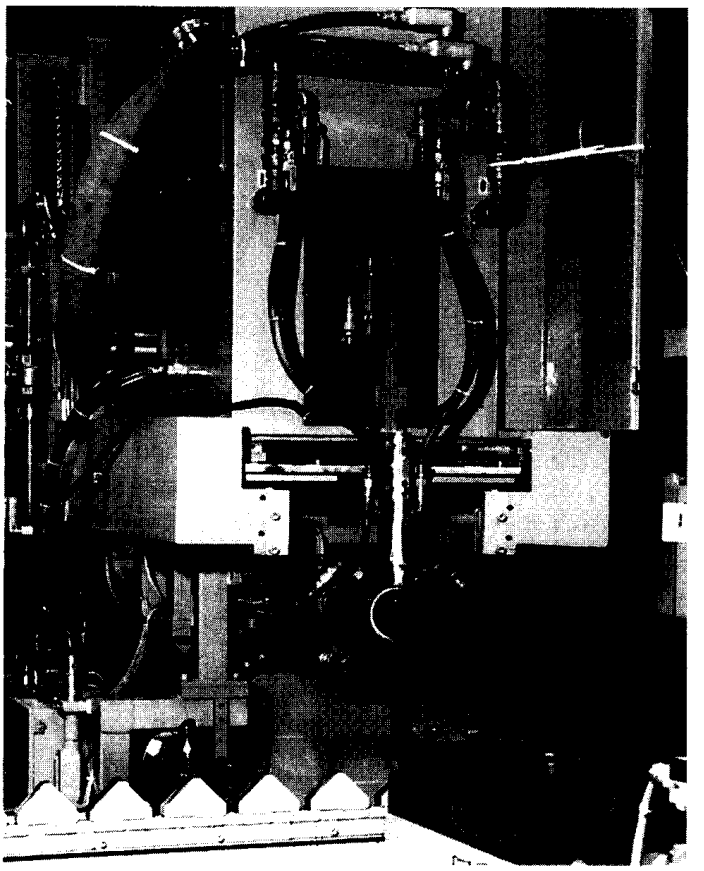

Figure 5.25 Closeup of a movable inductor to harden trailer axle ends. The inductor hardens each end of the axle. The total heating time is less than 8.0 sec.

frequency may change slightly. This occurs because the reactance of the part-to-coil air gap changes as the coupling gap changes. This change in frequency is usually insignificant as far as the process or case depth is concerned.

Several different case depth requirements may be necessary on a single component. If the differences in case depth and workpiece geometry are not significantly different a single-frequency scanner can be used. Deeper case depths can be achieved by increasing the power or increasing the heat time. Caution must be used when increasing the power to obtain the desired depth. This is because induction heating heats the skin of the part and the higher frequencies have a shallower penetration depth. Slight overheating can be compensated for by allowing the surface to cool before quenching. In the induction heating industry single-frequency scanning is the most common because it is very flexible with regard to the parts it can process; it can utilize fairly simple machine concepts and represents a low capital cost for the equipment.

As discussed in the Chapter 3, it can be effective to use a dual-frequency (or bifrequency) design concept. In these cases, a low frequency is used during the stage when the workpiece surface layer retains its magnetic properties (below Curie point). In the next heating stage, when the workpiece becomes nonmagnetic and the pene-

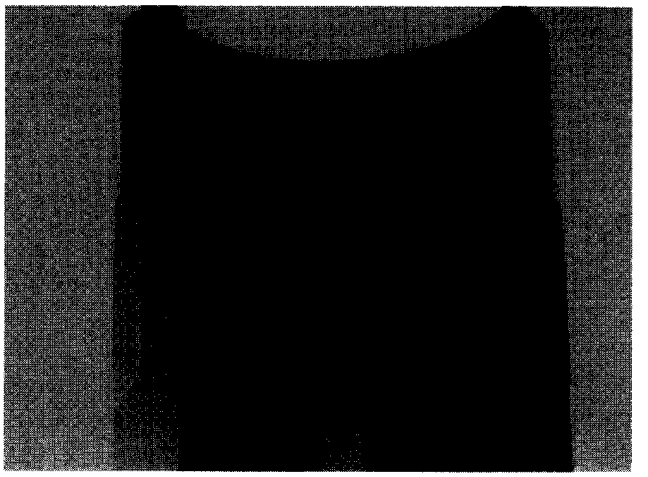

Figure 5.26 Cross-sectioned trailer axle etched to show hardness pattern.

tration depth is increased as much as eight times, it is more efficient to use a higher frequency (see Figure 5.27).

Another reason for using a dual-frequency design is to accommodate a component that has selected areas with different case depth requirements that cannot be achieved by adjusting the power level. A dual-frequency scanner can be used to harden selected areas of the part to scan with different frequencies using different power supplies. The part can be indexed to another station or the second inductor can be mounted above or below the first inductor.

Another example of dual-frequency scanning is a preheat of a large fillet or radius on an axle shaft, or in heating the root of a gear. Preheating is done when a

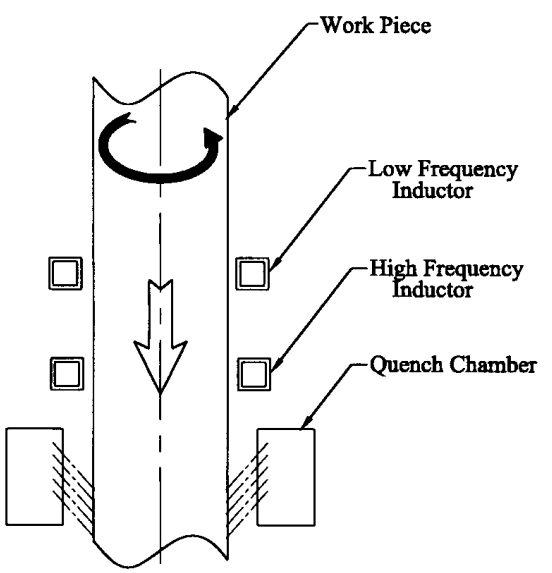

Figure 5.27 Dual-frequency vertical scan hardening. Separate power supplies are used, each with its own inductor.

large change in the part cross-section will not allow a single pass of the inductor to heat deep enough. Preheating can be done by scan heating selected difficult to heat areas of the part, then adding a soak time; when the final heat is applied, those areas will be heated more deeply. This preheat may be done at the same frequency or at a lower frequency.

The material of the part being heated may also dictate a preheat condition. Certain materials such as cast irons or steels that have a pronounced tendency to crack sometimes require a slower heat or more time at temperature before quenching. In this case the whole part could be scanned to preheat it using single or multiple passes.

Dual-frequency scanning is an excellent choice for irregular shapes (e.g., racks and gears) where preheating is required, or where selected areas require different case depths. Although a dual frequency approach provides important capability to an induction system, its utilization is limited to specific applications. Some of the main drawbacks of the dual frequency approach deal with its complexity and high cost, as it is necessary to have two different power supplies instead of a single one. In some cases it is possible to use one dual-frequency power source; however, the cost of these variable freqency power supplies is still high. Therefore, it is cost-effective to use a single frequency power supply and provide multiple pases for preheating of critical areas, where a deeper case depth is required.

d. Obtaining Uniform and Nonuniform Hardness Patterns when Scanning. As with all induction applications the correct frequency and power level are critical for obtaining the desired depth of heating and providing the required hardened case depth. Assuming the power and frequency have been chosen correctly, the controlling factor for case depth in scan hardening is the rate of scanning, which in this case is the time at heat. Many scanning applications range in scan speed from 0.25 in./sec (6 mm/sec) to as fast as 2 in./sec (50 mm/sec). It is important to remember that quenching must follow the heating. If the scan speed is too slow the part may cool below the critical temperature before it enters the quench, resulting in formation of upper transformation products and low hardness. Many times dwells are added at the start and end of each scan program to compensate for the weaker fields at the beginning and end of the inductor due to electromagnetic end effect.

When scanning symmetrical parts such as pins or simple shafts often a single speed and power level are used. The geometry of the part being heated has a tremendous influence on the resultant case depth. Figure 5.28, left shows a nonuniform hardened pattern, due to the shape of the part being nonuniform. Such a pattern is not within the required minimum and maximum case depths and is not acceptable. The inductor is designed around the largest diameter of the part. The inductor loses efficiency when the air gap is increased. In the part shown, there is an undercut at this diameter change; this also adds additional complexity. Sharp corners have a distinct tendency to overheat due to the buildup of eddy currents in this area. The electromagnetic edge effect may cause the corners to overheat while the undercut area has insufficient heat. In this case it would be advantageous to use a single-shot inductor.

Often slight local overheating is not objectionable as long as the overheating of the corners does not result in excessive grain growth or severe grain boundary

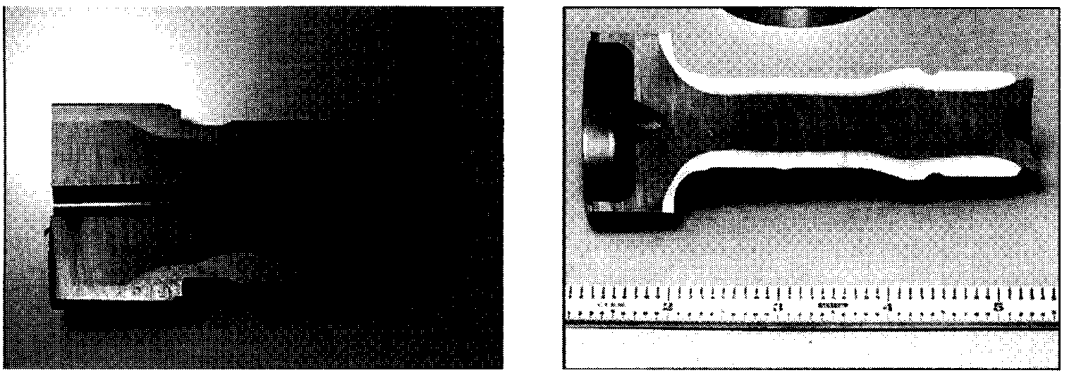

Figure 5.28 An unacceptable nonuniform hardness pattern due to the nonuniformity of the workpiece, scanned with a single-turn inductor (left). An acceptable hardness profile achieved with a single-shot inductor (right). (Courtesy of INDUCTOHEAT, Inc.)

liquation. The use of preheating of fillets and undercuts and changes in scan speed are an effective means of controlling the pattern during scanning of irregularly shaped parts.

The more complex the workpiece, the more complex is the machine control scanning program. If a nonuniform hardness pattern is not acceptable even with the use of these techniques, it may be necessary to use a profiled single-shot inductor.

When using a single-shot inductor the air gap around the part can be consistent. Quenching is also an issue with irregularly shaped parts. Quench barrels designed to quench each area are required. See Figure 5.28, right.

5.1.4.2 Progressive Inductors

Progressive heating is used especially for long parts. Long parts are typically heat treated horizontally because they are more readily processed in a horizontal manner. However, progressive heating is not limited by horizontally processed parts. Sometimes scanning inductors are used for progressive heating, although there may be cases when a part is statically heated to a certain temperature and then moved to another static inductor for the next heating stage.

The inductors for progressive heating follow the same design principles as conventional scanning or static inductors.

As mentioned earlier, progressive heating is used to heat parts in different heating stages. The different stages may have different power levels and frequencies. When using different frequencies for these various stages the coil design should change as well. Just as the depth of current flow in the part is related to the frequency, so is the depth of current flow in the inductor. The wall thickness (i.e., copper tubing wall) of the inductor needs to be adjusted to accommodate the frequency of each particular inductor. As the frequency is decreased the wall thickness should increase. Selecting the proper wall thickness for inductors is discussed later in the chapter.

Typically, a lower frequency is used for preheating inductors, a medium frequency is used for midheat inductors, and a medium to high frequency is used for final heat inductors. In many cases, the preheat inductors will have a wider coil turn configuration than the midheat and final heat coils. This takes place due to a lower

power density and allows the accommodation of the wall thickness and higher currents when using the lower frequencies. Figure 5.29 shows a typical progressive coil arrangement for through hardening of 25 to 50 mm (1 to 2 in.) diameter solid bars (notice the width of turns and the wall thickness of the copper tubing).

As an example of progressive through hardening and tempering, Figure 5.30 shows the induction equipment capable of processing wire from 6 to 12 mm in diameter at a rate of 35 m per minute. Because of the speed of the wire, the progressive coil arrangement must be quite long. In this application, the wire is preheated with medium frequency inductor about 1.5 m (60 in.) long. The next heating is to achieve the hardening temperature and is done with a high-frequency [2.4 m (94 in.) long] inductor, and then quenched. Figure 5.31 shows the final hardening coil and copper bus arrangement. After quenching the wire is tempered with a medium-frequency [1 m (38 in.)] inductor. See Figure 5.32 for a closeup of the temper coil.

5.1.4.3 Single-Shot Inductors

Single-shot inductors are made of tubing or machined from solid copper, but unlike scanning inductors they produce an axial rather than a circumferential current path (Figure 5.33). Because the current flow is axial, rotation must be used to produce a uniform case depth through the circumference of the part. For single-shot inductors rotation speeds range from 120 to 500 rpm. Shorter heating times require faster rotation speeds; there should be at least five rotations per heat, depending on the size of the inductor legs. Appendix F shows the dynamics of the temperature profile during the heat treating cycle. Typically, they have two horseshoe-shaped loops that join the two legs. These legs of the inductor conform to the area of the part to be heated. This type of inductor requires the most care in manufacturing because it must operate at very high power densities. The brazed joints must mate accurately. With a single-shot inductor the electromagnetic fields can be shaped to produce the exact hardness pattern desired although altering that shape is not always easy. Laminations and other types of magnetic flux concentrators are often used along with profiling of the copper in order to provide the required pattern. Figure 5.34 shows a case hardened axle shaft using a single-shot inductor with laminations along the length. Figure 5.35 shows a typical machine for hardening and tempering of axle shafts. On this machine the hardening and tempering is done at different single shot-stations with separate power supplies.

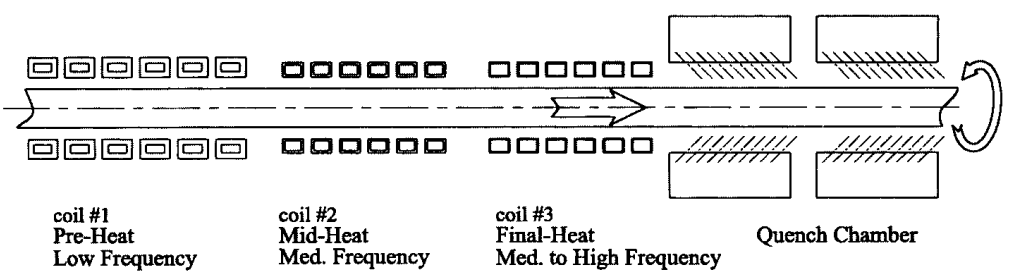

Figure 5.29 Horizontal progressive coil arrangement for through hardening of a solid round bar. In this case preheating is done with a low frequency; the coil wall thickness changes depending on the applied frequency.

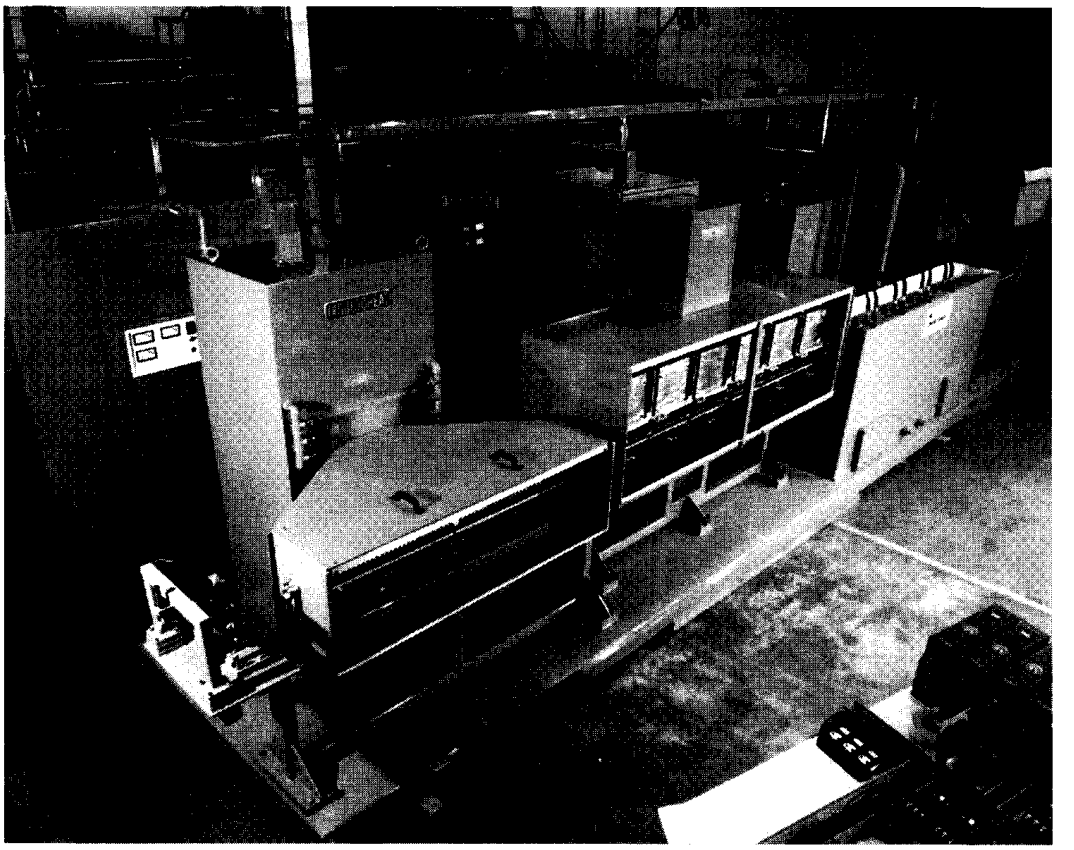

Figure 5.30 This system provides preheat, final heat, quench, and immediate tempering of wire diameter from 6 to 12 mm at a rate of 35 m per minute. (Courtesy of INDUCTOHEAT, Inc.)

Single-shot inductors should be used when the workpiece has an irregular shape or varying diameter, radius, and fillets (see Figure 5.36). When scan quenching is used some areas of an irregular workpiece may not quench adequately. These problems may make single-shot hardening a better choice. Typically, quench blocks with a staggered hole pattern are directed at the part, with the intent to completely cover the part with quench fluid. For the most effective quenching the quench blocks are very close to the inductor. Due to the close proximity to the induction heating coil these quench blocks are usually made of a nonmetallic material.

Single-shot hardening is also the best choice when shorter heat times are desired. Average heating times for single-shot hardening applications range from 2 to 17 sec. The same size component may take from 15 to 50 sec to scan heat (see Figures 5.36 and 5.37).

Single-shot inductors are designed to produce a specific heat treatment pattern. The heat cycle for single-shot inductors is usually much shorter than for other inductor styles. This leads to higher production rates, however, it also requires high coil power. Higher power is required because the entire workpiece is being heated at once. The use of high power combined with a complex geometry can shorten the life of the inductor. For this reason a single-shot inductor has a shorter life than a scan inductor.

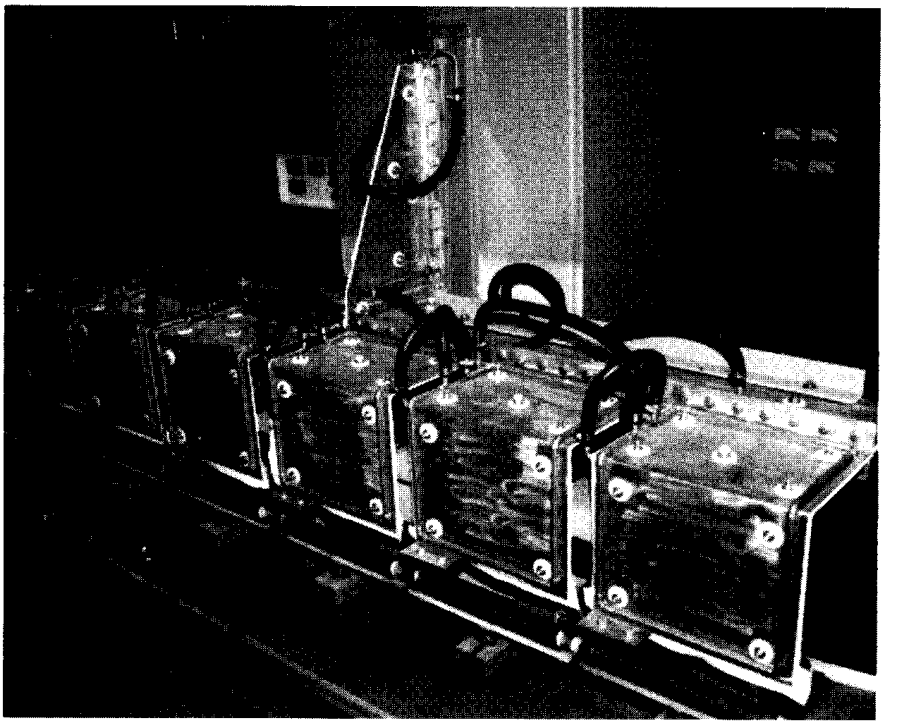

Figure 5.31 High-frequency final heat coils in a parallel circuit; total coil length is over 2.4 m long. (Courtesy of INDUCTOHEAT, Inc.)

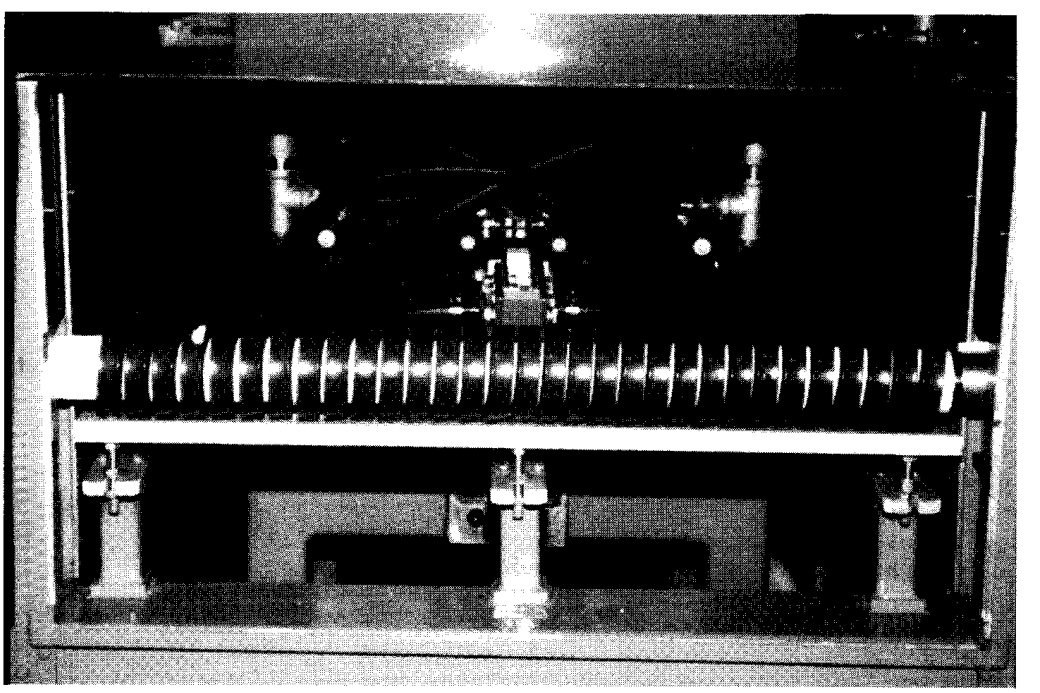

Figure 5.32 Closeup view of multiturn medium frequency coil used to temper wire. (Courtesy of INDUCTOHEAT, Inc.)

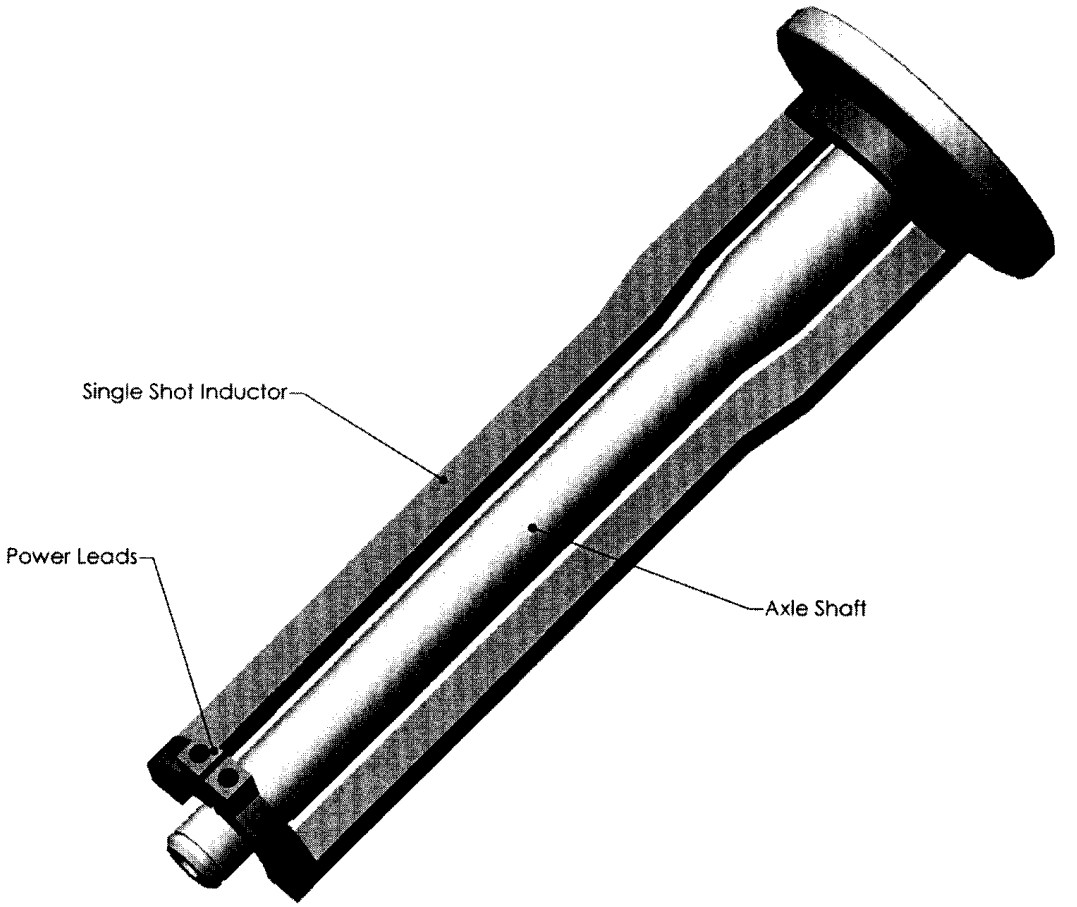

Figure 5.33 Single-shot inductor for hardening an axle shaft.

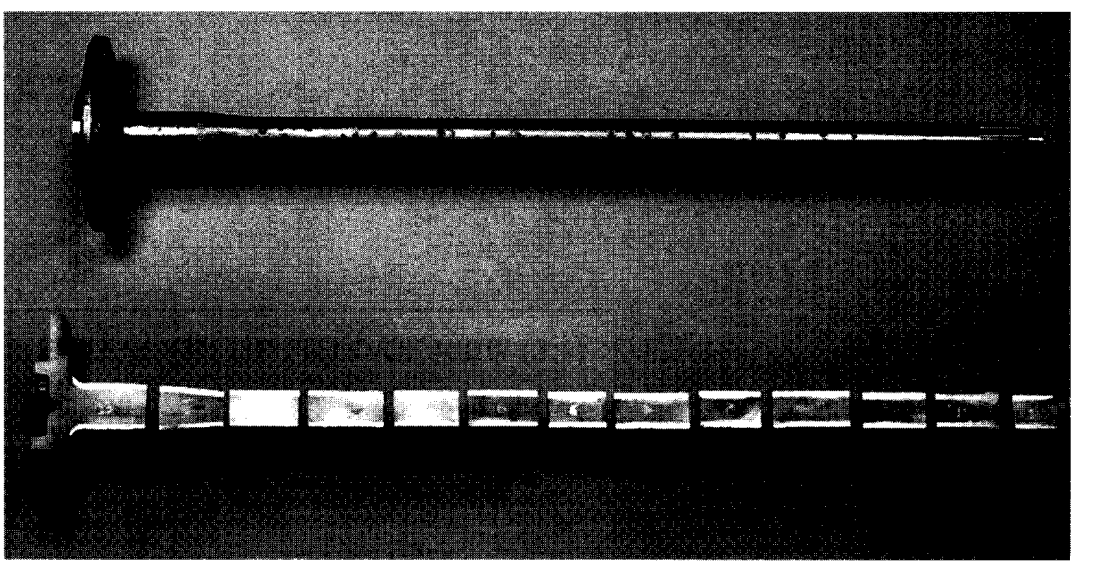

Figure 5.34 Axle shaft (sectioned to show hardness pattern) hardened and tempered with single-shot inductors. The shaft's average diameter is 1–3/8 in. (35 mm) and length over 30 in. (770 mm), hardened using an 800 kW power supply. (Courtesy of INDUCTOHEAT, Inc.)

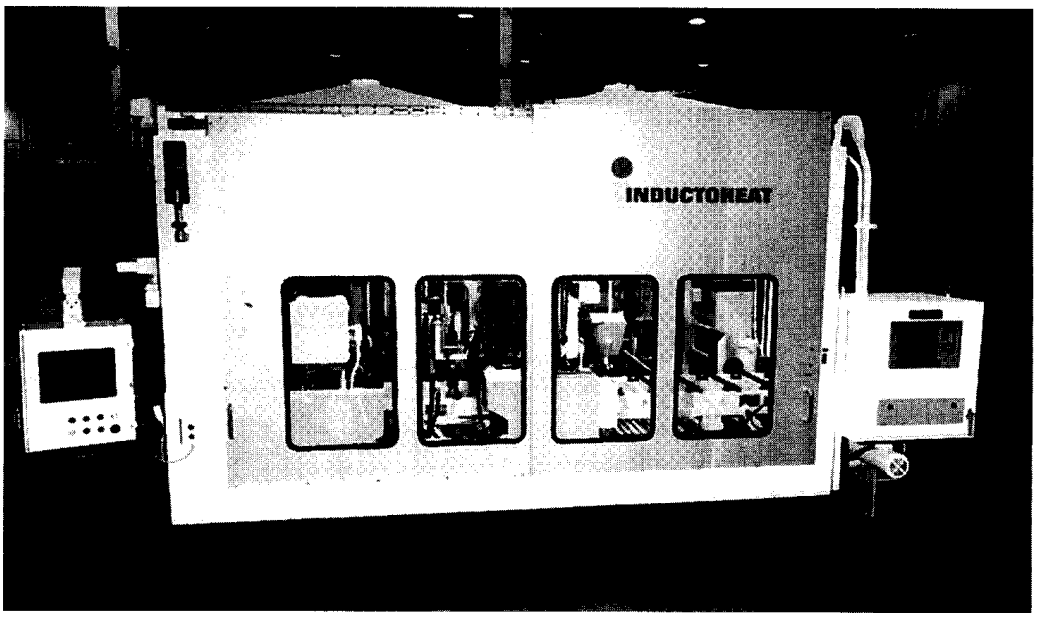

Figure 5.35 Shown is typical equipment used for single-shot hardening and tempering of axle shafts. The equipment is capable of processing over 175 pieces per hour and at full capacity is able to deliver over 1 MW of power.

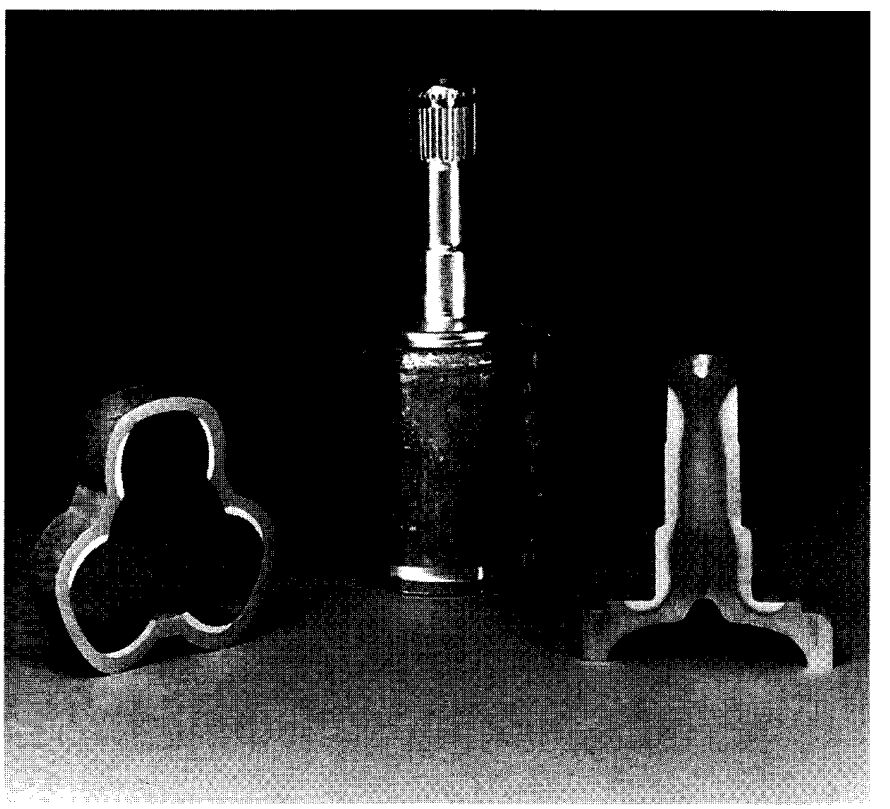

Figure 5.36 Single-shot inductors used for both track (lobes) and shaft of this automotive component. Part is sectioned and acid etched to show hardness pattern. Tracks are all hardened at the same time using 250 kW/30 kHz; stem is hardened using 135 kW/10 kHz. (Courtesy of INDUCTOHEAT, Inc.)

Figure 5.37 Single-shot inductor to harden three tack lobes simultaneously (left). The Shaft of the part also being heated with a single-shot inductor (right). (Courtesy of INDUCTOHEAT, Inc.)

Electrically speaking, it is always important to keep in mind that the inductor is the weakest link in an induction system and could be likened to a fuse. For this reason most inductors have a separate coil-cooling circuit and a separate part-quenching circuit. The inductor will fail if power is increased to the point at which water cannot adequately cool it. Additional cooling passages may be needed with single-shot coils. A high-pressure booster pump is almost always required. Information on the design for inductor cooling is discussed later in this chapter.

5.1.4.4 Special Inductors

The main considerations for choosing an inductor style are the shape of the part, the area to be heated or the desired heat-treated pattern, and the material handling to be used for production. (i.e., will the part be moved into the coil, will the coil index into the part, is rotation of the part required, or how is the part transferred after heat treatment).

Over the years induction practitioners have established what is called a family of special or specialty inductors. Common names have been coined to describe their appearance or function. Some of these include pancake, clamshell, hairpin, split-return, channel, and internal heating inductors (ID inductors).

Pancake inductors are used for selective heating of flats, disks, plates, and large mill rolls in the papermaking industry. The term pancake is used to describe the typical flat round shape of the inductor. This type of inductor has the appearance of an electrical stovetop burner. The center turn of the pancake coils is usually left out to eliminate current cancellation. Figure 5.38 shows a pancake coil for heating a flat circular pattern of a workpiece.

A pancake inductor may not be the best choice when heating the end of a bar or any workpiece that requires even heating, due to the above-mentioned current cancellation effect in the center of the inductor. In cases such as this a modified pancake coil is used.

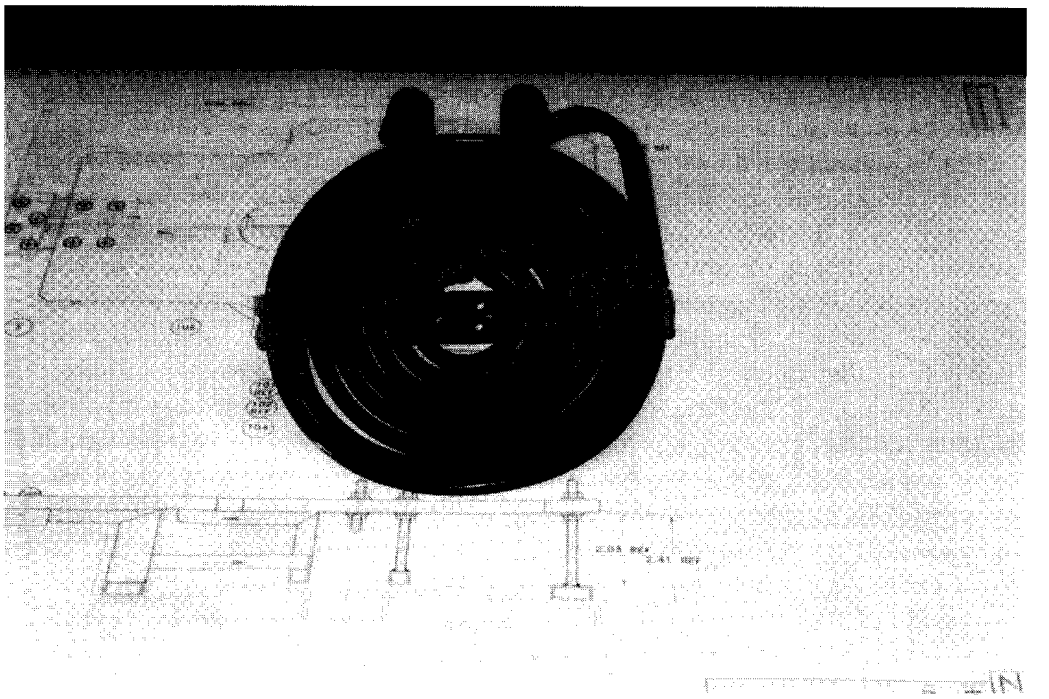

Figure 5.38 Pancake inductors used to heat flats, discs, and plates, producing a wide heating zone.

Figure 5.39 shows what is commonly referred to as a butterfly inductor. This inductor style gets its name because it resembles the shape of a butterfly. The butterfly inductor uses two pancake inductors (the "wings"). The turns are wound so that the center turns of the coil are all in the same direction (the "body"). This center area

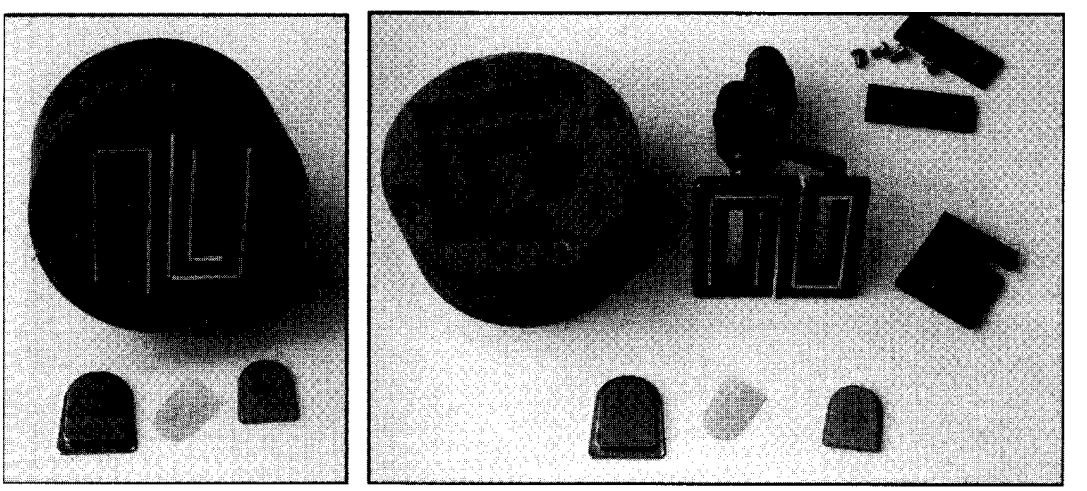

Figure 5.39 Modified pancake inductor called a butterfly inductor used to bond metallic rearview mirror buttons (shown below inductor) to windshield of automobiles (left). Disassembled inductor with flux concentrator, which allows center turns of the coil to focus heat (right).

where the currents are traveling in the same direction is the main area for heating, the even current distribution providing an even heating profile in the workpiece. The center area also has maximum power density. If heating the end of a bar, rotation is required for even heating when using this type of coil.

The inductor shown in Figure 5.39 is used to heat rearview mirror "buttons." When the button reaches a uniform temperature (around 290°F) it bonds an adhesive between the button and the windshield. This inductor has a U-shaped flux concentrator around the center turns of the coil to improve coil efficiency in the center of the coil as well as to ensure that the outer turns of the coil do not couple to the part (see Figure 5.39, left).

When hardening irregular shapes that will not allow an inductor to encircle a part or workpiece such as the lobes of cam shafts with a sharp nose and moderate base circle, or the eccentric journals of certain crank shafts, a split or clamshell inductor can be used. The term "clamshell" is used to describe these coils because they are typically hinged on one side and open and close so the part can be loaded in the correct heat position, simulating a clam opening and closing. For hardening applications the quenching can be integrated through the inductor. The profile of the inductor can follow the profile of the part being heated to maintain a consistent air gap. This results in an even temperature profile around the perimeter of an irregularly shaped part (see Figure 5.40). Often locating pins are required on the inside of the inductor or on some other areas of the part to ensure the correct location is maintained throughout the heating and quenching cycle.

The benefits of an even pattern on an irregularly shaped part are sometimes shadowed by the disadvantages for production intent inductors. If locating pins are

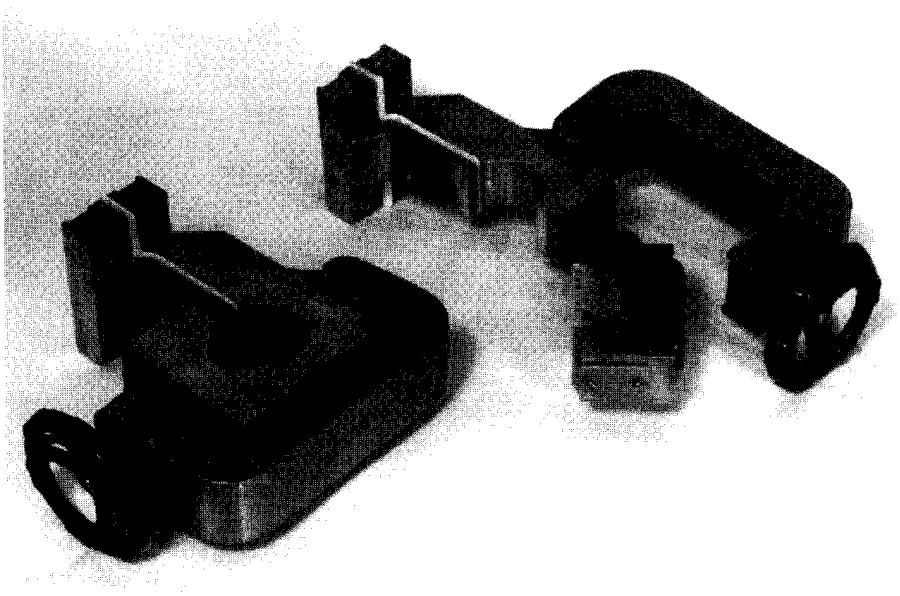

Figure 5.40 Clam shell or split inductor with integrated quench, for hardening cam shaft lobes. Camshaft is manually loaded and clamped in position before heating cycle begins.

used inside the coil they are typically ceramic and subject to breakage due to part handling and thermal shock from heating and quenching.

When the inductor is closed, it must be clamped to ensure a good electrical contact is made to carry the high currents. A special silver alloy is used in this contact area to lower the resistivity of the clamping area of the coil. This area of the coil has a limited life due to wear and contaminants, which can lead to excessive overheating and even arcing, which ultimately leads to premature coil failure.

Recent developments have been made with the split coil design to eliminate the contact area of the two halves of the inductor. In this case the life of the coil may be drastically increased.

Inductors that are formed of bent copper tubing to conform to a part or workpiece are sometimes referred to as hairpin inductors. This name is derived from the resemblance of the inductor's loop shape to a lady's hairpin. Because the typical size of this type of inductor is relatively small usually high frequency is used (i.e., 70 kHz or higher). Hairpin inductors are often shaped during manufacturing using the workpiece as a pattern and documented after an acceptable heat treat pattern is obtained.

A split-return inductor has a main leg of the inductor and equally splits into two legs to form the return legs of the coil (see Figure 5.41). Split-return inductors

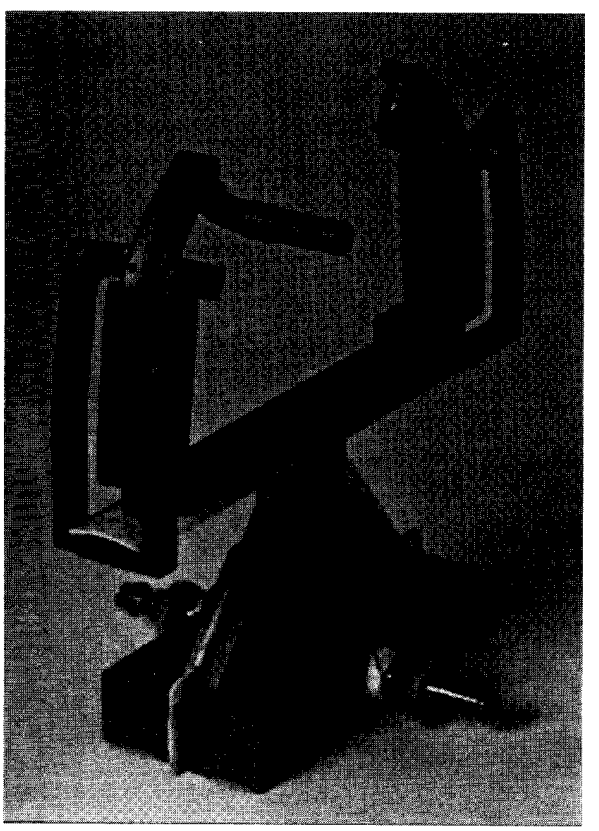

Figure 5.41 Split-return inductors produce a narrow band of heating from center leg of coil. This inductor hardens edges of brake shoes. Center leg of inductor also has integrated quench holes and a flux concentrator to increase efficiency.

produce a unique current distribution in the coil as well as in the workpiece. Because current flows through the center leg and splits into the outer legs, the current is twice as high in the center leg of the coil. Respectively, the power density under the main leg is four times higher coupled than the power density under the return legs. This ratio can be even bigger if the copper tubing for the return legs is bigger in size or a flux concentrator is added, compared to the main leg (see Figure 5.42). The result is very high current density in a narrow band of the workpiece. The eddy currents induced from the outer legs of the coil are usually insignificant to the workpiece. These inductors are typically used for heating a selected edge of a part.

For applications where a longer heating time with lower power density is required a channel type inductor is used. Some examples of these applications include through hardening, annealing, and tempering. The channel inductor gets its name from its similarity to a long channel. This shape allows parts to be passed through the coil in a number of ways such as a conveyor, carousel, turntable, or any indexing system.

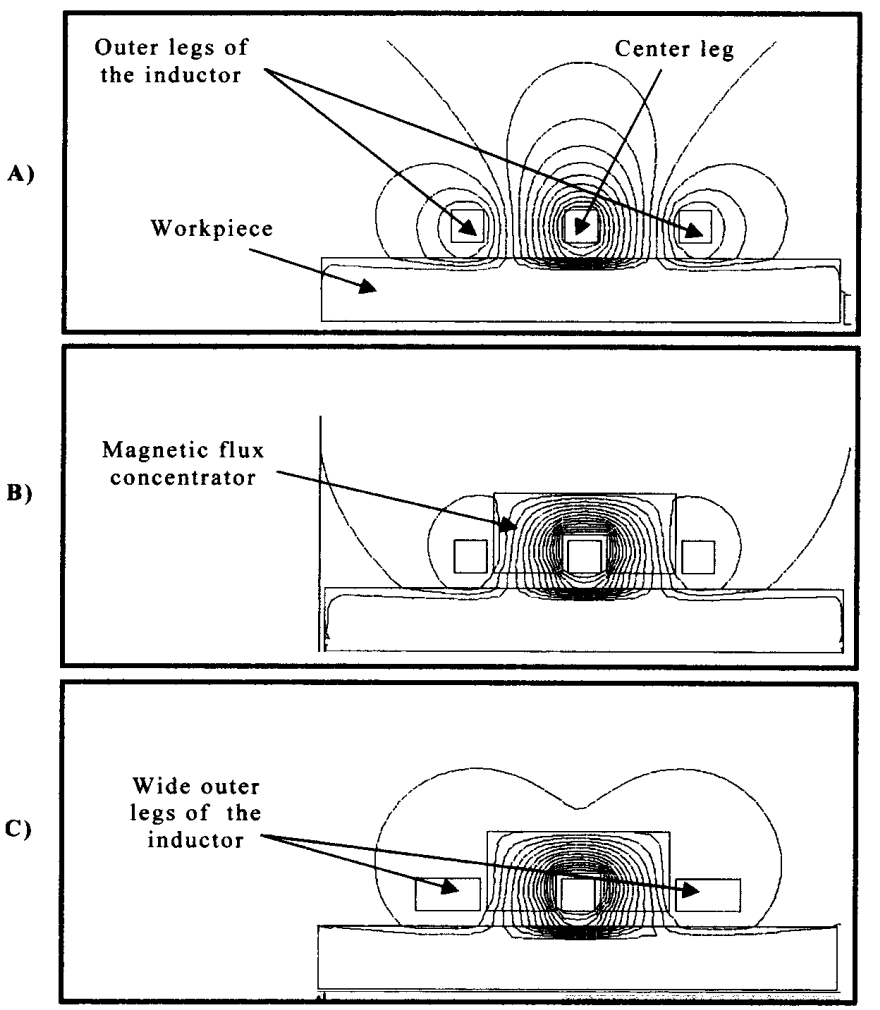

Figure 5.42 Computer graphics of the field distribution in the split-return coil.

The channel coil is a modified hairpin coil with the crossover ends bent away to allow the part to pass through by indexing or continuous feeding of parts. As well as part clearance the crossover ends have to be high enough so as not to influence the heating of the part at the ends of the coil. If a wider area of heat is desired the number of turns can increase to match the area to heat. The areas of the workpiece that are closest to the coil will receive the greatest heat. Since the parts are in the coil for a relatively long time (for smaller components 1 to 2 min) the temperature will equalize. These coils are often used for through hardening, annealing, and tempering applications. However, if a specific case depth is required, rotation of the workpiece may be required for even case depth.

5.1.4.5 Specifics of Designing Inductors for Heating Interior Surfaces

When heating the interior of a workpiece is required, ID or internal inductors are used. The highest current flow is on the inside of any inductor; the weakest field when heating an internal area of a part is the area closest to the coil. For this reason there are some special considerations when designing an internal inductor. Generally speaking internal inductors are not as efficient as inductors designed for outside diameter heating. The real coil coupling is larger than the actual air gap between the internal surface of the workpiece and the coil's outside diameter. The highest current density is on the inside diameter of the bare coil, which with internal heating is the farthest from the heated surface. The use of a flux concentrator installed inside the inductor is often required to improve electromagnetic coupling and shift the coil's highest current density closer to the heated workpiece.

Internal inductors are typically made from tubing and spiral-wrapped the same way a spiral coil is wrapped. A classical internal tubing type coil is shown in Figure 5.43. As explained above, the tubing should be as thin as possible to allow maximum

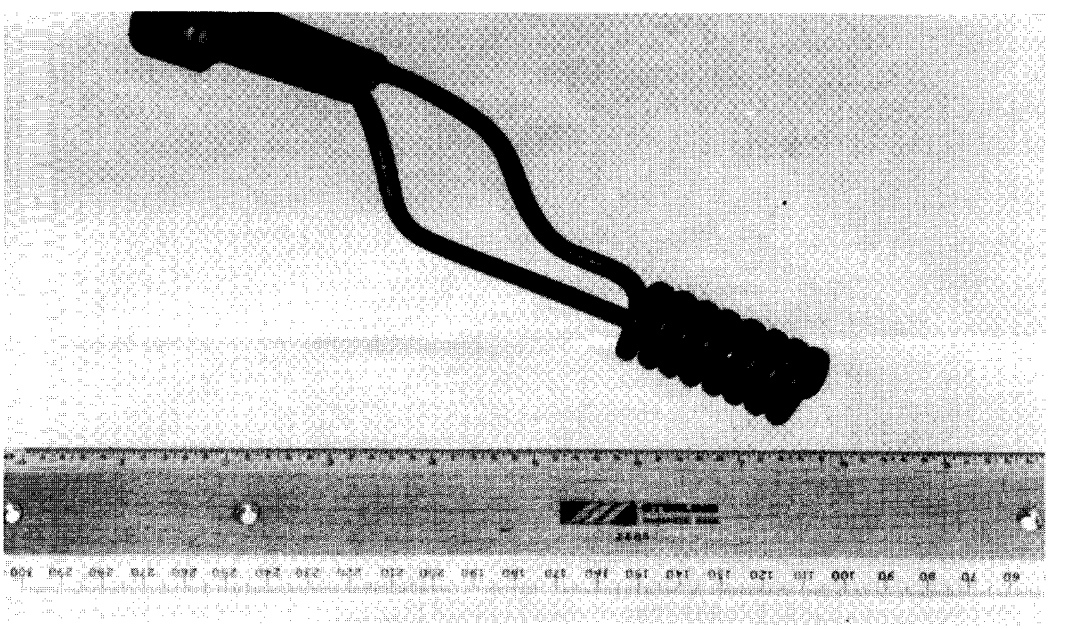

Figure 5.43 Classical small internal high-frequency inductor: coil is made of 1/8 in. diameter copper tubing and has 5/8 in. outside diameter.

coupling to the workpiece. The tubing may be flattened or if possible rectangular tubing can be used. (See Figure 5.44).

Coil turns with tighter windings generate an increased magnetic flux density in the workpiece. In contrast, due to end effect internal coils with a uniform winding provide more intensive heating of the central part of the inside surface of the workpiece resulting in a deeper hardness pattern there. This results in a thumbnail hardness pattern with a deeper case depth in the center. Hardness uniformity can be improved by spreading the coil's center turns (Figure 5.44). Since the center return leg of the ID inductor usually goes through the center of the coil, the smallest outside diameter of the ID coil is typically limited to about 16 mm (5/8 in). If the heated part requires a coil with a smaller outside diameter then a hairpin coil can be used.

In order to provide the same case depth, higher frequencies are used for hardening internal surfaces compared to hardening outside surfaces. In addition, higher power densities are required due to the inefficiency of the internal coil configuration.

When high-power density is combined with small tubing and inefficient heating it can result in coil overheating and, ultimately, premature coil failure. In many cases high-pressure pumps are used to provide adequate cooling water flow.

Often the inductor head can be machined from a solid copper bar. This not only provides a very rigid and robust coil it also allows the wall thickness to be designed to the specific application. Coil cooling and quench holes can be integrated as well. Figure 5.45 shows a typical internal heating inductor to harden the internal helical ring gear of an automotive transmission.

5.1.4.6 Induction Proximity Heating of Flat and Plane Surfaces

Induction heat treating of flat and plane workpieces can be done using longitudinal flux inductors, transverse flux coils, travelling wave inductors or specially designed coils that apply the principle of the proximity heating. The first three techniques are discussed in Sec. 7.6. The longitudinal flux inductor is the most popular approach to heat strips, slabs and plates. These inductors are very similar to classical solenoid cols for heating cylindrical bars and billets, with the exception that the coil is formed as a rectangular solenoid. With appropriate design parameters, longitudinal flux inductors provide efficient and uniform heating of the entire workpiece.

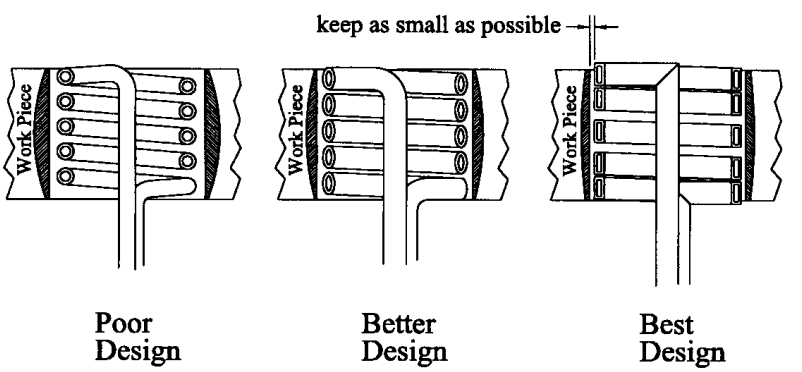

Figure 5.44 Internal heating inductors. Air gap should be as small as possible; rectangular tubing with larger spacing in the center area provides a uniform pattern.

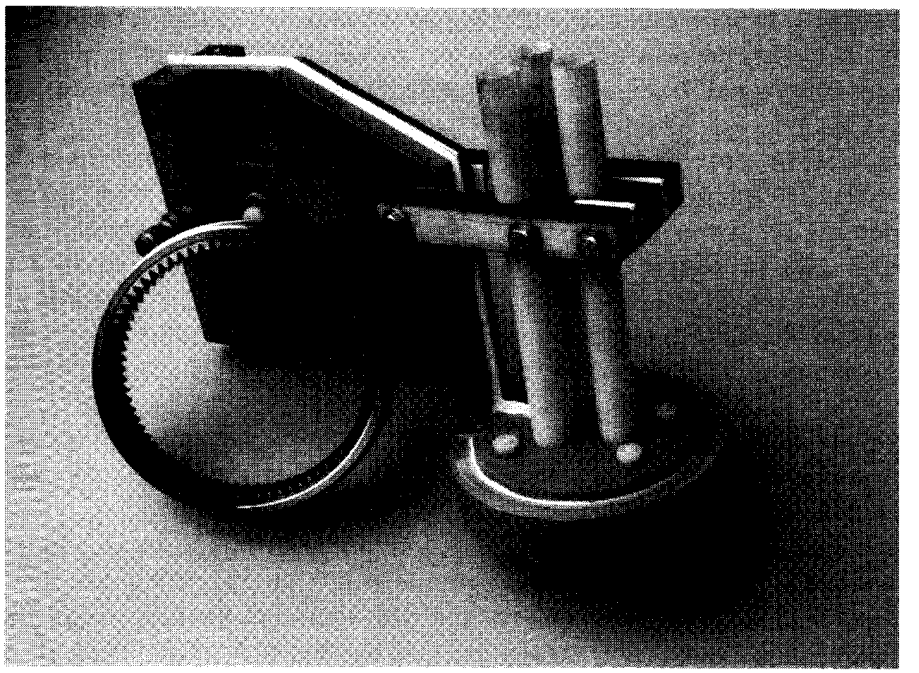

Figure 5.45 Internal inductor for hardening internal ring gear of automotive transmission; coil cooling and quench integrated in inductor head. (Courtesy of INDUCTOHEAT, Inc.).

It is sometimes desirable to heat only selected areas of a flat part. Heating of a particular area of a part can be accomplished by using C-core inductors (Sec. 7.9.2.5) or by proximity heating. Proximity heating implies the inductor that instead of encircling the whole part is placed in close proximity to the area that is required to be heated. Figure 5.46 shows the cross-section of an inductor that provides the selective heating of a flat bar using a pancake inductor. Besides pancake inductors, other special types of coils including channel coils, butterfly and split-return inductors can be used for selective heating of flat parts.

5.1.4.7 Inductors with Inserts

As mentioned earlier, heat treatment by induction is a particularly preferable choice for a high-volume production environment when it is required to heat a certain part

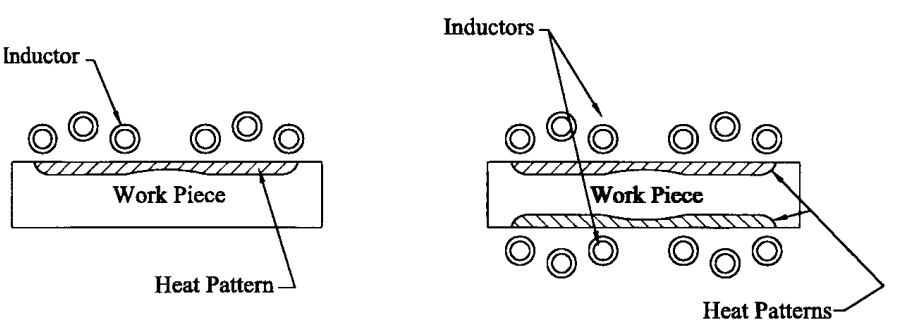

Figure 5.46 Pancake inductors to heat one or both sides of a flat bar.

or a few similar parts. In such cases, an induction coil can be optimized for a certain part or family of closely related parts. However, in some small shops it is often required to heat many small batches of parts, which can have different shapes and sizes.

It would not be cost effective to have several dozen coils dedicated to every single part. In addition, it is often time consuming (even with quick-change coil design) to install a new coil, load match it with the inverter, then run, for example, 30 or 40 parts, and then replace it with a new coil to run another 30 or 40 parts. Significant downtime, essential capital cost to have all those coils, and the necessity to store and maintain them would be noticeable shortcomings of conventional induction heat treatment compared to furnace batch heat treatment.

In these cases, it is often beneficial to use inductors with changeable inserts. Figure 5.47 shows a variety of inserts that allow one to heat treat different parts using the same inductor.

The physics of induction heating using inserts is quite obvious and is illustrated in Figure 5.48. Alternative current flowing within the induction coil produces a time-varying magnetic field that, in turn, induces the eddy currents flowing within the insert in the opposite direction. Due to the electromagnetic proximity effect, eddy currents have a tendency to follow the path of the source (coil) current. As discussed in Section 3.1, eddy currents have to make a loop. However, the slot within the insert breaks the natural eddy current flow forcing them to complete a loop on the internal surface of the insert.

Current flow on the inside surface of the insert creates its own magnetic field that, in turn, induces currents within the workpiece, which provides a heating effect as in a conventional induction heating system.

Inserts are typically made from copper tubing or fabricated from solid copper. It is important that the radial thickness of the inserts should be at least six times that of the current penetration depth. Otherwise, there will be an eddy current cancellation inside the insert resulting in low total efficiency. Water-cooling of inserts is usually required.

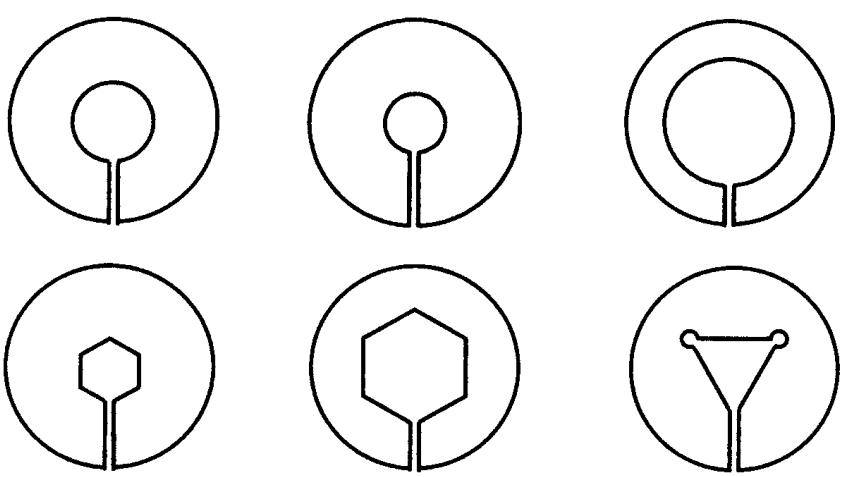

Figure 5.47 Sketch of changeable inserts dedicated for heating a variety of parts using the same inductor.

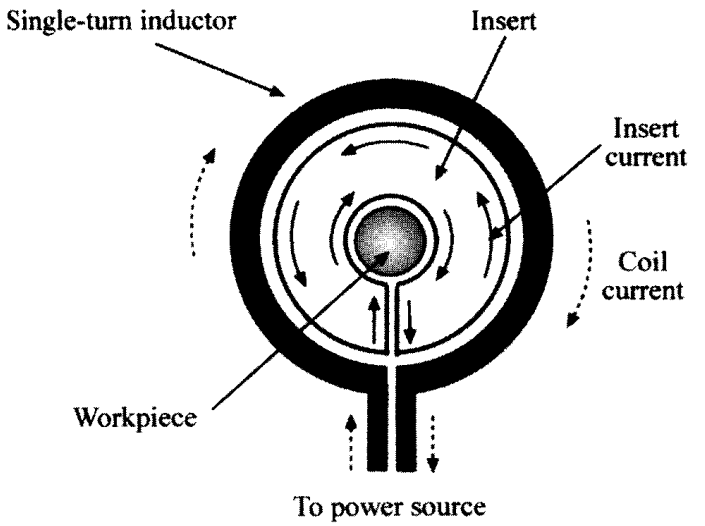

Figure 5.48 Current distribution within the changeable inserts.

Inserts provide a cost-effective solution when it is necessary to heat a variety of small batches. It is easy to maintain and store them. One noticeable advantage of using inserts deals with the fact that inserts simplify a load tuning of the inductor and power supply, significantly reducing the required time to switch from the heating of one batch of parts to another.

In order to reduce inductance, the slot opening should be as small as possible and should be chosen based on eliminating an arcing problem. Often an electrical insulator is placed inside the slot of the insert.

One of the main shortcomings of inductors with inserts is their low efficiency. The intensity of heating and efficiency of the inductor can be improved by fabricating the thickness of the inserts' OD larger compared to its thickness on the ID surface.

5.1.4.8 Coupling Gaps

Reliable operation of coils requires a gap between the workpiece and the inductor. This gap is referred to as the coupling gap. Sometimes this gap is called an air gap, but only in cases where there is nothing located between the coil and the part (i.e. the refractory liner is absent). A proper, more universal, way to describe the gap is as a coupling gap. For the most efficient heating the coupling gap should be held to a minimum. The strength of the magnetic field grows as the gap is decreased. It is sometimes necessary to allow extra inductor-to-part clearance to allow for workpiece tolerances, material handling, and in some cases thermal expansion in the workpiece itself. The length of the part and the required pattern are also considerations for extra clearance, because parts have a tendency to grow longitudinally; if the pattern length is not from end to end, it may result in bowing (e.g. when scan hardening only portions of a long shaft).

The frequency of the power supply being used will have an effect on the coupling gap. Higher frequencies require closer coupling. This is largely due to the fact that coil efficiency is more sensitive to coil-to-workpiece coupling at higher frequencies, and more forgiving at lower frequencies. In induction heat treating

Table 5.4 Typical Coil-to-Workpiece Gaps for Surface Hardening and Through Hardening of Small Parts with Various Heating Frequencies

Frequency	1–6 kHz	10–30 kHz	50–500 kHz
Coupling gap (mm)	13–6	6–3	3–1
Coupling gap (in.)	0.5–0.25	0.25–0.12	0.12–0.04

applications coupling gaps may be as small as 0.03 in. (0.75 mm) to as large as 2 in. (50 mm). Since the majority of hardening applications use high to medium frequencies, they generally have smaller air gaps. In other applications such as tempering or through hardening of large shafts and bars the coupling gaps can be larger. This is due to the fact that lower frequencies will allow a larger gap than is typically required for this type of coil. In induction tempering applications larger coupling gaps (to some extent) provide more uniform heating. In general larger coupling gaps will help to protect the coil and give more clearance through the coil for material handling. Table 5.4 shows a trend that indicates higher frequencies having smaller coupling gaps. However, as mentioned, those gaps vary for different heat treating applications. Table 5.5 shows larger coupling gaps used for other lower frequency heat treating applications; however, these are not limited to the shown gaps in Tables 5.4 and 5.5.

5.1.4.9 Profiled Inductors

When static or single-shot coils are used it is sometimes necessary to profile or relieve the inductor to obtain a uniform hardness or heat pattern. Figure 5.49, left shows that the electromagnetic end effect of a conventional single-turn coil design will result in a thumbnail-shaped heat treat pattern. In contrast, when the inductor is shaped as shown in Figure 5.49 it forces a higher flux density at the ends of the pattern, which would otherwise be the weakest area of heat. The depth of contour of the inductor is related to the applied frequency, magnetic field intensity, and the desired heat treat pattern. When using higher frequencies (e.g., 450 kHz) the depth of contour may be as small as 0.015 in. (0.4 mm) whereas lower frequencies (e.g. 8 kHz) would require a depth of about 0.14 in. (3.5 mm) to make a significant difference in the pattern profile.

This type of profiling of the inductor is similar to changing the spacing of a multiturn coil. Uniformly wound multiturn inductors also have the strongest field in the center of the coil. To obtain a uniform heating profile for static heating, the gap between turns can be spread apart or the coil can be made barrel-shaped with the

Table 5.5 Typical Coil-to-Workpiece Gaps for Through Hardening, Annealing, and Tempering of Moderate Size Parts With Various Heating Fequencies

Frequency	180 Hz–1 kHz	1–3 kHz	3–10 kHz
Coupling gap mm	50–25 mm	25–13 mm	13–6 mm
Coupling gap in.	2–1	1–1/2	0.5–0.25

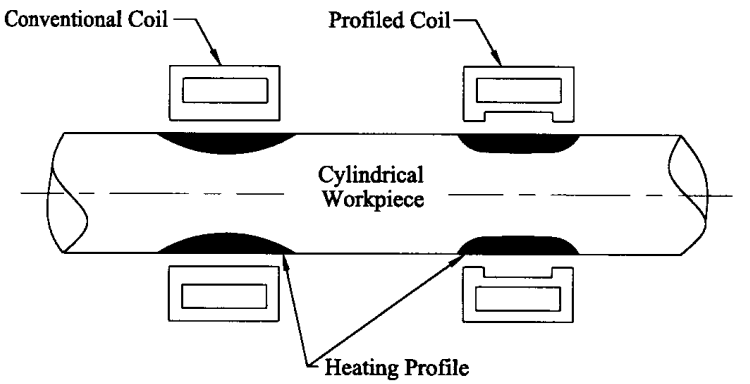

Figure 5.49 Conventional single-turn coil compared to profiled coil and heating profiles.

center turns having a larger coupling gap compared to the end turns. See Figure 5.50 for a comparison in profiling of single- and multiturn coils.

When designing the inductor it is important to maintain enough copper wall to accommodate the contouring and still be thick enough to carry the coil currents. More about copper wall thickness is discussed later in this chapter.

Mathematic modeling and previous experiences are used to determine the exact amount of profiling to be done.

5.1.4.10 Inductors for Heating of Irregular Shapes

Generally speaking the area of the workpiece closest to the inductor will achieve the highest heat because the flux field is strongest in that area. However, if the workpiece has an irregular shape (e.g., parts with flanges, undercuts, shoulders, etc.) there are some special considerations. Often the inductor may have to be relieved around the edges and corners. When there are large changes in masses of metal, the coupling gap will change to compensate heat sink and flux robbing effects in order to obtain uniform heating. Obviously the areas of less mass will take less energy to heat. This is compounded by the fact that the electrical current tends to take the shortest path (least path of resistance), which often is the smallest area or diameter of the part.

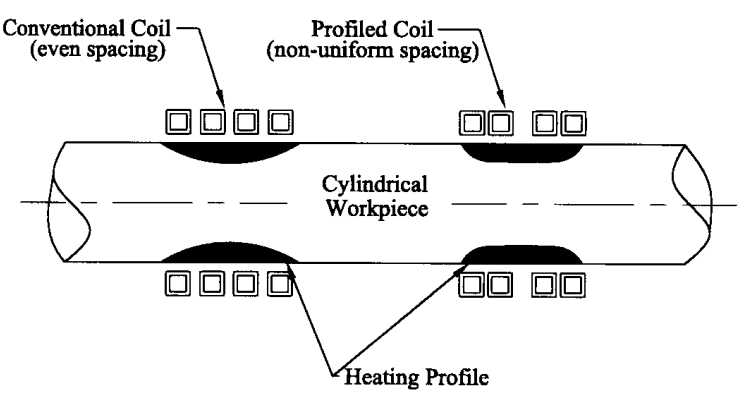

Figure 5.50 Profiling can be done with multiturn inductors by nonuniform spacing of turns.

The heat treat pattern specifications and workpiece geometry determine the basic shape and profile of the inductor. Figure 5.51, left shows an inductor that (due to an electromagnetic ring effect) would primarily heat the smaller diameter of the workpiece and would not properly harden the fillet area. It is possible to redistribute a hardness pattern by changing the shape of the inductor and coil decoupling in the area of the part's smaller diameter. Figure 5.51, middle shows a heattreat pattern through the corner fillet and on the smaller diameter of the part. This is accomplished by maintaining a relatively small gap on the perpendicular surface and having a larger gap on the smaller diameter. In this same example, if both diameters of the part require a heated pattern the inductor would also have a smaller air gap on the larger diameter; see Figure 5.51, right.

5.1.5 Striping Phenomena, Barber Pole Effect, and Snakeskin (Soft-Spotting) Phenomenon

When discussing the specifics of induction hardening, it is necessary to mention some unusual effects that are observed in induction heat treatment: the striping phenomena and barber pole effect [110, 203].

Generally speaking, there are two types of stripes. Both phenomena appear when only a single-shot heat mode is used. Although the appearance of both phenomena is almost identical, the physics behind each of them are quite different. The striping phenomenon type A is a more common form and appears when a multiturn coil is applied. A combination of small inductor-to-workpiece air gaps, relatively high-power densities, and coil turns wound loose might result in an uneven stripe-type temperature distribution along the workpiece length. Proper coil design can eliminate this undesirable phenomenon.

The type B striping phenomenon typically occurs during intensive induction hardening of carbon steels and irons where short time and high-power densities are used. This phenomenon can be seen even in the case of a single-turn coil with a conventional cylindrical load. Because of this effect, the workpiece area under the coil may unexpectedly start to heat nonuniformly (Figure 5.52). Shortly after the heating cycle begins, alternating hot areas (bright stripes) and cold areas (dark stripes) become visible. These bright and dark stripes encircle the cylinder and thus have the shape of rings.

The type B striping phenomenon has never been obtained by mathematical modeling. It has been viewed only in practical applications or during laboratory

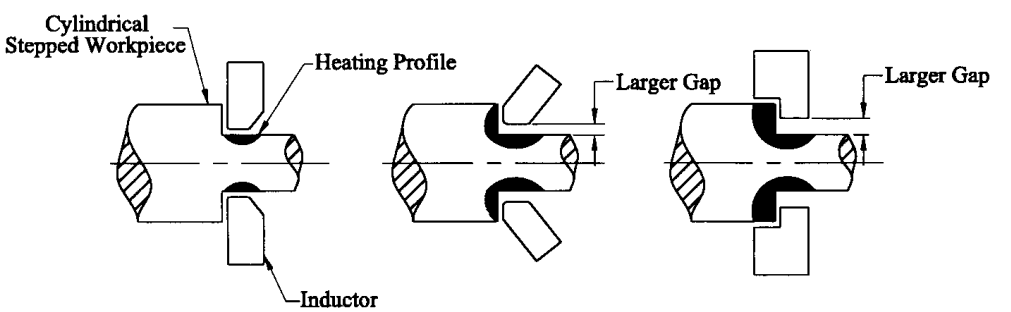

Figure 5.51 Coupling gaps as they relate to irregularly shaped parts.

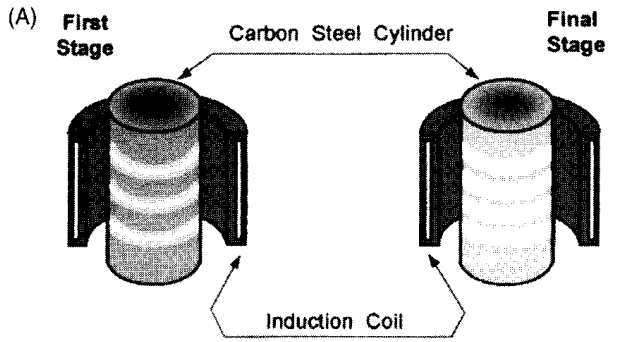

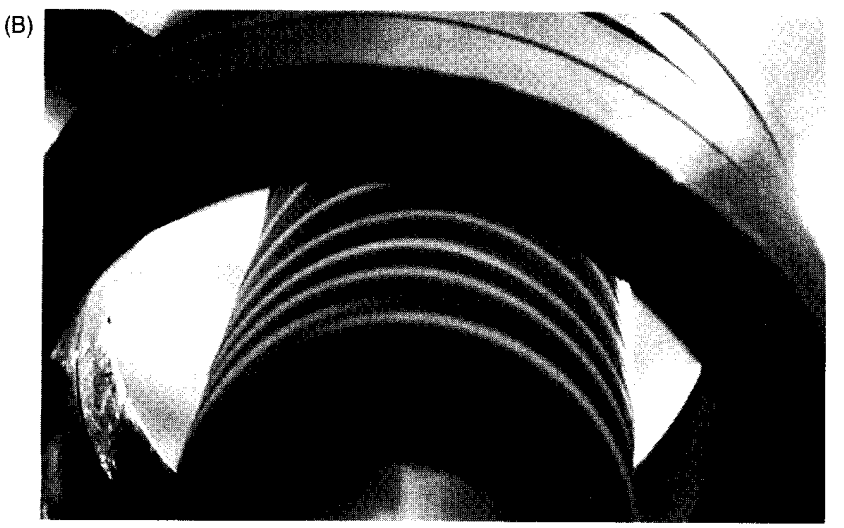

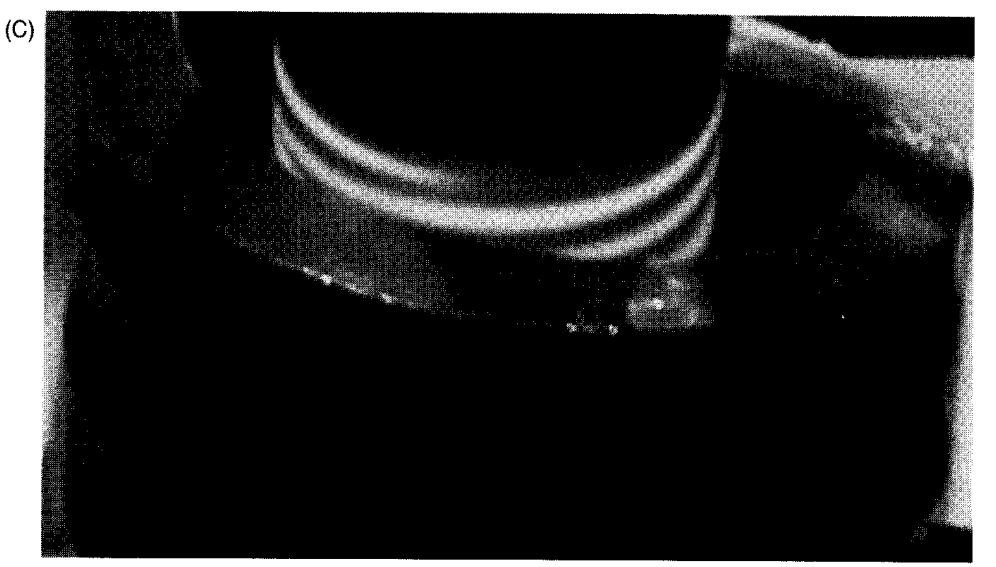

Figure 5.52 Striping phenomena in induction heating of carbon steel cylinder.

experiments on the induction heating of magnetic metals. In some applications striping suddenly occurs and then disappears. There is no single explanation of this phenomenon. The only attempt to explain it was made by M. Lozinskii [2] in the early 1940s; it was a very simple description based on the knowledge available to induction heat treaters at that time. It should be mentioned that Lozinskii's hypothesis concerning striping has a certain logic and can be accepted as an introduction to this effect. However, from our point of view, that explanation oversimplifies the mechanism of the type B striping phenomenon. Since that time, there have been no further attempts to explain this effect. Therefore, we briefly introduce Lozinskii's hypothesis along with our own point of view, which is based on modern experience and new theoretical knowledge accumulated at INDUCTOHEAT during the development of various induction heat treatment processes.

Assume that a magnetic cylinder is located inside a single-turn inductor (Figure 5.52). As a result of the electromagnetic field produced by the induction coil, eddy currents will flow within the workpiece. Due to the skin effect, these eddy currents will appear primarily in the surface layer of the workpiece located inside the coil and cause the surface temperature of the workpiece to increase.

Realistically speaking, any workpiece has certain nonuniformities, microscopic defects, impurities, and nonhomogeneities. These include structural/mechanical nonuniformities, metallurgical nonhomogeneities, and so on. As a result, different surface regions of the workpiece will be heated slightly differently. Some will reach the Curie temperature first and lose their magnetic properties. The relative magnetic permeability of these areas will dramatically drop to unity ($\mu_r = 1$). This leads to a significant increase in the penetration depth in those areas. The resistance of these nonmagnetic regions will drastically decrease compared to neighboring surface areas that retain their magnetic properties. As a result, the density of the induced currents in the low-resistance regions will increase. This leads to an increase in power density and heat sources in these areas. At the same time, there will be a redistribution of eddy currents in the workpiece surface. Eddy currents induced in areas that retain their magnetic properties (dark rings) will have a tendency to rush to complete their loops through the lower-resistance paths (bright rings). This current redistribution leads to a further heat source reduction in the magnetic areas with low temperature (dark rings) and appears as additional heat sources in the nonmagnetic areas with high temperature (bright rings). Therefore, a chain reaction somewhat similar to positive feedback will occur. As a result, one can view in the workpiece a mixture of ring-shaped stripes. Hot bright stripes will alternate with the relatively cold dark stripes. Experience shows that usually the thickness of the bright and dark stripes depends primarily on the frequency and power density and equals 1 to 3 current penetration depths in hot steel.

In addition to the current redistribution, the type B striping phenomenon is a result of several other electromagnetic and heat transfer effects, including the electromagnetic edge effect of joined materials with different properties (EEJ effect; see Section 3.1.7). The EEJ effect occurs when two different metals are located in a common magnetic field [203, 256].

Experience shows that striping can appear in several different ways. However, in the great majority of cases, very narrow bright stripes (rings) will appear at the beginning of the heating cycle (Figure 5.52). With time, the narrow stripes will widen. At this stage, the maximum temperature will move from the center of each

ring toward the edges of each bright hot ring. During the heating process, the stripes sometimes move back and forth along the workpiece surface area under the coil. When the length of the heating cycle is increased, typically the striping effect will not be pronounced and temperatures will equalize in the workpiece surface.

The appearance of the stripes depends on a complex function of the frequency, magnetic field intensity, and thermal, electrical, and magnetic properties of the steel. However, as mentioned above, it has been observed only when high-power density is applied. If the power density is relatively low, then the temperature will equalize between the neighboring bright (high-temperature) and dark (low-temperature) rings because of the thermal conductivity of the steel.

The barber pole effect can occur with both a single and multiturn coil with a rotated part. Similar to the type B striping phenomenon, the barber pole effect also has never been obtained by mathematical modeling. It has only been viewed in practical cases of induction heating.

There are different types of the barber pole effect. With the first type, during heating instead of a straight heat pattern, a shifted or squeezed temperature profile suddenly appears (Figure 5.53). When the next part is heated, the barber pole effect could disappear and may never be seen again.

There is another phenomenon also called the barber pole effect. However, its appearance is quite different from the previous one. In the second type, a combination of hardened and soft (partially hardened) circles could appear. Experience shows that this effect has something to do with one of three factors or a combination of all of them: part rotation, scan speed, and quenching features.

If a barber pole effect appears steady, it is possible to eliminate it by reducing the scan speed, and/or changing the part rotation. The part rotation should be smooth without significant wobbling.

Steam pockets can also result in the appearance of the barber pole effect. This requires the spray quenching block to be redesigned taking into consideration the geometrical features of the part.

The snakeskin (soft-spotting) phenomenon takes place with small coil-to-workpiece gaps, a substantial pressure of the quenchant, and sparsely located spray nozzles. There is a combination of "soft" and "hard" spots that can be seen by the naked eye on the workpiece surface (Figure 5.54). Proper design of the quenching block and enlarged coil-to-workpiece gaps will eliminate this phenomenon.

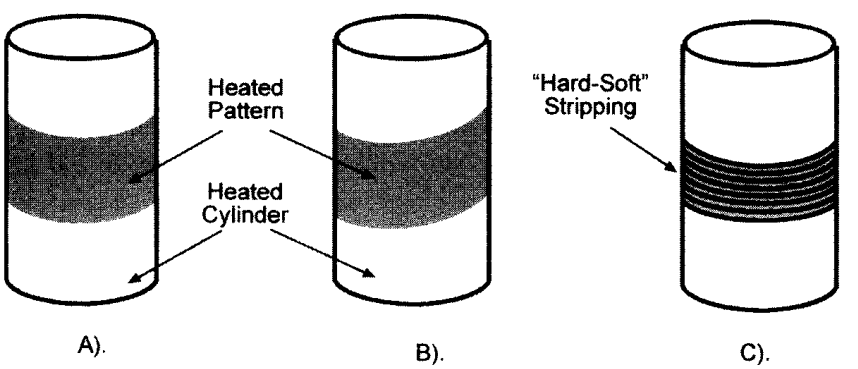

Figure 5.53 Barber pole effects.

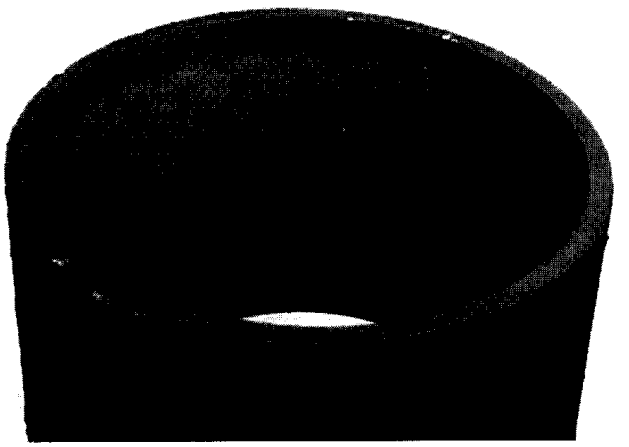

Figure 5.54 Snakeskin pattern.

5.1.6 Quenching and Spray Quench Design for Inductors

Up to now, we have discussed the heating process during induction heat treatment. In heat treat applications such as hardening, the two main stages are that the temperature be raised above austenizing temperature and that the part is immediately quenched. In providing a required microstructure of the heat treated part, a proper quenching is just as important as proper heating. The quench arrangement must be designed for rapid heat removal to develop the desired hardness and metal structure. Nonintensive quenching results in soft perlite- and bainite-type metal structures. Uneven quenching makes the distortion and cracking problems more pronounced.

As an example, Figure 5.55 shows the dynamics of the induction heating of a carbon steel cylinder and its cooling during quenching. With induction heat treatment of carbon steel, the quenching must typically begin immediately after the required austenizing temperature is reached. As shown in Figure 5.55, after 5.0 sec of heating the surface layer reaches its required final temperature. The core temperature does not rise significantly because of several factors such as a pronounced skin effect, the quite intensive heating process, and short heating time. Because of these factors the heat soak from the surface of the workpiece toward its core is not sufficient.

After the heating stage is complete, the quenching process begins. In the first stage of quenching the high temperature of the workpiece surface layer begins to lessen. Figure 5.55 shows that after 2 sec of quenching the surface temperature will be reduced by as much as 660°C. This results in a workpiece surface temperature of 320°C. At this point, the maximum temperature will be located at a distance of 3 mm inward from the surface. It is necessary to note that at this stage two heat transfer phenomena will take place: the cooling of surface layers as discussed above; and the heating (soaking) effect of the core. After 6 sec of quenching the surface temperature will decrease almost to the temperature of the quenchant. At the same time, the core is still quite warm. Core temperature is about 400°C (752°F).

In some cases, heat treaters do not cool the part completely. After the part is unloaded from the induction coil, it is kept for some time on the shop floor at the ambient temperature. During that time, the heat of the warm core soaks toward the

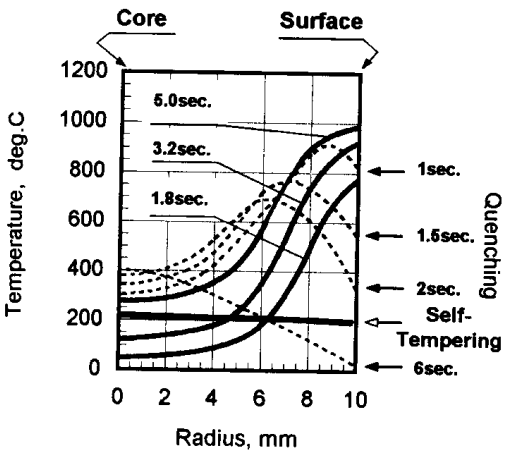

Figure 5.55 Dynamics of induction heating of a carbon steel cylinder (20 mm OD) and its cooling during quenching (F = 40 kHz): — heating; - - - quenching.

surface. In time, the temperature distribution within the part will equalize. In this case, the remaining heat is used for a slight temper back, which gives the part a nonbrittle structure.

The rate of cooling during the quenching process depends on several factors, including type of quenchant, temperatures, flow rate, geometry, and material properties of the metal.

Noticeable efforts in developing different quench media have been done by G. E. Totten, H. Tensi, H. Boyer, C. Bates, and others [18, 367–369]. Different types of quenchants have been used. These include water, polymer-types, oil, forced air, and in some cases self-quenching (mass quenching). Due to space limitation and the availability of several excellent texts devoted to quenchants quenching is not discussed in detail here.

At the same time, certain aspects related to the specifics of spray quenching that is the most popular approach will be indicated below. There are three factors that greatly affect the quench design: the required heat treat pattern, the style of the inductor and the workpiece geometry. It is important to remember that in the case of spray quenching, the classical cooling curves widely published in literature that represent three stages of quenching (the vapor blanket stage, the boiling stage and the convection heat transfer stage) cannot be applied directly. Due to the nature of the spray quenching, the first two stages are greatly suppressed. At the same time, cooling during the convection stage is more severe with spray quenching than represented by classical cooling curves. Detailed study of the specifics of spray quenching has been conducted in [217].

Spray quenching works best if the workpiece is rotated during the quenching operation. This will ensure uniformity in quenching. When rotating irregularly shaped parts such as gears, the speed of the rotation is slowed down for quenching; this reduction in speed is required to evenly quench the root of the gear. In contrast, if the rotation is too fast the quench fluid might not be able to provide a proper quenching in certain areas of the tooth (i.e. root region) resulting in an unacceptable hardness pattern. The ability to provide identical impingement is another considera-

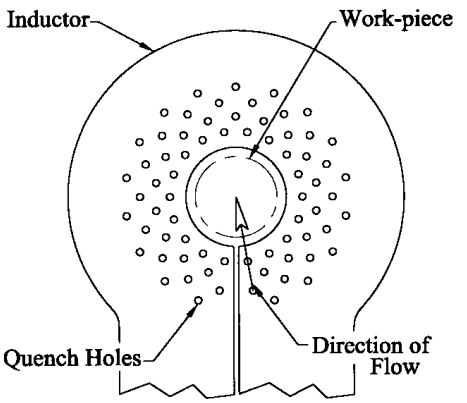

Figure 5.56 Typical staggered quench hole pattern for single-turn scan inductor.

tion when quenching complex shaped parts. Small orifices are required to agitate quench, to prevent steam pockets from developing on the surface being quenched. The intensity of quenching depends upon the flow rate, the angle at which the quenchant strikes the workpiece surface, temperature, purity, and type of quenchant.

The quenching pattern is generally conformed to the part, just as the inductor is. When using a single-shot inductor it is preferable to quench from two sides of the workpiece. The quench holes are typical placed facing the part at 3/16 to 1/4 in. intervals and have a staggered pattern. Figure 5.56 shows a typical scanning quench hole arrangement. The orifice size is related to the shaft or workpiece diameter, as well as the quenching area, and the air gap between the quench block and the workpiece surface (see Table 5.6). To maintain quench pressure at the point of impingement the quench device should be as close as practical to the workpiece surface.

As described earlier, in many cases the quench is built into the coil (Figure 5.20). In other cases a barrel or quench block is separate from the coil (Figure 5.21). In all cases it is important to move into the quenching position as quickly as possible, before the part's surface temperature cools below the critical hardening temperature unless intermedient soaking is required.

It is imperative to remember that since the quenchant (i.e., water or water-based polymers) hit the surface of the workpiece that has a temperature well above the boiling point of water, certain amount of water will be evaporated and should be compensated for.

Table 5.6 As the Workpiece Diameter Increases the Orifice Size Should Also Increase to Help Provide a More Uniform Quench

Shaft Diameter (in.)	Shaft Diameter (mm)	Orifice Size (in.)	Orifice Size (mm)
0.25–0.50	6.5–13	0.046–0.063	1–1.5
0.50–1.50	13–38	0.063–0.094	1.5–2.5
> 1.50	> 38	0.125–0.156	3.5–4

5.1.7 Cooling of Induction Coils and Tubing Selection

Because of the high currents and power applied to the coil in a majority of induction heating applications, inductors are water-cooled. The water-cooling flows through the inductor during operation.

Certain heat treating patterns can demand fabrication of small or intricate coils. Copper tubing used for coil fabrication is naturally profiled for water-cooling. For induction surface hardening and selective hardening applications coils are typically made from copper tubing or are made from a solid copper block with a machined water passage. In either case all efforts must be made to remove all restrictions in the water passages to allow a smooth water flow to avoid turbulence which can lead to steam pockets. When copper tubing or water passage becomes too small or restricted, overheating will occur. The overheating will eventually cause the copper to fail (or melt); this would mean that the temperature of the copper would be in excess of 980°C (1800°F). The volume of water-cooling is directly related to the amount of power and the frequency applied to the coil. A formula that expresses adequate water flow in the coil is:

$$\text{gpm} = \frac{PK_1K_2}{K_3\Delta T},$$

where gpm = gallons per minute, P is total coil power kW, K_1 is the tubing coefficient (for the great majority of high-frequency induction heat treating applications $K_1 = 0.5$, $K_2 = 3415$ is a conversion constant that is derived from Btu/kWh, and K_3 is a conversion constant that represents the heat capacity of water, normally 40°F or less, to allow for proper cooling of the copper. ΔT can be measured by the use of an inline thermometer as close to the inductor as possible.

In some cases the water passage size will not allow the above-calculated gpm to be achieved, and coil life can suffer. The use of a high-pressure booster pump can increase water flow; however, keep in mind that it is flow not pressure that is the critical factor.

In most heat treating applications the workpiece surface is being heated to an excess of 850°C (1562°F). The intensive radiant heat from the part can be detrimental to the coil, as well as the copper heating from the Joule losses. In induction heat treating the coil is in close proximity to the workpiece for maximum efficiency (refractory coil liners are not typically used). The air gap between the workpiece and the coil could be as small as .03 in. (0.75 mm). With the hot workpiece located so close to the coil, the design of the cooling passage is very critical. It is obvious that the coil cooling should be as close as possible to the heating face, particularly if magnetic flux concentrators are applied.

The heating face wall thickness should increase as the frequency decreases. This fact is directly related to the current penetration in the copper and holds true for both solid machined and tubing coils. There are some cases where water-cooling of the inductor can be eliminated. For example, low-power density coils made from litz-wire, and used for low-temperature preheating of magnetic parts are very efficient; air cooling is often sufficient to cool this type of coil. In other cases a large mass of copper (in the coil) can provide sufficient cooling, when short heat times (less than 1.5 sec) and high frequency (above 150 kHz) are applied. In the former case it is not necessary to use water-cooling, because the penetration depth in the copper is shal-

low combined with the fact that the heat time is short, therefore under these conditions the copper simply does not have time to significantly heat up; the heat that is generated is dissipated by the large mass of copper. For quick estimation of penetration depth in the copper, δ_1 can be calculated with the formula:

$$\delta_1 \text{for inches} = \frac{2.75}{\sqrt{F}}, \text{ or } \delta_1 \text{ for mm } = \frac{70}{\sqrt{F}}$$

where **F** is frequency, Hz.

The most effective thickness of the conductive part of the tubing wall (d_1) can be calculated as $d_1 > 1.6\delta_1$. A tubing wall of the induction coil smaller than $1.6\delta_1$ results in coil efficiency reduction. In some cases the tubing wall can be much thicker compared to the above-mentioned ratio. This is because it may not be mechanically practical to use a tubing wall thickness of 0.25 mm (0.01 in.). Some guidelines for wall thickness are shown in Table 5.7. As shown with the formula above, the penetration depth is the actual depth at which the current flows in the copper surface. The rest of the coil serves other mechanical purposes such as cooling, quench pocket design, and support against mechanical flexing caused by electromagnetic forces.

5.1.8 Inductor Mounting Styles

In order to accommodate a variety of heated parts while providing high efficiency and required harden patterns, inductors are frequently changed and considered perishable tooling. The dilemma is that an operator should be able to quickly change inductors and provide a reliable, low-resistive contact between the coil and power supply. The electrical connection between the inductor and the transformer or bus is sometimes referred to as the mounting foot.

There are several standard types of mounting feet that have been developed over the years. A precision-machined keyed foot ensures a good electrical contact. It is usually fastened with four 3/8-16 or $\frac{1}{2}$-13 stainless steel bolts (see Figure 5.57). When fast or frequent changeover is needed due to a wide family of parts requiring different inductor designs, a quick-change type mounting foot is often recommended. This can be in the form of a toggle clamp, dove tail, or pneumatic. A quick-change type can also be keyed for repeatable coil-to-part setup as shown in Figure 5.58. One of the main advantages of this type of mounting foot is that no special tools are required. When inductors are constructed of tubing, compression type fittings can be used. Because the fittings are carrying the current, special conductive sealant is used to ensure the connection does not leak coil coolant (see Figure 5.59).

Table 5.7 Copper Tubing Standard Wall Thickness

Copper Wall Thickness (mm)	Copper Wall Thickness (in.)	Frequency (kHz)
0.75–1	0.032–0.048	450–50
1–2	0.048–0.090	25–8.3
1.5–4	0.062–0.156	10–3
4–6.5	0.156–0.250	3–1

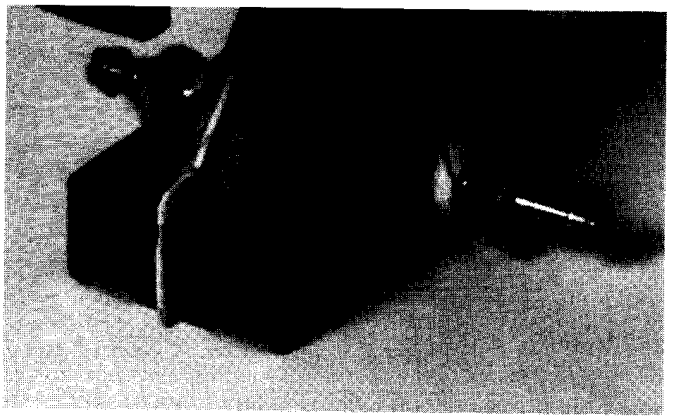

Figure 5.57 Standard keyed bolt on style mounting foot.

In all cases, to ensure a good electrical contact (avoid arcing), the contact areas must be clean and free from nicks, burrs, and scratches. Care must be used to avoid damaging the inductors when changing, handling, and storing them.

5.1.9 Accessory Equipment and Work Handling

Because of the ability to heat parts quickly, induction heating readily lends itself to many standard machine types. It requires integrating the coil design, quenching, and part holding fixtures to the chosen work handling. In automatic systems the work handling transfers the part through the heating and quenching processes as

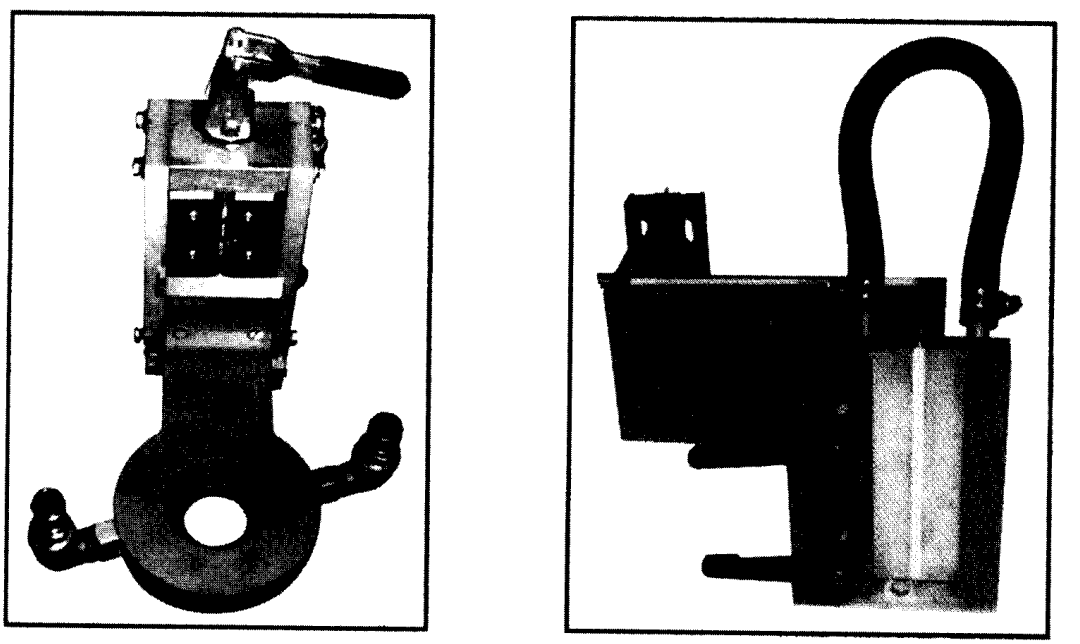

Figure 5.58 Quickchange mounting styles: toggle clamp type (right); dovetail-type quick clamp (left). (Courtesy of INDUCTOHEAT, Inc.)

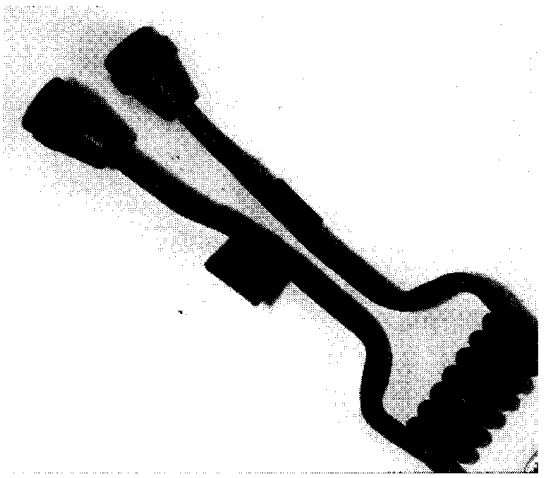

Figure 5.59 Compression fitting type coil connection type.

well as preheat and postheat operations such as loading and unloading (accessory equipment).

Often, to add automation, robots and gantries are used. Hoppers and magazine feeding are some other common ways to present parts for induction heat treat. Conveyors can be used for feeding or unloading and also in some cases used in the heating and quenching operations. Rotary tables can be used where large or small parts are passed through a channel inductor, for example.

5.1.9.1 Robots and Gantries

The use of robots and gantries is common for modern high-production equipment. Larger irregularly shaped parts often use robots or gantries for loading and unloading of induction equipment (Figure 5.60), mainly because these heavy cumbersome parts are not located near conveyors or other part transfer equipment. The time to manually load these types of parts would not be cost efficient. Robot and gantry loading can be done with virtually any size or shape component and in some cases can be added after the induction equipment is installed.

Many systems are designed with the option of using the induction equipment with or without the robot. This allows manual production to continue in the event that the robot is out of service.

5.1.9.2 Hoppers and Magazines

Magazines and hoppers are used when the same or a similar family of parts is to be processed. When referring to magazines it typically means that a given quantity of parts is loaded into a cartridge and the parts are dropped either into the coil for heating or onto a conveyor system for transferring to the work coil.

Hoppers are typically thought of as a tub of randomly oriented parts and could even handle random part sizes as well. From the hopper, the parts have to be sorted and oriented before they are presented to the induction system. This can be done in a number of ways such as by vibration, magnetically, or by specially designed mechanical fingers. After sorting the parts are indexed into the coil for heating and quenching.

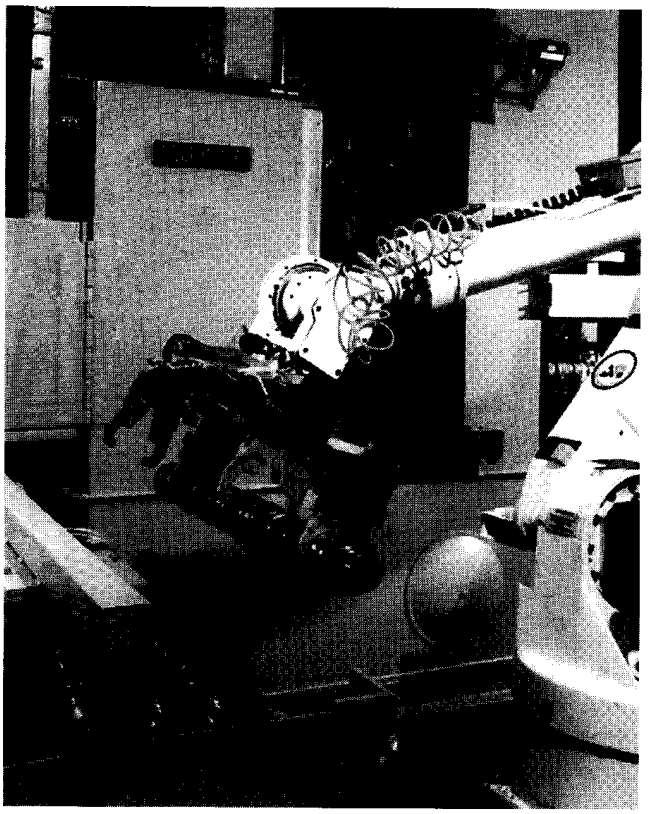

Figure 5.60 The large cam shaft uses a robot for loading and unloading into the induction system.

5.1.9.3 Conveyors

There are many types of conveyors used for a number of induction applications, often in combination with other feeding and loading equipment. Conveyors can be belt-, chain- or cam-driven; they operate in a continuous mode or can be indexed via servomotor or mechanical cam switches. The considerations for choosing a conveyor are usually determined by the application for which it is being used. It must stand up to harsh conditions of hot parts and continuous quenchant being sprayed on it. Stainless steel mesh or chain is commonly used for prevention of belt corrosion. If plain carbon steel belts or conveyors are used too close to the inductor there is the possibility of inductively heating the belt as well as the workpiece.

Figure 5.61 shows different conveyors for different applications. The left picture shows a conveyor that must handle extreme temperatures and its function is to carry the part away after heating. The picture on the right must handle lower temperatures, however, it is in close proximity to the inductors and its function is to index the parts through the inductor for heating.

5.1.9.4 Rotary Tables

Rotary tables usually have nests for a given number of parts and after loading the table, it is rotated like a carousel. This type of equipment is very popular with cellular-type systems mainly because the unheated parts are loaded and heat treated

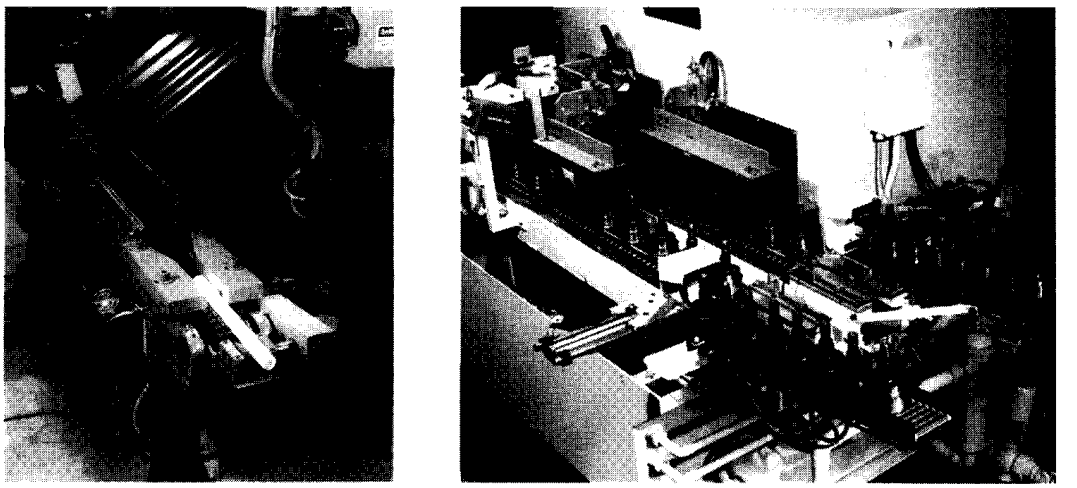

Figure 5.61 Exit conveyor designed to remove hot bars from induction system (left); indexing conveyor to transfer parts through tempering inductors (right). This system processes two different part sizes simultaneously. (Courtesy of INDUCTOHEAT, Inc.)

parts are unloaded in almost the same area of the equipment. Rotary tables are also used where high volume or high production is required, because a large number of parts can be passed through a coil very quickly. Figure 5.62 shows a schematic of a rotary table system for producing a high volume of annealed ball studs. As mentioned above, many times several different kinds of work-handling equipment are used in the same processes and combined to make a completely automated system. In the example the complete system to anneal ball studs utilizes many work-handling systems in addition to a rotary table. See Figure 5.63 for the complete system.

5.2 INDUCTION HEAT TREATMENT OF CRANK SHAFTS, CAM SHAFTS, AND AXLE SHAFTS

5.2.1 Crank Shaft Heat Treatment

Heat treatment plays an important role in the manufacturing of quality crank shafts, and induction heat treatment is a traditionally popular choice for their hardening and tempering. Crank shafts are widely used in internal combustion engines, pumps, compressors, and the like and belong to the group of the most critical auto components, typically weighing between 30 and 85 lbs depending upon the engine. In addition, the weight of some crank shafts can exceed 2000 lbs (e.g., crank shafts for the ship industry or stationary engines of power generators).

A crank shaft, typically cast or forged, comprises a series of crankpins (pins) and main journals (mains) interconnected by webs/counterweights (Figure 5.64). Steel forgings, nodular iron castings, microalloy forgings, and austempered ductile iron castings are among the materials most frequently used for crank shafts [370–371]. High strength and elasticity, good wear resistance, light weight, small torsion vibration, geometrical accuracy, short length, and low cost are some of the most important crank shaft requirements.

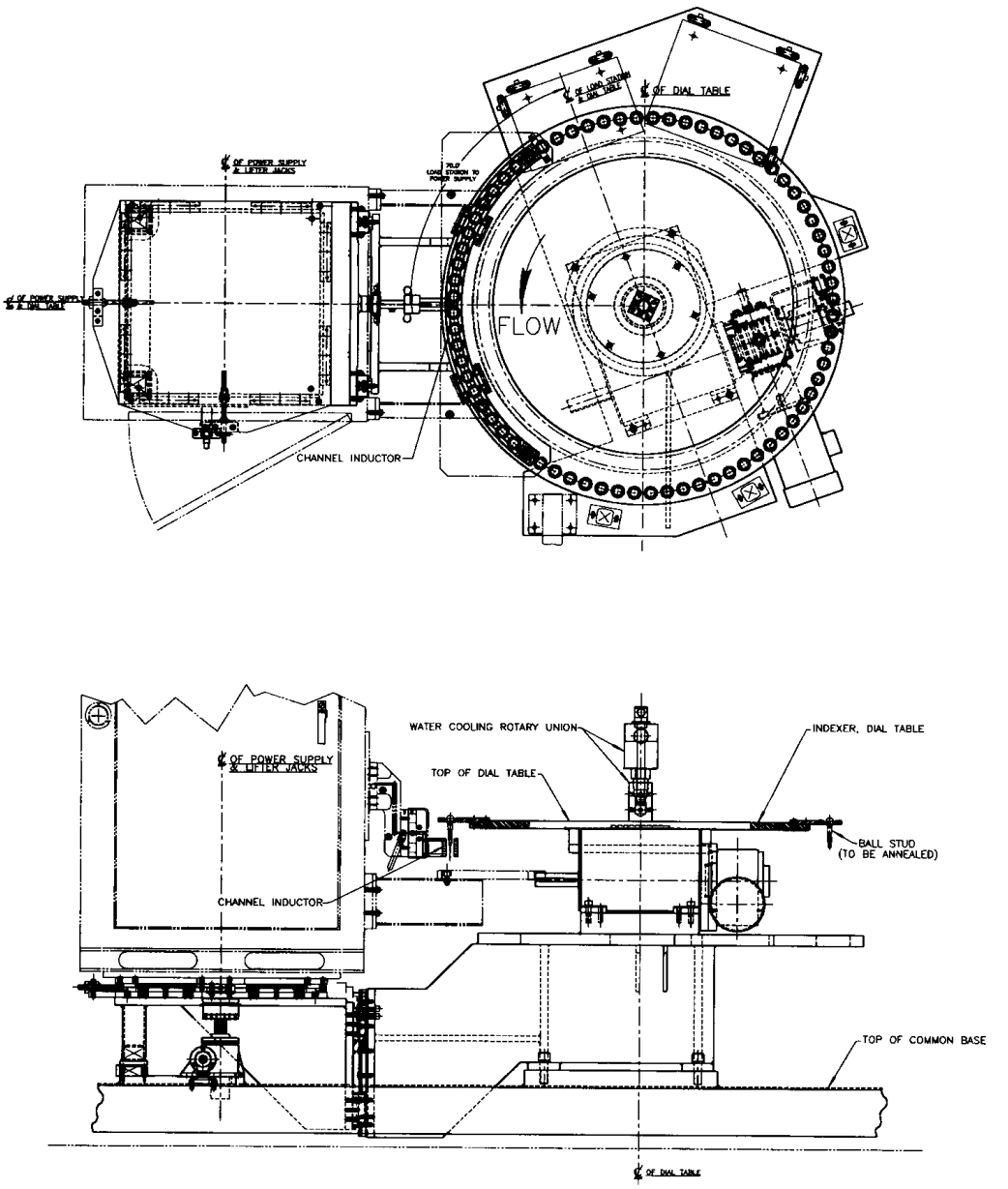

Figure 5.62 Rotary table for annealing ball studs. (Courtesy of INDUCTOHEAT, Inc.)

5.2.1.1 Conventional Technology with the Required Crank Shaft Rotation

Crank shafts belong to the group of parts that have a cylindrically shaped area to be hardened. In addition, the existence of large adjacent counterweights (webs) excludes the possibility of using conventional encircling-type coils. Inasmuch as the diameters of the crank's journals (mains and pins) are much smaller compared to the external dimensions of the counterweights, the conventional encircling-type coils could not freely pass from one heat treated feature to another.

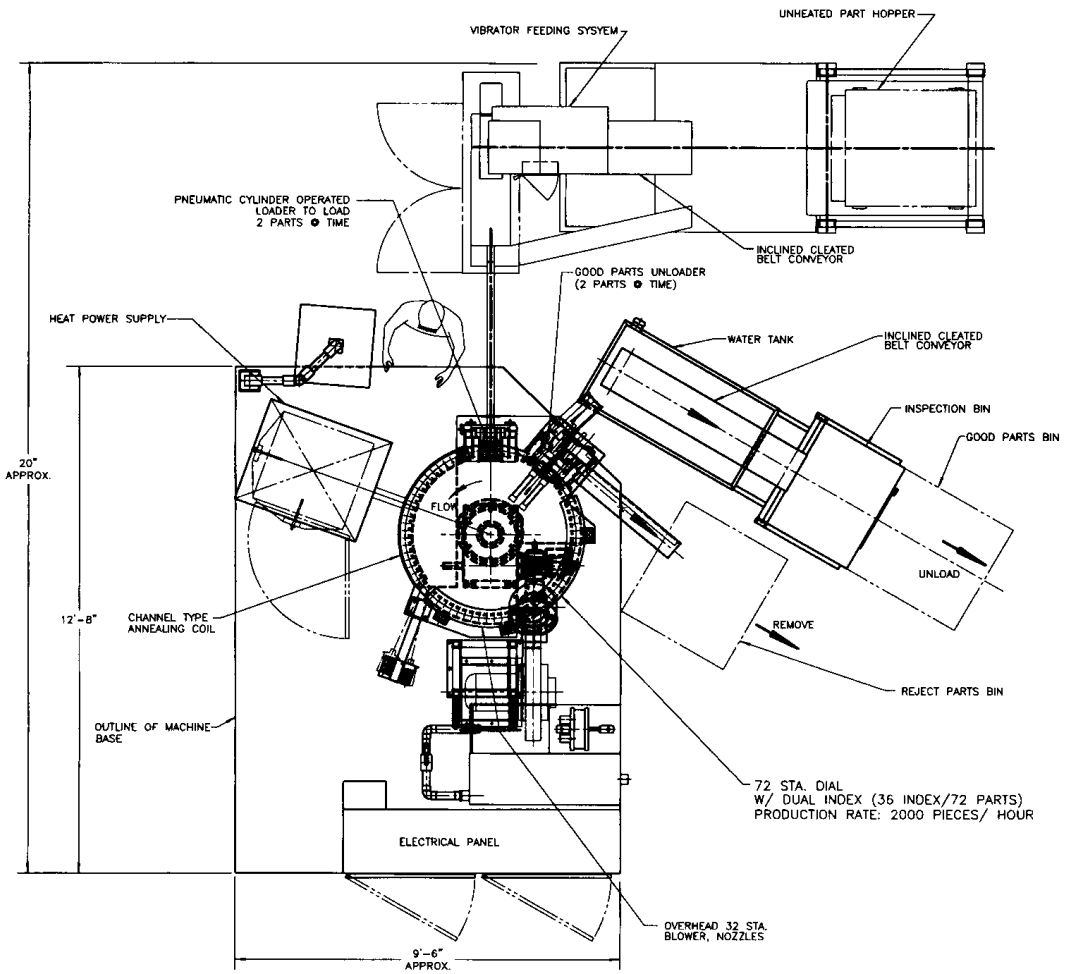

Figure 5.63 Rotary table from Figure 5.62 combined with accessory equipment for loading, sorting, and unloading. (Courtesy of INDUCTOHEAT, Inc.)

Specially designed clamshell or split inductors (see Section 5.1.4.4) were developed and extensively used for induction hardening of crank shafts in the early 1940s and middle 1950s. Short coil life, poor reliability, and low production rate of the clamshell coils were some of the main drawbacks of those inductors. The short coil life resulted from the inherent necessity of breaking the current paths by having high current (middle and high frequency) contacts.

From the 1960s to the year 2000, the majority of existing induction crank shaft hardening machines utilized U-shaped inductors, which required a crank shaft rotation during heating. According to that process each crankpin and main journal was heated by bringing a U-shaped inductor close to the pin or main bearing surface while the crank was rotated about its main axis. Since the pin axis was offset radially from the main axis, the pin orbited the main axis (Figure 5.65).

The crank shaft's rotational speed typically varies between 24 and 32 rpm [372]. Consequently, the U-shaped inductor, as well as some other quite massive components of the induction hardening machine (including the output transformer of the power supply, water-cooled coil, buswork, cables, etc.) which often weigh over 2000 lbs [372], traveled with the orbital motion of the connecting-rod journals.

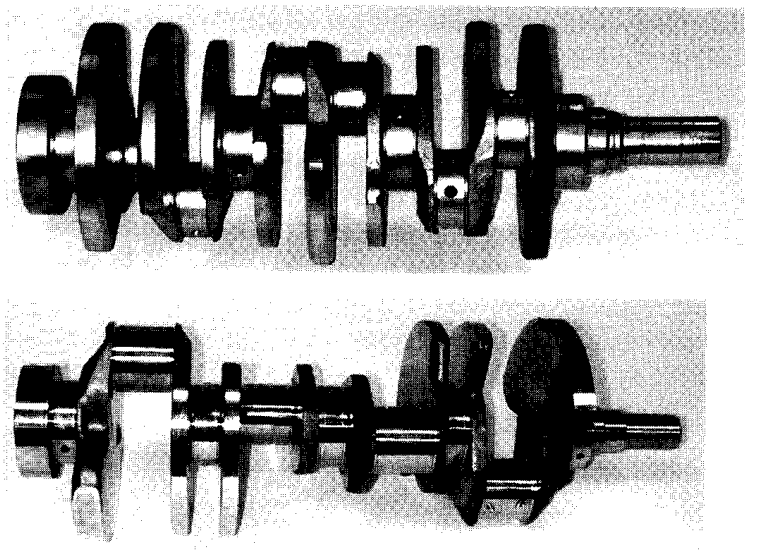

Figure 5.64 V-6 and V-8 crank shafts.

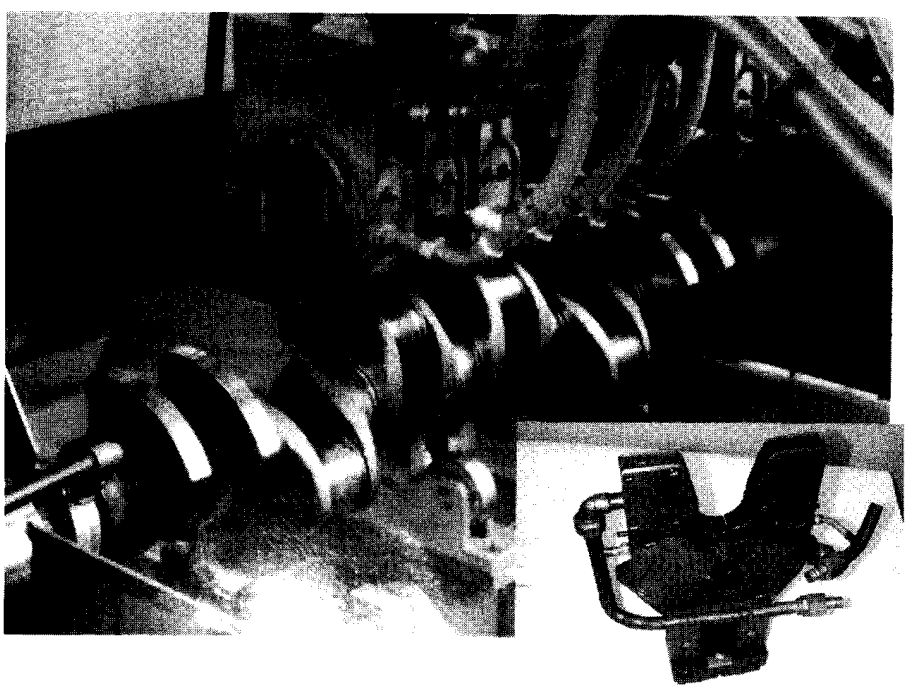

Figure 5.65 Conventional rotational-type crank shaft hardening machine with U-shaped coil.

The circular orbital motion of such a heavy system needed to be maintained quite precisely with a special control tracking system providing power variation for each heated crank's feature during its rotation. All these resulted in a quite complex, sensitive, bulky, noisy, and costly design for conventional induction hardening machines (Figure 5.66).

Equipment maintainability, reliability, hardened pattern repeatability, and substantial machine downtime are other concerns expressed by users of that technology. Although the U-shaped coils typically lasted longer compared to the clamshell coils, their short lifetimes were still considered a problem. Typically, U-shaped coils used in a conventional process did not last longer than four weeks and sometimes their coil life was as short as two weeks. There are several factors that led to short coil life while using U-shaped coils.

- It was necessary to have a quite small air gap between the coil and surface of the heat treated feature (in some cases less than 0.5 mm). The combination of such small air gaps, relatively prolonged heat time (7 to 20 sec), crank shaft surface temperature (often exceeding 920°C), and a moist working environment provided a favorable condition for stress-corrosion development in the copper coil.

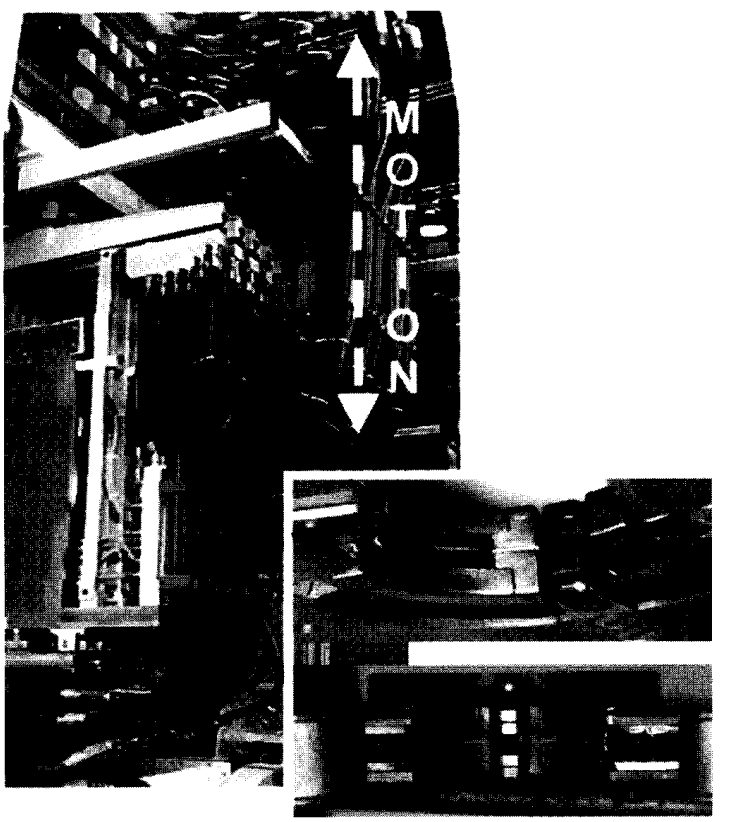

Figure 5.66 Flexible cables of induction crank shaft hardening systems required crank shaft rotation and close look at complexity of U-shaped inductors.

- Complex-brazed coil geometry with numerous joints in combination with significant heat exposure and the existence of electromagnetic forces created a favorable condition for stress-fatigue coil failure mode and crack development, particularly in the heat exposed brazed joint areas of the inductor.
- Due to the small air gap, the coil often had accidental physical contact with a rotating crank surface (coil "ridding" on the crank shaft journals). This resulted in physical damage of the coil (coil abuse), often causing premature coil failure, which took place due to uncontrollable wear of the carbide guides (locators) or, in other approaches, to an error of the noncontact coil position tracking system.

Most U-shaped inductors required the use of carbide guides. These locators have several disadvantages.

- They require specific time-consuming setup training and experience in the proper adjustment of the locators and still allow for human error.
- Carbide guides ride on the pin/main surface at high temperature and introduce foreign inclusions into journal surfaces that in some cases may create a stress riser. This particular factor, however, can be dismissed if severe final grinding is used.
- It is necessary to monitor wear of carbides and their location. Otherwise the hardened pattern can be shifted or the induction coil can rub the crank shaft surface, which shortens the coil life.
- Each locator is simply one more part that can go wrong.

High maintenance cost and the inductors' short life led to the users of crank shafts with rotational technology spending an average $2 per crank shaft as a maintenance fee (based on V-6 crank shaft manufacturer's practice).

When applying a U-shaped coil there is an asymmetric heating pattern and, at any given time, heat is applied to only one-half of the crank shaft feature. The second half of the pin/main undergoes a soaking–cooling mode. The asymmetrical heating nature of U-shaped inductors can result in nonuniform hardness profiles and possibly an egg-shaped distortion of the heated feature.

In order to improve the above-mentioned drawbacks and some other customer concerns regarding the conventional crank shaft hardening process requiring crank shaft rotation, a nonrotational technology has been introduced [260, 262, 264, 266, 267, 271].

5.2.1.2 Stationary Hardening Process for Crank Shafts (SHarP-C Technology)

The stationary hardening process for crank shafts (SHarP-C technology) has been considered by many heat treat experts as a revolutionary induction heat treating system. This technology eliminates the need to rotate or move either the inductor or the crank shaft during heating and quenching cycles while at the same time eliminating high current contacts when using encircling clamp-type coils (no flexible cables to wear out as well).

According to a stationary hardening process, an inductor consists of two coils (Figure 5.67): a top (passive) coil and a bottom (active) coil. The bottom coil, being active, is connected to a medium- or high-frequency power supply, and the top coil

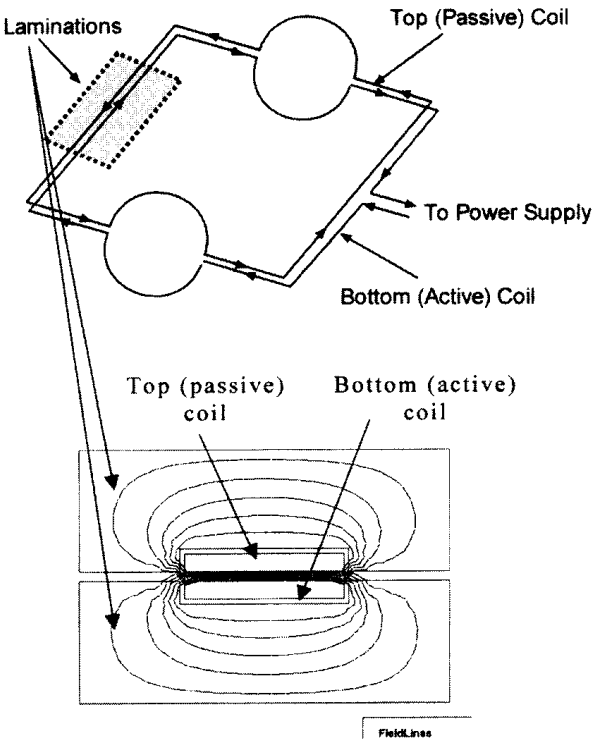

Figure 5.67 Circuit of nonrotational crank shaft hardening process and magnetic coupling of top and bottom coils.

(passive) represents a short circuit (a loop). The bottom coil is a stationary coil, whereas the top coil can be opened and closed. Each coil has two semicircular areas where the crank shaft's features will be located.

Thanks to a lamination pack that serves as a magnetic flux concentrator, both coils can be tightly coupled electromagnetically. After loading a crank shaft into the heating position the top coil moves into a "closed" position and the power is applied from the power supply to the bottom (active) coil. The current starts to flow in the top coil. Being electromagnetically coupled to the top coil, a current flowing in the bottom coil will induce eddy currents that start to flow in the top coil. Those induced currents will be oriented in the opposite direction from that of the source current. If the design parameters have been chosen correctly, the difference between the source current flowing in the bottom coil and the current induced in the passive coil will be negligible (less then 3%).

The SHarP-C coil design has several modifications. The case described above was a "passive-active" style. Another popular approach is called an "active-active" approach. According to an INDUCTOHEAT's patented "active-active" approach both the top and bottom coils are connected to one of two output transformers of an inverter. Both output transformers are phase locked providing currents flowing in the respective coils that is oriented in opposite directions. This approach does not require lamination packs at all for providing tight electromagnetic coupling and allows one to control the current in the top and bottom coil separately.

Any heated feature of the crank shaft (main, pin, oil seal) "sees" the SHarP-C inductor as a classical encircling cylindrical coil with induced eddy current flow along the circumference of the heat treated feature (there is a common eddy current loop). Therefore, the heating is efficient and symmetric, and the hardness profile is consistent, including the so-called fishtail area (or split region of the coil). In traditional induction systems there is a distortion of the electromagnetic field in the fishtail area due to current cancellation phenomena. As a result of several electromagnetic solutions these undesirable phenomena have been eliminated.

Figure 5.68 shows a CrankPro machine, which realizes a SHarP-C Technology. The advantages of the nonrotational hardening systems were recognized immediately by the customer's materials, manufacturing, and quality engineers. Some of the superior advantages include the following [260, 262, 264, 266, 267, 271].

1. The stationary method of heating without crank shaft rotation provides several practical benefits such as simple operation, superior reliability, maintainability, compactness, and cost reduction. Depending upon customer preference, crank shafts can be handled and heat treated vertically or horizontally.
2. Reduction of total indicated runout (TIR) distortion is traditionally one of the most important factors in the heat treating of crank shafts. Shape/size distortion directly affects the amount of metal required to grind. There are several factors that affect crank shaft distortion including metal properties, hardness profile, residual stresses, and so on. One of

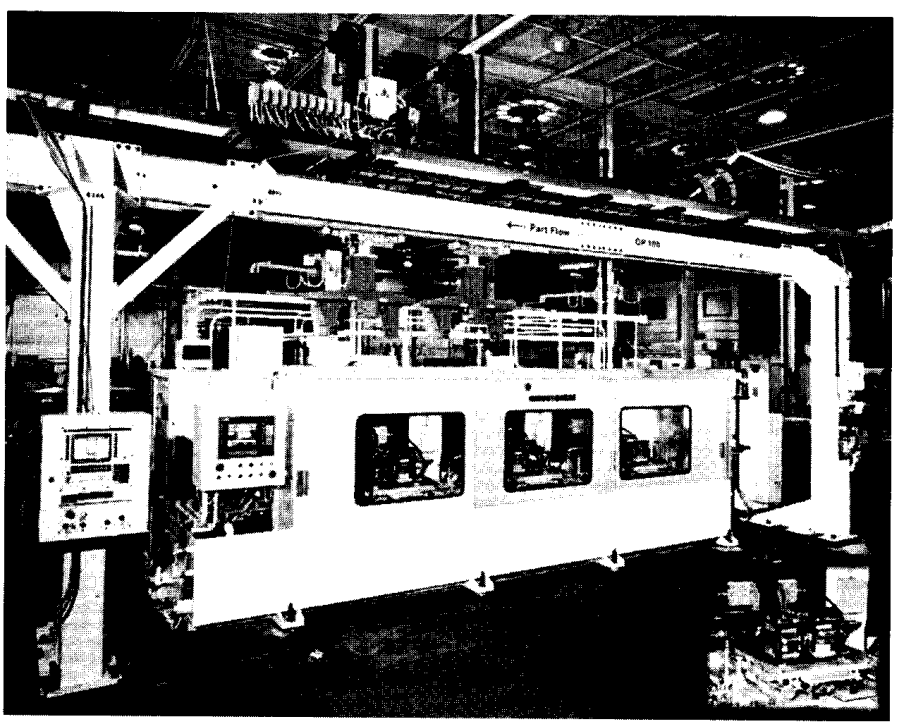

Figure 5.68 CrankPro machine utilizing advanced SHarP-C Technology which eliminates the need to rotate or move either inductor or crank shaft during heating and quenching cycles.

the most important factors that has a pronounced effect on distortion is the amount of heat generated within the crank shaft body (including mains, pins, and counterweights). The greater the amount of heated metal, the greater the metal's expansion, which in turn causes greater distortion. One of the noticeable advantages of SHarP-C technology is a short heat time, typically in the range of 1.5 to 4 sec (compared to 7 to 20 sec for the conventional process). Due to such a short heat time, only a small mass of metal will be heated. The heat-affected zone is minimized. This results in minimization of metal expansion and, obviously, in minimization of size and shape distortions (typically distortion is less than 0.025 mm).

3. Short heat time improves the metallurgical properties of the hardened zone by reducing grain growth, decarburization, and oxidation of the pin/main surface. The hardened zone is clearly defined and crisp without the fuzzy transition zone that is present when longer heat times are utilized (Figure 5.69). The case depth consists of a fine-grained martensitic microstructure with a negligible amount of retained austenite and without any traces of free ferrites. With the conventional process, significant amounts of free ferrites are often observed by customers when studying hardening case profiles (Figure 5.70). In addition, the existence of free ferrite at the pins/mains surface is detrimental to wear resistance and some other important properties of pins and main journals.
4. Short heating time can also lead to the phenomenon known as induction super hardening, where hardness is increased by 2 to 4 points HRC over the normal maximum hardness for a given grade of steel. This may allow a user to apply the lower steel grade (the lower carbon content) without sacrificing the desired surface hardness and hardness profile of the product.
5. SHarP-C technology is not very sensitive to the irregular shape of pin/main adjacent masses (webs/counterweights). The coil design combines a number of innovative electromagnetic solutions, which makes this technology practically insensitive to differences in adjacent masses. The hardness patterns shown in Figure 5.69 illustrate this feature.
6. With regard to electromagnetic effects, any heated feature of the crank shaft (main, pin, oil seal) "sees" the SHarP-C inductor as an encircling closed-form coil with induced eddy current flow along the circumference of the heat treated feature (there is a common eddy current loop). However, when using the conventional U-shaped induction coil design approach, the heat sources are limited to local eddy current loops only, which results in reduction of coil efficiency especially above the Curie temperature. The electrical efficiency of the SHarP-C coil is therefore higher than that of the U-shaped coil. In addition, the new coil is much less sensitive to variations of the air gap between the part and coil compared to conventional technology and allows a much larger air gap between the coil and journal surface.
7. Inasmuch as the heating time of the new technology is three or four times shorter compared to that of the conventional process, the thermal coil efficiency when using this new approach is higher as well (lower radiation and convection losses).

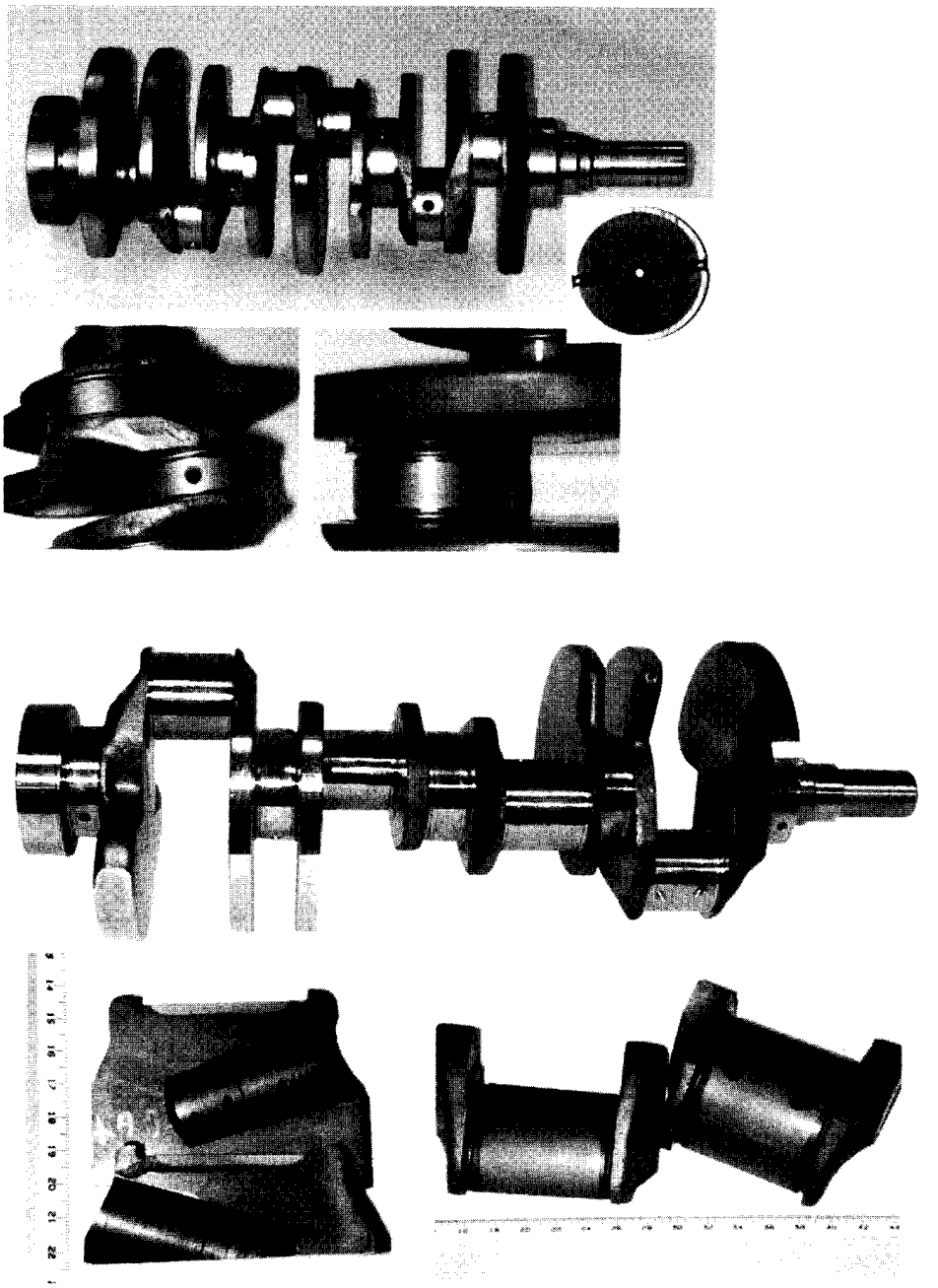

Figure 5.69 Hardness patterns on V-6 and V-8 carbon steel crank shaft journals resulting from the stationary induction hardening process (SHarP-C technology).

8. Controllability of the stationary crank shaft hardening process is superior. It is possible to modify the hardness profile along the circumference of the pins and the mains as well as across the width of the heat treated journal. This feature can also be used to prevent localized under- or overheating. For example, an area often considered as a trouble area is the oil hole region. Oil holes are often angled (skewed oil hole) relative to

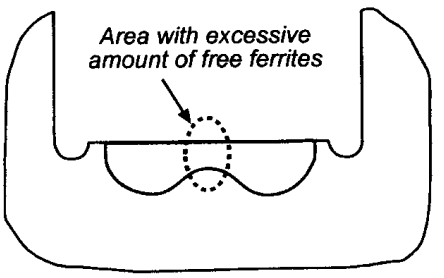

A. *Double hump pattern is typical for conventional induction hardnening machine which utilizes "U"-shaped coil and crankshaft rotation during heating*

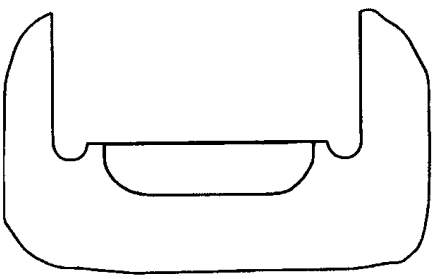

B. *A typical hardness pattern of an advanced crankshaft induction hardnening machine utilizing SHarP-C technology*

Figure 5.70 Crank shaft surface hardness patterns.

the surface, thus there is less metal mass on one side of the hole than on the other. Due to the lack of metal mass on one side, there is a danger of metal overheating in this area and, as a result, there is a possibility of crack initiation or even local melting there. The advanced coil design concept used in the SHarP-C process significantly decreases the induced power density in this area and eliminates these unpleasant surprises. In addition, when the counterweight to the left of a journal is not identical to that on the right, the heating can be controlled in order to prevent pattern drift from one side to the other. This improved ability to control heat "across the journal width" is quite limited in conventional induction hardening processes and can also be used where there is an asymmetrical bore as well.

9. Hardness of the top-to-bottom and left-to-right cross-sections can also be controlled. This includes the so-called fishtail area (or split region of the coil), where in traditional induction systems there is a distortion of the electromagnetic field due to a current cancellation phenomenon. As a result of this fishtail phenomenon a soft spot or "necking" of the hardening pattern could appear. As seen in Figure 5.69, there are no soft spots or hardness pattern necking evident in the stationary hardening process. In addition no double-hoop pattern is seen using the stationary hardening process (Figure 5.70).
10. Reduction of the residual heat of the crank shaft due to short heat time is another noticeable benefit of the SHarP-C technology. In many cases, the advantage of having less residual heat buildup alone can allow one to save a noticeable amount of money and floor space due to the elimination

of the special cooling systems. As an illustration, Figures 5.71 through 5.73 show a comparison of time–temperature profiles according to the SHarP-C process in comparison to a conventional technology. Figure 5.72 shows the temperature distribution along the journal radius prior to quenching. Results shown in Figures 5.71 through 5.73 were obtained using the induction heating software, ADVANCE. For comparison purposes, it has been assumed that surface temperature prior to quenching is the same whether using a conventional approach with a required crank shaft rotation or advanced nonrotational technology.

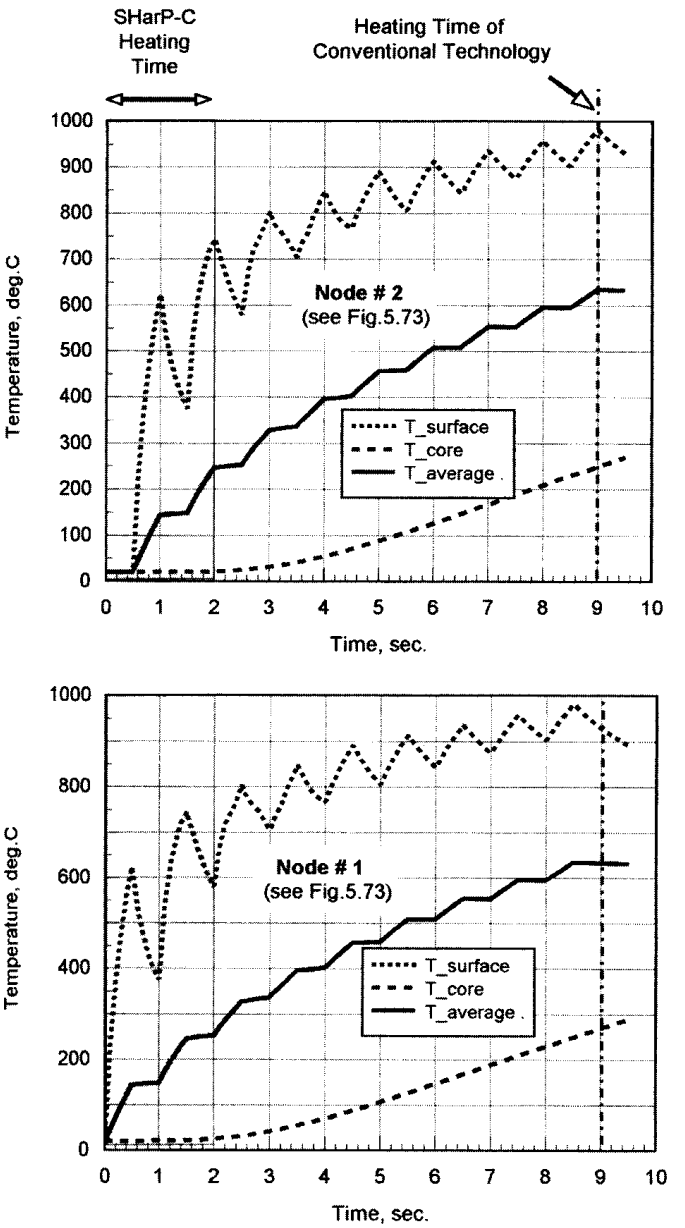

Figure 5.71 Time–temperature profiles using U-shaped inductors.

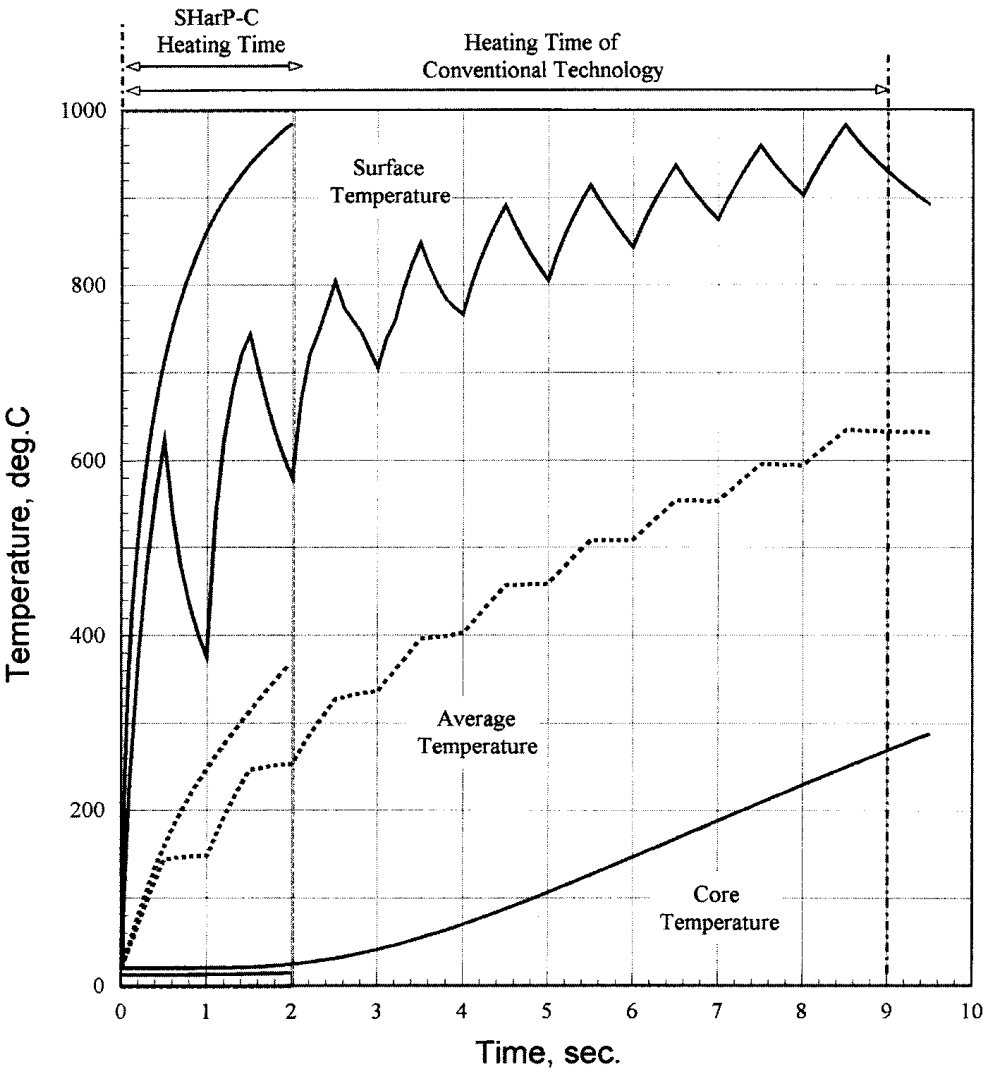

Figure 5.72 Comparison of time–temperature profiles of SHarP-C technology and conventional process using U-shaped inductor.

11. In order to increase coil electrical efficiency, the rotational crank shaft hardening technology must apply a variety of lamination packs located in close proximity to the heated surface (air gap between the heated surface and surface of the laminations is often less than 0.5 mm). The combination of radiation and convection heat exposure from the hot crank shaft surface, along with the inherently long thermal cycling (three to four times longer compared to the thermal cycle of the SHarP-C process) also shortens the life of these lamination packs and results in their premature degradation. Heating-cooling cycles, electromagnetic end effects, and substantial electromagnetic forces also decrease the lifetime of laminations. With the advanced stationary coil design, these laminations are unnecessary. These advanced coils utilize special flux concentrators that are much more durable, have less chance of magnetic saturation, and are

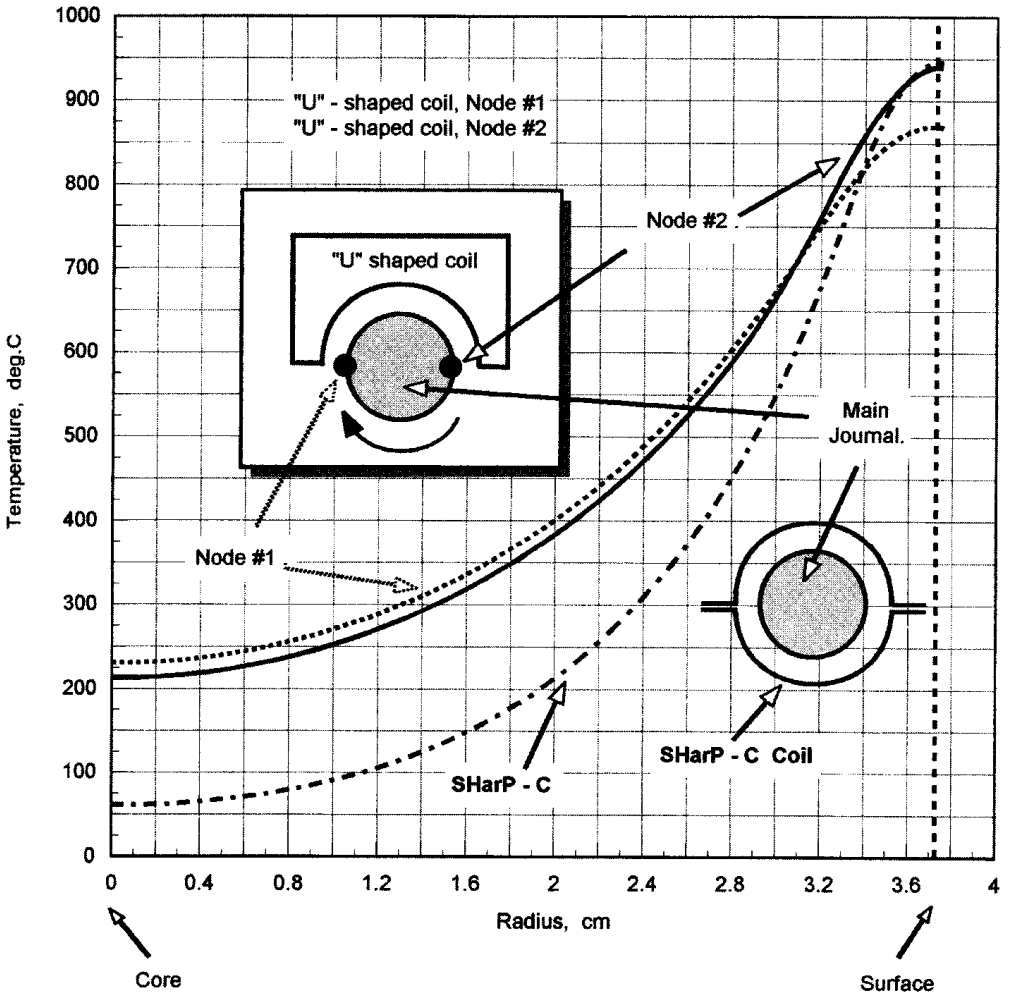

Figure 5.73 Comparison of temperature profiles along radius of main journal using conventional process and SHarP-C technology.

not exposed to as much heat or magnetic forces as the laminations used by conventional methods.

12. Although the SHarP-C process provides both hardening and tempering, some customers prefer to use long time–low temperature furnace tempering instead of short time–higher temperature induction tempering. In these cases based on customer preference, it is possible to utilize a non-rotational induction machine for hardening only and use an existing furnace/oven for tempering.
13. Coils are much more robust and rigid when CNC-machined from solid copper without any brazed parts. This precludes inductor distortion. There are far fewer components involved in the novel coil design, meaning higher reliability because of the smaller number of parts that can go wrong. The SHarP-C coil-to-journal air gap is noticeably larger compared to air gaps required by the rotational crank shaft hardening process. This creates a favorable condition to reduce stress corrosion and

stress fatigue induction coil failures. SHarP-C technology allows tooling life to be increased by at least four times.

14. Due to the electromagnetically "closed form" of the inductor, the coil power factor is very high and coil field exposure (coil external magnetic field) is negligible.
15. SHarP-C technology provides essential energy savings for the user.
    - Higher coil efficiency is one reason for improved energy savings.
    - Shorter heat time and smaller mass of metal being heated result in a noticeably reduced residual heat of the crank shaft, which is another factor for energy savings [because electrical energy is not wasted for heating in main/pin internal areas that do not require phase transformation changes (Figure 5.73)].
    - After completion of crank shaft heat treating, for safety and handling purposes, it is required to cool the crank shaft down. Therefore, the cooling process should reduce all extra energy introduced into the crank shaft. This is why the nonrotational short heat time approach will require spending much less energy for the cooling/quenching station.
    - Tempering is another area where a new approach provides energy savings. The electrical efficiency of a SHarP-C coil for induction tempering is typically in the range of 96 to 98%. The energy is localized in the areas of the crank shaft where it is needed. In contrast, the efficiency of tempering furnaces is lower due to the necessity of heating whole crank shafts and significant heat losses into the surrounding area during furnace/oven heating operation.
16. There are only three crank shafts in float with the CrankPro machine which utilizes nonrotational technology compared to 120 to 250 crank shafts in float with a conventional process. This results in low risk of rejection with this novel process.
17. Scale reduction minimizes filtration requirements.
18. SHarP-C technology is space-saving technology. Figure 5.74 illustrates the compactness and space saving of the new induction hardening/tempering system compared to the conventional approach.
19. A static method of heating without the necessity for crank shaft rotation is ergonomically attractive and creates some additional advantages that affect other aspects of the crank shaft induction hardening/tempering process.

Final Remarks Regarding SHarP-C Technology

In general, the SHarP-C crank shaft hardening/tempering technology provides several principal benefits compared to the conventional approach requiring crank shaft rotation during heating and quenching.

1. Because there is no rotation of a crank shaft involved during the heating/quenching process, it is not necessary to move heavy structures often weighing over 2000 lbs through the orbital path during heating. There are no high-current electrical contacts or flexible cables to wear out. There is open–close action only with far fewer moving parts.

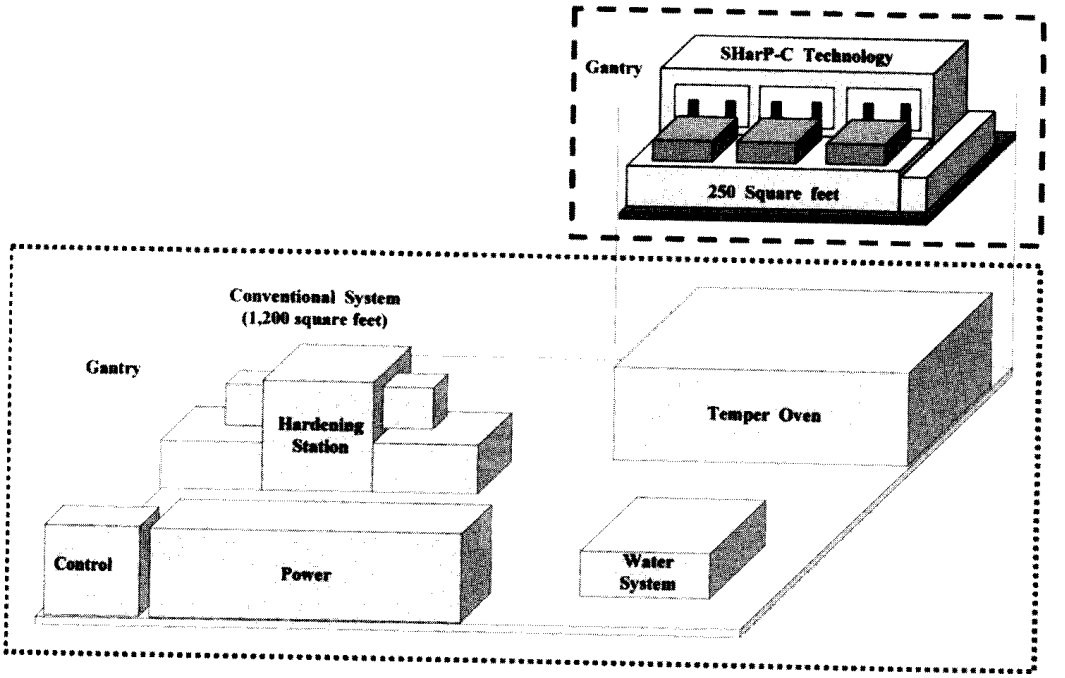

Figure 5.74 View of installed plant floor space of SHarP-C crank shaft hardening machine requiring only 20% of the conventional system (250 sq ft vs 1200 sq ft).

2. Induction coils are much more robust and rigid, being CNC-machined from solid copper without any brazed parts. This eliminates inductor distortion and hardness pattern drift. There are far fewer components involved in the novel coil design, meaning higher reliability because of the smaller numbers of parts that can go wrong. The SHarP-C coil-to-journal air gap is noticeably larger compared to air gaps required by the rotational crank shaft hardening process. This creates a favorable condition to reduce stress corrosion and stress fatigue induction coil failures. SHarP-C technology allows tooling life to be increased at least four times.
3. No wearing of the locators/guides is involved. The SHarP-C process utilizes inductors that do not require contact guides or complex and expensive noncontact coil positioning tracking systems of any kind. The coils are much less sensitive to coil–journal air gaps and to variation of adjacent masses as compared to existing technology.
4. Accurate CNC coil shaping and utilization of the quick-change pallet approach guarantee that coils are automatically aligned with respect to the crank shaft after coil replacement. No time-consuming process adjustments are required to tweak each coil after replacement. Unitized construction allows quick, error-free, production-ready factory installation and startup.

   Indisputable fact. One of our customers started up a V-6 CrankPro machine without help. The simplicity and robustness of the machine allowed the startup without requiring any extra support.

5. Crank shaft pins and mains have superior microstructural properties as compared to conventional crank shaft induction hardening processes utilizing U-shaped coils. These include the noticeable reduction of grain growth, decarburization, and oxidation of the pin/main surface. The hardened zone is clearly defined and crisp (Figures 5.69, 5.75 and Appendix I) without the fuzzy transition zone that is present when longer heat times are employed. The case depth consists of fine-grained martensitic microstructure with a negligible amount of retained austenite and without any traces of free ferrites. Essential surface compressive stresses obtained when applying SHarP-C technology are imperative for prevention of surface crack development.

Although the stationary hardening process is a cost-effective and space-saving technology, it has limited utilization for hardening of crank shafts with split-pins. This novel crank shaft hardening/tempering process is designed with ergonomics in mind, including a compact design with significantly reduced floor space requirements (Figure 5.74). There is easy access to all parts of the machine. CrankPro machines are easy to operate and maintain with significant reduction of industrial noise and a major improvement in coil life.

SHarP-C technology provides remarkable energy savings. Studies show that in some cases a total energy saving cost can exceed $260,000 per year.

Studies show that availability of the CrankPro machine is noticeably higher compared to machines that require a crank shaft rotation. The lifecycle cost of conventional crank shaft heat treatment equipment is 3.32 times higher compared to advanced SHarP-C technology.

5.2.3 Induction Hardening of Cam Shafts

Cam shafts are used in engines and comprise several irregularly or eccentricly shaped features. Typically the shaft or "stick" has a series of these irregular shapes

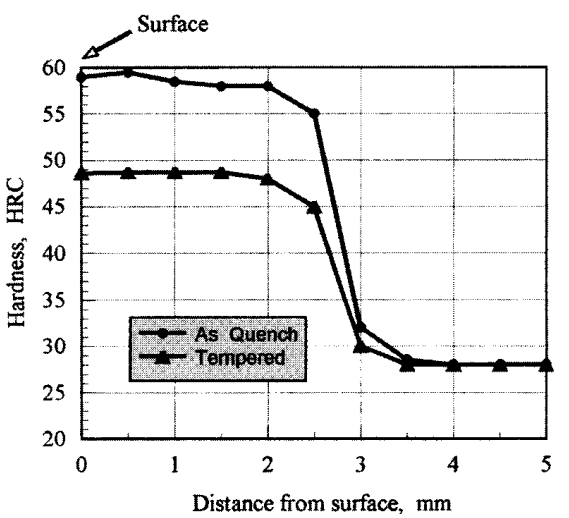

Figure 5.75 Hardness profile.

(lobes) as well as concentric features (journals). Figure 5.76 shows common names for the important geometrical shape of a typical cam. In most cases these features require wear-resistant properties because of the high rpm of most engines as well as the moderate load being applied. Depending on application and economical reasons there are several materials for the manufacturing of cam shafts including cast iron, nodular iron, gray cast iron, plain carbon steel, or alloyed steels. There is a large variety of sizes and shapes of cams and cam shafts that require surface or case hardening. In the past the hardening of cam shaft lobes was accomplished with flame and then submerging in an oil bath. This not only caused excessive distortion; it also caused an undesirable heat-affected zone (transition zone).

Medium- to high-frequency induction hardening has eliminated many of the problems of flame hardening. Induction hardening is used for cam shafts as large as ship and train cams to as small as cams for lawnmower engines. The size of the cam shaft usually influences the method of the induction process. For material handling purposes large cam shafts for ship or locomotive engines are typically processed in a horizontal manner. More commonly, automotive and truck cam shafts are processed vertically. As discussed earlier there are some quenching issues with horizontal applications, especially with irregularly shaped components. Therefore when practical it is desirable to process the cam shaft in a way that will allow proper quenching.

The typical modes of heating for cam shafts are scanning each feature, static heating of each feature, simultaneous heating of all or a series of features at one time (using a multiturn inductor), or several single-turn inductors connected in series or parallel.

The choice of scanning each feature is usually made when production volumes are low and the power available is limited. Traditionally, the size of the power supply is smaller for scanning. This results in a lower initial capital cost of the machine.

An advantage to scanning is the ability to vary the power and scan speed for obtaining a uniform hardness profile, as opposed to a single-shot profile that requires heating the whole feature at once. The main disadvantage of using the scanning mode is a noticeably longer cycle time compared to heating the whole feature at the same time.

A single-turn static heating inductor is commonly used when the lobes to be hardened are the same size and shape and are close together. Figure 5.77 shows an example of this. Flux concentrators are often on the top and bottom of the inductor, to help eliminate the heating of adjacent features (see Figure 5.78). If the previously hardened lobe heats due to the proximity of the induction field it can have undesir-

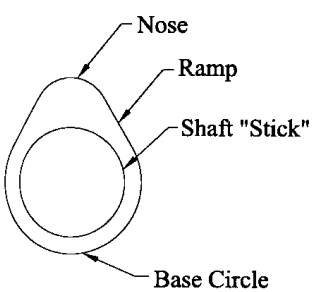

Figure 5.76 Typical cam lobe shape.

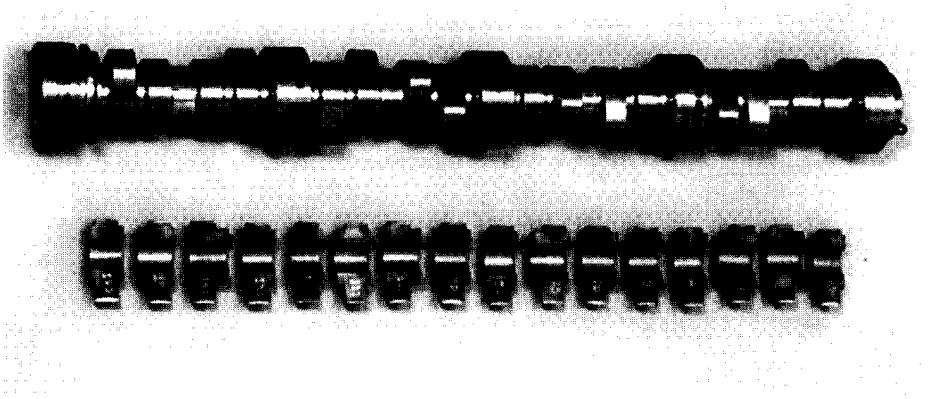

Figure 5.77 Cam shaft with lobes close together. (Courtesy of INDUCTOHEAT, Inc.)

able tempering and leave soft spots on the lobe. The use of flux concentrators focuses the heat to only the lobe within the inductor.

An effect of magnetic flux concentrators on the distribution of a magnetic field when heating a cam shaft lobe is discussed in Section 5.9. In other cases where the lobes are farther apart, the heating of the adjacent features does not take place.

To increase cycle time more than one lobe may be heated simultaneously. This can only be done if the spacing is the same between the lobes. For example, the cam shaft shown in Figure 5.16 was hardened with a four-turn coil, which provided hardening of eight lobes requiring only two heating cycles. Although this drastically

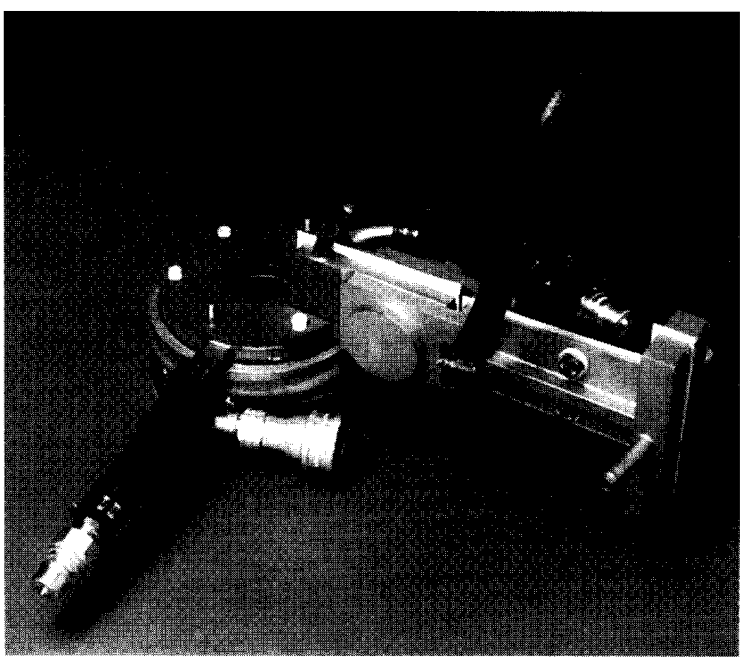

Figure 5.78 Single-turn cam shaft coil with flux concentrators, for hardening lobes that are close together.

increases the production rate, it also requires more power, due to the fact that four lobes are being heated at one time.

In order to harden truck cam shafts similar to the one shown in Figure 5.79, both a multiturn inductor (three turns) to heat the inlet, injector, and exhaust lobes, and a single-turn inductor (with flux concentrators) to heat the bearings are used. After the lobes are heated they are quickly lowered into a quench barrel. (see Figure 5.80). The single-turn coil has the quenching mechanism incorporated within it. Figure 5.60 shows equipment used to process such cam shafts.

When the hardness pattern profile cannot be achieved using the above-described methods, as a last resort clamshell or split inductors are used, as shown in Figure 5.40. Figure 5.81 shows a cam shape that would not lend itself to a conventional encircling coil. The nose of the lobe would be overheated, because of the close proximity to the inductor. In this case a clamshell-type inductor would give a uniform hardness profile; this type of coil is described in Section 5.1.4.4. Due to their nature they are usually reserved for manual loading and unloading.

The SHarP-C coil arrangement as discussed in the previous section will also provide uniform hardening of cam shaft lobes. Because of the ability to open and close the coil for loading and unloading it can have the same profile as the cam lobe, thereby producing an even heating around the perimeter of the lobe.

5.2.4 Hardening Shafts

Surface hardening of shafts is one of the most common applications for induction heat treating. The geometry of the part readily lends itself to pass through a coil or a series of coils. The size and length of the shaft can be relatively large to very small. As mentioned earlier, longer shafts have more distortion when the surface is raised to hardening temperatures. To minimize the distortion (due to thermal expansion) it is

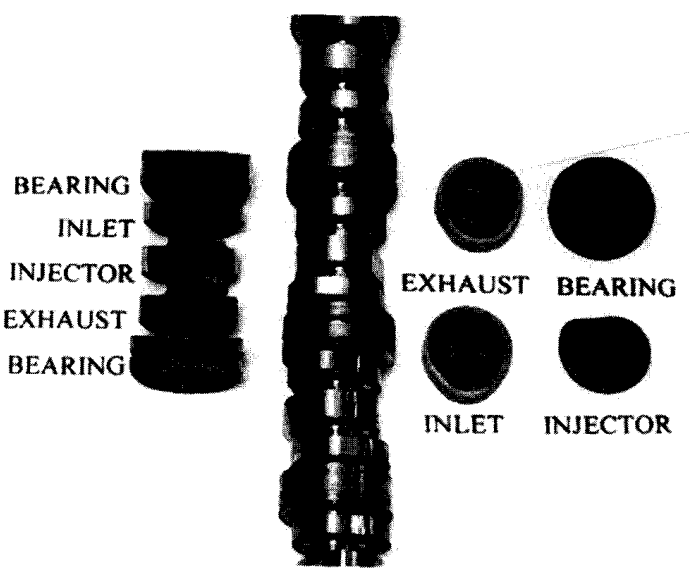

Figure 5.79 Cam shaft with all features hardened. (Courtesy of INDUCTOHEAT, Inc.)

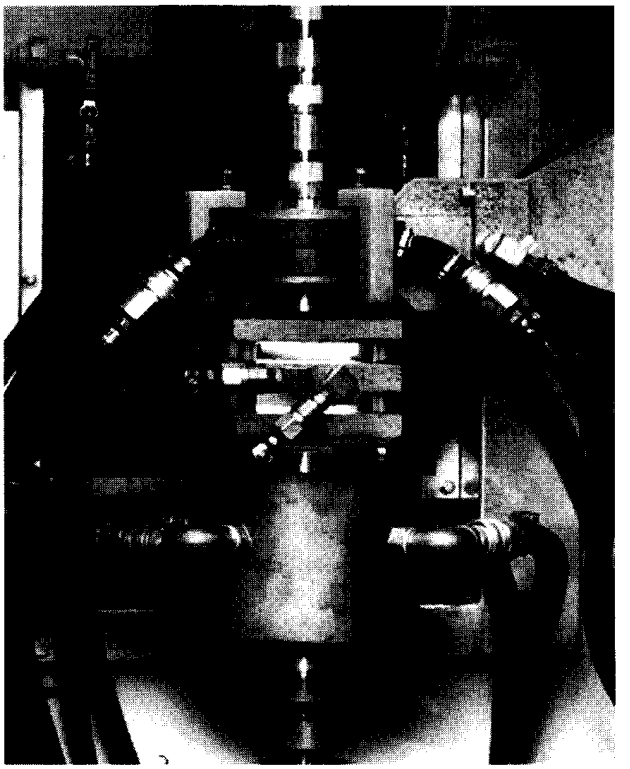

Figure 5.80 Inlet, injector, and exhaust lobes hardened with a three-turn inductor and bearings hardened with a single-turn inductor (above the three-turn inductor).

important to heat the part as quickly as possible, to eliminate the heat soaking into the core.

In the example shown in Figure 5.34, a single-shot inductor has been used to heat the axle shaft very quickly. There are also rollers in the center of the shaft to support it as well as help control distortion (keep the shaft from bowing in the center). This roller assembly is similar to what is referred to as a "steady rest"

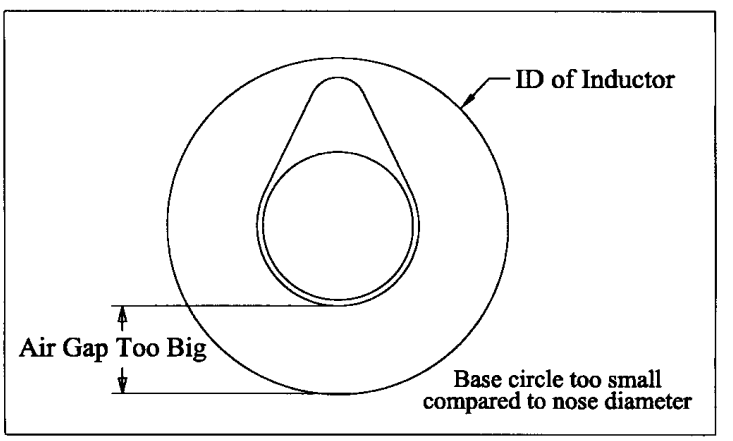

Figure 5.81 The shape of this lobe does not lend itself to a conventional style coil. Overheating of the nose will occur while underheating base circle.

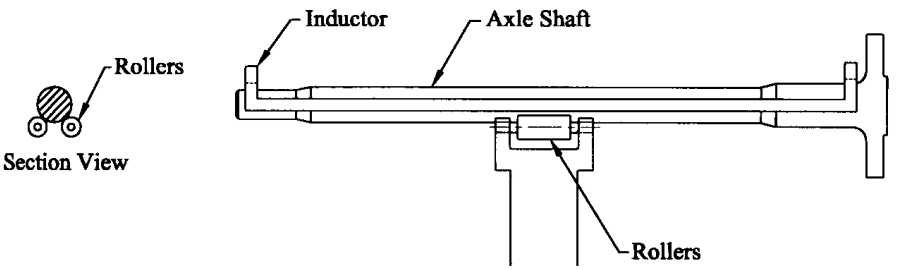

Figure 5.82 For long shafts rollers are added for support and to help control distortion during the hardening operation.

when turning a long part in a lathe. Because of the close proximity to the inductor these rollers are made of either ceramic or stainless steel. See Figure 5.82 for an example of the coil and roller arrangement.

Another possible cause for distortion when hardening shafts is the eccentricity of the inductor and quench system compared to the workpiece. If the inductor is closer to the part in one area it will cause a hotter surface temperature in that area. Even with rotation of the part it will continue to be the hottest area, because it will continue to be the closest to the coil. This nonuniform heating will also cause uneven quenching. Uniform quenching is important when trying to minimize distortion.

As with other long parts it is common to process shafts horizontally, because the material handling is easier, especially when scan hardening. See Section 5.1.5.1 for the subject of horizontal versus vertical scan hardening. When practical for shorter shafts [less than 800 mm (30 in.)] vertical processing is a common choice.

Certain features of the shaft may be a deciding factor for inductor style such as grooves, cross-holes, thin-walled parts, and the required hardness profile at the pattern ends. The shaft in Figure 5.83 has grooves, cross-holes, and thin areas. It must be heated quickly to prevent through hardening in the thin areas. The quenching must be uniform in the grooves to prevent cracking. A single-shot inductor can accommodate both concerns. Single-shot inductors are described in Section 5.1.4.3.

Key ways and snap ring grooves at the ends of shafts are also concerns for overheating of corners and underheating in the bottom of the groove. There are some special considerations about these critical areas, and they are discussed in Section 5.8.

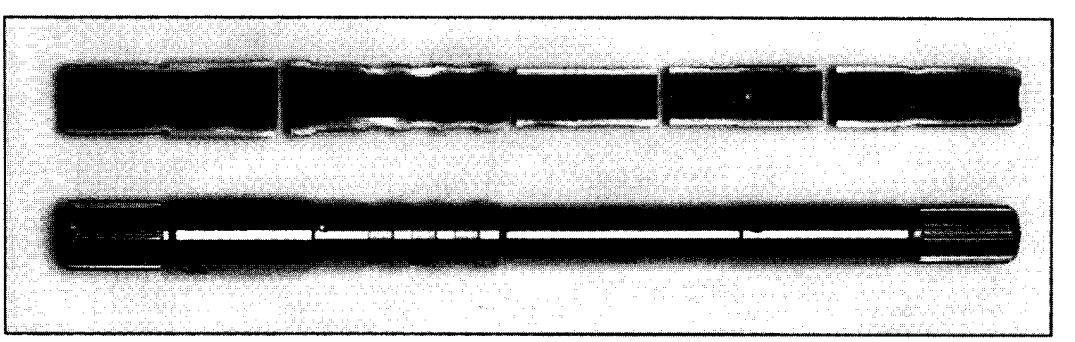

Figure 5.83 Shafts with thin walls, grooves, and special pattern terminations require some process and inductor considerations. (Courtesy of INDUCTOHEAT, Inc.)

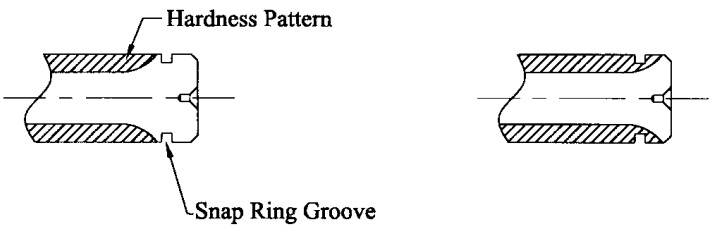

Figure 5.84 Typical hardness patterns at end of shaft with snap ring. Because of stress risers in sharp corners, either entire groove is hardened or groove is not hardened at all.

Care must be taken when hardening snap ring grooves. If only half the groove is hardened it will cause undesirable stress risers in the groove. Figure 5.84 shows typical pattern requirements at the ends of shafts with snap ring grooves. Figure 5.85 represents a typical bar shaft that is induction hardened and tempered with a single-shot inductor.

5.3 RESIDUAL STRESSES AND CRACKING IN INDUCTION HEAT TREATING

Heat treating specialists often face the necessity of making a reasonable compromise between maintaining the required hardness and obtaining tough and ductile microstructure in the metal that has the desirable distribution of residual stresses. Stresses that appear during heat treating can be divided into three general groups; initial,

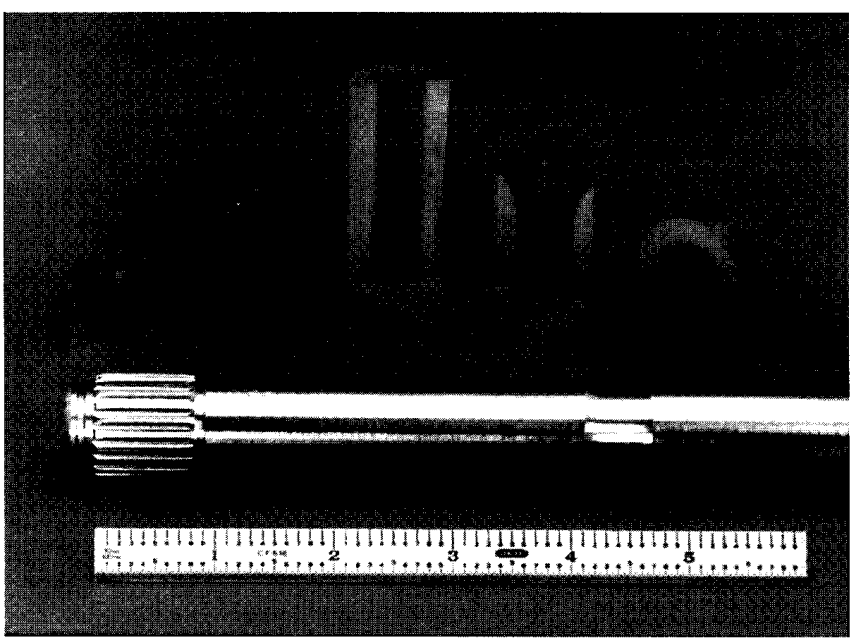

Figure 5.85 Bar shaft hardened and tempered with single-shot inductor. Pattern at end of shaft extends through snap ring groove. (Courtesy of INDUCTOHEAT, Inc.)

transitional and residual stresses. The distribution and value of initial stresses depends upon the operations that have taken place prior to heat treatment. Transitional stresses appear during heating and cooling and, depending upon the application, may partially or totally disappear after the process of heat treatment is completed. Residual stresses are a product of initial and transitional stresses. Let's examine how stresses appear during induction hardening. The mechanism of formation of residual stresses here is different than in other heat treatment processes including carburizing and nitriding.

Generally speaking, there are two different types of stresses: thermal stresses and stresses due to phase transformation. Thermal stresses are caused by different magnitudes of temperature and temperature gradients. Phase transformation stresses occur due to microstructural changes taking place as a result of the formation of austenite, bainite, or martensite. The total stress is a combination of both components. At different stages of heat treating the impact of both components on total stresses is different. Stresses are closely related to cracking. Appendix C shows INDUCTOHEAT's "fish bone" diagram of cracking during and after induction hardening.

Figures 5.86 and 5.87 illustrate the dynamics of stress appearance (macroscopically speaking) during induction hardening of a carbon steel cylinder [2, 12, 203, 243]. At the first stage of the heating cycle, the section of the cylinder located under the coil will try to expand. The temperature of the workpiece at this point is relatively low (less than 500°C/932°F). During this stage, carbon steels have a nonplastic condition and cannot easily expand. As a result, stresses build up within the workpiece.

The temperature rise will cause the appearance of increasing compressive stresses at the surface (Figure 5.87). In the temperature range of 520°C (968°F) to 750°C (1382°F) the steels undergo plastic volumetric expansion and the stresses start to decrease. Finally, when the temperature exceeds 850°C (1562°F), the steel surface freely expands, and the diameter of the heated area becomes greater than its initial diameter. Because the yield point of the surface layer is considerably lowered at elevated temperature (which is in the austenite state), the material will flow plastically. As a consequence, the stresses at the surface significantly decrease.

After the quenching fluid is sprayed onto the heated surface, the outside layer quickly loses its plastic properties and a pronounced maximum of tensile stresses appear at the surface of the workpiece (Figure 5.87). This maximum typically occurs just above M_s temperature. The appearance of martensite reduces the surface tensile stresses and leads to the compressive stresses at the surface. Finally, when the entire part is cooled down, a complex combination of compressive and tensile stresses exists within the workpiece body (Figure 5.86).

There is always a balance of residual stresses in the workpiece. If certain areas have compressive residual stresses, then somewhere else must have tensile stresses. The compression stresses in the surface are typically useful. They provide certain protection against crack propagation caused by microscopic scratches. In addition, these residual stresses are very beneficial to the parts that experience bending and torsion applied stresses during their service life.

It is imperative to mention that the maximum tensile residual stresses are located (Figure 5.86) just below the hardened case depth. It is a dangerous area of the part. This maximum is primarily responsible for subsurface crack initiation.

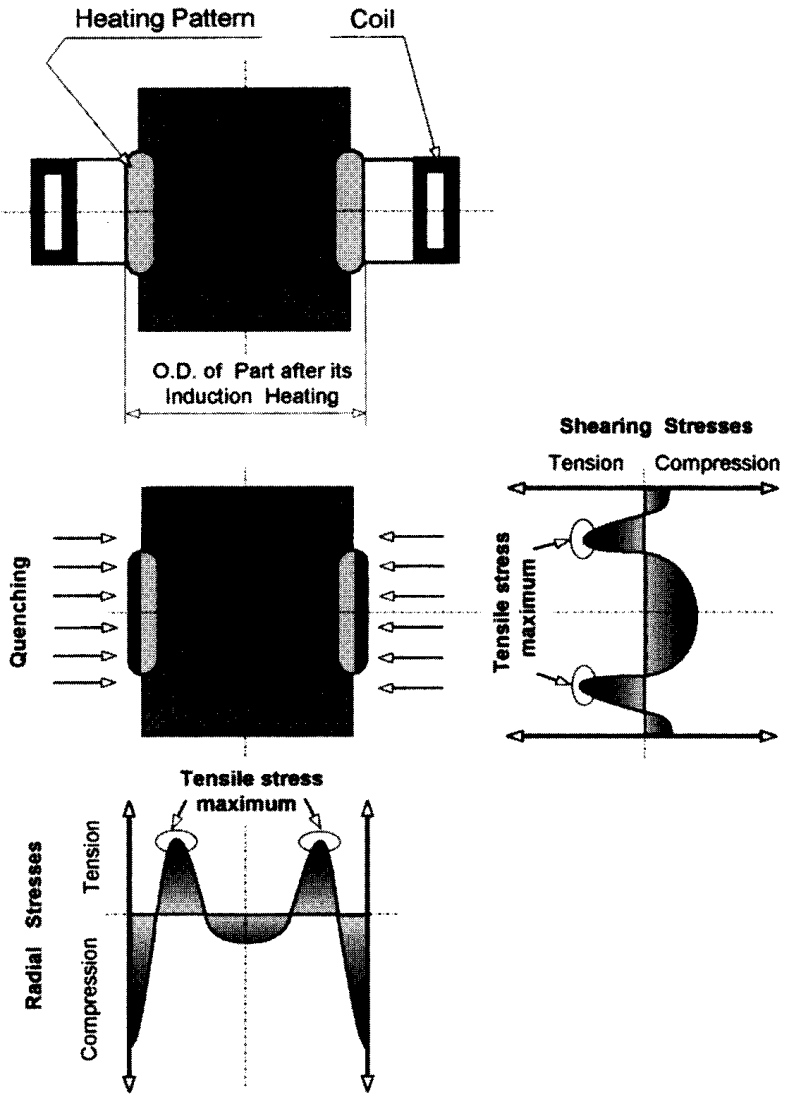

Figure 5.86 Formation of residual stresses after induction hardening.

In the case of induction heat treatment of complex-shaped bodies, the residual stress distribution is more complex. Xray analysis allows one to reveal three-dimensional distribution of residual stresses. Heat treat practitioners know that mild quenchants decrease the rate of cooling during martensitic transformation reducing the probability of crack initiation. At the same time, some researchers including N. Kobasko [473] and K. Schepelyakovskii [376] believe that the effect of the cooling rate within the martensitic range on crack development appears as a bell-shape curve. According to this phenomenon, both a slow cooling rate that represents mild quenching as well a a very high cooling rate that represents severe quenching prevent quench cracking and minimize distortion.

The overall residual stress condition increases brittleness and notch sensitivity, which reduces part reliability. Therefore it is necessary to relieve some stresses on the

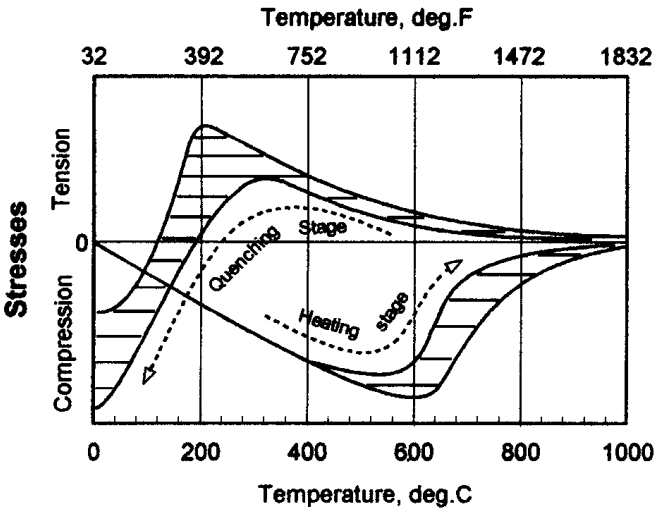

Figure 5.87 Stresses at surface of carbon steel cylinder during heating–quenching cycle.

part while trying to keep useful compressive stresses at the surface and removing the tensile stresses farther away from applied stresses. The process of stress relieving during tempering is discussed in Section 5.5. Besides tempering, final grinding also has a pronounced effect on the final residual stress distribution.

5.4 GEAR HARDENING

In recent years, gear manufacturers have increased their technological knowledge of the production of quality gears. This knowledge has led to many improvements including lower noise, lighter weight, and lower cost as well as increased load-carrying capacity to handle higher speeds and torque with a minimum amount of generated heat.

This section concentrates on induction gear/pinion hardening only. Induction tempering of gears is discussed in Section 5.5.

Not all gears and pinions are well suited for induction hardening. External spur and helical gears, worm gears, and internal gears, racks, and sprockets are among the parts that are typically induction hardened (Figure 5.88). Conversely, bevel gears, hypoid gears, and noncircular gears are rarely heat treated by induction.

In contrast to carburizing and nitriding, induction hardening does not require heating the whole gear. With induction the heating can be localized only to the areas where metallurgical changes are desired (e.g., flank, root, and gear tip can be selectively hardened) and the heating effect on adjacent areas is minimum. Depending upon the application a tooth hardness typically ranges from 42 to 60 HRC.

One of the goals of induction gear hardening is to provide a fine-grained fully martensitic layer on specific areas of the gear to increase hardness and wear resistance while allowing the remainder of the part to be unaffected by the process. The increase in hardness improves contact fatigue strength as well. A combination of increased hardness, wear resistance, and the ability to provide a fine martensite

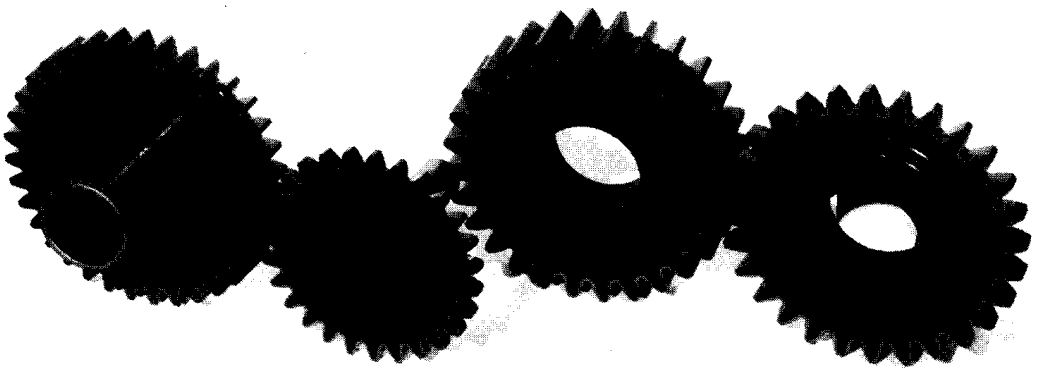

Figure 5.88 Typical induction hardened gears.

structure, often allows the substitution of inexpensive medium- or high-carbon steel or low-alloyed steel for more expensive highly alloyed steels.

As mentioned earlier, it is not always possible to obtain a fully martensitic case depth. Depending upon the kind of steel, the presence of some amount of retained austenite within the case depth is unavoidable (unless cryogenic treatment is used). This is particularly true for steels with high carbon content and cast irons.

Up to a certain point, some amount of retained austenite does not noticeably reduce the surface hardness. However, it brings some ductility and provides better absorption of impact energy which is imperative for heavily loaded gears. In addition, having an unstable nature, retained austenite has a tendency with time to transform into martensite. It introduces additional compressive residual stresses and increases the surface hardness. From this perspective, a small amount of retained austenite is not only harmless but may even be considered beneficial in some cases. However, an excessive amount of retained austenite can be detrimental because it may noticeably reduce the surface hardness, weaken bending fatigue properties, and can result in the appearance of a crucial amount of brittle untempered martensite during gear service life.

Another goal of induction gear hardening deals with the ability to provide significant compressive residual stresses at the surface. This is an important feature, since it helps to inhibit crack development as well as resist tensile bending fatigue.

The kind of steel/iron used, its prior microstructure, and gear performance characteristics (including load condition and operating environment) dictate the required surface hardness, core hardness, hardness profile, gear strength, and residual stress distribution

5.4.1 Material Selection and Required Gear Conditions Prior to Heat Treatment

Steel selection depends upon features of the gear working conditions, required hardness, and cost. Low-alloy and medium-carbon steels with 0.4 to 0.55% carbon content (i.e., AISI 4140, 4340, 1045, 4150, 1552, 5150) are quite commonly used for gear heat treatment by induction.

When discussing induction hardening it is imperative to mention the importance of having "favorable" metal conditions prior to gear hardening. Hardness repeatability and the stability of the hardness pattern are grossly affected by the consistency of the microstructure prior to heat treatment (referred to as microstructure of a "green" gear) and the steel's chemical composition [203, 211–213, 379].

"Favorable" initial microstructure, including a homogeneous fine-grained quenched and tempered martensitic structure with hardness of 30 to 34 HRC leads to fast and consistent metal response to heat treating with the smallest shape/size distortion and a minimum amount of grain growth. This type of initial microstructure results in higher hardness and deeper hardened case depth compared to the ferritic/perlitic initial microstructure.

If the initial microstructure of the gear has a significant amount of coarse perlite and most importantly coarse ferrites or clusters of ferrites, then these microstructures cannot be considered favorable because gears with such structures will require longer austenization time and/or higher austenizing temperatures to make sure that diffusion-type processes are completed and homogeneous austenite is obtained. Ferrite is practically a pure iron and does not contain the carbon required for martensitic transformation. Pure ferrite consists of less than 0.025% carbon. Large areas (clusters) of free ferrite require a long time for carbon to be able to travel and diffuse into the poor carbon area of the ferrite. Otherwise, clusters of ferrites will act as one huge grain of ferrite that will be retained in the austenite and upon quenching a complex ferritic–martensitic microstructure with scattered soft and hard spots will take place.

In opposition to quenched and tempered prior microstructure, steels with large carbides (i.e., spheroidized microstructures) have poor response to induction hardening and also result in the need for prolonged heating and higher temperatures for austenization. Longer heat time leads to grain growth, the appearance of coarse martensite, data scatter, an extended transition zone, and essential gear shape distortion. Coarse martensite has a negative effect on tooth toughness and creates favorable conditions for crack development.

As opposed to other heat treating techniques, heat treatment by induction is appreciably affected by variation in the metal chemical composition. Therefore favorable initial metal condition also includes tight control of the specified chemical composition of steels and cast irons. Wide compositional limits cause surface hardness and case depth variation. However, tight control of the composition eliminates possible variation of the heat treat pattern resulting from multiple steel/iron sources. Segregated and banded initial microstructures of "green" gears should be avoided.

The surface condition of the gear is another factor that can have a distinct effect on gear heat treating practice. Voids, microcracks, notches, and other surface and subsurface discontinuities as well as other stress concentrators can initiate crack development during induction hardening when the metal goes through the expansion–contraction cycle; thermal gradients and stresses can reach critical values and "open" notches and microcracks. Conversely, a homogeneous metal structure with a smooth surface free of voids, cracks, notches, and the like improves the heat treating conditions, and positively affects important gear characteristics such as bending fatigue strength, endurance limit, gear durability, and gear life.

Medium and high frequencies have a tendency to overheat sharp corners, therefore gear teeth should be generously chamfered if possible for optimum results in the heating process.

Because gears provide transmission of motion and force, they belong to a group of the most geometrically accurate power transmission components. A gear's geometrical accuracy and ability to provide a required fit to its mate greatly affect gear performance characteristics. Typical required gear tolerances are measured in microns, therefore the ability to control such undesirable phenomena as gear warpage, ovality, conicality, out-of-flatness, tooth crowning, bending, growth, shrinkage, and the like plays a dominant role in providing quality gears.

This is why hardness pattern consistency, minimum shape/size distortion, and distortion repeatability are among the most critical parameters that should be satisfied when heat treating gears.

5.4.2 Overview of Hardness Patterns

The first step in designing an induction gear heat treatment machine is to specify the required surface hardness and hardness profile. Figure 5.89 shows typical locations of gear profile measurements. In some cases, depending upon the type of gear and its application, some customers create specific procedures for gear profile measurements.

Insufficient hardness as well as an interrupted (broken) hardness profile at tooth contact areas will shorten gear life due to poor load-carrying capacity, pre-

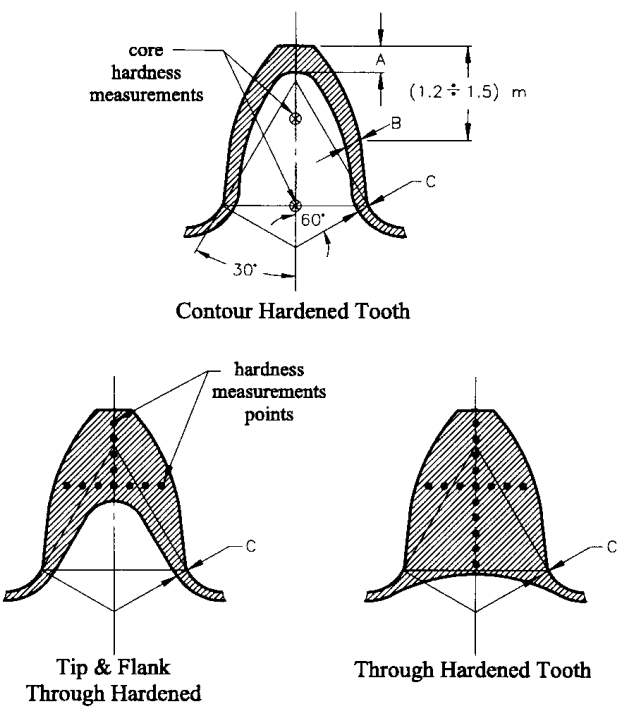

Figure 5.89 Typical locations of gear profile measurements. Depending on type of gear and its application, specific procedures are created for these measurements.

mature wear, tooth bending fatigue, rolling contact fatigue, pitting, and spalling, and can even result in some plastic deformation of the teeth.

A through hardened gear tooth with a hardness reading exceeding 60 HRC is too brittle and will often experience a premature brittle fracture. Hardened case depth should be adequate (not too large and not too small) to provide the required gear tooth properties.

There is a common misconception that a uniform contour profile is always the best pattern for all gear hardening applications. It is not. In many cases, a certain hardness gradient profile can provide a gear with better performance.

Operating load condition (whether there are occasional, intermittent, or continuous loads) has a pronounced effect on the type of gear, tooth geometry, and hardness profile. Loads lasting up to 30 minutes per day are considered occasional loads. Loads lasting several minutes per hour are considered to be intermittent-type loads. Continuous loads last from 10 to 24 hours [211, 381].

Let's briefly evaluate a variety of hardening patterns (Figure 5.90) and their effect on gear load-carrying capacity and life [252, 258].

Pattern A is a flank hardening pattern that has been used since the late 1940s for hardening large gears (with teeth modulus of eight and larger). The hardened pattern occupies the tooth flank area and ends prior to the tooth fillet. This pattern provides the required wear resistance, but the typical failure mode of gears with this type of pattern is a bending fatigue caused by repeated loading. A crack typically initiates in the tooth root/fillet area. In the harden–nonharden transition region, the residual stresses change from compressive in the hardened area to tensile in the nonhardened area. The maximum tensile residual stresses are located just below the end of the hardened pattern. A combination of applied tensile stresses with

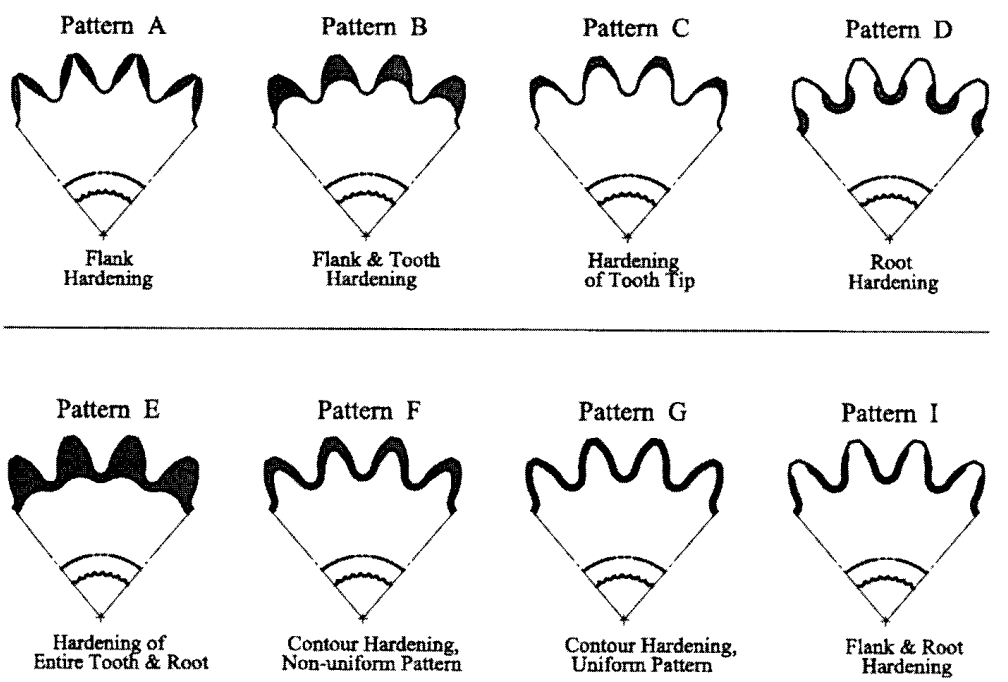

Figure 5.90 Induction hardening patterns of gears.

tensile residual stresses creates a favorable condition for early crack development in the root/fillet area particularly for heavily loaded gears. Therefore when Pattern A is obtained, a mechanical hardening (i.e., roll or ball hardening) is typically required to harden the fillet area and develop within that area useful compressive residual stresses that will resist bending fatigue. When mechanical hardening is not used, it is typically recommended that one uses a pattern that hardens the root areas as well, such as that pictured in Pattern I.

Pattern B is a flank and tooth hardening pattern. This pattern has a shortcoming similar to the previous one, featuring a poor load-carrying capacity yet can be used in cases where wear resistance is of prime concern. Patterns E, F, and G provide better results when a combination of wear, tear, and bending fatigue resistance is required.

Pattern C is a tooth tip hardening pattern. In this case, the gear has minimum shape distortion. In addition, the application of gears with this pattern is extremely limited because the two most important tooth areas (flank and root) are not hardened. As a matter of fact, due to unfavorable residual stress distribution, the bending fatigue strength of a gear with this pattern, as well as Patterns A and B, can even be 25% lower compared to gear strength prior to hardening ("green" gear) [213]. In most cases, Patterns F and G would be better choices.

Pattern D is a root hardening pattern. The maximum bending stresses are located in the tooth fillet area, therefore this pattern provides good fillet/root strengthening, meaning a combination of hard surface, sufficient case depth, and compressive stresses. The root is essentially reinforced, thus the maximum tensile residual stresses are shifted far away from the root/fillet surface to a depth where tensile residual stresses will not complement tensile applied stresses during service and create bending fatigue fracture. However, application of this pattern is quite limited. Since the tooth flank is not hardened, this pattern provides poor wear resistance that may result in removal or displacement of metal particles from the gear surface. Theoretically, it is possible to imagine the necessity of using this pattern as well as the previous one; however, it is more practical to use another pattern, such as Pattern I.

Pattern E is one of the most popular induction hardening patterns, particularly for small-size gears and sprockets. Because the body of the tooth is through hardened, some quench cracking may occur. In addition, there is a danger of having a brittle fracture in gears with through hardened teeth, particularly those subjected to shock loads. The core should be able to withstand impact loads and prevent plastic deformation of the gear teeth. It should also have some ductility. This is why a low-temperature tempering is often applied. The core strength is measured by its hardness. Low-temperature tempering lowers the final hardness down to 52 to 58 HRC and provides some ductility and toughness to the gear teeth. This pattern offers good resistance to wear and pitting.

Patterns F and G are popular patterns for medium-size gears in many applications. According to Pattern F, a case depth in the tooth root area is typically 30 to 40% of the depth in the tooth tip. Slightly larger hardness depth at the tooth pitch line compared to the root is beneficial as a preventive action against spalling and pitting. It is very important to harden the entire gear perimeter, including the flank and root area. An uninterrupted hardened pattern of all contact areas of the tooth indicates good wear properties of the gear, plus it typically ensures the existence of

uninterrupted distribution of desirable compressive stresses at the gear surface. Because gear teeth are not hardened through, a relatively ductile tooth core (30 to 44 HRC) and a hard surface (56 to 62 HRC) provide a good combination of such important gear properties as exceptional wear resistance, toughness, and bending strength, and provide superior gear durability.

Pattern I is one of the most popular choices for induction hardening of large gears and pinions (i.e., gears with 300 mm and even larger OD) with coarse teeth (modules greater than eight). This pattern provides an exceptional combination of fatigue and wear strength as well as resistance to shock loading and scuffing (severe adhesion wear where metal particles transfer from one tooth to another tooth), which is very important for heavily loaded gears and pinions experiencing severe shock loads. It is recommended that for these applications surface hardness should not be very high, typically in the range of 55 to 59 HRC. If surface hardness exceeds 61 to 62 HRC, the gear might be too brittle and could experience some tooth bending failures.

5.4.3 Coil Design and Heat Mode

The variety of required hardness profiles calls for different coil designs and heat modes [203, 252, 258]. Development, including coil design, is largely based on induction principles, the result of mathematical evaluation and experience with previous jobs. The development establishes not only process parameters, including cycle times and power levels, but also coil geometry.

5.4.3.1 Tooth-by-Tooth and Gap-by-Gap Inductors

Generally speaking, gears are induction heat treated by either encircling the part with a coil (so-called spin hardening, Figure 5.91) or, in larger gears and pinions, heating them "tooth-by-tooth" or "gap-by-gap" (Figure 5.92) [203, 211, 252, 258, 263, 277, 278].

Tooth-by-tooth and gap-by-gap techniques require a high level of skill, knowledge, and experience in order to obtain the required hardness pattern. These techniques can be realized by applying a single-shot or scanning mode. Scanning rates can be quite high, reaching 15 in./min and even higher. Both tooth-by-tooth and

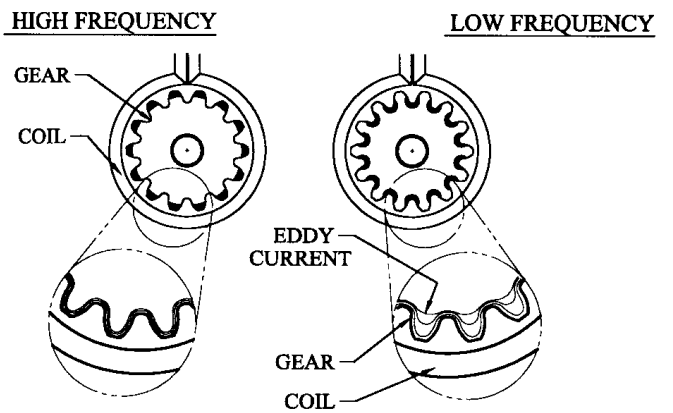

Figure 5.91 Frequency influence on hardness profile with encircling induction coil.

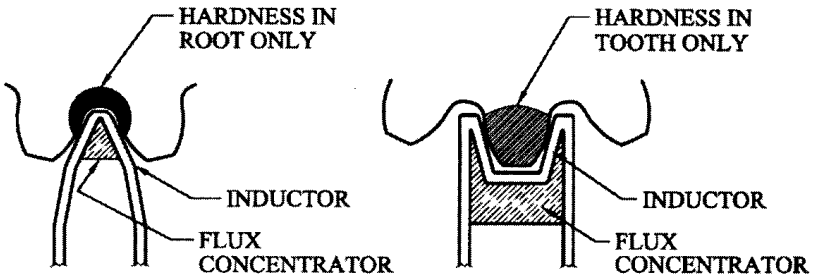

Figure 5.92 Gap-by-gap and tooth-by-tooth induction hardening.

gap-by-gap techniques are typically not very suitable for small and fine pitch gears (modules smaller than six).

Coil geometry depends upon the shape of the teeth and the required hardness pattern. According to the tooth-by-tooth technique, an inductor encircles a single tooth or is located around it. Such an inductor design provides Patterns B and C.

Gap-by-gap techniques require the coil to be symmetrically located between two flanks of two adjacent teeth. This inductor can be designed to heat only the root and/or flange of the tooth, leaving the tip and tooth core soft, tough, and ductile. There are many variations of coil designs applying these principles. Probably one of the most popular is the inductor shape shown in Figure 5.93. This type of inductor was originally developed in the 1950s by the British firm, Delapena. Figure 5.94 shows the pattern profile for gap-by-gap induction hardening.

As one can see from Figure 5.95, the path of the induced eddy current has a butterfly-shaped loop. The maximum current density is located in the teeth root area (the center part of the butterfly). In order to further increase the power density induced in the root, a magnetic flux concentrator is applied. A stack of laminations or powder-based magnetic materials is typically used as flux concentrators here. Laminations are oriented across the gap. The phenomena of magnetic flux concentration, materials selection, and general requirements of magnetic concentrators are discussed in detail in Section 5.9 of this book.

Although the eddy current path has a butterfly shape, when applied with a scanning mode, the temperature is distributed within gear roots and flanks quite uniformly. At the same time, since the eddy current makes a return path through the flank and, particularly through the tooth tip, proper care should be taken to prevent overheating the tooth tip. Overheating of the tip can substantially weaken the tooth.

Gears heat treated by using the tooth-by-tooth or gap-by-gap techniques can be fairly large, having outside diameters of 100 in. or more, and can weigh several tons. These techniques can be applied for external and internal gears and pinions. There is a limitation to applying these methods for hardening internal gears. Typically, it is required that the internal diameter of the internal gear exceeds 8 in., and in some cases 10 in. or more.

Both tooth-by-tooth and gap-by-gap hardening are time-consuming processes with low production rates. Power requirements for these techniques are relatively low and depend upon the production rate, type of steel, case depth, and tooth geometry. Modest power requirements can be considered an advantage, because if

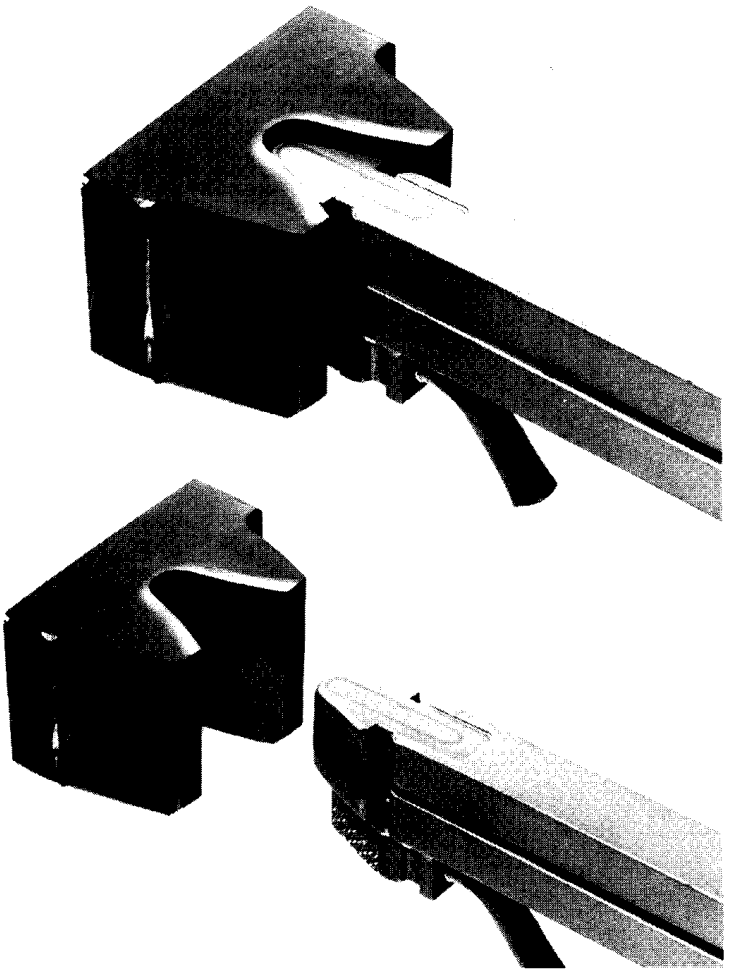

Figure 5.93 Gap-by-gap inductor and gear. (Courtesy of INDUCTOHEAT, Inc.)

spin hardening is used, a large gear would require an enormous amount of power which could diminish the cost effectiveness of the heat treating process.

Applied frequencies are usually in the range of 1 to 30 kHz. At the same time, there are some cases when a frequency of 70 kHz and even higher frequencies have been used. For example, the NATCO submerged technique [373] applied a radio frequency of 450 kHz.

Pattern uniformity is quite sensitive to coil positioning. The coil should be symmetrically located in a gap between two teeth. Asymmetrical coil positioning results in a nonuniform hardness pattern. For example, an increase in the air gap between the coil copper and the fillet surface on one side will result in a reduction of hardness and shallower case depth there. Shallow case depth can diminish the bending fatigue strength of the gear. Excessive wear of the working (contacting) side of the gear tooth can also occur.

A decrease of the air gap can result in local overheating or even melting of the gear surface. Some arcing can occur between the coil and the gear surface. Precise coil fabrication techniques, rigidity of the inductor, and careful alignment are required. Special locators should be used to ensure proper inductor positioning in

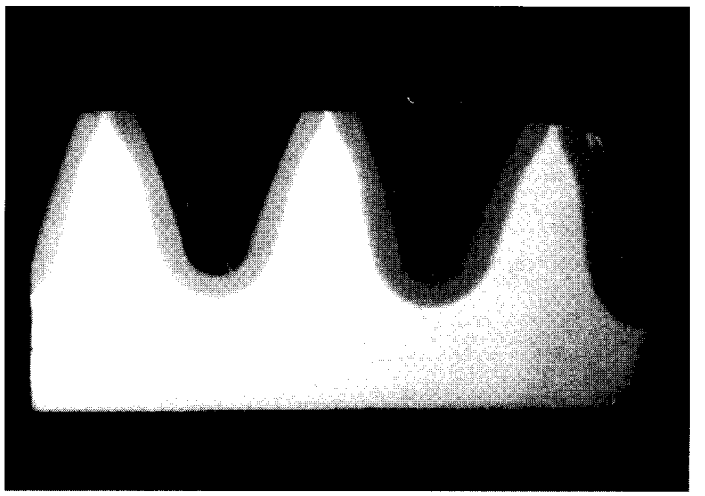

Figure 5.94 Gap-by-gap pattern profile. (Courtesy of INDUCTOHEAT, Inc.)

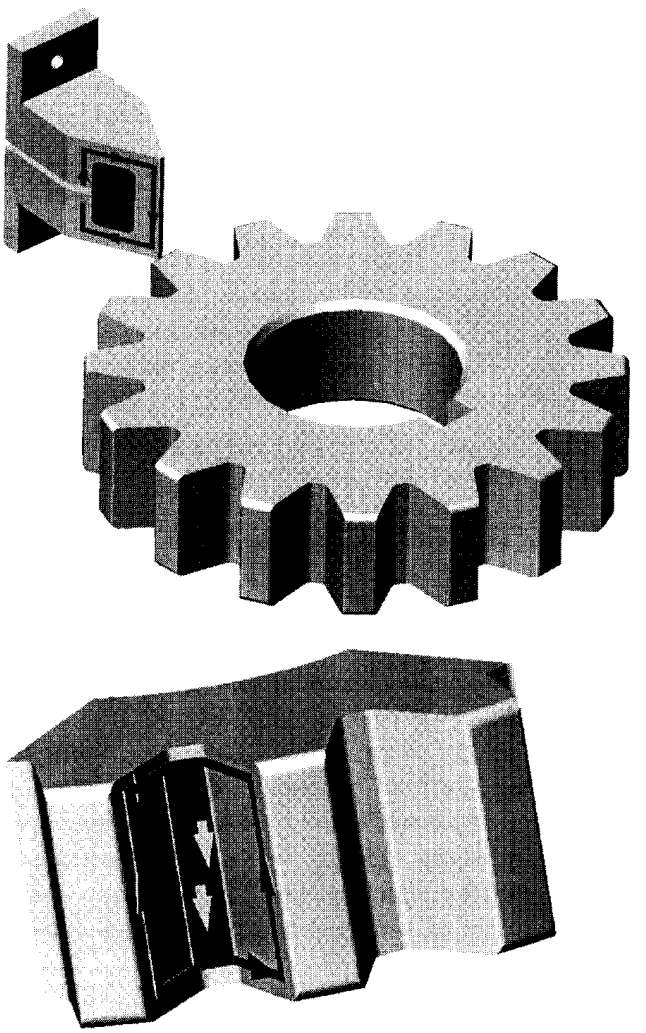

Figure 5.95 (A) Current flow on gap-by-gap inductor; (B) path of induced eddy currents has butterfly-shaped loop.

the tooth space. Thermal expansion of metal during heating should be taken into consideration when determining the proper coil-to-gear-tooth air gap.

There can be an appreciable shape/size distortion when applying tooth-by-tooth or gap-by-gap techniques for hardening large gears and pinions. Shape distortion is particularly noticeable in the last heating position. The last tooth can be pushed out 0.1 to 0.3 mm. In some cases, distortion can also be minimized by hardening every second tooth or tooth gap. Obviously this will require two revolutions to harden the entire gear. Therefore final grinding is often required. There is a linear relationship between the volume of required metal removal and grinding time. Thus excessive distortion leads to a prolonged grinding operation and increases the cost. Heat treat distortion can also be compensated for during previous stages of gear design and manufacturing.

Even though there might be appreciable distortion when applying induction hardening to large gears and pinions (e.g., mill, marine and large transportation gears, etc.), this distortion is not as significant compared to carburizing or nitriding. Both carburizing and nitriding operations require soaking of gears for many hours (in some cases up to 30 h or longer) at temperatures of 850°C (1562°F) to 950°C (1742°F). At these temperatures the large masses of metal expand to a much greater extent compared to a case when only the gear surface layer is heated. The expansion of a large mass of metal during heating/soaking and its contraction during cooling/quenching after carburizing results in much greater gear shape distortion compared to the distortion after induction hardening.

In addition, large gears being held at temperatures of 850°C (1562°F) to 950°C (1742°F) for many hours have little rigidity; therefore they can sag and have a tendency to follow the movement of their supporting structures during soaking and handling. During induction hardening, areas unaffected by heat as well as areas with temperatures corresponding to the elastic deformation range serve as shape stabilizers and lead to lower, more predictable distortion.

It is necessary to mention here that due to small coil–workpiece air gaps (0.5 to 1.5 mm) and harsh working conditions, these coils require intensive maintenance and have a relatively short life compared to inductors that encircle the gear.

When designing this type of induction heating process, particular attention should be paid to electromagnetic end/edge effects and the ability to provide the required pattern in the gear face areas (gear ends) as well as along the tooth perimeter (see Section 5.7).

When a single-shot mode is used, an active coil length has approximately the same length as the gear width. A single-shot mode is more limited in providing a uniform face-to-face hardness pattern compared to the scanning mode.

For the scanning mode, the coil length is typically at least twice as short as the gear thickness. In order to obtain the required face-to-face temperature uniformity, it is necessary to use a complex control algorithm, "Power and Scan Rate versus Coil Position." A short dwell at the initial and final stages of coil travel is often used. Thanks to preheating due to thermal conductivity, the dwell at the end of coil travel is usually shorter compared to the dwell at the beginning of travel.

When applying the scanning mode for hardening gears with wide teeth, two techniques can be used: a design concept where the inductor is stationary and the gear is moveable, and a concept that assumes the gear is stationary and the inductor is moveable.

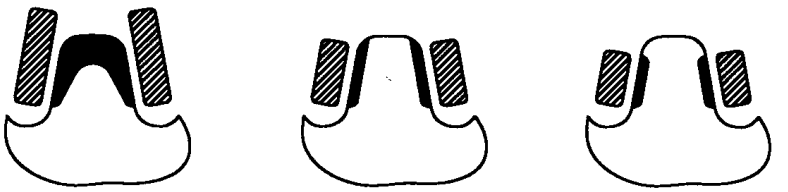

Figure 5.96 Effects of coil geometry on tooth-by-tooth hardness patterns.

Figures 5.96 and 5.97 show the effect of coil geometry on tooth-by-tooth hardness patterns [2].

One typical concern when applying tooth-by-tooth or gap-by-gap hardening techniques is the problem of undesirable heating of the areas adjacent to the hardened area (tempering back). Concern of tempering back is particularly pronounced for Patterns A, D, and I when using gap-by-gap hardening, and Patterns B and C with tooth-by-tooth heat treating. Generally speaking, there are two reasons why undesirable tempering back can take place.

The external magnetic field coupling phenomena of the inductor typically take place when hardening tooth-by-tooth (Patterns B and C), and often can be fixed relatively easily. The application of magnetic flux concentrators to the induction coil (Figure 5.98) results in a drastic reduction of the external magnetic field. In cases with medium-sized tooth gaps, the allocation of concentrators can be difficult due to space limitations. The undesirable heating of the flanks of adjacent teeth can also be reduced by applying thin copper shields (copper caps); see Figure 5.99 [2]. The physics and application features of magnetic flux concentrators and shields are discussed in Section 5.9.

Another cause typically takes place when applying gap-by-gap hardening techniques (particularly for Patterns A, D, and I) and deals with thermal conductivity phenomena. As discussed in Section 3.2.2, heat is transferred by thermal conduction from a high-temperature region of the workpiece toward a lower-temperature region. According to Fourier's law, the rate of heat transfer is proportional to the temperature difference and the value of thermal conductivity. Most metals have relatively good thermal conductivity. During hardening, the surface temperature reaches a relatively high value and exceeds the critical temperature A_{c3}. Therefore when heating one side of the tooth (i.e., Patterns A, D, and I) there is a danger that the opposite side of the gear tooth will be heated by thermal conductivity to an inappropriately high temperature, resulting in undesirable tempering back of previously hardened areas.

Figure 5.97 Effects of coil geometry on tooth-by-tooth hardness patterns.

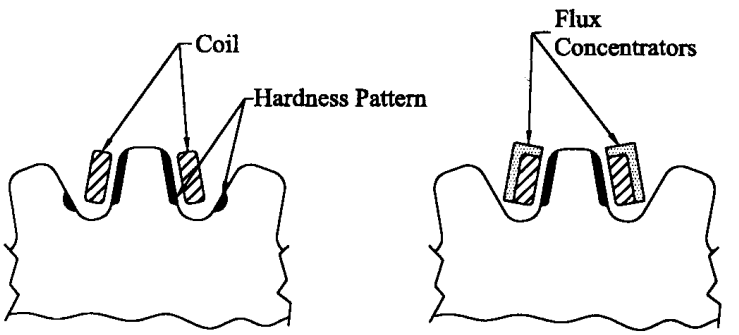

Figure 5.98 Application of flux concentrators to inductor drastically reduces the external field.

Whether a hardened side of the tooth will be softened due to tempering back depends upon several factors, including the applied frequency, gear module, tooth shape, heat time, case depth, and other pattern features. In the case of shallow and moderate case depth and large teeth, the root of the tooth, its fillet, and the bottom of the tooth flank are typically not overheated due to thermal conductivity. The massive area below the tooth root serves as a heat sink, which helps to conduct excessive heat and protects the hardened side of the tooth from tempering back.

Conversely, the tooth tip and top of the tooth flank can be considered as a troubled area as far as tempering back is concerned. This takes place because there is a relatively small mass of metal at the tooth tip. In addition, heat has a short distance to travel from one (heating) side to the other (already hardened) side of the tooth (Figure 5.100).

In order to overcome the problem of tempering back, additional cooling blocks can be used. Additional cooling protects already hardened areas while heating unhardened areas of the gear (Figure 5.101). Even though external cooling is applied, depending on the tooth shape and process parameters, there still may be some unavoidable tempering back. This tempering back is typically insignificant and acceptable.

Tooth-by-tooth and gap-by-gap techniques can harden gears submerged in a temperature-controlled tank of quenchant. This technique was applied in the origi-

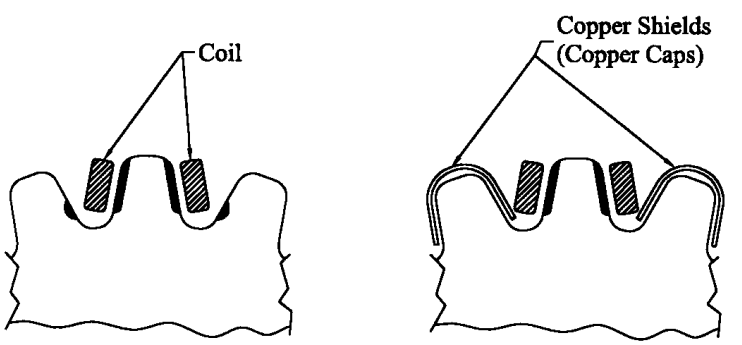

Figure 5.99 Undesirable heating of adjacent teeth can be reduced by applying thin shields (copper caps).

(A)

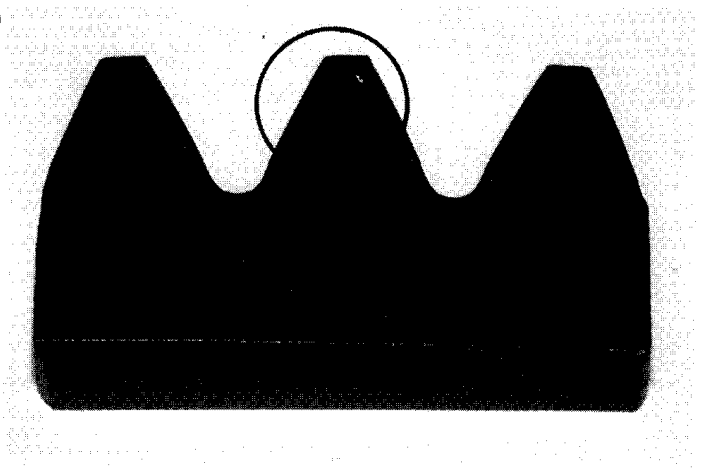

(B)

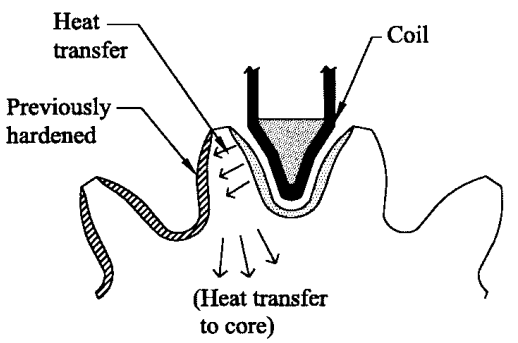

Figure 5.100 (A) Tip of tooth flank can be a trouble area as far as temper back of the adjacent tooth, because of the relatively small mass of metal at the tooth tip; (B) sketch of tempering back phenomenon.

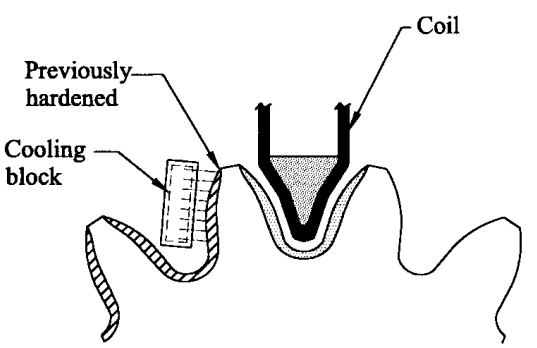

Figure 5.101 To overcome tempering back of previously hardened tooth, cooling blocks are added.

nal Delapena induction hardening process. In this case, quenching is practically instantaneous and both controllability and repeatability of the hardness pattern is improved, although additional power is required. The fact that a gear is submerged in quenchant also helps to prevent the tempering back problem as well as crack development in the tooth root. In addition, the quenchant serves as a coolant to the inductor. Therefore, in submerged hardening an induction coil does not have to be water-cooled.

5.4.3.2 Gear Spin Hardening (Encircling Inductors)

Spin hardening of gears utilizes a single or multiturn inductor that encircles the part and requires gear rotation. It is typically used for gears with fine- and medium-sized teeth and is considered less time consuming and more cost effective than the previously discussed processes. Therefore it is strongly recommended to use spin hardening whenever it is possible. Unfortunately, spin hardening is not a cure-all and sometimes cannot be easily used for medium-sized helical and bevel gears and large module gears due to an enormously large amount of required power and difficulties in obtaining the desired hardness pattern.

Gears are rotated during heating to ensure an even distribution of energy across their perimeter. Rotation rates are chosen to suit process requirements.

When applying encircling coils, there are five parameters that play a dominant role in obtaining the required hardness pattern: frequency, power, cycle time, coil geometry, and quenching conditions. Proper control of these parameters can result in totally different hardened profiles.

Figure 5.102 illustrates a diversity of induction hardening patterns that were obtained on the same carbon steel shaft with variations in time, frequency, and power. As a basic rule, when it is necessary to harden the tooth tips only, a higher frequency and high power density should be applied (Figure 5.91, left). When hardening the tooth root, a lower frequency and lower power density should be used (Figure 5.91, right). A high power density generally gives a shallow pattern; conversely, a low power density will produce a deep pattern.

In addition to the process parameters mentioned above, hardness pattern uniformity and repeatability depend strongly upon the relative positioning of the gear and coil and the ability to maintain gear concentricity to the induction coil.

There are several ways to accomplish quenching for spin hardening of gears. One technique is to submerge the gear in a quenching tank. This technique is applicable for large-size gears. Small and medium gear sizes are usually quenched in place, using an integrated quench. The third technique requires the use of a separate concentric quench block (quench ring) located below the inductor.

As a general remark, it has been reported [111, 374] that more favorable compressive stresses within the tooth root were achieved with the gear spin hardening technique than with the tooth-by-tooth or gap-by-gap approaches.

Figure 5.103 shows three of the most popular design concepts of the induction gear heat treating processes that employ encircling-type coils: conventional single frequency concept (CSFC), pulsing single frequency concept (PSFC), and pulsing dual frequency concept (PDFC). All three concepts can be used in either a single-shot or scanning mode.

a. Conventional Single Frequency Concept (CSFC) The conventional single frequency concept [203, 252] is used for hardening gears with medium and

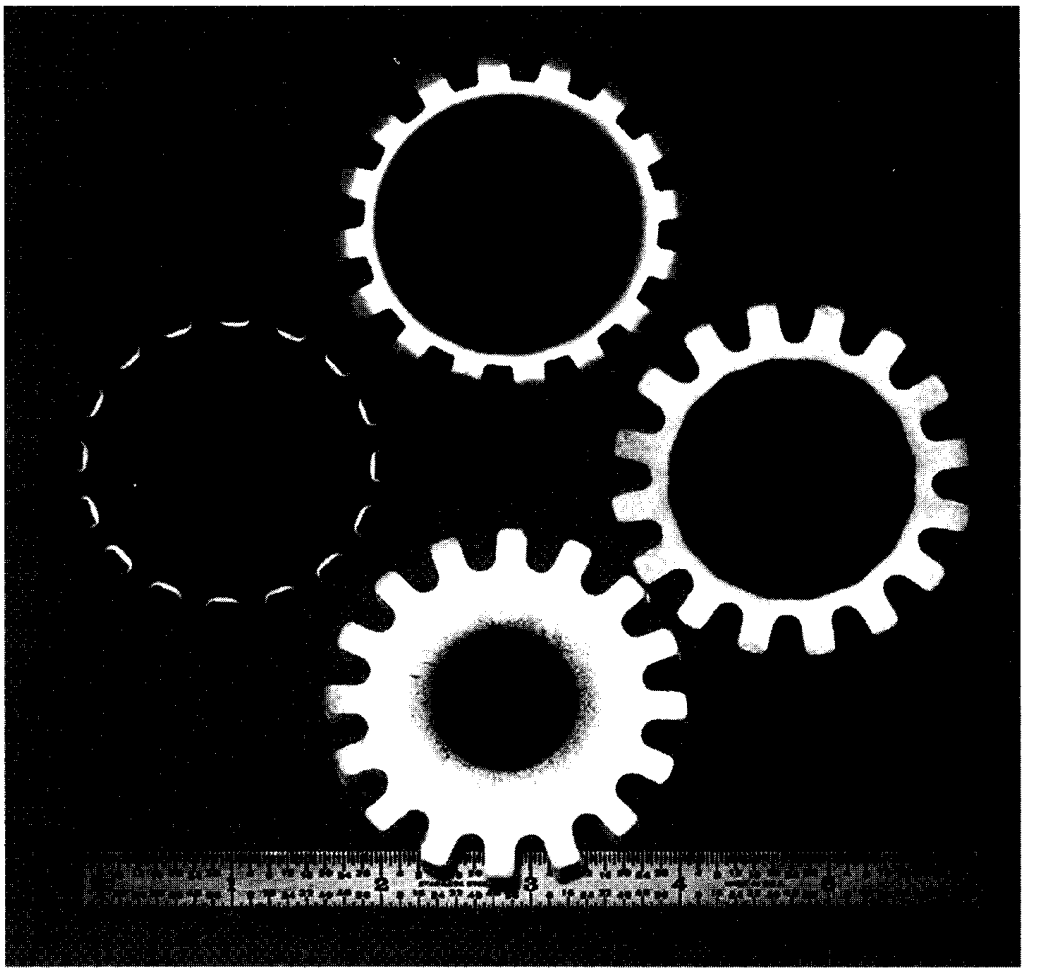

Figure 5.102 Diversity of induction hardening patterns, with variations in time, frequency, and power. (Courtesy of J. LaMonte, INDUCTOHEAT Inc., Madison Heights, MI.)

small teeth. As one can see in Figure 5.90 (Patterns B and E), the teeth are often through hardened. Quite frequently CSFC can also be successfully used for medium-size gears. As an example, Figure 5.104 shows an induction gear hardening machine that applies this concept. The gear being heat treated in this application is an automotive transmission component with helical teeth on the inside diameter (ID) and large teeth on the outside diameter (OD) for a parking brake. Both the inside and outside diameters require hardening (Figure 5.105). The hardening of the inside diameter gear teeth requires a higher frequency than the outside diameter. Therefore a frequency of 10 kHz was chosen for OD heating and 200 kHz was chosen for ID heating. After the heat is off, quenchant is applied to the hot gear in place; that is, no repositioning is required. This practically instantaneous quench provides a consistent metallurgical response. During quenching there is minimal or no rotation to ensure that the quenchant penetrates all areas of the gear evenly. Quenching reduces the gear temperature to the quenchant temperature or temperature suitable for gear handling.

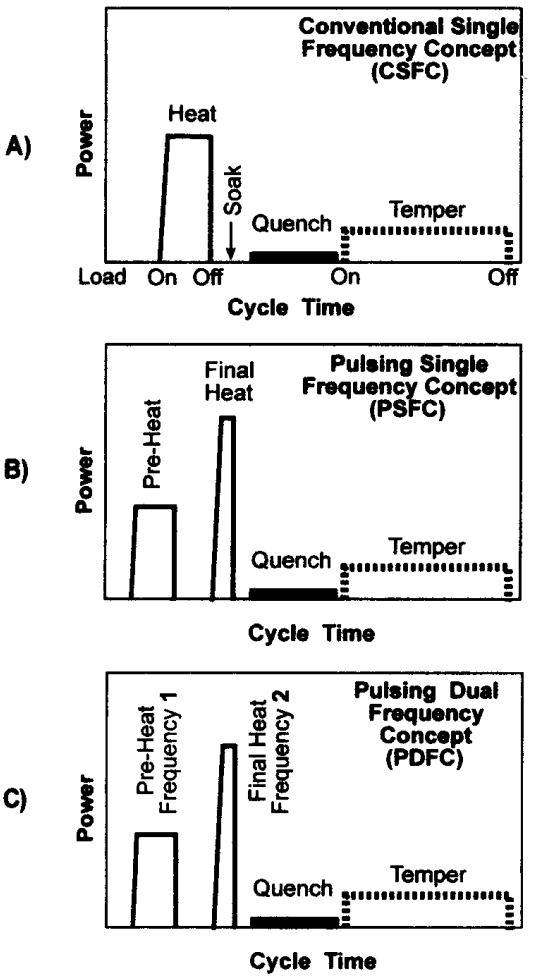

Figure 5.103 Concepts of gear hardening by induction.

On the machine referred to above (Figure 5.104) gears are conveyed to the machine, where they are then transferred by a cam-operated robot to the heat treating station. Parts are monitored at each station and accepted or rejected based on all the major factors that affect gear quality. This includes energy input into the part; quench flow rate, temperature, quench pressure, and heat time. An advanced control/monitoring system verifies all machine settings to provide confidence in the quality of processing for each individual gear. Precise control of the hardening operations and careful attention to the coil design minimize part distortion and provide the desirable residual stresses in the finished gear. The hardened gear is inspected and moved to the next operation.

Although CSFC is the most suitable for small- and medium-size gears, there are cases when this concept can be successfully used for large gears as well. As an example, Figure 5.106 shows an induction machine for hardening large gears. A multiturn encircling inductor is used for hardening gears with a major diameter of 27.6 in. (701 mm), root diameter 24.3 in. (617 mm), and thickness 3.125 in. (79 mm). In this particular case, it was in the customer's best interest to harden and temper in the same coil using the same power supply. In other cases it might not be the best solution.

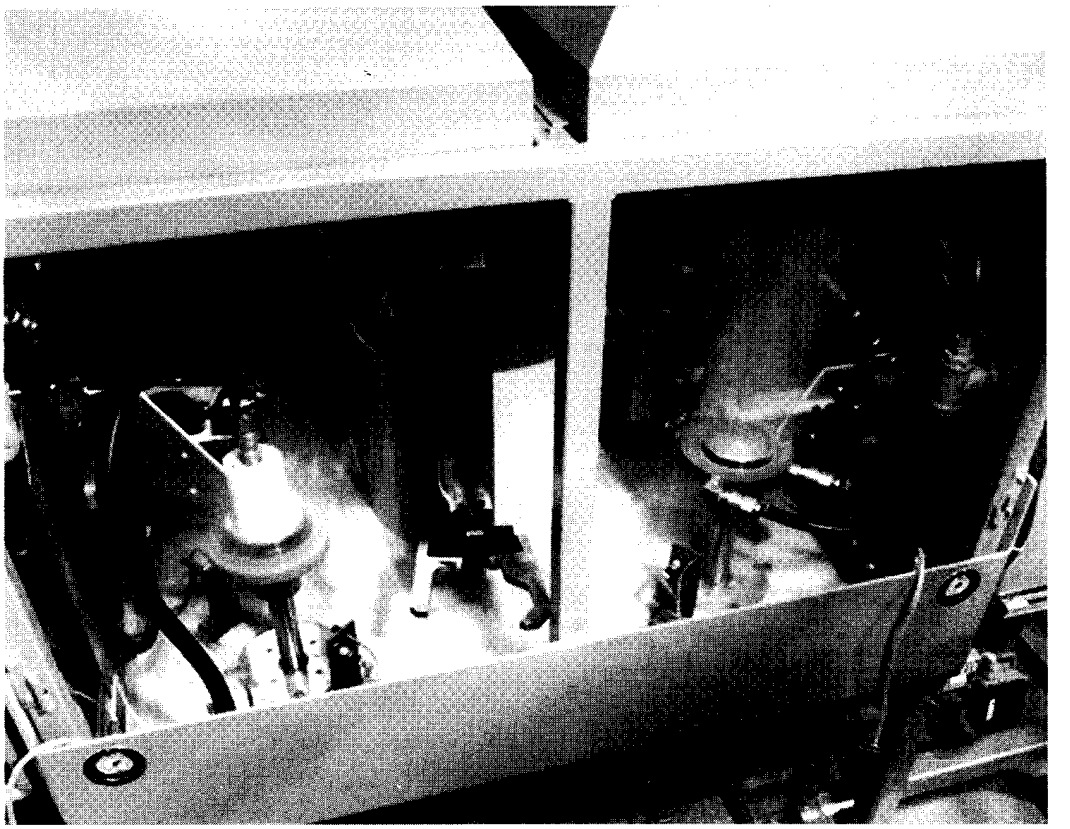

Figure 5.104 Equipment used to harden OD and ID of gear.

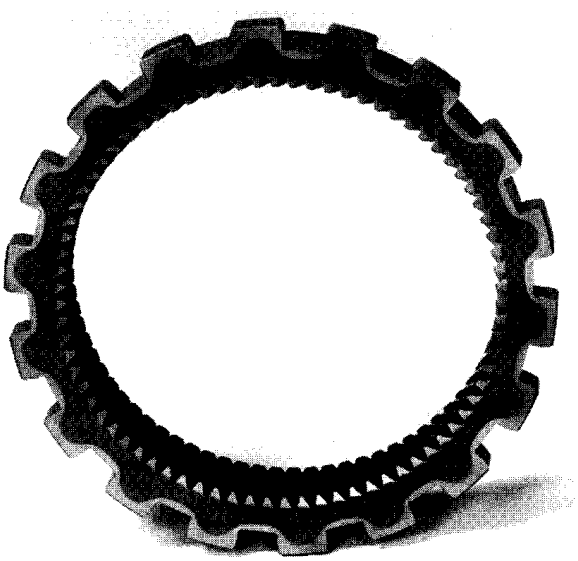

Figure 5.105 Some gears require hardening both OD and ID. (Courtesy of INDUCTOHEAT, Inc.)

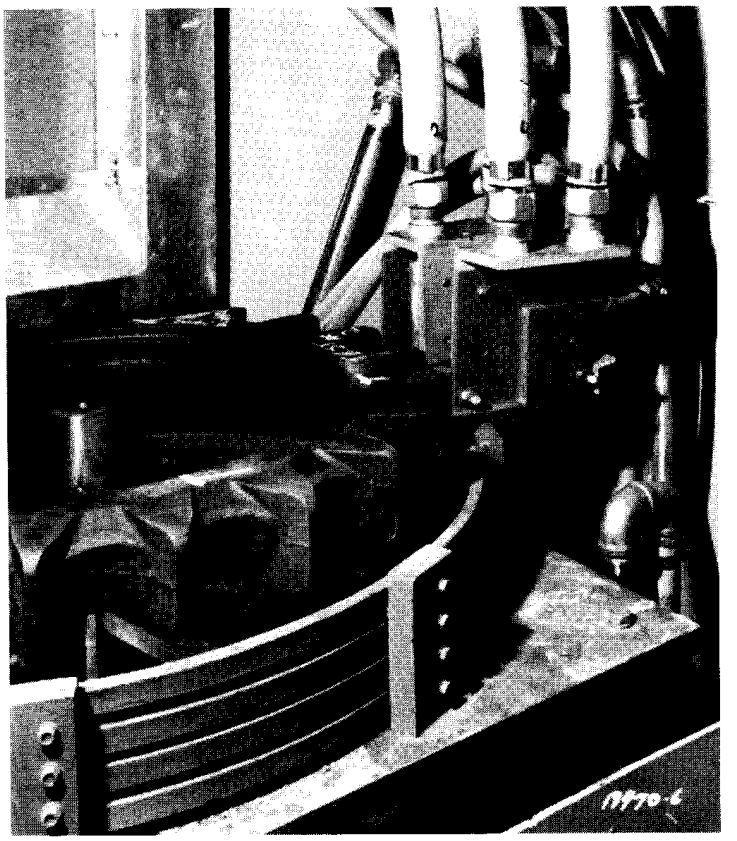

Figure 5.106 Induction equipment for hardening large gears. (Courtesy of INDUCTOHEAT, Inc.)

Quite often, in order to prevent problems such as pitting, spalling, tooth fatigue, and endurance, hardening the contour of the gear (contour hardening) is required. In some cases, this can be a difficult task due to the difference in current density (heat source) distribution and heat transfer conditions within a gear tooth.

Two main factors complicate the task of obtaining the required contour hardness profile. With encircling-type coils, the root area does not have good coupling with the inductor compared to the coupling at the gear tip. Therefore it is more difficult to induce energy into the gear root. In addition, there is a significant heat sink located under the gear root (below the base circle, Figure 5.91).

b. Pulsing Single Frequency Concept (PSFC). In order to overcome these difficulties and to be able to meet customer specifications, the pulsing single frequency concept was developed (Figure 5.103B). In many cases, PSFC allows the user to avoid the shortcomings of CSFC and obtain a contour hardening profile. Pulsing provides the desirable heat flow toward the root of the gear without noticeable overheating of the tooth tip. A well-defined, crisp, hardened profile that follows the gear contour (Patterns F and G) can be obtained using high power density at the final heating stage.

A typical "dual pulse" contour hardening system, which applies a pulsing single frequency concept has been discussed in [203, 209, 210]. This machine is designed to

provide gear contour heat treatment (including preheating, final heating, quenching, and tempering) with the same coil using one high-frequency power supply. Figure 5.103 illustrates the process cycle with moderate-power preheat, soaking stage, short high-power final heat, and quench followed by low-power heat for temper.

Preheating ensures a reasonable heated depth at the roots of the gear, enabling the attainment of the desired metallurgical result and decreasing the distortion in some materials. Preheat times are typically from several seconds to a minute, depending on the size and shape of the gear. Obviously, preheating reduces the amount of energy required in the final heat.

After preheating, there might be a soak time ranging from 2 to 10 seconds to achieve a more uniform temperature distribution across the teeth of the gear. Final heat times can range from less than 1 second to several seconds.

As a general rule, for both CSFC and PSFC techniques the higher frequency is called for by finer pitch gears which typically require a smaller case depth. Figure 5.107 shows a unitized induction hardening system capable of providing both CSFC and PSFC gear hardening. Figure 5.108 shows a double sprocket hardened by the induction machine shown in Figure 5.107.

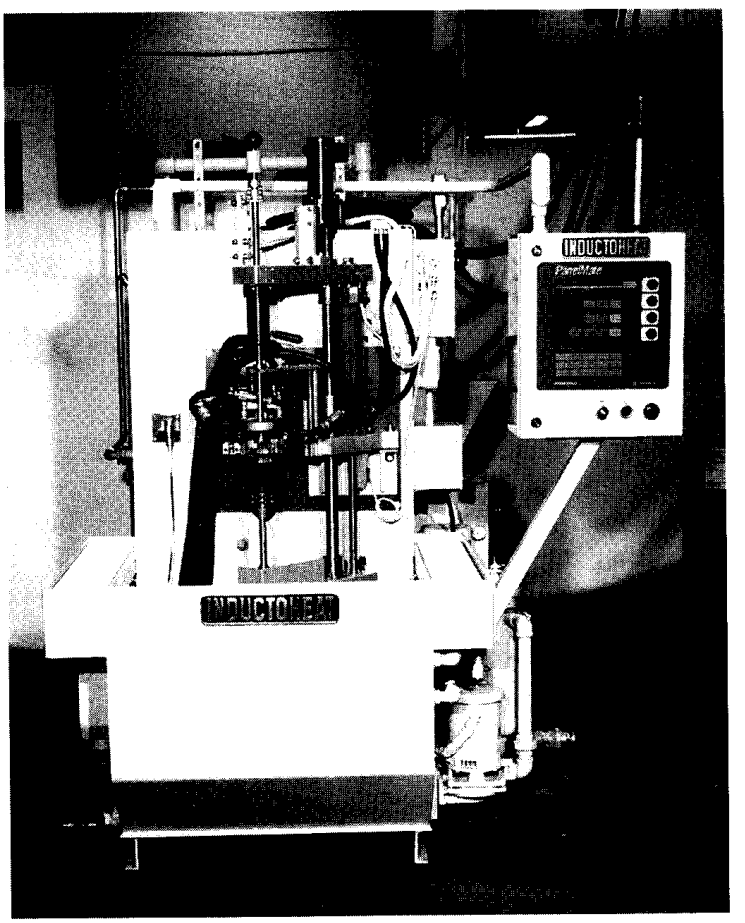

Figure 5.107 Unitized induction system capable of providing both CSFC and PSFC gear hardening.

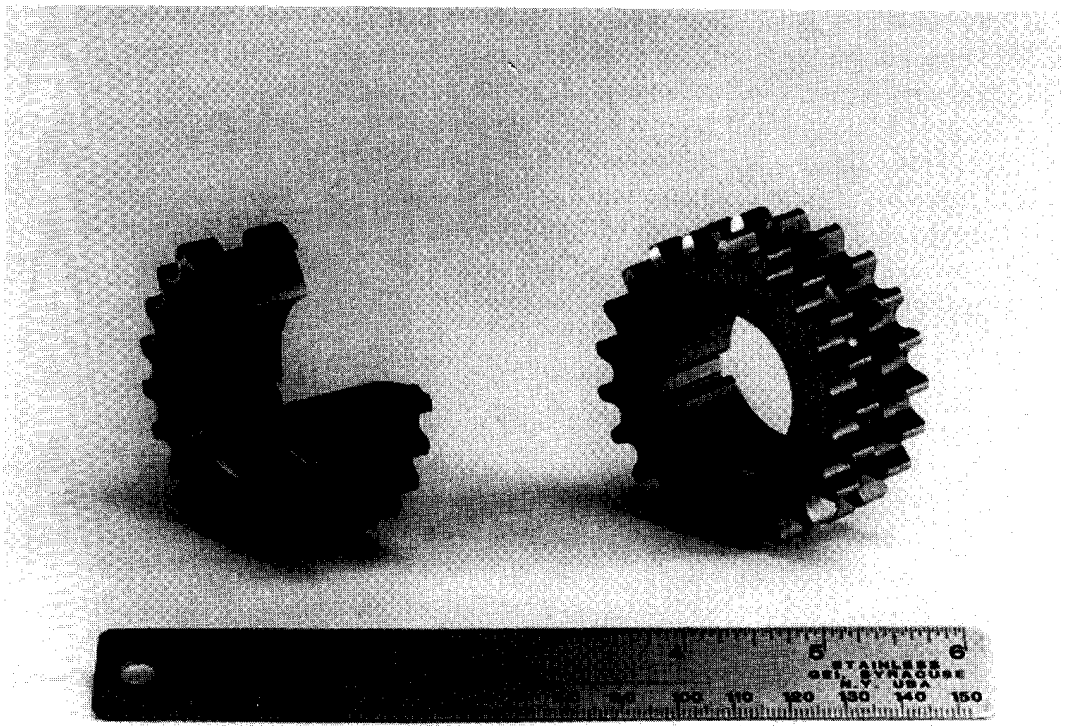

Figure 5.108 Double sprocket hardened by equipment shown in Figure 5.107.

c. Pulsing Dual Frequency Concept (PDFC). A third concept, the pulsing dual frequency concept, is not new. The idea of using two different frequencies to produce the desired contour pattern has been around since the late 1950s. This concept was primarily developed to obtain a contour hardening profile for helical and straight spur gears. Several companies, including Contour Hardening, INDUCTOHEAT, Inc., and others, have pursued this idea, and several different names and abbreviations have been used to describe it [2, 115, 203]. INDUCTOHEAT built its first prototype contour hardening machine that applied a dual frequency concept in 1986. Obviously, since that time, the process has been refined and several innovations developed. However, regardless of the differences in nomenclature and the slight process variations, the basic idea is the same.

According to PDFC (Figure 5.103C), the gear is preheated within an induction coil to a temperature determined by the process features. This temperature is usually 350 to 100°C below the critical temperature A_{c1}. Preheat temperature depends upon the type and size of the gear, tooth shape, prior microstructure, required hardness pattern, acceptable distortion, and the available power source. It should be mentioned that the higher the preheat temperature, the lower the power required for the final heat. However, high preheat temperatures can result in increased distortion.

As in previous gear spin hardening concepts, PDFC can be accomplished using a single-shot mode or scanning mode. The scanning mode is typically applied for longer gears.

Preheating is usually accomplished by using a medium frequency (3 to 10 kHz). Depending on the type of gear, its size, and material, a high frequency (30 to 450 kHz) and high power density are applied during the final heat stage. For the final heating stage, the selected frequency allows the current to penetrate only to the desired depth. This process gives excellent repeatability.

Depending upon the application, two coil design arrangements can be used when applying the scanning or single-shot modes. In the first arrangement (Figure 5.109), one coil and two power supplies are utilized to harden the gear. The sequence of operations is as follows:

1. Location of the gear within the induction coil;
2. Beginning of gear rotation;
3. Low frequency voltage is applied to the induction coil;
4. The coil begins to move along the gear length and preheats the full length of the gear;
5. After completion of the preheating stage, the coil is disconnected from the low frequency source;
6. Upon returning to the initial position, a high-frequency voltage is applied to the coil and a second scanning cycle begins;
7. The gear is heated to the hardening temperature and quenching is applied simultaneously or the gear is quenched after completion of the heating stage.

The first approach has many limitations including low reliability and complexity, therefore, in a great majority of cases, the PDFC process utilizes another type of coil arrangement.

For the second coil arrangement (Figure 5.110), two coils and two power supplies are utilized. One coil provides preheating and another coil, final heating. Both coils work simultaneously if the scanning mode is applied. In the case of a single-shot mode, a two-step index-type approach is used.

Quenching completes the hardening process and brings the gear down to ambient temperature. In some cases, dual frequency machines produce parts with lower distortion and a more favorable distribution of residual stresses compared to other techniques.

As mentioned above, when applying high frequency (i.e., 70 kHz and higher) it is important to pay special attention to gears with sharp corners. Due to the electromagnetic edge effect (discussed in Sections 3.1.7 and 7.5.3), high frequency has a tendency to overheat sharp edges and corners. This results in weakened teeth due to

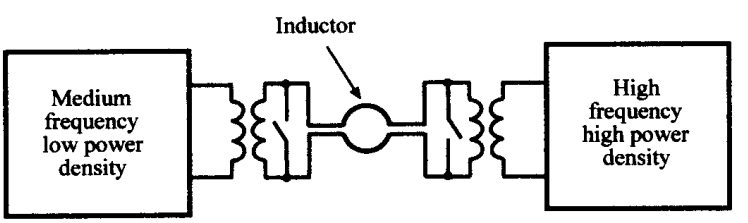

Figure 5.109 Using one coil and two inverters for gear hardening.

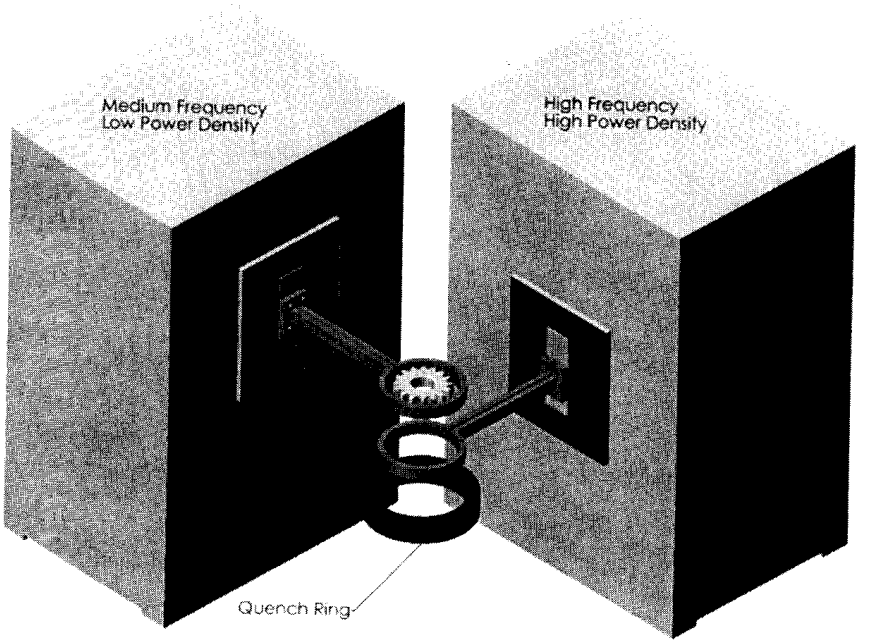

Figure 5.110 One coil is used for preheat and the second coil is for final heat.

decarburization, oxidation, grain growth, and sometimes even local melting of sharp edges. Therefore, in order to improve the life of a gear, the sharp edges and corners should be broken and generously chamfered.

The main drawbacks of the PDFC process are its complexity and high cost, as it is necessary to have two different power supplies. In some cases, it is possible to use one dual-frequency power supply instead of two single-frequency inverters; however, the cost of these variable frequency devices is high, and their reliability is low.

A 4-in. spur gear induction contour hardened using the PDFC approach is shown in Figure 5.111. As one can see from Figure 5.103 the hardness pattern of an induction hardened gear is quite similar to the hardness pattern obtained using carburizing. At the same time, the induction contour hardening process is accomplished in a much shorter time with a much simpler processing procedure. Figure 5.112 shows a comparison of processing steps required for induction heat treating versus carburizing [203, 210, 375].

5.4.4 Lightening Holes

Gears are often produced with holes to reduce the weight of the gear. In induction hardening of gears with internal lightening holes, including hubless spur gears and sprockets, cracks can develop below the case depth in the interhole areas (Figure 5.113). This crack development results from an unfavorable stress distribution during or after quenching. Proper material selection, improved quenching technique, and modification in gear design and/or required hardness pattern can prevent crack development in the lightening hole areas.

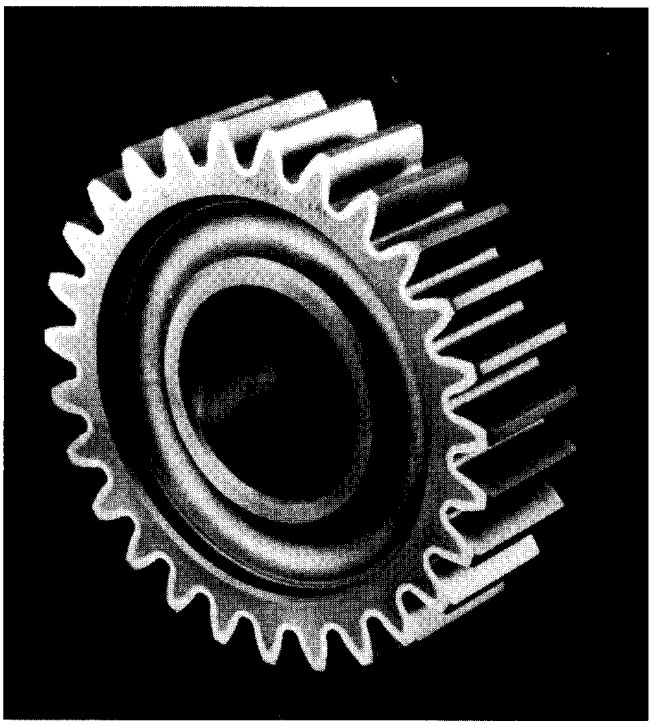

Figure 5.111 Four-inch spur gear contour hardened using PDFC. (Courtesy of INDUCTOHEAT, Inc.)

5.4.5 Powdered Metal Gears

Special attention should be paid when designing induction hardening machines for powdered steel gears. These gears are affected to a much larger extent by variations in the material properties of powdered metals as compared to gears made by casting or forming. This is because the electrical resistivity, thermal conductivity, and magnetic permeability strongly depend on the density of the powdered metal. Variations in the porosity of the powdered steel lead to scattered hardness, case depth, and residual stresses data (see Sec. 5.6).

5.4.6 TSH Technology for Gear Hardening

Impressive results can be achieved not only by developing a sophisticated process, but also by using existing processes with a combination of advanced steels. Through and surface hardening (TSH technology) is a synergistic combination of advanced steels and special induction hardening techniques [376]. These steels were invented by Dr. K. Shepelyakovskii [376] and distributed by ERS Engineering [479]. The new low-alloyed carbon steels are characterized by very little grain growth during heating into the hardening temperature range. They can be substituted for more expensive standard steels that are typically hardened by conventional induction or carburizing.

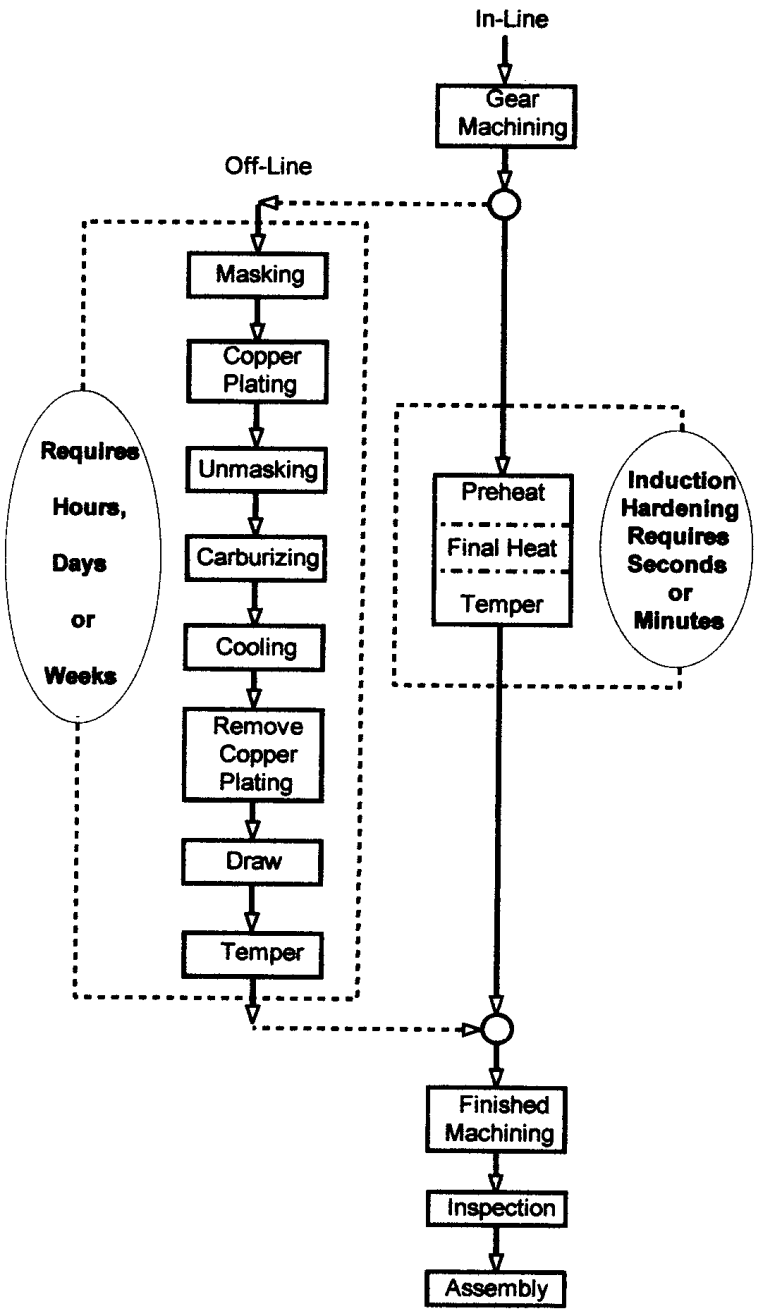

Figure 5.112 Steps required for carburizing versus steps for induction hardening. (From Refs. 209, 210, 375.)

The main features of TSH technology include the following.

- TSH steels are relatively inexpensive, incorporating significantly smaller amounts (3 to 8 times less) of alloying elements such as manganese, molybdenum, chromium, and/or nickel.
- They require a lower induction hardening frequency (1 to 10 kHz), which reduces power supply cost.

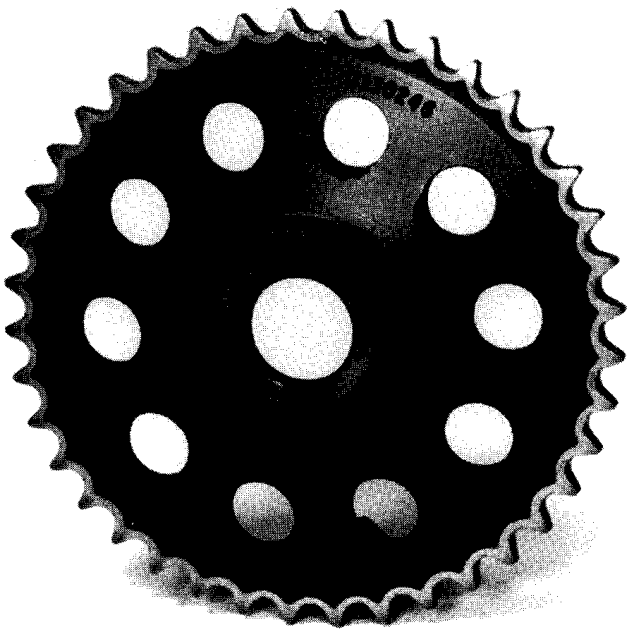

Figure 5.113 Holes in gears can cause unfavorable stress when induction hardening, resulting in cracks. Material selection and quench are important to reduce risk of cracks.

- They exhibit high surface compressive residual stresses (up to 600 MPA/85 ksi).
- The hardened depth is primarily controlled by the steel's chemical composition and initial microstructure. This makes the heat treating process repeatable and robust.
- They exhibit fine grain size (see Figure 5.114).
- They show a reduced chance of overheating part edges and sharp corners due to end effect.

Figure 5.115 shows an induction heat treated gear made from TSH steel. One of the unique features of that gear is that instead of using a two-step approach (first OD heat and then ID heat or vice versa) that gear has been heated and quenched in a single step using only one inductor. OD and ID teeth have fine-grained martensite with a hardness of 62 HRC. The microstructure of the core is a combination of very fine perlite and bainite having a hardness of 30 to 40 HRC.

TSH technology gears are stronger and more durable than some made of conventionally heat treated standard steels. Typical applications include gears, bushings, shafts, bearings, and coil and leaf springs [376, 377].

5.5 TEMPERING

Tempering is performed after steel is hardened, but it is still an important metal heat treatment process.

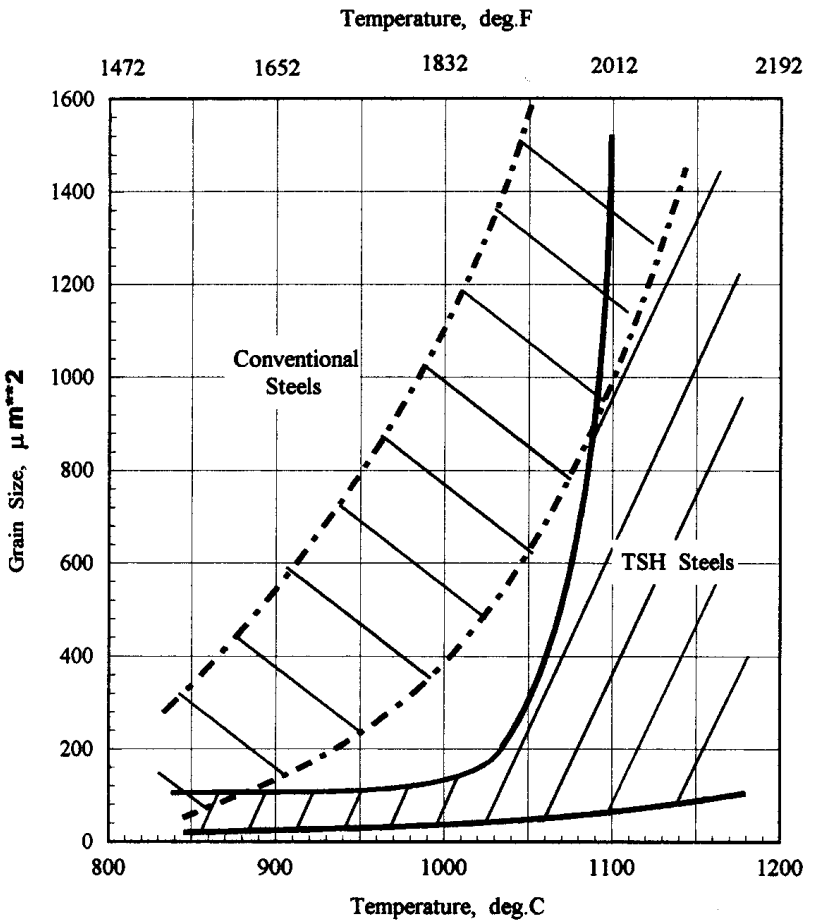

Figure 5.114 Grain growth for TSH steels versus that of conventional grades [376].

A variety of microstructures and mechanical properties of steel can be produced by tempering. The main purposes of tempering are to increase the steel's toughness and ductility, to relieve internal stresses, to eliminate brittleness, and, in some cases, to improve shape stability and homogenization [2, 6, 12, 151, 153, 203, 243, 257, 259, 383].

The transformation to martensite through quenching creates a very hard and brittle structure. This untempered martensite is typically too brittle for commercial use because it promotes notch sensitivity and crack development. It is also characterized by a high level of internal residual stresses. Reheating of the steel for tempering after hardening decreases or relaxes these stresses and produces a tempered martensite microstructure. In other words, by tempering it is possible to improve the mechanical properties of the workpiece and reduce stresses caused by the previous hardening stage without losing too much of the achieved hardness. Tempering temperatures are always below the lower transformation temperature (the A_1 temperature). The induction hardened steel parts shown in Figure 5.116 are all good candidates for induction tempering.

A conventional way of tempering is to run the parts through a tempering furnace (gas-fired or infrared), which is typically located in a separate production area and therefore requires extra space, labor, and time for part transportation.

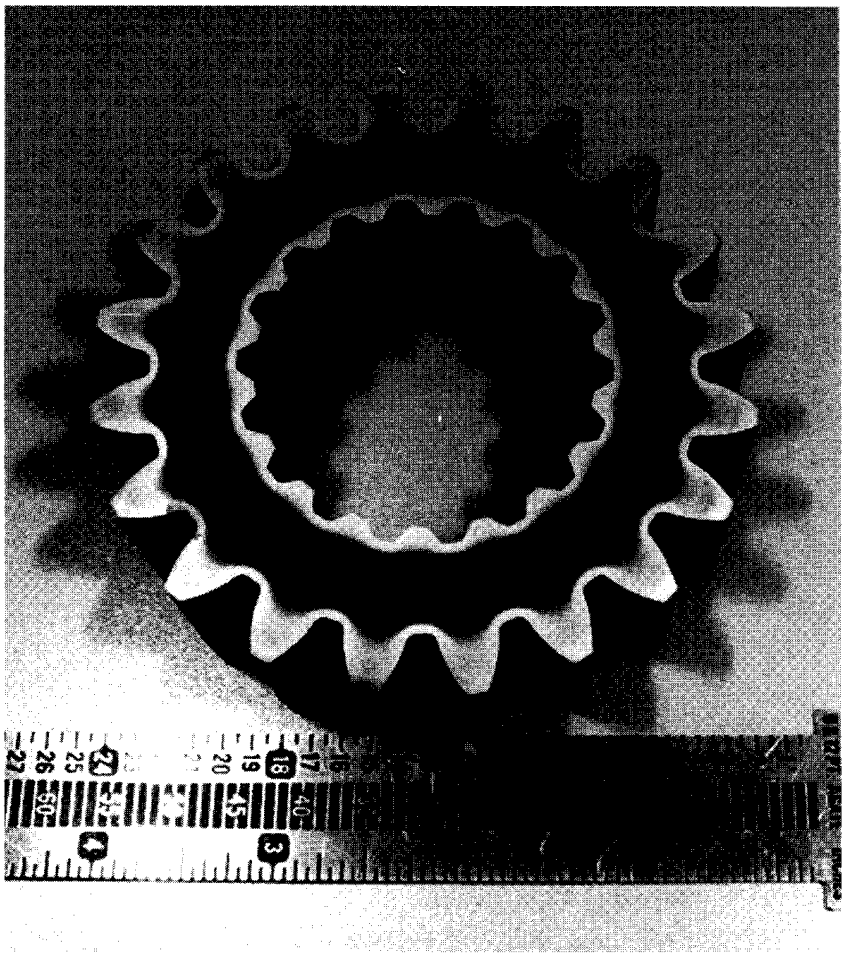

Figure 5.115 Induction heat treated gear made from TSH steel.

Tempering in the furnace is a time-consuming process that may take two to three hours. Short-time induction tempering was developed to overcome these drawbacks.

Time and temperature are two of the most critical parameters in short-time induction tempering. However, temperatures higher than those used for furnace tempering must be used to provide a similar effect. There are several ways to determine the time–temperature correlation between conventional long-time, lower-temperature furnace tempering and short-time, higher-temperature induction tempering, including, for example, the Hollomon–Jaffe equation, the Grange–Baughman tempering correlation, and modifications of these correlations created by Semiatin and coworkers [6, 385, 386].

Most correlations were derived by the tempered hardness estimations obtained from different time–temperature cycles. It has been found that time–temperature parameters are correlated in a logarithmic form of $T(C + \log_{10} t)$, where T is temperature in degrees Kelvin, C is a material constant, and t is the time in seconds. For plain and low-alloyed carbon steel, values of a material constant C are between 10 and 20, depending upon the particular metal. Figure 5.117 shows a time–temperature correlation for furnace tempering versus tempering by induction.

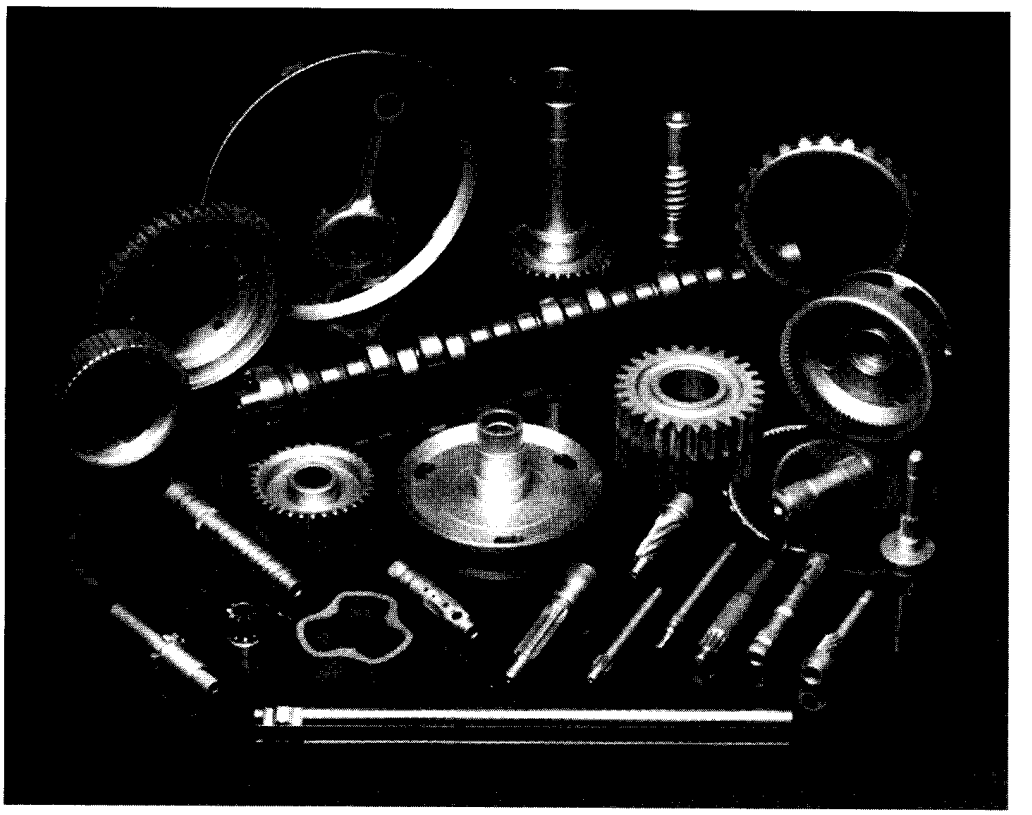

Figure 5.116 Induction hardened steel parts that are good candidates for induction tempering. (Courtesy of INDUCTOHEAT, Inc.)

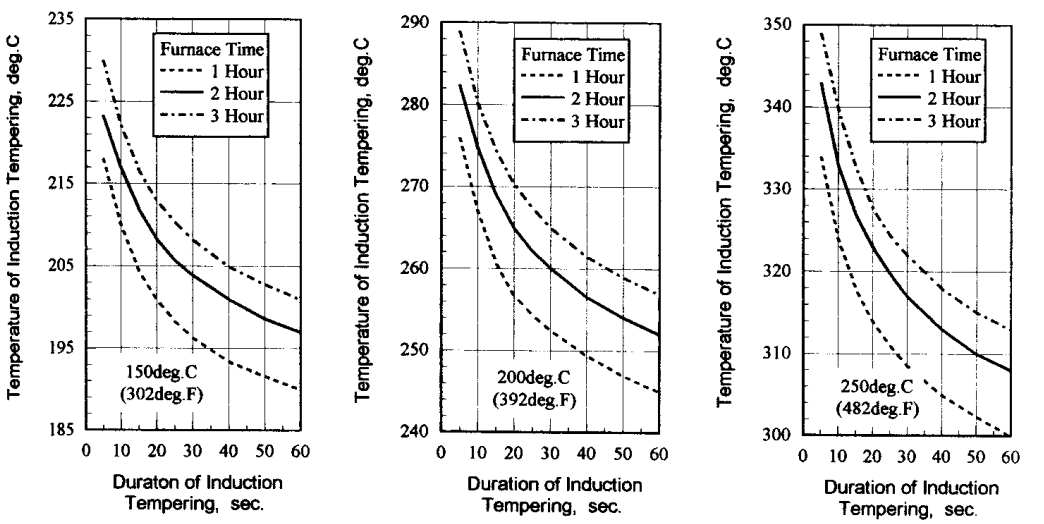

Figure 5.117 Time-at-temperature for oven versus induction temper.

Although the determination of parameters for an induction tempering process might look straitforward, it should be understood that the above-mentioned correlations can serve as a rough estimate only because there are several factors which could shift the curves shown in Figure 5.117. Some of these factors are: the chemical composition of the steel, the microstructure prior to tempering, the grain size, the hardness profile prior to tempering, the heating rate, temperature gradients, and the cooling rate following the induction tempering. The last factor is often one of the most important ones. In addition, it is frequently overlooked when determining tempering parameters.

Induction tempering is a continuous process of heating and subsequent cooling (soaking). Therefore metal tempering conditions are affected by both stages: heating and cooling. Although the maximum tempering temperature is achieved at the heating stage, the cooling stage is typically much longer (unless intensive water-cooling is used immediately after heating). Because tempering is a function of both parameters, time and temperature, both factors will affect the metal tempering conditions.

The time required for induction tempering of case hardened parts is typically two to four times that of induction hardening. There are some rare cases of tempering thin parts [i.e., strips and plates with thickness less than 1.6 mm (1/16 in.)] where tempering time might be equal or even less compared to heat time for hardening.

Tempering is always a reasonable compromise between maintaining the required hardness and obtaining low stress, with tough and ductile microstructure in the metal. Induction tempering temperatures depend upon the application and are usually in the range of 120°C (248°F) to 600°C (1112°F). If the carbon steel is heated to less than 100°C (212°F), there is no change in microstructure, and no induction tempering will occur. Low-temperature tempering of carbon steels typically occurs at 120°C (248°F) to 300°C (572°F). The main purposes of low-temperature tempering are stress relieving and generation of tempered martensite. The hardness reduction in this case typically does not exceed 1 to 3 points HRC.

If carbon steel is tempered at above 600°C (1112°F), practically all of the residual stresses existing in the part will be removed and significant changes in microstructure may result that can lead to a significant loss in hardness. The hardness reduction may exceed 15 points HRC, and the maximum hardness may drop to 36 to 44 HRC. Note that tempering an alloyed steel at above 600°C (1112°F) may not result in a significant hardness loss.

There is always a balance of residual stresses in the workpiece. If in certain areas of the part there are compressive residual stresses, then somewhere else within the workpiece there must be tensile stresses. As mentioned above, surface compressive residual stresses are usually considered to be beneficial. They provide protection against the propagation of cracks caused by microscopic scratches and delay fatigue cracking, and improve the performance of parts that experience bending and torsional stresses during service.

It is imperative to note, however, that a maximum tensile residual stress is located just beneath the hardened case (see Figure 5.86). This is a zone of potential danger, where most subsurface cracks initiate because the applied stresses are maximum at the part surface and then drop off. Therefore, one of the important "duties" of tempering is not only the reduction of tensile stresses, but also the shifting of the maximum of these stresses toward the core away from applied tensile stresses.

Tempering is needed to relieve some of these stresses, ideally, to remove or substantially reduce subsurface tensile stresses, while retaining the beneficial surface compressive stresses.

Tempering does make iron and steel more ductile, reducing the possibility of cracking. However, it is important to minimize the time between the quench and temper operations. Too long a delay or "transient time" may allow residual stresses to produce distortion and/or cracking, which would reduce or eliminate the benefits of tempering. This is why it is important to keep transition time under two hours.

It is imperative to mention here, that for plain carbon and low-alloy steels, an increase in tempering temperature results in consequent reduction of the hardness (Figure 5.118, top). However, it might not be true for some alloy steels, thanks to the phenomenon of a temper embrittlement or "secondary hardening" (Figure 5.118, bottom) [6, 14, 21].

Basically, there are two ways to temper in induction processing: self-tempering, where residual heat in the part is exploited, and induction tempering, where the hardened part is reheated for tempering.

5.5.1 Self-Tempering ("Slack Quenching")

The principle of self-tempering after induction hardening is illustrated using the example discussed in Section 5.1.2.1 (Figure 5.55). During the initial stage of induction heating, an intensive heating of the surface layers takes place. As shown in

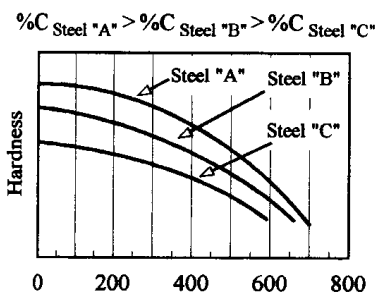

A). Plain carbon steel and low alloyed steel

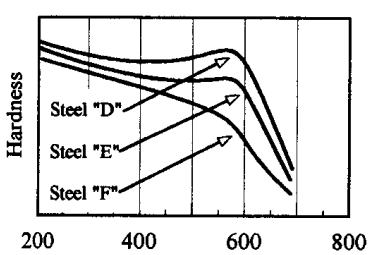

B). Alloyed steel

Figure 5.118 Hardness versus tempering temperature.

Figure 5.55, after 5 sec of induction heating the surface reaches the required final (hardening) temperature, which is a function of the material being processed and heat intensity. The temperature at the center of the part, however, does not increase significantly, for several reasons, including skin effect, high power density, and short heating time. The time is insufficiently long to allow much heat to be conducted from the surface to the core of the cylinder.

During the initial quenching stage, the high temperature of the surface layer will begin to fall. After 2 sec of spray quenching, the surface temperature will be drastically reduced. The maximum temperature of the part will be at some distance beneath the surface. However, note that the temperature at the center of the part will increase because more time is allowed for heat conduction.

After 6 sec of quenching, the surface temperature has decreased almost to that of the quenchant, but a considerable amount of heat is still retained in the interior of the cylinder (the temperature at the core exceeds 400°C/752°F). If at this moment the supply of quenchant is cut off, the surface of the part will begin to be heated again due to the accumulated heat inside the workpiece. And after a certain time, the surface temperature will increase to a value higher than it was when the quench was turned off (see the "self-tempering" curve in Figure 5.55). With proper selection of quenching conditions, this retained heat can be used to temper the workpiece. Self-tempering temperatures typically do not exceed 260°C (500°F) to 290°C (554°F) and are usually in the 210°C (410°F) to 240°C (464°F) range.

Several precautions must be taken to ensure that the self-tempering process is performed correctly. The energy introduced to the part and the heating time must be monitored to ensure a constant amount of residual heat. Quench flow, quench time, and quench temperature also should be monitored and held within close tolerances to ensure a consistent surface temperature after reheating of the part. In many cases an infrared pyrometer is used to monitor the surface tempering temperature.

It is easy to use self-tempering if the part has a large mass and single-shot induction hardening is applied. Self-tempering is more difficult to apply if the part has a complex shape or is scan hardened, because core temperatures will vary over the length of the part. The amount of heat stored as well as the heat sink beneath each section of the hardened case must be the same; otherwise, the temperatures obtained after the heat soak will be different and the result of the self-temper will be unacceptable.

In some applications, a quench–soak cycle can be used to obtain special properties and microstructures. This multistep method consists of a heatup, first quench, first self-temper, second quench, and final self-temper.

5.5.2 Induction Tempering and Its Features

The induction tempering method can be applied to those parts that cannot be self-tempered. There are several major questions to answer when determining the parameters of the induction tempering process:

1. The mode of induction tempering,
2. Coil design, and
3. Frequency/power selection.

Since tempering temperatures are always below the Curie point, the workpiece is always magnetic and the induced eddy currents heat the part not only due to the Joule effect. However, there will be an appreciable amount of heat generated by hysterezis losses as well.

There are three modes of induction tempering: single-shot, scanning, and progressive. When the same coil is used for hardening and tempering, the tempering mode matches the hardening mode. Otherwise, the progressive mode is typically used.

5.5.2.1 Coil Design and Process Parameters

It is possible to harden and temper parts in the same coil using the same power supply. In some cases, it is the best concept and has an obvious low capital cost advantage and less tooling to store. In other cases, it might not best suit customer requirements. There are several reasons why in a great majority of cases, the same coil (inductor) is not used for both hardening and tempering.

- In induction hardening, to obtain the required hardness pattern for a workpiece of complex shape (e.g., gears, CV joints, etc.) it is necessary to redistribute the electromagnetic field so as to introduce more energy in certain areas.
- The power densities used during hardening are much higher than those used for tempering. In tempering, it is necessary to heat the surface at a much lower rate to obtain a "gentle" temperature gradient from the heated surface to the case depth. Too high a power density could cause the surface temperature to exceed the optimum tempering temperature, which would result in an unacceptably soft surface.
- Depending upon the type of power supply, load-matching problems might occur when trying to run at very low power levels on an inverter designed for a hardening application.
- Unlike coils used for induction hardening, temper coils almost never require the use of magnetic flux concentrators, because there is no essential gain in coil efficiency in low-temperature tempering applications and there could be a decrease in efficiency.
- It is often preferable to use a lower frequency for tempering because the tempering temperatures are always below the Curie point. As a result, the heated part retains its magnetic properties and the skin effect is pronounced. In addition, the relative magnetic permeability of steel during induction tempering is more than 10 times higher than the permeability of steel even during the magnetic stage of induction hardening. This takes place because the power densities used in induction hardening are much higher than the power densities used during induction tempering, resulting in much lower magnetic field intensities used for tempering as compared to hardening (Figures 5.119 and 5.120). Therefore, the magnetic permeability of steel/iron during the tempering stage (due to low magnetic field intensity) is much higher than the magnetic permeability during hardening (which has relatively high magnetic field intensity) for the same grade of metal using the same frequency. This results in a noticeably smaller eddy current penetration within the workpiece for tempering as compared to the depth even

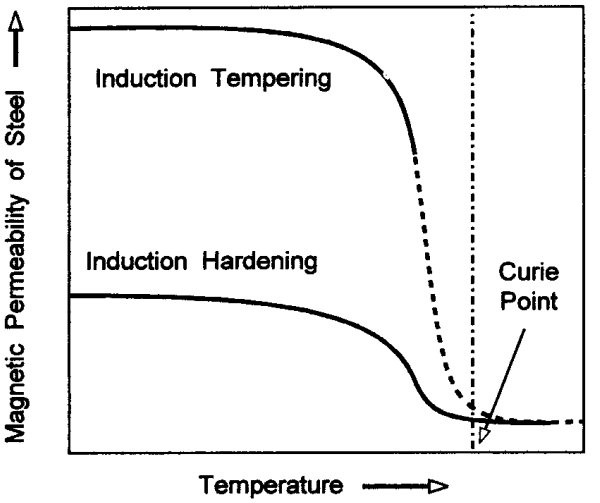

Figure 5.119 Magnetic permeability versus temperature.

during the magnetic stage of hardening. For example, during the magnetic stage of hardening applications (at temperatures of 400°C (732°F) to 500°C 932°F), the relative magnetic permeability, depending upon the application, is typically within a range of 6 to 18. During induction tempering the relative magnetic permeability at the same temperatures for the same grade of metal heated with the same frequency, is within a range of 40 to 150 depending upon the application. In some cases it can even be higher. Therefore, in order to heat a part for tempering to the same depth as hardening, it is wise to use a lower frequency.

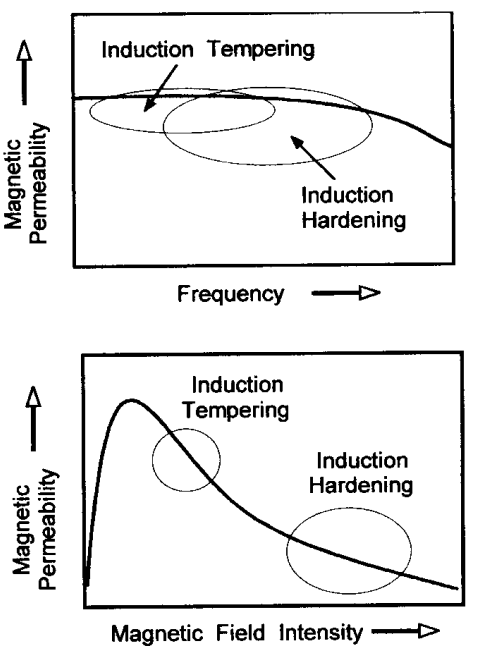

Figure 5.120 Magnetic permeability versus frequency and magnetic field intensity.

- As shown in Figures 5.119 and 5.120, both the frequency and magnetic field intensity used in induction tempering result in a much higher permeability, compared to the value during induction hardening. Therefore to increase the current penetration depth in the part during induction tempering, it is more effective to use a lower frequency. (The typical induction coil designed for hardening at a high frequency would be likely to perform poorly in a low-frequency tempering operation, and vice versa.)
- In addition, it is highly recommended that the temper inductor should not heat only the selected hardened area but a much larger region or even the entire workpiece. A loosely coupled multiturn coil can be used for this purpose.
- The time required for induction tempering of case hardened parts is typically two to four times that of induction hardening. The production and power supply utilization might suffer if the same coil were used for hardening and tempering.
- Heating for tempering with a separate coil and dedicated power supply is a more costly solution from a capital investment point of view, but at the same time, it has several noticeable advantages. The current distribution and power density can be optimized specifically for the tempering operation. A separate, loosely coupled, encircling or channel-type, single- or multiturn coil can be used effectively for this purpose. Equipment can be used very effectively for high production: one hardening machine can operate in conjunction with two or three tempering machines.

There is a common misconception that low-temperature tempering removes all internal residual stresses. It does not. However, it significantly decreases those stresses. It also shifts the location of the potentially dangerous, maximum tensile residual stresses farther away from the surface and the applied loads. In as- hardened steel or cast iron, the tensile stress maximum is typically located just beneath the hardened case (Figure 5.86).

Tempering is a diffusion-type process, therefore the time needed to complete it is much longer than that for hardening and quenching. It may take seconds to induction harden a part but tens of seconds or even minutes to induction temper it.

To induction temper complex-shaped parts (e.g., gears or other critical components), the choice of frequency, power density, and coil geometry is dictated by the need to apply enough energy to certain areas of the component. For example, in gear tempering, the challenge is to induce a sufficient amount of energy into the root of the tooth without overheating its tip.

The root is the most critical area of a gear because that is where the maximum concentrations of both residual and applied stresses are located. As a result, fatigue cracks and distortion occur primarily in the root area. This is why the root area is a primary target of induction tempering for stress relief. However, several factors complicate this task. Two factors are similar to hardening and were discussed above.

- One of them deals with poor electromagnetic coupling between the encircling-type coil and the tooth root compared with the tooth tip. This makes it more difficult to induce energy in the root.
- A second factor deals with the existence of the heat sink phenomenon in the root. There is a significantly larger heat sink located under the gear root (under the base circle) compared to the tooth tip.

- The third factor derives from the fact that the tempering temperatures are always below the Curie point. Therefore, the gear is magnetic and the skin effect is always pronounced (Figure 5.119). This results in a power surplus in the tip of the tooth compared to that in the root. In addition, the use of high frequency for induction tempering will result in more power in the tip of the tooth compared to the root and there will be a tendency to overheat edges, sharp corners, and areas that have better coupling with the inductor. In order to overcome these difficulties, low frequency, loose coil coupling, and low power density should be used for tempering.

As discussed above, it is possible to harden and temper gears in the same coil using the same power supply. In some cases, it is the best concept (particularly for fine tooth gears) and has an obvious low capital cost advantage and less tooling to store. In other cases, it might not best suit customer requirements.

In order to overcome the above-mentioned difficulties, induction equipment manufacturers have created several new design concepts that have resulted in the development of advanced induction gear tempering machines.

Two examples of induction tempering of complex-shape parts are shown in Figures 5.121 and 5.122. The part shown in Figure 5.121 has been hardened on a portion of its inside surface. This is the type of application in which induction tempering is most effective. The tempering coil is positioned around the part, so that the temperature can slowly increase from the outside surface toward the hardened (shaded) layer on the inside. Proper energy/temperature control enables tempering without overheating the hardened region of cross-groove disks (Figure 5.122).

A tempering coil of similar design can be applied to a hollow part that has been hardened on its outside surface. In this case, however, the coil is positioned inside the hollow center of the workpiece.

The spindle in Figure 5.123 requires a special tempering coil that will allow a predetermined amount of energy to be induced into each hardened section, so that all sections are heated to the same required tempering temperature. Because of the wide variation of mass distribution in this part, an inductor designed to heat only the hardened case (as was used for hardening) is not recommended.

Because of the different heat sink effects, the inductor also should induce heat into areas that have not been hardened, such as the flange. These areas will serve as a heat buffer and may even be heated to slightly above the tempering temperature. Note that heat also will be induced into the transition zone beneath the case, where the tensile residual stresses are at a maximum.

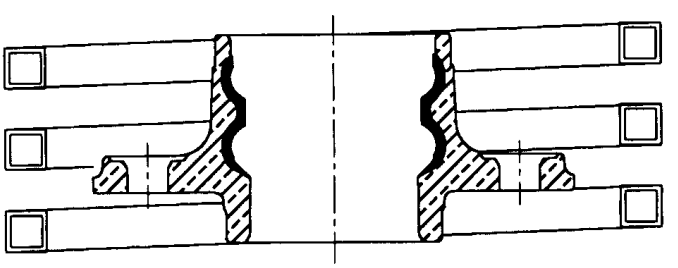

Figure 5.121 Induction tempering of part hardened on the inside.

(A)

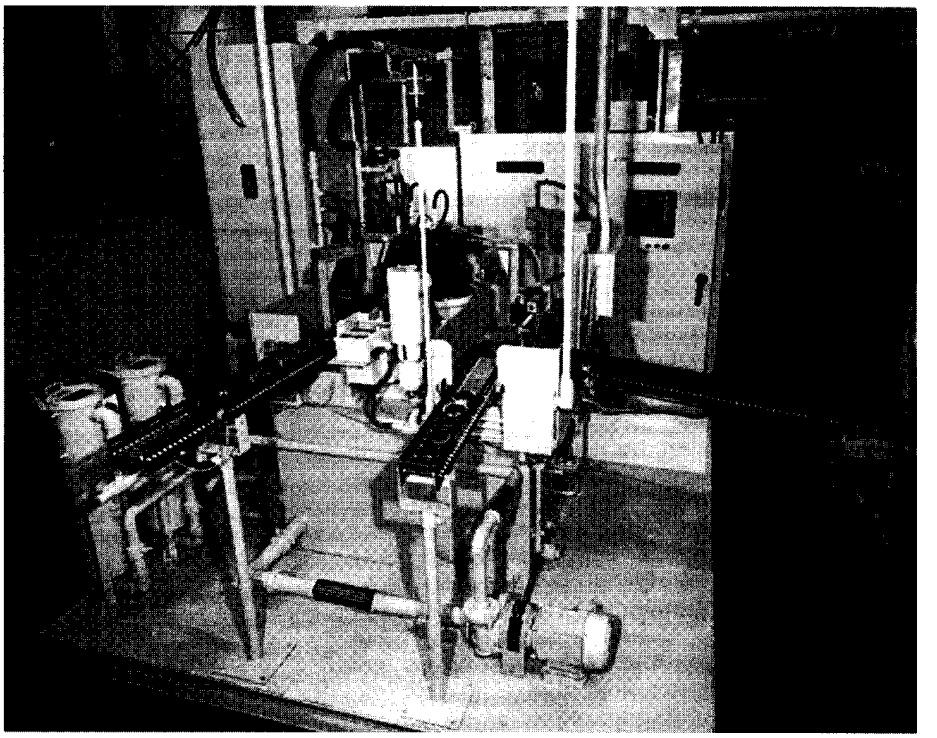

(B)

Figure 5.122 (A) Induction equipment for complex-shaped parts; (B) parts heated (for temper) from the outside, with hardness pattern on the ID.

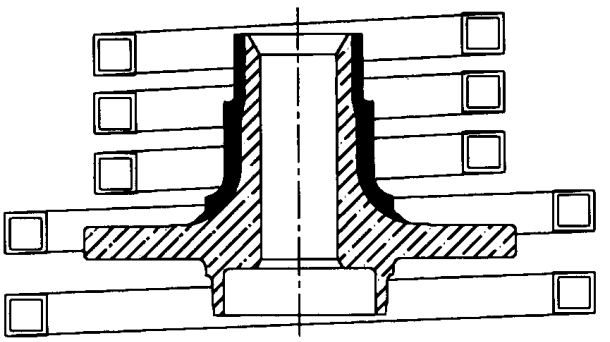

Figure 5.123 Induction tempering of part hardened on the outside.

Because the temper inductor is loosely coupled to the workpiece, the heating of hard-to-reach areas is facilitated. Its coils also lightly heat even edges, grooves, and other critical regions of a part. Through heating of a part without overheating its surface is possible by adopting a heat–soak cycle.

Figures 5.124 and 5.125 show a channel inductor used to temper a variety of parts having complex shapes and mass distributions such as CV joints, which are hardened both inside the bell and on the outside of the shaft (Figure 5.36).

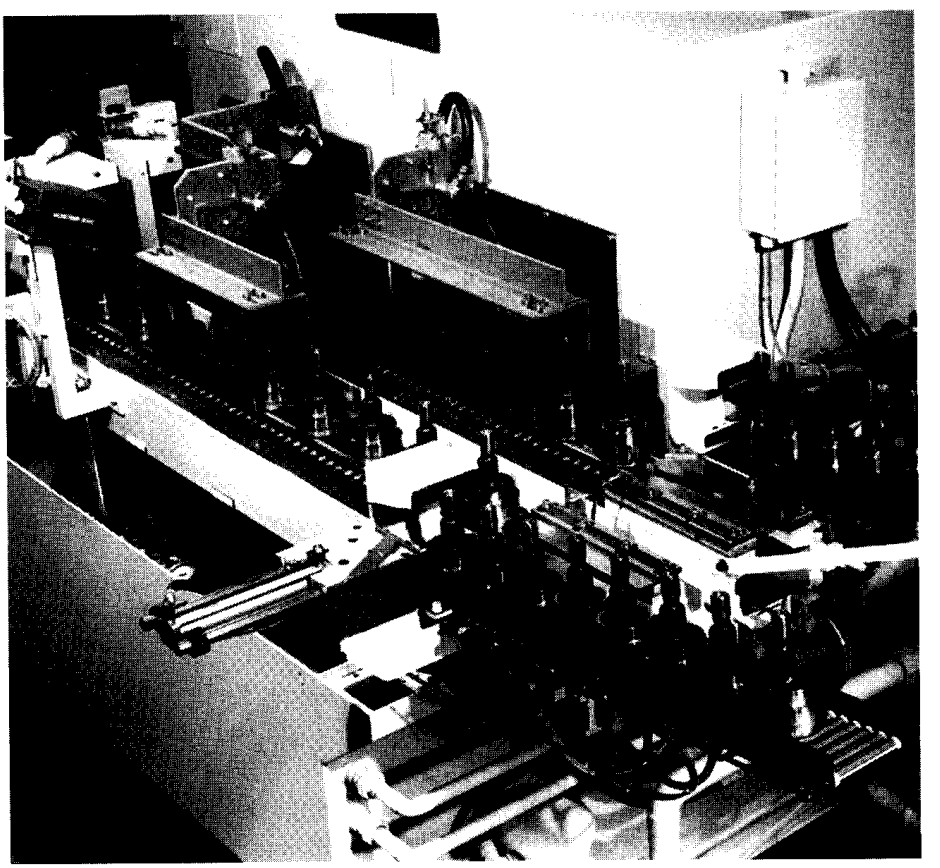

Figure 5.124 Channel inductors are used to temper a variety of complex parts.

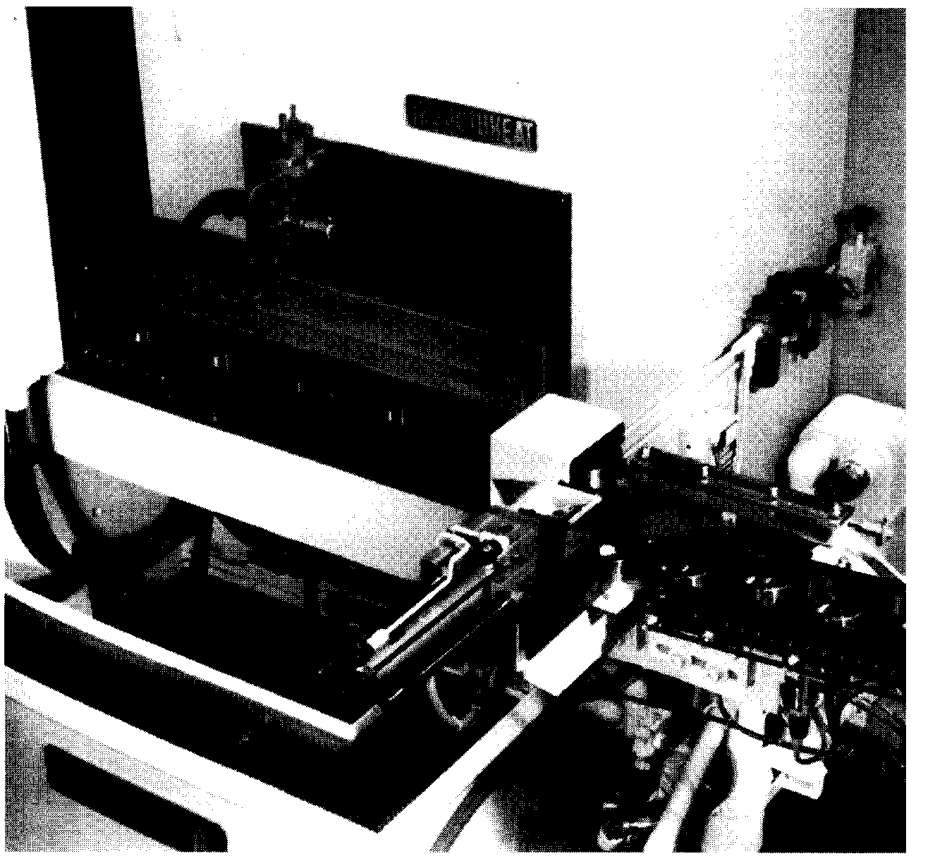

Figure 5.125 Single-turn inductor used to temper cross-grooved parts.

As a rule of thumb, the heating time for tempering is at least twice the hardening cycle time (heating plus quenching). This means that an induction heat treating machine can have one station for hardening (heat and quench) and two stations for tempering. The indexing time between the two tempering stations acts as a soak.

A cooling cycle may follow the completion of the tempering. The cooling station can be incorporated in the tempering machine, or separately on an exit conveyor. Use of a separate cooling station reduces the complexity of the tempering machine. The correct process parameters for induction tempering can be found by hardness measurements and by microscopic evaluation of the part's microstructure.

5.5.2.2 C-Core Tempering Inductors

Figure 5.126 shows some variations of one of the oldest coil designs for induction tempering. It is a C-core tempering coil. The induction heater consists of a typical transformer-type design with one or several C-shaped magnetic cores. Laminated low-carbon steel thin sheets are used for core fabrication. One or several multiturn induction coils are wound around the C-core to create the common magnetic flux. The intensity of heating of the C-core inductors depends upon the strength of that magnetic flux.

Due to some known limitations these types of heaters are not as popular and not as widely used as the inductors shown in Figures 5.121 to 5.125. There are still

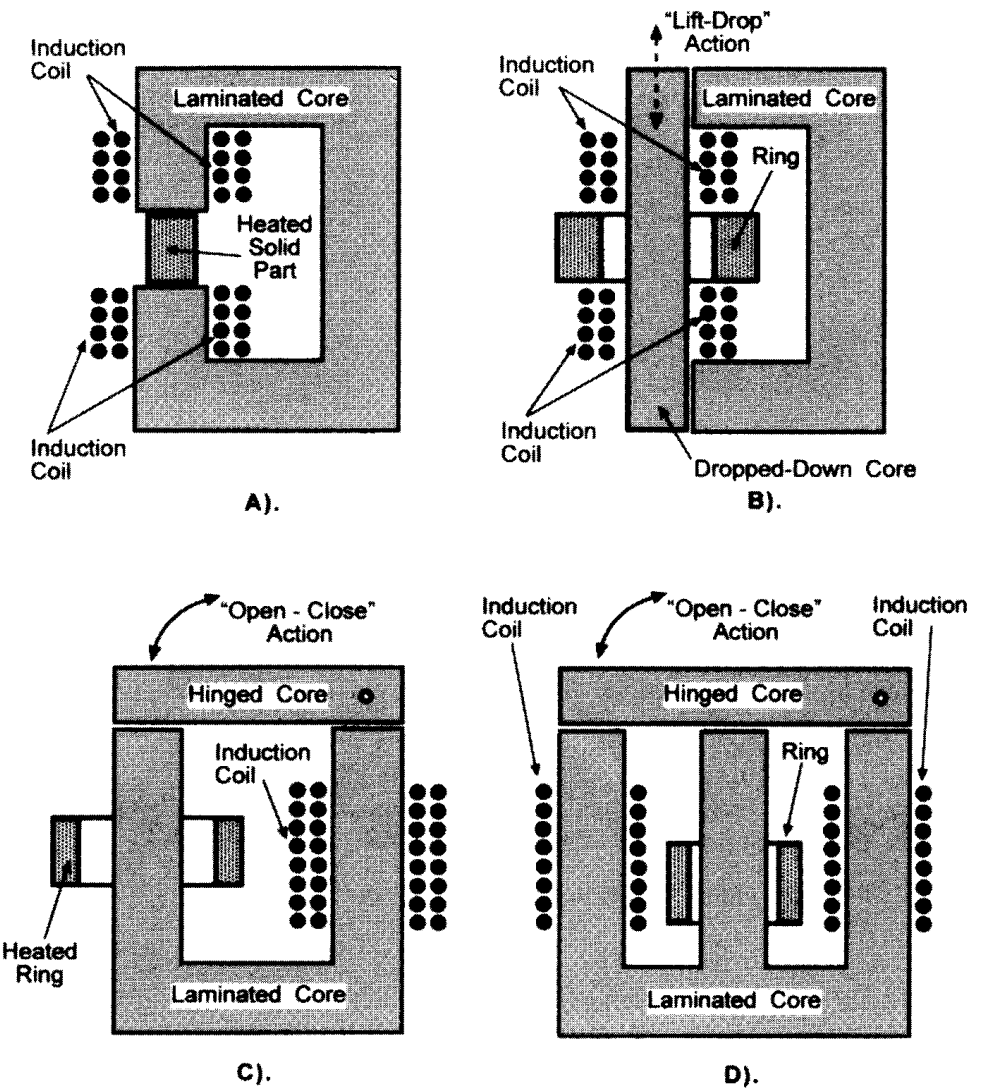

Figure 5.126 Some design variations of C-core coils for induction tempering applications.

quite a few induction applications, including shrink fitting and tempering of steel/cast iron solid and ring-shaped parts where these types of inductors can be used quite effectively.

There are certain approaches to using this technique, the first dealing with the induction heating of solid workpieces. With this approach, a part is located within the open space of the C-shaped core (e.g., see Figure 5.126A). Therefore the heated part becomes part of the magnetic circuit. The major portion of the magnetic flux induced by the multiturn coils and diverted by the magnetic core will close the magnetic loop through the magnetic workpiece. As the workpiece is magnetic and is not laminated the induced eddy currents will heat it quite effectively due to the Joule effect. In addition, considering the fact that the workpiece is in a magnetic state, there will be a substantial amount of heat generated by hysteresis losses as well as in the inductors shown in Figures 5.121 to 5.125, or any other induction application where the heated workpiece is magnetic.

Among other factors the effectiveness of C-core coils depends upon the gaps between the core and workpiece. Smaller gaps result in higher efficiency. To ensure minimum gaps special clamping devices are applied.

The second approach to using C-core inductors is applicable to the ring/tube-shaped parts that are placed around a certain portion of the core (see Figure 5.126B, C, and D). In this case, the heated part represents the secondary winding of a transformer.

Both approaches apply low frequency (single- or multiphase). The most commonly used frequencies are in the range of 50 to 500 Hz. Higher frequencies lead to a reduction of the electrical efficiency of the induction system due to the high losses in the laminated C-core.

Figure 5.127 shows a plot of the electromagnetic field of a C-core inductor for induction heating two different workpieces: a solid cylinder (i.e., carbon steel billet, 60 mm OD, 100 mm long, Figure 5.127A to D) and a ring/tube-type workpiece using line frequency.

Figure 5.127B and C shows a plot of the magnetic field lines when a carbon steel cylinder is in a magnetic state (below the Curie temperature). Figure 5.127C is a magnified version of the magnetic line distribution within the magnetic billet shown in Figure 5.127B. Figure 5.127D shows the magnetic field distribution when the workpiece is in a nonmagnetic state.

Because the temperature range of all tempering applications is below the Curie point, the carbon steel/iron workpiece is always magnetic and as shown in Figure 5.127B and C it acts as a continuation of the C-core. Actually, instead of the C-shaped core there will be an O-shaped core. It is much easier for magnetic flux to complete its loop through a magnetic body of the heated workpiece than through the air. This is why a majority of the magnetic flux lines pass through the workpiece. There is a negligible amount of leakage flux.

Pneumatic and hydraulic clamps are used in order to ensure a minimum air gap between the billet's buttends and the C-core faces, which in turn provide a high inductor electrical efficiency.

The C-core consists of numerous laminated carbon steel plates. Laminations should be thin enough from an electromagnetic point of view. For low-frequency applications, individual lamination is typically 0.2 to 0.5 mm thick. Because laminations are electromagnetically thin, there will be a current cancellation of eddy currents induced in each lamination (see Figure 5.128A) and, therefore, the Joule losses will be small enough and will not generate a large amount of heat.

Practically the same magnetic flux conducted by the laminations will be conducted by the magnetic workpiece. However, the workpiece is electromagnetically thick and will not experience current cancellation. Therefore, due to Joule and hysteresis losses there will be a significant amount of heat generated within the workpiece and the workpiece will be heated quite effectively.

It should be mentioned here that from an electromagnetic point of view there is practically no difference between the conventional induction heating of billets using a solenoid coil or the C-core inductor. In both cases it is possible to observe similar electromagnetic effects, including skin and end effects (Figure 5.127B and C).

The use of line or low frequency results in larger eddy current penetration depth into the heated part and, therefore, in a smaller surface-to-core temperature difference compared to using medium or high frequencies.

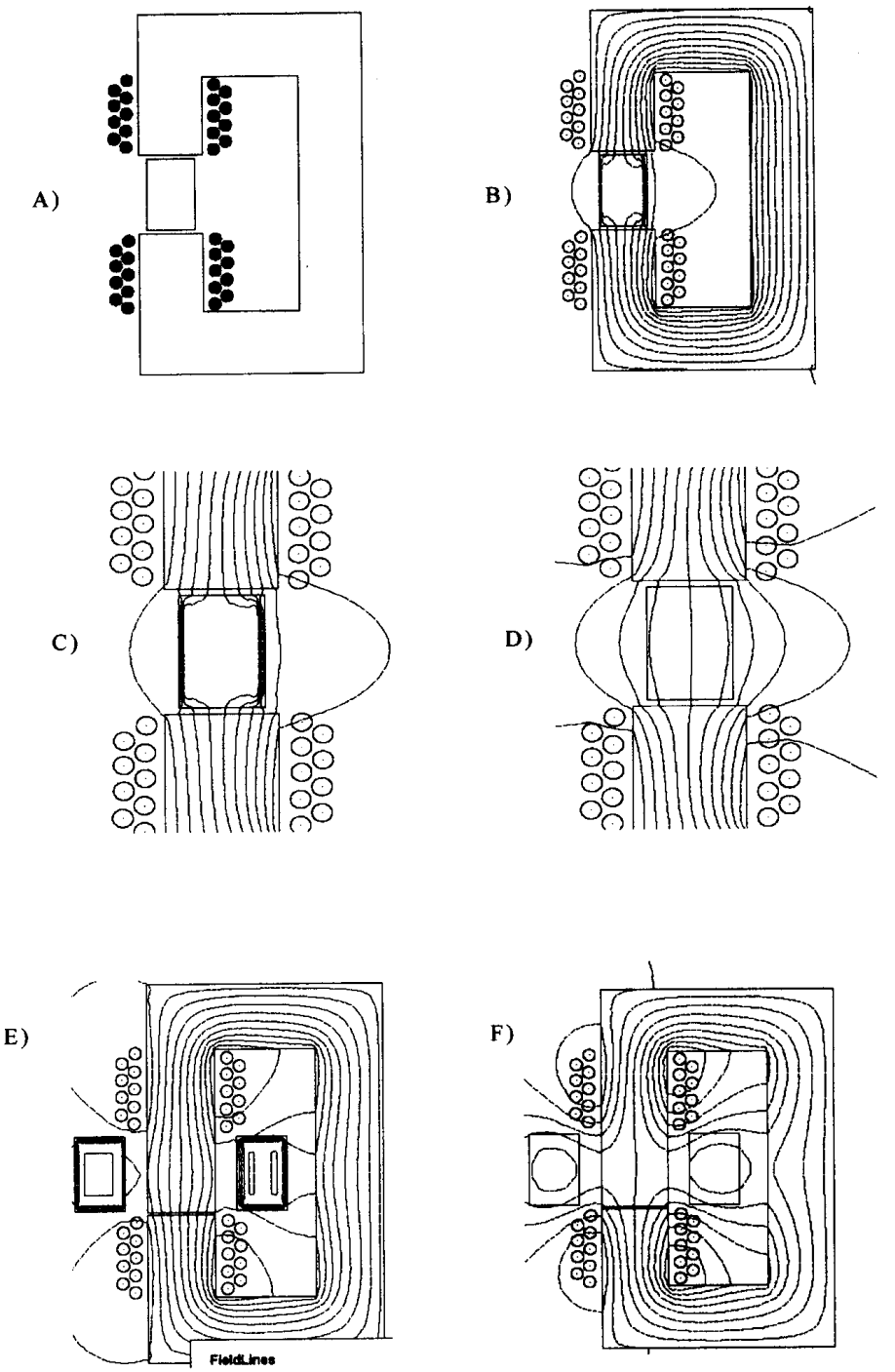

Figure 5.127 Plots of electromagnetic field of C-core inductor.

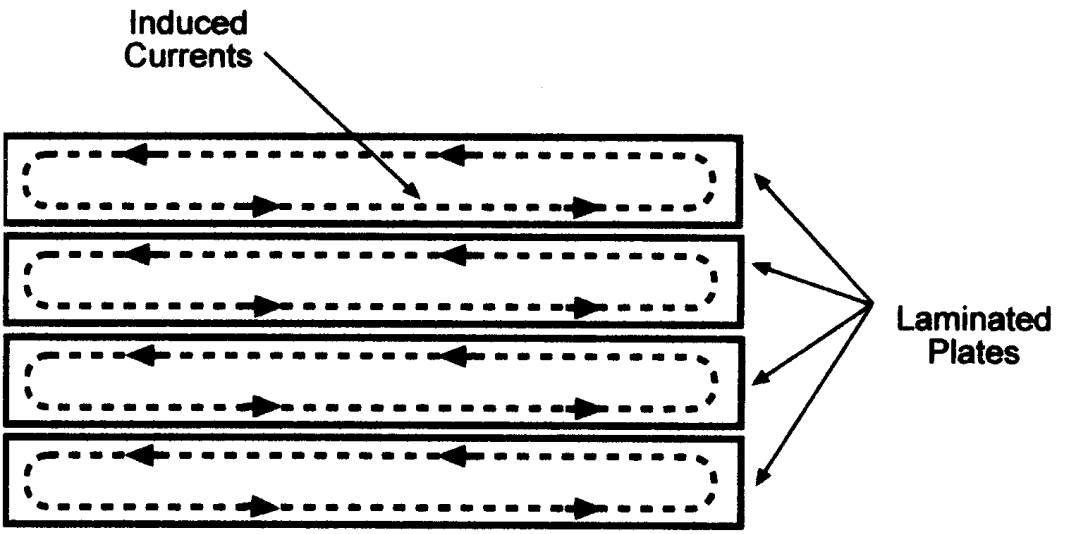

Figure 5.128 Eddy current distribution within laminations.

Note that occasionally there are some attempts to heat billets to higher temperatures than the temperatures of the tempering range. This includes induction billet heating from an ambient temperature to temperatures of forging and rolling applications. Some of these applications are discussed in Section 7.5.

Figure 5.127D shows the magnetic field when heating a nonmagnetic billet in a C-core inductor. As one can see, a nonmagnetic cylinder cannot conduct a magnetic field the same as a magnetic body. Figure 5.127D shows that when the workpiece is in a nonmagnetic state, there are fewer magnetic lines crossing the part, meaning a noticeable increase of magnetic flux leakage and a significant reduction of both the heat intensity and electrical efficiency of the inductor. The taller the nonmagnetic billet and the larger the air gap between the billet's buttends and the C-core faces, the lower is the efficiency of the C-core inductor.

As in the case of induction heating with a conventional solenoid coil, the electromagnetic end effect when using a C-core inductor varies depending upon whether the workpiece is in a magnetic or nonmagnetic state.

A C-core inductor can be used for heating both magnetic and nonmagnetic ring/tube-shaped parts. Practically all the features discussed above with respect to the induction heating of magnetic/nonmagnetic solid cylinders hold true when heating ring/tube-shaped parts in a C-core inductor. For example, it has been reported that it took 5 min to uniformly heat a carbon steel tube (140 mm OD, 100 mm ID, 350 mm long) using line frequency from ambient temperature to the hardening temperature of 1000°C.

The distribution of the magnetic field lines when heating a carbon steel ring/tube-shaped part (Figure 5.126B) in a magnetic state is shown in Figure 5.127E and in a nonmagnetic state in Figure 5.127F. One can conclude from comparison of both figures that, when heating a ring/tube-shaped workpiece, the density of the eddy currents induced on the outside diameter is similar to the density of eddy currents induced on the inside diameter.

This phenomenon might be misleading. People observing the heating process might assume that there is a uniform current density distribution within the ring/tube

wall and therefore temperature uniformity through the wall has been achieved as well. As can be seen from Figures 5.127E and F, there is still a skin effect within a heated ring/tube wall. The eddy current density decreases from the ring outside diameter towards the core and then it begins to increase again as the ring inside diameter is approached.

C-core tempering inductors have several beneficial features. These include

- the ability to use line and low frequencies leads to system simplicity and low-cost power supplies;
- radial temperature gradients are quite small (particularly when heating the ring/tube workpiece);
- the heated part does not need to be rotated;
- the process provides the required temperature uniformity for medium- and large-size (200 mm OD and even larger) ring/tube shaped parts, including ring gears and bearings. Long length/height is typically not a problem. There are cases of heated tubes being as long as 1 m or longer;
- design simplicity;
- high electrical efficiency (typically 85 to 95%); and
- high inductor power factor ($\cos\phi = 0.75$ to 0.85).

The wide utilization of C-core inductors is limited by several shortcomings, such as:

- relatively poor automation capabilities and complication in handling certain types of parts for inline processing;
- ineffective for heating asymmetrical complex-shaped workpieces;
- low production rate;
- large air gaps can result in reduced coil efficiency and temperature non-uniformity as well as local overheating of lamination faces;
- equipment is noisy (85–90 db);
- coils are expensive;
- not suitable for tempering selective areas;
- for solid parts with different sizes/shapes it is necessary to have adjustable laminated ends (inserts); and
- if an inverter is not used there could be problems associated with process control, power factor correction, and phase balancing (when a single-phase inductor is used).

5.5.2.3 Final Remarks on Induction Tempering

The decision to induction temper should be carefully weighed. Studies show that sometimes, regardless of the similar hardness pattern, the properties of the tempered parts subjected to high-temperature/short-time tempering could be different than parts subjected to low-temperature/ long-time tempering.

For example, in a comparison of the properties of carbon steel parts processed with both types of tempering, it has been shown that regardless of the identical hardness (48 HRC) the tempered carbon steel part (0.8% C) subjected to the high-temperature/short-time tempering (30 sec at 465°C) showed three times higher brittle strength compared to a part tempered for 3000 sec at 350°C. The improvement in brittle strength considerably extends the impact toughness. Similar results have been obtained for some alloyed steels, including chromium steels.

One hurdle to the acceptance of induction tempering is that some metallurgists are not comfortable with short-time/high-temperature tempering. They feel that an oven that heats the entire part and holds it at temperature for hours is more reliable.

Although both methods can provide the tempered parts with different properties, it does not mean that one tempering method is better than another. The proof of any production process is how well the part performs in service. The high-temperature/short-time induction tempered part, like any other machine component, should be thoroughly tested and evaluated for reliability.

Fatigue and failure test data for induction and furnace tempered parts should be compared. It is important to remember that the surface tempering temperature alone is not a valid indication of proper tempering.

If tempering has been done correctly, there will be only a slight reduction in hardness, which will be more than offset by the benefits obtained: internal stress relief, improved ductility or toughness, shifting of the dangerous maximum of tensile stresses farther away from the applied stresses, and improved machinability. Other benefits of inline induction tempering may include single-part processing, savings in investment cost, environmental friendliness, low floor space requirements, maintenance and labor savings, high energy efficiency, and precise control and monitoring.

Figure 5.129 shows a new generation of compact inline induction tempering machines. Such systems are a direct replacement for furnaces and require less than

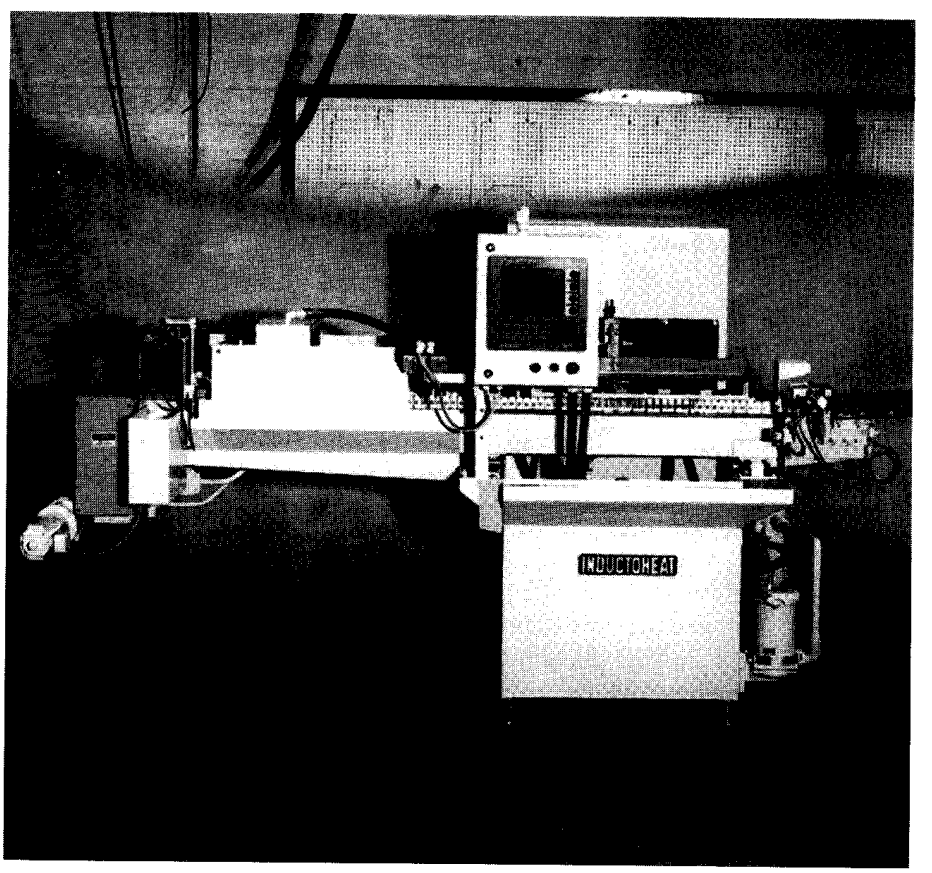

Figure 5.129 New generation of compact inline induction tempering.

half the floor space. Sophisticated design allows simplified operating conditions, increased reliability, and decreased maintenance requirements. Many of the parts processed on these machines have multiple hardened areas with both inside and outside surfaces case hardened. Production rates of the machines shown in Figure 5.129 are from 60 to 150 pieces per hour. Whole families of similar parts can be run using a single coil design.

The quenched hardness is in the 60 to 63 HRC range; the tempering process uniformly heats the entire part to a temperature of 190°C (375°F) to 232°C (450°F). The total maximum variation in part temperature is approximately 19°C (30°F). The final part hardness is 56 to 60 HRC. Due to the advanced coil design concept the tempering coil electrical efficiency is in the range of 85 to 93%.

5.6 INDUCTION HEAT TREATING OF POWDER METALS

Induction heat treating of the powder metals (and particularly induction hardening) has several principal particulars compared to heat treating of wrought steel. These features primarily deal with a marked difference in material properties that in turn affect the metal response to a particular heat treatment. Table 5.8 shows the effect of density reduction and porosity increase on some material properties and their influence on the induction heat treatment process.

Low density and essential porosity are major causes for poor heat treatment results. When induction heat treating powder metal products, it is good practice to have its density at least 7.0 g/cm^3 (0.25 lb/in.^{3}). This will help to obtain consistent heat treat results, particularly when hardening ID surfaces that have cuts, sharp corners, and other stress risers. Sometimes, the density of a powder metal part is expressed as a ratio of its actual density to the density of pure iron, 7.87 g/cm^3. Low-density powder metal parts are prone to cracking because the gases penetrate into the subsurface areas of the part through the interconnected pores. Low-density and porous powder metal parts have poor thermal conductivity and, therefore, require using quenchants with severe cooling rates.

Table 5.8 Effect of Powder Metal Density Reduction and Porosity Increase

Property	Change	Influence on Induction Heat Treatment Process
Thermal conductivity	Decrease	Less soaking action from high-temperature toward low temperature regions. Larger temperature gradients and thermal stresses during heating. Slower cooling during quenching
Electrical resistivity	Increase	Larger current penetration depth
Magnetic permeability	Decrease	Larger penetration depth and lower coil electrical efficiency
Hardenability	Decrease	Inconsistency of heat treatment, variation of surface hardness and case depth

In addition, a high copper content makes the cracking problem even more pronounced. This takes place due to reduction of toughness and elongation and increase of brittleness. Inconsistent and unstable heat treatment results (including a variation of the surface hardness, case depth, and crack development) often take place when porous parts have a low density.

It should be mentioned that although it is strongly recommended that induction hardened parts should have a density of not less than 7.0 g/cm^3 (0.25 lb/in.^{3}), there are several successful applications where an OD hardening has been conducted on the powder metal parts with density reduced down to 6.8 g/cm^3.

Obviously, density and porosity are not the only factors that affect the process of heat treatment of powder steels and irons. Other factors include the material composition, homogeneity of the powder metal parts' microstructure (the rate of material segregation), surface conditions, and features of the heat treat process, as well as features of prior processing including degree of sintering and graphite segregation.

Morphology of parts and the kind of alloying techniques (i.e., whether alloying elements have been added by admixed method, diffusion-alloyed technique, prealloyed method, or hybrid-alloyed technique) have a marked effect on the heat treat result. Material segregation and chemical and microstructural heterogeneity as well as the existence of large foreign inclusions may serve as subsurface stress risers making the powder metal part liable to subsurface crack development and inconsistent hardness pattern.

It is quite common for powder materials to absorb 2% oil by weight. Therefore intensive ventilation is required, as well as the need to make sure that the reusable quenchant is clean enough. Oil quenching is often applied when hardening powder metal parts, which have particular requirements for dimension stability and control of shape distortion and for parts prone to cracking. Other quench media include water-based polymer quenchants and water.

Carbon, copper, nickel, and molybdenum are the most commonly used powder metal alloying elements. Detailed discussion on the effect of different alloying elements on the critical temperatures, powder metal hardenability, and major heat treat properties can be found in [14, 19, 387, 474].

When determining process parameters for induction hardening of powder metal parts the higher energies and higher frequencies are often chosen compared to heat treatment of wrought metals of similar composition. Preheating is also often used to obtain required results.

5.7 ELECTROMAGNETIC END AND EDGE EFFECTS IN INDUCTION HARDENING AND TEMPERING

Nonuniformity of the heating pattern at the coil or workpiece ends is related to the distortion of the electromagnetic field in those areas. This distortion is called the electromagnetic end effect. As discussed in Section 3.1.7, the electromagnetic end effect can result in either over or underheating of the workpiece ends. Basically, it is a function of frequency, coil-to-workpiece geometry, and material properties. Note

that existence of magnetic flux concentrators as well as electrically conductive constructions (e.g., tooling) could also have a noticeable impact on the appearance of the end effects.

Inasmuch as most induction hardening applications utilize a single-coil arrangement, we now briefly discuss the appearance of an electromagnetic end effect in such cases. The differences in appearance of the end effects for induction hardening and tempering occur due to the following.

- The workpiece retains its magnetic properties for a whole tempering cycle. In contrast, at the final and the most critical part of the heating cycle for hardening, a dual-properties phenomenon takes place (see Section 3.3.2).
- Power density used in induction hardening is much greater compared to power densities used for tempering. Therefore even during the magnetic stage of heating a heated body acts differently because magnetic permeability is a function not only of temperature and frequency but also magnetic field intensity.
- In the majority of induction hardening applications the inductor-to-workpiece air gap is quite tight and typically in the range of 1.0 to 6 mm. In contrast, air gaps between the tempering coil and workpiece are much greater and usually in the range of 5 to 20 mm. Figure 5.130 shows an effect of the air gap on the eddy current density distribution in the workpiece.
- Finally, in induction hardening applications the chosen frequency is five to ten times higher and the heat time is two to four times shorter compared to induction tempering.

Figure 5.131 shows the distribution of the coil current and induced eddy current for different coil locations relative to the end of the heat treated part [2, 203]. When low frequency is applied, the eddy current distribution and heat pattern are different.

Electromagnetic end and edge effects during tempering are somewhat similar to end effects taking place in the first heating stage of the mass heating applications (see Sections 7.1, 7.2, 7.4, and 7.5).

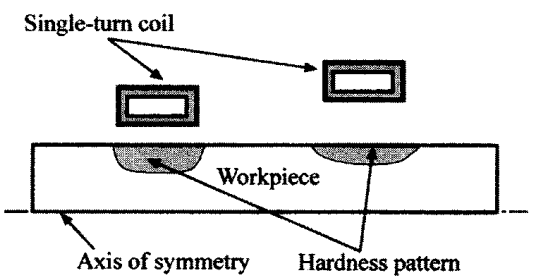

Figure 5.130 Influence of coil-to-workpiece air gap on hardness pattern.

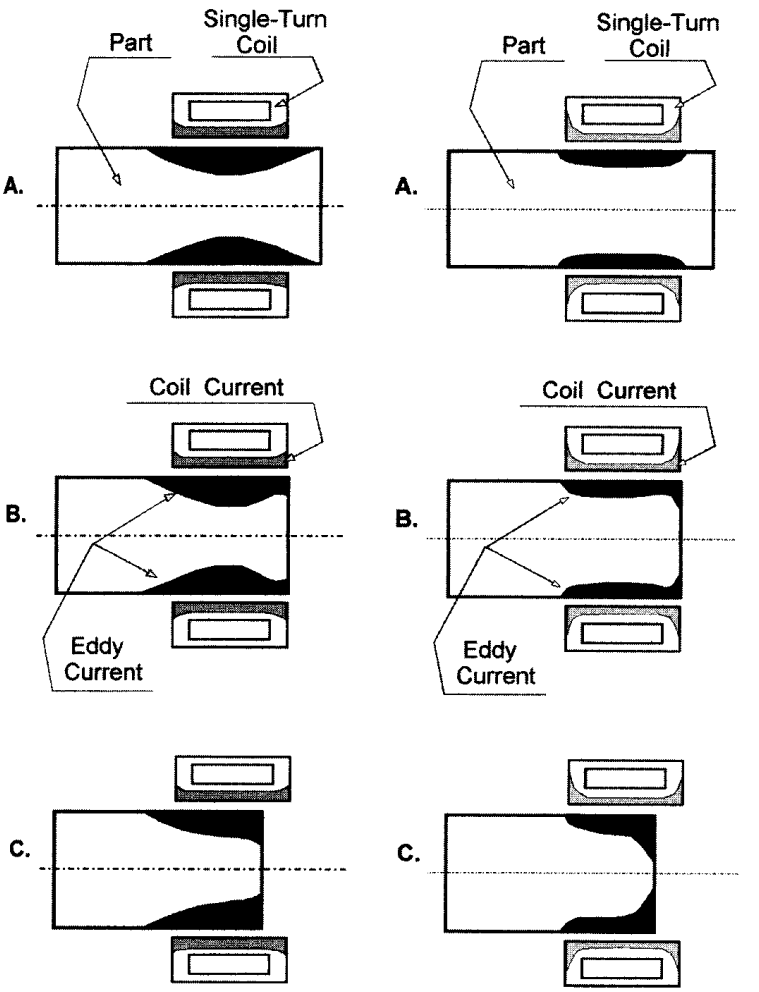

Figure 5.131 Electromagnetic end effect in induction heat treating, low frequency (left) and high frequency (right).

5.8 LONGITUDINAL AND TRANSVERSE HOLES, KEY WAYS, GROOVES, AND VARIOUS ORIENTED HOLLOW AREAS

In some applications heat treating by induction could face certain difficulties. Typical examples would be applications where the part (workpiece) contains longitudinal and/or transverse oil holes, key ways, grooves, undercuts, various orientations of hollow areas, and sharp corners (Figure 5.132) [109, 203]. These features are not considered to be exotic ones as they are constituents of cam shafts, crank shafts, and transmission parts as well as many other components that need to be heat treated.

The existence of these features can result in an undesirable appearance of hot and cold spots, shape distortion, grain boundary liquation, and even crack. In these cases it is necessary to carefully evaluate the eddy current and temperature fields in order to choose a frequency, power density, and coil design that will allow one to achieve the required heat uniformity and to meet customer specifications.

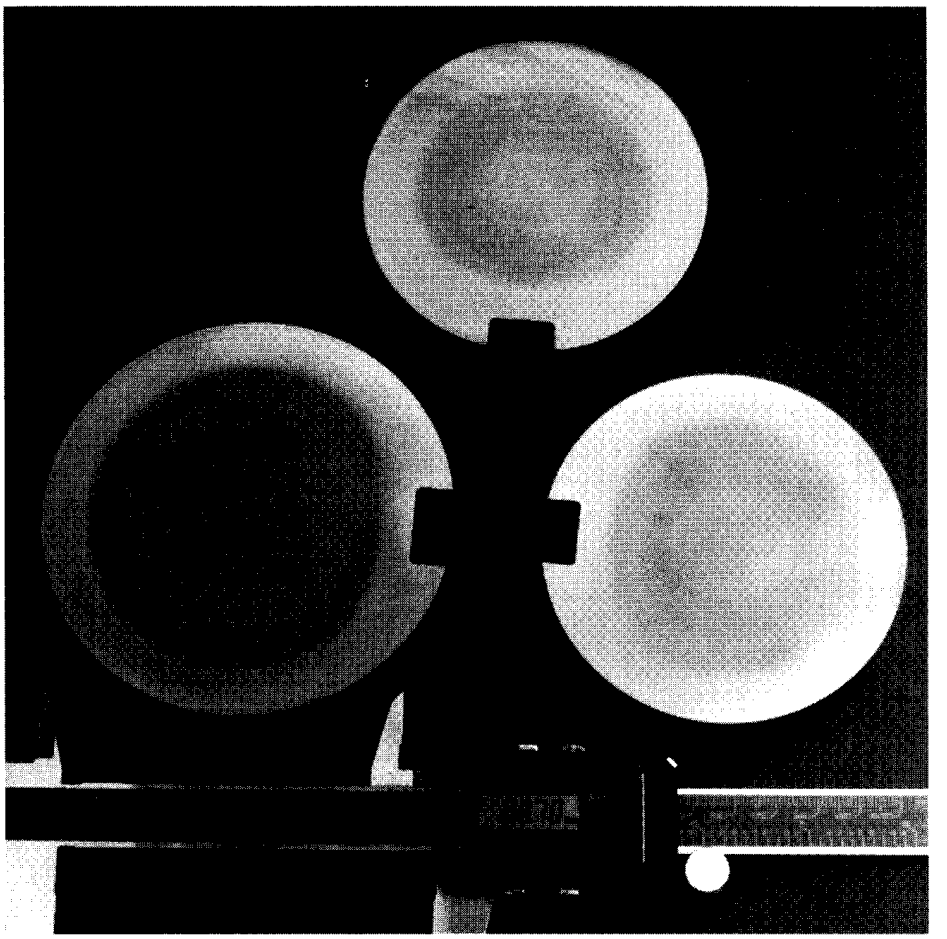

Figure 5.132 Induction heat treatment of parts with holes, keyways, and sharp corners. (continued on pages 353 and 354)

5.8.1 Longitudinal Holes and Longitudinally Oriented Hollow Areas

The existence of longitudinal holes or longitudinally oriented hollow areas within the part (Figure 5.133) can cause a redistribution of eddy current flow, resulting in overheating of some regions of the part (so-called hot spots). Figure 5.134 (left), shows a segment of a cylindrical part and the normal current flow within it. This current distribution is typical if the heated workpiece is solid or if a hole is located way below the surface, so that the current does not interact with it in any way.

In contrast, if a longitudinal hole is located within the current penetration depth, it blocks the normal eddy current path and leads to a current redistribution (Figure 5.134, right). Because of that redistribution, overheating or even local melting can take place in areas between the part's surface and the hole.

There are two factors that cause the overheating effect: an increase of power density in that area due to the redistribution of induced current, and the lack of adjacent mass in that area. As a result, less heat soaks from the surface of the part toward its core. The decrease in this heat soaking is due to the thermal conductivity. As one can see, these factors may coincide and result in the overheating of certain areas of the part.

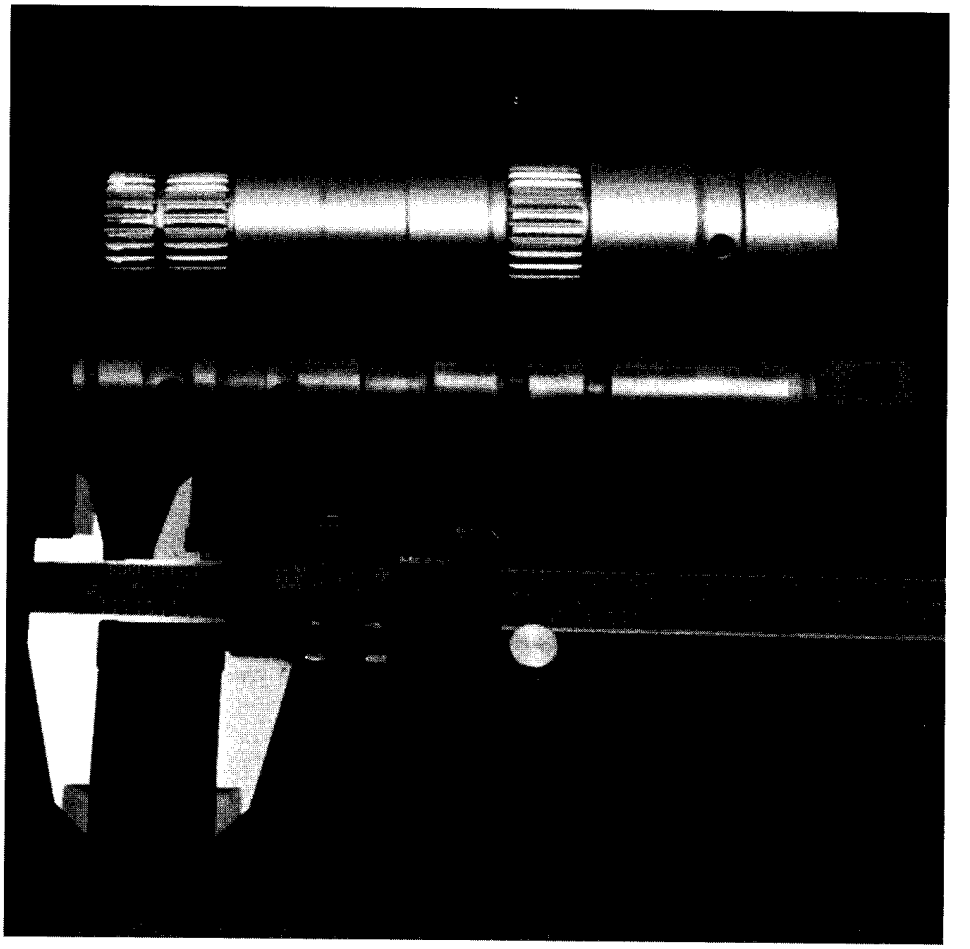

Figure 5.132 (B)

In different applications the influence of both factors may be different. If a longitudinal hole is located near the part surface within one current penetration depth, then the first factor typically prevails and is primarily responsible for the heat surplus in that area (Figure 5.135, hole A). Intense heating with higher power density makes this overheating more pronounced.

When the hole is located within one or two current penetration depths (Figure 5.135, holes B and C), then both factors have approximately the same influence on the heat surplus. If the longitudinal hole is located within two or three current penetration depths and the heat cycle time is relatively long (8 to 12 sec or more), the second factor makes a major contribution to the overheating of the area. When the hole is located within three to five current penetration depths or more under the surface of the part (Figure 5.135, hole D), the heat surplus due to the existence of a longitudinal hole is minor and the probability of overheating is very small.

5.8.2 Transverse Holes

Transverse holes can also cause a redistribution of eddy current flow (Figure 5.136). Unlike the case of longitudinal holes, eddy current redistribution due to transverse

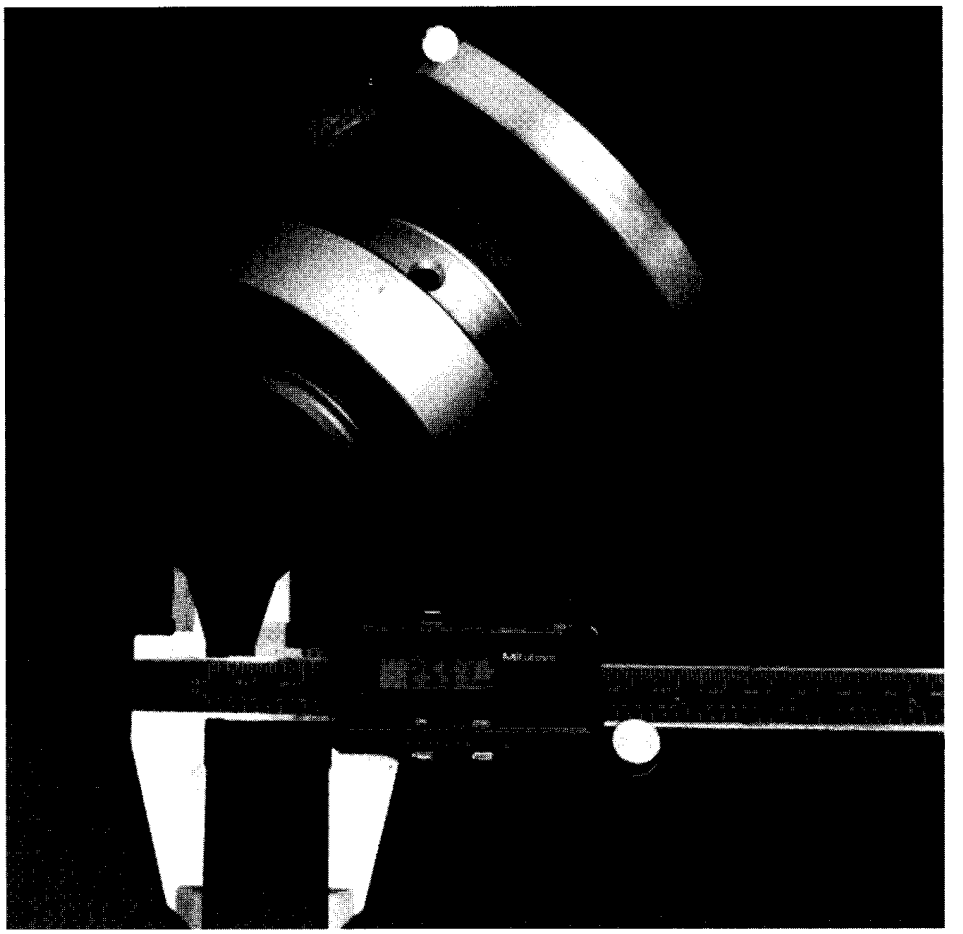

Figure 5.132 (C)

holes can result in both under- and overheating of the hole edges (Figure 5.136A). Because of the current concentration, overheating can occur at the hole edges parallel to the eddy current flow. On the other hand, the hole edges that are perpendicular to the eddy current flow will be underheated. With an increase of both the inside diameter of the transverse hole and the frequency, the nonuniformity of the temperature distribution along the perimeter of the hole will be more pronounced.

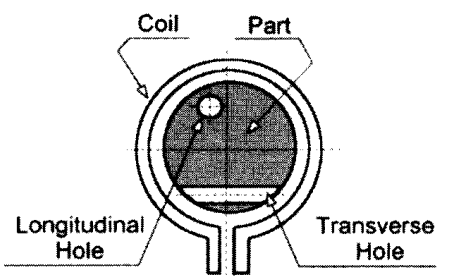

Figure 5.133 Longitudinal and transverse holes in induction heat treating.

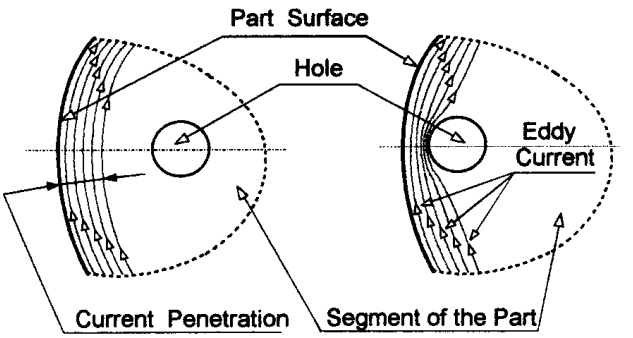

Figure 5.134 Eddy current redistribution as result of longitudinal hole.

These heat nonuniformities can cause grain boundary liquation, cracks, and distortion in the vicinity of the hole edges. Generous chamfering of the hole is helpful in eliminating the appearance of crack there and is strongly recommended.

Besides the temperature nonuniformity along the hole perimeter, there might be a noticeable heat pattern distortion along the height/length of the hole. This distortion results in a nonuniform case depth in the hole area surroundings (Figure 5.137). Obviously, a combination of chosen frequency, heat intensity, and hole diameter tremendously affects the pattern in the hole area. Table 5.9 shows combinations of frequencies and the straight hole diameters that typically would not result in a noticeable distortion of the case pattern for steel and iron.

It is possible to obtain a relatively uniform temperature distribution along the perimeter of the medium-size hole by putting a plug in the hole. If the plug is made of the same metal as the part, the heat nonuniformities will be negligible and the temperature distribution can be considered uniform (Figure 5.136B). Despite their use in avoiding over- and underheating at the hole edges, steel plugs present problems because it is often difficult to insert them and later remove them after the heat treatment because they may become welded in the hole.

An alternative to the use of steel plugs is the use of copper plugs. In this case, a nonuniform current distribution still occurs and can lead to local over- and underheating. However, the overheating/underheating phenomenon is opposite to that

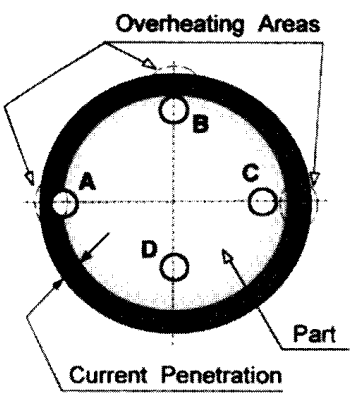

Figure 5.135 Overheating areas due to longitudinal holes.

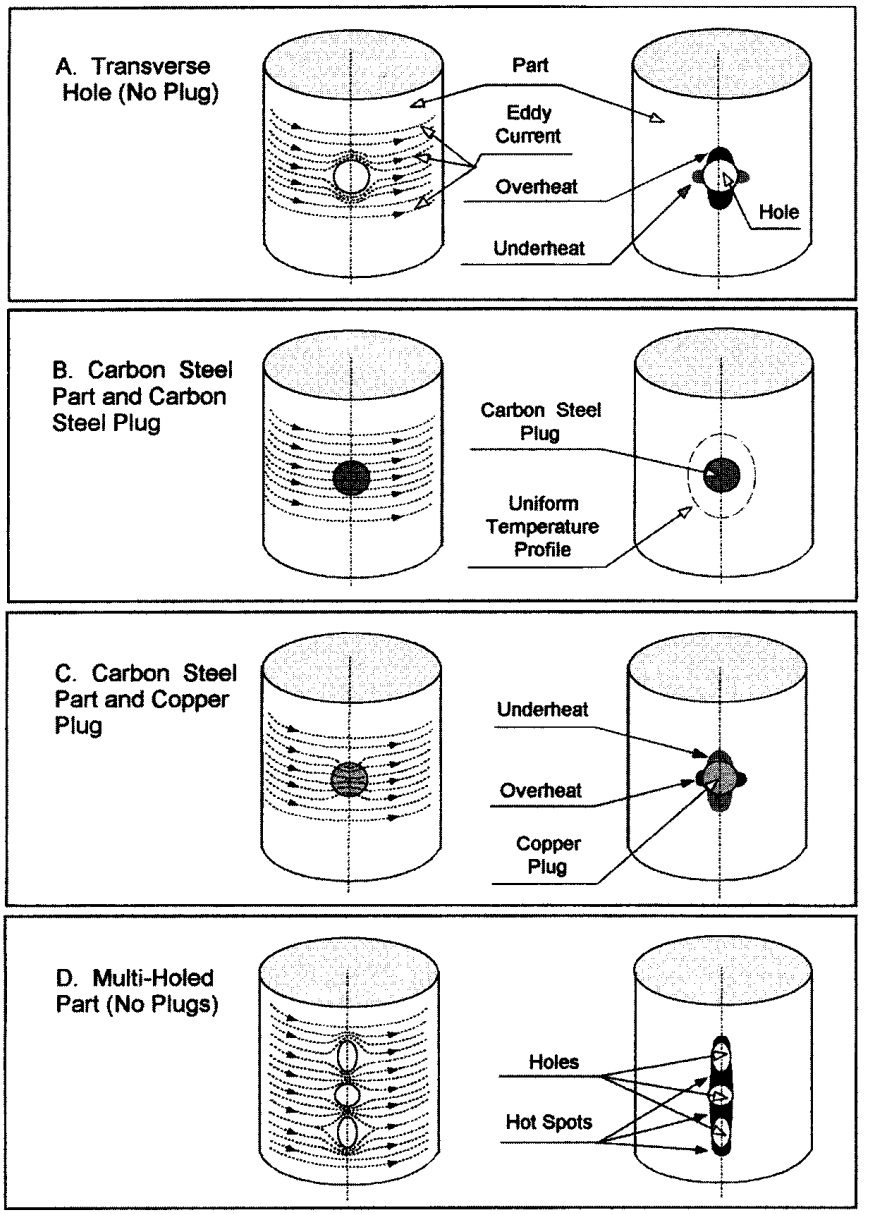

Figure 5.136 Eddy current distribution and heat nonuniformities appear due to transverse holes.

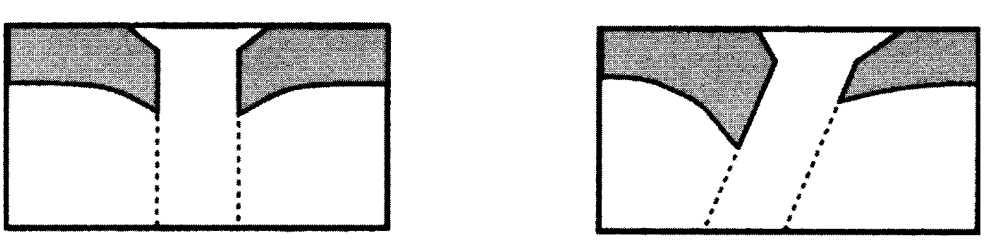

Figure 5.137 Differences in hardening patterns of straight (left) and angled (right) holes.

Table 5.9 Typical Combinations for Distortion-Free Case Patterns

Frequency (kHz)	Hole OD (mm)
3	5
10	3.5
30	2

seen without any plugs. Figure 5.136C shows that the eddy currents will gather in the copper plug from the neighboring carbon steel regions. This takes place because the electrical resistivity of the copper is much less (approximately a factor of 10) than the resistivity of any steel and it is much easier for the eddy currents to flow through the low-resistance copper than through the high-resistance steel. Therefore, when copper plugs are used, the hole edges that are parallel to the eddy current flow are underheated and the hole edges that are perpendicular to the current flow are overheated. An actual distortion of the hardness patterns due to the use of copper plugs is shown in Figure 5.138. Note that when using copper plugs (Figure 5.136C) overheating of the hole edges is much less pronounced compared to the case when plugs are not used (Figure 5.136A). At the same time, the copper plugs eliminate the appearance of cracks in the hole areas during induction heating and quenching.

Figure 5.138 Use of copper plugs prevents overheating around holes.

In some applications, instead of metal plugs, water-soaked wooden plugs have been used. Because wood is not electrically conductive, the wooden plugs do not change the eddy current distribution in the hole edge areas. Therefore there will still be regions with high and low current densities as shown in Figure 5.136A. However, the use of water-soaked wooden plugs allows one to decrease the overheating of the hole edges up to a certain point due to the heat transfer from the high-temperature regions into the water-soaked wood by thermal conduction. In addition, when using any plug there is a limited access of the quenchant into the hole overheated area. Therefore the probability of cracking is reduced because of the reduction of the thermal gradients.

5.8.3 Special Considerations

Special care should be taken in the case when the heat treated part contains angled holes or when there is a combination of closely spaced transverse holes. The temperature field in angled hole areas combines the features of nonuniform temperature distribution along the perimeter of the transverse hole and an overheating effect due to the increase of current density and the lack of mass on one side of the hole. The sharper the angle of the hole results in a more pronounced distortion of the heat treat pattern in the hole area as well as the hole area becoming more pronounced due to overheating, grain boundary liquation, and cracking.

Certain difficulties can appear when the part consists of several closely located holes (Figure 5.136D). Applying induction heat treatment in such cases could cause a sequence of cold spots (poorly heated areas) and very hot spots (almost melted areas). In such cases, quite often alternative heat treatment processes can be recommended.

Key ways can be considered extreme cases of longitudinal holes (Figure 5.139). Size, shape, and orientation of key ways with respect to current orientation (which depends upon the coil orientation) have a substantial effect on the ability to obtain the required temperature profiles within the key way area and to avoid undesirable hot and cold spots in these areas.

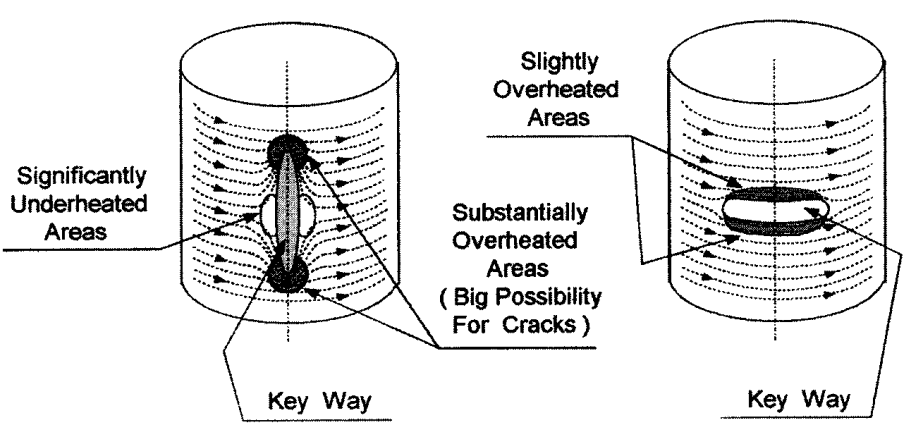

Figure 5.139 Sketch of key ways in induction heat treating.

Inserting plugs into holes and taking them out are very delicate and time-consuming processes. A popular attitude among heat treaters who deal with parts containing holes is that if there is a possibility of avoiding nonuniform heating of the hole edges without using plugs (e.g., by using a special heating regime, coil design, and/or frequency choice), then the extra development effort required is justified. Therefore plugs should be used only as a last resort.

When discussing heat nonuniformities due to electromagnetic end and edge effects, longitudinal and transverse holes, and temperature field nonuniformities due to key ways, sharp edges, and corners, it is necessary to mention that smooth chamfers on edges and rounding of sharp corners can be a great help in decreasing the possibility of overheating and cracking. The repeatability of machined chamfers, their depth, and location are of great importance.

Experience at INDUCTOHEAT, Inc. during heat treating of different parts with the above-mentioned features shows that, surprisingly, in many cases the proper choice of design parameters (applied frequency, power density, coil geometry, etc.) allows the heat treater to obtain the required heat treating pattern even in cases that seem unsuitable for heat treating by induction. For example, in some cases, even such complicated-shape parts as a ball bearing cage, which consists of a number of closely located large holes, can be surface hardened or contour hardened by induction instead of using time- and space-consuming carburizing processes.

Grooves and undercuts require special attention because they result in redistribution of the case pattern due to electromagnetic end and edge effects as well as thermal edge effects. The case pattern in the undercut area depends upon the application and the coil design. Often product engineers prefer to have a slightly lower hardness in the undercut area. Instead of a fully martensitic microstructure they sometimes prefer to have a martinsitic–bainitic structure. This provides some ductility in the undercut area and allows reducing the probability of cracking and overheating by reducing the thermal gradients during heating and quenching cycles.

5.9 MAGNETIC FLUX CONTROL TECHNIQUES: ELECTROMAGNETIC SHIELDS, MAGNETIC SHUNTS, AND MAGNETIC FLUX CONCENTRATORS (INTENSIFIERS)

Before embarking on a discussion of controlling magnetic flux, we take a few moments to examine the definition of magnetic flux and establish how we observe the result of flux control techniques. *Flux* is a term used to describe the rate of transfer of fluid, particles, or energy across a given surface interface. *Magnetic flux* is a measure of the total number of magnetic field lines crossing a chosen surface (Figure 5.140).

Although magnetic flux lines cannot be seen, they can be represented in mathematical calculations and graphs. Because an isolated magnetic source or monopole has never been observed to exist in nature, the net flux or divergence of the magnetic flux density vector ($\mathbf{B}$) is always equal to zero (i.e., $\nabla \bullet \mathbf{B} = \mathbf{0}$). This simply means that the lines of a magnetic field are closed loops and for a given volume the number of lines entering the volume will equal the number of lines leaving.

There is a mathematical proof that states that the divergence of the curl of a vector is always equal to zero (i.e., $\nabla \bullet (\nabla \times \mathbf{V}) = \mathbf{0}$). This implies that we could

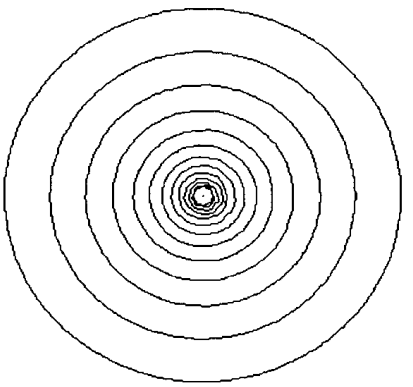

Figure 5.140 Lines of constant magnetic vector potential A_z in the current-carrying conductor surroundings.

define a vector **A** whose curl is equal to the magnetic flux density vector **B** (i.e., $\nabla \times \mathbf{A} = \mathbf{B}$). This is, in fact, what has been done in order to create a visualization of the magnetic field lines. The vector **A** is referred to as the magnetic vector potential and a plot of constant values of the vector **A** produces a visualization of the magnetic field with the density of the lines representing the strength of the magnetic field. This is all done in spite of the fact that the vector **A** cannot actually be measured in nature.

With the above-mentioned method of observing the field lines we can move on to the question of interest which is, "Can the position of these lines be altered in any way?" The answer to this question is yes. The position of the field lines and the strength of the field in a given area can be modified in several ways. The density of the lines can be changed by changing the cross-sectional area through which the flux is flowing. The location of the lines can be changed by the use of special materials that provide a different path or restrict the path of the magnetic flux. A third way that the flux lines can be changed is by the presence of other current-carrying conductors in the vicinity of the existing field; this is called the proximity effect (Figure 5.141).

5.9.1 Electromagnetic Shields

In the area of induction heating, magnetic fields are generated for the purpose of heating metal. Often the field will heat not only the desired workpiece but also metal in areas adjacent to the coil, workpiece, and transmission lines. Further problems can occur as the magnetic field couples into enclosure walls causing excessive heating and into control or power wiring causing disturbances in control, metering, or power circuit operation. For these reasons it is often necessary to use magnetic shields to reduce the effect of the magnetic field and to protect other structures, components, controls, or equipment in the immediate area.

The effectiveness of a magnetic shield is determined by comparing the field strength of the incident wave and the reflected or attenuated wave. The common formula used is

$$\mathrm{SE(db)} = 20 * \log \mathrm{F1/F2},$$

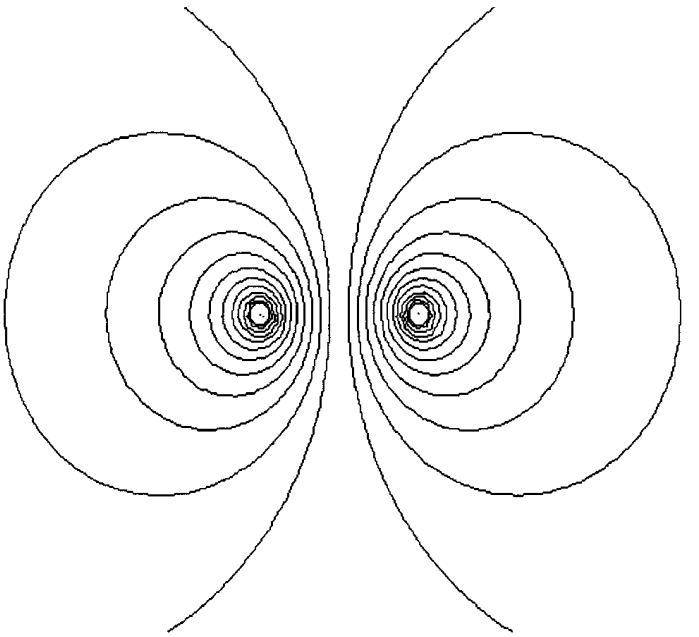

Figure 5.141 Magnetic vector potential field distribution of two conductors located in close proximity.

where F1 and F2 are the field strengths of the incident and attenuated waves, respectively [407]. Higher numbers represent a better shield. A 40 (db) attenuation would represent a field strength of the reflected or attenuated wave (F2) of 100 times less than the field strength of the incident wave (F1). A specific area may be shielded from an electromagnetic field by either reflecting the wave or absorbing the energy. Common materials used for the purpose of reflecting the wave would be copper or aluminum. The main materials used for absorption would be steel or high-permeability conductive materials.

At higher frequencies, shielding by reflection is very effective. Absorption may be used but is most often unnecessary. When reflection is the primary mechanism a relatively thin shield can produce quite good results. Often a thin copper or aluminum foil may be used above 100 kHz for a 60 db attenuation and one reference depth for frequencies as low as 10 kHz for a 40 db attenuation. At frequencies below 10 kHz, absorption is the only real choice. Materials should be highly permeable and the minimum thickness should be about four times the reference depth of the frequency for a 35 db attenuation.

$$\text{Absorption (db)} = 8.68 * \text{S.D.}, \quad \text{where S.D.} = \text{Shield thickness/Reference Depth.}$$

The effectiveness of a given shield is evaluated by the equation:

$$\text{SE(db)} = \text{R(db)} + \text{A(db)} + \text{B(db)}.$$

This equation includes the effects of reflection and absorption as well as a factor that is used for reflection on very thin shields at high frequencies (Figure 5.142).

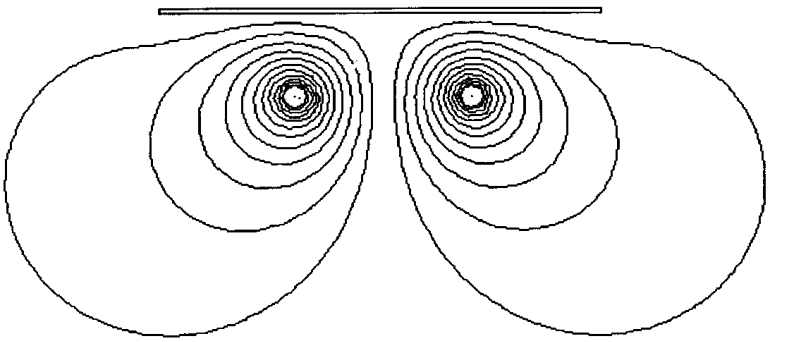

Figure 5.142 Effects of copper shield on magnetic vector field distribution (compare with Figure 5.141).

For shields operating by the principle of reflection the location of the shield may have a large impact on its effectiveness. For shields operating by the absorption principle the losses are independent of the distance between the shield and the source. Shields utilized in the presence of very strong electromagnetic fields can be a major source of power dissipation in the system and may require water-cooling. When shields are used around solenoid inductors they can also reduce the inductance of the circuit. When the circuit inductance of a heating coil is reduced by an external shield, the power supply or tank circuit will need to supply extra current to achieve the same level of power to the load.

When the inductor is a DC line choke for a chopper circuit the inductor turns should be increased to return to the original design inductance in order to prevent discontinuities of the current waveform during circuit operation.

Figure 5.143 shows the typical attenuation versus shield thickness for a copper shield and illustrates the rule of thumb of using a shield that is equal in thickness to four times the material reference depth at the given frequency. Figure 5.144 gives an indication of how the shielding effectiveness falls off with a given thickness of shield as the frequency is lowered. The effectiveness of the shield pictured in Figure 5.142

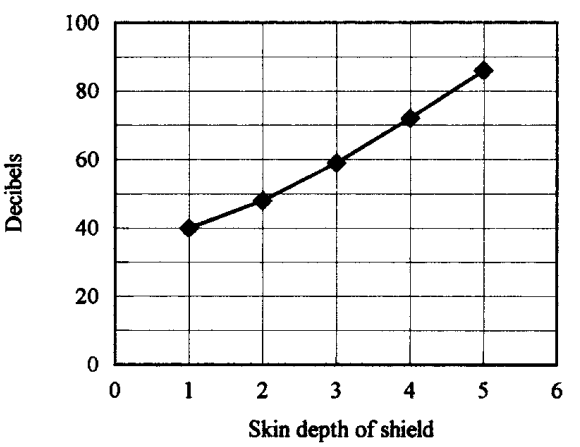

Figure 5.143 Attenuation versus skin depth at 10 kHz.

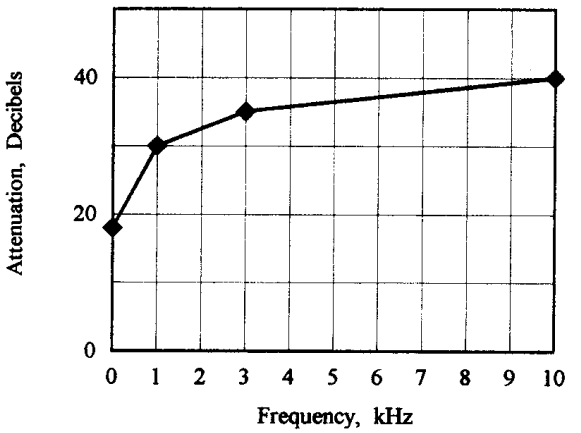

Figure 5.144 Attenuation versus frequency (shield equals one skin depth).

could be doubled simply by increasing the length to include the full area of coverage of the magnetic field. In attempting to shield an inductor this may require a shield that extends at least one and one half times the inductor diameter beyond the center line of the inductor.

Table 5.10 shows a brief comparison for shielding effectiveness of different materials at a 10 kHz frequency, assuming that the two conductors in the examples above form an induction coil to be shielded.

5.9.2 Magnetic Shunts

A magnetic shunt generally consists of a large stack of thin steel laminations placed along the axis of an inductor and parallel to it. The shunt provides a parallel, low-reluctance path for the magnetic flux. Shunts can reduce the external magnetic field and prevent heating of surrounding metal structures when used in conjunction with a heating or melting coil. Shunts also can be a source of significant power dissipation in the system and are most often cooled by water.

Table 5.10 Shield Effectiveness at 10 kHz Frequency[a]

Case	Description (in.)	Flux Density (Gauss)
1	No shielding	40.0
2	.125 Copper shield	1.16
3	.125 Aluminium shield	1.18
4	.125 Stainless shield	4.0
5	.125 Mild steel shield	4.7
6	.125 Mag. Mat'l. (perm. = 60)	20.0
7	.66 Stainless shield	0.89
8.	.4 Concentrator @ coil	27.0
9	.4 Conc. and Cu shield	5.5

[a] Calculations at 3 in. from coil surface using relatively short shield.

5.9.3 Magnetic Flux Concentrators

The same magnetic material may be used for a shield, shunt, or concentrator depending on the desired effect. The intent with a concentrator is to make the magnetic field more intense in certain areas during the heating process.

Magnetic flux concentrators (flux intensifiers) have become an acknowledged standard in induction heat treatment design [143–147, 154, 203]. Modern, high-permeability, low-power-loss materials are now routinely used in a manner similar to that of magnetic flux diverters (cores) in power transformers or motors. A traditional function of flux concentrators in induction heat treatment has been to improve the magnetic coupling efficiency (by loss reduction) and to obtain effective selective heating in workpiece areas that are difficult to heat. Successful development of powdered metal concentrators based on Fe, Ni, Co, and other elements have dramatically increased the popularity of magnetic flux concentrators.

5.9.3.1 Physics of the Magnetic Flux Concentration

Let us examine what happens when a magnetic flux concentrator is applied [143, 203]. Without a concentrator, the magnetic flux would spread around the coil or current-carrying conductor and link with the electrically conductive surroundings (e.g., auxiliary equipment, metal support, tools, etc.). The flux concentrator forms a magnetic path to channel the main magnetic flux of the inductor in a well-determined area outside the coil. Figure 5.145A shows the current distribution in an isolated conductor. The current redistribution within this conductor after locating a conductive load (i.e., workpiece) near the conductor can be observed in Figure 5.145B. Due to the proximity effect, a significant part of the conductor's current will flow near the surface of the conductor that faces the load. The remainder of the current will be concentrated in the sides of the conductor.

When an external magnetic flux concentrator is placed around the conductor (Figure 5.145C), practically all of the conductor's current will be concentrated on the surface facing the workpiece. The magnetic concentrator will squeeze the current to the "open surface" of the conductor—in other words, to the open area of the slot (slot effect). Current concentration within the coil surface facing the workpiece results in good coil workpiece coupling and therefore improves the coil efficiency. The actual current distribution in the conductor (Figure 5.145C) depends on the frequency, magnetic field intensity, geometry, and material properties of the conductor, the workpiece, and the concentrator.

There is a common misconception that the use of flux concentrators automatically leads to an increase in efficiency. Flux concentrators improve the efficiency of the process partly by reducing the coupling distance between the conductive part of the coil and the workpiece, but also by reducing the stray losses (by reducing the reluctance of the air path). However, because the flux concentrator is an electrically conductive body and conducts high-density magnetic flux, there is some power loss generated as heat within it due to the Joule effect. This phenomenon could cause a reduction of electrical efficiency and the need to design a special water-cooling system to remove the heat from the concentrator. The first two factors will counteract the third, and the change in electrical efficiency will be a result of all three factors. In some applications, efficiency can actually be reduced. However, the appropriate use of a magnetic flux concentrator will typically allow an increase in process effi-

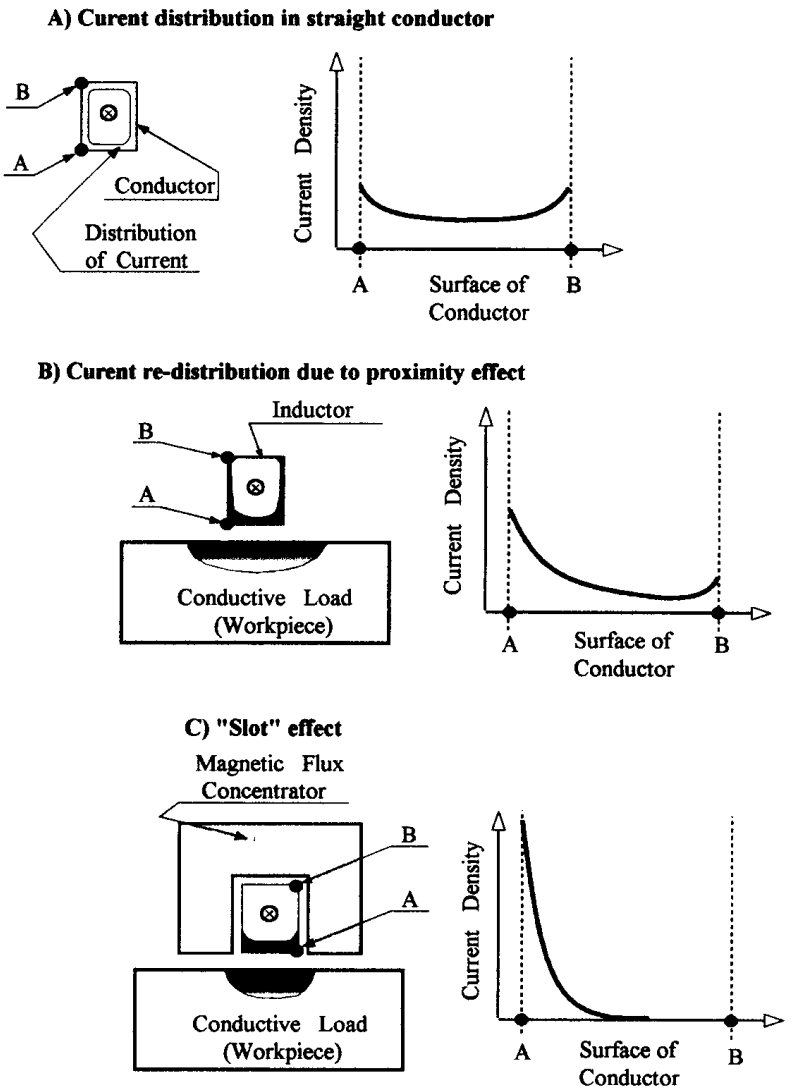

Figure 5.145 Effect of magnetic flux concentrator on current distribution.

ciency to be achieved. This can also result from the flux concentrator's ability to localize the magnetic field in a specific area. Because of this, the major portion of the magnetic field will not propagate behind the concentrator and the heated area will be localized. As a result, the heated mass of metal will be smaller, therefore, less power will be required to accomplish the desired heat treatment.

5.9.3.2 Design and Application Features

In most cases the application of magnetic flux concentrators does not require re-engineering of the induction system. However, when a concentrator is used, higher power densities will be generated on the inside diameter of the coil (Figure 5.145C). If the original coil design is susceptible to stress cracking over time due to the copper work hardening, this condition will occur sooner. Therefore consideration must be given to the coil ID, wall thickness and the location of quench holes, which are

frequently located near the coil surface edges. The propagation of stress fractures can almost always be minimized or eliminated by a well thought out coil design. From another side, impedance of the straight coil can be much different compared to a coil with a flux concentrator. Therefore, after the flux concentrator has been installed in the straight coil, it is necessary to check that the load properly matches the power supply.

Using a magnetic flux concentrator leads to an increase in power density not only in the induction coil but also in the workpiece areas that must be heated selectively. Because of this, the slot effect plays a particularly important role in the proper design of coils for selective induction hardening, including channel, hairpin, odd-shaped, spiral–helical, and pancake inductors. Special care should be taken when applying flux concentrators to a multiturn coil. With this type of coil the voltage across the coil turns can be significant, and a short current path can develop through the concentrator. In this case, the reliability of the electrical insulation of concentrators plays an essential role in the coil design.

One of the major problems in the induction hardening of steel up to the austenite temperature range is that of undesirable heating of adjacent areas that have previously been hardened (the so-called temper back or annealing effect of adjacent parts). This is particularly important in the induction hardening of crank shafts, cam shafts, gears, and other critical components [154, 203]. The complexity of this problem arises from the fact that, due to electromagnetic field propagation, the eddy currents are induced not only in the workpiece that is located under the inductor but in adjacent areas as well. A sketch of an induction carbon steel cam shaft hardening system is shown in Figure 5.146.

Figure 5.147 shows the magnetic vector potential field distribution around a two-turn cylindrical induction coil. Without a concentrator, the magnetic flux would spread around the coil and link with electrically conductive surroundings, which include neighboring areas of the part (e.g., cam lobes, journals) and possibly areas of the machine or fixture. As a result of induced eddy currents, heat will be produced. This heat can cause undesirable metallurgical changes in these areas. At different stages of the heating cycle, the extent of the heating rate of the adjacent areas can vary.

At the first stage of the heating cycle, the entire workpiece is magnetic, the inductor has good efficiency, and intensive heating of the areas located under the coil takes place. Because of better coupling, any surface areas of the workpiece located

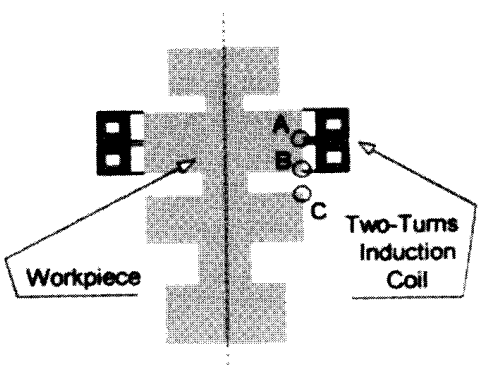

Figure 5.146 Sketch of induction surface hardening system.

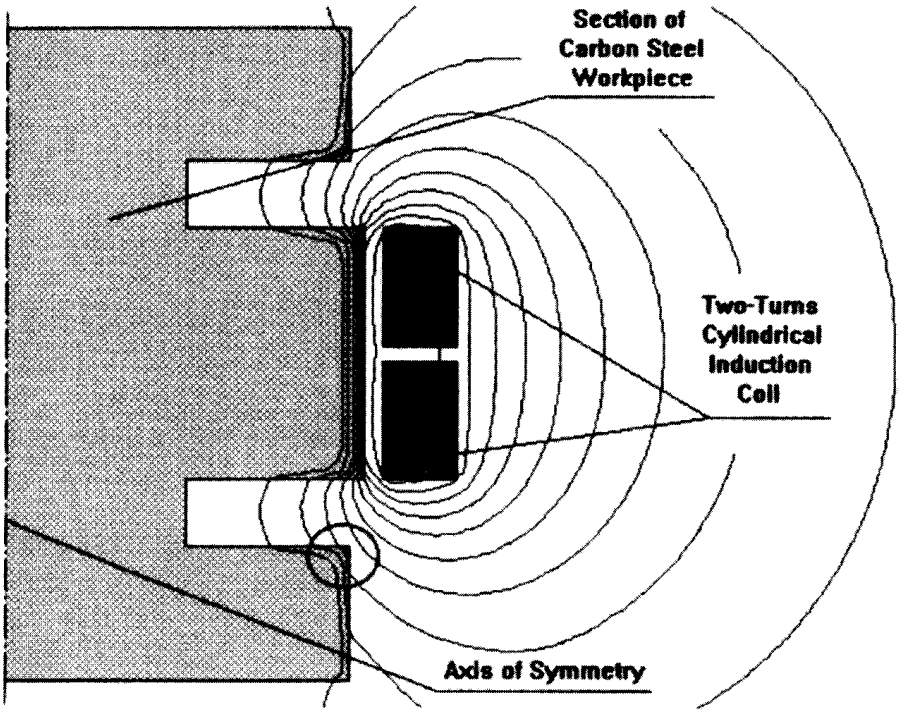

Figure 5.147 Magnetic vector potential field distribution around two-turn cylindrical coil.

under the coil (Figure 5.146, regions directly adjacent to the coil turns) will have much more intense heating than any other areas in the coil surrounding.

After a short time, the surface reaches the Curie temperature, the magnetic permeability drops to 1, the surface layer becomes nonmagnetic, and its heating intensity drastically decreases. At this stage, the coil will not have as good a coupling factor as it had during the first stage, when the whole workpiece was magnetic. Although the surface of the part has lost its magnetic properties, the adjacent areas retain theirs. Consequently, the coupling factor of these areas will not decrease, and a greater portion of the electromagnetic field will link with the adjacent areas.

In addition, in order to have a short cycle time and to keep the heat intensity of the surface area located under the coil within the same range as during the first stage of heating, the system can automatically increase the coil power after the surface temperature passes the Curie point. This also will result in additional heating of magnetic parts located in the coil surroundings, which leads to the temper back of these areas.

After a magnetic flux concentrator is located around the inductor (Figure 5.148), a much smaller portion of the electromagnetic field of the coil will link with adjacent areas. For example, in the induction surface hardening of carbon steel cam shafts, appropriate use of magnetic flux concentrators allows a four- to twelvefold reduction in the power density induced in adjacent cams compared to using a bare coil.

Therefore magnetic flux concentrators allow de-coupling of the induction coil and the adjacent electrically conductive areas. This eliminates undesirable heating of these areas and as a result the temper back (annealing) effect.

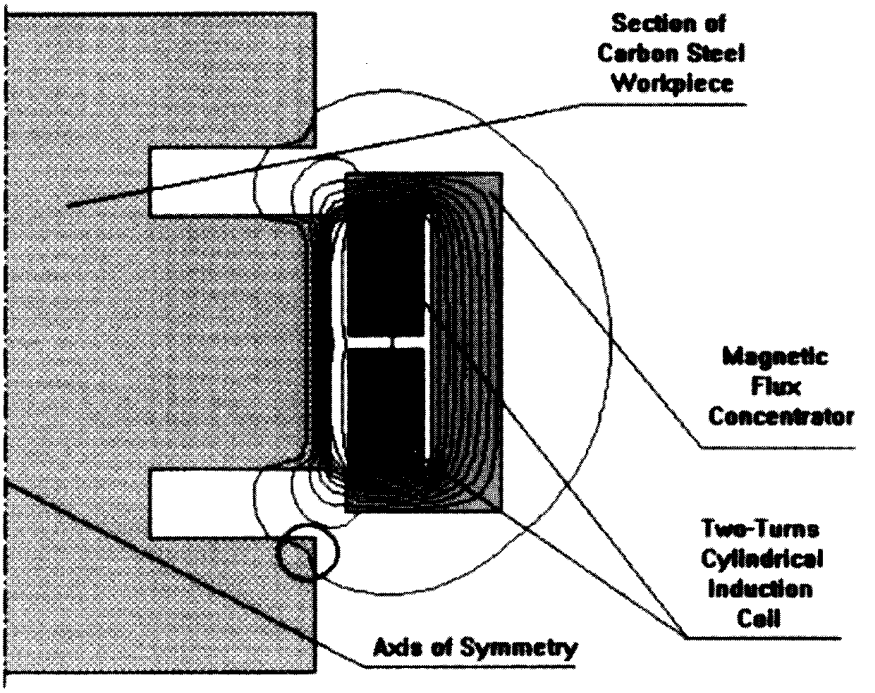

Figure 5.148 Effect of magnetic flux concentrator.

As one can see from Figures 5.147 through 5.149, because of the magnetic field redistribution, a bare induction coil cannot provide the required heating pattern in the workpiece. The areas with high power density are observed in adjacent areas of the part but not in the required area. With the addition of a flux concentrator at the coil edges, practically all of the coil's current will be concentrated on the surface facing the workpiece. The magnetic flux concentrator will squeeze the current to the "open internal face" of the coil. Current concentration within the coil surface facing the workpiece results in good coil–workpiece coupling, with a consequent improvement in process efficiency. At the same time, the correct choice of flux concentrators and their location, geometry, material properties, and frequency allows the designer to decrease the heat intensity in the adjacent areas of the workpiece and, therefore, avoid their undesirable heating. In contrast to locating concentrators only at the end areas of the coil, the application of a C-shaped flux concentrator which warps around the coil will lead to some coil efficiency improvement. However, this will of course increase the cost of the design.

In some heat treatment applications, several coils are involved. Because of the relatively small distances between coils, strong magnetic ties can form between coils. This can lead to some negative electromagnetic effects (e.g., power transfer between coils). From another perspective, the stray flux might cause an undesirable temperature profile in the workpiece. In these applications, magnetic concentrators can be used as electromagnetic shields, which will eliminate undesirable coil interactions and their negative results. In general, the effectiveness of magnetic flux shields depends on various parameters such as frequency, magnetic field intensity, material properties, and the geometry of the induction system. Care should be taken at the

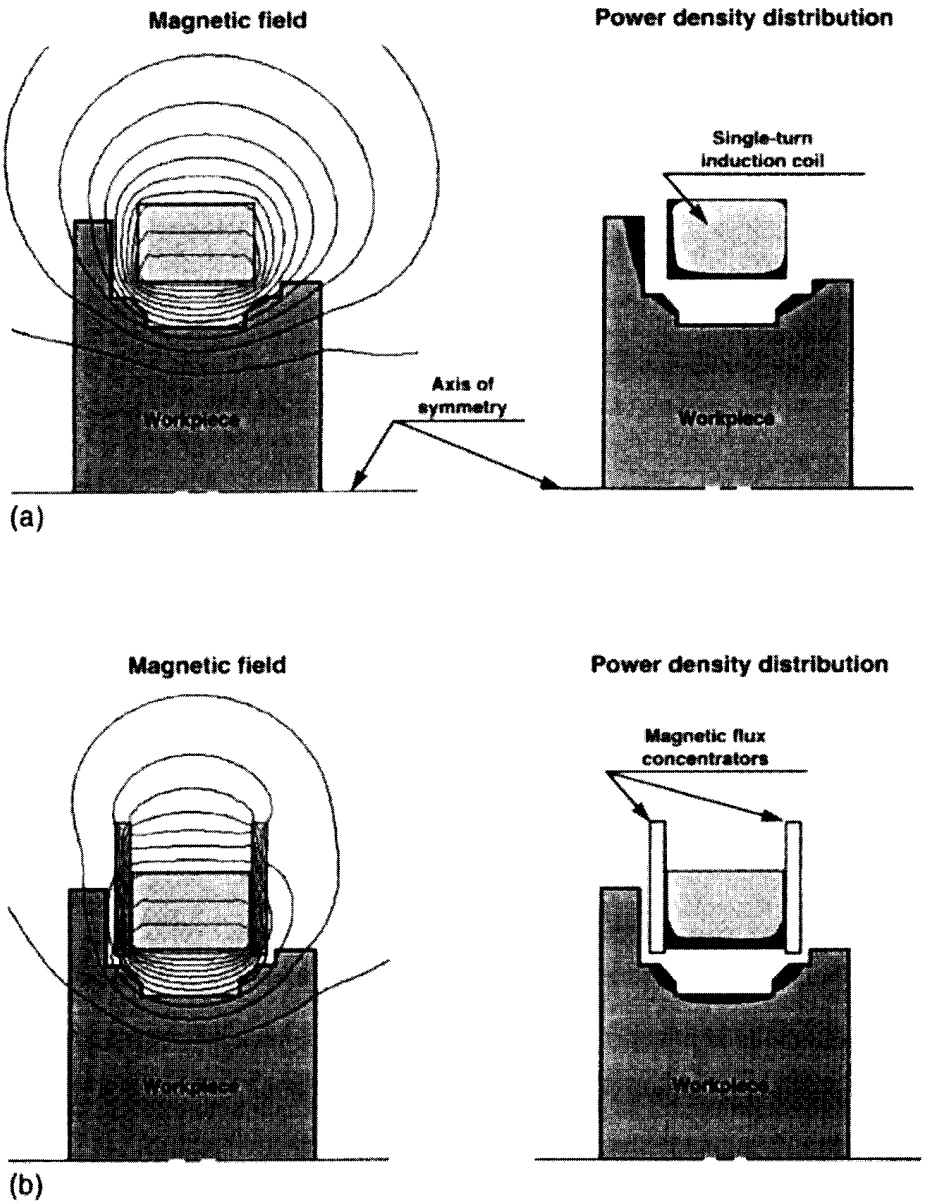

Figure 5.149 Magnetic vector potential distribution (A) without flux concentrator versus (B) with flux concentrator.

corners of flux concentrators because of their tendency to overheat due to electromagnetic end effects.

Manufacturers of induction heat treatment equipment have found the development and use of flux control technology increasingly important in reducing the size and improving the quality of induction heat treatment systems. Before beginning a project, detailed mathematical modeling and lab tests should be conducted to determine the cost effectiveness of using flux concentrators in a particular application. Different applications may call for different flux concentrator materials (e.g., laminations, Alphaflux, Fluxtrol, Ferrotron, Alphaform, etc.). Interested readers will find an analysis of the use of various materials for flux concentrators in

References [143–147, 154, 203]. Here we give only a short description of the features of using flux concentrators based on materials obtained from Fluxtrol Manufacturing Inc., Alpha 1, and many years of experience using flux concentrators at INDUCTOHEAT, Inc.

5.9.3.3 Selection of the Flux Concentrator Materials

The choice of concentrator material depends on several factors where the higher the value, the better the situation, including [203] relative magnetic permeability, electrical resistivity, thermal conductivity, Curie point, saturation flux density, and ductility. Other important factors rely on lower values for a better situation including hysteresis and eddy current losses. Additional factors that should be considered include the ability to be cooled and to withstand high temperatures; resistance to chemical attack by quenchants, machinability, formability, ease of installation and removal, and cost, which is dependent on the concentrator material, frequency, power density, and geometry of the heat treating system.

In heat treating, the materials typically used as magnetic flux concentrators are *soft magnetic* in nature, meaning that they are magnetic only when an external magnetic field is applied. In an electromagnetic field these materials can change their magnetization rapidly without much friction. They are characterized by a tall and narrow hysteresis loop of small area.

Magnetic materials that are soft magnetic usually have a uniform structure, low anisotropy, and magnetic domains that are randomly arranged. Random arrangement corresponds to a minimum energy configuration when the magnetic effects of the domains cancel each other. Therefore, the overall result is zero magnetization. The magnetic domains can be easily rearranged by applying an external magnetic field. The direction of domain rearrangement corresponds to the direction of the applied field. In this case, the magnetic materials behave as a temporary magnet [16, 39–46].

As mentioned above, magnetic materials used for flux concentrators should have both a high slope of magnetic permeability and a high saturation flux density. In addition to the magnetic permeability there are other important material properties of the concentrator material such as electrical resistivity and thermal conductivity. Magnetic materials with high electrical resistivity reduce the eddy current losses of the flux concentrator, thereby reducing its temperature increase. High thermal conductivity flux concentrators usually have a longer life because they are not subject to local overheating. Local overheating can be caused by heat radiation from the heated workpiece or high-density flux in certain areas of the magnetic concentrator.

One of the most important magnetic properties of concentrator materials is hysteresis loss. This quality is derived from the magnetization curve [16]. A typical magnetization curve, representing the magnetization process of magnetic materials, shows

1. A cycle of magnetization in one direction,
2. A reversal of the applied magnetic field, which results in demagnetization of previously magnetized material and its magnetization in the opposite direction, and
3. Another reversal process resulting in magnetization in the original direction.

Hysteresis loss is characterized by the conversion of electromagnetic energy into thermal energy due to rearrangement of the magnetic domains during the hysteresis cycle. This loss should be as small as possible because it signifies a temperature rise in the flux concentrator, which can cause a loss of its magnetism, and therefore, a reduction in coil efficiency.

Hysteresis loss is proportional to the area of the hysteresis loop and the frequency. Materials used for flux concentrators should have a coercive force as small as possible. A perfect flux concentrator with maximum efficiency would have no magnetization remaining after the external magnetic field has decreased to zero. A wide opening in the magnetization curve and a high frequency correspond to a high value of hysteresis loss. The flux concentrator properties can be determined from the manufacturer's data sheet or can be measured with the appropriate test equipment.

The types of materials most commonly used in induction heat treatment for flux concentrators and flux diverters [143–147, 154, 203]:

1. Laminations,
2. Electrolytic iron-based materials,
3. Carbonyl iron-based materials,
4. Pure ferrites and ferrite-based materials, and
5. Soft formable materials.

Laminations have been adapted for use in heat treatment from the motor and transformer industry. Grain-oriented magnetic alloys used in laminations are nickel–iron alloys and cold- and hot-rolled silicon–iron alloys. Packets of laminated steel punchings are used effectively from line frequency to 30 kHz. However, there are cases where laminations have been successfully used at higher frequencies (i.e., 100 kHz plus). Laminations are insulated with mineral and organic coatings and must be electrically isolated from each other and used at the proper frequency. The thickness of the individual laminations should be held to a minimum to keep eddy current losses in the concentrators low. Generally, laminations are 0.06 to 0.8 mm thick. Thin laminations are used for higher frequencies. Laminations with a thickness greater than 0.5 mm are typically used for frequencies below 1 kHz. Compared to most available magnetic flux concentrator materials, laminations have the highest relative magnetic permeability and saturation flux density. This is considered an important advantage. When laminations are applied, there are some problems that can occur. Laminations are particularly sensitive to aggressive environments such as quenchants, which lead to rust and degradation problems. Degradation of the magnetic properties of laminations is caused by an increase of coercive force and hysteresis loss. If the laminations are not firmly clamped, the punchings could start vibrating, resulting in mechanical damage, noise, and subsequent failure of the coil or process. Care should be taken with the corners of laminations and their ends, because of their tendency to overheat due to electromagnetic end effects.

One of the main advantages of using laminations is that they are relatively inexpensive and can withstand high temperatures better than other materials. Lamination packets can also be used to support the induction coil while remaining insulated from it. Another advantage of laminations deals with the fact that laminations have a high relative permeability and exceptionally high saturation flux density (1.4 1.9 Tesla). No other kind of magnetic flux concentrators,

including any types of magneto-dielectric materials and ferrites have such a high saturation flux density. This means that laminations better retain their magnetic properties in strong magnetic fields existed for example in some induction heating applications.

Electrolytic iron-based materials [145,146] were developed in the 1980s and early 1990s specifically for induction heat treatment applications. They can be machined by conventional methods, come in different sizes, and are available in two types of alloys with relative permeability up to 56. Some alloys are rated for higher frequencies (50 to 450 kHz) and others for lower frequencies (50 Hz to 50 kHz). They do not significantly degrade over time and can be easily removed and replaced for coil repairs.

Carbonyl iron-based materials came to the induction industry from products developed for the radio industry in the 1960s. They are easily machined but are available in only a few sizes having a low permeability ($\mu_r = 15$). These products were developed for the higher frequencies (200 to 450 kHz) and are easy to machine because of their high plastic content [145–146]. They cannot be soft soldered and must be acid etched. They have temperature characteristics similar to those of the electrolytic products but usually produce case depths about 10 to 20% less than the electrolytic products and laminations.

Other materials are pure ferrites or ferrite-based. Ferrites are dense ceramic structures made by mixing iron oxide (FeO) with oxides or carbonates of one or more metals such as nickel, zinc, or magnesium. They are pressed, then fired in a kiln at high temperature and machined to suit the coil geometry. In relatively weak magnetic fields ferrites have very high magnetic permeability ($\mu_r = 2000$ plus). Ferrites are quite brittle materials and this is their main drawback. Other disadvantages of ferrites are their low saturation flux density (typically 3000 to 4000 Gauss), low Curie point (approximately 220°C or 450°F), poor machinability, and the inability to withstand thermal shocks. Because of their high resistance, ferrite-based magnetic concentrators are particularly attractive for use in high power density magnetic fields or with high frequencies (50 kHz and higher).

Some concentrator materials are provided in a soft formable state (e.g., Alphaform [147] that can be easily molded to a desired shape for development purposes and later machined, if desired, to exact tolerances. Alphaform is an advanced composite of insulated iron microparticles, space-age polymers, and a thermally sensitive catalyst.

In some applications, magnetic flux concentrators can be made from a single material. Others may be constructed of several materials. For example, in a split-return coil, laminations can be located in the middle area of the coil and iron- or graphite-based materials can be placed at the coil ends. Such designs are cost effective and electrically efficient because they take into account the field distortion due to the electromagnetic end effect that results in additional losses within laminations at the coil ends.

5.9.3.4 *Advantages and Drawbacks of Using Magnetic Flux Concentrators*

As stated earlier, the use of magnetic flux concentrators delivers substantial benefits to the modern heat treater, such as

- reducing the operating power levels required to obtain the desired heating of pieces;
- improving the electrical efficiency of the process and decreasing the amount of energy used;
- making it possible to selectively heat specific areas of the workpiece;
- obtaining a superior heat pattern (i.e., more consistent hardness of the workpiece or more uniform heat patterns) and improving the physical and metallurgical properties;
- minimizing geometric distortion of the workpiece;
- preventing undesirable heating and annealing of adjacent parts;
- reducing the number of rejected parts, rework, and scrap;
- improving equipment life;
- reducing cycle time; and
- eliminating the negative biological effects of electromagnetic field exposure on humans.

Adding a flux concentrator to an existing inductor will result in additional expense. A common saying among people who deal with induction is that if a good part can be produced without a flux concentrator, there is no reason to add to the coil cost.

One of the major concerns with using magnetic flux concentrators has to do with the reliability of their installation. Typically, flux concentrators are soldered or screwed or sometimes simply glued to the induction coil. With time, due to different factors, there can be unexpected shifting or movement of the concentrator to an improper position. Usually, magnetic concentrators are located in areas with high magnetic flux density. Because of this, concentrators are affected by electromagnetic forces. Over time, as a result of those forces, the concentrator can become loose.

In addition to electromagnetic forces, this looseness can take place due to unstable temperature conditions. During the operation cycle, the flux concentrator could be heated to 250°C (482°F); then during quenching it could be cooled to the ambient temperature. In typical surface hardening applications, such heating–cooling cycles trigger an expansion–reduction of the volume of the flux concentrator. Unstable temperature conditions can also result in the flux concentrator moving or relocating itself in an improper position. As a result, the heating and hardening patterns will change.

Unexpected changes in the hardening pattern can cause very serious damage. For example, in the automotive industry this can result in the car being recalled for replacement of the defective part. To prevent such a situation, the flux concentrators should be examined from time to time and repaired if necessary. In some cases, special monitoring systems can be installed to indicate changes in concentrator operation; however, such monitoring systems substantially increase the cost of the equipment.

5.9.3.5 Case Studies

The following examples illustrate some of the practical benefits and features of using flux concentrators in various heat treatment applications [144, 203].

Application 1. Single-Shot Hardening of Long Shafts.

PURPOSE. To increase the torsional strength of the shaft by case hardening to a depth of one-fourth of the shaft diameter (one-half the radius).

Single-shot applications can increase productivity by heating the entire hardened area at one time. This application will require a larger power supply. When the power input is too low, the heat is conducted too deep; when the power is too high, the surface overheats. By using a flux concentrator, the power requirement is minimized and better control is established over process parameters such as cycle time and pattern termination at the ends of the heated zone. Lower power also increases the life of the inductor. The shaft shown in Figure 5.150 (a dummy for test purposes only) was heated with less than 250 kW. Quench blocks have been removed to permit viewing of the heated area.

Application 2. Channel Coil for Continuous Processing.

PURPOSE. To anneal parts that are moving through a long channel on a chain conveyor.

In multiple-station processes where conveyor speed is constant through all stations, the induction processing operation can be tuned to the constraints of the system by adjusting either the power input or the length of the inductors. Applications such as shell case and spark plug annealing are aided by flux concentrators on the channel coils (Figure 5.151), which increase the amount of energy that actually reaches the workpieces. Thus both the power requirement and coil length can be reduced. Figures 5.152 and 5.153 show the effect on magnetic field lines and current density, respectively, with and without a flux concentrator.

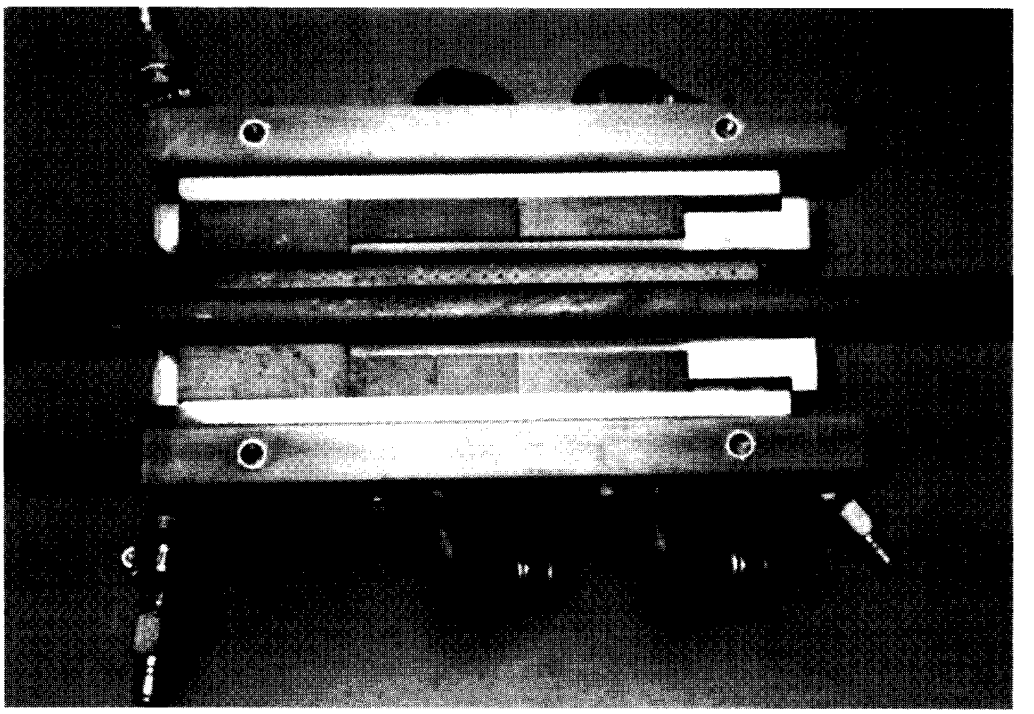

Figure 5.150 Single-shot induction hardening coil for long shafts.

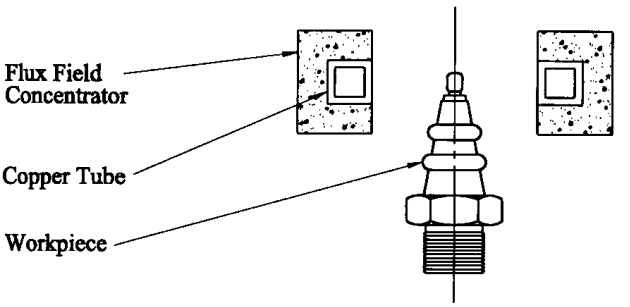

Figure 5.151 Flux concentrators can be used on channel coils to optimize continuous multi-station setups.

Application 3. Single-Shot Hardening of the Drive Stem.

PURPOSE. To increase the strength of the torque-transmitting component; to harden into fillet area and up to, but not into, the snap-ring groove.

Traditional scanning methods for induction hardening have created several problems, including (1) overheating of the corner of the large diameter near the fillet, (2) formation of a shallow and/or weak pattern in the fillet, and (3) a long tapered pattern terminating below the snap-ring groove.

The single-shot inductor enhanced heating characteristics but still did not consistently harden to specified depths over the entire part. Hot bands were observed at each end of the stem, and underheating occurred on the corner of the large diameter, in the fillet, and in the shank. With the addition of flux concentrators, the shank, large diameter, and fillet between them were heated at the same rate to produce the required hardness pattern. With the flux concentrators placed correctly at the top of the inductor, the pattern termination near the snap-ring groove was sharper and more controllable. The improved heating pattern was clearly visible in

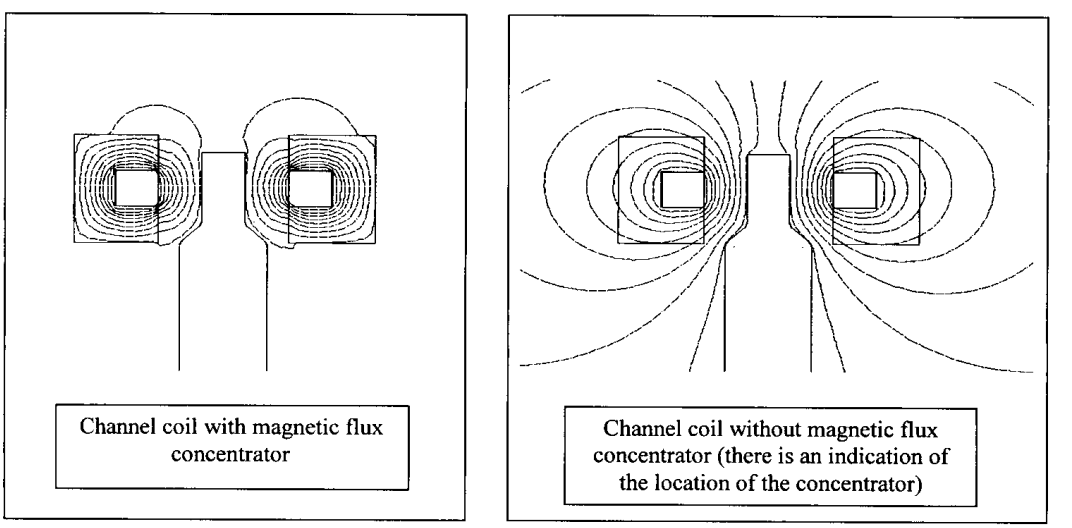

Figure 5.152 Effect of magnetic flux concentrator on magnetic field distribution (parameters are set to represent a vacuum).

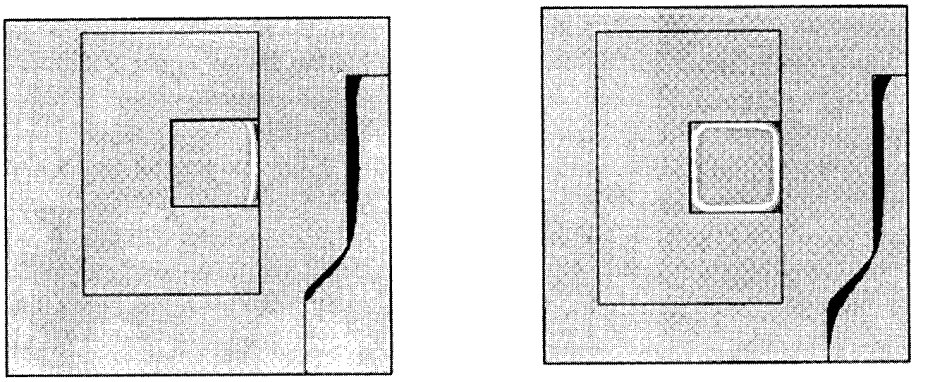

Channel coil with magnetic flux concentrator

Channel coil without magnetic flux concentrator (there is an indication of the location of the concentrator)

Figure 5.153 Effect of magnetic flux concentrator on current density distribution in workpiece end zone.

the parts as they were heated. Figure 5.154 shows the cut samples, the effects of improper heating (through heating at the top of the stem), and the improved pattern produced by the inductor after adding flux concentrators.

As inductor designers gain experience and familiarity with families of workpiece configurations, inductors can be designed with flux concentrator materials installed during initial fabrication (Figure 5.155). Minor changes are all that may be required for final pattern development. Typical heat time for short stems like this, at 10 kHz, is 6 sec at 100 kW.

Application 4. Hardening a Valve Seat.

PURPOSE. To improve surface wear to avoid marking by the valve.

Using a magnetic concentrator in this case turned an almost impossible development task into a fairly reasonable one. There were some obvious complexities. First, the diameters adjacent to the seat were the same size as the seat's outside diameter. The heat pattern produced by a simple inductor small enough to pass

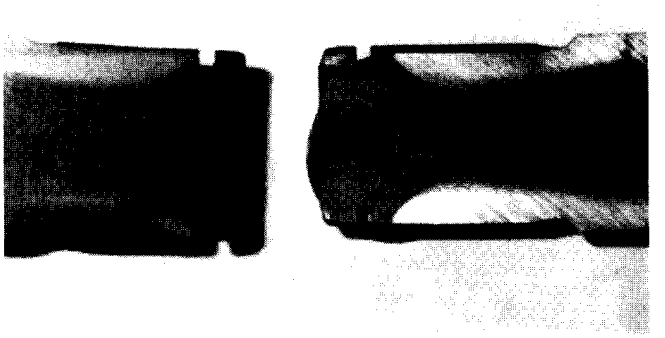

Figure 5.154 Use of flux concentrators is common when controlling hardness patterns at ends of parts.

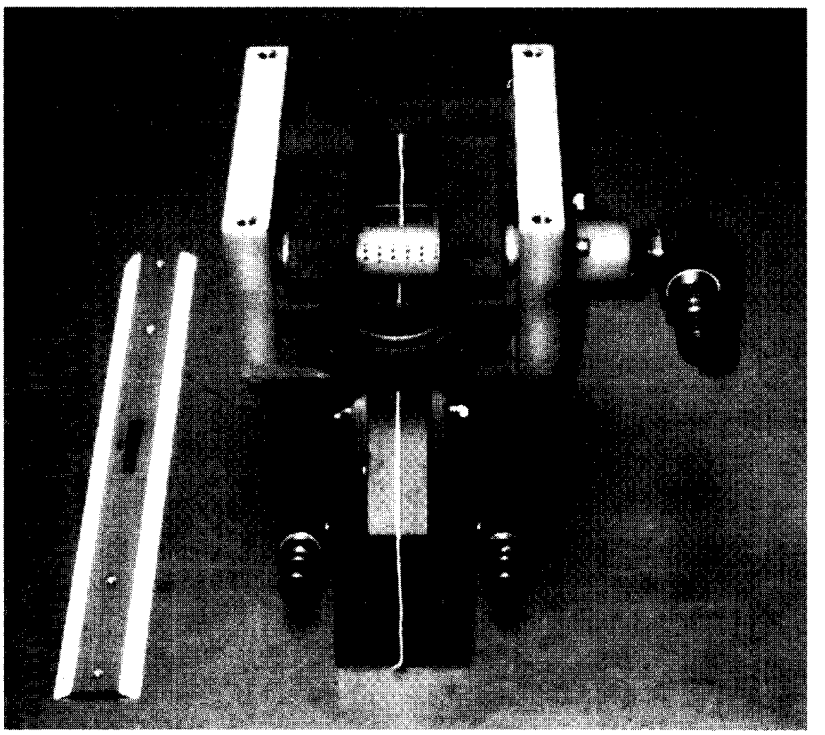

Figure 5.155 Flux concentrators are designed as part of inductors.

through these bores will not reach the outside diameter on the surface of the valve seat. Second, the tube inside the seat must not be hardened, yet the field intensity in a round inductor is greatest within the bore of the coil.

Magnetic flux concentrator material applied in the center and top of the inductor protects the center tube. It causes the heated pattern to flatten out across the seat and "pushes" the pattern across the entire surface. The pattern shown was accomplished with a 400 kHz unit at 6.0 kW in 4.0 sec. Figure 5.156 shows the placement of the powdered iron concentrator.

Application 5. Surface Hardening of Rocker Arm Tip.

PURPOSE. To improve surface wear on the nodular iron rocker arm.

Previous methods of heating rocker arm tips usually involved a circular inductor that heated the entire end of the rocker arm. The pattern was not optimal, and the time required to conduct heat to the center of the wear surface was excessive. A split-return type inductor improved results, and the use of flux concentrators allowed the wear surface to reach the hardening temperature before the remainder of the workpiece was appreciably heated. Heating time for this application was 1.0 sec at 27 kW at a frequency of 25 kHz.

From the examples described above, one can conclude that when choosing a magnetic flux concentrator for a particular application, the selection factors discussed here should be carefully considered. At the same time, major attention should be given to the location of the concentrator, its shape, and applied frequency. When many factors are involved in obtaining the required heating pattern, the computational ability of the induction heat treatment manufacturer becomes an ultimate advantage over companies that relay upon intuition and the experience of past mistakes.

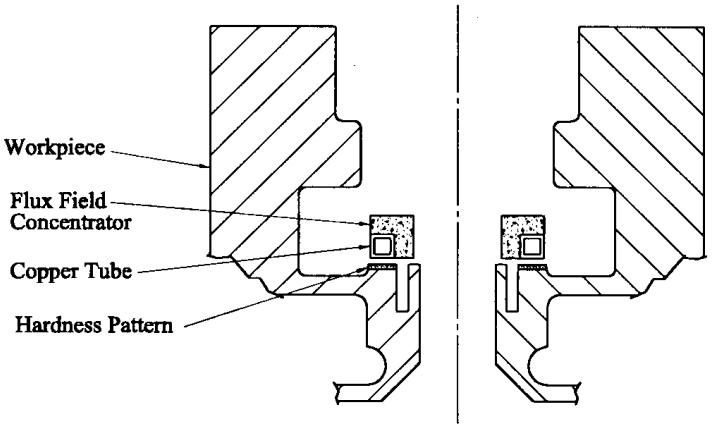

Figure 5.156 Placement of iron-based concentrator for induction heat treatment of complex-shaped part.

5.10 HEAT TREATING COIL FABRICATION, STORAGE, AND MAINTENANCE

5.10.1 Coil Fabrication

Inductors or coils are typically made of copper because of its high electrical conductivity and, therefore, low power loss. Other important reasons for using copper in coil manufacture are that copper is relatively inexpensive and has good thermal and mechanical properties. Oxygen-free high conductivity (OFHC) copper is commonly used for high-power or high-frequency applications. Coils made of OFHC copper are expected to have a longer life than coils constructed of commercial grade copper.

Because certain areas of the coil carry higher currents the location of coil cooling is critical. Coil cooling, wall thickness, and copper tubing selections are discussed in Section 5.1.7.

For multiturn coils made from copper tubing, the tubing is typically annealed to provide some ductility and is wrapped around a mandrel. When sharp bends or small diameters are required, sand or other fillers are packed into the tubing cavity to keep it from collapsing when being formed.

In addition to carrying the current the rest of the coil serves other mechanical purposes such as cooling passage and quench pocket design, and support against mechanical flexing caused by electromagnetic forces. At higher frequencies, coil currents are typically lower. As the frequency is lowered, more attention must be paid to coil support and brazed joints. There is also more vibration at lower frequencies, especially at the turns near both ends of the multiturn solendoid coil or split-return inductor. Nonmagnetic metal studs held together with an insulator can be added for support.

Brazed joints and copper may work-harden and develop fatigue from the on–off cycling of power. The clearance in silver-based solder joints should be held to a minimum. The solder should flow due to a capillary action into joints. Critical joints that are in or near the working area of the coil can be overlapping or tongue-in-groove joints. Figure 5.157 is an example of a tongue-in-groove joint commonly used on single-shot inductors. Common joint designs are described in Section 6.1.

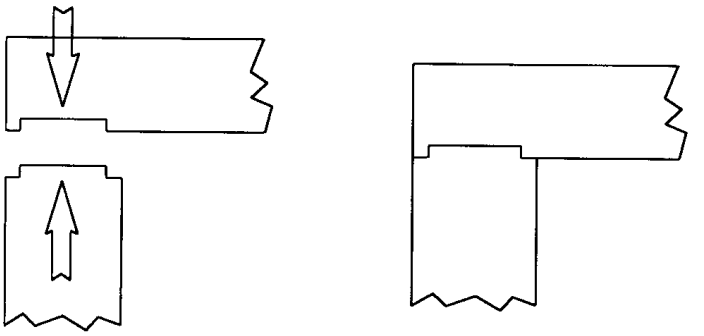

Figure 5.157 Example of type of tongue-in-groove joints commonly used on critical areas; joints should accurately mate and have minimum clearance for assembly.

The areas that do not participate in the actual heating can be fabricated with less precision. These include cooling tubes, covers for water pockets, studs for coil support, and any other items that are not expected to carry current.

Commonly used silver solder contains 35 to 45% silver. Experience in using silver solder with this silver content has shown that it flows well and has relatively low electrical resistance which is important for minimization of Joule losses in joint areas.

After brazing, the rest of the inductor is assembled and any coil protection added. There are several common ways to protect induction coils from the sometimes harsh environment to which they are exposed. Epoxy coating is often applied to multiturn inductors for isolation purposes (between turns). When a more abrasive coating is required for wear, a thin layer of ceramic is flame-sprayed onto the selected area of the inductor. This not only acts as an insulator but also adds good wear properties for cases where the part could come in contact with the inductor. In addition, ceramic or refractory cast liners can be added when space is available. One advantage to a liner is that it can usually be replaced, if damaged, without removing the inductor from the equipment, thereby reducing equipment downtime.

An important feature when designing and fabricating an induction coil is the consideration of the electromagnetic field in the immediate vicinity of the inductor. The use of the low-resistive nonferrous materials (preferably nonelectrically conductive materials) in the area close to the inductor is recommended. The fasteners and washers used to connect the buswork to the inductor should also be nonferrous but preferably nonconductive. The rule of thumb is that ferrous materials should be located at least one coil diameter from the coil. More precise recommendations can be obtained by using numerical modeling.

5.10.2 Heat Treating Coil Maintenance and Storage

Heat treating inductor maintenance can be summarized in five categories: maintaining the tooling and part holding devices, keeping the inductor clean, providing a visual inspection for monitoring a deterioration process, maintaining good electrical contacts, and maintaining spares.

Consistent Workpiece Holding

Because heat-treating coils that are made from copper are an electrical as well as a mechanical device and are in close proximity to hot parts and quenchants, they are subjected to deterioration and wear. The tooling, which holds the workpiece during heating, should be robust, corrosion resistive, and provide a consistent coil-to-part location. Care should be used when manually loading parts, to avoid damaging the inductor.

Keeping the Inductor Clean

Most hardening applications produce some amount of scale from the part as it is heated and quenched. The scale (small metallic flakes) combined with the quench medium can stick or cling to the inductor. If this is allowed to build up on or within the coil it can cause arcing or premature failure of the inductor. Wiping or washing off the coil on a regular basis is recommended. The application and its cleanliness will determine the frequency of cleaning. A mild soap can be used to clean the inductor. If a brush is used it should have plastic bristles; a wire brush can leave metal bristles in the coil, which could be detrimental.

Visual Inspection

Routine visual inspections should be done to look for deterioration or arcing of the coil. High-powered inductors can develop cracks in the heating face; this is more likely to happen when the inductor has quench holes drilled through the heating area of the coil. Cracks in the coil will cause a loss of efficiency, because the current will have to travel around the crack. This will be more noticeable at higher frequencies, because in effect it is like having a larger air gap between the workpiece and the inductor. If the crack in the inductor becomes large enough it will eventually cause a water cooling leak and be unable to process parts.

Maintain Electrical Contacts

There are two basic ways to install an inductor: either several bolts are used or, for frequent changeover, a quick-change type can be used (see Figure 5.58). The types of mounting feet are described in Section 5.1.8.

For many heat treating applications 10 to 12 mm ($\frac{3}{8}$ to $\frac{1}{2}$ in.) brass or stainless steel bolts are used for the inductor-to-bus connection. The stainless steel bolt should be tightened to approximately 35 to 40 ft lbs. Overtightening of the bolts can pull the threads from the soft copper, but undertightening will not produce a good electrical contact and lead to arcing and premature failure. Scheduled inspection of the fasteners to check for tightness is important. Higher power and lower frequencies require a more frequent inspection for tightness, due to more vibration when the heat is applied. Figure 5.158 shows the results of a loose connection.

If a tapped hole is to be used at the connection point, stainless steel threaded inserts should be utilized to maintain the threaded hole. Heavy-duty washers are recommended to ensure that adequate force is applied in the right areas and to distribute the force over a larger area. Figure 5.159 shows the results of not using the proper washers.

When using a quick-change arrangement it is important to maintain and inspect the clamping features such as springs and stainless steel clamp bars.

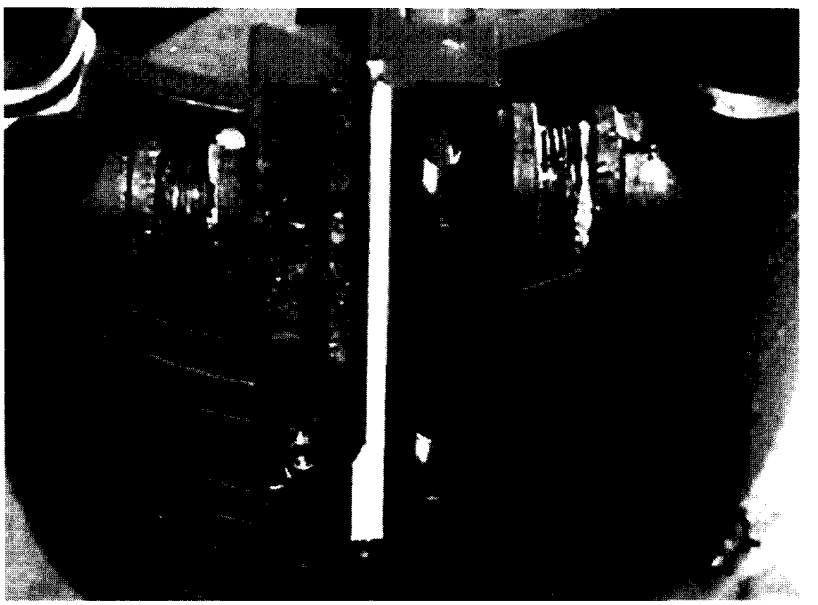

Figure 5.158 Results of loose connection between bus and inductor.

In all cases the electrical connection surfaces must be clean and free from nicks, burrs, scratches, and arc marks.

Besides keeping the surfaces clean providing good electrical contacts, coating with a thin silver plating is often done in an effort to keep the resistivity low at the connection joint. In addition, the plating prevents the copper from corroding, which could cause a poor contact.

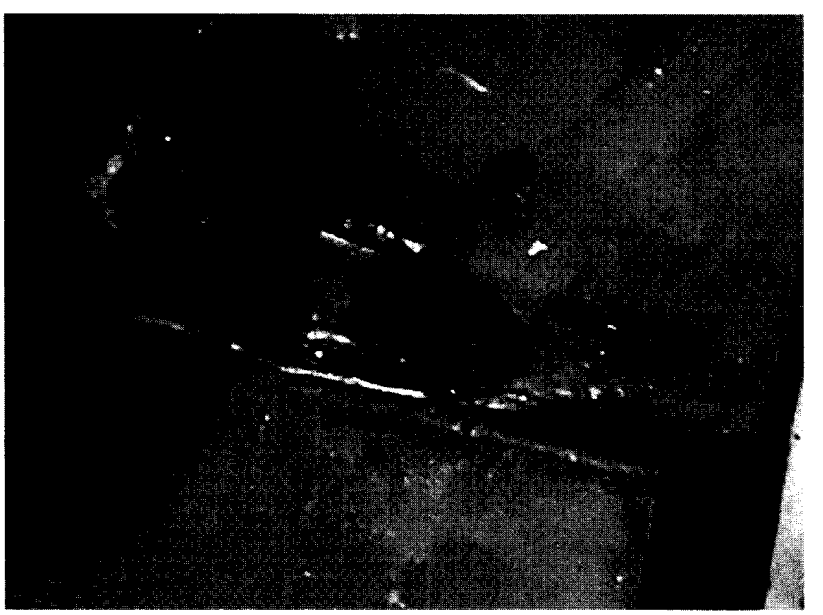

Figure 5.159 Results of not using correct washer: washer that was used has melted.

Spares

As with any critical component in production it is important to have and maintain spares, to minimize equipment downtime. It is recommended to have at least two of each inductor on hand. In the event that one inductor is being repaired, there will still be one on the equipment and one spare in storage. It is important to keep inductors stored (when not in operation) in a way that they stay clean and undamaged. If adequate protection is provided, the shipping containers often can be used as a storage device. Figure 5.160 shows an example of a shipping container that is commonly used to store inductors. The container also provides a label to describe the contents; the label includes vendor identification numbers and the customer's part and tooling number. These are not only used for inductor storage, but also to ship the inductor back and forth for any maintenance repairs.

5.11 BASICS OF METALLOGRAPHIC SAMPLE PREPARATION AND MODERN EQUIPMENT FOR MICROSTRUCTURAL ANALYSIS

5.11.1 Introduction

Metallography is a critical part of quality inspection of heat treated parts. Induction hardened materials present specific challenges when it comes to sample preparation and quality inspection. The hardened surfaces of induction hardened parts can be analyzed simply by sectioning the part and macroetching it, or by using a complete

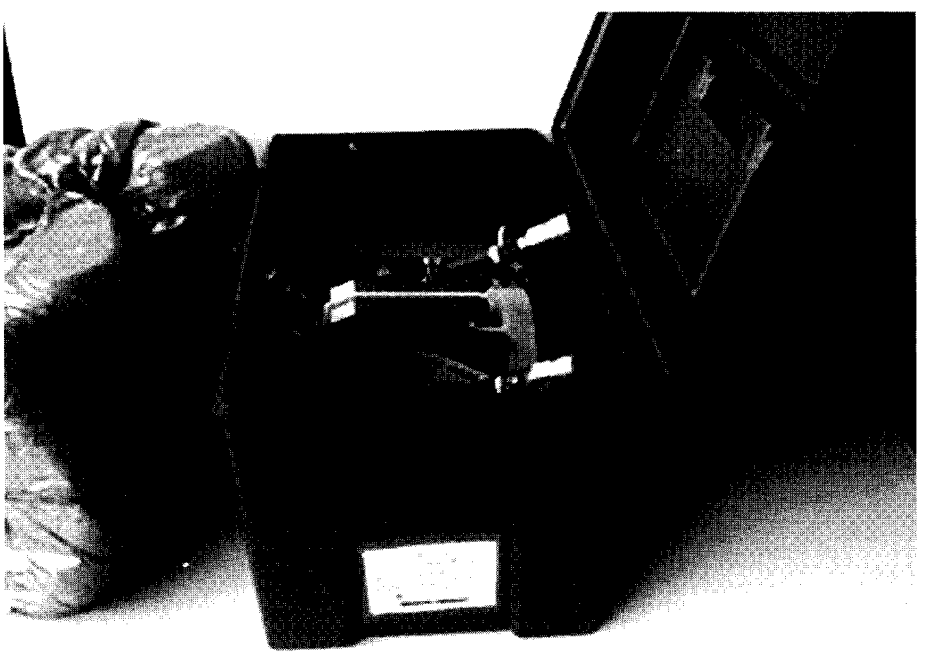

Figure 5.160 Shipping containers can be used as storage devices to provide protection for inductor when not in use. Labels provide information such as inductor, tooling, and serial number.

metallographic preparation and examining the microstructure at high magnification. This section concentrates on preparing induction hardened parts for visual and hardness examination. Each step in the metallographic process is examined in detail with tips on getting the best results in the least amount of time. Each induction hardened sample is slightly different. Some have very deep case depths and others have thinner areas of hardened material. The process of metallography is typically the same whether the depth is extreme or not. Examining an induction hardened sample allows the engineer to evaluate the depth of the case hardened area, the microstructure, and if any defects may have been caused by the process (e.g., cracking, decarburization, carbide formation, etc.). When a sample is prepared for examination it can also be tested to determine physical properties. Using hardness and microhardness testing allows the engineer to determine if the sample attained the correct hardness and whether the hardness depth is correct.

There are many types of nondestructive methods for inspecting induction hardened parts. Some of them can even be conducted while the sample is being produced. These types of tests are very effective but they have to be verified by destructive means—metallography. Metallography allows the technician and/or engineer to view the sample and verify several different characteristics that could affect the part's performance. Metallography plays a critical role in the development and ongoing inspection of induction hardened parts. During setup several factors have to be measured accurately to ensure that the correct depth of hardening is obtained. Other factors that need to be verified are core hardness, microstructure, and inspection for defects.

5.11.2 Theoretical Background of Sample Preparation

The technical definition of metallography is: "Metallography or microscopy consists of the microscopic study of structural characteristics of a metal or an alloy." This process can also include ceramics, plastics, composite materials, and various other types of materials. Metallography encompasses the preparation of samples for the study of the material.

The history of metallography began with a gentleman named Henry Clifton Sorby in the late 1800s. He was a scientist who was curious about metals and their structures. Using very simple methods and a primitive microscope, he managed to see structures in ferrous metals and theorize about how each type of structure was formed. Many other scientists added to this type of research and metallography was accepted as a vital part of quality inspection techniques.

There are varying degrees to which metallography is taken depending upon what type of information is being collected. The goal in metallography is to proceed through the metallographic process without changing the appearance or structure of the material. Therefore a metallographer must take careful precautions to avoid overheating the sample, and applying the correct grinding and polishing steps during these processes. A person examining the microstructure with a microscope should see the same structure that was there when the sample was started. This is extremely important when dealing with induction hardened or heat treated parts. They typically contain higher amounts of carbon and extreme care needs to be taken because these types of samples are easily burned during the sectioning or grinding process.

The following sections contain many procedures and helpful hints that will aid in acquiring the best possible results in your metallographic laboratory.

5.11.3 Stages of Sample Preparation, Basic Guidelines, and Rules of Thumb

There are several stages of sample preparation covered in this section. Discussion of each subject includes explanations, methods, and helpful hints that can cut preparation time and produce high-quality samples for examination. There are two approaches to metallography: research and production/quality control. This section covers both these areas but the main focus is on the quality control aspect. Emphasis is placed on preparing the samples for a typical evaluation in a heat treat facility or similar situation. Metallographers are always under pressure to reduce the number of steps so that the samples can be viewed more quickly; however, samples have to be in a condition that will allow the scientist or engineer to make a judgment on the quality of the sample. The sample has to be prepared properly so that structures are not misinterpreted because of changes to the sample or simply not being able to see the structures clearly enough to review the sample's status. There are many ways to prepare a sample but we focus on procedures that maximize a metallographer's time and resources. Keep in mind that a metallographer should not sacrifice quality when samples are being evaluated. The ultimate goal of any metallographer is to provide a well-prepared sample for evaluation and to use all resources to their best advantage.

5.11.3.1 Sectioning

The first step in metallography is to remove a representative sample from the original. This can be done using several different methods, but the most effective for the metallographer is the sectioning machine. A typical sectioning machine consists of an abrasive wheel and a coolant system to keep the sample cool during the cutting process. Sectioning machines are available in many different sizes, from units that use 3 in. blades to units that use 20 in. blades. Figure 5.161 shows a sectioning machine that has a builtin coolant tank along with a cutting area which allows the operator to work in a safe environment. It is extremely important that coolant be introduced into the cutting area in order to keep the sample at a reasonable temperature. If not, the surrounding area where the cut is taking place will be affected by the heat generated from the cut-off blade. Sectioning induction hardened samples can present many unique problems. Samples that have very thick induction hardened areas will often contain residual stresses that cause the part to pinch down during the cutting process. Even when the part is clamped down on both sides, these stresses are so great that they can pinch down on the blade causing the machine to stop or the blade to break. There are certain techniques that can help when this type of problem is encountered. Oscillating the blade through the cutting area can alleviate this situation; this technique also aids in cooling the sample during cutting. Pulse cutting can also be used to section difficult parts. The machine is set up to apply cutting force and then release the force for a desired amount of time. This also allows the coolant to penetrate into the cutting area and allows the swarf to be cleaned away. Coolant should be introduced onto the blade near the cutting area to allow the water to penetrate into the cutting area. Oscillation or pulse cutting allows more coolant to reach that area. Coolant that is used in a metallurgical saw should have a rust

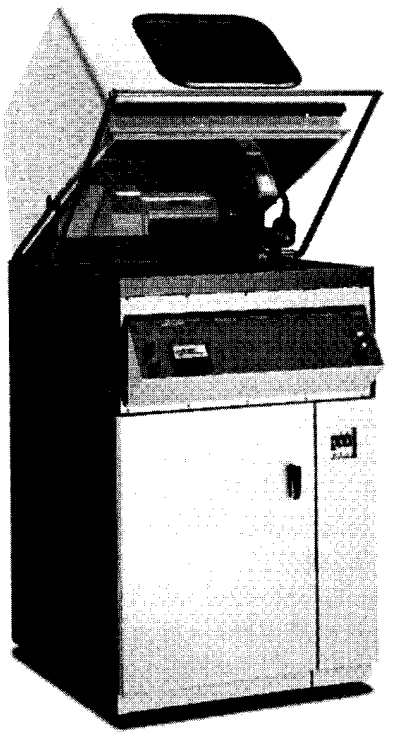

Figure 5.161 Sectioning machine. (Courtesy of LECO Corp.)

inhibitor and/or a lubricant. The rust inhibitor protects many of the internal parts and helps keep ferrous samples from rusting too quickly. Most metallurgical saws contain a tank that acts as a collection area for particles that build up from the cutting blade and from the sample itself. Baffles or some type of separation system help keep these particles from being recirculated into the cutting area. Also available are magnetic-type systems, which remove particles that can be attracted to a magnet. These types of systems help keep the coolant clean and also reduce maintenance.

One of the most important selections an operator can make is the selection of the cut-off wheel. An operator can have access to the most sophisticated equipment and if the wrong blade is used, then the results will not be acceptable. The key to choosing the correct blade is to match the blade to the material that is being sectioned. For example, when cutting a material that is 45 HRC, an operator should choose an abrasive blade that is designed to cut this hardness range. There are several types of blades that can be used including silicon carbide, aluminum oxide, and diamond. Silicon carbide abrasive blades are used mostly for nonferrous materials including aluminum and titanium. Aluminum oxide wheels—the most commonly used wheel—are used on ferrous materials. There is a wide variety of blades for different hardness of materials.

Abrasive cut-off wheels are constructed of abrasive particles, which are held together using different bonding systems. The main bonding systems are resin, rubber, and a combination of both. Resin-bond wheels are considered to be hard wheels: wheels that do not break down as quickly. Rubber-bond wheels are considered to be soft wheels and are designed to break down more easily. For

harder materials the rubber bond allows particles to break away from the wheel so that new cutting edges can be exposed on the surface of the wheel. Because the sample is harder, the cutting particles dull down more quickly. If they are not allowed to break away from the wheel, their cutting efficiency starts to diminish and instead of cutting, they generate heat. Cutting softer materials does not require that the particles be allowed to break away as easily as they are not getting dull as quickly. This is a delicate balance and an operator may need to try several types of wheels before a good choice can be made. Most manufacturers will have charts or tables that show the hardness range that certain blades will cut. When cutting very hard materials such as 60+ HRC, then a decision has to be made on what is important when cutting the sample. If the microstructural integrity is important, then use a soft blade and be prepared to use more blades than normal to get excellent results. If the priority is just to cut the sample and burning is not a critical issue, then a harder blade can be used. This will allow the blade to be used longer, but the resulting cut could get quite hot and affect the evaluation. There are many choices in the metallographic field for cut-off wheels and there is usually one ideally suited for the metallographer's particular application.

Diamond wheels are typically used for cutting extremely hard materials. Diamond blades come in different sizes from 3 up to 12 in. or larger. They can be run at different speeds depending upon the metallurgical saw. Low-deformation saws run at slower speeds to decrease the amount of deformation, whereas the typical metallurgical saw runs at higher speeds to increase the cutting rate. Diamond blades are quite expensive but they are designed to last much longer than abrasive wheels. Diamond wheels can be used to cut softer materials but since the diamonds stay in place on the wheel they can accumulate debris and cause the wheel to "load up." The debris or metal coats the edge of the wheel and the diamonds cannot cut properly. The wheel must then be dressed using a dressing stick. The dressing stick is an abrasive material that cleans the interstices between the diamond particles. Diamond wheels offer superior performance on materials such as ceramics, carbides, cermets, and other extremely hard materials.

Care should be taken when cutting samples for metallurgical examination. A manual cut-off machine, such as the one shown earlier, should be used according to the manufacturer's specifications. Some cut-off machines will have an amperage meter on the unit. This allows the operator to monitor the amount of pressure that is being applied. The pressure should be light at first until a groove has been formed; then the pressure can be increased. As the sectioning is coming to an end the pressure should be reduced. This will allow the blade to cut easily through the final area of the sample. Excessive pressure can cause blade breakage, deflection of the blade, and burning of the sample. When cutting a sample and the blade is not making steady progress through the part, simply try to apply a little more pressure to see if the blade will break down and start to cut. If this does not work then a different abrasive blade should be tried.

Abrasive cutting is indispensable to the laboratory. To the metallurgist, the quality of the cut is paramount and wheel life is secondary. To the manager, just the opposite may be true. With all of the options that are readily available regarding types of abrasive and bonds, a happy compromise can be reached. A well-equipped metallographic laboratory should have a variety of wheels available for different applications.

5.11.3.2 Mounting

Most samples that have been sectioned are not really suitable for grinding and polishing. The sharp edges and awkward shapes are not conducive to safe handling of the sample at grinding speeds of 300 rpms or higher. Odd shapes also make preparing a good sample even more difficult. Mounting a sample allows the metallographer to handle the specimen safely and the mounting material also supports the sample so that edges and other features can be examined at higher magnifications. The two most common methods of mounting samples are hot and cold mounts. Hot mounting is a term used to describe a technique that uses a mounting press, where heat and pressure are used to fuse the mounting material into one homogeneous material. Cold mounting describes the process of mixing two or three different components so that a chemical reaction occurs and forms a hard material. Mounting presses typically take 8 to 12 minutes to produce a normal size mount. Only one or two mounts can be made at a time so there is some downtime waiting for mounts to be completed. Cold mounts, on the other hand, can be made several at a time and this allows the metallographer to process several mounts at once. One could ask why a lab technician would choose to use a mounting press over the cold mounting materials. Cold mounting materials can be expensive and some contain hazardous materials that can cause odors in the lab. If a laboratory is going to produce a large number of mounts in a year, then it is preferable to purchase a mounting press because the consumables are much less expensive. Also hot mounting produces very good mounts with excellent edge retention.

A mounting press consists of a base unit with a heater that is wrapped around a mold cylinder. This is where the sample is placed and covered with some type of granular or powder mounting material. Pressure and heat are applied to form the plastic material around the sample. Hydraulics can be used to apply pressure and electricity is used to generate heat around the mould cylinder. Pressure must be maintained during the heating process so the material coalesces properly. Most mounting presses automatically keep the pressure maintained during the cycle, around 4200 PSI. Some mounting materials require less pressure and adjustments are normally made manually using the interface. Some type of cooling is applied—air or water—and the mount can then be ejected. Some presses are capable of making two mounts at one time by using a spacer between the mounts. Figure 5.162 shows a typical mounting press.

a. *Choosing a Mounting Material.* There are several features that separate the different types of mounting materials. For a harder sample, a mounting material with high hardness characteristics should be chosen. For induction hardened parts, the focus is normally on the surface of the sample. When choosing a mounting material, the material should stay in contact with the sample and be hard enough to keep the sample edge from rounding. The grinding and polishing procedure has some influence on this, but choosing the right mounting material will certainly help.

Epoxy thermosetting powder is one of the best mounting materials because it adheres to the sample and edge retention is excellent. Other choices include Bakelite, diallyl phthalate, and Lucite mounting materials. Bakelite is the economic choice and is widely used in metallography labs around the world, as it performs very well in most everyday applications. Diallyl phthalate is typically glass- or mineral-filled and

Figure 5.162 Mounting press. (Courtesy of LECO Corp.)

this increases its abrasion resistance. This makes it a very good mounting material for harder substances such as carbides, tool steels, and induction hardened parts. Epoxy thermosetting powder, Bakelite, and diallyl phthalate are thermosetting mounting materials, which means that they solidify during the heating cycle in the mounting press. The material goes through a transformation during the heating cycle and is a solid when the maximum temperature is reached. The mounts can be ejected hot but the best results are achieved when the samples are allowed to cool under pressure.

Lucite is a thermoplastic mounting material. Thermoplastic materials differ from thermosetting materials in that they cure during the cooling cycle rather than the heating cycle. Care must be taken that the cooling cycle is slow because a fast cooling rate will cause the material to solidify too quickly and unmelted resin will be trapped in the center of the mount. Air cooling is the best approach when making Lucite mounts. Lucite is a clear mounting material and is not intended for use with hard samples. It is best used with softer materials, and where edge retention is not a concern. The ability to see the sample and be able to grind to a certain location can be very important. When examining an induction part that has a defect or crack on the surface, for example, Lucite would allow the operator to grind to that particular area and examine it closely. Care must be taken when grinding Lucite because it grinds away fairly easily and it is very easy to grind past the area of interest.

b. *Cold Mounting Materials.* Another choice for mounting samples is cold mounting materials such as epoxy, acrylics, polyesters, and others. As in the thermosetting materials, there are choices between harder materials such as epoxy and the convenience of the acrylics. Once again epoxy is the best choice for most applications. It sets up very hard, flows very well, and works effectively for a variety of samples. Epoxies can be purchased with varying curing times. There are versions that have cure times of up to 72 hours and some as quick as 30 to 40 minutes. Epoxy can be cured in a vacuum to remove bubbles in the materials and

also to fill in cracks, voids, and pores in different types of materials. Edge retention for epoxy is excellent so it is a very good choice for induction hardened parts when the edges of the sample are of interest.

Another choice is acrylic mounting material, which provides the convenience of a short curing time. The material is normally mixed in a 2:1 powder-to-liquid ratio and the cure time is 10 to 15 minutes. It provides good edge retention and many mounts can be made at once. Acrylics can also be cured in a pressure vessel to provide a clearer mount with fewer bubbles. Acrylic materials are excellent for making larger mounts such as 2 in. or irregularly shaped mounts. Acrylics should be mixed in a well-ventilated area or under a fume hood due to the volatile fumes generated during the mixing process. There are other choices such as polyester and others, but they are used much less than the two mentioned previously. There are many choices available to the metallographer but one should choose the best material for the particular mount. Special attention should be paid to the hardness of the material, edge retention, flow characteristics, and other special considerations.

5.11.3.3 Grinding

Grinding is probably the simplest procedure and the most overlooked step in metallography. At first glance the metallographer is simply removing a layer of material with a grinding paper and then moving on to another one. Although this may seem simple it is actually a complex process where material is removed and a layer of structural deformation is introduced into the material. The whole concept revolves around removing the previous layer of structural deformation and replacing it with a thinner layer of deformation. This is completed using smaller and smaller abrasive particles to grind the sample. The most common form of grinding is with silicon carbide papers that are placed on a platen and rotated at approximately 300 rpms. Belt grinders, like the one shown in Figure 5.163, are often used for heavier material removal. Belts and papers come in different sizes, and grit sizes vary from product to product. There are two types of grading systems for silicon carbide; aluminum oxide papers and abrasive disks. There is an ANSI (American National Standards Institute)/CAMI (Coated Abrasives Manufacturers Institute) grading system and there is a FEPA (European Federation of Abrasive Producers) grading system, which matches the ANSI system up to 220 grit and then the FEPA's numbers get

Figure 5.163 Belt grinder. (Courtesy of LECO Corp.)

larger. FEPA designations typically start with a "P" and are sometimes called P-grades. ANSI/CAMI are the more typical grit sizes that we relate to in the United States. There are several comparison charts that show how each grade corresponds to the other. These grit size designations apply to belts, wheels, and disks of all sizes.

The first step in grinding is to get the sample flat so that the subsequent steps can be focused on removing the structural deformation. When a sample comes off a sectioning procedure, 180 grit papers or the equivalent will get the sample flat and remove the sectioning deformation. In some cases coarser grit may be needed, but most metallographic samples can be started in this way. Using a belt grinder for the first step is only recommended when the sample is going to be prepared manually. If the sample is going to be prepared automatically a belt grinder should be avoided. It is best to let the automatic machine perform that operation because the subsequent steps can be shorter and more effective. The second goal in grinding is to remove structural deformation. A coarse enough grit size should be used at each step to remove the previous step's structural damage and to leave a thinner layer of disturbed material. A typical grinding procedure might consist of 180, 320, and 600 grit, and then one or two polishing steps to finish the sample. The most common grinding material is silicon carbide, and the second most used is aluminum oxide. Water is used as the coolant during grinding. Grinding can be performed using manual or automatic methods. It is important during the grinding process that sufficient coolant be applied to keep the sample cool.

Grinding samples manually requires some expertise and feel for the process. It is very easy to bevel a sample and compound that error by trying to grind in another direction. It is important that an operator find a procedure that works for him or her. A good way to start is to gently press the sample onto a grinding paper and hold it in place for a few seconds. After lifting the sample, examine the grinding scratches and make sure they are going in the same direction. Rotate the sample 90° and grind the sample once again. After a few seconds examine the sample again and see if all of the scratches are going the same direction. If they are, then you have successfully removed the previous deformation on the sample. The operator can proceed with this method on the finer papers and—after using 600 or 800 grit—clean the sample and examine it closely for flatness.

One common mistake is to put too much pressure on the sample while grinding. Heavy pressure will most likely cause more problems than produce a good sample. Gentle even pressure will remove the right amount of material and produce a very good surface finish so that polishing can be accomplished. This method can be used on a stationary grinder such as the one in Figure 5.164, or it can be used on a rotating wheel. When using silicon carbide it is important that the operator understand that this type of abrasive does not last for an extended period of time. Each silicon carbide paper has abrasives embedded in the surface and as each piece of abrasive becomes dull its cutting efficiency goes down rather quickly.

Grinding can be considered a microscopic version of a milling machine. Each fixed abrasive particle acts as a machine tool, except there are thousands of machine tool points on a fixed abrasive paper as opposed to one large machining point on a milling machine. The effective cutting life of a silicon carbide paper is only about 60 seconds. After this the sample is not getting effectively ground but rather burnished,

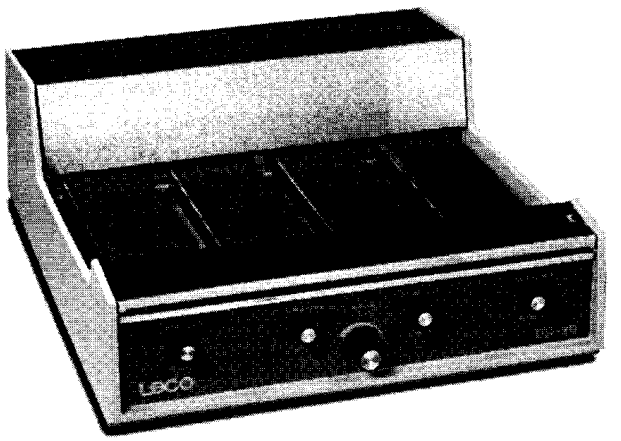

Figure 5.164 Stationary grinder. (Courtesy of LECO Corp.)

which can cause more structural deformation. Grinding induction hardened samples is not too much different than grinding other samples. The unique aspect of induction hardened parts is the hardness difference between the surface and the inner core of the sample. Emphasis should be on keeping the sample flat and, because the surface of the sample is most likely the area of interest, edge retention is the most important factor. Using good techniques during the grinding process will allow the operator to move smoothly through the polishing process and ensure success for a well-prepared sample. If attention is paid to this area of metallography, the sample will be flat and scratch-free, making it much easier for the technician or metallurgist to evaluate the sample.

New methods of grinding are coming into the metallographic market every year. New advances in bonding diamond and other abrasives to other types of materials have enhanced wheel life and convenience to the end user. One of these is a diamond–resin bond product that uses a metal mesh backing. Since diamond is extremely hard it does not break down as do other abrasives. It can be used for extended periods of time and can be used in conjunction with a magnetic plate, which holds the wheel in place during the grinding process. These types of systems will cost more money at the beginning of the process, but they will work for longer periods of time, and overall will be more efficient due to shorter grinding times, less downtime, and more productivity from the lab.

5.11.3.4 Polishing

Although grinding procedures can be very simple and most labs perform similar operations, this is where big differences occur from one lab to another. Lab A can be preparing the same material as Lab B and the grinding steps are similar. The polishing steps, however, can be quite different. For one thing there are more choices when it comes to polishing. Most labs depend upon the experience of people who have worked there before them. This can be good or it can be bad, depending upon the expertise of the advisor. Lab A may polish the sample using four or five polishing steps and Lab B may use only two. There is no guarantee that the samples from Lab A will look better than the samples from Lab B. The variables involved with polish-

ing are many and experience and knowledge go a long way. Some of the variables include polishing materials, polishing cloths, speed, pressure, and duration of polishing. For induction hardened parts the polishing procedure usually focuses on polishing the induction hardened area of the sample so that the edge, and the fine microstructure of the tempered martensite region can be examined. If the outer edge of the sample is prepared properly, then the core will also be polished well enough for visual examination.

Intermediate polishing is the first step in the polishing process. This section is designed to recommend the best and most efficient procedures, therefore we do not discuss the use of alumina until final polishing. Although alumina is still used quite often in metallurgical labs because it is inexpensive, it does not perform as well as diamond. Extra polishing time is needed with alumina to get the same effects as those provided by diamond. So our focus is on processing the sample quickly and getting the best results possible. A typical intermediate polish using a diamond compound or suspension would be 9, 6, or 3 microns. For induction hardened parts [which are typically harder (in the 40 to 55 HRC range)] it is recommended to use the 6 or 3 micron diamond. This intermediate step will remove the structural deformation from a 600 or 800 grit grinding step in less than two to three minutes of polishing. For an intermediate polishing step a "hard" polishing cloth is recommended. This means that the polishing cloth will not compress when pressure is applied on the sample. This is very important when the sample edges are meant to be flat. Using a polishing cloth with a nap or one that compresses will polish the sample unevenly. The mounting material will abrade away slightly faster and the sample's edge will protrude from the mount. This condition will not allow the metallographer to view the edge of the sample under high magnification.

For induction hardened samples this is very important so care must be taken to choose the correct polishing cloth. Table 5.11 shows various polishing cloths and their recommended uses There are many more polishing cloths than those listed in the table, but even this list shows the variety available. Many of these cloths are obtainable with plain back or PSA (pressure sensitive adhesive). Plain back cloths have to be attached to the polishing wheel by means of a clamping system or by using a double-sided adhesive disk. A PSA cloth (adhesive on the back side) is much simpler to use as you only have to remove the liner on the back and stick it onto the wheel. PSA cloths tend to cost more but the convenience and time savings far outweigh the expense.

Diamond polishing abrasive that is used in the metallographic laboratory can come in several different forms. There are two different types of diamond that can be used for polishing samples, monocrystalline and polycrystalline, both of which are manmade. For induction hardened samples the monocrystalline diamond should be used. Polycrystalline diamond is very useful for preparing ceramics and other difficult to prepare materials. It is typically more expensive and is not available in a variety of forms. Monocrystalline can be purchased as a paste, a suspension, or spray. There are differing opinions about what form is the easiest to use but a good recommendation is that paste is very good for charging a new polishing cloth. The diamond paste material adheres to the cloth better and applies a large amount of diamond in a small amount of material. Suspensions are an excellent way of adding diamond to an existing polishing cloth. They normally come in forms that have a sprayer or pump spray, which allows the operator to

Table 5.11 Polishing Cloths and Uses

Cloth	Construction	Uses
Canvas	Duck cloth	Rough polishing, loose abrasives
Cotton	Tightly woven cotton cloth	Rough polishing, alumina, or diamond
Billiard	100% virgin wool, sheared pile	Rough polishing, alumina, or diamond
Red Felt	100% virgin wool, plucked pile	Intermediate polishing, diamond
Nylon	Napless nylon	Intermediate polishing, diamond
Silk	Woven silk, hard cloth	Intermediate polishing, diamond (excellent for keeping samples flat)
Pan W (Pellon)	Textile type cloth	Intermediate polishing, diamond
Velveteen (Selvyt™)	Medium nap cloth	Intermediate or final polishing
Suede	Rayon flock	Intermediate or final polishing
Lecloth	Rayon fibers/cotton back	Final polishing
Velvet	Synthetic velvet, long nap	Final polishing/soft materials
Imperial Cloth	Synthetic fiber	Final polishing/colloidal silica

apply it directly to the polishing wheel. An extender of some type should also be used to make sure that the polishing cloth does not dry out during the polishing step. Samples can get quite hot during polishing and the extender acts as a coolant and a lubricant.

The techniques that are used to polish samples are quite varied. Manual polishing should be performed on a rotating wheel. This provides the best approach as far as speed and repeatability for the manual operation. The sample should be held firmly in one hand and rotated in the opposite direction of the polishing wheel. It is also recommended that the sample be rotated slightly during the polishing process. Moderate pressure needs to be applied during the polishing process and extender needs to be added to make sure the sample does not overheat. A polishing cloth should be moist but not dripping with extender. Using too much extender flushes the diamond from the wheel and it may also cause the sample to hydroplane on the polishing cloth. A speed of 200 to 250 rpms should be used for the intermediate polishing step. After the sample has been polished on the intermediate step, the sample should be cleaned before moving on to the final polishing step.

The final polishing step should be run using a wheel speed of 150 to 200 rpms with slightly lighter pressure. This step should be completed on a cloth that has a softer nap, which allows the diamonds or other polishing abrasive to contact the sample in a gentler fashion. This combination produces a superior surface finish for visual inspection. The time spent on the final polishing step should be kept to a minimum. Excessive polishing on a soft polishing cloth can cause the edges of the samples to become rounded. The mounting material will abrade away more quickly than the sample's edge so care must be taken when running the final polishing step.

This final step has to be determined by the metallographer: where the process stops depends upon what type of information is needed and how fast. Does the end-user need a photomicrograph? Does the end-user plan on performing microindentation tests? Will the sample be etched to determine the grain structure or other features? All of these questions determine when to end the metallographic process. In most cases where a visual examination is needed, a one-micron final polish will provide an excellent look at the sample while minimizing the number of steps. One-micron scratches will still be visible but they will not affect the visual examination. If photomicrographs or microindentation tests are to be run, then a final step of 0.05 micron colloidal silica or gamma alumina would provide an excellent finish. Photomicrographs can be taken and there will be a minimum of structural deformation on the surface, ensuring the photomicrograph will look very professional. Most final polishing steps are done with a slower wheel speed, light pressure, and a napped cloth that provides an excellent polishing surface. Colloidal silica, which is a 0.05 micron silica solution, works extremely well on all types of samples. Gamma alumina, which is also 0.05 micron material, works well and is very economical to use. Alumina comes in a powder form, or a slurry which comes ready to use. Colloidal silica only comes in liquid form and is also ready to use.

The methods that we have talked about so far have used manual methods to achieve a polished sample. Automation provides a better, more repeatable method for achieving these same results but faster and without using as many consumables. Multiple samples can be processed at one time and this is important in a high production area such as induction hardening. Hundreds or thousands of parts are processed each day so to meet quality requirements many samples have to be run in a short period of time. If a batch of material—whether it's going into the furnace or waiting to be shipped—has to be checked and they are waiting for samples in the lab, then it is costing the company money. The ability to process these types of samples through the metallographic laboratory is very important. This is where automation can truly pay for itself in a very short period of time. Applying pressure using an automatic grinder/polisher (such as the one shown in Figure 5.165) will give excellent

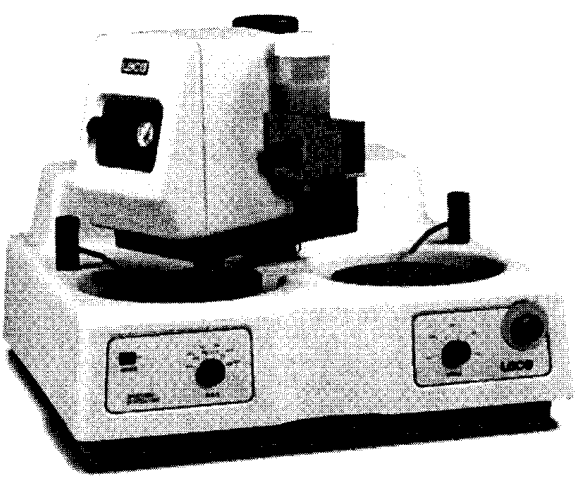

Figure 5.165 Semi-automatic grinder/polisher. (Courtesy of LECO Corp.)

results and little training is needed. Typically three to six samples are run at one time, and the process may include three or four grinding steps depending on the hardness of the material. One or two polishing steps follow, and all of the samples are completed at one time. This type of production is needed in some labs where several hundred mounts are completed weekly. This is also helpful when preparing samples that are not mounted in a thermosetting material. Holding large samples and applying pressure can be very difficult and the results are sometimes not repeatable. Sample holders designed to hold these large samples can be made and several samples can be processed simultaneously, depending upon their size.

Grinder/polishers are available in many different sizes and are suitable for a wide variety of applications. See Table 5.12 for an overview of the different procedures. The volume output of the lab will determine what level of automation is needed. Larger volume labs need a machine with programmable features so that procedures can be run quickly with little operator intervention. Lower volume labs can utilize less-automated equipment since their output is not as great.

5.11.3.5 Cleaning

Cleaning samples and sample holders can be a tedious process during metallographic preparation, but it is a very important part in obtaining excellent results. During the grinding steps, samples and sample holders should be rinsed thoroughly after each step. Bringing an abrasive particle from the previous step can cause damage especially when the smaller abrasives are being used. It becomes even more important when polishing steps are being performed. When a 6-micron diamond particle is dragged onto a 1-micron diamond polishing step, the results can be pretty disastrous. Some procedures recommend ultrasonic cleaning between

Table 5.12 Procedures for Grinding/Polishing Induction Hardened Samples[a]

Grinding	Wheel Speed (rpm)	Time (sec)	Head Speed (rpm)	Direction	Pressure (lbs)
180 grit SiC	250	60	150	CW	20
320 grit SiC	250	60	150	CW	20
600 grit SiC	250	60	150	CW	20
Polishing					
Pan W Cloth/ 6 micron Diamond/ extender	200	540	125	CCW	50
Red Felt Cloth/ 1 micron Diamond/ extender	200	120	125	CCW	50
Imperial cloth/ colloidal Silica/water	150	120	75	CCW	30

[a]Procedures done using the Spectrum System 2000 grinder/polisher.

each step. This is an excellent way to ensure that diamond particles are not carried from one step to another. For most labs, rinsing and swabbing with a cotton ball will provide enough cleaning to keep polishing cloths from being contaminated. For induction hardened parts this is probably not as critical, because most examinations are of the macro variety and the general thickness of the induction hardened area is the most common feature that is examined. When a sample is polished so that the microstructure can be examined then cleaning becomes very important. Contamination of a polishing cloth can be very frustrating. Some cloths can be cleaned with a brush, but typically the cloth must be removed from the wheel and discarded. This is a costly situation that can be avoided by just following some simple procedures during the preparation process. During the cleaning process it is a good idea to dry the samples so that they can be viewed clearly. When the samples are wet an operator cannot discern whether the samples are flat and properly ground or polished. Spraying the samples with alcohol (ethanol preferably) and blowing them dry using a hair dryer (or with a blast of air), allows the operator to see any problems that may be occurring on the samples.

The final cleaning step is probably the most important since it is the step just before examination. A sample that has just been finished with the polishing step should be cleaned using a cotton ball and lots of clean water, and then sprayed with alcohol and carefully dried. The drying process can be very important also. Using compressed air from an air line can be too aggressive and blow the alcohol all over the sample instead of drying it slowly and evenly. Using a hair dryer produces better results because the air flow is more even, and the hot air makes the alcohol evaporate very quickly. Using acetone, rubbing alcohol, or even methyl alcohol can work, but they present some problems of their own. Acetone dries very quickly, too quickly for metallographic applications. Rubbing alcohol contains water and when the alcohol part of the material dries, the water remains as small spots on the sample's surface. Methyl alcohol can also have more water than ethanol. Each of these materials can work, but the best choice is ethyl alcohol.

When cleaning samples that have been polished using colloidal silica, the procedure should include a gentle scrubbing using a cotton ball. Colloidal silica can leave a film on the surface of the sample if it is not cleaned properly. This film will prohibit the technician or engineer from seeing the sample clearly at high magnification. Colloidal silica cannot simply be rinsed from the sample, and if alcohol is used, it can cause the colloidal silica to dry out even faster. The sample should have a bright luster in the as-polished condition: if any dull areas or patches of staining are present, than a second cleaning is recommended.

5.11.3.6 Etching

Etching induction hardened samples is fairly straightforward inasmuch as most materials are ferrous materials with moderate amounts of carbon. Etching can be performed on a sample that has been ground flat or one that has been polished to a mirror finish. To simply see the shape and thickness of the induction hardened area a macro etchant can be used to darken that particular area. Of course the etchant used will depend upon the chemistry of the sample. For most ferrous materials the following etchants can be used.

Macroetching:		
1. Ethanol (96%)	90 ml	1–5 min
Nitric Acid	10 ml	
2. Distilled Water	50 ml	10–30 min
Hydrochloric Acid	50 ml	
Microetching:		
1. Ethanol (95%)	100 ml	Immerse 5–15 sec
Nitric Acid	1–10 ml	2% Nital is the most common etchant for steels
2. Ethanol (96%)	100 ml	Variable immersion time
Picric Acid	2–4 grams	Use caution when handling picric acid. See instructions for storage and handling precautions

There are many other etchants that can be used on induction hardened parts and they can be found in various books and handouts. An excellent source of material is the *ASM Metals Handbook* or *ASM Metallography and Microstructures*, Volume 9. These etchants can reveal the microstructure so that phases such as ferrite, pearlite, martensite, and carbides can be seen and documented. Please be sure to follow the safety instructions that are given for each etchant. Some etchants can be stored and used later, whereas others need to be disposed of properly right after they are used. Mixing of etchants can be dangerous; proper eye protection, gloves, and lab coat are recommended for safe handling of chemicals. Always be sure what the reaction of two chemicals will be before they are mixed together. Check with a chemist so that accidents can be avoided before they happen.

5.11.4 Basic Review of Hardness Testing Technique and Apparatus

Hardness testing is one of the most recognized procedures for testing materials and characterizing their properties. It is one of the fastest tests that can be run without destroying the part to get the results. There are several different types of hardness tests that have been used over the past 150 years. Hardness testing allows the scientist or engineer to determine the surface condition of the material. Surface hardening, such as induction hardening, is normally verified with some type of hardness test. This ensures that the surface of the material has reached a specific hardness or that the core hardness of the material has remained at a specified hardness to extend the fatigue properties of the part. Today's hardness testers consist of an indenter, an applied load, and depending upon which test is being run, a direct measurement or an eyepiece reticle for measuring an indentation size. Some parts have to be sectioned so that inner areas can be tested for hardness. In an induction hardened part there may be several measurements taken: at the surface to determine whether wear characteristics will be met, another to see how deep the hardness region actually is, and one to check the core hardness to make sure that the original material there has not been affected by the induction hardening process. Depending upon the method being used, several indents may be needed to fully characterize the hardness profile. Some hardness tests can be performed directly on the finished parts to check the hardness. Other samples need to be sectioned to further characterize the material and some may need to be mounted, ground, and polished to perform more precise types of hardness tests. Hardness testing is an invaluable tool for processes that involve

induction hardening. A great deal of information can be gathered in a very short amount of time. This information can show whether a process has been successful, especially during the testing phase of the process.

5.11.4.1 Types of Hardness

There are several types of hardness tests that people involved in induction hardening might use in their daily operation. Rockwell®-type hardness testing is the most common type and is widely recognized around the world. Rockwell-type testing involves using an indenter (typically a diamond), and a specified test load (usually 150 kg), to force the diamond into the sample or part. The resistance to that penetration is the hardness characteristic that is measured. Rockwell-type testing is considered a macrohardness test, which means that the load applied is greater than 1000 grams. Rockwell-type can be used with a ball indenter, which comes in sizes of 1/16, 1/8, $\frac{1}{4}$ and $\frac{1}{2}$in. Some Rockwell-type testers can be configured to use lower loads (such as 15, 30, and 45 kg); these machines are referred to as "twin" testers." They can perform a variety of hardness tests to match different hardnesses and thicknesses of materials. The condition of the surface of the sample has to be carefully controlled so that there are no changes in the hardness at the surface of the material. The surface of the sample should be clean, flat, and oil-free. The sample should be perpendicular to the indenter to perform a valid test.

The other types of hardness tests are microindentation hardness tests, which involve making an indentation with a light load. The length or length and width are then measured using a measuring eyepiece to determine the hardness number. The typical loads for a microindentation hardness tester are 1000 grams and below. The most used load is 500 grams, and two indenters can be used on most machines. Vickers and Knoop diamond indenters are used on microindentation hardness testers with a wide variety of loads.

5.11.4.2 Correlation Between Different Types of Hardness

In many situations the hardness scales that are used may not be exactly what the operator is looking for in the test results. Many times microhardness testing is completed and the results need to be posted using another hardness scale, that is, HRC. Conversion charts are available in ASTM E-140 Hardness Conversion Tables for Metals (Table 5.13 gives an example). These charts should be used with care since many materials do not match the criteria for the tables. There are several charts in ASTM E-140 that can be used for other types of materials. It is important that the operator read the specification and understand the limitations of the conversion charts. Most newer testers that have digital capability will have builtin hardness conversions and this can make the results easy to obtain. Even if a system has this type of capability, an operator should still be familiar with the rules governing conversion numbers. Many scales do not overlap each other and this can be quite confusing. Microhardness is converted to other scales quite often and in this case covers many scales. For instance, a case depth study that starts in the HRC 50 range may end up in the high HRB range when the core is reached. Because the HRB and HRC ranges do not overlap, the operator must change from HRC to HRB as the material gets softer. Whenever a conversion is used in a laboratory report or when reporting a hardness number, the value should be reported as a number that has been converted from another hardness number. It is always best to use the hardness

test that is being requested, but many times that is not possible. It is important that the person receiving the report be notified that the number was the result of a conversion chart. According to ASTM, "The conversion values, whether from tables or calculated from the equations, are only approximate and may be inaccurate for specific application." This statement reinforces the fact that conversion numbers are approximations and should be treated as such. If the data are critical to a specific application and have to be documented, then a specific hardness test should be run and conversions should probably be avoided in this situation. Most manufacturers of hardness testing equipment will have either hand-size conversion charts or will provide wall charts. These are helpful when quick comparisons are needed in the lab area.

5.11.4.3 Hardness Testers

There are several different types of hardness testers associated with induction hardening that can be used in a lab. The most useful and productive would be the Rockwell-type hardness tester. Given that it has several different scales for testing the surface hardness of materials, it is well suited to many different applications. The most attractive features of a Rockwell-type hardness tester are the speed and direct results given by the machine. A part can be checked quickly and easily and the test is very repeatable. As stated before, Rockwell-type testing involves forcing an indenter, typically a diamond, into the material using a specified load. For Rockwell C, which is the most common scale, the diamond indenter is forced into the material using a 150 kg load. The process begins when the indenter contacts the testing surface and applies what is called a minor load. This load forces the indenter into the material and establishes a "set" position. The major load is then applied and the distance that the indenter moves is measured very precisely. The hardness is then shown on a dial indicator, or a reading is shown on a screen. Hardness tests can be completed on whole parts or on pieces that have been sectioned from a larger sample. The same principle applies to testing of softer materials using ball indenters.

Another common scale is the Rockwell B scale, which is a $\frac{1}{16}$ in. ball with a 100 kg load. This provides testing capability of slightly softer materials when Rockwell C is not applicable. Other ball indenters that are available are $\frac{1}{8}$, $\frac{1}{4}$ and $\frac{1}{2}$ in. and combining these with different loads such as 60, 100, and 150 kg loads can provide many options for testing materials of different hardnesses.

Parts that are tested can be flat or round, but they must be held perpendicular to the indenter. Flat pieces must be of sufficient thickness to make sure that the indenter does not penetrate through the sample and into the anvil. Round pieces can be tested using an appropriate V-anvil for the size part being tested. There are correction factors available on ASTM charts for round parts and, depending upon the size of the parts, a correction factor may have to be added to obtain a correct hardness number. A similar situation occurs when testing the inner diameter of a pipe or similar shaped material. Correction factors exist for this situation where it may mean subtracting a number depending upon the diameter of the inner opening. It is very important that calibration checks are run on the Rockwell-type hardness tester using a set of high-quality Rockwell-type hardness test blocks. Proper maintenance can ensure that your machine will work for many years. Calibration checks can be performed quickly and are definitely recommended for certain quality programs, such as BSI, ISO, and so on. For information on Rockwell-type hardness

testing, please refer to ASTM Specification E-18 which describes all of the procedures involved in performing these tests. ASTM E-18 provides many guidelines for successful testing of your samples.

Another type of hardness testing that is used in induction hardening areas is microhardness testing (Table 5.13). This type of test differs from Rockwell-type testing in that an indentation is made and then a visual reading is performed to obtain the size of the indentation. These types of tests are run on samples that have been ground and polished. Lighter loads such as 1000, 500, 300 g, and so on are used to make a series of indentations to determine the hardness depth (Figure 5.166). Typically indentations are made starting near the surface of the sample and placed at measured intervals until the core material is reached. This provides a profile of the hardness as a function of depth, and helps determine the true hardness at the surface of the sample. Microhardness testers are smaller units and they can be somewhat delicate. Rockwell-type testers (Figure 5.167) can sometimes be found on the manufacturing floor, but microhardness testers should be used in a fairly clean environment for the best possible results. Once again periodic calibration of these units is very important in obtaining repeatable and accurate results.

Microhardness calibration test blocks are available for most scales and come in many different configurations for Knoop and Vickers testing (Figure 5.168). Calibration test blocks are available for different load and hardness ranges. It is recommended that similar hardness and load ranges be used for calibration. For example, if an operator is testing samples using a 500 g load with a Vickers indenter, then a test block using a 500 g load with a similar range of hardness should be used. This ensures that the results will be accurate and repeatable. Indents are made using a dwell time of 10 to 15 sec if the material is in the upper hardness range. Some softer materials need longer dwell times so there is time for the material to plastically deform. A sample that is to be used for microhardness testing in the majority of cases must be prepared using metallographic techniques. It is very important that the surface of the sample be flat and optically clean so that measurements can be taken on each indentation. Knoop and Vickers indentations have to be measured very carefully. The Knoop microindentation requires a very precise measurement because the tips of the indentation are difficult to see if the sample is not prepared properly.

Table 5.13 Automatic Microhardness Testing

No.	Distance	Hardness	Distance	Hardness
1	99.9926	788.8	Average	632.5
2	200.000	797.1	Standard Deviation	140.0
3	300.000	766.7	%RSD	22.13
4	400.000	730.6	Maximum	797.1
5	500.00	668.3	Minimum	428.8
6	600.000	626.9	Sum	6325
7	700.000	560.6	Count	10
8	800.000	507.3		
9	900.000	449.4		
10	1000.00	428.8		

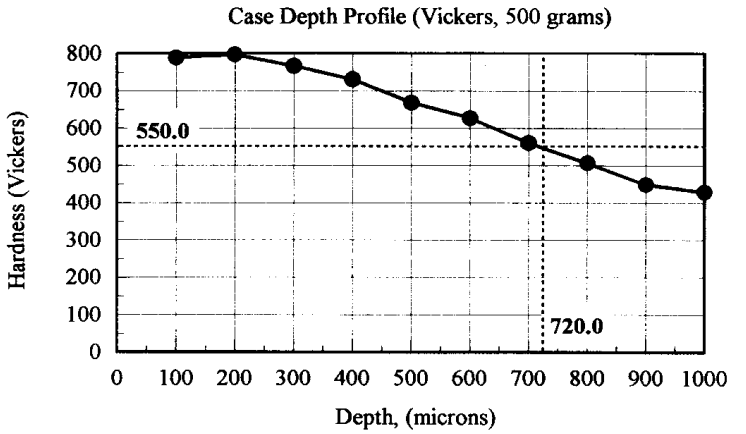

Figure 5.166 Case hardness profile.

A difference of a few microns can change the hardness reading by 20 to 40 Knoop points, which is equivalent to one Rockwell C point. That difference can mean being within specification or on the outside. Also it is very important on digital micro-indentation hardness testers that the unit be zeroed properly before measurements are taken. The normal procedure is to move the measuring lines together so that the inner part of each line contacts the other. When the band of light disappears from between the two lines, then the unit can be reset or zeroed. It is also very important to focus the eyepiece before any measurements or calibrations are completed. This will enable the operator to see the lines and perform subsequent measurements more accurately.

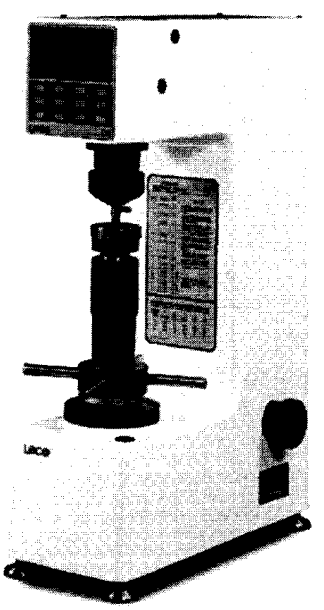

Figure 5.167 Rockwell-type hardness tester. (Courtesy of LECO Corp.)

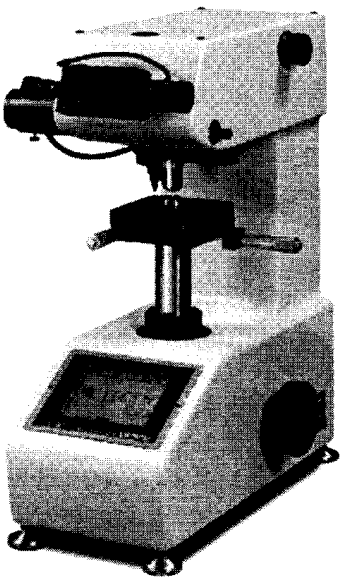

Figure 5.168 Microindentation hardness tester. (Courtesy of LECO Corp.)

Other types of hardness testing are Macro Vickers (Figure 5.169) and Brinell hardness testing. Macro Vickers testing is very similar to microindentation testing, except the loads are heavier. They start out at 1 kg and may go up to 50 kg. The diamond indenter is larger to accommodate the larger loads, and the indentation must be measured through a measuring eyepiece. The indentation is quite large but

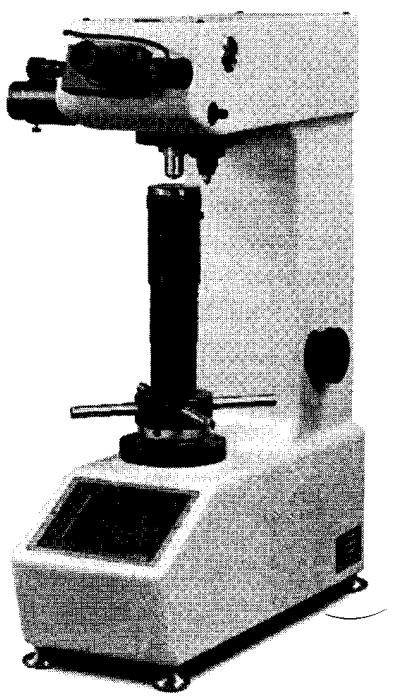

Figure 5.169 Macro Vickers hardness tester. (Courtesy of LECO Corp.)

the same types of measurements are made and the hardness is calculated from these measurements. Brinell hardness testing uses even heavier loads and is often used in the foundry and heavy manufacturing industry. A Brinell tester can use up to a 3000 kg load with a 10 mm ball indenter. The Brinell tester is used for materials where there are thick sections and a hardness is needed on a larger surface area. For example, gray cast iron has graphite, ferrite, perlite, and carbide phases in the microstructure so some tests (such as Rockwell-type tests) may not include all these phases, whereas Brinell makes a very large indentation that would most likely include several or all of these phases. Typically Brinell is not used in induction hardening because of the limitations on how hard the material can be for testing. If the material is too hard, as in induction hardening, then the 10 mm ball may distort before the material starts to deform.

5.11.5 Microscopes and Principles of Microscopic Analysis

Microscopes are a very important part of the metallography lab. They allow the operator to view prepared samples and determine if the microstructure in the induction hardened area meets the standard that was established for that sample. Two types of microscopes may be needed in the induction hardening area: the stereo microscope, which can be used to view samples at lower magnifications, and a microscope that allows the operator to see the samples at higher power.

Stereo microscopes are normally used to look at the thickness of the induction hardened sample, and to view the sample for cracks on the surface of the part. Stereo microscopes allow the operator to see samples with depth of field, revealing surface features that normally could not be seen. Sample preparation may not be needed for this type of analysis. The stereo microscope is an excellent inspection tool for any lab and can be used for a wide variety of materials. The main use for stereo microscopes is to examine failures and their fracture surfaces. It is fairly simple to operate and can be equipped with a camera or some type of system to document what is seen through the eyepieces. An external light source is needed to illuminate the sample and this is normally done using fiber optics. This provides the maximum amount of light and allows the operator to focus the light on the area of interest. Fiber optics provide the most efficient way of transferring light from the source to the sample.

Metallurgical microscopes are used to examine samples that have been ground and polished. These samples can be examined at higher magnifications. Typically induction hardened samples are etched to reveal the microstructure for examination. Metallurgical microscopes utilize reflected light to examine the samples at high magnification, which means that light is projected up through the objective (as seen in Figure 5.170), and it reflects off the sample back into the objective and up into the eyepiece for the operator to view. Metallurgical microscopes can be configured in two different ways: the objectives are positioned over the stage plate where the sample is placed (upright), or positioned under the stage where the sample is placed upside down so that the sample is facing downward (inverted; Figure 5.171). There are positive and negative aspects of both configurations. The upright metallurgical microscopes have some advantages in that they are usually less expensive and the operator can see where the sample is located under the objective. One problem area is that the sample must be leveled somehow so that it is perpendicular to the objective. Otherwise the sample will not stay in focus as the stage is moved

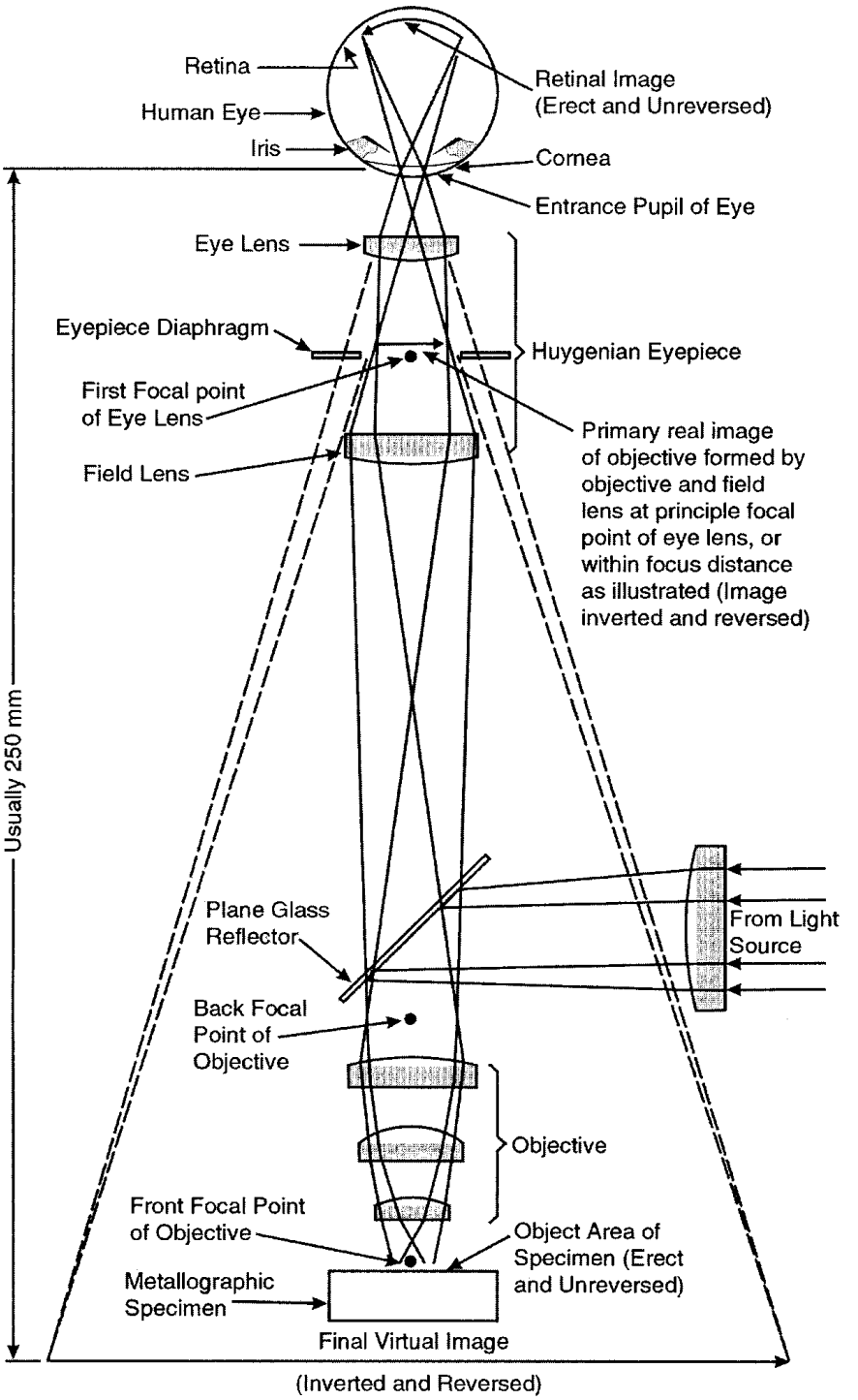

Figure 5.170 Metallurgical microscope. (Courtesy of Olympus Corporation.)

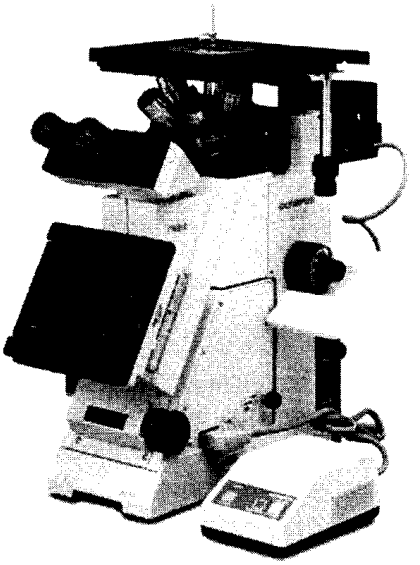

Figure 5.171 Inverted microscope (metallograph). (Courtesy of LECO Corp.)

from area to area. Another disadvantage is the limited amount of space that is available under the objective. The stage can only be moved down so far and that limits the height of the sample that can be used. Inverted microscopes or metallographs can accommodate almost any size sample and the sample does not have to be leveled at all. As long as the sample is flat, it will stay perpendicular to the objective while the stage is being moved from area to area. Inverted microscopes are convenient in a metallurgical lab because an operator simply places the sample on the stage and starts reviewing the sample. It is difficult sometimes to see where the sample is located because it is inverted, but with practice even this becomes second nature.

Each type of microscope can be outfitted with different features and controls. The types of features that may be needed on a microscope are aperture diaphragm, field diaphragm, green filter, neutral density filters, widefield eyepieces, and so on. There are many different choices when looking at microscopes, but it is important to know that the most significant feature on the microscope is the objectives. These provide the image that is seen in the eyepieces, so if the objectives are not of good quality, the image will be affected. It is important to choose the best objectives possible, especially if higher magnifications are going to be used.

The ability to document samples has changed greatly over the past years. A microscope set up with a large-format camera was the norm and produced excellent results, as long as the operator was skilled in taking photomicrographs. Long setup times and wasted film caused many laboratories to limit the amount of pictures that were taken. Polaroid film is still used quite often today and in trained hands can produce excellent results.

Many laboratories have gone to video systems, which are great for presentations and training. A video camera is mounted onto the microscope via a camera coupler, and the signal is sent to a video monitor where the image can be reviewed. Video printers were developed to capture the image seen on the monitor and print it

out on a 4 × 5 in. piece of paper. This was much easier to set up and typically faster than Polaroid film, but the resolution was limited by the camera and the printing device. High-magnification photomicrographs were grainy and sometimes the colors were not the same as the sample. Improvements continue in this area, but they have not reached the level of quality that Polaroid film can provide. As today's technology advances month to month, digital cameras have taken a large role in documenting samples. Digital cameras allow the operator to capture images of samples and store them on a computer or external storage device. The images, which can be several hundred kilobytes all the way up to several megabytes, are viewed on a computer and the images can be adjusted so that colors match those seen in the microscope. The most convenient aspect of digital imaging is that the images can be incorporated into generated computer-generated reports. It is important to note that these printed images are not the same as viewing a Polaroid photomicrograph. For the clearest, sharpest picture, Polaroid photomicrographs are still the best choice. Another benefit of digital imaging is archiving images onto a memory system. This allows the operator to save images so they can be viewed later, as well as categorizing them into cabinets and file folders. Searches can then be made for specific images or groups of images that can be searched for by using key words. Other types of digital cameras use media devices that store images on a small disk, and these disks can be inserted into a floppy disk adapter. The images can then be transferred into a computer for storage or printing.

Other types of packages can be added to a microscope system including measuring systems and image analysis systems (Figure 5.172). These products take the image from the video or digital camera and integrate them into a software-based system. A measuring module allows the operator to view the sample on the computer monitor and make measurements directly on the screen. The resulting image can then be saved or printed in a report. Simple measurements include coating thickness, particle size, diameter, angles, and other feature measurements. Making the measurements on the computer monitor allows the operator to see the entire sample and training becomes simplified because everyone can see exactly how the measurement was completed. This type of system can be integrated with the image archiving software and function as a complete archiving/measurement software package. Templates can be overlaid on the video screen so that measurements that are made repeatedly can be moved around and adjusted, rather than drawing new measuring lines each time. An excellent application for this is the measurement of induction hardening depths and welds. Multiple measurements can be taken on the sample and the results can be reported in a table format or on a graph.

Image analysis systems are another way that microscopes can be integrated with camera systems for measuring. Image analysis applications include grain size, area percent, coating thickness, cast iron analysis, and many others. The measurements made on image analysis systems can be done manually or automatically. When a sample is on the video screen, the particles of interest are detected using 256 gray levels. For instance, if a coating thickness application is being used to measure the depth of the induction hardening, then the layer of hardened material (which is darker) is detected and multiple measurements can be taken automatically, where instead of drawing each line manually, many lines are drawn across the layer. Image analysis systems also are set up to construct very detailed reports showing the data in a number of configurations. An autostage can be added so multiple field

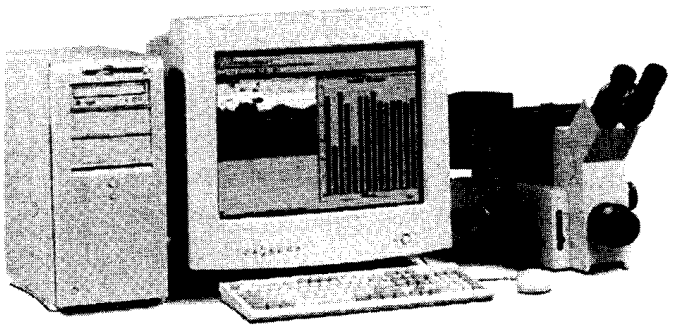

Figure 5.172 Image analysis system. (Courtesy of LECO Corp.)

analysis is available. This allows the operator to examine an entire sample for inclusions, area percent, grain size, and the like.

There are many ways to examine an induction hardened part but the most conclusive is to section the part, grind and polish the area of interest, perform physical and mechanical tests, and examine it under a microscope. This offers conclusive evidence that the part has been processed correctly and that it will perform as it was designed to do in the field. Taking these simple steps will ensure that quality standards are met and exceeded when induction hardened parts are produced.

6

Special Application of Induction Heating

6.1 JOINING APPLICATIONS

In the manufacturing process there are a number of ways to join two parts; some of the conventional methods include brazing, soldering, welding (TIG, spot, rolling resistance), screwing, bolting, and riveting. Screws, bolts, and threaded items provide a mechanical bond and are utilized when an assembly must be capable of being relatively easy to take apart. Components that do not require disassembly are welded, brazed, or soldered as these processes create permanent joints [316].

Induction heating is commonly used to join metal components. Typical induction joining applications include, but are not limited to, brazing, soldering, friction welding, bonding, and shrink fitting. The pieces being joined can be of the same material or two distinctly different materials.

In the cases of brazing, soldering, and friction welding (Figures 2.49 and 2.50) both joined metal components must be heated to approximately the same temperature. In contrast, when bonding and shrink fitting only one metal component might be heated. Metal threaded inserts that are heated by induction, and then pressed into a thermal set plastic component are a good example of using induction heating for joining.

6.1.1 Brazing and Soldering by Induction

Brazing and soldering are two of the most popular induction joining applications. These are accomplished in a similar manner to other induction processes (e.g., hardening) except that quenching usually does not apply. The typical components required for both induction brazing and soldering would include the following: a heating coil, a power supply, the components to be joined, a filler material, and flux if required. In most cases the parts to be brazed, as well as the filler material, are located and held in a fixture and moved into close proximity to an induction coil with heat applied.

Soldering is typically distinguished from brazing by the temperature at which the filler material melts. If the melting temperature of the filler is less than about 450°C (840°F) then the joining process is called soldering. If the filler material melts at a higher temperature, then the joining process is considered to be a brazing process. In addition to the differences in joining temperatures, the processes of soldering and brazing are distinguished by a metallurgical reaction between the filler and base metal. Intermetallic phases are typically formed in the joint area after a soldering operation, in contrast to solid solutions being formed as a result of brazing [317].

In the past, the processes of brazing and soldering have been conducted using flame heating (i.e., torch), or in lower temperature applications using special heating devices such as a soldering gun.

Induction brazing and soldering have several advantages compared to heating the workpieces with a flame. Because the joint is heated in a localized area, the remainder of the workpiece will not be significantly affected by temperature. This can be critical, for controlling shape distortion, surface corrosion, and oxidation of brazed components. Brazing and soldering by induction can also noticeably reduce grain growth, as well as toxic fumes and excessive radiant heat, and are usually accomplished without the use of a protective atmosphere. However, if required, the induction coil can be easily placed in a chamber that contains a protective gas atmosphere (e.g., argon, a mixture of hydrogen and nitrogen, etc.) or in a vacuum.

Induction heating is one of the most economical ways to heat many styles of joints for a wide variety of brazing/soldering applications. Induction brazing/soldering also produces clean high-quality joints with a minimal amount of scrap or brazing spatter of the filler material, because only the desired area is heated for a relatively short time.

One of the biggest advantages of induction brazing/soldering is the ability to automate the process and once the process is developed, there should be no need for intervention by the operator, because with induction the energy input is well controlled, producing reliable and consistent results [314].

Instead of both words, brazing and soldering, in this section we use the word "brazing" and assume that all discussions hold true for soldering as well, unless mentioned specifically.

6.1.1.1 Overview of Metal Joining Principles

The term brazing is used to describe the joining of two pieces of material (magnetic or nonmagnetic metals), using a special filler material. In a certain way, brazing is similar to welding. However, with welding the filler material is often the same as the pieces being welded and the pieces are actually fused together. In brazing applications, the temperature required for the filler material to melt is much lower than with welding and the process relies upon capillary action.

Brazing may be the only way to bond certain types of dissimilar materials. For instance, it is quite common to braze a stainless steel or brass stud onto a copper component. This allows the design of individual components to facilitate specific design intents. The process of welding different materials on the other hand can become difficult and power consuming, because the components as well as the filler materials are heated to the melting point to fuse them. If different metals are used

they can have different melting points and, therefore, in some cases the materials may not be compatible.

As mentioned earlier, brazing of metals is accomplished by melting the filler material. In all cases the filler material has a lower melting point than the liquidus temperatures of the components being joined.

Brazing, providing a permanent metallurgical bond between two or more pieces (an atomic bond at the interface takes place), is accomplished through the following stages. The joint area is heated to a temperature lower than the melting point of the workpieces, but higher than the melting point of the filler material. After reaching a certain temperature, during both the soldering and brazing processes the surface of the base metal undergoes a diffusion-type chemical reaction with the liquid filler. In the case of soldering, this reaction takes place within a few microns, whereas during the brazing operation (which utilizes higher temperatures) it propagates to a much greater depth. When the filler material reaches its liquid state it flows into the air gap of the joint through capillary action. The liquid almost immediately becomes a solid and the joint is complete.

The specifics of joints have a pronounced effect on the quality of brazing. Properly designed joints in combination with the correct brazing technique produce strong and reliable joints. In some cases the ductility of the joint will add better sheer strength. Sometimes, the brazed joint can be stronger than the joined materials. For example, it has been reported [313] that it is possible to have a brazed stainless steel joint, which has a tensile strength of 130,000 pounds per square inch.

6.1.1.2 Types of Joints

There are two basic joint designs: *butt* and *lap* joints and variations of each (Figure 6.1). The terms are self-explanatory and describe the specifics of joints. A butt joint has two pieces simply butted up against each other. This is the simplest and most common type of joint for fast noncritical applications. To improve strength and surface area a lap joint is used, which utilizes the effect of overlapping the two joint pieces to provide additional strength.

For obtaining even greater strength and durability, combinations of both joints are used. These are referred to as *butt-lap* and *modified butt-lap* joints (see Figure 6.2). These types of joints are usually self-supporting, meaning that in many cases no clamping or special fixtures are required. It is obvious that a more complex design will require more preparation prior to the joining operation (e.g., machining and cleaning of the pieces as well as degreasing of surfaces to be joined).

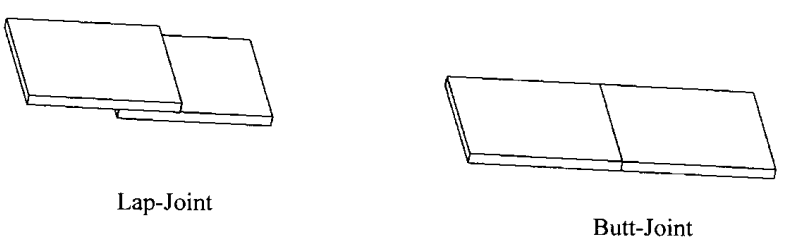

Figure 6.1 The two basic types of joints are lap and butt.

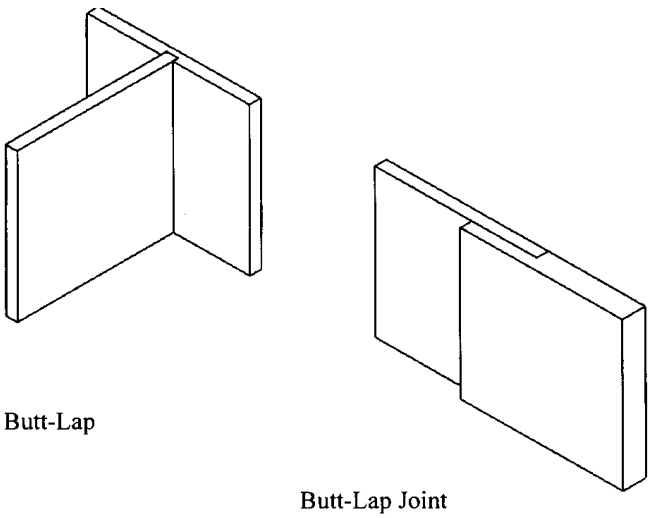

Figure 6.2 Butt-lap and modified butt-lap joints.

When pieces are cut or machined with angles in the joint area they are referred to as *mitered* or *scarf* joints. The miter joint is a variation of the butt joint (see Figure 6.3). This type of joint offers greater surface area for the bond, which improves strength, however, it is sometimes difficult to achieve the exact matching angles required. It is also more difficult to maintain the position of the pieces, because they are not self-supporting as are other joints. One of the most common uses for a mitered joint is making a 90° bend in copper tubing.

When using a lap or scarf joint the stress points in the joint are not concentrated in a single area, as in a butt joint. Another way of distributing the stress is to create a fillet or build up the filler material at the joint area. This can easily be done on the majority of lap joints and on some butt joints.

Because brazing relies on capillary action to form the bond, the clearance between mating components (joint gap) is held to a certain optimum value. It is important to recognize that joint gaps are not constant during a brazing cycle. It is

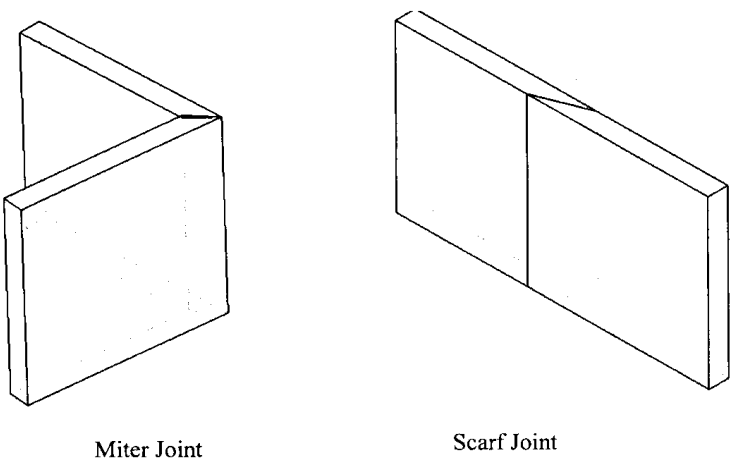

Figure 6.3 Miter and scarf joints.

generally agreed that joint gaps are specified at ambient temperatures. In most cases a clearance of 0.05 to 0.25 mm (0.002 to 0.01 in.) is desirable (Figure 6.4). If the clearance is less than the optimal value, it may not allow the filler material to flow. If the gap is too large the joint will have a poor load-bearing capability and the proper capillary action might not take place due to weakening of the capillary force. Filler materials for brazing applications are not generally intended to be gap fillers. Because the gap is so small a brazed joint is almost invisible. However, it should be clear that the optimal value of the joint gap in addition to other factors (e.g., brazing temperature, type of the base metal, etc.) depends upon a particular filler material. Table 6.1 shows preferred joint clearances for some brazing filler materials that are recommended in [318]. The proper clearance combined with the proper heating and suitable joint design ensures a strong and accurate bond.

6.1.1.3 Size and Shape Factors

For all forms of brazing it is very important to pay attention to the size and shape of the component to be brazed. Obviously as the workpiece size becomes larger, more energy is required to heat it to brazing temperature. Because induction brazing uses a dedicated power supply, the amount of power available is limited to the maximum rating of the power supply.

Induction brazing usually requires a separate coil for a particular application that is dedicated to a specific part. However, depending upon the features of the workpiece geometry of the brazed components, families of parts can sometimes be brazed utilizing the same coil.

If the size or shape of a component does not allow the induction coil to be positioned close enough to the joint area, undesirable heating can occur in adjacent areas to the joint.

In some cases, brazed components are dramatically different in size, mass, and shape. For example, thin-walled tubes or pipes may be brazed to a solid block. In these cases, slower heating with lower power levels is often used and the pulse

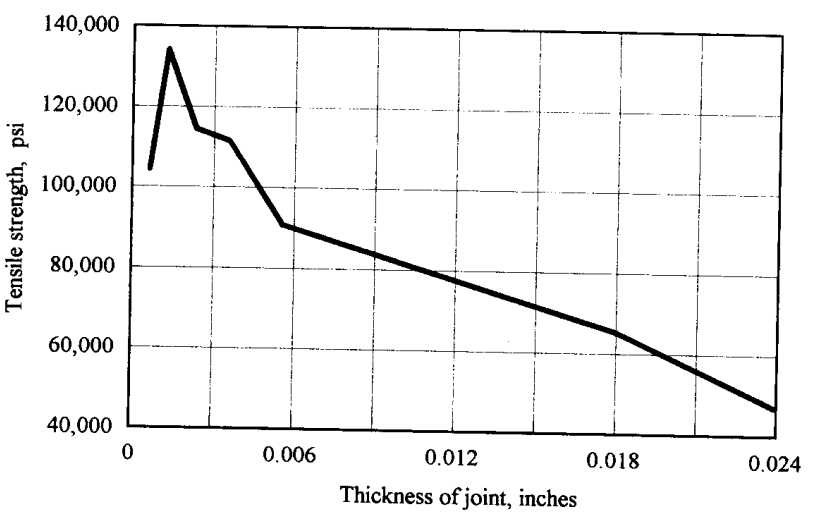

Figure 6.4 Effect of joint thickness on tensile strength. (From Ref. 313.)

Table 6.1 Preferred Clearance of Selected Brazing Fillers

Brazing filler	Joint clearance	
	mm	in.
Al–Si alloys[a]	0.15–0.61	0.006–0.024
Mg alloys	0.10–0.25	0.004–0.01
Cu	0–0.05	0–0.002
Cu–P	0.03–0.13	0.001–0.005
Cu–Zn	0.05–0.13	0.002–0.005
Ag alloys	0.05–0.13	0.002–0.005
Au alloys	0.03–0.13	0.001–0.005
Ni–P alloys	0–0.03	0–0.001
Ni–Cr alloys[b]	0.03–0.61	0.001–0.024
Pd alloys	0.03–0.1	0.001–0.004

[a]If joint length is less than 6 mm (0.24 in.), gap is 0.12 to 0.75 mm (0.005 to 0.03 in.); if joint length exceeds 6 mm (0.24 in.), gap is 0.25 to 0.6 mm (0.01 to 0.024 in.).
[b]Many different nickel brazing filler metals are available, and joint gap requirements may vary greatly from one filler to another.
Source: Ref. 318.

heating mode can be utilized in order to minimize local overheating and the appearance of hot spots.

6.1.1.4 *Frequency Selection*

As with any induction application the success of the brazing operation is greatly affected by the coil design, frequency choice, and the ability to have enough power for the job to be done without overheating the brazed components or unnecessarily increasing the heat time.

As discussed in Section 3.1.2, due to the skin effect phenomenon, the greatest portion of the induced current is localized within a thin surface layer of the workpiece called the current penetration depth. Frequency selection for brazing utilizes the same guidelines as for other induction heating applications of similar geometry (e.g., induction heating of bars or tubes). As has been discussed in Chapter 5, a high frequency is applied in order to obtain a "shallow" heating pattern, whereas lower frequency results in "deeper" heating.

At the same time, frequency selection for brazing is often not as straightforward as for conventional induction heating applications. This is because of the existence of various cross-sections of components being brazed together within the same assembly. Deep and slow heating may be required for one component that comprises the joint, and shallow and intense heating may be required for the other half of the joint.

Brazing different materials together using the same power supply may result in noticeably different depths of heating and heat intensity experienced by the different brazed components. This is due to the fact that the electrical resistivity and magnetic

permeability of the material directly affect the penetration depth at a given frequency. In addition, the electromagnetic coupling between the induction coil and the heated metal that greatly affects the metal's ability to be heated by induction also depends on the magnetic permeability and electrical resistivity of the different metals. Therefore, each electrically conductive component might be heated differently while using the same frequency and the same applied power.

It should also be taken into consideration that in addition to differences in the electromagnetic properties the difference in thermal conductivity of the different metals leads to a different rate of heat transfer (heat soaking). This results in differences in the heat dissipation within the components resulting in different masses of metal being heated. The arrangement of the induction coil can usually compensate for the differences in the ability of components to be heated by redirecting the electromagnetic field and induced eddy current in order to provide uniform heating.

The selection of frequency, required power, and coil design are concerns when brazing dissimilar materials, but it is also important to consider the variations in mechanical properties of materials. For example, it is wise to remember that the rates of thermal expansion of various materials can be different. This feature should be taken into consideration when designing the holding fixtures and choosing proper joint gaps because during the heating cycle the joint gap might be either opened or closed resulting in disturbance of the required filler flow.

High frequency is often chosen for brazing applications, largely because in many cases thin wall or small pieces are being joined. In addition, a high frequency allows one to better localize the heat.

When induction brazing thin components, care must be taken to select a frequency that will not result in eddy current cancellation. This will prevent the component from appearing as an electromagnetically thin body (see Section 3.1.2). It is also important to keep in mind that the resistivity of the metals changes as the part temperature increases. Therefore the final brazing temperatures should be taken into consideration when selecting the operating frequency. Table 6.2 shows the minimum economical diameters for various frequencies for nonmagnetic brazing and soldering applications.

6.1.1.5 Types of Inductors and Coil Design Features

In addition to the selection of the operating frequency and required power the other main considerations when conducting a brazing operation are the inductor design and method by which the components are fixtured (or held together) during the joining operation. It is advantageous to place the coil as close to the joint as possible, however, it may be more desirable to have a looser coupling gap to allow for slower but more uniform heating.

Typically inductors for brazing are somewhat simpler in design compared to heat treating inductors. Brazing inductors are commonly made from water-cooled copper tubing configured to conform to the brazed joint area. The size and shape of the coil tubing depend on the geometry of the brazed component, the frequency, and the required power. The tubing wall thickness depends on the operating frequency; its selection is discussed in Chapter 5.

In a well-designed induction brazing system, the areas of the components that are being joined and the filler material are supposed to reach a brazing temperature all at the same time. Therefore, part of the secret to success for induction brazing

Table 6.2 Minimum Diameters for Various Frequencies[a]

Material	Final temperature °C (°F)	60 Hz dia. mm	1 kHz dia. mm	3 kHz dia. mm	10 kHz dia. mm	50 kHz dia. mm	200 kHz dia. mm	400 kHz dia. mm
Aluminum:								
soldering	650 (1200)	94	22	13	7	3	2	1
Brass:								
soft soldering	260 (500)	76	18	11	6	2.5	1.5	0.8
silver soldering	650 (1200)	91	22	13	8	3.5	2.3	1.2
Copper:								
brazing	980 (1800)	78	19	11	6	3	2	1
silver solder	650 (1200)	66	16	9	5	2.3	1.5	0.75
Lead:								
soft solder	260 (500)	170	40	25	13	6	4	2
Zinc:								
soft solder	260 (500)	91	22	13	8	3.5	2.3	1.2

[a]For induction brazing and soldering applications of solid bodies.

deals with choosing the optimal combination of frequency, power density, and a coil geometry that provides uniform heating regardless of the different materials and/or variations of cross-section of the components.

There is an optimal value of coil length (in the case of a horizontal coil arrangement) or height (for a vertical arrangement). Too short an inductor might result in local overheating and prolong the heating time. In contrast, if the inductor is too long then more mass of metal will be heated, resulting in excessive distortion and higher energy consumption.

As discussed in Section 3.3.2, the highest coil electrical efficiencies are obtained when there is a good coupling (small gap) between the induction coil and the heated workpiece. However, in induction brazing the desire to minimize the coil-to-workpiece air gap in order to obtain the highest coil efficiency might be misleading. It is imperative at this point to provide some case studies supporting the latest statement.

Case Study 1. It should be clear at this point that, in order to achieve uniform heating when brazing dissimilar materials, the inductor design should provide compensation for the differences in heating characteristics of each component. This is especially true when one of the materials is nonmagnetic and the other component to be brazed is magnetic. Figure 6.5 shows a sketch of an induction brazing system providing brazing of two components. One of them is made from magnetic material (carbon steel) and the other from a nonmagnetic metal (copper). On the left side of Figure 6.5, a multiturn inductor with uniform spacing has been chosen to do the brazing operation. As one might expect, the magnetic material will better attract the magnetic field resulting in much greater heat intensity and heat generation compared to the nonmagnetic material.

The situation worsens because the nonmagnetic metal is copper, which has a much lower electrical resistivity than carbon steel. This leads to an even lesser ability of the copper to be heated by induction compared to the steel.

In addition, the copper is not only a good electrical conductor but also a good thermal conductor having much higher thermal conductivity than steel, which has a relatively low thermal conductivity. Therefore, copper soaks the heat much quicker than steel resulting in a larger mass of the copper component being heated due to thermal conduction.

Due to these three factors more heat generation will be required within the copper component in order to obtain similar heating conditions to the steel, and the use of a coil arrangement shown in Figure 6.5 (left) will produce a noticeable over-

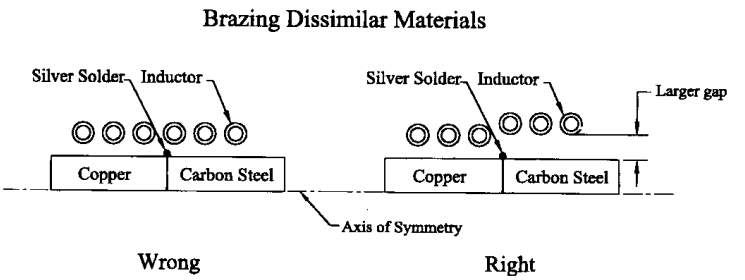

Figure 6.5 Brazing dissimilar materials requires different coil configurations. Notice the larger air gap in the carbon steel area.

heating of the carbon steel, while significantly underheating the component made from copper. The right side of Figure 6.5 shows an alternative coil arrangement where a number of coil turns are decoupled in the area of the carbon steel component resulting in a larger air gap and decreased field intensity in the area of the carbon steel component. This coil arrangement will produce a reasonably uniform heating pattern.

Case Study 2. Care must be taken when brazing pieces together that have different cross-sections. Such an arrangement is shown in Figure 6.6. In this example, a thin-walled tube is being joined with heavy-wall tubing made from the same metal. Similar to the previous case, if a multiturn coil with a uniform coupling gap is chosen, a noticeable overheating of the tube with the thin wall will occur. As a result of redistributing the electromagnetic field due to weakening the coil coupling in the area of the thin tube, it will be possible to obtain reasonably uniform heating.

Case Study 3. Figure 6.7 shows a brazed joint that not only has a different thickness but also a different shape and mass altogether. The left figure shows a uniform spacing between the inductor and the two components to be joined. The thin area of this assembly will be heated more intensely compared to the heavy mass of the flanged component. This will occur not only due to the smaller mass of the thin-wall tube component but also due to an electromagnetic ring effect (see Section 3.1.5) appearing in the coil. In Figure 6.7, right, the heat is redirected toward the larger mass area of the flange by trying to weaken the ring effect and take advantage of the electromagnetic proximity effect (see Section 3.1.3). This coil arrangement will achieve the required temperature uniformity.

It is sometimes necessary to heat not only the joint area but also the adjacent mass of the workpiece as well. When a multiturn coil is used the redistribution of the

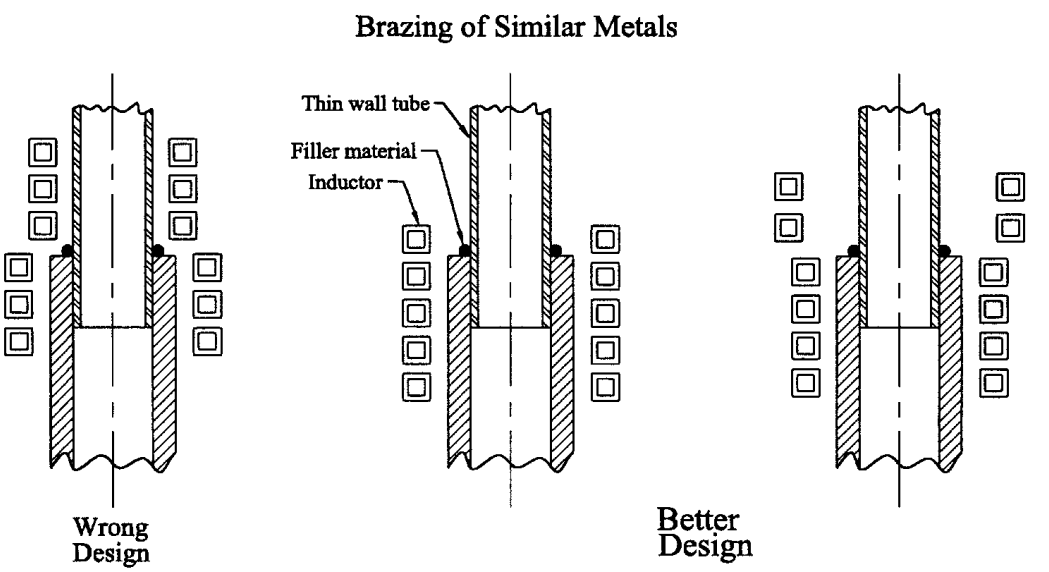

Figure 6.6 Uniform coupling gap would produce overheating of the thin-walled portion of the tube while underheating the thick wall. Heat should be concentrated into the heavy wall, due to the large mass in that area.

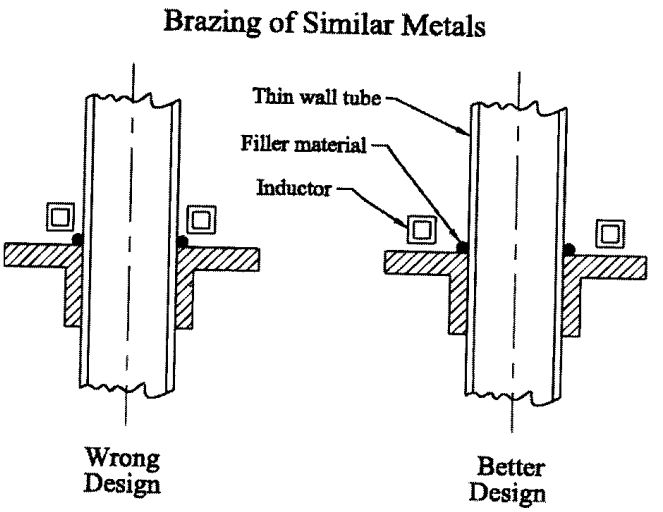

Figure 6.7 Overheating of the thin wall area, due to a smaller mass and placement of the inductor (left). Induction coil should be placed to allow uniform heating of the entire joint area (right).

electromagnetic field can be achieved by varying air gaps between certain turns and the brazed components and also by adjusting the spacing between turns. This will also allow one to provide higher power densities in specific areas of the workpiece. Making the distance between turns smaller, the coil space factor will be improved (see Section 3.1.7.1) resulting in increased power density in that area. However, if the power density is too high the coil space factor can be decreased in certain areas providing the required power density reduction there.

When a single-turn coil is used, it is possible to have the effect of power density redistribution by profiling the inductor in a similar manner to hardening coils as discussed in Section 5.1.5.

Some complex assemblies might have certain features located in close proximity to a joint that could be damaged if heated. In these cases magnetic flux concentrators and/or magnetic shields can be added to the coil (see Section 5.9). In other cases, water-cooled chiller blocks can be added (if there is sufficient space available) to the areas of concern. The latter may require increasing the power in order to provide the desired heating condition of the brazed joints.

There is a wide variety of shapes and sizes of inductors to suit the particular brazing or soldering application. In the case of frequent coil changes, quick coil change adaptors similar to those used in hardening applications may be utilized [361]. These adapters allow the inductors to be quickly replaced with a new setup, which will produce joints of the required quality while enabling the induction joining machines to run a variety of components.

Multi- or single-turn encircling coils are used when one joint at a time is to be brazed (Figures 6.8 and 6.9). Rotation of the workpiece is sometimes used when practical, to achieve a more uniform heat. However, many assemblies cannot be rotated due to their size or complexity of geometry. Pancake, channel, and hairpin coils (Figure 6.10) are also commonly used when assemblies to be brazed are presented to the induction coil on a continuous basis, such as a conveyor or rotary table.

Figure 6.8 Brazing inductors are often simple in design.

6.1.1.6 Overview of Filler Materials and Flux Selection

As mentioned earlier the filler material always has a lower melting point than the base materials being joined. Selection of the filler material plays an important role in producing a successful brazing operation. The choice of filler material depends on physical properties, melting characteristics, and the forms of filler material available [313]. Fillers used for the purpose of soldering are sometimes called solders and, filler materials used for brazing are often called brazes.

Hundreds of brazing alloys (filler materials) are specifically designed for an endless variety of metal joining applications that have a wide range of material properties including melting point, flow point, fluidity, and wetting characteristics. The wetting characteristics establish the proper flow of the filler material into the joint due to capillary action.

The filler material is an alloy of two or more metals. The chemical or metallurgical composition of the alloy dictates its physical properties including melting/fluiding characteristics. The alloy is designed and developed to achieve the desired brazing action based on the special requirements for the particular application. For example, when brazing or soldering electronic devices electrical resistivity and thermal conductivity may be a consideration, or in other cases corrosion resistance may be an important feature. In some cases there may be requirements for a certain

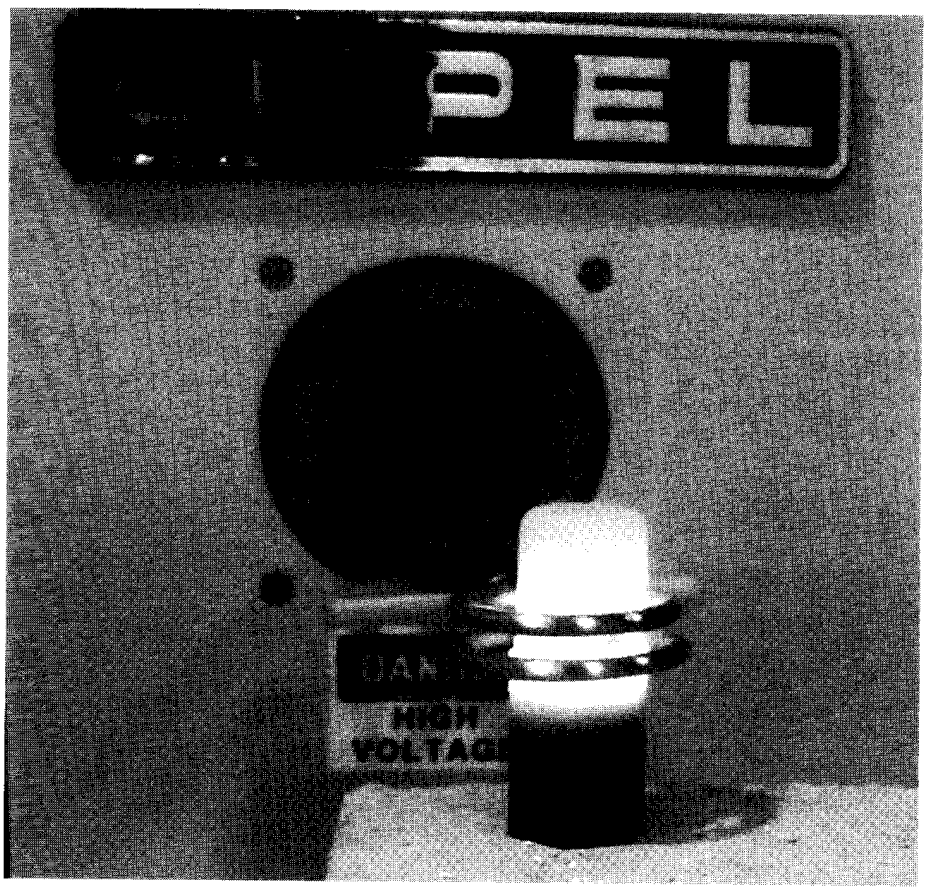

Figure 6.9 Induction brazing of a brass cap to a steel body using two-turn encircling inductor.

chemical composition that will provide features, such as avoiding toxic fumes, high dross, brittleness, volatility, poor fatigue resistance, and so on. In cases of exposure to human consumption (i.e., food or drinking water industries) a lead-free filler can become a critical factor. In other cases, the visual appearance of the brazed parts or cost may be the decisive factors affecting the choice of the filler material.

It is important to remember that since the filler is an alloy, it will have a different melting temperature, as well as solidus temperature compared to the "pure" metals comprising the alloy. The range of filler liquidus temperatures usually allows one to choose the best filler material for the size and clearances of a particular joint. Some alloys have a very narrow window of liquidus temperatures whereas others are designed to cover a larger temperature range.

In soldering and brazing applications the fillers (solders or brazes) can be categorized based on the principal alloying element. Table 6.3 lists principal filler alloying elements and the approximate applicable temperature range [313–318].

It should be clear that the temperature ranges shown are for reference purposes only. In order to obtain more precise information regarding a particular filler material it is strongly recommended that the filler supplier be contacted.

It is imperative to distinguish the terms *flow point* and *melting point*. The flow point is the state at which the material flows, which is different than the melting

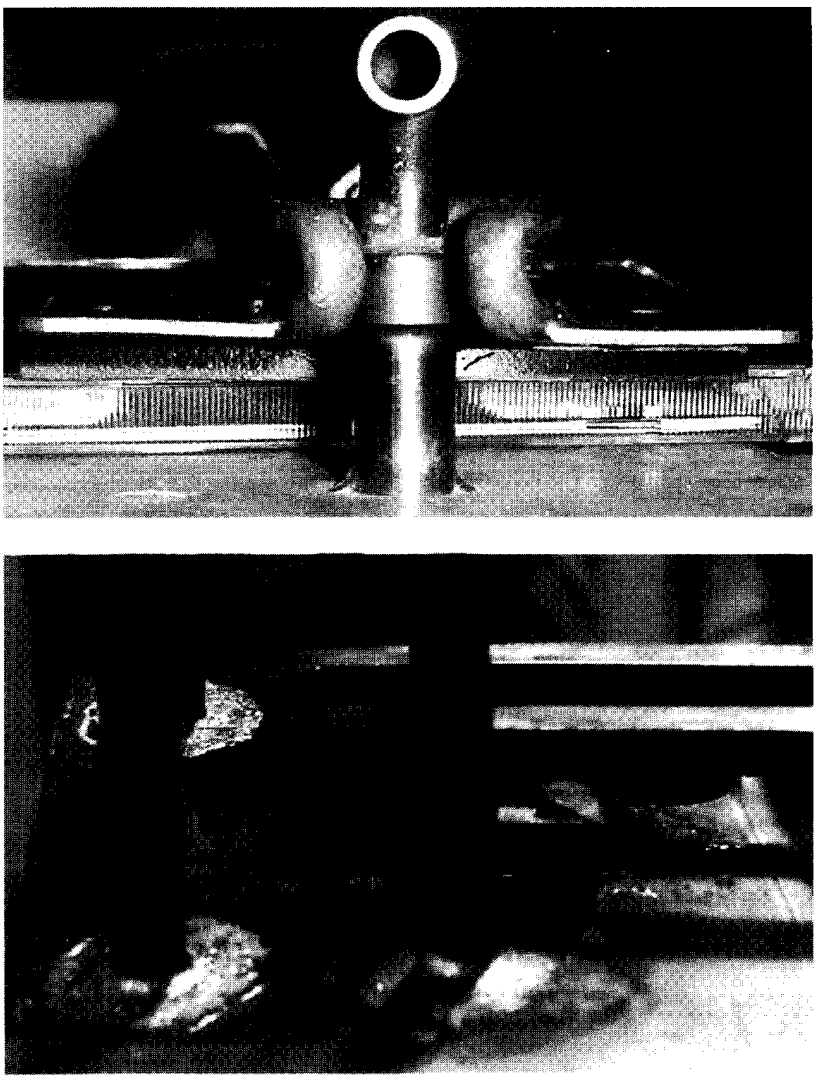

Figure 6.10 Induction brazing applications. (Courtesy of Lepel.)

point (liquidus point), which is the point at which the material starts to melt. The flow point can be a consideration when there is more than one joint to be brazed in an assembly or when a component is held in a brazing position in an unfavorable way for the filler to flow freely.

If there are a number of joints on an assembly, one might consider using a higher melting point filler on the first joint and a lower melting point filler on the second [316]. Filler suppliers often provide a list of typical applications for a particular filler as well as heating methods, melting temperatures, flow point, and chemical composition.

The forms and shapes of filler materials that are available should also be taken into consideration. Filler material is available in coils or spools of wire, lengths of rod, strips, powder, and preforms (e.g., shims, stamped shapes, washers, rings, shaped wire, slugs, and fillings) [313]. When it is necessary to provide high produc-

Table 6.3 Principal Filler Alloying Elements and Approximate Applicable Temperature range

Soldering							
Element		Ga	Bi	In	Sn	Pb	Au
Temperature range	°C	< 40	50–140	60–200	120–230	210–310	170–350
	°F	< 105	122–284	140–392	252–446	410–590	338–662
Brazing							
Element		Al	Ag	Au	Cu	Ni	Pb
Temperature range	°C	530–570	610–850	830–940	700–1040	880–1100	Appr.1200
	°F	986–1058	1130–1562	1526–1724	1292–1984	1616–2012	Appr.2192

Source: Ref. 313–318.

tion, automated brazing/soldering processes are required and custom forms of fillers are developed to produce consistent results (see Figure 6.11).

Fluxes also play an important part in a brazing/soldering operation. Being a chemical compound, flux helps protect the filler materials as well as the base metal from oxidation during the heating cycle [313]. Thanks to fluxing of the joint area the oxides that form during heating will be dissolved and absorbed. This is essential to allow the proper wetting condition in order to bond the materials. Fluxing is applied to the clear and degreased surface just prior to the brazing operation.

There are several fluxes available on the market. Just as the filler material is, they are designed for specific applications that include temperature range and filler material alloy content. Common forms of fluxes are paste, powder, and liquid. It is important to have no oxidation in the joint, therefore the flux is applied liberally. The necessity of using flux can be eliminated when brazing of clean parts is conducted in a protective atmosphere or in a vacuum.

6.1.1.7 Fixturing and Handling

Fixturing and handling of the parts to be brazed is just as critical as the uniformity of heating and selection of the proper filler and base materials. The best scenario for brazing from a fixture perspective is when the components are self-aligning and the design of the joint and components holds itself together during the entire brazing cycle. Cases such as this call for the simplest fixture.

As mentioned earlier, it is common for assemblies to be held or clamped together to maintain their alignment during the heating and cooling/solidification cycles. In some cases, the weight and geometry of the components themselves are sufficient to hold components together. A well-designed fixture allows correct positioning of the parts in the induction coil during the heating cycle. Nonmagnetic

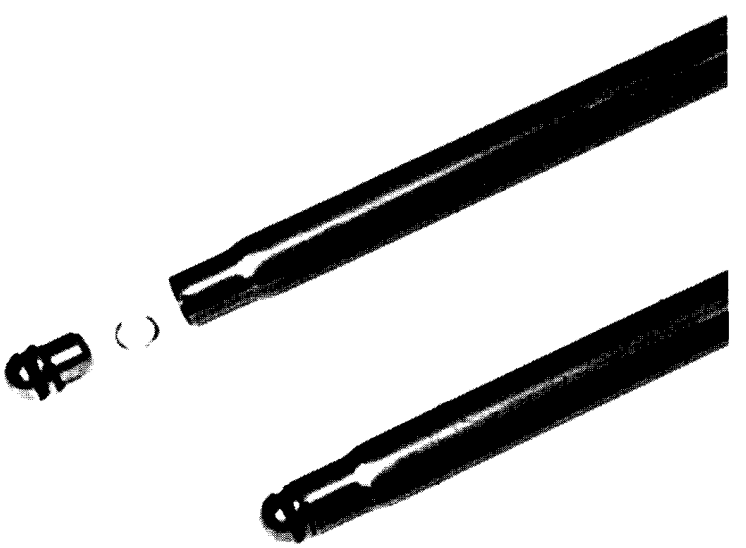

Figure 6.11 Parts to be brazed using custom-formed filler. (Courtesy of INDUCTOHEAT, Inc.)

metals, high-temperature plastics, ceramics, and heat-resistant composites are used as materials for making fixtures.

There are several basic ways to automate induction brazing equipment. Manually loading a magazine, conveyor feed, or rotary table arrangements are the most common. This approach usually represents a low production and/or low capital cost of brazing/soldering machinery. The operator assembles the components and either the filler material is hand-fed or a preformed filler is put in place. The operator also might use certain types of clamps or other holding devices if necessary. Figure 6.12 shows manually assembled and loaded equipment (in this particular case, the clamping of the components is not required).

When high production is required, a completely automated system may be used. Such a system would assemble the components, feed the filler material, or place preform filler and hold the part until the joint has solidified. The heating can be done at an individual station or at more than one station for multiple brazed joints. When the part's geometry will accommodate, a continuous feed system can be utilized. In cases such as this, through feed or channel-type inductors are utilized. Examples of both approaches are shown in Figures 6.13 and 6.14.

6.1.1.8 Summary

For all successful brazing applications there are some preparations before the actual brazing begins. The following steps are crucial for achieving a good consistent joint.

Basic Steps and Preparations for Brazing/Soldering

1. Parts to be brazed should have the proper clearances (not too big and not too small) so the filler material can flow freely due to capillary action. This will produce a strong joint.
2. Parts should be clean and free from any contaminants such as oxidation, oil, grease, scale, and the like.

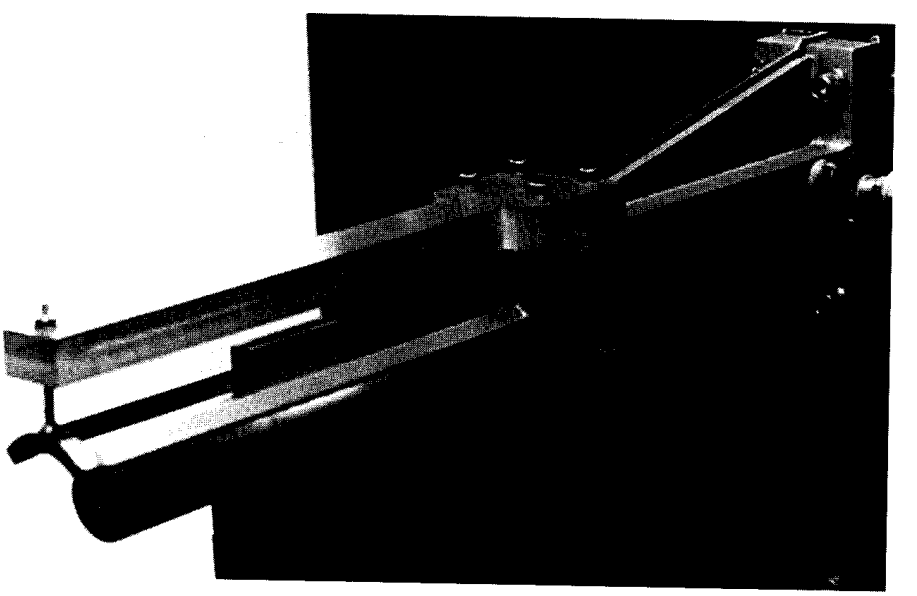

Figure 6.12 Manually loaded induction brazing application. The vane is brazed onto the shaft in seconds. (Courtesy of INDUCTOHEAT, Inc., Madison Heights, MI.)

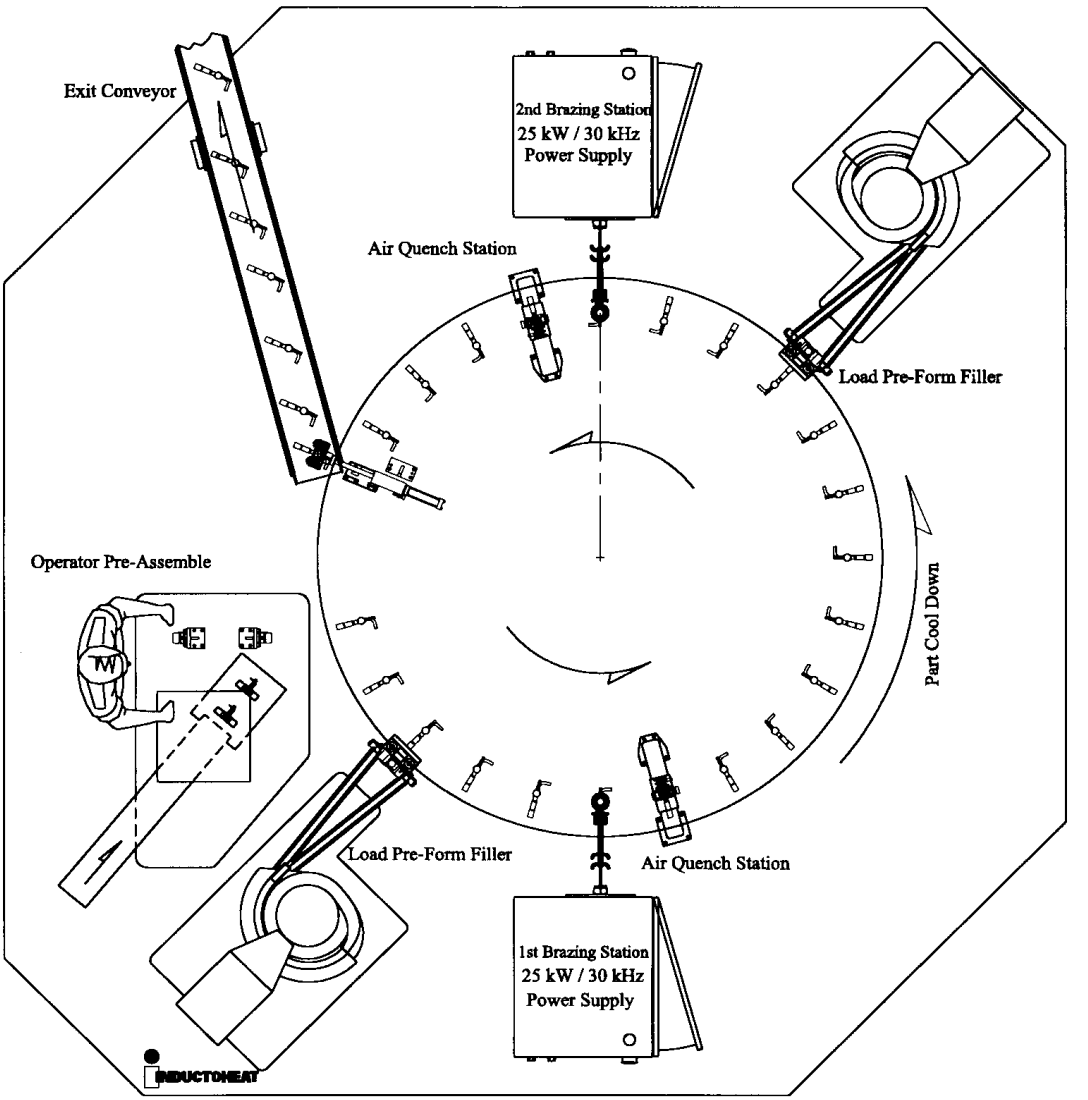

Figure 6.13 Automatic induction brazing station for brazing two areas of a brass valve assembly.

3. The parts should be properly fluxed. Fluxing the part will help keep the joint clean and free from oxidation and corrosion during the brazing process. A proper flux can be of help for creating a quality joint.
4. Fixtures or some way of holding the parts together during the heating cycle are required to keep the parts aligned.
5. Heating the piece to be joined and the filler material to simultaneously reach the required brazing temperatures is also necessary.

When brazing components, the selection of the proper heat time is important. If the heat time is too long, then shape distortion and surface oxidation can occur. However, if the heat time is too short, the flux might not be able to provide the required wetting conditions for brazing. The main difference between brazing by induction compared to other brazing operations deals with the fact that the heat is

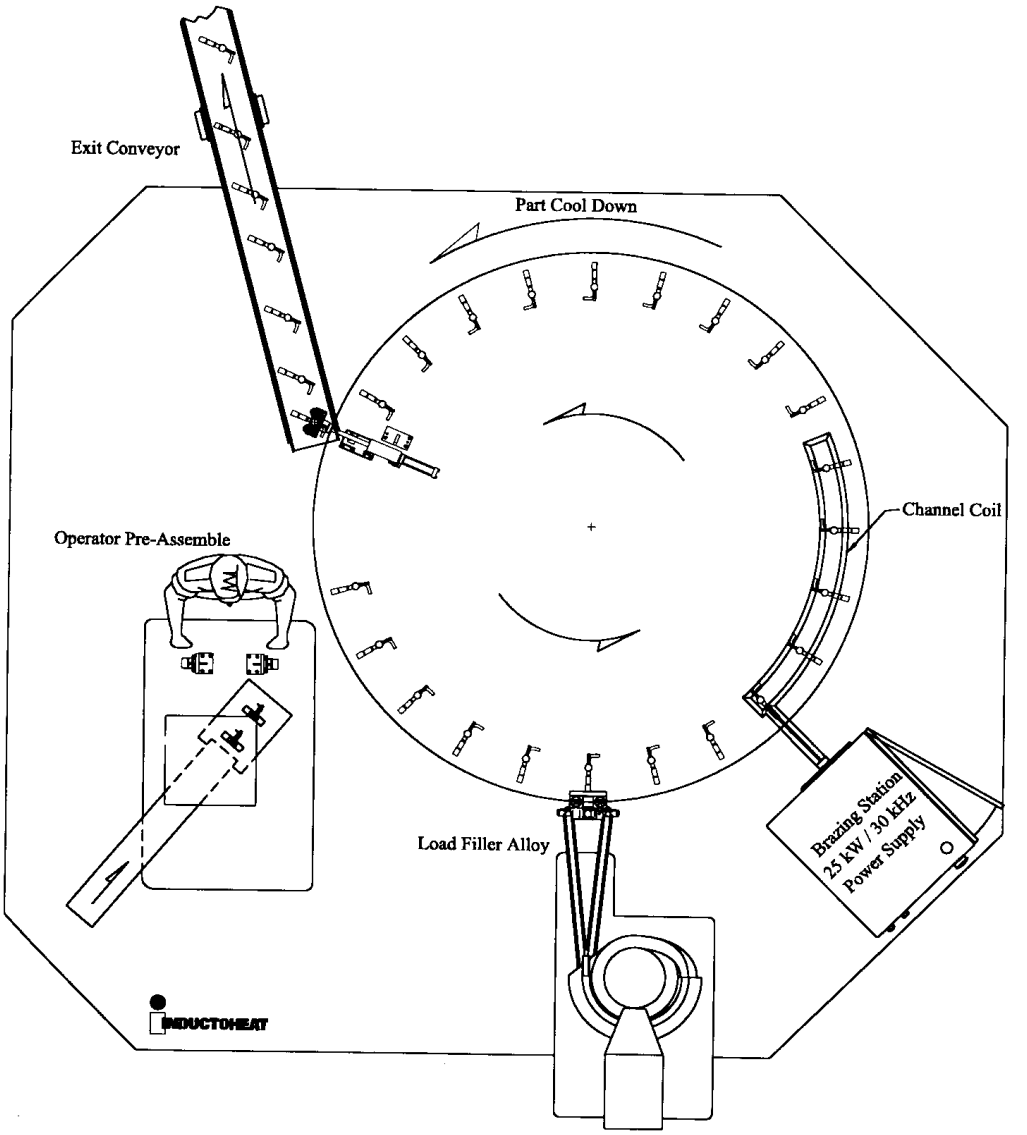

Figure 6.14 When the joint will allow it and high production is required, a channel type coil can be used in this automatic brazing system.

generated within the brazed body, and can be very accurately controlled. Induction heating has several advantages for brazing and soldering applications.

6.1.2 Bonding

In addition to brazing and soldering, bonding is another popular approach to join two or more materials. In contrast to brazing and soldering, bonding is a much more universal industrial joining technique because the components being joined do not have to be metals. Plastic materials, ceramics, glasses, and other nonmetallic materials can be bonded as well.

In different industries and, in particular, in the automotive industry, a common goal is to reduce the weight of the final assemblies. One way to accomplish this is to utilize plastic components. Some components require stronger properties only in certain areas of assembly. In these cases, plastic is bonded to some other materials such as ceramics, steel, brass, or another plastic with different properties.

In bonding applications, a bonding effect is provided by an adhesive material. Adhesive itself is not an electrically conductive material and cannot be heated by induction. Therefore, when bonding by induction is applied, at least one of two joining components should be electrically conductive (or several components should be electrically conductive when bonding a multicomponent structure). Electrically conductive components will be heated by induction providing the heat flow due to a thermal conduction to adhesive material that has physical contact with it. Sometimes a process of bonding requires the presence of an applied pressure between joint components.

Adhesive bonding provides several principal benefits to the users of this technology. This includes [363–366] the following.

- Adhesive bonding provides a lighter structure than welded, brazed, and particular structures that rely upon mechanical fasteners (e.g., bolts, screws, etc.).
- Adhesive bonding can be applied to those assemblies that cannot be brazed, soldered, or welded (e.g., ceramics or plastic materials) and cannot use mechanical fasteners due to the possibility of being damaged.
- When bonding the metal components, adhesive bonding does not accelerate corrosion development. The use of mechanical fasteners, however, would require drilling holes for fasteners, distracting an entity of the metal, removing a protective corrosion-resistive layer of coating, and raising the possibility of having a galvanic reaction of two dissimilar metals that have been joined. The latter two features also hold true when welding is applied. Because adhesive bonding is not electrically conductive material and does not require distracting the surface coating it eliminates the possibility of galvanic reaction.
- Adhesives provide good shock and vibration absorption with certain damping ability and can accommodate a thermal expansion.
- Welds, brazed joints, and fasteners (e.g., bolts, screws, etc.) are known for their ability to lead to uneven distribution of stresses in the joint areas. The presence of stress-raisers may negatively affect fatigue strength properties of the component. In contrast, adhesive bonds provide a more uniform distribution of stresses.
- Because adhesive bonding requires low temperatures (typically in the range of less than 230°C (450°F), thermally induced mechanical strain does not exceed the elastic limit of most applicable metals (e.g., steel) and it does not introduce a permanent shape distortion of the joint assembly as is the case when brazing and welding are applied.
- Adhesive bonding is corrosion resistive, as adhesives prevent metal components from being exposed to moisture and aggressive entrapping dirt.

Although there are numerous adhesives available to meet an almost endless variety of bonding applications, a majority of adhesives can be divided into two large groups [363–366]: thermoplastic and thermosetting. Thermoplastic adhesives soften

when heated and get hard when cooled down. Thermosetting adhesives form a joint bond due to a chemical reaction called the polymerization process. In both cases, induction heating is effectively used whether to accelerate a polymerization process or to provide a required softening of the adhesive.

Induction bonding is often performed on sheet metals or thin metal strips (e.g., brass strips). The manufacture of electrical connectors may serve as a typical example of induction bonding. Because the adhesive bonding process belongs to the group of low-temperature applications where the maximum temperature does not normally exceed 230°C (450°F), the power requirements are usually relatively small. Many bonding applications are done with power less than 10 kW and using the frequency that ranges from 10 to 200 kHz. It should be understood, however, that as with all induction heating applications, the power and frequency are greatly affected by the size, shape, and material of the components being bonded and the required heated mass.

At this point, for illustration purposes, two studies of typical induction bonding applications are discussed below.

Case Study 1. Joining a Rubber Gasket to a Brake Pedal Support. One challenge for automotive companies is joining dissimilar materials, such as securing a rubber gasket to a brake pedal support. One option is to use mechanical methods such as fasteners, rivets, or clips. However, these will add cost and require additional manufacturing. Gluing can be impractical and messy.

The induction bonding machine shown in Figure 6.15 utilizes induction heating to "heat stake" or bond a rubber-type gasket to a metal automobile brake pedal

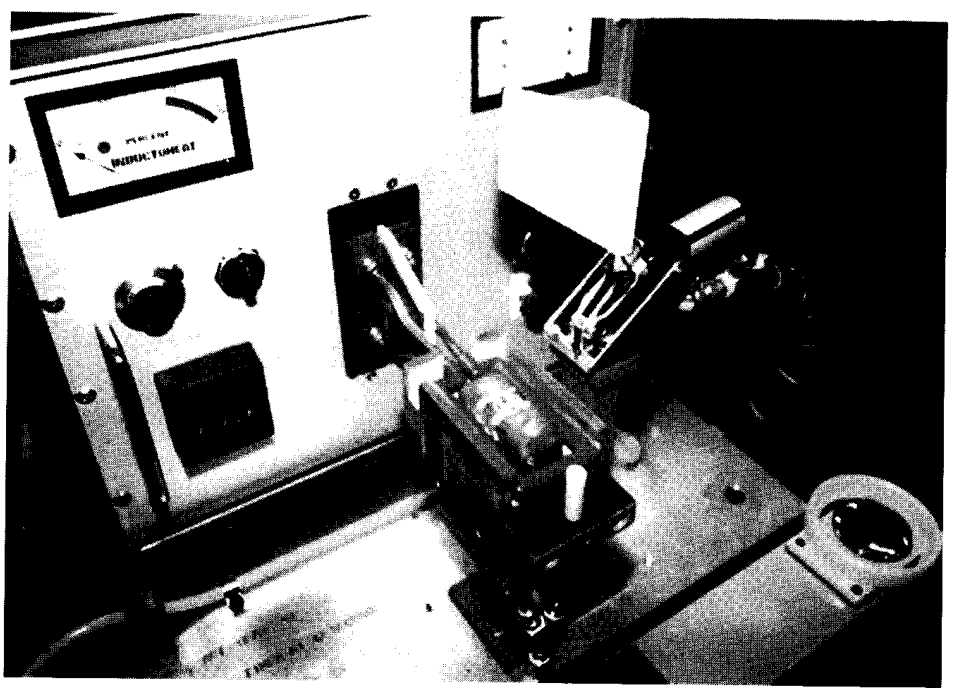

Figure 6.15 Induction bonding system. Rubber gasket is bonded to metal brake pedal support in 4 sec, using 2 kW/30 kHz. (Courtesy of INDUCTOHEAT, Inc., Madison Heights, MI.)

support. This bonding operation prepares the pedal for its next step in the assembly process. The fixture's components include: a table structure which supports a 5 kW, 30 kHz power supply, an induction heating coil, a part support for locating the brake pedal, a clamping device, and palm buttons to start the cycle.

In order to keep the capital equipment cost down, the fixture is manually loaded and unloaded. To process a part the operator loads a brake pedal and a gasket on the part supports. This automatically locates the part directly above the induction coil. A system was developed to produce 500 parts per hour. The heating cycle begins by heating the part to approximately 204°C (400°F), which bonds the gasket to the pedal. The entire process takes about 4 sec and uses about 2 kW per cycle. In this case induction bonding was chosen largely because it has a very quick cycle and the temperature can be accurately controlled, which is crucial as the rubber can deteriorate if it exceeds a certain temperature [363]. The operator then manually removes the processed part and prepares for the next machine cycle.

Case Study 2. Induction Hem Flange Bonding. Induction hem bonding systems provide a fast and reliable partial cure of adhesives that delivers an adequate strength to maintain a dimension stability of the assembly during material handling. For example, inner and outer automotive door panels, deck lids, lift gates, and hoods require being held together, maintaining their positions until they are completely joined.

One way to do this is to spot weld. However, spot welding creates numerous problems. One of them deals with the necessity to have a subsequent grinding operation. Not only does this add another operation, it also, as mentioned above, becomes a stress-riser and a source for corrosion initiation because the finish coating would be partially removed during spot welding and grinding.

An alternative approach would be to apply one-part epoxy adhesives in combination with an induction curing. Figure 6.16 shows the steps in the induction hem bonding process.

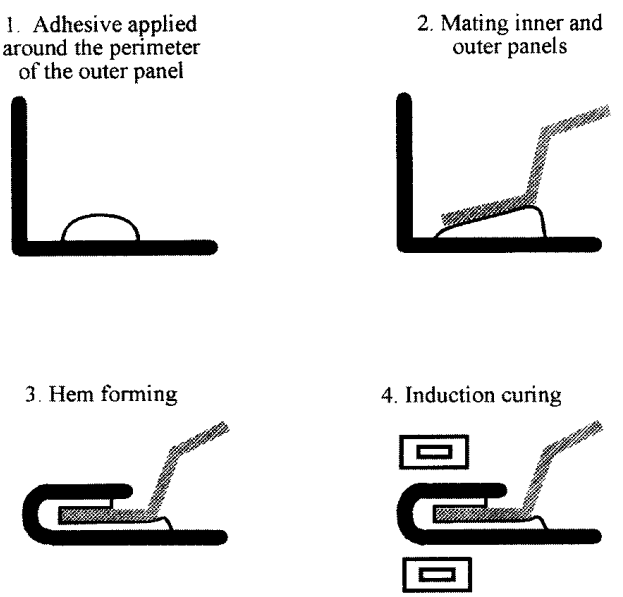

Figure 6.16 Induction hem bonding process steps.

An example of practical utilization of this technology is shown in Figure 6.17. The induction system hem bonding of automotive door panels consists of a 100 kW/10 kHz solid-state power supply, induction coil assembly, and modular fixture. Modular fixture design makes it easy to incorporate in a new or existing closure panel assembly line. The door panel nest is machined from high-temperature durable material.

The fixture comes complete with the necessary base, part nest, clamps, and pneumatics. The fixture base is available with a panel lifter mechanism, grout plates, wheels or air cushions, and an instachange coaxial cable adapter for fast fixture changeover. It can also be designed for full periphery or spot curing of the panels.

6.1.3 Cap Sealing

Induction cap sealing is a variation of the induction bonding process described in Section 6.1.2. It is a noncontact process by which a foil disk or "seal" is bonded to a container. This unique process can be used with almost any style container, jar, and closure for sealing foods, drugs, beverages, chemicals, and so on. The innerseals must meet the stringent requirements of the Food and Drug Administration (FDA) and can be used on containers of all compositions.

Innerseals are available in many variations to meet nearly any standard or customized packaging need. There is virtually no limit to the size of container finish they will seal.

Innerseals consist of specially treated aluminum foil bonded to various types of proprietary films for use with virtually any type of container or closure (HDPE, PE, PET, PETE, PETG, PVC, PP, Barrex, Barrier, Styrene), including most thermo-

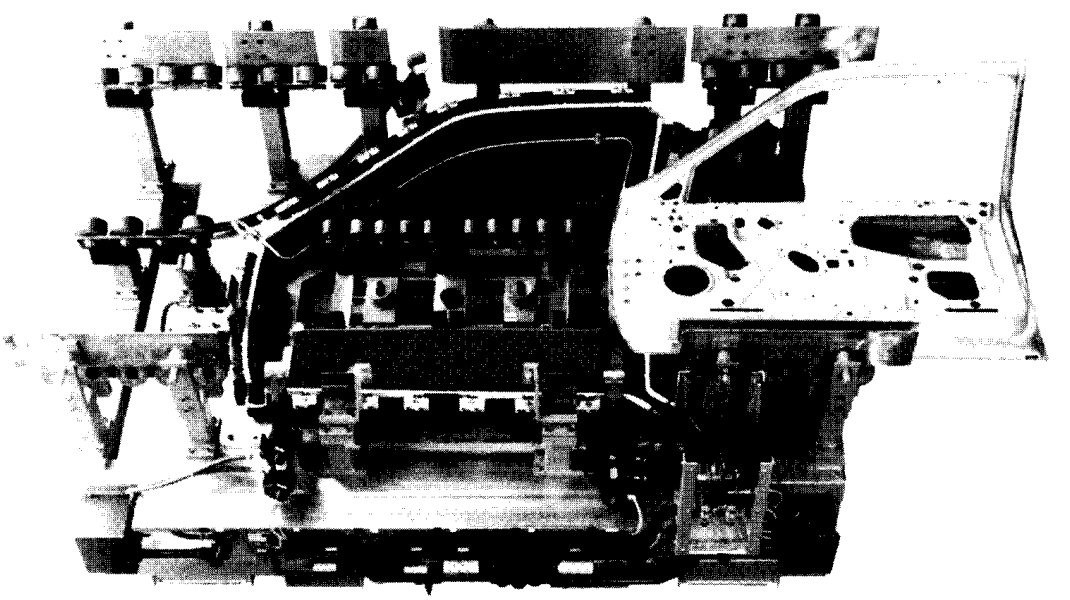

Figure 6.17 Full or partial periphery cure fixture showing panel lifter mechanism. This is known as hem bonding in the automotive industry. (Courtesy of INDUCTOHEAT, Inc., Madison Heights, MI.)

plastic containers as well as glass. They will provide tamper-evident hermetic seals suitable for use with foods, drugs, beverages, alkalies, acids, oils, organic solvents, flammables, powders, pellets, and many other products. They are particularly effective for products that must be kept free from contamination, oxidation, and moisture [324].

This process was developed to prevent leakage of chemicals from plastic bottle caps (Figure 2.53). The cap is supplied with a foil innerseal, ready to load into the capper. The container is filled and capped in the standard packaging operation. The capped container is transferred down the conveyor line and passes underneath a conveyor-mounted induction sealing head at line speeds up to 300 ft/min. The sealing head is designed to inductively heat the foil layer of the innerseal structure evenly to prevent liner damage. The electromagnetic field generated by the sealing head penetrates the cap and the aluminum foil layer as the container passes underneath. This is a noncontact process. As the field penetrates the electrically conductive foil, it induces an eddy current flow that quickly generates heat. Temperatures of 85°C (185°F) to 180°C (356°F) are typical to activate the heat seal coating [324]. After leaving the induction field, the foil cools, and the heat seal film bonds to the container finish leaving a hermetically sealed container. When the cap is removed, the aluminum foil remains bonded to the lip of the container.

The induction liner is normally supplied to the closure manufacturer in coil strip form, similar to conventional lining materials. The foil innerseal is then die-cut and inserted into the closure with a die-cutting system by the closure manufacturer. Although available in a variety of forms, the innerseal is supplied in two structures, each with several basic parts (see Table 6.4):

1. An aluminum foil layer, generally 0.025 mm (0.001 in.) thick;
2. A heat-sealable polymer film laminated to the foil, 0.025 to 0.05 mm (0.001 in. to 002 in.) thick;
3. A backing material of paper, pulp, or foam bonded to the foil either permanently with adhesives or temporarily with wax varying from 0.15 to 0.9 mm (0.006 in. to 0.035 in.) thick.

Induction sealing equipment is far less costly, requires less maintenance, and is much easier to install than other types of sealing equipment. The one-step sealing process itself is also low in cost; no extra handling or double operations are required since the capped containers merely pass underneath the induction sealing head without actual physical contact (Figure 2.53). The innerseal wafer combines the innerseal and a resealable cap liner for one-step insertion in the cap, resulting in a combined low cost.

Table 6.4 Bonding Materials for Innerseals

Wax bonded	Single element
Pulp board backing	Paper or foam
Wax coating for temporary bond	Adhesive
Aluminum foil	Aluminum foil
Heat-sealable film	Heat-sealable film

The inductively bonded foil seal will eliminate product leakage; prevent tampering, pilferage, and adulteration; lengthen shelf life; prevent evaporation; and enhance customer confidence.

6.1.4 Shrink Fitting

Shrink fitting parts together is a way of joining components without the use of a filler material. Instead, the phenomenon of thermal expansion of materials during heating and contraction during cooling is used to provide a mechanical bond between the two pieces.

Not every part can be shrink fitted. Most often this process is applied to cylindrical-shaped hollow parts such as ring gears, roller bearings, and the like. During a shrink fitting process, an external part is heated to provide temporary expansion for a slip or snug fit at assembly (Figure 6.18).

If the parts were only press-fit together without heating, there could be deformation of the assembly. After inserting the second part into an already heated and sufficiently expanded external part, the assembly is cooled to ambient temperature and the components are permanently locked together, unless heated again. Shrink fitting is a reversible process.

In many cases, shrink fitting is the most cost-effective way to assemble parts. The outer race is heated and expands relative to the inner race; the ball bearings are slipped into place and allowed to cool, resulting in contraction.

Because for most shrink fitting applications the entire part is required to be heated rather than selective areas, low power density and frequency are used. Typically for shrink fitting applications the applied frequency ranges from as low as line frequency to 10 kHz. Depending upon the geometry and the material of the components the temperature suited for shrink fitting ranges from about 120°C (250°F) to 400°C (752°F). Single- or multiturn solenoid coils or C-core type inductors (see Sections 5.5.2.2 and 7.6.3.5) are the most commonly used for shrink fitting applications.

Figures 6.19 and 6.20 show an eight-station automatic induction shrink fitting system that consists of a rotary-indexing unit powered by a hydraulic motor. C-core inductors powered from a line frequency power source provide the heating of truck

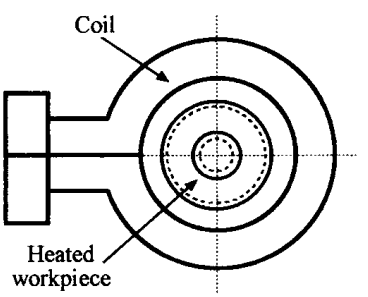

Figure 6.18 Expansion–contraction of workpiece during "heating–cooling" cycle (solid line represents geometry of heated part; dotted line represents geometry of cold part.)

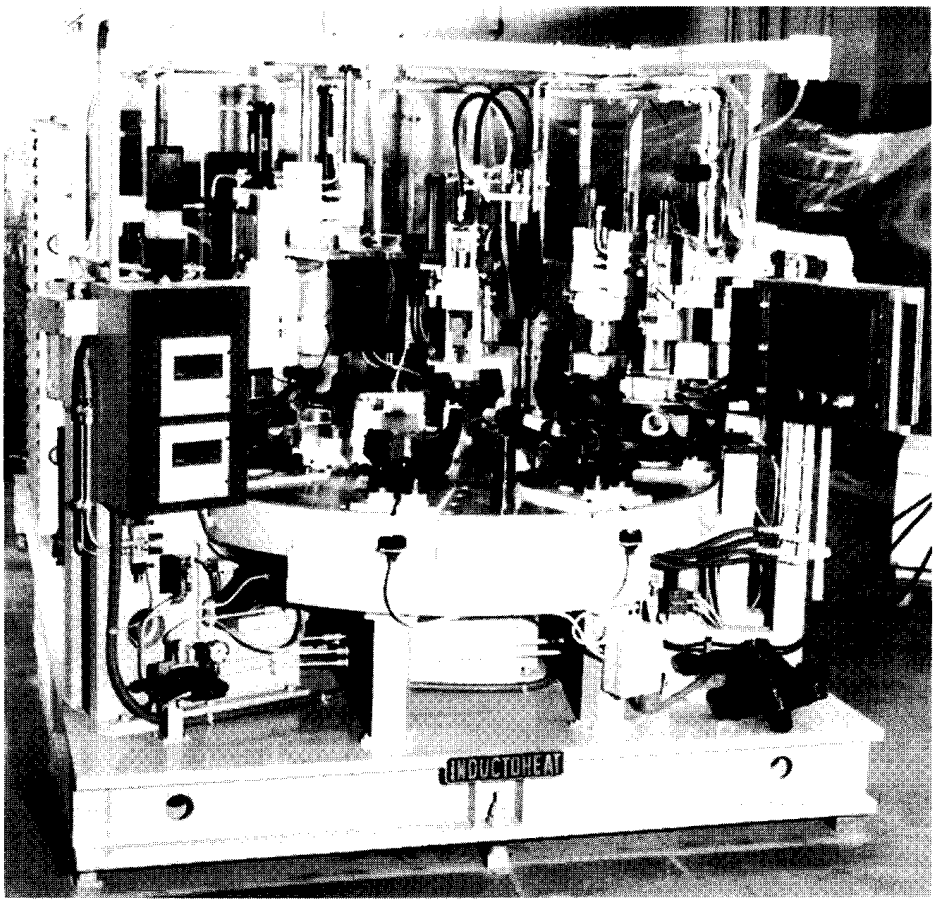

Figure 6.19 Compact shrink fitting system for assembling truck steering knuckles. Machine consists of eight stations and produces one knuckle every 120 sec. (Courtesy of INDUCTOHEAT, Inc., Madison Heights, MI.).

knuckles to a temperature of 343°C (650°F) to 371°C (700°F) in two stages. The preheat station heats the knuckle for a minimum of 40 sec prior to the final heating cycle to obtain 371°C (700°F). The knuckles have a heat soak of approximately 30 sec prior to spindle insertion. A closeup view of the knuckles can be seen in Figure 5.3. The machine is manually loaded and unloaded. The table is tooled to accommodate either right or left-hand knuckles.

The machine stations shown in Figures 6.19 and 6.20 are arranged as follows.

- Station 1—load and unload,
- Station 2—idle station,
- Station 3—pre-heat station,
- Station 4—final heat station,
- Station 5—spindle insertion,
- Station 6—cooldown of knuckle,
- Station 7—idle station, and
- Station 8—push test (to test spindle insertion).

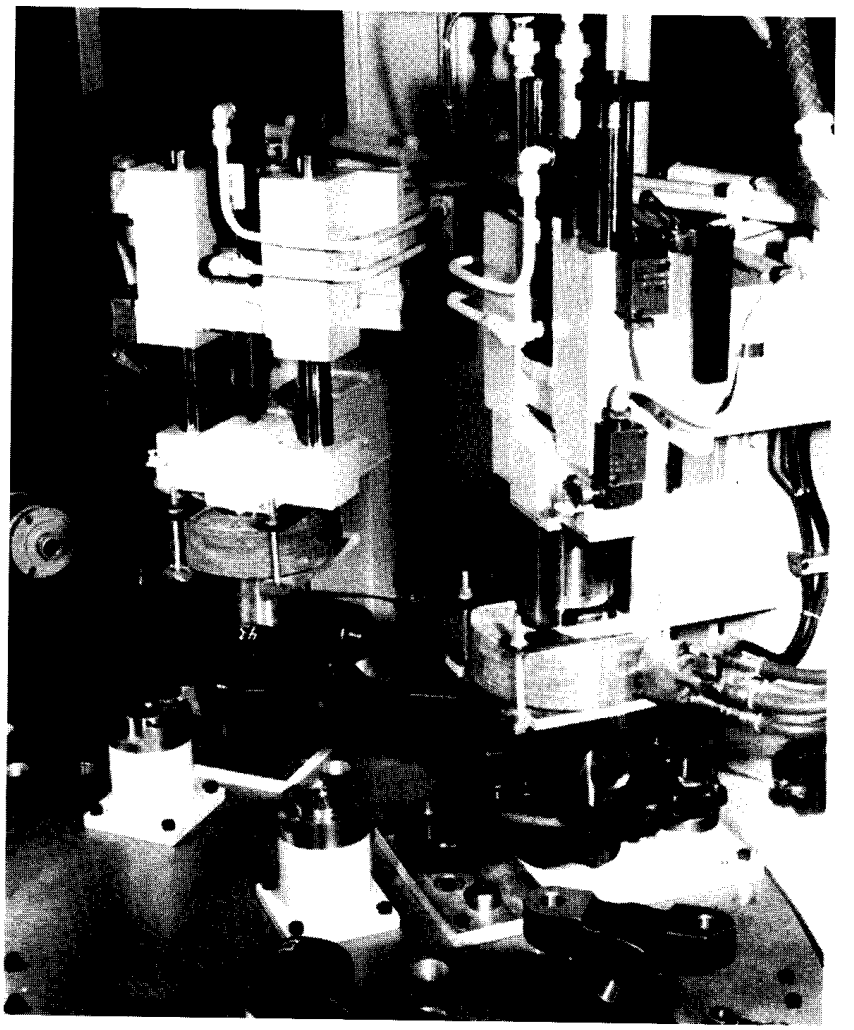

Figure 6.20 Closeup view at heating stations 3 and 4 providing preheat and final heat using C-core inductors powered from line frequency power source. (Courtesy of INDUCTOHEAT, Inc., Madison Heights, MI.)

The machine produces one knuckle every 120 sec. Forced water-cooling is used to cool the assembled parts to less than 90°C (195°F) before removal from the machine. The temperature of the part is controlled throughout the cycle by an optical pyrometer, to ensure quality.

6.2 INDUCTION MELT-OUT

Induction melt-out, or lost-core as it is often called, is a technology that involves inserting a cast metal core into an injection press and overmoulding it with a thermoset or thermoplastic material. The core, which is formed from a metal such as a tin–bismuth alloy having a relatively low melting point (about 132°C/269°F), is then

heated and eventually melted out of the part, often with the assistance of a hot glycol or oil bath to ensure removal of the smaller particles.

The idea of producing hollow parts by moulding them around another material and then removing the center material has been around for hundreds of years. The novel thinking in the induction melt-out concept is the use of a low-temperature melting alloy metal core over which a plastic or composite material is moulded, with the core subsequently being melted out of the part by the use of induction technology rather than simply hot oil or glycol. The use of induction shortens the time of core removal from hours to minutes.

Some of the major advantages of this process include, but are not limited by, internal dimensional accuracy, good quality of the internal and external surfaces of the complex-shaped parts, and the ability to produce parts in a high-volume production environment (Figure 6.21). This technology has also been referred to as MCT or metal core technology as defined in one publication [294].

The utilization of totally dense, dimensionally accurate, low melting temperature metal cores, overmoulded, and melted out allow one to produce hollow plastic components having complex internal geometry. A typical system of this type would include a power supply and induction coil, a robotic material handling system, and a large tank with a pumping system for transferring the molten metal from the melt-out tank surrounding the induction coil back to the injection moulding press. The system shown in Figure 6.22 includes three 150 kW power supplies. Three heating coils are mounted in a small tank containing hot glycol or oil and a robot to place the part into the inductor and often to move the part back and

Figure 6.21 Automotive intake manifolds produced by induction melt-out technology.

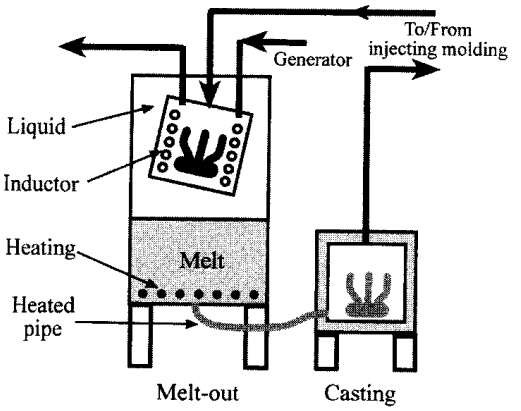

Figure 6.22 Induction melt-out system.

forth to facilitate removal of smaller pieces of metal inside the plastic part. Care must be taken to avoid overheating the metal and burning the plastic part. To prevent this, the part is strategically located in a certain orientation with holes at critical locations to allow the molten metal to easily flow out of the plastic part. Electromagnetic forces play an important role in helping to remove the molten particles. Depending upon the part geometry, a frequency is typically in the range of 6 to 30 kHz.

A casting machine is used to cast the cores to the required shape and a conveyor system is utilized to transport the cast cores to the injection molding machine. The injection molding machine must also be supplied with the required plastic material to mould around the core [293, 294].

From the induction heating standpoint the types of parts produced with this technology range from automotive intake manifolds (Figure 6.21) to wheelchair wheels on down to tennis shoes. For each part an induction heating coil must be designed for optimum performance in terms of time to melt the core completely out of the plastic part without overheating the metal and burning the plastic in the process.

Successful systems operating in the field regulate the inductor voltage near 800 to 1200 volts (rms) at the selected frequency and allow the power to fall off from the start of heating until the point where the metal is completely removed from the part and the load is simply the inductor itself. Melt rates of about one pound per second can be achieved.

Due to the very large diameter of many of the systems, a relatively small number of turns may be required to properly tune the power supply to the inductor. This necessitates a special design using many parallel turns to cover the required length to heat the entire part and balance the currents of the parallel turns.

In the initial design of a melt-out or lost-core system an evaluation must be made of the required frequency to successfully heat the smallest sections of the metal within the part. This consideration is often assisted by the use of a hot glycol or oil bath that will aid in melting the small slivers that the induction process may not completely remove. Some unfortunate penalties with the hot metal, glycol, and oil systems are the growing environmental and safety concerns with the use and disposal of potentially dangerous material.

6.3 MOTOR ROTOR HEATING

In the production of small and moderate size motors (Figure 6.23), induction heating is used for a variety of applications, such as the following [308].

- Die-cast aluminum bond breaking (thermal shocking) to improve electrical efficiency.
- Lamination bluing for rust prevention.
- Rotor heating for motor shaft insertion and shrink fit assembly.
- Motor frame heating for disassembly when open frame motor posts are heated to soften the epoxy. This enables the motor frame to break apart and the parts to be salvaged.
- Epoxy curing for component assembly. Curing epoxy used in the assembly of stator in housing and also for field ring magnet bonding.
- Varnish curing.
- Motor shaft bearing hardening when shafts are processed two at a time in a vertical scanning machine.
- Preheat for die casting.
- Heating for wire stripping.

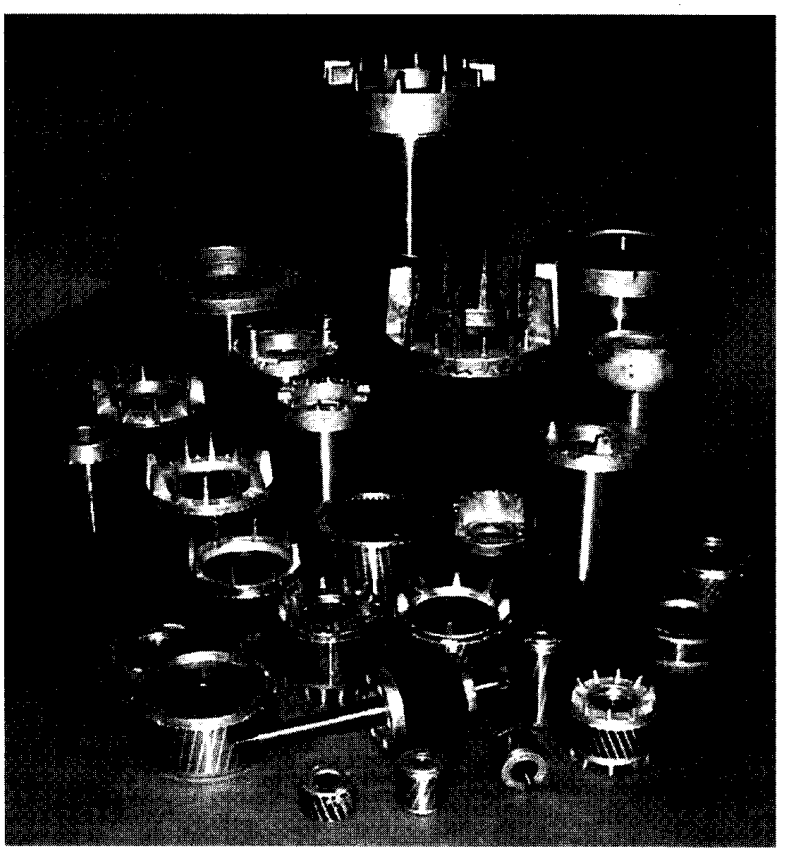

Figure 6.23 Small- and moderate-size motor rotors.

As an example, Figure 6.24 shows an INDUCTOHEAT–IHS 100 kW/1 kHz inline induction rotor heater consisting of an adjustable load magazine, electric actuator charge system with water-cooled charge lance, solenoid-type encapsulated heating coil, rotor up-ending device, pick and place unit, operator shaft drop location with automatic motor shaft positioner, and spray quench cooldown system. This induction system provides heating of rotors with diameter ranges from 57 mm (2.25 in.) to 115 mm (4.5 in.). Rotor stack height ranges from 16 mm (0.63 in.) to 155 mm (6 in.) up to 510°C (950°F) at a production rate of 240 rotors per hour.

In the past, fuel-fired ovens and furnaces have been widely used for rotor heating applications. During the last decade, induction began to dominate this market. There are several reasons why manufacturers of small- and moderate-sized rotors have turned to induction.

Fossil fuel-fired ovens and furnaces can consume valuable floor space, contribute to disagreeable working environments, and involve large quantities of product maintained in process. Startup, shutdown, and in some cases product changeover are time-consuming and costly processes.

As a result of gases escaping from the aluminum, furnace heating can produce hot spots and blisters on the die-cast rotors. Such undesirable effects cannot be tolerated due to the rotor-to-stator clearance of 0.05 mm (0.002 in.) to 0.08 mm (0.003 in.). Induction heating noticeably reduces or eliminates these problems providing some additional attractive features compared to furnace heating that have been indicated in [308]. Some of these features are discussed below.

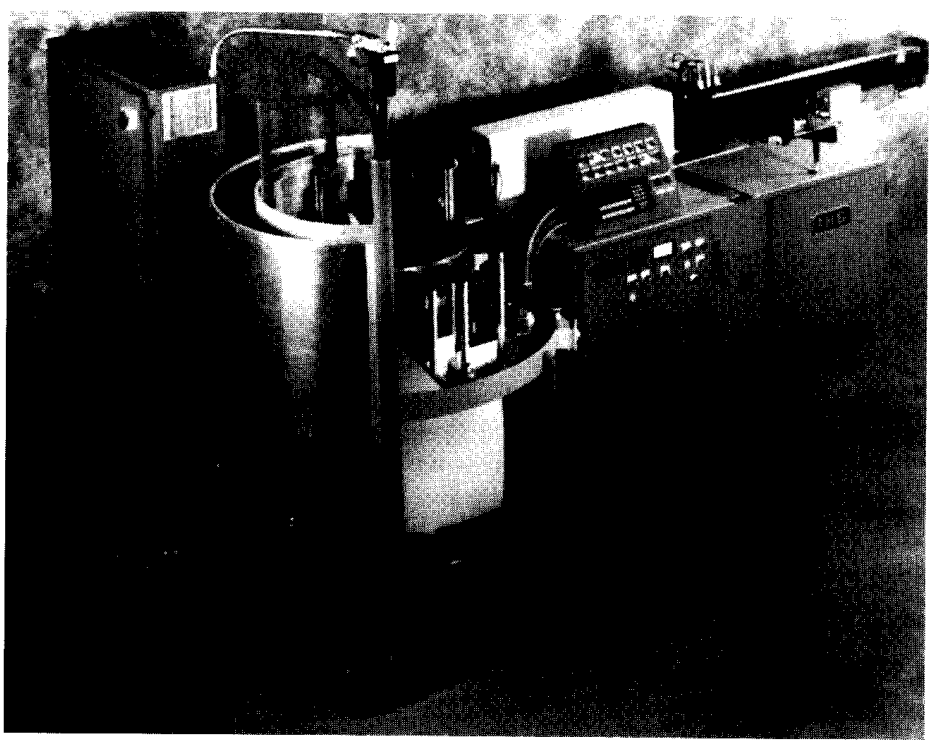

Figure 6.24 100 kW/1 kHz inline induction rotor heater with automatic coil cleanout.

Floor Space and Manpower Requirements

Furnace heating often requires two operators and floor space requirements can vary from 37 m^2 (400 ft^2) to as large as 93 m^2 (1000 ft^2). In comparison induction equipment in most cases occupies from 2.3 m^2 (25 ft^2) to 4.6 m^2 (50 ft^2) of floor space and generally requires only one operator (Figures 2.52, 6.24–6.26).

Working Environment

Induction systems can be placed directly in the manufacturing process line. They occupy minimal floor space and do not produce excessive heat or noise. Systems are PLC or computer controlled and require minimal setup and operator input.

Work in Progress

Furnace heating times can be as long as 8 to 10 hours with potentially thousands of parts tied up in process. The heating time of induction rotor heating typically ranges from one to two minutes. Production cycle times with induction ranges from 4.5 to 15 seconds per rotor. In most cases there are only 10 to 20 rotors in process.

Process Control and Quality

Power levels and frequency are easily controlled and therefore are repeated for each rotor heated. The energy induced in each rotor is the same every time. This high level of repeatability makes it ideally suited to the shrink fitting process. Heating for shrink fit assembly of the shaft requires that the rotors be consistently heated to the specified temperature in order to provide for the proper bore expansion of 0.05 mm (0.002 in.) to 0.08 mm (0.003 in.).

Motor manufacturers that have heated rotors by induction with consequent quenching report a significant reduction of rpm variation between motors. The reduction in variation differs between motor types but can be on the order of ±300 rpm for conventionally processed motors down to ±100 rpm using the induction heating and quenching process [308].

Efficiency

Fractional horsepower motor manufacturers comment that rotors in their product area have shown an efficiency improvement of up to 2% when processed through an induction heating system.

There are several design approaches using induction to heat rotors. According to one approach motor rotors are placed end to end on a locating vee and indexed into the induction coil or carried through the machine on vertical spindles. Figure 6.25 shows an IHS Corp. 350 kW inline indexing conveyor, vertical rotor heating system for thermal shocking and lamination bluing. Rotors are carried through the machine on vertical spindles. The heating coil assembly is lowered over the rotors and then raised as the conveyor indexes forward. Rotors are conveyed through the cooling section where high velocity air-cools the rotors to room temperature.

Another approach to heating motor rotors by induction utilizes a carousel-type arrangement where the parts are heated to the required temperature as they progress through the coil and are ready at the exit, after cooldown, to proceed to the next assembly operation. As an example, Figure 6.26 shows a 350 kW rotary index, vertical rotor heating system that provides computer control for thermal shocking and lamination bluing. Rotors are rotated through the heating coil, spray quench,

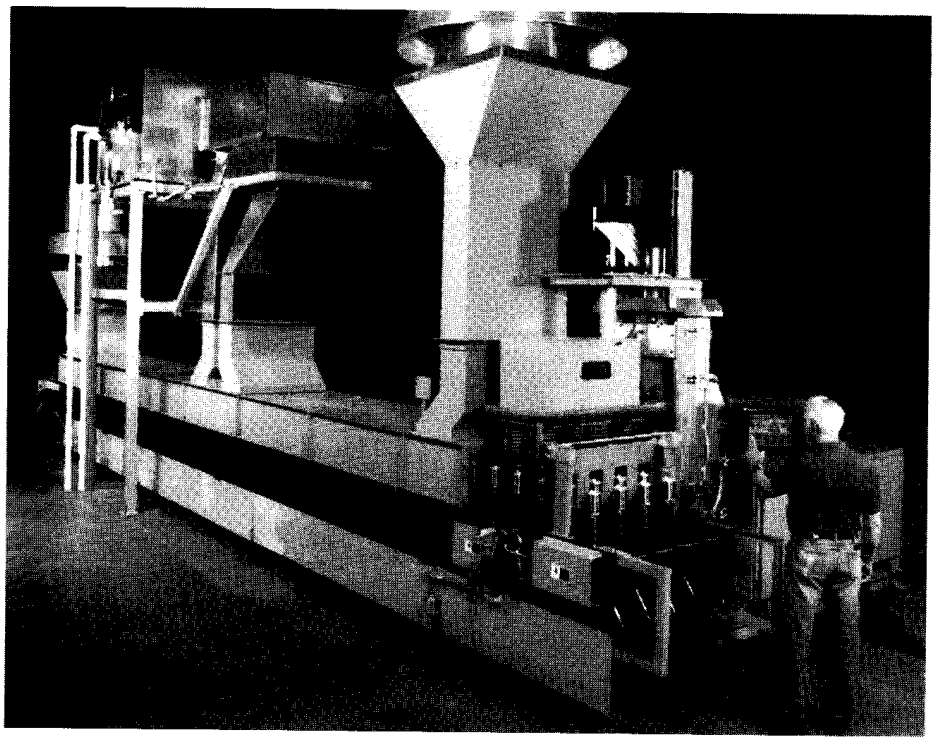

Figure 6.25 350 kW/1 kHz inline indexing conveyor, vertical rotor induction heating system with computer control for thermal shocking and lamination bluing. Rotor size range: diameter, 90 mm (3.5 in.); stack height, 64 mm (2.5 in.) to 127 mm (5 in.); overall length, 102 mm (4 in.) to 204 mm (8 in.); bore size, 25 mm (1 in.) to 32 mm (1.25 in.); nominal temperature, 510°C (950°F).

and air-dry stations. A single operator or pick and place robot may provide the load/unload operation.

In some cases, the induction rotor heating systems are similar to forge billet heaters (Figure 6.27) or inductors used for preheating of semisolid slugs.

6.4 DIE HEATING

Extrusion dies can be designed and produced to run in production without extensive trials and tests. However, some extruders (e.g., extruders of aluminum alloys) experience difficulty in beginning the extrusion process if the dies are not properly preheated to a uniform temperature near the required running temperature. For example, in the case of aluminum extrusion, dies are usually preheated to a nominal temperature of 425°C (800°F) to 550°C (1020°F).

There is the requirement then on extrusion systems to heat not only the billet to be extruded, but also the die and/or die assembly that will be used in the extrusion press. In order to accomplish this preheating of the die and tooling, a variety of different types of ovens and heaters may be used. Chest ovens, drawer ovens, rotary ovens, pot oven, infrared, and induction heaters may be used.

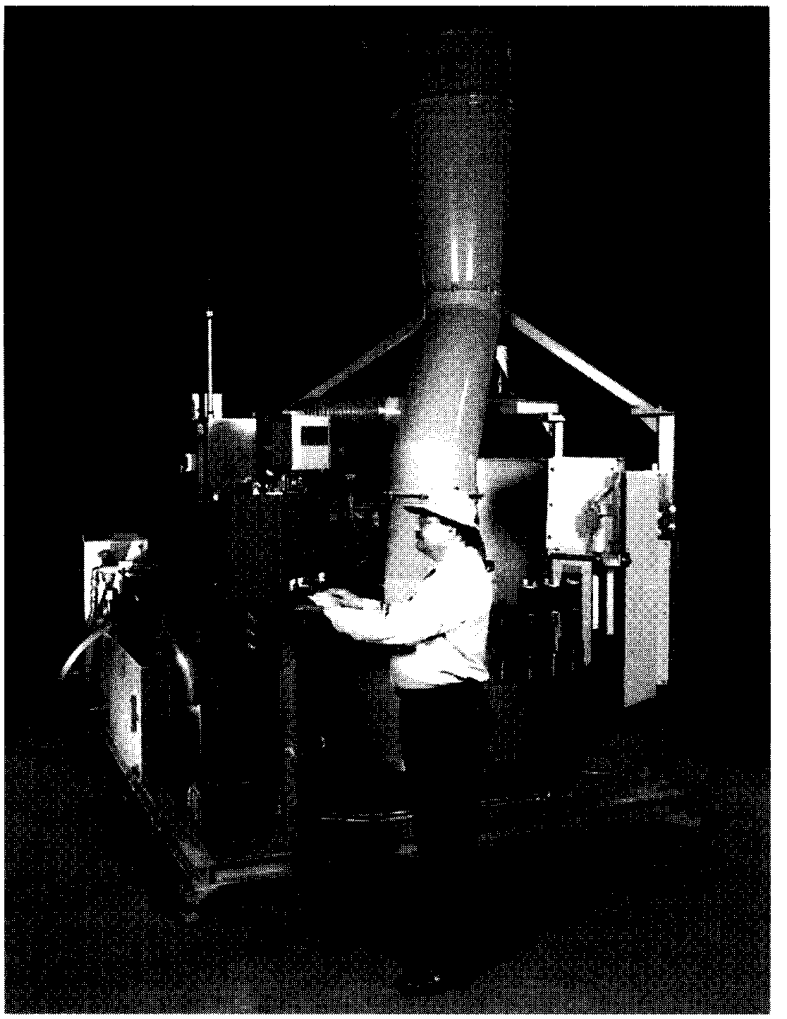

Figure 6.26 350 kW/1 kHz rotary index, vertical rotor heating system for thermal shocking and lamination bluing. Rotor size range: diameter, 66 mm (2.6 in.) to 86 mm (3.4 in.); stack height, 57 mm (2.25 in.) to 152 mm (6 in.); overall length, 114 mm (4.5 in.) to 230 mm (9 in.); bore size, 21 mm (0.81 in.) to 40 mm (1.57 in.); nominal temperature, 510°C (950°F); production rate, 300 rotors/h. (Courtesy of INDUCTOHEAT–IHS, Fort Worth, TX.)

On earlier systems it was common to heat a number of dies at the same time in a stack. Later systems have leaned in the direction of heating and very accurately controlling the temperature of one individual die in the pot-type oven.

Typical chest ovens holding a number of parts for several hours are common but are associated with a variety of problems such as uneven heating, oxidation, poor surface quality, and aging of dies. In these types of ovens, dies are held for hours inside the oven, as the heat is transferred by radiation and, convection and, in cases of multiple dies in one oven, conduction within the stack. Large chambers with recirculating fans assist in trying to equalize the temperature across the die volume. Opening or closing the ovens to insert and remove dies obviously causes greater variation in systems where multiple dies are heated. Heating and holding for extended periods of time also result in deterioration of the die surface, production of poor quality extrusions and shortening of the die life.

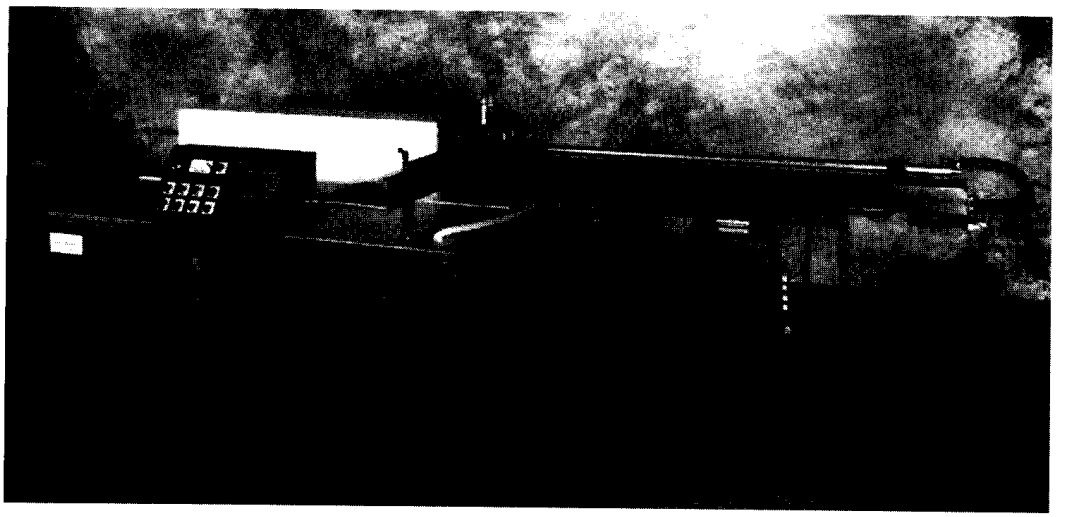

Figure 6.27 200 kW inline rotor heater consists of an adjustable load magazine, electric actuator charge system with water-cooled charge lance, and solenoid-type encapsulated induction coil. Rotor size range: diameter, 57 mm (2.25 in.) to 114 mm (4.5 in.); stack height, 16 mm (0.63 in.) to 152 mm (6 in.); nominal temperature, 510°C (950°F); production rate, 500–750 rotors/h. (Courtesy of INDUCTOHEAT–IHS, Fort Worth, TX.)

Reducing the effects of holding dies for too long a time in the ovens is important. One method of reducing the time required for heating the die to the working temperature is the use of induction as a means of preheating the die. The die is positioned between two spiral-wound pancake-type induction coils. The pancake coils have the desirable feature of heating more efficiently toward the extremes of their diameter so that the die is heated from the outer diameter with the heat conducting toward the center of the die. This is usually accomplished with a relatively low frequency (less than 1 kHz). A typical 330 mm (13 in.) die assembly can be heated and soaked to over 485°C (900°F) in about 30 min. The induction is used as a preheater to bring the die up to temperature before placing it into a conventional die oven to soak or equalize the temperature across the volume of the die.

An induction system typically consists of a power supply, induction heater and a mechanism for moving either the coils or the die into close proximity in order that the heating may be accomplished most efficiently with the required temperature uniformity.

Figure 6.28 shows a commercial induction system to preheat dies that have been manufactured by Inductoheat Banyard. Systems like this offer a variety of loading options (top, bottom, or side loading) and provide high efficiency, low noise, short heating cycles to the required temperature, and increased die life. Extensive trials have shown that induction die heaters provide the required uniform heating of the entire die, with minimal temperature differentials maintained throughout the heating cycle. Typical curves showing temperature uniformity during the heating cycle are shown in Figure 6.29.

Induction die heaters are very compact. Table 6.5 shows space dimensions and utility specifications of the heater that is shown in Figure 6.28.

Optical pyrometers are often used to eliminate the possibility of overheating the die and to allow a soaking cycle if the dies are not required for immediate use.

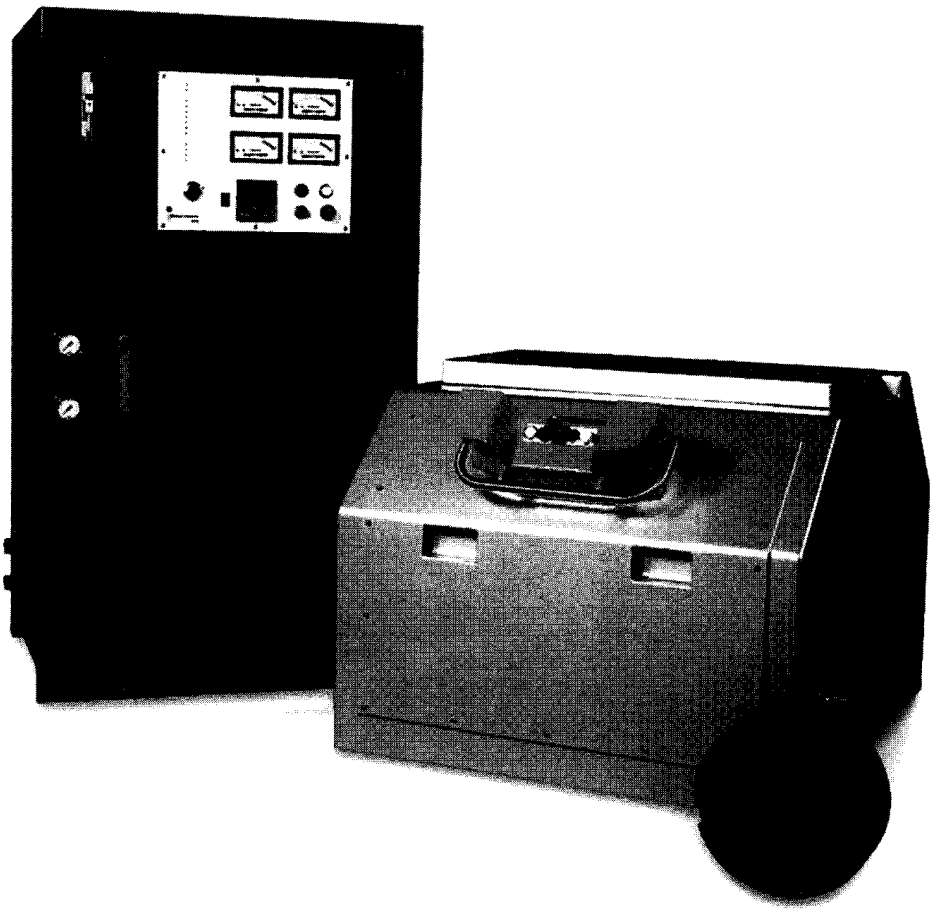

Figure 6.28 Induction die heater. (Courtesy of Inductoheat Banyard, UK.)

Since these systems heat up to eight times faster than conventional die heating ovens there is much less concern regarding oxidation and the energy requirement is only about 12 kWh for a typical heating cycle. The controllability and temperature uniformity at the end of heating meets the specification. Startup and shutdown time of the die heater is drastically reduced. In production operation dies may be taken directly from the induction die heater to the extrusion press or may be placed in a soaking chamber where they may be stored for later use.

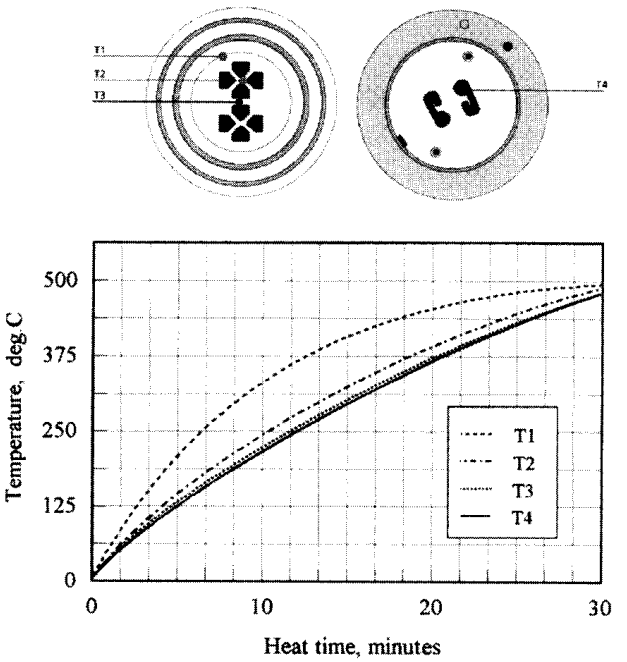

Figure 6.29 Typical temperature–time profiles of induction heating of dies for aluminum extrusion. (Courtesy of INDUCTOHEAT Banyard, UK.)

Table 6.5 Dimensions and Utility Specifications of Heater Shown in Figure 6.28

Type of power supply		SP-12 100 kW/3 kHz
Input voltage		380/480V, 3-phase, @ 50/60 Hz
Input power		110 kVA
Cooling water	Inverter	90 LPM
	Coils	90 LPM
Power supply dimensions		1650 mm(high) × 915 mm(wide) × 762 mm(deep)
Die heating enclosure		1200 mm × 1000 mm × 820 mm

Design and process features of induction die heater:
Rigid steel construction with removable cover plates for easy maintenance
Fully insulated pneumatically operated lid
Fully enclosed system housing die support, induction coils, pneumatics, and cooling water distribution
Linear bearing system for accurate coil positioning
Numerous presettable heating recipes with automatic power-time adjustment
Facility to introduce inert gas to eliminate the possibility of oxidation

7

Induction Mass Heating

This chapter is devoted to a discussion of the use of induction heating principles for a large group of applications referred to as mass heating. This term applies to a variety of applications where metal is heated for forging, forming, extrusion, coating and the like. Typically it is required to heat the workpiece uniformly within its body. However, it is sometimes necessary to heat certain areas of the workpiece selectively and care must be taken to provide uniformity in the temperature distribution. Certain applications such as extrusion may require a nonuniform end-to-end temperature profile. All of the most typical applications of mass heating are discussed in this chapter.

7.1 APPLICATIONS, DESIGN APPROACHES AND FUNDAMENTAL PRINCIPLES OF INDUCTION MASS HEATING PRIOR TO METAL HOT WORKING

Temperature greatly affects the formability of metals. Heating of a component through to temperatures that correspond to the plastic deformation range creates a favorable condition for metal to be subsequently forced by various means into a desired shape. The most popular metal hot working processes for which induction mass heating is applied are as [279].

Forging: Billets or bars are heated fully or partially, either in cut lengths or continuously, and are forged in presses, hammers (repeated blows), or upsetters (which gather and form the metal). Steel components by far represent the majority of forged parts. At the same time, aluminum, copper, brass, bronze, cobalt, nickel, and titanium as well as some other metals and alloys are also inductively heated and forged for a number of commercial applications.

Forming: Hot forming includes a variety of metal working operations generally encompassing bending, expanding, and spinning. The versatility of induction heating is that it can selectively heat through specific areas of the workpiece or can heat areas to different temperatures providing required temperature gradients, making it a popular choice for hot forming operations.

Extrusion: Extruding is the process of forcing or squeezing metal through a die. Both ferrous and nonferrous metals are heated by induction prior to extrusion.

Rolling: Bars, billets, rods, slabs, blooms, strips, and sheets are processed in rolling mills. These components are made from ingots or continuous cast metals and their alloys.

The goal of using induction heating in all of the above-mentioned applications is to provide the metal workpiece at the hot working stage with the desired (typically uniform) temperature across its diameter/thickness as well as along its length and across its width (see Section 2.2.1).

The required heating temperature depends upon the metal and the specifics of the metal working process. Table 7.1 shows a list of commonly required

Table 7.1 Commonly Required Temperatures when Heating Selected Ferrous Alloys

Alloys	Temperature (°C)	Temperature (°F)
Nickel alloys	880–1230	1616–2246
Low-carbon steel	1100–1300	2012–2372
Medium- and high-carbon steel	1050–1220	1922–2228
Typical Forging Temperatures Plain Carbon Steels		
AISI 1010, 1015	1315	2400
AISI 1020, 1030	1288	2350
AISI 1040, 1050	1260	2300
AISI 1060	1182	2160
AISI 1070	1150	2100
AISI 1080	1204	2200
AISI 1095	1177	2150
Alloy Steels		
AISI 4130	1204	2200
AISI 4140	1232	2250
AISI 4320	1232	2250
AISI 4340	1288	2350
AISI 4615	1204	2200
AISI 5160	1204	2200
AISI 6150	1204	2200
AISI 8620	1232	2250
AISI 9310	1232	2250

temperatures for selected ferrous metals and alloys prior to hot working [17, 279, 431]. Commonly required temperatures for selected nonferrous metals are shown in Table 7.2.

In some cases, the initial temperature of the product prior to induction heating is the ambient temperature. In other cases, the initial temperature is nonuniform, for example, due to uneven cooling of the slab, transfer bar, strip, or bloom as it progresses from the caster. Surface layers, and particularly the edge areas, become much cooler than the internal regions.

In the past, fuel-fired furnaces that utilized natural gas, fuel oil, or liquid petroleum gases were often used because of the low cost of fuel. However, in recent decades producers are shifting their preference toward induction heating systems and this tendency continues to grow at an increasing pace. There are several reasons for this shift.

First, fuel-fired furnaces demand a very long heating tunnel to achieve the desired temperature uniformity. The large required space often presents a problem in plants due to the limited space available on the shop floor, particularly when it is required to incorporate the heating system into an already existing production line. For example, it is frequently required to locate a slab or transfer a bar edge reheater into the limited space between an existing caster and rolling mill.

On the other hand, heating in fuel-fired furnaces results in a significant metal loss and poor surface quality (due to scale formation, decarburization, oxidation, coarse grains, etc.). Scale reduction and improved surface quality of heated parts leads to longer die life and minimum postprocessing operations.

Finally, fuel-fired heating increasingly faces environmental restrictions (air pollution) and restrictions from an ergonomic perspective because operators are exposed to hot air blasts and unstable work flow.

These are only some of factors that have resulted in induction heating becoming a more popular approach for through heating of slabs, blooms, billets, bars, tubes, strips, wires, rods, and other components made of both ferrous and nonferrous metals.

Induction mass heating applications are typically more power demanding and time consuming than induction heat treating. The power ratings of induction heating machines range from less than one hundred kilowatts up to dozens of megawatts. The success of an induction mass heating system is based on an in-depth under-

Table 7.2 Commonly Required Temperatures when Heating Selected Nonferrous Alloys

Alloys	Temperature (°C)	Temperature (°F)
Aluminum alloys	360–560	680–1040
Copper alloys	680–960	1256–1760
Titanium alloys	830–1070	1526–1958
Magnesium alloys	320–380	608–716
Stainless steel (2xx and 3xx)	1100–1250	2012–2282
Tungsten	about 1350	about 2462

standing of the process features. This is imperative for developing the sophisticated design concepts and precise engineering that lead to the achievement of a reasonable commercially acceptable compromise among often contradictory process requirements and design criteria [50, 251, 255, 256, 261, 268, 270]. The most important features dealing with electromagnetic and thermal phenomena are discussed in respective sections of this chapter where a certain feature has a critical impact.

Cylindrical and rectangular solenoid (helical) multiturn induction coils are most often used in induction mass heating applications.

The four basic heating modes in induction mass heating (Figure 7.1) are as follows [279].

Static heating: In the static heating mode the component (workpiece) such as a billet or slab is placed into an induction heating coil for a given period of time while a set amount of power is applied until the component reaches the desired heating conditions. Upon reaching the required thermal conditions, the heated component is extracted from the induction heater and delivered to the metal forming station. The next cold workpiece is loaded into the coil and the process repeats.

Progressive multistage heating: This heating mode occurs when two or more heated workpieces (e.g., billets) are moved (via pusher, indexing mechanism, walking beam, etc.) through a single coil or multicoil induction heater. Therefore, components or their different parts are sequentially

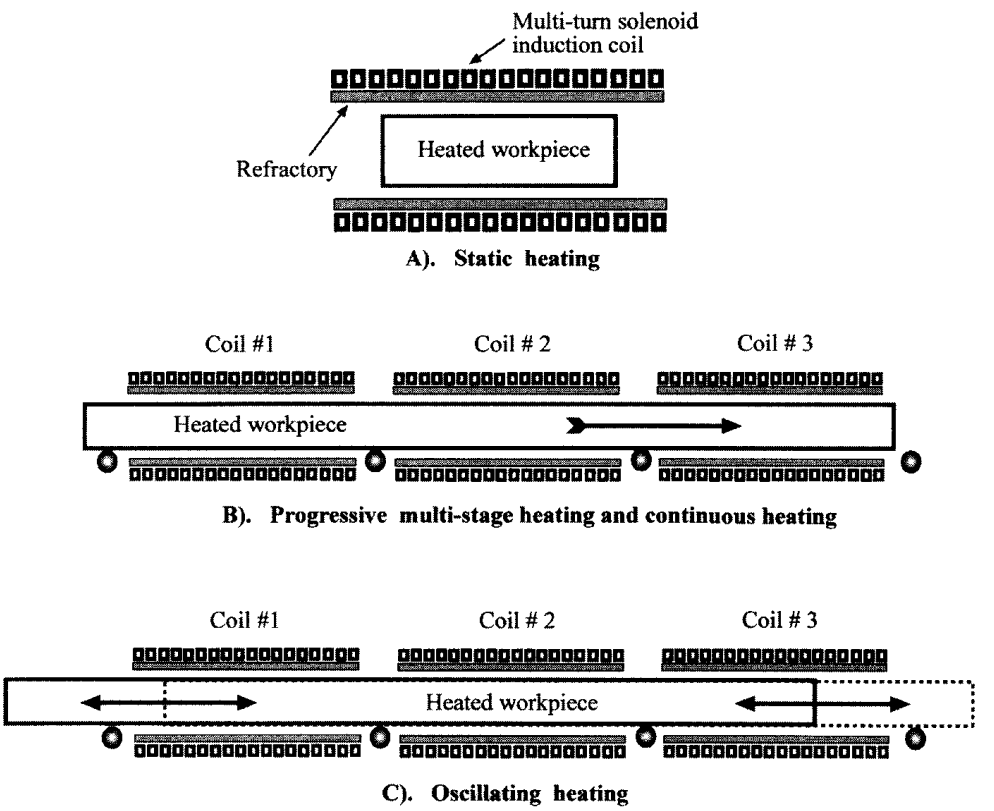

Figure 7.1 Four basic heating modes used in induction mass heating.

heated (in a progressive manner) at certain predetermined heating stages inside the heater.

Continuous heating: With the continuous heating mode the workpiece is moved in a continuous motion through one or more induction heating coils. This heating mode is commonly used when it is required to heat long components such as bars, slabs, strips, tubes, wires, blooms, and rods.

Oscillating heating: In this heating mode a component moves back and forth (oscillates) during the process of heating inside a single coil or multicoil induction heater with an oscillating stroke featuring a space-saving design approach.

When designing modern induction mass heating systems, temperature uniformity of the heated component is only one of the goals. Additional design criteria include maximum production rate, minimum metal losses, and the ability to provide flexible and compact systems that have high electrical efficiency. Other important factors include quality assurance, process repeatability, automation capability, environmental friendliness, reliability, and maintainability of the equipment. The last criteria, but not the least, is the competitive cost of an induction heating system.

One of the challenges in induction heating arises from the necessity to provide the required surface-to-core temperature uniformity. Due to the physics of the process, the workpiece core tends to be heated more slowly than its surface. The main reason for the heat deficit in the core of the heated component is the skin effect that has been discussed in detail in Section 3.1.2. It is assumed that the reader is familiar with the materials presented there.

As discussed in Section 3.1.2, the skin effect depends upon the metal properties and frequency of the induction heating power. Due to this effect, 86% of the power is induced within the surface layer ("skin" layer), which is called the current penetration depth and can be calculated according to Eqs. (3.6) and (3.7). Current penetration depths of nonmagnetic metals and carbon steels versus frequency and temperature are shown in Tables 3.4 and 3.5 (Chapter 3).

According to the skin effect, the induced current decreases from the surface towards the internal area of the heated body. The core heats due to thermal conductivity. The nature of the heat transfer phenomena and a description of its three modes (thermal conduction, convection, and radiation) were discussed in Sec. 3.2.2).

It has been pointed out that in induction mass heating, the heat transfer by convection and radiation reflects the value of surface heat loss. This heat loss varies with temperature. The analysis shows that convection losses are the major part of the heat loss in low-temperature applications such as induction heating of tin, lead, and aluminum alloys. In hot working applications (including induction heating of steel, titanium, and nickel), radiation losses are much greater than convection losses (Figure 3.42) representing the major portion of total heat loss from the workpiece surface. Section 3.2.2 provides a means of estimating the surface heat losses.

It is typically much easier to provide surface-to-core temperature uniformity for metals with high thermal conductivity such as aluminum, silver, or copper. Metals with poor thermal conductivity, including stainless steel, titanium, and carbon steel require extra care in order to obtain the desired temperature uniformity. This "extra care" includes proper selection of heat mode, frequency choice, process time, and other parameters.

Figure 7.2 shows the typical time–temperature curve for static induction heating of a nonmagnetic solid cylinder. As one can see, immediately after heating begins, the surface temperature and average temperature begin to rise. In contrast, there is a delay before the core temperature starts to grow. If the material properties vary according to a linear function with temperature and surface heat losses are absent, there will be a linear region where all three temperatures are represented by three straight lines (Figure 7.2, solid lines). The surface-to-core temperature difference in this area is proportional to the power density during the heating cycle, the frequency, geometry, and material properties of the heated component.

As soon as power is cut off, the surface temperature decays rapidly due to heat transfer toward a cooler core and there is a corresponding rise in the core temperature. It is during the soaking stage that the surface-to-core differential decreases and the heated component approaches the temperature uniformity that is required for hot working.

In reality, the surface-to-core temperature differential starts to decrease before the soaking stage begins. This temperature differential starts to decline during the heating stage (Figure 7.2, dotted curve representing surface temperature). This takes place due to the increasing surface heat loss with temperature and the depth of induction heating during the heating cycle. Because the electrical resistivity of most metals increases with temperature, there is an increase of the current penetration depth.

It is important to note that the soaking stage can be performed when the heated workpiece is inside the induction coil and/or during the workpiece transfer stage to the hot forming machinery. The latter approach allows minimizing the total process time.

It should be mentioned that the time–temperature profiles are more cumbersome than those shown in Figure 7.2. In order to improve the performance of an induction heating machine and reduce the heating time while providing the required

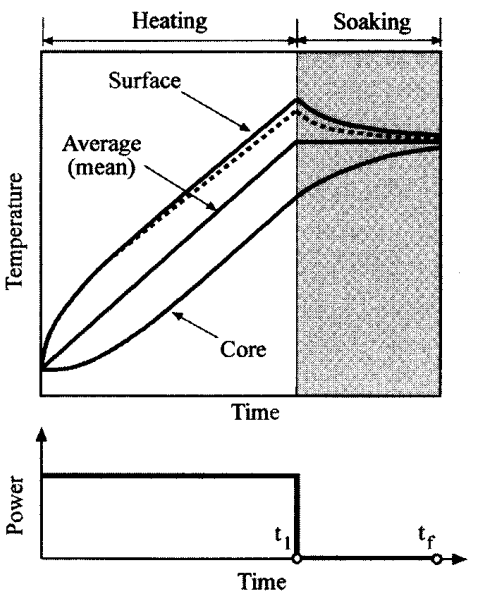

Figure 7.2 Time–temperature profile during static heating of a nonmagnetic solid cylinder.

surface-to-core temperature uniformity, power pulsing can be applied. Power pulsing refers to a technique that applies short bursts of power to maintain a desired surface temperature or a maximum allowable surface-to-core temperature difference. Pulse heating consists of a series of "Heat ON" and "Heat OFF" cycles until the desired uniformity is obtained (Figure 7.3). Depending upon the particular application, the process time reduction with pulse heating can exceed 40%.

The heating time can be reduced even more when applying accelerated heating (Figure 7.4). Obviously, in order to provide this type of heating it is necessary to have a power supply that allows a gradual reduction of output power. The features of modern power supplies, aspects of their load matching, principles of process control, and monitoring are discussed in detail in Chapter 8.

The accelerated heating approach may have several modifications. Figure 7.5 shows one of the modifications of accelerated heating that is particularly useful when heated bars, slabs, or billets have a tendency to crack. Longitudinal and transverse cracks may be a concern when heating irons and high-carbon steels. These cracks appear due to excessive thermal stresses (thermal shocks) that appear when thermal gradients exceed the maximum permissible levels. These levels vary depending upon the metal chemical composition, microstructure, and temperature.

Although it has been mentioned above that the curves shown in Figures 7.2 through 7.5 illustrate typical time–temperature profiles that take place during static heating, these curves are practically identical for progressive multistage heating and continuous heating modes as well. For multistage or continuous heating, the time axis represents the length of the induction heating line or coil length. Bursts of power can represent the power of inline coils that may have different lengths, windings, and/or can be individually fed from different power supplies with the ability to adjust the output power and frequency.

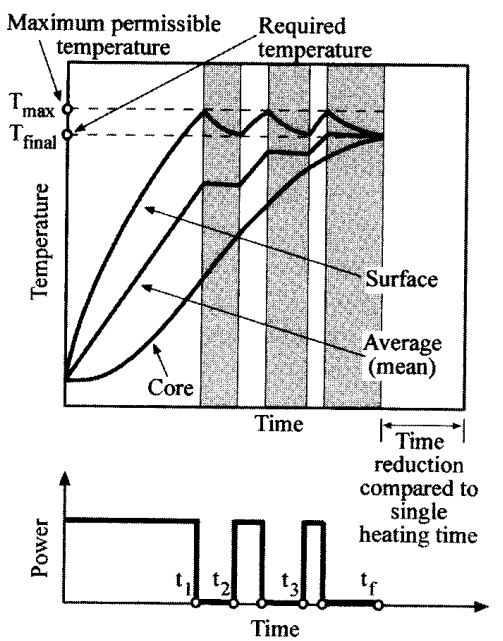

Figure 7.3 Power pulsing.

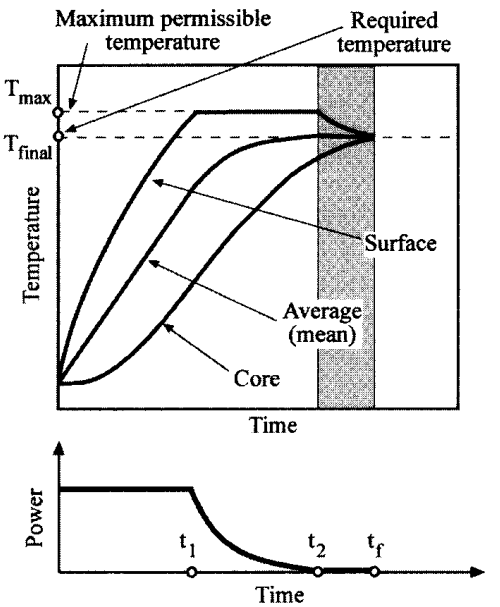

Figure 7.4 Accelerated heating.

The selection of power, frequency, and coil length in induction mass heating applications is highly subjective, depending upon the type of heated metal, required temperature uniformity, time of heating, and so on. Frequency is one of the most critical parameters in these applications. If the frequency is too low an eddy current cancellation within the heated body will take place resulting in poor coil efficiency.

However, when the frequency is too high, the skin effect will be highly pronounced resulting in a current concentration in a very fine surface layer compared to

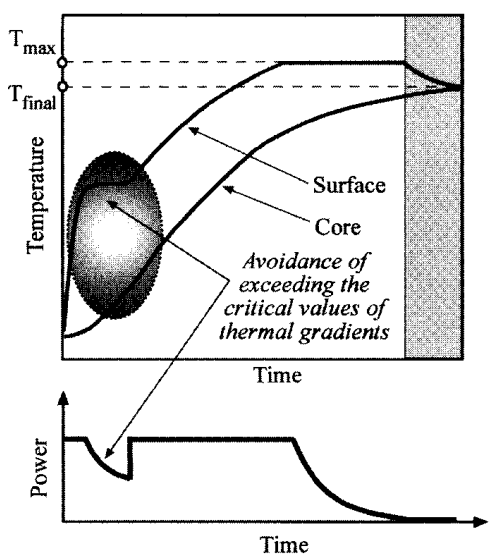

Figure 7.5 Modification of accelerated heating.

the diameter/thickness of the heated component. In this case, a long heating time will be required in order to provide sufficient heating of the internal areas and the core. Prolonged heat time results in an increase of the radiation and convection heat losses that, in turn, reduce the thermal efficiency of the induction heater and diminish the main advantage of induction heating. Frequency is always a reasonable compromise.

In the following sections several tables are introduced consisting of the minimum diameter/thickness of the selected metals versus frequency and temperature for efficient induction heating. As a rule of thumb, when heating solid cylinders, current cancellation will not take place if the ratio of workpiece diameter to current penetration depth is greater than four.

The determination of the length of the coil line is another important step in specifying an induction heating system. In determining how long the coil line needs to be, the time required for heating the workpiece to an acceptable temperature condition is actually being determined. Heating time is a complex function of various factors including the size of the workpiece, frequency, heating mode, power density, maximum permissible temperature, material properties, and the required surface-to-core temperature uniformity.

Numerical computation (e.g., using ADVANCE software and some other numerical codes) can be very helpful in conducting an accurate estimation of the coil length as well as other important coil design parameters. The procedure for rough estimation of the required power was discussed in Section 3.3.1.

A ballpark number for determining the minimum heat time and coil length when heating carbon steel cylinders from ambient temperature to temperatures in the forging range can be obtained using the following empirical formulas [279].

$$\text{Minimum heat time} = 25 \times D^2 \tag{7.1}$$

$$\text{Minimum coil length} = 0.03 \times (\text{lbs/hr}) \tag{7.2}$$

where D is the diameter of the solid cylinder (in inches), time measured in seconds, and coil length measured in inches.

Coil design is of course an extremely important factor in developing an efficient induction heating system. As mentioned earlier, solenoid-type (helical) multiturn coils are most often used in induction mass heating applications.

The electrical efficiency and coil coupling discussed in Section 3.3.1 have a marked effect on the coil's ability to deliver heating power to the workpiece. Smaller gaps between the surface of the heated workpiece and the coil result in better electromagnetic coupling and, consequently, higher coil efficiency. However, it is wise to remember that according to Eq. (3.29), the total efficiency of the induction coil is a product of both coil electrical efficiency and coil thermal efficiency.

Nearly all through heating induction coils consist of thermal insulation (also called refractory or liners) between the coil and the heated workpiece protecting the coil windings from heat exposure and providing a thermal barrier, thus reducing the chance of thermal shock and minimizing heat loss in water recirculating through the induction coil.

The thermal refractory can drastically decrease the heat losses from the surface of the heated workpiece. At the same time, the use of a refractory necessitates larger coil-to-workpiece gaps, which in turn deteriorates the electromagnetic coupling between the induction coil and the heated workpiece, leading to a reduction of

coil electrical efficiency (Figure 3.44). Thus the refractory allows one to improve coil thermal efficiency, but it also reduces coil electrical efficiency. In the great majority of mass heating applications and, in particular, in heating prior to hot working, it is advantageous to use a refractory. Its minimum thickness is usually about 12 mm (0.5 in.).

Different materials can be used for manufacturing refractory. These include castable (i.e., Visil), silicon carbide, Alumina, H-91, Zircar, and other fibrous ceramic materials.

There are two principal approaches to building coils that can be categorized as the open-wound or refractory-encased approach [425]. The open-wound method provides more convenient repair in the event of failure but the choice is never that simple.

Replaceable refractory liners are commonly utilized in the construction of open-wound coils (Figure 7.6). Coils with replaceable liners have lower repair time and cost compared to cast coils.

Although the encased-coil using a castable refractory offers durability and longer life it still follows recommended maintenance routines that should not be neglected. To repair a cast coil it must be shipped to a service center where it is broken down to the bare coil. Then the coil must be repaired, reinsulated, and recast. This process is time consuming considering that the operator can replace refractory liners on site in a matter of minutes [430].

Self-supporting internal water-cooled skid rails to protect the liner surfaces must be robust enough to carry the full load of heated billets with minimal deflection but from another perspective should be transparent enough to the electromagnetic field that they will not be significantly heated. Water-cooled rails occupy space inside the coil and consume additional coolant increasing the kilowatt losses. These rails terminate beyond the open-wound coil box envelope and extra expansion of longer rails must be accommodated.

In order to extend the life of water-cooled rails, they are wear coated. In the past, stellite was applied to the surface of the rails as a wear coating. This required an application process that works by fusing this material to the surface of the rail by heating with an oxygen acetylene torch. By replacing this with a less labor-intensive

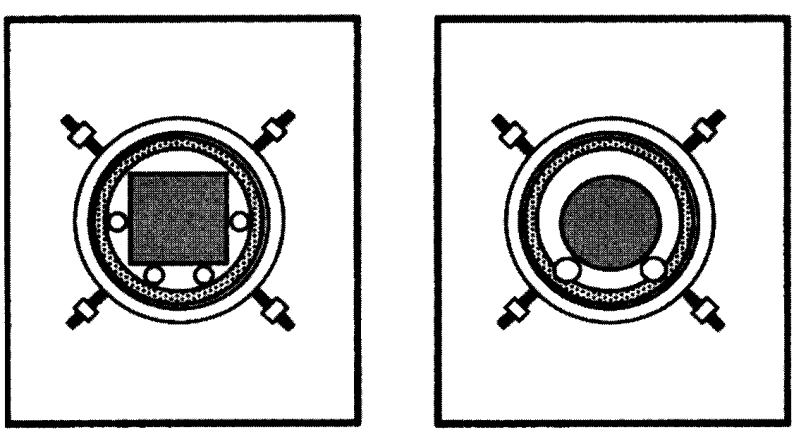

Figure 7.6 Open-wound type coil (side view).

plasma coating process, it is possible to apply a wider variety of materials, including tungsten carbide, stellite, and chrome carbide providing longer rail life.

In addition to water-cooled alloy skid rails, various ceramic materials have been developed for use as wear plates. Ceramic liners are embedded into the refractory surface and have been successful in many applications. For high wear/high-temperature applications the liners are manufactured from special alloys. In addition to improved alloys, new tubing may be provided with an extra heavy wall section that affords a much thicker wear area comparable to welding an additional layer of material to the top side of the water-cooled rail. These rails also utilize a plasma-applied wear coating on the surface to afford additional wear resistance and longer life [425, 430].

In applications where refractory liners are made from materials with extremely high wear-resistant properties, some end users actually skid or convey the billets across the surface of the ceramic liner thus eliminating the use of skid rails and any cold spots resulting from their use.

Most manufactured liners are round. For cylindrical billets a round-shaped liner naturally suits the coil geometry. However, when heating square billets this mismatch of shapes may result in a noticeable increase of the coil opening in addition to space allowances for the skid rails and thermal insulation. This reduces the electromagnetic coupling between the coil and billet. Longer coils call for a larger thickness of the refractory to ensure mechanical strength.

In order to optimize the design, the manufacturers of induction heating systems have developed different procedures. For example, Newelco windings are plastic coated for insulation purposes before being set in a high-quality refractory cement. After the winding is positioned in a carefully prepared and assembled box, a former is centrally inserted through it to create the coil tunnel. The refractory is poured around the winding in such manner that air pockets are eliminated, after which the refractory is aged following controlled procedures. The profile of the former is such that recesses along its length allow for small bore skid rails to be positioned prior to casting. Rails being half-sunken into the refractory directly take the load of the material being carried [425, 438].

The end boards of the coil boxes are carefully recessed to enable the rails to be terminated within the total envelope so these coil units can be shorter and butted against each other. Gaps between individual coil units manufactured by Newelco are designed to be only 12 mm. This ensures sufficient latitude for changing from one unit to another while avoiding the larger energy-sapping gaps inevitable with open-wound coils. It also follows that minimal gaps and closeness of the tunnel walls to the billet decrease atmospheric attack and hence scale generation.

Sufficient radial clearance has to be allowed for the largest size heated workpiece, taking into consideration the existence of the skid rails, the thermal expansion of the workpiece that is being heated, and its actual shape, because some workpieces can bow (i.e., long bars, rods, and slabs).

The coil space factor K_{space} is an important parameter of the coil design and should be as high as possible. The coil space factor represents how tightly the coil turns are wound. The space between turns should be as small as possible yet large enough to leave room for electrical insulation. The coil turn space factor for a multiturn coil can be determined according to Figure 3.33 and is typically in the range of 0.7 to 0.9.

High-conductivity round and square copper tubing known as oxygen-free high-conductivity copper (OFHC) is commonly used for coil fabrication because it is naturally profiled for water-cooling and because copper is a good electrical conductor having mechanical properties suited for coil fabrication. In some rare cases, copper tubing does not provide a large enough area for energy transfer. To compensate for tube constraints, a thick copper strip is sometimes brazed to the external water-cooling copper tube.

Coil windings are designed to accommodate the tube size, coil geometry, number of turns, and overall length with the workpiece size, shape, production rate, and load-matching with the power supply.

Coil cooling is a very important aspect of induction heater design. It is obvious that coil cooling should be as close as possible to the heating face. Tube wall thickness is chosen based on the system operating frequency. The heating face wall thickness should increase as the frequency decreases. For example, a system with low operating frequency requires a thicker wall tube than a high-frequency system. This fact is directly related to the current penetration depth in the copper (δ_1) and holds true for both tubing coils and coils made from copper sheet. The coil electrical losses will be minimum if the copper tubing wall thickness is greater than $1.6\delta_1$. A coil tubing wall smaller than $1.6\delta_1$ results in a reduction in coil efficiency and an increase of coil tubing power losses.

In some cases the tubing wall may be thicker than that calculated according to the above-mentioned procedure. This is because it may not be mechanically reliable to use too-thin wall tubing due to the mechanical flexing caused by electromagnetic forces. As the frequency is lowered, more attention must be paid to coil support as there is more vibration at lower frequencies, especially at the turns near both ends of multiturn solenoid coils.

The procedure for water-cooling calculations is similar to that discussed in Chapter 5.

High-dielectric epoxies and some nylons are often used as dielectric insulating materials that eliminate arcing between coil windings. A fluidized bed process or an electrostatic coating process can provide dielectric insulation. In certain cases, some ceramic coatings afford both protection from high-temperature exposure and suitable dielectric strengths.

7.2 IN-LINE INDUCTION HEATING OF LONG CYLINDRICAL BARS AND RODS

7.2.1 Electrothermal Nature of Inline Induction Heating

Modern techniques for producing long products such as cylindrical and rectangular shaped bars and rods integrate three stages of production: casting, reheating, and rolling into a continuous line [119, 169, 251, 256, 268].

Depending upon the process parameters, an induction bar/rod heating system may consist of one or several inline induction coils (Figure 7.7). The challenge with inline induction heating arises from the fact that the surface-to-core temperature profile continues to change as the bar passes through the line of induction coils. Due to the skin effect, the bar core tends to be heated slower than its surface. At the

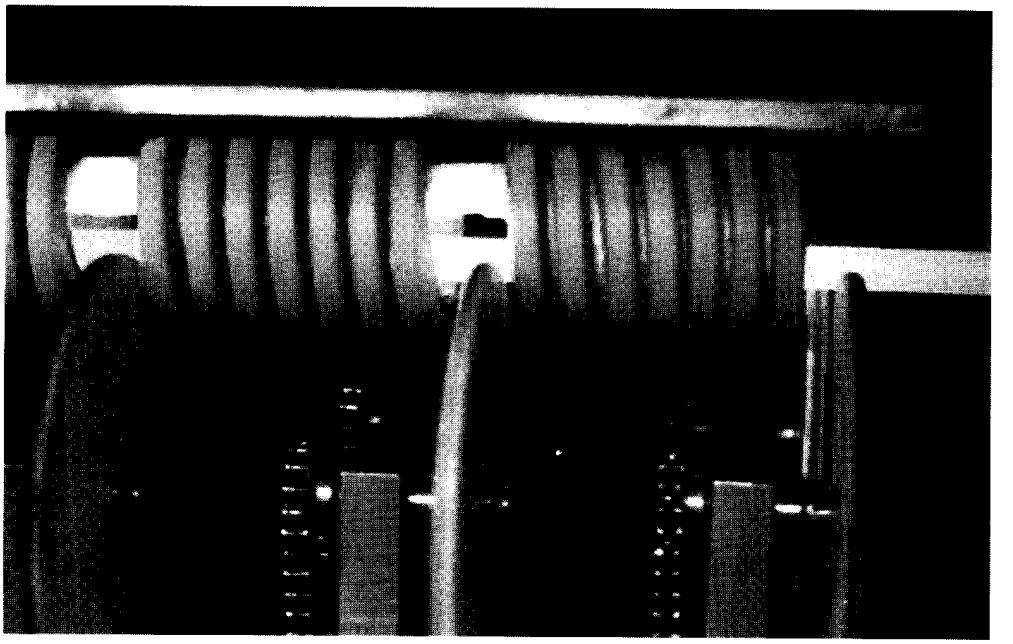

Figure 7.7 Depleted uranium rod heating using an inline multicoil induction heater. (Courtesy of Inductoheat–I.H.S. Corp., Fort Worth, TX.)

same time, the leading and trailing ends have a tendency to heat faster than the body of the bar (see Appendix H).

Experience gained on previous jobs and the ability to provide accurate mathematical modeling of the process serve as a comfort factor when designing new inline induction heating systems.

By combining advanced software with a sophisticated engineering background, modern induction heating specialists possess the unique ability to analyze in a few hours, complex technological problems that could take days or even weeks to solve trying to set experiments or physical modeling using the pilot models. Numerical computation methods (see Section 3.4.3) allow manufacturers of induction equipment to determine comprehensive details of the process that would be extremely difficult, if not impossible, to determine experimentally.

As an example, Figure 7.8 shows the results of the transitional and final heating conditions of a 76 mm (3 in.) diameter carbon steel bar and its surface-to-core temperature profile along the induction line. Coil parameters are: ID is 152 mm (6 in.); refractory thickness is 12 mm (0.5 in.); coil length is 1 m (40 in.); number of coils is 8; gap between coils is 0.3 m (12 in.), frequency is 1 kHz; and production rate is 65 mm/sec (2.56 in./sec).

At the first stage the entire bar is magnetic and the skin effect is pronounced. All power induced in the bar appears in the fine surface layer which typically doesn't exceed 6 mm (0.25 in.) for frequencies 500 Hz and up. Thanks to the relatively low temperature at this stage, the surface heat losses due to radiation and convection are relatively low. Both factors lead to a rapid increase in temperature at the surface with practically no change at the core. Intensive surface heating results in a significant surface-to-core temperature gradient.

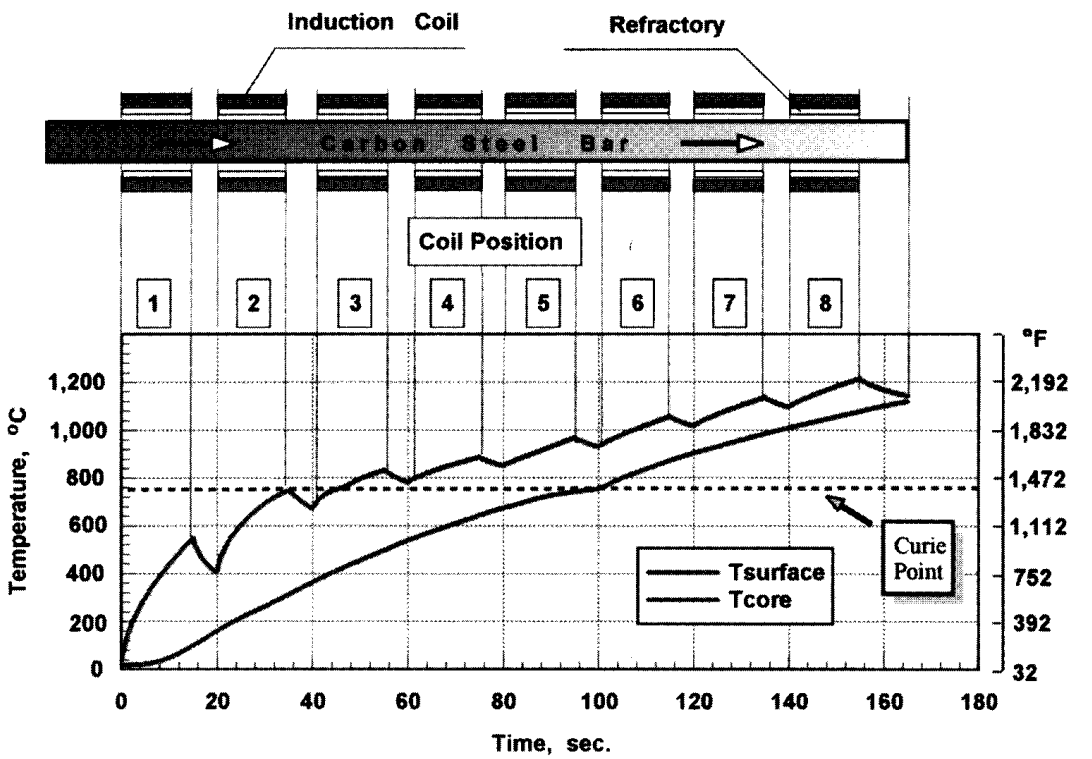

Figure 7.8 Inline induction bar heating.

Figure 7.9 shows a typical temperature profile and power density (heat source) distribution along the radius of the bar after exiting Coil #1 (scales of power density profiles are different for various coil positions). The temperature profile does not match the heat source profile because of thermal conductivity, which spreads the heat from the surface toward the core.

During the first heating stage, the coil efficiency is quite high (typically +80%) and continuously rising due to an increase in steel electrical resistivity with the temperature (Figure 3.2). Because the surface temperature is still below the Curie point, the magnetic permeability remains high and its slight reduction does not affect the climb in electrical efficiency. After a short time, the coil efficiency reaches its maximum value and the efficiency starts to decline.

The second stage takes place when the surface temperature passes the Curie point (i.e., after exiting Coil #3, Figure 7.9) and the intensity of heating noticeably decreases. This takes place primarily due to the following reasons.

- The surface of the carbon steel bar loses its magnetic properties and the relative magnetic permeability drops to 1. As a result, the power density induced within the bar will also decrease.
- The specific heat has its maximum value (a peak) near the Curie point (see section 3.2). The value of the specific heat denotes the amount of energy that must be absorbed by the metal to achieve the required temperature.

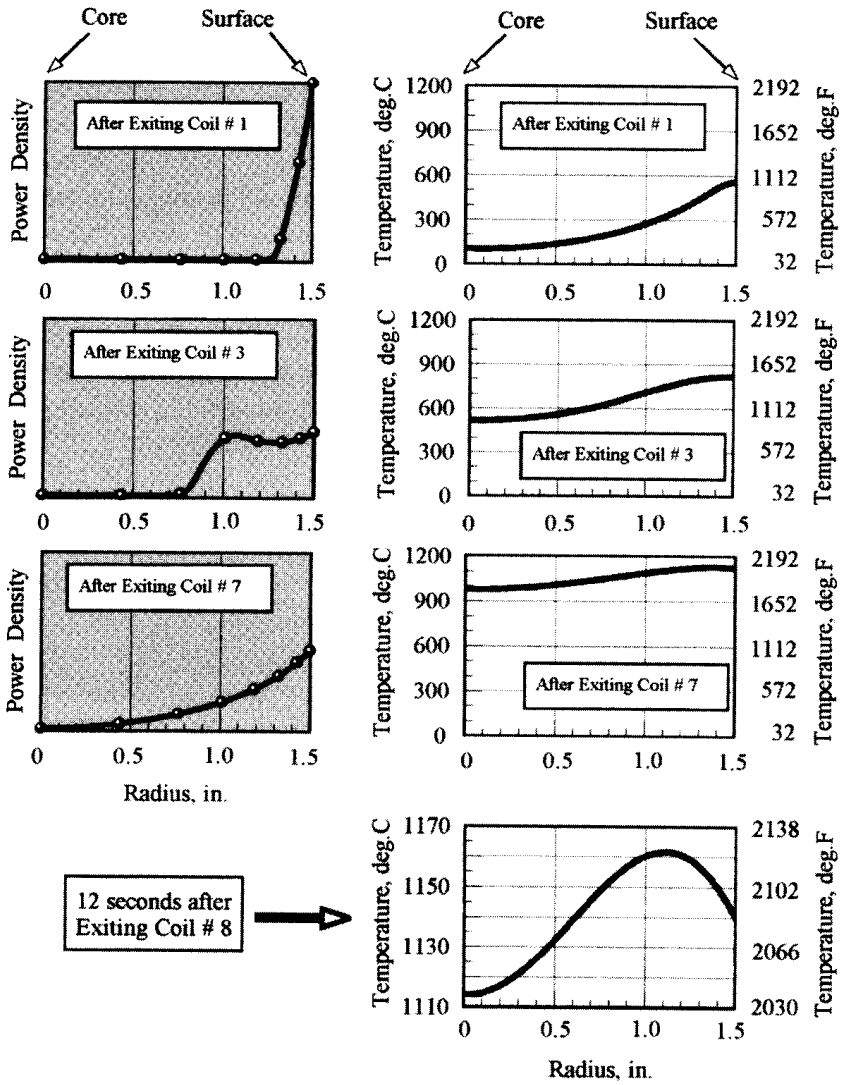

Figure 7.9 Power density and temperature profiles at different positions of the bar in an inline induction heater.

At this stage, the electrical resistivity of the carbon steel increases approximately two or three times compared to its value in the initial stage. At the same time, the decrease in magnetic permeability is much more pronounced (30 times or more). Both factors cause an increase of current penetration depth of 6 to 12 times. A significant portion of the power is now induced in the internal layers of the bar. The bar surface becomes nonmagnetic while the internal layers retain their magnetic properties. The second stage exists as long as the thickness of the nonmagnetic layer is less than the penetration depth in hot steel.

The induced eddy current and power density distribution along the radius of the bar have a unique wave-shaped form. Because of its complexity, this wave-shaped phenomenon is typically overlooked and is not discussed in most publications devoted to induction heating. The phenomenon can be analyzed only by applying sophisticated computer software. Figure 7.9 shows that after exiting Coil #3, the

greatest power density is located at the surface. Then the power density decreases toward the core. However, once it reaches a certain distance from the surface, the power density starts to increase again, due to the remaining magnetic properties of the steel below the surface. The nature of this phenomenon has been discussed in detail in Section 5.1.2.1.

Finally, the thickness of the surface layer with nonmagnetic properties exceeds the penetration depth in hot steel and the wave-shaped distribution of induced power will finally disappear. The power density will then have its classical exponential distribution (i.e., after exiting Coil #7, Figure 7.9).

Implementation of advanced numerical software allows the designer to optimize the process parameters and build a competitive edge inline induction heater similar to those shown in Figure 7.10.

7.2.2 Longitudinal and Transverse Cracks

Longitudinal and transverse cracks are often a concern when designing induction systems for heating steel bars with high carbon content (i.e., carbon steel of 0.6% C and higher). These cracks appear due to thermal stresses (thermal shocks) and poor thermal conductivity of high-carbon steels. Thermal stresses are caused by different magnitudes of temperature and temperature gradients [255, 256, 439].

Experience shows that most of these cracks take place during the initial heating stage, when the internal areas of the bar have a nonplastic condition. A "soft" start is required to avoid the appearance of cracking. The ability to accurately predict surface-

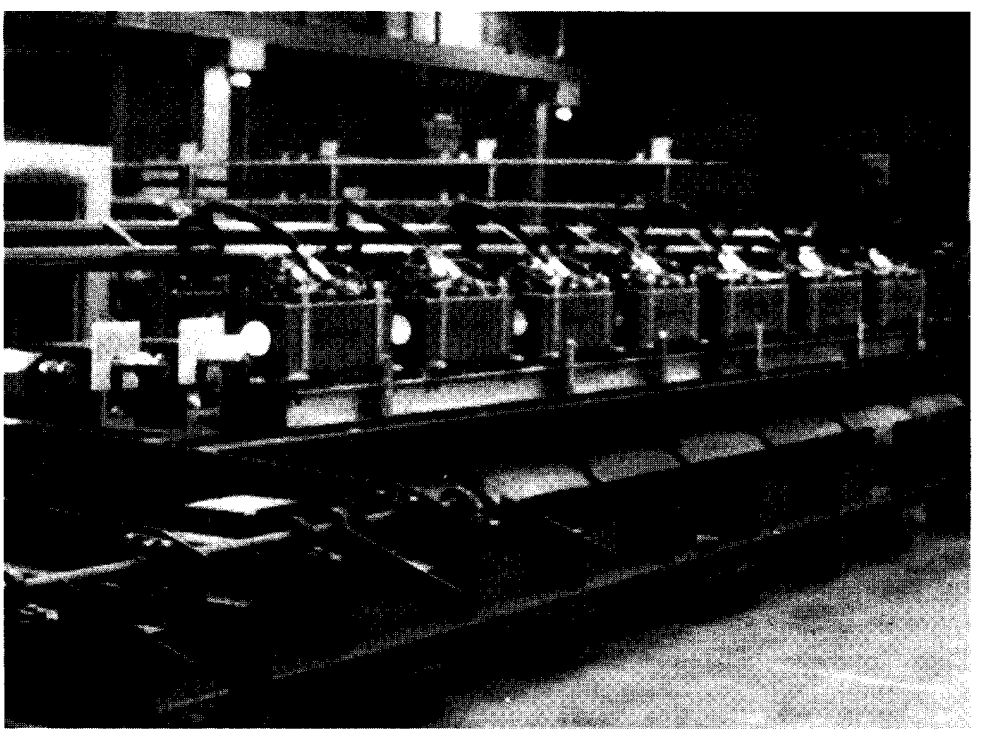

Figure 7.10 Inline induction steel bar heater. (Courtesy of INDUCTOHEAT, Inc., Madison Heights, MI.)

to-core temperature gradients at different heating stages allows the manufacturer to choose appropriate design parameters and eliminate dangerous temperature gradients that might result in crack development. At the same time, the ability to predict the temperature profiles along the induction line allows one to avoid surface overheating and minimize the duration of high-temperature at the bar surface. This leads to the reduction of metal loss due to scale, oxidation, burns, and decarburization.

7.2.3 Transient Processes and Nose-to-Tail Temperature Profiles

As mentioned earlier, surface-to-core is only one component of the thermal conditions specified by the customer. Another component is the "nose-to-tail" temperature profile. Transient processes that take place in continuous-type induction bar heaters are primarily responsible for the appearance of nose-to-tail temperature nonuniformity [50, 120, 169, 171, 198, 255, 256]. Transient processes include startup and shutdown states. Let's consider as an example, the shutdown process that takes place when the last bar or rod continuously moves through the induction heater. In this case, the transient end effect appears.

Figure 7.11 shows the power density distribution along the length of the stainless steel bar (OD = 76 mm/3 in.) for different positions of its end inside the induction coil (ID = 152 mm/6 in.; coil length = 280 mm/11 in.; frequency = 5 kHz) while the voltage of the inductor is constant. The dotted curve corresponds to the extreme values of the specific power density in the end zone of the bar. It is obvious that the end zone will be overheated compared to regular areas.

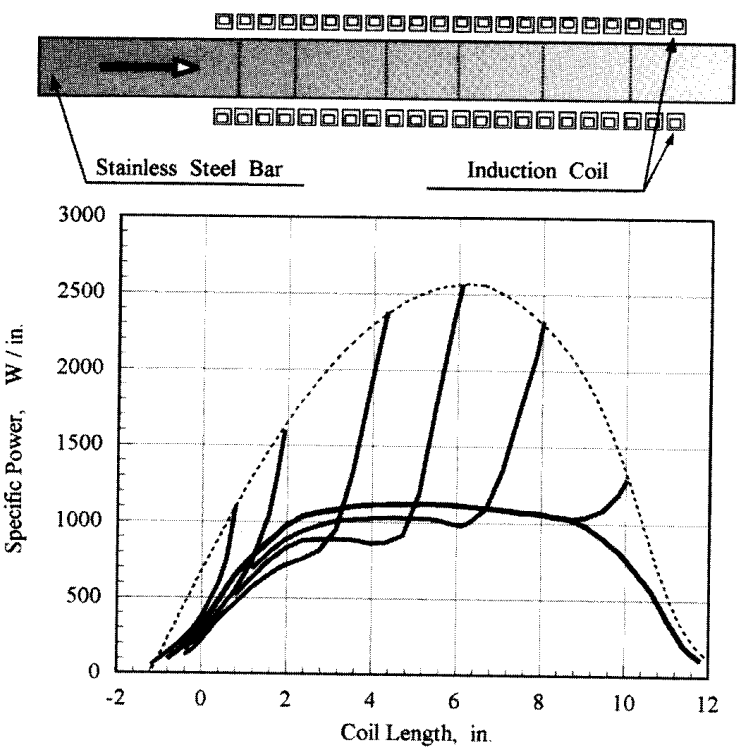

Figure 7.11 Distribution of a specific power density along the length of a stainless steel bar at different positions inside the induction coil (transient state).

With increasing frequency and/or power density, the surplus of the heat sources induced within the billet end area will increase as well. It should be mentioned here that the power density distribution and temperature distribution along the bar end effect area are not the same. Due to the additional heat losses from the bar end and the soaking action of thermal conductivity, the longitudinal temperature nonuniformity will not be as marked as the nonuniformity of the power density. Figure 7.12 shows the temperature profiles resulting from a transient end effect during inline induction heating of titanium bars of diameter of 25.4 mm (1 in.) traveling at a speed of 50.8 mm/sec (2 in./sec) using a frequency of 30 kHz.

As one might expect, due to the transient end effect and depending upon material properties and process parameters, the end of the bar can be not only overheated but underheated as well. For example, when heating a magnetic bar, the maximum temperature can occur at a distance of 40 mm (1.5 in.) to 75 mm (3 in.) from the buttend of the bar. Examples of transient end effect in the bar leading end zone when heating selected metals are in Appendix H.

The transient end effect in the bar end zone is similar to the end effect during a static heating (Section 3.1.7); however, there are several features that make this process unique and must be taken into account when designing contemporary induction heating equipment. One of the main features deals with the variation of coil current (in the case of constant coil voltage) or coil voltage (in the case of constant coil current) or both (in the case of constant or regulated coil power) when the leading end of the first bar or trailing end of the last bar moves through the induction coil.

In addition to the transient electromagnetic end effect there is a transient thermal effect that takes place when the leading end of the first bar moves through the inductor. During the startup process the transient thermal effect occurs due to a fluctuating temperature of the refractory. The startup process begins with a cold refractory (or in the case of an intermediate start, the refractory is partially heated). This results in increased heat losses from the bar surface due to radiation and convection and requires a special control algorithm that provides extra coil power to compensate for these losses.

It is imperative to recognize that in addition to the temperature nonuniformity that occurs in the areas of the leading end of the first bar and trailing end of the last bar, there might be other situations that would result in the appearance of nose-to-tail temperature nonuniformity.

When bars travel end-to-end through an induction heating line the nose-to-tail temperature uniformity is not a problem. However, there is often a 0.1 m (4 in.) to 0.25 m (10 in.) or larger air gap between the leading and following bars. The existence of these air gaps could result in a noticeable temperature nonuniformity along the length of the bar as well.

Obtaining the required temperature distribution along the length of long products that travel one after the other with a certain air gap requires the ability to manage the electromagnetic end effects of two bars placed inside an induction coil of finite length.

Figure 7.13 shows a sketch of the power density distribution along the bar length when two bars are located in the middle of a multiturn inductor.

In the case of nonmagnetic metals (i.e., certain stainless steels, titanium, or carbon steels heated above the Curie point), there is typically a surplus of induced

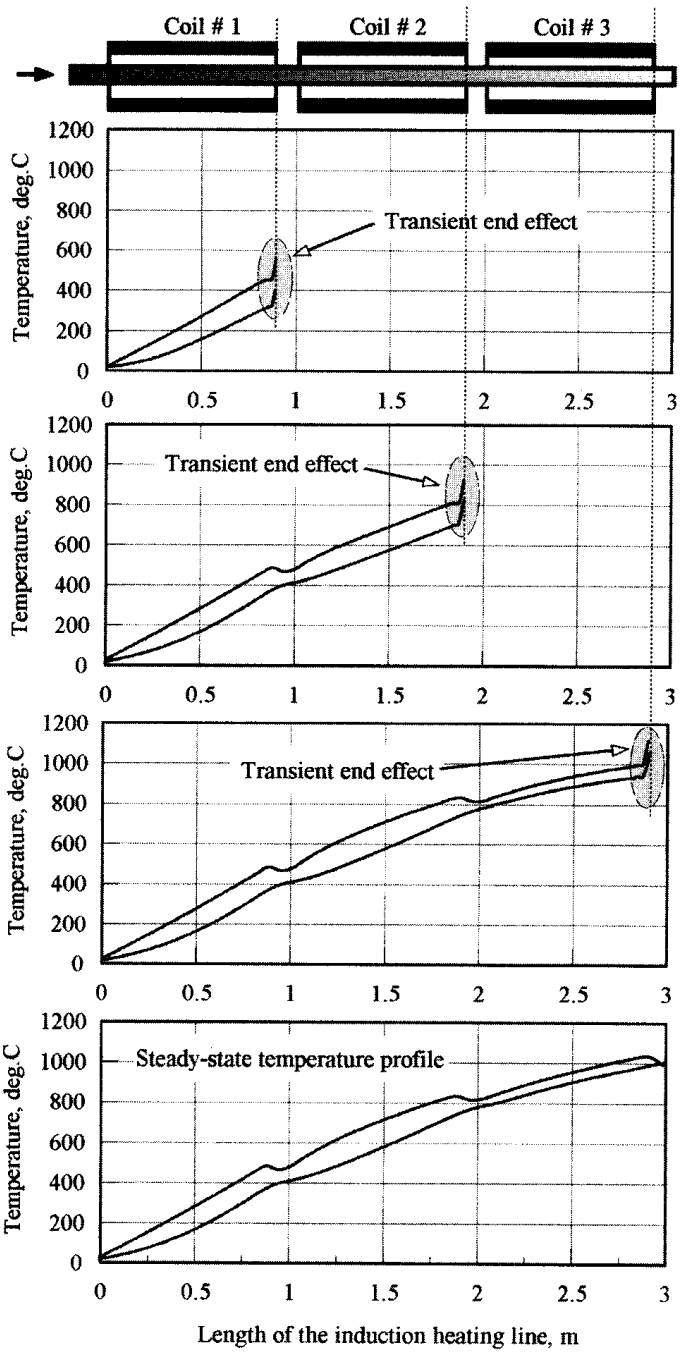

Figure 7.12 Inline induction heating of titanium bar with diameter of 25.4 mm (1 in.) using frequency of 30 kHz at 50.8 mm/sec (2 in./sec).

power in the bar end area. This power surplus depends upon the air gap, frequency, power density, electrical resistivity of the metal coil/bar geometry, and the air gap between the bars. Higher frequency, more intensive heating, and a larger air gap between the bars lead to a greater surplus of heat sources induced in corresponding end areas of the bar.

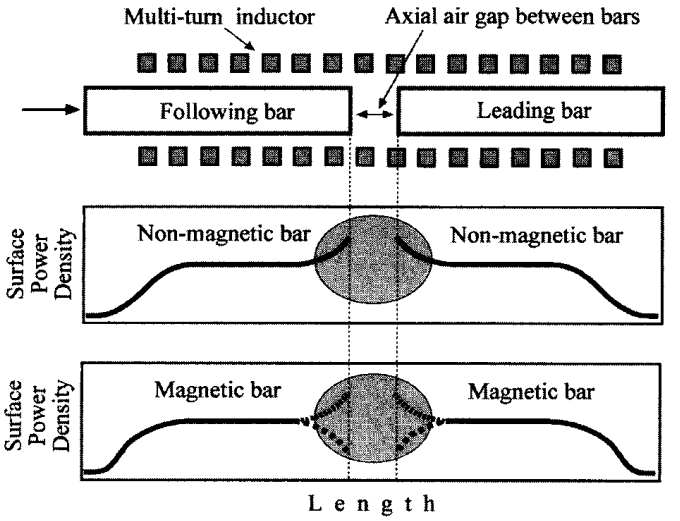

Figure 7.13 Sketch of surface power density distributed along the length of two bars located in the middle of a multiturn coil.

The end effect in magnetic bars has several features compared to a nonmagnetic bar. The electromagnetic end effect in ferromagnetic metal is mainly affected by two factors: the demagnetizing effect of eddy currents which tends to force the magnetic field out of the bar, and the magnetizing effect of the surface and volumetric currents, which have a tendency to gather the magnetic field within the bar (see Sec. 3.1.7).

The first factor causes an increase in power at the bar's end (similar to the end effect of a nonmagnetic bar). The second factor causes a power reduction at the bar's end. Therefore, the ends of ferromagnetic bars, even inside a long inductor, may be either over- or underheated. Studies show that the power deficit causing an underheating of the end area will be pronounced for high magnetic permeability steels that are heated with relatively low or moderate power density.

As previously mentioned, Figure 7.13 shows the power density distribution when two bars are located in the middle of a multiturn inductor and statically heated there. In reality, this power density distribution undergoes a continuous change as the bar passes through the inductor, and its power density profile becomes more complex. In some cases it can have a unique wave-shaped power distribution along the bar length having a local surplus of power in the end of a bar, however, in the region adjacent to the end there will be a power deficit compared to the power induced in the body of the bar or vice versa.

The task of obtaining nose-to-tail temperature uniformity is typically a more difficult one compared to minimizing the surface-to-core temperature gradient. Clear understanding of the intricacies of the process and applying a sophisticated control algorithm can significantly minimize the nose-to-tail temperature nonuniformity. Remarkable success in developing sophisticated control algorithms for inline induction heaters has been achieved by Dr. Edgar Rapoport and his coworkers [195, 197, 198, 207, 238, 239, 395].

7.2.4 Energy Efficiency of Inline Bar and Rod Heaters

Induction heating manufacturers pay special attention to maximization of energy efficiency of equipment and reduction of cost. Coil efficiency of induction bar heaters is a complex function of several design parameters including the gap between coil ID and bar OD properties of the heated metal, length of the coil, and applied frequency, with the last-mentioned being the most prominent. Figure 7.14 shows that there will be high coil efficiency when the frequency corresponds to a ratio of cylinder OD to current penetration depth δ greater than four ($OD/\delta > 4$). The use of a frequency that results in a ratio of $OD/\delta > 6$ will only slightly increase the coil efficiency.

The use of very high frequencies (frequency > F2) tends to decrease the total efficiency due to higher transmission losses and high heat losses as it will require a long heat time to provide the required surface-to-core temperature uniformity. If the chosen frequency results in a ratio $OD/\delta < 3$ (frequency less then F1, Figure 7.14), the coil efficiency will dramatically decrease. This is due to the cancellation of induced eddy currents circulating in the opposite sides of the solid cylinder. Table 7.3 shows minimum bar/billet diameters as a function of frequency and temperature for efficient induction heating of selected metals.

Highly effective solid-state power supplies, tapered low-loss coils, sophisticated refractory, and short bus bars are some of the factors that can minimize energy loss.

It is often required that an induction heating line processes bars of several different diameters. The specified cross-section range to be processed in a given set of induction coils and how many coil sets are needed requires consideration of a number of factors and also affects the energy efficiency of the system. The coil heating efficiency is largely a matter of the fill factor (area of the workpiece to be heated compared to the inside diameter of the coil windings). As the fill factor decreases, the efficiency decreases requiring more power. Energy demands rise as the heating efficiency is reduced.

On the other hand, the saving in energy cost by using a number of coil sets that are oriented on certain bars is diminished by the capital cost of investing in several sets of coils. There is also a production loss due to the time required to change coil lines, although advanced quick change design features discussed in the following sections can minimize this downtime.

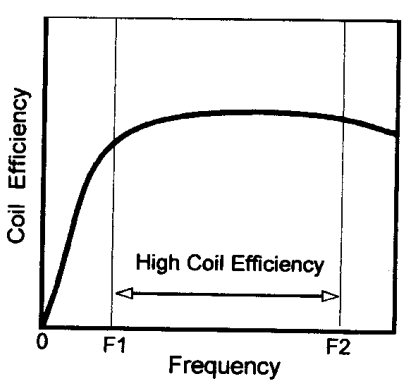

Figure 7.14 Coil efficiency versus frequency for induction heating of a solid cylinder.

Table 7.3 Minimum Bar/Billet Diameters (mm) for Efficient Induction Heating

		Frequency (kHz)						
Material	Temp. (°C/°F)	0.06	0.2	0.5	1	2.5	10	30
Copper	900/1652	68	35	23	17	11	5	3
Aluminum	500/932	68	35	23	18	11	5	3
Brass	900/1652	102	56	35	26	17	8	5
Titanium	1200/2191	304	168	105	74	47	23	13
Tungsten	1500/2732	168	92	58	43	27	14	8
Steel	1200/2192	253	140	94	65	41	20	12

A careful analysis of the product mix is necessary to determine how often the bar size may change and what the duration of each product run will be. These answers will help the user to determine the value of the second and possibly the third coil set. Note that below the Curie point the heating efficiency is not as greatly affected by the bar size variation; thus it may be worthwhile to change only the so-called "above Curie" coils.

In the case of the induction system shown in Figure 7.10, the smallest bar size was less than 5% of the total production mix. Therefore, in that particular case, it was cost effective for the customer to use the coil set designed for heating "big runners" to heat the small size bars as well, which under normal conditions would require separate coil sets.

If the product range (variety of bar/rod sizes) is too great, the ability to properly guide the smaller bars may be jeopardized. This can lead to jam-ups, unacceptable temperature nonuniformity at the given production rate, and excessive scale formation having a negative impact on the cost of coil maintenance and operation.

Additional sets of coils will be of little or no value if they are not readily available when needed. They must be stored in a designated area of the tool crib and properly identified as to the size of the bars they will process, the direction of bar flow through the coil, and, in some cases, their position on the coil line (assuming there are several coils inline).

In most instances, frequency selection when specifying an induction inline bar heater is a compromise because bar processing companies can rarely utilize a dedicated bar size with a particular induction heating system. In consequence it is often necessary to heat a bar that is too large or too small for a single frequency and therefore the efficiency of the induction machine suffers. Some of the solid-state inverters lend themselves to a dual-frequency configuration for the load circuit that to a large extent can overcome this problem. A typical example would be for a heater to be able to operate at 10 and 3 kHz or 3 and 1 kHz. Such approaches typically require installing dual capacitor banks. A detailed discussion of solid-state power supply design is provided in Chapter 8.

A dual-frequency design concept of an induction bar heater allows one to improve the overall efficiency of an induction heating system. This concept utilizes a low frequency in the initial heating stage, when the bar retains its magnetic properties. In the next stage, when the bar becomes nonmagnetic, it is more efficient to use a higher frequency to avoid a current cancellation and drastic reduction of the coil efficiency.

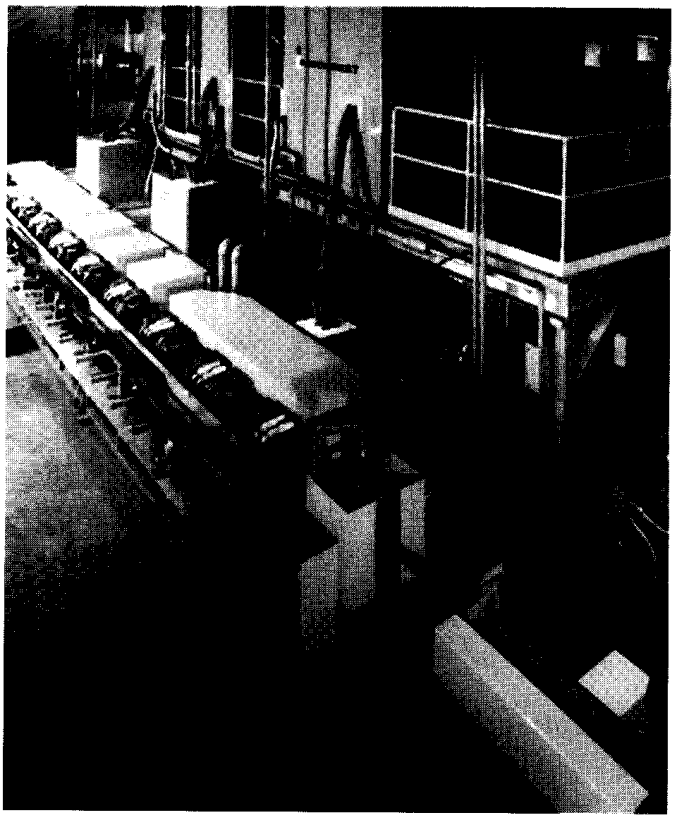

Figure 7.15 Dual frequency (1 and 3 kHz) inline induction steel bar heater. (Courtesy of INDUCTOHEAT, Inc., Madison Heights, MI.)

As an example, Figure 7.15 shows an inline induction heater for carbon steel bars. The bars are 6.1 m (20 ft) long and of various diameters ranging from 38 mm (1.5 in.) to 51 mm (2 in.), with a production rate of 7500 kg/hr (16,500 lb/hr). The system consists of 9 coils. A frequency of 1 kHz is used at the initial heating stage. The final heating is provided by two 750 kW/3 kHz solid-state power supplies. The bars are unloaded from railroad cars outside and placed on a bar bundle table and then fed end to end through the building wall to a bar feeder rack. The bars escape one at a time and are fed through the induction heating line. The bar handling system also includes a reversing system and unloads the table that is used when there is a press stoppage.

The specifics of induction heating rectangular or round-cornered square (RCS) bars are discussed in Section 7.5.

7.3 BILLET HEATING

7.3.1 Induction Heating of Steel Billets

The main goal of induction heating of steel billets is to raise the billet temperature to the level where it would be plastic enough to be forged, rolled, warm formed, or

extruded. The final temperature is typically in the range of 1050°C (1922°F) to 1260°C (2300°F) depending on the steel chemical composition and particularities of the postheating metal processing operation. The required surface-to-core and nose-to-tail temperature uniformity in billet heating applications is commonly specified as ±20° to ±50°C.

Depending upon the size of the billet, the heat time ranges from dozens of seconds (for smaller billet sizes) to dozens of minutes (for large billets).

There are two basic heating modes used in induction billet heaters: multistage or static heating. The majority of induction steel billet heaters utilize a progressive multistage heating mode where billets are moved end to end through a single coil or multicoil induction heater. Multiturn solenoid-type (helical) coils are the type most often used for billet heating applications.

A schematic of a typical multistage induction steel billet heater and a photo of a 1000 kW/1 kHz induction billet heating installation are shown in Figures 7.16 and 7.17, respectively. As one can see, modern induction billet heaters are compact unitized systems that incorporate a solid-state power supply, induction coil(s), an operator control panel, and a material handling system.

The standard range of induction billet heaters is a 200 kW/1 m through 3200 kW/12 m long induction coil, at frequencies of 500 Hz up to 10 kHz depending upon the geometry of the billets.

Surface-to-core temperature uniformity can be improved and/or coil length can be shortened when profiled coils are used instead of conventionally designed inductors. As shown in Figure 7.18, one of the main features of profiled coils deals with nonuniform winding of the copper turns along the coil length. The winding of coil turns for the initial heating stages is much tighter than in the final heating stages. In addition, smaller coil copper tubing sizes can be used in the initial stages resulting in higher current density there. Both factors result in initially more intensive heating and greater heat flow into the billet's core than when utilizing a conventional coil design. After the billet surface reaches a maximum temperature, the heat intensity is reduced to the levels that will only compensate for heat losses from the billet's

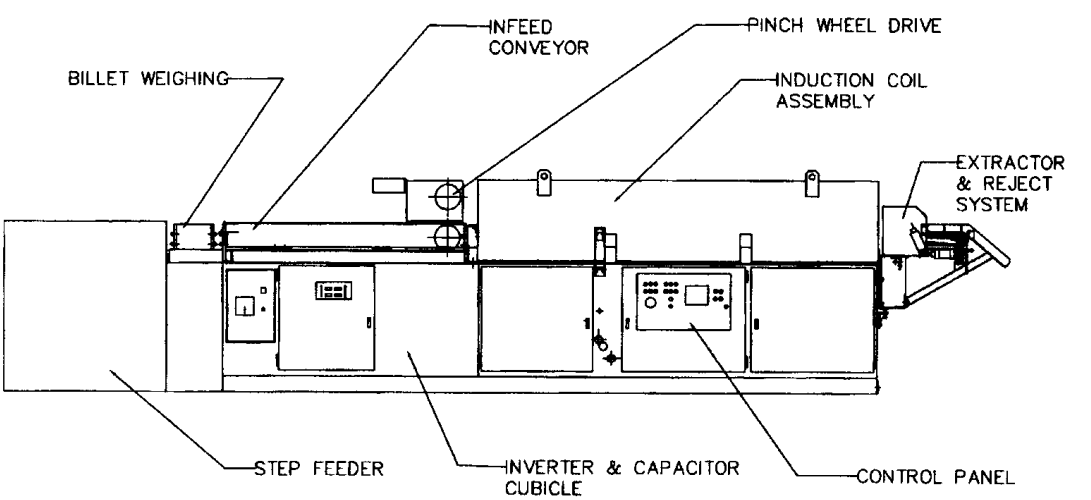

Figure 7.16 Schematic of Radyne's induction billet heater.

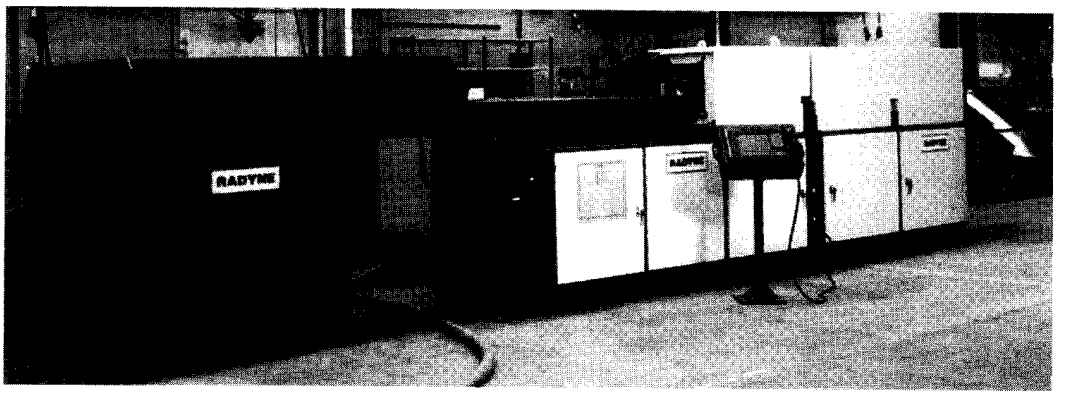

Figure 7.17 Contemporary induction billet heater.

surface (due to radiation and convection) and heat soaking toward the colder core (due to thermal conduction). Loose coil windings in combination with utilization of the larger size coil copper tubing is used at the final heating stage (Figure 7.18).

Obviously, the process of fabrication of the profiled coils is more complex and time consuming compared to a conventional inductor. However, the advantages gained may compensate for the extra cost of these type coils. One of the main concerns when using a profiled coil design deals with the necessity to avoid the appearance of large surface-to-core temperature gradients that might result in

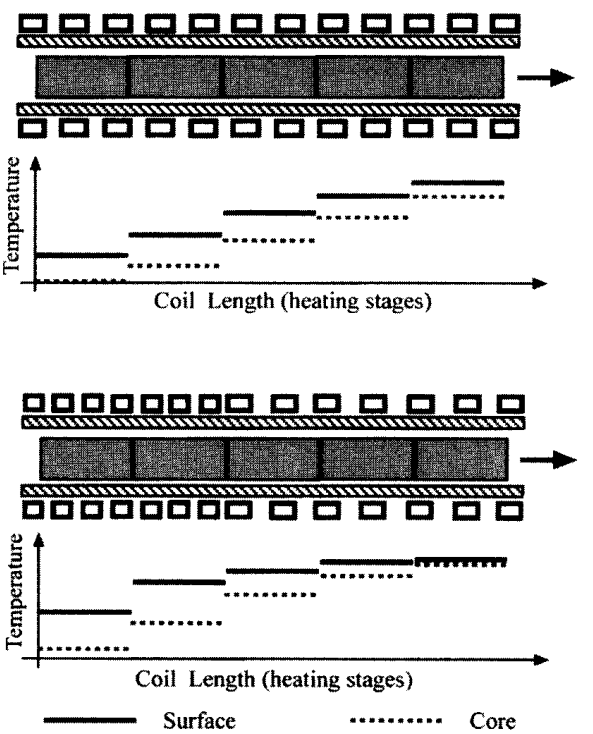

Figure 7.18 Conventional (top) and profiled (bottom) coil design for induction billet heater.

crack initiation (e.g., longitudinal cracks) when heating medium and, particularly, high-carbon steel billets [255, 256, 439].

The recommendations discussed in the previous section regarding frequency selection in bar heating applications hold true in billet heating as well. A quick rough estimate of the required coil power can be obtained using the procedures described in Section 3.3.1. More accurate calculations can be done using numerical computation.

The use of numerical computation is obviously preferable since it allows one to predict more accurately how different factors may influence the transitional and final heating conditions of the billet and what must be accomplished in the design of the induction heating system to improve the effectiveness of the process and guarantee the desired heating results [50, 169, 198, 238, 239, 268, 270].

An in-depth understanding of the induction billet heating process provided by numerical modeling allows manufacturers of induction heating equipment to build the optimum system for the forger: a system with the ability to meet exacting temperature requirements for precision forging. Additional benefits for a forger may include:

- Obtaining an optimized energy efficient induction system,
- Increased output of pieces forged,
- Reduction of scrap,
- Improved as-forged finish of the workpiece,
- Reduction of press loads and increased die life, and
- Ability to more readily obtain net and near-net shapes.

Last but not least, a major advantage provided by modern induction billet heaters is the minimization of shop floor space required. This compactness factor becomes increasingly important in a modern forge shop.

As an example, Figure 7.19 illustrates the results of computer modeling showing the distribution of the steady-state temperature profile and magnetic field intensity along the length of a single coil induction billet heater consisting of four end to end carbon steel billets. The billets are indexed using a pusher system one after the other through the single coil inductor. Most of the time, the billets are immobile in the inductor and move only when the leading billet heated to the final temperature exits the coil and a new billet is inserted.

The parameters of the induction system are:

- Billet geometry: OD = 80 mm (3.1 in.), length = 230 mm (9 in.);
- Coil geometry: ID = 152 mm (6 in.), length = 990 mm (39 in.), Number of turns = 50;
- Refractory geometry: thickness = 20 mm (0.8 in.), thermal conductivity = 0.028 W/°C;
- Frequency = 2.4 kHz.

As one can see, the distribution of the magnetic field intensity is quite different compared to the field intensity that can be calculated using the simple formula of $H = I * N/L$ (where H is magnetic field intensity, I is coil current, N is number of turns, and L is coil length) that is typically used in simplified calculations.

The distribution of magnetic field intensity and temperature along the billet length are caused by several electromagnetic and thermal effects. This includes the longitudinal end effect, thermal edge effect, edge effect of joined materials, and so

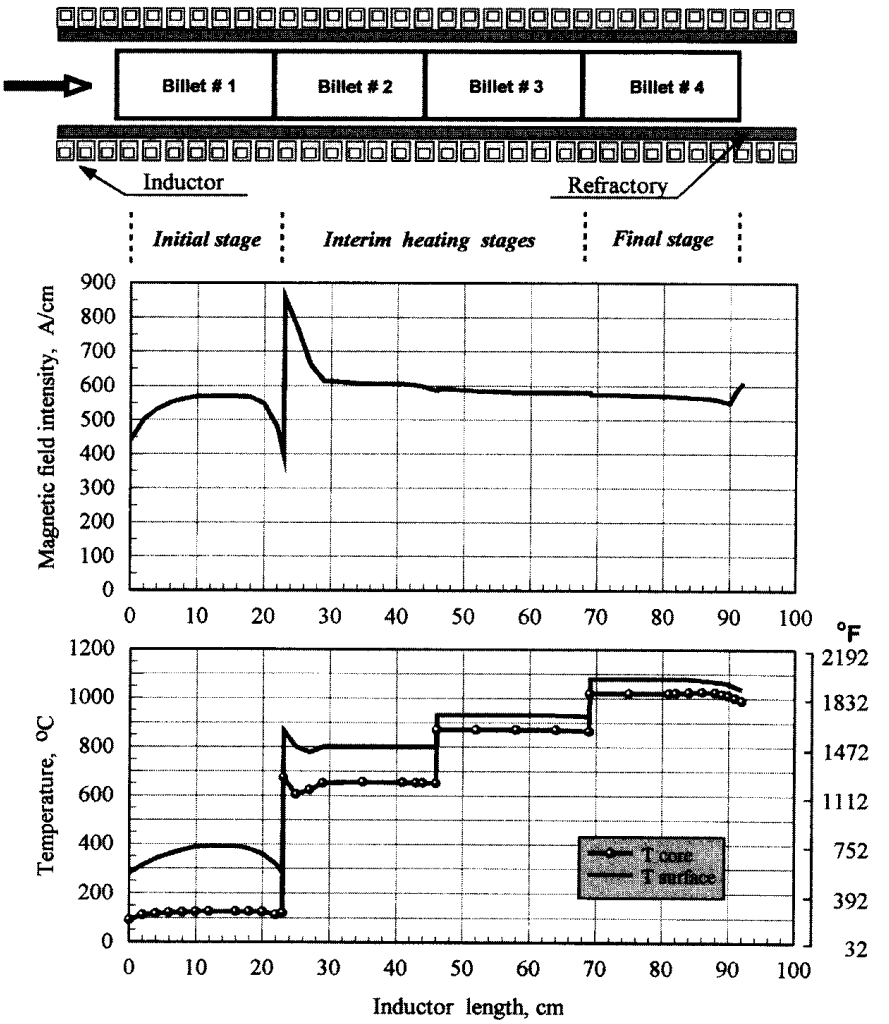

Figure 7.19 Distribution of the temperature and magnetic field intensity along the length of four inline carbon steel billets heated in a single multiturn coil.

on. Inasmuch as the nature of these effects has been discussed in detail in Section 3.1.7, it is assumed that the reader is aware of these phenomena. Here we describe the general tendencies of the appearance of these effects and their influence on the process of induction carbon steel billet heating using Figure 7.19 as an example.

The magnetic field in the tail end (left end) of billet #1 is formed by the end effect of a magnetic body. Depending upon the frequency, power density, physical properties of the heated metal, and geometry of the induction system, the ends of a ferromagnetic body may be either overheated or underheated. In the present case, the electromagnetic end effect results in the underheating of the tail end of billet #1 ($0 < Z < 8$ cm).

In the area where billet # 1 (heated below the Curie temperature) is brought into contact with billet #2 (surface temperature of this billet exceeds the Curie point) the electromagnetic effect of joined materials takes place. The magnetic field intensity at the central parts of both billets is approximately the same, meaning that the

electromagnetic field at the central parts of these billets is close to homogeneous. However, at the area of the ends of billets that are brought into contact drastic distortion of the electromagnetic field takes place.

At the end of the nonmagnetic billet (tail end of billet #2) the magnetic field intensity and power density are sharply increased. In contrast, both parameters are sharply decreased in the area of the magnetic billet (leading end of billet #1). Therefore, local longitudinal temperature gradients occur due to the electromagnetic effect of joined materials with different properties.

It is necessary to note here that the initial axial temperature distribution of billet #2 was not uniform (due to the above-described effects when this billet was in the previous heating stage). An increase of power density on the left end of billet #2 will approximately compensate for the initial underheating.

The effect of the joined materials also takes place at the area where billets #2 and #3, as well as billets #3 and #4 are brought into contact. The temperature of all three billets is above the Curie point; thus the relative magnetic permeability of these billets equals 1. At the same time, the electrical resistivity of these billets is different because they are heated to different temperatures. Therefore, the different resistivities result in a slight variation of the magnetic field intensities.

The magnetic field in the leading end (right end) of billet #4 is formed by two counteracting end effects: the electromagnetic end effect of the nonmagnetic body and the thermal edge effect that primarily represents the heat losses in the billet's leading end area. The thermal edge effect takes place due to Lambert's law (cosine law). According to this law, the thermal radiation is not only a function of the metal, its surface condition, and temperature but is also a function of the workpiece shape and surroundings. The thermal edge effect can be taken into account by standard computation procedures that use radiation shape factors (also called view factors or angle factors) [26–35].

As shown in Figure 7.20, the thermal edge effect takes place in the trailing end (left end) of billet "A" as well. The thermal radiation losses are a function of the fourth power of temperature. Therefore, since the temperature of billet "C" is much greater than the temperature of billet "A", the thermal edge effect in the end area of the billet that is located in the final heating stage is significantly more pronounced compared to the thermal edge effect of the billet located in the initial heating stage.

As one can see from Figure 7.19, a surplus of power induced in the area of the leading end (right end) of billet #4 only partly compensates for the thermal edge effect resulting in underheating of the leading end of that billet.

A uniform temperature distribution along the length of billet #4 that is located in the final heating stage may be achieved by properly choosing the parameters of the induction system, such as coil overhang, coil windings, and the like.

The electromagnetic effect of joined materials with different properties may have a greater influence on the final temperature distribution than shown in Figure 7.19, especially in cases when designing induction heating equipment that will operate below or just above the Curie temperature.

Since billets located in different heating stages have different temperatures, one of the key questions in modeling an induction billet heater is how to treat the heat flow in the axial direction (i.e., from billet "A" to billet "B"; Figure 7.20). Realistically, there are no butt end surfaces of billets that are perfectly smooth. Instead, the surface roughness provides the major impact in the heat flow through

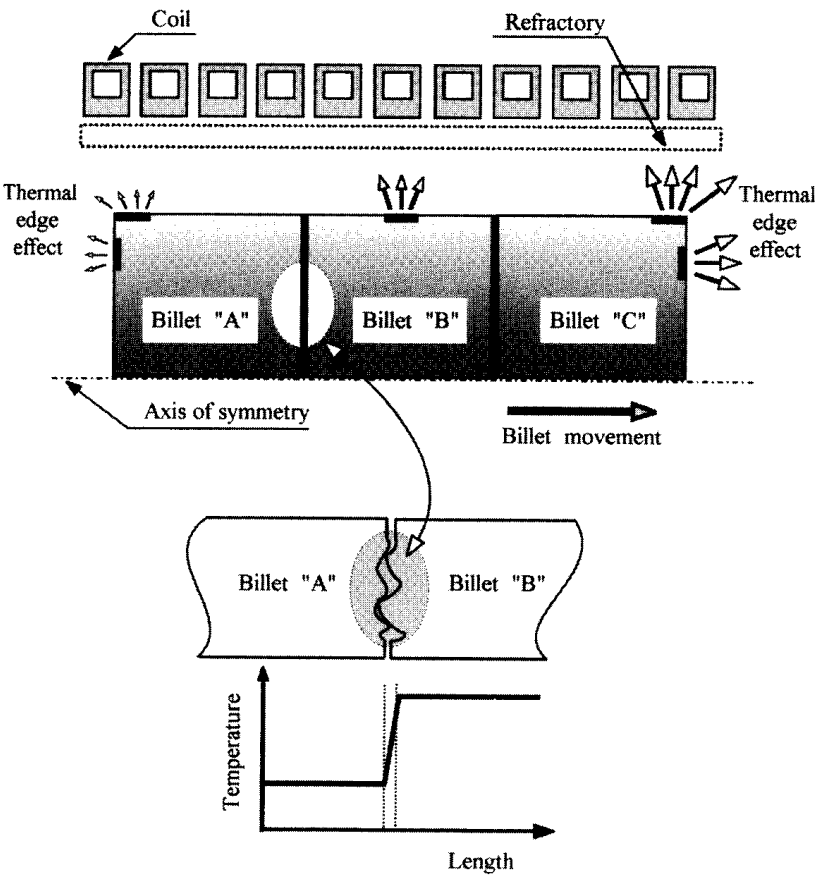

Figure 7.20 Thermal edge effect in billet heating.

the contact area of two billets. There are two principal contributions to the heat transfer in the area of the contact:

- The heat flow through the air pockets, and
- The thermal conduction through the solid-to-solid points of contact.

The first factor represents the major resistance to heat flow through the contact area, inasmuch as the air is a poor thermal conductor. The experience of modeling induction billet heaters shows that from an engineering perspective, it is legitimate to assume that the heat flow through the contact area of two billets is absent. At the same time, a quick estimate of the heat flow can be conducted using a method based on the thermal contact resistance approach discussed in [436].

Figure 7.21 shows a UNIFORGE® unitized billet heating system that in the last decade became the defacto standard of induction billet heating machinery and has been designed and optimized based on extensive study using numerical computation. This rigid and compact system incorporates a solid-state power supply, induction coil(s), operator control panel, built-in annunciator panel for simplified status/fault diagnostics, and a material handling system. The unitized construction of the UNIFORGE® eliminates the need for interconnections between separate components typical of conventional heating systems, saving floor space and installation time. Power and frequency combinations are available from 100 to 1000 kW

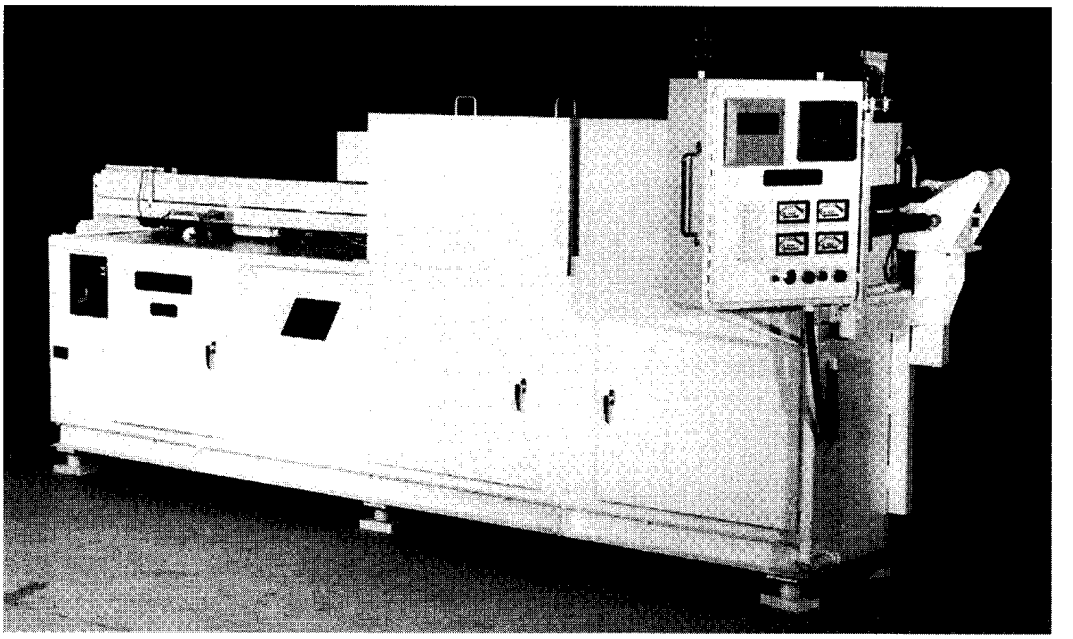

Figure 7.21 UNIFORGE unitized induction billet heater. The power of a single module is up to 1000 kW with a frequency range of 500 Hz to 30 kHz. (Courtesy of INDUCTOHEAT, Inc., Madison Heights, MI.)

operating at frequency range from 500 Hz to 30 kHz. External, visibly mounted water pressure gauges, as well as door-interlocked disconnect switches and fast-acting semiconductor type fuses mark some of the safety features. Each water circuit consists of a water pressure differential switch and reset temperature switches. Remarkably, this one megawatt billet heating system measures only 6.8 m (268 in.) in length.

System availability is another important factor that should be taken into consideration when evaluating the performance of a modern induction billet heater. As mentioned in the previous section devoted to induction heating of long bars, the coil efficiency is largely a matter of the fill factor. This results in the necessity in some cases of utilizing several sets of coils in order to accommodate the practically minimum clearance that would result in good coil to billet electromagnetic coupling. The ability to keep production loss due to the time required to change coil sets to a minimum is essential for modern billet heaters. The use of quick-change tooling in forging applications is similar in principle to that of heat treating (see Sec. 5.1.8), but the size and style are quite different. There are several design approaches that provide quick-change capability. According to one of them, the induction billet heater might consist of one or several coils that may include replaceable refractory liners, special alloy wear coated rails, electric quick disconnects, and water quick disconnects, all situated upon a common support structure [402, 405].

Utilizing a common aluminum support structure with four lifting points, one at each corner, enables the entire coil assembly to be lifted as a whole. Guide pins facilitate alignment during installation and act as protective support legs when the coil is offline. The pins protect the electrical bus connection pads from damage. Electrical connections are then made via bus pads secured to a receptacle extending

from the receiving pads. Connections are reduced to a pair of connectors that can be locked into place via a single nut or alternatively via a pair of pneumatic clamping devices.

Valve-actuated quick disconnects are then used to quick-connect the water circuits. The quick disconnects are designed to prevent reconnection errors. Drain circuits are then individually monitored through a series of flow switches. Removing and installing a quick-change forging coil is simplified in the following steps [405].

1. Unlock or release the electrical quick disconnects.
2. Unsnap the cooling water quick disconnects.
3. Attach the lifting assembly to the lifting points and lift.
4. Place assembly in storage or maintenance and connect to replacement assembly.
5. Lift another coil assembly from storage.
6. Lower the replacement coil assembly online.
7. Lock the electrical quick disconnects.
8. Snap on the cooling water quick connects.

This simple operation allows one to reduce the change over time to minutes resulting in a drastic reduction of the amount of lost production time.

When frequent coil change is required the twin track approach is beneficial. According to this approach, an induction billet heater integrates a twin track with a common aluminum base support to eliminate offline storage space and further simplify changeover operation. In this case, complete coil lines are stored on a parallel track that is in direct alignment with the operating coil assembly. Steps 3 through 5 of the above-described procedure are simplified to merely sliding the operating coil out and the new one into position. Most of the twin track systems house two assemblies but can be designed to be capable of housing several assemblies.

One of the most frequent causes of downtime with induction heaters of steel billets is coil breakdown to earth. This is usually caused by scale particles finding their way to the coil turns and causing a flashover. As a result the power supply trips or coil damage can occur. By limiting the coil output to 1200 volts and using an advanced coil fabrication technique this effect can be minimized [400–402, 405].

As mentioned earlier, the majority of induction steel billet heaters utilize a multistage heating mode where billets are moved end to end through a single coil or multicoil inductor typically by means of one of three basic billet feed systems: pinch roll drive, pusher, or walking beam [402].

The most widely used type of billet feeder is a pinch roll drive. The billet is fed through the heater by adjustable drive rollers with speed control (see Figure 7.16). When the equipment is used for heating short billets, they can be discharged from the heater by means of slide rails. Roller extractors are used if it is necessary to discharge long billets (i.e., over 200 mm).

Billet pushers can be of the pneumatic or hydraulic types. Heated billets are usually discharged at the end of the heating operation by gravity using two adjustable slide rails but, if necessary, an automatic transfer mechanism can be provided to convey the billets from the heater to the press.

Care should be taken with the billet exit. If they are tipped at the exit, care should be taken to allow for the tipping action. Bell mouths, if not correctly designed, can result in cooling of the exit billet and this may result in severe billet

sticking. The possibility of billet sticking rises when the billet temperature exceeds 1260°C (2300°F). Because of the limited coil length and interrupted pushing, it is possible that billets longer than about 150 mm may not be evenly heated unless special precautions have been taken [400–402].

One of the drawbacks of this type of feeder is that when the run is finished it is impossible to empty the heater automatically. So it has to be done manually by means of a hand pusher or other special devices. The subject of billet emptying devices is discussed in Section 7.7.

Walking beam feeders are built on the same principle as walking beam furnaces. The lift, transfer, and lower motions are smoothly actuated through mechanical linkages. As the billets are not touching each other, the sticking problem is virtually eliminated and conventional requirements as to the quality of the billet end shear are eliminated. At the end of a run, the heater can be emptied automatically. For large throughputs, twin track walking beam machines are utilized, so that two lines of billets pass side by side through the same inductor. Due to the cost of a walking beam system and its complexity, wide utilization of this type of system is limited. A detailed discussion on the subject of material handling is provided in Section 7.7.

The heart of the billet heating system is the electrical control system. At the present time, most manufacturers of induction billet heaters use the advanced Allen Bradley CPU, coupled with an Allen Bradley Panelview HMI. This combination lends itself toward giving the operator full control over the billet heating system and shows all preset conditions, logs any faults that may occur, and provides full production and running data. (e.g., power, information about the product being run, and temperatures, as well as an extensive shift and accumulated part count showing all accepted and rejected parts under temperature, over temperature, and press rejects).

Running in the background is the product code storage system, which allows manual input, storage, recall, running, and changing any or all of the programmed parameters required to run the perfect part. An HMI Control System is shown in Figure 7.22. Siemens and Mitsubishi are alternative systems.

Contemporary design of induction heating equipment should optimize not only steady-state but transient processes as well. Transient processes include startup and shutdown states as well as standby or the holding condition that occurs when it is necessary to hold the billet in the induction heater during the downtime of the forging, rolling, or extrusion equipment. Induction heating manufacturers have developed a variety of techniques to optimize transient processes. For example, Newelco has developed one of the most impressive techniques for conducting prolonged standby conditions. Newelco billet heaters are specifically designed to minimize the disruption to forging, rolling, or extrusion caused by the inevitable occasional break in activity caused by necessary adjustment or die changes. Their unique coil design allows the reduction of the gap between coils to a minimum of about 12 mm. This is an important design feature when it is required to hold hot billets inside the induction heater for a long time. In order to do so, the power connections to the coils are switched, reducing the coil voltage down to the levels that will compensate the surface thermal losses of the billet located in the second stage from the coil exit. The temperature of the billets will be practically unchanged with time, so that when the heater is restarted only the first billet is outside the

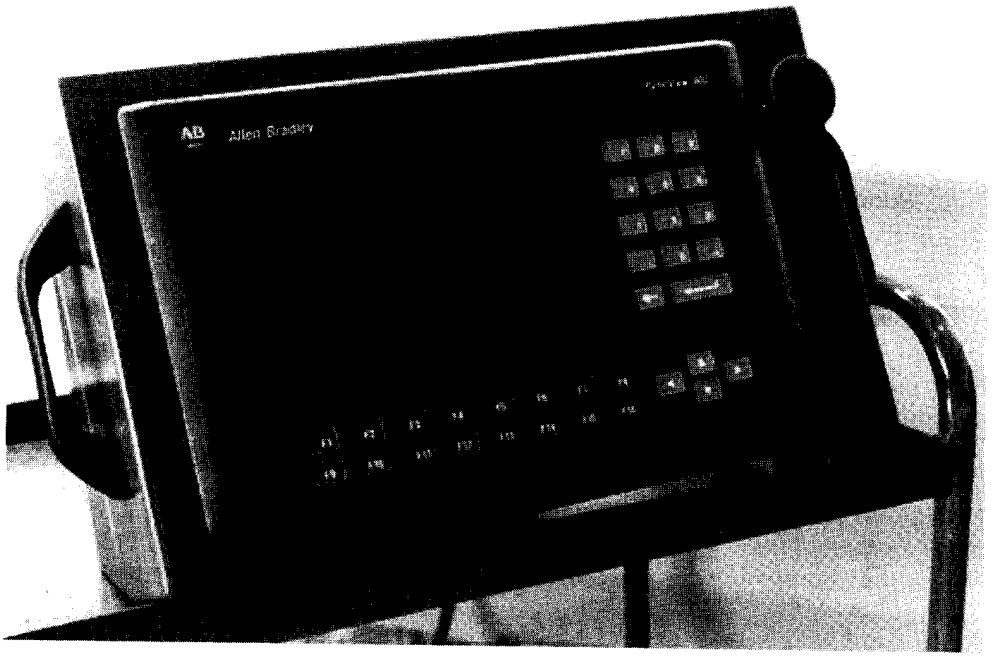

Figure 7.22 HMI control system.

forging temperature range being heated to lower than required temperature. Obviously, this is only one of the possible approaches to optimize the standby state of the billet heater and its recipe can be modified depending upon the application and particular requirements.

Progressive multistage heating is the most popular mode used for induction heating of steel billets. At the same time, there are applications where it is advantageous to use a static mode of heating instead of a progressive multistage mode or combination of both progressive and static heating modes. According to the static heating mode only one billet is heated in the coil. It is imperative at this point to provide a case study using as an example the world's largest induction billet heating installation for the extrusion of carbon steel and stainless steel tubes built by Inductotherm S.A., Belgium (previously called Elphiac) [420]. The construction of this installation, of a total rating of 33,000 kW, represents a major achievement in the field of billet heating equipment for the manufacture of seamless extruded steel tubes.

The extruded steel market is a special area. Steel tubes can be classified into two categories depending on manufacturing process: welded tubes made from steel strip and nonwelded, or seamless, tubes made from billets. In this second category, a further distinction can be made between rolled and extruded tubes.

Rolled tubes are obtained from a hot billet that is successively pierced and rolled. Extruded tubes are also made from a hot billet that is successively pierced and then extruded in a horizontal press. Extruded tube is particularly suitable for industries that have exceptionally high safety requirements, as is the case of the chemical and petrochemical industries, as well as the nuclear industry.

Most of the billets prepared for extrusion are induction heated. The special feature in the extrusion tube fabrication process concerns the fact that the surface of the steel billets is coated with a viscous glass film that acts as a lubricant during extrusion. It is important to take this coating into consideration when designing induction heating equipment, because its existence drastically affects the heat losses from the billet surface.

The tube works comprises two production lines [420]:

- One line with a 2000 tonne press extrudes 120 billets per hour and produces a maximum of 22 t/hr of steel tubing having outside diameters between 30 and 130 mm; the billets from which the tubing is made have diameters from 130 to 230 mm and lengths from 250 to 870 mm;
- A second line with a 5500 tonne press extrudes 75 billets per hour and produces a maximum of 57 t/hr of tubing having outside diameters between 40 and 240 mm; in the case of this line, the billet diameters range from 200 to 400 mm and a length of 0.48 to 1.4 m.

Induction systems have been supplied for both lines for heating billets prior to piercing and before the metal's extrusion.

The piercing of the metal requires that the steels should be heated to a temperature of about 1200°C (2192°F). For the 2000 tonne line, the process of heating is achieved thanks to three horizontal 3300 kW/50 Hz inline induction heaters that operate in parallel.

On the other hand, mixed heating is used in the 5500 tonne line. First, a rotary hearth furnace preheats billets up to a temperature of 850°C (1562°F), while the final heating from 850°C (1562°F) to 1200°C (2192°F) is carried out in three horizontal 3000 kW/50 Hz inline induction heaters also operating in parallel. These three groups of heaters are generally made to work at a constant production rate but, in the event of any irregularity of the line, they will immediately provide a hold or standby mode of operation.

During the piercing operation, the billet cools down and must be reheated prior to extrusion. This reheating from about 900°C (1652°F) to 1250°C (2282°F) takes place in two rows of vertical inductors in which each billet is individually reheated using a static heating mode. These inductors thus take into account an initially nonuniform temperature profile and enable the temperature of all the billets to be raised to the same level and with required uniformity for the extrusion process.

The 2000 tonne line comprises seven 650 kW vertical reheating inductors among which six operate continuously with the seventh being held in reserve. In the case of the 5500 tonne line, it comprises eight 1200 kW vertical inductors among which seven inductors operate continuously with the eighth being held in reserve.

The Prepiercing Horizontal Inline Induction Heaters

Each horizontal inline induction heater (Figure 7.23) is supplied with three-phase current through three step-down single-phase transformers, fitted with secondary taps and associated voltage adjustment devices with contactors and divider reactor. Such adjustment facilitates operating flexibility including frequent changeovers when it is required to provide the holding (standby) operational mode of the heater in the event of irregularities of the production line. A computer controls and optimizes the

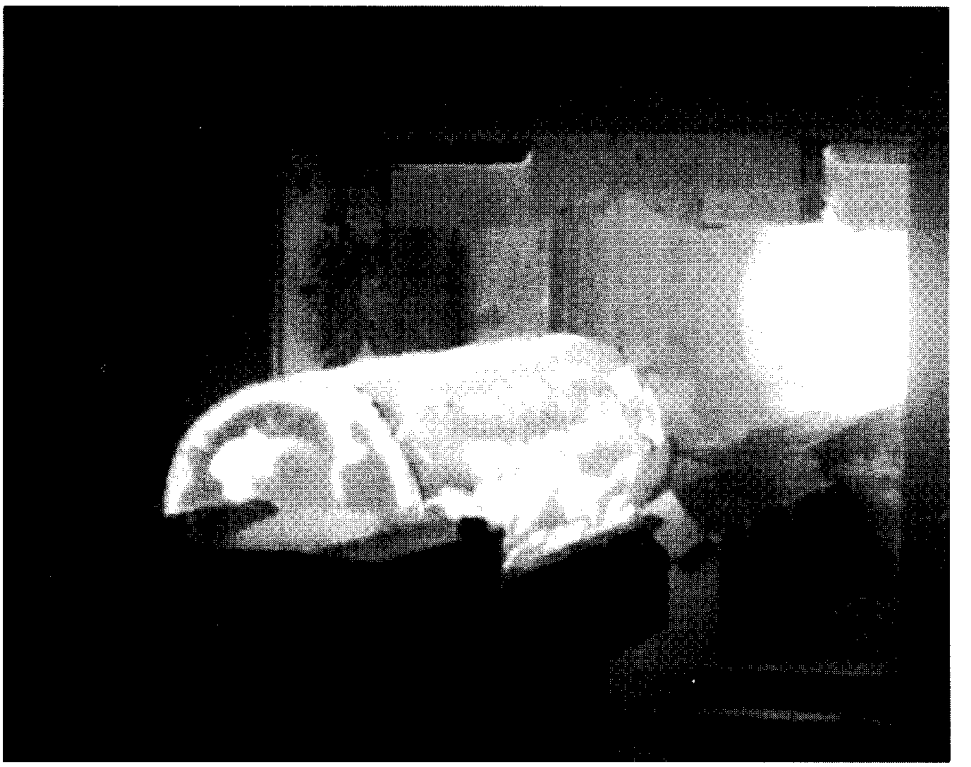

Figure 7.23 Prepiercing horizontal inline billet heater. (Courtesy of Inductotherm S.A. Belgium, previously called Elphiac.)

process of heating. The inductors and compensating capacitor banks all operate at the standardized maximum voltage of 600 V/50 Hz.

The heating zone of each of horizontal inline heater is seven meters long and comprises five inline induction coils aligned along a metal chassis. Each inductor is coated with refractory cement having a high alumina content and is fitted with a sole plate of heat-resistant steel capable of expanding freely. Two infrared pyrometers constantly monitor the temperatures of critical zones.

In the case of the 2000 tonne line, the billets are charged from pallets, and in the case of the 5500 tonne line, a roller track carries the billets after their passage through the rotary hearth furnace. After stopping at one of the measuring stations, the billets are distributed among the three horizontal inline induction heaters by means of transverse moving trolleys. After being delivered, the billets are subsequently moved into the appropriate heater.

The pusher that operates in small steps or fractional billet lengths is used to charge billets into the heater and ensure the required temperature uniformity along the billet length. The pusher is long enough to automatically empty the charged heater when required. For safety reasons, hydraulic jacks operating with a non-flammable water–glycol mixture carry out all movements.

At the entry to the inductors of the 5500 tonne line, fed with billets preheated to 850°C (1562°F), a small electric resistance holding furnace is located. This furnace maintains the temperature of the billet until it is fully inserted into the first inductor by the step-by-step action of the pusher.

At the exit of each horizontal induction heater, there is also an electric resistance holding furnace to maintain the billet leading end temperature until its tail end has completely left the last coil. This furnace also enables the differences in the production rates between the press line and the heaters to be evened out.

Billets are taken out of the electric resistance furnace by a tongs extractor that pulls them through an automatic separating mechanism. Only one billet is drawn onto a transverse moving trolley serving all three horizontal heaters, to be made available to a press or be rejected. This acceptance or rejection decision is taken by an optical pyrometer located in the discharge holding furnace.

A programmable automatic controller carries out the total control of the operation. This includes the sequential control of the pusher movements, extractor tongs, and trolleys, as well as the tracking of the billets. The heating cycles are controlled by a process control computer that utilizes an induction heating mathematical model that optimizes the process in each individual case as a function of production instructions, temperature profile, and the billet's identification number. In the event of a delay at the press, the induction heater will automatically change over to a holding mode.

The Pre-Extrusion Vertical Induction Billet Heaters

In order to feed the 2000 tonne press, six vertical 650 kW/50 Hz coils plus a standby inductor reheat 22 tonnes of steel billets per hour (maximum production rate) from 900°C (1652°F) to 1,250°C (2282°F). These inductors are designed to handle billets ranging from 130 to 240 mm in diameter. In order to maintain reasonably high coil efficiency when heating billets with different diameters, extracoil sets with different coil ID are used.

Similar to the 2000 tonne press, in the case of the 5500 tonne press there are seven 1200 kW/50 Hz plus one standby vertical coil that can reheat 57 tonnes of steel billets per hour (maximum production rate) from 900°C (1652°F) to 1250°C (2282°F). These inductors are designed to handle billets ranging in diameter from 200 to 420 mm using several coil sets. It is also possible to heat cold billets from 20°C (68°F) to 1250°C (2282°F).

Each vertical inductor is supplied with a single-phase current through a step-down transformer having secondary taps associated with a voltage-regulated system. The inductors consist of three tapings to adapt the length of the coil to that of the heated billet. Each vertical inductor consists of two infrared pyrometers (Figure 7.24).

The billet transfer, tipping, and charging mechanisms are located below the platform and operate as follows [420].

- The billets to be reheated are brought to the vertical cells by means of a trolley conveyor (2000 tonne line) or a roller track (5500 tonne line); the billet is brought in front of the vacant furnace either by the stoppage of the trolley (2000 tonne line) or by a retractable stop on the roller track (5500 tonne line).
- The billet is then transferred sideways by the tipping of the trolley platform (2000 tonne line) or by a canted diverting arm inserted into the roller track (5500 tonne line); the billet rolls off into an intermediate station and then

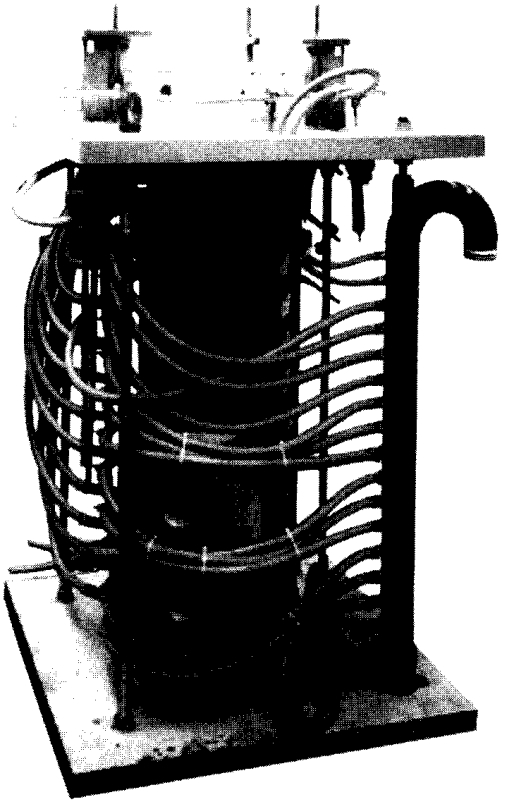

Figure 7.24 Pre-extrusion vertical billet heater. (Courtesy of Inductotherm S.A. Belgium, previously called Elphiac.)

onto a horizontal cradle; this cradle forms part of a rocking hanger which pivots 90° and sets the billet vertically over a charging jack.

- The charging jack is installed at basement level and raises the billet vertically into the inductor; it moves through its full travel so that the lower end of the billet is always positioned at the same level in the inductor, while its upper end is in the zone where the taps are located. All the jacks operate with a nonflammable mixture.

The heating operation is automatically started once the billet is completely charged. The process of heating is controlled as a function of the required energy and is readjusted as a function of the initial temperature and the transient temperature measured by pyrometers during the heating cycle. This approach ensures that all billets are heated to the required extrusion temperature whatever the temperature variation at charging is.

When the heating cycle is completed the programmable controller generates a signal checking whether the press is available to accept the billet. Otherwise, the inductor changes its heat mode over to hold mode.

Billet discharge occurs by the lowering of the jack followed by the 90° pivoting of the hanger, thus bringing the billet into a horizontal position on the cradle (Figure 7.25). The cradle then tips and spills the billet onto the trolley conveyor that takes it to the extrusion press.

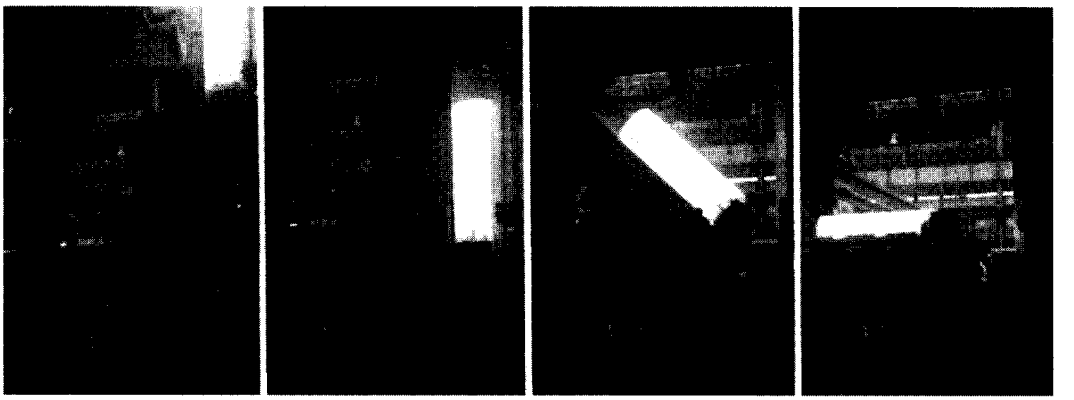

Figure 7.25 Billet discharge sequence after heating billets statically in a vertical inductor. (Courtesy of Inductotherm S.A. Belgium, previously called Elphiac.)

7.3.2 Induction Heating of Nonferrous Billets

Induction heating of nonferrous billets (i.e., aluminum, copper, brass, magnesium, silver, titanium, etc.) comprises the same basic design approaches as the heating of steel billets. Actually, for some light metals such as titanium, for example, the frequency selection and obtained temperature profiles are quite similar to stainless steel billet heating as discussed in the previous section, because both titanium and stainless steel (2xx and 3xx series) are nonmagnetic metals and the average values of electrical resistivity and thermal conductivity of both metals are quite similar (Figures 3.2 and 3.39). This similarity certainly does not mean that design procedures for induction heaters of titanium and stainless steel billets are identical. For example, induction heating of titanium billets almost always requires the use of a protective atmosphere and lower final temperatures compared to steel heating applications.

In contrast to titanium, the process of heating copper and aluminum alloys requires at special design approach compared to steel billet heaters. The principal differences arise because aluminum and copper are better electrical and thermal conductors than steel and titanium. For example, the electrical resistivity of copper is 38 times (ambient temperature) to 15 times (at temperature of 900°C/1652°F) lower than that of stainless steel. At the same time, the thermal conductivity of copper is 15 to 20 times higher compared to stainless steel.

According to formulas (3.6) and (3.7), the low value of electrical resistivity results in a small current penetration depth making it possible to apply much lower frequencies and often even using a line frequency when heating billets made from low-resistive metals such as aluminum and copper without facing the danger of eddy current cancellation. An ability to utilize line heating is obviously an attractive approach. Because frequency conversion is not required when line frequency is used it results in lower capital cost of the equipment. Table 7.3 (Sec. 7.2) consists of minimum bar/billet diameters for efficient induction heating for selected metals.

In addition, because the line frequency inductors are known for low "volts per turn" values, the ability to apply a multilayer multiturn coil design is advantageous from the perspective of load-matching the coil to a line frequency transformer.

As has been discussed earlier and according to formulas (3.25) and (3.26) (Sec. 3.3.1), low electrically resistive metals are known to have a low coil electrical effi-

ciency. As an example, Figure 7.26 shows the coil electrical efficiency and coil power factor ($\cos\Theta$) versus frequency when heating cylindrical billets made from selected metals (carbon steel AISI 1045, nonmagnetic stainless steel 304, titanium alloy Ti6Al4V, aluminum, and copper). Coil and billet geometry in all cases was the same: billet's geometry = 0.1 m (4 in.) diameter and 0.5 m (20 in.) long; coil geometry = 0.15 m (6 in.) ID and 0.56 m (22 in.) long.

Drastic reduction of the coil electrical efficiency when heating stainless steel and titanium alloy at a frequency less than 500 Hz indicates that eddy current cancellation takes place. As one can see from Figure 7.26, for that particular geometry the coil electrical efficiency does not significantly change with frequency and its maximum value is below 45% when using a conventional single-layer coil design. With a properly selected frequency, coil efficiency when heating stainless steel and titanium alloy billets is in the range of 68 to 75%. As expected, carbon steel billets at temperature below the Curie point feature the maximum coil electrical efficiency of exceeding 85% at frequencies above 500 Hz. It is important to note that during heating of magnetic billets some reduction of coil electrical efficiency particularly at frequencies below 200 Hz is not due to a current cancellation but to reduction of the billets' resistance to an eddy current with lower frequencies.

Low coil electrical efficiency when induction heating low-resistance metals forces manufacturers of induction heating equipment to use nontraditional design approaches.

While discussing induction heating of such metals as copper, silver, and aluminum, it is important to mention that because the thermal conductivity of those metals is high it is easier to obtain a uniform temperature distribution within the

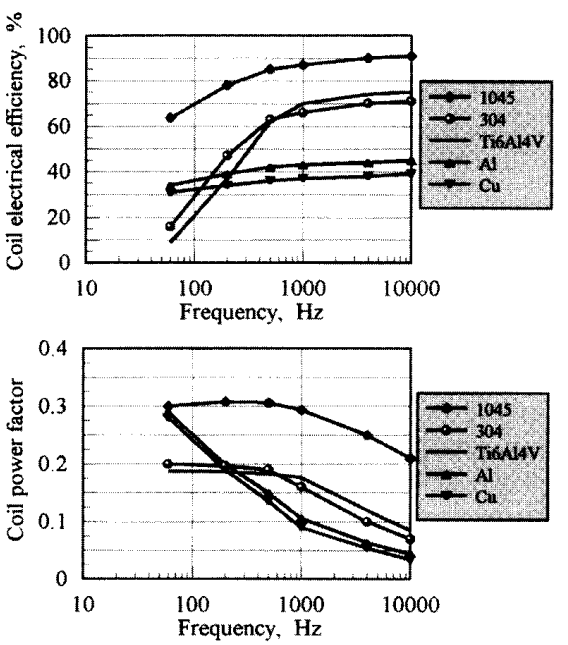

Figure 7.26 Coil electrical efficiency and power factor versus frequency when heating cylindrical billet 0.1 m (4 in.) OD, 0.5 m (20 in.) long at 550°C (1022°F).

heated billet thanks to an intensive soaking action from high-temperature regions toward low-temperature areas.

Another feature when heating billets made from aluminum and copper alloys deals with the fact that those metals are heated to much lower temperatures compared to steel. Table 7.2 (Sec. 7.1) shows the list of commonly required temperatures for selected nonferrous metals.

This section concentrates on the discussion of aluminum billet heaters as a typical representative of a family of low-resistive, high thermally conductive metals assuming that the majority of the design features will be similar for induction heating of billets made from copper, brass, gold, and silver.

The first industrial inductor for heating of light metal billets is believed to have been produced to fulfill the needs of the aluminum industry around 1950 [399]. Conventional single-layer solenoid-type coil design similar to inductors used for heating steel billets has been used for heating aluminum billets. As mentioned earlier, one of the main drawbacks of conventional coil design for heating aluminum billets as well as any low electrically resistive metals has to do with low coil electrical efficiency. In the past several years attempts have been made to try to improve coil efficiency when heating low-resistive alloys.

As illustrated in Section 8.13.4 (Figure 8.97), the power loss in induction heating systems includes losses in power supply, capacitors, transmission losses, loss of power induced in the coil surroundings (i.e., laminations, water-cooled liners, rollers, etc.), thermal losses from the billet's surface, and actual losses in coil windings. When heating nonmagnetic low-resistive metals such as aluminum, the power loss in the coil windings is greater than all other losses combined. Therefore, an ability to reduce losses in coil turns represents the main avenue toward improving the total efficiency of an aluminum billet heater.

An obvious way to decrease power losses in coil windings is to reduce coil resistance R_{coil} that in a simplified way can be determined as follows: $R_{coil} = \rho_{coil} * L/A$, ρ_{coil} is the electrical resistivity of the coil windings, L is the length of current-carrying conductor, and A is the area through which the current flows.

Generally speaking, ρ_{coil} can be reduced using low-resistive metals. Unfortunately, there are not too many options in using different metals for coil fabrication, as copper is one of the metals with the lowest electrical resistivity.

Theoretically speaking, the phenomenon of superconductivity can be used to drastically reduce the value of ρ_{coil} and, therefore, significantly improve coil efficiency particularly when heating low-resistive metals. Study shows that due to the phenomenon of superconductivity when heating aluminum billets, a coil electrical efficiency can be increased from about 45 up to 88%. Unfortunately, in order to create a condition for the existence of the superconductivity phenomenon it is required to have the temperature below about −250°C (−425°F). In order to create such low-temperatures, it would be necessary to use liquid nitrogen for cooling coil turns instead of water. Such an approach would result in a significant increase of the capital cost of the induction heater leading to difficulty in providing a cost-effective, reliable, and robust system. In addition, it is necessary to mention that although the coil electrical efficiency can be noticeably improved when cooling with liquid nitrogen, a system total efficiency can still suffer due to a poor efficiency of the cryogenic system itself.

Instead of trying to use different metals for coil fabrication, the coil resistance can be minimized by increasing the area of current flow. For example, it is common practice to use the Litz-wire technology in transformer design or when fabricating low-temperature pancake-type inductors for domestic cooking.

Litz-wire is a low-resistive stranded conductor consisting of numerous individually isolated fine copper wires. Study shows that the utilization of the Litz-wire cables for induction coil fabrication can improve the coil efficiency of aluminum billet heaters from about 45 up to 65% (using the above-mentioned example). However, the main drawback for wide utilization of the Litz-wire cables for coil fabrication in induction billet heaters is the difficulty of providing reliable cooling of Litz-wire cables that carry high currents.

In the late 1970s the research and development of multilayer line frequency inductors was completed by the Capenhurst Research Center, UK. This technology has been exclusively licensed to Inductoheat Banyard Ltd. (Figure 2.43). During the intervening years, Inductoheat Banyard Ltd. has refined the technique of designing and manufacturing multilayer coils. Figure 7.27 shows a multilayer disc-pair copper winding. Further theoretical study devoted to the development of multilayer coils was reported in [172]. The study shows that properly designed multilayer coils could allow one to reduce coil losses as much as 25%, particularly in the case of a single-phase coil design. Figure 7.28 shows an assembly line of multilayer induction coils.

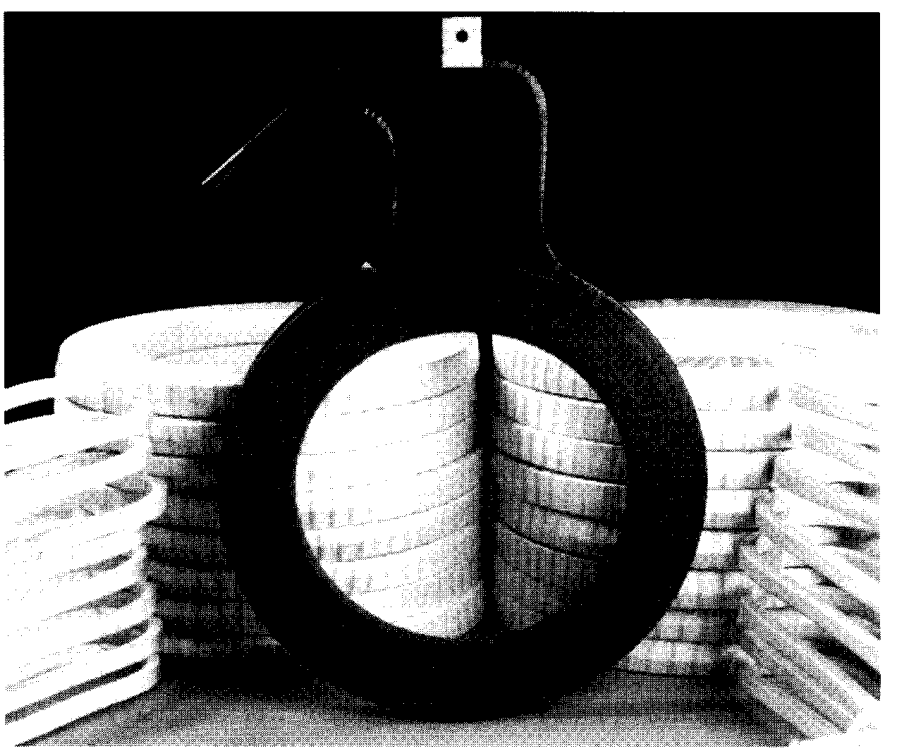

Figure 7.27 Multilayer disc-pair copper winding. (Courtesy of Inductoheat Banyard Ltd., UK.)

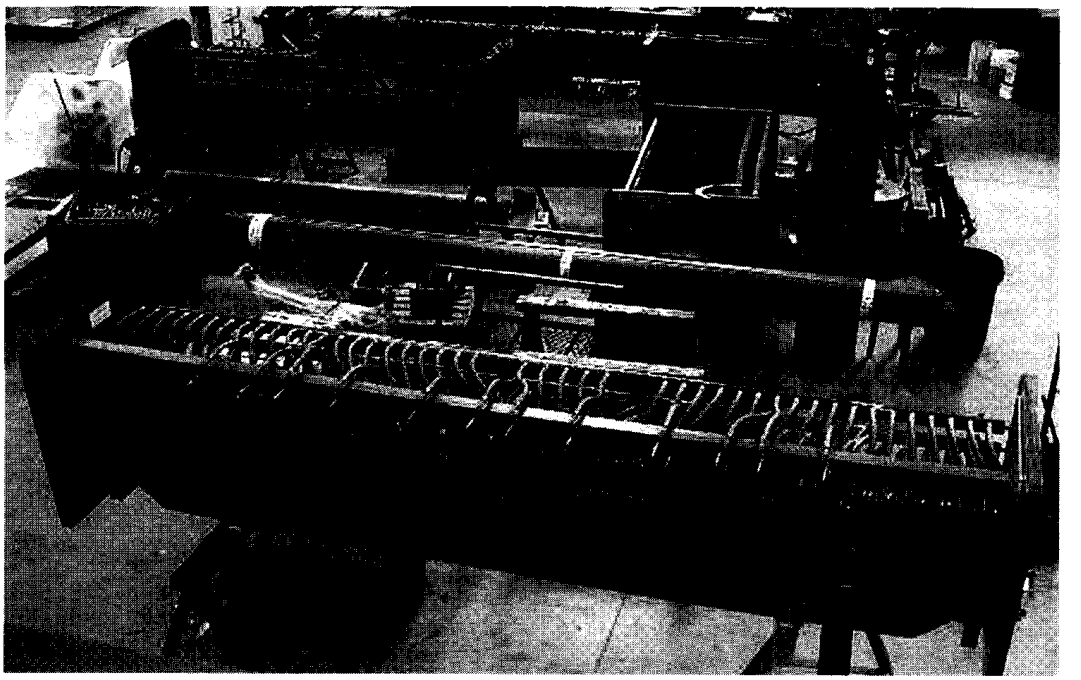

Figure 7.28 Multilayer coil fabrication/repair facility. (Courtesy of Inductoheat Banyard Ltd., UK.)

High-efficiency multilayer coils started to replace their less efficient single-layer predecessors in the late 1970s and early 1980s. A popular type of induction billet heater at that time was based on using a multilayer multiturn water-cooled coil connected to three single-phase transformers designed to provide the required kVA at the operating voltage of the coil. The transformers were provided with an offload tap switch to allow the secondary voltage and therefore the coil voltage to be varied. Because power density was voltage dependent, the taps allowed the induction heater to be set up to closely match the throughput of the extrusion press. In reality, the great majority of extruders set the heater to maximum and allowed it to go into the holding or standby stage while waiting for the next billet to be called by the press.

Another feature of the three-phase induction heater is that by setting each of the phases to a different voltage and, therefore, to a different power density, it is possible to achieve a stepped temperature profile along the length of the billet, which approximates a crude taper. Figure 7.29 shows a sketch of such a heater and the type of temperature profile it is capable of producing. Contact thermocouples positioned at depth of the current penetration on billets' end faces are used for dynamic and static temperature monitoring [399].

An advantageous ability of induction heating to provide a tapered temperature profile (longitudinal thermal gradient) along the billet's length is imperative for heating aluminum billets prior to extrusion.

Generally speaking, there are two different types of extrusion: cold extrusion and hot extrusion. Induction heating is used for the heating of billets prior to hot extrusion, that is, the process of forcing a heated metal (e.g., aluminum, copper, steel, etc.) using a hydraulic force to flow through a shaped die opening. Pressure of

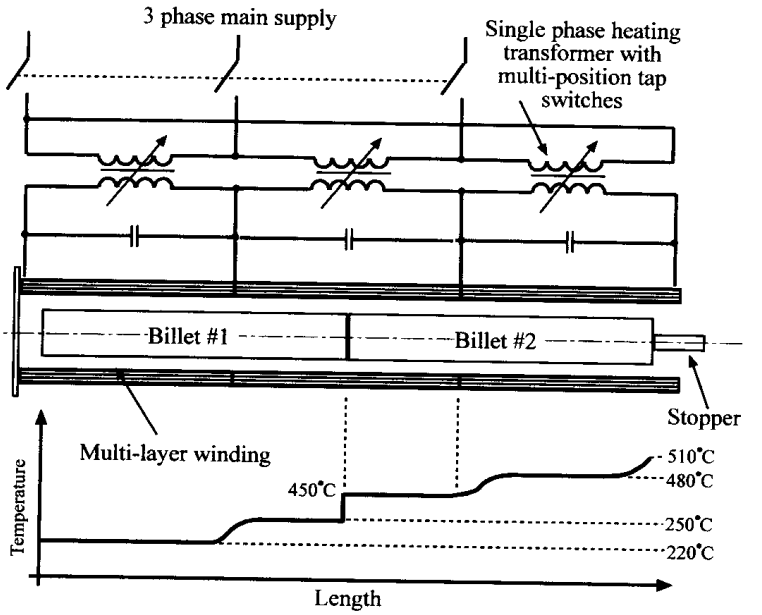

Figure 7.29 Electrical circuit of a three-phase multilayer induction heater for aluminum billets (top) and temperature profile (bottom) along the billet length.

the extrusion presses generally ranges from 500 to 5500 tonnes. Hot extrusion is used to produce long, straight metal products of constant cross-section, such as bars, solid and hollow sections, tubes, and wires that cannot be formed by cold extrusion [434, 435]. The geometry of aluminum billets that feed to the extrusion press typically ranges from 100 to 600 mm in diameter and up to 1.6 m in length.

There are basically two methods for hot extrusion: forward or direct extrusion and backward or indirect extrusion. In direct extrusion, the ram travels in the same direction as the extruded section and there is a relative movement between the billet and container. A typical metal flow pattern for direct extrusion is shown in Figure 7.30. The temperature of the extruded product varies during the extrusion process, depending on the process features including the type of extruded alloy, metal flow, ram speed, billet/container interface friction, and geometry of the extruded products. These temperature changes during hot extrusion greatly affect the mechanics of the process itself as well as the structure and properties of the extruded product.

After the heated billet is loaded into the preheated container and the beginning of the extrusion, there will be a rise in the billet temperature (Figure 7.31). There are two major sources for heat generation during extrusion:

Heat generation due to a plastic deformation, and
Heat generation due to internal shear and friction between the deforming metal and the container.

Studies show [414–416] that if ram speed is constant and the billet has been heated uniformly, the exit temperature of the extrudate rises rapidly particularly during an initial stage of the ram travel. It is beneficial to maintain the temperature of the extrudate leaving the die area at a certain optimum level, a process called an isothermal extrusion. This process provides several important benefits including a

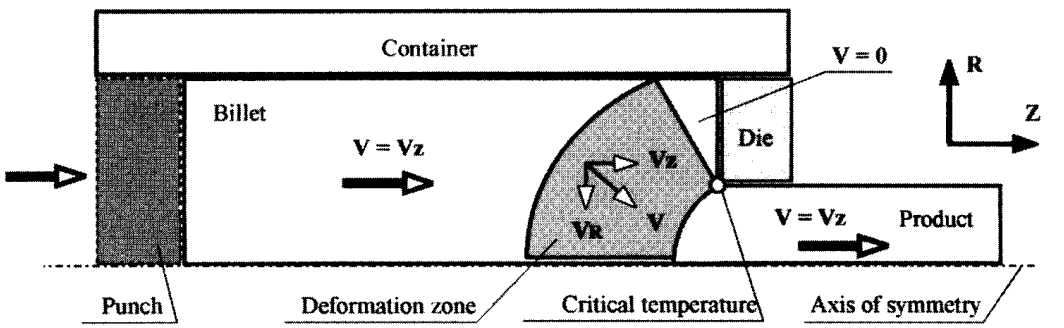

Figure 7.30 Metal flow during direct hot extrusion. (V is the velocity of the metal flow).

maximization of the quality of the extruded products resulting in more consistent product shape, microstructure, and mechanical properties. In addition, the die experiences more consistent load during the whole extrusion cycle leading to longer die life and potentially higher press production.

Isothermal extrusion can be achieved by

- Reducing the ram speed during extrusion (Figure 7.32, top): This approach results in increased cost of the extrusion press due to the necessity of having a sophisticated press control;
- Extruding at a constant ram speed a billet that has a nonuniform temperature profile. The billet should have a hot nose and cooler tail (Figure 7.32, bottom). This can be achieved by selective cooling of the uniformly heated billet, the so-called taper-cooled billet (e.g., using the water shower sprayed on the surface of the uniformly heated billet) or by heating the billet with a temperature gradient along its length. The latter process is called an isothermal extrusion of the taper-heated billet.

Therefore, nonuniform temperature profiles compensate for the heat generated during extrusion. There are several ways to obtain taper heated billets. Realization of one approach has been illustrated in Figure 7.29 using a specific induction heater arrangement. According to another approach, the hybrid approach, the billet can initially be preheated uniformly to a subfinal temperature that strongly depends upon the type of extruded alloy and extrusion practice (generally about 400°C/

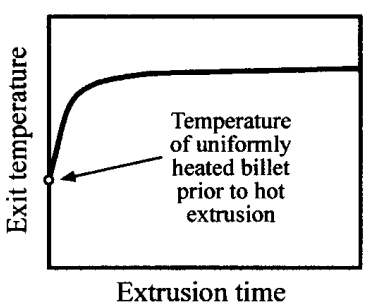

Figure 7.31 Typical exit temperature variation of aluminum products during direct extrusion (assuming a uniform temperature distribution within the billet prior to extrusion).

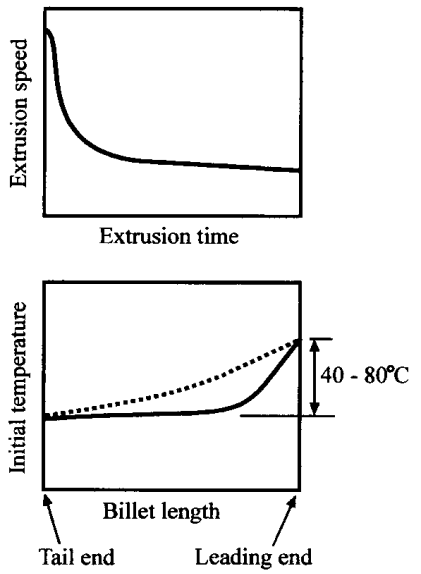

Figure 7.32 Typical variation of extrusion speed (assuming uniform initial temperature, top) and taper heating for isothermal extrusion (bottom).

752°F) using a gas- or oil-fired furnace and then finally heated using a compact and lower-power taper heating inductor. The taper heating inductor can be located between the gas-/oil-fired furnace and press. Figure 7.33 shows the influence of the nonuniform temperature profile prior to extrusion on the temperature change during direct hot extrusion of the aluminum alloys [200, 201, 205, 206].

Applications requiring certain temperature gradients upon heating call for a special design philosophy, the inverse design concept that has been developed by INDUCTOHEAT, Inc. This induction heating design philosophy requires considering induction heating not as a standalone process, but as part of an integrated system including all elements of the system: the process of induction heating, and the change in the billet temperature profile during its transportation from the heater to the extrusion press and plastic deformation, while taking into consideration the features of the particular metal forming technology (i.e., forging, rolling, extrusion, etc.).

INDUCTOHEAT's inverse concept allows designers to obtain the optimal output parameters (including end-product quality, maximum production, minimum equipment cost, maximum overall efficiency, minimum downtime, etc.) not only for induction heating machinery as a standalone process, but for optimization of the whole integrated process of induction heating–plastic deformation using the complex criteria.

Figure 7.34 shows the basic idea of INDUCTOHEAT's inverse design concept that heavily relies on the ability to use mathematical modeling of different technological operations [200]. The inverse design concept for direct hot extrusion of aluminum alloy billets includes these steps:

1. Determination of the optimal temperature pattern of tamper heated billet that will ensure an isothermal extrusion;
2. Evaluating heat transfer actions during billet transportation from the heater to extrusion press;

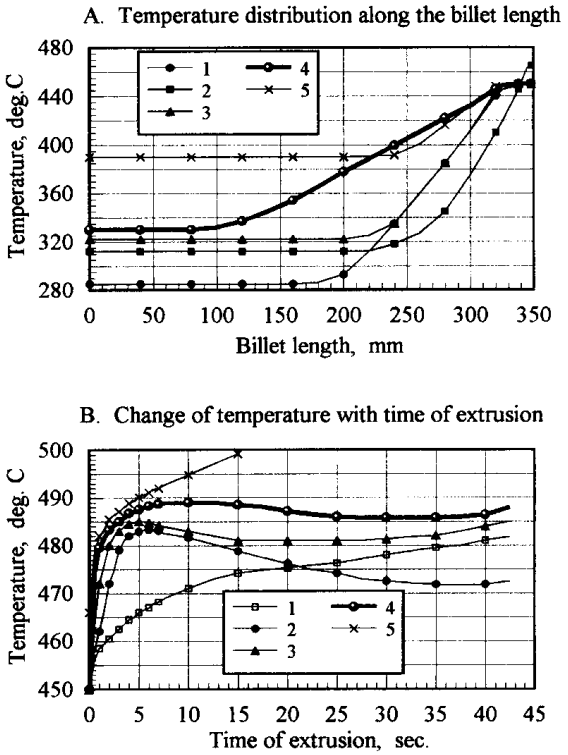

Figure 7.33 Initial temperature distribution prior to extrusion (top) and its influence on the temerature change during hot direct extrusion (bottom).

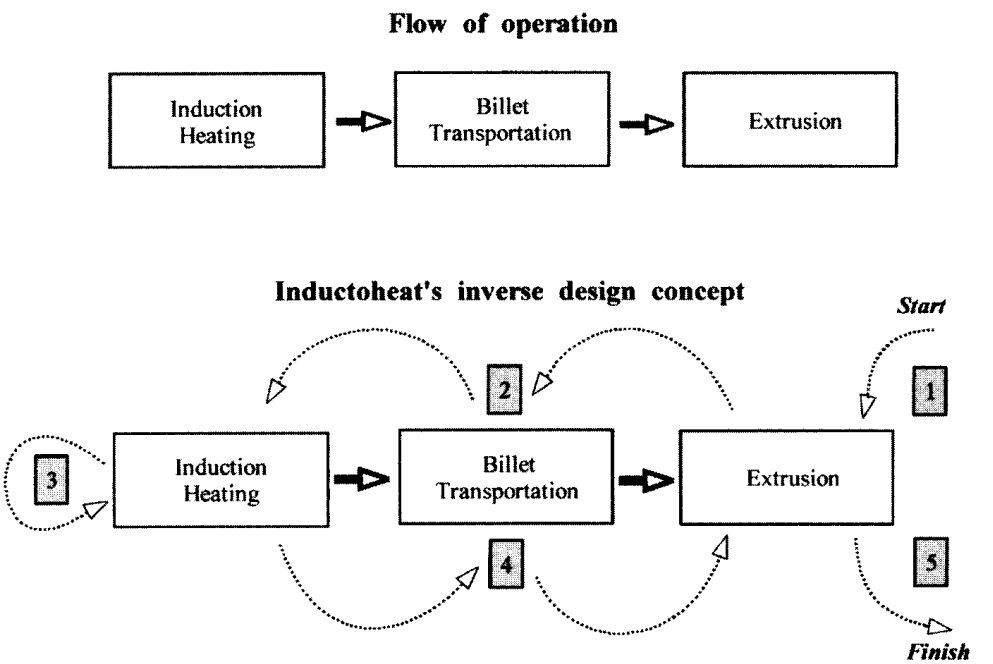

Figure 7.34 INDUCTOHEAT's inverse concept for induction taper heated billets prior to direct hot extrusion.

3. Taking into consideration the existing natural limitations in obtaining the required temperature pattern due to electromagnetic end effect, thermal edge effect, and other physical phenomena. Obtaining the best "realistic" temperature profile that can be obtained as a result of induction heating;
4. Simulation of how this realistic heat pattern will be distorted during billet transportation to the press. As soon as the billet obtains a certain temperature gradient, it starts to lose it due to the high thermal conductivity of aluminum that carries the heat from the hotter end of the billet toward its cooler end. If the soak time is sufficiently long, the billet temperature will eventually be uniform along the entire length. Therefore, a desire to heat metals that have high thermal conductivity in taper heated billets can create some concerns; and
5. Re-evaluation of the results of extrusion according to the "new" hot extrusion condition.

Induction billet heaters typically process presawn billets that were either obtained in standard length or were sawn to length immediately prior to being loaded into the heater. Although the first method was, at one time, by far the most popular method of operation, the second method has over the years increasingly gained in popularity. From the inductor design perspective, the only difference was that hot and cold billet handling needed to cater to two-part billets, and the control system needed to know the length of each billet being loaded and unloaded regardless of whether it comprised one or two pieces.

It is imperative to mention at this point that both sawing and shearing systems have their advantages and disadvantages [399]. The cold saw is a more straightforward process that produces precise square-faced billets, which is an important factor in preventing air inclusions during extrusion. On the other hand, as many as six billets can be in process prior to extrusion, and saw swarf can present a disposal problem. The hot shear has the advantage of being able to cut a billet to length just prior to its being loaded into the press, although the process in terms of mechanisms is more complicated and, if an unplanned alloy change is required, a hot log of aluminum has to be unloaded and disposed of. The face squareness, although much improved on modern shears, it is not as precise as a sawn face.

Today there are still many induction aluminum and copper billet heaters operating in conjunction with inline billet saws, enabling optimum billet length and their resultant improvement in yield to be practiced.

The more efficient multilayer coil technology also enabled log heating by induction to become economically viable. Because of the increased clearance necessary in a log heater to accommodate bow, the single-layer coil became less efficient to the point where it was very expensive to run.

The induction log heater is the type where the log of 5 m or more long is moved forward at the present speed while the induction coil is energized. Operation of such a system is shown in Figure 7.35 [399, 437]. Note that the temperature profile (temperature gradient) resulting from this type of operation is linear. This is vital to the successful operation of a heater of this type where the length of the billet to be sheared is unknown until the log reaches its final temperature. The accuracy of this

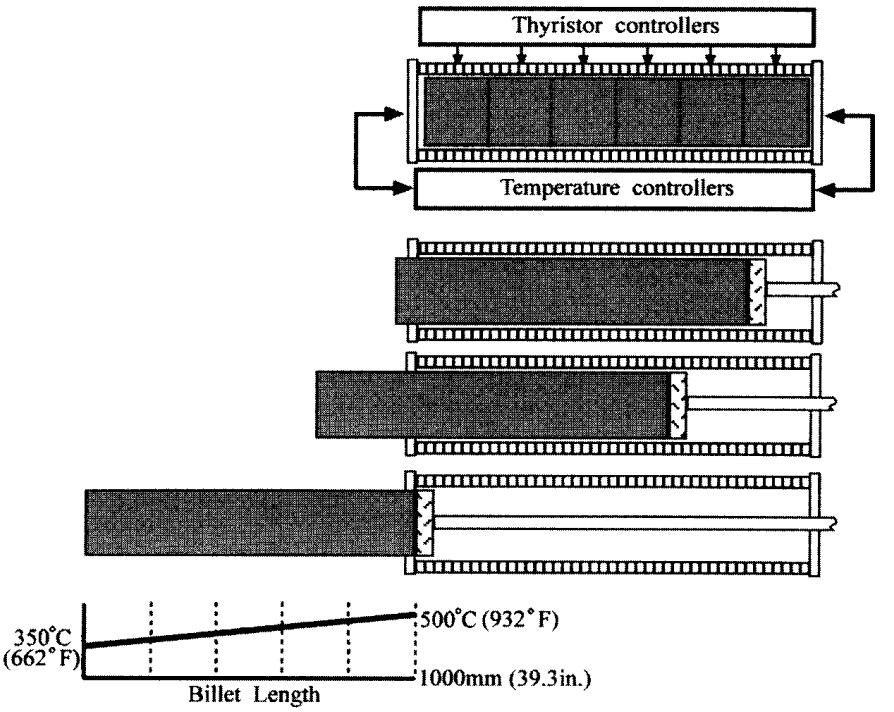

Figure 7.35 Dynamic taper heating. (Courtesy of INDOCTOHEAT Banyard Ltd., UK.)

type of heater depends upon the log being returned into the coil at a position coincident with its position prior to a billet being sheared. This repetition ensures process continuity without deviation from the required temperature profile. Obviously, if it is necessary, the linear thermal profile can be modified to match another required temperature gradient along the billet length.

A major step forward in induction billet heater design was the introduction of solid-state power switching and control. All electromechanical devices are prone to periodic failure and the main contactor used to switch a billet heater ON and OFF is no exception. Another component prone to periodic failure was the transformer tap switch. Solid-state switching (Figure 7.36) solved both the contactor and tap switch problems and at the same time opened the way to today's sophisticated induction heater power control that is discussed in Chapter 8 of this textbook.

Combined with thyristor-switched, variable power control, coil phase subdivision and logic control permit this type of induction heater to be used to impart a uniform or taper temperature profile to a billet or log in the following ways.

- Taper heating an aluminum log prior to shearing is done by advancing the log through the induction coil at uniform speed.
- An aluminum billet can be taper heated in an induction coil subdivided into, for example, six sections. Each section is controlled by contact thermocouple and the temperature changes in steps throughout the length of the billet. Figure 7.37 shows a six-phase thyristor power switching device. Utilization of special circuits allows eliminating a harmonic issue.

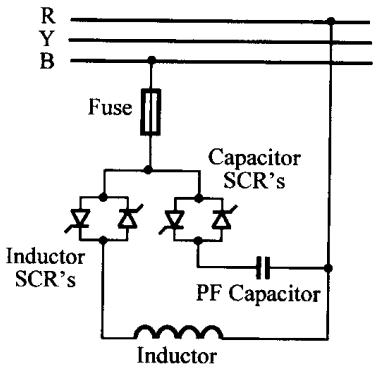

Figure 7.36 Thyristor switching ciruit. (Courtesy of Inductoheat Banyard Ltd., UK.)

- A simplification of the above system uses a short nose heater to raise the temperature of typically one-third of the billet length. Figure 7.38 shows six side entry thermocouples that provide a temperature monitoring of taper heated billets when the static heating mode is used. Figure 7.39 shows an Allen Bradley Panelview man–machine interface in combination with a specialized monitoring system for "policeman control" over the temperature.
- The dynamic heating system moves the billet and water-cooled flux extender to compensate for varying billet lengths into the energized induction heater at controlled speed to achieve the desired temperature profile.

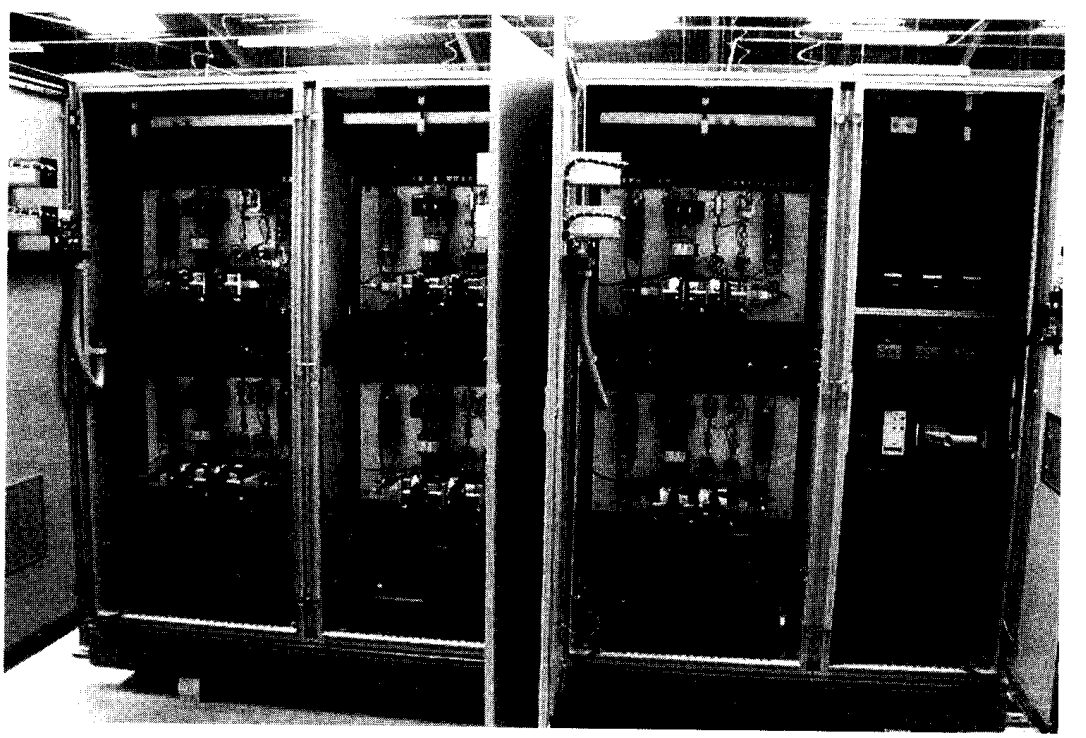

Figure 7.37 Inductoheat Banyard's 6-phase thyristor power switching device.

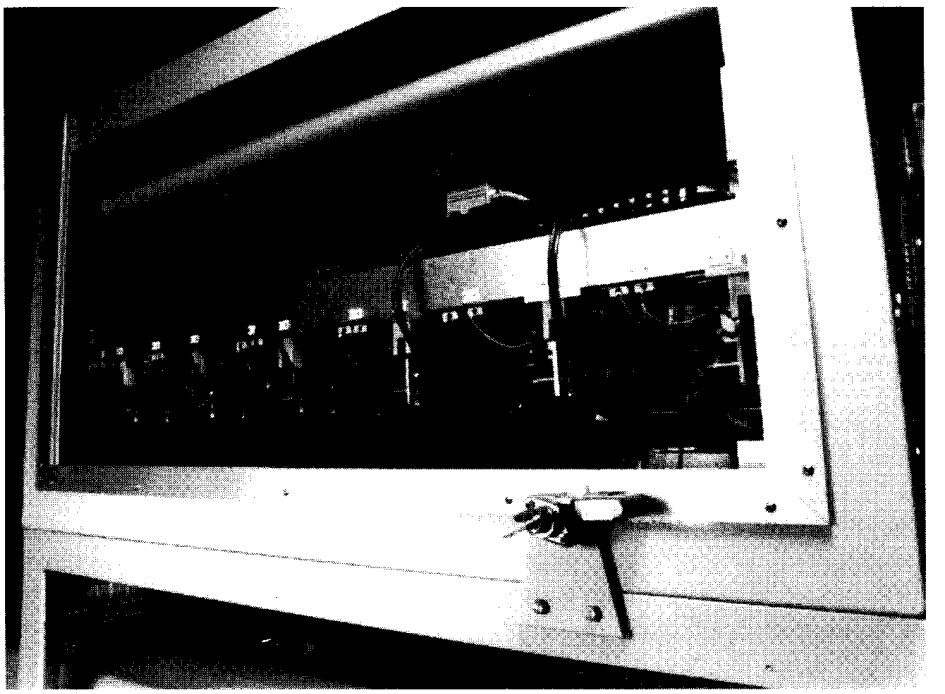

Figure 7.38 Side-acting thermocouples with visual accessibility for inspection and maintenance. (Courtesy of Inductoheat Banyard Ltd., UK.)

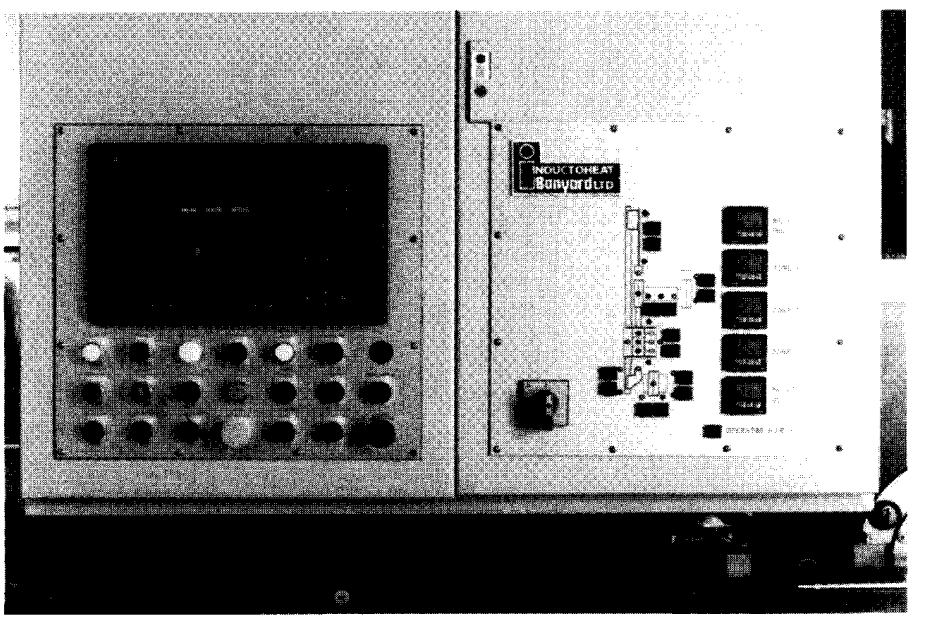

Figure 7.39 Allen Bradley Panelview man–machine interface includes heater illuminated indication assistant and billet temperature indication. (Courtesy of Inductoheat Banyard Ltd., UK.)

Figure 7.40 shows the state-of-the-art "flying-loader" noncontact single-shot dynamic taper aluminum billet heater manufactured by Inductoheat Banyard, Ltd.

In a high-production environment where it is required to heat large aluminum billets of about 1.6 m (63 in.) long and 0.8 m (32 in.) diameter, an inline multicoil design concept similar to induction heaters used for the bar/rod heating applications discussed in the previous section can be applied. According to this concept, the induction heater consists of several inline coils. The billets are pushed sequentially through the coils. However, most of the time the billets are immobile in the induction heater and move only when a new billet arrives. The overall length of the induction line can be up to 12 m (40 ft) long.

Normally, the heating process is controlled by the output temperature of the billet located in the final heating position. By using the thermocouples at the final position of the inline heater, the control system allows one to obtain the optimal output parameters of the induction heating installation for the particular type of billet.

However, the modern aluminum industry is required to meet the needs of a variety of different billet mixtures including alloys, geometry, and required final temperatures. This production mix has an essential negative influence on the effectiveness of any heating system, especially when the mixture consist of several groups of billets. In the most complicated case (but certainly not an exotic one) each group could consist of a low quantity of billets (i.e., a group of one or two billets) that must be heated for hot extrusion.

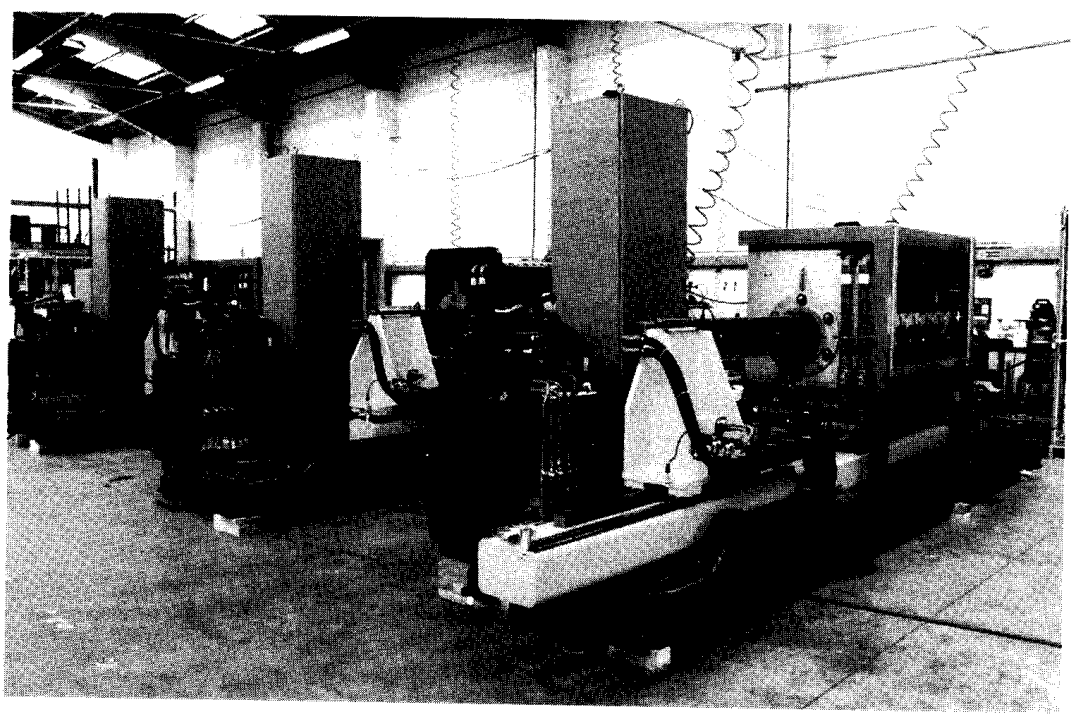

Figure 7.40 "Flying-loader" single-shot noncontact dynamic taper aluminum billet heater (billet OD = 228mm). (Courtesy of Inductoheat Banyard Ltd., UK.)

With gas or resistive heating, a change in the required final temperature can take more than one hour to set up the process. This leads to significant extrusion equipment downtime. When dealing with these billets' mixture, nothing can compare to the flexibility of induction heating.

Traditionally, induction heating machines used several "dummy" billets in the line to achieve the desired temperature profiles of the billets during the billet mixture change. There are some obvious limitations with this traditional approach, including the

Large number of "dummy" billets required,
Energy required to heat the large number of "dummy" billets,
Problems of rejection and storage of hot "dummy" billets, and
Appreciable downtime of extrusion equipment.

An alternative advanced approach developed by Dr. E. Rapoport and co-workers [170, 195, 207, 238, 239] allows the optimization of induction heater operation. In order to illustrate that approach, let's consider the simple example shown in Figure 7.41. The induction heater consists of six inline coils (C1 through C6). Normally, five billets are progressively heated in this heater. Let's assume that, due to a production mix, after heating a group of five billets (group #1), it is

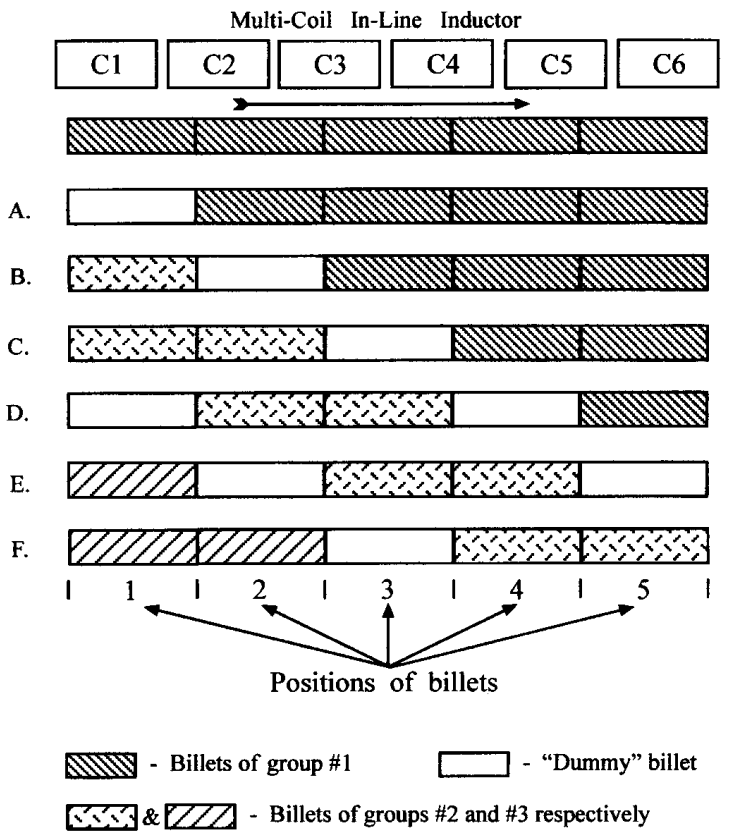

Figure 7.41 Advanced approach to optimizing transient processes with inline induction heating of large aluminum billets.

necessary to heat the group of two billets (group #2) up to the final temperature (T_2) that is higher than the required final temperature of group #1 (T_1). Then, after heating two billets of group #2, it is necessary to heat a group of five billets (group #3) to the temperature T_3 that is lower than T_1 ($T_3 < T_1$). Due to the significant inertia of the gas-fired or resistance furnace, that simple change in the production mix causes significant downtime.

A proposed alternative solution allows one to significantly decrease that downtime and increase productivity of the heater. According to this approach, each group of heated billets is divided by a single "dummy" billet. When the first billet of the new group is pushed into the first coil, the microprocessor computes the location of all billets including the "dummy" billet. The process of heating group #1 billets is conducted as a function of the temperature of the output billet. At the same time, the heating of new billets (group #2) is controlled as a function of input energy required providing a necessary heat. This energy is calculated as a function of the final temperature, geometry, and chemical composition of the group #2 billets.

With time, the last billet of group #1 will be at the final heating position. In this case, the power of coils C5 and C6 will be controlled as a function of the temperature of the output billet. The group #2 billets will be located in the coils C2 through C4. Therefore, the power of these coils will be controlled as a function of the required energy.

A new "dummy" billet will be placed after the last billet that belongs to group #2 followed by incoming billets of group #3. When the first billet of group #2 is at the final heating position, the microprocessor will switch control of the coils with those billets as a function of the new required temperature (T_2). Similar to the previous stage, the heating process of billets that belong to group #3 will be performing as a function of their required energy.

The above-described approach minimizes downtime of the extrusion presses and allows one to develop a highly flexible, efficient, and precise induction heating system that can handle the wide range of the billets' mixture. For example, several single billets that require different heating recipes can be heated simultaneously inside the same induction heater.

7.4 BAR/BILLET/ROD END HEATING

Although many of the bars, billets, or rods being manufactured today lend themselves to processes in which entire workpieces are heated and fed into a roll former or other type of forming machine, in some cases it is required to hot form only a certain part of the workpiece, for example, its end. Therefore, in cases like this it is required to heat only the end area of the workpiece. Some examples of these types of parts are "sucker rods" for oil country goods or various structural linkages in which an eye or a thread may be added to one or both ends of the bar.

Induction bar end heating is generally accomplished by placing the end of the bar in a multiturn coil and heating it for a specified amount of time. The choice of design parameters when heating ends of bars, billets, and rods is similar to cases when it is necessary to heat a whole body. Table 7.3 (Sec. 7.2) shows a minimum bar diameter as a function of frequency and temperature for efficient induction heating of selected metals. At the same time, there are some specifics.

As with all through heating applications a sufficient time is necessary to obtain a required surface-to-core temperature uniformity, and the choice of frequency affects not only temperature uniformity but the overall efficiency of the system as well. Some bar heating applications require a specific temperature profile along the length of the workpiece, including sharp or gradual cutoff of the heat or certain length of the transition zone (temperature profile of the transition zone).

In its simplest form, a single-shot heat mode with manual loading can be used to heat the end of the bar by placing the workpiece into the proper position within a coil allowing appropriate power at a given frequency to do its work to provide the required production.

Heating time can be roughly estimated by one of the long-standing rules of thumb discussed earlier or more accurately using numerical modeling. The power required could be estimated by using a production rate and specific heat approach or the heat content techniques discussed in Section 3.3.1.

In continuous bar heating applications using inline inductors it is easier to predict the expected steady-state temperature distribution and obtain the required temperature profile in the bar than in the case of bar end heating applications. Basically, this is because, as has been shown above, each part of the bar in end-to-end progressive heating experiences the same magnetic flux with respect to time as it is being heated. On a bar end heater it is a much different story, and more variables are involved in obtaining the required temperature profiles within the bar end.

Multiple bar ends can be heated in a single-turn or multiturn oval coil (Figure 7.42), as well as in a channel-type coil, also sometimes called a slot or skid coil (Figures 7.43 and 7.44), or in two, three, four, or more coil arrangements configured from individual conventional solenoid coils [117, 203, 285]. Multiple coils are used to increase the production rate.

In the case of a channel coil (Figures 7.43 and 7.44), typically the magazine-loaded bars are removed by carriers, for example, on a belt, and the end of the bar to be heated passes through the channel coil. Upon leaving the coil, the end of the bar is at the required temperature, and the bar moves to the forging operation.

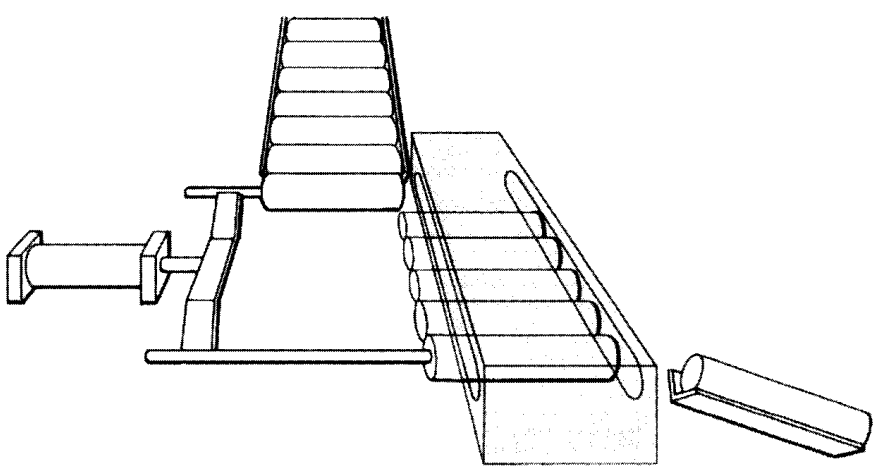

Figure 7.42 Oval coil bar end heater.

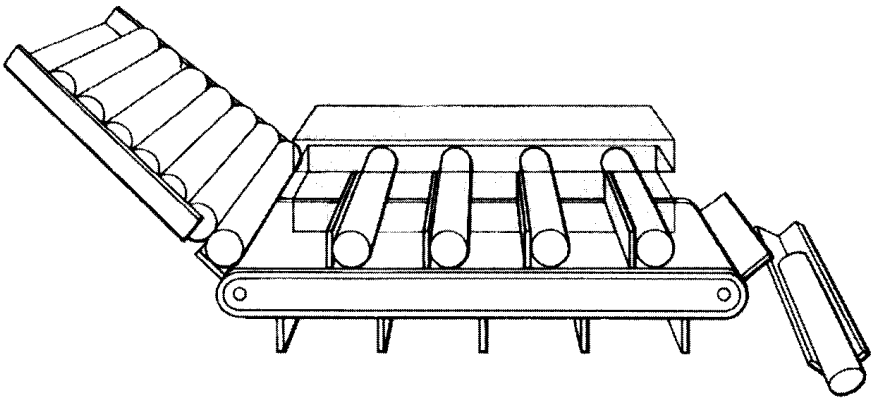

Figure 7.43 Channel coil bar end heater.

Efficiency suffers when using channel-type coils and a further detriment is the uneven heating along the bar perimeter. Due to the electromagnetic proximity effect (Sect. 3.1.3), the heat is induced into the areas of the bars closest to the coil at a greater rate than the areas that are located farther away (Figure 7.45). This phenomenon may result in a noticeable temperature nonuniformity that can cause problems during the subsequent metal forming operation.

Low heating intensity and subsequent increase of the heat time results in a more intensive soaking action within the bar cross-section that is conducted because of thermal conductivity. However, some undesirable effects may occur. First, an increase in the heat time leads to a favorable condition for formation of an unaccep-

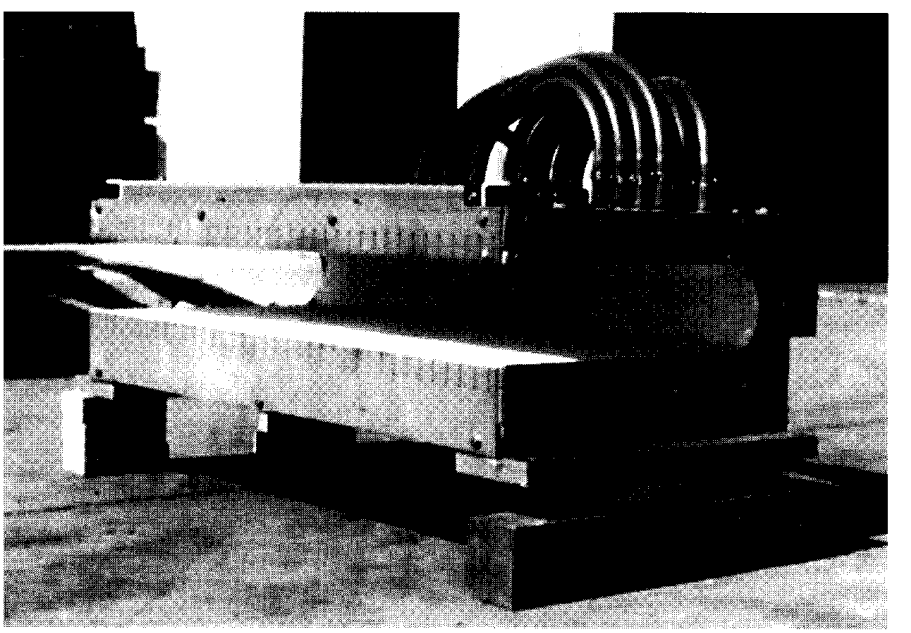

Figure 7.44 Channel coil bar end heater. (Courtesy of Inductoheat–I.H.S. Corp., Fort Worth, TX.)

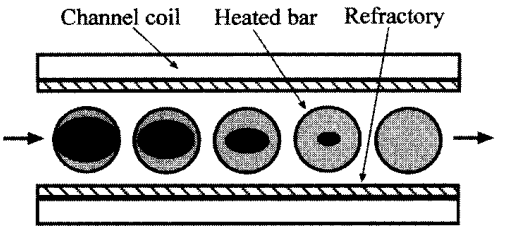

Figure 7.45 Heat nonuniformity when heating bars in a channel coil.

table amount of metal loss due to scale. On the other hand, letting the heat soak through the bar cross-section will result in heat soak along its length providing undesirable heating of the cold end. This leads to energy waste. Often, heat intended for the billet ends up heating the fixture, resulting in premature equipment failure and reduced reliability due to the effect of excessive heat.

The oval coil is a more efficient way of bar end heating than the channel coil. In the case of the oval coil design (Figure 7.42), bars are loaded into a magazine from which they are pushed, one at a time, into the upper end of an inclined oval coil. They roll down as previous bars are removed.

When using the channel coils, there might be the added complication of having to insert the parts into the coil at a fixed depth and holding them at that relative location while bars travel through. By the time a bar reaches its final heating position inside the coil it will have obtained the required thermal condition and will be pushed out for delivery to the forming machine.

Nevertheless, for a high production rate (i.e., up to 1800 pieces per hour or even higher) both oval- and channel-type inductors become virtually the most suitable possibilities and are often employed with auto handling. It should be mentioned, however, that these types of coils are not very well suited to heat bars with long heated lengths.

It is important when applying the oval or channel coil design concepts to pitch the heated workpieces as close together as possible; however, the mechanical aspects of the machine may constrain having a very small pitch. While in process, it is important to keep the heated parts centered within the coil; otherwise, an additional uneven heating problem might occur due to the proximity effect.

The choice of a particular type of induction bar/billet/rod end heater arrangement depends upon the application and the customer's preference. However, because the highest efficiency and the best temperature uniformity are obtained with a solenoid coil, every effort should be made to use it wherever possible.

In addition to the variety of coil arrangements, the loading/unloading operation can be fully automated, semiautomated, or manual; the choice depends on the required production rate and the cost of equipment.

For low outputs, components may be indexed through several solenoid coils. At the same time, as the production rate increases, the number of coils rises, and time lost in the index process becomes progressively more significant. It should be noted that although the time when bars are not within the coils during indexing leads to extra heat losses and subsequently requires a higher installed power compared to the case where the heated components remain within the coil. Nevertheless, the time when heated bars are outside the coil is still valuable in providing the required heat

uniformity and avoiding surface overheating since surface-to-core soaking action continues during indexing.

Manual or semiautomated designs where the operator simply removes the hottest bar and replaces it with a cold bar before it is moved to the forming hammer, press, or upsetter is the least expensive approach. Figure 7.46 shows two typical semiautomatic loading/unloading methods using multiple solenoid coil arrangements. As an example, Figure 7.47 shows Radyne's 700 kW/3 kHz 10-station semiautomatic bar end heater, producing 400 bar ends per hour heated up to 1232°C (2250°F). It has single-load and unload positions.

The fact that in the induction bar end heater the bar is only partially inserted in the heating coil leads to the difficulty of using analytical and equivalent circuit coil design methods to compute this process, because those methods are based on the assumptions of an infinitely long coil and symmetrically located workpiece within the coil. Such assumptions are not valid for the induction bar end heater, which in most cases cannot be considered an infinitely long system. As a result of such limitations, those computation techniques have limited use in providing an accurate prediction of the power density and temperature distribution within the heated end of the bar end. From another perspective, the extreme end of the workpiece offers no thermal path for the conduction of heat, whereas its cold end provides a ready heat sink and easy conduction path.

Although there is a variety of bar end heating coil design arrangements and alternatives, the basic principles in obtaining the required temperature profile within the bar end are quite similar. Consequently, we discuss the features of the design and operation of the induction bar end heater by analyzing a conventional multiturn solenoid coil design (Figure 7.48).

In the case of the induction bar end heater, the temperature distribution within the bar is affected, among other factors, by the electromagnetic end effect which represents a distortion of the electromagnetic field in the extreme end of the bar and

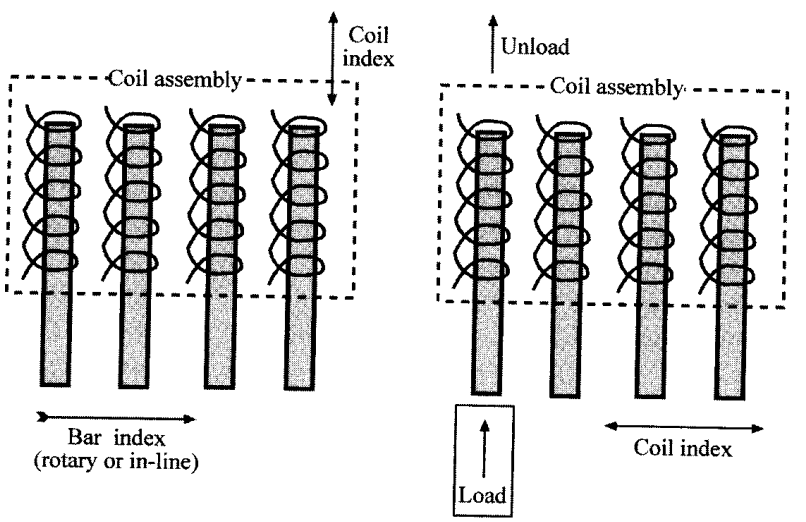

Figure 7.46 Two typical semiautomatic loading/unloading approaches using multiple solenoid coils.

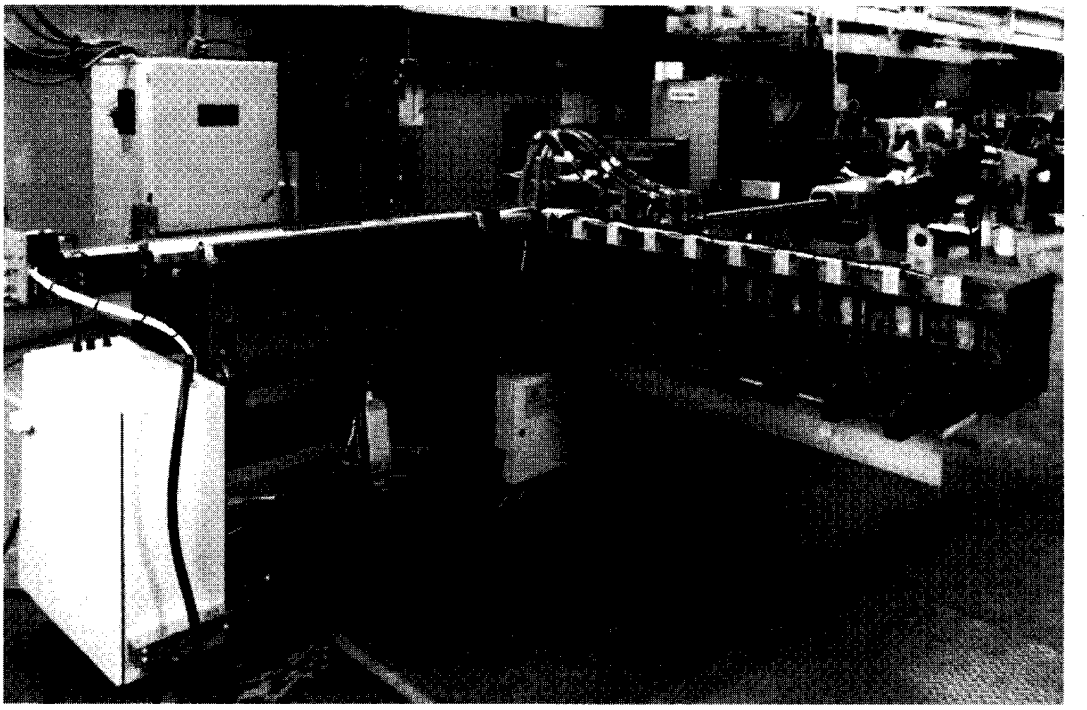

Figure 7.47 Radyne's 700 kW/3 kHz 10 station semiautomatic bar end heater. Producing 400 bar ends an hour up to 1232°C (2250°F). Single load and unload position.

induction coil end zone (Figure 7.48). These end effects may be illustrated by the curves in the lower diagram of Figure 7.48, zone *"a"*.

As discussed in Section 3.1.7, the electromagnetic end effect in the extreme end of the cylindrical bar is defined by four variables; $\mathbf{R}/\delta$, the skin effect; σ the coil overhang; the ratio $\mathbf{R_i}/\mathbf{R}$, and coil turn space factor K_{space}, where $\mathbf{R}$ is the radius of the bar and $\mathbf{R_i}$ is the inside radius of the coil; and δ is the current penetration depth.

An incorrect combination of these factors can lead to under- or overheating the extreme end of the bar. Studies show that when heating carbon steel bars the electromagnetic end effect area may extend toward the central region of the bar no farther than 1.5 times the bar diameter. Higher frequency and large coil overhang lead to a power surplus in the extreme end of the bar. As a result, noticeable overheating may take place in that area. Low frequencies, large coil-to-bar radial gaps, and small coil overhang will cause a power deficit at the extreme end of the bar, which will therefore be underheated.

We point out here that a uniform power distribution along the extreme end of the bar will not correspond to its uniform temperature profile because of the additional heat losses (radiation and convection losses) at the bar's extreme end area compared to its central part. By the proper choice of design parameters, it is possible to obtain a situation where the additional heat losses at the end of the bar are compensated for by the additional power (power surplus) due to the electromagnetic end effect. This will allow the designer to obtain a reasonably uniform temperature distribution within the required heated area of the bar.

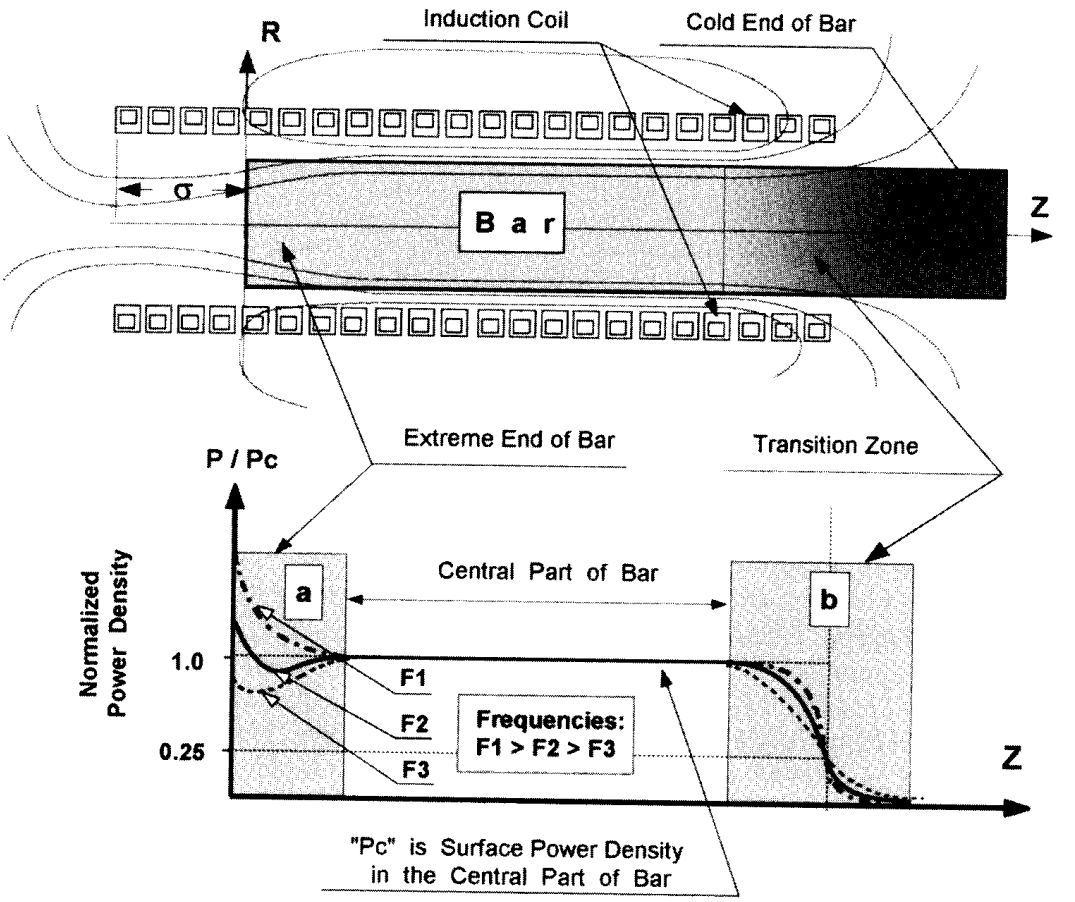

Figure 7.48 Sketch of induction heater and power distribution along the length of the bar.

The magnetic field distribution in the bar near the right end of the coil (the so-called "cold end") shown in Figure 7.48 (zone b) affects the heat transition zone and primarily depends on the radii ratio $\mathbf{R_I/R}$ and the skin effect, with the latter being most prominent. Due to the physics of the electromagnetic end effect in that area, there is always a power deficit under the coil tail end at any frequency.

As discussed in Section 3.1.7 and Appendix D, in the case of a long multiturn induction coil with a long homogeneous nonmagnetic bar (zone b), the density of the induced eddy current in the bar area located under the coil tail end is only half that in the central part. Therefore, the power density in that area is only one-fourth of the power in its central part. Typically, the length of zone b is equal to 0.5 to 3.5 times the coil radius.

It should be emphasized that in order to compensate for the power deficit within the bar area located near the cold end of the bar (zone b), the extreme end of the coil should be extended farther toward the bar cold end. In other words, the coil length should be longer than the required uniformly heated area of the bar end.

Another important feature that defines the coil length is the fact that in zone b, which is often called the transition zone, there is a significant temperature gradient along the length of the bar. As a result, heat is conducted from the high-temperature

region of the bar toward its cold area, the heat sink phenomenon (zone b). This phenomenon is more pronounced when heating metals having high thermal conductivity (e.g., Al, Cu, etc.). The proper choice of coil geometry, power density, and frequency will allow one to compensate for this cooling effect and obtain the required uniform temperature profile for the bar with a minimum transition zone.

Often, there is a limitation on the permissible length of the transition zone. A short cycle time, high power density, small coil-to-workpiece radial gap, and high frequency help to make this zone shorter.

The fact that in the induction bar end heater the bar is only partially inserted in the heating coil leads to the difficulty of using analytical and equivalent circuit coil design methods to compute this process, because those methods are based on the assumptions of an infinitely long coil and symmetrically located workpiece within the coil. Such assumptions are not valid for the induction bar end heater, which in the great majority of cases cannot be considered an infinitely long system.

From another perspective, the extreme end of the workpiece offers no thermal path for the conduction of heat, whereas its cold end provides a ready heat sink and easy conduction path. Heat flow occurring due to the heat sink effect not only leads to redistribution of the temperature pattern but also affects the amount of mass being heated that would in turn affect the amount of energy required to heat the bar end. Over the years, some recommendations have been developed for providing a rough estimate of the heat sink effect. As an example, Figure 7.49 shows an equivalent additional distance added when determining heated mass and required power.

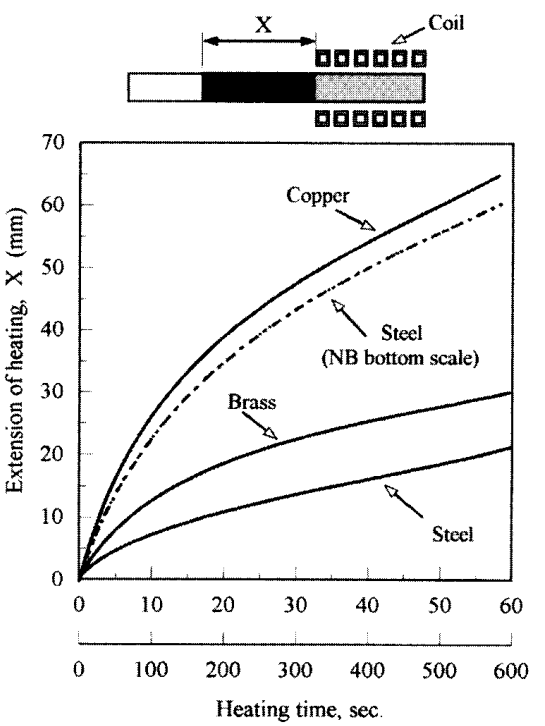

Figure 7.49 Equivalent additional distance that should be added when determining a heated mass and required power in bar end heating applications. (From Ref. 472.)

Restrictions of the analytical and equivalent circuit coil design methods as well as recommendations for rough estimation of the of heat sink effects result in the limited use of these techniques. An accurate prediction of the power density, temperature distribution within the bar ends, and required coil design parameters can be conducted using numerical analysis.

As an example, Figure 7.50 shows a sketch of an induction carbon steel (AISI-SAE 1035) bar end heater that will be modeled using a numerical technique. The outside diameter of the bar (OD) is 25.4 mm (1 in.). The dynamics of the induction carbon steel bar end heating process are shown in Figure 7.51.

The analysis of the results of numerical modeling shows that in the first heating stage the whole bar is magnetic (cycle time < 3 sec), and its relative magnetic permeability is high (Figure 7.51). Therefore, the skin effect is pronounced ($\mathbf{R}/\delta > 20$). At the same time, due to a relatively low temperature, the heat losses from the bar surface are relatively low. Because of the pronounced skin effect, the induced power appears in the fine surface layer of the bar. No power is induced into its inner layers. The core of the bar is heated from the surface only by thermal conductivity. Consequently, the surface of the bar is heated much faster than the core. This stage of heating is characterized by a high-temperature gradient along the radius of the bar.

With time (cycle time about 5 sec), as a result of surface temperature rise, the surface of the bar starts to lose its magnetic properties and the relative magnetic permeability in the surface layer drops to 1. Furthermore, because of the temperature rise, the electrical resistivity of the carbon steel increases to approximately 1.5 to 2.5 times its initial stage value. The decrease of relative magnetic permeability and increase of electrical resistivity cause a noticeable increase in the penetration depth. As a result, an essential portion of power is now induced in the internal layers of the bar. This stage can be characterized as the biproperties stage of the bar. In this stage the bar surface becomes nonmagnetic; however, the internal area of the bar and its core remain magnetic. The surface-to-core temperature difference here is not as significant as it was in the first stage.

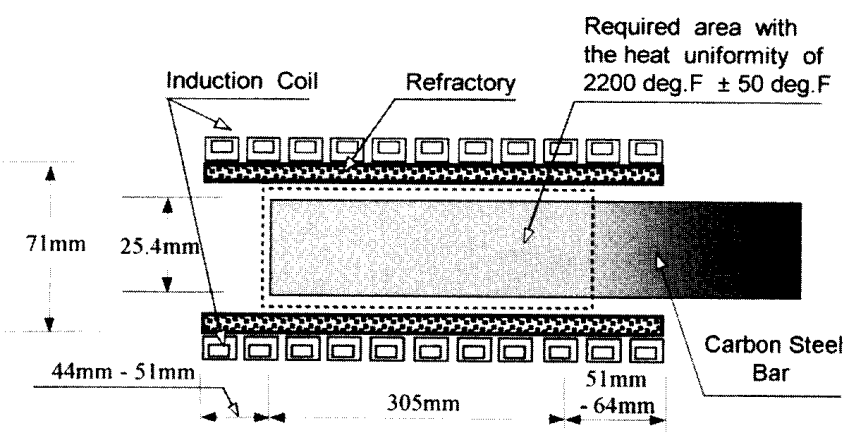

Figure 7.50 Geometry of induction bar end heater: Frequency = 9 kHz; heat cycle = 36 sec; coil turns = 9 turns; length of billet = 0.46 m (18 in.)

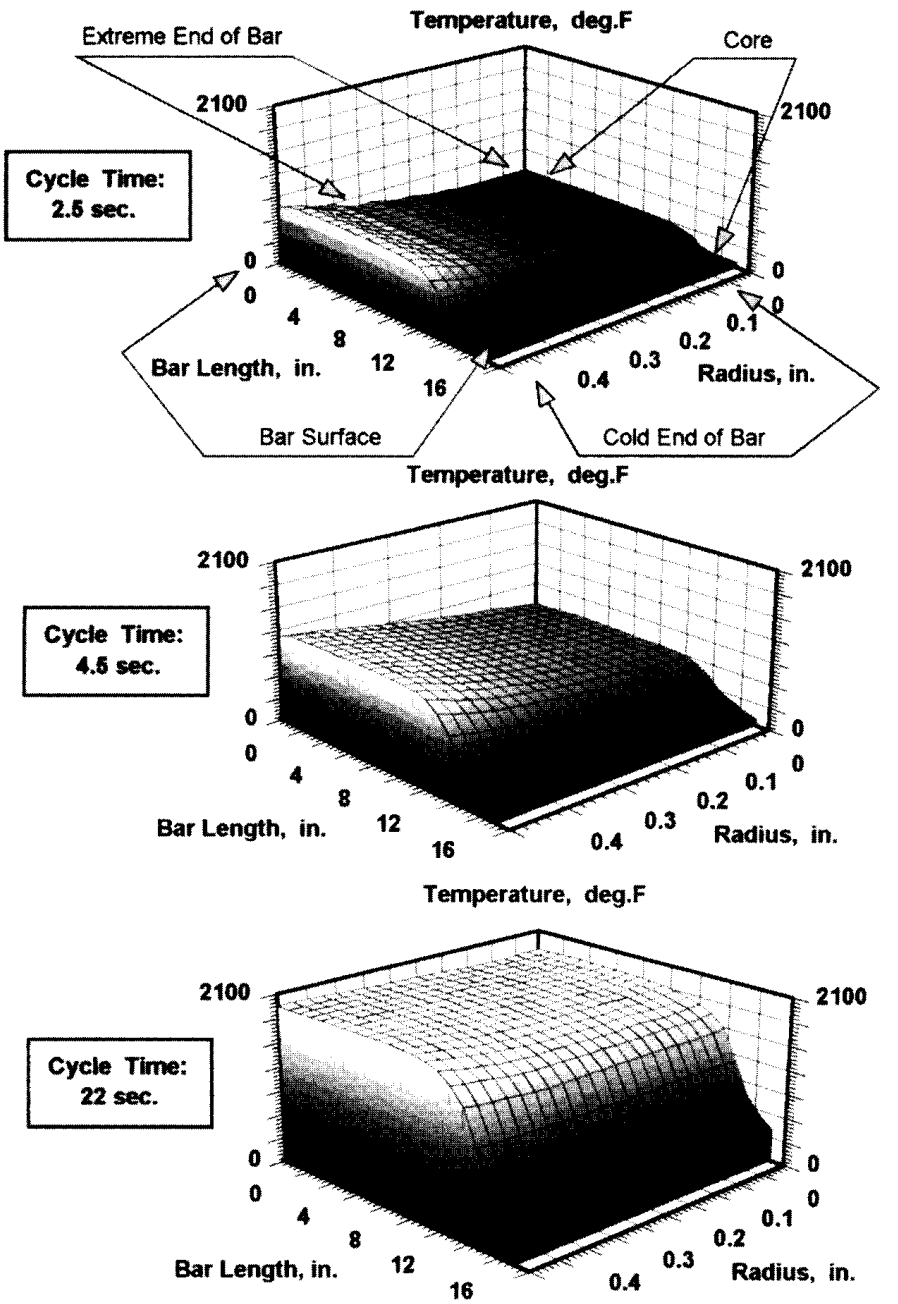

Figure 7.51 Dynamics of induction carbon steel bar end heating.

Finally (cycle time approx. 15 sec), the total bar area located under the coil, including the core of the bar, becomes nonmagnetic. The penetration depth becomes quite large and the skin effect becomes less pronounced ($\mathbf{R}/\delta < 2.5$). As a result, a significant amount of energy is induced within the internal area of the bar, and the core starts to heat noticeably more intensely than in the previous two stages. Furthermore, the heat losses from the bar surface become relatively high (primarily due to radiation losses). Because of the large penetration depth, increased heat losses

from the surface of the bar, and thermal conductivity within the bar, the temperature profile within the radius will equalize (cycle time of 22 sec).

Often, the need for a bar end heater involves equipment that can be used for a wide range of workpiece sizes. The coil arrangement in Figure 7.50 can provide satisfactory results in induction end heating for bar diameters as small as 9.5 mm (3/8 in.).

Obtaining required temperature uniformity along the length of the bar by choosing a proper coil overhang is only one of the possible design approaches. Figure 7.52 shows a variety of end heating design concepts that provide uniform heating using a multiturn solenoid coil.

One of the examples of a commercial induction bar end heater is shown in Figure 7.53. This inexpensive portable induction system (Unipower UPF) can be used in forging applications as well as for bright annealing of stainless steel tubing, upsetting, stress-relieving pipe and rod, and other induction heating applications. These machines with output frequencies of 1 to 30 kHz provide output power of 25 to 400 kW.

Unipower UPF systems have a built-in control, output transformer (depending on the application), and heat station for standalone operation. They have a broad power-matching capability to deliver full power throughout the heating cycle. Precise power settings are ensured within 2% accuracy with 10% line voltage variance. All the controls necessary for independent operation are built into the machine or located on an optional remote operator's panel. Controls include a single meter

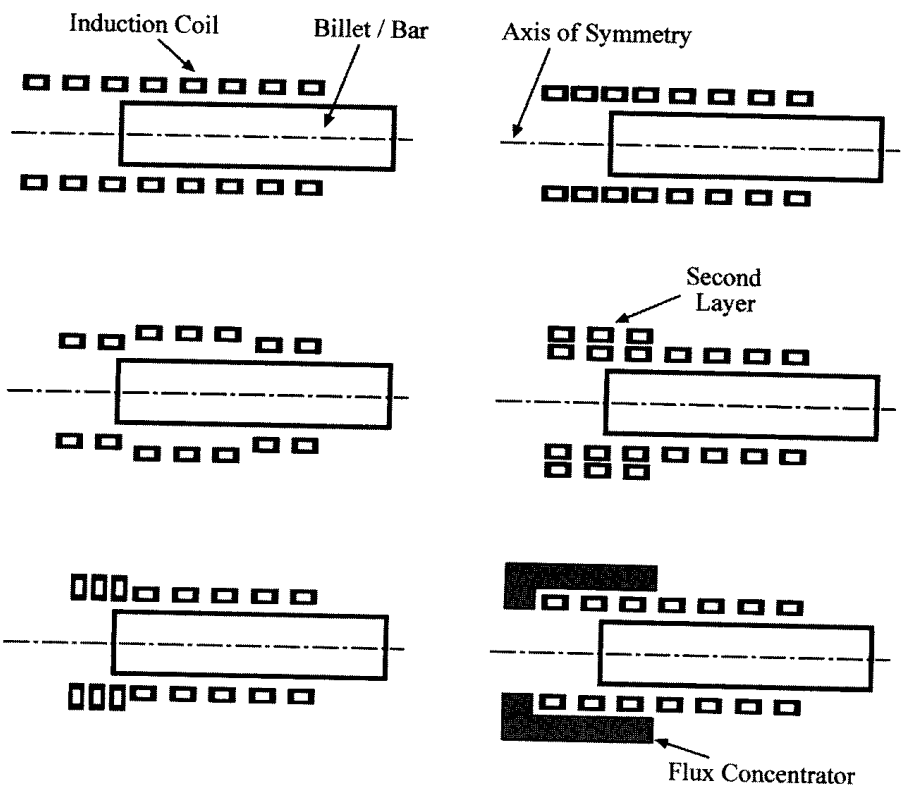

Figure 7.52 Basic concepts of induction bar end heaters.

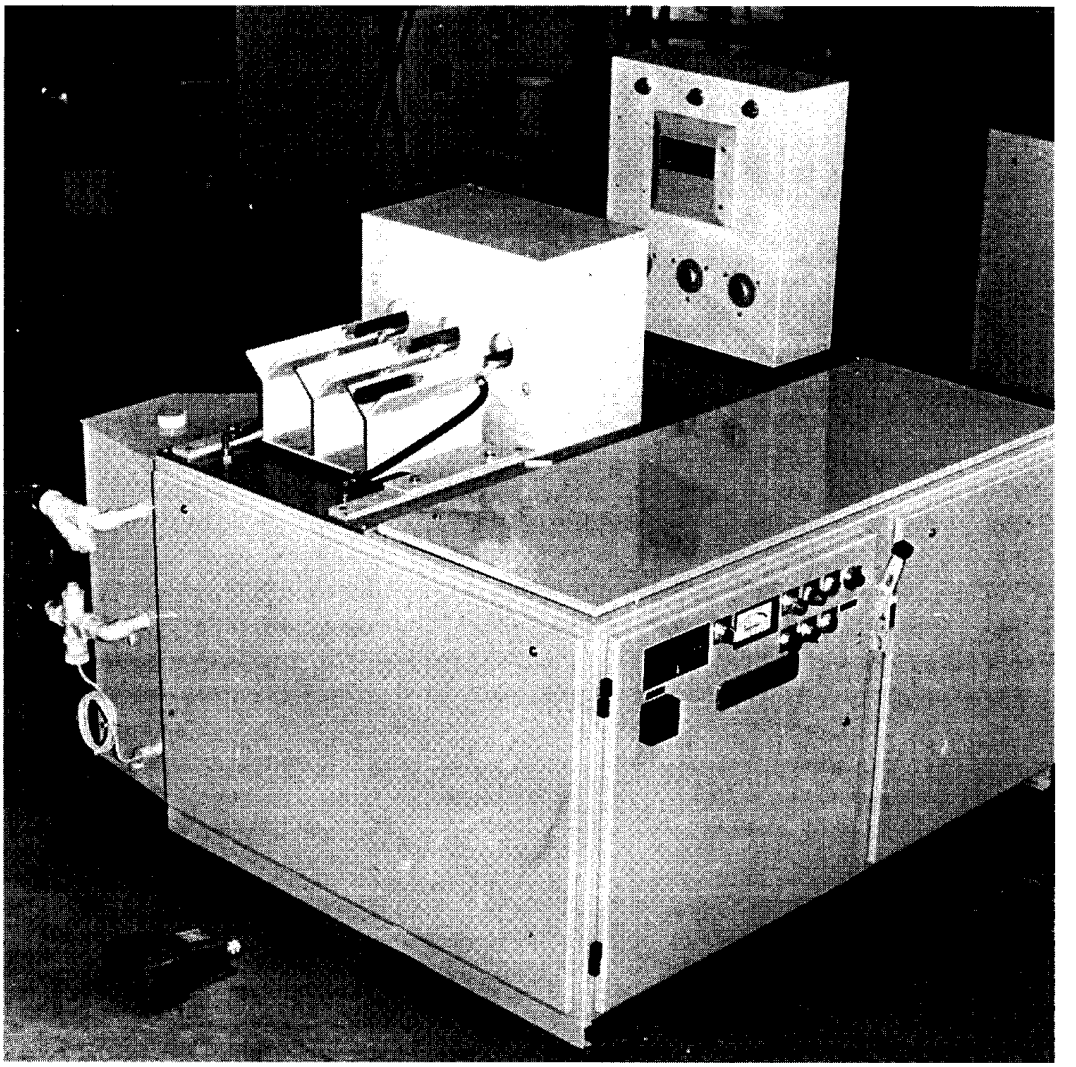

Figure 7.53 Low-cost portable induction bar end heating system UNIPOWER UPF. (Courtesy of INDUCTOHEAT, Inc., Madison Heights, MI.)

with a selector switch for monitoring kilowatts, volts, or frequency; light-emitting diodes to indicate heat status, kilowatts, capacitor volts, output volts, and output current limits; a manual/timed/auto selector switch; and built-in digital timer. Optional equipment includes a side-mounted water recirculating system, additional heat levels, and special coil assemblies. The input power factor of such systems is 0.94 under all operating conditions.

Figures 7.54 through 7.56 show other types of induction bar end heaters. Figures 7.54 and 7.55 show Radyne's unique award-winning bar end heating installation supplied to an automotive plant in the USA to manufacture 600 flanged axles per hour. The robots sequentially load and unload the 16 induction coils. Robots 1 and 2 automatically sequentially load bars into solenoid coils and robots 3 and 4 unload heated bars and place them in accept or reject position. This arrangement achieves high production and high efficiency in combination with

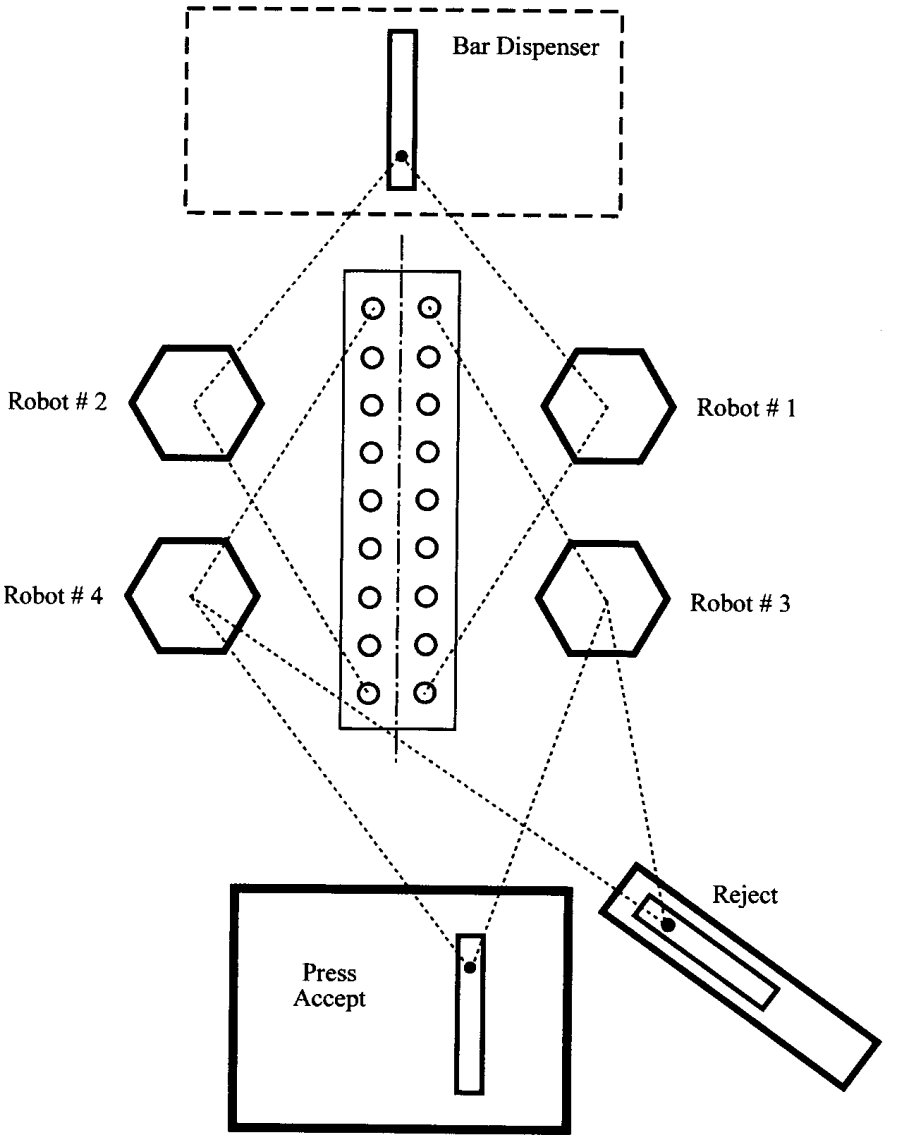

Figure 7.54 Sketch of unique Radyne's award-winning induction bar end installation.

required heat uniformity. This unique installation was the winner of the 1991 British National Committee for Electroheat's Innovation competition. The 2000 kW/3 kHz installation heats bars up to 50 mm diameter and 1 m long with heated lengths up to 380 mm for upset forging. The final temperature is 1260°C (2300°F) with a surface-to-core tolerance of 16°C (30°F). Since the first equipment was commissioned, the customer has experienced higher efficiency over the previous heating system, very accurate temperature profiles, longer die life, improved quality, and high reliability.

Utilizing the Unipower, Uniforge, and ForgeMaster design concepts, the power supply, matching components, and heating coil are all grouped together in a single package that can easily be moved from place to place.

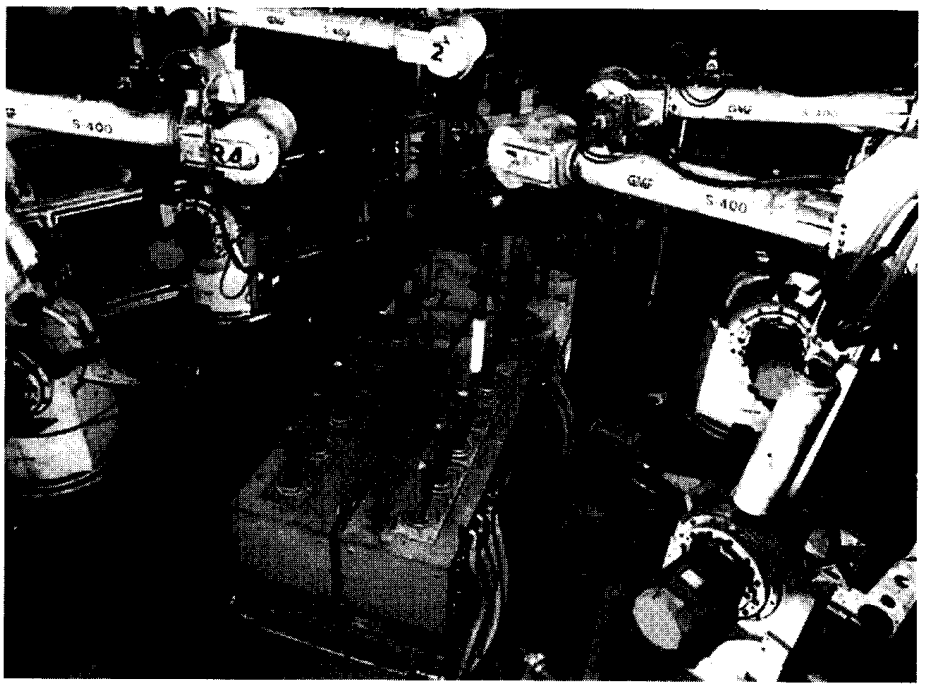

Figure 7.55 Radyne's award-winning 2000 kW/3 kHz induction bar end heater supplied to an automotive plant to manufacture 600 flanged axles per hour.

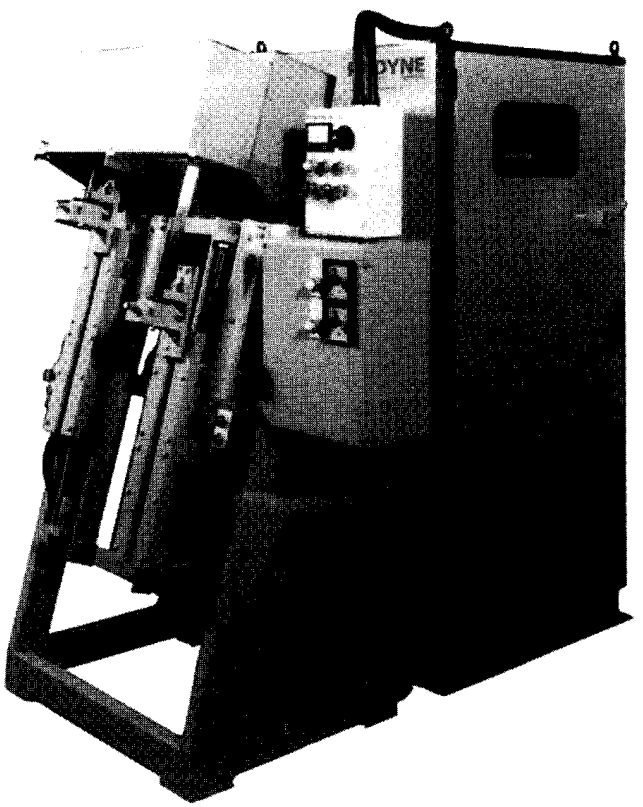

Figure 7.56 100 kW Vertical induction bar end heater. (Courtesy of Radyne Ltd., UK.)

7.5 SLUG HEATING FOR SEMISOLID PROCESSING

Semisolid metal (SSM) casting was originally developed at MIT in the 1970s. SSM casting has several advantages compared to casting in the fully liquid stage. This includes a lower level of product porosity and higher flow viscosity during casting [249, 250, 282–284]. The former provides laminar flow during casting. This results in higher quality of cast products by prevention of the entrapment of gas. Figure 7.57 shows samples produced by semisolid casting of aluminum alloys. The semisolid metal casting process consists of preheating a metal slug up to a semisolid condition (partially liquid and partially solid) followed by the casting process.

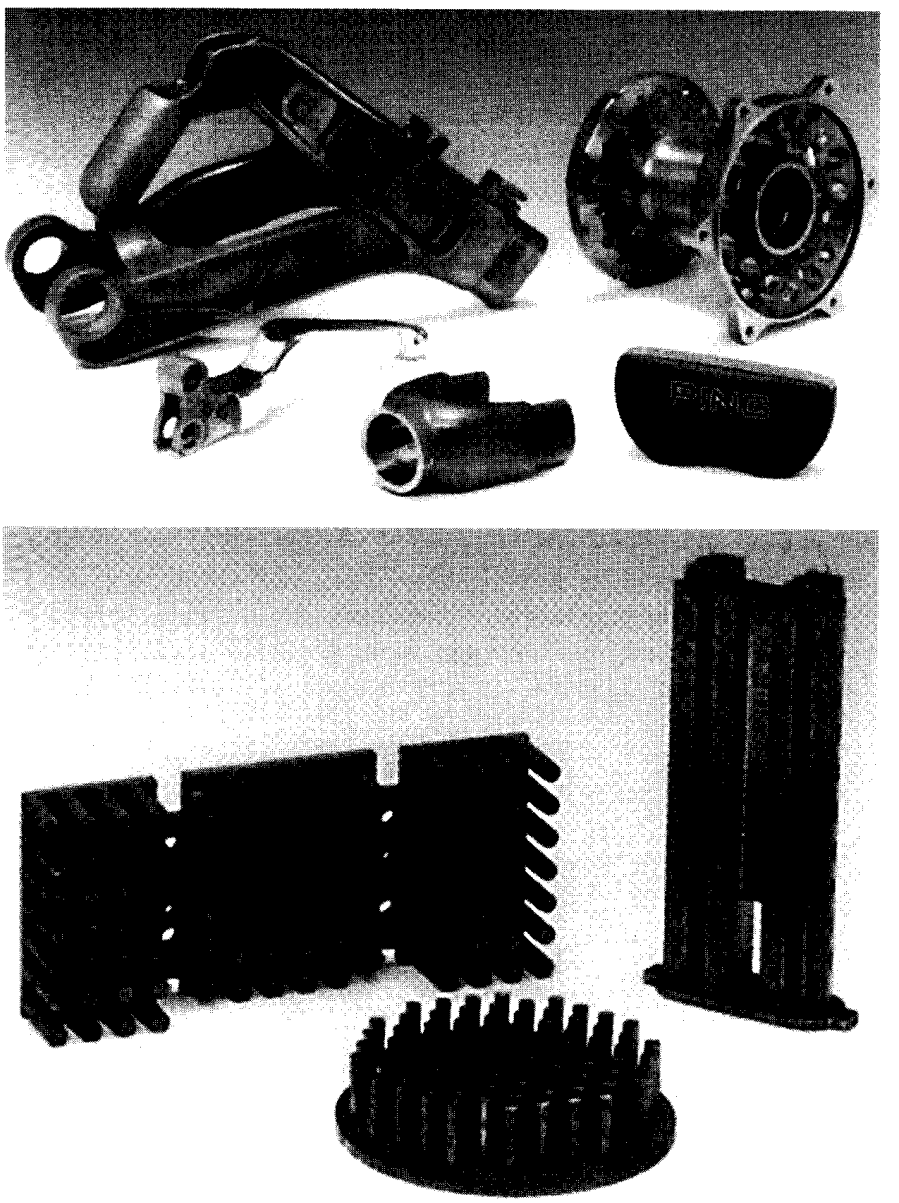

Figure 7.57 Samples of parts produced by semisolid casting of aluminum alloys.

7.5.1 Nature of Semisolid Processing and Basic Phenomena

Several metal alloys have been used for SSM casting, including copper, magnesium, nickel, and ductile iron. However, most of the commercial success in SSM forming centers around aluminum alloys, in particular, alloys 356 and 357. In aluminum alloys a typical liquid fraction of about 0.5 is optimum. Figure 7.58 shows a sliced aluminum alloy slug in a semisolid state.

During the SSM casting process, it is very important to obtain a uniform temperature, which affects the uniformity of the liquid fraction, throughout the slug. Distribution of solid fraction compared to liquid fraction should be as uniform as possible. The need for a uniform liquid fraction distribution is demonstrated by the rheology curve shown in Figure 7.59 [282]. At a liquid fraction of about 0.5, the rheology of the semisolid alloy changes rapidly with only a small change in liquid fraction. Thus if the semisolid slug has an end-to-end or surface-to-core variation in the liquid fraction, this will have a negative impact on the casting behavior, and also on the quality of the castings produced. If the liquid fraction exceeds its optimal value then a significant amount of liquid metal might drip out of the slug leading to unnecessary metal loss. In addition, an excessive amount of the liquid fraction can introduce some slag handling problems.

Practice shows that the best results of semisolid casting of aluminum alloys are obtained when the ratio of slug length to slug diameter is 1:2 to 1:3. An attempt to cast long slugs (i.e., with a ratio of 1:6) may result in a segregation problem.

Consequently, a heating method that can provide a suitable temperature profile throughout the slug must be chosen. Other parameters that must be considered include the heating time, the level of control and temperature consistency, repeatability, the floor space occupied, amount of metal loss, and capital cost.

Induction heating has been identified as the process that best meets these criteria, and so it is used by many commercial SSM casters. There are two types of induction coil arrangements: vertical and horizontal (Figure 7.60). There are no principal differences between these two approaches from electromagnetic and heat transfer perspectives.

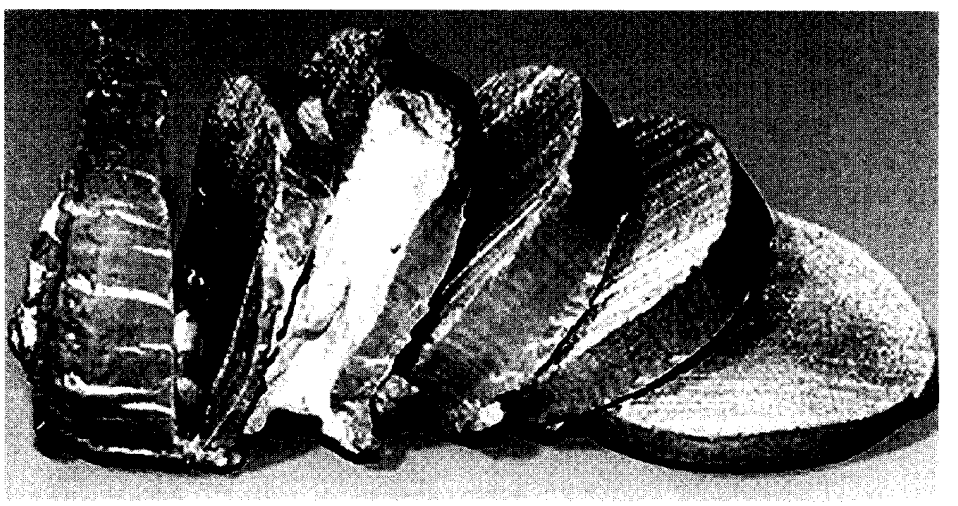

Figure 7.58 Sliced aluminum alloy slug in semisolid stage.

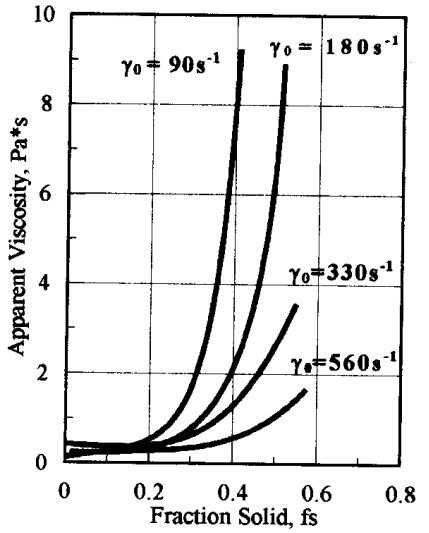

Figure 7.59 Rheology curve (Al:4.5%, Cu:1.5%Mg, $\varepsilon = 0.03\ K_{s-1}$).

Figure 7.61 shows a horizontal coil arrangement. As one can see, the coil design and system design are very similar to that of a conventional billet heater described in previous sections. The only difference lies with the use of "boats" for carrying the semisolid billets.

At this point, the vertical approach is the most popular due to equipment compactness and significantly lower capital cost. In a vertical coil arrangement (Figure 7.62) slugs are placed on ceramic pedestals and heated to the semisolid casting temperature. Once semisolid, the slugs are transferred to the shot sleeve of a real-time controlled horizontal die casting machine and cast in reusable steel dies.

As mentioned earlier, the quality of semisolid castings is greatly affected by the ability to achieve temperature uniformity within the slug. Depending on the alloys, the required temperatures for aluminum slugs are typically in the range of 575 to 595°C with a required uniformity of ±3°C.

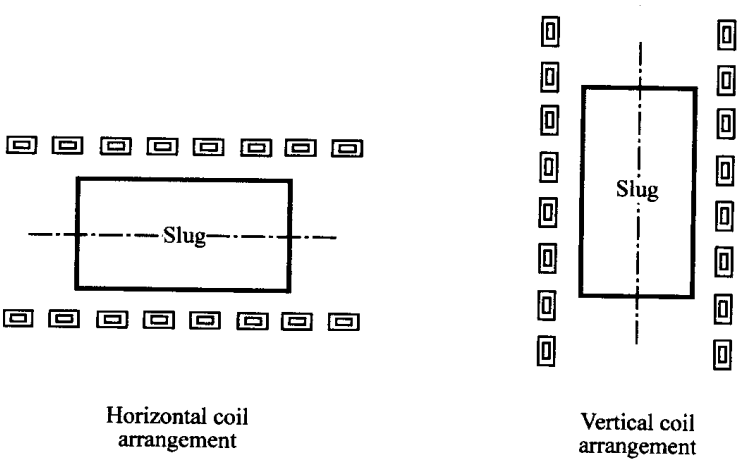

Figure 7.60 Two basic types of induction coil arrangments for heating SSM slugs.

Figure 7.61 Fragment of horizontal coil arangement for semisolid heating. (Courtesy of Inductoheat–I.H.S. Corp., Fort Worth, TX.)

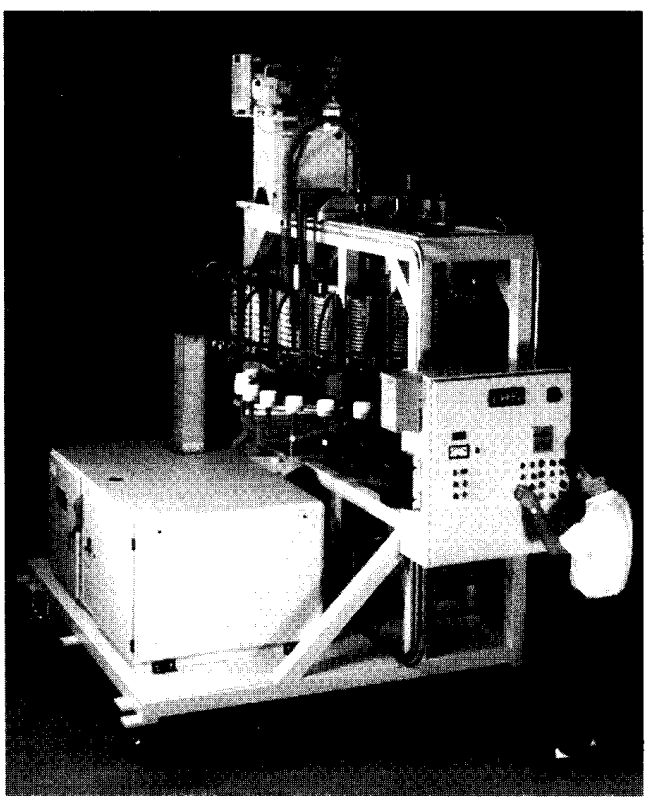

Figure 7.62 High production compact induction heating machine for semisolid forming. (Courtesy of INDUCTOHEAT–I.H.S., Fort Worth, TX.)

As mentioned in Section 3.1.7, the nonuniformity of the heating profile at the coil and slug ends is related to the distortion of the electromagnetic field in those areas [249, 250]. The end effect has unique features when induction heating of slugs for semisolid processing. Prior to discussing these features, it is imperative to outline some basic principles of the electromagnetic end effect phenomenon concentrating on its specifics when heating aluminum slugs prior to SSM casting.

The electromagnetic end effect can result in either over- or underheating of the workpiece ends. The required temperature distribution along the end of the slug depends on the frequency, the coil and slug geometry (including the slug-to-coil air gap and coil overhang), the material properties of the slug, power density, cycle time, and coil space factor.

Electromagnetic end effects may be illustrated by the curves in the lower diagram of Figure 7.63 and are basically defined by three variables; $\mathbf{R_{SLUG}}/\delta$, σ_{SLUG}, and $\mathbf{R_{COIL}}/\mathbf{R_{SLUG}}$, where σ is the coil overhang, $\mathbf{R_{SLUG}}$ is the radius of the slug, and $\mathbf{R_{COIL}}$ is the inside radius of the coil.

Generally speaking, there are two extreme cases of the appearance of an electromagnetic end effect. Let's first consider what happens with the power density distribution in the area located at the left end of the slug in Figure 7.63. An inap-

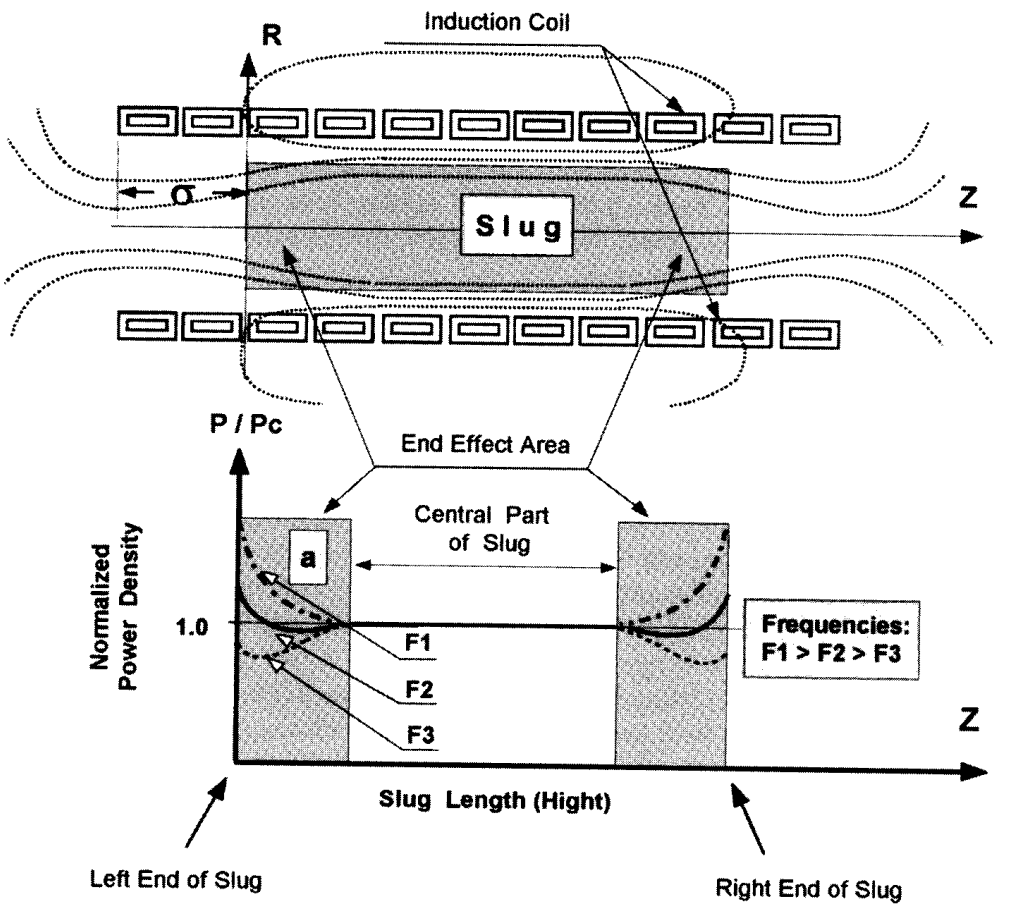

Figure 7.63 Sketch of electromagnetic end effect areas of the slug (horizontal coil arrangement). "Pc" is surface power density in the central part of the slug.

propriate combination of the above-mentioned factors can lead to under- or overheating of the end of the slug. Generally speaking, the electromagnetic end effect area can extend toward the central region of the slug to a distance of 4 times the slug's radius. For typical conditions of induction heating of aluminum slugs for semisolid forming, the end effect area extends toward the central region of the slug no farther than 0.5 to 1.2 times the coil radius.

Higher frequency and larger coil overhang lead to a power surplus in the end area of the slug. As a result, significant overheating may take place in that area. A low frequency and small coil overhang will cause a power deficit at the end of slug, which will, therefore, be underheated compared to its central area.

A uniform power distribution along the length/height of the slug will not correspond to a uniform temperature profile. This is the result of additional heat losses (due to radiation and convection) at the slug end area compared to its central part. By the proper choice of design parameters, it is possible to obtain a situation where the additional heat losses at the end of the slug are compensated for by the additional power (power surplus) due to the electromagnetic end effect. This allows one to obtain a reasonably uniform temperature distribution along the length (in the case of horizontal coil arrangement) or height (for vertical coil arrangement) of the slug.

The choice of frequency is defined not only by the required temperature profile in the slug, but also by the requirement for providing a high electrical efficiency of the induction system with minimum electromagnetic forces (Lorenz force). During induction heating, aluminum slugs experience forces that are directed out of the coil. Under normal process conditions, slugs consist of a significant amount of liquid fraction. Excessive electromagnetic forces may result in uncontrollable removal of liquid metal from the inductor and slug shape distortion. Moreover, if the slug is situated asymmetrically inside the induction coil, it may be accidentally ejected from the inductor by the electromagnetic field. Therefore, special attention should be paid to the minimization of these forces.

It is important to understand that the temperature profile in the slug is formed not only by the skin effect and electromagnetic end effect but by the thermal edge effect as well. Thermal edge effect takes place due to Lambert's law (cosine law).

When discussing the end effect one should notice that this effect is markedly different at different stages of the heating cycle. For example, at the beginning and at the end of heating the rates of the end effect are different. This is due not only to the change of electrical resistivity of the aluminum, but also to several unique features of the SSM induction heating, including the "elephant foot" effect, slug tilting (sagging), and surface erosion phenomena. Figures 7.64 and 7.65 show shape distortion of aluminum slugs that reached a semisolid condition in vertical and horizontal coil design approaches, respectively.

Proper handling of end and edge effects and the correct choice of design parameters including application of flux concentrators and flux extenders will allow one to obtain the required longitudinal temperature uniformity.

7.5.2. Shortcomings of Mathematical Modeling of Induction Heating for Semisolid Casting

Mathematical modeling is a major factor in the successful design of an induction heating system. During the last decade a considerable amount of knowledge has been

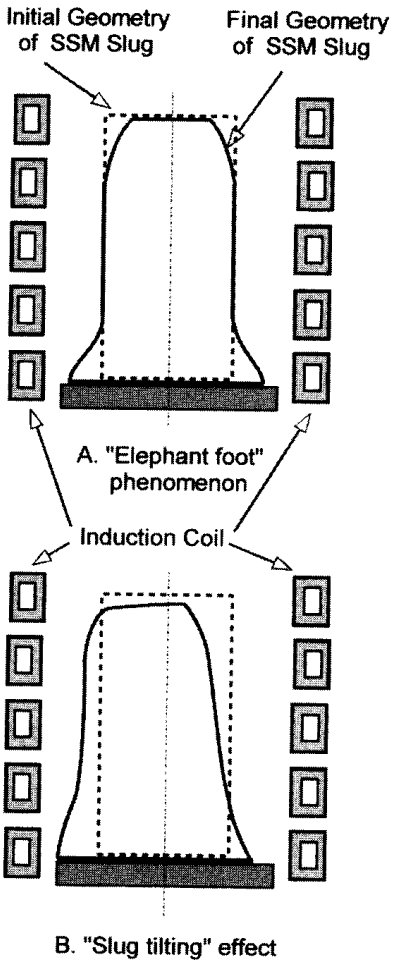

Figure 7.64 "Elephant foot" phenonomenon (A) and "slug tilting" effect (B) using vertical coil arrangements.

accumulated on the computation of the induction heating process by using numerical techniques for a variety of applications (Sec. 3.4). Unfortunately, the features of heating by induction for semisolid forming generate several limitations to using practically all existing commercially available software. The following example illustrates this statement. The existence of the elephant foot phenomenon (Figures 7.64 and 7.65) is an indication that the slug has obtained a semisolid condition. As a result of this phenomenon, the coil-to-slug radial air gap will not be the same along the coil length/height. Variation of the air gap changes the electromagnetic coupling between the coil and different areas of the slug. The power density distribution along the slug length/height will vary compared to the distribution within an "ideal" cylindrical body.

In addition to the elephant foot phenomenon, the slug tilting effect and surface erosion of certain surface areas (i.e., at the top of the slug) can make the situation even more complex. Due to tilting (Figures 7.64 and 7.65), certain slug areas will have better coupling with the inductor than the areas located on the opposite side of the slug. Somewhat similar to positive feedback, the areas with better coupling will have more intense heating that will result in more intense tilting.

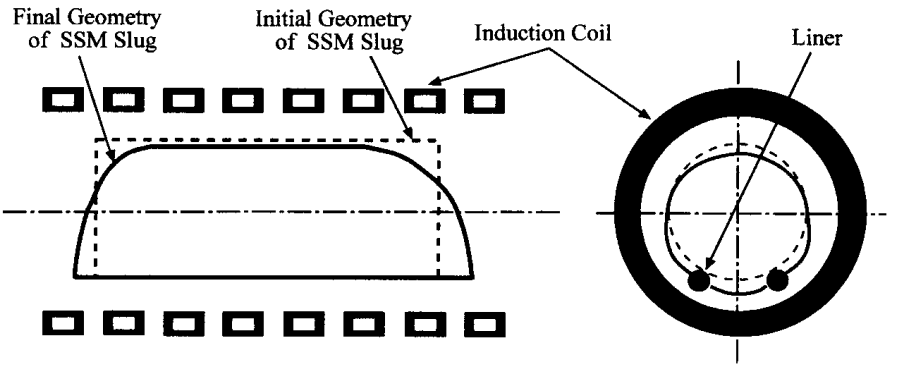

Figure 7.65 Shape distortion of semisolid slug that takes place with horizontal coil arrangement.

Due to surface erosion at the top of the slug and the elephant foot phenomenon at its bottom, the length of the eddy current paths at the top, bottom, and central areas of the slug will be different. This will result in different resistance to eddy current flow in different surface areas of the slug and, therefore, in a different amount of Joule losses that appear within the slug body. In other words, from the electromagnetic perspective, the slug will be seen by the magnetic field as a number of disks made from metals with different electrical conductivity. As mentioned above, the elephant foot phenomenon, tilting effect, and surface erosion do take place in both horizontal and vertical coil arrangements.

It is very important to remember that any computational analysis can at best produce only results that are derived from initial modeling assumptions. Even a cursory look at a computer-simulated magnetic field distribution (Figure 7.66)

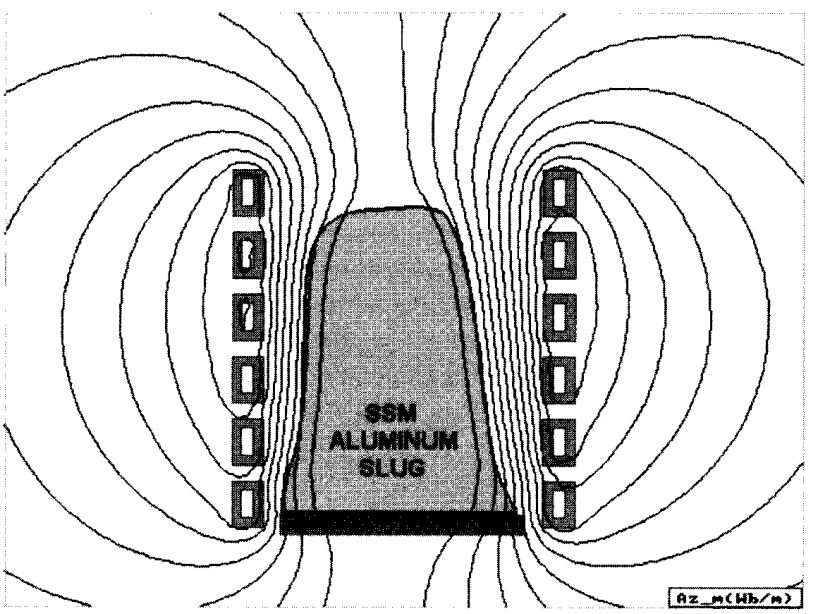

Figure 7.66 Computer graphic of magnetic vector potential distribution.

reveals the danger in underestimation of the features of SSM heating from a computational perspective by using overly simplified assumptions such as considering a slug's geometry as a "perfect" cylinder. This assumption was valid in conventional induction heating prior to forging or extrusion; however, in SSM they can lead to an incorrect mathematical model that will not be able to provide the required accuracy. In order to adequately simulate an induction heating of SSM, the computational model should couple electromagnetic, heat transfer, phase transformation, and metal flow phenomena. The last would allow one to take into consideration the shape distortion of the slug being in a semisolid state. The development of software that will be able to take all four interrelated phenomena into account is a very complex task even for modern computers. Therefore, the recommendations obtained from conventionally coupled electromagnetic heat transfer software should be applied only for cases where elephant foot, slug tilting, surface corrosion phenomena, and other effects are not pronounced (as is sometimes the case with small slugs).

Another factor that affects the accuracy of any computer modeling is the availability of reliable material property data. There are a number of handbooks available providing material properties where one can find information regarding density, thermal conductivity, electrical resistivity, and specific heat of most metals. Unfortunately, such information for SSM is very limited. In some instances, SSM property data exist but due to measurement complexity and cost to conduct such a measurement, the reliability of those data, especially in the most critical stages such as the spherodization stage, is quite poor.

Therefore, the results of SSM modeling using a conventional electromagnetic heat transfer coupling approach can be considered to be basic guidelines or ball park numbers and should be used in conjunction with the individual's engineering background and experience in induction heating for SSM processing.

7.5.3. Technological Aspects of Commercial Induction Heating Systems for SSM Forming

One of the traditional induction heating machines for heating aluminum alloy slugs is shown in Figure 7.62. It is a compact high-production carousel-style induction heater. This heater is built by I.H.S., Fort Worth, Texas and powered by a 350 kW/1 kHz power supply, and uses 24 pedestals and 18 induction coils. The cold slugs are loaded onto ceramic pedestals, and indexed to the first induction coil. The coils are lowered around the slugs and the power applied. After a preset time, the current is turned off and the coils are raised. The pedestals are then indexed forward by one position, the coils are lowered, and the process repeated (Figure 7.67). In this manner, the slugs index from coil to coil until, at the final heating position, the temperature and liquid fraction of the slugs are suitable for the SSM casting process.

This induction heater has been designed to match the throughput of the horizontal casting machine, which typically operates at a cycle rate of between 30 and 90 sec, depending upon the size of the castings and number of cavities being cast. This style of heater can heat aluminum slugs up to 5 kg (12 lb) in weight at this rate.

As all the coils are connected in series (Figure 7.68A), two different designs of coils are used to provide the optimum heat cycle: fast heating and soaking. The fast heating coils have a greater number of turns, and are used to rapidly heat the slugs to the solidus temperature. The soaking coils (so-called "power coils") have fewer turns

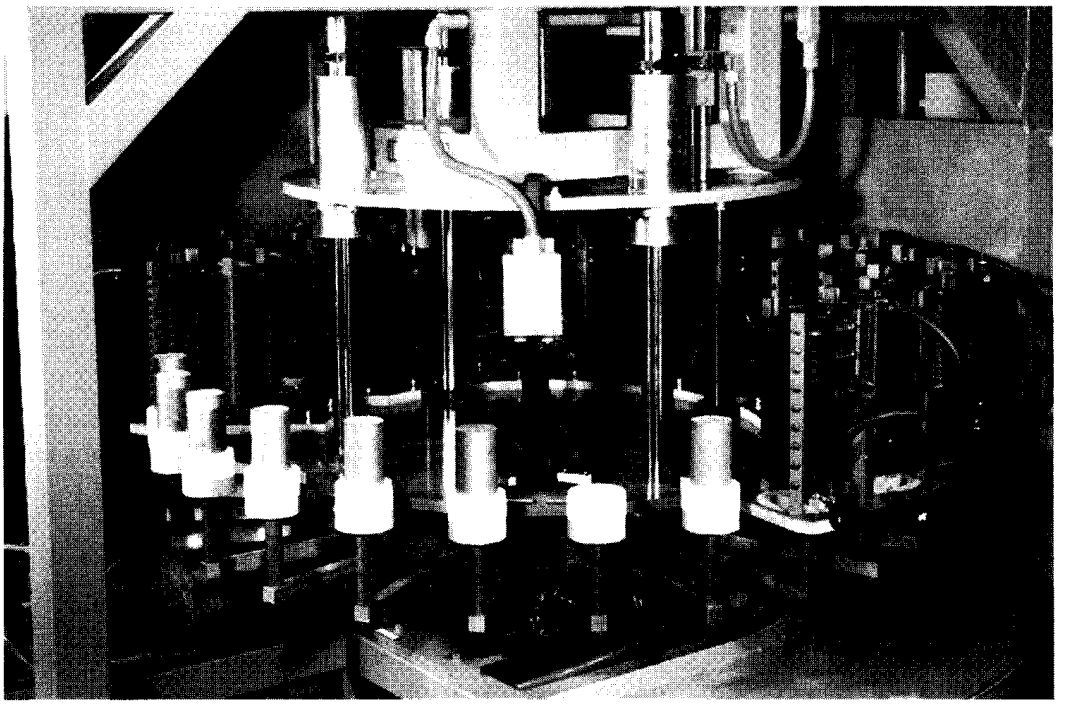

Figure 7.67 Slugs stand on ceramic pedestals with vertically oriented induction coils. (Courtesy of INDOCTOHEAT–I.H.S., Fort Worth, TX.)

("holding coils"), and so heat the slugs slowly providing isothermal holding. This ensures that sufficient time is provided for the heat to conduct from high temperature areas toward regions wth lower temperature (i.e., from the surface to the center of the slug), ensuring a uniform temperature distribution. The longer heating time provided by the soaking coils is also used to complete the process of homogenization and spheriodization of the alpha-aluminum particles from the equiaxed dendrites found in the electromagnetically stirred SSM feed material [282].

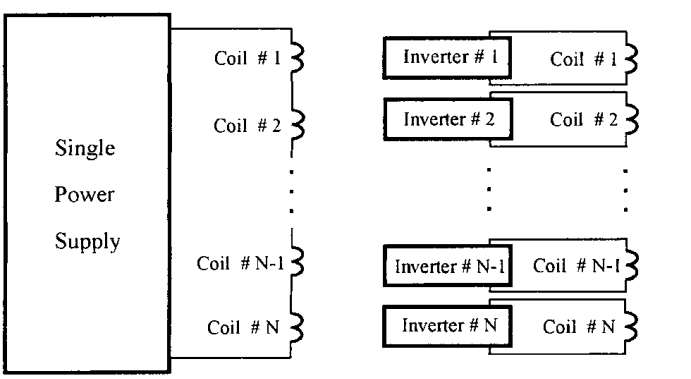

Figure 7.68 Use of a single or multipower supply approach for heating SSM slugs that can be used in both vertical and horizontal coil arrangements.

A multicoil machine design concept allows one to properly handle electromagnetic end effects while the slug progresses from one heat position to another.

Minimum heating times are suggested for all slug sizes. Typical recommended heating times for 76 mm (3 in.), 90 mm (3.5 in.), and 100 mm (4 in.) diameter slugs are listed in Table 7.4.

The induction heater in Figure 7.67 also utilizes an automated unit for cleaning any debris remaining on the pedestal once the semisolid slugs have been removed. Debris can include drips or small pieces that were knocked off the semisolid slug during heating. This ensures that the pedestal is clean once it returns to the slug loading position, so that the cold slug will sit squarely on the pedestal. Devices such as the pedestal cleaning device are important to ensure problem-free operation of the induction heater in a fully automated semisolid metal casting cell.

Heating trials were performed using the carousel-style induction heating system described above [249, 250]. Slugs 140 mm (5.5 in.) in length were cut from 76 mm (3 in.) diameter alloy A356 VELVET flow SSM feed material produced by Ormet Corp. These slugs were heated to semisolid temperature using induction coils that were approximately 282 mm (11.125 in.) long. The heater used a heating time of 42 sec per coil, and an indexing time of 10 sec. Slugs stood on ceramic pedestals with the induction coils oriented with a vertical axis. Once the slugs exited the final soaking coil, a type-K thermocouple was used to measure the temperature of the top, center, and bottom of the slug. Table 7.5 shows a longitudinal temperature profile at optimal slug position.

These data show that the proper handling of electromagnetic end effects results in a uniform top-to-bottom temperature profile with minimal appearance of the elephant foot effect and surface erosion. In contrast, incorrect handling of end effects can lead to a situation where the end of the slug that has the largest coil overhang would have a significantly higher temperature and liquid fraction compared to optimal whereas the rest of the slug might not have any liquid fraction at all.

In [117] one can find a description of the physics of the impact of the coil overhang on the slug's top-to-bottom temperature uniformity. These results indicate that it is very important to control the electromagnetic end effects in order to obtain temperature uniformity of the slug, its liquid fraction, and tilting.

Different applications call for different design approaches. Some of them are shown in Figures 2.44, 7.69, and 7.70. These machines as well as the machine shown in Figure 7.62 utilize one power supply that feeds all coils connected in series (Figure 7.68A). This approach allows one to significantly reduce capital cost. In some cases, the cost reduction exceeds three times.

Table 7.4 Recommended Slug Heating Times

Slug Diameter (in.)	Optimum Heating Times (min)
3.0	9
3.5	12
4.0	16

Source: Ref. 249.

Table 7.5 Longitudinal Temperature Profile

Top Temperature, °C (°F)	Center Temperature, °C (°F)	Bottom Temperature, °C (°F)
586 (1087)	583 (1081)	582 (1080)

As an alternative, Figure 7.68B shows another approach where each coil is powered from an individual power source. Therefore each coil is individually tailored to the required heating condition. This approach provides superior controllability of the surface-to-core temperature uniformity during the heating process allowing slugs to be held within the inductor for a relatively long time. This feature is important in cases when the casting machines experience downtime.

However, the obvious drawback of this approach is a significantly higher capital cost. Another disadvantage is that this approach (Figure 7.68B) has lower controllability in obtaining the required temperature uniformity along the length (for horizontal coil arrangement) or height (for vertical coil arrangement) of the slug compared to the approach shown in Figure 7.68A.

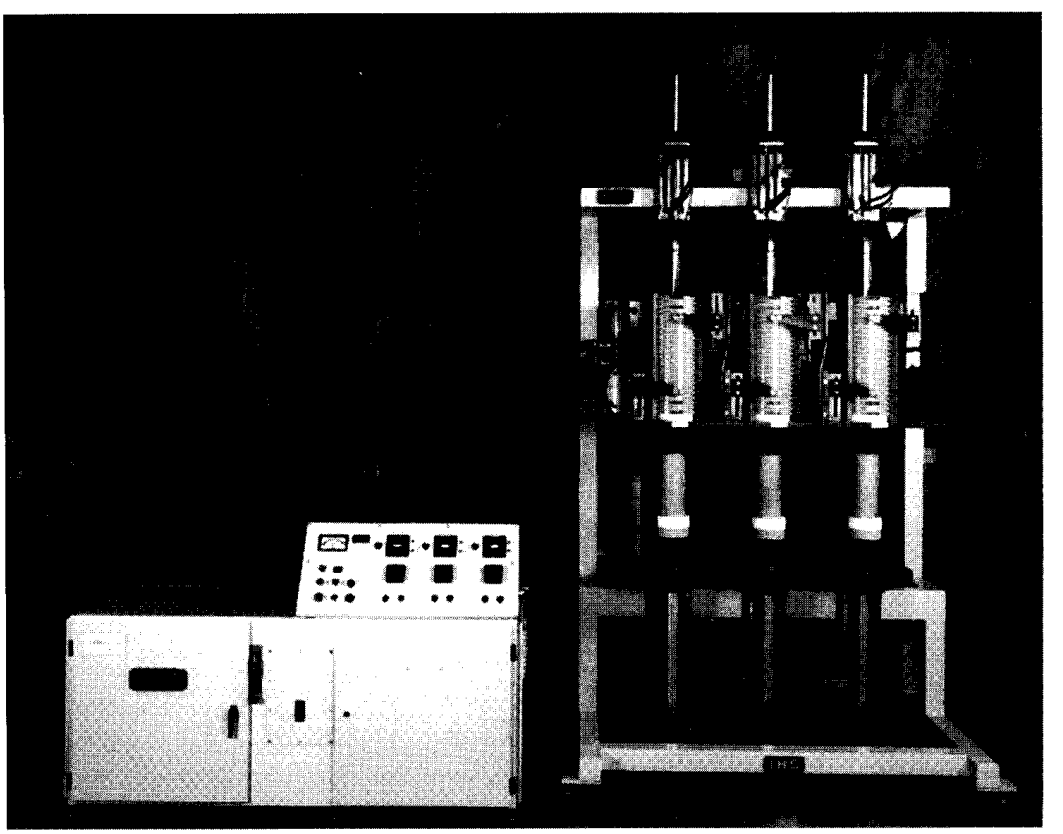

Figure 7.69 Low production induction heating machine for semisolid forming. (Courtesy of INDUCTOHEAT-I.H.S., Fort Worth, TX.)

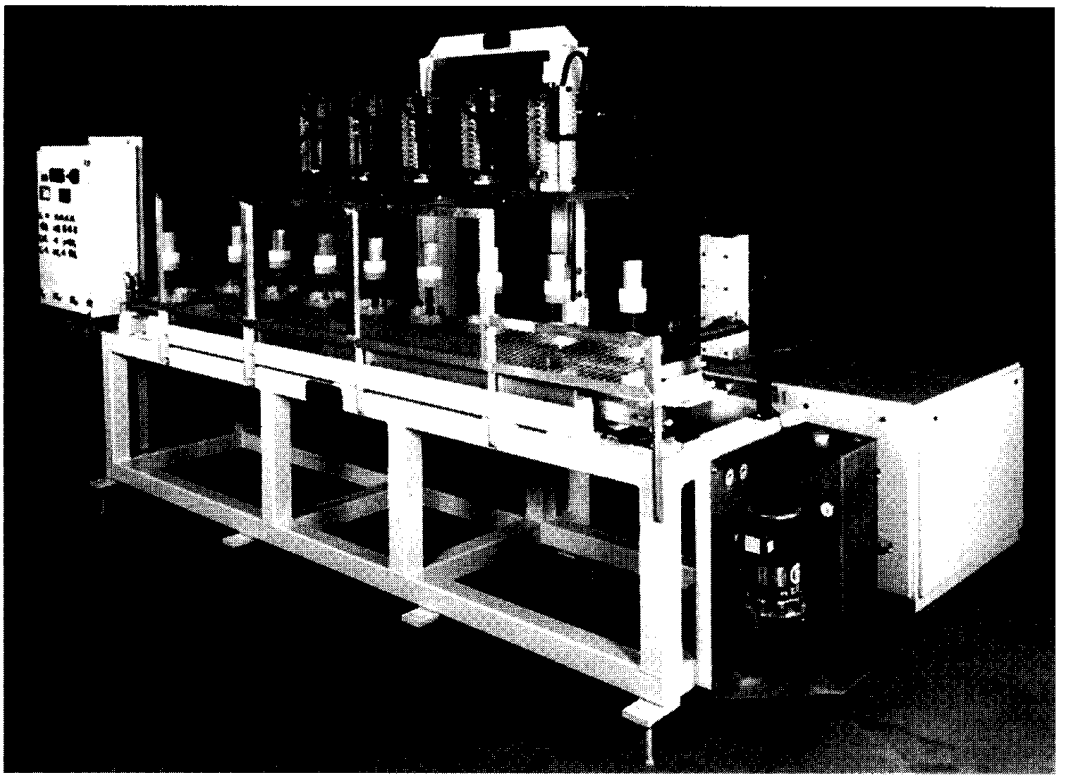

Figure 7.70 Five-coil induction heating machine for semisolid forming. (Courtesy of Inductoheat–I.H.S. Corp, Fort Worth, TX.)

7.6 INTRICACIES OF INDUCTION WIRE/CABLE/ROPE HEATING

7.6.1 Specifics of Design Criteria and Coil Arrangements

There are several approaches to heat wires, cables, and ropes including gas furnaces, electrical resistance heaters, infrared furnaces, electric ovens, molten lead baths, salt baths, and induction heaters.

Growing environmental concerns for global warming in combination with a continuous increase of the cost of natural resources (e.g., natural gas) have resulted in heating by induction becoming the dominant approach for heating of both ferrous and nonferrous wires, cables, and ropes [265]. Thanks to induction, the use of molten lead and salt baths for heating of wire products has practically been eliminated. The use of a protective atmosphere is often required by a process specification and induction heating is well suited for this requirement.

Quick response and the ability to provide a practically instantaneous change in the process operating parameters to accommodate the required temperature of the wire/cable being processed at speeds up to 5 m/sec (1000 ft/min) is another benefit of compact induction systems compared to fluidized beds, infrared heaters, and gas furnaces.

The extensive use of induction for heating wire and cable products in a variety of applications (Figure 7.71) has led to the development of a wide range of process concepts. As one can see from Figure 7.71, in addition to traditional applications

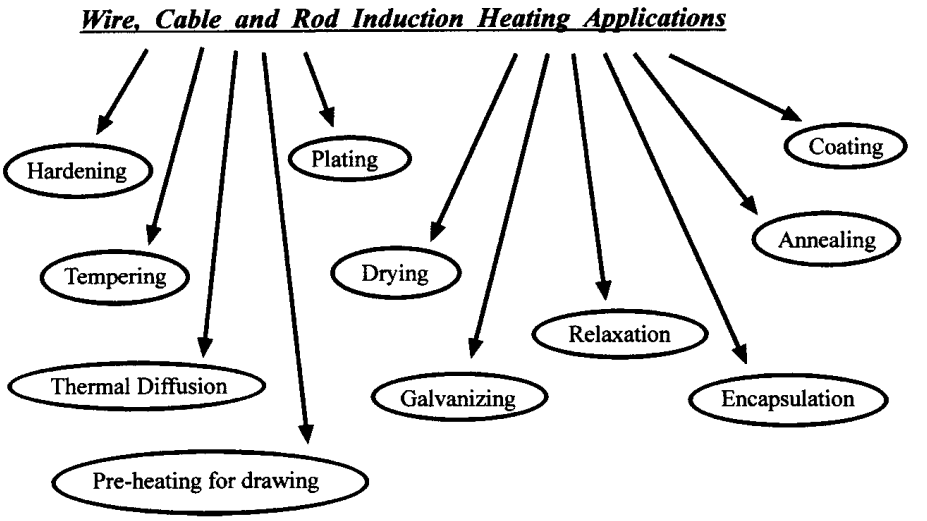

Figure 7.71 Most typical wire, cable, and rod induction heating applications.

(e.g., hardening, tempering, stress-relieving, see Figures 5.30, 5.31, and 5.32) there are other unique applications including wire/cable heating prior to encapsulation (e.g., PVC covered electrical cables), tire cord diffusion, and wire heating prior to metallic or organic coating [272, 273].

Wire/cable heating prior to encapsulation is typically applied to aluminum alloy wires. The wire is preheated as it leaves the payoff roll and the induction coil is positioned on the catenary of the wire line. The wire passes through the induction coil where it is heated to 120°C (248°F) and then immediately passes to the encapsulation process where the PVC flows evenly over the wire.

Tire cord diffusion requires simultaneous heating of typically 10 to 24 wires running in parallel and heated to a temperature of 600°C (1112°F) to melt the surface coatings of copper or zinc alloys which diffuse into the base wire to provide a barrier for rust formation. Wire diameters typically range from 0.8 mm (0.031 in.) to 2 mm (0.08 in.), and the process is described in [272, 273].

The physical nature of wire processing makes it reasonable to use continuous-feed material handling. As mentioned in Section 7.1, continuous induction heating is the case where the workpiece is moved in a continuous motion through one or more inline induction heating coils.

Often it is required to induction heat multiple wires running in parallel or process several cables consisting of many wires and strands (Figures 7.72 and 7.73). The great majority of induction wire/cable heating applications apply solenoid-type (helical) multiturn coils (cylindrical or rectangular shape) similar to coils used for induction heating of bars, billets, and slabs. Depending upon the application, coil turns can be connected in series or in parallel.

Most design criteria discussed in Section 7.1 are applicable for wire, cable, and rope heating, however, some of the criteria have different interpretations and particularities with regard to induction heating of wire products. For example, in most single wire processing applications with wire diameters less than 3 mm (1/8 in.) the entire wire is usually heated through and the criterion of obtaining surface-to-core temperature uniformity is not an issue.

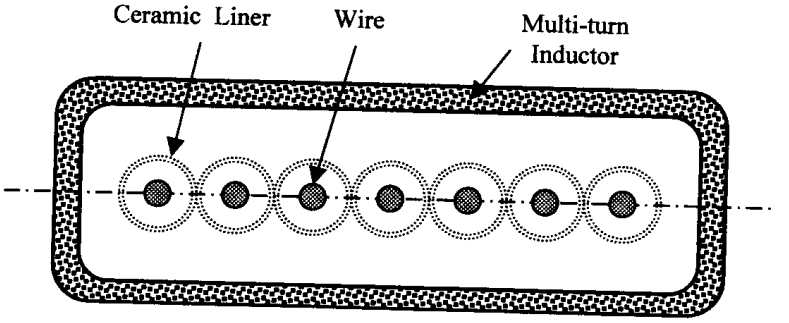

Figure 7.72 Sketch of transverse section of multiwire cable induction heating system.

Therefore, when heating multiple wires running in parallel or multistrand cables, the criterion of providing an equal temperature in all wires regardless of their position inside the inductor becomes critical. The former is a result of the fact that external and internal wires of the cable may be heated differently due to the electromagnetic proximity effect (discussed in Section 3.1.3) resulting in different electromagnetic coupling of the external and internal wires (Figure 7.73, right).

Several process features and physical phenomena distinguish induction heating of multiple wires and cables from conventional induction heating of solid cylinders, bars, and single wire heating.

7.6.2 Energy Efficiency

7.6.2.1 Frequency Selection

Coil electrical efficiency is a complex function of several design parameters including the gap between coil-ID-to-wire-OD, properties of heated metal, coil length, number of wires/strands, and frequency, with the former being the most prominent not only from the required heating energy perspective but due to equipment cost as well.

In the case of induction heating of a single rod or wire, there will be higher coil efficiency when the applied frequency corresponds to a ratio of wire OD to current penetration depth (δ) greater than four (wire OD/$\delta > 4$; see Figure 7.14). Similar to bar heating applications, the use of a frequency that results in a ratio of wire OD/$\delta > 6$ will only slightly improve the coil efficiency. At the same time, the use of very

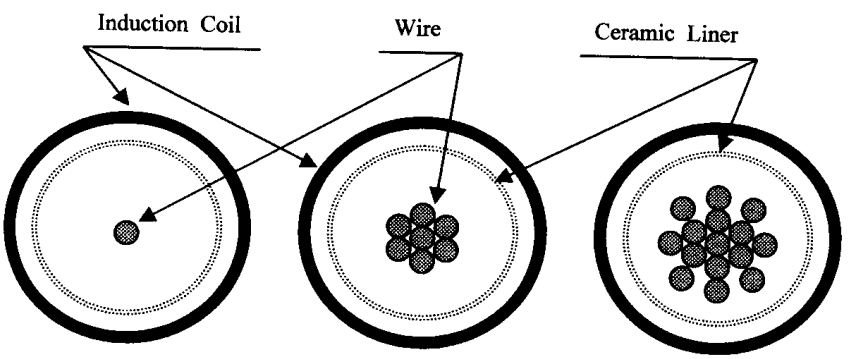

Figure 7.73 Sketch of transverse section of multistrand cable induction heating system.

high frequencies (frequency > F2) will decrease the total electrical efficiency due to higher transmission loss [265].

If the chosen frequency results in a ratio of wire outside diameter to current penetration depth less than 3 ($OD/\delta < 3$), the coil electrical efficiency will dramatically decrease. This is due to the cancellation of induced eddy currents circulating in the opposite sides of the single wire (see Sec. 3.1.2). Table 7.6 shows minimum diameters for efficient heating of single processing wires. As shown below in the case of heating multiple wires and multistrand cables, efficient heating can be achieved using lower frequencies or smaller size wires compared to the heating of a single wire.

Analysis of Figure 7.74 shows that coil efficiency proportionally increases with the number of wires/strands heated in the same coil. In some cases, it is possible to gain an improvement in coil electrical efficiency of +30% compared to the heating of a single wire.

Since the capital cost of a power supply usually decreases with a frequency reduction, the ability to use a lower frequency inverter can result in significant cost savings for the user.

Table 7.6 Minimum Wire Diameters for Efficient Heating when Processing Single Wires

		Frequency (kHz)						
Material	Temp. (°C/°F)	1	2.5	10	30	70	200	500
Aluminum	100/212	11.6	7.3	3.6	2.1	1.4	0.8	0.5
	250/482	14.1	8.9	4.4	2.5	1.7	1	0.6
	500/932	17.9	11.4	5.4	3.3	2.1	1.3	0.8
Copper	100/212	9	5.7	2.8	1.6	1.1	0.6	0.4
	500/932	13.8	8.7	4.4	2.5	1.6	1	0.6
	900/1652	17.7	11.2	5.4	3.2	2.1	1.2	0.8
Brass	100/212	16.6	10.5	5.1	3	1.9	1.2	0.7
	500/932	22	13.9	7	4	2.6	1.5	1
	900/1652	26	16.8	8.4	5	3.2	1.9	1.2
Tungsten	100/212	14	8.9	4.4	2.5	1.6	1	0.6
	900/1652	33	21	10.6	6.1	4	2.4	1.5
	1500/2732	43	27	14	8.1	5.4	3.1	2
Nonmagnetic	100/212	53	33	16.8	9.7	6.3	3.8	2.4
stainless steel	800/1472	64	39	19.4	11.8	7.6	4.5	2.9
	1200/2192	65	41	19.6	12.2	8	4.7	3
Medium Carbon Steel (1040) at Different Magnetic Field Intensities (H)								
H, A/mm								
10	100/212	2.1	1.3	0.65	0.37	0.25	0.15	0.1
	500/932	4.2	2.6	1.3	0.75	0.5	0.29	0.19
80	100/212	5	3.2	1.6	0.92	0.6	0.36	0.22
	500/932	10.3	6.5	3.3	1.9	1.24	0.73	0.46
160	100/212	6.8	4.3	2.2	1.25	0.82	0.48	0.3
	500/932	13.9	8.8	4.4	2.5	1.66	0.98	0.6

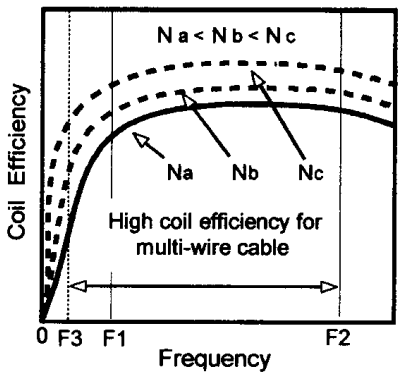

Figure 7.74 Coil efficiency of a multiwire cable induction heater versus frequency, where N is the number of heated wires in one coil.

As shown in Figure 7.74, the minimum recommended frequency for heating of multiple wires (Figure 7.74, frequency F3) is shifted toward the use of lower frequencies compared to induction heating of a single wire (frequency F1).

7.6.2.2 Ferrous and Nonferrous Wires

As discussed in Sections 7.1 and 7.2, different metals have different ways of being heated by induction. Metals with high electrical resistivities are heated with higher coil efficiency than metals with low electrical resistivity (assuming that there is no current cancellation).

In the induction heating of magnetic wires such as carbon steel wire, several unique aspects are encountered compared to nonmagnetic metals. In contrast to induction bar/billet heating when heating magnetic wires/cables instead of three stages of the heating cycle there are only two stages.

At the first stage, the wire is magnetic, current penetration is small, skin effect is pronounced, and coil efficiency is quite high (typically 80% or even higher). At the beginning of the heating cycle, the current penetration depth into the carbon steel wire will start to increase slightly because of the increase in electrical resistivity of the metal with temperature. With a further rise of temperature (after exceeding the temperature of about 550°C or 1022°F), magnetic permeability starts to noticeably decline resulting in a marked increase of current penetration depth. The first stage exists as long as the wire temperature is below the Curie point.

As discussed in Section 3.1, near the critical temperature A_{c2} known as the Curie point, the permeability drastically drops to unity because the metal becomes nonmagnetic. As a result, the current penetration depth will increase significantly (up to 15+ times). This may lead to the eddy current cancellation within each single wire and, as a result, to a drastic reduction of the coil efficiency. In cases such as this, the application of a dual-frequency design concept can be beneficial. This concept makes use of low frequency in the initial heating stage, when the steel retains its magnetic properties. In the final stage, when the wire becomes nonmagnetic, it is more efficient to use a higher frequency. At this point it would be imperative to provide a case study where it is required to heat 3.18 mm (1/8 in.) carbon steel single wire to the temperature above the Curie point using different frequencies.

A comparison of time–temperature profiles of induction heating of 3.18 mm (1/8 in.) carbon steel wire using a single 10 kHz frequency and dual 10/200 kHz frequencies is shown in Figure 7.75. The graphs shown in Figure 7.75 are the results of computer modeling using ADVANCE software developed specifically for induction heating applications.

As can be seen from the top graph of Figure 7.75, with a frequency of 10 kHz, the final temperature of the wire experiences a small change whereas the coil power increases more than five times (from 17 to 90 kW). The only noticeable difference

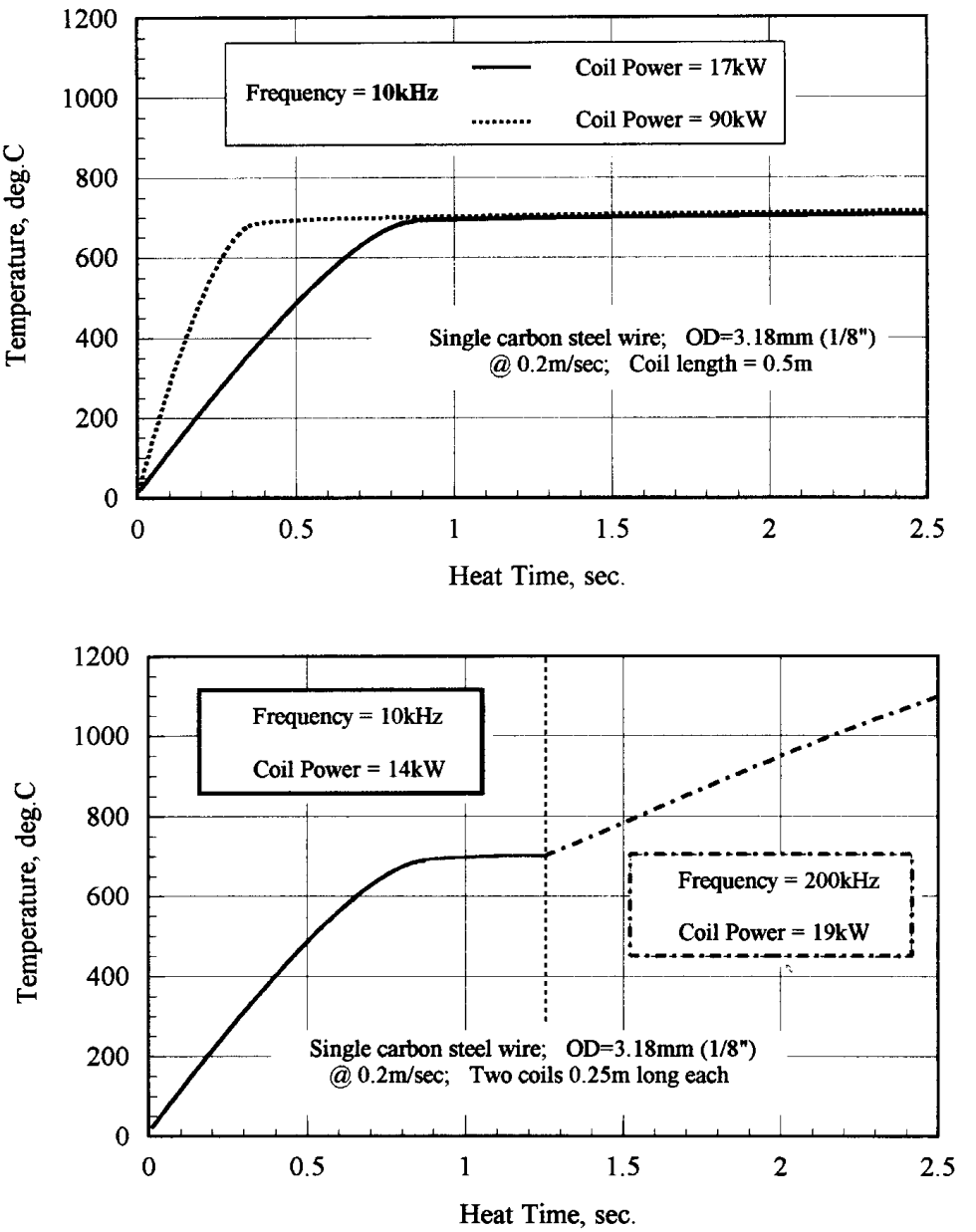

Figure 7.75 Comparison of time–temperature profiles of induction heating of a 3.18 mm (1/8 in.) carbon steel wire using a single 10 kHz frequency and dual 10/200 kHz frequencies.

deals with the slope of the time–temperature curve. This change takes place during the first heating stage when a wire is magnetic. Then, after reaching the Curie temperature, there is no noticeable temperature rise. This occurs due to a phenomenon of eddy current cancellation induced within the wire when its temperature exceeds the Curie point.

In contrast, the bottom graph of Figure 7.75 shows remarkable improvement in the ability to heat a 3.18 mm (1/8 in.) carbon steel wire above the Curie temperature using a dual-frequency approach. Power of 14 kW/10 kHz has been used for heating the wire below the Curie point and power of 19 kW/200 kHz has been used for heating above the Curie temperature. The total required power is 33 kW (compared to 90 kW using a single frequency of 10 kHz).

Generally speaking, in this particular case, there can be several basic scenarios regarding different frequency options for induction heating of 3.18 mm (1/8 in.) carbon steel wire up to temperature above the Curie point: (1) a single relatively low frequency (i.e., 10 kHz), (2) a combination of a low frequency and a high frequency (i.e., using a dual-frequency 10/200 kHz), and (3) a single relatively high frequency (i.e., 200 kHz). Table 7.7 shows the advantages and disadvantages of each option.

This case study stresses the importance of avoiding a current cancellation when choosing a power supply operating frequency. It is sometimes required that the single wire induction heater should be able to heat a variety of wire sizes to different temperatures using a single frequency. In cases like this, in order to avoid eddy current cancellation, it is necessary to choose a frequency which would guarantee that for any combination of wire sizes and final temperatures, the ratio of wire diameter to current penetration depth should exceed at least 3.8 when processing a single wire. It is wise to remember that while calculating the current penetration depth (see formulas (3.6) and (3.7) the values of electrical resistivity and relative magnetic permeability of the metal should correspond to their values at the highest temperature that appears during the heating process.

Table 7.7 Frequency Options for Induction Heating

Frequency (kHz)	Advantages	Drawbacks
10	Low cost	Does not provide a required heating of 3.18 mm (1/8 in.) steel wire above the Curie temperature almost regardless of the applied power
10 and 200	Energy savings. Low required power. Good temperature uniformity. Cost effective	Two inverters with two different frequencies are required
200	Low required power	Costly if a high power is required. Potential problem with temperature uniformity when heating multistrand cables and utilizing electromagnetically short coils

It should be mentioned, however, that in some cases it makes economical sense to choose the frequency based on so-called "big runners" (wire sizes that represent the highest production, i.e., 70% of total production or more). If there is an insignificant difference in the sizes of the big runners and smaller wires, then, in order to minimize the capital cost of the system, the choice of frequency can be determined by optimizing coil efficiency when heating the big runners with an accepted efficiency reduction while processing the smaller sizes.

Thus far we have discussed the features of induction heating of carbon steel wires heated below and above the Curie temperature. Nonferrous wires/cable/ropes such as aluminum, copper, tungsten, brass, and so on can also be successfully heated using induction. However, coil efficiency when heating nonferrous wire is noticeably lower compared to magnetic metals.

7.6.2.3 The Factor of System Geometry

The geometry of the induction system has a distinct effect on coil efficiency. Similar to bar heating, the gap between the inside diameter of the coil (coil ID) and the surface of the wire/cable plays an important role in determining the coil electrical efficiency. Smaller air gaps result in better coil-to-wire electromagnetic coupling and thus higher coil efficiencies. At the same time, the minimum value of the coil-to-wire air gap is dependent upon the ability to safely process all the required wire/cable sizes through the induction coil with no danger of touching and damaging the coil copper or refractory. Wire vibration, the method of wire reel joining, wire tension, wire size, and some other factors relate to the stability of wire progress through an induction coil. All these factors affect the minimum clearance value for wire processing through the inductor.

In addition to the coil opening, the coil length is another geometrical factor that has a marked effect on coil electrical efficiency and, therefore, on required power. Long and tightly wound coils are more efficient when heating both ferrous and, particularly, nonferrous wires compared to short and sparsely wound coils.

For nonferrous wires it is recommended to have a coil length at least five times the coil inside diameter. If the coil length is less then three times the coil ID, then the coil efficiency reduction can be quite appreciable due to a nonhomogeneous magnetic field and a prolonged end effect zone.

For electromagnetically short coils the use of magnetic flux concentrators (i.e., laminations or metal powder-based materials) may noticeably improve the coil efficiency particularly when heating nonferrous wires. If the coil length is five times longer than the coil ID then a further increase in the coil length will not provide any significant improvement in coil efficiency. The former statement might not hold true when heating ferrous wires below the Curie temperature. In cases such as this, an increase in coil length results in a reduction of magnetic field intensity and, therefore, in an increase of the relative magnetic permeability (see Figure 3.8). A gain in magnetic properties due to a reduction of magnetic field intensity leads to a coil efficiency increase. In addition, it makes the skin effect more pronounced by reducing the current penetration depth and allows the use of a lower frequency compared to a short coil without sacrificing coil electrical efficiency.

7.6.3 Commercial Aspects of Induction Wire, Cable, and Rope Heaters

Because the response of an induction heater to changes in process parameters is practically instantaneous, the ability to provide consistent heating creates a special requirement for the control system. Typically one of two control methods is applied in induction wire heating systems.

- A closed-loop control system with feedback from an output temperature sensor or line speed meter. Wire speed is detected to verify the pounds per hour throughput and to set the control algorithm for the process.
- An open-loop system utilizing feedforward controllers. These controllers compute a line speed and required coil power based on the wire size, its production rate, and required final temperature.

The ability to control individual wire speed when heating multiple side-by-side wires running in parallel allows the user to heat different wire sizes to different temperatures within the same coil (Figure 7.72). Depending upon process-specific requirements, kind of metal, required tensile strength, and customer preference, a PLC or PC can be used to compute the required coil power and speed. Aspects of process control and monitoring are discussed in detail in Section 8.14.

Infrared pyrometers are used for temperature measurement and verification. Section 4.3 is devoted to discussion of infrared pyrometry. It should be pointed out here that the accuracy of temperature readings is affected by the ability to accurately focus the sensing head on the heated part. Therefore there is a potential problem in accurately focusing a pyrometer on the wire surface. Sometimes, due to process features, a wire cannot remain in a stable position inside the inductor and could move "up-down" and "left-right". Therefore there is a danger that the wire could move out of view of the temperature sensor resulting in a false signal.

All these result in the fact that closed-loop control systems have not been as widely used for wire heating applications as open-loop systems with a controller.

In addition to traditional process parameters that may include power/energy, coil current, voltage, line speed, and the like, a monitoring system of a wire/cable induction heater provides information regarding the quench flow rate and quench temperature when using aqua or gas quench.

As an example, Figure 7.76 shows a typical inline induction heater (manufactured by the INDUCTOHEAT Mass Heating Division) with a thermostatically controlled holding chamber and the ability to heat 18 wires (side by side running in parallel) in a hydrogen/nitrogen protective atmosphere [265].

A typical arrangement of a induction machine manufactured by Radyne Corporation for wire heating prior to encapsulation is shown in Figure 7.77 [272]. The induction coil length is dependent upon the speed of the process and the depth of heating required through the wire cross-section. The induction coil length is generally in the range of 0.5 m (20 in.) to 1 m (40 in.). The system consists of three induction coils (each to suit a different wire diameter range) all on a common slide operated by pneumatic cylinders. Water-cooling of the coils is achieved by separate cooling of each coil assembly and solenoids automatically changing the cooling flow from one coil set to another as required. The system is rated at 125 kW at 10 kHz.

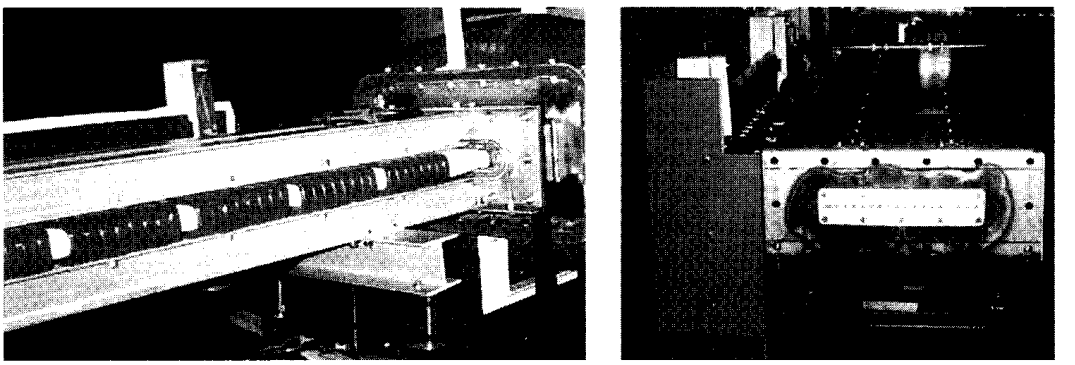

Figure 7.76 INDUCTOHEAT's 18 wire inline induction heater capable of operating in a protective atmosphere.

Continuous hardening and tempering of steel wire has several technological features and is important in certain wire applications such as the production of deformed bar for reinforcing concrete structures. For applications like this Radyne Corporation has registered the "High Bond" process. In the High Bond Process [272] wire is heated to austenizing temperature of approximately of 950°C (1742°F), followed by a quenching operation with water, and then reheated to

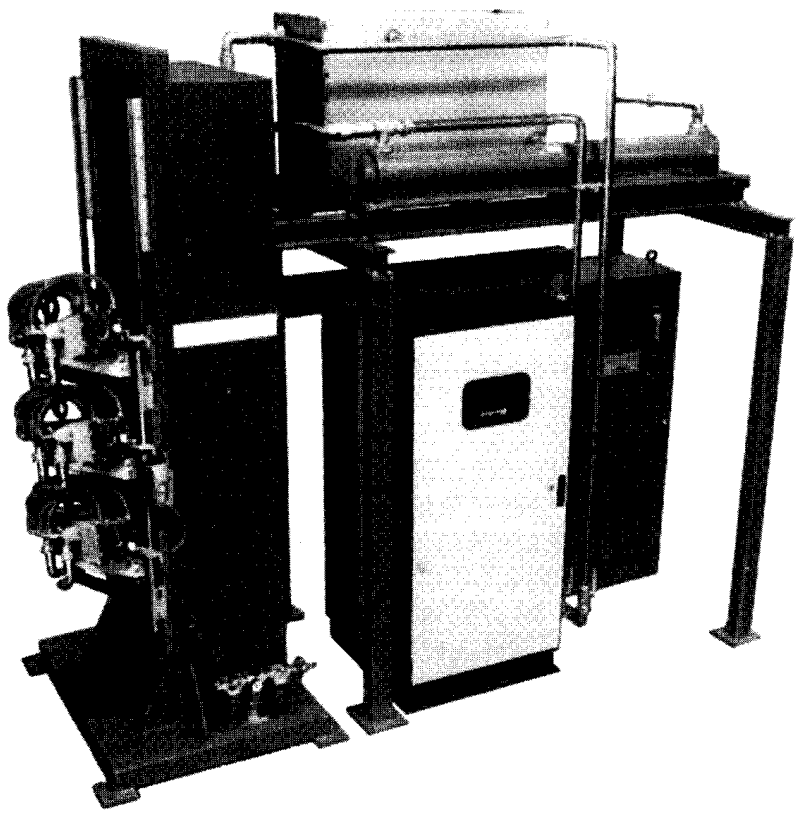

Figure 7.77 Radyne's three-coil 125 kW/10 kHz compact induction system for heating wires prior to encapsulation.

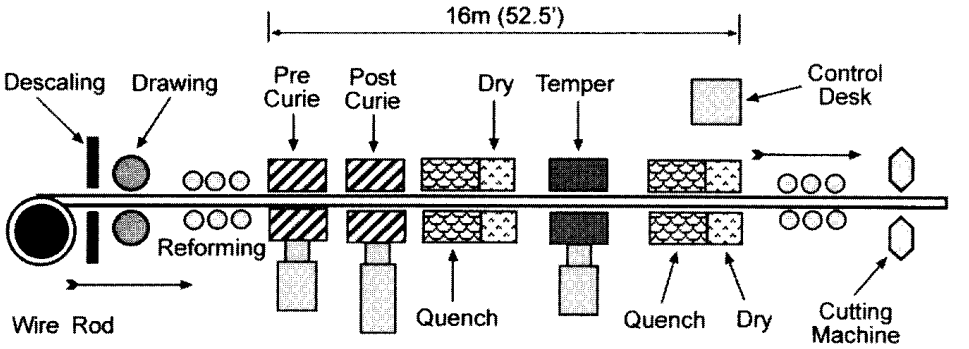

Figure 7.78 High Bond wire heat treatment line. (Courtesy of Radyne Corp.)

between 350°C (660°F) and 450°C (842°F) for final temper, the temperature being dependent upon the final product tensile strength requirements.

A typical line, as shown in Figure 7.78, has the capability to continuously harden and temper wire sizes from 5.1 mm (0.2 in.) to 13 mm (0.512 in.) at speeds of up to 70 m per minute (230 fpm). The line has a total length of 16 m (53 in.); the wire, being uncoiled, passes through an induction coil operating at an output frequency of 10 kHz to heat the wire to Curie temperature and then to austenizing temperature using a coil operating at an output frequency of 50 kHz. The wire is then quenched, generally using water (although a polymer quenchant may also be used), drained through an air wipe, and reheated for the tempering operation.

All coil lines are 1.8 m (63 in.) and the induction power source ratings are entirely dependent upon the production rates required. Finally, a second quench and air wipe follow the temper heating process prior to final cooling of the wire. The process is dynamically controlled using line speed and power level as convergent parameters ensuring constant temperatures at varying line speeds in order to produce consistent products.

7.7 TUBE AND PIPE HEATING

7.7.1 Specifics of Induction Heating of Tubular Products

The extensive use of tubing in thousands of products being manufactured today demands a wide range of process concepts. For example, in automotive manufacturing alone, new applications for tubing are being advanced at an expanding rate. From small and medium size tubular parts such as stabilizer bars to cam shafts, intrusion beams, and structural rails, steering columns, axles, and shock absorbers, the list continues to grow. On the other hand, oil and gas lines with their high-pressure requirements represent another specific area of large size tubular products where heating by induction has proven effectiveness. Figure 7.79 shows a variety of tube and pipe applications where heating by induction can be productively used.

In order to better suit a particular heating requirement, a variety of coil arrangements and frequency/power selection is used. Design of some tube/pipe inductors has been adapted from heat treating applications; others are quite similar

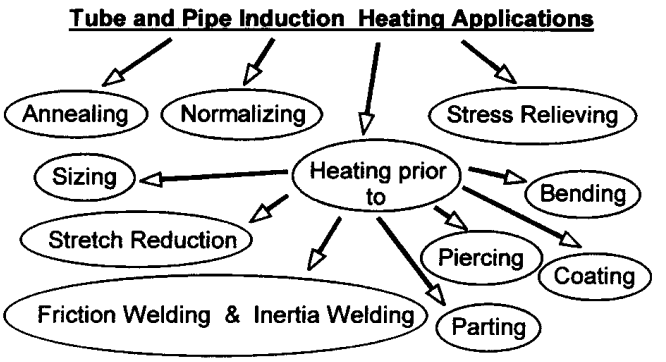

Figure 7.79 Induction heating of tubular products.

to designs used in bar/billet heating. For example, Figure 7.80 shows a 350 kW/1 kHz induction system for heating ends of tubes for upsetting or offset steel tube fitting.

Although there are many similarities, there are several process features and physical phenomena that distinguish induction heating of tubular products from induction heating of solid cylinders. The specifics of maximizing coil efficiency represent one of these features.

The coil efficiency of an induction tube/pipe heater is a complex function of several design parameters including coil ID to tube OD air gap, metal properties, coil length, tube wall thickness, and frequency with the last-named being the most critical factor. As can be seen in Figure 7.81, in the case of induction heating of a solid cylinder, there will be high coil efficiency when the applied frequency (**F2**) corresponds to a ratio of cylinder OD to current penetration depth δ greater than four ($OD/\delta > 4$. The use of a frequency that results in a ratio of $OD/\delta > 6$ will only slightly increase the coil efficiency. At the same time, the use of very high frequencies (frequency > **F3**) tends to decrease the total efficiency due to higher transmission losses and high heat losses as it will require a long heat time to provide the required surface-to-core temperature uniformity. If the chosen frequency results in a ratio $OD/\delta < 3$ (frequency less than **F2**), the coil efficiency will dramatically decrease. This is due to the cancellation of induced eddy currents circulating in the opposite sides of the solid cylinder.

Figure 7.81 shows that there is a difference in the optimal frequency for induction heating of tubular workpieces as compared to solid cylinders. In induction tube and pipe heating, the optimal frequency, which corresponds to maximum coil efficiency, is shifted toward lower frequencies (frequencies are between **F1** and **F2** for tubes instead of **F2** to **F3** for solid cylinders). The frequency appropriate for heating hollow cylinders typically provides a current penetration depth larger than the tube wall thickness (except for heating of tubes with small diameters). This condition can result in a noticeable increase in coil efficiency. In some applications, it is possible to gain an improvement in electrical efficiency of 10% to 16%. In others, the increase in coil efficiency is less pronounced and may not be noticeable.

The total gain in electrical efficiency when applying a lower frequency is not only derived from improvements in coil efficiency, but is also the result of lower bus bar losses and short heat time, as well as a reduction of transformer and capacitor losses.

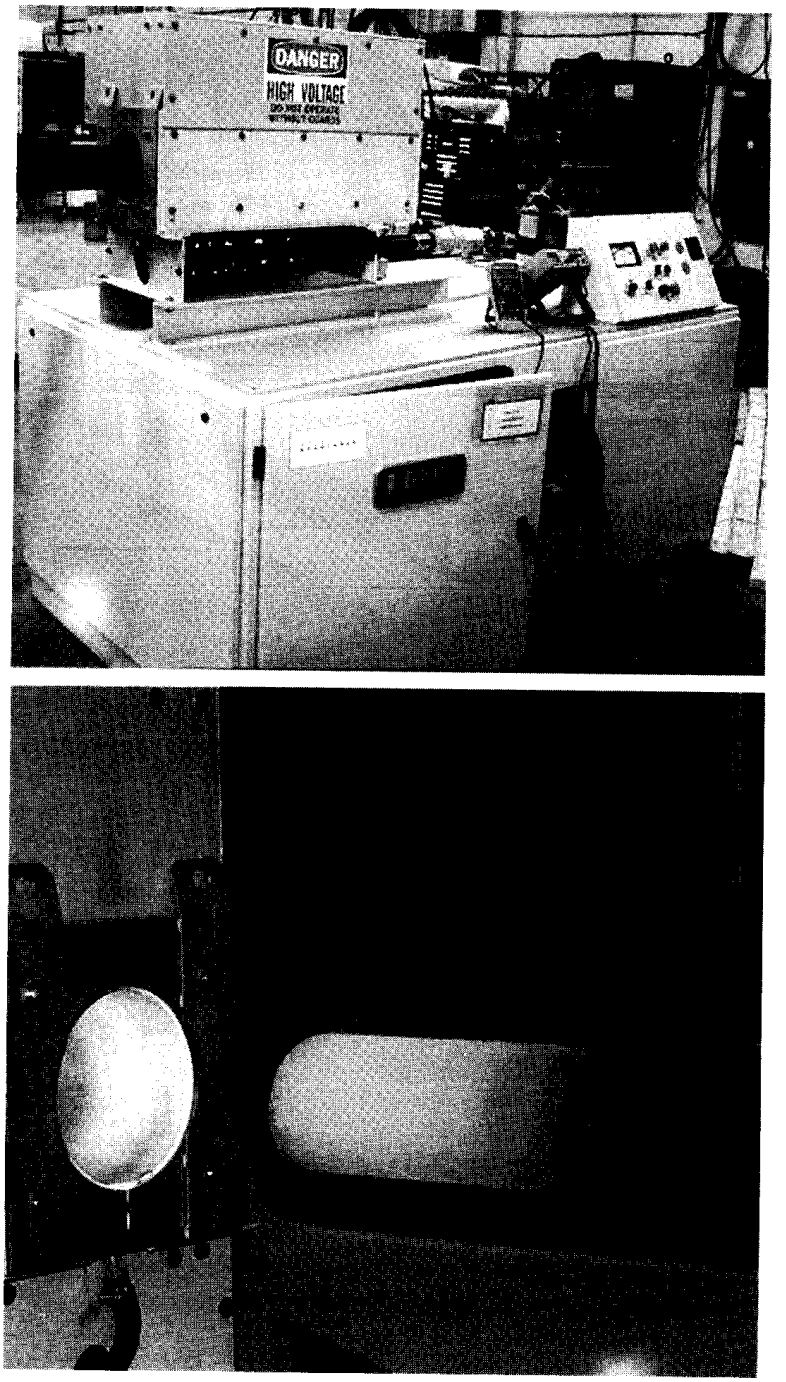

Figure 7.80 Compact 350 kW/1 kHz induction system provides heating of the ends of carbon steel tubes to a temperature of 1260°C (2300°F) to produce offset tube fittings. The system is capable of processing tubes with OD ranging from 0.1 m (4.15 in.) to 0.143 m (5.625 in.) and heated length of 0.2 m (8 in.) to 0.61 m (24 in.). (Courtesy of Inductoheat–I.H.S., Fort Worth, TX.)

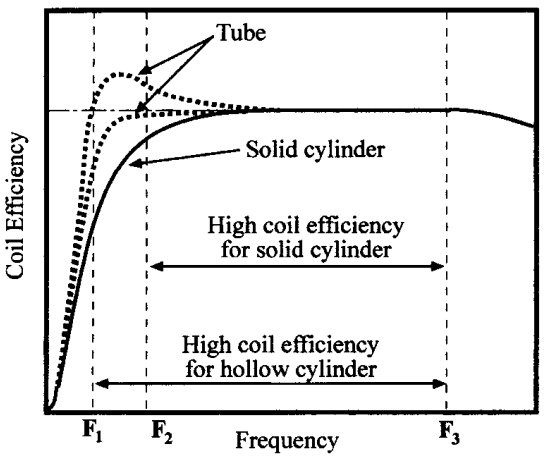

Figure 7.81 Coil electrical efficiency versus frequency.

Another advantage of using lower frequencies deals with improved overall system cost effectiveness, as typically, the cost of lower frequency power supplies is lower than that of higher frequency power supplies.

Numerical computation allows one to select the optimum frequency for a particular application. At the same time, in order to obtain a quick rough estimate of the most appropriate frequency, several simplified formulas are in use in the tube/pipe industry. For example, in the case of electromagnetically long solenoid-type inductors some typical formulas are shown below [390]:

$$\text{Frequency} = 34.6\frac{\rho}{A_m h}(\text{Hz}), \tag{7.3}$$

where

ρ = electrical resistivity of heated metal, ($\mu\Omega$*in),
A_m = average diameter; A_m =(Tube OD $-h$) (in),
h = wall thickness (in);

$$F_{\text{optimal}} = 8.65\frac{\rho 10^5}{A_m h}\ (\text{Hz}), \tag{7.4}$$

where the units are ρ ($\Omega * m$), $A_m(m)$, $h(m)$ [4]. Table 7.8 consists of frequencies obtained by using the formula recommended in [4].

It should be taken into consideration that in cases when induction heaters cannot be considered to be electromagnetically long inductors, but electromagnetically short inductors, the values of the optimum frequency will be higher than the values shown in Table 7.8.

It is necessary to mention that in tube and pipe heating, audible noise can be a dominant factor that greatly affects the selection of frequency, because certain tubes and pipes exposed to certain frequencies at high-power density emit resonant sound waves.

As has been mentioned earlier, regardless of frequency when heating a solid cylinder there is no eddy current flow in its core. However, when heating a hollow cylinder there is the flow of eddy current on both OD and ID surfaces. Figure 7.82

Table 7.8 Optimum Frequencies for Some Tubes/Pipes Using Solenoid-Type Inductors[a]

Tube OD mm (in.)	Wall Thickness, mm	Optimal Frequency, kHz		
Nonmagnetic Stainless Steel		20°C (68°F)	800°C (1472°F)	1200°C (2192°F)
12.7 (0.5)	1	51	85	92
	2	28	47	50
	3	21	34	37
25.4 (1)	1	25	41	44
	2	13	21	23
	3	8.9	15	16
	5	5.9	9.8	11
50.8 (2)	1	12	20	22
	2	6.1	10.1	11
	3	4.2	6.9	7.5
	5	2.6	4.3	4.7
76.2 (3)	1	7.9	13.2	14.3
	2	4	6.7	7.2
	3	2.7	4.5	4.9
	5	1.7	2.8	3
102 (4)	1	5.9	9.9	10.6
	2	3	5	5.4
	3	2	3.4	3.6
	5	1.2	2.1	2.2
Brass		20°C (68°F)	400°C (752°F)	900°C (1632°F)
12.7 (0.5)	1	4.8	8.4	15
	2	2.6	4.6	8.2
	3	1.9	3.4	6
25.4 (1)	1	2.3	4	7.2
	2	1.2	2.1	3.8
	3	0.84	1.5	2.6
	5	0.6	1	1.7
50.8 (2)	1	1.1	2	3.5
	2	0.6	1	1.8
	3	0.4	0.7	1.2
	5	0.25	0.43	0.8
Copper		20°C (68°F)	500°C (932°F)	900°C (1632°F)
2.7 (0.5)	1	1.33	3.7	6.3
	2	0.73	2	3.4
	3	0.54	1.5	2.5
25.4 (1)	1	0.64	1.8	3
	2	0.33	0.92	1.6
	3	0.23	0.64	1.1
50.8 (2)	1	0.31	0.87	1.5
	2	0.16	0.44	0.8
	3	0.11	0.3	0.51

[a]Under the assumption that these coils can be considered electromagnetically long coils.

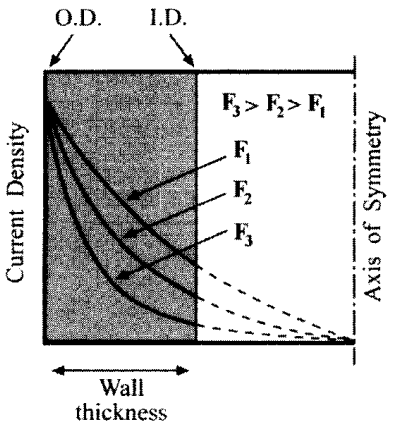

Figure 7.82 Current density distribution along the tube wall.

shows the current density distribution along the wall thickness of a nonmagnetic tube.

While discussing the current density distribution along the wall thickness of the tube it is imperative to mention a subtle phenomenon that does not have a wide practical use in induction tube heating. However, it is important to keep this phenomenon in mind from an academic perspective in order to have a complete understanding of the physics of the process. This phenomenon has been discussed in [51].

In some cases, the current density distribution along the wall thickness of the hollow cylinder may have an upside-down bell shape (arc shape). This phenomenon takes place under certain conditions. The first condition deals with the fact that the current penetration depth should be much greater than the tube wall thickness. The second condition is that an internal magnetic flux concentrator be placed inside of the heated tube. Figure 7.83 shows the distribution of current density along the tube wall thickness as a function of frequency assuming that a highly permeable magnetic flux concentrator has been placed inside the tube.

As would be expected, in addition to the frequency and properties of the heated material, the eddy current distribution along the tube wall thickness depends upon the air gap between the tube ID and the flux concentrator as well as the magnetic permeability of the concentrator. Figure 7.84 shows the effect of relative magnetic permeability on current density distribution. An evaluation of this phenomenon in a particular case can be done using numerical computation.

7.7.2 In-line Induction Heating of Tubes and Pipes and Their Applications

A continuous-feed multicoil induction heater similar to inline systems used for bar/rod/wire heating applications is a popular approach when it is required to through heat long tubular products. The range of heat treatment processes of steel tubes and pipes suitable for inline induction heating include hardening and tempering. As an example, Figure 7.85 shows a time–temperature profile of an induction hardening system of carbon steel tubes (tube OD = 127 mm, wall = 12.7 mm, at 3t/hr) that is

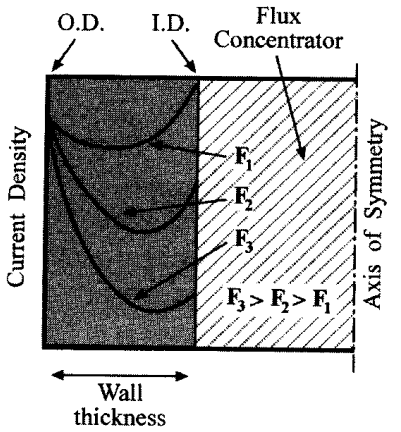

Figure 7.83 Current density distribution along the tube wall as a function of frequency when a highly permeable magnetic flux concentrator is placed inside the tube.

required to heat the tube through and consists of three inline coils and a water-spray quench chamber.

Whole body annealing of carbon steels as well as annealing of other metals such as titanium, copper, and stainless steel is equally suitable for inline annealing by induction.

Gas quench bright annealing of stainless steel tubes is another example of the effective use of an inline design approach [397]. Stainless steel tubing is used in decorative-type hardware, food processing, and other areas where a shiny bright appearance is important. The system shown in Figure 7.86 was installed in 1987 [397]. Stainless steel tubing is heated by induction to a temperature of about 1150°C (2100°F) and than goes into a 6.1 m (20 ft) long hydrogen–nitrogen gas quench tunnel.

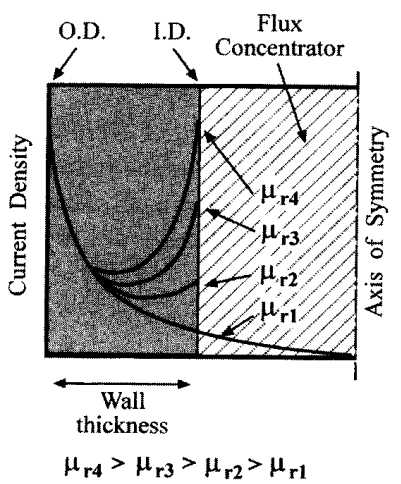

Figure 7.84 Effect of relative magnetic permeability of an internal flux concentrator on the current distribution along the tube wall.

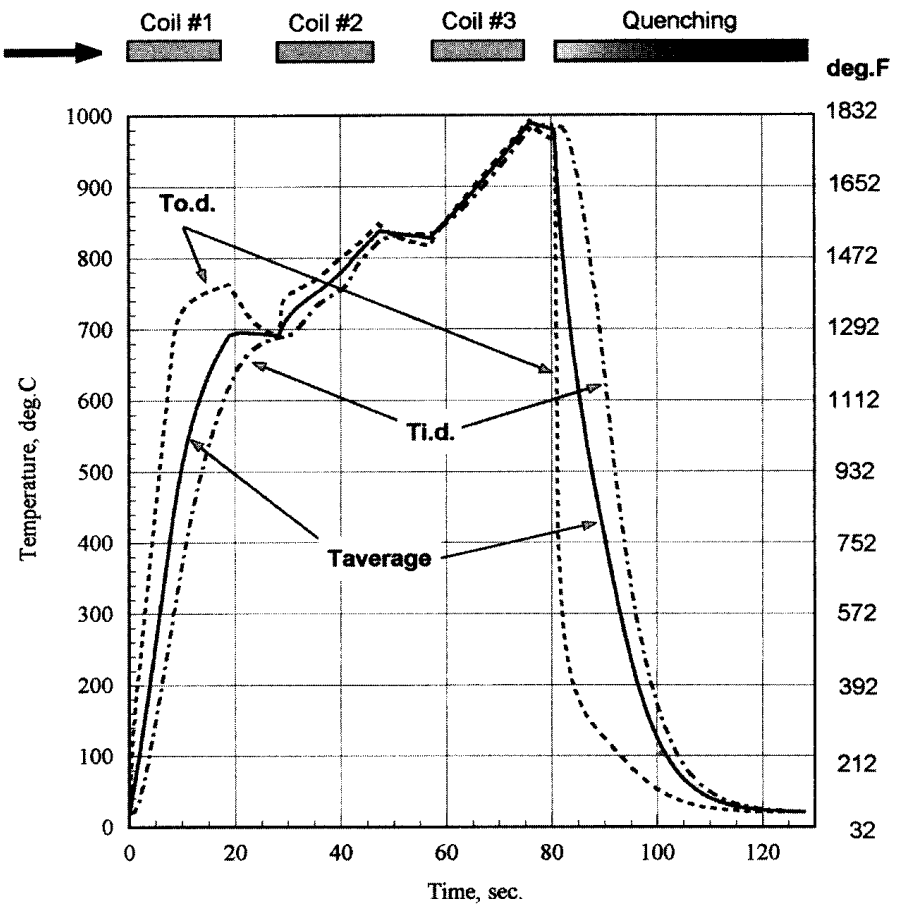

Figure 7.85 Inline induction hardening of carbon steel tube: tube OD = 5 in. (127 mm); wall = 0.5 in. (12.7 mm); Tube ID = 4 in. (101.6 mm); at 3t/hr; frequency = 3 kHz; coil length = 1.31 ft (0.4 m); distance between coils = 7.9 in. (0.2 m).

During the operation of the gas quench, nitrogen is used to purge the system of all oxygen. As purging continues, hydrogen is then fed into the system. Such an arrangement prevents the possibility of explosion that might occur should an excessive hydrogen and oxygen leak develop.

When designing bright annealing induction systems, it is important to have a sufficiently long quench tunnel so that when the tube exits the chamber its temperature is below the oxidizing point; otherwise the tube surface will tarnish as it reacts with the oxygen in the air. This phenomenon will not occur if the temperature of the stainless steel tube is below about 300°C (572°F) as it emerges from the gas quench tunnel. Therefore, in order to be on the safe side, it is typically required that the exit temperature from the gas quench zone not exceed 250°C (482°F) and often it is less than 150°C (302°F).

To maximize circulation and, hence, quench efficiency, quench gas is fed into two different locations in the tunnel. The tunnel has a water-cooled jacket that functions as a heat exchanger, helping to cool the quench gas that comes in contact with the tunnel's inner surface. Although the entire line is airtight, the possibility of gas contamination exists at the entrance to the heating line and the exit from the

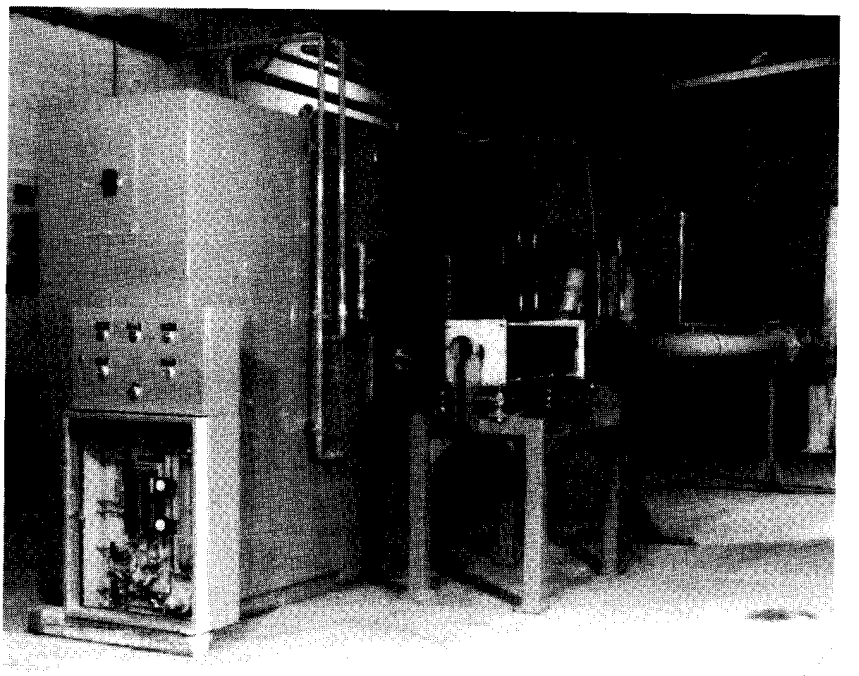

Figure 7.86 Gas quench induction bright annealing system for stainless steel tubing (304, 304L, 316, 316L grades). Tube ranges from 12.5 mm to 53 mm OD with a maximum throughput of 300 kg/hr (662lb/hr). The system has been operating since 1987. (Courtesy of Inductoheat Inc., Madison Heights, MI.)

quench tunnel. Consequently, the quench gas is kept under positive pressure. Hydrogen that "bleeds" is burned off at the entrance to the heating coil. In some cases, argon is used instead of nitrogen.

Stainless steel bright annealing systems often consist of a holding zone that is located between the induction heater and the quenching tunnel. The stainless steel tube maintains its temperature in this zone providing favorable conditions for the completion of the diffusion-type processes, ensuring that the required microstructural conditions have been achieved. A separate low-power induction coil or electric furnace can be used to hold the required temperature at the desired level by compensating for the radiation and convection heat losses from the tube surface in the holding zone.

After exiting the quench tunnel the tube temperature is much below the levels where surface contamination can occur during contact with air or moisture, therefore the tube is cooled down for handling purposes using a water spray system.

The success of induction bright annealing of stainless steel tubes using a gas quench is greatly affected by the quality of the gas. As the dewpoint rises, the gas contains more moisture and the corresponding volume of hydrogen has to be increased. Otherwise, the process will not provide the required quality and surface appearance, because the chrome in the stainless steel and the moisture react together forming an oxide, Cr_2O_3.

Induction heating can be advantageously used for annealing of not only steels but light metals as well, for example, copper tubes. Copper tubes are utilized for

water plumbing, consumer goods, transport, textile, and industrial machinery industries. One of the world's fastest copper tubing growth areas is in the production of tubing for the air conditioning and refrigeration industry. These industries dictate particular requirements for thin wall ACR copper tubing [307]. These include:

- Small eccentricity of wall thickness;
- Accurate dimensional tolerance;
- Maximum heat transfer area;
- Cleanliness of the tube inside wall; and
- Proper grain size and anneal properties of the tube to allow easier bending.

Due to several advantages, induction high-speed copper tube annealing systems (Figure 7.87) are replacing the older bell-type and roller hearth furnaces. As has been reported in [307], with induction the major saving over the conventional roller hearth furnace occurs where the second layer winding operation is eliminated. This not only saves the cost of the equipment purchase of a second layer wind machine, but also reduces operating costs and provides greater productivity. The exposure to mechanical damage of fully annealed product handling is also eliminated. Table 7.9 provides a comparison of a conventional roller hearth furnace to an induction annealing system for light wall, inner groove feed, ACR copper tubing.

After the tube is heated to the annealing temperature (for phos deoxidized copper it is about 700°C (1292°F)) it enters the holding or dwell zone to produce

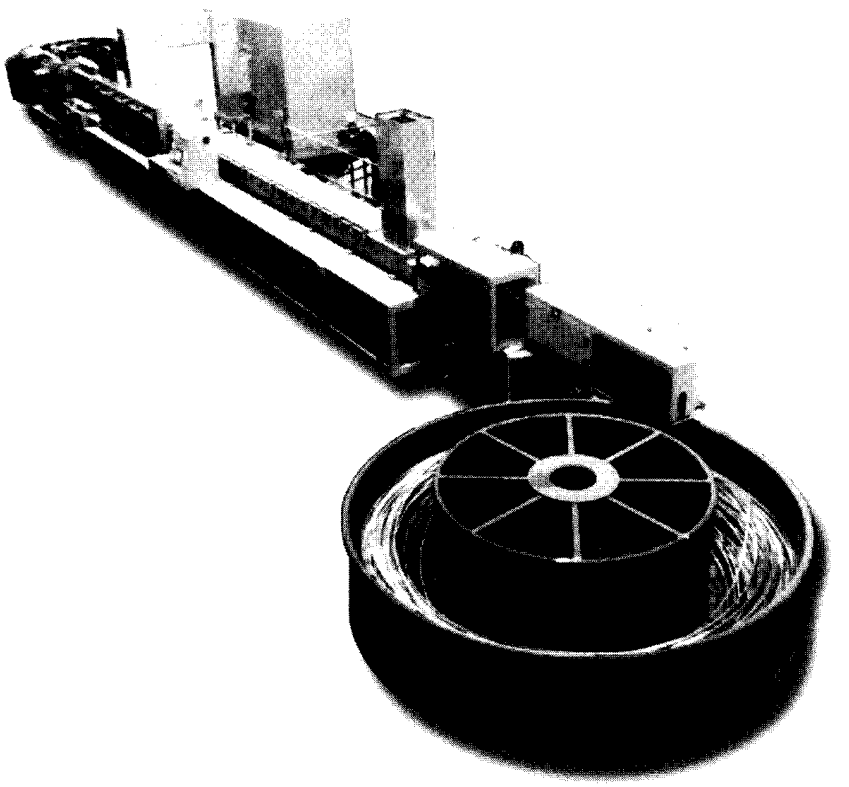

Figure 7.87 Basket-to-basket induction annealing system of ACR copper tubing. (Courtesy of Inductoheat Australia.)

Table 7.9 Operating Comparison of Conventional Furnace and Induction Strand Annealing for Light Wall, Inner Groove Feed, ACR Copper Tube

Comparisons	Roller Hearth Annealing Furnace	Induction Strand Annealing Line
Direct labor	2 man h/ton	1.25 man h/ton
Energy standby losses during zero production periods	50 kW	0 kW
Energy consumption on 12.7 mm OD × 0.38 mm wall	233 kWhr/ton	167 kWhr/ton
Protective atmosphere consumption	24,000ft^3/hr	50ft^3/hr
Floor space	600 m^2	160 m^2
Number of layer winding operations	1.75	1
Layer winding machine purchased	2	1
Loss of tube per coil length after anneal	0 meters	2 meters
Flexibility for automation	Difficult	Simple
Incremental expansion	Difficult	Good

Source: Ref. 307.

full-grain recrystallization. Thereafter, the tube enters the rapid quench station where the temperature is rapidly brought down to a conventional handling temperature. The typical layout of an induction basket-to-basket ACR copper tube annealing system is shown in Figures 7.88 and 7.89. This system was produced by Inductoheat Australia in collaboration with Mitsui Engineering & Shipbuilding Co.

When designing induction annealers for light wall copper tubing (i.e., wall thickness can be as low as 0.3 mm) running at standard line speeds of 200 to 500 m/min (3.33 m/sec to 8.33 m/sec), automatic tension control is of the utmost importance to avoid tube marking. This is achieved by a variable-speed driven

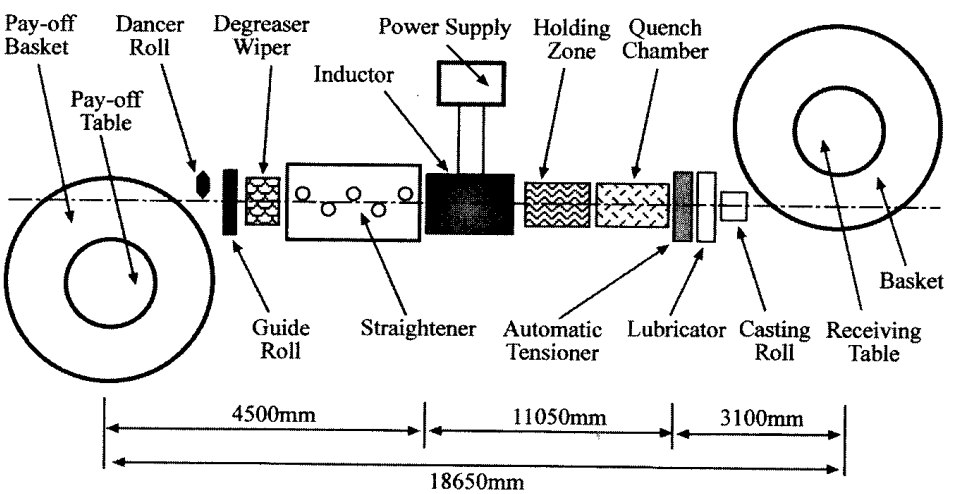

Figure 7.88 Typical layout of an induction copper tube annealer (300 m/min). (Courtesy of Inductoheat Australia.)

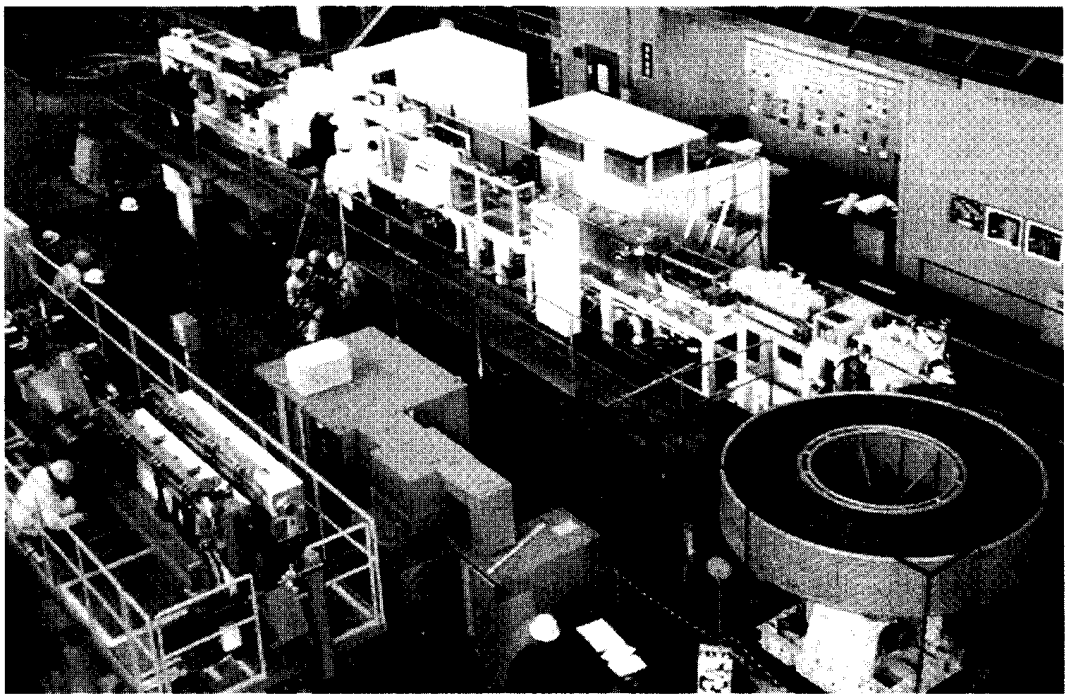

Figure 7.89 Induction basket-to-basket ACR copper tube annealing system built by Inductoheat Australia in collaboration with Mitsui Engineering & Shipbuilding Co.

caterpillar type system, which constantly and precisely controls the copper tube tension during the annealing operation and minimizes any occurrence of jamming. A detailed description of the system shown in Figure 7.89 can be found in [307]. Table 7.10 provides a typical annealing specification for phos deoxidized copper tube with an annealing grain size of 0.015 to 0.025 mm running at 300 m/min (5 m/sec) rated speed. The annealing temperature is about 700°C (1292°F). The power rating of this system is 600 kW.

Metallic and nonmetallic coating of tubular steels also often calls for the use of inline induction heating. The main purpose of metallic coating of carbon steel tubes is to improve resistance to corrosion, oxidation, and abrasion.

Galvanizing is one of the most popular metallic coating techniques. A fine zinc or zinc alloy layer is deposited on the OD surface of a steel tube, developing

Table 7.10 Typical Annealing Specification

Wall Size (mm)	Weight (kg/m)	Speed (m/min)	Energy Consumption (kW hr/ton)	Limiting Factor	Comments
12.7 ⌀ × 0.48	0.1648	300	202	kW	1. One induction coil size is used for all tube sizes
12.7 ⌀ × 0.38	0.1316	300	167	Speed	
11.2 ⌀ × 0.38	0.1155	300	192	Speed	
9.52 ⌀ × 0.38	0.0976	300	239	Speed	2. Adjustable grain size is instantly available

a metallurgical bond that provides a dual-action protection mechanism. A detailed discussion of the physics and nature of metallic coating is described in Section 7.6.

Nonmetallic coating represents a wide range of different coating techniques including, but not limited by, primers, paints, epoxies, polymers, heat-cured powders, and the like. Because some of the features of nonmetallic coating are described in Section 7.6.1.2, the present discussion is limited to a description of one coating process: the three-layer pipe coating that includes all of the most important aspects of nonmetallic coating [306, 388].

Three-layer coating systems provide specified performance properties for the external protection of steel pipes designed for safety and lifelong transmission service. The multilayer pipe coating combines a fusion bond epoxy film (which has excellent adhesion and chemical resistance properties), the extruded intermediate adhesive copolymer layer, and the extruded multilayer polyethylene top layer. This combination provides corrosion protection and strong physical and mechanical performance, even at elevated temperatures. The mechanical properties of surface coating include a relatively high impact strength and penetration resistance. Steel pipes that have a three-layer coating have a range of impressive performance properties, such as

- Low permeability to water vapor and gases;
- Mechanical protection against handling and transportation damage;
- Superior resistance to cathodic disbonding;
- Outstanding dielectric properties;
- Heat-aging resistance because of stabilization against oxidation damage;
- Strong resistance to environmental conditions such as corrosive soils, salt water, microorganisms, and spreading plant roots; and
- Good outdoor resistance due to carbon-black addition.

As has been reported in [306, 388], the three-layer coating has practically no adverse effects in the circumferential welded area where one pipe is joined to another. There are no limitations on infield pipe bendability using the conventional cold bending methods up to 2% of the outside diameter. This pipe coating method also causes minimal pollution problems during the application.

The sequence of the three-layer nonmetallic coating operation consists of the steps shown in Figure 7.90. This process includes:

1. Abrasive mechanical descaling of the pipe surface, together with a profiled surface pattern, to achieve good epoxy bonding properties;
2. A thin-film epoxy primer of about 0.05 mm fusion bond coated by an electrostatic powder spray method on the inductively preheated surface;
3. The extruded and wrapped copolymer layer, with 0.25 mm applied as an intermediate layer, producing strong adhesion between the epoxy primer and the polyethylene top coating; and
4. The extruded and multiwrapped polyethylene top layer. A thickness of 2.7 mm or more is applied.

Uniform heating is paramount for good coating properties. Inline induction heating is the most suitable method for this coating process. It is essential to provide a clean oxidefree surface and obtain a constant application temperature. Typically,

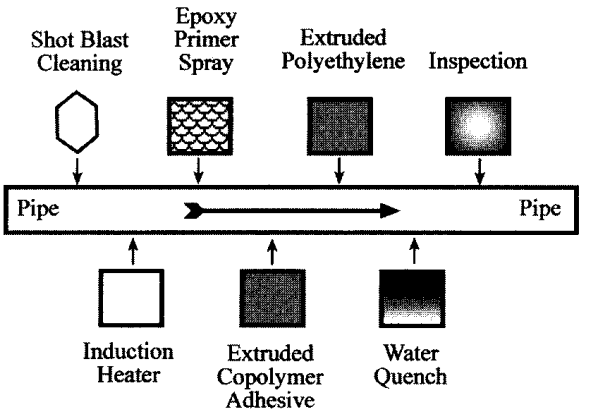

Figure 7.90 The stages of three-layer pipe coating.

the pipe is heated to about 210°C (410°F) on the outside surface before entering the coating system. It may seem that only the pipe surface needs to be heated, as that is the area to be coated. However, surface radiation and the cold well effect (soaking effect) of a heavy-wall pipe are important considerations in determining the total mass to be heated.

As the pipe emerges from the induction heater, radiation and convection heat losses occur over a large surface area. These losses may be relatively insignificant compared to the heat loss from the surface due to the soaking action of the inside wall of the pipe. If the system is designed to heat through the pipe wall, then the phenomenon of thermal conduction from OD to ID is eliminated resulting in a sound engineering design and minimal possibility of a reject after coating. The downside of heating through the wall is an increase of energy consumption that adds to the total operating cost. Therefore, the total wall thickness should be heated unless the wall thickness becomes very heavy and the coating operation can be located very close to the exit of the induction coil.

Figure 7.91 shows induction coils and a solid-state power supply for heating of pipes used for oil and gas lines prior to application of a three-layer polyethylene coating. This system is quite large. The coils are normally maneuvered into the heating position with the aid of casters or wheels, and jacked up for correct pass line height. They are housed in a steel frame to ensure robust performance and long life. Some systems are built with a coil mounted on a frame, permanently located in the line, and are moved in and out of position by a crane.

Typically, one coil is designed with the ability to heat several different pipe sizes. Flexibility of the power supply to allow operation under varying load conditions is an important factor.

An important step in designing the coating processes is to determine the pipe coating speed achievable with different wall thicknesses and different diameters. Figure 7.92 illustrates the results of tests to indicate the possible coating speeds per 1000 kW of power operating at a frequency of 1 kHz using an INDUCTOHEAT-style power supply [306, 388]. Usually, a computer model is made of the various pipe diameters and wall thicknesses for accurate kilowatt sizing related to the desired coating speed.

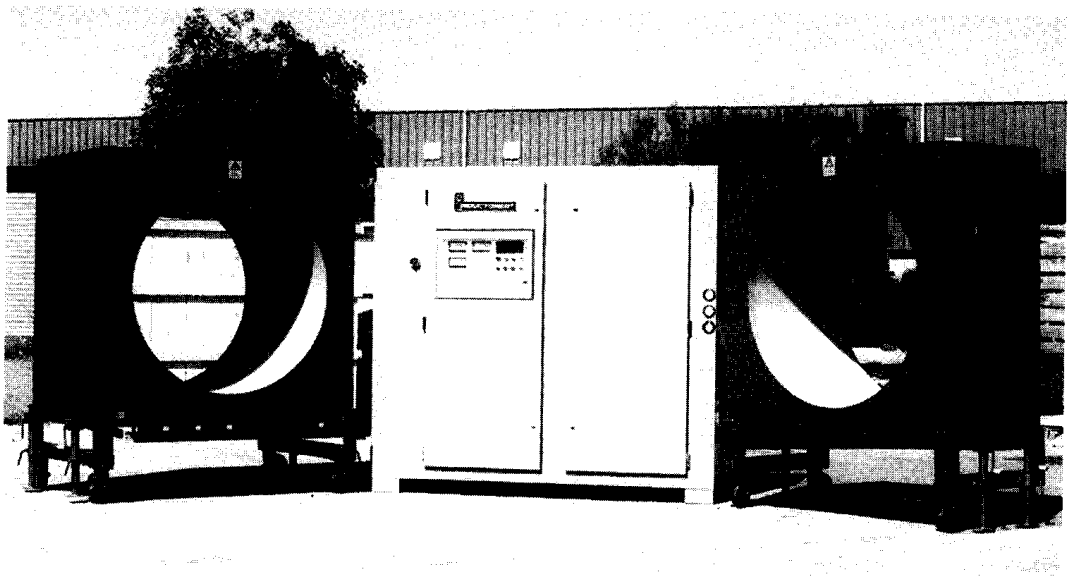

Figure 7.91 Induction heating system for pipe coating. (Courtesy of Inductoheat Australia.)

7.7.3 Selective Heating of Tubular Products and Case Studies of Typical Applications

The ability of induction to concentrate the heat within a certain area of the workpiece is widely used to selectively heat tubular products. Such applications as localized stress relieving (Figure 7.80), brazing, parting, friction welding, bending, annealing of welds, and others are typical candidates for selective induction heating. Figure 2.49 shows some samples of friction-welded tubular parts that have been selectively preheated by induction.

Figure 7.93 illustrates some thermal features of selective heating of hollow cylinders, where a two-turn solenoid-type induction coil has been used as an exam-

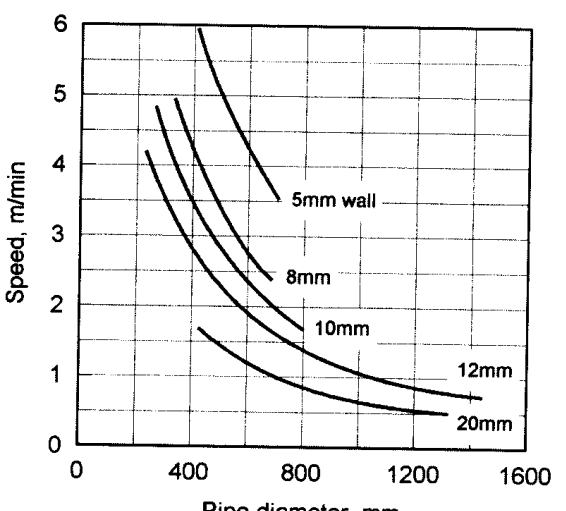

Figure 7.92 Test results of possible coating speeds per 1000 kW of power operating at a frequency of 1 kHz as a function of pipe OD and wall thickness. (From Ref. 388.)

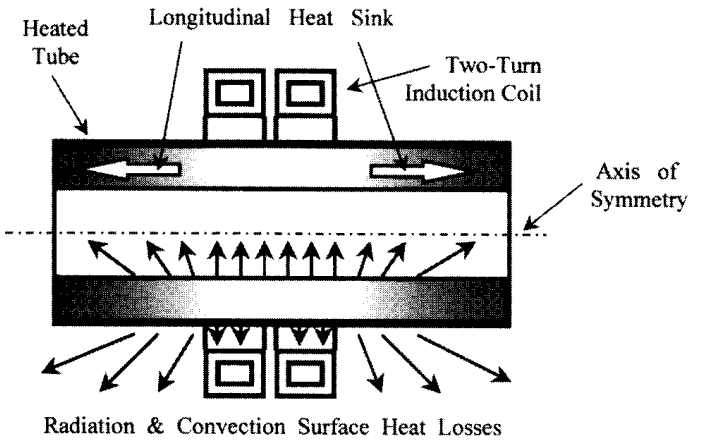

Figure 7.93 Radiation and convection surface heat losses in selective heating of tubes.

ple. The maximum temperature will be observed under the inductor in the middle of the heat zone. As a result of radiation and convection heat losses, there will be cooling from the OD and ID surfaces. Of course, cooling from the ID surface will be much less pronounced compared to cooling from the OD surface. This is primarily true due to significantly lower radiation losses from the ID surface.

Another important feature that strongly affects the required power, coil design, and frequency choice is the existence of transition zones and the cooling effect due to the longitudinal heat sink from the cold ends of the tube (Figure 7.93). It is important to recognize that, somewhat similar to bar end heating applications, the existence of transition zones and heat sink phenomena are primarily responsible for mistakes in determining the required coil power and temperature profiles when calculations are based on simple formulas using one-dimensional numerical computation approaches or uncoupled numerical software (see Sec. 3.4.3.5). Without knowing the length of the transition zone and temperature profiles within these zones, it is very difficult to make a reasonably accurate estimate of the total mass of the heated metal and, therefore, to determine the required power to heat a tube to the final temperature in the desired time. The use of two-dimensional coupled software allows one to overcome this.

As an example, Figure 7.94 illustrates the dynamics of selective induction heating of a 1045 carbon steel tube with OD = 152mm (6 in.) and wall 15 mm (0.6 in.) using a 1 kHz power supply prior to the tube parting operation. The optimal algorithm of power variation applied to the induction coil was also obtained during the numerical computation. Typically, the design procedure for determining the coil geometry and algorithm for power variation includes several computations. As a result of computer modeling, the influence of the different factors on process parameters can be evaluated and optimized. For example, in some tube parting applications it is wise to use a single-turn coil instead of a multiturn coil arrangement.

The choice of coil length is another critical issue, which can be quite contradictory when designing induction heating systems for such applications as tube parting. It is quite clear that a shorter coil results in a smaller mass of metal to be heated and, therefore, leads to a lower coil power requirement. From another perspective, the coil electrical efficiency is a function of not only the frequency, material

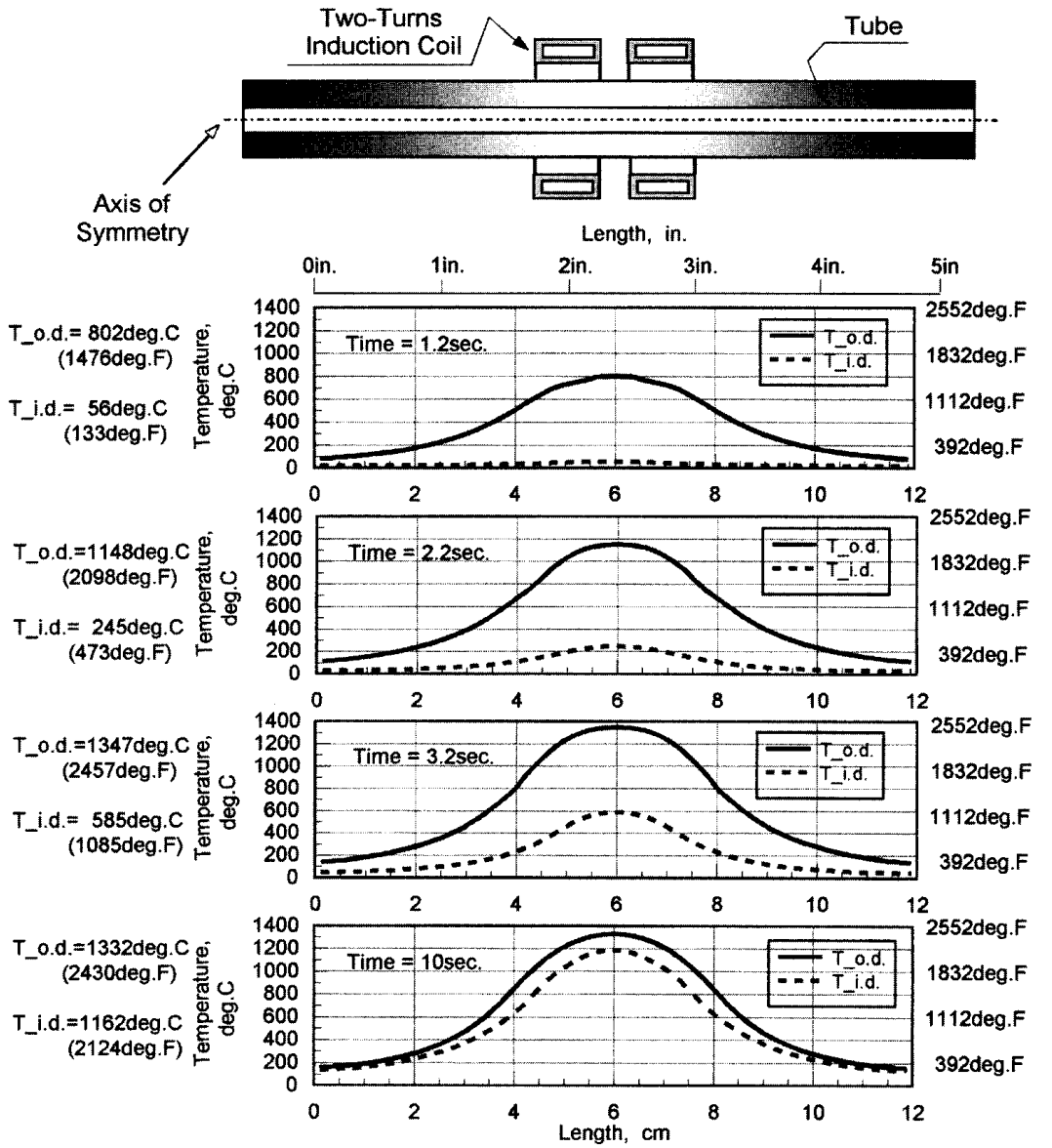

Figure 7.94 Temperature profiles at different stages of induction heating of carbon steel tube: OD = 152 mm (6 in.) at 1 kHz.

properties of heated metal, and coil-to-copper air gap, but is also a function of the coil length. Shortening the coil length results in a decrease of the coil electrical efficiency. Therefore, the choice of coil length is always a reasonable compromise.

When heating selective areas, it is sometimes desirable to have a short longitudinal transition zone. In cases such as this, the ability of a flux concentrator to localize the magnetic field in the required area in combination with a short heat time can be a definite benefit.

In addition to friction welding and parting, the ability of induction to provide selective heating is effectively used for localized stress-relieving (Figure 7.95) as well as for tube end heating prior to swagging or upsetting (Figure 7.80) or for pipe/tube

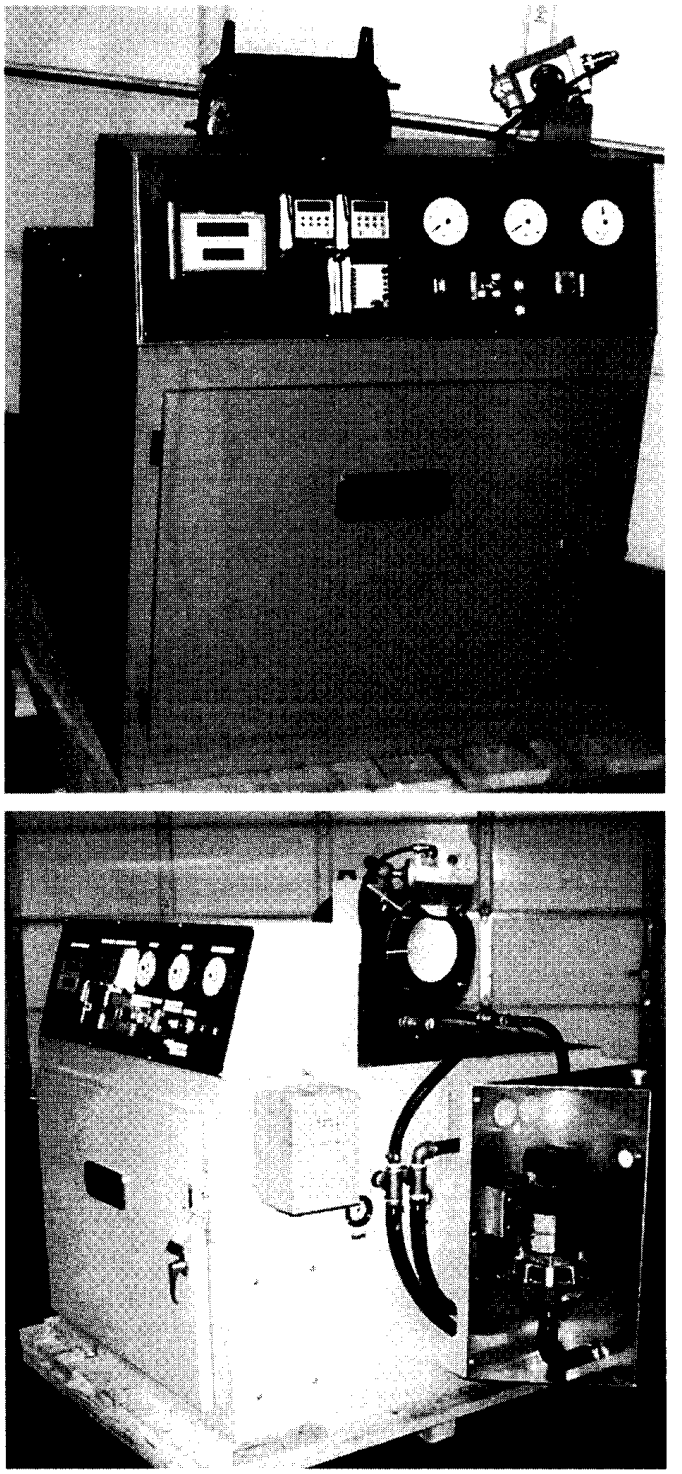

Figure 7.95 I.H.S. Model LFS–200 kVA, low cost line frequency pipe end stress-relief induction system for threading, designed to operate from a 480 volt, 60/50 Hz single phase. The system includes an SCR power contoller with input line capacitor, kilowatt/current/power factor metering, primary transformer, power factor regulator, UNICOOL water recirculating system, and optical pyrometer for temperature sensing.

bending applications where it is required to heat a narrow band of metal around the area to be bent. Induction bending is usually performed on steel pipes/tubes with outside diameters varying in the range of 0.1 m (4 in.) to 1 m (40 in.). At the same time, there are examples of induction bending installations that are capable of bending much larger pipes (e.g., 1.5 m (60 in.) OD and even larger) [394].

The sketch shown in Figure 7.96 illustrates the principle of an induction bending machine. After positioning the pipe and firmly clamping both its ends, power is applied to the solenoid-type inductor that provides a circumferential heating of the pipe area to be bent. Upon achieving the appropriate temperature distribution to provide sufficient ductility of the metal at the heated band where the actual bending will take place, the pipe is pushed forward through the coil at a certain speed. The pipe's leading end, being clamped to the pivot arm, experiences a bending moment. The bending arm can pivot up to 180°. In induction bending of carbon steel pipes, the length of the heated band is usually within the range of 25 mm (1 in.) to 50 mm (2 in.) with the required temperature range from 800°C (1472°F) to 1080°C (1976°F). As the pipe passes through the inductor, it bends within the hot and ductile bend area according to the radius of the pivot radial arm while being supported on each side by a cold nonductile rigid section. Depending upon the application, bending speeds can vary from 12.7 mm (0.5 in.)/min to 150 mm (6 in)/min. In some bending applications, where larger radii are required, instead of a pivot radial arm a set of bending rolls that provide a bending force is used [276, 391–394].

After completion of the bending operation, the pipe is cooled down to ambient temperature using a water spray, forced air, or natural cooling in air. The process of stress-relieving or tempering can be conducted in order to obtain the desired post-bend properties of as-quenched steel pipes.

It is important to emphasize here that induction heating provides fast localized circumferential heating of selected areas of the pipe, consuming a minimum amount of energy compared to other hot bending processes that require heating the entire pipe. There are also other important benefits provided by induction tube bending. These benefits include, but are not limited to, high predictability of shape distortion (ovality) and wall thinning. Minimization and predictability of wall thinning are particularly critical when producing tubes and pipes for such industries as nuclear, or oil and gas lines with high-pressure requirements.

Oil and gas pipeline ratings are based on the wall thickness. During bending the outer side of the bend is in tension and has a reduced cross-section, while the

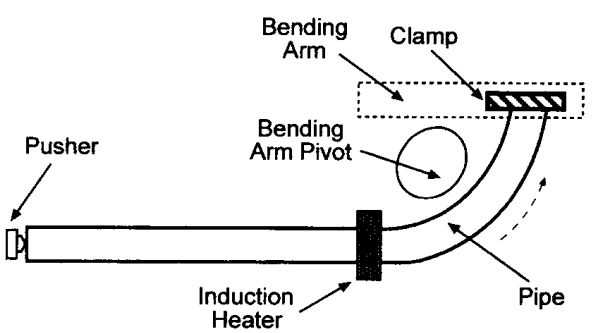

Figure 7.96 Sketch of an induction tube bending machine.

inner side of the bend is in compression. When conventional heating is used to make the bend, the outer side of the bend area section is often reduced by as much as 20% or more resulting in a corresponding reduction of the total pipeline pressure rating [388]. The pipe bend becomes the pressure-limiting factor in the total pipeline. With induction heating this cross-section reduction is reduced to typically 11% due to very even heating, an optimized bending program through a computerized bending machine, and a narrow plasticized (ductile) zone. Therefore, induction heating not only reduces production cost and increases the quality of the bend, but also reduces the total pipeline cost.

Other important advantages of induction bending deal with the fact that it is a nonlabor-intensive process, has little effect on surface finish, and has the ability to bend small radii, producing multiradius curves/multiple bends in one pipe and bending of thin-walled tubes [391–393].

Rapid induction heating of the localized areas is used not only for bending steel tubes but for bending some light metal hollow products, such as aluminum tubes as well. However, there is a different phenomenon involved in bending aluminum tubes compared to steel. According to the process of retrogression heat treatment (RHT process) that has been patented by Alumax Extrusions Inc. [408], induction heating provides rapid heating of selective areas of age hardenable aluminum alloy extrusions (i.e., 6000- and 7000-series alloys in various tempers and particularly the –T6 temper) to a temperature range from 315°C (600°F) to 538°C (1000°F) within a few seconds. The purpose of heating is to provide a full or partial softening of the heated zone after its rapid quenching to ambient temperature. Bending is typically done at room temperature with conventional tools and lubricants. It has been reported that even thin-walled aluminum tubes of 6061-T6 have been successfully bent using induction heating in combination with the RHT process to a radius-to-ID ratio of one tube diameter [408].

Seam annealing and stress-relieving represent areas that utilize induction to provide selective noncircumferential heating of certain areas of pipes. Figure 7.97 shows a seam annealing inductor design that utilizes a split-return coil for annealing straight welded steel tubes. When the tube has been welded, the metallurgical structure in and around the weld zone (the heat-affected zone) is altered to produce a Widmanstatten-type structure which occurs when metal has been heated to a very high temperature. This structure is an undesirable nonhomogeneous brittle structure that consists of coarse elongated grains "shooting" into the matrix. Brittle martensitic areas are formed in the welded zone as a result of self-quenching (mass quenching) due to the thermal conductivity of the heated zone by conduction to adjacent unheated cold areas. The narrower the heat-affected zone, the faster the cold sink effect will occur, the coarser the grain structure will be formed, and the more brittle the welded area will be.

In order to anneal a weld it is required to heat the weld zone to a minimum temperature of about 600°C (1112°F). The inductors are typically mounted in the mill line immediately after the welding and scarfing operations. In addition to the coil geometry, inductor-to-tube air gap, and frequency, the required heating power depends upon the rate of tube processing and the width of the zone to be heated. Typically this zone can vary from 12 mm ($\frac{1}{2}$ in.) to 50 mm (2 in.) depending on pipe diameter, wall thickness, and so on.

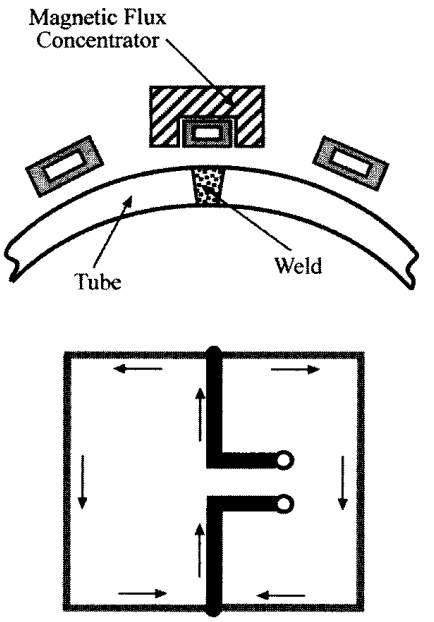

Figure 7.97 Split-return seam annealing inductor (top) and diagram of its electrical ciruit (bottom).

When determining the required power, consideration must also be given to the residual temperature of the weld zone, keeping in mind that the amount of residual heat after induction welding is noticeably greater than the heat generated as a result of contact or laser welding.

The split coil or clamshell inductor shown in Figure 7.98 represents an inductor design approach that is typically used for localized annealing of large oil and gas pipes having circumferential welds in a field environment. The coil is assembled around an existing pipe and disassembled after heating the weld area.

7.8 SLAB, PLATE, BLOOM, AND RECTANGULAR BAR HEATING

7.8.1 General Remarks

Induction heating is often the most popular approach to the heating of rectangular shape workpieces (Figure 7.99). Workpieces of this general shape, including slab, bloom, plate, and rectangular bar, are referred to in this section as slab. Specific reference is made to a particular shape where it applies.

Although there are several different coil arrangements available to heat a slab by induction, the great majority of applications apply longitudinal flux inductors (rectangular solenoids) (see Figures 7.100 and 7.101). As mentioned in Section 3.1.7, due to the geometry of rectangular slab, induction heating of such workpieces has several features compared to the heating of cylinders. These include several electromagnetic effects and the peculiarity of heat transfer phenomena. Therefore, it is imperative to outline here the specifics of electromagnetic end and edge effects taking

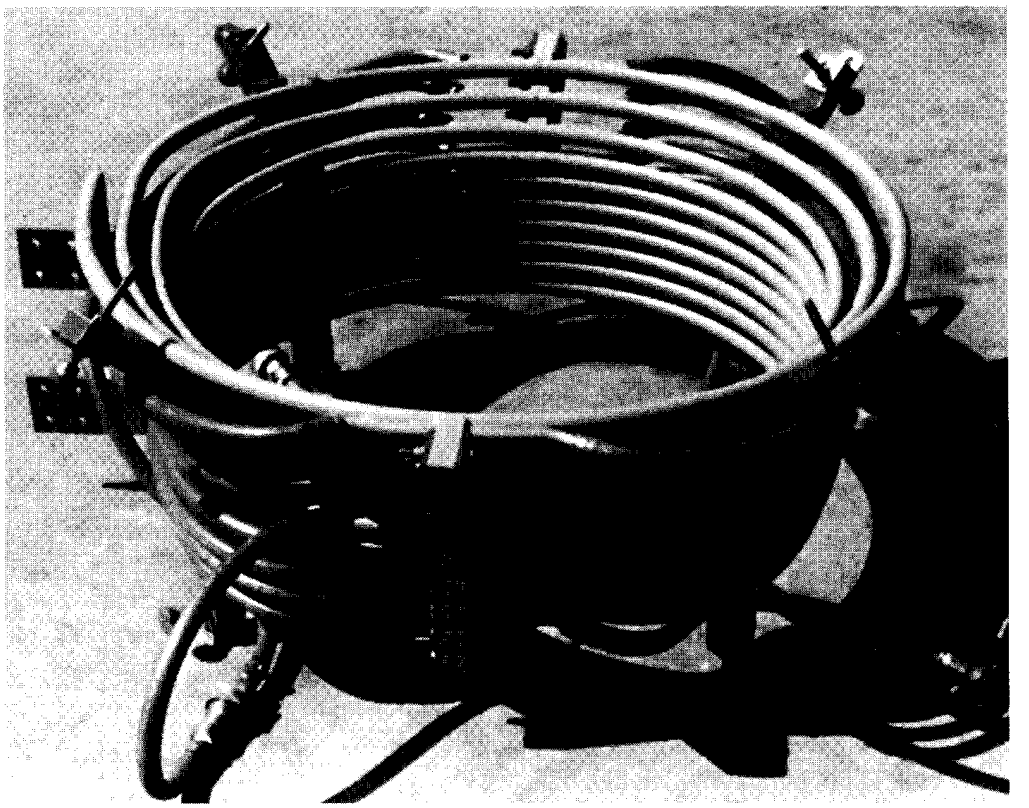

Figure 7.98 Split coil (clamshell inductor) for pipe joint weld annealing.

place when heating rectangular bodies (previously discussed in Sec. 3.1.7). Later in this section an in-depth study of these effects is provided as well.

Suppose a slab is placed in an initially uniform magnetic field (Figure 7.102). If the slab's length a and width b are much larger than its thickness d, the electromagnetic field in the slab can be viewed as an area consisting of three zones: central part, area of the longitudinal end effect, and area of the transverse edge effect (Figure 7.102) [51, 53, 120–123, 190–194].

In the central part, the electromagnetic field distribution corresponds to the field in the infinite plate. Basically, end and edge effects have two-dimensional space distributions excluding only the zone of three-edge corners where the field is three-dimensional and the corresponding field distribution is the result of a mixture of both the electromagnetic end and the edge effects.

In the longitudinal flux induction heating of long or continuously fed rectangular slabs the difficulty in obtaining heat uniformity is caused by a combination of the skin effect, electromagnetic edge effect, and electromagnetic end effect.

The core-to-surface temperature difference is a result of the skin effect. The temperature difference between the edge area and central part of the slab is caused by the combination of the electromagnetic transverse edge effect and additional heat losses at the edge area. Due to the electromagnetic edge effect, a surplus or shortage of power in the edge area can occur. With the proper choice of design parameters, it is often possible to obtain a proper power distribution that will provide a reasonably

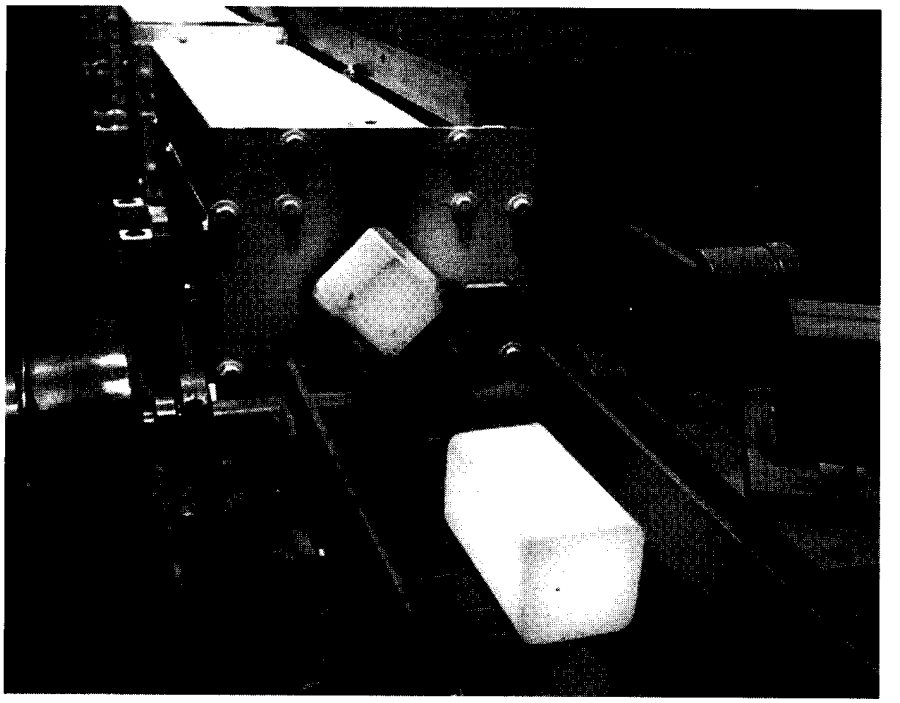

Figure 7.99 Induction heating of round-cornered square billets.

uniform temperature profile along the slab width. This reasonably uniform temperature distribution is often called a quasiuniform temperature profile. In this case, the additional heat losses at the edge area are compensated for by the additional power generated there due to the electromagnetic edge effect.

The electromagnetic end effect in slab heating applications is primarily responsible for temperature differences between the end areas of the slab (nose and tail of the slab) compared to its central part.

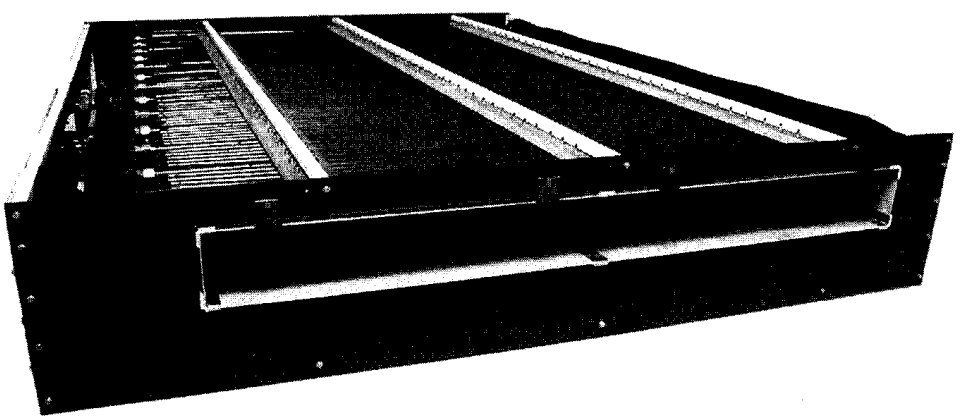

Figure 7.100 Longitudinal flux inductor (rectangular solenoid) for induction heating of slabs, plates, strips, and sheets.

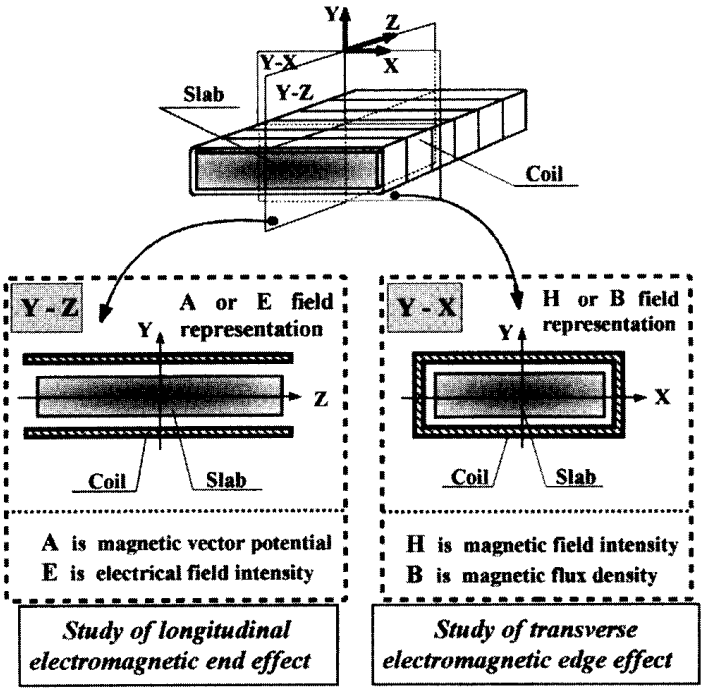

Figure 7.101 Field representation for induction slab heating using rectangular solenoid coils.

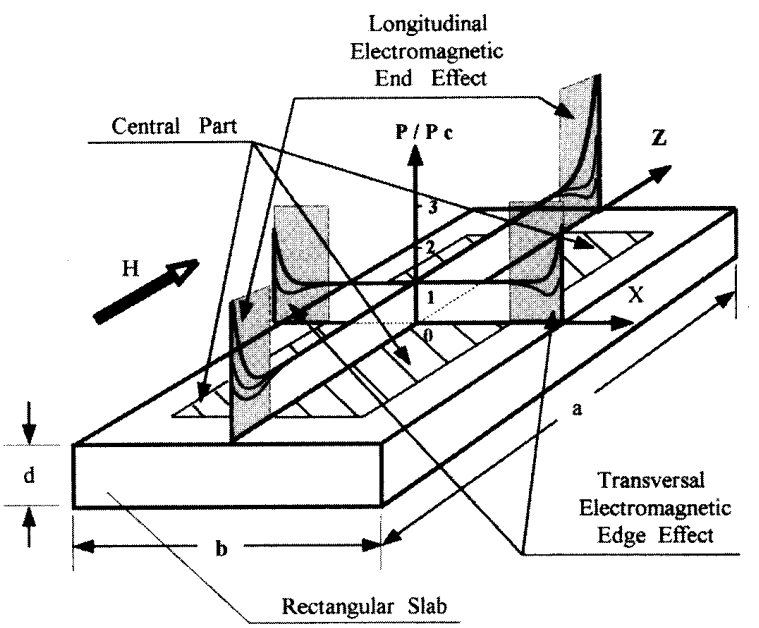

Figure 7.102 Electromagnetic end and edge effects of the slab.

Due to the complex nature of electromagnetic edge and end effects, the reasonably precise evaluation of the induction slab heating process should be done by numerical simulation. A transverse edge effect can be studied using B or H field representation (Figure 7.101). In contrast, it is easy to study the electromagnetic end effect using A or E field representation (see Sec. 3.4.3).

The choice of frequency has a major effect on the temperature profile within the slab's body. Thermal gradients along the length, thickness, and across the width greatly depend upon the chosen frequency. Similar to induction heating of cylinders, the temperature distribution along the thickness of the slab is affected by the skin effect (see Sec. 3.1.2) which in turn directly depends upon the frequency as well.

When heating a rectangular shaped body, it is convenient to quantify the skin effect in the slab, using the ratio of d/δ, where d is the thickness of the slab and δ is the current penetration depth calculated according to formulas (3.6) and (3.7). More uniform temperature profiles along the slab thickness correspond to a lower ratio of d/δ. If d/δ is much greater than 6, the temperature distribution along the slab thickness will be noticeably nonuniform. An increase of the cycle time, in combination with the power density reduction, leads to more uniform heating because thermal conductivity "helps" to equalize the thermal gradients. At the same time, an increase of the cycle time leads to an increase in heat losses. Equipment floor space requirements increase with corresponding increases in cycle time as well.

Importantly, as in the case of heating cylinders, the choice of frequency affects not only the required temperature profile within the slab, but also coil electrical efficiency. There is an optimal frequency value ($F_{el.eff.}$) that corresponds to the maximum value of coil electrical efficiency. The use of a frequency higher than the optimal will only slightly change the efficiency. However, a significantly higher frequency (i.e., $d/\delta \gg 25$) tends to decrease the total electrical efficiency due to higher transmission and power losses in the coil turns. If the chosen frequency is noticeably lower than the optimal value ($F_{el.eff.}$), the electrical efficiency can dramatically decrease due to cancellation of the induced currents circulating in the opposite sides of the slab cross-section.

High coil efficiency will be obtained if the ratio of slab thickness d to penetration depth δ is 2.5 or more. The optimal frequency that corresponds to the maximum coil efficiency while heating infinitely wide slabs can be determined as follows [53,122,123]. A nonmagnetic slab or a magnetic slab heated above the Curie temperature:

$$\frac{d}{\delta_{\text{non-magn.}}} \simeq 3 - 3.5; \tag{7.5}$$

a magnetic slab:

$$\frac{d}{\delta_{\text{magn.}}} \simeq 2.6 - 3.1, \tag{7.6}$$

where $\delta_{\text{non-magn.}}$ is the current penetration depth in a nonmagnetic slab, and $\delta_{\text{magn.}}$ is the current penetration depth in a magnetic slab. Table 7.11 shows the minimum slab thickness for efficient slab heating of a variety of metals.

While discussing heating, efficiency, it is imperative to mention that smaller air gaps and tighter windings of coil turns improve the coil efficiency. The higher ratio of

Table 7.11 Minimum Thickness (mm) for Efficient Heating of Nonmagnetic Wide Slabs and Plates Using Longitudinal Flux Indicators

		Frequency (kHz)					
Material	Temp. (°C/°F)	0.06	0.5	1	2.5	4	10
Aluminum	100/212	31	10.7	7.6	4.8	3.8	2.4
	250/482	37	12.9	9	5.8	4.6	2.9
	500/932	48	16.6	11	7.4	5.9	3.7
Copper	100/212	24	8	6	3.7	2.9	1.9
	500/932	36	12.6	8.9	5.6	4.4	2.8
	900/1652	48	16.7	11.8	7.5	5.9	3.7
Brass	100/212	44	15	10.9	6.9	5.4	3.4
	500/932	59	20	14	9.2	7.3	4.6
	900/1652	73	25	17.9	11	9	5.7
Silver	100/212	24	8.5	6	3.7	3	1.9
	300/572	31	11	7.8	4.9	3.9	2.4
	800/1472	43	14.9	10	6.6	5.2	3.3
Nonmagnetic stainless steel	100/212	143	49	35	22	17.5	11
	800/1472	174	60	42	27	21.3	13
	1200/2192	180	63	44	28	22	14
Tungsten	100/212	38	13	9	5.8	4.6	2.9
	900/1652	90	31	22	13.9	11	7
	1500/2732	120	42	30	18.6	14.7	9
Titanium	100/212	131	45	32	20	16	10
	600/1112	192	66	47	30	23	14.9
	1500/2732	218	75	53	33	26	17

b/d (where b is the width of the slab) also corresponds to the higher coil electrical efficiency (assuming the same slab-to-coil gap).

In the past, coil calculations for heating blooms and bars/billets with a square cross-section were conducted using formulas for equivalent cylinders (cylinders with equivalent diameters). An error in such calculations is usually within 6 to 10%. A calculation error increases with the higher ratio of b/d. If $b/d > 1.5$, such an assumption should not be used. Contemporary software providing numerical simulations offers better results.

As discussed in Section 3.1.6, any current-carrying conductor placed in a magnetic field experiences the force. The intensity of this force and subsequent magnetic pressure in some cases might be so significant that it can result in coil shape distortion and even banding of bus bars and copper tubing used for coil manufacturing. Electromagnetic vibration and industrial noise are other undesirable side products of those forces. Therefore, in order to provide a rigid and reliable coil design, the existence of electromagnetic forces and pressure should be taken into consideration, particularly with induction heaters that have a noncylindrical shape inasmuch as inductors for heating cylinders have a greater natural rigidity (Figure 3.29). Rectangular inductors for heating slabs with low electrical resistivity (i.e., aluminum or copper slabs) that utilize high power densities are particularly sensitive to this problem.

This text is not intended to provide a detailed discussion of this subject. The nature of electromagnetic forces and pressure as well as acoustic vibration in induction heating applications are discussed in [191, 421, 428].

7.8.2 Longitudinal Electromagnetic End Effects of Rectangular Workpiece

The longitudinal electromagnetic end effect in the induction slab heating system is quite similar to the electromagnetic end effect that occurs in cylinders. This effect may be illustrated by the curves in Figures 7.103 and 7.104. In the case of a multiturn solenoid inductor with a long homogeneous slab (Figure 7.104, zone "b"), the density of the induced power under the coil cold end ($Z = L_2$) is approximately four times less than in the central part (see Sec. 3.1.8). When heating slabs that travel "butt to butt" through the induction coil in a progressive manner, the electromagnetic end effect does not lead to temperature non-uniformity because each part of the slab experiences the same magnetic field with respect to time as the slab is being heated.

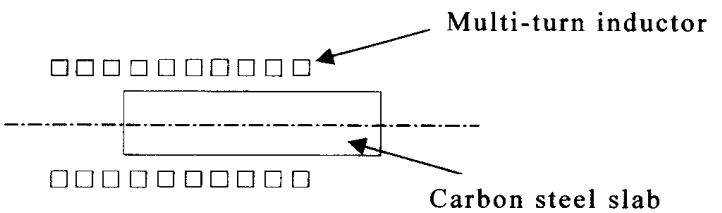

a) A sketch of the longitudinal cross section of an induction slab heater

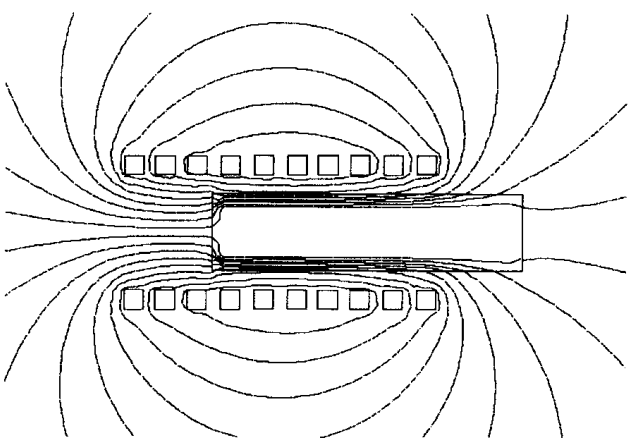

b) Computer graphics of the field distribution in axial direction of the induction slab heater

Figure 7.103 Longitudinal eletromagnetic end effect of a ferromagnetic slab (carbon steel) heated in a multiturn solenoid inductor.

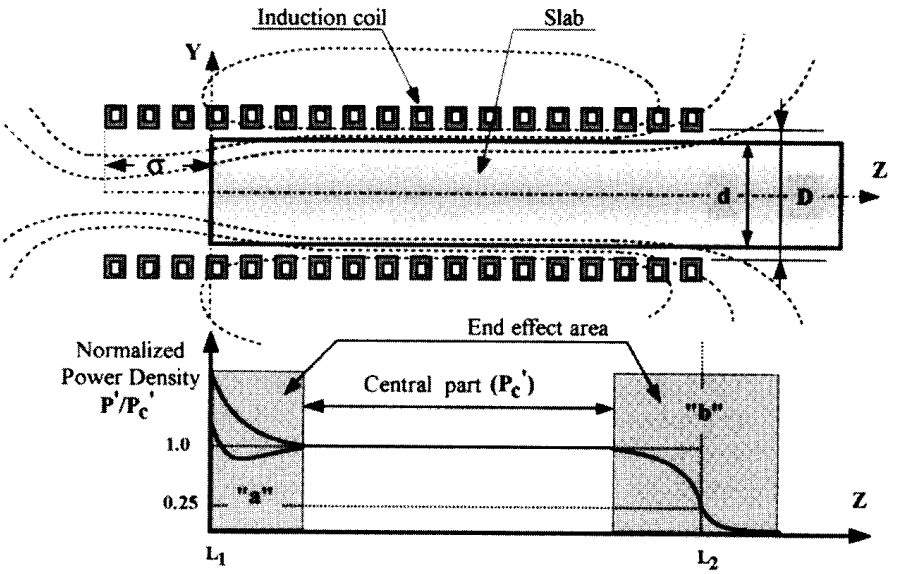

Figure 7.104 Longitudinal eletromagnetic end effect in the slab.

7.8.2.1 Nonmagnetic Slab

Basically, the electromagnetic end effect of the nonmagnetic slab (Figure 7.104, zone "a") is defined primarily by four variables:

d/δ = skin effect,
σ/d = Normalized coil overhang,
D/d = Thickness ratio, and
K_{space} = Space factor of coil turns,

where δ is the penetration depth; σ is the coil overhang (distance between the end of the coil and the end of the slab (Figure 7.104); d is the slab thickness; D is the height of the induction coil (coil opening); and K_{space} represents how tightly the coil turns are wound.

Higher frequencies and larger coil overhangs lead to additional power (or heat sources) at the corresponding end of the slab (so-called "power surplus"). This is why the combination of pronounced skin effect and significant coil overhang causes overheating at the end area of a nonmagnetic slab. Figure 7.105 (slab left end) shows the results of a computer modeling that illustrates this condition.

When the frequency is low (skin effect is not marked) and coil overhang is small, instead of a surplus a power deficit at the slab end will occur. By the proper choice of coil overhang and frequency, it is possible to obtain a condition where the surplus of heat sources caused by the electromagnetic end effect can be offset by the additional heat losses from the slab's end. As a result, the temperature distribution along the slab's length will be reasonably uniform.

Figure 7.106 shows the normalized power distribution along the length [122, 123] of a typical aluminum slab for different coil overhangs, where Pc′ corresponds to the integrated power densities in the slab central area. The distribution of power shown in Figure 7.106 was obtained by integrating the volumetric power densities (power per unit volume) along the slab thickness.

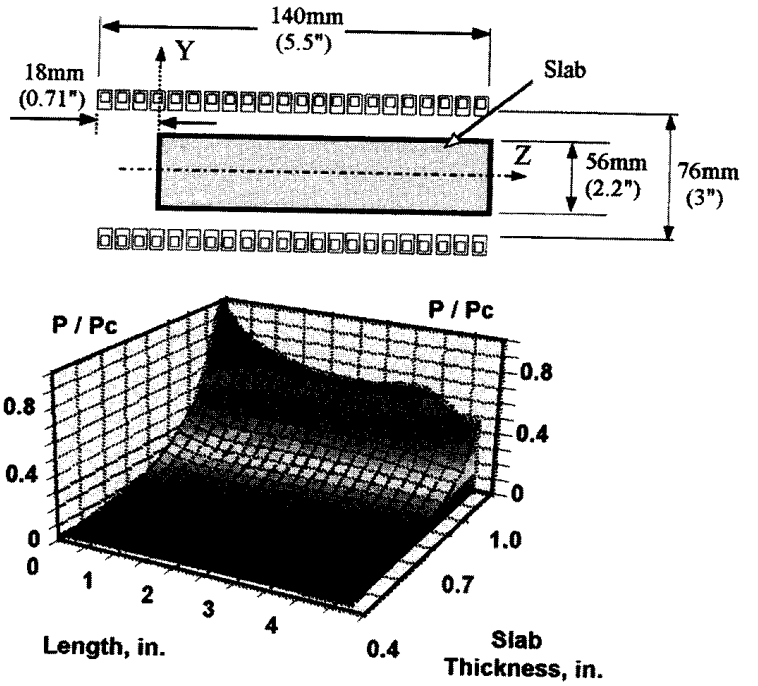

Figure 7.105 Normalized power density distribution P/Pc in the cross-section of the stainless steel slab (frequency = 1 kHz).

In the case shown in Figure 7.106, the power distribution along the slab length can be considered reasonably uniform if $\sigma/d = 0.7$(approx.). As one can see from Figure 7.106, under this condition at the slab butt end there is a local surplus of power, however, in the adjacent region there is a power deficit. Therefore, thermal conductivity will "try" to equalize this localized heat difference. In addition, the butt

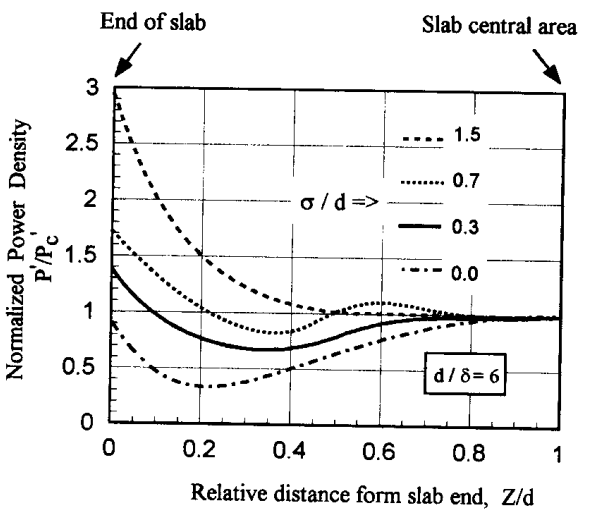

Figure 7.106 Normalized power density distribution along the end effect zone of the stationary heated aluminum slab ($d/\delta = 6$) as a function of coil overhang.

end area of the slab has additional heat losses due to radiation and convection compared to its central area. These additional heat losses will also somewhat compensate for a surplus of power in that area resulting in a nearly uniform temperature distribution along the slab's length.

In the case of the nonmagnetic slab, with a positive coil overhang $\sigma/d > 0$, the power density always increases towards the slab end and a surplus of power at the slab's butt end takes place compared to the area near the butt end. This is true for any frequency and any kind of nonmagnetic slab, including aluminum, copper, stainless steel, titanium, and so on. However, this does not automatically guarantee overheating of the end area because the heat losses from the slab end can exceed the surplus of power in this area. In addition, a region with a power deficit just before the butt end area (depending upon a combination of the skin effect d/δ, the thickness ratio D/d, and the coil space factor K_{space}) might exist and be quite significant acting as a heat sink. Therefore, in cases such as this an underheating of the slab ends can occur regardless of the power surplus there.

7.8.2.2 Magnetic Slab

The end effect in a magnetic slab has several features compared to the nonmagnetic one. As discussed in Section 3.1.1.2, magnetic materials have a tendency to gather the magnetic flux lines because of magnetic permeability μ_r. In engineering calculations, relative magnetic permeability of the nonmagnetic slab can be considered as equivalent to that of air and it is assigned the value of one. By contrast, μ_r of the carbon steel can vary, for example, from 1 to over 300, depending on the magnetic field intensity, temperature, and frequency. Generally speaking the electromagnetic effect in a ferromagnetic slab is mainly affected by two factors (as is also the case in the induction heating of magnetic cylinders; see Secs. 3.1.7 and 7.2.5):

1. the demagnetizing effect of eddy currents, which tend to force the magnetic field out of the slab; and
2. the magnetizing effect of the surface and volumetric currents, which have a tendency to gather the magnetic field within the slab.

The first factor causes an increase in power at the slab's end (similar to the end effect of a nonmagnetic slab). The second factor causes a power reduction there.

Therefore, unlike those of the nonmagnetic slab, the ends of the ferromagnetic slab, even in a uniform magnetic field (large coil overhang), may be either overheated or underheated. Figure 7.107 shows that there will be more of a power deficit at the slab end area with higher μ_r. A decrease of μ_r leads to a reduction of the power deficit in the end area. Therefore, instead of the power deficit (e.g., for $\mu_r > 40$, for conditions of the case shown in Figure 7.107), a surplus of power can occur ($\mu_r < 20$). In this case, the end effect in a magnetic slab will be similar to that of a nonmagnetic one. The rule of thumb is that low magnetic permeability leads to a tendency to shift the electromagnetic end effect of the magnetic slab toward the nonmagnetic one.

Since relative magnetic permeability of the magnetic slab varies along its length, the skin effect d/δ also varies accordingly in the slab axial direction. The curves of Figure 7.107 show how the power density distribution along the slab length is affected by variations in μ_r.

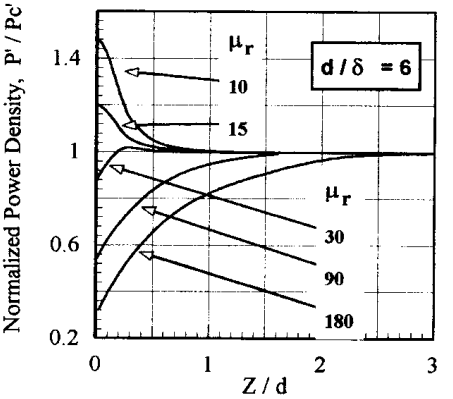

Figure 7.107 Electromagnetic end effect of the magnetic slab $\sigma/d = 1.5$.

In conclusion, regarding electromagnetic end effects that occur with statically induction heated slabs, plates, or blooms we can say that in the case of a magnetic slab, it is possible to provide the required temperature profile along the slab length by choosing the proper coil overhang and frequency. However, if the skin effect is not pronounced and low power densities are used, then the slab end area might be underheated at any value of coil overhang.

In order to provide required temperature uniformity along the length of the slab it will be necessary to use another way to control the electromagnetic field distribution (e.g., using tighter winding of turns near the slab ends compared to its central area, applying magnetic flux concentrators, and/or utilizing multilayer windings in the end areas compared to a single-layer winding in its central part).

If the magnetic slab is heated above the Curie temperature then during the heating cycle end effects of both the magnetic and nonmagnetic slab take place. In the beginning of heating, only the end effect of a magnetic body will take place. As soon as the temperature of the slab exceeds the Curie point, the end effect of the nonmagnetic slab will occur. When the slab surface temperature reaches the Curie point but the areas under the surface still remain magnetic, a mixture of end effects of both magnetic and nonmagnetic bodies will take place.

7.8.3 Electromagnetic Transverse Edge Effect

As mentioned above, in addition to the distortion of the magnetic field in the slab's end areas, a similar distortion occurs at its edges on the transverse cross-section of the slab. This phenomenon takes place due to the electromagnetic transverse edge effect (Figure 7.102 [53, 92, 120–123, 190–194]) that plays a major role in obtaining the required temperature profile across the slab width.

7.8.3.1 Parameters Related to Transverse Edge Effect of Nonmagnetic Slab

The maximum value of the eddy current density is located on the surface of the slab's central part (it does not, however, mean that the maximum temperature is always located there). The more pronounced the skin effect, the better the induced current matches the contour of the slab. Figure 7.108 shows the distribution of the electric

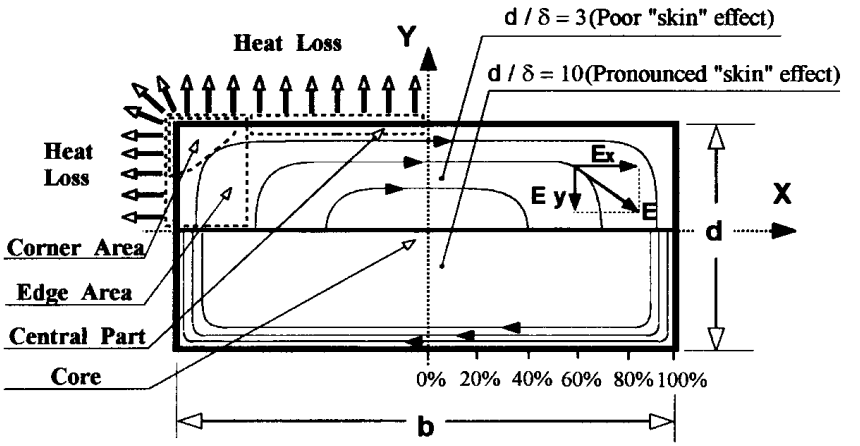

Figure 7.108 Distribution of the electric field intensity (E) in the transverse cross-section of the slab.

field intensity in the slab's cross-section with pronounced skin effect ($d/\delta = 10$, where the slab thickness d divided by penetration depth δ is equal to 10) and when skin effect is not pronounced ($d/\delta = 3$).

If the skin effect is pronounced ($d/\delta > 5$), then the current and power density are approximately the same along the slab perimeter, except in the edge areas (Figure 7.108, bottom half of the slab cross-section), where the distortion of induced power takes place.

Even though heat losses at the edge or corner area are higher than heat losses at the central part, the corners and edge areas can be overheated compared to the central part. This occurs because in the central part the heat sources penetrate from two sides (from two surfaces) and at the edge areas the heat sources penetrate from three sides (two surfaces and the edge). The phenomenon of edge overheating usually occurs in the induction heating of magnetic steel, aluminum, silver, or copper slabs where the skin effect is typically pronounced.

If the skin effect is not pronounced ($d/\delta < 3$), then underheating of the corners and edges will occur. In this case, the path of eddy currents in the slab cross-section does not match the contour of the slab and most of the induced currents close their loops earlier, without reaching the corners and the edge areas (Figure 7.108, top half of the slab cross-section). As a result, the power densities and heat sources in the edge areas will be less than the corresponding values in the central part of the slab. For example, in induction heating of thick titanium slabs (using the low frequency), in the final heating stage the temperature of the corners and edge areas could often be 20% lower compared to the temperature of the slab's central part.

As an example and in order to qualify a distortion of power density distribution due to transverse edge effect, Figure 7.109 shows a normalized power density distribution within a transverse cross-section of a nonmagnetic slab for two different cases $d/\delta = 3$ and $d/\delta = 10$.

It should be mentioned here that, from an electromagnetic perspective, in transverse cross-section the slab corner should be treated as a special area. Due to a principle of current discontinuity, no eddy currents exist in the actual corner of the

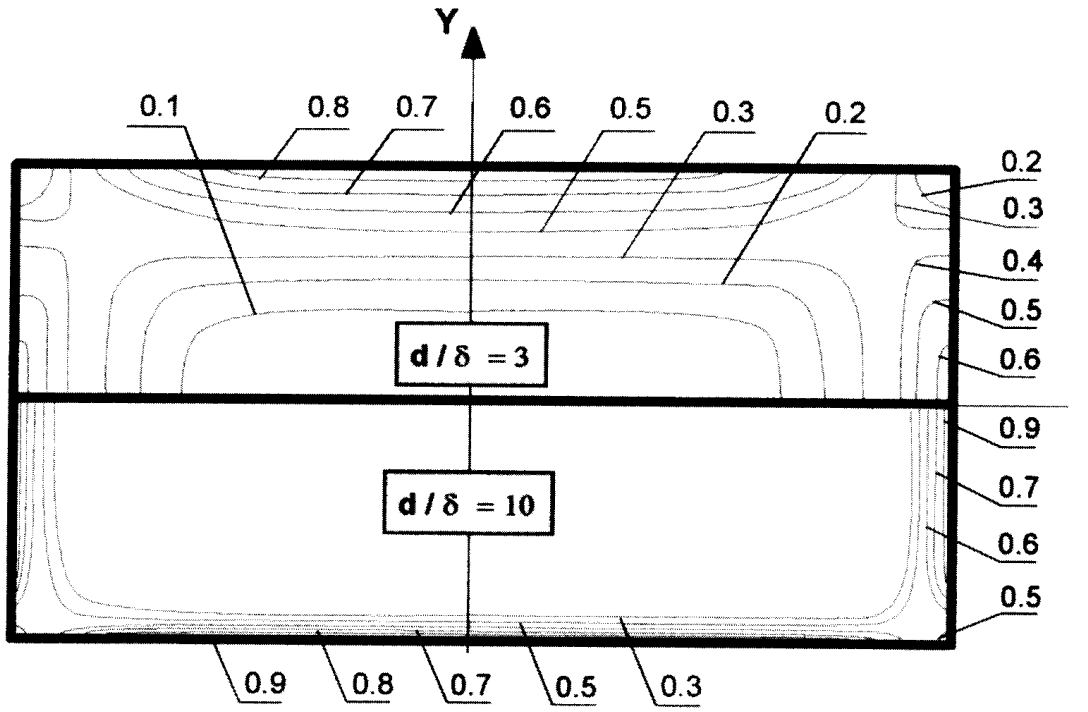

Figure 7.109 Normalized power density distribution in the slab cross-section.

slab. However, as discussed above, regardless of this phenomenon, corners are often overheated when relatively high frequency is used.

The specific power density P_t' [W/m^2] is used as a parameter to allow analysis of the transverse electromagnetic edge effect in the slab transverse cross-section. P_t' can be obtained by integrating the volumetric power density P [W/m^3] along the slab thickness and, as a result, plotting a distribution of integrated power across the width of the slab.

$$P_t'(X) = \int_0^d P(X, Y)\, dY. \tag{7.7}$$

Figure 7.110 shows the distribution of the normalized power $P_t'/P_{t,c}'$ across the width of the nonmagnetic slab, as a function of the skin effect d/δ and ratio b/d (where $P_{t,c}'$ is the integrated power density in the central part of the transverse cross-section of the slab and b is the slab width). When $d/\delta \geq 6$, the curves rapidly fall toward the slab's central part and their values decrease from maximum to unity. In this case, overheating of the slab edges will typically occur [53, 92, 121–123, 193].

If the skin effect is not pronounced (i.e., $d/\delta < 2.5$), a marked power reduction is observed in the sub-edge area resulting in a noticeable deficit of heat sources. If heat losses are absent and $d/\delta \cong 3.14$, the power deficit in the subedge area is compensated by its surplus near the edge as shown in Figure 7.110.

Studies show [53] that the edge effect area does not extend from the slab edge toward its central part more than the slab thickness and usually is (1.5 to 4.0)*δ long. Normally the length of the edge effect zone does not depend upon the width of the

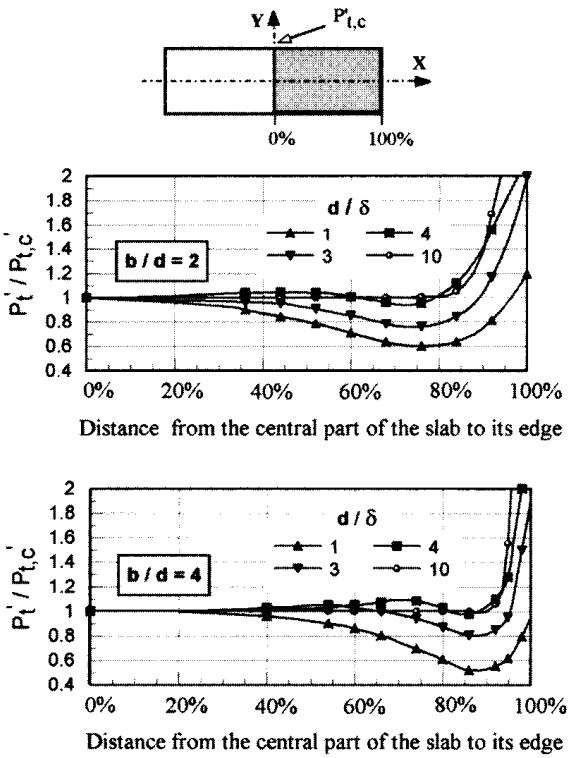

Figure 7.110 Transverse edge effect of nonmagnetic slab.

slab, particularly when $b/d > 4$. When $b/d < 2$, edge effect zones from both sides might overlap.

7.8.3.2 Specifics of the Transverse Edge Effect of Magnetic Slab

In the case of an infinitely long magnetic slab, the relative magnetic permeability μ_r varies only within the slab thickness. As discussed in Sections 3.1.1 and 7.5.2, μ_r of carbon steel can vary, for example, from 1 to over 300, depending on the magnetic field intensity H, temperature, and frequency.

It is important to note that realistically speaking, the μ_r of the magnetic slab changes along its thickness, length, and width, therefore the skin effect d/δ varies throughout the slab as well. To more easily present edge effect analysis in a magnetic slab, the penetration depth is evaluated using the value of μ_r at the central part of the slab surface. Due to the variation of μ_r within the magnetic slab, from a quantitative perspective the edge effect is not the same as for the nonmagnetic slab [53, 92]. Figure 7.111 shows a comparison of the electromagnetic transverse edge effect in a magnetic and nonmagnetic slab.

7.8.3.3 Dynamics of Transverse Edge Effect During Heating Cycle

The dynamics of transverse edge effects can be viewed in Figure 7.112. Two polar processes shown in that figure represent induction heating of a thick carbon steel slab and, alternatively, induction heating of a titanium slab of the same geometry. The line frequency power source has been chosen in both cases. Both slabs were 0.71 m (28 in.) wide and 0.18 m (7 in.) thick. Such large size slabs were chosen to facilitate a

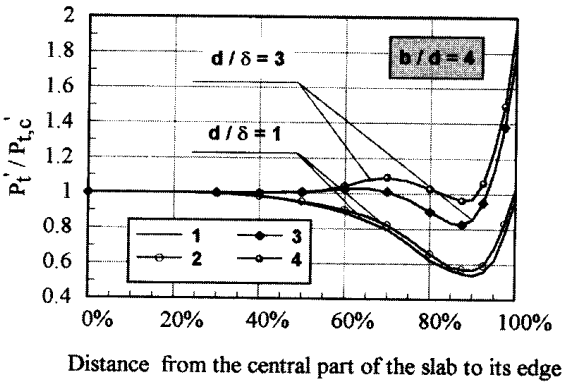

Figure 7.111 Comparison of the transverse edge effect in nonmagnetic (curves 1 and 3) and magnetic (curves 2 and 4) slabs.

demonstration of the specifics of the induction slab heating process. An analysis of the dynamics of temperature profiles with time is provided in the slab transverse cross-section by plotting the temperature of the most interesting areas; for example,

- Location #1 corresponds to the half-thickness of the slab surface;
- Location #2 represents the slab corner;
- Location #3 corresponds to the half-width of the surface; and
- Location #4 denotes the center of the slab.

The process of induction heating of a carbon steel slab from an ambient temperature or a temperature below the Curie point to a temperature above it, involves several features that require a special design concept. Numerical computation analysis shows that in the first stage of heating, the entire slab is magnetic (time is less than 125 sec) and the skin effect is pronounced, featuring an extremely large ratio of slab thickness to penetration depth that exceeds the value of 50 even though line frequency is used.

It should be mentioned here that the heat losses from the slab surface are relatively low at this stage. Due to the transverse edge effect, the edge area and particularly the slab corner will be heated much faster than any other areas of the slab including the surface of its central region (Figure 7.112).

The maximum temperature will be located near the corner, despite the fact that there is not any current induced in the actual corner of the slab (because of a current discontinuity principle discussed earlier).

The beginning of the second stage of heating is characterized by high-temperature within the slab. The corner area reaches the Curie temperature first and after that the heat intensity in this area significantly decreases. This takes place mainly due to the following reasons.

1. Specific heat has its maximum value (peak) near the Curie point (see Figure 3.40). The value of the specific heat denotes the amount of energy that must be absorbed by the slab to achieve the required heat. Therefore, this peak leads to a reduction of the heat intensity in the corner when its temperature approaches the Curie point.

2. Steel in the corner area loses its magnetic properties and the μ_r drops to 1. In addition, during the heating cycle, the electrical resistivity of the carbon steel

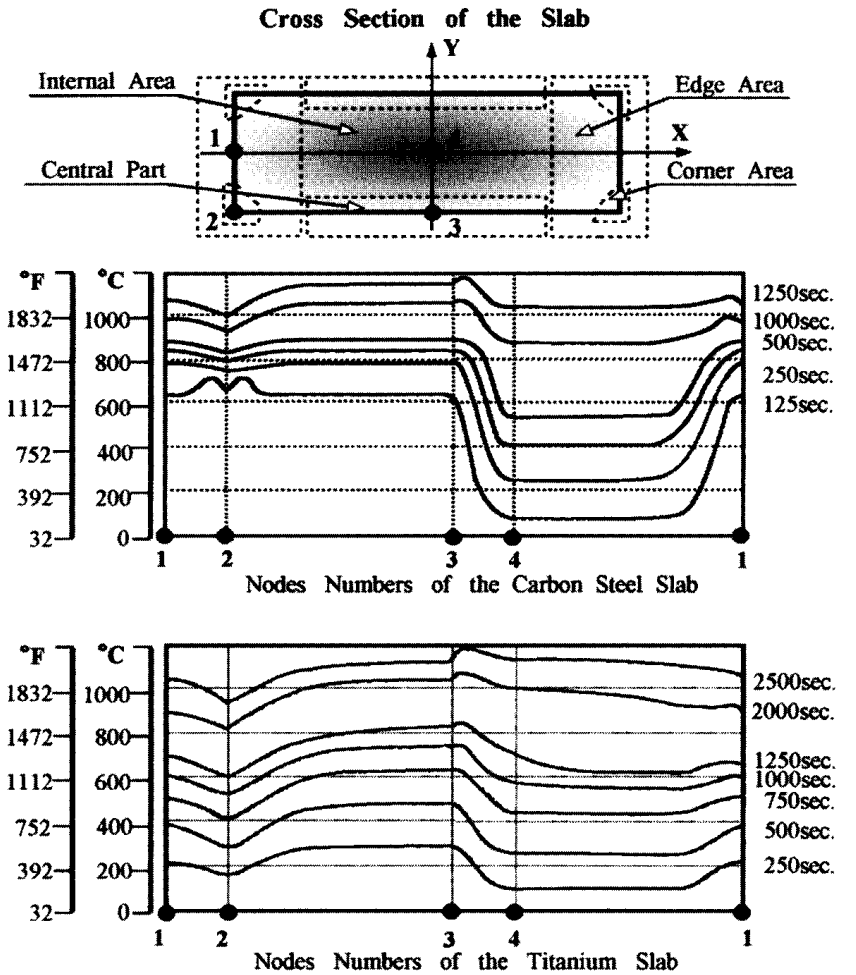

Figure 7.112 Time-dependent processes in line frequency (60 Hz) induction heating of titanium and carbon steel slabs. Slab geometry: 0.71 m (28 in.) wide × 0.18 m (7 in.) thick.

increases approximately two to three times, compared to its value in the initial stage. Both factors (reduction of μ_r and increase of electrical resistivity ρ) cause an increase of current penetration depth δ. As a result, the skin effect in the corner area becomes less distinct and redistribution of heat sources takes place.

3. Surface heat loss increases with temperature. Because the corner of the slab became the hottest area, the heat losses in that area will also be the largest.

During the second heat stage, due to thermal conductivity and increased penetration depth, the temperature of the subsurface area rises more rapidly compared to the first stage of heating, and the local equalization of the temperature profiles will take place within the edge area.

With time, the surface of the slab becomes nonmagnetic representing the final heating stage (time $\cong$ 300 sec) and the skin effect in the slab will be noticeably less pronounced compared to its value in the first stage of heating. The heat sources at the central part of the slab will be greater than in its edge area. In addition, the heat losses at the edge area are greater than the heat losses in the central part of the slab.

As a result, the temperature in the slab central part will start to rise much faster than in its corner.

Finally, the underheating of the slab edges compared to the central part causes the corners to become the coldest area within the slab (time $\cong$ 1200 sec). Even the slab core is heated to a higher temperature than its corners.

In order to avoid undesirable temperature nonuniformity along the slab perimeter, using a dual-frequency approach similar to the one discussed in Sections 7.2 and 7.6 is effective. With a dual-frequency approach, a low frequency is used in the first heating stage when most of the slab remains magnetic. As soon as the surface temperature of the slab exceeds the Curie point, a higher frequency is applied. The latter statement represents a noticeable difference in the necessity of applying a dual-frequency approach when heating cylinders compared to heating rectangular shaped bodies.

As discussed in Sections 7.2 and 7.6, when heating a solid cylinder the principal reason for using a dual-frequency approach is to avoid an eddy current cancellation when heating above the Curie point. However, when heating rectangular workpieces, there is an additional criterion for using a dual-frequency approach, one that deals with the need to control the electromagnetic transverse edge effect and, thus, the ability to provide a required temperature distribution along the perimeter.

Therefore, in slab or rectangular bar heating applications a dual- or a multi-frequency design concept allows one to combine the high overall electrical efficiency and short cycle time with the required temperature uniformity within the slab.

For example, a dual-frequency design has been successfully used in the induction heating of steel alloy RCS bars. Radyne Ltd. (England) for Kanthal Corp., Halstammer, manufactured the system in 1991. The induction heating coil assembly consists of nine inline coils and two power supplies: a 600 kW/0.5 kHz and a 300 kW/1 kHz. The rectangular alloy steel bars are 4 in. sq and 3 m (10 ft) long with the overall length of the coil assembly being 9 m (30 ft). The bars are heated from ambient temperature by using 0.5 kHz up to 650°C (1200°F) and then 1 kHz, to increase the temperature to 1120°C (2050°F). The production rate is one bar every three minutes.

For comparison purposes, Figure 7.112 also shows the line frequency induction heating of a thick nonmagnetic (titanium) slab. The geometry of the titanium slab is the same as that of the previous example of the carbon steel slab.

Due to the material properties of the titanium (its electrical resistivity is higher than that of the magnetic carbon steel but its relative magnetic permeability is one), the skin effect is not pronounced at any stage of the heating cycle. Because of this, the heat intensity in the slab corner as well as in the entire edge area will be less than in the central part of the slab even at the beginning of the heating cycle (the first heating stage).

With time, the thermal difference between the edge area and the central part of the slab becomes more marked. Finally, the slab corners become the coolest areas of the slab. The slab's internal areas and even its core will have noticeably higher temperatures compared to its corners (Figure 7.112). Obviously, in this particular case the use of such a low frequency as the line frequency might be the best choice for reducing the total cycle time and heating the slab's internal areas and, in particular, its core as quickly as possible. At the same time, low frequencies are not the best choice for obtaining uniform temperature profiles within the thick nonmagnetic slabs

that have high electrical resistivity. The use of a higher- or dual-frequency approach would be the better choice in cases when high-temperature uniformity is required.

Figure 7.113 shows two-dimensional temperature profiles in a quarter of 0.15 m RCS stainless steel bar with 20 mm radius using a dual frequency approach. Significant temperature gradients occur within the bar cross-section. It is important to have a clear understanding of the magnitude of these gradients during the intermediate, and particularly, during the initial, heating stage. With intensive heating, longitudinal and transverse cracks occur as a result of the significant thermal stresses (thermal shocks) caused by different magnitudes of temperature and temperature gradients.

Appendix G shows the importance of the soaking/cooling action that takes place during slab/bar transportation to the next operation.

7.8.4 Design Concepts of Induction Slab Heating Systems and Case Studies of Commercial Installations

Depending upon the process requirements there are typically three major design concepts of the induction slab heating systems: static heating, inline continuous heating, and oscillating heating (Figure 7.1). The name of each concept is fairly self-explanatory and indicates the specifics of slab movement during the heating cycle (see the discussion in Sec. 7.1).

7.8.4.1 Static Heating

According to the static heating design concept a slab is statically heated without any movement during the heating cycle. This design concept is very similar to the static heating of cylindrical billets. An induction heater can consist of one or several coils. Figure 7.114 shows an example of a multicoil induction system that statically heats 0.15 m (6 in.) carbon steel square bars to 1250°C (2282°F). This induction heating system consists of a 2000 kW/1 kHz solid-state power supply feeding six single-shot inductors. The number of inductors depends upon the required production rate.

7.8.4.2 Inline Continuous Heating

The continuous slab heating concept assumes that heating is done in one or various stages and the slab is being progressively moved through the induction heating line. The continuous heating approach is often used for slab reheating after continuous casting. In such an application, the inductor is located just before the mill and should be able to compensate for the previous cooling effects and heat loss in the continuously cast slab and provide the hot mill with a uniformly heated slab.

Figure 7.115 shows an induction heater consisting of six progressive coils that is capable of heating long rectangular steel bars running at 80 imperial tons/hr. This system is powered by six solid-state inverters each operating at 1.65 MW/1 kHz with total power of 9.9 MW (built by Radyne Ltd., UK).

Sometimes one of the major difficulties in developing induction reheating systems after continuous casting deals with nonrectangular (i.e. trapezoidal) cross-sections of bars and slabs and with the nonuniform temperature profiles that exist before the induction reheating stage.

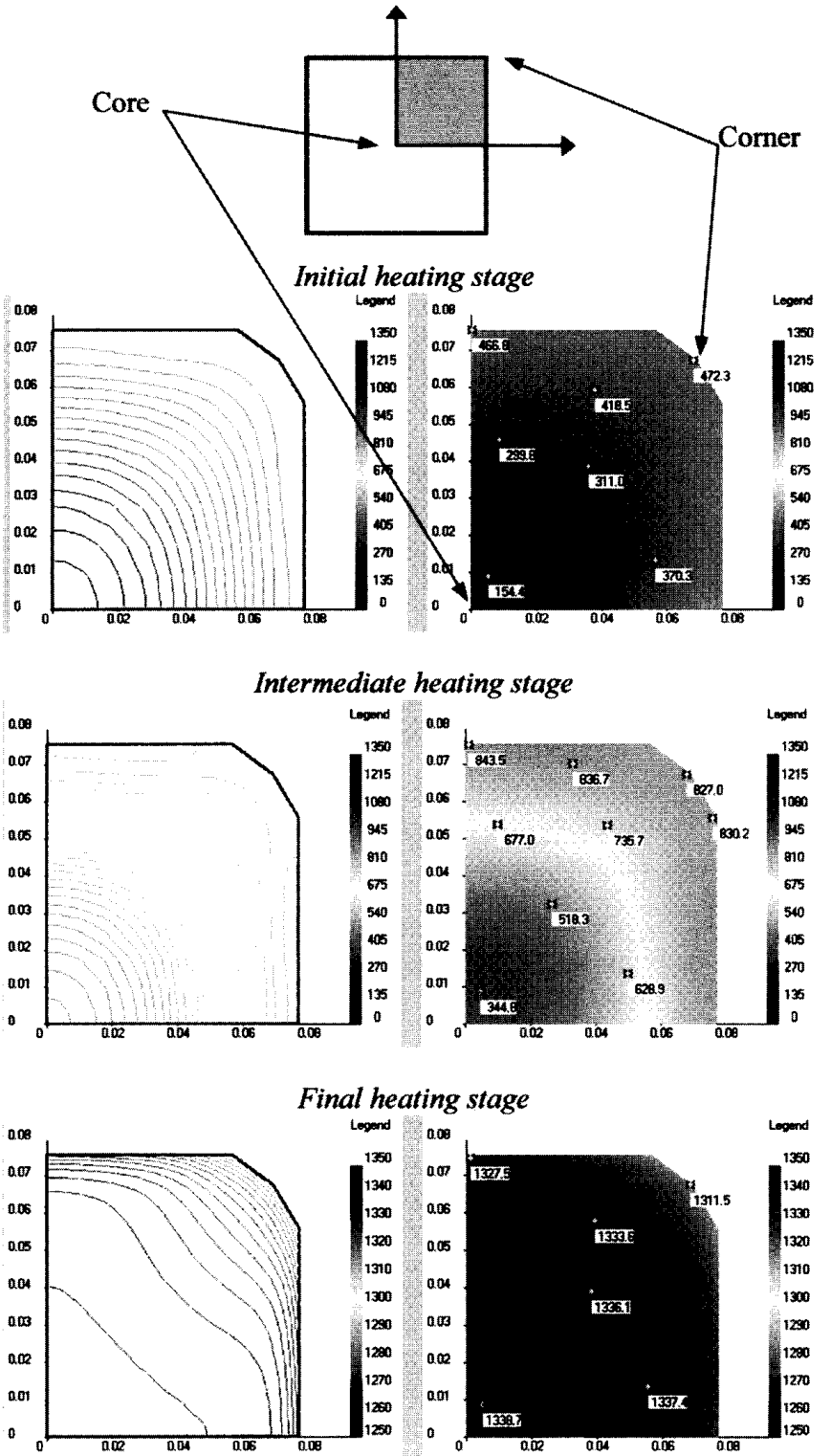

Figure 7.113 Dynamics of temperature distribution (°C) in quarter of 0.15 m (6 in.) RCS stainless steel bar (301 series) using dual frequency (500 Hz and 3 kHz). Required temperature is 1315°C (2400°F).

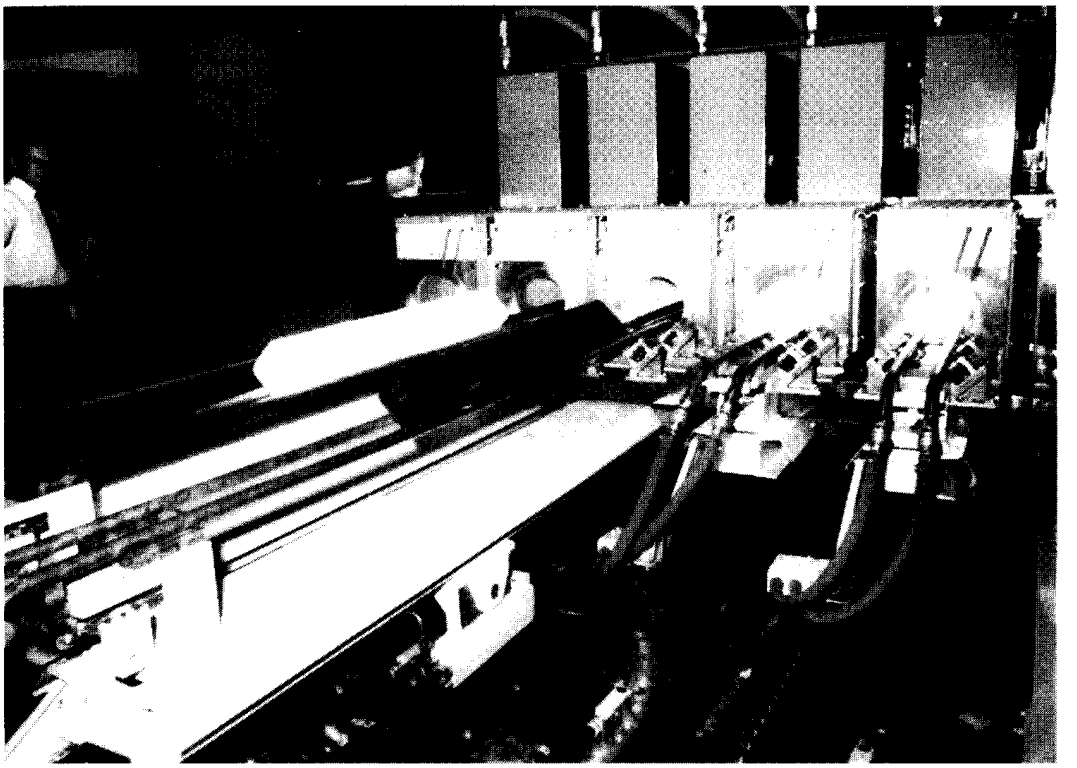

Figure 7.114 Radyne's 2000 kW/1000 Hz solid-state power supply feeding six single-shot inductors heating 0.152 m (6 in.) square billets to 1250°C (2282°F).

When heating slabs or bars with a trapezoidal cross-section the temperature of the sharp corner can be significantly different compared to the temperature of the rest of the body. The sharp corner can be easily underheated or greatly overheated and even melted, depending upon the heated metal, geometry of the slab, chosen frequency, and specifics of the refractory design. The choice of frequency is often based on the particular geometry of the sharp corners.

At this point we provide a case study of the continuous inline induction reheater of the trapezoidal cross-section long aluminum bars. One of the leading Venezuelan aluminum producers turned to induction for reheating concast aluminum bars in the mid-1980s. [119]. It was necessary to reheat both rectangular and trapezoidal shaped aluminum alloy bars after continuous casting before rolling. An original, line frequency induction reheater was chosen first, one that required no special power supply, which held down the cost.

However, line frequency induction heating falls short of several process requirements. Due to limited temperature control and an inability to meet temperature uniformity requirements (particularly in the case of bars with trapezoidal cross-sections), it was particularly difficult to handle the required temperature of the sharp corners.

In addition, due to the nature of the continuous casting process, and because of the heat losses during transportation of the bar from the caster to the reducing mill, the temperature profile within the bar cross-section entering the reheating stage was

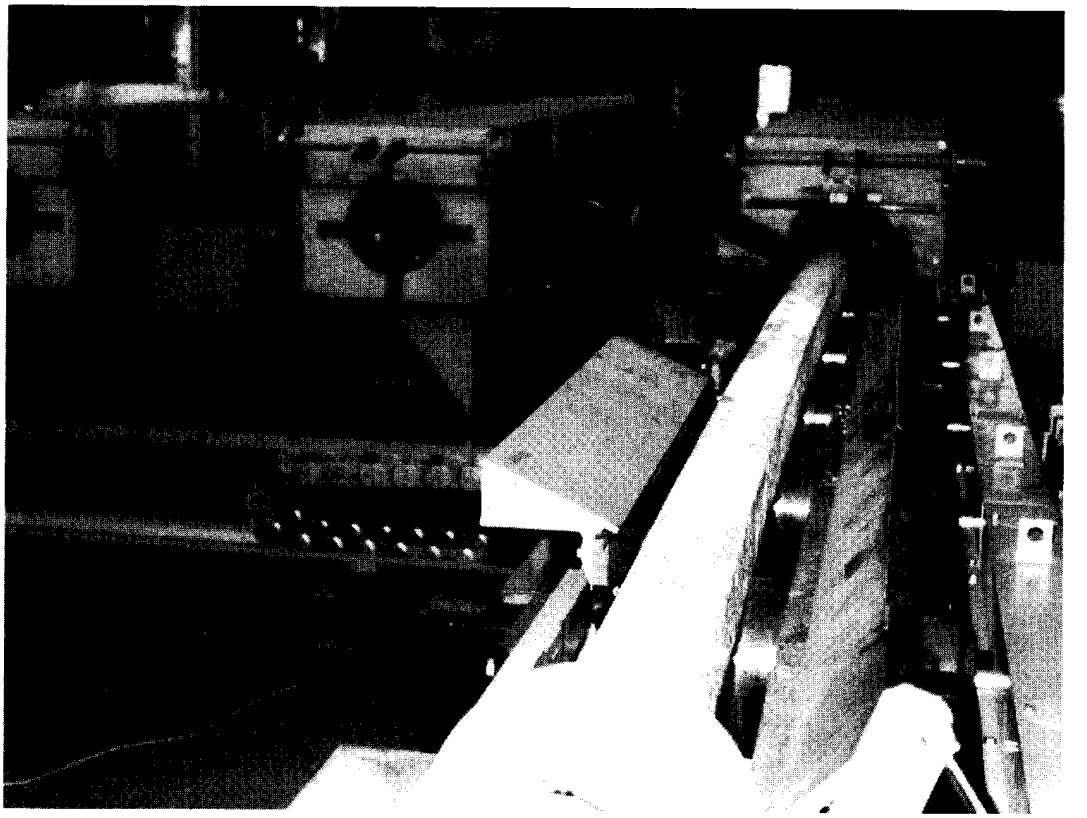

Figure 7.115 An induction heater consisting of six progressive coils capable of heating long rectangular steel bars running at 80 imperial tons/hr. The system is powered by six solid-state inverters each operating at a rate of 1650 kW/1 kHz with a total power of about 9900 kW. (Courtesy of Radyne, Ltd., UK.)

nonuniform. Surface layers of the bar, and especially the areas of sharp corners, became much cooler than internal regions.

The aluminum manufacturer requested INDUCTOHEAT, Inc. to analyze a possible improvement to the existing line frequency induction system. After extensive evaluation based on a proprietary computer modeling and experience gained from previous jobs, it was found that for that particular geometry of trapezoidal shaped aluminum bars, the optimal choice was a longitudinal flux coil network operating at 700 Hz/750 kW.

The net result was a compact induction reheating system that has been in production since 1987, using minimum floor space, of approximately 1.5 m (60 in.) long (Figure 7.116). The induction system was able to process the cast bars of both rectangular and trapezoidal cross-sections at a production rate of 12.8 m/min (42 ft/min). The final temperature after induction reheating was 520°C (970°F) ±6°C [119].

7.8.4.3 Oscillating Heating

According to the oscillating design concept, the slab moves back and forth (oscillates) during the heating (Figure 7.1) inside the induction heater with a certain oscillation stroke.

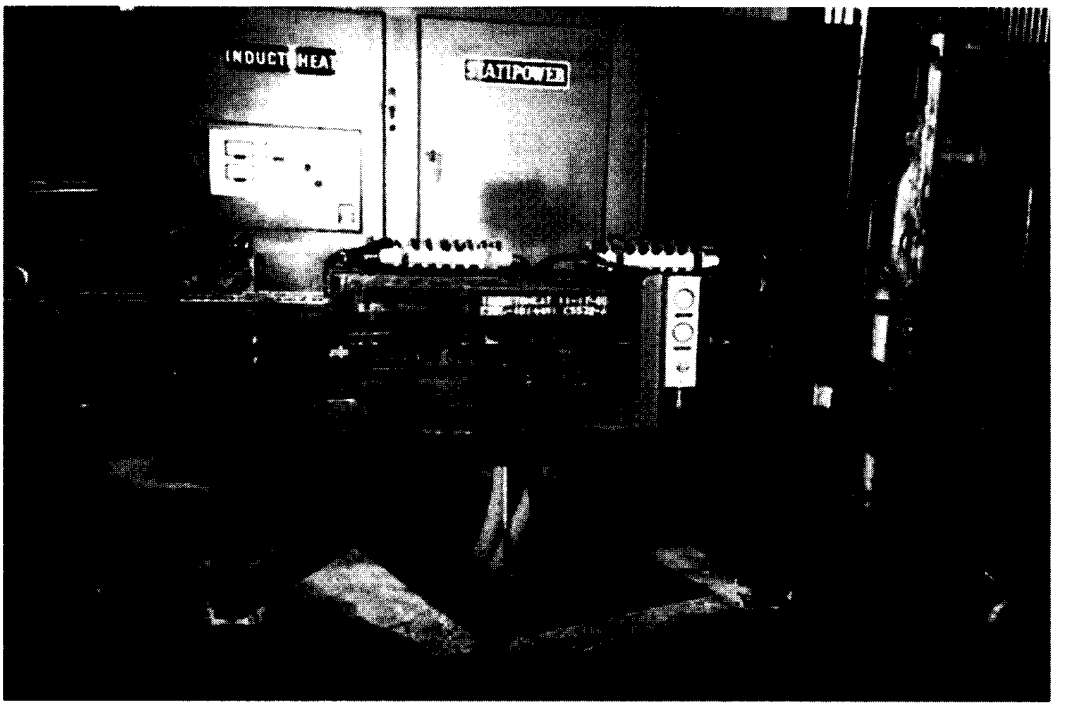

Figure 7.116 Inline induction system (750 kW/700 Hz) for reheating trapezoidal cross-section aluminum bars after continuous casting and prior to reducing mill. (Courtesy of INDUCTOHEAT, Inc., Madison Heights, MI.)

Oscillating heating provides several principal benefits compared to continuous or progressive inline heating, including:

- Minimum shop floor requirements while providing a high production rate,
- Relative ease of operation in both the heating and holding modes,
- System flexibility, and
- Higher overall efficiency due to minimized radiation heat losses.

The nature of oscillating induction heaters requires proper handling of the electromagnetic edge effects as well as electromagnetic and thermal end effects; otherwise the slab end and edge areas could have essentially different temperatures compared to its central area and internal regions. In addition, the phenomenon of "thermal striping" could appear.

If the initial temperature of the slab is uniform, then, in order to provide a uniform final temperature distribution within the slab, it is necessary to ensure that each region along the slab width and length absorbs the same amount of energy during the process cycle. After continuous casting a temperature distribution within the slab is nonuniform depending upon slab geometry and features of the casting process (i.e., production rate and specifics of cooling). Slab edges tend to cool faster than the central areas and, particularly, its core.

As an example, Figure 7.117 shows a typical initial temperature distribution in a quarter of a continuously cast slab prior to induction reheating. Therefore, it is often required during reheating to redistribute energy induced within the slab in such

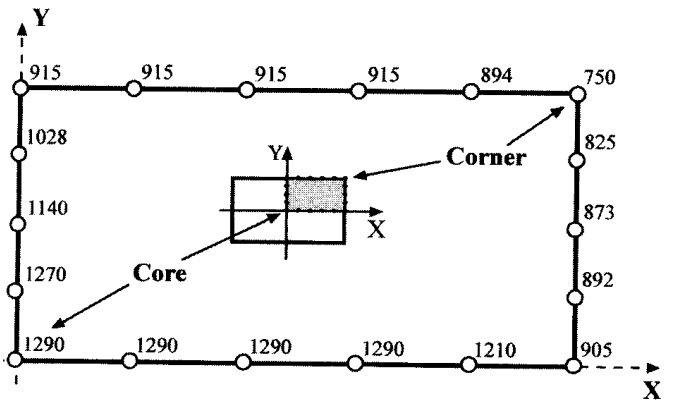

Figure 7.117 Nonuniform temperature distribution (°C) in a quarter of the continuously cast slab prior to induction reheating.

a way that would allow one to compensate for its nonuniform initial temperature profile.

The world's largest oscillating induction heater (Figure 2.46) was engineered and manufactured by INDUCTOTHERM Corp. for Geneva Steel, Utah, in August 1995 [275]. After installing the world's largest continuous caster, Geneva Steel was looking for a method to reheat large slabs that required 800 to 1000 PIW (pounds per inch width). This reheating system was to feature the lowest capital cost possible bringing the added capacity online in the shortest time possible. Slabs were produced in a continuous caster which was capable of producing 1.8 m (71 in.) wide through 3.2 m (126 in.) wide single slabs or 1.07 m (42 in.) wide through 1.6 m (63 in.) wide twin cast slabs. Figure 7.118 shows induction heating of .6 m (63 in.) wide twin slabs. All slabs were 0.22 m (8.7 in.) thick [275]. It was required that an induction reheater should be inline with the existing caster and the rolling mill.

This task was accomplished by a 42,000 kW induction oscillating system (Figures 2.46 and 7.118) with the capacity to reheat 500 short tons per hour from a bulk input temperature of 1090°C (1994°F) to a bulk output temperature of 1260°C (2300°F). This unique induction slab heating system was designed, manufactured, and delivered to Geneva Steel within a five-month period [275]. Geneva Steel completed construction and installation within one month. Total time from inception of the contract to beginning startup of the equipment was six months.

The induction reheater heats two slabs side by side, four slabs side by side and end to end, three slabs end to end, two slabs end to end, or one large single slab. The overall length of the reheater is 14 m and the overall width is 4 m.

Seven solenoid coils are placed inline with one another at a distance of 1.71 m center to center. Each coil can deliver up to 6000 kW/110 Hz of power to the slab (Figure 7.119). Slabs go through an oscillation stroke of 1.71 m and continue to oscillate until the required time at the surface temperature, time at holding power, and mill push rate are met.

Slabs exit the induction reheater one at a time as they proceed to the rolling mills, therefore, slabs must enter the reheater one at a time which requires a split

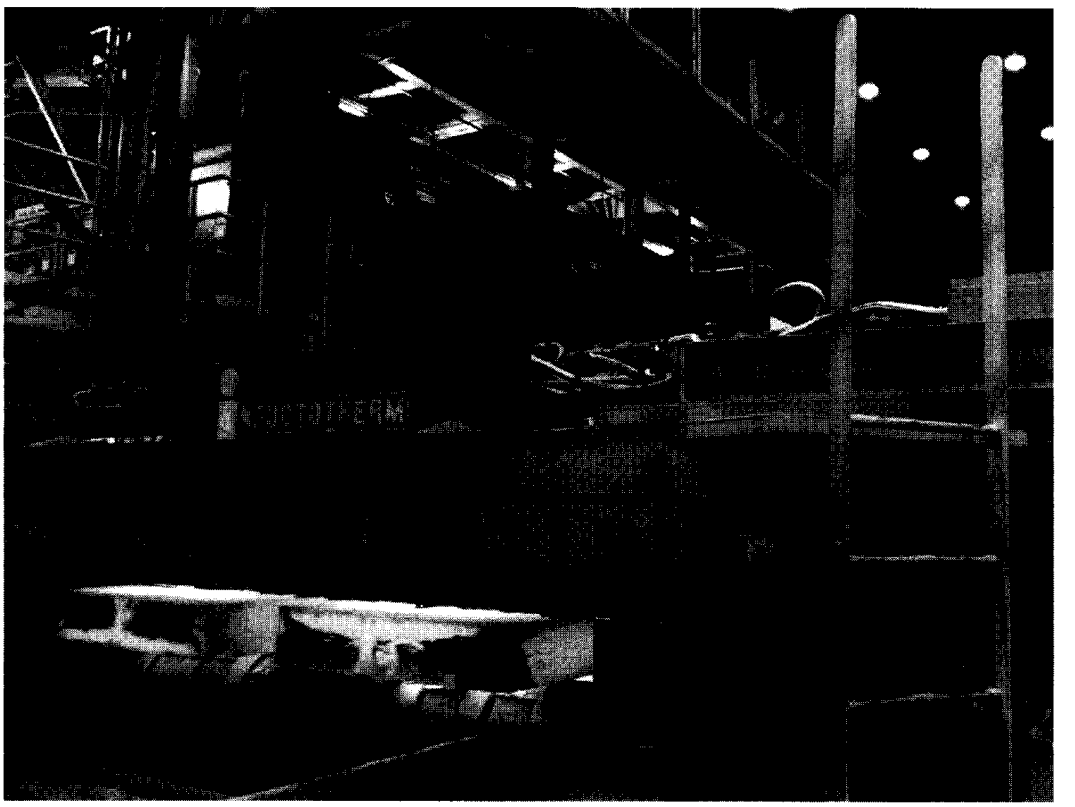

Figure 7.118 Inductotherm's 42,000 kW induction oscillating system is capable of heating a large single slab (3.2 m wide, 0.22 m thick) or two smaller slabs side by side.

roll line with individually driven rolls. Since slabs are entering the reheater individually, they are at different bulk heat values. Control is focused on only the hottest slab in the furnace, thereby avoiding the possibility of melting a slab accidentally.

One of the obvious concerns when designing a multimegawatt system is the possibility of noticeable external magnetic field exposure. This is why specially designed patented magnetic shunts have been developed. Without magnetic shunts, the magnetic field would spread around the coil supporting structure.

Magnetic shunts allow containment of a magnetic field inside the coil and not spread outside the coil. All components supporting the induction coils, including support rolls, remain unaffected by the magnetic field of the coil. Although the power delivered to an induction coil is about 6000 kW, the level of the magnetic field exposure outside the coil is quite low. Actual field measurement indicates 20 microtesla at a 0.3 m range from the coil [275].

Magnetic shunts concentrate energy directly into the slab resulting in a coil electrical efficiency increase of 3 to 5% compared to the inductors without shunts. In addition, the coil with magnetic shunts has a significantly higher mass than the coil without shunts. This added mass greatly reduces the mechanical resonance frequency and vibration on the inductor, which in turn increases the inductor's rigidity.

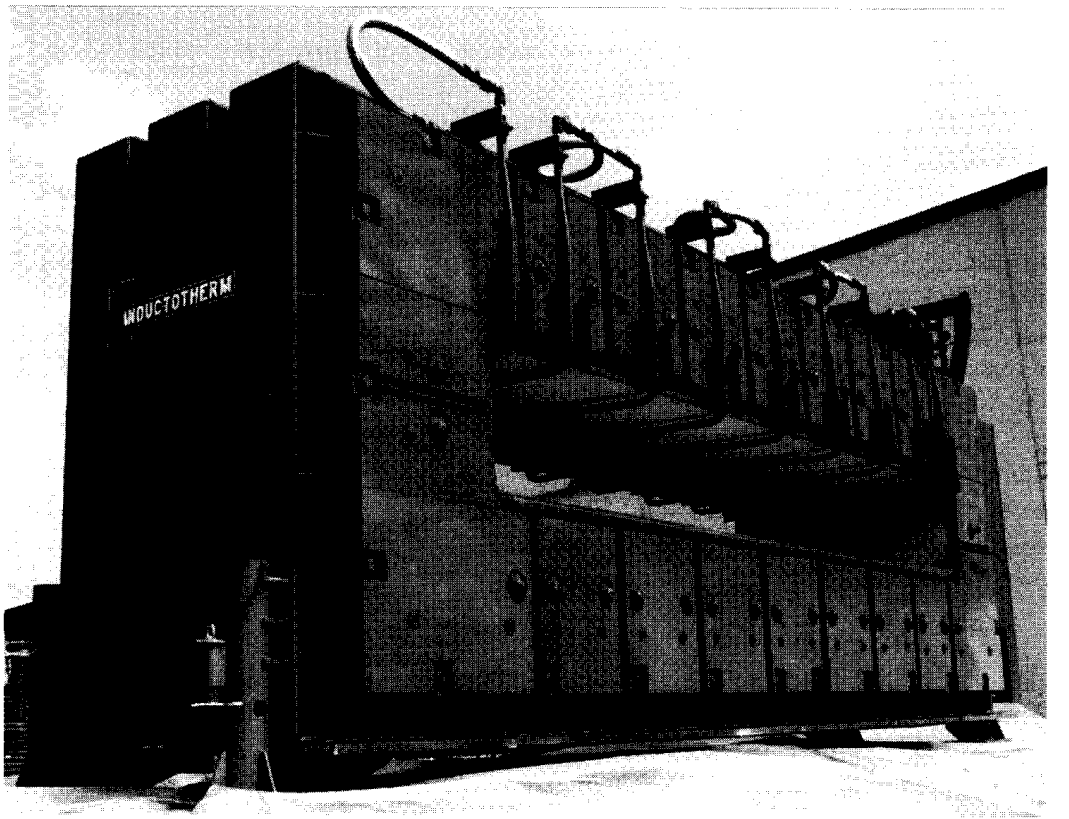

Figure 7.119 Unique 6000 kW/110 Hz induction coil provides heating of the world's largest steel slab. Slab geometry: 3.2 m (126 in.) wide and 0.22 m (8.7 in.) thick. (Courtesy of Inductotherm Corp.)

7.9 INLINE INDUCTION HEATING OF STRIP, SHEET, PLATE, THIN SLAB, AND TRANSFER BAR

Induction heating of thin slabs, plates, and strips is very similar to the heating of rectangular bars and thick slabs, which was discussed in the previous section. At the same time, there are some specific features regarding design concepts, selection of process parameters, and applications that make it unique. In this section we do not repeat the basic principles and phenomena, which were already discussed in Section 7.8. It is assumed here that the reader is already familiar with them.

Instead of using the words plate, sheet, strip, thin slab, and so on, in this section we use the word "strip" assuming that all discussions hold true for plate, sheet, and thin slab as well, unless mentioned specifically.

The strip heating recipes vary depending upon the process features. However, regardless of the specifics, induction heating provides the technology to alter heating rates and heating times requiring a much smaller floor space and shorter startup and shutdown times compared to conventional furnace heating that relies on heat transfer by convection and/or radiation. An ability to provide strip heating under a protective atmosphere is another advantage of induction heating.

Conventional induction strip heating applications include, but are not limited to, full or process annealing, galvanizing, galvannealing, galvaluming, preheating

prior to the reducing mill, or furnace heating, tempering, stress-relieving, paint curing, lacquer coating, and drying.

During the last decade the most intensive use of induction for heating of strips has been observed in strip coating applications. The popularity of coated metal strips and in particular low-carbon steel strips has soared through the efforts of strip producers to find more durable and environmentally friendly coatings (both metallic and nonmetallic). At the present time, it is possible to apply solvent-based, water-based, and powder coatings as well as coatings with no solvents at all. Each approach requires a different process in terms of pretreatment, curing, and so on. For example, during the last decade the use of clear coats has increased dramatically to provide basic protection from finger marking on plain metallic coated material.

Such metal coating processes as galvanizing, galvaluming, galvannealing, and tinning represent the most popular metallic coating processes and occupy the highest volume of coated metal strips used for the needs of industries such as the domestic appliance, automotive, and construction industries. Thus the following discussion is primarily concentrated on these processes.

7.9.1 Strip Coating Processes

7.9.1.1 Metallic Coating of Strips (Galvanizing, Galvaluming, Galvannealing, Tinning)

The main purpose of metallic coating of ferrous strip is to improve resistance to oxidation, corrosion, and abrasion. These goals can be achieved by depositing a layer of a certain metal on the strip surface. Pure zinc and zinc alloys are the most popular choices for metallic coating. Aluminum and its alloys are also used in combination with zinc to improve corrosion protection and/or formability.

Metallic coating has a dual-action protection mechanism [173, 296–303, 432, 469, 476–478].

1. In order to prevent the surface of a carbon steel strip from rusting and oxidation when it is exposed to air and humidity, the metallic coating simply provides a physical and chemically stable barrier that isolates the surface from contact with oxygen, water, or aggressive atmosphere.
2. In addition to serving as a physical protection barrier, a metallic coating conducts the anodic reaction to steel (so called cathodic protection).

The second part means that if the protective metallic coating layer is accidentally disrupted (i.e., due to microporosity or appearance of small scratches) creating a favorable condition for corrosion, then because of the galvanic reaction the metallic protective layer becomes the anode and the steel acts as the cathode. As a result, the carbon steel is not dissolved and corroded. Instead of developing a rust formation in the steel, the metallic coating layer undergoes an electrochemical reaction when a positive current starts to flow from the metallic coating through the medium that acts as an electrolyte to the carbon steel providing an electrolytic or cathodic protection.

The slow rate of zinc corrosion compared to corrosion of iron ensures long-lasting protection of iron coated with zinc. Figure 7.120 illustrates the mechanism of the rust prevention action of metallic coating as compared to a nonmetallic coating. The life of a galvanized coating is directly proportional to the coating thick-

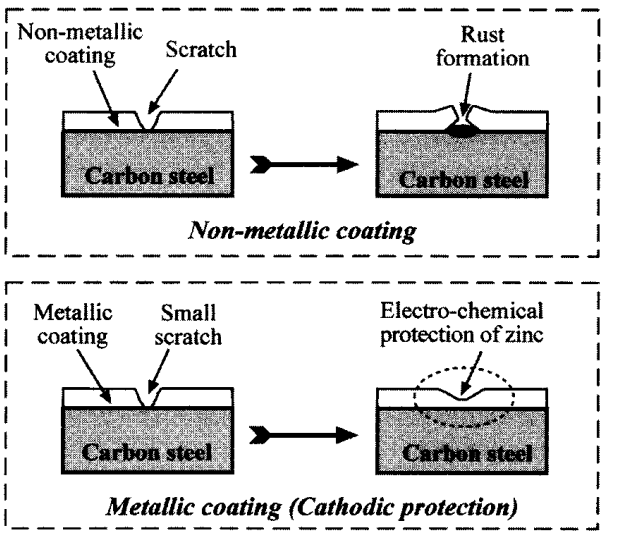

Figure 7.120 Comparison of metallic and nonmetallic coatings.

ness. It is wise to remember that not all metals are suited to provide such an active electrochemical protection of the carbon steel. Only metals that have an electronegative position with respect to a carbon steel potential can do so. If two metals are coupled to create an electrochemical cell then the potential difference is responsible for the corrosive reaction. The greater the difference in the potentials the more intense the galvanic corrosion of the metal. Table 7.12 shows potentials and types of reactions for selected metals in the electrochemical (galvanic) series [432].

Table 7.12 Electrochemical (Galvanic) Series of Selected Metals

Metal	Reaction	Potential, V
Silver	$Ag^{+} + e^{-} \Rightarrow Ag$	+0.8
Aluminum	$Al^{+3} + 3e^{-} \Rightarrow Al$ (0.1f NaOH)	−1.706
Gold	$Au^{+} + e^{-} \Rightarrow Au$	+1.68
	$Au^{+3} + 2e^{-} \Rightarrow Au^{+1}$	+1.29
	$Au^{+3} + 3e^{-} \Rightarrow Au$	+1.42
Chromium	$Cr^{+2} + 2e \Rightarrow Cr$	−0.557
	$Cr^{+3} + e^{-} \Rightarrow Cr^{+2}$	−0.41
	$Cr^{+3} + 3e^{-} \Rightarrow Cr$	−0.74
Copper	$Cu^{+} + e^{-} \Rightarrow Cu$	+0.522
	$Cu^{+2} + e \Rightarrow Cu^{+}$	+0.158
	$Cu^{+} + 2e^{-} \Rightarrow Cu$	+0.34
Iron	$Fe^{+2} + 2e^{-} \Rightarrow Fe$	−0.409
	$Fe^{+3} + 3e^{-} \Rightarrow Fe$	−0.036
Magnesium	$Mg^{++} + 2e^{-} \Rightarrow Mg$	−2.375
Lead	$Pb^{+2} + 2e^{-} \Rightarrow Pb$	−0.126
Titanium	$Ti^{+2} + 2e^{-} \Rightarrow Ti$	−1.63
	$Ti^{+3} + e^{-} \Rightarrow Ti^{+2}$	−2.0
Zinc	$Zn^{+2} + 2e^{-} \Rightarrow Zn$	−0.763

Source: Ref. 432.

The galvanization process applies the above-described advantages of metallic coating. According to this process a thin layer of pure zinc or zinc alloy is deposited on a carbon steel surface.

There are two types of continuous galvanizing lines: hot dip and electrolytic. According to the electrolytic galvanizing process, zinc is electrolytically deposited on the strip surface. This process is relatively expensive and typically handles strip widths of 0.5 m (20 in.) to 1.8 m (72 in.). One of the main shortcomings of electrolytic galvanizing is its ability to provide only a light coating. The maximum coating thickness obtained as a result of electrolytic galvanizing is about 0.0043 mm (0.00017 in.).

The continuous hot dip galvanizing process consists of three stages [300]. During the initial stage the process of cleaning and pickling takes place. During this stage different types of surface contaminants (including grease, dirt, oil, mill scale, drawing lubricants, etc.) are removed. Annealing or heat treating of the steel that is preheated to a certain temperature represents the second or intermediate stage. During the final stage of the hot dip galvanizing process, the heated strip passes through a molten zinc pot where the zinc coating is applied (Figure 7.121). As a result of a metallurgical reaction that takes place between a molten alloy coating and hot carbon steel, an alloy layer is created. This alloy layer binds the coating to the carbon steel.

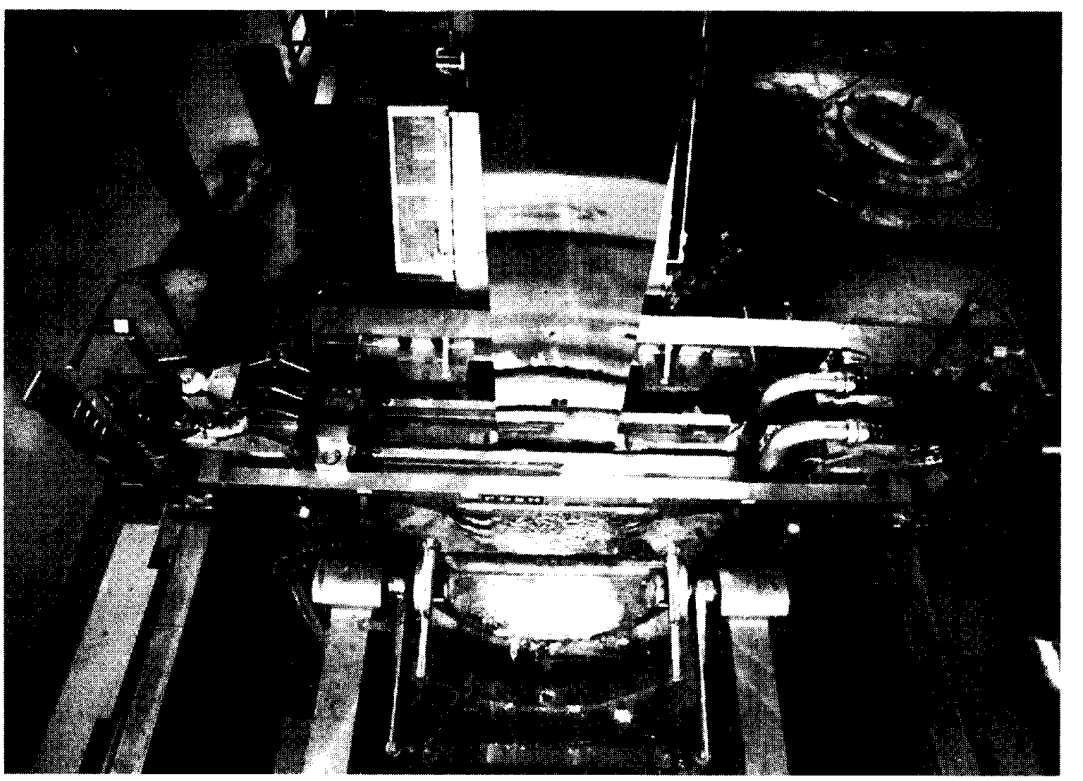

Figure 7.121 Low carbon steel strip passes through an inductively heated molten zinc pot (top view).

Induction can be effectively suited to heat the strip prior to entering the coating pot. This can be as simple as preheating the strip (if the strip is chemically cleaned beforehand), or can be integrated with a combination of chemical and mechanical processes to condition the steel strip prior to entering the coating pot. In hot dip galvanizing lines, induction heating is used not only to preheat the strip but to provide heating of a melted zinc pot as well (Figure 7.122).

The great majority of galvanizing lines apply a hot dip approach. The low-carbon steel strips and sheets of thickness range 0.2 mm (0.008 in.) to 4.5 mm (0.175 in.) and width range 0.5 m (20 in.) to 1.9 m (75 in.) are typically used in hot dip galvanizing lines. Strip processing speed typically ranges from 7.6 m/min (25 FPM) to 200 m/min (490 FPM). The thickness of the hot dip zinc coating is typically within the range of 0.5 oz. to 2.75 oz for each sq.ft of strip [300]. Coating weights that refer to the total coating on both sides of the strip can vary between 0.25 oz/sq.ft (0.011 mm/0.000425 in.) to 4 oz./sq.ft (0.18 mm/0.007 in.). The coating thickness is controlled by the speed of the strip and the "air knife" wiping system. The air knife is located just above the zinc melting pot representing a complex apparatus (Figure 7.123). Air, steam, or nitrogen can be used as the wiping medium. The air knife blows the excessive amount of coating alloy off the strip surface down into the melting pot before the coating is solidified.

Depending upon the specifics of cleaning, pickling, and strip heat treating the hot dip galvanizing processes can be divided into several basic types: the gas pickling process (being the oldest and almost disappeared at the present time), the United States Steel process, the wheeling process, the Sendzimir process, and their modifications [300]. Production rate of the hot dip galvanizing lines typically ranges from 20 t/hr to 50 t/hr.

Induction heating has gained much importance in the area of post coat heat treatment of the steel strip as well. To describe a post coat heat treatment suppliers around the world use various names and trademarks, but in essence the heat treatment is commonly described as Galvanneal or Zincanneal. In the present text, this process is referred to as galvannealing. Galvannealing involves

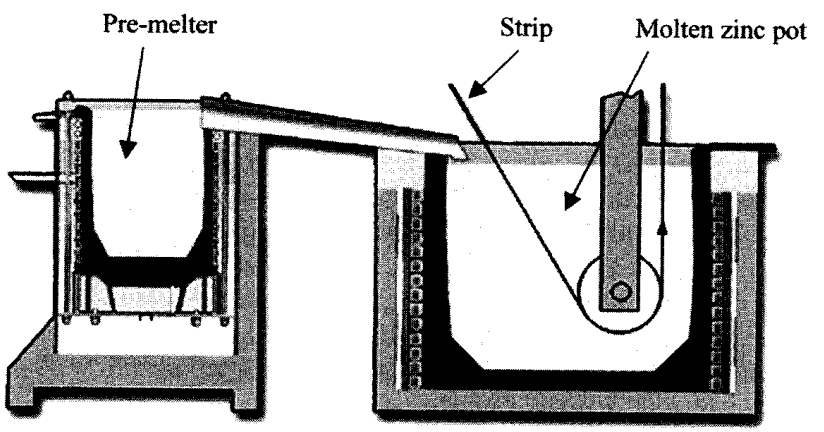

Figure 7.122 Extended coreless coil design with premelter. Strip passes through a molten zinc pot where the zinc coating is applied.

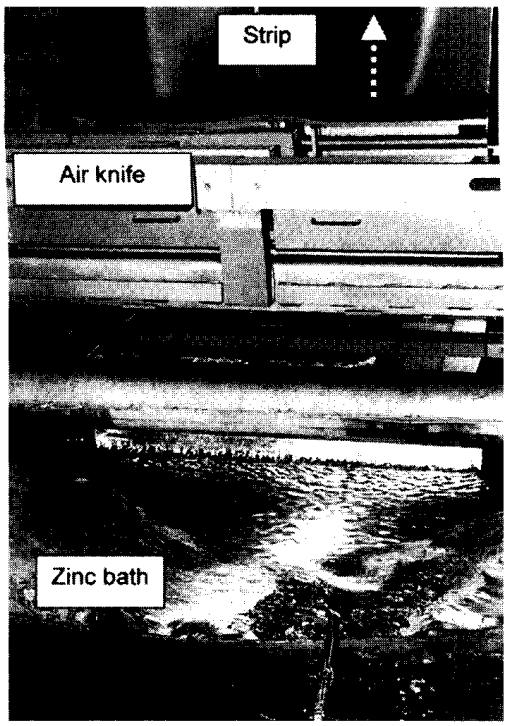

Figure 7.123 The coating thickness is controlled by the speed of the strip and the air knife located just above the zinc melting pot.

heating the coated strip from the zinc melting point (about 420°C) to temperatures in the 500°C (932°F) to 580°C (1076°F) range, holding/soaking at that temperature for a defined period of time, and then cooling the strip down for additional treatment.

When coating with zinc containing a certain amount of aluminum, the aluminum adheres to the steel strip first and provides an alloy layer that inhibits the migration of iron into the zinc. This latter is a time-consuming action responsible for the length requirements of the holding (soaking) zone. This action depends upon the local concentration gradient of the iron in the zinc layer.

A uniform temperature distribution across the strip width during the holding (soaking) stage is critical for obtaining the required quality of coated strip. Normally, the strip has a uniform transverse temperature profile after exiting a molten zinc pot. However, due to the thermal edge effect and specifics of air/gas flow resulting from operation of the air knife, the strip edges have a tendency to be cooler compared to the central part of the strip prior to entering an induction postheating system and holding zone. This phenomenon of edge underheating should be compensated for when choosing the design parameters of the induction postheater.

It should be emphasized that the strip cooling after exiting a holding/soaking zone also plays an important role in obtaining the required structure of the coating layer since upon cooling, the zinc layer "freezes" into a different lattice structure. After solidification of the metal coating, a hard coating can come into contact with guiding rollers without developing marks at the strip surface.

This heat treatment produces a uniform matte gray zinc finish ideal for metal fabrication and offers improved weldability and paintability of the subsequent operations compared to galvanized strips.

Depending upon the requirements of a particular process, instead of pure zinc, the binary zinc–aluminum alloys or ternary zinc–iron–aluminum alloys are often used for coating material. Numerous recipes of metal coatings and trademarks have resulted in various coatings used in hot dip coating processes (e.g., Galfan, Galvalume, Alusi, Alupur, Galflex, etc.).

The induction heating principle can be used not only for induction strip pre- and postheating but also for designing the holding chambers, which are designed to be moved on and off the line as required. Figure 7.124 shows a sketch of a strip galvannealing line.

Conventional solenoid coils, inductors with "doors", and advanced doorless coils that provide a side opening are available for this operation. Figure 7.125 shows a strip galvannealing line that consists of a pot of molten zinc alloy and induction reheater (postheater) of coated strip that uses two doorless inductors and a holding (soaking) zone. Frequencies of 30 to 120 kHz are the most commonly used for galvannealing applications.

Figure 7.126 shows one of two induction heating boosters. A 1200 kW/30 kHz IGBT inverter powers each booster. The system is installed in the horizontal passline of an L-shaped annealing gas furnace and designed to minimize production losses due to transitions caused by changing the strip size (i.e., strip gauge) or annealing cycle [303].

The noticeably long response time of gas furnaces produces a significant amount of scrap when a production transition occurs. Scrap may be caused by either underheating heavier gauge strips or overheating lighter gauge strips until new process parameters are established when strip sizes, or thermal cycles are changed.

Induction heaters provide a unique characteristic of practically instantaneous response to a change in process parameters to reduce this time lag and decrease production loss during the transient time that results in higher yields. Because of this seamless transition, a wide variety of strip gauges can be run at the same line speed.

The induction booster shown in Figure 7.126 was built by INDUCTOHEAT's Mass Heating Division. Coils were manufactured from specially designed heavy wall rectangular internally water-cooled tubes. Each coil was fabricated with no welds inside the furnace casting. It was placed inside the steel furnace casting and thermally insulated from the surrounding 705°C (1300°F) atmosphere consisting of a mixture of about 94% nitrogen and 6% hydrogen. As shown in Figure 7.126, in order to minimize heat losses into the hot atmosphere, the inductor is thermally insulated outside as well as inside. The bus connection that carries current from the 1200 kW/30 kHz inverter is sealed gastight against atmosphere leakage. Atmosphere leakage is dangerous if leaks are to the outside as the hydrogen can form an explosive mixture if allowed to collect. If the leak is formed outside to inside, the air will cause the strip at elevated temperature to oxidize immediately. Since zinc will not adhere to an oxidized strip, this means a loss in production.

This type of induction heater can also be used to increase furnace capacity even when not used for transitions by applying additional energy in order to process more throughput of strip.

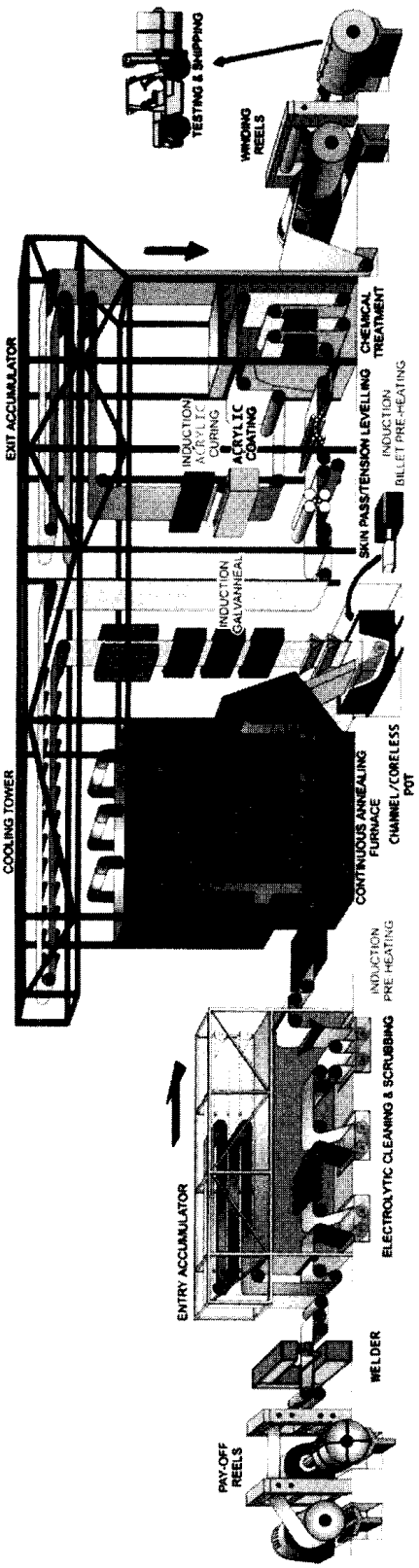

Figure 7.124 Sketch of the strip galvannealing line. (Courtesy of Inductoheat Australia.)

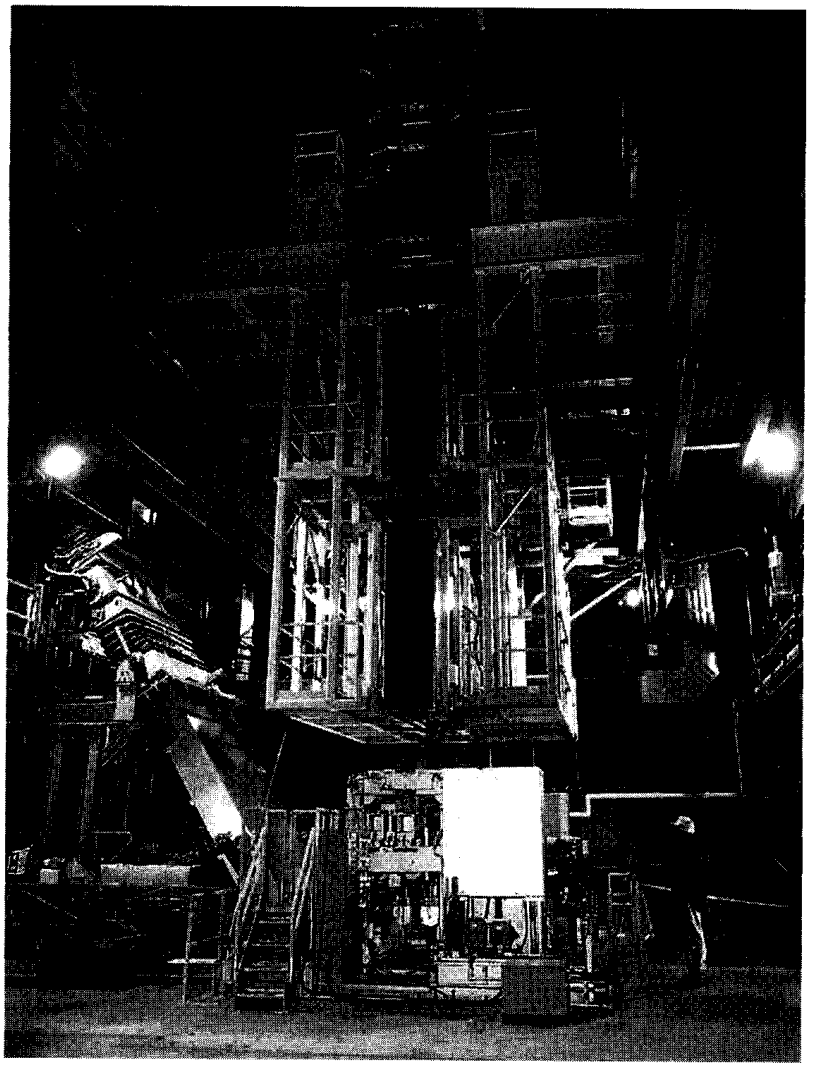

Figure 7.125 INDUCTOHEAT's strip galvannealing line consisting of a pot of molten zinc alloy, induction strip reheater utilizing two doorless inductors, and holding zone.

Tin plating (tinning) represents another form of metallic coating of carbon steel strips and sheets. Tin-plated strips are primarily used by the food industry [173, 300]. The corrosion resistance of tin is much greater than that of carbon steel. Tinning lines accept carbon steel strip from the "double reduced" tinplate or temper mill and process it by welding, cleaning, pickling, plating, reflowing, chemical treating, and coiling or shearing.

The thickness of tin-plated strips (also referred as tinplate) typically ranges from 0.1 mm (0.04 in.) to 0.92 mm (0.036 in.) with a maximum strip width of 1.1 m (43 in.). It has been reported that a maximum speed of some tinning lines can be as high as 610 m/min (2000 FPM). There are two basic types of tinning lines: acid-type (i.e., Halogen and Ferrostan lines). Tin plating is accomplished as a bonding process due to electrolytic reaction of electrolysis with the tin being cathodic to the carbon steel [173, 300].

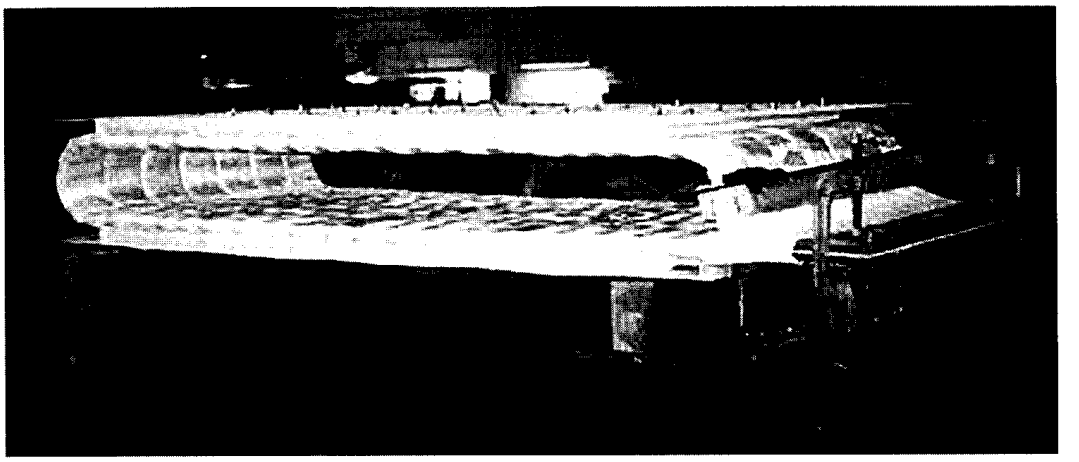

Figure 7.126 Induction booster that minimizes transition losses. (Courtesy of INDUCTOHEAT, Inc., Madison Heights, MI.)

An important part of the process of tin-plating deals with the necessity to remelt (reflow) a tin layer (melting point of tin is about 231°C/448°F). The specific appearance of the strip surface can be achieved by a tin reflow process that provides certain optic and aesthetic properties (e.g., a glossy surface). In addition, it provides a good bonding between the coating layer and base metal (carbon steel). It was also found that dull, not reflowed, tin corrodes at a faster rate than highly polished reflowed tin.

The most long-lasting protection of a carbon steel strip against corrosion can be obtained by applying not just a metallic coating but a combination of metallic and nonmetallic coatings.

7.9.1.2 Nonmetallic Coatings

Paint/coating lines represent a multizone system where the metal strip (i.e., steel or aluminum) is coated with a variety of coatings that includes primers, paints, epoxies, and polymers. In these applications, induction has been used for strip preheating prior to coating or heating after coating for curing, or a combination of both.

There is a fundamental difference between induction heating and convection/radiation furnaces used for strip heating in paint/varnish/organic coating lines. The difference lies in the ability of induction to heat internally, beneath the coating, leaving the surface soft and allowing the solvents to evaporate much more rapidly than curing with convection or radiant heating, which heats from the outside in [296]. When heating the outside first, the surface of the coating is cured and hardened, trapping the solvents between the substrate and the coating skin, making it far more difficult and time consuming for the solvent to evaporate from the coating. In addition, because induction heats the substrate inside-out, there are no pin holes in the coating.

The process dictates the heating requirements and, in general, the required temperatures are relatively low (i.e., from 50°C/122°F to 280°C/536°F) but the temperature uniformity is very tight and critical. For these types of applications the solenoid-type coils fed from power inverters with a frequency of 6 to 30 kHz

are typically utilized (Figure 7.127). The organic coating processes consist of solvent-based wet paints, water-based wet paints, and dry powder coatings. Figure 7.128 shows an example of strip processing lines that provides organic coating [296].

It is important to remember that in some cases (e.g., curing of water-based solutions) there is a limitation on a maximum heating rate. In water-based solutions, the solids can be dispersed as a result of extremely intensive heating leading to a vaporization of the water carrier. On the other hand, solvents can be flashed off at a lower temperature and the profile stepped up to a higher temperature for curing [301].

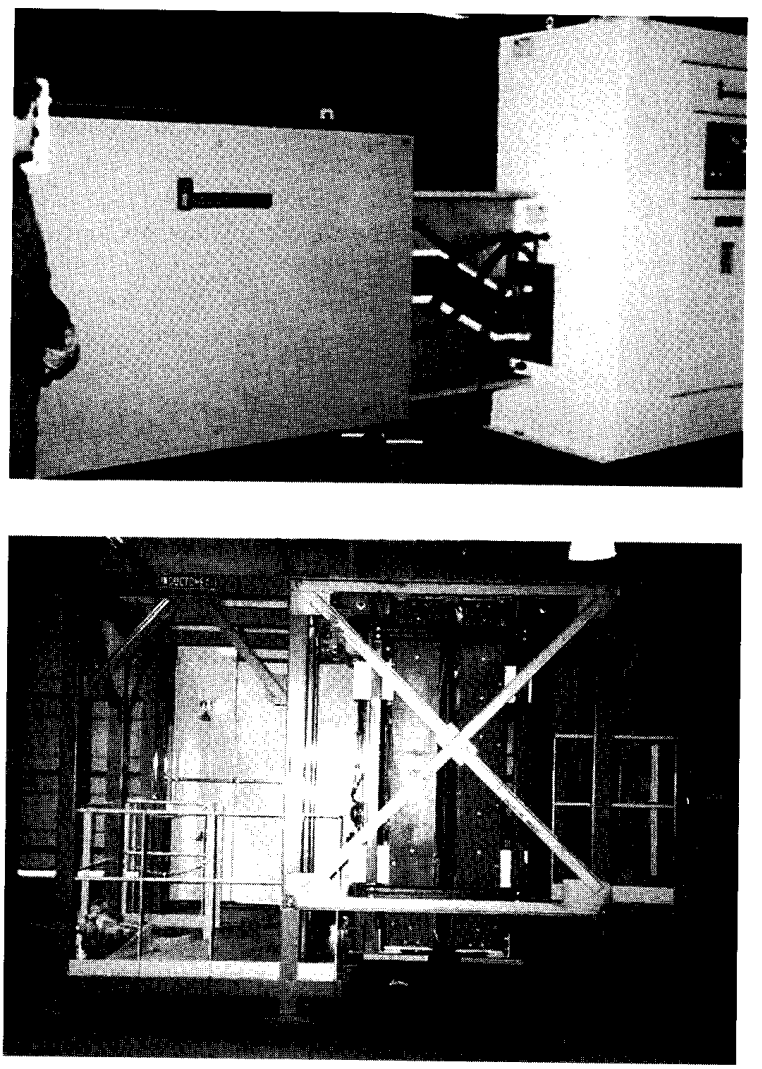

Figure 7.127 INDUCTOHEAT's 800 kW/6 kHz power supply and coil. Strip thickness: 0.3 to 2.3 mm, strip width: 200 to 1550 mm at 42.4 MTH heating after coating, temperature rise: from ambient temperature to 150°C (302°F) to cure a water-based paint type coating of the hot dip galvanized strip.

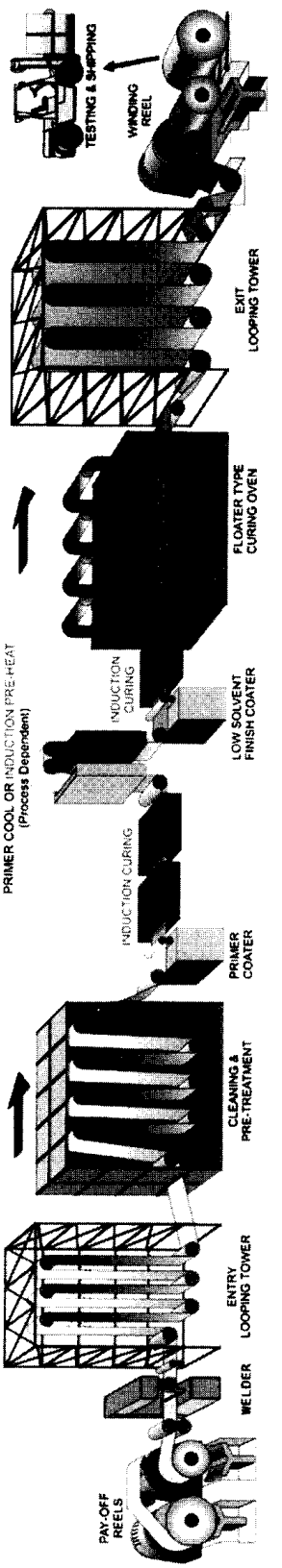

Figure 7.128 Sketch of the strip process line that applies organic coating. (Courtesy of Inductoheat Australia.)

7.9.2 Coil Design Approaches for Heating Strips, Plates, Sheets, and Thin Slabs

A particular strip/thin slab/plate heating application calls for a specific coil design. There are several basic induction heating coil designs [121–123]:

1. Longitudinal flux inductors (solenoid type coils),
2. Transverse flux inductors,
3. Traveling wave coils,
4. Channel-type coils, and
5. C-core inductors.

Generally speaking, these designs are distinguished by the orientation of the main magnetic flux with respect to the strip. Each of the inductors has certain advantages and all have been used either alone or in combination with others.

Electromagnetic end and edge phenomena discussed in Section 7.5 take place in strip heating as well. Careful control and the use of these effects help overcome the problem of obtaining high electrical efficiency and uniform temperature distribution. However, unlike the case of induction heating of slabs or thick plates [92, 121–123, 203], the heat source nonuniform distribution along the strip thickness does not typically cause a surface-to-core temperature nonuniformity, because the thermal conductivity of the metal is able to quickly equalize the temperature nonuniformity within the strip thickness.

Therefore, when designing strip heating lines the major concern is the ability to provide temperature uniformity across the strip width. The temperature distribution along the strip width is primarily affected by a distortion of the electromagnetic field in its edge areas. This is another instance of the electromagnetic edge effect that should be carefully taken into consideration when designing induction strip heating equipment.

No single type of coil will provide acceptable heating results in all strip-heating applications. Therefore the selection of the best type of coil and its specific design must rely on a detailed analysis of the application.

7.9.2.1 Longitudinal Flux Inductor (Solenoid Coil)

A longitudinal flux inductor can be described as a solenoid induction heater (Figure 7.129) similar to that used in the induction heating of slabs (see Sec. 7.5). The strip is surrounded by the induction coil. An alternating current flows through the coil turns and produces a longitudinally oriented time-variable magnetic field that induces

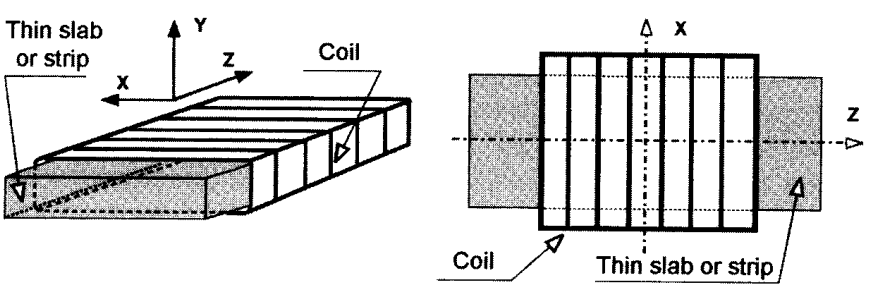

Figure 7.129 Longitudinal flux induction heater.

eddy currents to circulate within the strip thickness and produce heat by the Joule effect.

Traditionally, longitudinal flux induction heaters have high electrical efficiency and the required uniformity of temperature across the strip width. As in the case of induction heating of slabs (Sec. 7.5), high coil efficiency will be obtained if the ratio of strip thickness d to penetration depth δ is 2.5 or more. The optimal value of the frequency that corresponds to the maximum coil efficiency can be determined as follows [53].

A nonmagnetic strip or a magnetic strip heated above the Curie temperature:

$$\frac{d}{\delta_{\text{non-magn}}} \cong 3 - 3.5, \tag{7.8}$$

a magnetic strip:

$$\frac{d}{\delta_{\text{magn}}} \cong 2.8 - 3.2, \tag{7.9}$$

where $\delta_{\text{non-magn}}$ is the current penetration depth in the nonmagnetic strip, and δ_{magn} is the current penetration depth in the magnetic strip.

The use of a frequency higher than the optimal value will only slightly change the coil efficiency. However, the use of frequencies higher than optimal might be a preferable choice in cases when it is necessary to have higher heating intensity in the strip edges compared to the strip central part. This is typically the case with strip reheating when the strip's edge areas have a lower initial temperature than the central part.

Note that sometimes the strip thickness is not the same across the strip width and depends upon a previous rolling process. In cases like this, the "best" frequency might be different from a recommendation based on an assumption of equal thickness.

It is wise to remember that the use of very high frequencies tends to decrease the total electrical efficiency due to higher power losses in the coil copper and bus bars. If the chosen frequency is noticeably lower than the optimal value, the coil efficiency will dramatically decrease due to a cancellation of the induced currents circulating in the opposite sides of the strip cross-section.

Longitudinal flux inductors are normally less demanding with a tight air gap, and they do not require big adjustments of the heater for strips with different widths and thicknesses. These types of inductors are particularly efficient when used for low-temperature induction heating of magnetic strips when the final temperature of the strip is below the Curie point.

Solenoid inductors are effectively used for heating nonmagnetic low-resistivity (e.g. aluminum, copper, brass, etc.) thin slabs, plates, and thick strips as well. Table 7.13 shows the minimum thickness for efficient heating of some nonmagnetic strips. A dual-frequency approach (discussed in Secs. 7.2 and 7.3) is also very useful here.

As one can see from Table 7.13, these applications can be handled by solid-state power supplies such as the Statipower and Statitron that have been specifically developed for load conditions typical of strip heating applications.

In the case of heating thin nonmagnetic stainless steel strips or thin magnetic strips above the Curie point, a solenoid-type inductor might require high power at

Table 7.13 Minimum Thickness (mm) for Efficient Heating of Nonmagnetic Thin Slabs, Plates, and Strips Using Longitudinal Flux Inductors

		Frequency (kHz)					
Material	Temp. (°C/°F)	2.5	10	30	70	200	500
Aluminum	100/212	4.8	2.4	1.4	0.9	0.53	0.34
	250/482	5.8	2.9	1.7	1.1	0.65	0.42
	500/932	7.4	3.7	2.1	1.4	0.82	0.52
Copper	100/212	3.7	1.9	1.1	0.7	0.42	0.26
	500/932	5.7	2.9	1.6	1.1	0.64	0.4
	900/1652	7.3	3.7	2.1	1.4	0.82	0.52
Brass	100/212	6.9	3.4	2	1.3	0.78	0.48
	500/932	9.2	4.6	2.6	1.7	1	0.65
	900/1652	11.3	5.6	3.3	2.1	1.3	0.8
Titanium	100/212	17.7	8.9	5.1	3.4	2	1.2
	600/1112	29	14.8	8.6	5.6	3.3	2.1
	1500/2732	33	16.8	9.7	6.4	3.8	2.4

frequencies in the megahertz range, which can be provided by tube generators. The use of tube generators in the megawatt range can lead to a variety of problems such as safety concerns, low reliability, and low efficiency yet they are the only choice until megahertz range frequency solid-state power supplies can be developed.

The process of induction heating of magnetic strips from ambient temperature, or a temperature below the Curie temperature, to a temperature above the Curie point has several features that could call for special design of the induction system.

At the beginning of the heating cycle (the first stage), the whole strip is magnetic and the heating process is very efficient when using a longitudinal flux inductor assuming that the frequency has been selected appropriately. After the strip temperature approaches the Curie point, the heat intensity will significantly decrease and the heating process will become inefficient. To avoid this, one could use not just a dual-frequency but also a dual-inductor approach. According to this approach, a solenoid-type inductor can be used for induction heating of the strip to the temperatures below the Curie point. In the second stage when the carbon steel becomes nonmagnetic, it is more efficient to use another type of inductor, for example, the transverse flux inductor or traveling wave inductor discussed in the next section.

It is important to keep in mind that formulas (7.8) and (7.9) allow one to determine the optimal frequency that corresponds to the maximum coil efficiency when heating uncoated strips or strips with a nonelectrically conducted coating (e.g., paint). At the same time, in many cases it is required to heat strips that have a metal coating (Figure 7.130). For example, it is often required to induction heat a carbon steel strip (e.g., low-carbon steel of 1008 or 1010 being the base metal) that has a zinc–aluminum alloy coating. If the thickness of the metal coating is comparable to the current penetration depth in the coating alloy (ratio $d_{\text{coating}}/\delta_{\text{coating}} \geq 1.5$) then, regardless of the existence of the base metal, electromagnetically speaking, the magnetic field will see only the metal coating (Figure 7.131) and the existence of the base

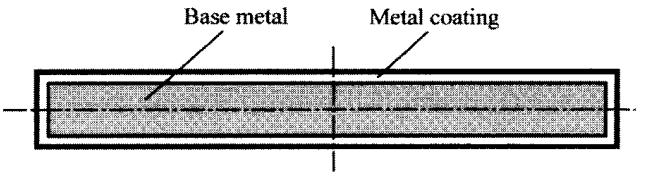

Figure 7.130 Sketch of transverse cross-section of metal coated strip.

metal will be taken into consideration only in thermal calculation when determining the required power.

If the thickness of the metal coating is less than 5% of the current penetration depth then electromagnetically speaking the metal coating will be practically transparent to the magnetic field. The magnetic field will see the base metal only. In this case, the existence of the coating will be taken into consideration only in thermal calculations when the required power will be determined.

If the ratio $1.5 \geq d_{\text{coating}}/\delta_{\text{coating}} \geq 0.05$) there will be a complex distribution of induced eddy current along the strip thickness dealing with the dual-properties (biproperties) phenomenon. The current density distribution may have a waveshape (waveform) that is different from the classical exponential distribution similar to the phenomenon discussed in Sections 3.3.2 and 5.1.2.1. The use of sophisticated numerical computation (e.g., ADVANCE software) would be necessary in cases such as this in order to determine the required process parameters such as coil efficiency, coil power factor, required power, coil current, and so on.

At this point, it would be useful to emphasize that in the case of using longitudinal flux inductors the temperature uniformity across the strip width depends upon several factors, one of which is the *frequency*. The effect of the frequency has already been discussed above. Generally speaking, too low a frequency results in underheated edges. In contrast, too high a frequency results in overheated edges. There is a range of frequencies that can produce a reasonably uniform transverse temperature distribution. It is important to clarify what we mean by "too low a frequency" and "too high a frequency." For example, is a frequency of 10 kHz a high frequency or a low one? As one can conclude from the discussion conducted in Section 3.1.2 this is not the correct question. A frequency of 10 kHz may be considered to be a very high frequency in some strip applications and in others it may be considered to be a low frequency. Whether a frequency is too high or too low

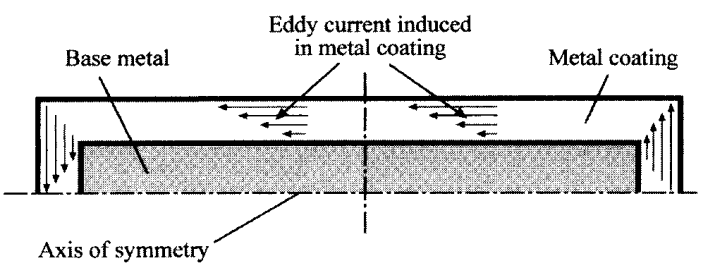

Figure 7.131 Eddy current distribution within top portion of transverse cross-section of metal-coated strip when the thickness of the metal coating is comparable to the current penetration depth in the coating alloy.

depends upon the ratio of strip thickness-to-current penetration depth (d/δ). If this ratio is less than 1.6, the frequency is too low, resulting in poor coil efficiency and significant edge underheating. If the ratio is 20 or higher, then the frequency is very high, resulting in high coil efficiency, but at the same time leading to overheated edges as well as high equipment cost and possible load matching problems. The most appropriate frequencies for strip heating applications typically result in a ratio d/δ of 2.6 to 8.

Another factor that can affect the transverse temperature profile is the *shape of the strip inside the induction coil* (Figure 7.132) and whether the coil is electromagnetically long or short. If the strip is not perfectly even while it progresses through a multicoil induction line, the transverse temperature nonuniformity can be magnified. In addition, the strip width has a marked effect on the temperature profile. For example, wider strips may develop a different temperature distribution than narrower strips even though the "shape" of the strip inside the induction coil is similar. If the induction coil is electromagnetically short or consists of a number of electromagnetically short sections, then such a coil might be more sensitive to variation of the strip shape and strip width inside the coil. Making electromagnetically long coils/sections can help decrease the sensitivity of heating conditions to the strip shape/width. The use of magnetic flux concentrators/diverters (i.e., ferrites) is a step toward transferring electromagnetically short coils to electromagnetically long coils without actually changing the coil geometry.

The third factor that affects transverse temperature uniformity is an *inconsistent strip thickness*. Quite often, strip processing companies have several suppliers of strip that is manufactured by different mills. Every mill can supply strip in the range of width and thickness but may have certain peculiarities regarding the strip thickness uniformity. The thickness across the strip width can affect the temperature profile in two ways:

- Thinner areas will have a smaller mass of metal that will be heated, therefore, those areas will be heated to higher temperatures compared to thicker areas resulting in high local temperatures: local hot spots. This phenomenon is frequency independent.
- A second phenomenon typically takes place only in cases when the chosen frequency results in the ratio d/δ less than 2.6. In this case, eddy current cancellation can take place in thin areas of the strip (two opposite currents induced on opposite sides of the strip can cancel each other). Therefore,

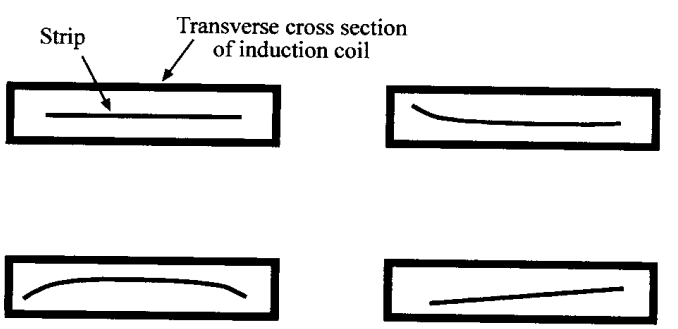

Figure 7.132 Variety of shapes of the strip inside an induction coil.

from one side, the thin areas have a lesser amount of metal to be heated, resulting in a tendency to experience hot spots. On the other hand, the existence of current cancellation in those areas leads to the appearance of cold spots. The final thermal condition in thin areas of the strip when using a relatively low frequency will depend upon which factor is stronger.

The fourth factor is related to strips that are nonmetallic and, in particular, to metal coating. *Coating thickness may vary* across the strip width and under certain circumstances can lead to the appearance of a nonuniform transverse temperature profile. The coating thickness can vary in several ways:

1. Different sides of the strip could have equal but different thickness (Figure 7.133);
2. The coating thickness can vary uniformly from edge to edge of the strip (Figure 7.134); and
3. The coating thickness is generally uniform, however, there are some localized areas (patches) that have different coating thicknesses (Figure 7.135).

The effect of variations in the coating thickness on transverse temperature distribution has a complex electromagnetic–thermal nature and depends upon the frequency, material properties, and thickness of the coating and base metal. These can be studied using numerical computation methods.

A longitudinal flux induction heating is the most widely used approach for induction strip heating applications, featuring high electrical efficiency, a low shop floor space requirement, cost effectiveness, high production rate, robustness, and very little required maintenance. Such systems have been used effectively for a variety of strip processing applications including galvanizing, galvaluming, galvannealing, and tin reflow lines. Among the design criteria that are typical for conventional induction heating systems, there are some specific design criteria, including the necessity of avoiding the vibration marks or striping phenomenon. If this phenomenon is present, the surface of the strip may unexpectedly develop coating marks.

Section 5.1.6 discussed a striping phenomenon that takes place during induction surface hardening. There are several different types of striping phenomena, due to the different nature and various factors responsible for the appearance of stripes. Some stripes are caused by a barber pole effect and others appear due to the use of multiturn coils. These striping phenomena can occur in induction strip coating applications such as galvanizing and tin reflow and are somewhat similar to the striping phenomenon occurring in induction hardening.

The stripes occurring during induction hardening are transversely oriented, but stripes appearing during induction heating of the coated strip are longitudinally

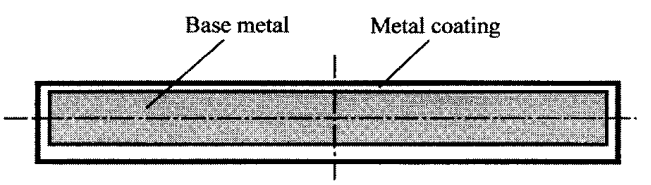

Figure 7.133 Nonuniform coating of strip.

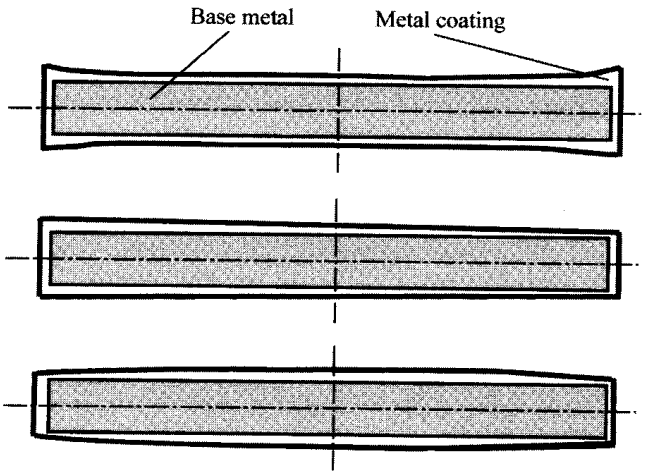

Figure 7.134 Nonuniform coating of strip.

oriented (Figures 5.52A,B and 7.136). The striping occurring during induction heating of a coated strip can be seen even with a single-turn coil and low-intensity magnetic field. Shortly after the heating cycle begins, alternating bright and dark areas on the strip surface become visible. These bright and dark stripes are somewhat similar to standing waves. In some applications, striping suddenly occurs and in others it disappears. One of the possible explanations of this phenomenon has been published in [297] and is related to elastic buckling of the strip. This buckling take place due to a complex distribution of the magnetic forces (magnetic pressure) acting on the strip (Figure 7.136A and Sec. 3.1.6). Forces that provide pulsating magnetic pressure on strip edges in the direction where thin strips have little stiffness result in elastic buckling of the strip (Figure 7.136B).

It has been found that the appearance of the coating marks depends upon a complex function of frequency, strip width and thickness, coil power, type and thickness of the coating, strip flatness, the tension of the strip, and its natural mechanical vibration frequency. As one can see, this phenomenon has a complex nature associated with mechanical vibration and electrodynamics. Due to the complexity and interrelation of the different factors it is difficult to create a universal mathematical formula that would allow one to determine conditions that would avoid this undesirable phenomenon. The experience of successfully designed projects allows a manufacturer of induction strip heating lines to build an inherently stripe-

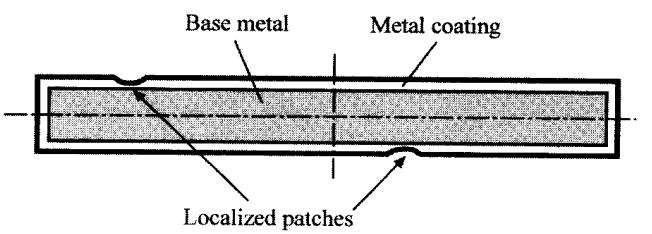

Figure 7.135 Localized areas (patches) that have different coating thicknesses.

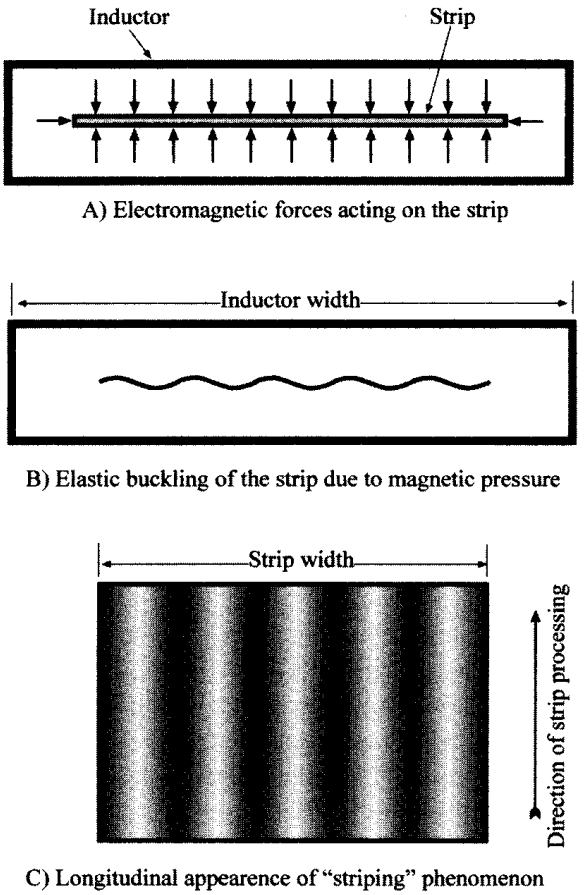

Figure 7.136 Striping phenomena in induction heating of coated strip.

free process. An approximate estimation of the buckling mechanism applied to a steel strip can be provided using the formula proposed in [297]:

$$f \cong 2\pi \frac{a}{\lambda^2} \sqrt{\frac{E}{12 \times \text{Density}}}, \tag{7.10}$$

where

a = Thickness of the strip (mm);
f = Mechanical buckling frequency, in this case electrical frequency (Hz);
λ = Mechanical wavelength (m) (i.e., two times the strip pattern pitch);
E = Young's module (N/m^2);
Density = Specific density (kg/m^3).

One of the major difficulties in induction strip heating design is caused by the geometry variation of the products (i.e., strip thickness or width) that are heated in the same coil. However, the problem of providing a uniform transverse temperature distribution is not nearly as pronounced with a longitudinal flux inductor as with other types of induction coils (i.e., transverse flux or traveling wave inductors).

7.9.2.2 Transverse Flux Induction Heater (TFIH)

The transverse flux inductor (Figure 7.137) is one of the oldest induction heating techniques, having been developed for use in the induction aluminum alloy strip heating industry in the early 1940s. The principles of the process, simulation procedures, and experience of industrial utilization of transverse flux induction heaters were reported by R. M. Baker and M. Lamourdedieu as early as 1950 [124–127]. This process was established as a way to overcome the low efficiency problem of induction heating of thin nonmagnetic strips and films in solenoid (longitudinal flux) inductors.

In the conventional transverse flux induction heater (TFIH), the strip passes through induction coil pairs that are located on both sides of the strip, as shown in Figure 7.137. These coil pairs create a common magnetic flux. This magnetic flux passes perpendicularly through the strip width. Unlike the longitudinal flux induction heater, in the transverse flux induction heater the induced eddy currents are circulated in the plane of the strip not just within the strip thickness. This allows induction heating of a thin strip to be carried out with high power densities using low, and sometimes even line, frequency. TFIH systems typically require less floor space compared to solenoid coils. The transverse flux inductor often utilizes external magnetic flux concentrators (i.e., laminations or other high-permeability materials).

Electrically efficient heating can be provided when the coil-to-strip air gap is relatively small and the strip thickness is 1.5 to 2 times the penetration depth or less. Without satisfying the latter condition, the transverse flux effect will disappear and conventional proximity heating (similar to heating with two pancake coils) will take place. Proximity heating is known for having lower coil efficiency compared to longitudinal flux and in particular transverse flux heating.

The most difficult problem in utilizing transverse flux inductors is obtaining temperature uniformity across the width of the strip. The heat time of TFIH is typically quite short ranging from a fraction of a second to 10 seconds, therefore the thermal conductivity does not have a chance to equalize the temperature gradients across the strip width (as in the case of induction heating of bars and billets). This is why with TFIH the temperature profile typically follows the power density distribution very closely.

The eddy current paths in the strip match the shape of the transverse flux induction coils. Therefore, when the current reaches the edge, it must flow along the strip edge (Figure 7.138). Because of this natural phenomenon, in cases where coil width is

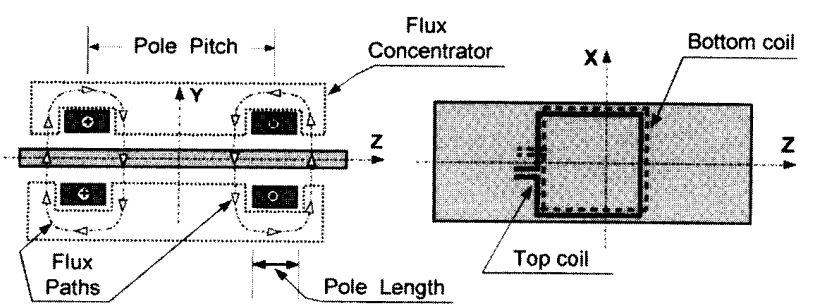

Figure 7.137 Sketch of conventional transverse-flux induction heater (TFIH).

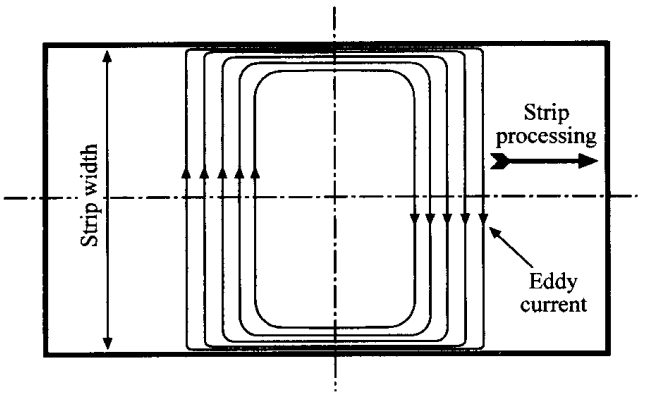

Figure 7.138 Eddy current flow in conventional transverse flux inductor.

greater than the width of the strip, the current's concentration will be higher in the strip edge area compared to the strip central area and, as a result, the strip edges will be overheated. However, if coil transverse overhang is negative (i.e., strip width is greater than the coil width) then the strip edge areas will be underheated because the eddy current will not reach the strip edges. Obviously, somewhere between these extreme cases there is a condition for reasonably uniform heating. Figure 7.139 shows three of the most typical temperature profiles across the strip width.

In addition to the electromagnetic properties of the heated metal, strip geometry and transverse coil overhang, there are four other factors that have a major impact on the coil electrical parameters (i.e., coil efficiency and coil power factor) and greatly affect the temperature profile across the strip width:

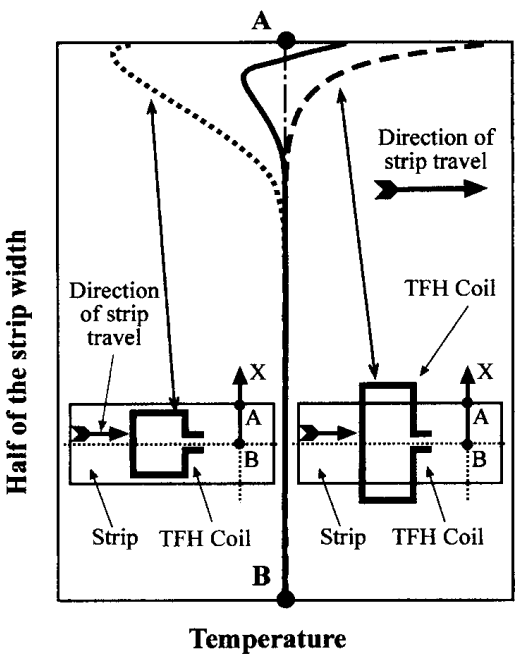

Figure 7.139 Typical temperature profiles across the strip width using conventional transverse flux inductor.

- Pole step (pole pitch),
- Pole length,
- Coil opening, and
- Frequency.

In-depth theoretical work and mathematical modeling devoted to TFIH have been conducted at Hannover University, Germany [289, 290, 441, 442], Padua University, Italy [292, 295, 442], as well as at Inductotherm Corp. [190], INDUCTOHEAT, Inc. [92, 121–123, 194, 203, 418] and in [124–139, 287–290]. Figure 7.140 shows the results of evaluation of coil efficiency and coil power factor of a transverse flux induction heater for a 6 mm thick strip made from three different metals (aluminum, titanium, and stainless steel) [288]. The parameters of the TFIH were: pole length = 90 mm; pole pitch = 180 mm; and coil-to-strip air gap = 37 mm. Figure 7.141 shows the coil efficiency and coil power factor of TFIH of titanium strip (1 mm thick) as a function of the skin effect for four different pole pitches (0.1 m, 0.14 m, 0.18 m, and 0.26 m) [288].

As one can see from Figures 7.140 and 7.141, the curves representing the coil power factor have a well-defined maximum. This feature is critical for load-matching the inductor to the power supply. At the same time, the maximum of the coil efficiency curves is not as pronounced as the maximum of the coil power factor.

Several different formulas have been developed in the past for selecting the frequency that provides high electrical efficiency using transverse flux induction heating for a nonmagnetic strip [124–131, 194, 419].

$$F = 24.5 \times 10^6 \frac{\rho h}{\tau^2 t}, \tag{7.11}$$

where ρ is electrical resistivity, Ω cm; h is the coil opening, in., τ is the pole step of the coil (pole pitch) in., and t is the strip thickness, in., or

$$F = 1.58 \times 10^8 \frac{\rho h}{\tau^2 t}, \tag{7.12}$$

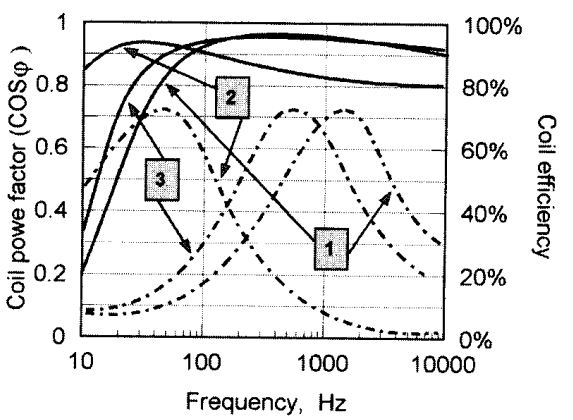

Figure 7.140 Coil efficiency (solid lines) and coil power factor (dotted lines) of TFIH of a 6 mm thick strip made from different metals as a function of frequency: 1 = titatium 2 = aluminum, and 3 = stainless steel. (From Ref. 288.)

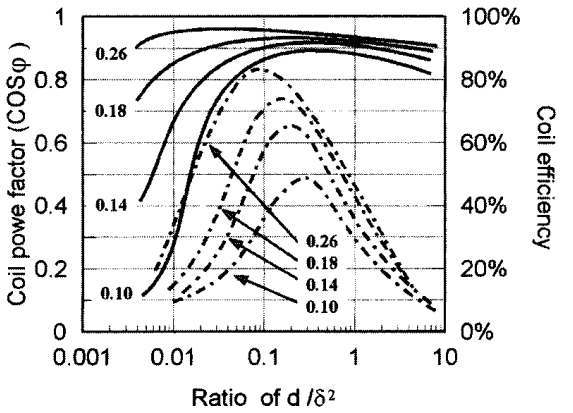

Figure 7.141 Coil efficiency (solid lines) and coil power factor (dotted lines) of TFIH of titanium strip (1 mm thick) as a function of $d/(\delta * \delta)$ different pole pitches: 0.1 m, 0.18 m, and 0.26 m (ratio of pole length to pole pitch = 0.5, ratio of half air gap to pole pitch = 0.23). (From Ref. 288.)

where ρ is electrical resistivity, Ω cm; h is the coil opening, cm; τ is the pole step of the coil (pole pitch), cm; and t is the strip thickness, cm.

One of the transverse flux inductor design parameters that has a significant influence on current, and therefore on the heat source distribution in the plane of the strip, is the shape of the induction coil. Over the last four decades, different complex-shaped transverse flux coils have appeared quite regularly [124–141, 287–290]. This includes diamond-shaped coils, J- and O-type coils, pairs of U-shaped coils (Figure 7.142), and so on. In some cases, in order to provide the required thermal profile, the poles of the TFIH were deliberately shifted (Figure 7.143).

Theoretically speaking, some of the TFIH coils were suitable for a broad production mix (including variation of strip width and thickness) and immune to unstable strip positioning inside the inductor. However, in practice, most of these coils have noticeable limitations in providing the required temperature repeatability and uniformity across the strip width when the strip width and thickness vary widely

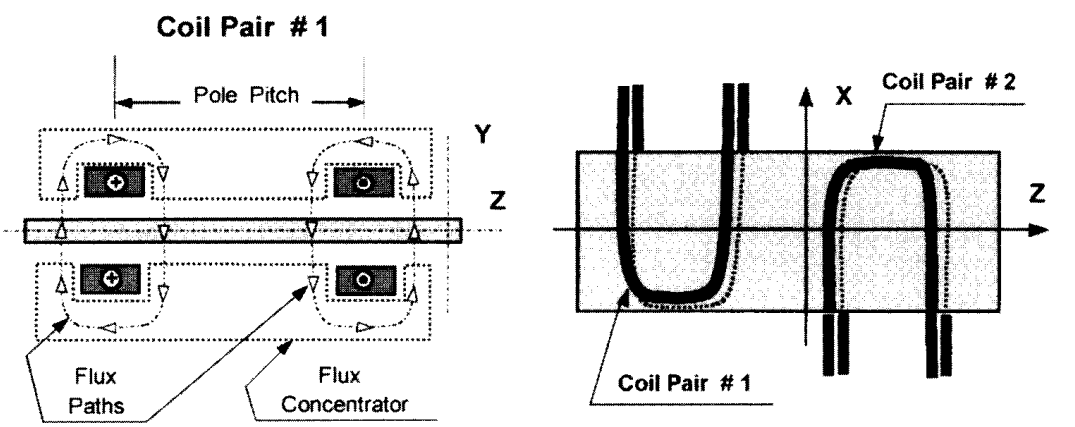

Figure 7.142 U-shaped approach of transverse-flux induction heater.

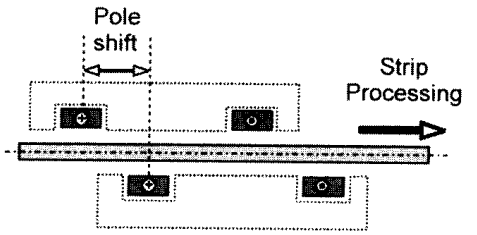

Figure 7.143 Pole shift of transverse flux induction heater.

or when the strip moves left to right or up and down inside the transverse flux inductor.

One of the possible solutions for designing a TFIH line that would be less sensitive to strip movement in the transverse direction would be to build moveable coil pairs so they could trace the strip movement. However, this approach drastically increases the capital cost of the transverse induction heater.

One of the most practical uses of the transverse flux inductors is probably the edge reheating of the plates, strips, slabs, and transfer bars. In applications such as these, the natural tendency of wide transverse flux induction heaters to overheat edges that is typically considered as an undesirable feature and concern works advantageously. Extensive R&D studies conducted at Inductotherm Corp. and INDUCTOHEAT, Inc. [418] show the effectiveness of using the transverse flux principle for edge reheating of flat workpieces. A properly designed TFIH allows one to obtain high coil electrical efficiency in the range of 70 to 85% in combination with a generous coil opening and the inductor's ability to produce repeatable temperature profiles that would be practically immune to variation of the strip, slab, or transfer bar width, thickness, and positioning inside the inductor. In this case, the maxima of the curves that correspond to coil efficiency and coil power factor shown in Figures 7.140 and 7.141 are shifted toward the lower frequencies. Figure 7.144 shows the variation of coil efficiency and coil power factor of a particular TFIH coil

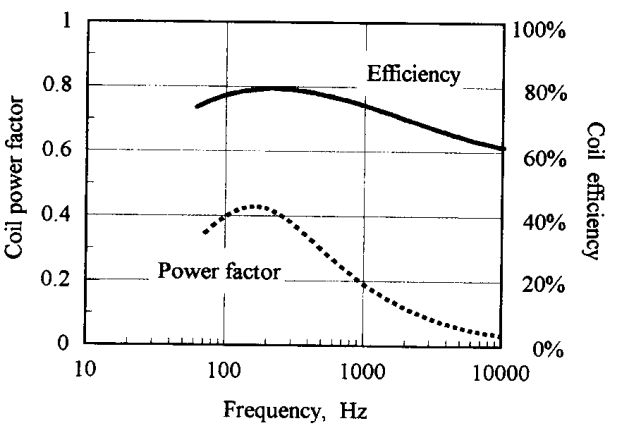

Figure 7.144 Coil effciency (solid curve) and coil power factor (dotted curve) of transverse flux induction edge heater for carbon steel transfer bars (25 mm/1 in. thick) at 900°C. (From Ref. 418.)

design as a function of frequency for a 25 mm (1 in.) thick carbon steel transfer bar heated to a temperature of 900°C [418].

7.9.2.3 Traveling Wave Induction Heater (TWIH)

The traveling wave inductors are not as commonly used for strip heating applications as transverse flux heaters or particularly longitudinal flux inductors. The main reasons for this are the complexity of the process and the fact that there has not been enough experimental and research work done in developing the traveling wave induction heating process.

One of the most extensive works in the area of theoretical development and commercial implementation of induction traveling wave heaters has been conducted by the scientific group of Drs. A. Rashepkin and I. Kondratenko (Kiev, Ukraine) [291]. Figure 7.145 shows a strip-processing line for annealing of copper alloys using a traveling wave induction heater. Marked theoretical development has also been conducted by Drs. S. Lupia, F. Dughiero, and coworkers (Padua University, Italy) [295, 440].

The fundamental concept of this process is quite simple [10,121] and is similar to that of the conventional three-phase electric machine where the strip takes the place of the rotor and the induction coil can be considered a stator (Figure 7.146). The inductor turns are located quite close to each other and carry multiphase currents. The coils are located in the slots of the flux concentrator (e.g., laminated low-carbon steel packs). The inverse connections of the middle phases and the

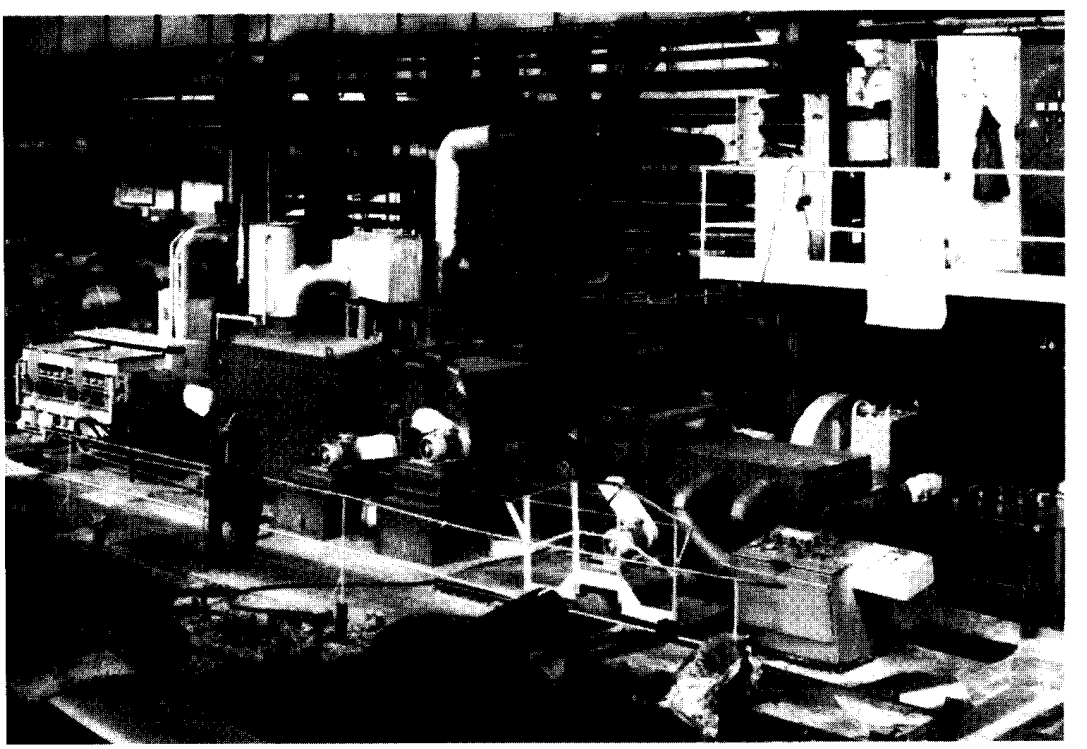

Figure 7.145 Using traveling wave inductors for heating thin copper and brass strips.

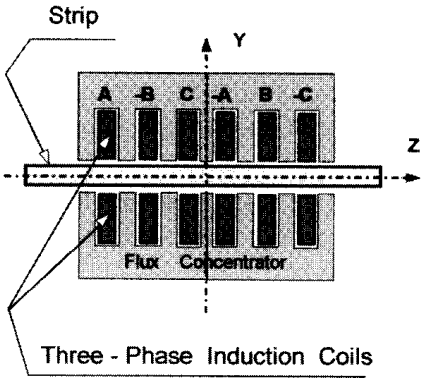

Figure 7.146 Traveling-wave induction heater (TWIH).

external magnetic flux concentrator have been used to reduce current cancellation in neighboring coils.

The three-phase current flows through the coil turns, producing traveling wave electromagnetic fields and corresponding heat sources in the strip. One of the main advantages of a traveling wave system is its low level of vibration and industrial noise compared to transverse flux inductors. This feature is primarily important when induction heating nonmagnetic (aluminum, copper, etc.) thin strips.

Electromagnetic force plays a major role in the appearance of industrial noise. Mathematically speaking, the electromagnetic force existing between two current-carrying bodies (i.e., plates) can be expressed as

$$F = \int_0^l \int_0^b \frac{\mu_0 B_m^2}{h} \sin^2(\omega t) dx\, dy = \frac{1}{2} bl \frac{\mu_0 B_m^2}{h} (1 - \cos(2\omega t)), \tag{7.13}$$

where B_m is a module of magnetic flux density; l is the length; b is the width; h is the height of the air gap; and ω is the angular frequency, $\omega = 2\pi f$. It is imperative to note that the electromagnetic force acts with a doubled frequency compared to the frequency of the electromagnetic field (see Sec. 3.1.7).

As shown in [291], in contrast to Eq. (7.13) in the case of a three-phase traveling wave inductor the electromagnetic forces can be expressed as

$$\begin{aligned} F &= \int_0^l \int_0^b \frac{\mu_0 B_m^2}{h} \sin^2(\omega t - ax) dx\, dy \\ &= \frac{1}{2} bl \frac{\mu_0 B_m^2}{h} \int_0^l (1 - \cos[2(\omega t - \alpha x)]) dx, \end{aligned} \tag{7.14}$$

where $\alpha = \pi/\tau$ and τ is the pole step (pole pitch) of the inductor. Assuming that $l = 2n\tau$, $n = 1, 2, \ldots$, (n is the number of poles), electromagnetic forces can be calculated as

$$F = \frac{1}{2} b \frac{\mu_0 B_m^2}{h} 2n\tau. \tag{7.15}$$

As one can see, formula (7.15) has only a static component and not a dynamic component (a dynamic component is a function of the frequency and is the major source of vibration and noise). Therefore, the major source of vibration is eliminated when using traveling wave inductors, making these inductors quieter compared to transverse flux inductors. They also allow one to prevent the "sucking" action when the strip is suddenly sucked in to one of the sides of the coil which sometimes takes place with transverse flux inductors (in cases when the tension force is not sufficient to stabilize the strip in the middle of the coil).

An important feature of TWIH deals with the fact that an electromagnetic traveling wave creates an electromagnetic force oriented in the direction of the strip travel (longitudinal direction). This force provides an additional tension, which can coincide with the applied tension or be opposite to it (depending upon phase switching). This helps to stabilize strip positioning inside the coil.

In addition to the described advantages, a traveling wave heater has some limitations that prevent wider use of this type of heater. A common shortcoming of both transverse flux inductors and the traveling wave heaters deals with the fact that in order to have high electrical efficiency, inductors require small air gaps between the coil and strip. This often leads to difficulties with respect to strip processing and mechanical design.

The second shortcoming is that even with the use of magnetic flux concentrators, because of the closeness of multiphase turns, there is magnetic coupling between the turns carrying currents with different phases and, therefore, there is magnetic field cancellation in adjacent sections. This leads to a reduction of the total electrical efficiency of the traveling wave inductor compared to the transverse flux or longitudinal flux induction heaters.

Finally, there is still the difficulty of producing a uniform temperature profile for a wide variation of strip width or requiring numerous sets of TWIH coils that accommodate a certain strip width.

Nevertheless, in cases when variation of the strip width is not significant, the TWIH approach has been used successfully. Figure 7.147 shows a multiphase induction traveling wave heater that consists of two line frequency multiphase inductors used for annealing copper and brass strips. This system was designed by the scientific group of Drs. A. Rashepkin and I. Kondratenko [291]. Table 7.14 shows the mea-

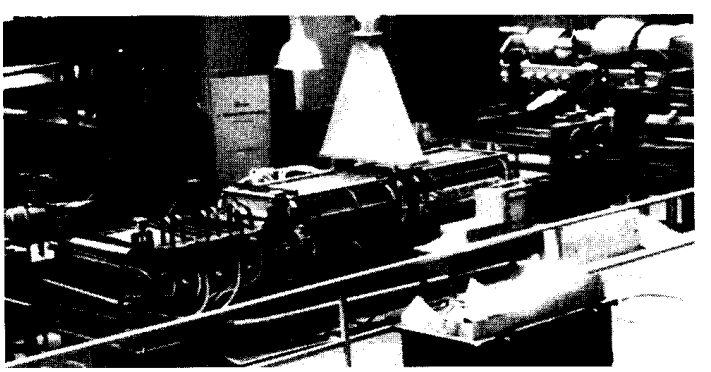

Figure 7.147 Multiphase traveling wave inductors used for annealing copper alloy strip.

Table 7.14 Parameters of the Traveling Wave Inductor for Copper and Brass Strips

Parameter	Unit	Value
Strip width	mm	620 ± 20
Strip thickness	mm	0.4 to 4
Total power	kVA	1,000
Voltage	V	220/380
Number of phases		Three-phase
Frequency	Hz	50
Production	kg/hour	4,000 to 10,000
Initial temperature	°C (°F)	20 (68)
Final temperature	°C (°F)	700 (1292)
Energy required	kW*hr/ton	50 to 80
Electrical efficiency	%	not less than 85%
Power factor ($\cos\varphi$) of inductor		0.5 to 0.75

Source: Ref. 291.

sured parameters of the traveling wave heater that has been in production since 1994 (Figure 7.147).

7.9.2.4 Channel-Type Coils

Among a variety of applications requiring induction heating of thin slabs, plates, and strips, there are applications that do not require heating a whole body but only certain selected areas. Induction reheating of edge areas of continuously cast slabs is one example where selective induction reheating is required. There are several approaches to reheat edges of the rectangular workpiece, including the following.

- Solenoid longitudinal flux coils fed by the current of a frequency higher than that required for uniform heating can be used. Due to the electromagnetic transverse edge effect, the edge areas will be heated at a much greater rate than the central area.
- Naturally, transverse flux and traveling wave heaters can also be effectively used to reheat edges. As discussed above, edge overheating is a major concern when utilizing these types of inductors. Therefore, in cases where edge areas initially have lower temperature than the rest of the workpiece and where it is required to reheat edge areas primarily, this disadvantage can be turned into an advantage since both approaches (TFIH and TWIH) have a tendency to induce more power in the edge areas compared to the rest of the workpiece.
- Utilization of channel-type inductors creates another possibility for providing selective heating of the edge areas.

A channel-type inductor is tunnel-shaped and the thin slab or plate is processed through the coil set (Figure 7.148). These channel coils are similar to the channel inductors discussed in the heat treating section of this text. The slab areas located under the coils will be heated, because of the proximity effect. These coils have not been widely used for strip heating applications but rather for induction heating of thin slabs and plates.

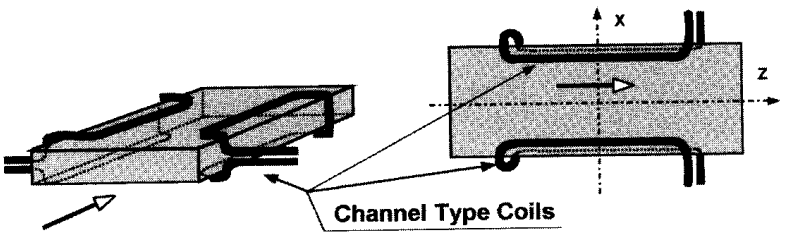

Figure 7.148 Channel-type inductor.

The main advantage of the channel-type inductor is the ease of entry and exit for the workpiece. Magnetic flux concentrators (i.e., laminations) are often used to increase the electrical efficiency of this type of heater and concentrate the magnetic field in the area required to be heated. Flux concentrators increase the coil's efficiency, and eliminate electromagnetic field exposure. However, even with flux concentrators, the efficiency of this type of inductor is lower than the longitudinal flux coil and particular TFIH.

The efficiency of a channel inductor is quite sensitive to the air gap between the coil and slab. If there are significant variations in slab width, one or both of the channel coils can be made flexible enough that the channel inductors can be moved in and out and adjusted to the workpiece geometry. This keeps the induction heater efficient and allows various heating patterns of the slab edge for different production mixes.

7.9.2.5 C-Core Inductors

This type of inductor was discussed in detail in Section 5.5 in applications for induction tempering. Therefore, its coverage here is limited. The C-core induction edge heater is an alternative for applying the transverse flux principle in induction edge heating of thin slabs, plates, and thick strips.

One or several induction coils are wound around the core to create a common magnetic flux (Figure 7.149). Slabs or plates are passed through the opening (air gap) of the transformer. Due to the special location of the heater, eddy currents are mainly induced in the edge areas of the slab or plate, and the current density in

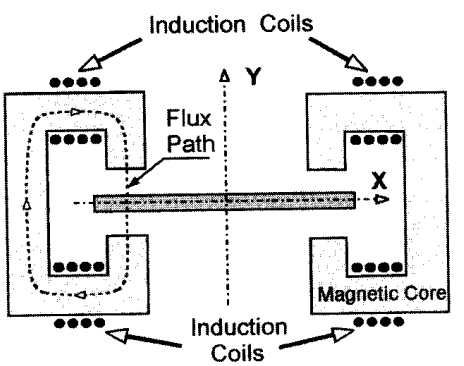

Figure 7.149 Transverse cross-section of C-core induction edge heater.

its central area is much lower. As a result, intense heating of the slab or plate edges takes place.

The efficiency of this type of induction heater depends primarily upon the air gap and material properties of the slab. The mechanical design of an adjustable inductor is obviously not an easy one and is quite expensive. However, several successful installations have been built with adjustable C-core edge heaters.

Additional difficulties appear when using this type of inductor for strip heating applications, primarily when heating of nonmagnetic strips. The problem deals with strip vibration, which can produce significant industrial noise. In some cases, strip can be sucked in to a side of the C-core.

7.9.2.6 Doorless Technology for Strip Processing Lines

The ability to move the induction coil from the heating position to an offline position is an important system requirement in such strip coating applications as galvannealing [246]. Prior to 1995 these systems commonly used a solenoid coil having a "door" with electrical contacts [411] that when closed conducted the full coil current (Figure 7.150). This coil with a door is actually a split coil (also called a clamshell inductor; see Sec. 5.1.4.4) that has been used in induction hardening since the 1960s [2].

In the split coil a good surface-to-surface contact has to be maintained between the faces of the movable part of the inductor that is called the hinge or door and the fixed part where the actual door opening contact takes place. Insufficient contact results in failure due to a local current concentration within the areas of local contacts, overheating, and the appearance of arcs, burns, and contact wear.

In order to improve contact and reduce power loss in the contact area, the contact faces are polished and silver alloy coated. In addition, substantial pressure is applied to provide a reliable contact.

Unfortunately, in strip coating applications, the air contains a substantial amount of dust. As a result of the open–close action of the coil doors a significant amount of zinc dust and other foreign elements builds up on the door opening contacts and operating mechanisms and causes well-known difficulties resulting in premature failure, particularly when using high frequencies and high voltages.

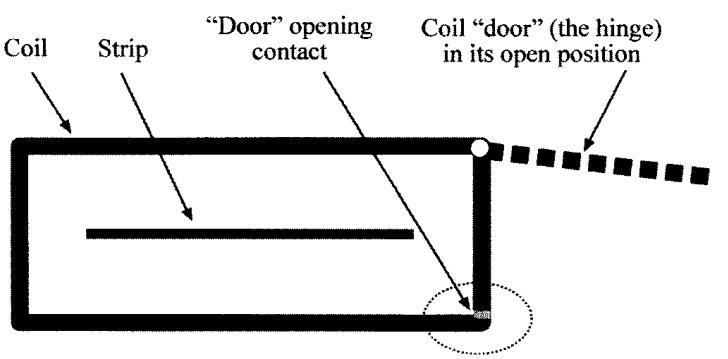

Figure 7.150 Transverse section of solenoid-type induction strip heater with "door."

The doorless induction coil [412] was developed to increase coil life and to eliminate the maintenance problems associated with high-frequency current interrupting the doored coil. Solenoid coils providing uniform heating and being the most efficient are often the preferable choice in the majority of strip heating applications. The doorless coil is a clever adaptation of this existing proven technology. Using two coils in series and rotating the interconnection bus so one coil is over the other, a doorless coil is obtained. As shown in Figure 7.151, from an electromagnetic perspective, a doorless inductor consists of two solenoid coils connected in series with the strip passing through them for heating to galvannealing temperatures. The gap between the interconnecting bus and coils allows passage of the strip without the necessity of having a door.

Removal of the door eliminates the need to make and break electrical connections each time the induction heating unit is moved offline. With the elimination of these high-current-carrying electrical connections, reliability is increased dramatically with significantly improved maintainability. To move the coil offline, air cylinders are used on each side of the interconnection bus to slightly spring it $2\frac{1}{2}$ in. in each direction providing a 5 in. gap that is typically sufficient for strip to pass through. However, if necessary, this doorless coil can easily provide a much greater gap. As an example, Figure 7.152 shows the open position of the doorless coil with several people standing inside.

This patented doorless coil eliminates the need to provide an electrical contact along areas that can be as long as 1 m in a split coil with a door.

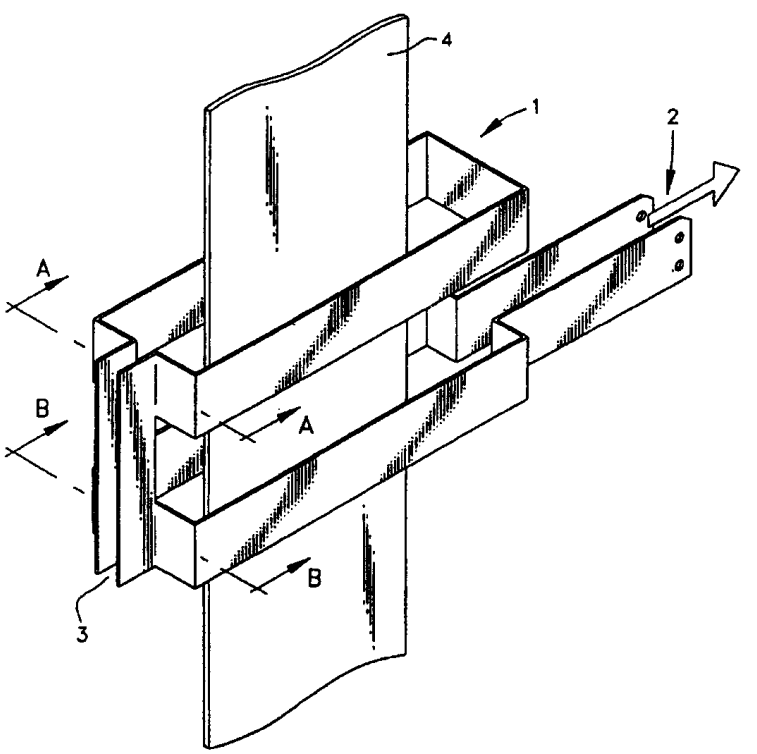

Figure 7.151 Sketch of INDUCTOHEAT's patented doorless coil for strip heating applications. (From Ref. 412.)

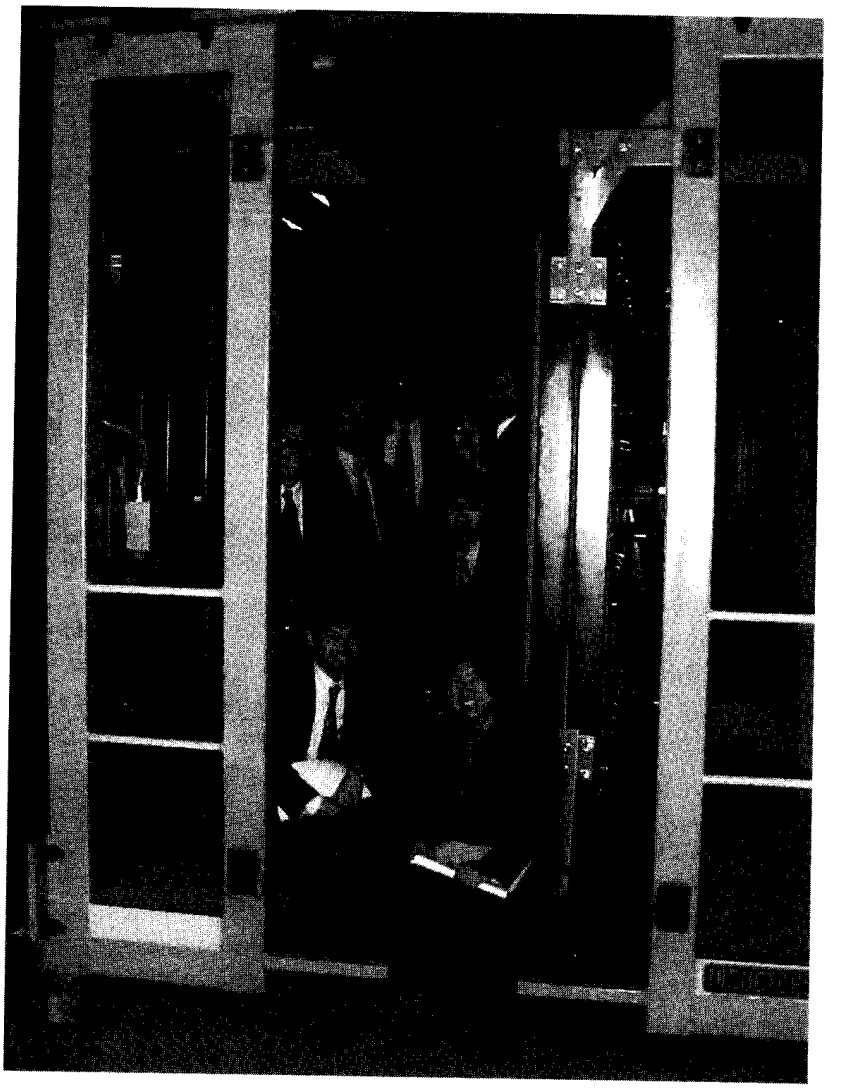

Figure 7.152 Open position of INDUCTOHEAT's patented doorless coil.

The doorless inductor is made from wide sheets of copper and consists of a nonferrous support frame, outer panels sealed with gaskets, and a bellows at the gap. The whole assembly can be connected to a dry air source for pressurization to completely eliminate zinc dust from the coil. Depending upon the application, the inductor may have an inner refractory liner.

Figure 7.125 shows two doorless inductors utilized in an induction strip reheater for INDUCTOHEAT's strip galvannealing line that also consists of a pot of molten zinc alloy and a holding zone.

Because from an electromagnetic perspective the strip is heated in a doorless coil in a manner practically identical to using a conventional solenoid coil, the efficiency of the doorless coil is about 93%, which is the same as the efficiency of a conventional solenoid-type longitudinal flux coil. With the power supply operating efficiency at 91%, the overall system efficiency is high as well: about 84%.

7.10 MATERIAL HANDLING

Material handling operations can be broken down into several basic phases:

1. Delivery of the part to the induction heater;
2. Transferring the part through the coil (in the case of continuous heating or progressive multistage heating) or holding the part in place (during static heating); and
3. Discharging the heated part from the induction heater.

Because there are many types of material handling systems available, the choice of a particular system depends on the application.

7.10.1 Billet Handling

Most continuous-type induction billet heaters or progressive multistage inductors heat through cylindrical or rectangular shaped billets while the billets pass end to end through one or several inline solenoid (helical) coils.

Prior to heating, the billets are sawed or sheared to the required length, typically in the range of 50 mm (2 in.) to 1 m (40 in.). The cross-section of the billets may vary from 12 mm (0.5 in.) to 400 mm (16 in.) diameter (or RCS) and sometimes even larger.

The specifics of the billets' geometry, weight, desirable surface conditions, and required production rate have a pronounced effect on the choice of handling system. A feeding system separates, orients, and delivers the billets to the induction heater. Often, a feeding system consists of a length detector to reject billets that are outside the design specification.

A pneumatic pusher, a cat track, or a twin opposed chain pinch wheel drive can be used to handle the billets. One approach is to feed cold billets automatically using a bin tipper to feed the billets into a vibratory mechanism, which may comprise an external or internal bowl feeder system (Figure 7.153). Alternately, a hydraulic step feeder could feed the billets up to an infeed conveyor (Figure 7.154). Hoppers, as shown in Figure 7.154, represent a large storage area specially designed to accept billets randomly dumped into the hoppers from tote boxes or other means.

Figure 7.155 shows a photo of a reciprocating step feeder [400–402]. This equipment comprises a large steel hopper in which three heavy-duty mechanical slides are layered in an angled and staggered formation to form a series of steps. Each step is individually actuated. In operation the lowest slide picks up a column of billets from the base of the hopper and the reciprocating motion elevates the column of billets up to the level of the next slide; the billets automatically take up position on the next step. The process is repeated until the billets slide from the top step onto the adjacent conveyor, which feeds directly into the continuous feed billet heater.

Step feeders are unlike vibratory bowl feeders, which are inherently self-destructive. Step feeders have a much longer life before major maintenance is required for the wear surfaces and slide mechanism. They are also much quieter in operation and do not create excessive dust.

The two common power sources used for step feeders are hydraulic power packs and electric motors. The electrically powered units offer further advantages in that they can be reverse-actuated with intermittent power to overcome jamming

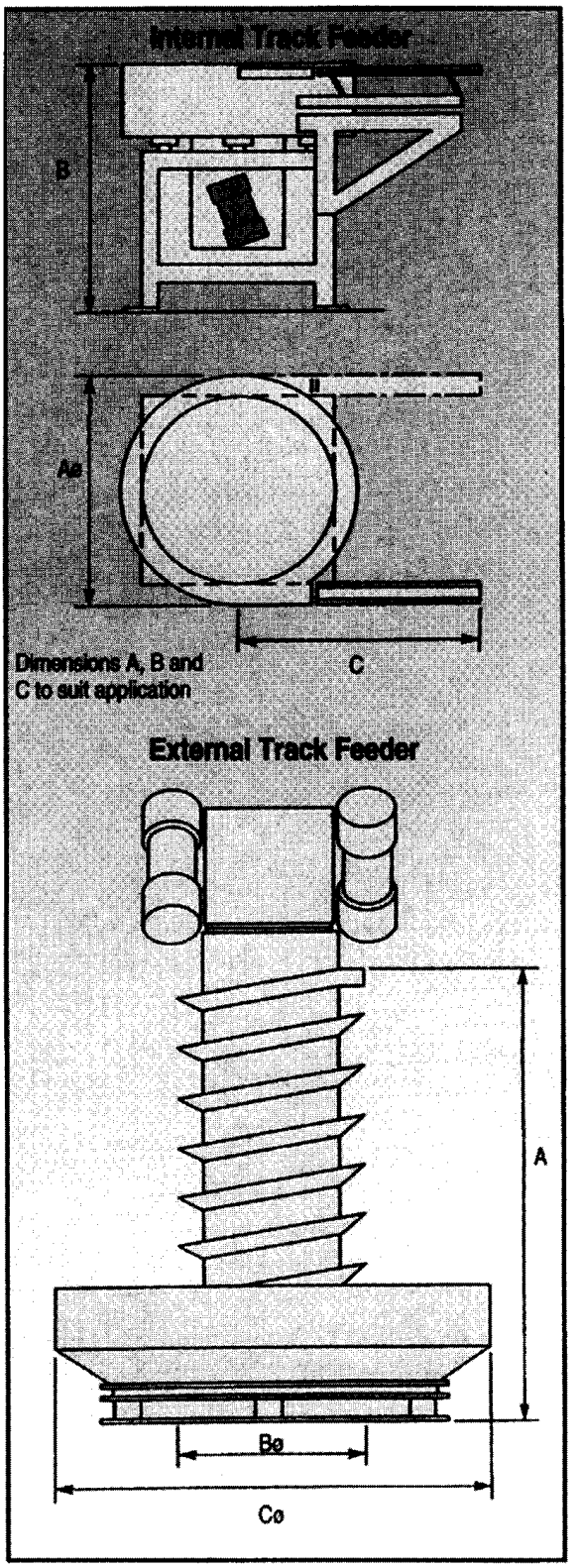

Figure 7.153 Schematics of internal and external track feeding systems.

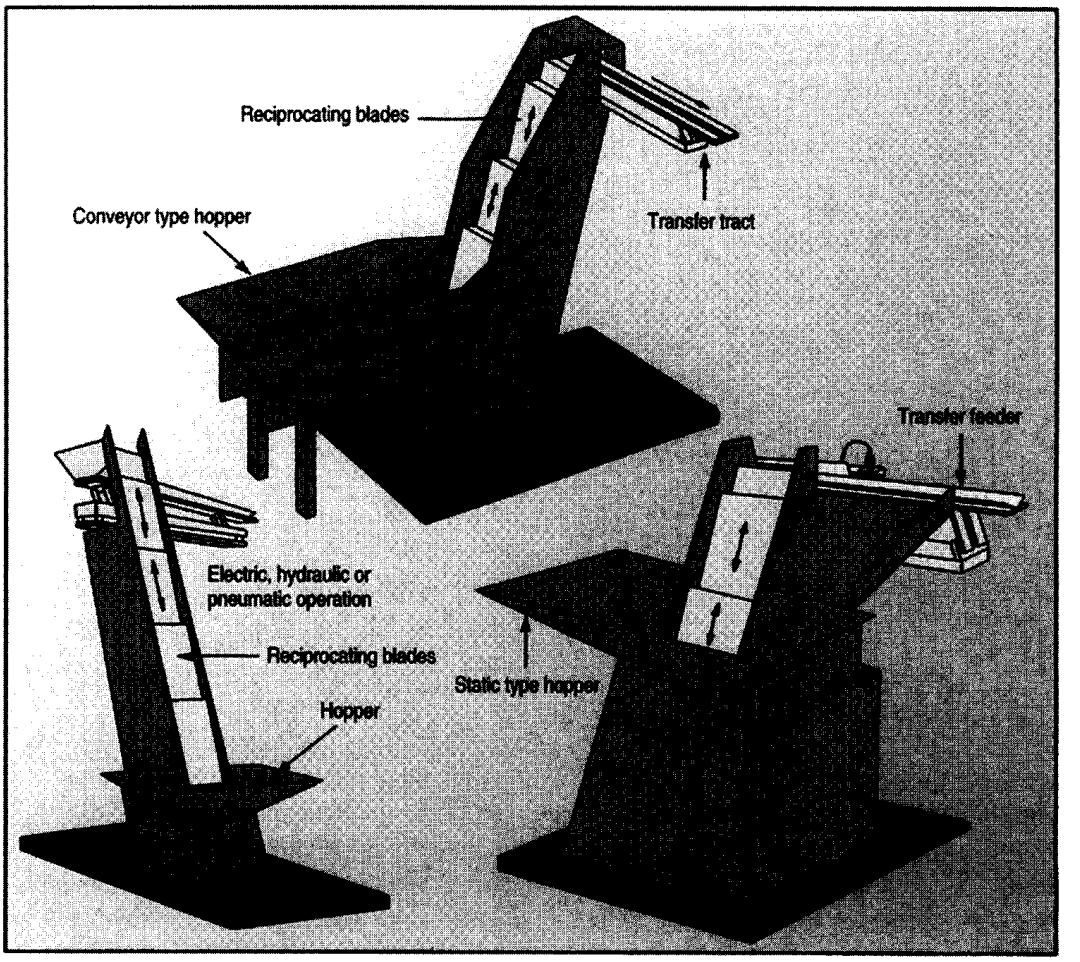

Figure 7.154 Three types of step feeding systems.

of billets, which can occur. Step feeders are particularly good for feeding round sections.

With some forging processes the weight of the cut billets is critical and must be within very close tolerances. This is particularly true for warm forging applications where waste material, in the form of flash, is not permissible and all of the billet material is used to form the part. The cut billets arrive at the weigh station, which has built-in load sensors. The billets are weighed and, provided they are within the weight tolerance required, are allowed to pass through to the next stage of the process. Out of specification billets are rejected at this point. This entire evaluation process can be reliably carried out in less than two seconds [400–401].

Virtually all standard induction billet heating systems incorporate a billet feed system for transporting the billets through a series of induction heating coils. The feeding device will either operate on an intermittent basis, utilizing a pneumatic or hydraulic cylinder as a "pusher," or on a continuous basis by means of a pinch wheel or pinch chain arrangement (Figure 7.156). The most common induction billet heaters installed in forge shops throughout the world today employ pinch drive systems.

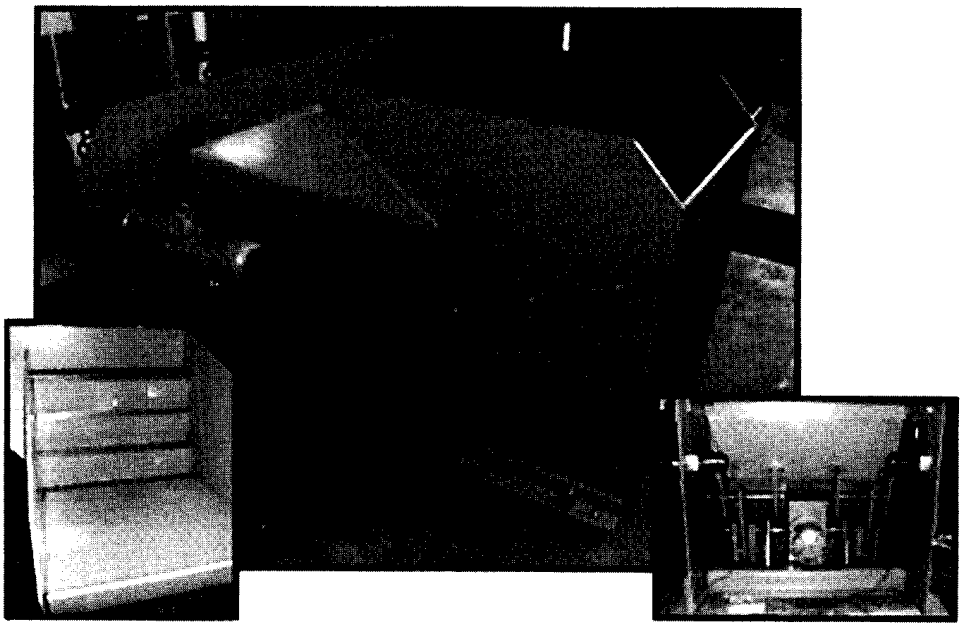

Figure 7.155 Step feeder.

Although this is certainly not a new concept and in fact has been established for many years, innovation has continued to the extent that the most up-to-date drives are extremely compact and capable of pushing very long and heavy columns of billet. For example, performance information for some standard drive units available from Radyne Ltd. (UK) is given in Table 7.15.

An additional feature that can be supplied to provide automatic adjustment on many standard pinch wheel drive assemblies is a pneumatic cylinder for adjusting the

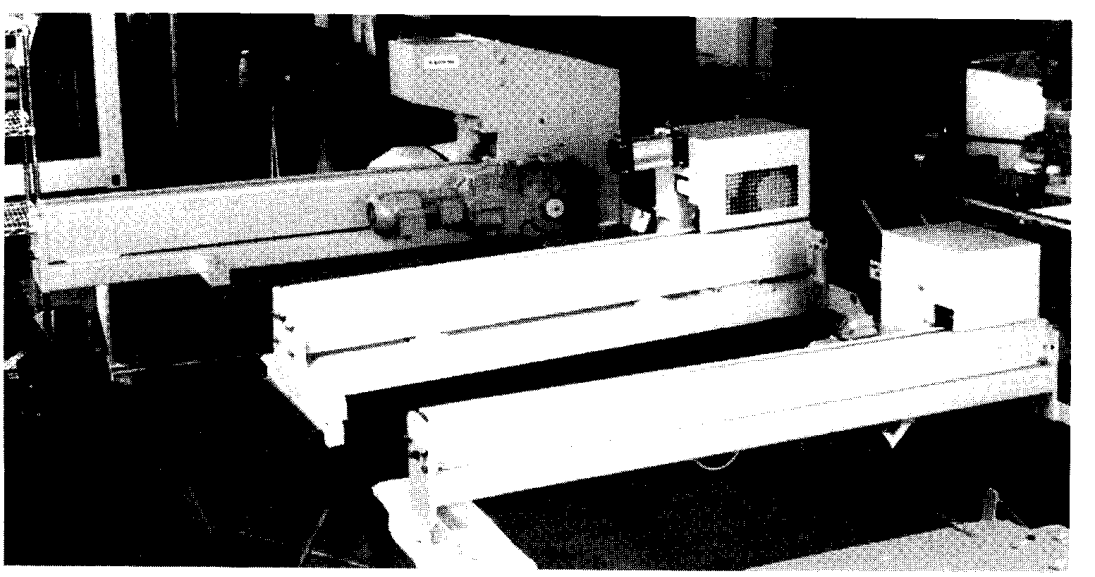

Figure 7.156 Radyne's ICF150, 385, 750 drive units.

Table 7.15 Radyne Ltd. Drive Unit Performance

Drive Unit	Max./Min. Billet Section, RCS and Diameter, mm (in.)	Max. Coil Length, m (ft)
ICF 150	10–65 (0.4–2.6)	2 (6.6)
ICF 385	20–102 (0.8–4)	3 (9.8)
ICF 750	45–152 (1.8–6)	6 (19.7)
ICF 750S	45–135 (1.8–5.3)	9 (29.5)
ICF 1500[a]	75–225 (3–8.9)	12 (39.4)

[a]See Figure 7.156.

position of the top wheel. The cylinder air pressure ensures that sufficient downward force is applied to the billets. This allows automatic adjustment of the top wheel over the full range of billet sections with which the machine has been supplied for processing.

This feature when integrated with an appropriate control system allows pre-stored information to be recalled so that power, speed, and billet section can be selected from the control panel menu system. This avoids the need for manual adjustment of the drive system when heating different billet sections. The ICF750 drive unit is shown with covers removed in Figure 7.157.

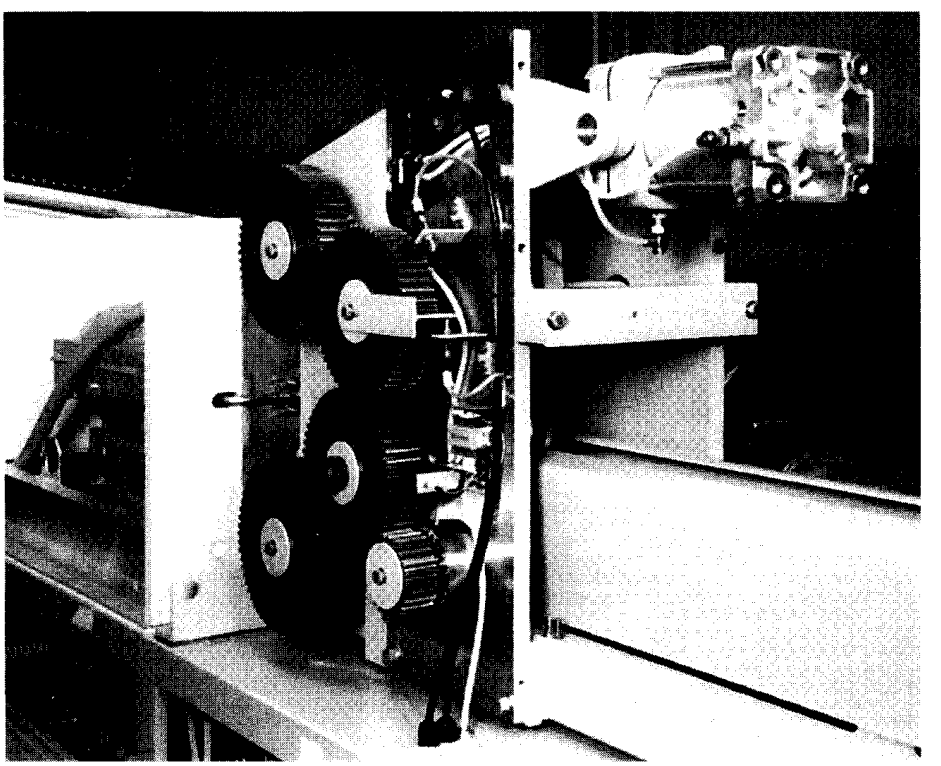

Figure 7.157 Radyne's ICF750 shown with the covers removed.

Figure 7.158 shows an alternative approach. The large continuous billet pusher gives a positive feed over a range of billet cross-sections and eliminates slippage [438].

The inability to forge all billets that are heated in the coil line and the difficulty of emptying the billet heater after a run are sometimes cited as disadvantages of continuous-feed billet heaters. A different cost-effective solution to solve these problems has been developed by suppliers of induction heating machinery. One of these approaches applicable to large continuous-feed billet heaters provides an appropriate number of specially designed beam sections. These sections have a combined length greater then the heaters' total coil length. The beam sections are designed to have the required mechanical strength to push a column of billets, while having sections which do not significantly heat when placed inside the induction coil. By using relatively short lengths, the beam sections are easily handled and intermediate sections interlock with each other to form a single continuous beam.

At the end of a production run the beam is simply fed into the billet heater in place of the billets with each section being manually interlocked with the preceding section as the heater continues to process the billets through the coil. When the final billet exits the coil, the heater is stopped, leaving the beam inside the coil. The manual control is then used to drive the beam until it is in the extractor [400–402].

The drive is then disconnected and the extractor is manually operated to pull the beam sections through the coil. When each section is completely clear of the extractor it is manually removed and the process repeated until the coil is completely empty. An example of the beam empty-out system in use is shown in Figure 7.159.

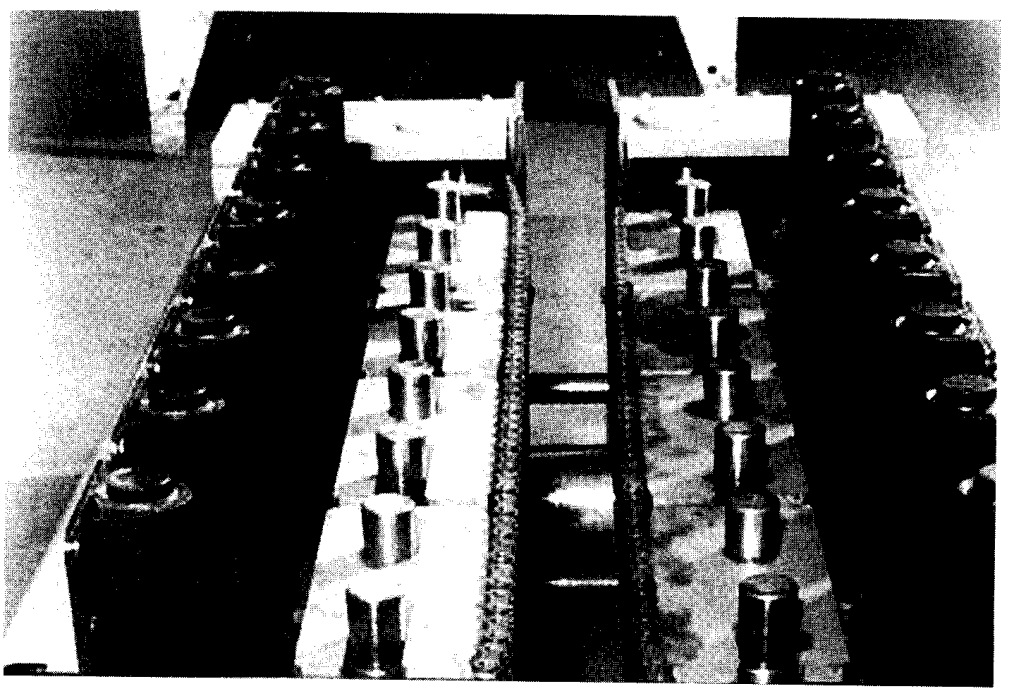

Figure 7.158 Large continuous billet pusher gives positive feed over range of billet. (Courtesy of Newelco Ltd., Wales, UK.)

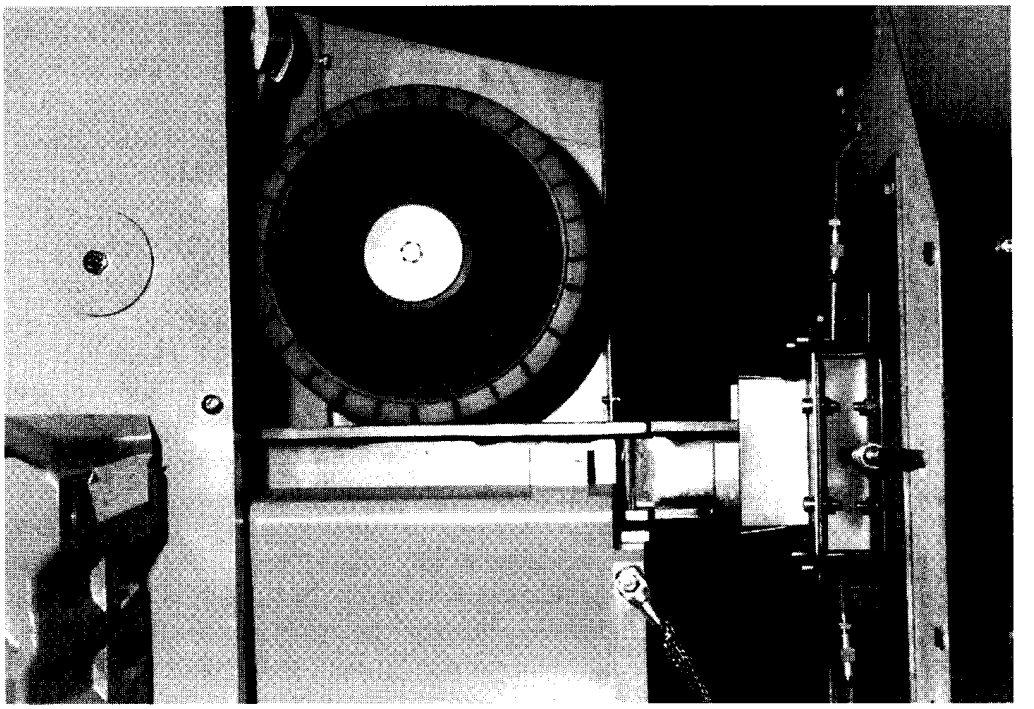

Figure 7.159 "Beam" empty-out system (Courtesy of Radyne Corp.)

Continuous-feed chain drive systems are also a popular choice when designing material handling machinery. Some of the new designs will automatically accept round and square billets with 25 to 150 mm cross-sections, and are capable of pushing a total billet load of up to 800 kg, which equates to a column length of 4.5 m for 150 mm square billets. Figure 7.160 shows a unique chain drive system and an empty-out system manufactured by Newelco (Wales, UK).

The variable-speed billet drive assembly is used to convey billets through the induction coils of the heater at a predetermined speed. The unit consists of the chain drive assembly as a pusher, a storage conveyor, and a reduction gearbox/electric motor.

The reduction gearbox/electric motor may be either an AC thyristor controlled unit or a DC solid-state controlled unit mounted upon a drive base plate. The output shaft of the reduction gearbox is fitted with two sprockets: the first is used to drive the storage conveyor and the other one drives the pusher via simple chain drives. The chain drive to the conveyor is fitted with a tensioner, whereas the tensioning of the pusher chain drive is by adjustment of the drive base plate.

The chain pusher consists of two endless triplex chain mechanisms, mounted horizontally, face to face, one above the other. A common drive shaft is used to drive the upper and lower chain mechanisms simultaneously. The lower chain mechanism is fixed and incorporates the common drive shaft, with the upper chain mechanism being adjustable. The upper chain mechanism has a pneumatic cylinder attached, which is fully retracted upon startup and automatically clamps the billets upon detection.

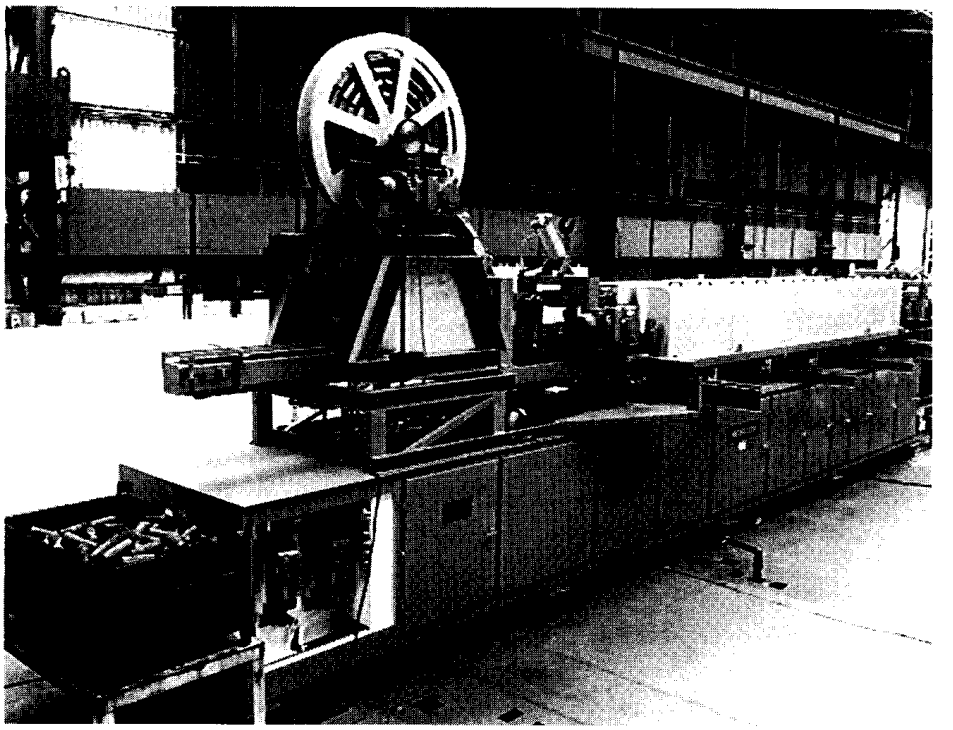

Figure 7.160 Advanced chain drive empty-out system. (Courtesy of Newelco Ltd., Wales, UK.)

To ensure that positive clamping of the billets takes place, and to allow for minor tolerances and distortion of the billets, compression springs and pressure plates are provided within the upper chain mechanism. The lower chain mechanism uses the rollers of the chain to run on hardened wear strips. This ensures that each billet is firmly gripped by the chains and that a positive forward movement takes place. These springs are tension-loaded during the assembly of the chain pusher and should not normally require further adjustment [438].

The storage conveyor consists of an endless triplex chain, which is driven via its drive chain and sprockets from the output shaft of the gearbox. This is arranged so that the storage conveyor is traveling between 1.5 and 2 times faster than the pusher, thus ensuring that the billets are always kept close together in the pusher, thereby avoiding gaps in the steel column being fed into the coils. The endless chain runs on mild steel wear plates and is tensioned by means of two tensioning bolts at the input end of the conveyor.

Whichever drive unit is fitted, the system comes with a speed indicator and speed controls mounted on the heater control panel. The speed indicator will be set during commissioning and if further adjustment is needed to compensate for subsequent errors. When a DC drive is fitted, a tachometer is used to feed back to the controller.

If an oversized or badly distorted billet should be presented to the chain pusher or if the billets should become jammed within the induction coils, an increased torque will be required. With the electronic drive control systems, the method of detecting excessive force buildup within the pusher is by an over-current method

incorporated in the drive electronics. Feedback sensors detect the rate of rise of current and this is set prior to a limiting point. The detector of this increased current switches off the drive and the medium frequency power as in the hydraulic drive method. A lost-motion detector is also provided. Figure 7.161 shows a close-up view of the chain drive system and an empty-out system.

The billet-emptying device is used to clear billets from the pusher and coils. The coil-emptying equipment is positioned above the billet storage conveyor and is integrated into the variable-speed drive unit.

The billet-emptying device is used in conjunction with a modified billet storage conveyor. A chain pusher with pneumatic adjustment is positioned at the front of the billet storage conveyor. The guide rails of the pusher and storage conveyor are split to prevent closure of the rails into the emptying device.

The billet-emptying device consists of a large wheel with specially designed stainless steel links to simulate billets that would pass through the heater. During normal production the links are wrapped around the wheel and held in position with a pneumatically operated safety brake. The links are also lifted off the storage conveyor with a pneumatically operated pinch roll.

During operation of the emptying system, the pneumatic pinch roll drives the links forward on the storage conveyor and under the chain pusher. To enable this to happen the safety brake is released and the wheel is free to turn; to prevent the wheel uncoiling under the weight of the links, a pneumatic resistance brake is applied to the wheel to maintain a constant withdrawal of the links [438].

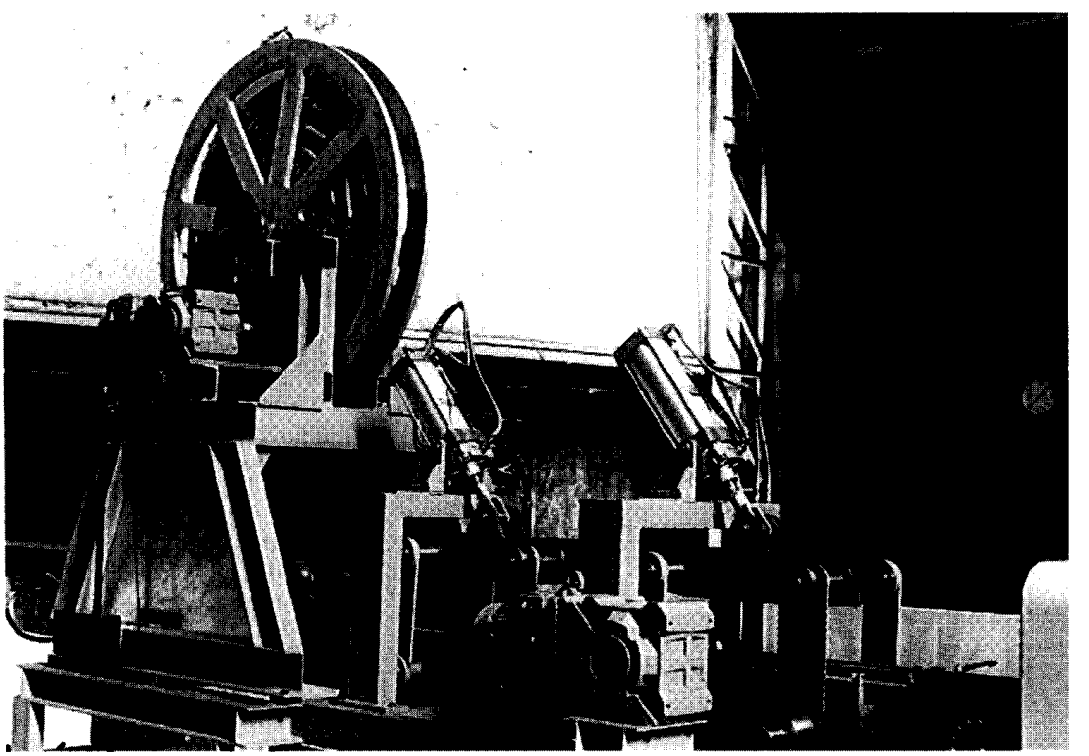

Figure 7.161 Close-up view of chain drive system and empty-out system. (Courtesy of Newelco Ltd., Wales, UK.)

When the links have been withdrawn to their designated position from the wheel, an AC thyristor controlled geared motor winds the links back.

The billets extractor is another important part of the billet handling system. Historically, extractor units were simply a means of delivering the heated billet to the forge press as quickly as possible to minimize heat loss.

The design of one of the popular billet extractor approaches is based on a pair of continuously running pinch rollers [400–402]. The lower roller is fixed at just over the billet base height. The upper roller is normally set at the top of the billet height; when the billet is detected the top roller is pneumatically powered down onto the billet. The extracted billet then is delivered onto a simple chain conveyor for final delivery to the forging press.

Where there is a quality assurance requirement, the billet temperature is monitored at the extraction stage to determine its suitability for the next operation (e.g., forging). If the preset requirements are met, the billet proceeds unimpeded to the forging press position. Out-of-specification or not-required billets are separated into a reusable bin for undertemperature and not-required billets or scrap bin for any overtemperature billets. The increasing use of better and more sophisticated pyrometers combined with modern computer-based temperature profiling of coils and the monitoring of temperatures along the coil has made this system increasingly reliable.

The reject signals from the PLC system are used to activate pneumatically operated diverters, which deflect the billets from the extractor conveyor via heavy duty plate chutes into the appropriate reject bin. A photo of a hot end reject system is shown in Figure 7.162.

7.10.2 Handling of Long Bars, Rods, and Tubes

In most induction heating systems the parts to be heated are delivered from an inline input conveyor, transfer mechanism, or automatic sorting hopper such as a bowl feeder or elevator conveyor-type feeder. As an example, Figure 7.163 shows an automatic bar handling system feeding a 6000 kW continuous induction bar heater.

Bar heaters are often fed with a bundle unscrambler, which sorts the bars and loads them one behind the other on an input conveyor. An alternative approach is to deliver parts to the induction heater by insertion from a transverse conveyor that indexes the parts across the axis of the heater.

Bar heaters are well suited for high-production type operations such as roll formers or other forming operations that can work directly from the hot bar or may be hot sheared into smaller length billets for use in automated hammers or presses.

Typically an unscrambler is combined with a feed conveyor to provide the bars in the correct orientation and at the correct speed for the coil line. Even the infeed portion from the scrambler to the coil line must be designed for a hot stock condition in the event that a hot bar must be backed out of the coil line and into the infeed reject bin.

The bar must proceed at a controlled speed through the induction heating coils in order to provide the correct surface temperature and surface-to-core differential temperature. When the bar arrives from the unscrambler, control of the bar speed transfers over to the induction heater and the infeed conveyor may slip on the part since it is running at a speed slightly faster than the induction heater in order to avoid any gaps in the bars being heated.

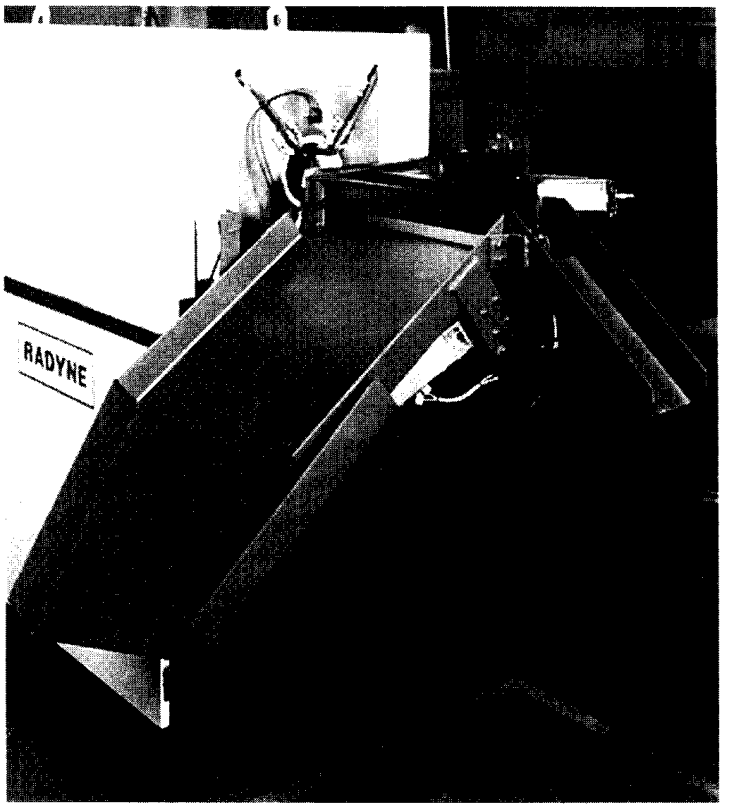

Figure 7.162 Hot end reject system.

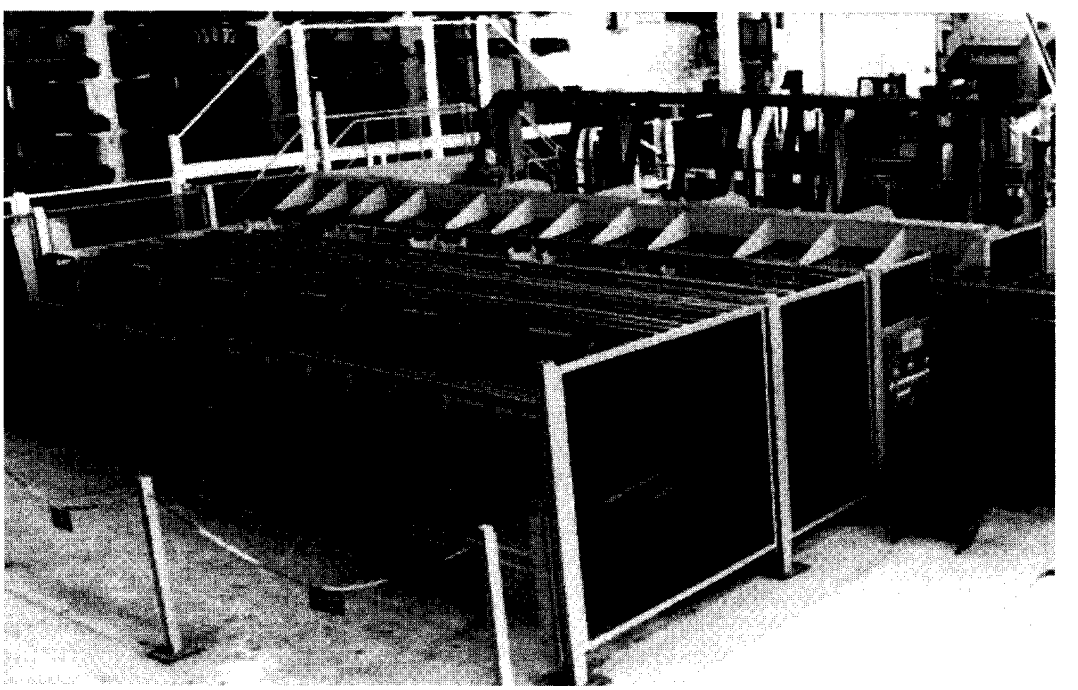

Figure 7.163 Newelco automatic bar handling system feeding a 6000 kW continuous induction bar heater.

If the drive speeds are not properly synchronized, significant gaps can exist from one bar to the following bar resulting in noticeable temperature differences at the bar ends. Bar ends may be under- or overheated depending on the bar geometry, type of heated metal, frequency, and power density used to heat the bar (Sec. 7.2.3).

Obviously any slowdown or stoppage of the material during the heating process can result in overheating and/or melting of the bar inside the heating coil. In order to prevent this from occurring, a motion-detecting wheel is often used to ride on the part during feeding of the bar through the coil line. The wheel has a number of holes drilled around its circumference and is fitted with a proximity switch to detect the motion of the wheel. If a stoppage of the wheel is detected, the power to the coil is turned off until the problem is corrected and normal line speed is resumed.

Parts typically ride on V-rolls rather than sliding on rails, as in the case of a billet heater (Figure 7.164). The V-rolls can accommodate round or RCS stock. The rolls are usually water-cooled in order to continually convey hot bar stock through the coil line. The upper roll may be pneumatically adjusted to allow entry of a new bar before the roller is pinched down on the bar. Wear rails are generally not required for bar heating lines as the bars are supported on the V-rolls rather than being pushed along the rails mounted in the heating coil.

It is sometimes necessary to reverse the direction of the bar drive system to allow oscillating a bar back and forth within the heating coils if delays occur in the forging process ahead. This may also be useful if problems occur in the feed process and bars must be removed from the entrance end of the coil line rather than simply passing them through the line.

On very long bar lines the drive systems may be either mechanically geared or electrically connected to ensure that the roll speed is synchronized for the correct feed rate. Bar handling systems consume a considerable amount of floor space in order to accommodate the full length of the bar at the infeed, in the coil line, and at the exit end of the system [410].

7.10.3 Slab, Plate, and Transfer Bar Handling

The heating of slabs for subsequent rolling operations presents a number of challenges due to the massive size of the metal to be transported and heated. Slabs may vary in length from 3 to 9 m and in width from 0.5 to 2.3 m (1.6 to 7.5 ft.). They may be from 25 to 300 mm (1 to 11.8 in.) thick and weigh more than 12,000 kg.

Slabs are conveyed on water-cooled rollers (Figure 2.46) that allow enough space between the rollers for installation of the heating coils. Because the clearance is relatively small, the location of the slab must be carefully controlled as it passes through the coil line in order to prevent damage to the refractory in either the vertical or horizontal direction.

Slabs may be heated in either a horizontal or vertical orientation depending on the geometry of the slab, application, and customer's preference.

It is also very important in slab heating to control the vertical orientation and shape of the slab as it enters and exits the induction heating coil. A 1 in. thick (25.4 mm) transfer bar could have as much as a 100 mm (4 in.) bend at the ends. This phenomenon is called ski-shaped, boat-shaped, or simply bowing, and could cause major damage to the heating coil. For this reason the guide rollers are used to prevent coil damage.

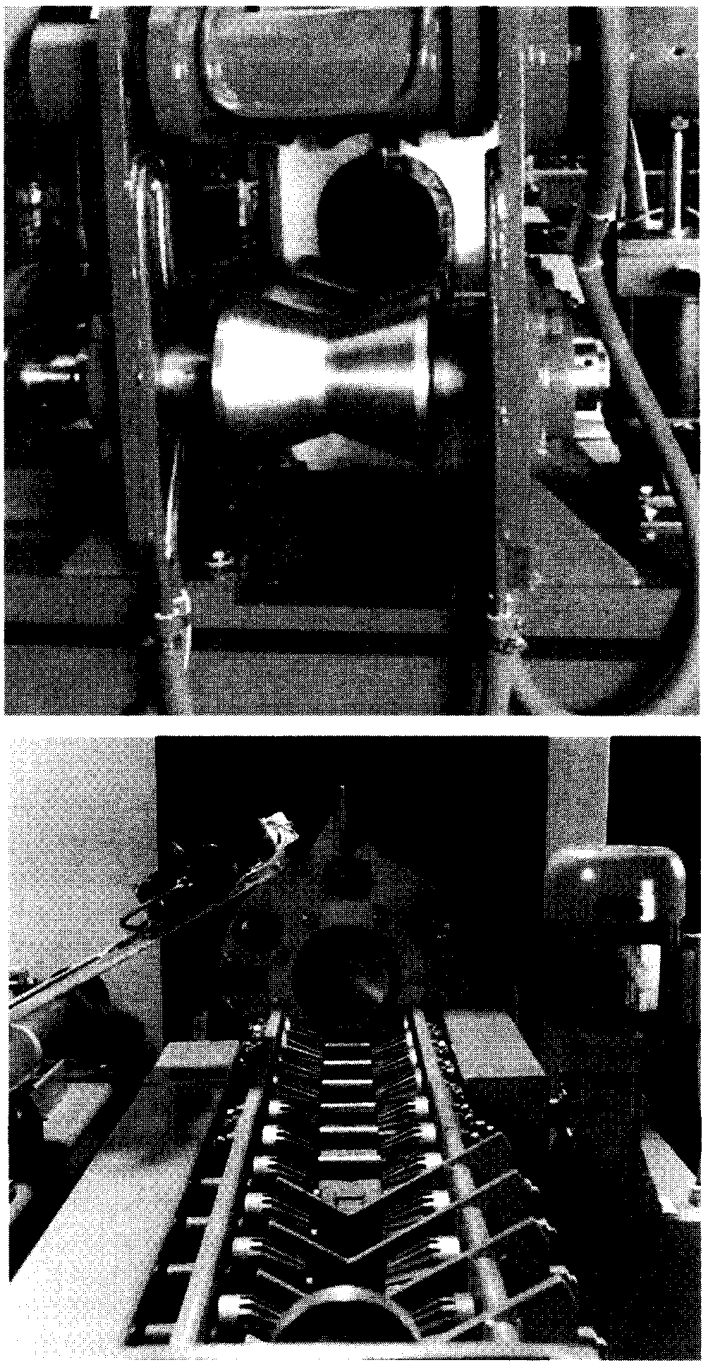

Figure 7.164 V-rolls used to support bars and billets for fast extractors and to transfer them between coils

If this bowing of the slab is not controlled, the coil opening must be greatly increased to prevent mechanical damage to the coil. This results in a noticeable reduction of coil efficiency and, therefore, a drastic increase in the required power to accomplish the heating of the slab or transfer bar. In slab heating applications the

required powers are measured in the range of megawatts, and thus even a slight coil efficiency reduction results in a marked waste of energy.

Care must also be exercised in handling short slabs or plates that may not be fully supported from one roller to the next. In these cases the use of short coils in combination with an extra support or using special guides may be required to assist the main mill rollers.

AC or DC drive systems must be adequately sized to transport the weight of the slab, but also protected to prevent large-scale damage to the system in the event that the slab becomes dislocated and the drive pushes the slab into the coil or part of the conveyor system.

Slab heating systems usually require very large amounts of power to accomplish the heating. Care must be taken in the system design to prevent the drive system and supporting framework from being affected by electrical noise or induction heating by an external magnetic field. The induction heating system of the world's largest carbon steel slab shown in Figure 7.118 utilized a total power of 42 megawatts. The system comprises seven coils of six Megawatts each. The Inductotherm Corp. has developed specially designed patented magnetic shunts for a dramatic reduction of the external magnetic field outside the coils. Actual field measurement indicated 20 microtesla at a 0.3 m range from the induction coil [275].

8

Power Supplies for Modern Induction Heating

Induction heating power supplies are frequency changers that convert the available utility line frequency power to single-phase power at a frequency appropriate for the induction heating process. They are often referred to as converters, inverters, or oscillators, but they are generally a combination of these. The converter portion of the power supply converts the line frequency alternating current input to direct current and the inverter or oscillator portion changes the direct current to single-phase alternating current of the required heating frequency.

8.1 POWER–FREQUENCY COMBINATIONS

Many different power supply types and models are available to meet the heating requirements of a nearly endless variety of induction heating applications [248, 320–329]. The specific application will dictate the frequency, power level, and other inductor parameters such as coil voltage, current, and power factor or Q. Figure 8.1 illustrates this power versus frequency relationship for common induction heat treating applications. Figure 8.2 illustrates this same relationship for induction heating prior to metal forming operations.

For purposes of efficient communication it is best to refer as needed to the glossary of terms found in Chapter 10. There you will find terms commonly used by induction heat treatment specialists that may be encountered in this section.

Frequency is a very important parameter in induction heat treatment because it is the primary control over the depth of current penetration as discussed in detail in Section 3.1. Frequency is also important in the design of induction heating power supplies because the power components must be rated for operation at the specified frequency. The power circuit must ensure that these components are operated with an adequate margin to yield high reliability at this frequency.

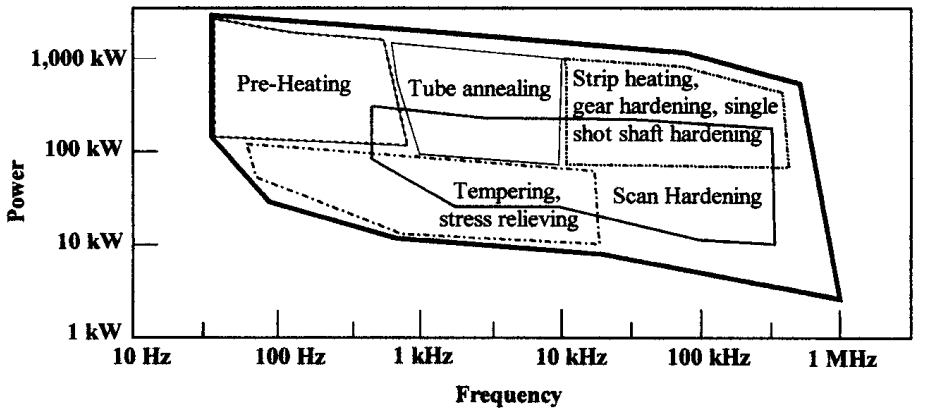

Figure 8.1 Power–frequency diagram for typical induction heat treating applications.

8.2 ELEMENTS OF POWER ELECTRONICS

To gain a fundamental understanding of the various induction heating power supply circuits it is first necessary to know the function of the power electronic components that are commonly used. These components include resistors, inductors, capacitors, transformers, and power semiconductors.

For those with little or no knowledge of electronics, a mechanical analogy may be helpful. Resistance is like friction in that it dissipates energy and creates heat. Inductance is like the inertia of a flywheel as it stores energy and opposes change. Capacitance is like a mechanical spring that stores energy while promoting change. When inductors, capacitors, and resistor are connected as shown in Figure 8.3A, a resonant circuit is formed that tends to oscillate at a single frequency determined by the value of the components. In like manner, when a flywheel mounted on a shaft with a bearing is mechanically connected to a spring as illustrated in Figure 8.3B it too will

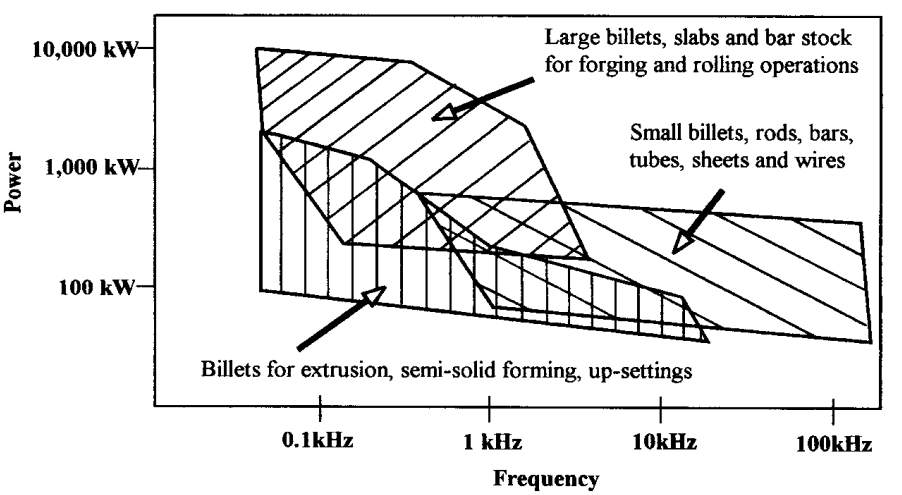

Figure 8.2 Power–frequency diagram for typical induction heating prior to metal forming operations.

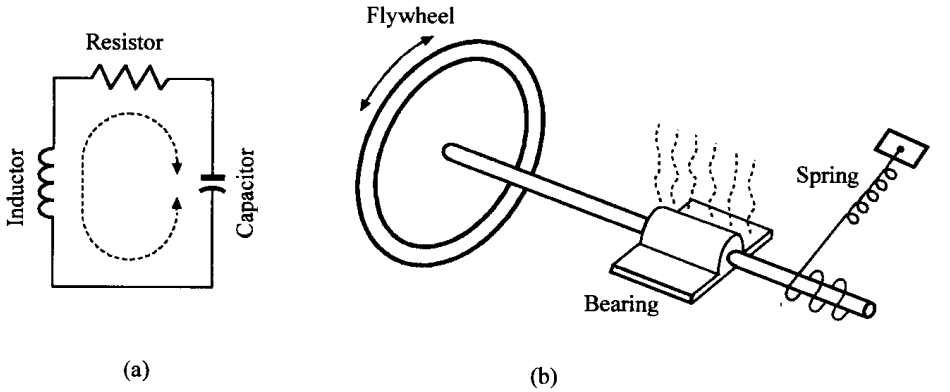

Figure 8.3 Resonant circuit and a mechanical analogy.

oscillate at a natural resonant frequency. The frequency of this oscillation is determined by the size of the flywheel and the spring. The friction of the bearing on the shaft will damp the oscillation and in the process produce heat, just as the resistance in the electrical circuit damps the oscillation and in the process develops heat.

A mechanical analogy can also be used to explain the function of a transformer as illustrated in Figure 8.4. In a mechanical system a gearbox is used to match the speed and torque requirements of two portions of the system. In an electrical system a transformer is used to match the impedance of two portions of a circuit. This means that a transformer can reduce voltage and increase current or alternately increase voltage and decrease current while maintaining the same volt amp product on both the input and output sides of the transformer.

8.2.1 Inductors

Most modern induction heating power supplies are of the "load resonant" type. This means that the inductive and resistive portion of the power supply circuit is actually provided by the induction heating coil and the resistance of the workpiece being induction heated. The geometry of this coil, which is usually dictated by the induction heating application, determines the value of circuit inductance and resistance.

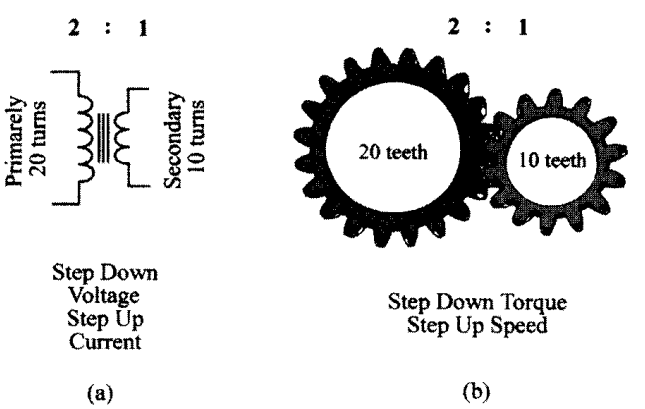

Figure 8.4 A mechanical analogy can be used to explain the function of a transformer.

The specific design and resulting parameters of various induction heating coils are covered in detail in Chapter 5.

8.2.2 Capacitors

Power capacitors used in induction heating equipment must be capable of withstanding high voltage while carrying high current at the induction heating frequency. These capacitors come in a variety of sizes and shapes as shown in Figure 8.5. Most are water-cooled and packaged in an aluminum case with large studs for power connection to bus bars. It is important that these capacitors be designed to have very low values of internal resistance and inductance to minimize power loss within the capacitor.

8.2.3 Vacuum Tubes and Power Semiconductors

Very early power supplies used high-power vacuum tubes in an oscillator circuit to generate the radio frequency that was used for induction heating. Modern induction heating power supplies utilize power semiconductors such as SCRs, diodes, and transistors to switch the direction of current flow from a direct current source to produce alternating current at a frequency suitable for induction heating. A simple explanation of what these power semiconductors do might be helpful for readers with little or no electronics background. These devices (often referred to by their

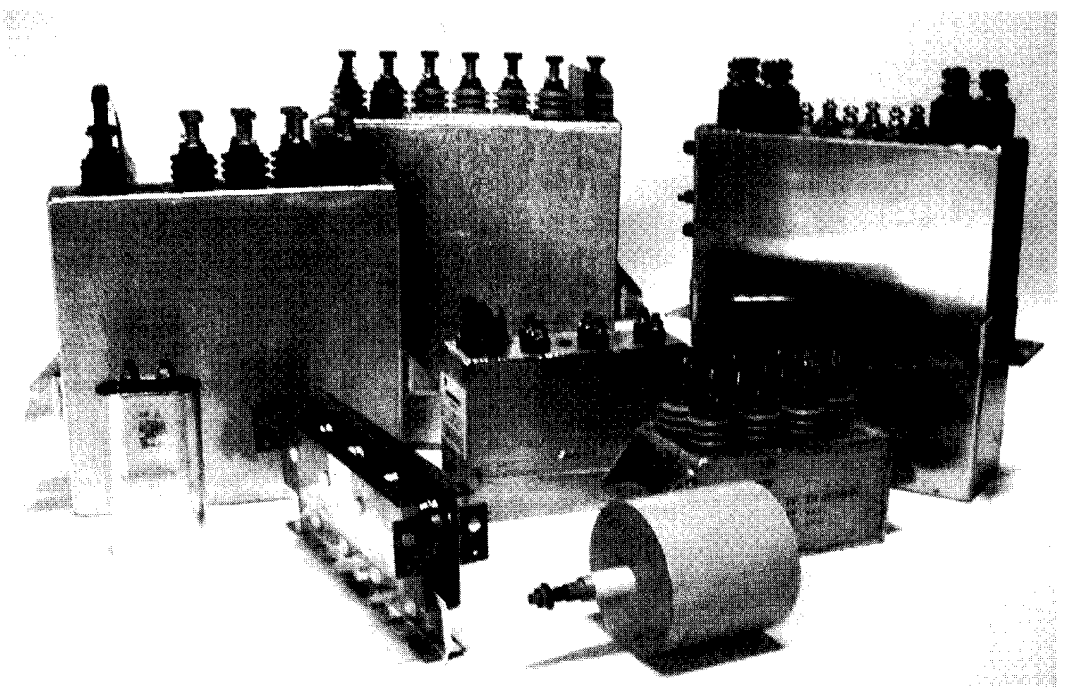

Figure 8.5 Power capacitors used in induction heating equipment come in a variety of sizes and shapes.

initials) are switches that open and close to control electric current much the same as a gate or door controls passage from one area to another.

8.2.3.1 SCR or Thyristor

The SCR (silicon controlled rectifier) or thyristor is like a gate with a simple latch that will only swing one way to open. If the gate is pushed in the opening direction and the latch is not released the gate remains closed and no one is allowed to pass through it. This is like an SCR when it is "OFF" or, in electronic terms, forward blocking. As soon as the gatekeeper releases the latch, the gate swings open and people begin to pass through to the other side. This is like the SCR when it receives a trigger pulse from the control circuitry and begins to turn "ON" and conduct current. If the people turn around and begin to push on the other side of the gate, it swings closed and latches, thus preventing passage in either direction. When the voltage reverses on an SCR it turns off and blocks current flow in the forward direction as well as the reverse direction. The symbol of the SCR and its waveshapes are shown in Figure 8.6.

8.2.3.2 Diode or Rectifier

The diode is the simplest power semiconductor. It is like a gate without a latch that only swings open one way. If pushed in one direction it opens allowing passage in that direction. If pushed in the opposite direction, it swings closed preventing passage in the reverse direction. When voltage is applied to a diode in the forward direction it will conduct current. When the voltage is reversed the diode begins to block the flow of current. The symbol of the diode and its waveshapes are shown in Figure 8.7.

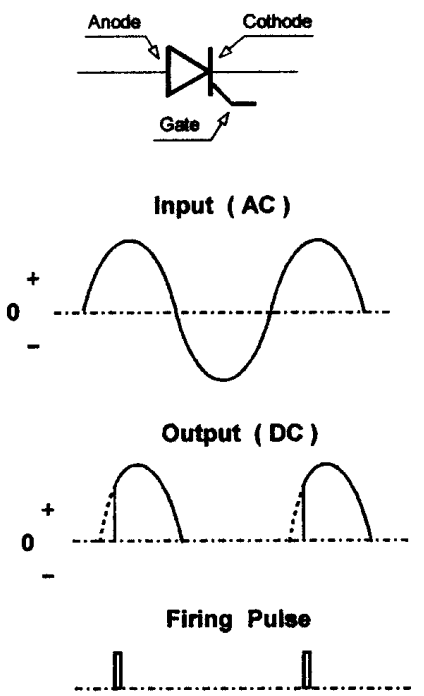

Figure 8.6 Symbol and waveshapes of thyristor.

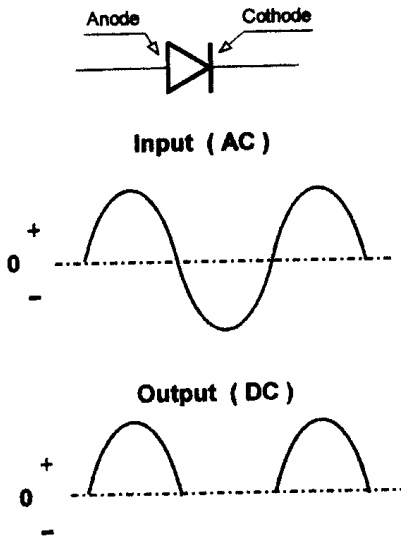

Figure 8.7 Symbol and waveshapes of diode.

8.2.3.3 Transistors

Transistors are a bit more complicated. They are like a one-way gate that is opened and closed by a gatekeeper. Imagine the gate to be actuated by a hydraulic cylinder controlled by a small valve that is easily switched by the gatekeeper. The small amount of force required by the gatekeeper to control the force of people pushing to get through the gate is like the electronic gain of the transistor. The force with which the people push against the closed gate is like the voltage applied to the transistor. The size of the gate opening limits the rate at which people can pass through to the other side, just as the size of the transistor limits the maximum current it can conduct.

For a transistor to be useful in an induction heating application it must (1) block high voltage, (2) carry high current, and (3) switch ON and OFF very quickly. In terms of the above analogy, the gate must be (1) strong (made of iron), (2) large in opening, and (3) still be able to open and close very quickly. To build a gate with one or two of these requirements is not a problem. To provide all three in one design is quite difficult. Large strong gates are difficult to open and close quickly. Large gates that move quickly must be light and are therefore not strong, and so on. The symbol and waveshapes for transistors are shown in Figure 8.8.

a. *MOSFET.* The MOSFET (metal oxide silicon field effect transistor) technology has provided one solution to this problem: a power transistor with relatively high voltage, high current, and very fast switching speeds. This is accomplished by placing thousands of very small, fast transistors that are all connected in parallel on a single chip of silicon, measuring about $\frac{1}{4}$in. on a side. As in the analogy, this is like having many small, strong, and rapid gates placed side by side to provide a wide section that can be quickly opened and closed. Larger MOSFET transistor modules combine many of these chips connected in parallel on a common mounting base.

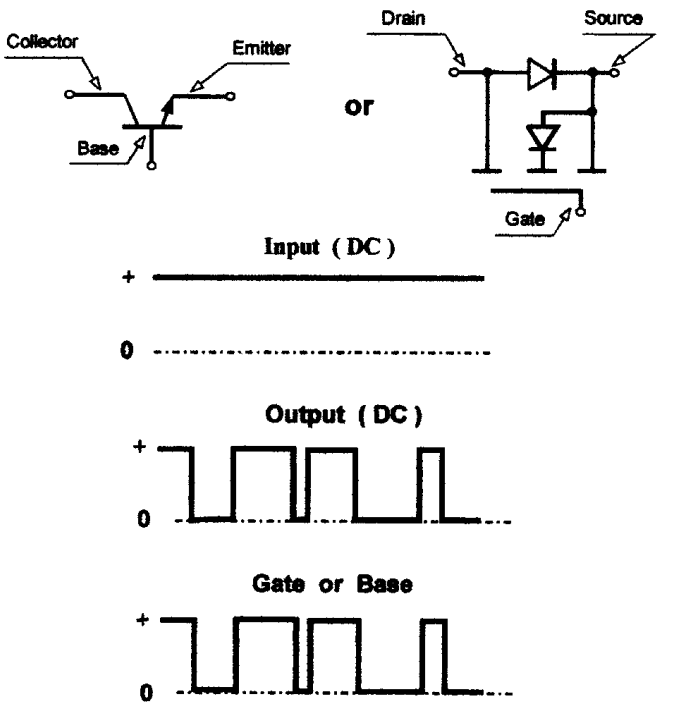

Figure 8.8 Symbol and waveshapes of transistor.

b. *IGBT.* In the IGBT (insulated gate bipolar transistor) two transistor technologies are combined to obtain high voltage, high current, and fast switching speeds. Bipolar transistors capable of handling relatively high voltage and high current have been available since about 1970 but are slow switching and require relatively high-power control signals. Small low-power MOSFET transistors with very fast switching speed and low-power control requirements have also been around for many years. Put the two technologies together with the MOSFET (insulated gate technology) on the control end and the bipolar on the power handling end and you have the best of both in the IGBT.

Figure 8.9 shows a dual 300 amp IGBT module (top left) and a dual 50 amp MOSFET module (top right). Below each is a sample of the same module type with the cover removed to show the multiple chip construction.

c. *Transistor Assemblies for More Power.* To obtain the high-power usually required for induction heating many transistor modules are often connected on a single heat sink as shown in Figure 8.10.

The inverter circuits that convert direct current to alternating current use solid-state switching devices such as thyristors (SCRs) and transistors. For high-power and lower frequencies, large thyristors are commonly used. For frequencies above 10 kHz or for low-power, transistors are used because of their ability to be turned on and off very quickly with low switching losses.

8.2.3.4 Vacuum Tube Oscillators

Vacuum tube oscillators have been used extensively for many years at frequencies above 300 kHz. However, the tube oscillators have a low conversion efficiency of

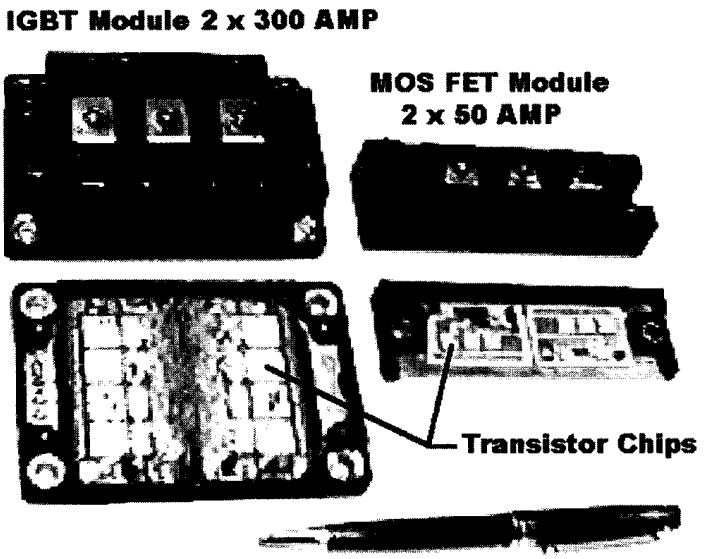

Figure 8.9 Dual 300 amp IGBT (top left) and dual 50 amp MOSFET module (top right).

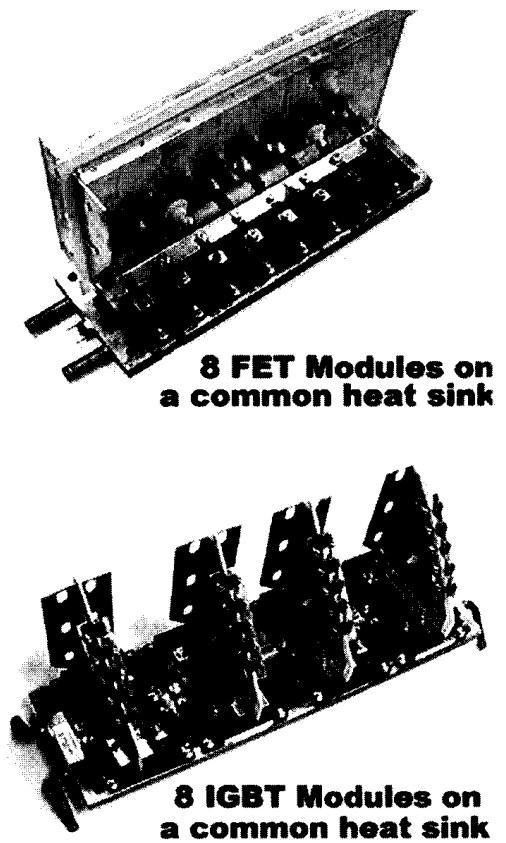

Figure 8.10 Multiple module assemblies.

typically 50 to 60% compared to 83 to 95% for an inverter using transistors. Power vacuum tubes have a useful life of 2000 to 4000 hours and are therefore a costly maintenance item. The high voltage (over 10,000 V) required for tube operation is more dangerous than the 1000 V or less present in typical transistorized inverters. These negative features of tube oscillators have brought about a dramatic move toward the use of transistorized power supplies in most heat treatment applications that require a frequency of less than 1 MHz.

8.2.3.5 Power–Frequency Application of Semiconductors and Vacuum Tubes

Figure 8.11 shows in graphical form the various power and frequency combinations that are covered by power supplies using thyristors, transistors, or vacuum tubes. There are obviously large areas of overlap where more than one type of power supply can be used.

8.3 TYPES OF INDUCTION HEATING POWER SUPPLIES

The power required for a given application depends on the volume and kind of metal to be heated, the rate of heating, and the efficiency of the heating process. Small areas heated to a shallow depth may require as little as 1 or 2 kW, whereas heating wide, fast-moving steel strips to temperatures above their Curie point may require many megawatts of induction heating power. It is, therefore, necessary to define the process and its power requirements by using the numerical techniques described in the computation section of Chapter 3 or by careful extrapolation from similar applications.

The geometry of the part and coil as well as the electrical properties of the material to be heated determine the specific coil voltage, current, and power factor. Defining these parameters is necessary to ensure that the output of the power supply is capable of matching the requirements of the coil. Most induction heating power supply systems have the ability to match a reasonable range of heating coil parameters.

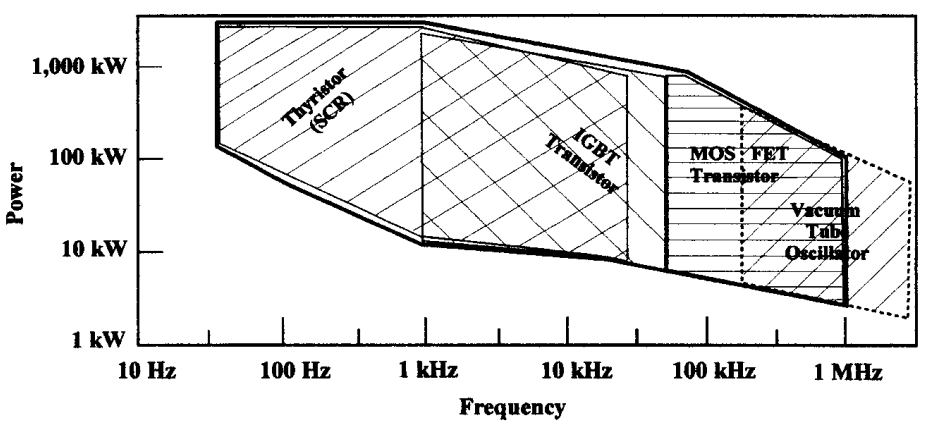

Figure 8.11 Power semiconductors used for induction heating.

Physical constraints imposed by the environment in which the induction heat treatment is to be done can also play an important part in the selection or application of the power supply. Each type of power supply, described in detail later in this section, has specific advantages that may directly affect its suitability in the overall induction heating system.

Floor space, machine design, and plant layout are important factors in many induction heat treatment installations. For example, in highly automated machines with a number of hardening and tempering stations, the very compact unitized construction of a transistor-based power supply with self-contained load-matching transformer and capacitors is a definite advantage. On the other hand, for installations requiring a long distance between the power supply and the work coil, the heat station or load-matching portion should be separated from the rest of the power supply and located at the work coil.

Many books and technical papers have been written about the detailed design and theory of operation of the various types of induction heating power supplies [320–322, 343, 353–355]. Inclusion of such detail here would likely be of little help to those primarily involved only in the selection or use of these power supplies. Therefore, the following paragraphs only categorize the most commonly used power circuit and control combinations. This gives some insight into the advantages and disadvantages of modern induction heating power supplies and their applications and features.

A very basic block diagram that applies to nearly all induction heating power supplies is shown in Figure 8.12. The input is generally three-phase 50 or 60 Hz at a voltage between 220 and 575 V. The first block represents the AC to DC converter or rectifier. This section may provide a fixed DC voltage, a variable DC voltage, or a variable direct current. The second block represents the inverter or oscillator section, which switches the direct current to produce a single-phase AC output. The third block represents the load-matching components, which adapt the output of the inverter to the level required by the induction coil. The control section compares the output of the system to the command signal and adjusts the DC output of the converter, the phase or frequency of the inverter, or both to provide the desired heating.

Figure 8.13 shows the principal design features of the inverter configurations most commonly used in induction heating power supplies. The two major types are the voltage-fed and the current-fed. The chart further subdivides each of these by the

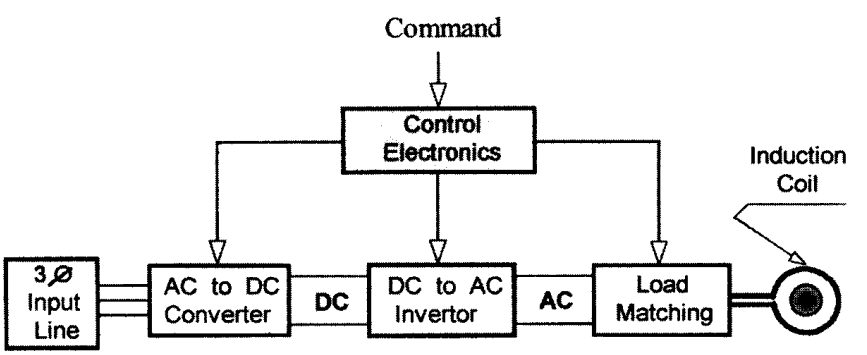

Figure 8.12 Induction heat treat power supply basic block diagram.

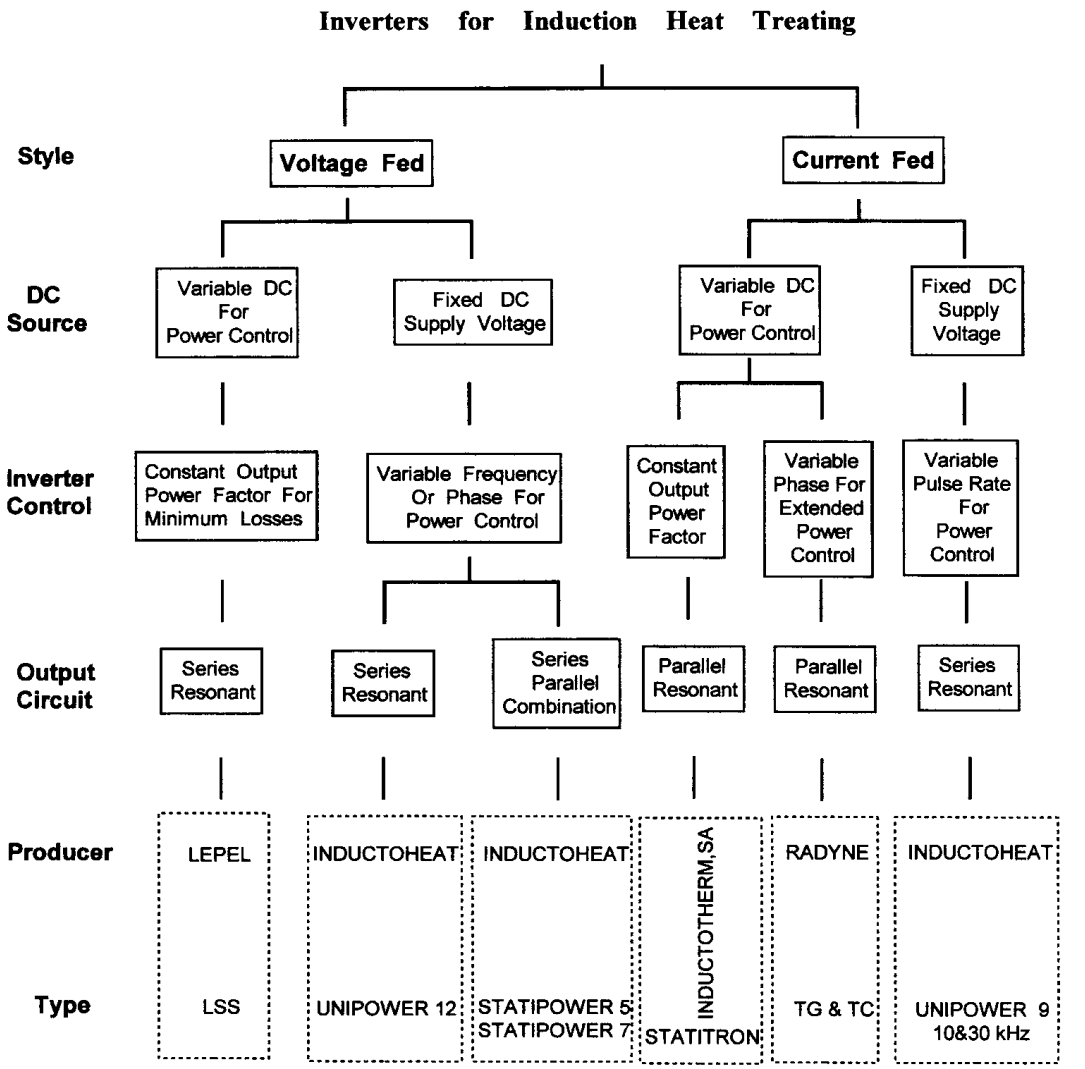

Figure 8.13 Induction heat treating inverters.

DC source (fixed or variable), the mode of inverter control, and the load circuit connection (series or parallel).

8.3.1 Rectifier or Converter Section

All of the power supplies outlined in the chart in Figure 8.13 have a converter section that converts the line frequency alternating current to direct current. [2, 3]. Nearly all induction heating power supplies use one of three basic converters. The simplest is the uncontrolled rectifier shown in Figure 8.14. The output voltage of this converter is a fixed value relative to the input line-to-line voltage, and the converter section provides no control of the output. The uncontrolled rectifier must therefore be used with an inverter section capable of regulating the power supply output.

The phase-controlled rectifier, shown in Figure 8.15, has thyristors that can be switched on in a manner that provides control of the DC output relative to the input

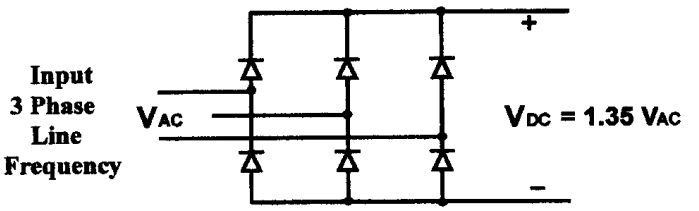

Figure 8.14 Uncontrolled rectifier.

line voltage. This relatively simple converter can be used to regulate the output power of the inverter by controlling the DC supply voltage. The circuit has some disadvantages. First, the input line power factor is reduced to values that are not acceptable to modern power quality specifications when the DC output voltage of the converter is less than maximum. (Sections 8.11 and 8.12 provide a detailed discussion of power quality issues.) Second, the control response time is necessarily slower because it is not able to respond faster than the frequency of the input line upon which it is acting. There are, however, schemes that require additional power components for alleviating both of these disadvantages [321, 351].

The third converter type has an uncontrolled rectifier followed by a switch mode regulator as shown in Figure 8.16. The switch mode regulator shown in the diagram is one of the simplest forms and is called a buck regulator [356]. The level of DC voltage or current at the output is regulated by rapidly switching the pass transistor on and off. The greater the ON-time/OFF-time ratio, the higher the output voltage or current. The converter can therefore regulate the output power of the inverter by controlling the supply of direct current. The input line power factor is the maximum at all power levels, and the response time can be very fast due to the relatively high switching rate of the buck regulator. Therefore, this converter overcomes the disadvantages of the simple controlled rectifier while being more complex, more costly, and slightly less efficient.

All the converters just discussed draw non-sine wave current from the input AC line. This means that there are harmonics or multiples of the line frequency present in the current waveshape. The harmonic distortion of the current waveshape can adversely affect supply transformers and other electronic equipment connected to the same line. In most heat treatment situations where the power supply rating is less than 600 kW and the plant power distribution system provides a low source impedance or "stiff line," a 6-pulse rectifier as described above is acceptable. For higher-power systems or where utility requirements require reduced harmonic content, a

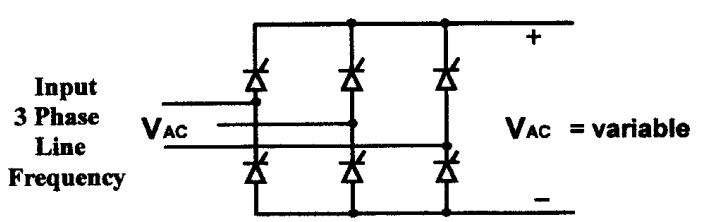

Figure 8.15 Phase-controlled rectifier.

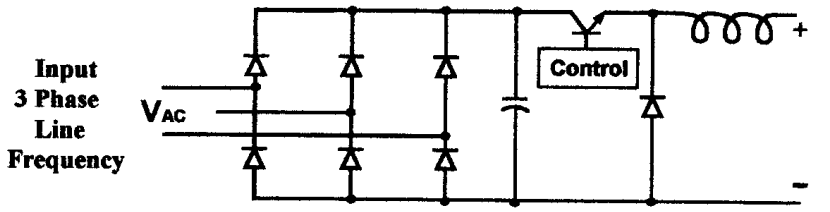

Figure 8.16 Uncontrolled rectifier with switch mode regulator.

12-pulse rectifier, which has a six-phase input and 12 rectifiers, can be used. The chart in Figure 8.17 compares the typical line current harmonics as a percentage of the fundamental for these rectifier configurations. As shown in the chart, the fifth and seventh harmonics are nearly eliminated in the 12-pulse case, resulting in a dramatic reduction of the total harmonic distortion of the line current. Use of higher pulse configurations such as 18 or 24 obviously leads to a further reduction but at considerable expense. Refer to Sections 8.11 and 8.12 for a more indepth discussion of line power quality including input power factor and harmonics.

8.3.2 Inverter Section

The inverter section of the power supply switches the direct current or voltage to produce a single-phase AC output. The two most common configurations are the full bridge and half bridge, which are used in both voltage-fed and current-fed inverters.

8.3.2.1 Full-Bridge Inverter

The most common inverter configuration is the full bridge as shown in Figure 8.18. Often referred to as an H bridge, it has four legs, each containing a switch. The output is located in the center of the H so that when switches S1 and S2 are closed, current flows from the DC supply through the output circuit from left to right. When switches S1 and S2 are opened and switches S3 and S4 are closed, the current flows in the opposite direction, from right to left. As this process is repeated, an alternating current is generated at a frequency determined by the rate at which the switches are opened and closed.

8.3.2.2 Half-Bridge Inverter

The half-bridge inverter, as its name implies, requires only two switches and two capacitors to provide a neutral connection for one side of the output circuit as shown

Inverter pulses	Order of harmonic							
	5th	7th	11th	13th	17th	19th	23rd	25th
6	17.5%	11%	4.5%	2.9%	1.5%	1%	0.9%	0.8%
12	2.6%	1.6%	4.5%	2.9%	0.2%	0.1%	0.9%	0.8%
24	2.6%	1.6%	0.7%	0.4%	0.2%	0.1%	0.9%	0.8%

Figure 8.17 Comparison of percentage of harmonics for 6-, 12-, and 24-pulse rectifiers as a percentage of the fundamental.

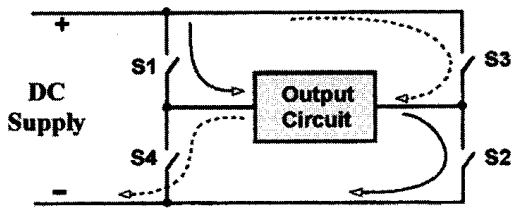

Figure 8.18 Basic full-bridge inverter

in Figure 8.19. The other side of the output circuit is then switched between the positive DC supply by S1 and the negative supply by S2, thus generating an AC voltage across the output. This configuration is used in place of the full bridge where lower output voltage or output power is desired.

8.3.2.3 Voltage-Fed Inverters with Simple Series Load

Voltage-fed inverters are distinguished by the use of a filter capacitor at the input of the inverter and a series-connected output circuit as shown in the simplified power circuit schematic of Figure 8.20. The voltage-fed inverter is used in induction heating to generate frequencies from 90 Hz to as high as 1 MHz. Thyristors or silicon-controlled rectifiers can be used to switch the current at frequencies below 10 kHz. Below 50 kHz, insulated gate bipolar transistors are commonly used. Above 50 kHz power, MOSFET transistors are usually chosen for their very fast switching speeds.

The voltage-fed inverter can be switched below resonance as illustrated by the bridge output voltage (Figure 8.21, trace 1) and the output current waveshape (trace 2). This must be the case when thyristor switches are used because diode conduction must follow thyristor conduction for sufficient time to allow the thyristor to turn off. This minimum turn-off time requirement limits the practical use of thyristors to frequencies below 10 kHz. The INDUCTOHEAT Statipower 6 is an example of this type of inverter [323].

Transistors do not require turn-off time and therefore can be operated at resonance as illustrated by the output current waveshape (Figure 8.21, trace 3). In this case, there is little or no diode conduction, and the transistor is switched while the current is at zero, thus minimizing switching losses and maximizing inverter power rating and efficiency. Operation at resonance means that the output power factor is unity and maximum power is being transferred from the DC source to the load. To regulate power in this case the DC supply voltage must be controlled. The LSS family of induction heating power supplies (produced by Lepel Corp.) is an

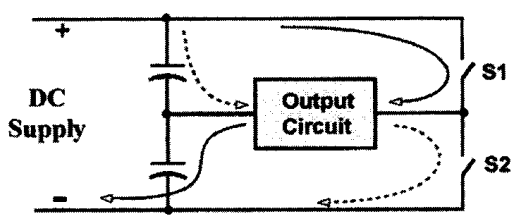

Figure 8.19 Basic half-bridge inverter.

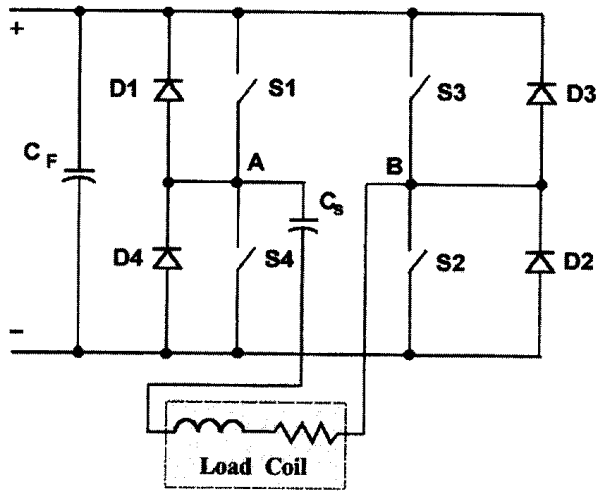

Figure 8.20 Voltage-fed series connected output.

example of this type; they are operated at resonance with power controlled by variable direct current supplied by a switch mode regulator [324].

Transistors can also be switched above resonance as illustrated in Figure 8.21, trace 4. In this case, the conducting switches (S3 and S4) are turned off prior to the

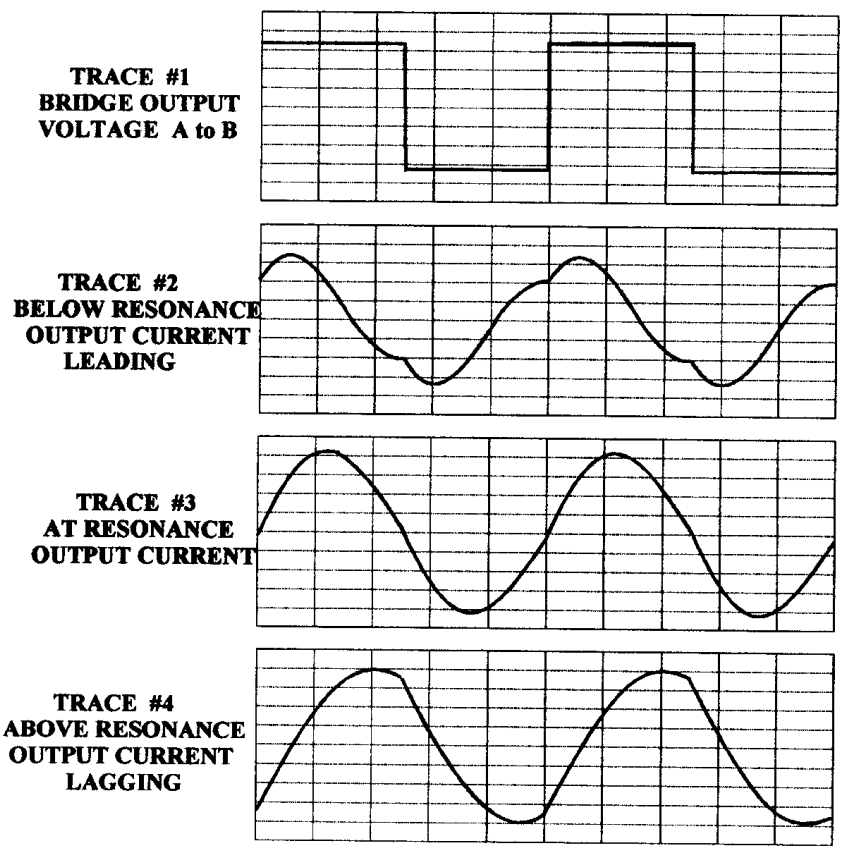

Figure 8.21 Voltage-fed inverter waveshapes with series connected output.

current reaching zero. This forces the current to flow in the diodes (D1 and D2) that are across the nonconducting switches (S1 and S2). These switches (S1 and S2) can then be turned on and will conduct as soon as the load current changes direction. This mode of operation minimizes transistor and diode switching losses while allowing the inverter to operate off resonance to regulate power. Control of inverter frequency relative to the natural resonant frequency of the load to regulate output power is discussed in Section 8.4.2.

The voltage-fed inverter supplies a square wave voltage at the output of the bridge, and the impedance of the load determines the current drawn through the bridge to the series load circuit. In nearly all heat treatment applications, an output transformer is required to step up the current available from the inverter to the higher level required by the induction heating coil. The secondary of this transformer is connected directly to the heating coil when the heating frequency is 30 kHz or less and the coil voltage is less than 250 V. In higher frequency applications where the coil voltage is necessarily greater, the series resonant capacitor is usually placed in the secondary circuit of the transformer and in series with the heating coil.

Figure 8.22 shows INDUCTOHEAT's portable induction heating power supply. This low-power (10 kW), high-frequency (20 to 40 kHz) unit is specifically designed for such heat treatment applications as preheating, soft soldering, brazing, shrink fitting, annealing, through hardening, and epoxy curing of small parts. Although capable of functioning as a low-power, inplace unit, the generator's small size and weight allow it to be hand-carried to wherever it is needed.

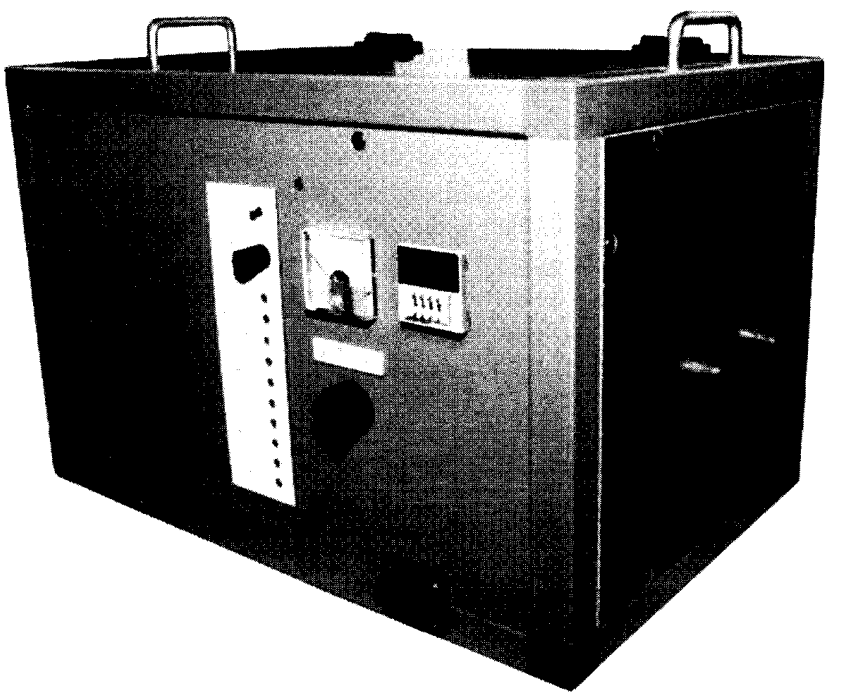

Figure 8.22 INDUCTOHEAT's portable benchtop induction power supply Unipower (5 to 10 kW/20 to 40 kHz) measures only 305 mm × 458 mm × 305 mm(12 in. × 18 in. × 12 in.)

The salient features of the voltage-fed inverter with a simple series resonant induction heating load are compared to those of the current-fed bridge inverter and summarized in Figure 8.23.

8.3.2.4 Voltage-Fed Inverter with Series Connection to a Parallel Load

A popular variation of the voltage-fed inverter for induction heating has an internal series-connected inductor and capacitor that couple power to a parallel resonant output or "tank" circuit as shown in Figure 8.24. The values of the internal series inductor and capacitor are selected to be resonant above the operating or firing frequency of the inverter with an impedance at this firing frequency that will allow sufficient current to flow from the bridge to permit full-power operation. A very important feature of this style of inverter is that the internal series circuit isolates the bridge from the load. This protects the inverter from load faults caused by shorting or arcing and from badly tuned loads, making it one of the most robust thyristor-based induction power supplies available for heat treatment.

A second feature of this series-parallel configuration is realized when the internal series circuit is tuned to the third harmonic of the firing frequency. The power supply is then capable of developing full power into the parallel tank circuit tuned to either the fundamental firing frequency or the third harmonic. For example, the INDUCTOHEAT Statipower 5 family of induction heat treating power supplies is produced in three dual-frequency models, 1 and 3 kHz, 3.2 and 9.6 kHz, and 8.3 and 25 kHz [325] with a power range of 10 to 1500 kW (Figure 8.25). Because load current is not used for commutation, this system can be operated with the output shorted for easy troubleshooting. Solid-state accuracy ensures output power regulation of ±1% with an input line variance of ±10%. Reliability is further enhanced by placement of 95% of all circuitry on one control board that is accessible without entering the high-voltage section of the power supply.

The voltage-fed inverter with series connection to a parallel load commonly uses thyristors for power switching in the bridge and has an unregulated DC input supply. Regulation of output power is accomplished by varying the firing frequency relative to the parallel load resonant frequency. The waveshapes present in this style of inverter are shown in Figure 8.26. Trace 1 shows the voltage waveshape at the output of the bridge. Trace 2 shows the bridge current to the load and trace 3 is the

Bridge Inverter Features	
Voltage Fed	**Current Fed**
DC Filter Capacitor Square Wave Voltage Sine Wave Current Series Resonant Output Load Current = Output I. Voltage x "Q" Best for low "Q" Loads	DC Inductor Sine Wave Voltage Square Wave Current Parallel Resonant Output Load Voltage = Output V. Current x "Q" Best for high "Q" Loads

Figure 8.23 Bridge inverter features.

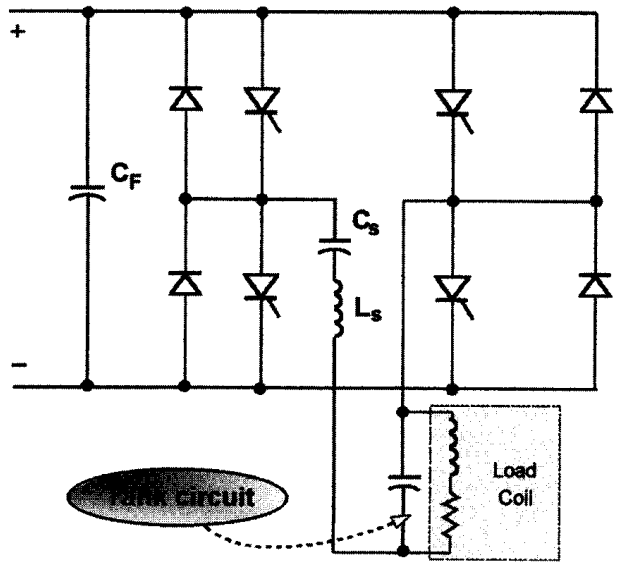

Figure 8.24 Voltage-fed inverter with series connection to parallel load.

Figure 8.25 Solid-state power supply Statipower sp5 & 7. Power and frequency combinations from 25 to 1300 kW/1 to 25 kHz. (Courtesy of INDUCTOHEAT, Inc.)

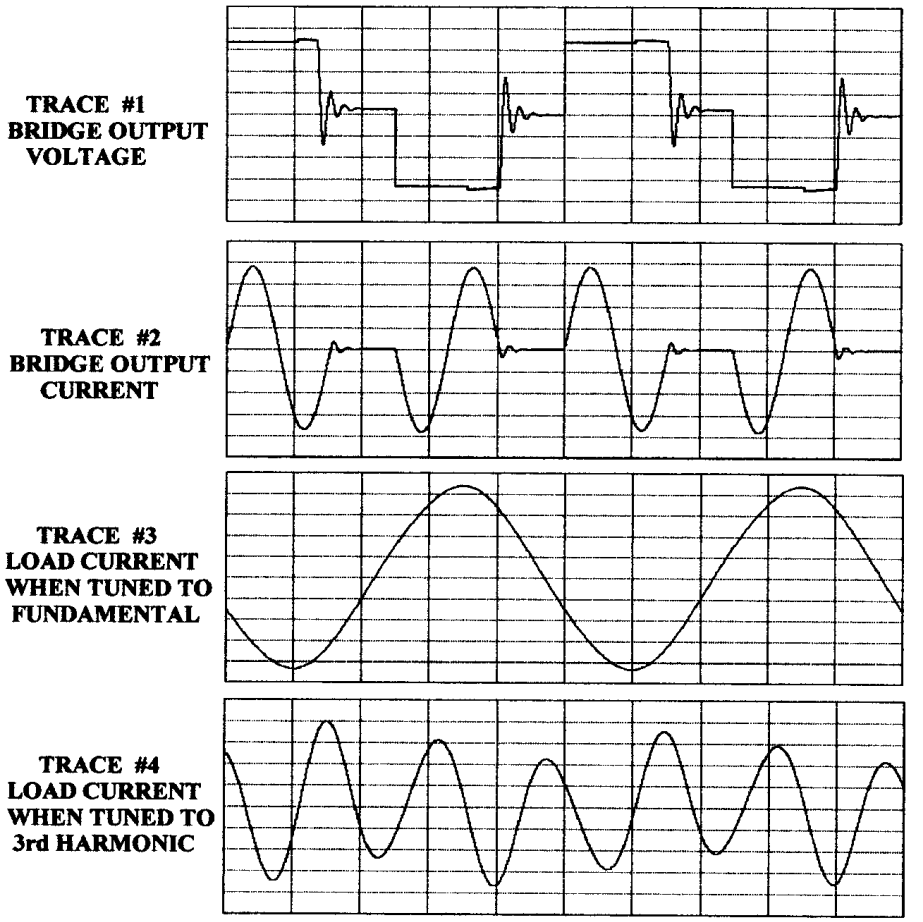

Figure 8.26 Waveshapes of voltage-fed inverter with series connection to parallel load.

load current and the current when the load is tuned to the fundamental or firing frequency. The corresponding waveshapes for operation with the load tuned to the third harmonic of the firing frequency are shown in Figure 8.26, trace 4.

8.3.2.5 Current-Fed Inverters

Current-fed inverters are distinguished by the use of a variable-voltage DC source followed by a large inductor at the input of the inverter bridge and a parallel resonant load circuit at the output as shown in the simplified power circuit schematic of Figure 8.27. Current-fed inverters are available in models that cover the entire 90 Hz to 1 MHz range of frequencies used for induction heat treatment. Thyristors are commonly used below 10 kHz, whereas transistors are chosen for the higher frequencies.

When the power switching is done with thyristors, the current-fed inverter must be operated above the resonant frequency of the parallel resonant load. As illustrated by the waveshapes of Figure 8.28, the voltage across the output of the bridge is a sine wave (trace 1) and the current (trace 2) is a square wave. It is interesting to note that this is just the reverse of the voltage-fed inverter, where the voltage is a square wave and the current is a sine wave. The DC bus voltage across the bridge after the large inductor L_{dc} (trace 3) resembles a full wave rectified sine wave. The

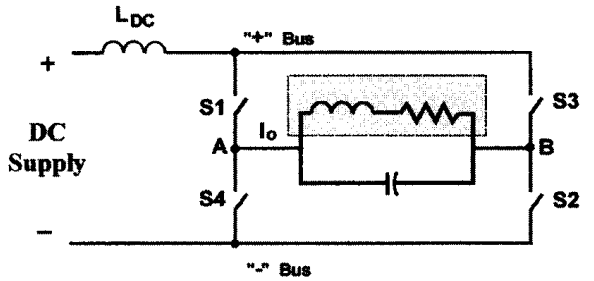

Figure 8.27 Current-fed full-bridge inverter.

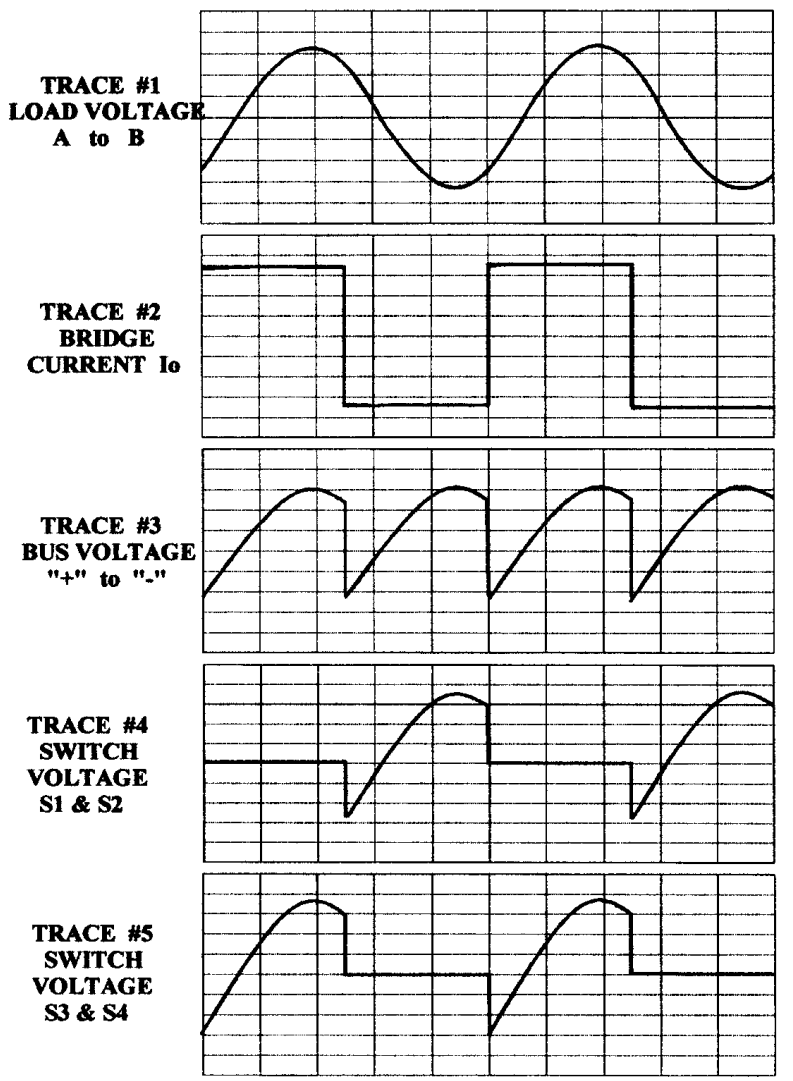

Figure 8.28 Current-fed inverter waveshapes above resonance.

bus voltage is forced negative from the time the bridge is switched until the load voltage reaches zero. This time must be sufficiently long to provide turn-off time to thyristors that are no longer conducting. The voltage across the thyristor switches is shown in traces 4 and 5 of Figure 8.28 with the negative portion of the waveshape noted as the turnoff time. The TG, TC, and ICF families of induction heat treatment power supplies (produced by Radyne Limited, UK) are of this design (Figure 8.29) and have been in use since 1970 [326].

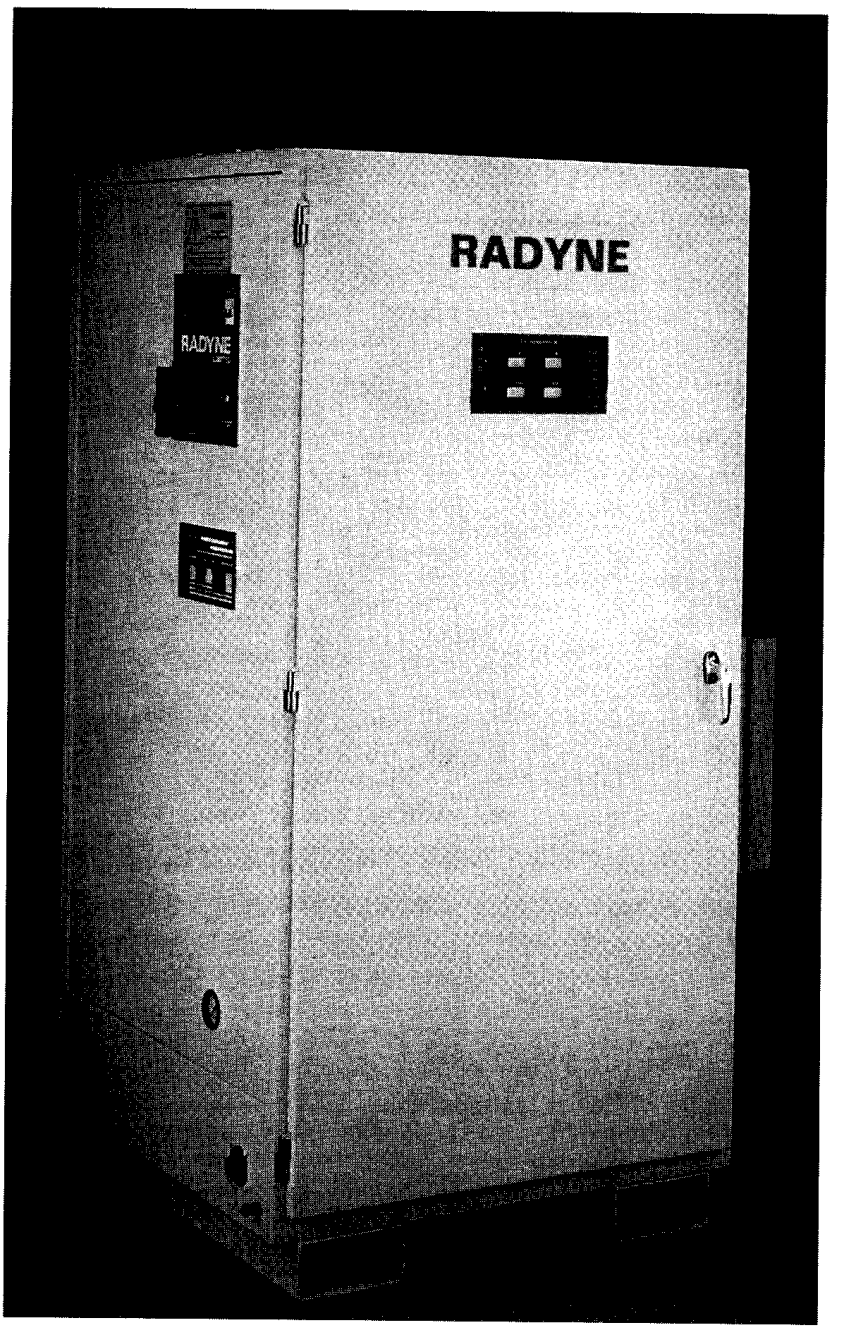

Figure 8.29 Radyne's TG-type solid-state power supply.

The current-fed inverter uses transistors at frequencies above 10 kHz because they can be switched very fast and do not require turn-off time. In this case the inverter can be operated at the resonant frequency of the parallel resonant tank circuit as shown in Figure 8.30. One diagonal of the bridge containing transistors T1 and T2 is turned on as transistors T3 and T4 of the other diagonal are turned off. This switching or commutation is done at a time when the voltage across the load, inverter bus, and transistors is zero. The inverter waveshapes obtained in this mode of operation are shown in Figure 8.31. Switching at zero voltage minimizes the switching losses in the transistors and therefore allows for higher frequency operation. When the inverter frequency is locked to the natural resonant frequency of the load, the output power must be regulated by controlling the input current to the inverter. This is accomplished by using one of the variable-voltage DC supplies described earlier. The Statitron III (produced by Inductotherm S.A., Belgium) uses MOSFET transistors in a current-fed configuration for heat treating at frequencies from 15 to 800 kHz with power levels up to 2 MW [327].

8.3.2.6 *Single Switch Inverter*

Another inverter configuration that has been used extensively for heat treating at 10 and 30 kHz uses only one thyristor and is referred to as a chopper or quarter bridge. Figure 8.32 shows a simplified circuit diagram. It is classified as a current-fed inverter because it has a large inductor in series with the DC supply to the inverter. Unlike the conventional full-bridge current-fed inverter, the chopper has a series-connected output circuit. When the thyristor is switched on, current flows both from the DC source through the large inductor and from the series load-tuning capacitor, discharging it through the load coil. The resulting load current pulse (Figure 8.33, trace 2) is nearly sinusoidal, with the first half-cycle of current passing through the thyristor and the second half-cycle through the diode. During this part of the period, current is rising in the input inductor. When current stops flowing in the diode, the energy stored in the input inductor causes direct current to flow in the output circuit, recharging the series load-tuning capacitor. The frequency of the output sine wave is determined by the series capacitor and the load coil inductance. It is this frequency that determines the penetration depth of the induction heating current. The firing rate of the inverter regulates the output power and therefore a simple fixed-voltage

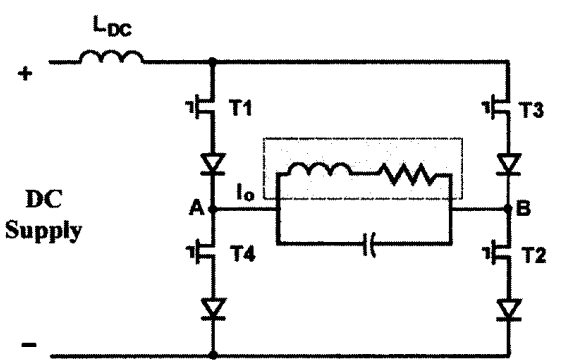

Figure 8.30 Current-fed full-bridge transistor inverter.

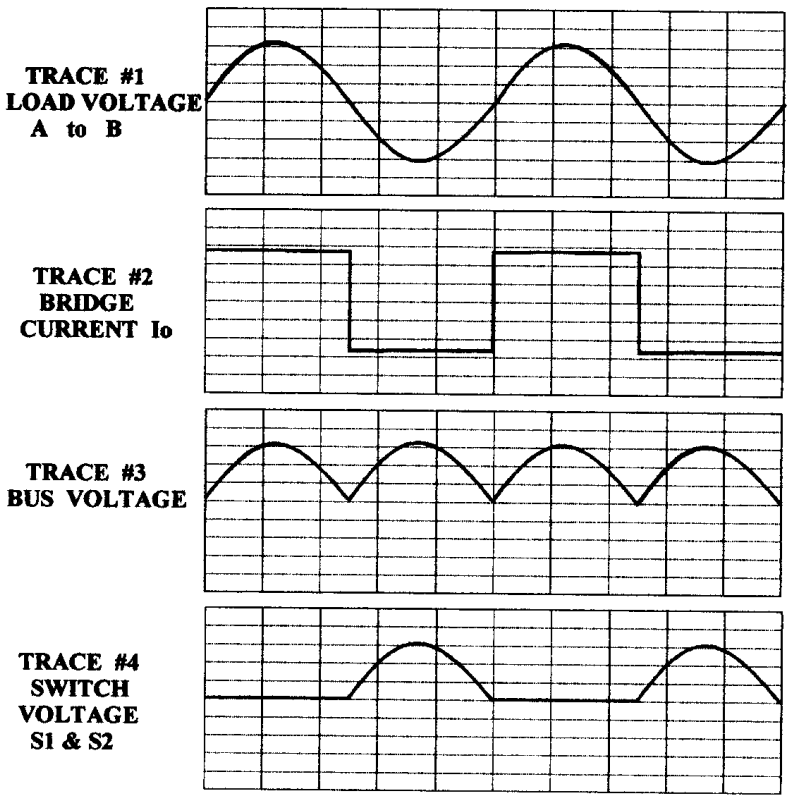

Figure 8.31 Current-fed inverter waveshapes at resonance.

DC source may be used. The INDUCTOHEAT Unipower 9 and Uniscan induction scan hardening machine both make use of this simple inverter [321, 328, 332–334].

8.3.3 Operational Considerations

Operational considerations that have an impact on the suitability of each type of power supply include initial cost, operating cost or overall efficiency, reliability, maintenance, flexibility, cooling water availability, and the power supply's impact on utility power quality.

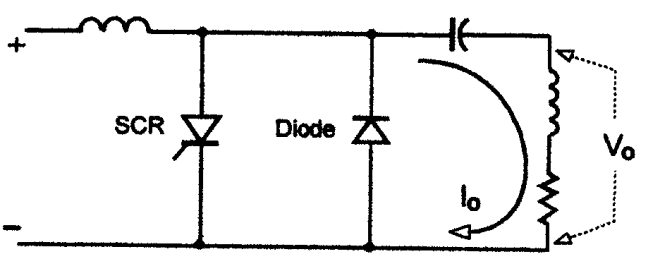

Figure 8.32 Current-fed chopper or quarter-bridge.

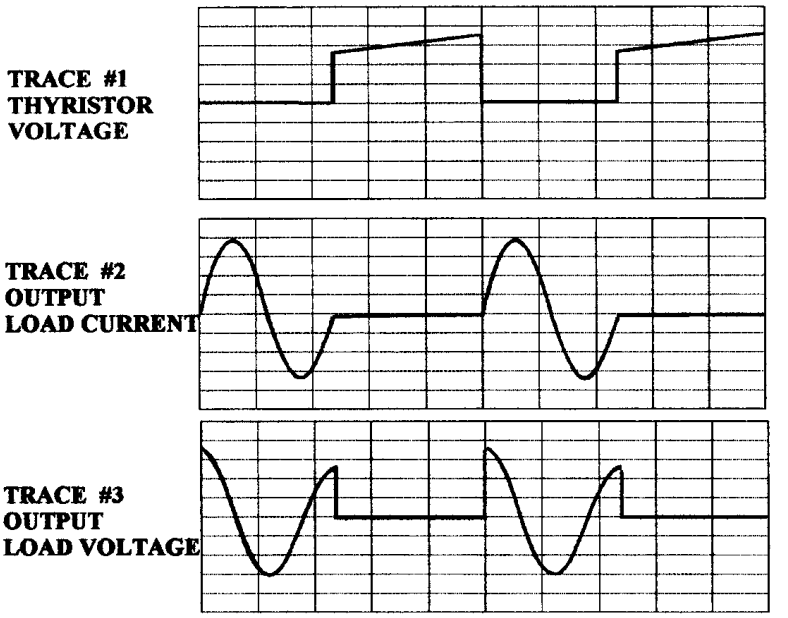

Figure 8.33 Current-fed chopper or quarter-bridge inverter waveshapes.

8.3.3.1 Initial Cost

Initial cost is important but should be a deciding factor only when all of the inverter types considered meet the other operational requirements. In general, the chopper or quarter-bridge power supply has the lowest purchase price. For power levels below 250 kW, the voltage-fed inverter with series resonant load is the next choice based on cost. The current-fed inverter has a low cost per kilowatt when high-power at low frequency is required. The most expensive is usually the voltage-fed inverter with a series connection to a parallel load. It has more power components per kilowatt than any other type of inverter in its frequency range but is the most robust and flexible for induction heating applications.

8.3.3.2 Operating Cost

Operating cost, which is usually determined by the power conversion efficiency, is also a consideration. Modern semiconductor-based induction heat treatment power supplies, however, all have reasonably high conversion efficiency compared to their motor generator and vacuum tube predecessors. Most have a conversion efficiency of 80 to 93% when running at rated output power. The conversion efficiency referred to here is that of the power supply from the input power connection to the output terminals and therefore does not include, in some cases, the output-matching transformer and load-tuning capacitors. Measurement and specification of power conversion efficiency can be accomplished in many ways with differing results. At one extreme, only the losses in the inverter portion are used in the calculation of efficiency. At the other extreme, all the losses from line to load are used by taking the ratio of the output power delivered to a calorimeter load to the input line power to the system. This method includes the losses in the inductor coil, which can be relatively high, resulting in a much lower stated efficiency. It is therefore essential

to know specifically what portions of the system are included in the specified efficiency to make direct comparisons of power supply efficiency.

8.3.3.3 Reliability and Maintainability

Reliability, maintainability, and a power supply's tolerance to input and load perturbations are functions of power component design margin and control circuit design rather than the general type of power supply circuit used. Without carrying out a detailed analysis of a power supply it is very difficult to assess its reliability. Barring this analysis, the best guide to equipment reliability is an assessment of the manufacturer's reputation, how long they have been in the business of producing induction heating power supplies, and the amount of their equipment in field use. Maintainability is affected by many features of power supply design, including the level of self-diagnostics provided, accessibility of components for inspection and measurement, and ease of component and subassembly removal and replacement. When power components, subassemblies, and control boards are interchangeable without adjustment or modification, electrical maintenance personnel with only minimal training can quickly and effectively accomplish troubleshooting and repair. Self-diagnostic systems can be very helpful in locating failures in a power supply. However, the inclusion of diagnostic circuitry, which can also fail, has a negative impact on reliability and, therefore, a balance between the level of fault diagnostics and power supply reliability is necessary. A very reliable power supply design should require only very basic fault indicators, whereas more failure-prone designs should be equipped with more extensive diagnostics to speed the repair process even though an incremental decrease in reliability will result.

8.3.3.4 Flexibility

The ability of a power supply to operate under varying load conditions or in different applications is an important factor in some situations. If the heat treatment machine is general-purpose such as a scan hardening machine used in a job shop, the ability to match a wide range of coils at more than one frequency is attractive if not essential. In this case, a dual-frequency power supply with a versatile load-matching system, including both transformer tap switches and dual-frequency capacitor banks, is recommended. The relatively new transistorized power supplies with external transformer tap switching are also attractive where their small size, light weight, and minimal cooling water requirements allow them to be portable and to be used by multiple machines. The Unipower 12 shown in Figure 8.34 is an example of such a multiple-application power supply [321, 329].

8.4 LOAD-MATCHING

8.4.1 Prelude to the Discussion of Load-Matching

A very important facet of induction heating that is often overlooked in the initial design stages is the ability to successfully deliver to the workpiece the maximum available power from a given power supply at the minimum cost. Circumstances do not always allow for optimal design of a complete induction heating system in which the power supply design is based on the application including the specific induction coil parameters. Quite often, the induction coil is designed to achieve the desired

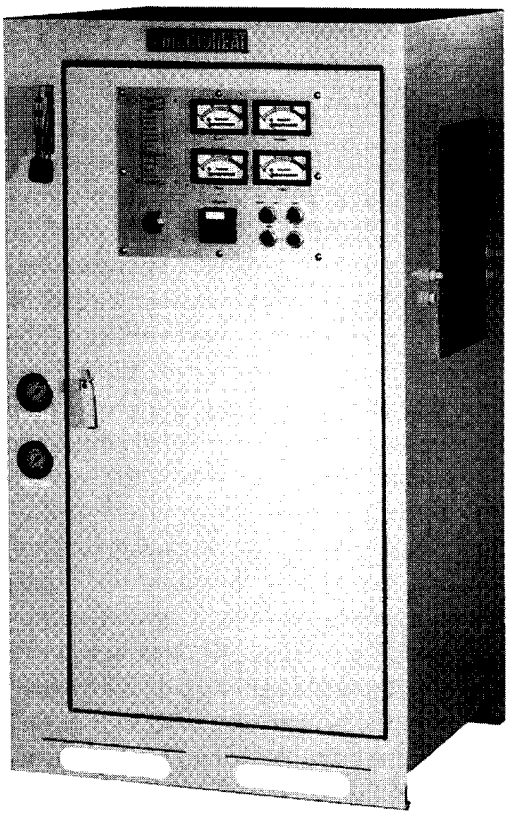

Figure 8.34 Multiple application solid-state power supply Unipower up-12 (3, 10, and 30 kHz frequency with output power ratings 25 through 200 kW).

thermal conditions and temperature profiles without regard for the power supply that will be used. When this is the case, a flexible interface is required to match the output characteristics of the power supply to the input characteristics of the induction coil and workpiece combination [330]. If this match is not provided, the power supply may not be able to deliver its rated power inasmuch as the coil requires more voltage or current than the supply can deliver.

There are many factors involved, any of which can cause complications in arriving at the stated goal. To facilitate this matching process, variable ratio transformers, capacitors, and sometimes inductors are connected between the output of the power supply and the induction coil. The adjustment of these components is commonly referred to as "load-matching" or "load-tuning."

8.4.2 Four Steps in Understanding Load-Matching for Solid-State Power Supplies

8.4.2.1 Step One

A common example of matching a power source and load would be a simple lighting circuit application where a 6 V light bulb is available for use on a 120 V power line (Figure 8.35). Obviously there is a need for some type of interface hardware to

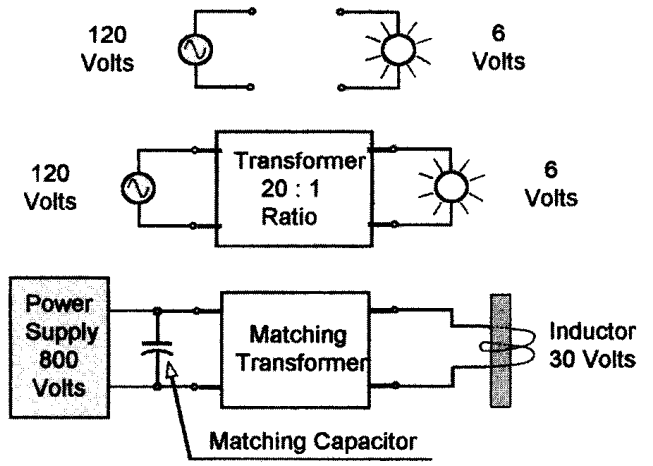

Figure 8.35 Load-tuning: impedance matching.

prevent the 120 V from destroying the light bulb. This would commonly be accomplished by inserting a transformer between the light bulb and the power line or a second solution would be to connect 20 of the bulbs in series across the 120 V line. Either solution would suffice and both require knowledge of the operating characteristics of the source and of the load to provide a successful match.

To apply a similar rationale in the induction heating arena we must begin with an understanding of the induction heating load circuit.

As illustrated in Figure 8.36, the generalized model for the induction heating coil and workpiece combination consists of the following components: R_p, the resistive component of the work coil copper; R_s, the reflective resistance of the secondary eddy current path in the workpiece to the primary circuit; X_{lp}, the primary reactance of the work coil; X_{ls}, the reactance of the secondary eddy current path reflected to the primary circuit; and finally, X_{lg}, the reflective reactance of the secondary air gap between the coil and the workpiece. The largest reactive component is X_{lg} [1, 4, 320, 360].

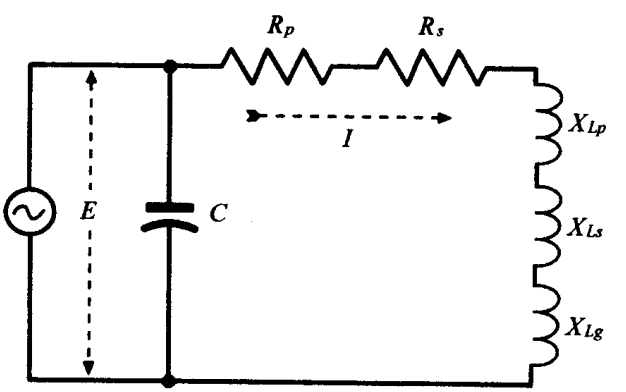

Figure 8.36 Typical equivalent circuit for an induction heating load.

In the parallel circuit shown, the load power dissipated is given by the formula

$$P = I^2 * (R_p + R_s).$$

The output current is the output voltage of the converter divided by the circuit impedance E/Z, where $Z = (R_p + R_s) + j(X_{lp} + X_{ls} + X_{lg})$.

This circuit would seem to be easy enough to analyze except for the fact that both resistance and the reactance of the circuit are nonlinear functions of several parameters such as coil–workpiece geometry, material properties, and frequency. Furthermore, the electrical resistivity and magnetic permeability of the metals are nonlinear functions of the temperature at the specific areas of the workpiece. At the same time, magnetic permeability is a nonlinear function of magnetic field intensity as well (Figures 3.2 through 3.11). As shown in Section 3.1, electrical resistivity and magnetic permeability vary during the heating cycle. In addition, for reasons of economics, modern metalworking processes require that workpieces of different sizes be heated in the same inductor. Combinations of the production mix and variation in material properties result in changing coil resistance and reactance, which affects the tuning and performance of the power supply.

Generally speaking, a change in coil resistance and reactance results in a change of the phase angle between the coil voltage and the coil current of a given circuit. Such a change can be characterized by the coil power factor, which refers to the cosine of the phase angle ($\cos\Theta$).

Power factors of different types of inductors are affected differently by various parameters. At the same time, for different frequencies and different coil-to-workpiece air gaps the power factor can be significantly different (i.e., $\cos\Theta = 0.02$, up to $\cos\Theta = 0.6$, which makes a Q-factor $((X_{lp} + X_{ls} + X_{lg})/(R_p + R_s))$ range from $Q = 50$ down to $Q = 1.7$.

Figures 8.37 through 8.40 illustrate the dynamic characteristics of the induction heating process for a typical carbon steel workpiece heated from room temperature to 1200°C (2200°F). Obviously, calculation and measurements for a dynamic process must be done at the specified time or temperature indicated or the results will be completely erroneous.

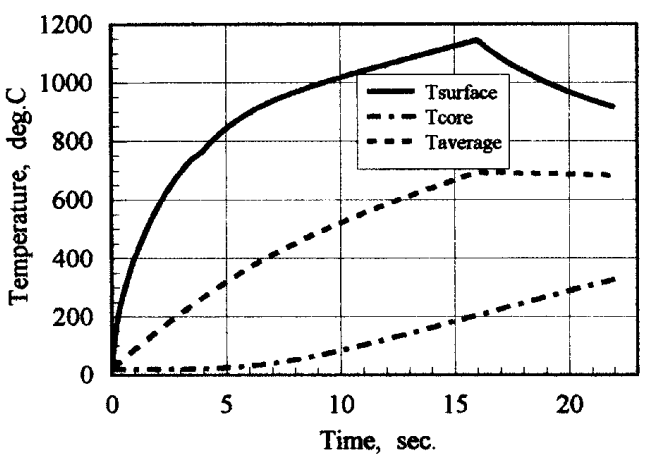

Figure 8.37 Typical workpiece temperature variation with time.

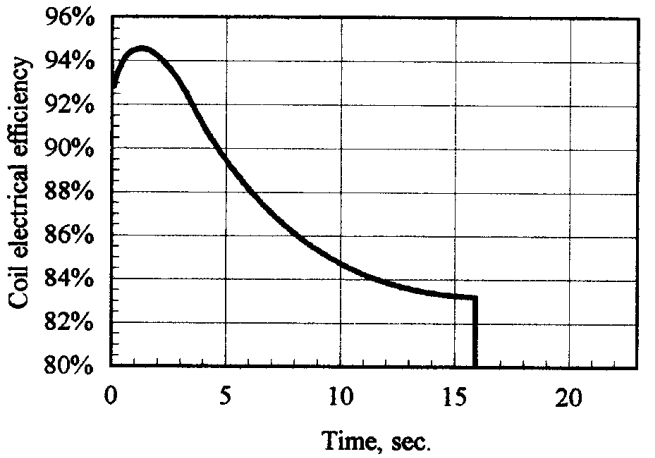

Figure 8.38 Variation of coil electrical efficiency with time.

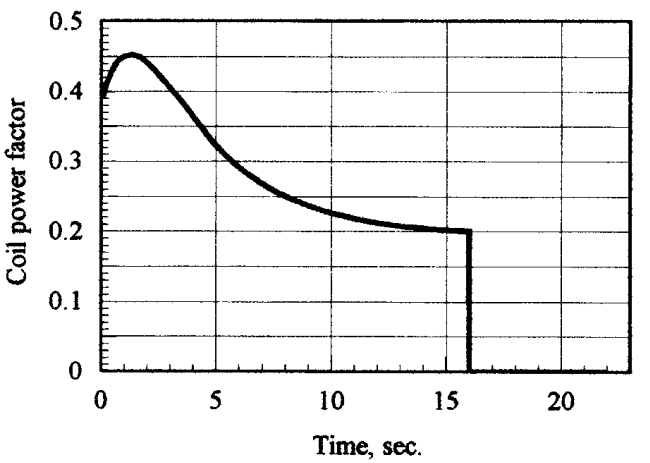

Figure 8.39 Coil power factor versus time.

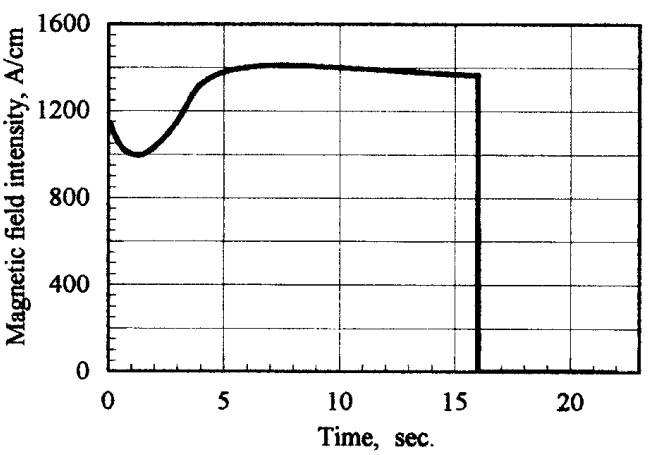

Figure 8.40 Magnetic field intensity versus time.

In addition to these factors the process itself usually requires that the part be heated at some frequency other than the line frequency. In conventional heat treatment, the applied frequency typically ranges from 200 Hz to 600 kHz. Since a relatively large current is required to successfully heat a workpiece, it is necessary to build power sources with extremely high output current capability or to use a simple resonant circuit to minimize the actual current or voltage requirement of the frequency converter.

A simple example may help at this point.

Example. Given an induction coil that requires 100 kW, 40 V, 10,000 A at 10 kHz and a power source that is rated at 100 kW, 440 V, and 350 A, are the two incompatible?

By using an isolation transformer we might select a ratio of 440:40 or 11:1 to match the power source's 440 V to the induction coil's 40 V. This would leave us with a current requirement of 10000/11 or 909 A, which is too high for the given power source.

By the addition of a specific capacitance to the load circuit it is possible to lower the current requirement and still accomplish the heating task. The addition of sufficient capacitance to tune the circuit to the unity power factor ($\cos \Theta = 1$) would result in a required current from the power source of 100 kW/440 V or 227 A, well within the limitations of our selected power source. This relaxes the requirements not only on the power source but also on interconnecting cables, contactors, and transformers operating in the area of the improved power factor.

As shown in the previous section, there are two basic types of resonant frequency converters that use parallel and series resonant circuits. Figure 8.41 shows the characteristics of series and parallel resonant circuits. Looking first at the parallel circuit, it is easy to see that if the capacitor value is equal to zero, then a given voltage applied to the circuit at a fixed frequency will result in a specific amount of power dependent on the circuit impedance. When sufficient capacitance is added to the

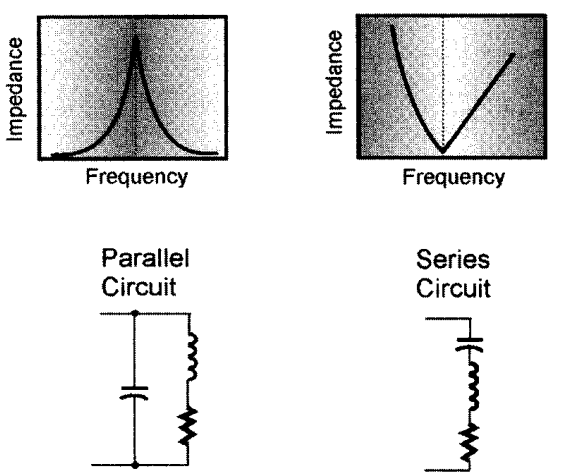

Figure 8.41 Resonance at parallel and series circuits.

circuit to tune the load circuit near resonance, the circuit impedance rises and the amount of current drawn from the power source falls off dramatically. The circuit voltage required to achieve a specific power level is the same as with the initial case of zero capacitance, but now the higher current required by the load is being supplied by the capacitors rather than the power source.

In a parallel-tuned load circuit we have a Q rise in current in the tank circuit compared with the input line from the power source (Figure 8.42). This analogy can be repeated for the case of the series circuit to realize that with the calculated change in circuit impedance the circuit current will be much higher for a given input voltage when the circuit is tuned near the resonant frequency because the impedance is approaching zero. The load coil current required for a given power is the same for the given load circuit regardless of whether the connection is series or parallel, but because the overall impedance has fallen and the required current is fixed, the required driving voltage is approximately a factor of Q lower than the coil voltage. Hence, we have a Q rise in current in the parallel circuit and a Q rise in voltage with the series-connected circuit (Figures 8.41 and 8.42). It is therefore imperative to have an understanding of what type of circuit connection exists in order to understand the effect that changes in value of the tuning components will have on the power source and workstation components.

8.4.2.2 Step Two

Turning now to look at the output power characteristic for a given load circuit versus the circuit operating frequency (Figure 8.43), it is easy to see that if we begin at a low frequency and gradually increase the operating frequency to the point of resonance, we will have an increase in output power. Beyond the point of resonance, an increase in the operating frequency will result in a decrease in the output power. This characteristic is often used to accomplish the required regulation mode for the power source. This process can be accomplished in the reverse direction as well when a "sweep down" control is utilized. For our discussion we describe a "sweep up" control while realizing that the same principles can be used in reverse for the "sweep down" control.

The goal in tuning the workstation is to deliver the required power to heat the workpiece without exceeding the maximum value of any of the power source para-

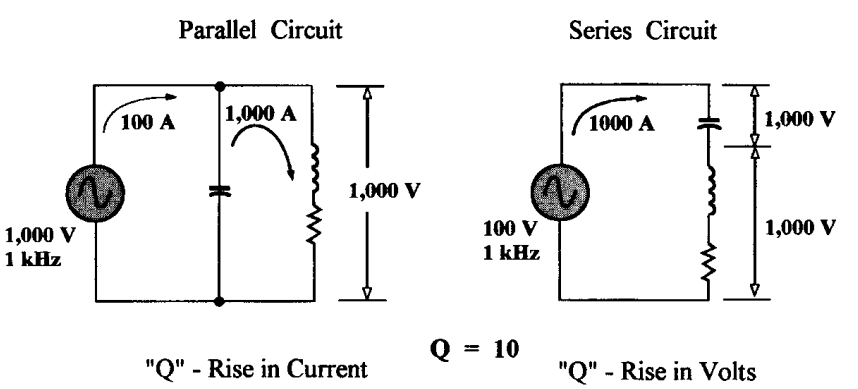

Figure 8.42 Parallel and series circuits.

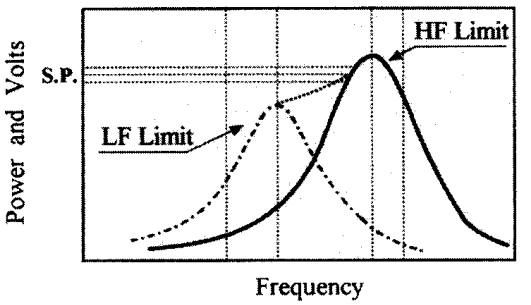

Figure 8.43 Power curves for series and parallel output circuits.

meters. Figure 8.44 is a schematic for a typical workstation with capacitors, an autotransformer, and an isolation transformer. It should be noted that a given heat station may use all of the above components or as few as one in addition to the heating coil.

A useful way to approach the tuning of a workstation is first to determine the ratings of the power source and record the available workstation hardware. The next step would be to make an estimate of the required coil voltage for the desired output power. This may be done with previous data or rule-of-thumb extrapolations. Selection of an isolation transformer ratio to yield the proper voltage match follows. The next step would be to set up the load in the work coil as it will be heated and use a load-frequency analyzer or signal generator to determine the resonant frequency of the load circuit [330,331]. Figure 8.45 shows INDUCTOHEAT's load-frequency analyzer, which is a solid-state portable instrument that quickly determines the resonant frequency of the induction heater without heating the workpiece. This analyzer eliminates hours of setup time and prevents the waste of production parts. Instead of guesswork, the load-frequency analyzer can easily and precisely determine the resonant frequency for any induction load or heat treatment system.

After obtaining a resonant frequency it is necessary to add or subtract capacitance from the circuit to match the tuned frequency of the workstation to the rated frequency of the power source. At this time it is useful to run a cycle and record data for use in extrapolating to the desired setup. Figure 8.46 shows a portion of the MathCAD solver sheet for use in extrapolations when tuning the workstation. Variables are presented for power, voltage, coil length, coil turns, frequency, and coil diameter. The variables P1, V1, L1, N1, F1, and D1 are the initial values recorded. The remaining variables are the desired values except for one variable that is chosen as the one to solve for. The equation can be solved manually for any of the given variables. An example at this point might prove helpful.

Example. From previous data:

$P1 = 100\,kW; \quad V1 = 30\,V; \quad F = 10\,kH;$

$N1, L1, D1 = 1.$

Desired: What voltage is required for the same power at 3 kHz?

$P2 = 100\,kW; \quad V2 = ?; \quad F = 3\,kHz$

$N2, L2, D2 = 1$ (same as above).

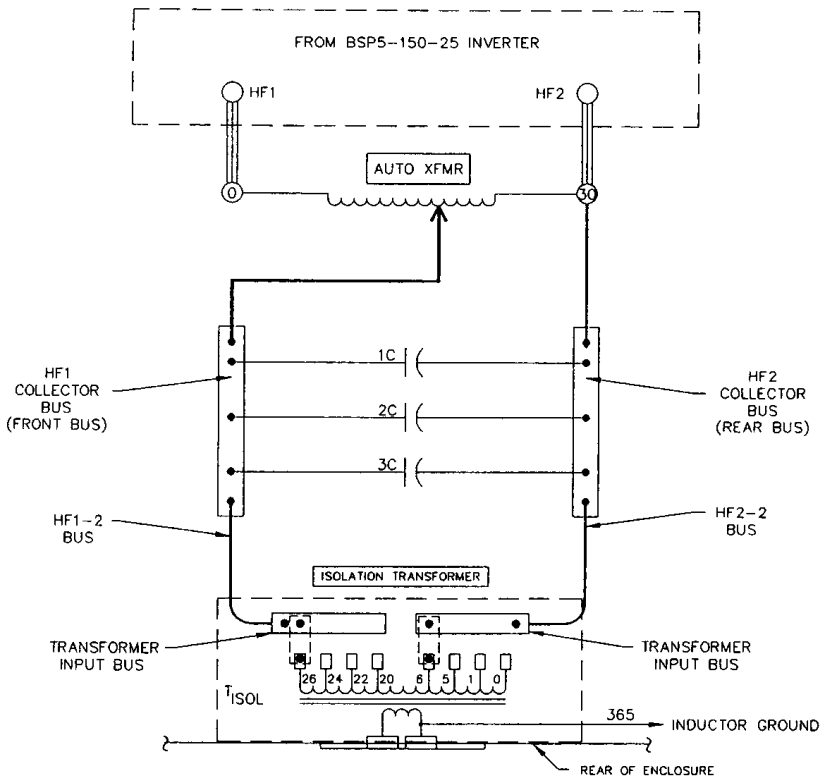

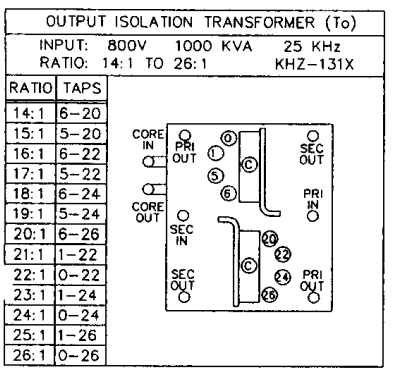

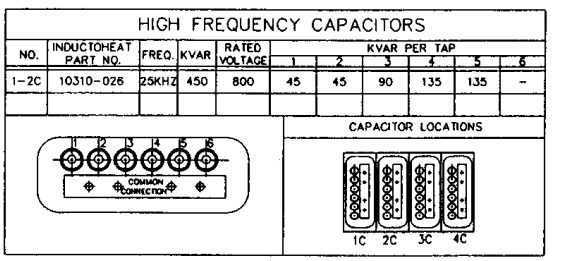

Figure 8.44 Typical load-tuning component interconnection.

Solve for V2.

Answer: 20 V (approximately).

Note. For most load-matching calculations, an answer within 10% is close enough to accomplish the job. Although not pleasing scientifically, it is very practical and will save considerable time probing for exact answers.

It may be profitable at this point to consider the effect of changes in various components or component values in the workstation. The induction coil may be varied in shape and size with respect to the workpiece being heated. The effect of changing a simple cylindrical coil and workpiece is shown in Figure 8.47. The value

Figure 8.45 Load-frequency analyzer. (Courtesy of INDUCTOHEAT, Inc.)

P1 := 100 P2 := 100

V1 := 30 V2 := 1

F1 := 10000 F2 := 3000

L1 := 1 L2 := 1

N1 := 1 N2 := 1

D1 := 1.5

To use this program:
1) input all values that are known
2) input 1's for all remaining variables
3) Insert the name of the variable that you are solving for in the Find(x) statement below.
4) The Answer is diplayed below

NOTE: TO INPUT VARIABLES, POINT WITH YOUR MOUSE TO THE NUMBER YOU WANT TO CHANGE AND CLICK THE LEFT BUTTON. THEN DELETE OR ENTER NUMBERS AS REQUIRED. CLICK ON THE NEXT POSITION OR PRESS RETURN.

Given

$$\frac{P1}{P2} = \left(\frac{V1}{V2}\right)^2 \cdot \left(\frac{F2}{F1}\right)^x \cdot \frac{L1}{L2} \cdot \left(\frac{N2}{N1}\right)^2$$

NOTE: VALUES OF x CAN RANGE FROM .65 FOR SMALL DIAMETER SHORT COILS TO 1.5 FOR LARGE DIAMETER MULTI TURN COILS .

Answer := Find(V2)

Answer = 20.285

P1 IS THE INITIAL POWER READING
V1 IS THE INITIAL RMS VOLTAGE READING
F1 IS THE INTIAL FREQUENCY
L1 IS THE INITIAL LENGTH
N1 IS THE INITIAL NUMBER OF TURNS
D1 IS THE DIAMETER

Figure 8.46 MathCAD solver routine for the extrapolations when tuning the workstation.

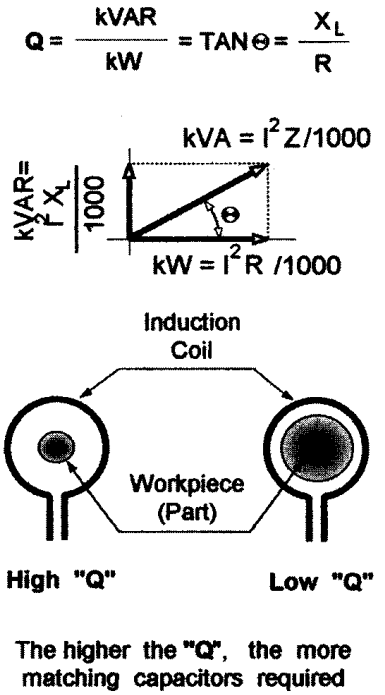

Figure 8.47 Definition of the parameter Q.

of circuit Q is directly affected by the part-to-coil coupling and will cause a need for increased capacitive volt amperes to balance the inductive portion of the circuit: the larger the gap between the part and the coil, the greater the required value of heat station capacitance (Figure 8.47).

The heat station isolation transformer can also be varied by physically changing tap connections to change the turns ratio. A change in this transformer will produce a significant change in the circuit inductance reflected to the primary side of the circuit and subsequently the amount of capacitance required to balance the load properly.

The amount of capacitance connected in the circuit can also be changed. Increasing the circuit capacitance will lower the resonant frequency of the circuit, and a decrease in capacitance will result in an increase in the load resonant frequency. There is sometimes confusion in recording the actual amount of capacitance in a given load circuit due to the use of the terms kVAR and microfarads to describe the quantity of capacitance. The term kVAR can be expressed by the formula

$$\text{kVAR} = 2\pi \text{F C V}^2/1000$$

and is obviously a function of the frequency F, microfarad value C, and operating voltage V of the capacitor. For a given capacitor, the kVAR rating is at the name plate frequency and voltage. If the capacitor is used at another voltage or frequency, the actual required microfarad value C will change according to the above formula.

One might ask what the real benefit of the kVAR term is. It can facilitate calculations when transformers are installed between the coil and the capacitor bank. As shown in Figure 8.48, if we have a load that has a Q value of 8, the required

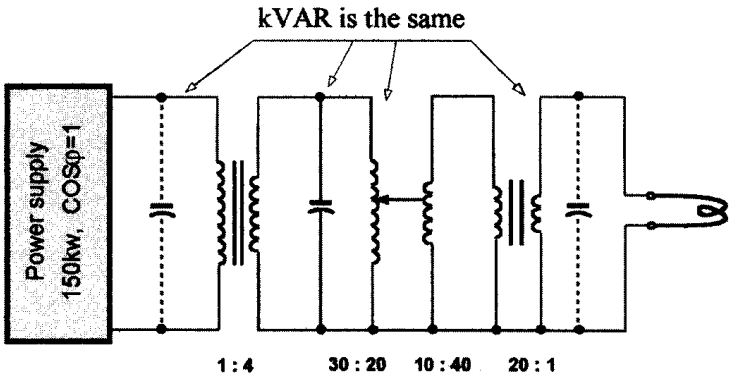

Figure 8.48 Schematic of induction system: power = 150 kW, Q = 8; Vo = 600 Volts, frequency = 10 kHz.

value of the load or tank capacitor is approximately the Q value multiplied by the required kilowatts. For a 150 kW unit this load would require 1200 kVAR of heat station capacitance at the rated voltage and frequency. This is true regardless of the position of the capacitor in the circuit. If the microfarad values were used here, then the effective microhenry value of the coil would have to be calculated through each of the transformer connections and then the capacitor microfarad value would be calculated.

One of the major causes of misapplication of this information is that most users assume that the kVAR value of the capacitor is constant, but, in fact, it changes in value as the operating frequency and voltage change. It is then necessary to specify the kVAR at the operating voltage and frequency and to select the capacitors so that they provide the required kVAR value at the desired voltage and operating frequency. For example, using the information above, if the circuit requires 1200 kVAR at 600 V and 10 kHz, then the nearest standard capacitor that would be acceptable would probably be a 2133 kVAR, 800 V, 10 kHz capacitor.

Manufacturers for many years have standardized on 220, 400, 440, and 800 V operating voltages to reduce the variety of capacitors produced and to match the existing standard output ratings of motor generators.

Another component that can be changed in the matching process is the autotransformer. A change in the tapping of this transformer will, for all practical purposes, affect the output voltage of the circuit but not the operating frequency. This is stated with the qualifier "for all practical purposes" because with solid-state power supplies the leakage reactance of the autotransformer may sometimes be significant. Care should be taken in choosing the placement of the autotransformer because it can greatly affect the required kVA rating of the transformer. As shown in Figure 8.49a, if the transformer is installed between the power supply and the capacitor bank it is operating at the power factor of the power source with relatively low current. If this same transformer is installed between the capacitor bank and the isolation transformer or work coil (Figure 8.49b), the current is much higher and the required kVA rating of the transformer is much higher, roughly Q times the kilowatt operating point of the power supply.

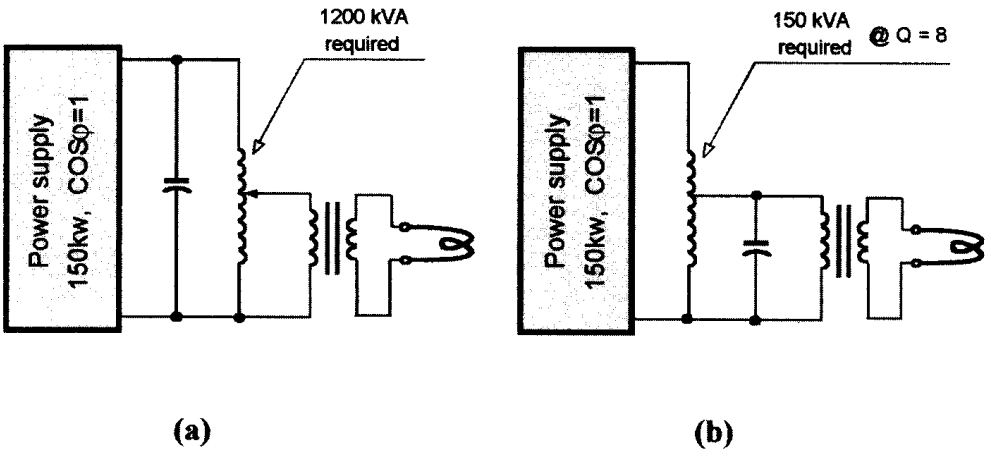

Figure 8.49 Features of the reactive power compensation due to different autotransformer location.

8.4.2.3 Step Three

Historically, for the motor generator set, tuning was approached by trying to add enough capacitance to read the unity power factor or zero phase angle on the panel meters. With solid-state power supplies, the power source often operates with a leading or lagging power factor, and any inductance added in the transmission lines becomes more of a factor. Often a reactance located in the power supply must be considered part of the tuned circuit. To complicate matters further, each type of power source has a variety of limiting conditions that could prevent delivery of maximum power to the workpiece. It is advisable, before purchasing a power supply, to check with the manufacturer as to how much reserve capacity is available in the power supply. More than one user has been cut short by buying a 150 kW power supply only to find out that the maximum power it will deliver into the load circuit is 90 kW. Figure 8.43 shows a typical tuning curve for a swept frequency power supply operating into a parallel tank circuit. This type of power supply most often begins at a lower frequency, called the low-frequency limit (LF in Figure 8.43) and begins sweeping up in frequency until the preset power level is attained or a limit is reached. Typical limits would include a high-frequency (HF) limit, a phase or low impedance limit, output voltage limit, output current limit, maximum power limit, and so on.

One complication that can arise as a result of mistuning the load is that the frequency may be increased beyond the resonant frequency of the tuned circuit. This results in confusing the control circuit, which is normally (for a "sweep up" control) in a mode of increasing the frequency to increase the output power. Since the power will decrease for an increase in frequency beyond the load resonant frequency, the power supply frequency will continue to increase until it reaches the high-frequency limit. This condition is referred to as "going over the hump". The remedy is generally to reduce the value of the heat station capacitor or vary the inductance to produce an increase in the load resonant frequency.

It should be noted that on power supplies with an output series capacitor this over the hump condition will result when the series capacitance is too small relative

to the kilowatt rating of the power supply. By adjusting the tank circuit capacitor and transformer or coil turns, it is possible to shift the curve in Figure 8.43 to the left or right to move away from expected limiting conditions. It should be noted that the power delivered is that shown on the curve and that if the curve is shifted too far to the left, a higher power than that desired may be delivered with no apparent control by the power potentiometer. Most solid-state converters will not run at a zero power output even though the potentiometer may be set to zero.

A transistorized current-fed power supply operating into a parallel tank circuit operates at a fixed frequency by phase-locking itself to the tank circuit resonant frequency. One might think that this would eliminate the need for tuning. Unfortunately, this is not the case. The problem of matching impedance and frequency still exists. Because the control will phase-lock to the load resonant frequency, the amount of capacitor connected in the circuit must be the amount that will tune the unit to the desired running frequency. Also, on many current-fed units the maximum allowable output current is only slightly higher than that which would be calculated for the unity power factor at full voltage. This means that unless the impedance of the tank circuit is exactly right to deliver full current at full voltage, the power supply will deliver less than full power to the load. This sometimes requires the insertion of a special tuning bus to adjust the impedance for the correct value.

If the current as a percentage of maximum is higher than the percentage of voltage, more inductance is required in the circuit. If the voltage is higher than the current, then inductance must be removed from the circuit. Another solution provided by the control of some current-fed inverters is to operate the inverter above the resonant frequency of the tank circuit. This reduces the load impedance to better match the output of the inverter.

Effort spent on load-matching can be reduced by using a power supply that has more rated capacity than required or one that can demonstrate the capacity to run at 120% of its power rating. This will ensure ease of tuning when the application calls for 100% power or less.

Another general guide in load-matching is to aim for an approximate voltage match as outlined in Figure 8.50.

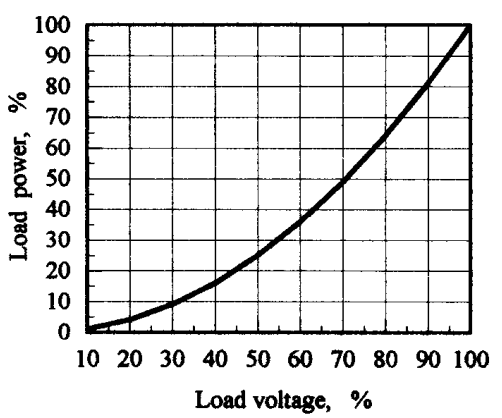

Figure 8.50 Load power versus load voltage.

Because the power varies as the square of the output voltage, striving for these values will give a setting that will allow easy adjustment to higher or lower values without continual limiting conditions.

8.4.2.4 The Final Step

A final caveat in load-matching has to do specifically with the transmission lines from the power source to the load-matching (or heat) station and those from the load-matching capacitors or output transformer to the heating coil. Large inductances in these areas can cause considerable problems because much of the voltage generated by the power supply is dropped across the high-inductance elements of the circuit and not across the load itself. This can result in a considerable reduction in allowable output power and possibly in the inability to complete the desired heating task. This inductance is particularly critical in the higher kVA portion of the circuit (between the matching capacitors and the coil), especially at higher frequencies and higher currents. A good practice is to minimize the transmission line inductance within the required cost and size constraints to stay below a 10% voltage drop and 5% kW loss.

8.4.3 Summary

In summary, although the induction heating process is a complicated dynamic process, the load-matching process need not be. If the information presented above is applied with careful collection of data during the process, the correct setup can be accomplished in a relatively short time by

- Starting with an estimated required kW and voltage,
- Establishing the correct resonant frequency,
- Running a test cycle and gathering data at a specified time in the cycle,
- Extrapolating from the existing readings to the desired readings,
- Resetting the component values, and
- Rerunning a cycle to evaluate the results.

8.5 MEDIUM- AND HIGH-FREQUENCY TRANSFORMERS FOR HEAT TREATING AND MASS HEATING

A transformer is an important part of the induction heating machine. Different types of transformers are used in inverters and heat stations [335]. The total efficiency of the power supply is primarily affected by the transformer's efficiency. Years ago, when motor generators were widely used, the design of isolation transformers was a straightforward process. Basic information, such as frequency, kilowatts, kilovolt amperes, and input/output voltages, was all that was required. Today, with many different types of solid-state inverters and heat stations, the task of designing efficient transformers becomes more complex. The successful design of contemporary transformers should involve such features as the current and voltage waveforms, which can be square, sinusoidal, or saw-tooth, and often contain harmonics.

The transformer's main purpose is to change one voltage to another, making it possible to operate a great variety of loads at suitable voltages. In a transformer the

turns of the primary and secondary coils are coupled closely together so that their respective turns ratios determine very closely the output voltages and volt ampere characteristics. The coils are usually wound on a core of laminated or ferrite magnetic material. In radio-frequency transformers used with vacuum tube oscillators there is no magnetic core. In this case the transformer is called an aircore transformer.

Transformer manufacturers including the Jackson Transformer Company provide the induction heating industry with a wide range of transformers and other magnetic products from line frequency to 800 kHz, from a few volt amperes to over a megawatt, and with water and air-cooled designs [335, 336]. Products include isolation, auto, current, potential, and RF transformers, along with AC/DC reactors and integrated magnetic devices. As a general rule, most of the magnetic devices are water-cooled. This is because of size limitations, cost factors, power requirements, and the frequency ranges they cover.

8.5.1 AC/DC Reactors

Alternating current reactor designs take into consideration any DC component, from a few Hertz to several hundred kiloHertz, water-cooled or dry, open construction or encapsulated. The legs of the inductors wound on magnetic cores have distributed gaps to minimize flux leakage and to reduce noise. The legs are normally encapsulated to minimize vibrations. They are available from a few microhenries to several millihenries and from a few amperes to several thousand amperes.

8.5.2 Variable Impedance Transformer

The variable impedance transformer (VIT) is a current-control device that requires very small signals to control a large amount of power. Its purpose is to provide stepless power to electric furnaces that have silicon carbide elements, vacuum furnaces for deposition of metal, plating power supplies, and load banks. The VIT is an integrated magnetic device in which the primary windings and the magnetic amplifier windings are placed on common cores. It can operate with large unbalanced loads or with an open-circuit phase. The VIT can withstand short circuits for prolonged periods of time without incurring component failure. It is available in single-, two-, or three-phase designs that provide from a few Hertz to 200 kHz, and from a few volts to 2000 V up to 500 kVA.

8.5.3 Heat Station Transformers

Jackson heat station transformers such as the 52V1, 51V1, and 531V1 have become the standard used in the heating, hardening, and annealing industry. 52V1 transformers (Figure 8.51) are normally used where the voltage needs to be stepped down from 5:1 to 22:1 or from 5:2 to 22:2 or other ratio combinations depending on customer requirements. The input voltages are from 220 to 1200 V, and frequencies from 500 Hz to 10 kHz. The kVA can range from 50 to over 10,000 kVA.

The construction of the windings as shown in Figure 8.52 can be either open or epoxy-encapsulated. The output connections (secondary terminals) are generally

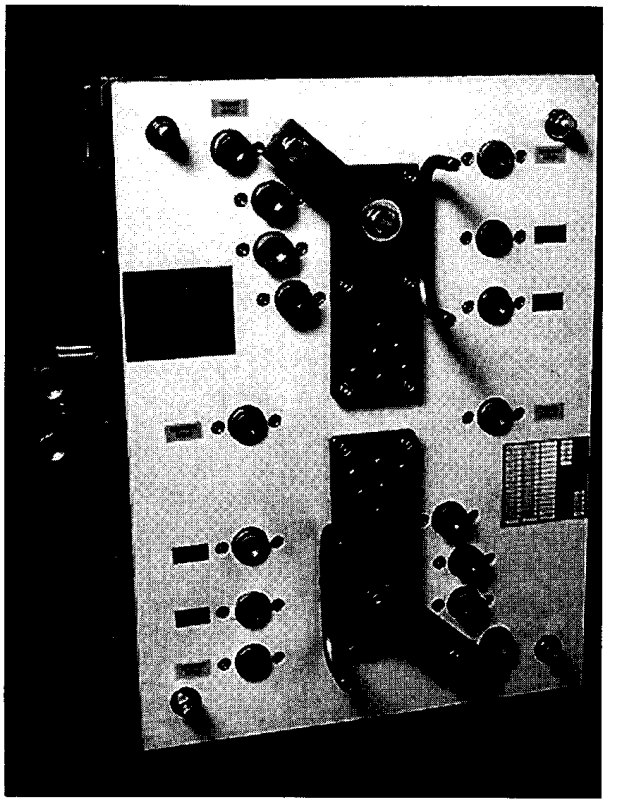

Figure 8.51 Heat station transformer. (Courtesy of Jackson Transformer Company.)

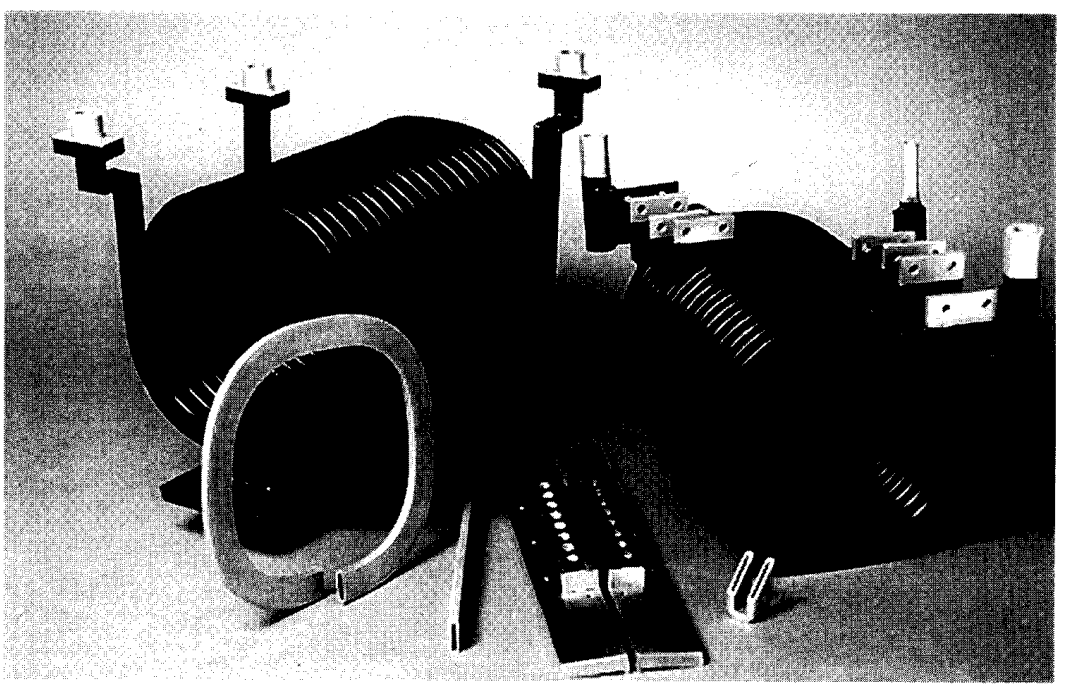

Figure 8.52 Epoxy-encapsulated windings of transformers. (Courtesy of Jackson Transformer Company.)

referred to as fishtails. The input side of the transformer, the primary winding, is tapped to cover the required turns ratio. The windings use rectangular copper tubing of the thin wall, which is acceptable because penetration depth of the current into copper at 10 kHz is only 0.7 mm (0.028 in.). A typical profile of the tubing used would be 6.35 mm × 25.4 mm × 1.2 mm (0.25 in. × 1 in. × 0.048 in.) wall. The primary and secondary windings are of an interleaved design to take advantage of the shape of the tubing and to reduce the resistance and impedance of the transformer. One of the unique features of this design is that the losses in the primary and secondary windings are equal. For a typical 22:1 ratio transformer there are 22 primary turns in series and there are 22 secondary turns connected in parallel in a one-turn construction.

The construction of the core uses thin permeable steel 0.15 or 0.18 mm thick (0.006 or 0.007 in.) of EE or EI-type laminations as shown in Figure 8.53. The core is water-cooled by means of copper cooling plates sandwiched between the steel laminations. It has been concluded after many tests that the flux generated by the ampere-turns in the magnetic circuit flows along the inside legs of the laminations just as current in a circuit takes the least resistive path. Therefore, the width of the outside legs of a shell-type transformer operated at medium frequencies can be less than one-half the tongue (center leg), as is required for low-frequency designs. The core losses of the outside legs will be higher than the losses of the center leg, which is acceptable, because the outside legs are cooled more effectively than the center. The core loss of the transformer varies as the square of the input voltage, inversely

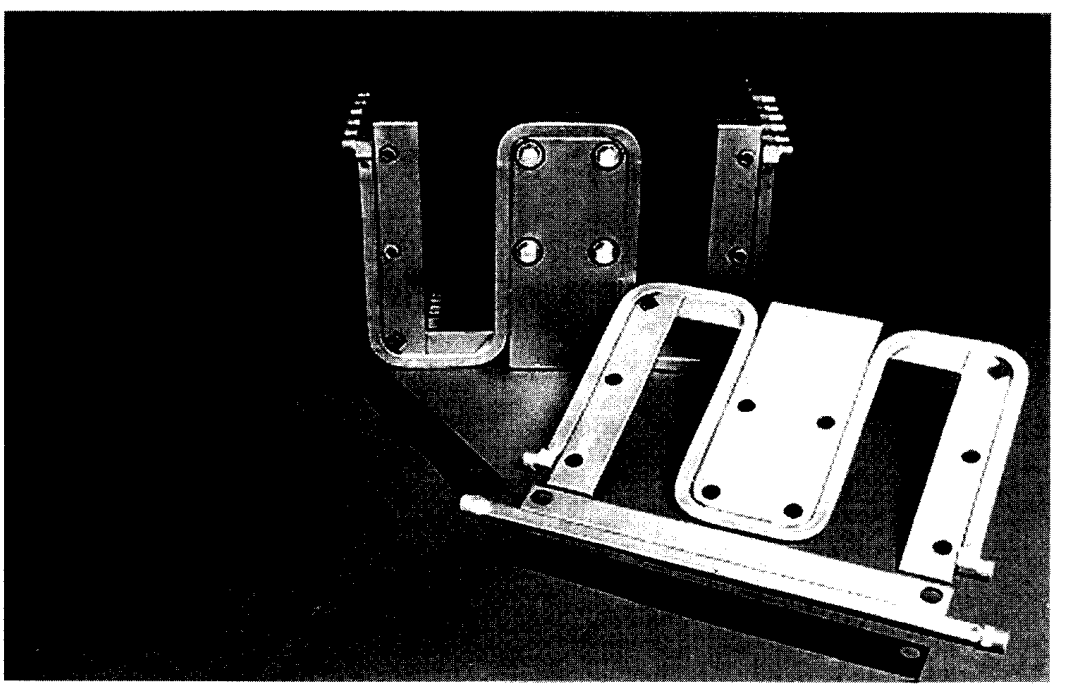

Figure 8.53 Thin permeable steel laminations (0.15–0.18 mm) are used for construction of transformer cores. (Courtesy of Jackson Transformer Company.)

as the square of the input turns, and approximately as the fourth root of the frequency.

8.5.4 Ferrite-Core Transformers

Ferrite-core transformers are similar to laminated core heat station transformers in that they can have an interleaved winding construction. The main difference is that in place of the steel laminations used in the core, ferrite material is used. The electrical resistivity of ferrites is much higher than laminations resulting in lower eddy current losses in the ferrite cores. Having a homogeneous ceramic structure and inherent low core loss, the ferrites are very attractive for transformer applications at frequencies above 10 kHz. Even though the ferrite core loss is low, they may still need to be water-cooled in some cases, because of the high frequencies at which they are used. In applications when the output power from the power supply is fairly low and the frequency is under 10 kHz, ferrites are more advantageous than steel because of the lower loss of the ferrite.

Another design of the ferrite core isolation transformer utilizes Litz wire for the primary winding on a water-cooled copper secondary. This construction has two noteworthy advantages. The primary has very low losses at high-frequency because the Litz wire minimizes skin and proximity effects. Secondly, the Litz wire primary is indirectly cooled by the secondary but is not in direct contact with the cooling water. This means that low conductivity cooling water is not required and the primary will not be affected by electrolysis.

8.5.5 Toroidal Transformers

Typically toroidal transformers are totally encapsulated as shown in Figure 8.54 and are used in through hardening, tempering, forging, and annealing. Normally the output voltages are higher than in the heat station transformers. In many instances the output voltage is equal to or much higher than the applied voltage. Input voltages can be from 100 to 2000 V or higher. The output voltages can range from 50 V to several thousand volts. Taps are provided within the voltage range. The frequencies can be from 200 Hz to 10 kHz. The kVA can range from 50 to 3000 kVA or higher. They are more efficient than laminated transformers and have virtually no air gaps. A disadvantage of being encapsulated is that they are not easily repaired and therefore are usually replaced when they fail.

Toroidal autotransformers are typically smaller in size and have lower exciting current, better regulation, and higher efficiency than an isolation transformer. This is because in an isolation transformer all the kVA are transferred to the secondary, whereas in an autotransformer only a portion of the total kVA is transformed; the rest flows directly from the primary to the secondary without transformation. The windings in an autotransformer are wound around the same core and are used to step up or step down the input voltage. The core of toroidal transformers consists of thin steel strip wound in a cylindrical or toroidal form. Water-cooled copper heat sinks are used on the flat surface of the cores to carry away the heat generated by the core. Without water-cooling, the physical size of the core would increase drastically. The windings are hand-

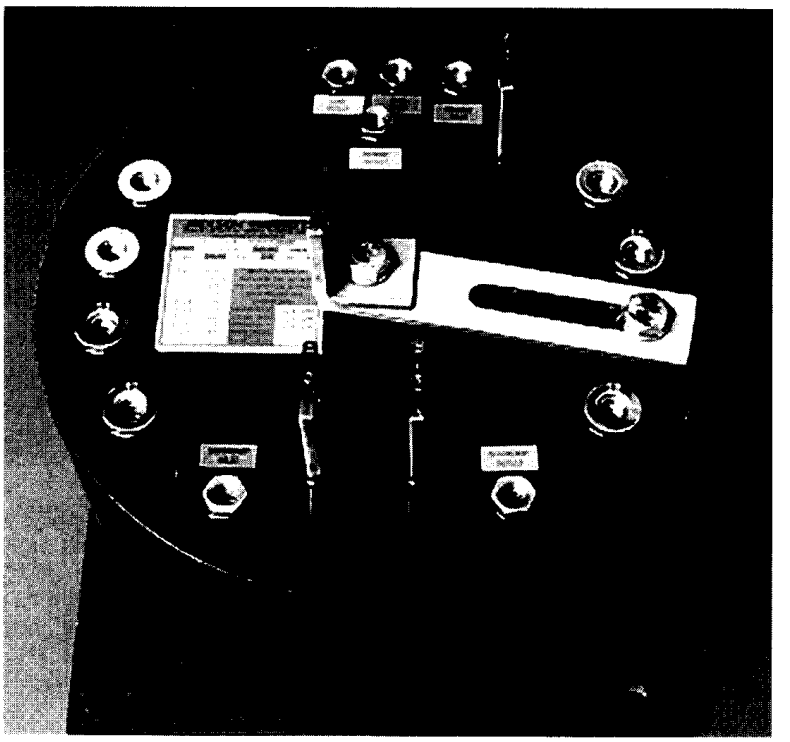

Figure 8.54 Totally encapsulated toroidal transformer. (Courtesy of Jackson Transformer Company.)

wound over the core, using round copper tubing, its size being determined by the design current.

8.5.6 Integrated Magnetic Transformers

The Jackson Transformer Company has developed and patented a method of combining a transformer and inductor in a single package whereby the inductor and the primary of the transformer have a common core [346]. This product is referred to as a transinductor and can be designed to provide a fixed inductance in the primary or secondary or both. Variable ratios can be provided on the transformer portion. By combining the two components the size of the product is reduced, the overall efficiency is increased, and the leakage flux of the magnetic device is minimized.

8.5.7 Rectangular (C-Core) Transformers

The construction of a rectangular transformer uses a C core and interleaved windings. Normally, the unit is epoxy-encapsulated as shown in Figure 8.55. The design of the rectangular core transformer is usually for low to medium frequency with input voltages from a few hundred to a few thousand volts, output voltages from a few hundred to a few thousand volts, and input power up to several thousand kilovolt amperes. Specific requirements for this type of transformer are low leakage, low inductance, and high efficiency.

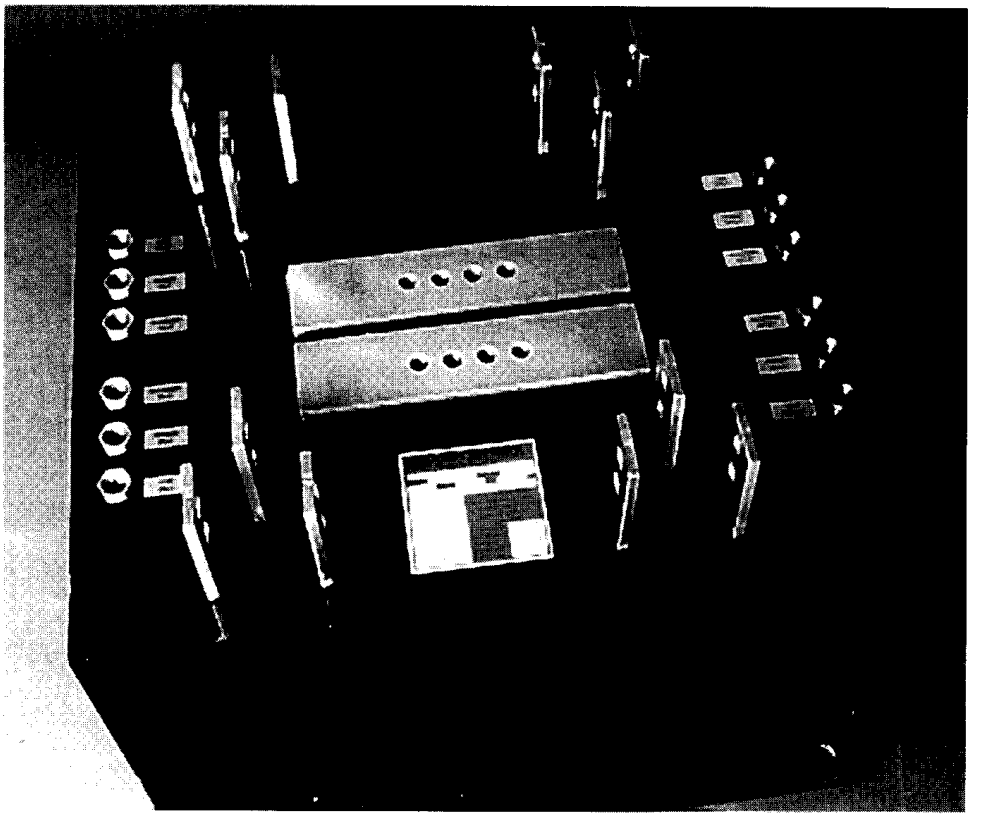

Figure 8.55 Rectangular (C-Core) transformer. (Courtesy of Jackson Transformer Company.)

8.5.8 Narrow-Profile Transformers

Narrow-profile transformers are designed to deliver high-power at medium frequencies within narrow physical constraints. A typical example as shown in Figure 8.56 is used for the rotational induction heating of bearing surfaces on an engine crank shaft. A series of narrow-profile transformers can be placed side by side for simultaneous induction heating of a number of different bearing surfaces on an engine crank shaft. The construction of this style of transformer uses the interleaved winding design and ferrite cores and is epoxy-encapsulated. This allows the transformer to achieve its narrow-profile, high-efficiency, low-leakage inductance and be completely protected from its harsh environment and physical abuse.

8.5.9 Air-Core Radio Frequency Transformers

The air-core radio frequency (RF) transformer shown in Figure 8.57 is normally referred to as a current transformer and is designed without any core material. The critical element in the design is to obtain the highest current transfer ratio from primary to secondary. Generally, the primary winding is encapsulated silicon rubber, which is a moisture-resistant material. This is required to prevent corona and voltage

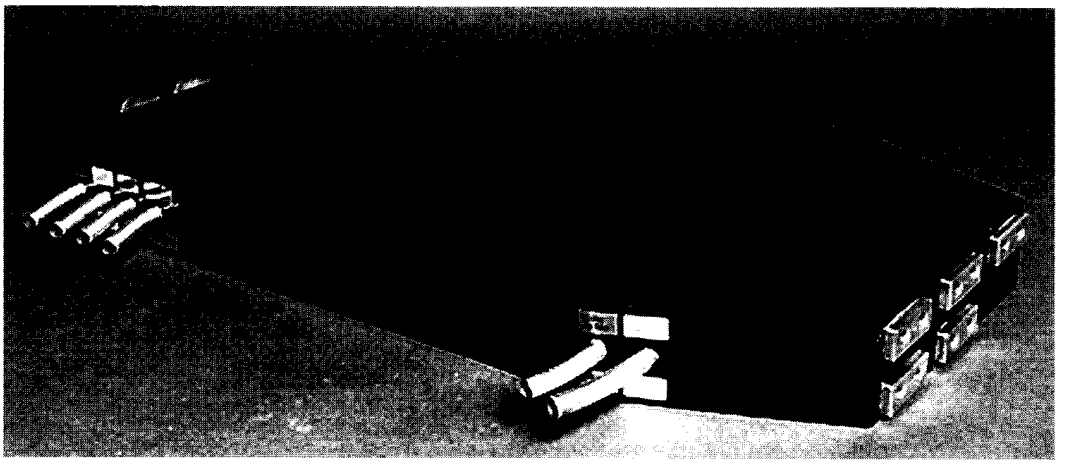

Figure 8.56 Narrow-profile transformer. (Courtesy of Jackson Transformer Company.)

breakdown because of the high dielectric stress between the primary and secondary. It is also required to protect the windings from the environment. Great care must be taken in the selection of material and construction. Manufacturing of this transformer is usually performed in a cleanroom environment.

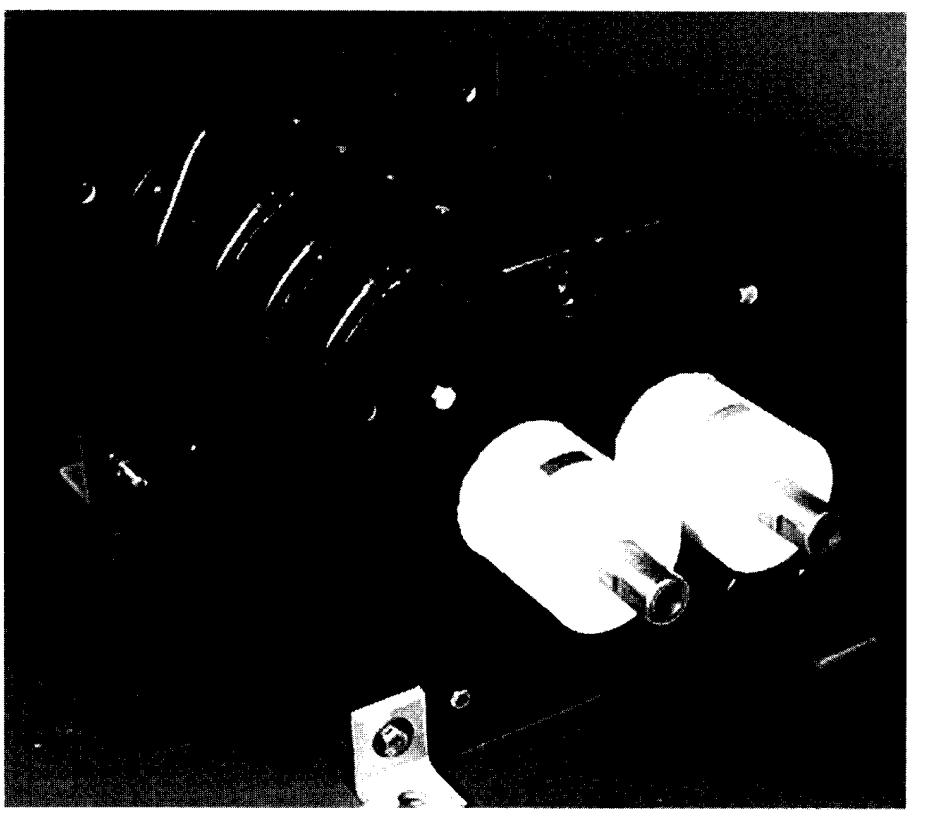

Figure 8.57 Air-core radio frequency (RF) transformer. (Courtesy to Jackson Transformer Company.)

8.5.10 Maintenance, Sizing, and Specification of Transformers

As a general rule, when transformers are water-cooled, most failures occur because of a breakdown of the insulation between the windings. Normally, this is due to lack of water, poor quality water, too high a water inlet temperature, or operation of the transformer outside its designed rating. Sometimes insulation breaks down because of the harsh environment to which the transformer is subjected. Another failure that commonly occurs is the melting of the output connection (fishtail). This can be caused by improper tightening or poor maintenance of the inductor (e.g., dirt or oxidation on the mating surfaces of the inductor or fishtail). Occasionally the core may fail due to lack of water, poor quality water, too many input volts per turn (voltage per turn exceeds core loss temperature limitation), and use at the wrong frequency. A well-designed water system will pay for itself with reductions in component failures and downtime. Proper maintenance of the inductor-to-transformer connections will also help greatly.

To properly size or specify a transformer this information is generally required:

- Input voltage to the transformer, power source wattage; the frequency range of the power source, and the frequency at which the transformer will operate;
- The turns ratio or the output voltage required at full load (or no load);
- The input kVA at the minimum and maximum turns ratios; and
- The expected efficiency (based on the kilowatt rating of the power source) or loss of the transformer.

It is also helpful to know any unique characteristics of the power source, type of waveform, and if any direct current will be present. The more information the designer has available, the more assurance the customer has of getting the proper, most efficient transformer.

8.6 SPECIAL CONSIDERATIONS FOR POWER SUPPLIES

As described in previous chapters there is a wide variety of induction heat treatment processes. These include selective surface hardening, annnealing, tempering, stress relieving, and through hardening. Prior to the use of induction heating these processes were accomplished by batch heating in a furnace. Induction heating allows for inline heat treatment using machines with these special power supply considerations:

- Less than 50% duty cycle,
- Rapid cycling of heat on and off,
- Precise control of power and time, and
- Minimum utilization of floor space.

8.6.1 Duty Cycle

The induction heat treating cycle in most cases consists of time to load the individual part or workpiece and move to the heating position, heat, quench, and unload the part. The heating portion of this cycle is usually less than 50% of the total cycle. This means that some portions of the power supply can be designed to safely take advantage of lower average losses that result from less than continuous duty operation.

The most significant factor is the sizing of the cooling system required for the power supply. This is discussed in more detail in Section 8.13 later in this chapter. Components of the power supply that heat and cool relatively slowly including the load-matching transformer and the internal interconnect cabling or bus bars; the DC choke can also be sized to take advantage of limited duty cycle operation. Some components such as power semiconductors, fuses, and circuit breakers cannot be derated because of a low duty cycle.

8.6.2 Rapid Cycling of Heat On and Off

The semiconductor modules of transistors and diodes used in many modern induction heating power supplies are subject to power cycling failure. During each cycle the semiconductor chip heats and cools, causing stress due to the thermal cycling: the higher the power dissipation in the semiconductor, the greater the change in temperature and the higher the thermal stress. Semiconductor manufacturers provide curves, as shown in Figure 8.58, that relate temperature excursion to the number of cycles that can be expected before failure. This means that the rating of the power semiconductor modules in terms of power supply output power must be less for a cycling operation than for continuous duty operation.

8.6.3 Precise Control of Power and Time

The heating time in many induction heat treating applications is very short to avoid conduction of heat outside the desired hardness pattern area. In contour hardening, for example, heat times of less than one second are common. This means that the control of heat time must have high resolution (typically 0.001 sec), and be repeatable and accurate. It also requires that the time required by the power supply to ramp up to set power at heat on and down at heat off must be short and repeatable.

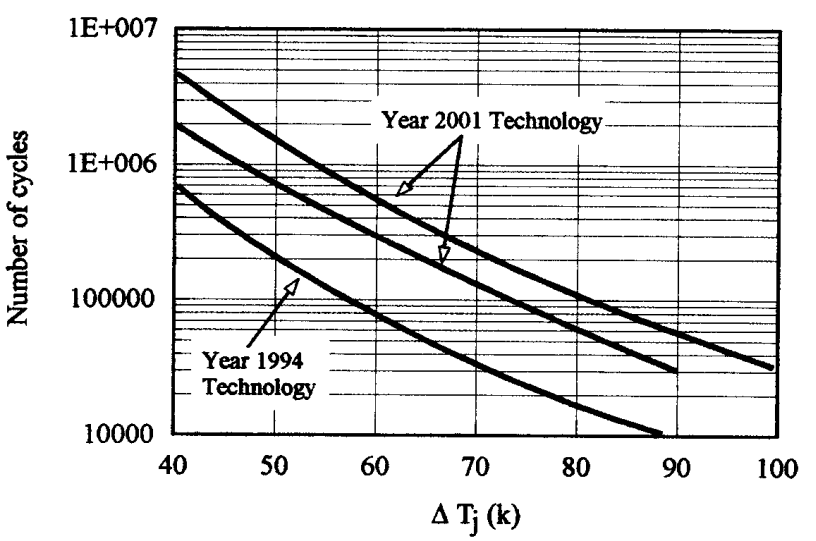

Figure 8.58 Power cycling of IGBT modules (accelerated reliability testing of IGBT modules)

8.6.4 Minimum Utilization of Floor Space

During the last years of the twentieth century, manufacturers of induction heat treating equipment made significant progress in developing highly efficient, compact heat treating systems [241]. The space savings were achieved by technical innovations in the area of electrical power devices, electronic systems, and equipment design. Many new induction heating power supply designs were introduced during this same time period. Most of these designs use relatively new MOSFET or IGBT fast switching power transistors. Other factors, which have also had a significant influence on the ability to conserve existing heat treat shop floor space, are improvements in concept and the continued growth of microprocessor technology resulting in sophisticated control/monitoring systems.

In general, transistorized power supplies are much more compact than the equivalent thyristor or vacuum tube equipment. For example; a newly developed heat station power supply shown in Figure 8.59 [357] is a 150 kW, 30 kHz, IGBT power supply that includes the inverter, heat station, load-matching transformer, and capacitors. It measures only 0.6 m × 0.6 m × 1.3 m (24 in. × 24 in. × 51 in.) and mounts on a standard heat station base.

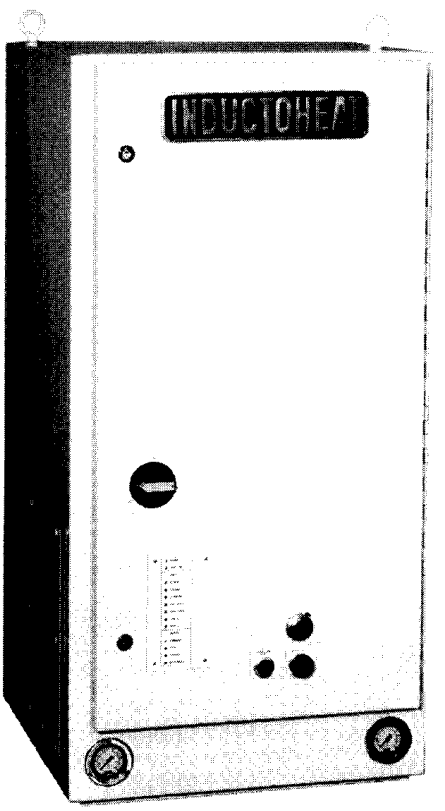

Figure 8.59 Transistorized induction heat station power supply Statipower hsps. 3, 10, and 30 kHz frequency with output power ratings of 25 through 200 kW.

The heat station power supply has had a major impact on the design of modern multistation automatic induction heat treating machines. In the past, the power supplies and their cooling water recirculating systems were mounted on a balcony above the machine to conserve floor space and minimize the distance between the power supply and its heat station. The new generation of power supplies has increased the power density from 1.0 to closer to 10 kW/ft^3. This has made a huge difference in the space requirements for induction heating machines.

Applications that in the past required expensive platforms and consumed large amounts of costly floor space can be done in less than half the space with no overhead clearance requirements. Figure 8.60 illustrates this dramatic reduction in size and complexity by photographically superimposing a new INDUCTOHEAT machine that uses transistorized HSP12 heat station power supplies for heat treating CV joints over the previous (1995) balcony-style system.

The transistorized heat station power supply is also used in compact cells such as the dual position cam shaft hardening cell shown in Figure 8.61. Two HSP12 200 kW/30 kHz heat station power supplies each provide power to two heating positions.

As one can see from Figure 8.62, INDUCTOHEAT's cam shaft hardening machine built in 2000 requires less than 15% of the shop floor space of a similar machine built in 1994. An appropriate combination of the design parameters such as frequency, power density, coil geometry, and so on, allows the heat treating practitioner to optimize system efficiency, minimize cam shaft distortion, and obtain the required hardness profile.

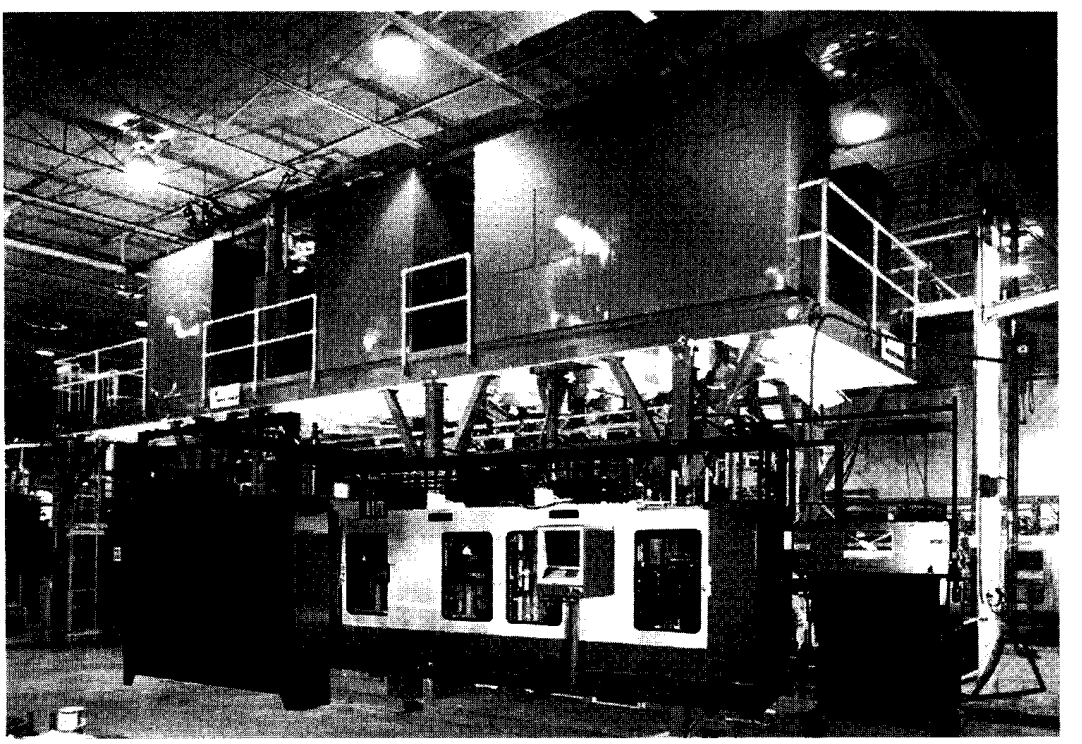

Figure 8.60 CV joint heat treating system with heat station power supplies superimposed over a similar system with balcony-mounted SCR power supplies.

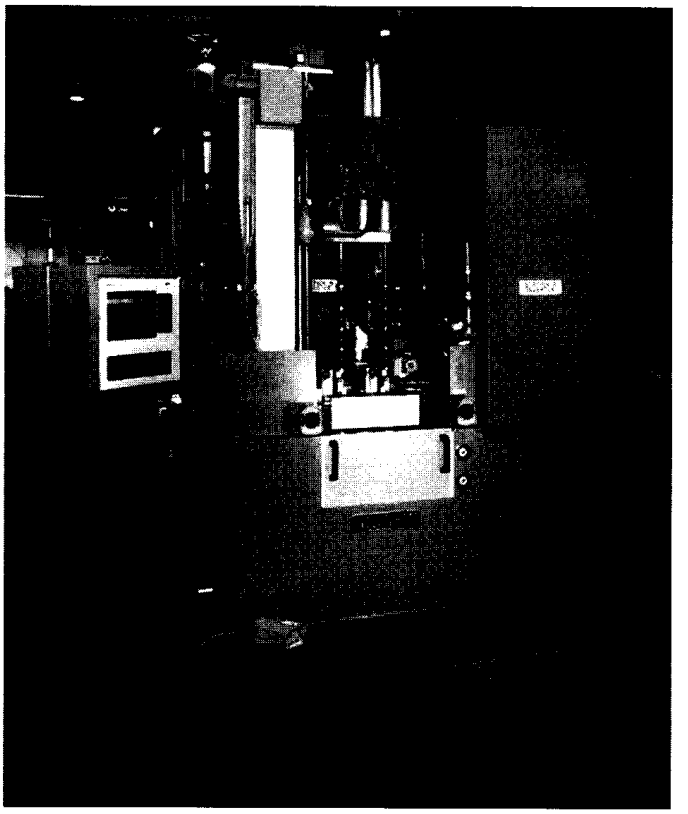

Figure 8.61 Heat treat cell for cam shaft hardening with two heat station power supplies. (Courtesy of INDUCTOHEAT, Inc.)

Other induction heat treating machines such as the Statiscan IV pictured in Figure 8.63 integrate all necessary functions including machine control, quench and cooling, process monitoring, and the power supplies into one unitized enclosure [358]. This general-purpose scan hardening machine has two transistorized power supplies each up to 300 kW at frequencies from 3 to 200 kHz.

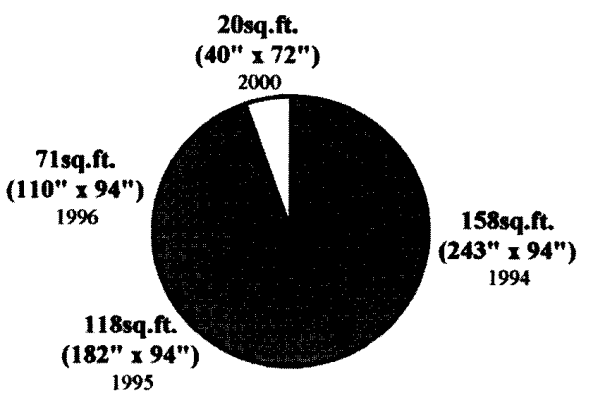

Figure 8.62 An evolution of the floor space requirements for cam shaft hardening machines. (Courtesy of INDUCTOHEAT, Inc.)

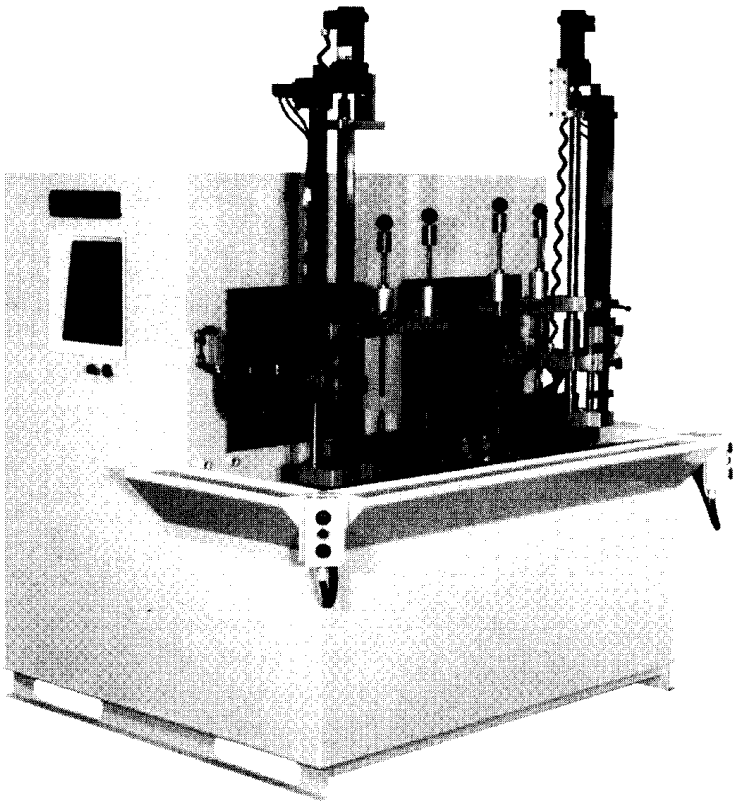

Figure 8.63 Unitized four-spindle vertical-scanning system for mid- and high-volume production, Statiscan-IV. (Courtesy of INDUCTOHEAT, Inc., Madison Heights, MI.)

The tempering process takes place after the part is hardened. The main purposes of tempering are to increase the steel's toughness, yield strength, and ductility; relieve internal stresses; improve homogenization; and decrease brittleness of the part.

It is important that the time from quench to temper be held to a minimum. If this "transient time" is long enough, the internal stresses may have enough time to allow shape distortion or cracking to take place. Therefore, a long transient time between quenching and tempering will decrease or eliminate the tempering benefits. Due to the desire to minimize that transient time, the tempering machine should be located near the induction hardening machine. Therefore, the problem of effective use of available floor space is very important in tempering by induction. In order to achieve efficient utilization of shop floor space, induction tempering is often accomplished as part of the hardening machine or as a separate machine located with the hardening equipment. As an example, Figure 8.64 shows a machine for inline induction tempering of constant velocity joints. The compact design of this machine is its primary advantage.

These advances in transistorized power supply design are only one factor in the space efficiency issue. As mentioned above, other factors involved are continued growth of microprocessor technology and innovations in design concept and mechanical components.

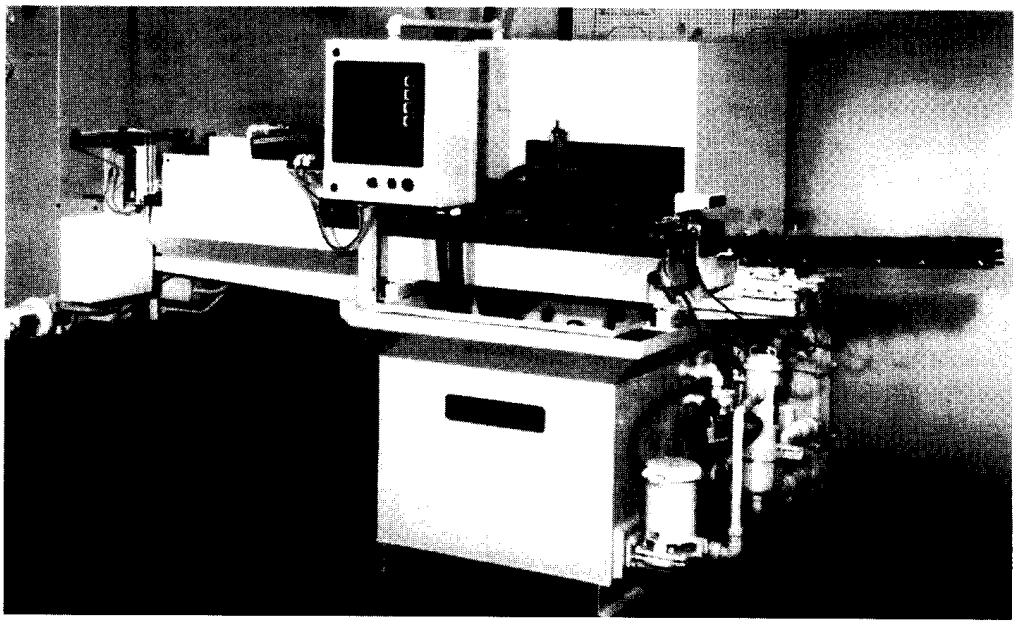

Figure 8.64 Unitized inline induction tempering machine. (Courtesy of INDUCTOHEAT, Inc.)

Equipment design has become holistic. The equipment now consists of a minimum of components and is more reliable, compact, and easier to operate and maintain. By designing with the whole system in mind, the floor space can be best utilized. For example, if the whole machine is more compact, the distance over which the water is pumped is shorter and the pump sizes can be smaller. All of these items work to the advantage of the purchaser by keeping cost and floor space to a minimum.

8.7 SPECIAL CONSIDERATIONS FOR INDUCTION BRAZING, SOLDERING, AND BONDING

The application of induction heating for joining operations including brazing, soldering, and bonding has been discussed in Section 6.1. The power supplies used for these applications have these special requirements and operational considerations:

- Low power,
- Medium to high-frequency,
- Small size, often portable,
- Load-matching flexibility,
- Load Q is typically high, and
- Operator manipulation of the heating coil is often required.

Joining operations require the heating of adjacent surfaces so that a filler material can be melted on these surfaces and then allowed to solidify to produce a solid joint. It is important therefore to be able to direct the heat uniformly into the areas to be joined without unnecessarily heating adjacent areas. This is done primarily by heating coil design but is also influenced by the characteristics of the

power supply. The area that is joined by induction brazing or soldering is usually kept small because it is more practical to precisely control the heating of small areas than larger areas. This means that the power required is relatively low, usually in the range from 1 to 50 kW.

Heating of only the surface of the workpiece implies, as discussed in previous chapters, that the frequency be relatively high. For example, for a penetration depth of 0.5 mm the heating frequency would be about 10 kHz for steel when using low power density at room temperature. To obtain the same penetration depth, 20 kHz is required to heat copper and 70 kHz for brass. An even more compelling reason to use high-frequency for brazing, soldering, and bonding is that the higher the frequency, the smaller the current needed to do the same heating. This means that the heating coil and the conductors carrying current to the coil become smaller at higher frequencies. At the same time the use of a higher frequency means magnetic components such as transformers used in the power supply and for load-matching at the heating coil can be made more compact and lighter because smaller magnetic cores can be used. Thus the use of high-frequency allows for the use of smaller, lighter, and more portable equipment while providing the shallow heating required by the application.

In many applications of brazing and soldering the process must accomplished in a confined and often difficult to reach location. A small portable power supply such as the 5 kW unit shown in Figure 8.65 may be hand-carried and placed where the heating is to be performed.

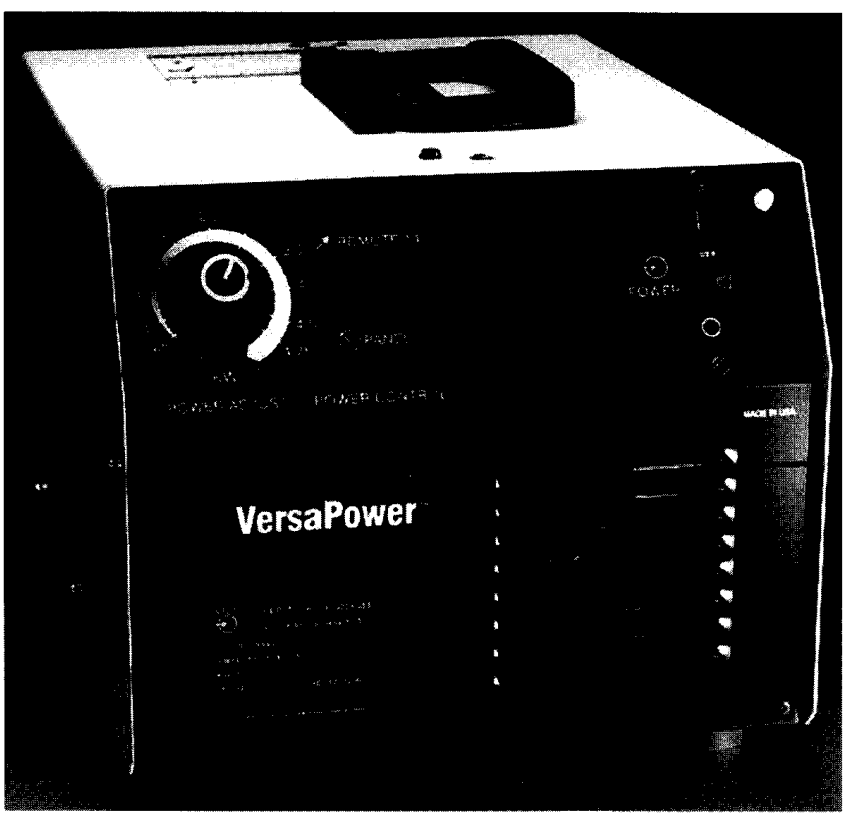

Figure 8.65 VersaPower power supply (MOSFET Bench Top) for 10 to 50 kHz applications. (Courtesy to Radyne Corp.)

Induction heating power supplies designed for brazing and soldering are capable of matching a wide variety of heating coils. Brazing and soldering coils are often fabricated by forming copper tubing around the part to be heated and then bending it by "cut and try" to obtain the desired heating pattern. Figure 8.66 shows the different sizes and shapes that are commonly used for this application.

Many of these coils have very loose coupling to the workpiece and often heat nonmagnetic material, which results in a high Q load. This means that the power supply must be capable of providing a high output kVA to kW ratio.

As explained in Section 8.3.2.5 the current-fed inverter easily will match high Q loads because the output circuit is parallel resonant and the high kVA is provided by the load capacitor rather than the power supply. The Radyne Flexitune shown in

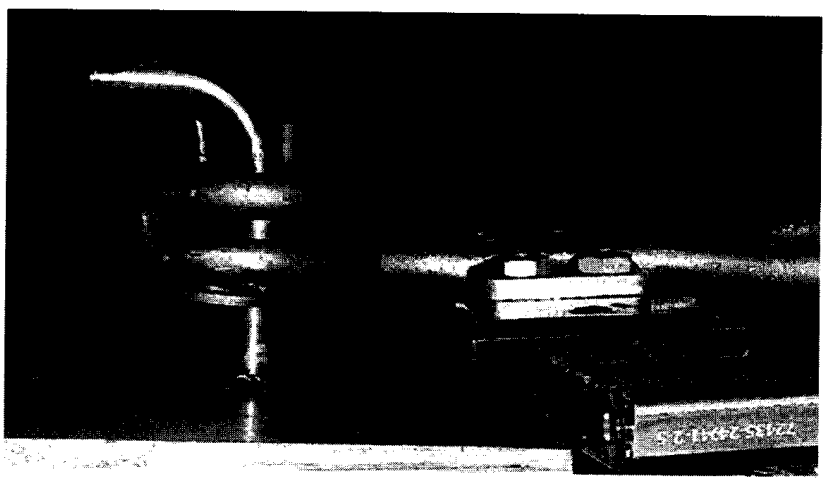

Figure 8.66 Brazing/soldering inductors.

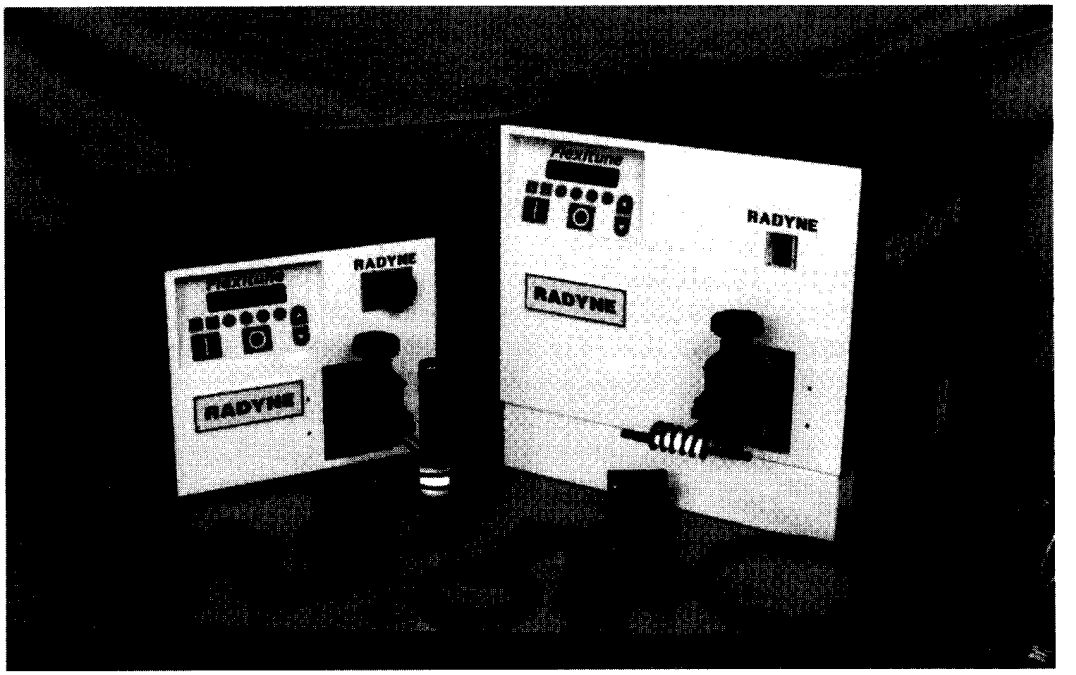

Figure 8.67 Radyne flexible general-purpose IGBT power sources for a wide variety of applications. Coil display illustrates flexibility of load matching: smaller cabinet, 5 or 10 kW at 20 to 60 kHz; larger cabinet, 15 at 20 to 60 kHz, 30 kw at 20 to 40 kHz.

Figure 8.67 is a compact current-fed power supply designed for low-power high Q applications such as brazing and soldering.

8.8 SPECIAL CONSIDERATIONS FOR INDUCTION HEATING POWER SUPPLIES IN MASS HEATING APPLICATIONS

Prior to 1970 the induction power supply used for heating large billets, bars, or slabs was single-phase line frequency. For somewhat smaller workpieces, frequency multipliers employing saturable reactors were used to provide 180 and 540 Hz. Still smaller billets, bars, and slabs required even higher frequencies that could only be provided by motor generator sets. Popular frequencies for these MG sets were 1, 3, and 10 kHz. In the late 1960s the development of the thyristor or SCR made practical solid-state power supplies for generating frequencies from 90 Hz to 10 kHz. By the mid 1980s power transistors became available that made possible the development of medium- and high-frequency transistorized induction heating power supplies.

The choice of which kind of power supply (thyristorized or transistorized) for mass heating depends primarily upon the frequency required but also upon the specific application. Transistorized power supplies are especially cost effective at frequencies of 10 kHz and above. In general, for these frequencies the transistorized power supplies are much more compact than the equivalent thyristor-type power supplies. Figure 8.68 shows a 1200 kW, 30 kHz transistorized power supply used for heating rods prior to coiling and quenching to make automotive coil springs. It

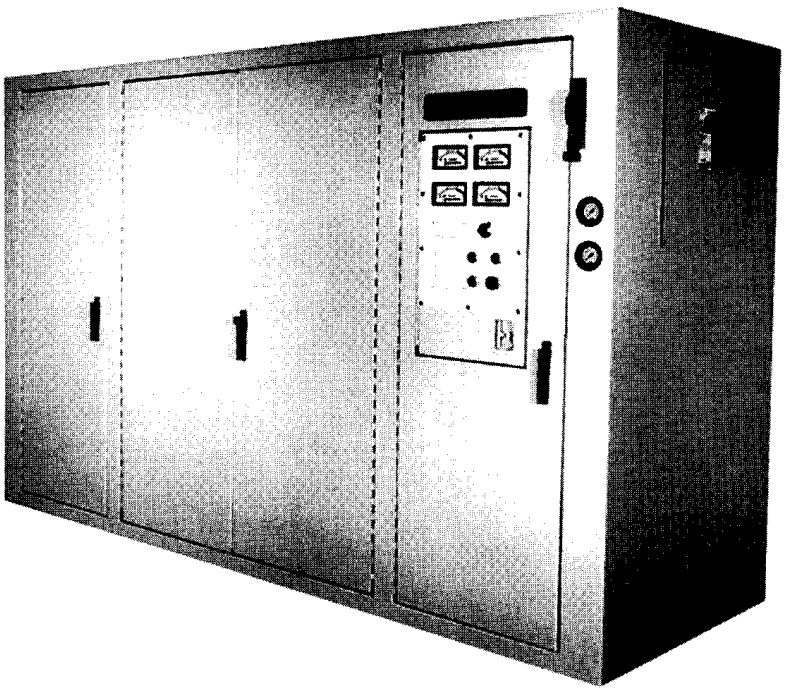

Output power at 30kHz	Input kVA (max.)	Water reqd. for 25psi pressure drop	Dimensions W x D x H in. (mm)	Shipping weight Pounds(kg)
400kW	525kVA	44 gpm (167 lpm)	72x36x90 (1829x914x2286)	2000 (907)
800kW	1050kVA	70 gpm (265 lpm)	100x36x90 (2540x914x2286)	3200 (1452)
1200kW	1575kVA	90 gpm (341 lpm)	100x36x90 (2540x914x2286)	4200 (1905)
1500kW	2000kVA	105 gpm (477 lpm)	138x36x90 (3505x914x2286)	5100 (2313)

Figure 8.68 High-power transistorized induction heating power supply Statipower SP-14: 30 kHz with models from 400 kW to 1.5 MW output power; 400 to 2000 V output voltage. Remote control can be accomplished by connection to the user interface provided. (Courtesy of INDUCTOHEAT, Inc.)

measures 0.91 m deep × 3 m wide × 2.3 m high (36 in. × 120 in. × 90 in.) and includes the IGBT inverter, load-matching isolation transformer, and load-resonating capacitors. Both technologies are used at 3 kHz, with SCRs still dominant at the higher power levels.

The induction heating power supplies used for most mass heating prior to forming applications have in common these characteristics:

- Low to medium frequency of operation,
- High power,
- Continuous duty,
- High efficiency, and
- Harsh operating environment.

As discussed in Chapter 7, selecting the optimum frequency is essential to minimize line length and output temperature differential surface-to-core. In some very high production applications use of more than one frequency is required. The system shown in Figure 8.69 for heating steel bars for forming grinding balls uses 1 kHz at the beginning of the line for heating the bars up to the Curie temperature. At this temperature the steel becomes nonmagnetic and the depth of penetration increases dramatically. The remainder of the coil line at the exit end is powered by 3 kHz to maintain high electrical efficiency. In this system the bars ranged from 38 to 50 mm (1.5 in. to 2 in.) in diameter and were heated to forging temperature at a rate of 7484 kg/hr (16,500 lb/hr).

Heating prior to forming requires uniform through heating of the workpiece and therefore demands much higher power than surface heat treating processes. Heating of small bars and billets (Figure 8.70) or small bar end heating systems (Figure 8.71) may require 100 kW or less at 10 or 30 kHz. However, most forging applications need at least 250 kW, although 1 MW power supplies are common. Heating of large slabs often requires multiple power supplies each producing many megawatts. One such system, shown in Figure 8.72, for heating carbon steel slabs (3.2 m/126 in. wide by 0.22 m/8.7 in. thick at 540 tons/hr), consists of seven coils each powered by a 6 MW power supply.

Heating of billets, bars, and slabs is most often a continuous process and therefore does not require derating of the power semiconductors as in power supplies

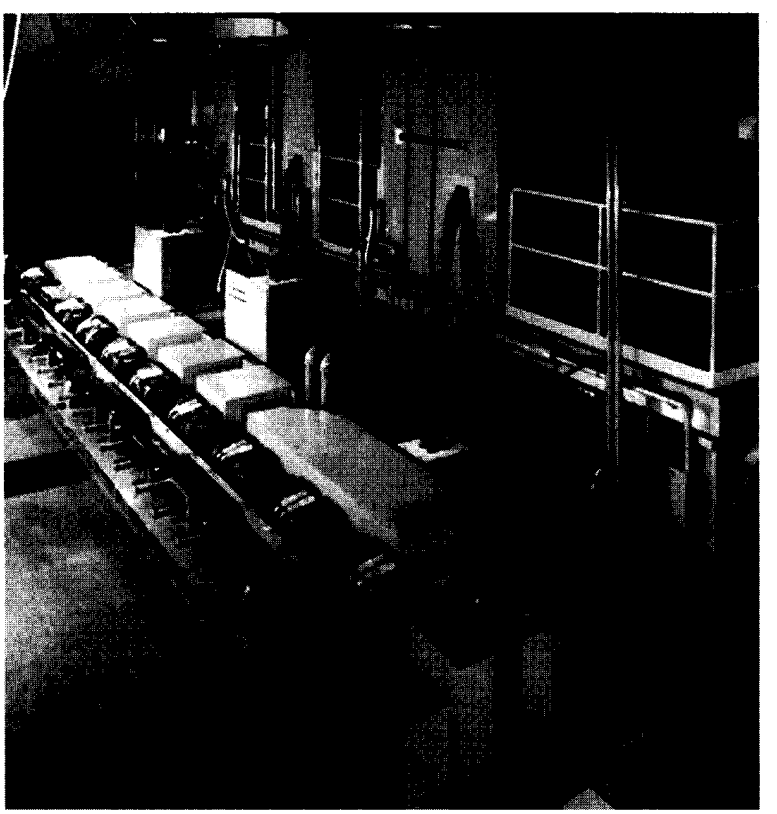

Figure 8.69 INDUCTOHEAT's dual frequency multicoil induction carbon steel bar heater.

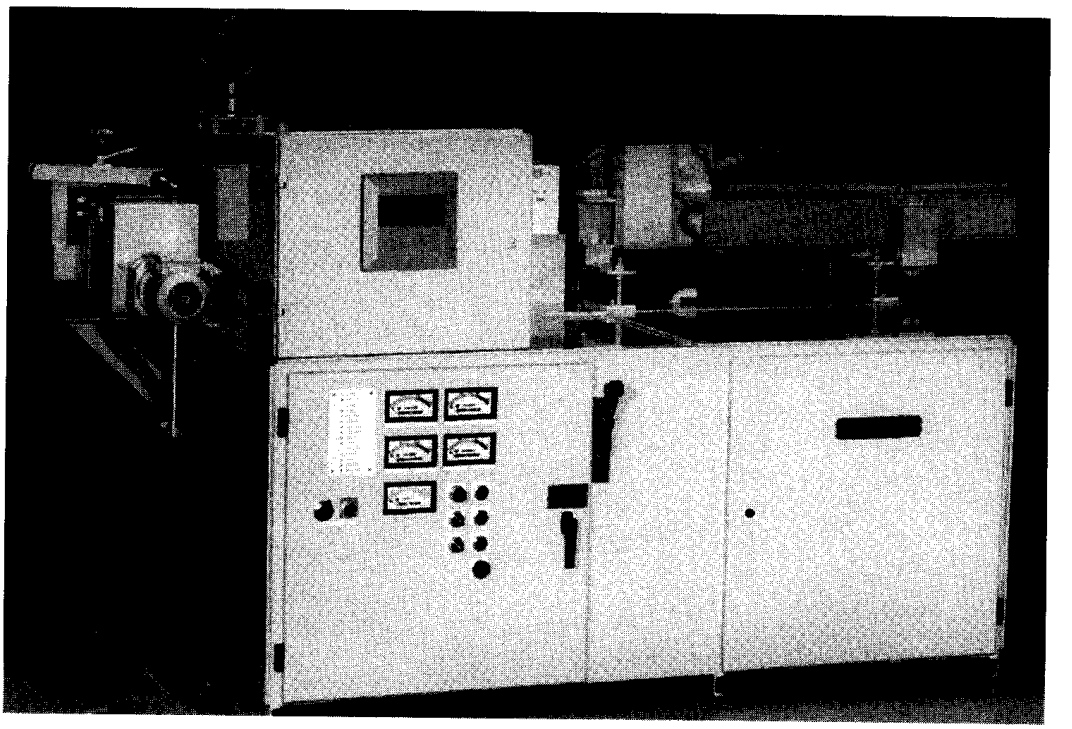

Figure 8.70 INDUCTOHEAT's compact small bar and billet heater.

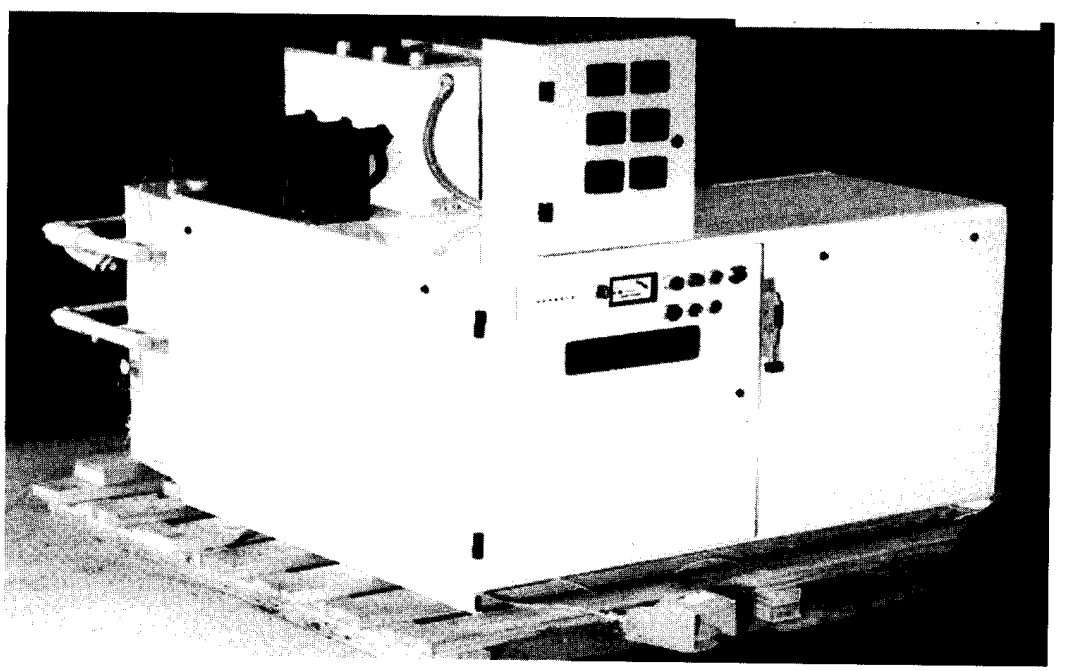

Figure 8.71 INDUCTOHEAT's compact bar end heater.

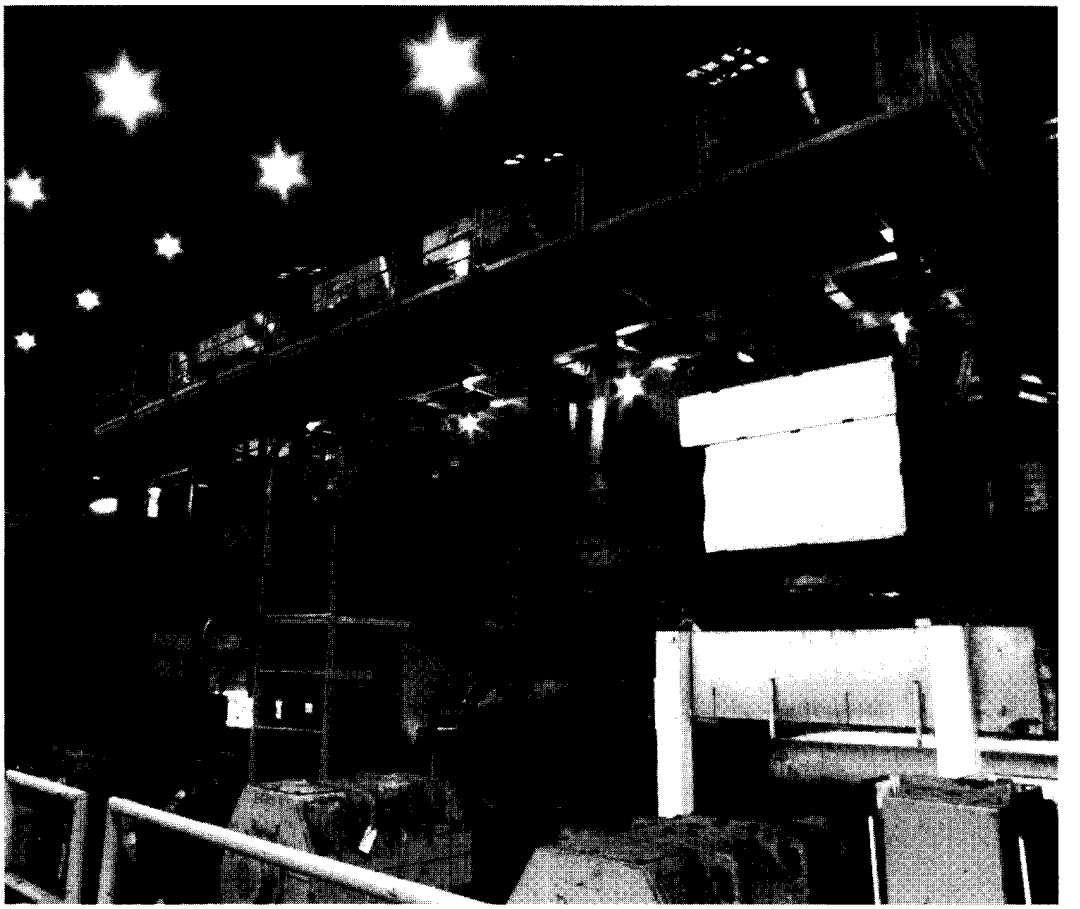

Figure 8.72 Inductotherm's induction heater of the world's largest carbon steel slab.

for induction heat treating. Continuous operation does mean that all components must be rated to operate at full power for many hours without overheating or degraded performance. It is important to note that water-cooled components stabilize at maximum operating temperature in minutes whereas non-water-cooled components may take hours to reach maximum temperature.

Power supply efficiency is very important in mass heating applications because the cost of electrical energy input is a significant portion of the production process cost [255]. The initial equipment cost is higher when low-loss power circuits and components are provided to increase power supply efficiency. This higher initial cost is offset many times over the life of the equipment by lower energy costs.

The operating environment must always be considered in the design of induction heating power supplies. This is especially true in the case of mass heating before forming where conductive dust from scale or die lube is blown through the air and cabinets must be well sealed to prevent this dust from collecting on high-voltage power components. Extremes of temperature are also common especially in cold climates where the lost heat from the heating and forming process is the major source of heat for the facility. The use of antifreeze to cool the power supply and coils may be necessary when the plant is shut down and the temperature is below freezing.

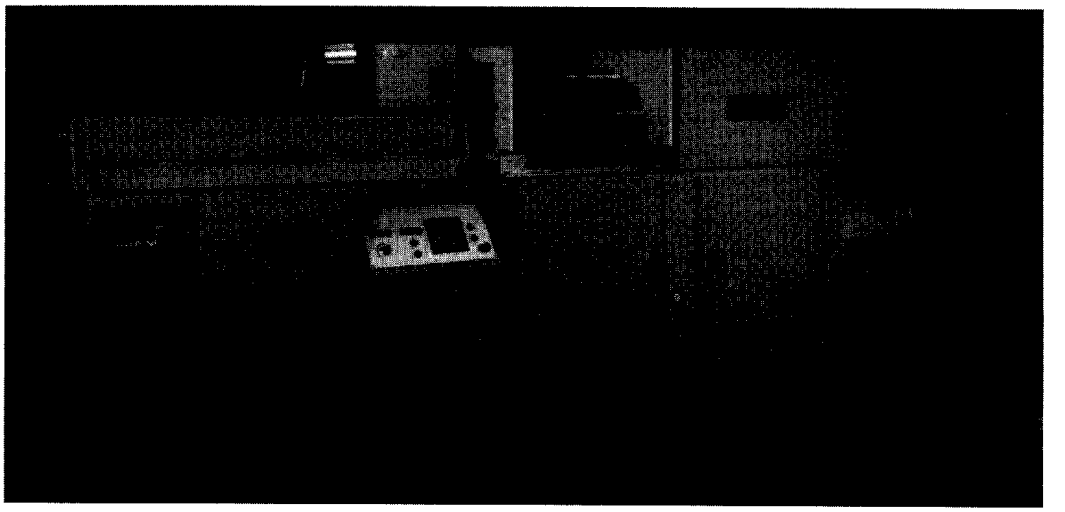

Figure 8.73 Radyne's induction heater for the forging industry.

Modern induction heating systems for forging are designed to minimize the floor space required [256]. The equipment must be at least as long as the heating coil length required to obtain the desired surface-to-core temperature within the workpiece plus infeed and outfeed mechanisms. The power supply and machine control electronics are usually packaged below the coil line resulting in a unitized heating system such as the Radyne ICF shown in Figure 8.73.

8.9 SPECIAL CONSIDERATIONS FOR INDUCTION HEATING POWER SUPPLIES IN STRIP PROCESSING APPLICATIONS

Induction heating of steel strips for galvanizing, galvannealing, galvaluming, annealing, and lower-temperature processes such as paint drying require power supply features most similar to mass heating applications such as forging. As in forging, a large amount of metal (measured in tons per hour) is heated continuously. Here the heating process is not interrupted to change from one role of strip to the next, or even to change strip thickness or width. Power supply efficiency is also very important because the cost of electricity is a large portion of the total process cost.

Strip heating differs from forging by the thickness of the workpiece that is heated. Where forging involves heating of billets, bars, or rods of relatively thick cross-section, in strip heating the workpiece thickness is measured in thousandths of an inch or fractions of a millimeter. This requires application of a much higher frequency to obtain acceptable heating efficiency. In most cases frequencies from 30 to 150 kHz are used.

The induction heating power supplies used for strip heating applications have in common these characteristics:

- Medium to high-frequency of operation,
- High power,

- Continuous duty,
- High efficiency, and
- Unusual and often harsh operating environment.

In some strip heating applications including organic coating and paint drying the strip is conveyed horizontally as shown in Figure 8.74. Here the power supply is adjacent to the heating coil and connected by a short, wide, horizontal bus to minimize voltage drop and power loss.

Induction galvannealing on the other hand is accomplished by passing the strip through a pot of molten zinc and then vertically through one or more heating coils located on a gantry high above the factory floor [246]. As shown in Figure 8.75, the coil and high-frequency inverter portion of the power supply are suspended from a movable gantry. The DC rectifier and control portion of the power supply (Figure 8.76A) is located conveniently on the factory floor and connected to the 100 kHz high-frequency inverter (Figure 8.76B) by low-loss cables that carry only direct current. This is obviously an application-specific design devised to meet the demanding physical requirements of the system while maximizing efficiency and maintainability. A module containing the high-frequency transistorized inverter, heating coil, and interconnecting bus is shown in Figure 8.77. This module is located directly above the pot of molten zinc and is therefore exposed to high ambient temperatures and electrically conductive zinc dust. In some installations this module is completely enclosed and air-conditioned to provide a friendlier environment for both the induction heating equipment and maintenance technicians.

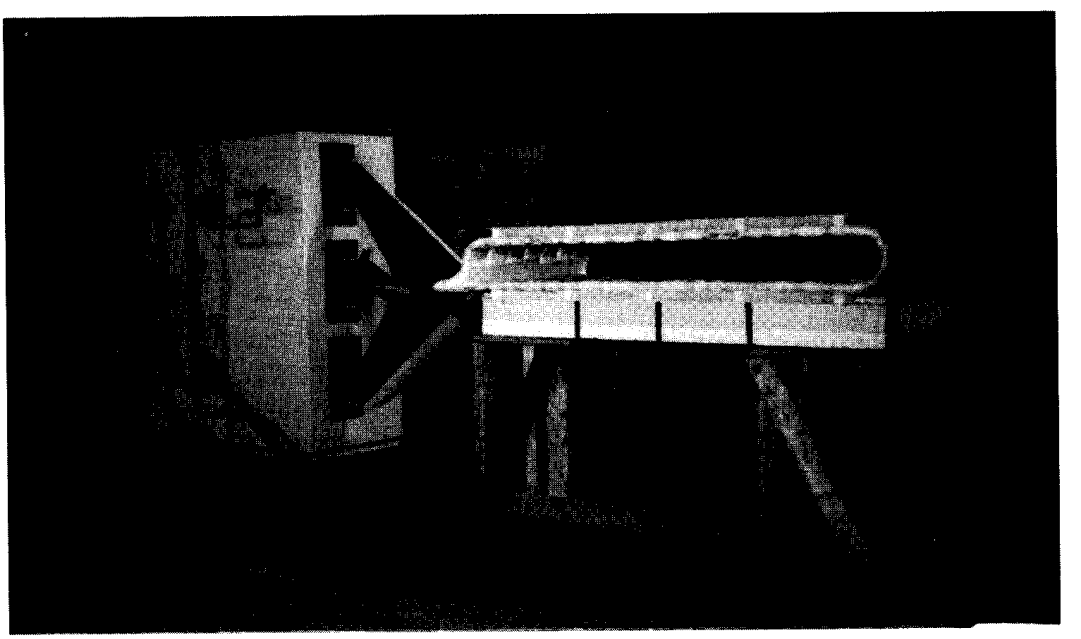

Figure 8.74 INDUCTOHEAT's induction heater of wide strips.

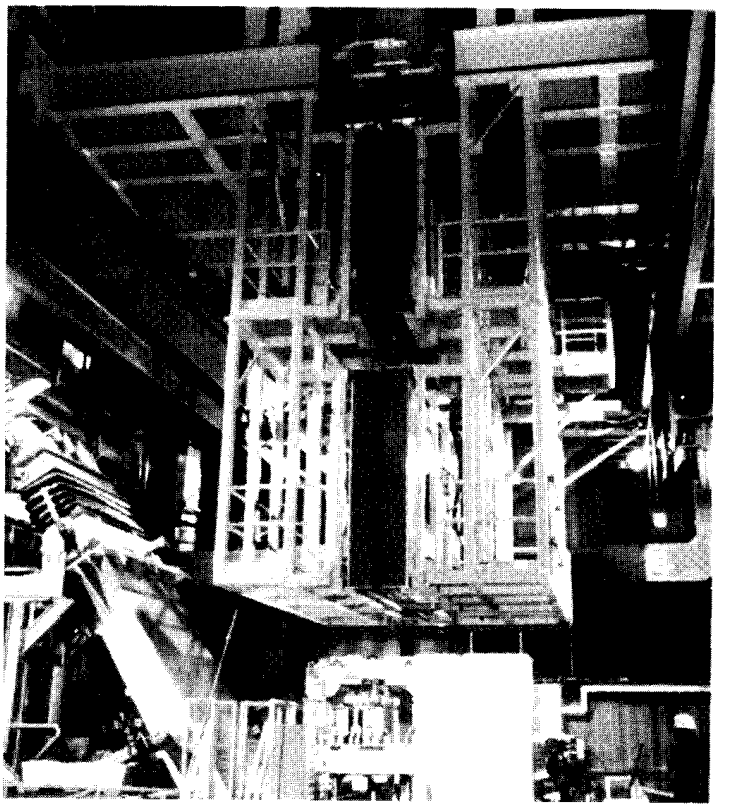

Figure 8.75 High-frequency "doorless" coil and "coreless" coating pot technology.

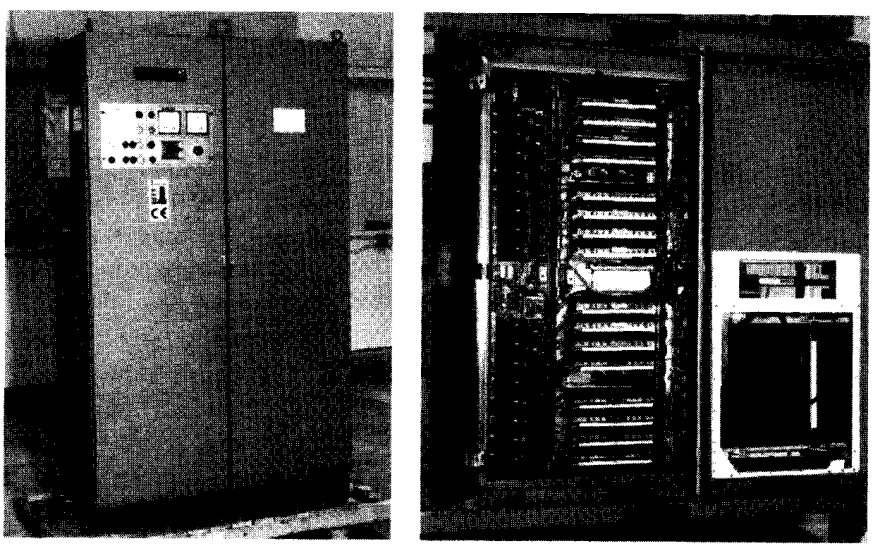

A) DC rectifier and control portion of the power supply

B) High frequency inverter (100kHz)

Figure 8.76 High-frequency transistorized power supply.

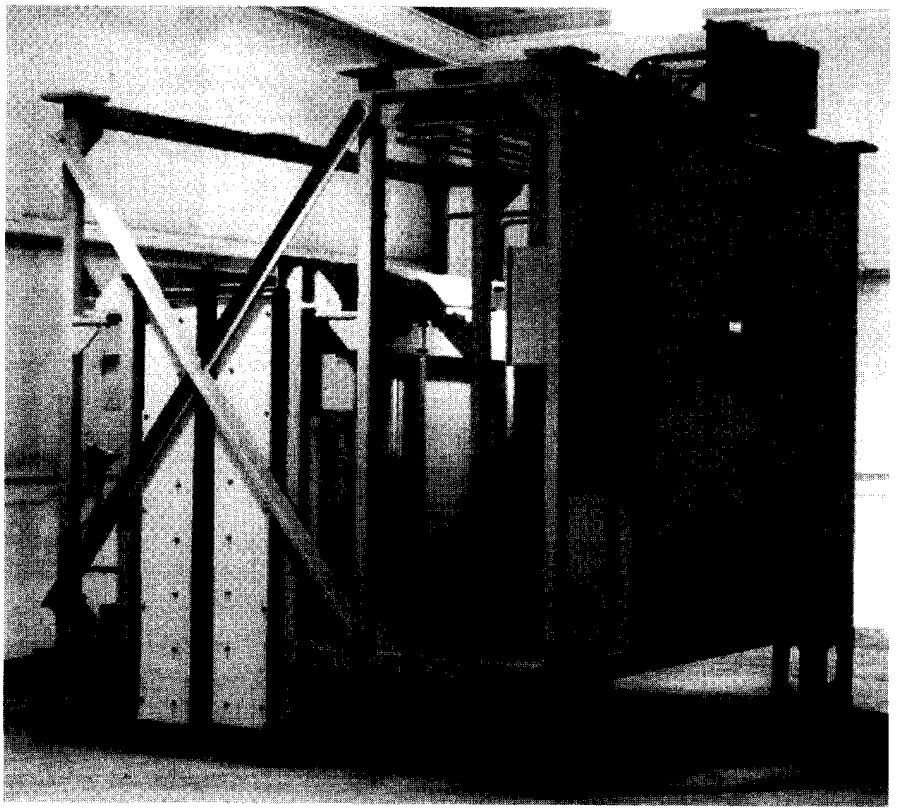

Figure 8.77 A strip heating module contains the high-frequency transistorized inverter, doorless induction coil, and interconnecting high-frequency bus. (Courtesy of INDUCTOHEAT, Inc., Madison Heights, MI.)

8.10 COMPARISON OF SOLID-STATE POWER SUPPLIES AND VACUUM TUBE OSCILLATORS

Prior to 1985, radio frequency vacuum tube oscillators dominated the market for RF induction heating power supplies [247]. The development of new high-frequency semiconductors (MOSFETs, IGBTs, and SITs) and other power components including high kVAR, low-inductance, low loss capacitors, and high-efficiency low-inductance transformers has made possible the design and production of a variety of different types of solid-state power supplies in the 50 to 450 kHz range. Offered initially in smaller kilowatt sizes, the development has continued on to include single power supplies of one megawatt or more. Applications include hardening, strip heating, crystal growing, galvannealing, and so on.

Today, because of greater efficiency, safety, smaller size, and lower cost, solid-state power supplies have replaced their predecessors in most applications. Because of differences in the characteristics of solid-state power supplies as opposed to the vacuum tube oscillator, it is necessary to use good judgment in the specific application requirements to facilitate a harmonious blending of application requirement and power supply performance characteristics.

8.10.1 Characteristics of Vacuum Tube Oscillators

The vacuum tube oscillator, as shown in Figure 8.78, has been the workhorse of the radio frequency range of induction heating equipment for many years. This equipment, although dependable with routine maintenance and tube replacement, was very inefficient (typically 50 to 60%) and often dangerous with very high voltage levels present in the power supply enclosure. It was often difficult to get a true reading of what level of power was actually being delivered to a given load; manual calculations of DC voltage and current levels or calorimeter measurements for a given coil or load configuration were often required.

The presence of very high voltages (15 to 20 kV) in the DC power section and sometimes nearly double that in peak AC voltage (AC + DC) on the plate circuit required the use of very long hose lengths on water circuits to prevent electrolysis and voltage breakdown across the length of the hose. Corona and arcing were often seen on problem installations due to the sheer magnitude of internal voltages.

Special care was required in the specification of the cooling system which required the use of deionized water for very low conductivity levels and a volume large enough to dissipate the full kW rating of the power supply because of internal tube and tank circuit losses.

One saving grace for this type of power supply is the fact that almost any configuration of work coil could be connected to the output and a reasonable amount of power would be delivered to the load. The setup was not always optimum but in most cases it did not need to be. The setup was generally quick and relatively painless. The waveform across the load for a radio frequency oscillator would be a high-frequency sine wave of voltage, modulated by the lower line frequency, which can have significant ripple, depending on the conduction angle of the input SCR controller (see Figure 8.79).

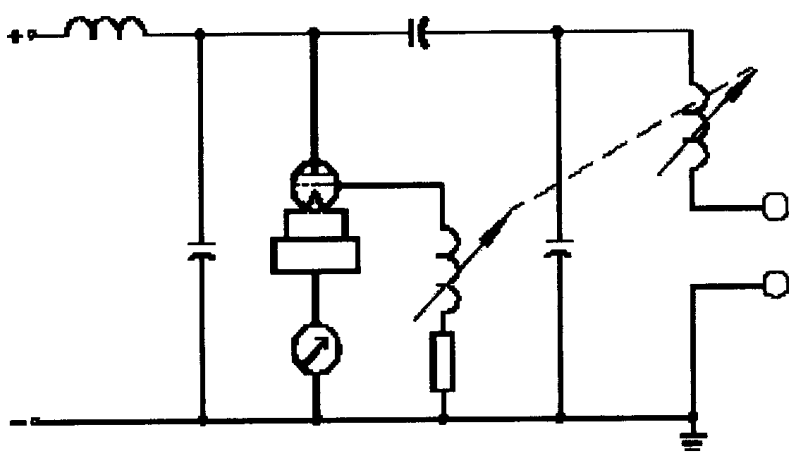

Figure 8.78 Vacuum tube oscillator power circuit.

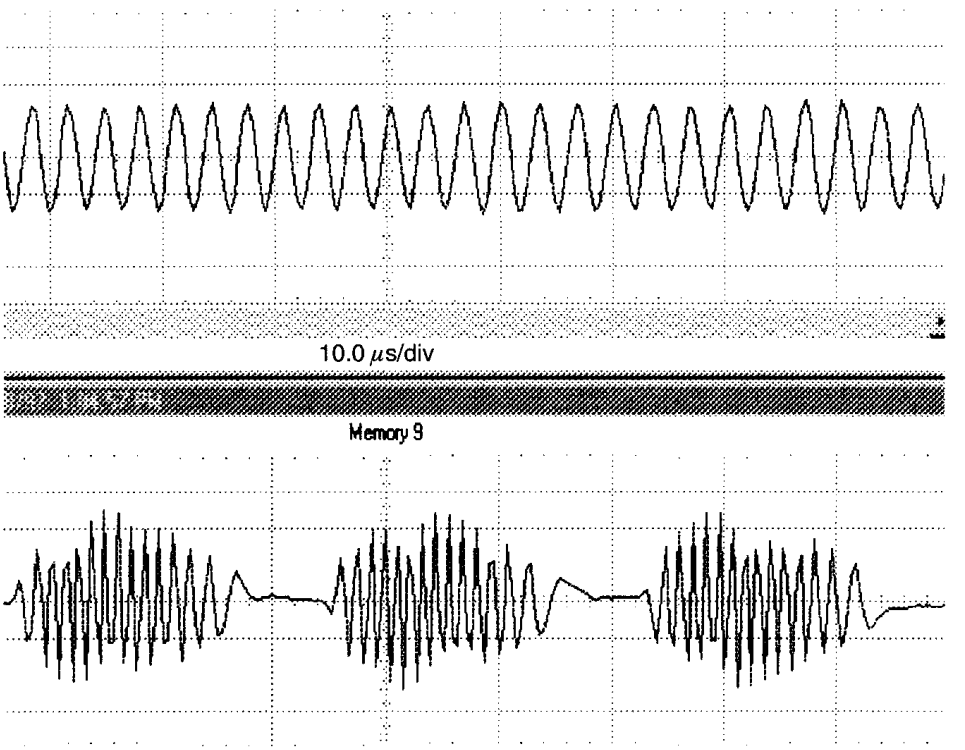

Figure 8.79 Output voltage waveform for solid-state inverter (top) versus vacuum tube oscillator (bottom).

8.10.2 Characteristics of Solid-State Radio Frequency Power Supplies

Solid-state radio frequency power supplies offer many advantages over the tube-style RF oscillator: smaller size, lower cost, higher reliability, greater efficiency, ease of control, and safety. Sophisticated control technology allows very precise timing of the switching of the semiconductors. This is critical to efficient operation because of the high switching losses that occur in semiconductors operating at high frequencies. The general design strategy is to operate at unity power factor by using a phase-locked loop electronic circuit to force the switching of the semiconductors to be the same as the load-resonant frequency. This allows switching to occur at very low levels of voltage or current, which leads to lower internal losses and very high efficiencies (85 to 90%). On continuous heating operations, this characteristic alone would dictate the use of a solid-state power supply since at high-power levels the payback in energy savings justifies a higher equipment purchase price in a very short time compared to the purchase of tube-type equipment.

The control electronics on the solid-state inverter give fast accurate response and high reliability, and are able to communicate with computer control and monitoring systems.

A comparison of the relative size of comparable power supplies is shown in Figure 8.80 for a solid-state radio frequency power supply versus the earlier tube-style RF oscillator.

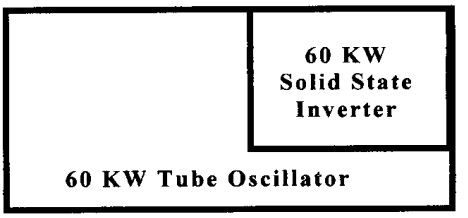

Figure 8.80 Relative size of solid-state power supply versus vacuum tube oscillator.

Two types of inverter circuit are generally used in transistorized RF power supplies, the voltage-fed circuit and the current-fed circuit.

8.10.2.1 Voltage-Fed Circuits

The voltage-fed circuit, as shown in Figure 8.20, utilizes a three-phase rectifier bridge input circuit feeding into a filter capacitor and transistor chopper circuit. Power control is achieved by varying the DC voltage level out of the chopper circuit and into the AC bridge which is switching at the load-resonant frequency and feeding a series-resonant load circuit. The voltage-fed circuit is typically used for power supplies (below 300 kW) at frequencies above 50 kHz and for larger sizes (1 megawatt or more) with frequencies at or below 50 kHz. The voltage-fed circuit switches a square wave of voltage across the series connected load, giving a sine wave of current at the load (see Figure 8.81).

8.10.2.2 Current-Fed Circuits

The current-fed circuit, as shown in Figure 8.30, utilizes a stepdown transformer feeding into an SCR-controlled rectifier circuit and a large smoothing choke which provides a constant level of DC current to the high-frequency AC bridge. Switching a constant DC current from the supply delivers an alternating square wave of current to the parallel connected load circuit and a sine wave of voltage is produced across the load circuit (see Figure 8.82). The current-fed circuit is used for 100 kW to 2 MW RF power supplies at frequencies above 50 kHz.

8.10.3. Load-Matching Considerations

A prime consideration for any induction heating application is the matching of the load circuit to the power supply in order to obtain the maximum power transfer to

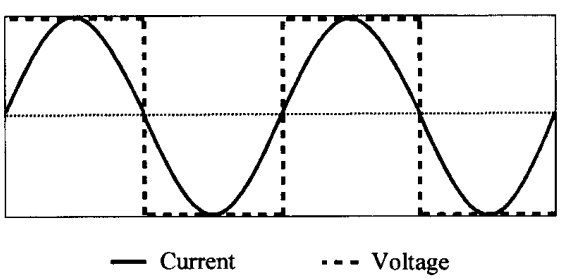

Figure 8.81 Waveforms of voltage-fed inverter with series connected load.

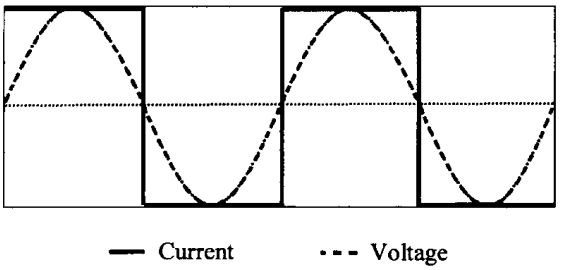

Figure 8.82 Waveforms of current-fed inverter with parallel connected load.

the load circuit. The two methods of connecting the capacitor and load coil would be a series or parallel arrangement (see Figure 8.41). The impedance curve for these circuits is different, but the power curve for either circuit is essentially the same (see Figure 8.43).

The load circuit for the tube-style RF oscillator is shown in Figure 8.83. It should be noted that because the tube-style oscillator is operating at very high voltage, it is less susceptible to problems with long transmission line runs to the heat station where the load-matching transformer is located. With the solid-state inverter, the operating voltage is lower and the transmission line impedance from the power supply to the load circuit becomes much more critical. For this reason, the solid-state radio frequency inverters are often separated into two enclosures, one being the DC power supply that may be mounted at a remote location, and the AC bridge and output section that must be mounted near the heating coil. On new installations this may easily be taken into account during the design stage to provide adequate space for the enclosure. On installations where a tube-style oscillator is being replaced, there may be a need for special considerations in interconnecting the larger AC bridge and output section of the solid-state unit into the same location as the smaller RF heat station. Figure 8.84 gives an idea of the relative difference for a 100 kW solid-state AC bridge/output section versus an RF heat station containing only the output transformer.

Another consideration is the fact that the Q of the load can affect the ability of the power supply to deliver the desired voltage to the load and may affect the ability of the control circuit to phase-lock during the startup phase of operation. These are not major problems and easily can be taken into account during the systems engineering portion of the initial design. If the system inductance is too low, a trombone

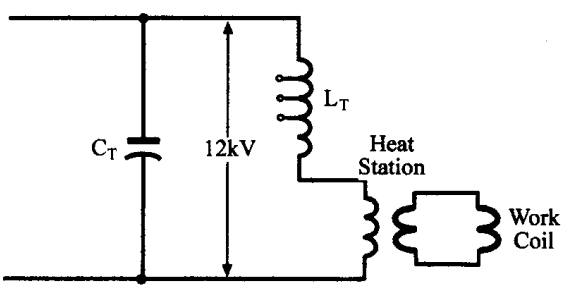

Figure 8.83 Load circuit for vacuum tube oscillator.

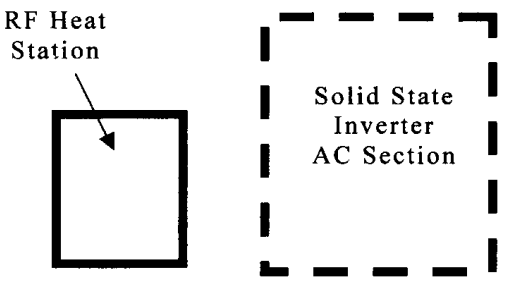

Figure 8.84 Comparison of a 100 kW solid-state AC bridge/output section versus an RF heat station containing only the output transformer.

bus (Figure 8.85) can be inserted in series with the bus connection to the coil. If the circuit Q is too low, a parallel inductance may be added to the output circuit to draw higher current from the power supply and simulate a higher Q operation.

A fact that has been observed since the development of the solid-state power supply is that many of the applications that had previously been relegated to the tube-style oscillator can be easily done with 30 to 50 kHz inverters. This can lead to very large cost reductions for the required power supply for these applications. On applications requiring the use of frequencies in the range of 50 to 450 kHz there are still marked advantages in going to a solid-state system, but the cost is significantly higher than the 30 to 50 kHz equipment. Operation at frequencies greater than 600 kHz with solid-state inverters is possible but the demand in the induction heating arena is limited to pipe and tube seam welding.

8.10.4 Conclusion

Due to smaller size, lower cost, higher reliability, greater efficiency, ease of control, and safety the solid-state radio frequency power supply is currently replacing the tube-style oscillator in the induction heating industry in much the same way that solid-state inverters have replaced the motor generator set. As with any new technology, there will be growing pains during the initial application as the nuances of each range of applications must be experienced.

The watchword in the application of solid-state radio frequency inverters is system engineering. Each application must be viewed as a complete system, taking

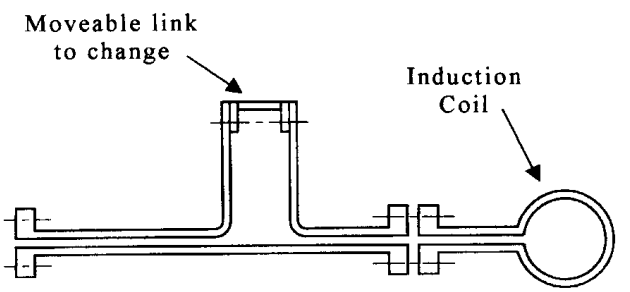

Figure 8.85 Trombone bus in solid-state inverter output bus.

into account the metallurgical requirements, production rate, ergonomics, safety, cost, reliability, and maintainability. It must be clearly understood that the heating coil, tooling, and transmission lines can be as critical to proper application as the design of the power supply itself. An understanding of the characteristics of the power supply used will help to determine how critical each of the remaining items is to a successful new application or power supply field replacement.

8.11 THE IMPORTANCE OF HAVING A GOOD POWER FACTOR

Induction heating power supplies are most commonly connected to three-phase, 400 to 480 V, 50 or 60 Hz in-plant distribution systems. The power drawn by the induction heating equipment from this distribution network can be a significant portion of the total plant load. Current drawn from the supply lines that is not a sine wave in phase with the supply voltage may cause a reduction in the power factor and contribute to supply distortion [349].

The input supply voltage can be considered constant whereas the amount of current drawn from the supply lines varies with the amount of power being used. When the supply and the load are both sine waves, the power used is the product of the voltage, current, and the phase angle between them:

where

$$\begin{aligned} \text{Voltage} \quad & v = V_{max} \sin(\omega t) \\ \text{Current} \quad & i = I_{max} \sin(\omega t + \theta) \\ \text{Power} \quad & p = V_{max} \sin(\omega t) I_{max} \sin(\omega t + \theta) \\ \text{Power factor} \quad & PF = \cos\theta. \end{aligned}$$

The power factor is also expressed as the ratio of watts used to the volt amperes supplied or at power levels more common to induction heating:

$$PF = kW/kVA.$$

Losses in the supply network including losses in distribution transformer windings, cabling, or bus bars and switch gear are directly proportional to the square of the current ($P = I^2R$). Therefore it is desirable to have the kVA be as small as possible and the power factor as high as possible to minimize unnecessary I^2R losses.

8.11.1 Full-Bridge Uncontrolled Rectifier

As described in Section 8.3.2.3 most voltage-fed induction heating power supplies have an uncontrolled rectifier where the rectifier does not control the output power of the power supply. Either the inverter controls power output or a form of post-rectification switch mode control (chopper) is used to control the DC supply to the inverter. The input power factor is very high as shown in Figure 8.86. In this case the current waveshape is not a sine wave and the difference between the input kVA and kW is due to the shape factor of the current waveshape. The schematic and waveshapes of 6- and 12-pulse full wave uncontrolled rectifiers are shown in Figures 8.87 and 8.88.

8.11.2 Full-Bridge Phase Controlled Rectifier

In most current-fed inverters the output power is controlled by the variation of the magnitude of the DC current by regulating the conduction phases of the rectifier. The diode rectifier is replaced by thyristors so conduction can be controlled. Here the input power factor is proportional to the output voltage. Figure 8.89 shows (A) the schematic, (B) line voltage, (C) DC voltage, (D) phase current and (E) line current waveshapes. In the phase-control mode, the gating of the thyristors is delayed, therefore, the switching between phases is forced by the angle of delay. Power drops rapidly with the increase of the retard angle. The chart of input power factor as a function of the phase-control angle is shown in Figure 8.90. Proper output load-matching is very important in current-fed inverters to maximize the input power factor.

Energy conservation is an important issue and power companies are beginning to change the power distribution regulations in order to raise the minimum limit for the power factor. Some countries are now requiring $\cos \Theta = 0.92$ and are soon going to 0.95. In most cases a progressive extra charge and in some cases penalties are imposed for operation with input power factors that are below these minimums. This will of course preclude the use of conventional full-bridge controlled rectifiers.

Care must be taken in the measurement of the power factor of induction heating installations. High-frequency harmonics and magnetic fields may affect some sophisticated electronic instruments used for automatic measurement of the power factor and consequently give erroneous readings. True rms instruments are most likely to provide accurate results.

The conventional method for correcting the factory input power factor is to provide line frequency capacitor banks across the incoming lines. This practice can cause undesirable results when used on systems that have significant loading by static power converter equipment, which includes induction heating power supplies. The harmonic distortion produced by the rectifiers can excite resonance between these power factor correction capacitors and other reactive components in the distribution network. The resulting high-frequency currents can exceed the ratings of the capacitors and other parts of the system causing unexpected damage.

Modern static VAR compensation equipment is available that is designed to correct the power factor to near unity while also suppressing undesirable harmonics. This equipment can be effective, however, it is a relatively costly solution. It is usually better to eliminate the source of the poor power factor than to correct for it.

8.11.3 Active Unity Power Factor Rectifiers

There are new rectifier circuits that employ IGBTs along with reactive components so that a pulse width modulation scheme can be used to control the conduction of

Number of pulses	Power factor (COS Θ)
6	0.955
12	0.989
24	0.997

Figure 8.86 Power factor for full wave rectifier.

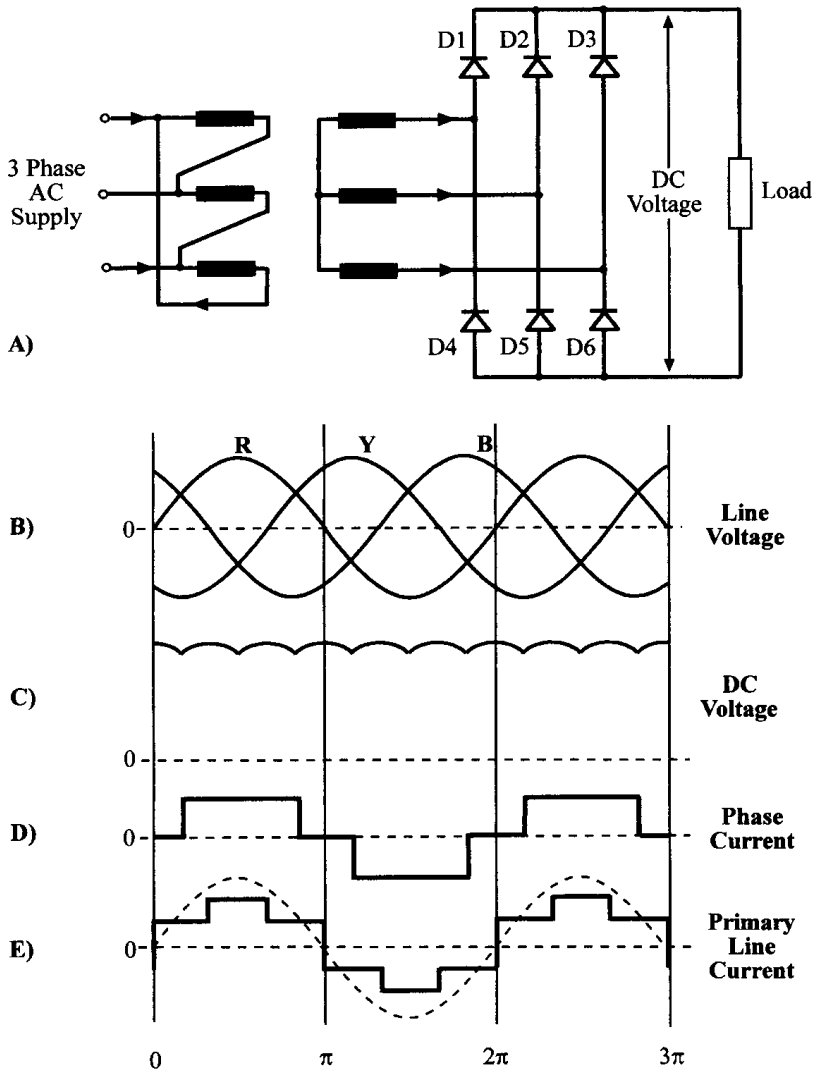

Figure 8.87 Power factor for full wave rectifier.

current from the input line. This type of rectifier is also capable of dramatically reducing the total harmonic distortion while using a simple three-phase supply. A description of this type of circuit is presented in Section 8.12.2.3.

8.12 HARMONICS AND THEIR REDUCTION

Induction heating power supplies convert AC input voltage into DC in a rectifier and switch the DC voltage or current to the output in a manner that provides a single-phase sine wave to be loaded. In the controlled rectifier, electronics controlling the switching of thyristors permit the output voltage to be varied thus controlling the output power (see Figure 8.89). For a detailed explanation of the rectifier section of the power supply refer to Sections 8.3.1 and 8.11.

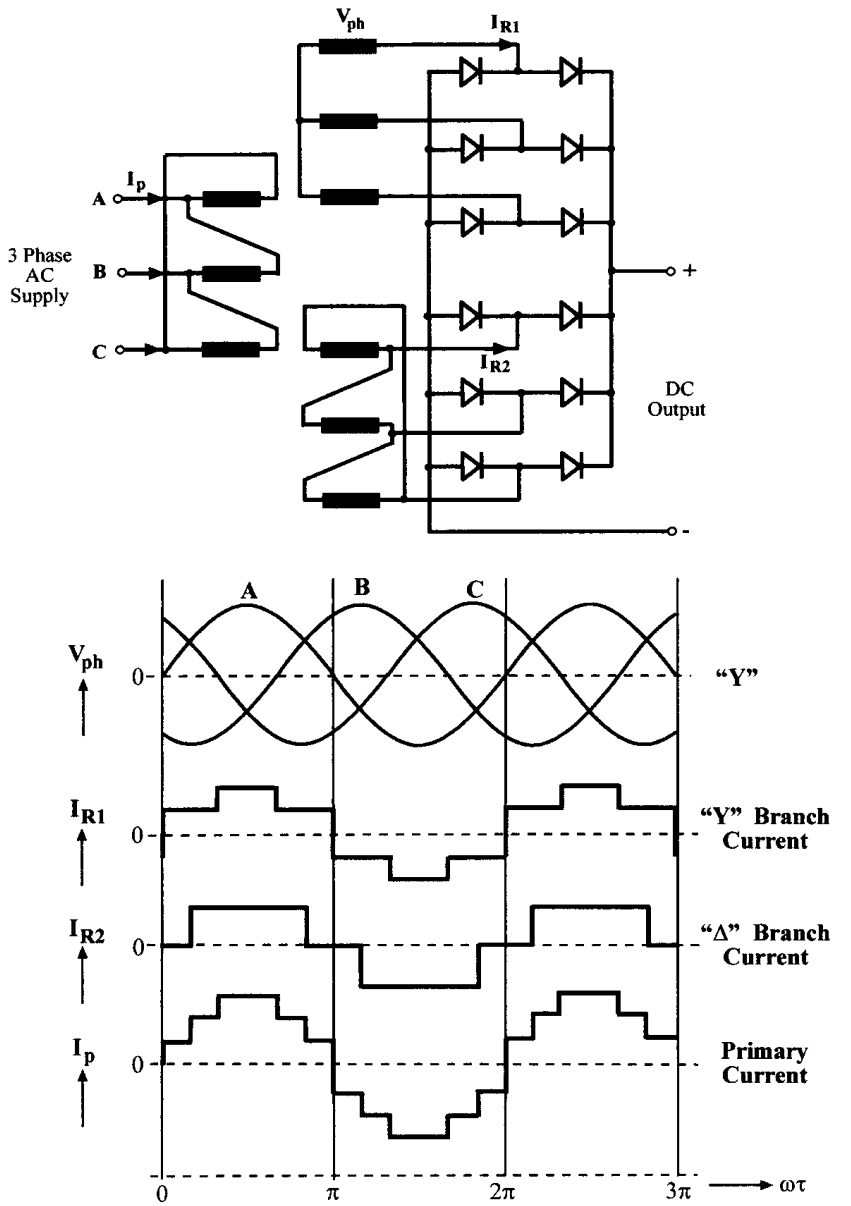

Figure 8.88 Twelve-pulse rectifier combining two three-phase bridges in parallel with an interphase reactor.

8.12.1 Nature and Cause of Harmonics

Whenever current flow in an AC circuit is switched on and off rather than permitted to follow the voltage waveform, high-frequency currents at integer multiples of the power system frequency (harmonics) are generated [350]. The switching of the full-bridge three-phase rectifier results in an input current waveform containing the sum of the current at the fundamental frequency (60 Hz), and higher-order harmonic currents (see Figure 8.91). The harmonics produced are the fifth (300 Hz), seventh (420 Hz), eleventh (660 Hz), thirteenth (780 Hz), and so on, following the pattern of

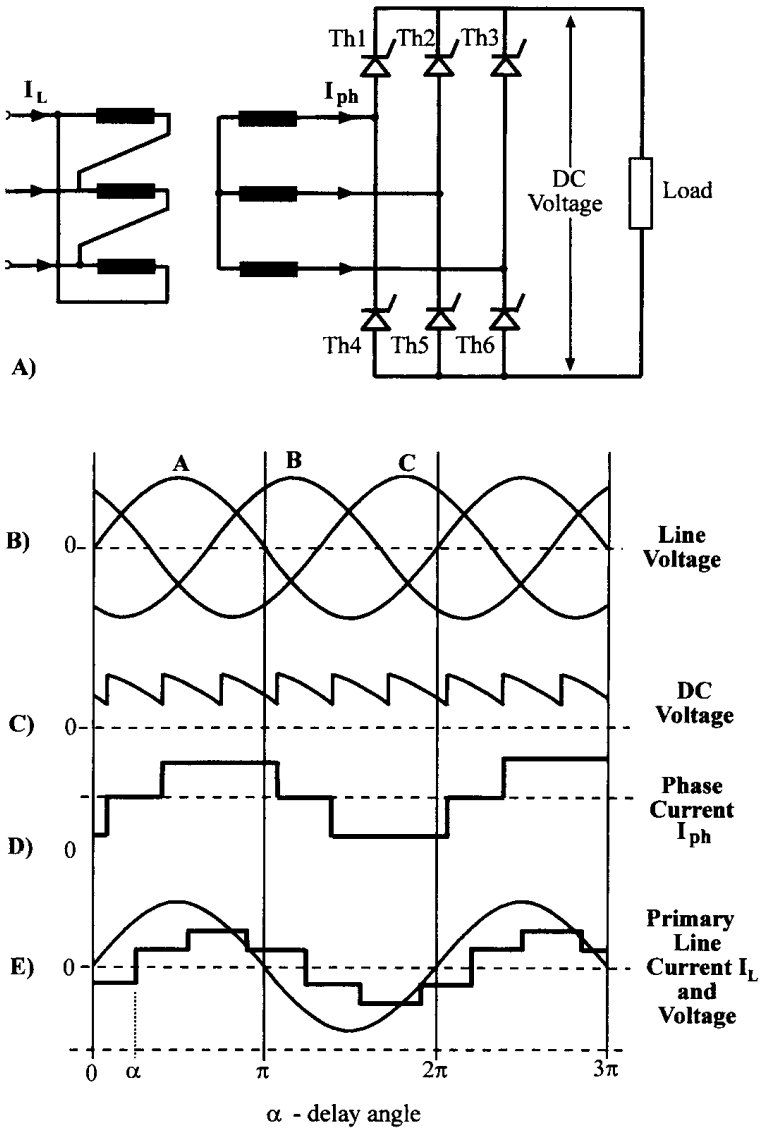

Figure 8.89 Three-phase fully controlled bridge converter.

$6N \pm 1$, with the magnitude of the harmonic decreasing as the harmonic order increases. The IEEE Standard 519-1992 defines the limits of voltage and current distortion that should be permitted in electric distribution systems [352]. A new revision of this standard is being prepared and is scheduled for completion in 2002.

8.12.1.1 Voltage Distortion

Unwanted harmonic currents are a concern because they cause losses and voltage distortion. Any current drawn from the power system results in a voltage drop equal to the product of the current and the impedance of the system. System impedance must be limited to prevent the voltage drop from reducing the voltage at the load to unacceptable levels and to limit voltage distortion that can cause problems for other electronic equipment on the same line. Unfortunately power systems are highly

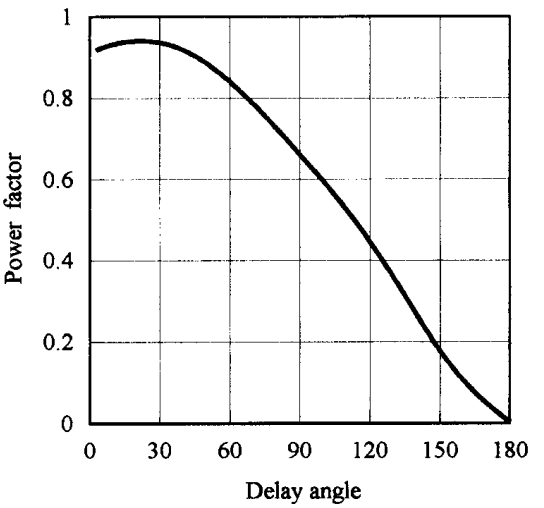

Figure 8.90 Variation of power factor as a function of delay angle.

inductive and their impedance to current flow increases with frequency. This means that relatively low-magnitude high-frequency currents can produce significant voltage distortion.

Total harmonic voltage distortion is the ratio of the total line to neutral harmonic voltage to the fundamental line to neutral voltage.

$$\text{Total harmonic distortion} = V_H/V_{L-N},$$

where V_H is the rms sum of all harmonics through the 25th. Table 8.1 summarizes the recommended voltage distortion limits.

8.12.1.2 Line Notching

Line notching occurs when two semiconductors with the same polarity in a rectifier are simultaneously conducting. This occurs in the interval when one rectifier is beginning to turn off while the other is turning on, a process known as commutation. The duration of this time is called the commutation interval. The recommended limits for line notching are provided in Table 8.1. Line notching is a concern because

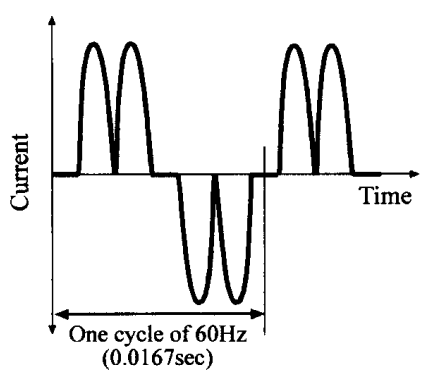

Figure 8.91 Typical phase-controlled rectifier input current waveform rich in harmonics.

Table 8.1 Line Notching and Distortion Limits for 460 V Systems

Class	Line Notch Depth (%)	Line Notch Area (V-μs)	Voltage Total Harmonic Distortion (%)
Special applications	10	16,400	3
General system	20	22,800	5
Dedicated system	50	36,500	10

it can cause noise problems in electronic computer and control equipment connected to the same distribution line.

8.12.1.3 Current Distortion

The line current waveshape typical of 6-pulse rectifiers is shown in Figure 8.92. The current is not drawn from the input line as a sine wave but as the sum of nearly constant current segments that when summed are equal to the current in the DC output of the rectifier. The stepped waveshape contains harmonics of the fundamental line frequency in the percentages shown in Figure 8.17. The total demand distortion TDD is the total harmonic current distortion given by

$$TDD = I_H/I_L,$$

where I_L is the maximum demand load current at the fundamental line frequency and I_H is the rms sum of the individual harmonic components up through the 25th.

Line current harmonics are a concern because they lead to live voltage distortion that can adversely effect other equipment on the same distribution circuit. Unwanted additional power losses can also be attributed to line current harmonics. Any components that must conduct these harmonic currents, including transfor-

Table 8.2 Current Distortion Limits for General Distribution Systems (120 Through 69,000 V)

	Maximum Harmonic Current Distortion in % of I_L[a] Individual Harmonic Order (Odd Harmonics)					
$I_{sc}I_L$	< 11	$11 \leq h < 17$	$17 \leq h < 23$	$23 \leq h35$	$35 \leq h$	TDD
< 20	4.0	2.0	1.5	0.6	0.3	5.0
$20 < 50$	7.0	3.5	2.5	1.0	0.5	8.0
$50 < 100$	10.0	4.5	4.0	1.5	0.7	12.0
$100 < 1000$	12.0	5.5	5.0	2.0	1.0	15.0
> 1000	15.0	7.0	6.0	2.5	1.4	20.0

[a] Even harmonics are limited to 25% of the odd harmonic limits. Current distortions that result in a DC offset (e.g., half-wave converters) are not allowed.
All power generation equipment is limited to these values of current distortion, regardless of actual I_{sc}/I_L, where: I_{sc} = maximum short-circuit current at PCC; I_L = maximum demand load current (fundamental frequency component) at PCC.

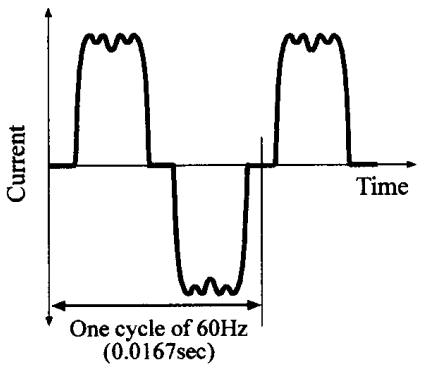

Figure 8.92 Distorted AC voltage waveform showing the effect of harmonic currents.

mers, switch gear, distribution bus, and cables, will have higher losses due to high-frequency effects. These high-frequency heating effects are eddy current losses, skin effect, proximity effect, and hysteresis losses: all these heating effects are described in previous chapters as the basis for induction heating. Another often-overlooked consequence of these line current harmonics is the error that they can cause in the trip level of circuit breakers.

8.12.2 Solutions to Power Factor and Harmonic Problems

Three possible approaches are available to solve rectifier power factor and harmonic problems.

8.12.2.1 Excess Installed Capacity

In some cases the installed power electronic (rectifier) load can be restricted to a small amount of the total load served by the distribution branch. This is practical where a small induction heating power supply is used in a plant or area of a plant that is primarily operating nonpower electronic loads. To provide excess capacity for the sole purpose of reducing harmonic distortion is seldom if ever economically feasible.

8.12.2.2 Filtering the Total Load

In some cases where there is a large amount of equipment with rectifier inputs it is practical to filter the entire plant or branch circuit. This can be accomplished by passive or active filtering components or by phase staggering of various loads to obtain harmonic cancellation. This approach requires careful planning and is often not practical because significant loads such as large induction heating power supplies may be turned on and off randomly, which means an adaptive system is needed.

8.12.2.3 Individual Power Factor and Harmonic Compensation

Relatively new rectification schemes use transistors to switch current from the input AC line. The circuit configuration shown in Figure 8.93 is very similar to the three-phase controlled rectifier described in Section 8.3.1 except the thyristors are replaced by IGBTs with series diodes. The principle of operation is to pulse-width modulate the conduction time of the transistors at a much higher frequency than the line frequency. The output voltage can be controlled while maintaining a near unity

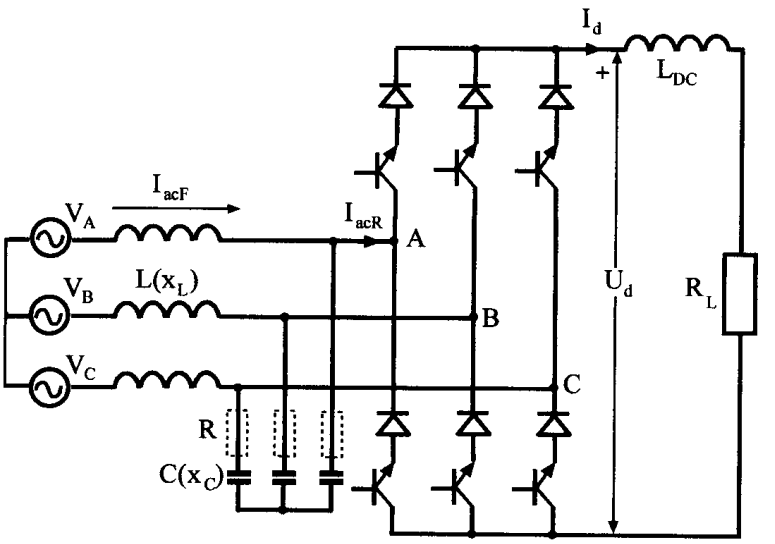

Figure 8.93 Three-phase PWM rectifier.

input power factor by providing the appropriate switching pattern to the transistors [351]. A simple LC filter in each line filters the high-frequency ripple caused by the switching of the transistors. Line harmonics are thus reduced to an acceptable value. Waveforms of typical pulse-width modulation patterns and input line voltage and current are shown in Figure 8.94.

The cost and complexity of this solution to the power quality problem can be greater than that of the high-frequency inverter portion of the induction heating power supply. The robustness and reliability of this approach using transistors, under inverter fault conditions, is significantly less than conventional rectifiers using high-power SCRs or diodes. Development of active rectifier circuits is being aggressively pursued and will undoubtedly become a viable solution to both power factor correction and harmonic reduction.

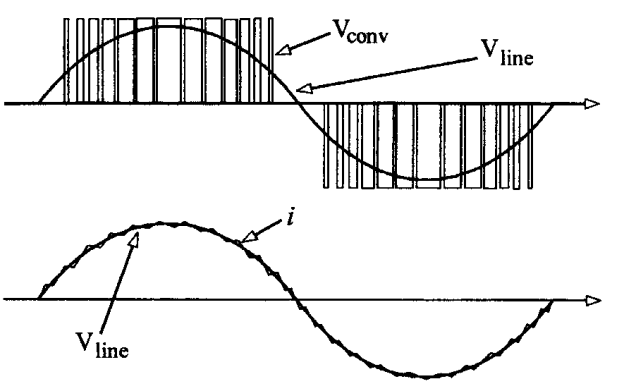

Figure 8.94 Circuit waveforms.

8.13 POWER SUPPLY COOLING

Water-cooling is the most common method used to remove the heat generated by losses in the induction heating power supply, the output bus bars or cables, and the induction heating coil. The water quality, temperature, flow rate, and other requirements vary depending upon the type of power supply and the application [347, 348].

8.13.1 Water Quality

In vacuum tube oscillators and power supplies using SCRs there is DC voltage potential between the water-cooled power components. This DC potential between components can cause leakage current to flow through the water in the hose connecting them. If not controlled to acceptably low levels this current can cause electrolysis, which over time will eat away the metal at one end of the water circuit causing a water leak. The metal eaten away from one end will try to deposit at the other end of the water circuit. The deposited material can form a blockage of the water circuit causing an overheating fault or component failure due to insufficient cooling. To protect against these modes of failure the leakage current must be controlled by limiting the conductivity of the water or by providing sufficient hose length between components at differing DC potential. The conductivity of the water used to cool vacuum tube oscillators and power supplies using SCRs with short interconnecting hoses is typically limited to a maximum of 40 micromhos. This requires that the water be distilled and deionized. The maximum conductivity can be raised 10 times to 400 micromhos where the interconnecting hose length is sufficient to limit the DC voltage potential to less than 20 volts per foot. This means 40 feet of hose must be used to connect across a DC bus potential of 700 volts.

Modern transistorized power supplies are usually designed to avoid direct contact between the cooling water and any DC voltage potential. This eliminates the possibility of damage caused by electrolysis. In this case water with high conductivity, even quenchant, can be used to cool the power supply. This approach has been very successfully used in INDUCTOHEAT's high- and medium-frequency power supplies. The HSP (heat station power supply) and UP12 (Unipower 12), which are often part of a unitized heat treating machine, have been in service since 1994 successfully using quench for cooling.

8.13.2 Cooling Water Flow Rate

The individual water-cooling circuits within the power supply are designed to provide the flow rate required to cool the various individual power components on the circuit. Components requiring the coolest water such as capacitors and power semiconductor heat sinks are placed close to the inlet, and bus bars and inductors that can tolerate higher temperatures are placed near the outlet end of the circuit.

Some circuits require much higher flow than others do because some components have higher power dissipation or are unable to tolerate significant temperature rise from inlet to outlet. The typical flow rate per circuit within the power supply is about 2 to 3 gpm. Obviously, large power supplies will have more cooling circuits and therefore higher flow requirements than smaller power supplies. All the individual water circuits within the power supply are connected in parallel to inlet and

outlet manifolds and the pressure inlet to outlet must be sufficient to guarantee the engineered flow rate. This pressure is usually specified to be a minimum of 25 or 30 psi and is usually monitored by a minimum pressure differential switch.

8.13.3 Cooling Water Recirculating Systems

Most induction heating power supplies are cooled by closed-loop water recirculating systems. These systems have a pump, heat exchanger, temperature control valve, tank, filter or strainer, and plumbing to interconnect all the components. A typical cooling water recirculating system is shown in Figures 8.95 and 8.96. Tables 8.3 and 8.4 show rating data applicable to these water-cooling systems.

8.13.3.1 Pumps

Most water recirculating systems are designed with centrifugal pumps. These pumps have well-defined pressure versus flow performance characteristics. Knowing where a pump is expected to operate is essential in sizing the system. The total water flow required must include the power supply, external bus or water-cooled cables, the heat station (if separate from the power supply), the inductor coil, and any other external components that are cooled by the system. The pressure required from the pump must include the drops across the power supply and other components and also the pressure drop across the supply and return lines.

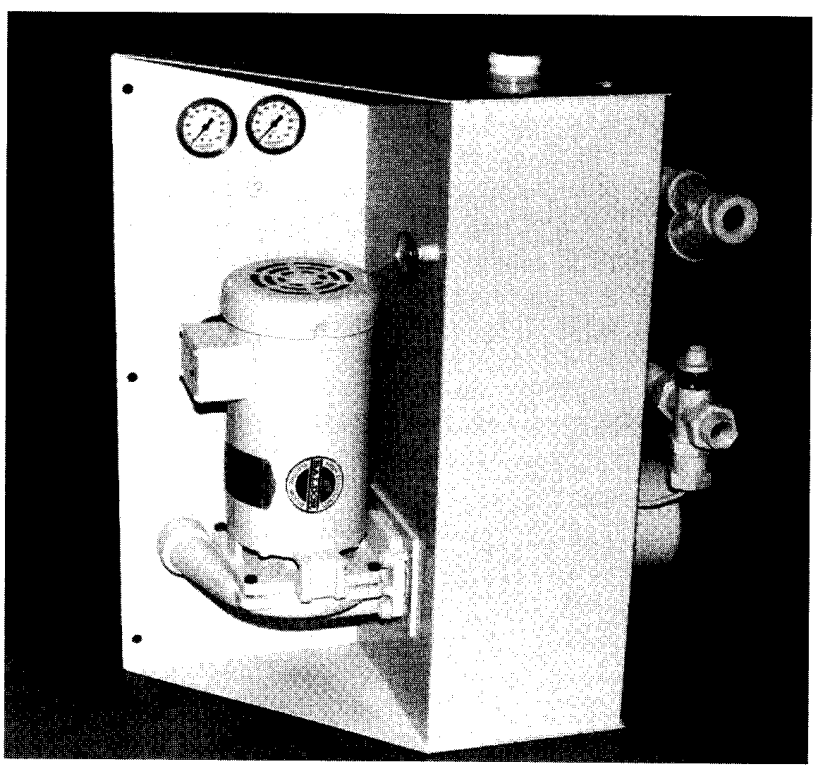

Figure 8.95 INDUCTOHEAT's bolt-on style compact closed-loop water-cooling and recirculating system.

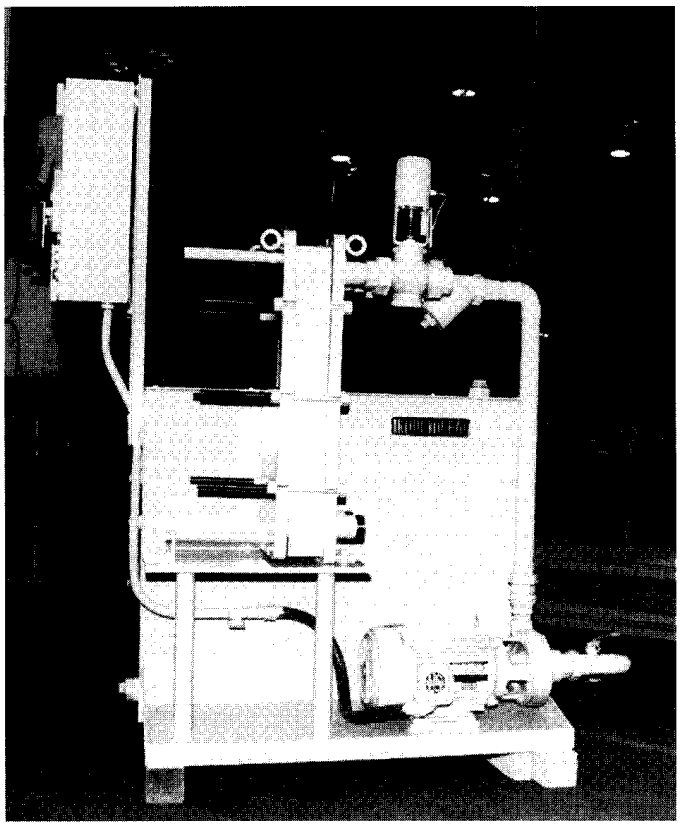

Figure 8.96 Standalone closed-loop water-cooling and recirculating system.

8.13.3.2 Heat Exchanger

The second item of importance in the recirculation system is the heat exchanger. Most systems use a water-to-water heat exchanger. Typically, modern systems are using plate-type heat exchangers that are compact and can be assembled from standard plates to provide the necessary capacity.

Most induction heating power supplies are designed to operate with a maximum inlet water temperature of 95°F (35°C). To properly size the heat exchanger one must know the power dissipated in kW or heat load in BTU/hr, the flow rate, and the "lead" which is the difference between the coolest water on one side of the

Table 8.3 Parameters of INDUCTOHEAT's Bolt-On Style Closed-Loop Water-Cooling and Recirculating System[a]

Model	Minimum Flow (gpm)	Heat Dissipation (BTU/hr)	Floor Plan Dimensions
UNICOOL	70	240,000	0.3 m × 0.6 m (12 in. × 23.5 in.)
UNICOOL	125	425,000	0.3 m × 0.6 m (12 in. × 23.5 in.)

[a]See Figure 8.95.

Table 8.4 Parameters of INDUCTOHEAT's Standalone Closed-Loop Water-Cooling and Recirculating System[a]

Model No.	Plant Water Flow (gpm)	Output Water Flow (gpm)	Heat Dissipation (BTU/hr)	Floor Plan Dimensions
46P0210	37	100	200,000	0.74 m × 1.3 m (29 in. × 53 in.)
46P0410	73	100	400,000	0.74 m × 1.3 m (29 in. × 53 in.)
46P0815	146	150	800,000	0.74 m × 1.3 m (29 in. × 53 in.)
46P1010	182	100	1,000,000	0.74 m × 1.3 m (29 in. × 53 in.)
46P1515	273	150	1,500,000	0.74 m × 1.3 m (29 in. × 53 in.)

[a]See Figure 8.96.

heat exchanger and the coolest water on the other side. The lead has a major impact on the size of the heat exchanger. A lead of 10°F is common, which requires that the plant-side water temperature be 85°F, or less.

An example showing the power losses in a typical induction heating system is given in Figure 8.97. As shown, an induction heating system with a power supply operating at 100 kW output and 90% efficiency will have 10 kW losses. The matching station and interconnecting bus with 85% efficiency will lose 15 kW, and the load coil with 70% efficiency will lose 25 kW. Thus the total power losses are: 10 kW + 15 kW + 25 kW = 50 kW. If the part is heated for 10 seconds and the entire cycle is 40 seconds, the duty cycle is 10/40 or 0.25. The heat load of the cooling system is then: 50 kW × 0.25 = 12.5 kW. To convert 12.5 kW to BTU/hr multiply by 3415 and the heat load is then 42,688 BTU/hr.

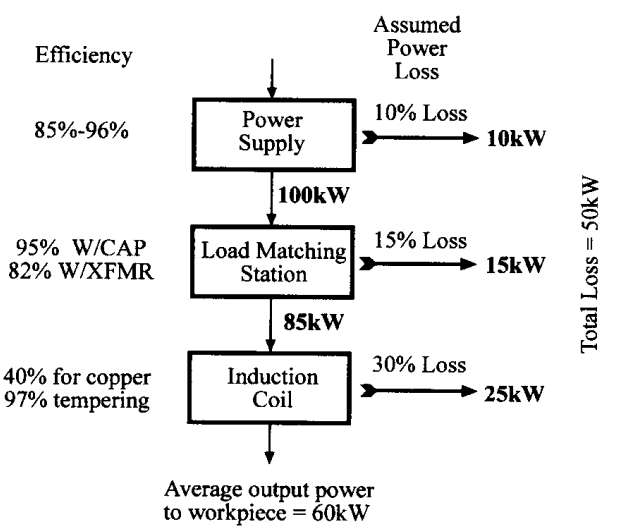

Figure 8.97 Power diagram for calculating cooling water requirements.

The flow 85°F water required to cool the above system using a well-designed heat exchanger can be calculated using the following.

$$\text{Flow (gpm)} = \frac{\text{Heat Load (BTU/hr)}}{500\,\text{Temperature Rise (°F)}} = \frac{42{,}688}{500 \times 10} = 8.5\,\text{g pm.}$$

It is important to note that the worst-case operating conditions for the system should be used in sizing the water-cooling system. For example, if it is possible that the duty cycle in the above system could be 0.5 for another application, the flow required would double to 17 gpm.

8.13.4 Common Water-Cooling Problems

Some of the most common problems associated with power supply cooling systems are outlined below.

1. Supply and return lines to and from the power supply are too small and introduce excessive pressure drop leaving too little differential across the power supply.
2. The cooling system is undersized for the application because the process is less efficient or has a higher duty cycle than the original application.
3. Filter or strainer has high pressure drop and needs cleaning or replacement.
4. Incorrect flow due to changes made to the water circuit connections during maintenance.
5. Heat exchanger efficiency poor or restricting flow and needs cleaning.
6. Ambient temperature and relative humidity too high and therefore cooling water temperature is too high.
7. Recirculating cooling water is too cold causing moisture condensation on high-voltage components.

8.14 PROCESS CONTROL, MONITORING, AND QUALITY ASSURANCE

8.14.1 Prelude to Discussion of Process Control and Monitoring

One of the most important features of a modern induction heating machine is the ability to effectively control and monitor the significant process variables. The control system should allow presetting a number of system input parameters with the expectation that, via a specified control algorithm, the result will be the desired system output. The monitoring system must be independent of the control system and should provide the operator with information about what is actually happening during the process. It should indicate whether the parameter values measured are essentially the same as the values recorded for a test piece that is known to be properly processed. If the values are the same or within acceptable limits, it may be inferred that the processing of the workpiece has been successfully completed [292, 293].

The features of a control and monitoring system are largely dependent upon the process being monitored and controlled. A metal heat treating process (i.e.,

surface hardening) is very different from a mass heating process (i.e., heating prior to hot forming or coating). The desired parameters to control in a heat treating process are the microstructure, hardness profile, and distribution of residual stresses within the part. These are controlled in order to produce certain desired mechanical properties of the part, which include wear resistance, tensile strength, fatigue strength, and ductility.

In a mass heating process the main parameter to control is the final temperature distribution and in some cases transient temperature gradients. Final temperature distribution is controlled for providing a workpiece that is easily formed as in a forging, rolling, or extrusion system, or coated with another material such as galvanizing, galvannealing, or paint curing.

The comparison of the main differences between typical metal heat treating and mass heating processes are provided in Table 8.5. The differences, as stated above, are many. Therefore the description of control and monitoring techniques is broken into two areas, heat treating and mass heating.

Table 8.5 Typical Metal Heat Treating and Mass Heating Processes

Feature	Heat Treating	Mass Heating
Cycle time	In most induction heat treating applications heat treat cycles are relatively short, on the order of seconds or tens of seconds.	Mass heating cycles are longer, often measured in hundreds of seconds and even minutes.
Frequency selection	Typically in the range of 6 to 70 kHz and sometimes as high as 600 kHz.	Frequencies of 50 Hz to 10 kHz are used for heating slabs, bars, and billets. Strip, sheet, and wire heating applications call for frequency range of 10 to 150 kHz.
	Single frequency (except gear hardening and some through hardening applications).	Often use more than one frequency to provide a desired temperature uniformity and high electrical efficiency.
Coil design	Single coil design. Coil has a few turns or single-turn coil.	Single or multiple multiturn coils sometimes as many as 30 coils on a given system.
Required power	20 to about 600 kW.	100 to 40,000 kW.
Phase connection	Single-phase systems.	Single- and multiphase systems.
Coil-to-workpiece air gap	2 m to 6 mm.	12 to 75 mm.

8.14.1.1 Specifics of Control and Monitoring of Induction Metal Heat Treating Processes

As described in Chapter 3 the induction metal heat treating process is a complex combination of electromagnetic, heat transfer, and metallurgical phenomena. Two of the most common applications of induction heat treatment are surface hardening and through hardening. Both applications involve heating the workpiece to the austenizing temperature, holding it at a temperature for a period long enough for completion of the formation of austenite, then rapidly quenching the metal to produce a very hard but brittle structure called martensite.

A subsequent but no less important step in the process is the tempering of the hardened material to relieve internal stresses and eliminate the brittleness that is characteristic of as-quenched martensite.

During the heating of the workpiece for hardening, significant metallurgical changes take place. These are covered in detail in Sections 2.1.1 and 2.1.2 but a brief review will help to understand the requirements of the control and monitoring system.

For a workpiece made from steel or iron, the metal goes through a change in crystalline structure when it is raised to a specific critical temperature resulting in a material called austenite (Figure 2.6). The material must then be quenched rapidly enough to cause a change again in the crystalline structure to a material called martensite (Figures 2.7 and 2.8). The required transformation temperature for a particular metal and the degree of hardness attained are a function of the material chemical composition, intensity of heating, the specifics of quenching, and prior microstructure (Figures 2.12, and 2.26 through 2.28).

In looking at the time–temperature isothermal transformation diagrams and continuous cooling diagrams for a typical material (Figures 2.7 and 2.8) it is apparent that if the material is cooled more slowly than the time necessary to miss the nose of the transformation curve, the material will change into a softer material. This softer material (i.e., ferritic–perlitic structures) will not provide the required properties in regard to such important mechanical properties as strength and wear resistance. It should be mentioned here that in the field of intensive induction heating the equilibrium phase transformation diagrams, time–temperature isothermal transformation diagrams (TTT or IT diagrams), and continuous cooling diagrams (CCT diagrams), are not always a reliable source when high-temperature gradients and short heating times are involved.

Proper control of this process involves not only heating the workpiece but also taking the necessary steps to ensure that proper cooling has taken place within the required time period.

A complication to this process occurs due to the thermal properties of the material being heated. Because heat transfers from the area where the heat source has been generated to the neighboring regions of the workpiece by thermal conduction and externally by convection and radiation, it is imperative that the combined heat flow effect result in the proper transformation and cooling temperatures for the material affected.

A heat treating system requires very close coupling gaps from the coil to the workpiece often with an inductor that very closely follows, within 2 to 5 mm, the contour of the workpiece.

In some cases, the development of the proper heat treating pattern requires the ability to precisely spin or move the workpiece at a specified rate while turning the high-frequency power ON and OFF to harden specific sections of the workpiece while leaving others unheated. The inductors are relatively delicate and protective circuitry must be incorporated to ensure that travel is immediately stopped if a workpiece touches the inductor.

In order to properly harden the workpiece it is also necessary to quench it properly. A specific minimum quench volume is required during a specific time interval. The quench medium must have the correct cooling curve and be of the correct concentration to effect the proper heat transfer.

In some cases the material may be properly heated but can only be quenched effectively to a certain depth within the workpiece because of the thermal properties and hardenability of the material used. Hardenability curves are useful in determining what hardness can be produced with a given material at a specified depth inside the workpiece (Figure 2.23). The workpiece material must have sufficient hardenability in order to develop the prescribed hardness pattern to the required depth.

In selective hardening applications, produced power must often be concentrated along certain sections of the workpiece, which requires the use of laminations or other types of flux concentrators, whose position and characteristics are critical to the hardening process.

The final step in the heat treating process is tempering or stress-relieving of the workpiece and requires that the desired areas of the workpiece be raised above some minimum temperature for a specific length of time. This results in a decrease in the hardness reading to some extent but produces a tough part that has a reasonable compromise among the hardness, toughness, and ductility.

Each phase of the process, heating, quenching, and tempering, must be precisely controlled and monitored in order to produce a properly heat treated part. Although the process may be successfully done with a minimum of monitoring equipment, safety and liability concerns force manufacturers to invest in systems that will document that they have done everything possible to control the process. In addition, every effort must be made to detect and remove defective parts before they reach the point of assembly in a critical subassembly.

8.14.1.2 Specifics of Control and Monitoring of Induction Mass Heating

In a typical mass heating system (i.e., inline bar, billet, slab, or strip heating applications) the applied frequency power is turned on continuously as the part traverses a coil that has very generous air gaps compared to the heating process. There is no rotation of the part required. This may seem like a relatively simple process in concept, however, the practical implementation requires much experience and technical foresight.

Materials are sometimes heated very close to the melting temperature. Much higher voltages are utilized on the multiturn coils, which can lead to problems with arcing, corona discharge, ground loops, and personnel safety hazards. Arriving at a stable process can sometimes be a challenge since a cold load (that occurred, e.g., during startup and shutdown stage), a hot load, and a continuously running load all require different power supply tuning to optimize performance.

The requirement for a specific distribution of temperature within the workpiece requires careful selection of frequency, power, and line length. Convection,

conduction, and radiation losses must be carefully calculated to ensure that the system will provide a part heated to the required specification. Improperly heated parts can cause major problems during the forging, hammering, or forming process.

Handling metal that is heated to forging temperatures can be difficult. Expansion of metal components in proximity to the hot metal and scale can cause mechanical problems. Personnel protection is a primary concern. Preventing damage to expensive equipment is an important secondary concern.

8.14.2 Meters and Meter Circuits

The task of measuring the wide variety of parameters seen in an induction heat treating or mass heating process can be a challenge. For many years it was possible to use simple analog d'Arsonval meters to measure most waveforms that might be seen in industrial power equipment. These meters utilize a permanent magnet and a vane or indicator that is mounted with a small coil of wire to a metal pin that allows the vane and coil assembly to rotate freely. When a DC current is passed through the coil of wire, the vane rotates or moves to indicate the magnitude of the current. For DC signals this type of meter provides a quickly responding visual indication of the value of the DC voltage or current being measured. AC voltage or current is measured by first rectifying the signal and then measuring the DC value of the rectified signal. This assumes that the AC signal is a perfect sine wave. A reading that may be referred to on the meter scale as root mean square (rms), is actually an average reading of the waveform with the meter scale multiplied to give the rms value assuming that the waveform is a sine wave.

Analog meters, on the other hand, are not always adequate to measure the waveforms that may occur at the output of an induction heating power supply. The waveforms are of higher frequency and may involve square waves or combinations of sine waves and pulses at different frequencies. The voltages may be relatively high, in the range of 2000 volts or even more. Internal to the power supply there may be triangular waves or pulses at different frequencies.

Certain types of analog meters are built with internal mercury switches that allow setting a pointer at a certain place on the meter scale. When the reading of the meter goes beyond the set point, the switch closes to indicate that the meter is reading above a minimum set point. On dual set point meters, a range can be set with one switch at the lowest acceptable reading and another switch at the highest acceptable reading. This type of meter would then allow the relay circuits to be interrogated to ensure that the meter reads above the lower set point and below the upper set point.

An alternative to the simple analog meter is a digital meter that is designed to give the actual rms value of a given waveform. These meters utilize special integrated circuits that will provide a DC output proportional to the true rms value of the waveform within certain limits. Used within their rating, these meters provide a very accurate measurement of the magnitude of the power supply waveshapes. The major problem with using the digital meters is that it often takes several seconds for the meter to respond with a correct reading. This can be a problem because often the heating time is less than the meter response time and it is not possible to get a correct reading during the machine cycle. Some manufacturers have

responded to this problem by providing both a quickly responding bar graph as well as the slowly responding digital readout of the value of the parameter, in the same meter housing.

Without much regard to the type of waveform being measured, some early techniques for measuring process parameters were as simple as a dual set point meter that would indicate if the parameter dropped out of the acceptable range during the cycle. On less critical variables this approach can still be the most prudent way to design the system. This approach is often used on programmable logic controller (PLC) systems with the analog readout being internal to the PLC rather than on a discrete meter.

This approach involves the design of an interrogation circuit in the machine control to check the variable during the time that it should be in the normal operating range. For such variables as flow and temperature this involves the designer's best guess as to the time it may take for the flow or temperature to stabilize before making an accept or reject measurement (Figure 8.98).

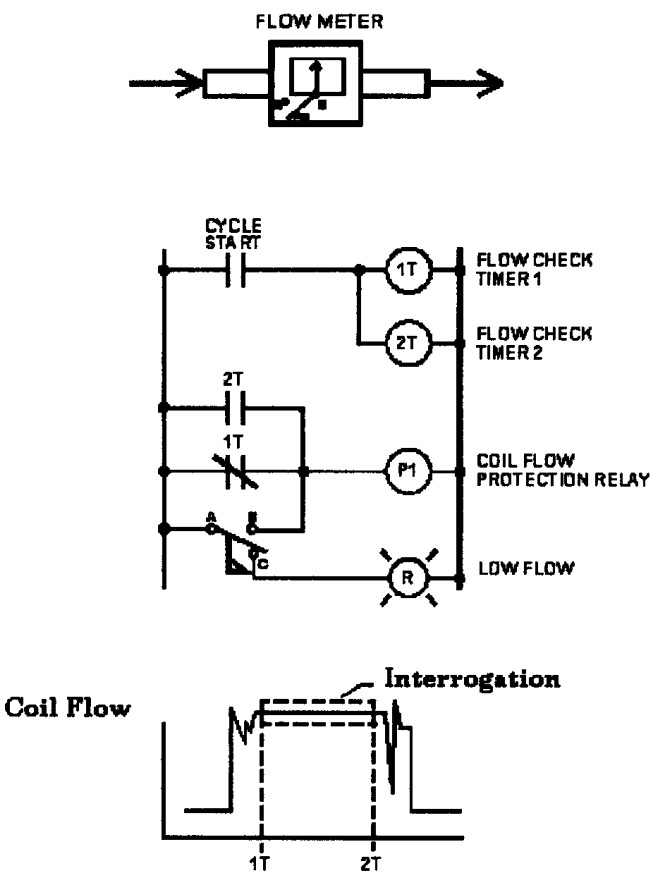

Figure 8.98 Simple interrogation circuit.

8.14.3 Features of Control/Monitoring Strategies for Induction Heat Treating Versus Induction Mass Heating

In terms of monitoring different types of processes the approaches would be significantly different. Possible guidelines for development of control and monitoring strategies are outlined below for induction heat treating and induction mass heating applications.

8.14.3.1 Induction Heat Treating

As described above, there are many variables in the induction heat treating process, but some are more important than others in terms of assuring consistent results.

A list of variables for the induction heat treating process would include:

1. Material chemical composition and properties,
2. Material geometry,
3. Induction coil geometry,
4. Part-to-coil location,
5. Frequency,
6. Active power, voltage, current, kVA,
7. Heat time,
8. Quench medium, temperature, purity, concentration, flow, and pressure,
9. Quench delay time,
10. Incoming part temperature,
11. Part temperature after heat,
12. Part temperature after quench,
13. Inductor and bus temperature,
14. Power component and heat station temperature,
15. Incoming line voltage,
16. Rotation, and
17. Scan speed.

As described in Chapter 3, the resistivity, thermal conductivity, specific heat, and relative magnetic permeability of the workpiece all change with temperature. Magnetic permeability is also affected by the magnetic field intensity used for heating the part. At first glance the changes in these parameters may appear to be very dramatic, but there are some factors that may mask the expected effect to a large extent. For hardening applications often running at 10 kW/in.^{2}, the change in relative magnetic permeability may often be only from 9 to 1 (Figures 3.10, 5.119, and 5.120). Because the current penetration depth varies as the inverse square root of the permeability change (Formulas 3.6 and 3.7), the actual change in inductance from a cold to a hot load may be relatively small. Sample calculations in Figure 8.99 illustrate this point.

As shown in Figure 8.99 the actual change in inductance and impedance from a cold load to a hot load is relatively small and is greatly reduced for higher power densities, which is the case for induction heat treating. The most interesting parameters from the standpoint of monitoring equipment would be the coil current, the energy input, and the system power factor. Even these will give only a partial picture of the induction heating process inasmuch as the quenching and tempering phases are as critical to the proper heat treating of the part as the heating phase. With this in

	Power density	
Parameter	Low (about 1kW/in^2)	High (about 10kW/in^2)
Inductance	-27%	-10%
Resistance	-81%	-65%
Impedance	-36%	-15%
Current	+132%	+66%
Power factor	-53%	-57%
Efficiency	-20%	-16%

Figure 8.99 Sample calculation results of actual change percentage of the process parameters when part has been heated from a "cold" stage to a "hot" stage for a low power density (heating prior to hot forming) and high power density (surface hardening).

mind, it would be desirable for the end-user to have equipment available that could monitor several parameters simultaneously in real-time and indicate which parameters may cause an improperly heated treated part.

Some manufacturers do a design of experiments (DOE) before purchasing equipment. In this way it is possible to determine the most significant variables in the process. The equipment design may then focus on controlling these parameters rather than the larger number of less significant variables that could be pursued.

Either past experience or a design of experiments approach may be used to select the most important variables to monitor and control during the heat treating process. Some variables are more consistent than others and can be monitored with very inexpensive circuitry. Others are critical with respect to their magnitude and timing relative to other parameters and more expense may be justified to ensure that these variables are more tightly monitored and controlled. The items in the preceding list of variables may be broken down as shown below for a given machine.

Simple Inexpensive Check or Check Seldom Required

1. Material chemistry/prior microstructure,
2. Material geometry,
3. Induction coil geometry,
4. Induction coil material and flux concentrator (if required),
5. Part-to-coil location,
6. Quench medium, temperature, purity, concentration, and pressure,
7. Incoming part temperature,
8. Part temperature after heat,
9. Part temperature after quench,
10. Inductor and bus temperature,
11. Power component and heat station temperature, and
12. Incoming line voltage.

More Expensive Monitor May Be Justified

1. Frequency,
2. Power, voltage, current, or kVA,
3. Heat time,
4. Quench flow,
5. Part temperature during heat,
6. Part rotation, and
7. Scan speed.

A heat treating system would require signature monitoring of the energy envelope during hardening and tempering. Quench timing, volume, and temperature would typically be monitored. Final part temperature during the heating and tempering process may also be monitored. If there is a concern for material growth during heating, strain gauges may be installed in tooling to measure force or percent elongation. This process could require up to 16 or more parameters to be monitored on a signature-type system to ensure correct magnitude and timing of all parameters.

8.14.3.2 Induction Mass Heating

For the mass heating process, there is little concern with timing conditions or turning the power supply ON and OFF except in cases of attempting to maintain line temperature for a short time during an equipment malfunction. Exit temperature is an important parameter and often is measured with a dual set point optical pyrometer to ensure the correct exit temperature. In order to prevent overheating or melting the workpiece in the event of a slowdown or stoppage in part motion, a stop motion detector is usually required. On reheating applications it is sometimes necessary to sense the incoming part temperature and reset the power supply output power to compensate for variations in the incoming temperature.

With certain types of material, rapid heating can cause cracking of the part during heating (e.g., induction heating of high carbon content billets and bars to forging temperatures or induction hardening of gray irons). For these materials a slow rampup may be required in the application of power to the workpiece.

Because the process is continuous there is little need to monitor the energy in short intervals. Total power consumption and cost of electrical power are major concerns and often warrant the installation of analog or digital watt-hour meters.

A list of variables for the induction mass heating process would include:

1. Material chemical composition and properties,
2. Material geometry,
3. Induction coil geometry,
4. Induction coil material,
5. Part-to-coil relative size,
6. Frequency,
7. Power, voltage, current or kVA,
8. Heat time,
9. Incoming part temperature,
10. Part temperature after heat and temperature uniformity,
11. Inductor and bus temperature,
12. Power component and heat station temperature,
13. Incoming line voltage, and
14. Production rate.

As in the case of induction heat treating, some variables are more consistent than others and can be monitored with inexpensive circuitry. Others are critical and more expense may be justified to ensure that these variables are more tightly monitored and controlled. These items may be broken down as shown below for a given machine.

Simple Inexpensive Check or Check Seldom Required

1. Material chemical composition and properties,
2. Material geometry,
3. Induction coil geometry,
4. Induction coil material,
5. Part-to-coil location,
6. Incoming part temperature,
7. Inductor and bus temperature,
8. Power component and heat station temperature, and
9. Incoming line voltage.

More Expensive Monitor May Be Justified

1. Frequency,
2. Power, voltage, current, or kVA,
3. Heat time,
4. Part temperature,
5. Part "stop motion," and
6. Production rate.

In short, there is no single answer for monitoring and controlling an induction heat treating or mass heating system. Each application is different and requires careful analysis of the process requirements and sensitivity of the process to variation in ambient conditions and input parameters.

8.14.4 Basic Principles of Feedback and Control Algorithms

In order to properly control a power supply or the output of an induction heating system it is necessary to use a variety of control algorithms. These may be comprised of open and closed loop control systems to accomplish the control of material transport, output power, and temperature.

The basic elements of a process control system are shown in Figure 8.100. A set point is applied to the system as the input at the summing point or feedback comparator. In a closed-loop system, the final controlled variable is measured and a signal proportional to its value is returned to the comparator. If the value is below the desired output value, the difference between the input signal and the control signal, or the system error signal, is fed into the final control element. The final control element then increases the value of the controlled variable until the error signal approaches zero and the value of the controlled variable approaches the ideal or desired value. This comparison and response of the system can be handled in a variety of ways that are described below.

8.14.4.1 Open-Loop Systems (Feedforward Control Systems)

A true open-loop system would run without feedback by simply setting an input variable and allowing the output variable to fluctuate within an acceptable range without feeding back any indication of magnitude, phase, frequency, temperature, and so on. A simple water valve might be an example of a completely open-loop system. If the valve is opened, the fluid may flow in the system from one point to another. If system pressure changes for some reason, the flow in the circuit may change because there is no feedback to automatically adjust the system input to

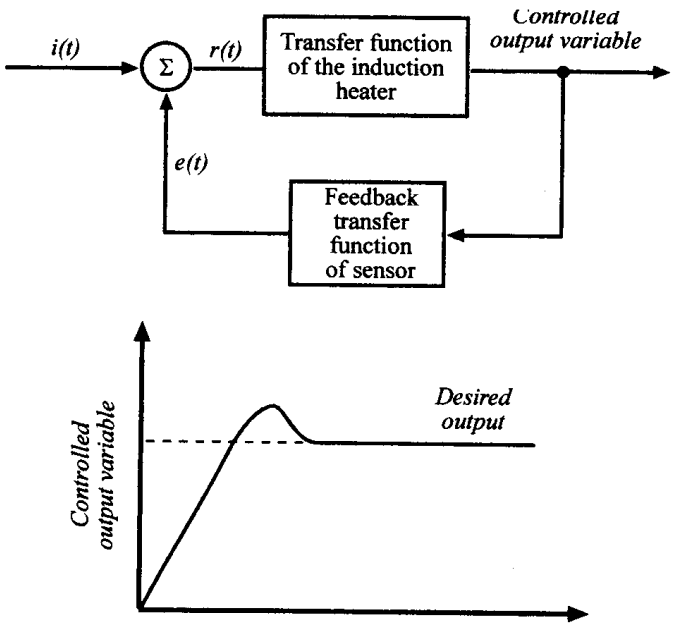

Figure 8.100 Basic feedback control system.

compensate for changes in the output variable. Some open-loop systems do measure an output variable but use it for registration purposes only.

Many open-loop systems are combinations of closed-loop components that provide a regulated input variable to the system but provide no measurement or feedback of the final critical system output variable. For example, an induction heating power supply may use regulation circuits to provide a very stable input power to the heating coils, whereas no measurement is made of the final exit temperature of the part. The system is running essentially open-loop with the assumption that stable input will provide stable output. A typical rotation motor drive would also be used in this fashion. The drive itself may utilize IR compensation to regulate the voltage to the motor armature but there is no measurement of the actual speed of rotation of the motor or any attempt to correct it to a desired value. The assumption is that once it is set it will remain the same for each cycle to be run.

One example of an effective use of an open-loop system would be wire and cable heating systems where it is very difficult to reliably measure the output parameter.

8.14.4.2 Closed-Loop Systems (Feedback Control Systems)

Obviously if we are really concerned about arriving at the right value for the controlled output variable it pays to measure it and to use it as a signal to stabilize the control response to make sure that the measured value is the desired value. This may be done on an induction heating system by measuring the part temperature and adjusting the controller response based on the difference between the actual measured temperature and the desired temperature. Once this measurement is made there are several common ways of using the error signal to change the value of the controlled output variable.

8.14.4.3 ON-OFF Control Algorithms

An ON-OFF control has two states. It is either fully ON or fully OFF. There is no intermediate state. If the value of the controlled output variable is below the lower set point the error signal will drive the control to turn fully ON, providing maximum power to the system until the value of the controlled output variable exceeds the upper set point (Figure 8.101). With this type of control the value of the controlled output variable will oscillate about the desired value with the rate of oscillation dependent on the system time response and the upper and lower set point levels.

This sounds simple, but can be problematic when trying to make small corrections. Unless an appropriate amount of hysteresis (control response delay) is added to the circuit, frequent ON-OFF cycling and hunting or oscillation of the supposedly controlled output variable can occur. This type of system works best when there is a relatively long time delay in system response.

8.14.4.4 P, I, D, PI, and PID Control Algorithms

A more sophisticated way of approaching the control on a system would be to implement proportional (P), integral (I), and/or derivative (D) types of control. These may be implemented individually or together depending on the specific application requirement.

a. *Proportional Control.* Proportional control is a term used to describe a control circuit that provides full controller output below a specified level. Above that level, the controller response to an error signal is diminished as the controlled output variable approaches the desired value (Figure 8.102). A proportional band is specified above and below the final desired value for the controlled output variable. When the controlled output variable is operating within the band a proportionally smaller response occurs to an error signal. The normal setup that is needed for a proportional type controller would be the manual reset and the gain (or bandwidth) setting.

The manual reset will change the position of the proportional band with respect to the set point to apply more or less output correction in response to an

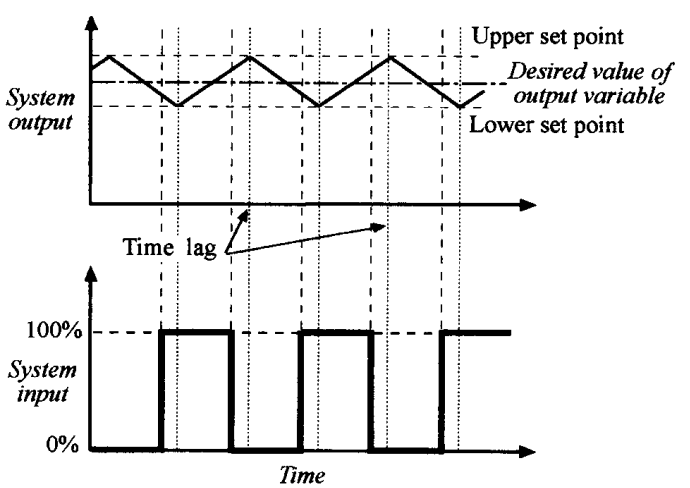

Figure 8.101 Simple ON/OFF control.

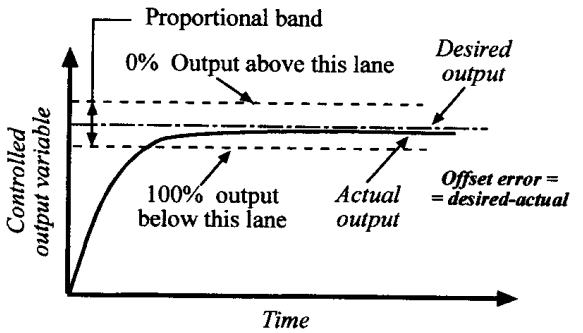

Figure 8.102 Proportional control.

error signal when the value of the controlled output variable is near the set point. An incorrect value for this setting will result in the actual value of the controlled output variable being more or less than the desired value.

The gain (or bandwidth) setting has to do with setting the level or amount of controller response to an error signal when the value of the controlled output variable reaches a specified percentage of the set point. Too low a value for the gain setting will result in droop error, or the actual value of the controlled output variable being less than the desired value. Too high a value for the gain setting will result in oscillation of the controlled output variable.

Proportional controllers are most useful where the process is stable and the set point is not often changed.

b. *Integral Control.* In the proportional mode the controller provides a response based on what the value of the error at a specific time. The integral feature is used with the proportional mode to provide a response signal in proportion to the previous history of the error signal. The response is based on the net area under the error curve and the response signal may be set by the integral gain setting to be equal to a proportion of the area under the error curve. The net effect is to allow the value of the controlled output variable to "home in" on the set point level over time.

c. *Derivative Control.* With the derivative mode of control the response is based on the "time rate of change" of the error signal. If the error is zero but is changing rapidly at that time, the derivative control portion of the system will apply a relatively large correction. The derivative mode of control by itsself is inherently unstable and is always used in combination with other types of control.

The most common combinations of these control modes would be proportional–integral (PI), proportional–derivative (PD), and proportional–integral–derivative (PID). Transfer functions for the various modes may be found in standard textbooks on process control [344, 345].

The response of these control modes can be set up to be either direct or reverse acting. This means that the response to the error signal for a direct acting system would be to increase system output when the error increases. Most often for temperature control a reverse acting system is required so that if the temperature is too high, the kW output to the load circuit is reduced.

8.14.4.5 PLC Controller

In the field of induction heating PLCs are used for controlling machine functions through ladder logic and a variety of analog and digital output modules and servo-motor drives. Often a separate controller would be used for specific PID loop functions within the induction heating system. PLCs are often used in an open-loop fashion for the heating portion of the system. An analog input signal is provided from the PLC to the power supply. The controlled output variable from the power supply would be the kW level. This is often measured at the PLC and an alarm circuit may be set to indicate if the actual and preset values do not correspond to each other but there is no attempt to reset the analog input to the power supply based on the measured kW.

Most PLC systems utilize the PLC for control as well as fault and diagnostic messaging, and a separate computer-based system may be used for signature-type monitoring of the process in real-time.

8.14.4.6 Controller Tuning

Ideally when a controller is set up for operation on an induction heating system the desire is to get the workpiece up to the required temperature as quickly as possible with very little overshoot. This same objective is held for a motor drive or positioning system. The goal is to move to position at a preset velocity and to arrive exactly at the chosen end point. A servo positioning system is easily able to accomplish this task.

On induction mass heating systems there is a considerable lag from the time an input signal is applied until the temperature of the part is stabilized. Coil lines may be 20 feet long with coils connected in parallel. It may take minutes for a part to traverse from one end of the line to the other. It is necessary to measure the response to a given change before attempting to make another change in the system's input parameters. Many systems that are envisioned to be a PID system to control the part temperature are actually running with the gain, reset, and proportional band settings adjusted to such a slow response that the system functions as an open-loop system. In the area of induction hardening, the cycles are much shorter and there is more likelihood of being able to accomplish closed-loop control.

For either type of system the general approach would be to attempt to use standard off-the-shelf controllers and tune them up on the production floor. This can become time consuming and costly so their use must be carefully reviewed to determine whether the benefits outweigh the additional cost associated with the control components and implementation costs.

8.14.5 Energy Monitoring

A simple energy monitor is shown in Figure 8.103. This monitor measures and displays the actual energy delivered to the induction coil in kilowatt seconds. It is a relatively inexpensive device. Once a heating pattern is developed and the correct power and heating time are established this information is preset into the monitor. The user then enters the acceptable lower and upper kilowatt second limits. If insufficient or excessive energy is applied to the load, the display will show "REJECT/UNDER" or "REJECT/OVER," respectively. Auxiliary contacts can be used to reject the part in automated lines or sound an alarm in manual operations.

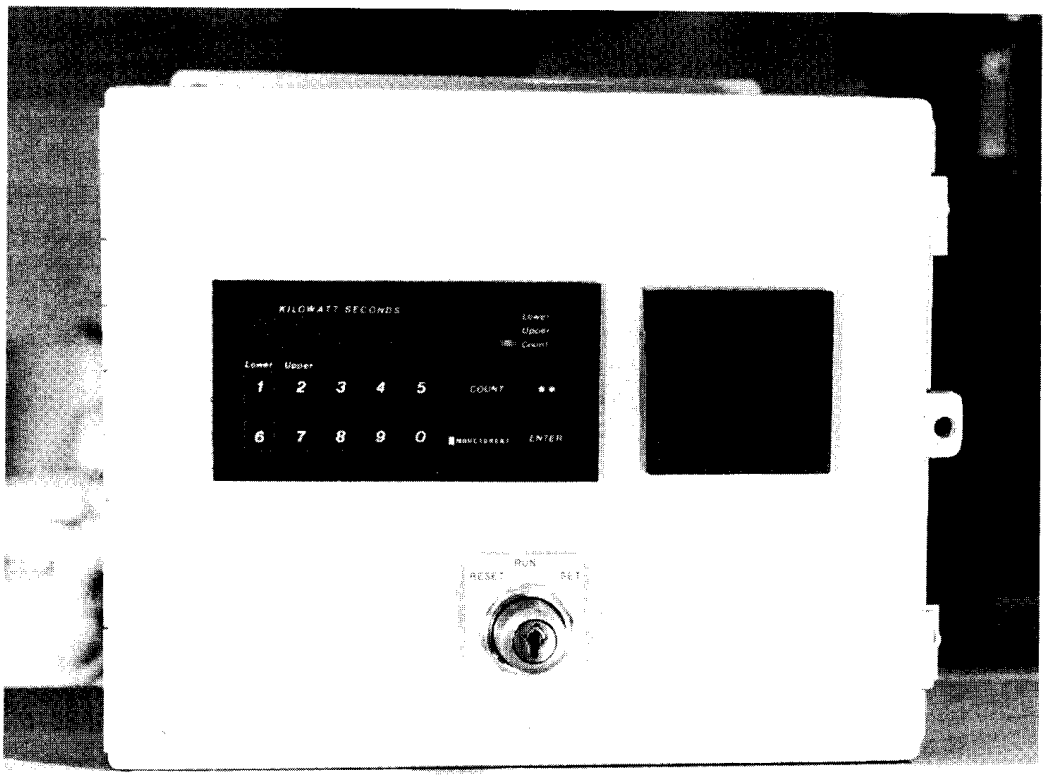

Figure 8.103 INDUCTOHEAT's energy monitor.

If the count falls within the preset range, the "ACCEPTABLE" indicator will be displayed. The energy monitor can be used as an induction process controller to turn off the power automatically when the desired amount of energy is delivered to the load. The energy monitor circuitry accurately measures and displays the output of the power supply. Although most earlier RF monitoring was on the input, fiber optics now make it possible to monitor the high voltages and frequencies on the output safely.

There is often debate with respect to the best location to monitor the voltage and current for the energy monitor. Ideally this should be done at the coil terminals to eliminate other components from masking energy changes or causing false indications of changes. The energy monitor system sometimes measures energy in this way. In most cases it is easy to monitor the coil voltage but rather difficult and/or expensive to monitor the coil current.

A reasonable alternative is to monitor the coil voltage and the primary current to the isolation transformer. The secondary current waveform is virtually identical to the primary current but phase-shifted 180° (a very small amount of additional phase-shift may be contributed by the output transformer magnetizing current). When the secondary current is used with an additional 180° phase-shift at the feedback current transformer and corrected for the output transformer ratio, the result is a negligible difference in the measurement between a system using primary current or a system using secondary current feedback (see Figures 8.104 and 8.105).

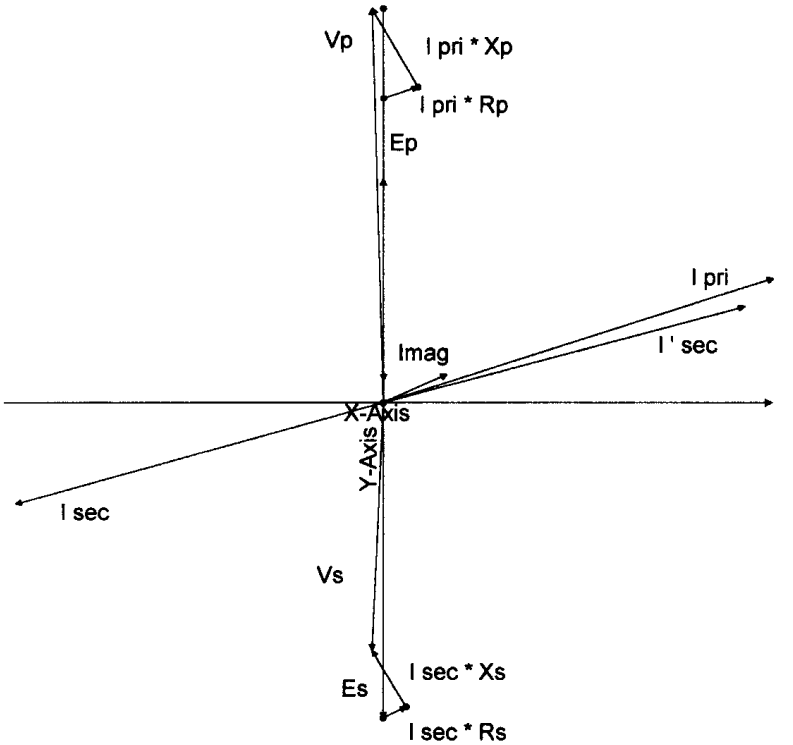

Figure 8.104 Example of the vector-phase diagram for energy monitoring. As a result of magnetizing current there is a phase shift.

Coil voltages may be considerably different from job to job. Therefore manufacturers will often standardize the design of energy monitor electronic circuits and feedback components for use on the primary of the output isolation transformer because the voltage range at that point is well known and remains the same from one

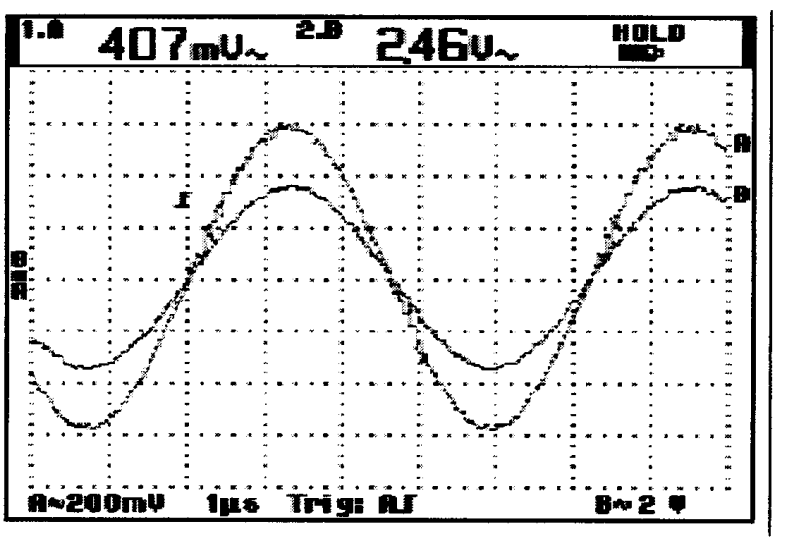

Figure 8.105 Scope diagrams for energy monitoring.

application to another. It is also more economical with respect to feedback component cost.

One of the most common application problems with energy monitors and other monitoring systems is the attempt to set the limits too close to the desired set point. Most power supplies will regulate the output power to within ±1 or 2% of the power supply's full-scale output rating. The energy monitor electronic circuitry and feedback components are similar to the power supply and typically give an output repeatability of ±1% of full scale. This means that the process could indicate ±3% for a system that is running in its normal regulation mode. The upper and lower set point limits must be set beyond this range or good parts may be rejected as being bad.

The desired setup method for the energy monitor would be to develop a good part on the heat treating system and then run parts at 5 or10% above and below this setting. The part should then be checked to see if it is in or out of spec. The desired upper and lower limits should be set just inside the limits that would cause the process to go out of specification. This will eliminate many problems of false tripping or rejection of good parts but will prevent any bad parts from entering the production line. Customers who try to set the energy monitor or signature system set points to too tight a range spend thousands of dollars each year on needless service calls.

8.14.6 Advanced Monitoring and Signature Analysis

With the advent of the programmable logic controller (PLC), a much larger number of points could be monitored in real-time during the heat treatment cycle. In the early 1980s, HWG Inductoheat in Germany developed the coil signature system, which was sold on many commercial machines and has been effectively applied for repeatable heat treatment processes.

The general idea of the signature concept is rather simple and can be described as follows. The monitoring system observes one of the unregulated variables related to the process and stores the most important parameters during the machine cycle. These values are compared to set points stored in the information bank within the PLC (ideal signature), and an output indication is given on the human–machine interface (HMI) readout. In normal performance all subsequent signatures of cycles are compared to the ideal one and must remain between the upper and lower limits (Figure 8.106). If any signature goes outside the limit area, the operator can see exactly during which part of the heat treatment cycle the signature was not repeated and the process exceeded the set limits. The operator knows immediately what the problem is and what should be done to adjust the machine to get the cycle signature back into the correct setup. It is not necessary for the operator to know in detail the electromagnetic, heat transfer, or quenching features of the process. He or she merely needs to know how to adjust the machine to get the signatures back to the ideal shape. Figure 8.107 shows an advanced commercial signature monitoring system, QA Ultra 8000, that has been used in the heat treating industry since 1991. This system verifies all machine settings to provide confidence in the processing quality of the part.

On this type of system a liquid crystal display (LCD) or other type of graphics display is utilized to give a real-time signature or display of the magnitude of a specific variable with respect to time. Many different variables can be monitored

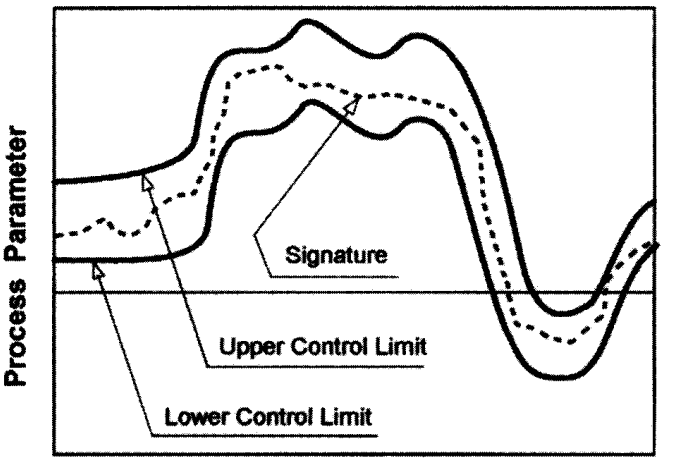

A) Signature of the process parameter

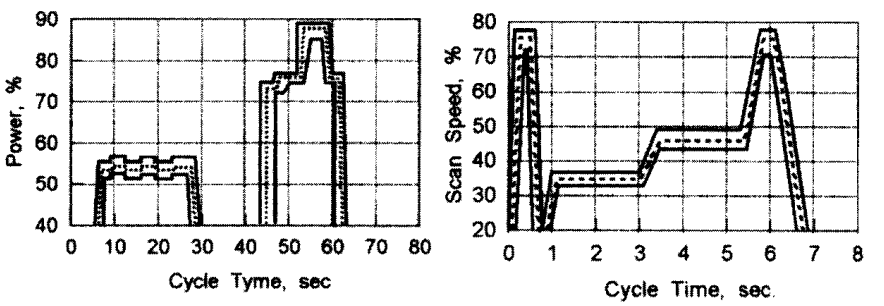

B) Examples of power signatures of power and scan speed

Figure 8.106 Control limits and signature sample.

and displayed simultaneously to give a complete picture of what is happening during the cycle. It is wise to remember that each parameter that is monitored adds cost to the machine.

For conventional induction hardening applications, from four to eight signatures are often sufficient to define the process. For example, scanning induction surface hardening typically requires the following signatures: scan speed, quench pressure, rotation speed, and power/energy. Single-shot hardening processes could require parameters such as rotation speed, quench pressure, power/energy, and quench flow. Because the part is not moving during the heating cycle, the scan speed is irrelevant to the process, although monitoring these parameters might indicate a tendency toward a failure of the machine index. Therefore, for maintenance, scan speed could be monitored. Other parameters that would be advisable to monitor with a signature system are shown in Figure 8.108.

More modern monitoring systems have been developed using computer systems to give virtually unlimited storage capability to hard disk or tape backup. The output gives a high and low set point display with the actual value being accumu-

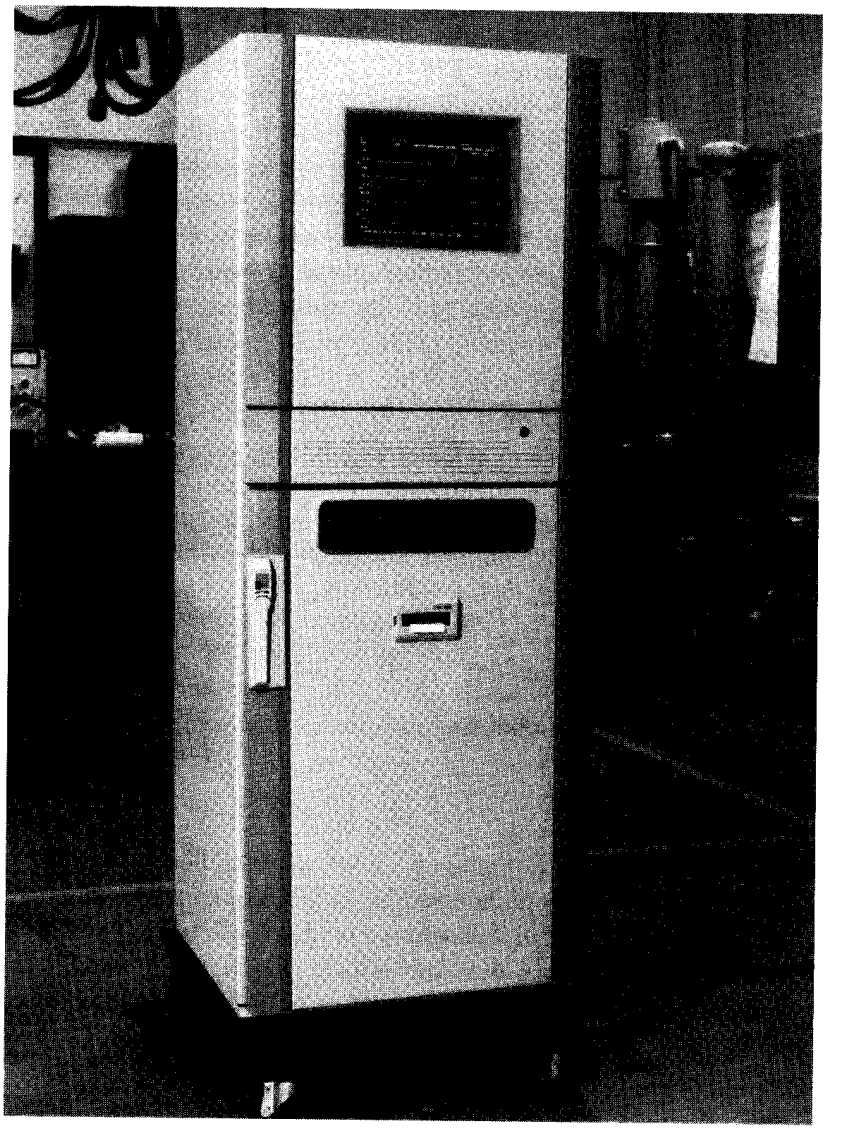

Figure 8.107 QA Ultra 8000 quality assurance monitor.

lated as the process is viewed. If any of the variables exceed the high or low set point the system will give warning of an unacceptable part and the operator can generally look at the screen and determine why the part is unacceptable. A variety of statistical process control (SPC) analyses can also be done on current data or data retrieved from past runs of a particular part.

8.14.7 Protective Devices and Safety Principles

There are several variables that have more to do with operator safety and prevention of damage to the equipment than prevention of improperly heating the workpiece. These would include water pressure, water flow, ground fault detectors, safety interlocks, door switches, over-current protection devices, over-temperature protection, and capacitor pressure and discharge circuits.

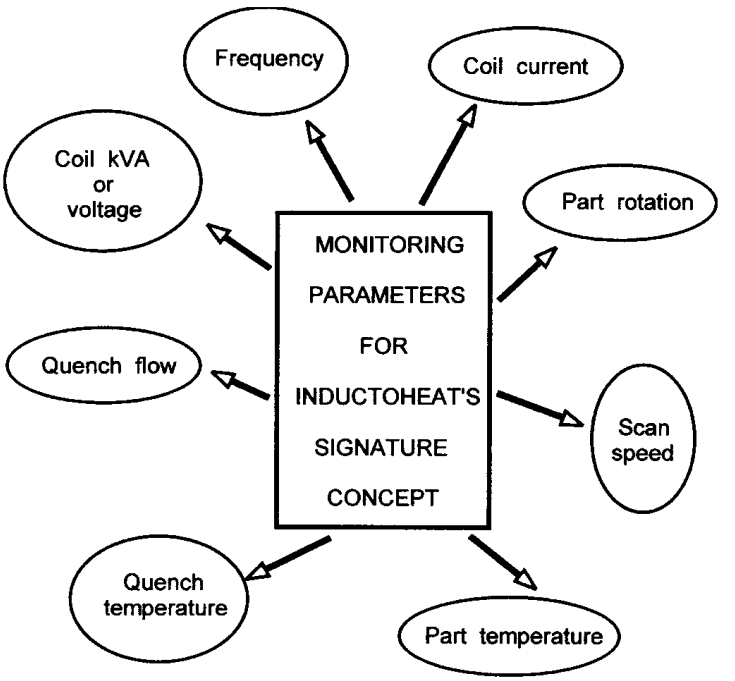

Figure 8.108 INDUCTOHEAT's typical monitoring parameters for the signature concept for induction hardening applications

Operator safety is of paramount importance in the design of any industrial equipment. Induction heating power supplies operate with high voltages and currents and with components that can store and discharge energy. Safety interlocks are included on doors and guarding to ensure that the system power is removed if an operator enters an enclosure or guarded area. Output isolation transformers are often grounded on the secondary to prevent operator contact with DC voltage in the event of a transformer failure.

With respect to equipment protection, ground fault detectors are used to prevent damage to equipment if a moving workpiece touches the induction heating coil. Water flow and temperature protection are included to prevent failure of semiconductors, transformers, capacitors, and water-cooled current-carrying conductors. Over-current protection may be in the form of fast-acting semiconductor fuses or electronic limit or trip circuits.

For the most part, this type of protection is set up to immediately turn off the HF output power and to remove all energy from the circuit. Latching control circuits are used with LEDs, LCD panels, or other types of displays to maintain a record of the circuit component causing the system to stop. Pressing a manual reset push button then resets the circuit.

8.14.8 Final Remarks

Different types of monitoring systems are available on the market. The choice of a particular monitoring system is a matter of operational features of the process, cycle time, technological requirements, and cost. In some applications a relatively simple

energy monitor will be sufficient. Other applications may require advanced signature monitoring devices.

For the purist in machine control techniques, the obvious next step in the monitor and control area is to move from the point of observing that a part was not properly hardened to taking corrective action as the problem is encountered. For example, the use of a servocontrol valve would allow the control to raise or lower the quench flow or pressure when the value drops below the control set point. In this type of system there typically would be two sets of set points around each signature; one pair of control set points, and one pair of alarm set points. If the control set point were exceeded, corrective action would be taken. If the alarm set point were exceeded, the part would be classified as unacceptable.

Although technically feasible, this high-tech monitoring hardware may add considerable cost to the induction heating equipment while at the same time reduce overall system reliability. In many instances the more prudent approach may be to utilize some of the basic monitoring and control techniques mentioned above, with general preventive maintenance and common sense to maintain consistent reliable results.

References

1. C. A. Tudbury, Basics of Induction Heating, Rider, New York, 1960.
2. M. G. Lozinskii, Industrial Applications of Induction Heating, Pergamon, London, 1969.
3. E. J. Davies, Induction Heating Handbook, McGraw-Hill, New York, 1979.
4. A. E. Slukhotskii and S. E. Ryskin, Inductors for Induction Heating, Energy Publications, St. Petersburg, Russia, 1974.
5. A. E. Slukhotskii et al., Induction Heating Equipment, St. Petersburg, Russia, 1981.
6. S. L. Semiatin and D. E. Stutz, Induction Heat Treatment of Steel, ASM International, Metals Park, OH, 1986.
7. Induction Heating, Course 60, ASM International, Metals Park, OH, 1986.
8. M. Orfueil, Electric Process Heating, Battelle Press, 1987.
9. S. Zinn, Elements of Induction Heating: Design, Control, and Applications, ASM International, Metals Park, OH, 1988.
10. E. J. Davies, Conduction and Induction Heating, Peter Peregrinus, London, UK, 1990.
11. A. D. Demichev, Surface Induction Hardening, St. Petersburg, Russia, 1990.
12. G. F. Golovin and M. M. Zamjatin, High-Frequency Induction Heat Treating, Mashinostroenie, St. Petersburg, Russia, 1990.
13. G. Vander Voort, Atlas of Time-Temperature Diagrams for Irons and Steels, ASM International, 1991.
14. Heat Treater's Guide: Practices and Procedures of Irons and Steels, ASM International, 1999.
15. J. Mortimer, Batch induction melting, *Foundry*, August, 1994.
16. P. Neelakanta, Handbook of Electromagnetic Materials, CRC Press, Boca Raton, FL, 1995.
17. Metals Handbook, ASM International, 2000.
18. G. Totten and M. Howes, Steel Heat Treatment Handbook, Marcel Dekker, New York 1997.
19. ASM, Metals Handbook, 9th ed., Vol. 4, Heat Treating, ASM, Cleveland, OH, 1991.
20. C. Brooks, Principles of the Heat Treatment of Plain Carbon and Low Alloy Steels, ASM International, 1996.

21. G. Krauss, Steels: Heat Treatment and Processing Principles, ASM International, 1999.
22. S. Avner, Introduction to Physical Metallurgy, McGraw-Hill, New York, 1964.
23. K. Thelming, Steel and Its Heat Treatment, Butterworth, London, 1975.
24. Atlas of Isothermal Transformation and Cooling Transformation Diagrams, ASM International, 1977.
25. D. Lavers, Current, force and velocity distributions in the coreless induction furnace, Ph.D. Thesis, University of Toronto, Canada, 1970.
26. B. Gebhart, Heat Transfer, McGraw-Hill, New York, 1970.
27. S. Patankar, Numerical Heat Transfer and Fluid Flow, Hemisphere, New York, 1980.
28. F. P. Incropera and D. P. Dewitt, Fundamentals of Heat Transfer, Wiley, New York, 1981.
29. R. F. Myers, Conduction Heat Transfer, McGraw-Hill, New York, 1972.
30. J. A. Adams and D. F. Rogers, Computer Aided Analysis in Heat Transfer, McGraw-Hill, New York, 1973.
31. W. M. Rohsenow and J. P. Hartnett, Handbook of Heat Transfer, McGraw-Hill, New York, 1973.
32. R. Siegel and J. R. Howell, Thermal Radiation Heat Transfer, 2nd ed., McGraw-Hill, New York, 1980.
33. J. A. Wiebelt, Engineering Radiation Heat Transfer, Holt, Rinehart & Winston, New York, 1966.
34. E. M. Sparrow and R. D. Cess, Radiation Heat Transfer, Wadsworth, Englewood Cliffs, NJ, 1966.
35. J. R. Howell, A Catalog of Radiation Configuration Factors, McGraw-Hill, New York, 1982.
36. W. C. Leslie, The Physical Metallurgy of Steels, McGraw-Hill, New York, 1981.
37. ASM, Metals Handbook, Vol. 2, Properties and Selection: Nonferrous Alloys and Pure Metals, ASM, Cleveland, 1979.
38. ASM, High Temperature Property Data: Ferrous Alloys, ASM, Metals Park, OH, 1988.
39. L. V. Bewley, Flux Linkages and Electromagnetic Induction, Dover, New York, 1964.
40. Encyclopedia of Physics, 2nd ed., VCH, 1991.
41. R. W. Chabay and B. A. Sherwood, Electric and Magnetic Interactions, Wiley, New York, 1995.
42. P. Hammond, Electromagnetism for Engineers, Pergamon, New York, 1978.
43. M. A. Plonus, Applied Electromagnetics, McGraw-Hill, New York, 1978.
44. I. E. Tamm, Fundamentals of the Theory of Electricity, Moscow, Russia, 1981.
45. W. H. Hayt, Jr., Engineering Electromagnetics, McGraw-Hill, New York, 1981.
46. H. G. Booker, Energy in Electromagnetism, Peter Peregrinus, London, UK, 1982.
47. N. N. Rao, Elements of Engineering Electromagnetics, Prentice-Hall, Englewood Cliffs, NJ, 1987.
48. R. Ehrlich, J. Tuszynski, L. Roelofs, and R. Storner, Electricity and Magnetism Simulations: The Consortium and Upper-Level Physics Software, Wiley, New York, 1995.
49. V. Nemkov, B. Polevodov, and S. Gurevich, Mathematical Modeling of High-Frequency Heating Equipment, 2nd ed., St. Petersburg, Russia, 1991.
50. V. Rudnev and K. Schweigert, Designing induction equipment for modern forge shops, *Forging*, Winter 1994, 56–58.
51. V. Nemkov and V. Demidovich, Theory of Induction Heating, Energoatomizdat, St. Petersburg, Russia, 1988.
52. D. Griffiths, Electrodynamics, Prentice-Hall, Englewood Cliffs, NJ, 1989.

53. V. Rudnev, Mathematical simulation and optimal control of induction heating of large-dimensional cylinders and slabs, Ph.D. Thesis, Department of Electrical Technology, St. Petersburg Electrical Engineering University, Russia, 1986.
54. G. Smith, Numerical Solution of Partial Differential Equations: Finite Difference Methods, 3rd ed., Oxford University Press, Oxford, UK, 1985.
55. K. J. Binns, P. J. Lawrenson, and C. W. Trowbridge, The Analytical and Numerical Solution of Electric and Magnetic Fields, Wiley, New York, 1992.
56. A. A. Samarskii, Theory of Finite Difference Schemes, Moscow, 1977.
57. S. V. Patankar and B. R. Baliga, A new finite-difference scheme for parabolic differential equations, *Num. Heat Transfer*, 1:27–30, 1978.
58. K. S. Demirchian and V. L. Chechurin, Computational Methods of Electromagnetic Field Simulations, Moscow, 1986.
59. J. C. Strikwerda, Finite Difference Schemes and Partial Differential Equations, Wadsworth & Brooks, Belmont, CA, 1989.
60. M. V. K. Chari, Finite element analysis of nonlinear magnetic fields in electric machines, Ph.D. Dissertation, McGill University, Montreal, Canada, 1970.
61. M. V. K. Chari and P. P. Silvester, Finite element analysis of magnetically saturated DC machines, *IEEE Trans. PAS* 90: 2362, 1971.
62. J. Donea, S. Giuliani, and A. Philippe, Finite elements in solution of electromagnetic induction problems, *Int. J. Num. Methods Eng.* 8: 359–367, 1974.
63. W. Lord, Application of numerical field modeling to electromagnetic methods of nondestructive testing, *IEEE Trans. Magn.* 19(6): 2437–2442, 1983.
64. W. Lord, Development of a finite element model for eddy current NDT phenomena, Electrical Engineering Department, Colorado State University, 1983.
65. C. Marchand and A. Foggia, 2D Finite element program for magnetic induction heating, *IEEE Trans. Magn.* 19(6): 2647–2649, 1983.
66. P. P. Silvester and R. L. Ferrari, Finite Elements for Electrical Engineers, Cambridge University Press, New York, 1983.
67. W. Muller, C. Kramer, and J. Krueger, Calculation of 2- or 3- dimensional linear or nonlinear fields by the CAD-program profi, *IEEE Trans. Magn.* 19(6): 2670–2673, 1983.
68. R. K. Livesley, Finite Elements: An Introduction for Engineers, Cambridge University Press, New York, 1983.
69. N. Ida, 3-D finite element modeling of electromagnetic NDT phenomena, Ph.D. Thesis, Colorado State University, 1983.
70. J. D. Lavers, Numerical solution methods for electroheat problems, *IEEE Trans. Magn.* 19(6): 2566–2572, 1983.
71. D. A. Lowther and P. P. Silvester, Computer-Aided Design in Magnetics, Springer, Berlin, 1986.
72. W. Lord, Y. S. Sun, S. S. Udpa, and S. Nath, A finite element study of the remote field eddy current phenomenon, *IEEE Trans. Magn.* 24(1): 435–438, 1988.
73. A. Muhlbauer, S. Udpa, V. Rudnev, and A. Sutjagin, Software for modeling induction heating equipment by using finite element method, Proceedings of the Tenth All-Union Conference on High-Frequency Application, St. Petersburg, Russia, Part 1, 36–37, 1991.
74. E. J. W. ter Maten and J. B. M. Melissen, Simulation of inductive heating, *IEEE Trans. Magn.* 28: 1287–1290, 1992.
75. J. M. Jin, The Finite Element Method in Electromagnetics, Wiley, New York, 1993.
76. S. Mandayam, L. Udpa, S. S. Udpa, and Y. S. Sun, A fast iterative finite element model for electrodynamic and magnetostrictive vibration absorbers, Proceedings of the Ninth Conference on Computation of Electromagnetic Fields, COMPUMAG, Miami, 8–10, 1993.

77. T. Dreher and G. Meunier, A 3D line current model of voltage driven coils, Proceedings of the Ninth Conference on Computation of Electromagnetic Fields, COMPUMAG, Miami, 50–52, 1993.
78. M. Hano, An improved finite element analysis of eddy current problems connected to voltage source, *IEEE Trans. Magn.* 29:2, 1993.
79. E. Thimpson, The finite element method, Class Notes CE-665, Colorado State University, Progress in 1978–1990.
80. O. C. Zienkiewicz and R. L. Taylor, The Finite Element Method, 4th ed., Vol. 1, Basic Formulation and Linear Problems, McGraw-Hill, New York, 1989.
81. L. J. Segerlind, Applied Finite Element Analysis, Wiley, New York, 1976.
82. C. S. Desai, Elementary Finite Element Method, Prentice-Hall, Englewood Cliffs, NJ, 1979.
83. S. J. Salon and J. M. Schneider, A hybrid finite element–boundary integral formulation of the eddy current problem, *IEEE Trans. Magn.* 18(2): 461–466, 1982.
84. T. H. Fawzi, K. F. Ali, and P. E. Burke, Boundary integral equations analysis for magnetic field analysis, *IEEE Trans. Magn.* 19(6): 2337–2339, 1983.
85. S. Cristina and A. Di Napoli, Combination of finite and boundary elements for magnetic field analysis, *IEEE Trans. Magn.* 19(6): 2337–2339, 1983.
86. C. A. Brebbia, The Boundary Element Method for Engineers, Pentech Press, London, UK, 1978.
87. K. R. Shao and K. D. Zhou, Boundary element solution to transient eddy current problems, *Eng. Anal.* 1: 182–187, 1984.
88. M. H. Lean, Electromagnetic field solution with the boundary element method, Ph.D. Thesis, University of Manitoba, Winnipeg, Canada, 1981.
89. Y. B. Yildir, A boundary element method for the solution of Laplace's equation in three-dimensional space, Ph.D. Thesis, University of Manitoba, Winnipeg, Canada, 1985.
90. T. Inuki and S. Wakao, Novel boundary element analysis for 3-D eddy current problems, *IEEE Trans. Magn.* 29(2): 1520–1523, 1993.
91. K. F. Wang, S. Chandrasekar, and H. T. Y. Yang, Finite element simulation of induction heat treatment and quenching of steels, *Trans. NAMRI/SME* XX: 83–90, 1992.
92. V. Rudnev, Characteristics of transverse electromagnetic edge effect in induction heating of magnetic and nonmagnetic slabs, in The Study of Electrothermal Processes, Cheboscary, Russia, 30–34, 1985.
93. V. Rudnev, D. Loveless, M. Black, P. Miller, Progress in study of induction surface hardening of carbon steels, gray irons and ductile (nodular) irons. *Industrial Heating*, March, 1996.
94. G. Roen, Metallurgical considerations in induction hardening, Proceedings of the Sixth International Induction Heating Seminar, Nashville, September, 1996.
95. A. Sverdlin and A. Ness, Fundamental Concepts in Steel Heat Treatment, Chapter 1 of Steel Heat Treatment Handbook, edited by G. Totten and H. Howes, Marcel Dekker, New York, 1997.
96. A. Sverdlin and A. Ness, The Effects of Alloying Elements on the Heat Treatment of Steel, Chapter 2 of Steel Heat Treatment Handbook, edited by G. Totten and H. Howes, Marcel Dekker, New York, 1997.
97. B.Liscic, Hardenability, Chapter 3 of Steel Heat Treatment Handbook, edited by G. Totten and H. Howes, Marcel Dekker, New York, 1997.
98. Surface Hardening of S.G. Iron, British S.G. Iron Producers' Association Ltd., 1984.
99. C. Walton, Introduction to Heat Treating of Cast Irons, ASM Handbook, Vol.4, Heat Treating, ASM International, 1991.
100. R. Elliott, Cast Iron Technology, Butterworth, London, UK, 1988.

101. I. Minkoff, The Physical Metallurgy of Cast Iron, Wiley, New York, 1983.
102. M. Fallon, The Surface Hardening of Cast Iron, BCIRA, UK, 1988.
103. G. Kurdyumov et al., Transformations in Iron and Steel, Nauka, Moscow, 1977.
104. C. Walton, Gray and Ductile Iron Castings Handbook, Gray and Ductile Iron Founders' Society, Cleveland, OH, 1971.
105. Ductile Iron Data for Design Engineers, QIT-Fer et Titane Inc., 1990.
106. V. I. Rudnev, The Art of Computation of the Induction Heating Process, INDUCTOHEAT Booklet, INDUCTOHEAT, Inc., Madison Heights, MI, 1994.
107. V. I. Rudnev, New induction heat technology in Russia, in Heat Treating: Equipment and Processes, Conference Proceedings, ASM International, 209–213, 1994.
108. INDUCTOHEAT Bulletin, UNIPOWER UPF, Self Contained Induction Heating System, INDUCTOHEAT, Inc., Madison Heights, MI, 1990.
109. V. I. Rudnev, R. L. Cook, and J. LaMonte, Induction heat treating: Keyways and holes, *Metal Heat Treating*, March–April 1996.
110. V. I. Rudnev, D. L. Loveless, and R. L. Cook, Mystery of unknown in induction heat treating of carbon steel: Striping phenomena, *Industrial Heating*, November, 1995.
111. Gear Research Institute, Review of Literature on Induction Hardening of Gears, Project A-1051 (C553), 1994.
112. American Gear Manufacturers Association, Gear Materials and Heat Treatment Manual, ANSI/AGMA 2004-B29, Section 5.2, Flame and Induction Hardening AGMA, 1989.
113. AGMA, Design Guide for Vehicle Spur and Helical Gears, ASNI/AGMA 6002-B93, AGMA, Section 3.
114. K. Namiki, T. Urita, I. Machida, and T. Takagi, The application of hardenability assured cold forging medium carbon steels to CVJ outer race, SAE Technical Paper 930965, SAE International.
115. J. M. Storm and M. R. Chaplin, Dual frequency induction gear hardening, *Gear Technol.* 10(2): 22–25, 1993.
116. Y. Matsubara, M. Kumagawa, and Y. Watanabe, Induction hardening of gears by dual frequency induction heating, *J. Jpn. Soc. Heat Treatment* 29(2): 92–98, 1989.
117. V. I. Rudnev and R. L. Cook, Bar end heating, *Forging*, Winter 27–30, 1995.
118. INDUCTOHEAT Bulletin, Bar Heating, INDUCTOHEAT, Inc., Madison Heights, MI, 1994.
119. V. I. Rudnev and W. B. Albert, Continuous aluminum bar re-heating prior to reducing mill, *33 Metal Producing*, January, 50, 1995.
120. V. S. Nemkov, V. B. Demidovich, V. I. Rudnev, and O. Fishman, Electromagnetic end and edge effects in induction heating, UIE Congress, Montreal, Canada, 1991.
121. V. Rudnev and D. Loveless, Induction slab, plate and bar edge heating for continuous casting lines, *33 Metal Producing*, October, 32–34, 43–44, 1994.
122. V. Rudnev and D. Loveless, Longitudinal flux induction heating of slabs, bars and strips is no longer "black magic," Part 1, *Industrial Heating*, January, 29–34, 1995.
123. V. Rudnev and D. Loveless, Longitudinal flux induction heating of slabs, bars and strips is no longer "black magic," Part 2, *Industrial Heating*, February, 46–50, 1995.
124. R. M. Baker, Transverse flux induction heating, *Elec. Eng.*, October, 922–924, 1950.
125. R. M. Baker, Transverse flux induction heating, *Trans. AIEE* 69(2), 711–719, 1950.
126. M. Lamourdedieu, Continuous heat treatment of aluminum alloy strip, *Metal Prog.*, October, 88–92, 1951.
127. M. Lamourdedieu, Continuous heat treatment of aluminum alloys of the Duralumin type, 80: 335–338, 1952.
128. R. C. Gibson and R. H. Johnson, High efficiency induction heating as a production tool for heat treatment of continuous strip metal, *Sheet Metal Ind.*, December, 889–892, 1982.

129. R. Waggott, D. Walker, R. Gibson, and R. Johnson, Transverse flux induction heating of aluminum alloy strip, *Metals Techn.*, 9, 493–498, 1982.
130. J. Blacklung, Induction heating in rolling mills, new ideas and applications, *Rev. Metall. Cah. Inf. Tech.* 84: 67–71, 1987.
131. N. Ross, R. Kaltenhauser, and G. Walzer, Transverse flux induction heating of steel strip, Electroheat Congress, Toronto, Canada, 110–119, 1992.
132. T. Yamagishi, Y. Kitajima, K. Nagahama, H. Ishii, and H. Ikeda, TFX Induction Heating CAL for Rolled Aluminum Sheet, Jpn. Light Metal Association, Tokyo, April, 1988.
133. R. C. J. Ireson, Induction heating with transverse flux in strip metal process lines, *IEE Power Eng. J.*, 3, March, 1989.
134. R. C. Gibson, W. B. R. Moore, and R. A. Walker, TFX—an induction heating process for the ultra rapid heat treatment of metal strip, ASM Heat Treatment and Surface Engineering Conference, Amsterdam, May, 1991.
135. R. C. J. Ireson, Developments in transverse flux (TFX) induction heating of metal strip, *Metallurgia* February, 58–68, 1991.
136. S. Wilden, Inductive high-capacity annealing furnaces for the continuous treatment of strips, *Metallurgia*, 43, August, 1989.
137. I. Oku, M. Inokuma, and K. Awa, Application of induction heating to continuous treatment for aluminum alloy strip, *J. Jpn. Inst. Light Metals*, 40, August, 1990.
138. S. B. Lasday, Work processing for continuous annealing of sheet by transverse flux induction heating at steel plant, *Induction Heating*, October, 43–45, 1991.
139. K. Standford, Transverse flux induction heating, *Eng. Digest*, September, 23–25, 1987.
140. P. W. Ainscow, Inductive heating for production of galvannealed steel strip, *Steel Times*, April, 173–175, 1992.
141. E. Balle, J. Calas, and A. B. Wilhelm, Lacquer coating line for tin mill products, *Iron Steel Eng.*, May, 36–38, 1991.
142. W. Kolakowski, Economical production of hot strip with the compact strip production process, Improved Technologies for the Rational Use of Energy in the Iron and Steel Industry, NEC, Birmingham, UK, 1992.
143. V. Rudnev and R. Cook, Magnetic flux concentrators: myths, realities and profits, *Metal Heat Treating*, March/April 31–34, 1995.
144. J. Lamonte and M. Black, How flux concentrators improve inductor efficiency, *Heat Treating*, June, 1989.
145. R. Ruffini, Production and concentration of magnetic flux for eddy current heating applications, Report presented to the 1992 International Federation of Heat Treatment and Surface Engineering, Beijing, China, 1993.
146. R. Ruffini, Induction heating with magnetic flux technology, *Modern Appl. News*, 1991.
147. Alpha 1 Induction Service Center, General Presentation, *Industrial Heating*, 54–55.
148. Handbook of Experimental Stress Analysis, Wiley, New York, 1963.
149. R. D. Cook, Finite Element Modeling for Stress Analysis, Wiley, New York, 1995.
150. A. J. Fletcher, Thermal Stress and Strain Generation in Heat Treating, Elsevier Science, London, UK, 1989.
151. K. Weiss, In-line tempering on induction heat treating equipment, Proceedings of the First International Induction Heating Seminar, Sao Paulo, Brazil, 1995.
152. General Presentation of HWG, Germany, 1993.
153. K. Weiss, In-line tempering on induction heat treating equipment relieves stresses advantageously, *Industrial Heating*, December, 1995.
154. V. Rudnev, R. Cook, and D. Loveless, Keeping your temper with magnetic flux concentrators, *Modern Application News*, November, 1995.
155. NANMAC Temperature Measurement Handbook, Vol. IX, NANMAC Corp., Framingham, MA, 1997.

156. J. Schooley, Thermometry, CRC Press, Boca Raton, FL, 1986.
157. Manual on the Use of Thermocouples in Temperature Measurement, ASTM, Philadelphia, 1993.
158. E. Magison, Temperature Measurement in Industry, ISA, Research Triangle Park, North Carolina, 1990.
159. B. Liptak, Temperature Measurement, Chilton, PA, 1993.
160. T. McGee, Principles and Methods of Temperature Measurement, Wiley, New York, 1988.
161. N. Anderson, Instrumentation for Process Measurement and Control, Chilton, PA, 1980.
162. K. Irani, Theory and construction of blackbody calibration sources, Mikron Instrument Co. Inc., SPIE, The International Society for Optical Engineering, Proceedings of the Spring Conference, paper number 4360–49, 2001.
163. D. DeWitt, Theory and Practice of Radiation Thermometry, Wiley, New York, 1988.
164. Infrared Non-Contact Temperature Measurement, Mikron Instrument Co., Inc., 1998.
165. V. Demidovich and V. Nemkov, Computation of induction heating of non-magnetic cylinders, Proceedings of VNIITVCh: Industrial Applications of High Frequency Currents, Vol. 15, 1975.
166. S. Salon and J. Schneider, A hybrid finite element – boundary integral formulation of Poisson's equation, *IEEE Trans. on Magnetics*, 17: 6, November, 1981.
167. A. Konrad, M. Chari, and Z. Csendes, New finite element techniques for skin effect problems, *IEEE Trans. on Magnetics*, 18: 2, March, 1982.
168. B. Ancelle, A. Nicolas, and J. Sabonnadiere, A boundary integral equation method for high frequency eddy currents, *IEEE Trans. on Magnetics*, 17: 6, November, 1981.
169. V. Rudnev, Optimal control of a continuous induction heaters at transient state operation, M.S. Thesis, Samara State Technical University, Samara, Russia, 1977.
170. L. Zimin, A. Procenco, E. Rapoport, and V. Rudnev, Software and optimal control of in-line multi-coil induction slab heater, *Journal of Elements and Systems of optimum Identification and Control of Technological Processes*, Tula, Russia, 1987.
171. N. Smirnov, Study of transient processes during induction heating operation, Ph.D. Thesis, St. Petersburg Electrical Engineering University, Russia, 1989.
172. A. Severianin, Study of electromagnetic processes and design parameters of multi-layer billet heaters, Ph.D. Thesis, St. Petersburg Electrical Engineering University, Russia, 1986.
173. Electromagnetic Induction and Electric Conduction, Centre Francais de'Electricite, 1997.
174. D. Brand, Metallurgy Fundamentals, Goodheart-Willcox Co., Inc., 1985.
175. J. Shackelford, CRC Materials Science and Engineering Handbook, CRC Press, Boca Raton, FL, 2001.
176. R. Honeycombe and H. Bhadeshia, Steels: Microstructure and Properties, Edward Arnold, UK, 1995.
177. M. Bauccio, ASM Metals Reference Book, 1997.
178. G. Vander Voort, Metallography Principles and Practice, ASM International, 1999.
179. C. Brooks, Heat Treatment, Structure and Properties of Nonferrous Alloys, ASM International, 1995.
180. C. Brooks, Principles of the Austenization of Steels, Elsevier Applied Science, UK, 1992.
181. L. Samuels, Light Microscopy of Carbon Steels, ASM International, 1999.
182. J. Davis, Alloying: Understanding the Basics, ASM International, 2001.
183. D. Bullens, Steel and Its Heat Treatment, Wiley, New York, 1948.
184. E. Bain and H. Paxton, Alloying Elements in Steel, ASM International, 1966.
185. J. Hollomon and L. Jaffe, Ferrous Metallurgical Design, Wiley, New York, 1947.

186. M. Grossmann and E. Bain, Principles of Heat Treatment, ASM International, 1964.
187. T. Spencer et al., Induction Hardening and Tempering, ASM International, 1964.
188. W. Feuerstein and W. Smith, *Trans. ASM*, 46, 1270, 1954.
189. R. Bozorth, Ferromagnetism, IEEE Press, 1993.
190. V. Peisakhovich, The calculation of induction heating processes of square billets, proceedings of VNIITVCh, Mashgiz, St. Petersburg, Russia, 1961.
191. L. Zimin, Specifics of Induction Heating of Rectangular Slabs, Utilization of High Frequency Currents for Industrial Applications, St. Petersburg, Russia 1973.
192. N. Pavlov, Engineering Calculations of Induction Heaters, Energy, Moscow, 1978.
193. V. Nemkov, V. Demidovich, and V. Rudnev, Utilization of Electromagnetic Edge Effects in the Induction Heating Applications, High Frequency Technique for Induction Heaters, Energoatomizdat, Moscow, 1988.
194. V. Rudnev, Characteristics of Electromagnetic Transverse Edge Effects in Induction Heating of Magnetic and Non-Magnetic Slabs and Strips, An Investigations of Electro-thermal Installations, Chebocsary, 1985.
195. A. Danilushkin, E. Rapoport, and V. Rudnev, Optimal Control of Induction Heating Equipment, Algorithmization and Automation of Industrial Systems, Samara, 1979.
196. V. Demidovich, V. Rudnev, and A. Stochniol, The Study of Edge Effects in Square Ferromagnetic Slabs, Trans. of St. Petersburg Electrical Engineering Institute, St. Petersburg, Russia, 1985.
197. V. Rudnev, Optimal control of a continuous induction heaters at transient state operation, M.S. Thesis, Samara State Technical University, Samara, Russia, 1977.
198. A. Danilushkin, V. Rudnev, and L. Sindjakov, Automatic System for Optimization of the In-Line Continuous Fed Induction Heater During Start-Up and Shut-Down Operation, Algorithmization and Automation of Industrial Systems, Samara, 1980.
199. V. Demidovich, V. Rudnev, and A. Nikanorov, Computation of Temperature Distribution Across the Width of the Inductively Heated Rectangular Slab, Moscow, 1987.
200. V. Rudnev, Advanced induction heating design for forging and extrusion, Proceedings of the First International Induction Heating Seminar, Brazil, March, 1995.
201. V. Rudnev and S. Kondrashov et al., An optimal control and computation of industrially coupled processes: Induction heater—Direct extrusion, Proceedings of the Conference of the Russian Federation: Automatic Control of Advanced Technological Processes, 1987.
202. V. Bukanin and V. Kaz'min, Mathematical Modeling of Induction Processes for Forging Industry, Electrotermia, Vol. 1, Moscow, 1983.
203. V. Rudnev, R. Cook, D. Loveless, and M. Black, Induction heat treatment: Basic principles, computation, coil construction, and design consideration, Chapter 11A of the Steel Heat Treatment Handbook, edited by G. Totten and M. Howes, Marcel Dekker, New York, 1997.
204. V. Nemkov, V. Demidovich, and V. Rudnev, An effect of operation conditions of the design features of induction heaters, *Journal of Electrotechnics*, Moscow, 3, 1986.
205. L. Zimin, V. Rudnev and S. Kondrashov, Software and adaptive control of technological complex: Induction heating—Plastic deformation of large aluminum billets, Proceedings of the Conference of the Russian Federation: The Contemporary Methods of Improving Technological Mechanisms, Chebocsary, Russia, 1987.
206. V. Rudnev and S. Kondrashov, CAD of Coupled "Induction Heater—Direct Extrusion," Modeling and Optimal Control of Industrial Systems, Samara, Russia, 1988.
207. E. Rapoport and V. Rudnev et al., Advanced Control of Induction Heaters Consisting of In-Line Multiple Inductors, Theory and Practice of Induction Heating, Energoatomizdat, Moscow, Russia, 1985.

208. L. Zimin and E. Rapoport, Optimal Control of Temperature Distribution During Induction Heating of Aluminum Slabs, Utilization of High Frequency Currents for Industrial Applications, St. Petersburg, Russia 1971.
209. M. Chatterjee, USA Patent # 4,639,279, 1990.
210. US Army project DDJ02–88-M-0009 and Department of the Navy contract N00019–90-pa-mg-013, principle investigator M. Chatterjee, 1990.
211. D. Dudley, Handbook of Practical Gear Design, Technomic Publishing, 1994.
212. M. Conyngham, Metallurgical aspects to be considered in gear and shaft design, *Gear Technology*, March/April, 1999.
213. G. Parrish and D. Ingham, The Submerged Induction Hardening of Gears, Heat Treatment of Metals, Vol. 2, 1998.
214. K. Shepelyakovskii and F. Bezmenov, New induction heating technology, *Advanced Materials & Processes*, October, 1998.
215. W. Smith, Structure and Properties of Engineering Alloys, McGraw-Hill, New York, 1993.
216. A. Sinha, Ferrous Physical Metallurgy, Butterworth, London, UK, 1989.
217. G. Golovin and N. Zimin, Technology of Heat Treatment by Induction, Mashinostroenie, St. Petersburg, Russia, 1990.
218. Metals Handbook, Volume 1: Properties and Selection of Irons and Steels, ASM International, 1978.
219. C. Walton and T. Opar, Iron Castings Handbook, Iron Castings Society, Inc., 1981.
220. P. Beeley, Foundry Technology, Butterworth, London, UK, 1972.
221. E. Rowardy et al., Hardening characteristics of induction heated ductile iron, *Trans. of the American Foundrymen's Society*, 61, 422–431, 1953.
222. F. Yakovlev, Features of induction hardening of magnesium-treated iron, *Russian Castings Production*, 8, 389–390, 1967.
223. ASTM Standard # A247.
224. W. Nicola and V. Richards, Age strengthening of gray cast iron, An AFS Research Report, 2000.
225. R. Heine et al., Principles of Metal Casting, McGraw-Hill, New York, 1967.
226. J. Davis, ASM Specialty Handbook: Cast Irons, ASM International 1996.
227. J. Wallace and P. Weiser, Trace Elements in Gray Iron, American Foundrymen's Society, 1965.
228. A. Gulyaev, Metallurgy, Metallurgiya, Moscow, 1977.
229. A. Troiano and A. Greninger, Metal Progress, Vol. 50, 303, 1946.
230. J. Hodge and M. Orehoski, *Trans. AIME*, 167, 1946.
231. A. Schmykov, Heat Treater's Handbook, Mashgiz, Moscow, 1961.
232. K. Andrews, Empirical formulae for the calculation of some transformation temperatures, *JISI*, 203, 721–727, 1965.
233. W. Steven and A. Haynes, The temperature of formation of martensite and bainite in low-alloy steel, *JISI*, 183, 349–359, 1956.
234. W. Stuhlmann, What the TTT-diagrams tell us, *Harterei-Techn. Mitt.*, 6, 31–48, 1954.
235. A. Griebel, Microstructure of induction hardened parts, *Heat Treating Progress*, April/May, 35–38, 2001.
236. M. Tisza, Physical Metallurgy for Engineers, SAM International, 2001.
237. G. Melloy, P. Slimmon, and P. Podgursky, *Met.Trans.*, 4, 2279, 1973.
238. E. Rapoport, Optimization of Induction Heating of Metals, Metallurgy, Moscow, 1993.
239. E. Rapoport, Alternative Approach for Solving Optimal Control Problems, Nauka, Moscow, 2000.
240. V. Rudnev, D. Mellon, Induction billet heaters engineered for isothermal extrusion, *Modern Metals*, September, 1995.

241. D. Loveless, V. Rudnev, R. Cook, and T. Boussie, Space saving induction heating innovations, *Industrial Heating*, March, 1998.
242. V. Rudnev, D. Loveless and J. LaMonte et al., A balanced approach to induction tube and pipe heating, *Industrial Heating*, June, 1998.
243. K. Weiss, V. Rudnev, R. Cook, D. Loveless, and M. Black, Induction tempering of steel, *Advance Materials and Processes*, August, 1999.
244. V. Rudnev, T. Boussie, D. Loveless, and R. Cook, Innovations in induction heat treating of carbon steels and modern ductile (nodular) irons, Proceedings of the Sixteenth Heat Treating Conference, ASM International, 1996.
245. V. Rudnev and V. Demidovich, Computation tools for everyday use in modern induction heat treating, Proceedings of the Seventeenth Heat Treating Conference, ASM International, 1997.
246. E. Rylicki, A. White, and V. Rudnev, High frequency strip galvannealing with a doorless inductor, Proceedings of Galvatech '97, 1997.
247. R. Cook, A comparison of radio frequency power supplies, Proceedings of the Seventeenth Heat Treating Conference, ASM International, 1997.
248. D. Loveless, Solid state power supplies for modern induction heat treating, Proceedings of the Seventeenth Heat Treating Conference, ASM International, 1997.
249. S. Midson, V. Rudnev, and R. Gallik, The induction heating of semi-solid aluminum alloys, Proceedings of the Fifth International Conference on the Processing of Semi-Solid Alloys and Composites, 1998.
250. S. Midson, V. Rudnev, and R. Gallik, Semi-solid processing of aluminum alloys, *Industrial Heating*, January, 1999.
251. V. Rudnev, D. Loveless, W. Albert, K. Schweigert, and P. Dickson, Want your bar at uniform temperature? *Forging Magazine*, June, 1999.
252. V. Rudnev, D. Loveless, B. Marshall, K. Shepeljakovskii, N. Dyer, and M. Black, Gear heat treating by induction, *Gear Technology*, March, 2000.
253. V. Rudnev, R. Cook, D. Loveless, and M. Black, Induction hardening basics for iron and steel, *Modern Application News*, June, 2000.
254. V. Rudnev, R. Cook, D. Loveless, and M. Black, Shops warm up to induction heat treating, *American Machinist*, June, 2000.
255. V. Rudnev, D. Loveless, K. Schweigert, P. Dickson, and M. Rugg, Efficiency and temperature considerations in induction re-heating of bar, rod and slab, *Industrial Heating*, June, 2000.
256. V. Rudnev, D. Loveless, K. Schweigert, and M. Rugg, New generation of induction heating machines for the forging/rolling industry, Proceedings of the Twentieth Heat Treating Conference, St. Louis, October, ASM International, 2000.
257. K. Weiss, V. Rudnev, R. Cook, D. Loveless, and M. Black, Induction tempering of steels, *Journal of the Chinese Society for Metal Heat Treatment*, 65, 2000.
258. V. Rudnev, D. Loveless, and B. Marshall, Gear heat treatment by induction, Proceedings of the Twentieth Heat Treating Conference, St. Louis, October, ASM International, 2000.
259. V. Rudnev, D. Loveless, J. Murray, and R. Escobedo, Intricacies of induction tempering for automotive industry, Proceedings of the Twentieth Heat Treating Conference, St. Louis, October, ASM International, 2000.
260. D. Loveless, V. Rudnev, L. Lankford, G. Desmier, and H. Madhanie, Advanced non-rotational induction crankshaft hardening technology introduced to automotive industry, *Industrial Heating*, November, 2000.
261. V. Rudnev, D. Loveless, K. Schweigert, E. Rylicki, and M. Rugg, Achieving uniform temperature through induction heating, *Metallurgia*, December, 2000.

262. D. Loveless, V. Rudnev, L. Lankford, G. Desmier, and H. Madhanie, Advanced Non-Rotational Crankshaft Induction Hardening and Tempering Technology, Heat Treatment of Metals, Vol. 2, Wolfson Heat Treatment Centre, UK, 2001.
263. V. Rudnev et al., Gear heat treating by induction, *Journal of the Chinese Society for Metal Heat Treatment*, 68, 2001.
264. D. Loveless, V. Rudnev, L. Lankford, G. Desmier, and H. Madhanie, Reducing the scale of crankshaft hardening, *Metallurgia*, April, 2001.
265. V. Rudnev, J. Murray, K. Schweigert, D. Loveless, and M. Rugg, Intricacies of induction wire/cable/rod heating, Proceedings of the 71st Wire & Cable Symposium, Atlanta, May, 2001.
266. D. Loveless, V. Rudnev, G. Desmier, L. Lankford, and H. Madhanie, Non-rotational induction crankshaft hardening capabilities extended, *Industrial Heating*, June, 2001.
267. D. Loveless, V. Rudnev, G. Desmier, L. Lankford, and H. Madhanie, SHarP-C is advanced non-rotational induction crankshaft hardening and tempering technology, Proceedings of Global Powertrain Congress GPC-2001, Section: Advanced Engine Design & Performance, 2001.
268. V. Rudnev et al., Induction Re-Heating of Slabs, Plate, and Bars for Continuous Casting Lines, Manufactura, July, Mexico, 2001.
269. D. Loveless, R. Cook, and V. Rudnev, Current Trends in Technology of Induction Thermal Treatment in the USA, Metallovedenie I Termicheskaya Obrabotka Metallov, Moscow, Vol. 6, 2001.
270. V. Rudnev, D. Loveless, K. Schweigert, E. Rylicki, and M. Rugg, New Generation of Systems for Induction Re-Heating, Millennium Steel, UK, 2001.
271. D. Loveless, V. Rudnev, G. Desmier, L. Lankford, and H. Madhanie, SHarP-C is advanced non-rotational induction crankshaft hardening and tempering technology, *Powertrain International*, 4: 3, 2001.
272. K. Spain, Advances in Induction Heating of Wire Products, Wire and Cable Technology International, Vol. 1, 2000.
273. K. Spain and R. Kirkwood, Induction wire heating, *Wire Journal*, 2, 1997.
274. K. Spain, Industrial heating systems for forging industry, *Industrial Heating*, 3, 10–12, 1997.
275. K. Kunda and V. Peysakhovich, Induction heating before rolling on the world's largest continuous caster, Proceedings of the International Congress: Electromagnetic Processing of Materials, Vol. 2, May, 231–238, 1997.
276. Recommended Standards for Induction Bending of Pipe and Tube, TPA-IBS-98, Tube and Pipe Association International, 1998.
277. J. Wolf, Progressive Induction hardening of gears submerged in quenchant, *Industrial Heating*, 8, 10–12, 1979.
278. Review of Literature on Induction Hardening of Gears, Gear Research Institute, 1994.
279. K. Schweigert, Induction Heating Prior to Hot Working, Proceedings of the 6th International Induction Heating Seminar, Vol.2, September, 1995.
280. V. Rudnev and K. Spain, Advanced induction heating for the modern metalworking industry, Proceedings of the Fifth Precision Forging Conference, SME, Romulus, October, 1999.
281. M. Flemings, Behavior of metal alloys in the semi-solid state, *Met.Trans.*, 22A, 957, 1991.
282. S. Midson, Semi-solid castings of aluminum alloys: A status report, *Modern Castings*, February, 41, 1997.
283. K. Young, High integrity high pressure casting process: Market demands and process development, CIATF Technical Forum, UK, June, 1997.
284. Althix Billets, Aluminum Pechiney, April, 1996.

285. A. Eveson, Induction bar end heating, Proceedings of the Sixth International Induction Heating Seminar, Nashville, 1995.
286. V. Rudnev, New technologies in forge and extrusion coil design, Proceedings of the Sixth International Induction Heating Seminar, Nashville, 1995.
287. A. Nikanorov, The study of induction heating of strips using a transverse flux heater, Ph.D. Thesis, St. Petersburg Electrical Engineering University, Russia, 1987.
288. V. Demidovich, A. Nikanorov, and A. Slukhotskii, Energy Parameters of Induction Transverse Strip Heaters, 1989.
289. A. Ruhnke, Systematic study of induction transverse flux heating, Ph.D. Thesis, University of Hannover, Germany, 1999.
290. A. Ruhnke, A. Muhlbauer, and A. Nikanorov, A thermal deformation of the strip during transverse flux induction heating, Proceedings of Compel, Vol. 19, 2 730–736,, 2000.
291. A. Rashepkin and I. Kondratenko, Induction strip heating using travelling wave heaters, Kiev, Ukraine, (unpublished report) 1999.
292. F. Dughiero, M. Forzan, S. Lupi, and M. Tasca, Numerical and experimental analysis of an electro-thermal coupled problem for transverse flux induction heating equipment, *Proc. IEEE Transactions on Magnetics*, 34: 5, September, 3106–3109, 1998.
293. J. Schut, Close up on lost-core—A puzzle with many pieces, *Plastics Technology*, December, 1991.
294. T. Kidd, New generation of "lost core" meltout for plastic one-piece automotive air intake manifolds, Proceedings of the Seventh International Induction Heating Seminar, 1997.
295. S. Lupia and M. Forzan, Comparison of edge-effects of transverse flux and travelling wave induction heating inductors, *Proc. IEEE Transactions On Magnetics*, 35: 5, September, 3556–3558, 1999.
296. Induction Solutions for Steel Strip for Heat Treatment & Coating, Inductoheat Australia, 2001.
297. W. Trakowski, G. Pawolleck, and P. Knupfer, The application of high frequency technology for the inductive heating of steel strip in galvannealing, Proceedings of Galvatech '95, 181–188, 1995.
298. Y. Hardy et al., Design of square temperature-time cycle for optimal galvannealed sheet, Proceedings of Galvatech '95, 193–198, 1995.
299. M. Beguin et al., Revamping of Segal's galvannealing section by high frequency (HF) induction and misting jets, Proceedings of Galvatech '95, 199–203, 1995.
300. J. Remley and W. Lordo, Process lines and their mechanical components, AISE Seminar, Nashville, December 2–5, 1997.
301. E. Rylicki, Organic paint curing using induction heating, Proceedings of the First International Induction Heation Seminar, Sao Paulo, Brazil, 1995.
302. D. Loveless and J. Lovens, Strip Heating Coil Apparatus with Series Power Supplies, US Patent #5,837,976, 1988.
303. A. White, Perspectives and specifics of galvanizing and galvannealing technology in the world market, Internal report of Inductoheat Group, 2002.
304. J. Powell, In-line induction heat treatment, Proceedings of the Australian Institute of Metals, Sydney, August, 1984.
305. J. Powell, Stress relieving of steel strand for pre-stressed concrete tendous by induction heating method, Proceedings of the Wire ASIA Conference, Singapore, October, 1982.
306. J. Powell, Induction heating of pipes before coatings, *Tube & Pipe Equipment*, September, 1996.
307. J. Powell, High speed ACR copper tube inline induction annealing, Proceedings of the International Tube Conference, Singapore, October, 1997.
308. J. Arnosky, Induction Heating in the Manufacture of Electric Motors, 2002.

309. Die Heating by Induction, Inductoheat Banyard, UK, 1999.
310. Induction Heating Application Note—Extrusion Die Heating, Inductoheat Pty. LTD, 1995.
311. M. Fielding, A review of systems for heating extrusion dies, *Light Metal Age*, August, 1998.
312. Guide to Induction Heating Equipment, BNCE Induction Heating Group, 1984.
313. The Brazing Book, Handy & Harman Publication, 1985.
314. B. Gramoll, Induction brazing, Proceedings of the Seventh International Induction Heating Seminar.
315. J. Libsch and P. Capolongo, *Lepel Review*, 1: 5, 1.
316. R. Gallik, Using induction heating for joining, *Industrial Heating*, December, 1996.
317. G. Humpston and D. Jacobson, Principles of Soldering and Brazing, ASM International, 1993.
318. M. Schwartz, Brazing, ASM International, 1987.
319. V. Rudnev, Magnetic fields in induction heating, Proceedings of the SME Induction Heating Clinic, December 7–8, Cleveland, OH, 1994
320. C. A. Tudbury, Basics of Induction Heating, Vol. 2, Rider, New York, 1960.
321. D. L. Loveless, R. L. Cook, and V. I. Rudnev, Considering nature and parameters of power supplies for efficient induction heat treating, *Industrial Heating*, June 33–37, 1995.
322. D. L. Loveless, An overview of solid state for induction heating, *33 Metal Producing*, August, 1995.
323. INDUCTOHEAT Bulletin, Statipower 6, 1991.
324. General Presentation of Activity of Lepel Corp. 1990.
325. INDUCTOHEAT Bulletin, Statipower 5, 1991.
326. General Presentation of Activity of Radyne Ltd., UK, 1992.
327. General Presentation of Activity of Elphiac, Belgium, 1990.
328. INDUCTOHEAT Bulletin, Unipower 9, 1991.
329. INDUCTOHEAT Bulletin, Unipower 12, 1993.
330. R. L. Cook, D. L. Loveless, and V. I. Rudnev, Load matching in modern induction heat treating, *Ind. Heating*, September 1995.
331. INDUCTOHEAT Bulletin, Load Frequency Analyzer, 1991.
332. INDUCTOHEAT Bulletin, Uniscan-1, 1991.
333. INDUCTOHEAT Bulletin, Uniscan-11, 1992.
334. INDUCTOHEAT Bulletin, Uniscan-1V, 1992.
335. W. E. Terlop and S. Cassagrande, Special transformer technology for medium and high frequency applications, Proceedings of the First International Induction Heating Seminar, Sao Paulo, Brazil, 1995.
336. General Presentation of Jackson Transformer Company, 1993.
337. R. L. Cook, R. J. Meyers, and V. I. Rudnev, Process monitoring for more effective induction hardening control, *Mod. Appl. News*, August, 1995.
338. R. J. Meyers, Induction control with smoke and mirrors, Proceedings of the International Heat Treating Conference: Equipment and Processors, ASM International, 295–297, 1994.
339. INDUCTOHEAT Bulletin, Energy Monitor: Quality Control Energy Monitor, 1993.
340. INDUCTOHEAT Bulletin, QA Ultra 8000, 1992.
341. INDUCTOHEAT Bulletin, Stativision, 1993.
342. P. J. Miller, Automation is key to efficiency for many truck auto makers, *Heat Treat*, May, 1982.
343. D. Oxbrough, Current fed inverters, Proceedings of the Sixth International Heating Seminar, Nashville, September, 1996.

344. C. Johnson, Microprocessor-Based Process Control, Prentice-Hall, Englewood Cliffs, NJ, 1984.
345. S. Heisler, Wiley Engineer's Desk Reference, Wiley, New York, 1998.
346. W. Terlop, US Patent # 5,163,173.
347. T. Boussie, Water system problems and solutions, Proceedings of the Sixth International Induction Heating Seminar, Nashville, September, 1995.
348. J. Kosniewski, Induction heating: The basics and beyond, Proceedings of the Ninth International Induction Heating Seminar, May, 2000.
349. E. Almeida, Power factor correction on induction heating systems, Proceedings of the Sixth International Induction Heating Seminar, Nashville, September, 1995.
350. D. Paice, Power Electronic Converter Harmonics, IEEE Press, Piscataway, NJ, 1996.
351. N. Mohan, T. Undeland, and W. Robins, Power Electronics-Converters, Applications and Design, Wiley, New York, 1995.
352. IEEE Standard 519–1992. IEEE Recommended Practices and Requirements for Harmonic Control in Electrical Power Systems, IEEE Inc., Piscataway, NJ, 1993.
353. W. Frank and C. Der, Solid state RF generators for induction heating applications, *IEEE IAS Conference Record*, October, 939–944, 1982.
354. K. Mauch, Transistor inverters for medium power induction heating applications, *IEEE IAS Conference Record*, October, 555–562, 1986.
355. P. Jain and S. Dewan, A performance comparison of full- and half-bridge series resonant inverters in high frequency high power applications, *IEEE Transactions on Industry Applications*, 26: 2, March/April, 1990.
356. K. Kit Sum, Switch Mode Power Conversion, Marcel Dekker, New York, 1984.
357. INDUCTOHEAT Bulletin, Statipower HSPS, 2000.
358. INDUCTOHEAT Bulletin, Statiscan IV, 2000.
359. J. Blinov, Unique applications of induction technology in Russia, Proceedings of the Ninth International Induction Heating Seminar, Clearwater Beach, FL, May, 2000.
360. A. Vasiliev, S. Gurevich, and J. Ioffe, Power Supplies for Electrothermal Equipment, Energoatomizdat, Moscow, 1985.
361. INDUCTOHEAT Bulletin, Insta-Change Coil Adapters, 2000.
362. Metals Handbook, Vol. 6, Welding, Brazing, and Soldering, ASM International, 1983.
363. Bonding dissimilar materials safely, cleanly and accurately, *Heat Treating*, January, 1992.
364. INDUCTOHEAT Bulletin, M-17 Hem Bonding by Induction, 1992.
365. F. Chang et al., Bonding automotive hoods to eliminate spot welds, *Adhesives Age*, February, 1986.
366. E. Stefanides, Epoxy cured by induction heating gives strong sheet metal joint, *Design News*, June, 1987.
367. G. Totten, C. Bates, and N. Clinton, Handbook of Quenchants and Quenching Technology, ASM International, Metals Park, OH, 1993.
368. H. Boyer and P. Cary, Quenching and Control of Distortion, ASM International, Metals Park, OH, 1988.
369. Proceedings of the Second International Conference on Quenching and the Control of Distortion, by G. Totten and M. Howes, et al., Eds. ASM International, Metals Park, OH, 1996.
370. N. Nallicheri, J. Clark, and F. Field, Material alternatives for the automotive crankshaft: A competitive assessment based on manufacturing economics, SAE International Congress, Detroit, February, 1991.
371. Steel's Technical and Economic Progress in the Production of Lighter and Smaller Engine Components, BRMDG study, AISI, 2000.
372. J. Lewis, Advanced controls eliminates case-hardening contacts, *Design News*, 5: 1, 2000.

373. American Metal Treating Co., General Presentation, 1999.
374. N. Okada et al., Bending fatigue strength of gear teeth hardened by an induction hardening process, *The Sumitomo Search* 4, November, 1970.
375. D. Mellon, Contour gear hardening using induction heating with RF and thermographic control, *Industrial Heating*, July, 1988.
376. K. Shepelyakovskii, Induction Surface Hardening of Parts, Mashinostroenie, Moscow, 1972.
377. K. Shepelyakovskii and F. Bezmenov, New induction hardening technology, *Advanced Materials & Processes*, October, 1998.
378. V. Rudnev et al., Progress in study of temperature and electromagnetic field behavior during induction hardening, Proceedings of the First International Conference on Induction Hardened Gears and Critical Components, Indianapolis, IN, 1995.
379. D. Medlin, Induction hardening response of 1550 and 5150 steels with similar prior microstructure on induction hardening, Proceedings of the First International Conference on Induction Hardened Gears and Critical Components, Indianapolis, IN, 1995.
380. M. Wiezbowski, Induction Hardening of Critical Powertrain Components, Proceedings of the First International Conference on Induction Hardened Gears and Critical Components, Indianapolis, IN, 1995.
381. L. Alban, Systematic Analysis of Gear Failure, ASM International, Metals Park, OH, 1985.
382. E. Buckingham, Analytical Mechanics of Gears, Dover, 1949.
383. G. Krauss, Heat treated martensitic steels: Microstructural systems for advanced manufacture, Yukawa Memorial Lecture, Kanda Gakushi Kaikan, Tokyo, Japan, December, 1994.
384. M. Uno, F. Nakasato, S. Kiyokoba, and K. Uno, The effect of pre-microstructures (ferrite and perlite grain sizes) on the hardness profile of induction-hardened layers of medium-carbon steels, *The Sumitomo Search*, 45, March, 1991.
385. J. Hollomon and L. Jaffe, Time-temperature relations in tempering steel, *Trans. AIME*, 162, 1945.
386. S. Semiatin, D. Stutz, and T. Byrer, Induction tempering of steel: Parts 1 & 2. Development of an effective tempering parameter, *Journal of Heat Treating*, 4: 1, June, 1985.
387. ASM powder metallurgy.
388. J. Powell, Induction heating prior to coating for value-added pipe, *Tube and Pipe Technology*, January, 1997.
389. R. Baker, Heating of non-magnetic electric conductors by magnetic induction longitudinal flux, *Trans. of AIEE*, January, 1944.
390. J. Vaughan and J. Williamson, Design of induction heating coils for cylindrical non-magnetic loads, *Trans. of AIEE*, 64, August, 587–592, 1945.
391. B. Gover, Exploring applications, bending methods for structural tubing, *Tube and Pipe Journal*, June, 22–24, 2000.
392. Brarnshaws Bender Ltd., The Induction Bending Process, *Tube and Pipe Journal*, June, 60, 2001.
393. B. Frank, Save money when ordering bends, *Tube and Pipe Journal*, June, 28–32, 2001.
394. J. Gillanders, Pipe and Tube Bending Manual, Fabricators & Manufacturers Association, 1994.
395. J. Boikov, Optimization of the in-line induction heaters, Ph.D. Thesis, Samara State Technical University, Samara, Russia, 1985.
396. J. Lu, Handbook of Measurement of Residual Stresses, CETIM, 1996.
397. B. Vinton, In-line gas quench system bright anneales Korean tube, *Heat Treating*, June, 1988.

398. J. Powell, Developments in ACR copper tube induction annealing, Proceedings of the Seventh International Induction Heating Seminar, St. Louis, Vol. 2, April, 1997.
399. B. Evans, Induction Billet heating an updated summary of latest technology, Proceedings of the Seventh International Induction Heating Seminar, St. Louis, Vol. 2, April, 1997.
400. M. Garaway, Current fed power supplies for induction billet heating, Proceedings of the Seventh International Induction Heating Seminar, St. Louis, Vol. 2, April, 1997.
401. S. Baskerville, The latest trends & applications of high power IGBT modules in induction heating, Proceedings of the Eighth International Induction Heating Seminar, Kissimmee, FL, November, 1998.
402. M. Garaway, Innovations in forging equipment design, Proceedings of the Tenth International Induction Heating Seminar, Clearwater Beach, FL, October, 2001.
403. G. Desmier, Beneficial new technologies in system design: From product to process, Proceedings of the Tenth International Induction Heating Seminar, Clearwater Beach, FL, October, 2001.
404. S. Baskerville, Power supplies; flexible tuning, reliability and maintainability, Proceedings of the Tenth International Induction Heating Seminar, Clearwater Beach, FL, October, 2001.
405. J. Stambaugh, Advanced coil designs for heat treating and forging, Proceedings of the Eighth International Induction Heating Seminar, Kissimmee, FL, November, 1998.
406. J. Robson, High power voltage FED series inverters & applications, Proceedings of the Seventh International Induction Heating Seminar, St. Louis, Vol. 2, April, 1997.
407. D. Gerke and B. Kimmel, EDN's Designer's Guide to Electromagnetic Compatibility, Cahners, Denver.
408. J. Benedyk, Retrogression heat treatment applied to aluminum extrusions for difficult forming applications, *Light Metal Age*, October, 1996.
409. J. Goodwill and T. Donohue, Induction heating for the steel industry, *Iron and Steel Engineer*, August 1999.
410. G. Bobart, Part Handling Systems and Process Control, Course 60, Lesson 8, ASM International, 1986
411. Scherer et al., US Patent 4,761,530.
412. H. Rowan, J. Mortimer and D. Loveless, USA Patent 5,495,094.
413. K. Laue and H. Stenger, Extrusion; Processes, Machinery, Tooling, ASM International, 1983.
414. A. Singer and J. Coakham, Temperature change occurring during the extrusion of aluminium, tin, and lead, *Journal of the Institute of Metals*, 89, 1960–1961, 177–182.
415. A. Singer and J. Coakham, Temperature changes associated with speed variation during extrusion, lead, *Journal of the Institute of Metals*, 89, 1960–1961, 225–231.
416. R. Akeret, A numerical snalysis of temperature distribution in extrusion, *Journal of the Institute of Metals*, XCV, 1967, 204–211.
417. T. Chandrupatla and A. Belegundu, Introduction to Finite Elements in Engineering, Prentice-Hall, Englewood Cliffs, NJ, 1997.
418. V. Rudnev, Evaluation of the electro-thermal parameters of induction transverse flux heater used for edge re-heating of transfer bars, Inductoheat's inter-company teport, INDUCTOHEAT, Inc., Madison Heights, MI, 2001.
419. W. Jackson, Transverse flux induction heating of flat metal products, Proceedings of the U.I.E. Conference, VII, 1972.
420. Induction Heating Installations for the Extrusion of Steel Tubes, Inductotherm S.A.–Elphiac Bulletin.
421. A. Sutjagin, The study of electro-magnetic forces, vibration and industrial noise, Ph.D. Thesis, Samara State Technical University, Russia, 1987.

422. V. Rudnev, Advanced computation techniques for everyday use in induction heating, Proceedings of the Seventh International Induction Heating Seminar, St. Louis, 2, April, 1997.
423. V. Rudnev, Fatal mistakes in benchmarking frequency selection, Proceedings of the Eighth International Induction Heating Seminar, Kissimmee, FL, November, 1998.
424. P. Dickson, Successful start-up techniques for mass heating systems, Proceedings of the Eighth International Induction Heating Seminar, Kissimmee, FL, November, 1998.
425. W. Albert and M. Black, Principal considerations in coil design and fabrication, Proceedings of the Ninth International Induction Heating Seminar, Clearwater Beach, FL, May, 2000.
426. J. Robson and G. Fielding, INDUCTOHEAT's Technical Manual, AUS-GEN, Series III, Inductoheat-Australia, 1999.
427. V. Rudnev and D. Mellon, Inverse design concept of induction billet heating for modern aluminum extrusion industry, Proceedings of the Sixth International Induction Heating Seminar, Nashville, September, 1995.
428. L. Zimin, A. Danilushkin and P. Rudnev, Optimal design of induction slab and bloom heating systems, Proceedings of the Eighth International Induction Heating Seminar, Kissimmee, FL, November, 1998.
429. E. Rapoport, Yu. Pleshivtseva, M. Livshitz, P. Rudnev, Unique Solutions for Typical Induction Mass Heating Problems, Proceedings of 8th International Induction Heating Seminar, Kissimmee, FL, November, 1998.
430. M. Cloonan, New technology in induction forging coil design, Proceedings of Forge Fair '94, Columbus, OH, April, 1994.
431. T. Byrer, (Ed.) Forging Handbook, Forging Industry Association, 1985.
432. CRC Handbook of Chemistry and Physics, 51 Edition, The Chemical Rubber C., 1971.
433. L. Canale, C. Brooks, T. Watkins and V. Rudnev, The effect of prior microstructure on the hardness and residual stress distribution in induction hardened steels, Proceedings of SAE International Off-Highway Congress, Las Vegas, March, 2002.
434. C. Pearson and R. Parkins, The Extrusion of Metals, Wiley, New York, 1961.
435. B. Avitzur, Handbook of Metal-Forming Processes, Wiley, New York, 1983.
436. J. Holman, Heat Transfer, McGraw-Hill, New York, 1990.
437. A. Bryant et al., Isothermal extrusion, *Light Metal Age*, April, 1999.
438. NEWELCO Billet Heaters, NEWELCO Bulletin, 1999.
439. B. Boley and J. Weiner, Theory of Thermal Stresses, Dover, New York, 1997.
440. V. Bukanin, F. Dughiero, S. Lupi and A. Zenkov, Edge effects in planar induction heating systems, Proceedings of International Seminar "Heating by Internal Sources," Padua, September, 2001.
441. A. Nikanorov, G. Nauvertat, H. Schulbe, B. Nacke and A. Muhlbauer, Proceedings of International Seminar "Heating by Internal Sources," Padua, September, 2001.
442. F. Dughiero, S. Lupi, A. Muhlbauer and A. Nikanorov, TFN—Transverse flux induction heating of non-ferrous and precious metal strips, Proceedings of International Seminar "Heating by Internal Sources," Padua, September, 2001.
443. H. McGannon, The Making, Shaping, and Treating of Steel, United States Steel Corporation, 9th ed., 1971, p.1132.
444. A. Jablonka, K. Harste, K. Schwerdtfeger, Steel Research, Vol. 62, 1991, p. 24.
445. G. Desmier, V. Rudnev, R. Cook, D. Loveless, L. Lankford, H. Madhanie, Induction Hardening and Tempering of Critical Powertrain Components: A SHarP-C Approach to Reversing the Trend of Price for Quality, Proceedings of Global Powertrain Congress GPC-2002, Michigan, USA, 2002.
446. K. Schroder, CRC Handbook of Electrical Resistivities of Binary Metallic Alloys, CRC Press, Inc., 1983.
447. A. Nayar, The Metals Databook, McGraw-Hill, 1997.

448. J. Carvill, Mechanical Engineer's Data Handbook, CRC Press, Inc., 1993.
449. A. E. Slukhotskii, Inductors for Induction Heating, Energy Publ., St. Petersburg, Russia, 1954.
450. Physical Values, Edited by I. Grigor'ev and E. Meilikhov, Energoatomizdat, Moscow, 1991.
451. V. Zinoviev, Thermal Properties of Metals at High Temperatures, Metallurgia, Moscow, 1989.
452. A. Buch, Pure Metals Properties, ASM International, 1999.
453. R. Lula, Stainless Steel, ASM International, 1986.
454. L. Hall, Survey of Electrical Resistivity Measurements on 16 Pure Metals in the Temperature Range 0 to 273°K, United States Department of Commerce, February, 1968.
455. G. Brady et al. Materials Handbook, McGraw-Hill, 1997.
456. T. Hicks, Standard Handbook of Engineering Calculations, McGraw-Hill, 1995.
457. E. Avallone, Th. Baumeister, Mark's Standard Handbook for Mechanical Engineering, McGraw-Hill, 1996.
458. A. Belegundu, T. Chandrupatla, Optimization Concepts and Applications in Engineering, Prentice Hall, 1999.
459. D. Peaceman, H. Rachford, The Numerical Solution of Parabolic and Elliptic Differential Equations, *J. Soc. Industr. and Appl. Math.*, Vol.3, #1, 1955.
460. E. Kolbe, W. Reis, Eine Methode zur Numerischen Bestimmung der Stromdichteverteilung, Wiss. Z. Hochshule Elektrotechnik, Ilmenau, Bd.9, #3, 1963.
461. R. Dudley, P. Burke, The Prediction of Current Distribution in Induction Heating Installations, IEEE Transactions of Industry Applications, IA-9(5), 1972.
462. O. Tozoni, Calculation Of the Electromagnetic Fields Using Computers, Kiev, Ukraine, 1967.
463. F. Grover, Inductance Calculations Working Formulas and Tables, Dover, New York, 1946.
464. P. Kalantarov, L. Tscheitlin, Inductance Calculations, Energoatomizdat, St. Petersburg, 1986.
465. M. Abramowitz, I. Stegun, Handbook of Mathematical Functions, Dover, New York, 1970.
466. L. Neiman, Skin Effect in Ferremagnetic Bodies, Gosenergoizdat, St. Petersburg, Russia, 1949.
467. S. Gurevich, A. Vasil'ev, B. Polevodov, General Tendencies of Mathematical Modeling of Induction and Dielectric Heating, Electrotechnica, Vol. 8, 1982, p.37–40.
468. A. Shamov, V. Bodazkov, Design and Maintenance of High Frequency Systems, Mashgiz, St. Petersburg, 1963.
469. R. Lerner, G. Trigg, Encyclopedia of Physics, VCH Publishers, 1990.
470. G. Totten, M. Howes, T. Inoue, Handbook of Residual Stress and Deformation of Steel, ASM International, 2002.
471. Tool Steel for Dies and Motors, edited by X. Luoping and L. Norstrom, Shanghai Jiao Tong University Press, 1998.
472. P. Simpson, Induction Heating, McGraw-Hill, 1960.
473. M. Aronov, N. Kobasko, et al, Practical Application of Intensive Quenching Technology for Steel Parts, Heat Treatment of Metals, Vol.1, 2000.
474. D. Herring, Heat Treating P/M Parts, Heat Treating Progress, June, 2002.
475. Metallographic Catalog, LECO Corporation, 1998.
476. Corrosion: Understanding the Basics, Edited by J.R.Davis, ASM International, 2000.
477. E. Stansbury, R. Buchanan, Fundamentals of Electrochemical Corrosion, ASM International, 2000.
478. ASM Handbook: Corrosion, Vol. 13, 1987.

479. TSH Steels and Advances in Induction Hardening of Pinions, Inter-company Report of ERS Engineering Corp., 2002.
480. S. Nasar, 2000 Solved Problems in Electromagnetics, McGraw-Hill, 1992.

Appendix A

PERIODIC TABLE OF THE ELEMENTS

Appendix B

CONVERSIONS

Temperature

Celsius to Fahrenheit and vice versa:	°C = 5/9 (°F − 32)	or °F = 9/5°C + 32
Celsius to Kelvin and vice versa:	°C = °K 273	or °K = °C + 273
Fahrenheit to Kelvin and vice versa:	°F = 5/9 (°K − 460)	or °K = 9/5 (°F + 460)
Rankine to Fahrenheit and vice versa:	°R = °F + 460	or °F = °R − 460
Rankine to Kelvin and vice versa:	°R = 1.8 °K	or °K = °R/1.8

Temperature Difference (Temperature Gradient)

1°C = 1°K = 1.8°F = 1.8°R

Multiplication factor	Symbol	Prefix
1 000 000 000 000 000 = 10^{15}	P	exa
1 000 000 000 000 = 10^{12}	T	tera
1 000 000 000 = 10^{9}	G	giga
1 000 000 = 10^{6}	M	mega
1 000 = 10^{3}	k	kilo
100 = 10^{2}	h	hecto
10 = 10^{1}	da	deka
1 = 10^{0}		
0.1 = 10^{-1}	d	deci
0.01 = 10^{-2}	c	centi
0.001 = 10^{-3}	m	mili
0. 000 001 = 10^{-6}	μ	micro
0. 000 000 001 = 10^{-9}	n	nano
0. 000 000 000 001 = 10^{-12}	p	pico
0. 000 000 000 000 001 = 10^{-15}	f	femto

Roman Numbers

1	**I**	11	**XI**
2	**II**	12	**XII**
3	**III**	13	**XIII**
4	**IV**	14	**XIV**
5	**V**	15	**XV**
6	**VI**	20	**XX**
7	**VII**	50	**L**
8	**VIII**	100	**C**
9	**IX**	500	**D**
10	**X**	1000	**M**

Fractions vs. Millimeters

Fractions	mm	Fractions	mm	Fractions	mm	Fractions	mm
1/64	0.397	17/64	6.747	33/64	13.097	49/64	19.447
1/32	0.794	9/32	7.144	17/32	13.494	25/32	19.844
3/64	1.191	19/64	7.541	35/64	13.891	51/64	20.241
1/16	***1.588***	***5/16***	***7.938***	***9/16***	***14.288***	***13/16***	***20.638***
5/64	1.984	21/64	8.334	37/64	14.684	53/64	21.034
3/32	2.381	11/32	8.731	19/32	15.081	27/32	21.431
7/64	2.778	23/64	9.128	39/64	15.478	55/64	21.828
1/8	***3.175***	***3/8***	***9.525***	***5/8***	***15.875***	***7/8***	***22.225***
9/64	3.572	25/64	9.922	41/64	16.272	57/64	22.622
5/32	3.969	13/32	10.319	21/32	16.669	29/32	23.019
11/64	4.366	27/64	10.716	43/64	17.066	59/64	23.416
3/16	***4.763***	***7/16***	***11.113***	***11/16***	***17.463***	***15/16***	***23.813***
13/64	5.159	29/64	11.509	45/64	17.859	61/64	24.209
7/32	5.556	15/32	11.906	23/32	18.256	31/32	24.606
15/64	5.953	31/64	12.303	47/64	18.653	63/64	25.003
1/4	***6.35***	***1/2***	***12.7***	***3/4***	***19.05***	***1***	***25.4***

Length

1 ft = 12 in = 0.33 yd = 0.3048 m = 30.48 cm = 304.8 mm
1 m = 100 cm = 1000 mm = 1.0936yd = 3.281 ft = 39.37 in
1 in = 0.0833 ft = 0.0278 yd = 0.0254 m = 2.54 cm = 25.4 mm
1 mile = 5280 ft = 1760 yd = 1609 m = 1.609 km = 0.869 miles (naut)
1 km = 1000 m = 10^6 mm = 0.621 miles = 1094 yd = 3281 ft

Area

1 ft^2 = 0.111 yd^2 = 144 in^2 = 0.0929 m^2 = 929 cm^2 = 929 mm^2
1 m^2 = 10^4 cm^2 = 10^{-6} km^2 = 1.196 yd^2 = 10.76 ft^2 = 1550 in^2
1 acre = 4840 yd^2 = 43560 ft^2 = 4047 m^2 = 4.047 km^2 = 0.4047 hectares

Volume

1 ft^3 = 0.037 yd^3 = 1728 in^3 = 0.0283 m^3 = 7.481 gallons(US) = 28.32 liters
1 gallons(US) = 3.785 liters = 4.0 quarters = 8.0 pints(US) = 0.1337 ft^3 = 0.00379 m^3
1 liter = 1000 ml = 0.264 gallons(US) = 61.02 in^3 = 0.001 m^3 = 0.0353 ft^3

Weight

1 kg = 1000 g = 2.205 lb = 35.274 oz = 0.001 tonne = 0.0011 ton
1 ton = 2000 lb = 0.907 tonne = 907 kg

Energy

1 kcal = 4187 joules = 3.968 Btu = $4.186*10^{10}$ erg
1 joules = $2.388*10^{-4}$ kcal = $9.478*10^4$ Btu
1 Btu = 1055 joules = 0.252 kcal

Flow

1 GPM(US) = 3.785 l/min = $3.785*10^{-3}$ m^3/min = 0.1337 ft^3/min
1 m^3/min = 264 GPM(US) = 35.31 ft^3/min = 1000 liters/min

Pressure

1 atm = 102325 Pa = 1.013 bar = 14.696 psi = 14.7 lb/in^2 = 10332 kg/m^2
1lb/in^2 = 703.1 kg/m^2 = 16 oz/in^2 = 0.0689 bar = 6895 Pa = 6895 N/m^2

Velocity (Speed)

1 ft/min = 0.3048 m/min = 0.00508 m/s = 0.0167 ft/s = 0.0183 km/hr
1 m/s = 3.281 ft/s = 3.6 km/h = 2.237 miles/hr

Density

1 g/cm^3 = 1000 kg/m^3 = 62.43 lb/ft^3 = 0.0361 lb/in^3
1 lb/in^3 = 1728 lb/ft^3 = 27.68 g/cm^3 = $2.768*10^4$ kg/m^3

Heat

1 cal = 0.003967 Btu = 4.186 joule (J)
1 joule = 0.000948Btu = 0.2389 cal

Thermal Conductivity

1 W/(m*K) = 0.578 Btu/(h*ft*°F) = $2.388*10^{-3}$ cal/(s*cm*°C) = 0.86 Kcal/(hr*m*°C)
1 Btu/(h*ft*°F) = $4.13*10^{-3}$ cal/(s*cm*°C) = 1.488 Kcal/(hr*m*°C) = 1.731 W/(m*K)

Specific Heat

1 J/(kg*°C) = $2.39*10^{-4}$ cal/(g*°C) = 0.4545 J/(lb*°C)
1 J/(lb°C) = 2.2J/(kg*°C) = $5.258*10^{-4}$ cal/(g*°C)

Electrical Resistivity

1 Ω*m = 100 Ω*cm = 39.37 Ω*in = 3.28 Ω*ft
1 Ω*in = 0.0254 = 0.0833 Ω*ft = 0.0254 Ω*m = 2.54 Ω*cm

Appendix C

INDUCTOHEAT'S "FISHBONE" DIAGRAM OF CRACKING

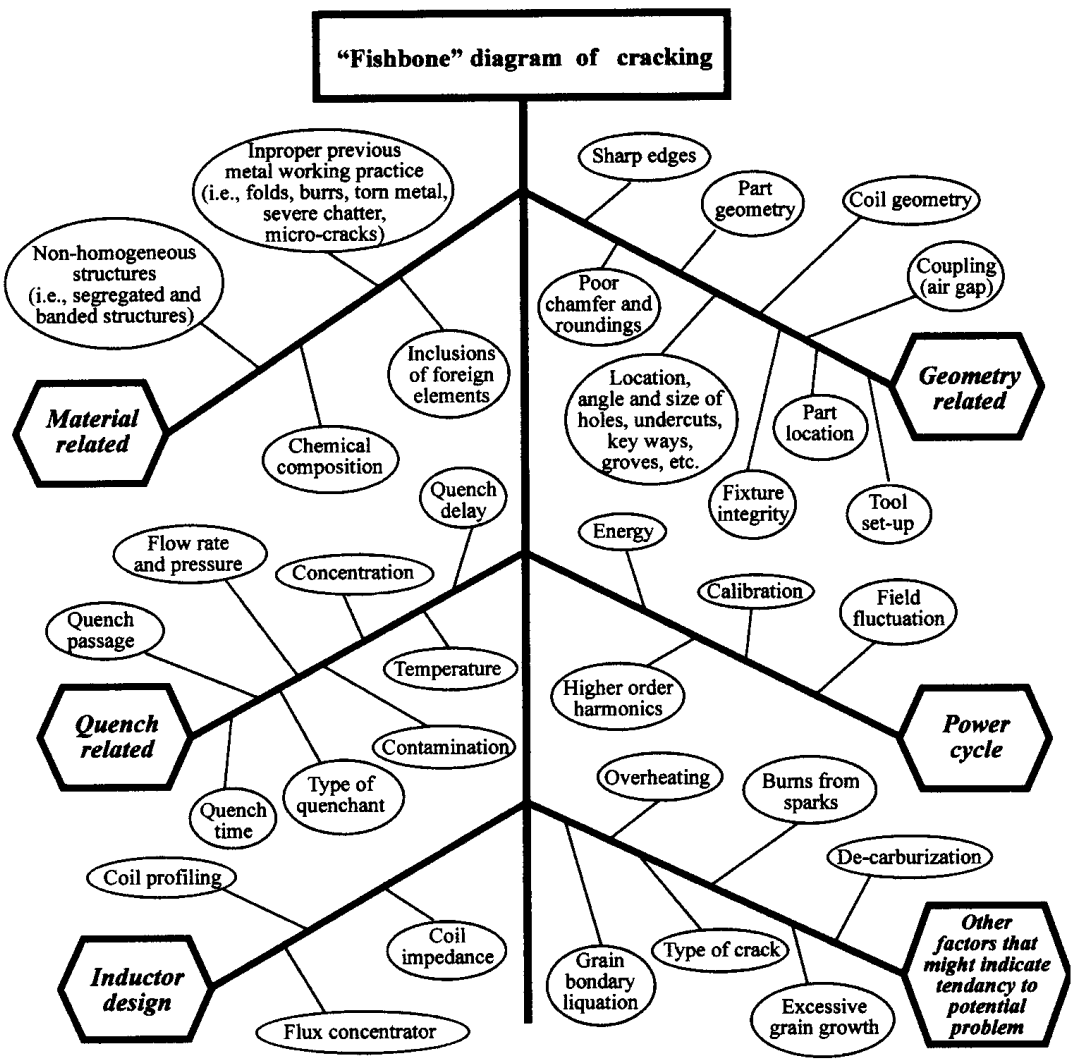

Appendix D

LONGITUDINAL ELECTROMAGNETIC END EFFECT

The distribution of the magnetic field along the axis in the end area of the empty "ideal" solenoid (helical) coil can be obtained relatively easily using an expression that describes the magnetic field distribution in a single loop of wire. The assumption of an "ideal" solenoid presumes the following conditions:

- The solenoid turns are tightly wound using thin wire.
- The coil current is uniformly distributed within each turn.
- There are no electrically conductive bodies located within close proximity of the solenoid.

Figure D1 shows the sketch of such an ideal solenoid of length l and radius R that has N tightly wound turns. A current carrying empty loop produces a B field along the loop axis with "z" component according to the following expression [42–45, 480]:

$$B_z = \frac{\mu_0 R^2 I}{2\left(R^2 + Z^2\right)^{3/2}} \tag{D1}$$

where Z is the axial distance from the loop to the area of interest, I is the loop current and μ_0 is the permeability of free space (a vacuum), $\mu_0 = 4\ \pi 10^{-7}$ H/m [or Wb/(A*m)].

The magnetic field at the center of the empty loop can be obtained by assuming $Z = 0$ in equation (D1). This results in

$$B_z = \frac{\mu_0 I}{2 R} \tag{D2}$$

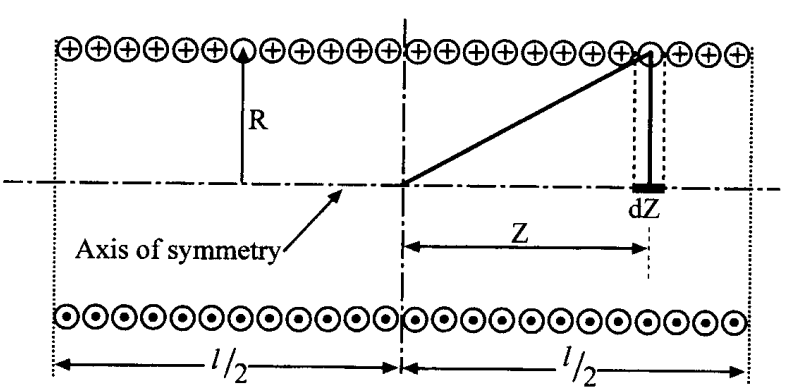

Figure D1 Sketch of a tightly wound multi-turn solenoid for end effect calculation.

The magnetic field distribution along the axis of an empty solenoid can be obtained by expansion of B_z of a single wire loop on a multi-turn coil. Taking into consideration the assumption of tightly wound solenoid turns the contribution of a small current carrying section "dZ" on the total field in the center of the solenoid will be

$$d\,B_z = \frac{\mu_0\,R^2}{2\,(R^2 + Z^2)^{3/2}}\,\frac{N\,I}{l}\,d\,Z = \frac{\mu_0\,R^2\,N\,I}{2\,l}\left(\frac{d\,Z}{(R^2 + Z^2)^{3/2}}\right) \tag{D3}$$

The total magnetic field in the center of the coil can be obtained by taking into account the contributions of all current carrying sections. Therefore, after integrating dB_z along the coil length the magnetic field along the coil center can be written as

$$B_z = \frac{\mu_0\,R^2\,N\,I}{2\,l}\int_{-L/2}^{L2}\frac{d\,Z}{(R^2 + Z^2)^{3/2}} \tag{D4}$$

After simple mathematical operations the total axial field in the center of the solenoid will be

$$B_z = \frac{\mu_0\,N\,I}{\sqrt{(4\,R^2 + l^2)}} \tag{D5}$$

If the length of the solenoid is much greater then its radius $l \gg R$ (electromagnetically long coil) then it is possible to neglect R with respect to l and (D4) can be rewritten as

$$B_z = \frac{\mu_0\,N\,I}{l} \tag{D6}$$

This is the well-known expression for the axial B field at the center of an electro-magnetically long solenoid. It is possible to show that by letting the corresponding limits in equation (D4), the equations (D1) and (D4) can be transformed into

$$B_z = \frac{\mu_0\,N\,I}{2\,\sqrt{(R^2 + l^2)}} \tag{D7}$$

For an electro-magnetically long coil (D7) can be approximated as

$$B_z = \frac{\mu_0\,N\,I}{2\,l} \tag{D8}$$

Therefore, a comparison of expressions (D6) and (D8) shows that at the ends of the empty coil the magnetic flux density B_z drops to one-half its value at the center. The same will be true for an electromagnetically long multi-turn coil with an infinitely long homogeneous non-magnetic workpiece.

Figure 3.32 (zone "b") shows the distribution of the magnetic field intensity along the coil length. As one can see the density of the induced current under the coil end is two times less than in the center. It means that the power density under the coil end is equal to a quarter of that in the center ($P_{end} = 0.25 * P_{center}$). The length of zone "b" depends on the skin effect in the heated workpiece, the ratio of coil inside

radius to workpiece radius and the coil turn space factor K_{space} and might be as long as five times the coil radius (if skin effect is not pronounced and the ratio of coil inside radius to workpiece radius in large) or twelve equivalent air gaps between the coil and the load (for pronounced skin effect and small air gaps).

Appendix E

REQUIRED INLET AND OUTLET QUENCH FLOW VS. PRESSURE

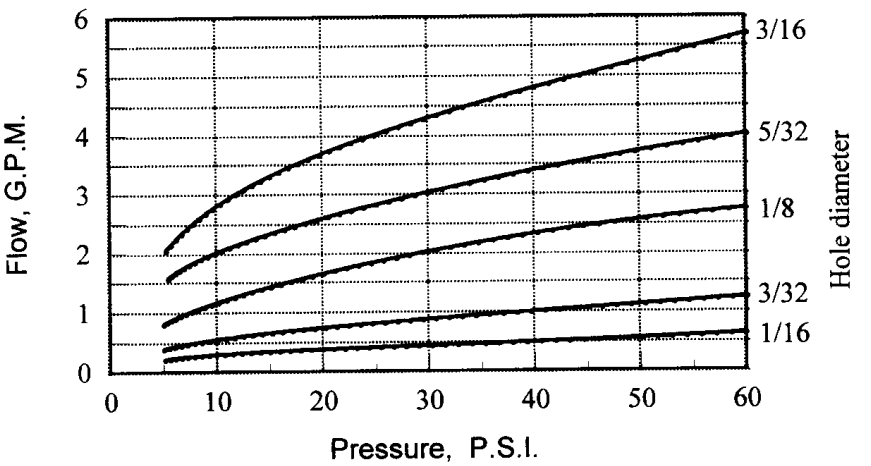

The number of quench holes is sometimes limited to the available quench inlet (i.e., the number and size of hoses and/or pump capacity, plumbing limitations, etc.). When estimating the number and size of holes versus the required flow one can refer to the above chart, finding the flow of a single orifice and multiplying it by the number of quench holes in the quench apparatus. The resultant amount of quench fluid can be determine by the size and number of quench holes. *Example*: At 20psi if there are 100–1/8" (3.1 mm) diameter quench holes the total flow estimate would be 1.7 * 100 = 170 gpm.

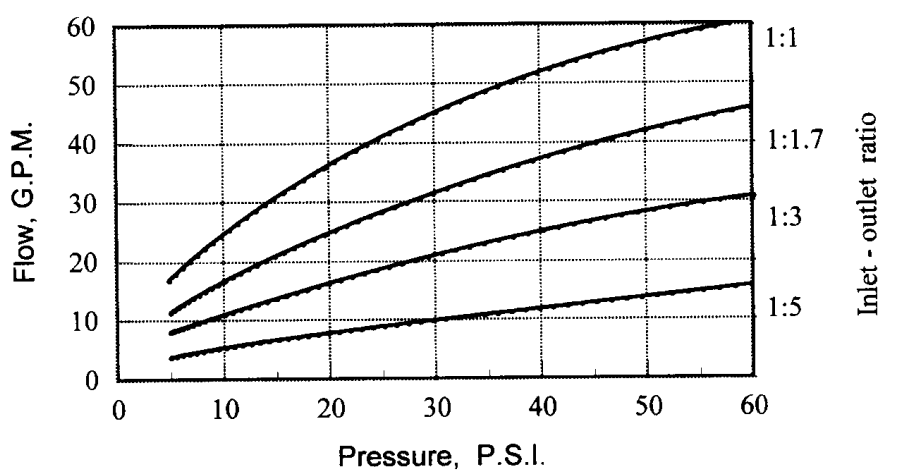

The quench inlet volume must be equal to or greater than the calculated outlet volume (quench holes). To insure constant flow and pressure (in order to keep the quench chamber full), it is usually advantageous to have a slightly larger inlet volume than the calculated outlet. The chart shows the effect of inlet-to-outlet ratio on quenchant flow versus pressure.

Example: @ 20psi with 1:1 ratio the flow will be 36 gpm
@ 20psi with 1:5 ratio the flow will be 8 gpm

Appendix F

DYNAMICS OF SINGLE-SHOT INDUCTION HEATING OF 40 MM (0.04 M) OD AXLE SHAFT

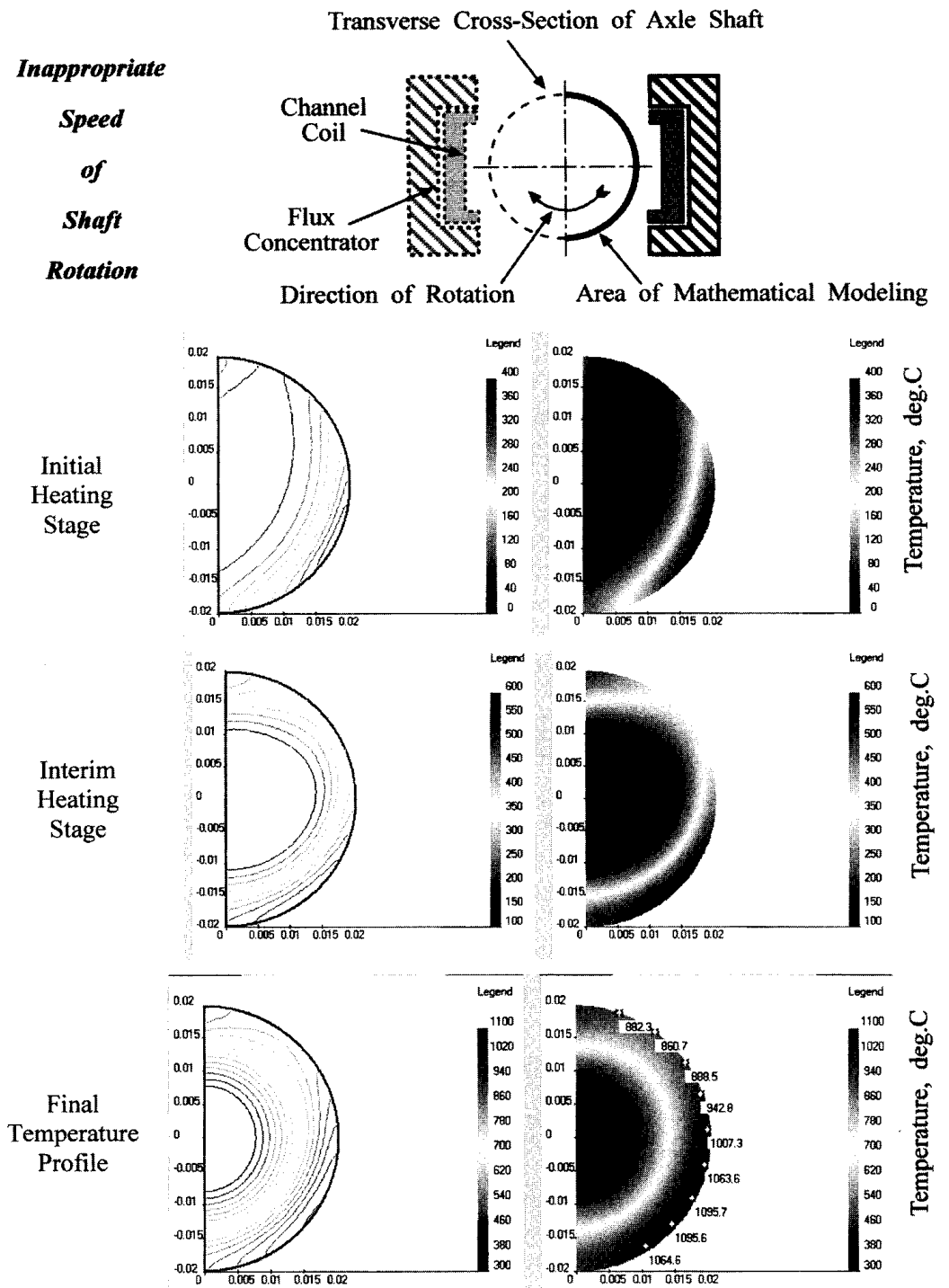

Appropriate Speed of Shaft Rotation

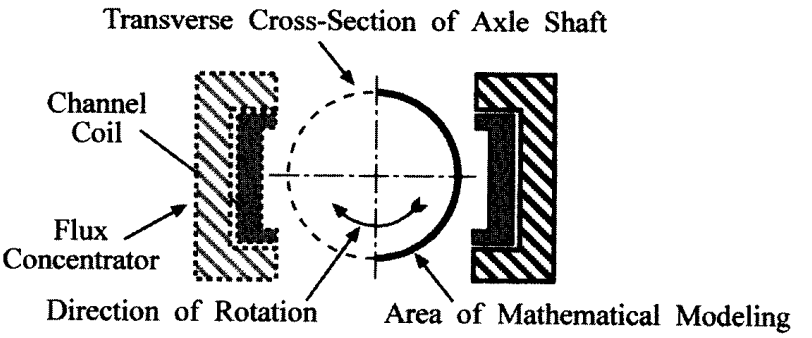

Initial Heating Stage

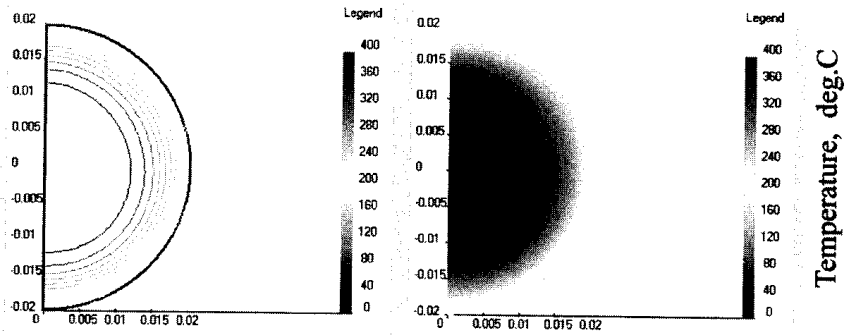

Interim Heating Stage

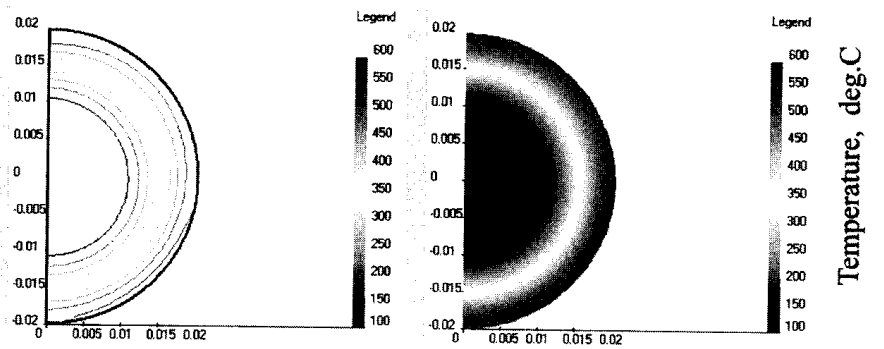

Final Temperature Profile

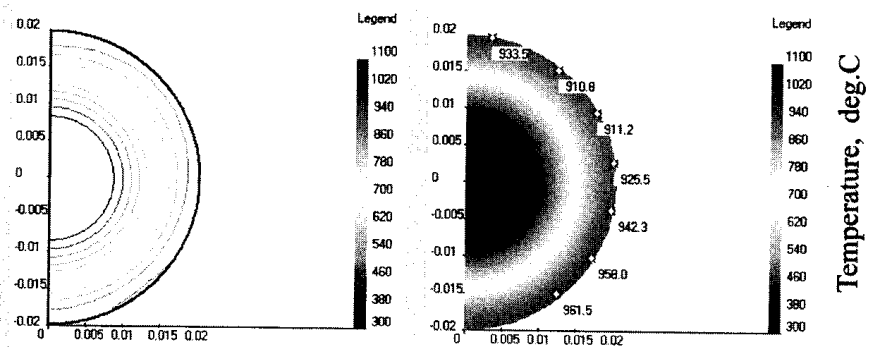

Appendix F (continued)

Appendix G

COOLING OF UNIFORMLY HEATED (1315°C/2400°F) 0.152 m RCS STAINLESS STEEL BAR (301 SERIES) DURING ITS TRANSPORTATION ON AIR

Radius of RCS bar is 6mm (0.25in.)

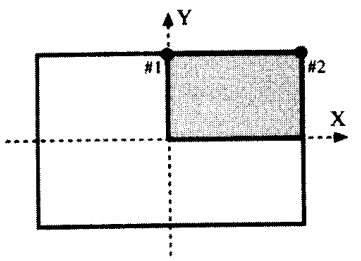

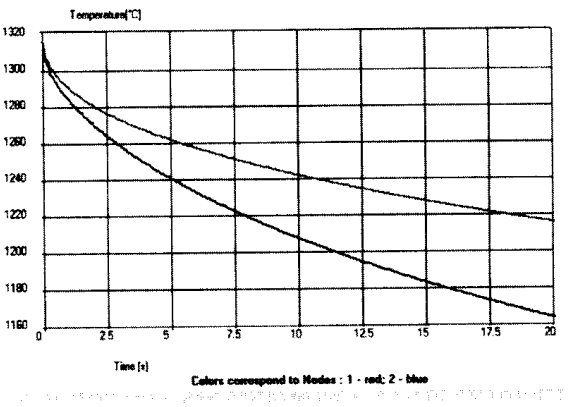

After 5 seconds of cooling

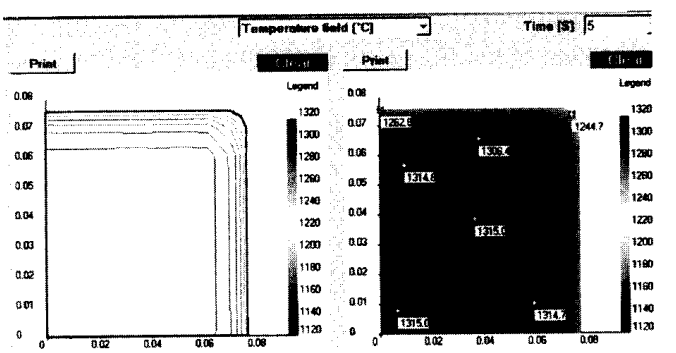

After 20 seconds of cooling

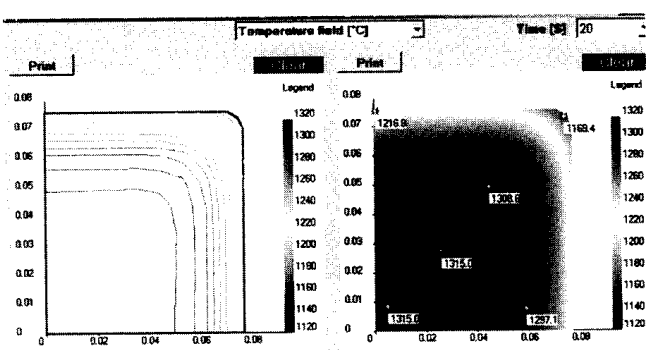

Radius of RCS bar is 20mm (0.75in.)

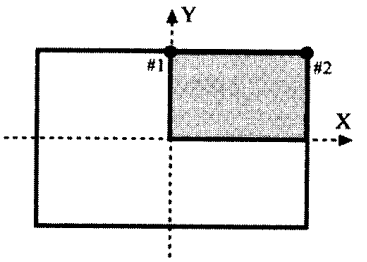

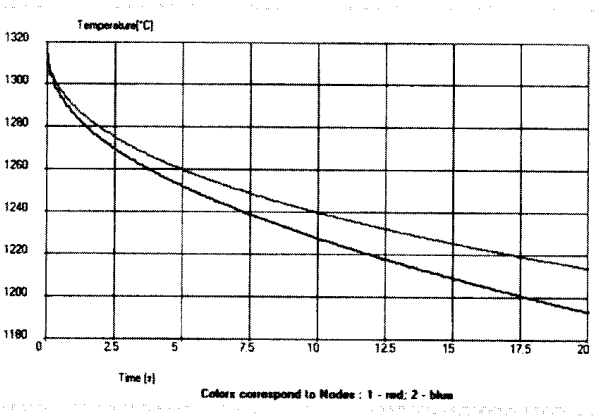

After 5 seconds of cooling

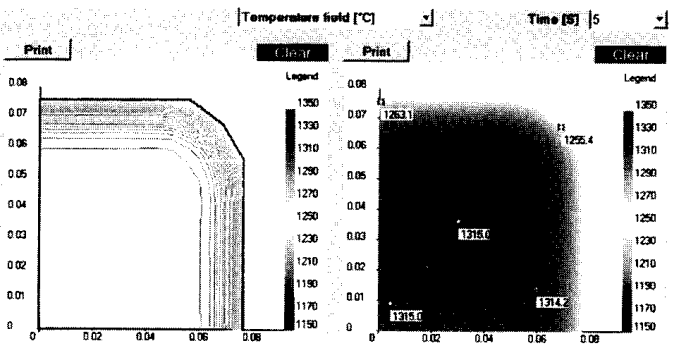

After 20 seconds of cooling

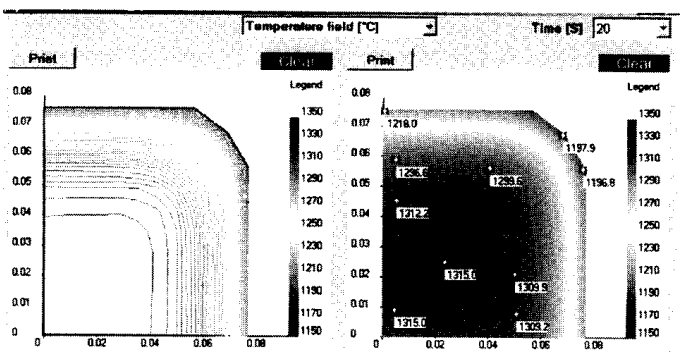

Appendix G (continued)

Appendix H

EXAMPLES OF TRANSIENT END EFFECT IN THE BAR LEADING END ZONE

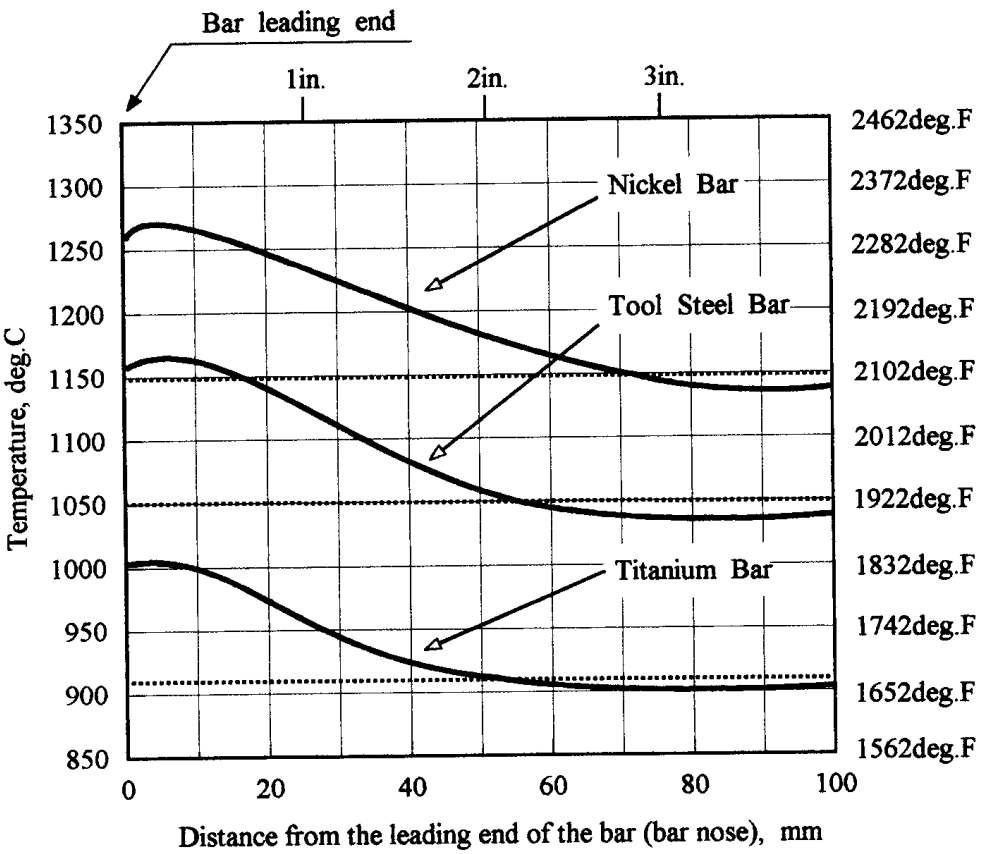

102 mm (4 in.) OD bars are continuously heated in multi-coil induction heater using frequency of 500 Hz.

Appendix I

TEMPERATURE DISTRIBUTION (°C) DURING HEATING AND QUENCHING OF A DOUBLE-PIN FEATURE OF THE V-8 CRANKSHAFT AND THE FINAL HARDNESS PATTERN USING SHarP-C TECHNOLOGY

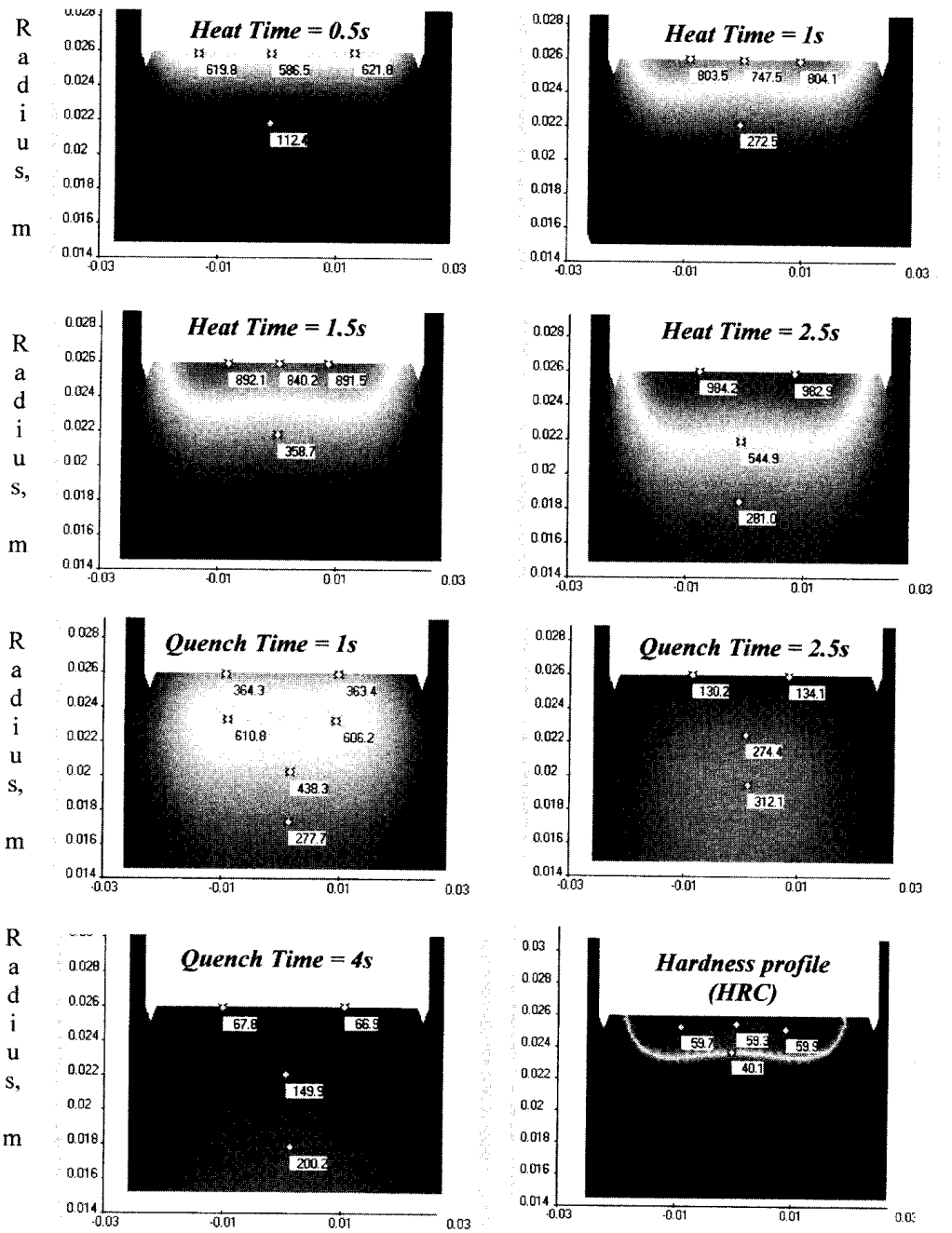

Index

About the Authors

Dr. Valery Rudnev is Group Director of Science and Technology at Inductoheat. He received his M.S. degree in electrical engineering from Samara State Technical University and his Ph.D. in induction heating from St. Petersburg Electrical Engineering University, Russia. He was the proud student of the honored professor Edgar Rapoport. Formerly, Dr. Rudnev was an associate professor teaching graduate and postgraduate courses. His areas concentration are electromagnetics, material science, heat transfer, mathematical modeling, and process development. He has 27 years of experience in induction heating. His credits include 15 patents and 112 scientific and engineering publications. He is a member of ASM, SME, AISE, IEEE Magnetics, and the New York Academy of Sciences.

Mr. Don Loveless is Group Vice President of Research and Development at Inductoheat. He received his electrical engineering degree from Western Michigan University. His responsibilities include development of high- and medium- frequency transformers, power electronics components, and development of thyristorized and transistorized power supplies including IGBT and MOS FET inverters for a wide variety of applications of induction heating. Mr. Loveless has 30 years of experience in induction heating. He has six patents and has authored 36 research and engineering publications. Mr. Loveless is an inventor of numerous design innovations. He is a member of IEEE Industrial Applications, ASM, IEEE Industrial Electronics, and Power Electronics.

Mr. Raymond Cook is Vice President of Engineering at Inductoheat. He is a registrated Professional Engineer in the State of Michigan, with a B.S. degree from Western Michigan University and an M.B.A. from Wayne State University, Michigan. Mr. Cook has been involved in the design and development of high-, medium-, and low-frequency solid-state inverters, machine and system design, load matching, process control, and monitoring for a wide variety of induction heating applications including hardening, annealing, tempering, and lost-core melt-out technology. Mr. Cook has 33 years of experience in induction heating and has written 24 research and engineering articles. He is a member of ASM.

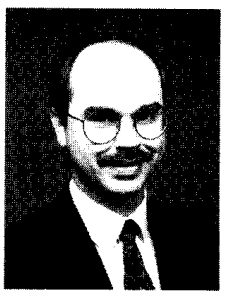

Mr. Micah Black is the induction heat treating coil design supervisor at Inductoheat. He graduated from Oakland Community College, Michigan. Mr. Black has 21 years of experience designing induction coils, fixtures, and quenching systems for various metal heat treating applications, including surface hardening, shrink fitting, tempering, stress relieving, brazing, and soldering. Mr. Black has been involved in the development of a number of advanced induction heating processes, such as inline tempering, heat treating of gears and critical components, induction hem bonding, and selective hardening of front-wheel-drive components. He is the author of 13 engineering publications. He is a member of ASM.

about the book . . .

This **reference** provides detailed descriptions of electromagnetic and heat transfer phenomena as well as current methods in the design and analysis of induction heat treating, mass heating, melting, and welding processes and equipment—exploring principles in load matching, process control, quality assurance, equipment monitoring, and system maintenance to improve the **reliability** and **efficiency** of induction heating systems and components.

Contains valuable photographs, magnetic field plots, and temperature profiles to navigate and avoid difficulties in system construction and installation.

The ***Handbook of Induction Heating*** covers methods to select the most appropriate power supply to enhance energy- and cost-efficiency, flexibility, and solidity in system function...model and simulate heating and cooling processes, as well as changes in material properties through heating cycles...estimate variations in principal process parameters, such as temperature, required power, optimal frequency, electrical current, and coil voltage...and compare mathematical techniques for calculating heat treating constraints, partial differential equations, and coupling approaches...and details heating of irregularly shaped products, such as billets, blooms, tubes, wires, and strips...common pitfalls in the utilization of commercially available software for computing induction heating parameters...and the latest techniques in surface and through hardening, tempering, stress relieving, normalizing, annealing, spherodizing, and sintering, as well as brazing, bonding, shrink fitting, and cap sealing.

Printed in the United States of America

MARCEL DEKKER, INC.
NEW YORK • BASEL

ISBN 0-8247-0848-2